



सत्यमेव जयते

INDIAN AGRICULTURAL  
RESEARCH INSTITUTE, NEW DELHI

I.A.R I.6.

GIP NLK—H 3 I.A.R.I. —10-5-55—15,000







THE  
PROCEEDINGS  
OF  
THE PHYSICAL SOCIETY

Section A

FROM JANUARY 1949 TO DECEMBER 1949

VOLUME 62



Published by  
THE PHYSICAL SOCIETY  
1 Lowther Gardens, Prince Consort Road,  
London S.W.7

# OFFICERS AND COUNCIL, 1949-50

## PRESIDENT

S. CHAPMAN, M.A., D.Sc. F.R.S. (1949- )

## VICE-PRESIDENTS

who have filled the Office of President

C. H. LEES, D.Sc., F.R.S. (1918-20)  
Sir FRANK SMITH, G.C.B., G.B.E., D.Sc., LL.D., F.R.S. (1924-26)  
Sir OWEN RICHARDSON, M.A., D.Sc., F.R.S. (1926-28)  
W. H. ECCLES, D.Sc., M.I.E.E., F.R.S. (1928-30)  
A. O. RANKINE, O.B.E., D.Sc., F.R.S. (1932-34)  
T. SMITH, M.A., F.R.S. (1936-38)  
ALLAN FERGUSON, M.A., D.Sc. (1938-41)  
Sir CHARLES DARWIN, K.B.E., M.C., M.A., Sc.D., F.R.S. (1941-43)  
E. N. da C. ANDRADE, Ph.D., D.Sc., F.R.S. (1943-45)  
Sir DAVID BRUNT, K.B.E., M.A., Sc.D., F.R.S. (1945-47)  
G. I. FINCH, M.B.E., D.Sc., F.R.S. (1947-49)

## VICE-PRESIDENTS

W. D. WRIGHT, D.Sc.	C. H. COLLIE, M.A., B.Sc.
W. JEVONS, D.Sc., Ph.D.	R. E. PEIERLS, C.B.E., M.A., D.Phil., D.Sc., F.R.S.

## HONORARY SECRETARIES

C. G. WYNNE, B.A. ( <i>Business</i> )	H. H. HOPKINS, Ph.D. ( <i>Papers</i> )
---------------------------------------	--

## HONORARY FOREIGN SECRETARY

E. N. da C. ANDRADE, Ph.D., D.Sc., F.R.S.

## HONORARY TREASURER

H. SHAW, D.Sc.

## HONORARY LIBRARIAN

R. W. B. PEARSE, D.Sc., Ph.D.

## ORDINARY MEMBERS OF COUNCIL

D. ROAF, M.A., D.Phil.	R. C. EVANS, M.A., Ph.D.
A. C. G. MENZIES, M.A., D.Sc.	L. C. MARTIN, D.Sc.
R. E. PEIERLS, C.B.E., M.A., Dr.Phil., D.Sc., F.R.S.	C. E. WYNN-WILLIAMS, D.Sc., Ph.D.
F. C. TOY, C.B.E., D.Sc.	A. G. QUARRELL, D.Sc., Ph.D.
J. H. AWBERY, M.A., B.Sc.	A. B. WOOD, O.B.E., D.Sc.
L. F. BATES, D.Sc., Ph.D.	WILLIS JACKSON, D.Sc., D.Phil., M.I.E.E.
	H. S. W. MASSEY, B.A., Ph.D., F.R.S.

## COLOUR GROUP

### Chairman

W. S. STILES, O.B.E., D.Sc., Ph.D.

### Honorary Secretary

R. G. HORNER, B.A.

## LOW-TEMPERATURE GROUP

### Chairman

F. E. SIMON, C.B.E., M.A., D.Phil.,  
F.R.S.

### Honorary Secretary

G. G. HASELDEN, Ph.D.

## OPTICAL GROUP

### Chairman

L. C. MARTIN, D.Sc.

### Honorary Secretary

G. S. SPEAK

## ACOUSTICS GROUP

### Chairman

H. L. KIRKE, C.B.E., M.I.E.E.

### Joint Honorary Secretaries

W. A. ALLEN, B.Arch., A.R.I.B.A.  
A. T. PICKLES, O.B.E., M.A.

## SECRETARY-EDITOR

Miss A. C. STICKLAND, Ph.D.

1 Lowther Gardens, Prince Consort Road, London S.W.7  
(Telephone : KENsington 0048, 0049)

# CONTENTS

## Part 1. January 1949

	PAGE
Editorial . . . . .	1
Dr. J. HAMILTON. Collision Problems and the Theory of Radiation Damping . . . . .	2
Dr. J. HAMILTON. Damping Theory and the Propagation of Radiation . . . . .	12
Dr. M. KROOK. Continuous $\gamma$ -Emission in Neutron-Proton Collisions . . . . .	19
Dr. E. J. BOWEN, Mr. E. MIKIEWICZ and Mr. F. W. SMITH. Resonance Transfer of Electronic Energy in Organic Crystals . . . . .	26
Mr. A. G. FENTON and Mr. E. W. FULLER. Further Experiments with an Adjustable Geiger-Müller Counter . . . . .	32
Dr. R. EISENSCHITZ. The Steady Non-Uniform State for a Liquid . . . . .	41
Dr. A. H. COTTRELL and Mr. B. A. BILBY. Dislocation Theory of Yielding and Strain Ageing of Iron . . . . .	49
Mr. R. HUBY. Investigations on the Binding Energy of Heavy Nuclei . . . . .	62
Reviews of Books . . . . .	71
Contents for Section B . . . . .	75
Abstracts for Section B . . . . .	75

## Part 2. February 1949

Dr. E. R. ANDREW. The Size-Variation of Resistivity for Mercury and Tin . . . . .	77
Dr. E. R. ANDREW. Critical Field Measurements on Superconducting Tin Foils . . . . .	88
Mr. F. BOOTH. On the Radiation from Transient Light Sources . . . . .	95
Mr. M. W. FEAST. On the Schumann-Runge O <sub>2</sub> Bands emitted at Atmospheric Pressure . . . . .	114
Mr. M. W. FEAST. The CN Tail Bands emitted by the Carbon Arc in Air . . . . .	121
Dr. S. P. SINHA. Ultra-Violet Bands of Na <sub>2</sub> . . . . .	124
Dr. F. C. FRANK. On the Equations of Motion of Crystal Dislocations . . . . .	131
Letters to the Editor :	
Mr. R. A. WEALE. The Resistivity of Thin Metallic Films . . . . .	135
Prof. N. F. MOTT. Note on the Slowing Down of Mesons . . . . .	136
Reviews of Books . . . . .	138
Contents for Section B . . . . .	139
Abstracts for Section B . . . . .	139

## Part 3. March 1949

Mr. E. BAUER. A Theory of Ultrasonic Absorption in Unassociated Liquids . . . . .	141
Mr. R. B. DINGLE. Second Sound and the Behaviour of Helium II . . . . .	154
Dr. R. SHUTTLEWORTH. The Surface Energies of Inert-gas and Ionic Crystals . . . . .	167
Dr. K. HUANG and Mr. G. WYLLIE. On the Surface Free Energy of Certain Metals . . . . .	180
Dr. R. C. PANKHURST. The Emission Spectrum of Sodium Hydride . . . . .	191
Dr. L. KELLNER. Bending Vibrations of a Linear Chain . . . . .	200
Letters to the Editor :	
Dr. F. C. FRANK. Sessile Dislocations . . . . .	202
Contents for Section B . . . . .	203
Abstracts for Section B . . . . .	203

## Part 4. April 1949

	PAGE
Dr. E. F. DALY and Dr. G. B. B. M. SUTHERLAND. The Performance of Infra-Red Spectrometers as Limited by Detector Characteristics . . . . .	205
Mr. J. EWLES and Dr. G. C. FARNELL. The Luminescence of Wetted Solids . . . . .	216
Mr. R. J. BRIGHT, Dr. D. A. JACKSON and Dr. H. KUFIN. The Resolving Power and Intensity Relationships of the Fabry Perot Interferometer with Silvered Reflecting Surfaces . . . . .	225
Miss M. E. PILLOW. Intensity Distribution for Bands of the $\gamma$ -System of $\text{MgH}^+$ . . . . .	237
Dr. E. P. GEORGE and Mr. A. C. JASON. Nuclear Disintegrations in Photographic Plates exposed to Cosmic Rays under Lead Absorbers . . . . .	243
Mr. D. E. BUNYAN, Dr. A. LUNDBY and Dr. D. WALKER. Experiments with the Delayed Coincidence Method, including a Search for Short-lived Nuclear Isomers . . . . .	253
Discussion on paper by Dr. F. C. CHAMPION and Dr. R. R. ROY entitled "The Scattering of Fast $\beta$ -Particles through Large Angles by Nitrogen Nuclei" ( <i>Proc. Phys. Soc.</i> , 1948, 61, 532) . . . . .	264
Letters to the Editor :	
Mr. T. S. MOSS. Infra-Red Photoconductivity in Layers of Tellurium and Arsenic . . . . .	264
Reviews of Books . . . . .	266
Contents for Section B . . . . .	267
Abstracts for Section B . . . . .	267
Corrigenda . . . . .	268

## Part 5. May 1949

Dr. A. H. COOKE. The Establishment of the Absolute Scale of Temperature below $1^\circ \text{K}$ . . . . .	269
Dr. D. J. PRICE. A Theory of Reflectivity and Emissivity . . . . .	278
Dr. E. H. PUTLEY. The Electrical Conductivity of Germanium . . . . .	284
Mr. J. E. R. HOLMES. Measurement of the Half-Life of $^6\text{He}$ . . . . .	293
Mr. L. L. GREEN and Mr. W. M. GIBSON. The Disintegration of Carbon by Fast Neutrons . . . . .	296
Mr. L. E. DRAIN. A Direct Method of Measuring Nuclear Spin-Lattice Relaxation Times . . . . .	301
Mr. J. D. ESHELBY. Uniformly Moving Dislocations . . . . .	307
Letters to the Editor :	
Mr. J. H. VAN DER MERWE and Dr. F. C. FRANK. Misfitting Monolayers . . . . .	315
Mr. J. S. JOHNSON and Dr. F. E. WILLIAMS: Dr. G. F. J. GARLICK. The Electron Trap Mechanism of Luminescence in Sulphide and Silicate Phosphors . . . . .	317
Reviews of Books . . . . .	319
Contents for Section B . . . . .	331
Abstracts for Section B . . . . .	331

## Part 6. June 1949

Mr. T. K. JONES, Dr. R. A. SCOTT and Dr. R. W. SILLARS. The Structure and Electrical Properties of Surfaces of Semiconductors.—Part I. Silicon Carbide . . . . .	333
Dr. A. J. ELLEMAN and Dr. H. WILMAN. The Structure and Epitaxy of Lead Chloride Deposits Formed from Lead Sulphide and Sodium Chloride . . . . .	344
Dr. E. W. KELLERMANN and Mr. K. WESTERMAN. On the Absorption Spectrum of Cosmic Rays . . . . .	356
Dr. S. M. MITRA and Mr. W. G. V. ROSSER. Momentum Spectrum of the Particles in Extensive Air Showers . . . . .	364

# Contents

V  
PAGE

Dr. H. ELLIOT. The Effect of External Quenching on the Life of Argon-Alcohol Counters . . . . .	369
Prof. W. HEITLER and Prof. L. JÁNOSSY. On the Absorption of Meson-producing Nucleons. . . . .	374
Dr. J. RZEWUSKI. Some Cut-off Methods for the Electron Self-Energy . . . . .	386
Letters to the Editor :	
Mr. R. P. HUDSON, Miss B. HUNT and Dr. N. KURTI. The Use of Liquid Helium in Magnetic Cooling Experiments . . . . .	392
Prof. E. N. DA C. ANDRADE. A Lantern Model to Illustrate Dislocations in Crystal Structure . . . . .	394
Mr. R. BOWERS and Dr. K. MENDELSSOHN. Viscosity and Superfluidity in Helium . . . . .	394
Dr. L. E. BEGHIAN and Mr. H. H. HALBAN. Electron Collection in High Pressure Methane Ionization Chambers. . . . .	395
Reviews of Books . . . . .	397
Corrigendum . . . . .	398
Contents for Section B . . . . .	399
Abstracts for Section B . . . . .	399

## Part 7. July 1949

Mr. C. H. MILLER, Mr. D. A. LONG, Dr. L. A. WOODWARD and Dr. H. W. THOMPSON. A Recording Spectrometer for Raman Spectroscopy . . . . .	401
Mr. L. L. GREEN and Mr. W. M. GIBSON. The Neutrons Emitted in the Disintegration of Lithium by Deuterons . . . . .	407
Professor N. F. MOTT. The Basis of the Electron Theory of Metals, with Special Reference to the Transition Metals . . . . .	416
Dr. N. R. CAMPBELL and Dr. L. HARTSHORN. The Experimental Basis of Electromagnetism—Part III: The Magnetic Field . . . . .	422
Dr. L. HARTSHORN. The Experimental Basis of Electromagnetism—Part IV: Magnetic Materials . . . . .	429
Mr. R. W. WRIGHT and Dr. J. P. ANDREWS. Temperature Variation of the Electrical Properties of Nickel Oxide . . . . .	446
Letters to the Editor :	
Mr. B. N. WATTS. Increased Sensitivity of Infra-red Photoconductive Receivers . . . . .	456
Dr. R. WILSON and Mr. G. R. BISHOP. The Decay Constant of Radio-Sodium, <sup>24</sup> Na . . . . .	457
Mr. F. K. GOWARD, Dr. E. W. TITTERTON and Mr. J. J. WILKINS. The Photo-Disintegration of Oxygen into Four Alpha-Particles . . . . .	460
Reviews of Books . . . . .	461
Contents for Section B . . . . .	463
Abstracts for Section B . . . . .	463

## Part 8. August 1949

Prof. G. I. FINCH. Steam in the Ring Discharge . . . . .	465
Mr. M. RYLE. The Significance of the Observation of Intense Radio-Frequency Emission from the Sun . . . . .	483
Mr. M. RYLE. Evidence for the Stellar Origin of Cosmic Rays . . . . .	491
Dr. R. R. ROY. Pair-Production in Different Elements by $\gamma$ -Rays . . . . .	499
Prof. M. G. EVANS, Mr. J. DE HEER and Dr. J. GERGELY. Structure and Diamagnetic Anisotropy of P-Benzoquinodimethane in Connection with those of P-Benzoquinone . . . . .	505
Dr. R. McWEENY and Prof. C. A. COULSON. The Computation of Wave Functions in Momentum Space—I: The Helium Atom . . . . .	509
Dr. R. McWEENY. The Computation of Wave Functions in Momentum Space—II: The Hydrogen Molecule Ion . . . . .	519

	PAGE
Letters to the Editor:	
Mr. K. H. SPRING. Electrons Ejected by Polarized Radiation. . . . .	529
Mr. E. SCHWARZ. Theory of Photoconductivity of Layers of Semi-Conducting Substances . . . . .	530
Reviews of Books . . . . .	532
Corrigendum . . . . .	534
Contents for Section B . . . . .	535
Abstracts for Section B . . . . .	535

### Part 9. September 1949

Prof. J. D. BERNAL. The Physical Basis of Life . . . . .	537
Mr. A. E. DE BARR. A Stereographic Projector . . . . .	559
Dr. R. STREET and Mr. J. C. WOOLLEY. A Study of Magnetic Viscosity . . . . .	562
Mr. P. J. GRANT and Mr. R. RICHMOND. The Decay of $^{170}\text{Tm}$ and $^{186}\text{Re}$ . . . . .	573
Dr. S. DEVONS. A Note on the $^{10}\text{B}(n, \alpha)^7\text{Li}$ Reaction . . . . .	580
Mr. W. M. GIBSON. The Neutrons emitted in the Bombardment of $^{10}\text{B}$ and $^{11}\text{B}$ by Deuterons . . . . .	586
Mr. C. ROBINSON. Three-Dimensional Design of Synchrotron Pole-Faces . . . . .	592
Reviews of Books . . . . .	597
Contents for Section B . . . . .	599
Abstracts for Section B . . . . .	599
Corrigendum . . . . .	600

### Part 10. October 1949

Mr. B. G. OWEN and Dr. J. G. WILSON. On the Ratio of Positive to Negative Particles in the Vertical Cosmic-Ray Beam at Sea Level . . . . .	601
Mr. D. J. BEHRENS. The Effect of Holes in a Reacting Material on the Passage of Neutrons . . . . .	607
Mr. F. K. GOWARD. Betatron Injection into Synchrotrons . . . . .	617
Mr. W. H. HALL, Dr. U. W. ARNDT and Mr. R. A. SMITH. A Geiger Counter Spectrometer for the Measurement of Debye-Scherrer Line Shapes . . . . .	631
Dr. C. GURNEY. Surface Forces in Liquids and Solids . . . . .	639
Mr. R. B. DINGLE. The Hydrodynamics of Helium II . . . . .	648
Dr. K. E. GREW. The Dependence of the Thermal Diffusion Factor on Temperature . . . . .	655
Letters to the Editor:	
Mr. R. WEALE: Dr. D. J. PRICE. A Theory of Emissivity and Reflectivity . . . . .	661
Mr. D. J. E. INGRAM. Hyperfine Splitting in Paramagnetic Resonance . . . . .	664
Reviews of Books . . . . .	666
Recent Publications Received . . . . .	666
Contents for Section B . . . . .	667
Abstracts for Section B . . . . .	667

### Part 11. November 1949

Prof. W. HEITLER and Prof. L. JÁNOSSY. On the Size-Frequency Distribution of Penetrating Showers . . . . .	669
Dr. A. DUPERIER. The Meson Intensity at the Surface of the Earth and the Temperature at the Production Level . . . . .	684
Mr. C. B. VAN WYK. On the Decay of $\tau$ -Mesons . . . . .	697
Miss J. JACOBS. Excited Electronic Levels in Conjugated Molecules—III: Energy States of Naphthalene . . . . .	710
Dr. H. G. WOLFARD and Dr. W. G. PARKER. A New Technique for the Spectroscopic Examination of Flames at Normal Pressures . . . . .	722
Dr. G. F. J. GARLICK and Mr. A. F. GIBSON. Dielectric Changes in Phosphors containing more than One Activator . . . . .	731

# Contents

	vii
	PAGE
Prof. A. RUBINOWICZ. Eigenfunctions following from Sommerfeld's Polynomial Method . . . . .	736
Letters to the Editor :	
Mr. B. V. THOSAR. Origin of Low-Energy Electron Lines in the $\beta$ -spectrum of $^{198}\text{Au}$ . . . . .	739
Mr. B. EISLER and Dr. R. F. BARROW. The Ultra-Violet Absorption Spectrum of $\text{SnO}$ . . . . .	740
Mr. W. H. HALL. X-Ray Line Broadening in Metals . . . . .	741
Dr. R. STREET and Mr. J. C. WOOLLEY. Magnetic Viscosity in Mn-Zn Ferrite . . . . .	743
Reviews of Books . . . . .	745
Corrigendum . . . . .	746
Contents for Section B . . . . .	747
Abstracts for Section B . . . . .	747

## Part 12. December 1949

Dr. J. HAMILTON. Radiative Reaction and Damping in Scattering . . . . .	749
Mr. J. W. GARDNER. Directional Correlation between Successive Internal-Conversion Electrons . . . . .	763
Dr. J. IRVING. Applications of the Peierls-McManus Classical Finite Electron Theory . . . . .	780
Dr. K. FUCHS. Perturbation Theory in Neutron Multiplication Problems . . . . .	791
Dr. D. Walker. Half-lives of $^{141}\text{Ce}$ and $^{169}\text{Yb}$ . . . . .	799
Mr. M. G. E. COSYNS, Miss C. C. DILWORTH, Dr. G. P. S. OCCHIALINI, Dr. M. SCHOENBERG and Miss N. PAGE. The Decay and Capture of $\mu$ -Mesons in Photographic Emulsions . . . . .	801
Dr. P. T. LANDSBERG. A Contribution to the Theory of Soft X-ray Emission Bands of Sodium . . . . .	806
Dr. G. F. J. GARLICK and Mr. D. E. MASON. The Luminescence Characteristics of Tin Activated Zinc Sulphide Phosphors . . . . .	817
Contents for Section B . . . . .	823
Abstracts for Section B . . . . .	823
Obituary Notices :	
WILLIAM BOWEN . . . . .	826
NORMAN ROBERT CAMPBELL . . . . .	826
CECIL LEWIS FORTESCUE . . . . .	829
EDWARD PHILIP HARRISON . . . . .	829
RICHARD ALBERT HULL . . . . .	830
CHRISTOPHER NOEL HUNTER LOCK . . . . .	831
WILLIAM BLAIR MORTON . . . . .	832
ALAN FARADAY CAMPBELL POLLARD . . . . .	833
WILLIAM GEORGE PYE . . . . .	834
MAX PLANCK . . . . .	835
WILLIAM NELSON STOCKER . . . . .	838
Index to Section A, Vol. 62 . . . . .	841
Index to Reviews of Books, Section A, Vol. 62 . . . . .	849
Proceedings at Meetings, 1948-49 . . . . .	viii
Report of Council for the Year 1948 . . . . .	xviii
Report of the Honorary Treasurer for the Year 1948 . . . . .	xxii



# PROCEEDINGS AT THE MEETINGS OF THE PHYSICAL SOCIETY

## SESSION 1948-49

13th October 1948

*Joint Science Meeting of THE COLOUR AND OPTICAL GROUPS*, at Northampton Polytechnic, London E.C.1. Mr. J. G. Holmes was in the Chair.

The following papers were read and discussed :

- " General Phenomena associated with Scattering of Light ", by E. W. H. Selwyn;
- " Atmospheric Haze Factors : An Approximate Calculation of the Diffuse Reflection and Transmission of a Layer of Scattering Particles ", by W. S. Stiles;
- " The Effect of Haze on Photography from the Air at Night ", by G. B. Harrison;
- " Scattering of Light in Photographic Materials ", by D. T. R. Dighton;
- " The Scattering and Absorption of Light in Coloured Paper ", by F. North.

---

14th October 1948

*The ninth meeting of THE ACOUSTICS GROUP*, at Imperial College, London S.W.7. Mr. H. L. Kirke was in the Chair.

The following paper was read and discussed :

- " The Accuracy of Measurements by Rayleigh Disc ", by W. West.

---

25th October 1948

*The sixteenth meeting of THE LOW TEMPERATURE GROUP*, at the Science Museum, London S.W.7. Sir Charles Darwin was in the Chair.

The following paper was read and discussed :

- " The Unattainability of Absolute Zero ", by F. E. Simon.

---

4th November 1948

*The tenth meeting of THE ACOUSTICS GROUP*, at the Royal Society of Arts, London W.C.2. Mr. H. L. Kirke was in the Chair.

A discussion was held on " Concert Hall Acoustics ".

H. Bagenal opened the discussion.

---

5th November 1948

*Extraordinary General Meeting*, at Imperial College, London S.W.7. The President, Professor G. I. Finch was in the Chair.,

The following special resolution was passed :

" That as from January 1949, or from such date as the Council may see fit, the *Proceedings of the Physical Society* shall be issued in two parts, which parts shall be entitled respectively *Proceedings of the Physical Society A* and *Proceedings of the Physical Society B* ; and further, that each Fellow and Student Member shall be entitled to receive either *Proceedings A* or *Proceedings B* (whichever he elects) on payment of the ordinary current subscription, and shall be entitled to receive both parts of the *Proceedings* on payment of an additional annual subscription not exceeding the current Fellowship subscription, the exact amount to be determined by the Council in accordance with the Articles of Association of the Physical Society.

*5th November 1948*

*Science Meeting*, at Imperial College, London S.W.7. The President, Professor G. I. Finch, was in the Chair.

The following were elected to Fellowship, the first two being transferred from Student Membership : David Noel Ferguson Dunbar, Peter Ewart Watson, Maurice Evan Bell, Charles Alexander Cochrane, Sheila Marion Crawford, Frederick Paulinus Cunningham, Gerard Field, Louis Jacob, Dominic Johnston, George Guy Macfarlane, Harrie Stewart Wilson Massey, Archibald George Peacock, Cyril George Wilson, J. G. Raynor Young.

The following papers were read and discussed :

"The Scattering of Fast Beta-Particles through Large Angles by Nitrogen Nuclei", by F. C. Champion and R. R. Roy;

"Beta Disintegration and Sargent Diagram", by N. Feather and H. O. W. Richardson

"Investigations using a Permanent Magnet Double Beta-Ray Spectrograph with Coincidence Counting", by N. Feather, J. Kyles and R. W. Pringle.

---

*10th November 1948*

*The forty-second meeting of THE COLOUR GROUP*, at the Lighting Service Bureau, London W.C.2. Dr. W. D. Wright was in the Chair.

The following papers were read and discussed :

"Measurement, Representation and Specification of Colour and Colour-rendering Properties of Light Sources", by G. T. Winch and H. R. Ruff;

"Fluorescent Lamp Artificial Daylight Units for Colour Matching", by G. T. Winch, W. Harrison and H. R. Ruff.

An informal report was given on the meeting of the Commission Internationale de l'Eclairage in Paris, July 1948, by members of the Colour Group who attended.

---

*25th November 1948*

*The seventeenth meeting of THE LOW TEMPERATURE GROUP*, at the Science Museum, London S.W.7. Sir Charles Darwin was in the Chair.

A lecture was given entitled "Irreversible Processes in Liquid Helium II", by Professor C. J. Gorter.

---

*25th November 1948*

*The eleventh meeting of THE ACOUSTICS GROUP*, at Imperial College, London S.W.7. Mr. H. L. Kirke was in the Chair.

The following paper was read and discussed :

"Apparatus for Acoustical Measurements at Low Frequencies", by R. S. Dadson and E. G. Butcher.

---

*3rd December 1948*

*Extraordinary General Meeting*, at Imperial College, London S.W.7. The President, Professor G. I. Finch, was in the Chair.

The following special resolution was passed :

"That Article 44 of the Articles of Association of the Society be altered as follows :—

Student Members shall be entitled to a copy of all publications issued by the Society upon such terms as the Council or a General Meeting of the Society may from time to time fix."

## *Proceedings at Meetings*

3rd December 1948

*Science Meeting*, at Imperial College, London S.W.7. The President, Professor G. I. Finch, was in the Chair.

It was announced that Council had elected the following to Student Membership : Peter John Cott, John Joseph Florentin, William Peter McKinney, Eric Shuttleworth, Donald Wesley Willis, Ronald Drayton Brown, Michael Onslow Bryant, Desmond Malone Burns, Ugo Camerini, Richard Hapgood Campbell, Peter Francis Chester, John Oswald Cope, Brian Arthur Evans, Cecil Bentley-Innes Glass, Stanley Hope, David John Ingram, Charles Hennie James Johnson, Aaron Klug, William Owen Lock, Ronald W. Maxwell, Hugh Muirhead, William Paterson Forsyth *Raffan*, Leonore Ritter, Michael Ian Scott.

The following were elected to Fellowship, the first-named being transferred from Student Membership : Raymond Jeffrey Slaughter, Mohammed Kashif Al-Ghita, Stanley Edgar Barden, Christopher Frederic Bareford, Albert Edward De Barr, David Robert Bates, Fathi Ahmed el Bedewi, Isaac Israel Berenblut, Arthur Cunliffe, A. Van Itterbeek, Max Krook, John Stewart Marshall, Bernard Wheeler Robinson.

The following papers were read and discussed :

“ Refractive Index in Electron Optics and the Principle of Dynamics ”, by W. Ehrenberg and R. E. Siday;

“ Measured Properties of Strong ‘ Unipotential ’ Electron Lenses ”, by G. Liebmann.

---

8th December 1948

*The forty-third meeting of THE COLOUR GROUP*, at Imperial College, London S.W.7. Mr. J. G. Holmes was in the Chair.

The following papers were read and discussed :

“ The Scotopic Visibility Function ”, by B. H. Crawford;

“ Visual Purple and the Photopic Luminosity Curve ”, by H. J. A. Dartnall.

---

9th December 1948

*Science Meeting*, at the Laboratories of Metropolitan-Vickers Electrical Co., Trafford Park, Manchester. The President, Professor G. I. Finch, was in the Chair.

The following papers were read and discussed :

“ The Structure of Electro-Deposits ”, by G. I. Finch;

“ Observations on Electrical Behaviour of Silicon Carbide Contacts ”, by E. W. J. Mitchell and R. W. Sillars;

“ Structure and Electrical Properties of Surfaces of Semiconductors—Part I : Silicon Carbide ”, by T. J. Jones, R. A. Scott and R. W. Sillars;

“ Some Experiences in the Application of the Electron Microscope to the Study of Steels ”, by J. Trotter and F. W. Cuckow;

“ The Structure and Epitaxy of Lead Chloride Deposits formed from Lead Sulphide and Sodium Chloride ”, by A. J. Elleman and H. Wilman.

---

16th December 1948

*The twelfth meeting of THE ACOUSTICS GROUP*, at Imperial College, London S.W.7. Mr. H. L. Kirke was in the Chair.

The following paper was read and discussed :

“ Jet-propelled Aircraft Noise ”, by S. C. Ghose.

---

17th December 1948

*The thirty-fourth meeting of THE OPTICAL GROUP*, at the Institute of Physics, London S.W.1. Professor L. C. Martin was in the Chair.

The following papers were read :

“ On the Theory of Aplanatic Aspheric Systems ”, by E. Wolf and G. D. Wassermann;

“ A General Method for the Calculation of the Chromatic Variation of Lens Aberrations ”, by H. H. Hopkins.

17th December 1948

*The third Annual General Meeting of THE LOW TEMPERATURE GROUP*, at the Science Museum, London S.W.7. Sir Charles Darwin was in the Chair.

The Minutes of the Second Annual General Meeting were read and confirmed.

The Report of the Committee for 1948 was presented.

The Officers and Committee for 1949 were elected.

Auditors were elected for the Special Fund.

The retiring President addressed the meeting.

Votes of thanks were recorded to the retiring Chairman and members of the Committee..

---

17th December 1948

*The eighteenth meeting of THE LOW TEMPERATURE GROUP*, at the Science Museum, London S.W.7. Sir Charles Darwin was in the Chair.

A discussion was held on "The Use of Thermodynamics Diagrams in Industry".. The subject was introduced by Professor D. M. Newitt.

---

14th January 1949

*Science Meeting*, at Imperial College, London S.W.7. The President, Professor G. I. Finch, was in the Chair.

It was announced that Council had elected the following to Student Membership : Jack Blitz, Brian Irvine Callin, John Anthony Champion, Robert Derek Craig, Gordon Arthur Dale, Cyril Henry Dix, Hector William Emerton, Donald Charles Field, Bernard Frank Figgins, Roy Sidney Gibbons, Donald Henry Grover, Raymond Frederick Hall, Leslie Jeffrey Hastewell, John Frank Hills, Walter Hopwood, John Arthur Hulbert, Arthur Langridge, Geoffrey Albert Lawrence, Albert John Manuel, Douglas Leonard Martin, Colyn Grey Morgan, Basil Leslie Morton, Edmund Gerard Muirhead, Frank Donald Stacey, Anthony Victor Stockley, John Thraves, Gerald Anthony Williams, John Francis Williams, Ronald John Wilson, Alan Neal Durham Young.

The following were elected to Fellowship, the first six being transferred from Student Membership : Patrick Bomyer, Sylvia Mary Gumbrell, Peter Donald Lomer, Lloyd Julian. Perper, Michael Somerset Ridout, Krishnarao Govindarao Torgal, James Brooking Brown, Klaus Fuchs, Alfred Claude Jessup, John Moffatt, Frank Dudley Stott, James Harold. Thorp, John Samuel Thorp, John Wilson.

The following papers were read and discussed :

"Travelling Wave Linear Accelerators", by R. B. R.-Shersby-Harvic;

"Theoretical Design of Linear Accelerators for Electrons", by W. Walkinshaw;

"Experimental Work on Corrugated Waveguides and Associated Components for Linear Electron Accelerators", by L. B. Mullett and B. G. Loach.

---

26th January 1949

*The thirteenth meeting of THE ACOUSTICS GROUP*, at the Institution of Electrical Engineers, London W.C.2. Mr. H. L. Kirke was in the Chair.

A demonstration was given on "The Development of Magnetic Tape Recorders", by B. E. G. Mittell.

The meeting was held jointly with the Radio Section of the Institution of Electrical Engineers.

---

4th February 1949

*Science Meeting*, at University College, London W.C.1. The President, Professor G. I. Finch, was in the Chair.

It was announced that Council had elected the following to Student Membership : Herbert Colin Bate, Alan E. Beck, Dennis Walter Bird, Walter Ernest Booth, James Graham Brown, Clifford Harry Champness, John Albert Chapman, David Michael Danziger,.

Mehmet Yusuf Dizioğlu, Kenneth Thomas Dolder, Arthur James Dyer, Roland Ernest Ford, Clifford Gregory, Dorothy Joyce Harrington, Benjamin Peter Howorth, David William Shaper Limbert, Max Lipsicas-Lipschitz, John Morgan, Eric Norman-Wilson, John Osborne, Alexander Tudor Pomeroy, John Samuel Pyett, Robert Shannon, Roman Stefan Sidorowicz, Alan Smith.

The following papers were read and discussed :

- "A Projection Model to Illustrate Crystal Structure with Surfaces of Misfit", by E. N. da C. Andrade;
- "The Mechanism of Dilatancy", by E. N. da C. Andrade and J. W. Fox;
- "The Effect of Pre-Strain on the Character of the Creep of Lead", by E. N. da C. Andrade and A. J. Kennedy;
- "The Thermal Etching of Single Crystals of Cadmium", by E. N. da C. Andrade and R. F. Y. Randall;
- "Viscosity and Density in the Supercooled Liquid State", by C. Dodd and Hu Pak Mi.

#### 12th February 1949

*The forty-fourth meeting of THE COLOUR GROUP*, held jointly with the BRITISH PSYCHOLOGICAL SOCIETY, at Tavistock House, London W.C.1. Mr. J. G. Holmes was in the Chair.

A discussion was held on the techniques and methods of interpretation of experiments in colour as carried out by physicists, physiologists and psychologists. The discussion was introduced by W. A. Allen, R. C. Oldfield, R. W. Pickford, L. C. Thomson and W. D. Wright.

#### 18th February 1949

*The fourteenth meeting of THE ACOUSTICS GROUP*, at Imperial College, London S.W.7. Mr. H. L. Kirke was in the Chair.

A discussion was held on the subject of "Applications of Ultrasonics". Mr. G. Bradfield opened the discussion.

#### 19th February 1949

*Science Meeting*, at Edinburgh University. The President, Professor G. I. Finch, was in the Chair.

The following papers were read and discussed :

- "Experimental Tests of a Wide-Angle Beta-Particle Spectrometer using an approximately Prolate Spheroidal Magnetic Field", by T. H. Braid and H. O. W. Richardson;
- "Tests of a Prism Spectrograph of High Resolving Power", by R. E. Siday and D. A. Silverston;
- "An Emission Microscope for Photoelectron Autoradiography", by (Miss) A. N. Barker, N. Feather and H. O. W. Richardson;
- "The Use of Proportional Counters to Investigate Beta-Disintegration", by S. C. Curran;
- "Electrons as Nuclear Projectiles", by B. Touschek;
- "A new Approach to the Theory of Elementary Particles", by M. Born and H. S. Green;
- "Film Transport in Liquid Helium II", by J. F. Allen;
- "A new Photoelectric Amplifier", by R. V. Jones;
- "Long-Range Molecular Forces", by J. Iball.

24th February 1949

*The nineteenth meeting of THE LOW TEMPERATURE GROUP*, at the Geological Society, London W.1. The meeting was held jointly with the Institution of Chemical Engineers. Professor F. E. Simon was in the Chair.

A Lecture was given on "Materials of Construction for use at Low Temperatures", by E. W. Colbeck.

11th March 1949

*Science Meeting*, at the Science Museum, London S.W.7. The President, Professor G. I. Finch, was in the Chair.

It was announced that Council had elected the following to Student Membership: Herbert Roy Barnes, Clive Keith Coogan, Jack Dutton, Arthur Abraham Fiöhllich, Brian Leonard Hart, Peter Arthur Lee, Colin Douglas McKenzie, Richard Leonard Mason, John Barlow Massey, Maurice George Mylroi, John Robert Pattison, Colin John Swanson, Peter Guy Towlson, Alan Reginald Watson, Donald Percy Dennis Webb, Kenneth Worthington.

The following were elected to Fellowship, the first thirteen being transferred from Student Membership: Edward Walter Bastin, Raymond Bowers, Richard Arthur Brown, Francis Maurice Comerford, Christian Ellis Coulman, James William Crawford, Robert Tudor Jarman, George Harry King, Eric Walter Lee, Charles Walter Morley, Michael William Ovenden, John Alexander Pryde, Geoffrey Cecil Pyle, Stanley Sumner Ballard, Max Born, Edward Colin Cherry, Claude Le Cointe, Ralph Forder Denington, Adam Wincety Gac, Hylton Judith Grenville-Wells, Arthur Ap Gwynn, Gordon Edward Hughes, Cecil Newton Kington, Anne Hutton Numbers, David Luther Phillips, Horace Hewitt Poole, Otto Pressel, Alec Radcliffe, Marion Amelia Spence Ross.

The following papers were read and discussed:

"Temperature Measurements of Flames containing Incandescent Particles", by H. G. Wolfhard and W. G. Parker;

"A new Technique for the Spectroscopic Examination of Diffusion Flames at Normal Pressures", by H. G. Wolfhard and W. G. Parker.

---

18th March 1949

*The Second Annual General Meeting of THE ACOUSTICS GROUP*, at the Royal Society of Arts, London W.C.2. Mr. H. L. Kirke was in the Chair.

The Minutes of the First Annual General Meeting were read and confirmed.

The Report of the Committee for 1948-49 was presented.

A proposal to make some alterations and additions to the Regulations of the Group was approved.

The Officers and Committee for 1949-50 were elected.

---

18th March 1949

*The fifteenth meeting of THE ACOUSTICS GROUP*, at the Royal Society of Arts, London W.C.2. Mr. H. L. Kirke was in the Chair.

The following paper was read and discussed:

"The Acoustics of Bells", by Ir. E. W. van Heuven.

---

21st March 1949

*Celebration of the Seventy-fifth Anniversary of the Foundation of THE PHYSICAL SOCIETY.*

The thirty-third Guthrie lecture was delivered at the Royal Institution, London W.1. by Professor A. O. Rankine. His subject was "Experimental Studies in Thermal Convection".

During the evening a *Conversazione* was held at the Rooms of the Royal Society.

*Proceedings at Meetings**23rd March 1949*

*The twentieth meeting of THE LOW TEMPERATURE GROUP*, at the works of Messrs. Petrocarbon Ltd., Eccles, Manchester. Professor F. E. Simon was in the Chair.

An introductory lecture was given outlining the scope of the works and describing the low temperature plant. The pilot plant and the works were then inspected.

---

*24th March 1949*

*The thirty-fifth meeting of THE OPTICAL GROUP*, at Imperial College, London S.W.7. Professor L. C. Martin was in the Chair.

The following papers were read and demonstrations given :

"The Design of a Class of Variable Power Systems", by H. H. Hopkins. The demonstration was given of a system with 2-inch aperture and 30-degree field for use with television cameras;

"German Infantry Range-finders", by E. Wilson.

---

*30th March 1949*

*The ninth Annual General Meeting of THE COLOUR GROUP*, at the Royal Photographic Society's rooms, London S.W.7. Mr. J. G. Holmes was in the Chair.

The Minutes of the eighth Annual General Meeting were read and confirmed.

The Report of the Committee for 1948-49 was presented.

The Officers and Committee for 1949-50 were elected.

A vote of thanks was given to retiring Committee Members.

---

*30th March 1949*

*The forty-fifth meeting of THE COLOUR GROUP*, at the Royal Photographic Society's rooms, London S.W.7. Dr. W. S. Stiles was in the Chair.

A discussion was held on Photoelectric Spectrophotometers and Tricolorimeters. The discussion was introduced by T. Vickerstaff.

The new Hilger Uvispek photoelectric spectrophotometer was demonstrated by Messrs. Hilger and Watts Ltd.

---

*22nd April 1949*

*The sixteenth meeting of THE ACOUSTICS GROUP*, at the National Hospital, London W.C.1.

The following paper was read and discussed :

"The Theory of Hearing", by T. Gold and R. J. Pumphrey.

---

*22nd April 1949*

*Science Meeting*, at the Science Museum, London S.W.7. The President, Professor G. I. Finch, was in the Chair.

It was announced that Council had elected the following to Student Membership : Max Theodore Christensen, Alan Derek Harold Cripps, Francis Peter Edmund Gardner, Bernard Lionel Ginsborg, Henry Ralph Harman, Harvey Douglas Keith, Alan Bernard Lidiard, John Langley Rogers, Alfred Philip Tatt, Alan Teviotdale, Bernard John West.

The following were elected to Fellowship, the first-named being transferred from Student Membership : Werner Freitag, Henry Ian Allgood, Frank Foster Evison, Richard L. Extermann, Arthur J. Good, Pierre A. Grivet, Arnold Charles Lynch, Ian Mackay, Roy Middleton, Velimir Vook.

The twenty-fifth Duddell Lecture was delivered by Professor K. M. G. Siegbahn (Nobel Institute for Physics, Stockholm), whose subject was "On Gratings".

*27th April 1949*

*The twenty-first meeting of THE LOW TEMPERATURE GROUP*, was held at the Laboratories of the British Oxygen Company, Morden, London S.W.19. Professor F. E. Simon was in the Chair.

An introductory lecture was given by P. H. Sykes. The work of the Development and Research Sections was outlined by P. M. Schuftan and A. M. Clark.

The laboratories were then inspected.

---

*6th May 1949*

*Annual General Meeting*, at the Royal Institution, Albermarle Street, London W.1. The President, Professor G. I. Finch, was in the Chair.

The Minutes of the Annual General Meeting held on 5th May 1948 were read and confirmed.

The Reports of the Council and the Honorary Treasurer and the Annual Accounts for 1948 were adopted.

The Officers and Council for 1949-50 were elected.

Votes of thanks were recorded to the retiring President, Officers and Members of Committees; to the Rector and Governing Body of Imperial College; the Director of the Science Museum; the Managers of the Royal Institution and the Royal Commission for the Exhibition.

---

*6th May 1949*

*Science Meeting*, at the Royal Institution, Albermarle Street, London, W.1. The President, Professor G. I. Finch, was in the Chair.

The following were elected to Fellowship, the first three being transferred from Student Membership: Jerzy Adam, Michael Julian Maurice Bernal, Stuart Astley Young, Arnold Maurice Dobson, Alan Sayed Farghaly, Frederick Charles Frank, Marjorie Elsie Pillow, Edmund James Pryor, John Douglas Swift, Harold William Taylor, Cyril Stanley Watt, Maurice Stafford Willis.

Prizes and Certificates awarded in the recent Craftsmanship and Draughtsmanship Competition were presented.

The Presidential Address was delivered by Professor G. I. Finch, whose subject was "Steam in the Ring Discharge".

---

*11th May 1949*

*The twenty-second meeting of THE LOW TEMPERATURE GROUP*, at the Science Museum, London S.W.7. Professor F. E. Simon was in the Chair.

A discussion on "The Use of Thermodynamic Diagrams in Industry" was introduced by D. M. Newitt.

---

*13th May 1949*

*The eighth Annual General Meeting of THE OPTICAL GROUP*, at Imperial College, London S.W.7. Professor L. C. Martin was in the Chair.

The Minutes of the seventh Annual General Meeting were read and confirmed.

The Report of the Committee for 1948-49 was presented.

The Officers and Committee for 1949-50 were elected.

Votes of thanks were given.



*Proceedings at Meetings*

13th May 1949

*The thirty-sixth meeting of THE OPTICAL GROUP*, at Imperial College, London S.W.7. Professor L. C. Martin was in the Chair.

The following paper was read :

"Notes on the Designing of Aspherical Magnifiers for Binocular Vision", by C. E. Coulman and G. R. Petrie.

A lecture was given by M. André Maréchal of the Institut d'Optique.

---

20th May 1949

*The seventeenth meeting of THE ACOUSTICS GROUP*, at the Royal College of Organists, London S.W.7. Mr. H. L. Kirke was in the Chair.

The following paper was read and discussed :

"The Development of a new Electronic Organ", by L. E. A. Bourne.

A demonstration was given.

---

2nd June 1949

*Science Meeting*, at the Science Museum, London S.W.7. The President, Professor S. Chapman, was in the Chair.

It was announced that Council had elected the following to Student Membership : David Spence Campbell, Reginald George Harlow, Roger George Jarvis, Derek Raynor, John Albert Bennett, Thomas Hamilton Braid, Norman Daniel Cowell, Kathleen Marjoria Gartwick, Michael Samuel Kisch.

The following were elected to Fellowship, the first two being transferred from Student Membership : Fritz K. Bowers, Cyril Scott, Frank William Cuckow, Antonius Mathias Johannes Friedrich Michels, Alexander John Moncrieff-Yeates, Leslie Walter Phipps, Walter Phipps, Denis Edwin Piper, Leonard Alfred Sayce, Harold Smith.

The twenty-sixth Duddell Medal, Prize and Certificate were presented to Dr. E. H. Land (Polaroid Corporation, Cambridge, Massachusetts), in recognition of his work on polarizing materials.

The twenty-sixth Duddell Lecture was then delivered by Dr. Land under the general heading of "A Colour Translating Ultra-Violet Microscope".

---

10th June 1949

*Science Meeting*, at the Science Museum, London S.W.7. The President, Professor S. Chapman, was in the Chair.

The 1949 Thomas Young Oration was delivered by Mr. T. Smith, M.A., F.R.S., whose subject was "The Contributions of Thomas Young to Geometric Optics, and their Application to Present-day Questions".

---

11th June 1949

*The thirty-third meeting of THE OPTICAL GROUP*, at Imperial College, London S.W.7. Professor L. C. Martin was in the Chair.

The following papers were read and discussed :

"The Computation of Large Numerical Aperture Telescope Objectives", by T. Smith;

"The Boundary Wave Theory of Image Formation", by L. C. Martin.

15th June 1949

*The forty-sixth meeting of THE COLOUR GROUP*, at the Institute of Ophthalmology, London, W.C.1. Dr. W. S. Stiles was in the Chair.

The following paper was read and discussed :

"The History of Artists' Pigments", by H. J. Plenderleith.

14-16th July 1949

*Science Meeting*, at the Cavendish Laboratory, Cambridge. In the absence of the President, the meeting was opened by Professor G. I. Finch.

It was announced that Council had elected the following to Student Membership : John Robert Gabriel, Frederick John Hiorns, Bruce Sween Liley, John Alexander McDonnell.

The following were elected to Fellowship, the first two being transferred from Student Membership : Joan Edwards, William Leslie Wilcock, John Raymond Drabble, Oliver William Humphreys, Kamal Mikhail Matta, Clifford Charles McMahon, Margarita Eileen Monk-Jones, John Maurice McLean Pinkerton, Sidney Joseph Wyard.

Papers were read under the following headings :

*The Regular Behaviour of Long and very Long Waves returned from the Ionosphere :*

"The Regular Behaviour of Long and very Long Waves returned from the Ionosphere", by J. A. Ratcliffe;

"Very Low Frequency Propagation", by S. B. Smith and K. W. Tremellen;

"The Effects of Sky-Wave on the Planning of Navigational Aids using Frequencies in the 70-130 kc/s. Band", by W. T. Sanderson;

"The Characteristics of Low-Frequency Radio Waves reflected from the Ionosphere, with particular reference to Radio Aids to Navigation", by C. Williams;

"Measurements on Long and very Long Waves", by R. N. Bracewell.

*The Regular Behaviour of Medium and Short Waves :*

"The Application of Ionospheric Data to Short-Wave Transmission Problems", by W. J. G. Beynon;

"(P', f) Records at Spitsbergen", by A. B. Whatman.

*The Irregular Behaviour associated with Solar Events :*

"Irregular Behaviour of the Ionosphere associated with Solar Events", by W. R. Piggott;

"Some Work at Cambridge on Radio Fade-outs", by K. Weekes;

"Les renforcements brusques des ondes très longues", by R. Bureau.

*The Formation of Ionized Regions :*

"The Formation of Ionized Regions", by K. Weekes;

"Theoretical Considerations regarding the Formation of the Ionized Layers", by D. R. Bates and M. J. Seaton.

*Irregularities in the Horizontal Plane in the Ionosphere :*

"Irregularities in the Horizontal Plane in Region E of the Ionosphere", by J. W. Findlay;

"Meteor Ionization in the Upper Atmosphere", by A. C. B. Lovell;

"Scattering of Radio Waves from Region E", by G. Millington;

"The Variations in Direction of Arrival of High-Frequency Radio Waves", by W. Ross;

"Diffusion des echoes su voisinage des fréquences critiques de F2", by R. Rivault.

# REPORT OF COUNCIL FOR THE YEAR ENDED 31<sup>ST</sup> DECEMBER 1948

## INTRODUCTORY AND GENERAL

1948 may in general be considered a satisfactory year for the Society. The membership has again risen considerably, the increase of the Fellows' annual subscription from two to three guineas having produced no serious losses. The financial position has improved, though publication costs continue to rise; the balance is still rather precarious, but steps have been taken which, it is hoped, will result in a further improvement in 1949.

The number of papers suitable for the *Proceedings* has so much increased that substantial changes in policy were necessary if undesirable delays in publication were to be avoided; it was therefore decided to divide the *Proceedings* into two Sections, A and B, each to be issued in monthly parts.

At the Annual General Meeting, Professor A. O. Rankine, who had been acting as Honorary Business Secretary, was succeeded by Mr. C. G. Wynne.

The continued generosity of the Royal Commission for the Exhibition of 1851 in providing accommodation for the Society's headquarters at 1 Lowther Gardens is once more gratefully acknowledged.

The Council again records the cordial thanks of the Society to the Rector and Governing Body of Imperial College and Professors Sir George Thomson and H. V. A. Briscoe for the great privilege of holding the Exhibition in the Physics and Inorganic Chemistry Departments of the College. For the use of the Lecture Theatres for Science Meetings of the Society and its four Groups the Council thanks the various bodies who gave them hospitality, in particular Sir George Thomson, Head of the Physics Department of Imperial College, the Director of the Science Museum, and the Managers of the Royal Institution.

## MEETINGS

The Annual General Meeting was held at the Royal Institution on 5th May. Reports of the Council and the Treasurer and the Accounts and Balance Sheet for 1947 were presented and adopted, and Officers and Council for 1948-49 elected.

Three Extraordinary General Meetings were held during the year. The first, on 5th May, when Professor Ernest Orlando Lawrence was elected to Honorary Fellowship of the Society. The second, on 5th November, was held to consider the proposed division of the *Proceedings*. A Resolution was adopted that the *Proceedings* be issued in two Sections, A and B, and that each Fellow and Student Member be entitled to receive either Section A or Section B on payment of the ordinary current Annual Subscription, and to receive both Sections of the *Proceedings* on payment of an additional annual subscription to be determined by Council. At the third, on 3rd December, an alteration to Article 44 was approved, viz., that Student Members be entitled to a copy of all publications issued by the Society upon such terms as the Council or a General Meeting of the Society may from time to time fix.

A two-day summer meeting at the Clarendon Laboratory, Oxford, was devoted to microwave spectroscopy, and a full-day meeting at the Research Department of Metropolitan-Vickers Electrical Co. Ltd., Manchester, in December to surface structure and electrical properties of semiconductors. At one of the nine meetings held in London the Society was delighted to welcome one of its Honorary Fellows, Professor R. W. Wood, who lectured on spontaneous deformation of crystals.

## MEMORIAL LECTURES AND AWARDS

### GUTHRIE LECTURE

The 32nd Guthrie Lecture was delivered at the Science Museum on 4th June by Sir George Thomson, who took as his subject "The Growth of Crystals".

**CHARLES VERNON BOYS PRIZE**

The 4th (1948) Prize was presented to Professor S. Tolansky at the Science Museum on 8th October, who delivered a discourse on his work entitled "Current Investigations with Multiple-Beam Interferometry".

**HOLWECK PRIZE AND MEDAL**

The 3rd (1948) award of the Holweck Prize of the Physical Society and Holweck Medal of the Société Française de Physique was to Professor Y. Rocard. The presentation took place at the Royal Institution on 5th May when Professor Rocard delivered a Holweck Discourse on "Sur les Conditions D'Auto-Oscillation des Systèmes Vibrantes".

**EXHIBITION OF SCIENTIFIC INSTRUMENTS AND APPARATUS**

The 32nd Exhibition was held at Imperial College on 6th to 9th April. The attendance was higher than in 1947 (about 9,400 excluding holders of members' and exhibitors' passes). The Catalogue was available in good time, and all orders were fulfilled before the opening of the Exhibition.

**PUBLICATIONS**

**PROCEEDINGS**

During 1948 a start has been made in decreasing the period which elapses between the time of submission of a paper for publication and its appearance in print. This has been made possible in part by the increase in paper allocated to the *Proceedings* and in part by the raising of the standard of presentation required for papers accepted for publication. The institution of "Letters to the Editor" has met with approbation and is now a regular feature of the *Proceedings*. These letters are not intended to be substitutes for detailed publication of completed work, but for preliminary announcement of the results where these may be of importance even without details of the methods, or of proposals for work to be undertaken later, or they may give short outlines of proposed new methods of attack, free for others to take up. It is not desired in general that they should be the sole medium of publication of slight researches which the author judges to be unworthy of longer publication.

In order further to expedite publication, from January 1949 the *Proceedings* is to appear monthly in two sections. It will be recalled that proposals for establishing a journal of Applied Physics had been considered and rejected. It was next proposed that the *Proceedings* should be separated into papers which deal with pure physics, and others with technological physics, but examination showed the impracticability of this mode of division. It led in particular to the disadvantage that papers on a given subject—say the motion of electrons in a field—would be found in both parts, according to the point of view adopted in the treatment. It was felt that workers would prefer all papers on a given field to be in one part, whether they were written with applications in mind or not. In consequence, it has been decided that Section A shall cover atomic and sub-atomic physics, including such subjects as crystal structure, quantum mechanics and spectra, whilst Section B deals with macroscopic physics, including such subjects as acoustics, optical design and radio.

Each member of the Society receives one part, at his choice, and may purchase the other at a reduced price. The cost of supplying both parts to all members would have involved raising the subscription to more than 4 guineas, and was unacceptable to the General Meeting held on 5 November.

**REPORTS ON PROGRESS IN PHYSICS**

Volume 11 (1946-47) was published in July 1948 and is in great demand. Some delay was experienced in despatching of orders because of the difficulty of obtaining the standard green cloth for binding. There is a long waiting list for some earlier issues of the *Reports*, viz., Volumes 1-3 and 5-9, which are out of print. The Society is anxious to buy second-hand copies of these Volumes.

Volume 12 (1948-49) is in active preparation and should be published during the summer of 1949.

## SPECIAL REPORTS

During the year the publication of the following reports was completed: *Report on Colour Terminology*, prepared by a Sub-Committee of the Colour Group of the Society; *The Strength of Solids*, a report of a summer conference held at the H. H. Wills Physical Laboratory of the University of Bristol in July 1947; *The Emission Spectra of the Night Sky and Aurorae*, a report of a conference arranged under the auspices of the Gassiot Committee of the Royal Society.

In general the sales of Special Reports are disappointing, and the Council of the Society has decided that in future the production of such Reports shall be kept to a minimum. There will, however, be published two reports of Symposia of the Acoustics Group, arrangements for which are already in hand.

## SCIENCE ABSTRACTS

*Physics Abstracts* (Section A of *Science Abstracts*), which is issued as part of the Fellowship subscription, continues to increase markedly in size and cost, but the Society has decided to continue its issue to Fellows as part of the subscription at present.

## REPRESENTATION ON OTHER BODIES

The following appointments of representatives in 1948 are reported:—

*National Committee for Crystallography*: Dr. H. Wilman.

*Journal of Scientific Instruments, Advisory Committee*: Mr. J. H. Awbery, Professor G. I. Finch, Dr. H. H. Hopkins, Mr. A. T. Pickles, Mr. E. W. H. Selwyn, Dr. A. C. Stickland, Dr. W. S. Stiles, Dr. W. D. Wright.

*British Standards Institution Sub-Committee on Temperature Measurement*: Dr. E. Griffiths.

*Royal Society National Committee for Physics*: Dr. A. C. Menzies.

*Royal Society National Committee for Scientific Radio*: Dr. W. J. G. Beynon.

*Faraday Society, Colloid and Biophysics Committee*: Professor J. T. Randall.

*Organization Committee for Symposium on Metallurgical Applications of the Electron Microscope*: Dr. A. G. Quarrell.

*British Standards Institution—Committee on Nomenclature and Symbols*: Dr. L. Hartshorn.

*Board of the Institute of Physics*: Dr. H. H. Hopkins, Dr. A. C. Menzies.

*British Standards Institution—Acoustics Industry Committee*: Mr. H. L. Kirke.

*Science Abstracts Committee of Management*: Mr. J. H. Awbery, Dr. A. G. Gaydon, Dr. A. C. Menzies, Dr. D. Roaf.

## OBITUARY

The Council records with great regret the deaths of the following: Dr. Irena Gimpel, Mr. T. H. Littlewood, Mr. G. L. Overton, Sir Clifford Paterson, Professor A. F. C. Pollard, Dr. J. H. Shaxby, Mr. E. W. Smith, Professor S. W. J. Smith (*Fellows*); and Miss Margaret Weiss (*Student Member*).

## MEMBERSHIP

As the following tables show, the membership of the Society continues to increase.

Roli of Membership		Hon. Fellows	Ex- officio Fellows	Fellows	Student Members	Total
Totals, 31st Dec. 1947		8	4	1469	384*	1865*
Changes during 1948	Newly elected	1		86	126	
	Transferred			39	39	
	Deceased			7	1	
	Resigned			56	27	
	Lapsed			2		
Net increase		1		60	59	120
Totals, 31st Dec. 1948		9	4	1529	443	1985

\* Amended figure.

The following is a summary of the membership during the past eight years :—

Year . . . . .	1941	1942	1943	1944	1945	1946	1947	1948
Newly elected Student Members	51	96	74	52	68	53	102	126
Transfers from Student Membership . . . . .	13	20	22	23	52	46	33	39
Newly elected Fellows . . . .	28	57	42	36	56	139	126	87
Net increase in Fellowship . .	6	57	36	55	80	165	137	60
Net increase in total Membership	37	140	73	63	75	160	179	120

## GROUPS

### COLOUR GROUP

The Group held its eighth Annual General Meeting for the presentation of the Committee's Report on the work of the Group in 1947-48. Mr. J. G. Holmes was re-elected as Chairman of the Group, Mr. R. G. Horner was elected as Honorary Secretary, and the Committee for 1948-49 was elected.

Nine Science Meetings, brief particulars of which are given in the *Proceedings*\*, were held during the year. One of them, on 13th October at Northampton Polytechnic, was held as a joint meeting with the Optical Group.

The Report of the Sub-Committee on Colour Terminology was published as a companion to the earlier Report on "Defective Colour Vision in Industry".

### OPTICAL GROUP

At the Seventh Annual General Meeting, which was held at Imperial College on 30th April 1948, Professor L. C. Martin was re-elected as Chairman of the Group, Mr. E. W. H. Selwyn was re-elected as Honorary Secretary, and the Committee for 1948-49 was elected.

Five Science Meetings, brief particulars of which are given in the *Proceedings*\*, were held during the year. One of them, on 13th October at Northampton Polytechnic, was held as a joint meeting with the Colour Group.

Papers read at the meetings of the Group have been published in the *Proceedings*† and in the *Photographic Journal*.

### LOW TEMPERATURE GROUP

The Third Annual General Meeting of the Group was held at the Science Museum on 17th December 1948, when Professor F. E. Simon and Professor D. M. Newitt were elected as Chairman and Vice-President respectively. Dr. G. G. Haselden was re-elected as Honorary Secretary and the Committee for 1948-49 was elected.

There were six Science Meetings held during the year, brief particulars of which are given in the *Proceedings*\*. The one held on 13th February 1948 was a joint meeting with the Institution of Chemical Engineers at the Institution of Civil Engineers, and the one held on 5th April was a joint meeting with the Institute of Refrigeration.

### ACOUSTICS GROUP

The Second Annual General Meeting of the Group took place at the Royal Institute of British Architects on 8th April, when Mr. H. L. Kirke and Dr. A. Wood were re-elected Chairman and Vice-Chairman respectively, Mr. W. A. Allen and Mr. A. T. Pickles were re-elected as Joint Honorary Secretaries, and the Committee for 1948-49 was elected.

Nine Science Meetings, brief particulars of which are given in the *Proceedings*\*, were held during the year.

### MEMBERSHIP

The membership of the four Groups on 31st December 1948 was as follows :—

	Colour	Optical	Low Temperature	Acoustics
Members of the Physical Society .	113	189	45	69
Members of participating bodies .	62	80	35	146
Members of subscribing firms and Societies . . . . .	33	75	—	—
Other members . . . . .	15	19	10	50
	<u>223</u>	<u>363</u>	<u>90</u>	<u>265</u>

\* *Proc. Phys. Soc.*, 1948, 61, vi-xv.

† *Proc. Phys. Soc.*, 1948, 61, 489, 494.

# REPORT OF THE HONORARY TREASURER FOR THE YEAR ENDED 31<sup>ST</sup> DECEMBER 1948

The accounts have been prepared on the same lines as last year, and show an excess of income over expenditure of £1067 4s. 2d., against a deficit in 1947 of £1992 7s. 8d.

All items of expenditure show increases due to the increased activities of the Society.

On the income side the increase in the rate of Fellows' subscriptions from two to three guineas has produced a considerably greater revenue, while receipts from the sale of publications show a general all-round improvement.

A publication grant of £1500 from the Royal Society (against grants totalling £1400 last year) and also a legacy of £500 from the will of the late William Lucas (Fellow 1891) are gratefully acknowledged.

For the first time in recent years the stocks of publications on hand at the opening and closing of the year have been included, thereby giving a more accurate indication of the operations in connection with publications.

Dividends and interest show a decrease, which is accounted for by the fact that during 1947 the Society sold £1000 3% Savings Bonds, while £400 Lancaster Corporation Stock was redeemed and the proceeds not re-invested. There is also a reduction in income due to nationalization of the railways. No change has taken place in the Society's investments during the year.

(Signed) H. SHAW,

*Honorary Treasurer.*

25th February 1949.

## SPECIAL FUNDS

### W. F. STANLEY TRUST FUND

	£	s.	d.		£	s.	d.
Carried to Balance Sheet	259	0	0	£338 19s. 1d. British Transport Stock	259	0	0
				1978/88			
	<u>£259</u>	<u>0</u>	<u>0</u>		<u>£259</u>	<u>0</u>	<u>0</u>

### DUDELL MEMORIAL TRUST FUND

#### CAPITAL

	£	s.	d.		£	s.	d.
Carried to Balance Sheet	374	0	0	£400 3½% War Loan Inscribed "B" Account	374	0	0

#### REVENUE

	£	s.	d.		£	s.	d.
Prize	20	0	0	Balance on 31st December 1947	13	19	11
Certificate	1	0	0	Interest on War Loan	14	0	0
Balance carried to Balance Sheet	6	19	11				
	<u>£27</u>	<u>19</u>	<u>11</u>		<u>£27</u>	<u>19</u>	<u>11</u>

# SPECIAL FUNDS (*contd.*) CHARLES CHREE MEDAL AND PRIZE FUND

CAPITAL							
Balance carried to Balance Sheet	£	s.	d.	£784 4% Funding Stock	£	s.	d.
	1866	10	0	£1500 2½% Consols	839	0	0
					1027	10	0
	<u>1866</u>	<u>10</u>	<u>0</u>		<u>1866</u>	<u>10</u>	<u>0</u>
REVENUE							
Balance carried to Balance Sheet	£	s.	d.	Balance on 31 December 1947	£	s.	d.
	86	11	10	Interest on Investments	17	14	8
					68	17	2
	<u>£86</u>	<u>11</u>	<u>10</u>		<u>£86</u>	<u>11</u>	<u>10</u>

## CHARLES VERNON BOYS PRIZE FUND

CAPITAL							
Balance carried to Balance Sheet . . .	£	s.	d.	£1132 16s. 10d. 2½% Consols "B" Account	£	s.	d.
	900	0	0		900	0	0
	<hr/>				<hr/>		
REVENUE							
Balance on 31 December 1947 . . .	£	s.	d.	Interest on Investment . . .	£	s.	d.
Prize . . . . .	15	10	3	Balance carried to Balance Sheet . . .	28	6	4
Certificate . . . . .	26	5	0		14	8	11
	1	0	0				
	<hr/>				<hr/>		
	£42	15	3		£42	15	3

## HOLWECK PRIZE FUND

CAPITAL							
	£	s.	d.		£	s.	d.
Balance carried to Balance Sheet . . . . .	575	0	0	£575 3% Defence Bonds . . . . .	575	0	0
REVENUE							
	£	s.	d.		£	s.	d.
Prize and Certificate . . . . .	107	12	6	Balance on 31st December 1947 . . . . .	8	13	8
Expenses . . . . .	66	19	6	British Council contribution to expenses . . . . .	25	0	0
Balance carried to Balance Sheet . . . . .	4	6	8	Interest on Investments . . . . .	20	5	0
				Sale of Investment . . . . .	100	0	0
				Grant from General Fund . . . . .	25	0	0
	£178	18	8		£178	18	8

## ADDENBROOKE BEQUEST

CAPITAL							
Balance carried to Balance Sheet . . .	£	s.	d.	£384 6s. 7d. 2½% Consols "D" Account	£	s.	d.
	337	0	0		337	0	0
REVENUE							
Balance carried to Balance Sheet . . .	£	s.	d.	Balance on 31st December 1947 . . .	£	s.	d.
	26	5	0	Interest on Investments . . .	16	13	0
					9	12	0
	£26	5	0		£26	5	0

## LIFE COMPOSITION FUND ON 31ST DECEMBER 1948

16 Fellows paid £10 . . . . .	£	s.	d.
1 Fellow paid £15 . . . . .	160	0	0
1 Fellow paid £15 15s. 0d. . . . .	15	0	0
17 Fellows paid £21 . . . . .	15	15	0
1 Fellow paid £25 4s. 0d. . . . .	357	0	0
1 Fellow paid £26 5s. 0d. . . . .	25	4	0
56 Fellows paid £31 10s. 0d. . . . .	26	5	0
1 Fellow paid £33 12s. 0d. . . . .	1764	0	0
1 Fellow paid £67 14s. 6d. . . . .	33	12	0
	67	14	6
	<u>£2464</u>	<u>10</u>	<u>6</u>



### INCOME AND EXPENDITURE ACCOUNT FOR THE YEAR ENDED\*31st DECEMBER 1948

[illegible]

\* The opening stock was not included in the Income and Expenditure Account last year but was taken direct to the General Fund.

# BALANCE SHEET AS ON 31st DECEMBER 1948

LIABILITIES			ASSETS		
	£	s. d.	£	s. d.	£ s. d.
SUNDRY CREDITORS					
LIFE COMPOSITIONS:					
As on 31st December 1947	2443	11 0	Investments at market value on 31st December 1939		
Add Payments during year	83	9 6	or cost:—		
	2527	0 6	W. F. STANLEY TRUST FUND:		
Less Transfer to Income and Expenditure Account	62	10 0	£338 19 1 3% British Transport Stock 1977/88		259 0 0
			DUDELL MEMORIAL FUND:		
SUBSCRIPTIONS:			£400 3½% War Stock		374 0 0
Members	587	9 11	CHARLES CHREE MEDAL AND PRIZE FUND:		
Publications	2391	6 8	£784 4% Funding Stock	839	0 0
			£1500 2½% Consols	1027	10 0
SPECIAL FUNDS:			CHARLES VERNON BOYS PRIZE FUND:		
W. F. Stanley Trust Fund	259	0 0	£1132 16s. 10d. 2½% Consols		1866 10 0
Duddell Memorial Trust Fund	380	19 11	HOLWECK PRIZE FUND:		
Charles Chree Medal and Prize Fund	1953	1 10	£575 3% Defence Bonds		900 0 0
Charles Vernon Boys Prize Fund	885	11 1	ADDENBROOKE BEQUEST:		
Holweck Prize Fund	579	6 8	£384 6s. 7d. 2½% Consols		575 0 0
Addenbrooke Bequest	363	5 0	GENERAL FUND:		
			£2100 2½% Consols	1437	10 0
GENERAL FUND:			£1750 3½% War Stock	1636	0 0
As on 31st December 1947	11013	1 5	£500 4% Funding Stock	535	0 0
Add Lucas Legacy	500	0 0	£2300 3% Defence Bonds	2300	0 0
Balance of Income and Expenditure Account	1067	14 2	£1910 16s. 3d. 3% British Transport Stock		
			1977 88	1533	0 0
					7441 10 0
					11,753 0 0
			(Market value on 31st December 1948: £12,836.)		
			Dividends due on Investments		64 1 5
			Inland Revenue—Income Tax recoverable		16 12 10
			Subscriptions due		151 11 6
			Sundry Debtors		1013 16 8
			Stock of Paper and Binding Material		
			Publications		1480 2 9
					7500 0 0
			Cash at Bank: Current Account		8980 2 9
			Deposit Account		2255 2 10
			Cash in hand		95 15 11
					81 15 10
					2432 14 7
					£24,411 19 9

We have audited the above Balance sheet and have obtained all the information and explanations we have required. We have verified the bank balances and the Investments. In our opinion such Balance Sheet is properly drawn up so as to exhibit a true and correct view of the state of the Society's affairs according to the best of our information and the explanations given to us and as shown by the books of the Society.

KNOX, CROPPER & Co.,  
Chartered Accountants

SPENCER HOUSE, SOUTH PLACE, E.C.2.  
25th February 1949.



# THE PROCEEDINGS OF THE PHYSICAL SOCIETY

## Section A

---

VOL. 62, PART 1

1 January 1949

No. 349 A

---

## EDITORIAL

Beginning with this issue the *Proceedings* will appear in two Parts, "A" and "B". This change has been dictated by the increasing volume of important communications which has proved too great even for the larger amount of space available since monthly publication began in January 1948.

It is intended provisionally to publish in Part A papers dealing with subjects such as the quantum theory, statistical mechanics, nuclear physics and cosmic rays, atomic physics, molecules, spectra, theories of solids, liquids and gases, surface phenomena, growth and properties of crystals, crystal structure, luminescence, electrodynamics, heat and thermodynamics, and standards. Part B will include subjects such as acoustics (including ultrasonics), optical design, electron optics, colour, elasticity and other mechanical properties of solids and liquids, crystal structure analysis, magnetic materials, refrigeration and liquefaction, electric discharges, radio, geo- and ionosphere physics, astrophysics, and solar physics. It is obvious that a hard and fast dividing line cannot at present be drawn, but we feel sure that in a short time each Part will develop a character of its own, so that the reader will have little difficulty in deciding with which he wishes to be supplied.

With this new arrangement we hope to be able, not only to give improved service to Fellows and other subscribers, but also to effect that speedy publication of important scientific papers which is so vital to the development of physics.

G. INGLE FINCH,  
*President.*

# Collision Problems and the Theory of Radiation Damping \*

By J. HAMILTON

Manchester University

*Communicated by L. Rosenfeld; MS. received 12th May 1948*

**ABSTRACT.** The relation between radiation damping theory and the problem of the radiationless collision of an electron with a field of force is discussed. It is shown that the divergence difficulties, such as appear in the damping treatment of Compton scattering do not arise, and the "cut-off" of damping technique is not necessary. The same result applies to the relativistic collision of two electrons.

## § 1. INTRODUCTION AND SUMMARY

It has been pointed out by Bethe and Oppenheimer (1946) that an uncritical application of the equations developed by Heitler and Peng (1942) for treating radiation damping, leads to incorrect results when applied to the radiationless collision of particles under a static interaction potential. It is, of course, clear that the damping theory was developed in order to treat the interaction of quantized fields with particles to a higher degree of accuracy than is possible by the conventional perturbation theory. It may, however, be of interest to discuss the relation between damping theory and collision problems from a general point of view. This should give some idea of the range of validity of the theory, and some guide as to its application to more complicated problems, such as *bremsstrahlung*.

The scattering of a particle by a central static field of force is considered in the non-relativistic case. This collision problem is treated by the same method as was used in an earlier paper (Hamilton 1947), to be referred to as I, to deal with the damped scattering of radiation by an electron. Thus it is possible to compare in detail the treatment of the collision problem and of Compton scattering. The equations which describe the change in the free particle system due to the presence of the potential energy can be written in the same form as the equations which connect the initial and final states in the damping theory treatment of Compton scattering. The first difference between the two cases is that infinite transverse self-energy terms have to be neglected in the Compton scattering problem before any reasonable equations connecting the initial and final states can be formulated.

A more important difference arises in the solution of these two sets of equations. In Compton scattering it is essential to limit the energy of the final states to a narrow band of values centred on the energy of the initial state. The excluded final states would give an infinite contribution of such a type that the scattering cross-section would vanish (cf. I, § 7(a)). Relativistic invariance is not violated by this procedure, as the breadth of this energy band tends to zero as the size of the enclosing box becomes infinite. If the final states to be considered in the collision problem be limited to a similar narrow band of energies it is shown that a result is obtained which is in agreement with the result got by applying

\* This paper forms part of a thesis presented to the University of Manchester for the Ph.D. degree.

the Born approximation, when the latter is valid. When the Born approximation is not valid, this limitation to a narrow band of final energy values is easily seen to be incorrect.

Further investigation of the collision problem shows that those final states which lie outside the narrow energy band do not give an infinite contribution; in fact they give just that contribution which is necessary to lead to the correct collision cross-section as deduced by the phase method. Thus, in general, a direct application of the equations which were developed to treat the damped scattering of radiation leads to results which have no greater accuracy or range of validity than those given by the Born approximation. It seems that, when there is no reason (such as divergency) for the limitation of the range of energy values of the final states, the Heitler-Peng equations, in their simple form, are no longer valid.

In §§2-4 the case of a central force of finite range is treated, and in §5 the modifications which are necessary in dealing with the Coulomb potential are indicated. In both these cases it is possible to simplify the calculations by using a simple relation which exists between the phase shift of the wave mechanical method of treating scattering, and the energy shifts which play an important part in the damping phenomenon.

In §6 the relativistic collision of two electrons (without the emission of radiation) is discussed. While the restriction to radiationless collisions makes the discussion of limited validity, it seems that there is no more serious convergence trouble for high energies of the final states when the lowest order relativistic interaction is used, than when the Coulomb interaction alone is used. Thus the parts of the interaction due to longitudinal and transverse photons, respectively, are not treated by different methods, as would be the case if the transverse part had to undergo a cut-off procedure; and the relativistic invariance is not violated.

It would be useful to have a general criterion which would indicate those cases in which it is essential to limit the possible energies of the final states. It is a fact that, so far as the electromagnetic field is concerned, this limitation has only been required in problems in which a change in the free photon configuration is considered (i.e. emission or scattering of a photon). This may be a general rule.

It might be expected from a correspondence principle argument that no damping problem in the usual sense arises in the collision of two electrons. In classical or quantum theory, damping expresses the reaction of the emitted or scattered entity on the emitter or scatterer. In the former, damping takes the form of certain reactive forces, while in the latter it can be regarded as arising from a re-normalization of the wave function of the initial state. The classical theory of electron collisions introduces no damping effect of this nature, and the same may be expected to hold for the non-relativistic quantum theory treatment.

That divergence troubles are absent from the simple treatment of the radiationless relativistic collision of two electrons is also to be expected. Møller (1931) has shown that the part of the interaction which results from the virtual emission and absorption of one photon, can be regarded as being due to the interaction of the currents which arise from the motion of the electrons. As it is possible to treat the motion of an assembly of charges and currents by the ordinary quantum mechanical methods without any difficulty, it is to be expected that no divergence of energy integrals will arise in the present treatment. It may be of interest

to remember that the relativistic interaction of the electrons can be regarded, by the correspondence principle, as arising from uniformly moving electrons, so that no acceleration of the electrons is involved, and no radiation reaction arises.

These arguments apply to the electromagnetic field only. The interaction of the charges and currents arising from the meson fields of nucleons cannot be treated by the ordinary quantum mechanical methods, and divergence difficulties are expected to occur in treating collisions involving these particles.

There is, of course, in principle, a distinction between the existence of divergence difficulties and the presence of a damping effect. Even if quantum electrodynamics were well behaved so that no divergent integrals arose, it would be possible to express the damping effects of emitted or scattered radiation. In that case the Heitler-Peng formalism would have to be altered so as to allow for those final states which lay outside the narrow energy band. In view of the above discussion it is possible to go further and state that such a modification would be particularly necessary in cases where the interactions are strong, and the damping is, therefore, really important.

The question of the effect of the emission of radiation on the collision of an electron with a field of force is not considered in the present paper. Bethe and Oppenheimer (1946) applied the Heitler-Peng equations to the *bremsstrahlung* process in which only one photon is emitted, and they found that the infra-red catastrophe appeared in a very troublesome way. As all the final states interact with each other in any damping treatment it is essential that all the physically important states are considered.

Ferretti and Peierls (1947) pointed out that this imposed a restriction on the validity of Bethe and Oppenheimer's treatment, due to the possible emission of many photons. They showed that for the single photon treatment to be valid, it is essential to enclose the system in a reflecting or periodic box of a size such that  $(e^2/\hbar c) \ln(E/p_{\min}) \ll 1$ , where  $p_{\min}$  is the lowest photon energy allowed by the size of the box, while  $E$  is the initial kinetic energy of the electron. Ferretti and Peierls showed that, if the size of the box be such that this condition holds, there is a damping correction to the radiationless scattering cross-section, which depends logarithmically on the linear dimensions of the box. They suggested that this was a meaningless result.

The *bremsstrahlung* problem has been partially investigated. It has been shown that, in the single photon case, the damping correction to the cross-section for radiationless collisions of the electron is just the total cross-section for collisions in which a photon is emitted. Although this correction does depend on the size of the box in the way Ferretti and Peierls suggest, it clearly has a very reasonable interpretation. A solution of the *bremsstrahlung* process for the case in which the box may be infinite appears to be very complicated.

## § 2. THE PHASE SHIFT

In this and the two following sections the collision of a particle with a central field of force of finite range is considered. Spherical polar coordinates are the most convenient. In order to show the connection between the phase shift of the wave function of the scattered particle and the change in the energy levels which occurs in going from the free particle system to the system in which the

potential energy acts on the particle, it is essential to enclose the particle in a large spherical box. This box is assumed to be impenetrable; its centre coincides with the centre of force, and its radius is denoted by  $R$ .

The motion of a free particle in such a box is given by the wave function

$$\Phi_p(r) = Cr^{-1} J_{l+1/2}(pr) Y_{lm}(\theta, \phi), \quad \dots\dots(1)$$

where  $J$  and  $Y$  are Bessel functions and spherical harmonics, respectively, and  $C$  is a normalizing constant;  $p$  is the radial momentum, and  $\hbar$  is taken as being unity. The asymptotic form of such a wave function is  $\Phi \sim r^{-1} \sin(pr - l\pi/2)$ . The boundary condition requires  $pR - l\pi/2 = n\pi$ , where  $n$  is an integer. Thus the  $p$  values are equally spaced by the amount

$$\Delta p = \pi/R. \quad \dots\dots(2)$$

This corresponds to an energy spacing, in the non-relativistic case, of  $\Delta E = (p/m)(\pi/R)$ , where  $m$  is the mass of the particle.

When the problem of the scattering of a free particle by the potential energy  $V(r)$  is solved by the normal methods, the result can be expressed by the asymptotic form of the wave function, viz.  $\Psi \sim r^{-1} \sin(pr - l\pi/2 + \delta_l)$ . If this scattering takes place within an impenetrable box of radius  $R$  a spectrum of  $p$  values is selected, given by  $p'R - l\pi/2 + \delta_l = n_l\pi$ . These new values of the momentum are related to the momentum values of the free particle by the equation

$$(p' - p)R = -\delta_l. \quad \dots\dots(3)$$

If  $\Lambda$  is the new energy value corresponding to  $p'$ , and  $E$  the original energy, then (2) and (3) give

$$\pi(\Lambda - E)/\Delta E = -\delta_l. \quad \dots\dots(4)$$

### § 3. THE BORN APPROXIMATION

As the potential  $V(r)$  is independent of angles and spin the coupling of the free states (1) which  $V$  introduces does not mix the angular momentum quantum numbers  $l, m$ . In what follows the case  $l=0$  will be treated. The method of treating damping theory developed in I will be followed, in so far as it is applicable to the scattering problem. Denoting the states of the free particle by the quantum number  $p$ , the equations giving the behaviour of the system when  $V(r)$  is introduced are (cf. I, eqn. (4))

$$(E_p - \Lambda)A_p + \sum_{p'} H_{pp'} A_{p'} = 0. \quad \dots\dots(5)$$

$E_p$  and  $\Lambda$  are the energies of the free and the coupled system respectively, the  $A_p$  are the normal amplitude functions, and  $H_{pp'} = \int_0^R r^2 dr \Phi_p(r) V(r) \Phi_{p'}(r)$ .  $\Phi_p(r)$  is given by (1) with  $l=0$ .

Following the treatment of Compton scattering (I, §6) new amplitude functions are introduced by the relation  $V_p = (\Lambda - E_p)A_p$ . Substitution in (5) gives

$$V_p = \sum_{p'} H_{pp'} V_{p'} / (\Lambda - E_{p'}). \quad \dots\dots(6)$$

If  $\Lambda$  lies in the region between  $E_{p''}$  and the next highest energy value, the sum in (6) can be split up, conveniently, into a sum over the  $2N$  values of  $E_{p'}$  situated symmetrically about  $E_{p''}$ , and a sum over the remaining  $E_p$  values.



The result of this separation gives

$$V_p = \sum_{[2N]} \frac{H_{pp''} V_{p''}}{\Lambda - E_{p''}} + \sum_{(E_{p''})} \frac{H_{pp'} V_{p'}}{E_{p''} - E_{p'}}, \quad \dots\dots (7)$$

where  $[2N]$  denotes the region about  $E_{p''}$ , and  $(E_{p''})$  the remainder. The details of the transition from (6) to (7) are given in the Appendix.

Equation (7) gives

$$V_p = H'_{pp''} V_{p''} \frac{m}{p'} \cot \{(\Lambda - E_{p''})\pi/\Delta E\} + \frac{1}{\pi} \int_{(p'')} \frac{H'_{pp'}}{E_{p''} - E_{p'}} V_{p'} dp', \quad \dots\dots (8)$$

where the second sum in (7) has been replaced by an integral.  $(p'')$  indicates that the principal value has to be used at  $p' = p''$ , while  $H'_{pp'} = RH_{pp'}$ .

According to the damping theory technique for radiation developed in I, the second term on the right hand side of (8) has to be neglected. In the radiation case this term is infinite. Neglecting this term in the present case will lead to the results obtained by indiscriminate application of the Heitler-Peng equations to collision problems.

Thus (8) gives  $V_p = H'_{pp''} V_{p''} (m/p'') \cot \{(\Lambda - E_{p''})\pi/\Delta E\}$ . Putting  $p = p''$ , it follows that

$$\tan \{(\Lambda - E_{p''})\pi/\Delta E\} = (m/p'') H'_{p''p''}, \quad \dots\dots (9)$$

or using (4),

$$\tan \delta_0 = -(m/p'') H'_{p''p''}. \quad \dots\dots (9a)$$

Allowing for the fact that the normalized functions  $\Phi_p(r)$  of (1) have a radial part given by  $\Phi_p(r) = (\pi p/R)^{1/2} r^{-1/2} J_{1/2}(pr)$ , (9a) gives

$$\tan \delta_0 = -\frac{1}{2}\pi \frac{8\pi^2 m}{\hbar^2} \int_0^\infty V(r) [J_{1/2}(pr)]^2 r dr \quad \dots\dots (10)$$

on re-introducing  $\hbar$ .

This agrees with the usual Born approximation for  $\delta_0$ , viz.

$$\delta_0 = -\frac{1}{2}\pi \frac{8\pi^2 m}{\hbar^2} \int_0^\infty V(r) [J_{1/2}(pr)]^2 r dr, \quad \dots\dots (11)$$

which is valid provided  $\delta_0 \leq 1$ .

It can be seen readily that (10) gives incorrect results if the right hand side is large. Consider a potential  $V(r)$  which is extremely strong where  $r < a$ , and which vanishes where  $r > a$ . Then the true value of  $\delta_0$  is approximately  $-(a/p)$ , but the right hand side of (10) is, in general, certainly not  $-\tan(a/p)$ .

Thus the technique used for the damping of radiation when applied to a collision problem gives a value for the phase which agrees with that derived by using the Born approximation, in cases where the Born approximation is valid; but it gives an incorrect result in cases where the Born approximation is not valid. It follows that the region of validity of the Heitler-Peng equations for collision problems is the same as that of the Born approximation.

#### § 4. THE EXACT SOLUTION

It remains to show that it is possible to take account of the second term on the right hand side of (8), and that this equation then leads to the correct value of the phase.

Equation (8) can be written

$$V_p = \lambda H'_{pp''} V_{p''} + \frac{1}{\pi} \int_{(p'')} \frac{H'_{pp'}}{E_{p''} - E_{p'}} V_{p'} dp', \quad \dots\dots (8a)$$

where  $\lambda$  is an eigenvalue to be determined.  $H'$  is independent of  $R$ , the radius of the box, and so is  $\Phi'_p(r) = R^{\frac{1}{2}} \Phi_p(r)$ . Actually  $\Phi_p(r) = \sqrt{2} \sin(pr)/r$ . To find the solutions of (8a) it is useful to study the properties of the homogeneous integral equation

$$W_p = \mu \int_0^\infty H'_{pp'} W_{p'} dp'. \quad \dots\dots (12)$$

Equation (12) will have a set of real eigenvalues  $\mu_\alpha$ , and a corresponding set of solutions  $W_p^\alpha$ . The functions  $W_p^\alpha$  are orthogonal, and if the  $\alpha$  form a discrete set, the  $W_p^\alpha$  can be normalized so that  $\int_0^\infty dp' W_p^\alpha W_{p'}^\beta = \delta_{\alpha\beta}$ . Then

$$H'_{pp'} = \sum_\alpha W_p^\alpha W_{p'}^\alpha / \mu_\alpha, \quad \dots\dots (13)$$

where the summation extends over all values of  $\alpha$ . However, the definition

$$H'_{pp'} = \int_0^\infty \Phi'_p(r) V(r) \Phi'_{p'}(r) r^2 dr, \quad \dots\dots (14)$$

remembering the orthogonal properties of the  $\Phi'_p(r)$ , suggests that  $\alpha$  denotes the continuous spectrum given by  $r$ , and that the  $W_p^\alpha$  are related to the  $\Phi_p(r)$ . If  $W_p^r = \pi^{-\frac{1}{2}} r \Phi'_p(r) = (2/\pi)^{\frac{1}{2}} \sin(pr)$  then

$$\lim_{P \rightarrow \infty} \int_0^P W_p^r W_{p'}^r dp = \pi^{-1} \lim_{P' \rightarrow \infty} \left\{ \frac{\sin P(r-r')}{r-r'} - \frac{\sin P(r+r')}{r+r'} \right\} = \delta(r-r') \quad \dots\dots (15a)$$

where  $\delta(r-r')$  is the Dirac  $\delta$ -function. Similarly, the other orthogonal relation holds, viz.

$$\lim_{R \rightarrow \infty} \int_0^R W_p^r W_{p'}^r dr = \delta(p-p'). \quad \dots\dots (15b)$$

Now (14) can be written in the form

$$H'_{pp'} = \int_0^\infty \frac{W_p^r W_{p'}^r}{\mu_r} dr, \quad \dots\dots (16)$$

which is analogous to (13). It follows that  $1/\mu_r = \pi V(r)$ . It can easily be verified that the  $W_p^r/\mu_r$ , thus defined are the solutions of equation (12).

To solve (8a) substitute  $V_p = \int_0^\infty dr a_r W_p^r$  (i.e. the solution of (8a) is expanded in terms of the solutions of (12)).

Using (16) and the orthogonality relations (15) this gives

$$\mu_r a_r = \int_0^\infty dr' a_{r'} \{ \lambda(r, r') + [r, r'] \}, \quad \dots\dots (17)$$

where  $(r, r') = W_p^r W_{p'}^{r'}$ ,  $[r, r'] = \frac{1}{\pi} \int_0^\infty dp' \frac{W_p^r W_{p'}^{r'}}{E_{p''} - E_{p'}}$ . Using  $E_p = p^2/2m$  gives

$$[r, r'] = -(2m/\pi p'') \begin{cases} \cos(r'p'') \sin(rp'') & r < r' \\ \sin(r'p'') \cos(rp'') & r > r' \end{cases}$$

and also  $(r, r') = (2/\pi) \sin(p''r) \sin(p''r')$ . Further, substituting  $\alpha_r = \mu a_r$ , (17) leads to the equation for  $\alpha_r$

$$\alpha_r = 2\{\lambda \sin(p''r) - (m/p'') \cos(p''r)\} \int_0^r dr' \alpha_r V(r') \sin(p''r') \\ - 2(m/p'') \sin(p''r) \int_r^\infty dr' \alpha_r V(r') \cos(p''r'). \quad \dots\dots (18)$$

From (18) it follows that if  $\alpha_r$  is everywhere finite then  $\alpha_0 = 0$ . By differentiation of (18) it is readily seen that  $\alpha_r$  satisfies the equation

$$d^2\alpha_r/dr^2 + \{(p'')^2 - 2mV(r)\}\alpha_r = 0. \quad \dots\dots (19)$$

As is well known the solution of (19), together with the condition  $\alpha_0 = 0$ , leads to the asymptotic form for large  $r$

$$\alpha_r \sim A \sin(p''r + \delta_0), \quad \dots\dots (20)$$

where  $A$  tends to a constant as  $r \rightarrow \infty$ . The asymptotic form of (15), on the other hand, is

$$\alpha_r \sim 2\{\lambda \sin(p''r) - (m/p'') \cos(p''r)\} \int_0^\infty dr' \alpha_r V(r') \sin(p''r'). \quad \dots\dots (21)$$

Comparing (20) and (21), it follows that  $\cot \delta_0 = -\lambda p''/m$ .

Thus  $\cot \delta_0 = -\cot \{(\Lambda - E_{p''})\pi/\Delta E\}$ , in agreement with the exact relation (4). Hence the additional term in (8a) gives a finite correction to the Born approximation—a correction which gives the exact result as deduced by the phase method.

Equation (21) yields the further relation for the phase

$$\sin \delta_0 = -2(m/p'')A^{-1} \int_0^\infty dr \psi(r) V(r) \sin(p''r), \quad \dots\dots (22)$$

where  $\psi(r)$  is the finite solution of (19) which has the asymptotic form  $\psi \sim A \sin(p''r + \delta_0)$ . Equation (22) can be verified by the usual methods.

Finally, it should be noted that the same method could be used for values of  $l$  other than zero, with a slightly more complicated analysis.

## § 5. THE COULOMB FIELD

The investigations of the previous sections can be carried through for the Coulomb interaction, with some slight modifications. It is well known that in this case the phase contains an additional factor  $(-\ln r)$ . This corresponds to the fact that  $H'_{pp}$  depends logarithmically on  $R$ , the radius of the enclosing sphere. It is therefore necessary to keep the radius  $R$  finite, but large. The connection between the phase shift and the energy difference, established in § 2, then holds (provided the  $\ln R$  term is included as being part of the phase). The  $p$  values now form a discrete set, and some integrations are to be replaced by summations.

In the Appendix it is shown that the transition from (6) to (7) can also be made in the Coulomb case. The last term in equation (8) is to be replaced by the summation  $\pi^{-1} \Delta p \sum_{p'} (H'_{pp'}) / (E_{p''} - E_{p'})$  where  $H'_{pp'} = \int_0^R \Phi'_p(r) V(r) \Phi'_{p'}(r) r^2 dr$ . Further, (15a) becomes  $\Delta p \sum_p W_p W_p^{r'} = \delta(r - r')$ . The modified form of (12),  $W_p = \mu \Delta p \sum_{p'} H'_{pp'} W_{p'}$ , has the solutions  $W_p^r$ . Equation (17) can be derived, with the modifications that the upper limit of the integration over  $r'$  is now  $R$ ,

while  $[r, r']$  is given by a summation over the  $p'$  values. Equations (18) and (19) follow easily, and (21) is replaced by

$$\alpha_R = 2\{\lambda \sin(p''R) - (m/p'') \cos(p''R)\} \int_0^R dr' \alpha_{r'} V(r') \sin(p''r').$$

From this it again follows that  $\cot \delta_0 = -\cot \{(\Lambda - E_{p''})\pi/\Delta E\}$ .

It is clear, therefore, that for the Coulomb interaction the damping theory cut-off is no more justified than it is for a static interaction of finite range.

## § 6. THE RETARDED INTERACTION OF TWO ELECTRONS

The result of the preceding section leads to the question of what part damping plays in the collision of two electrons when the retardation and velocity dependent effects are considered. It might be guessed that as the damping theory was developed for quantized fields, it will modify that part of the interaction which arises from transverse photons. On the other hand, it is difficult to see how such a treatment could avoid destroying the Lorentz invariant form of the total interaction (cf. Møller 1931).

Any investigation of the nature of the corrections to be applied to the first order perturbation method of treating the relativistic scattering of electrons must be mainly formal. Of the two reasons for this, the first is that the correction due to the emission of radiation is of the same order as any correction to Møller's (1932) collision cross-section. The other reason is that the matrix elements are very strongly dependent on the angle of scattering, if the latter is small; so that it is apparently impossible to apply perturbation theory to calculate the higher order corrections.

It is easiest to use a linear momentum representation (and a cubic periodic box). The fundamental equations (5) become

$$(E_c - \Lambda)A_{cl} + \sum_{c'l} H_{cl, c'l} A_{c'l} = 0, \quad \dots \dots (23)$$

where  $c, c'$  label the distinct energy levels, while  $l, l'$  denote the directions of the momenta and the spins of the two electrons in the initial and final states respectively.  $H_{cl, c'l}$  is the matrix element connecting the states  $(c, l)$  and  $(c', l')$ , and is composed of the Coulomb interaction matrix element, together with the compound matrix elements arising from the exchange of one transverse photon between the two electrons.

Substituting  $(\Lambda - E_c)A_{cl} = V_{cl}$ , and changing the summation over  $l'$  into an integration, equation (23) can be written as

$$V_{cl} = \pi\lambda \int dl' H_{cl, c'l} \rho(E_{c'l}) V_{c'l} + \int_{(E_c)} dE_{c'} dl' \frac{H_{cl, c'l} \rho(E_{c'l}) V_{c'l}}{E_c - E_{c'}}, \quad \dots \dots (24)$$

where  $\Lambda$  lies in the vicinity of  $E_c$ .  $\rho(E_{c'l})\Delta E_c dl$  is the number of final states in the range  $(\Delta E_c, dl)$ ;  $\Delta E_c$  is the interval between two discrete energy levels in the neighbourhood of  $E_c$ , while  $\lambda = \cot \{(\Lambda - E_c)\pi/\Delta E_c\}$ . (In the linear momentum representation there is no simple relation between  $\lambda$  and the phase.)

In the damping theory treatment of Compton scattering the second term on the right hand side of (24) is neglected, because the integration over the energy diverges. It can easily be seen that, in the Compton scattering case, the compound matrix element corresponding to  $H_{cl, c'l}$  behaves like  $(E_c)^{-\frac{1}{2}}$  as  $E_c \rightarrow \infty$ .

Suppose that in the problem of the collision of two electrons the initial momenta are  $\mathbf{p}_a, \mathbf{p}_b$ ; and the final momenta are  $\mathbf{p}'_a, \mathbf{p}'_b$ . Then the Coulomb matrix element is

$$4\pi e^2/[|\mathbf{p}_a - \mathbf{p}'_a|^2], \quad (\hbar = c = 1), \quad \dots\dots(25)$$

while the term in  $e^2$  due to the transverse photon field is (Heitler 1944, p. 98)

$$\frac{2\pi}{k} e^2 \left[ (\alpha^a \alpha^b) + \frac{(E_a - E'_a)(E_b - E'_b)}{k^2} \right] \frac{(E_a + E_b) - (E'_a + E'_b) - 2k}{\{E_a - E'_a - k\}\{E_b - E'_b - k\}} \quad \dots\dots(26)$$

$E_a, E_b; E'_a, E'_b$  are the initial and final energies of the electrons, while  $k = |\mathbf{p}_a - \mathbf{p}'_a| = |\mathbf{p}'_b - \mathbf{p}_b|$ . Conservation of energy is not assumed in calculating (25) or (26).

For  $k$  much larger than  $p_a, p_b$ , and the rest mass of the electrons, (26) takes the form  $(2\pi e^2/k^2)[\alpha^a \alpha^b + 1]$  and, for very large final energies,  $E_c \sim 2k$ . It is therefore to be expected that if the matrix element (25) gives no divergence difficulty in the energy integral occurring in equation (24), the same will apply to (26). As it is not permissible to neglect all but a narrow energy band in the case of the Coulomb interaction, it seems unjustified to apply the damping theory cut-off to the interaction given by (26). However, the general remarks on the essentially formal nature of any consideration of (26) at high energies should be remembered.

Finally, it may be noted that substituting the left hand side of (24) in the integral on the right hand side gives

$$V_{\bar{c}l} = \pi\lambda \int dl' \left\{ H_{\bar{c}l, \bar{c}l'} + \int_{(E_{\bar{c}})} dE_{c''} \int dl'' \frac{H_{\bar{c}, c''l''} \rho(E_{c''}l'') H_{c''l'', \bar{c}l'}}{E_{\bar{c}} - E_{c''}} \right\} \rho(E_{\bar{c}}l') V_{\bar{c}l'} + (\text{a term in } H.H.H.).$$

Here  $\int dE_{c''}$  is a convergent integral, but  $\int dl''$  gives rise to an infinity when  $l''$  is parallel to  $l$ , or to  $l'$  (in the centre of gravity system). Such a substitution method of approximating to (24) is therefore impossible, because of the strong angular dependence of the matrix elements.

#### ACKNOWLEDGMENT

I would like to express my sincere thanks to Professor Niels Bohr for facilities to work at the Institute in Copenhagen, where most of this work was completed. I am also indebted to Professor L. Rosenfeld for very useful discussions.

#### APPENDIX

The transition from equations (6) to (7) for finite range interactions can be justified as follows. Consider first the  $(E_{p''})$  region, which is the region remaining when the  $N$  terms higher and lower than  $E_{p''}$  are excluded.

On  $(E_{p''})$  the term  $1/(\Lambda - E_{p'})$  can be written

$$\frac{1}{\Lambda - E_{p'}} - \frac{1}{E_{p''} - E_{p'}} + (\Lambda - E_{p''}) \frac{\partial}{\partial E_{p''}} \left( \frac{1}{E_{p''} - E_{p'}} \right) \\ \frac{(\Lambda - E_{p''})^2}{2!} \frac{\partial^2}{\partial E_{p''}^2} \left( \frac{1}{E_{p''} - E_{p'}} \right) + \dots$$

The order of magnitude of the ratio of the second term on the right hand side to the first is  $|(\Lambda - E_{p''})/(E_{p''} - E_{p'})|$ ; and on  $(E_{p''})$  this is less than  $r/N$ , where  $(\Lambda - E_{p''})/\Delta E = r$ , and  $r = O(1)$ . Choosing  $N = KR^{(1+\epsilon)}$ , where  $0 < \epsilon < \frac{1}{2}$  and  $K$  is a constant, this ratio can be made negligible. Thus the second, and similarly the higher order terms on the right hand side of the series can be neglected compared with the first term. With this definition of  $N$ , it follows that  $N\Delta E = (\pi p''/m)R^{(1+\epsilon)}$  tends to zero as  $R \rightarrow \infty$ . Thus the breadth in energy of the region  $[2N]$  about  $E_{p''}$  which contains the  $2N$  energy levels tends to zero as  $R \rightarrow \infty$ .

For the region  $[2N]$  it is convenient to use the expansion

$$H_{pp'}V_{p'} = H_{pp''}V_{p''} + (E_{p'} - E_{p''}) \frac{\partial}{\partial E_{p''}} (H_{pp''}V_{p''}) + \dots \quad (A)$$

It is assumed that  $H_{pp'}V_{p'}$  does not vary rapidly on  $[2N]$ . Further

$$\sum_{[2N]} \frac{E_{p'} - E_{p''}}{\Lambda - E_{p'}} = -2N + (\Lambda - E_{p''}) \sum_{[2N]} \frac{1}{\Lambda - E_{p'}}.$$

If  $N$ , and so  $R$ , is sufficiently large, the last term gives

$$\{(\Lambda - E_{p''})\pi/\Delta E\} \cot \{(\Lambda - E_{p''})\pi/\Delta E\}.$$

It is therefore negligible compared with the term  $-2N$ . The first term on the right hand side of (A) gives the first term in (7) whose value is

$$H'_{pp''}V_{p''}(\pi/R\Delta E) \cot \{(\Lambda - E_{p''})\pi/\Delta E\},$$

where  $H'_{pp''} = RH_{pp''}$ .  $H'_{pp''}$  is independent of  $R$  provided

$$R \int_0^R \Phi_p(r)V(r)\Phi_{p''}(r)r^2 dr,$$

converges as  $R \rightarrow \infty$ . This is true when  $V(r)$  is a potential of finite range.  $R\Delta E$  is independent of  $R$ . The second term on the right hand side of (A) gives a term in (7)

$$-2N \frac{\partial}{\partial E_{p''}} (H_{pp''}V_{p''}) = -\frac{2N}{R} \frac{\partial}{\partial E_{p''}} (H'_{pp''}V_{p''}) = O(R^{-1+\epsilon}).$$

This can be neglected. Similarly it can be shown that the higher order terms in (A) do not contribute to (7).

When  $V(r)$  is of the form  $1/r$  it is essential to keep  $R$  finite, but it can be seen that by choosing  $R$  sufficiently large, the errors involved in going from (6) to (7) can be made as small as is desired.

#### REFERENCES

- BETHE, H. A., and OPPENHEIMER, J. R., 1946, *Phys. Rev.*, **70**, 451.  
 FERRETTI, B., and PEIERLS, R. E., 1947, *Nature, Lond.*, **160**, 531.  
 HAMILTON, J., 1947, *Proc. Phys. Soc.*, **59**, 917.  
 HEITLER, W., 1944, *Quantum Theory of Radiation* (Oxford: University Press).  
 HEITLER, W., and PENG, H. W., 1942, *Proc. Camb. Phil. Soc.*, **38**, 296.  
 MØLLER, C., 1931, *Z. Phys.*, **70**, 786; 1932, *Ann. Phys., Lpz.*, **14**, 531.

## Damping Theory and the Propagation of Radiation \*

By J. HAMILTON  
Manchester University

*Communicated by L. Rosenfeld; MS. received 12th May 1948*

**ABSTRACT.** It is shown that a careful examination of the concepts involved in radiation damping theory makes it possible to treat the propagation of energy from one atom to another through the electromagnetic field. An exact and continuous solution of the propagation problem is given.

### § 1. INTRODUCTION AND SUMMARY

IT has been suggested by Ferretti and Peierls (1947) that the quantum theory of radiation damping leads to incorrect results when it is applied to a problem which involves the propagation of radiation. They consider the resonance interaction of two atoms through the medium of the electromagnetic field; and they suggest that a consequence of the damping theory is that energy is propagated from one atom to the other at a velocity other than the velocity of light. They reach this conclusion after making use of the ideas of "roundabout transitions" and "intermediate" states which are involved in the application of damping theory to the scattering of radiation (Heitler and Peng 1942). The present paper is an attempt to show that there need be no difficulty in the propagation problem, provided these ideas are examined carefully; and, in addition, it is an attempt to obtain an exact solution for this problem.

It is assumed that there are two identical atoms A and B, which can interact by emitting and absorbing photons. For simplicity the states considered are: two, in which one atom is in its excited state and the other is in its normal state; and an infinity, in which both atoms are in their normal states and one photon is present. For such a system there need be no confusion due to "roundabout transitions". This type of transition can be defined as involving the emission and re-absorption of the same photon by the same electron, and it is clear that such a transition leads to an infinite self-energy term in the solution. No such transition arises in the simple treatment of the propagation problem. Having excluded these roundabout transitions, it is obvious that, if two distinct transitions lead from an observable initial state to an observable final state, there is no reason to neglect one of them.

The idea of "intermediate" states in the damping theory requires more detailed examination. The concept first arose in the treatment of the intermediate states occurring in Compton scattering. Those states have an energy which differs by a finite amount from the energy of the initial state for the scattering problem. Moreover, the energy spread of the final states tends to zero, as the enclosing "periodic" box becomes infinite; so the intermediate states cannot have the same energy as any of the final states. For scattering problems, therefore, the intermediate states are not observable; they have a mathematical meaning only. As a consequence, in the damping theory solution of scattering, the

\* This paper forms parts of a thesis presented to the University of Manchester for the Ph.D. degree.

possibility of the energy of the coupled system of particle and radiation being equal to the energy of an intermediate state is neglected. Further, in normalizing the total probability to unity, the possibility of the system being found in any intermediate state is neglected.

The intermediate states (states in which one photon is present and both atoms are unexcited) which may occur in the propagation problem are of quite different nature from those which have just been discussed. Any of the intermediate states in the propagation problem may be observed; so they are no more intermediate than they are final states. That they happen to be coupled to final states of another kind is incidental. Further, it is clear that they have to be considered in normalizing the total probability; and it will appear from the detailed solution that they give the major contribution to the normalization equation. There is, therefore, no basis for treating these states by the same method as was used for the intermediate states in the scattering problem.

It is shown that these considerations lead to a reasonable result for the propagation problem. The method of discrete energy levels developed in an earlier paper (Hamilton 1947), to be referred to as I, is used, and the treatment of the simple atomic emitter is followed closely. The presence of the second atom causes a splitting of the energy levels of the interacting system, a splitting which is inversely proportional to the separation of the atoms. This splitting makes it possible for the second atom to remain in its ground state for the correct time after the first atom starts radiating.

On the basis of Weisskopf and Wigner's solution for the atomic emitter, Kikuchi (1930) has shown that the electromagnetic disturbance which is emitted travels with the velocity of light. Wentzel (1933) shows in a similar manner how the propagation problem can be treated. The present solution differs from these in that the reaction of the second atom on the first is considered, and that the solution obtained for the excitation probability of the second atom is a continuous function of the time. Both the above authors make substitutions for the excitation of the second atom which are discontinuous in time.

## § 2. THE FUNDAMENTAL EQUATIONS

The system composed of two identical atoms A and B and any radiation is enclosed in a large cubic "periodic" box. It will be assumed that each atom has only one excited state, and states in which more than one photon occurs will be neglected. As was shown in I, the unperturbed states of such a system have a discrete energy spectrum; and it can be assumed that the distinct energy levels (which are highly degenerate) are equally spaced.

The unperturbed states to be considered are: (0) atom A excited and no photon present, (1) atom B excited and no photon present, (i) both atoms in their normal state and a photon "i" present. 0, 1, i, will be used to label these states. The effect of the coupling between the atoms and the radiation field can be expressed by the equations (cf. I, eqn. (11))

$$\begin{aligned}(E_0 - \Lambda)A_0 + \sum_i H_{0i}A_i &= 0, \\(E_1 - \Lambda)A_1 + H_{10}A_0 + H_{1i}A_i &= 0, \\(E_i - \Lambda)A_i + \sum_j H_{ij}A_j &= 0.\end{aligned}\tag{1}$$



The  $E$  denote the energies of the uncoupled states, the  $H$  are the usual matrix elements for emission and absorption of radiation, and the  $A$  are the amplitude factors describing the coupled states;  $\Lambda$  is the energy value of the coupled system. Different solutions of the set (1) will be denoted by the index  $\mu$ .

Following I, any state of the coupled system can be described by the wave function  $\Psi$ , which can be written in the form  $\Psi = \sum_{\mu} c_{\mu} \Psi^{\mu}$  where the  $c_{\mu}$  are constants depending on the initial conditions and  $\Psi^{\mu} = \sum_r A_r^{\mu} \exp \{-i(\Lambda_{\mu} - E_r)t\} \psi_r$ . The index  $r$  runs over 0, 1 and all the  $i$ , while the  $\psi_r$  are the wave functions of the uncoupled system.  $\Psi$  can also be written

$$\Psi = \sum_r a_r \psi_r, \quad \dots\dots (2)$$

where  $a_r(t) = \sum_{\mu} A_r^{\mu} \exp \{-i(\Lambda_{\mu} - E_r)t\}$  is time dependent. If the initial conditions are

$$a_0(0) = 1, \quad a_1(0) = 0, \quad a_i(0) = 0, \quad \dots\dots (2')$$

then  $c_{\mu} = \overline{A_0^{\mu}}$ .

Due to the positions of atoms A and B being different (both atoms are regarded as being massive and immovable), the matrix elements  $H_{0i}$ ,  $H_{1i}$  are not identical. They are related thus

$$H_{1i} = \exp \{i(\mathbf{p}_i \cdot \mathbf{r}')\} H_{0i}, \quad \dots\dots (3)$$

where  $\mathbf{r}'$  is the displacement vector of B relative to A and  $\mathbf{p}_i$  is the momentum of photon "i" ( $\hbar = c = 1$  throughout).

Elimination of the  $A_i$  from (1) gives

$$\left\{ \begin{aligned} \left\{ E_0 - \Lambda + \sum_i \frac{|H_{ci}|^2}{\Lambda - E_i} \right\} A_0 + \sum_i \frac{H_{ci} H_{1i}}{\Lambda - E_i} A_1 &= 0, \\ \left\{ E_1 - \Lambda + \sum_i \frac{|H_{1i}|^2}{\Lambda - E_i} \right\} A_1 + \sum_i \frac{H_{1i} H_{0i}}{\Lambda - E_i} A_0 &= 0. \end{aligned} \right\}$$

Taking  $E_0 = E_1$ , these equations give

$$(E_1 - \Lambda)^2 + (E_1 - \Lambda) \sum_i \frac{|H_{1i}|^2}{\Lambda - E_i} + \sum_{i,j} \frac{\{|H_{0i}|^2 |H_{1j}|^2 - H_{0i} H_{1j} \bar{H}_{0j} H_{1i}\}}{(\Lambda - E_i)(\Lambda - E_j)} = 0, \quad \dots\dots (4)$$

where the bar denotes the complex conjugate.

Using (3), any term of numerator of the last summation in (4) becomes  $|H_{0i}|^2 |H_{0j}|^2 \cdot [1 - \exp \{-i(\mathbf{p}_i \cdot \mathbf{r}')\} \exp \{i(\mathbf{p}_j \cdot \mathbf{r}')\}]$ . The summation  $\sum_i$  in (4) can be split up into a summation over the discrete energy levels, denoted by  $\sum_{E_i}$ , and a summation over all the states belonging to a fixed value of  $E$ , denoted by  $\sum_{[E_i]}$ .

Consider, for simplicity, that the excited state of either atom is a  $p$ -state with the magnetic quantum number zero. Then

$$H_{0i} = \text{const.} \int g(r) (z/r) \exp \{i(\mathbf{p}_i \cdot \mathbf{x})\} f(r) dV,$$

with an obvious notation. Thus for dipole radiation

$$H_{0i} = i p_{iz} \cdot \text{const.} \int g(r) f(r) (z^2/r) dV,$$

where  $p_{1z}$  is the  $z$ -component of  $\mathbf{p}_1$ . Hence

$$|H_{01}|^2 = (p_{1z})^2 C,$$

where  $C$  is independent of  $\mathbf{p}_1$ .

Denoting the angle between the axis  $OZ$  and  $\mathbf{r}'$  by  $\theta'$ , the angular summation of the term containing the exponential factor gives

$$\sum_{[E_1]} \exp \{ -i(\mathbf{p}_1 \cdot \mathbf{r}') \} |H_{01}|^2 = \overline{|H_{01}|^2} \cdot \left\{ \frac{\sin \alpha}{\alpha} + (3 \cos^2 \theta' - 1) \left( \frac{\sin \alpha}{\alpha} + 3 \frac{\cos \alpha}{\alpha^2} - 3 \frac{\sin \alpha}{\alpha^3} \right) \right\},$$

where  $\overline{|H_{01}|^2} = \sum_{[E_1]} |H_{01}|^2$  is the summation of  $|H_{01}|^2$  over all angles, and  $\alpha = |\mathbf{p}_1| r'$ .

If the zero of energy is taken as the energy of either of the atoms in its normal state, then  $|\mathbf{p}_1| = E_1$ .

It is convenient to write the angular summation in the form

$$\sum_{[E_1]} \exp \{ -i(\mathbf{p}_1 \cdot \mathbf{r}') \} |H_{01}|^2 = |H_{01}|^2 \{ G_1(E_1 r') \sin(E_1 r') + G_2(E_1 r') \cos(E_1 r') \},$$

where

$$G_1(E_1 r') = 3 \cos^2 \theta' / (E_1 r') - 3(3 \cos^2 \theta' - 1) / (E_1 r')^3; \quad G_2(E_1 r') = 3(3 \cos^2 \theta' - 1) / (E_1 r')^2.$$

Then

$$\begin{aligned} \sum_{[E_1]} \sum_{[E_j]} |H_{01}|^2 |H_{0j}|^2 [1 - \exp \{ -i(\mathbf{p}_1 \cdot \mathbf{r}') \} \exp \{ i(\mathbf{p}_j \cdot \mathbf{r}') \}] \\ = \overline{|H_{01}|^2} \cdot \overline{|H_{0j}|^2} \cdot \{ 1 - [G_1(E_1 r') \sin(E_1 r') + G_2(E_1 r') \cos(E_1 r')] \\ \times [G_1(E_j r') \sin(E_j r') + G_2(E_j r') \cos(E_j r')] \}. \end{aligned} \quad \dots\dots (5)$$

### § 3. THE ENERGY SUMMATION AND THE EIGENVALUE EQUATION

Assuming that the matrix elements  $H_{0i}$  vary slowly with the energy  $E_i$  in the important region (i.e. over the ordinary line width) it is possible to separate off energy summations in equation (4) of the type  $\sum_{E_i} 1/(\Lambda - E_i)$ . Assuming that the distinct energy levels  $E_i$  are equally spaced in the vicinity of  $\Lambda$  such a summation gives

$$\sum_{E_i} 1/(\Lambda - E_i) = (\pi/\Delta E) \cot \{ (\Lambda - E_s)\pi/\Delta E \} + \sigma, \quad \dots\dots (6)$$

where  $\Delta E$  is the spacing of the energy values, and  $E_s$  is one of the energy values  $E_i$  which lies close to  $\Lambda$ .  $\sigma$  is a correction arising from the  $E_i$  values which lie far from  $\Lambda$ . As the range of  $E_i$  values centred about  $\Lambda$  over which the summation is made is increased,  $\sigma$  is zero at first, and only becomes appreciable for ranges which are very many times greater than the line width of one of the atoms. Over such large ranges the matrix elements will vary appreciably with  $E_i$ , and (6) would have to be modified. In the extreme case of an infinite range of  $E_i$  values the term  $\sigma$  leads to the usual transverse self-energy of the bound electron. It is sufficient here to note that in the present problem  $\sigma$  can be neglected for ranges of  $E_i$  which are many multiples of the line width. Such a limitation will be used in what follows. Under similar conditions

$$\sum_{E_i} \frac{\sin(\Lambda - E_i)r'}{\Lambda - E_i} = \pi/\Delta E; \quad \sum_{E_i} \frac{\cos(\Lambda - E_i)r'}{\Lambda - E_i} = (\pi/\Delta E) \cot \{ (\Lambda - E_s)\pi/\Delta E \}.$$

The variation of  $G_1(E_1r')$ ,  $G_2(E_1r')$  with  $E_1$  in the energy summations occurring in (4) can be neglected, provided the "periodic box" is sufficiently large. These functions are therefore replaced by  $G_1(\Lambda r')$ ,  $G_2(\Lambda r')$  respectively.

Using these summations, (4) with the aid of (5) reduces to a quadratic equation for  $(\pi/\Delta E) \cdot |\overline{H_{01}}|^2 \cdot \cot \{(\Lambda - E_s)\pi/\Delta E\}$  whose roots are

$$(\Gamma/2) \cot \{(\Lambda - E_s)\pi/\Delta E\} = \frac{\Lambda - E_1 \mp \{G_2(\Lambda r') \sin(\Lambda r') - G_1(\Lambda r') \cos(\Lambda r')\} \cdot (\Gamma/2)}{1 \pm \{G_1(\Lambda r') \sin(\Lambda r') + G_2(\Lambda r') \cos(\Lambda r')\}}, \quad (7)$$

where the upper or lower signs are to be taken together, and  $\Gamma/2 = (\pi/\Delta E) \cdot |\overline{H_{01}}|^2$ .  $\Gamma$  is the ordinary line breadth of either atom (cf. I, § 5). According to (7) there will be two roots  $\Lambda$  lying in the energy range  $\Delta E$  between each two adjacent distinct values of  $E_1$ . As  $r' \rightarrow \infty$  equation (7) becomes

$$(\Gamma/2) \cot \{(\Lambda - E_s)\pi/\Delta E\} = \Lambda - E_1, \quad \dots\dots(7')$$

which is the eigenvalue equation for the photon emission of one atom. By the definition of the functions  $G$  it follows that

$$G_1(\Lambda r') \sim (1/\Lambda r') O(1), \quad G_2(\Lambda r') \sim (1/\Lambda r')^2 O(1),$$

provided  $\Lambda r' \gg 1$ .  $O(1)$  denotes a constant of the order of magnitude unity. Thus the roots of (7) differ from the roots of (7') by amounts of the order of  $\Delta E/(\Lambda r')$ , provided  $\Lambda r' \gg 1$ . As  $1/\Lambda r' \simeq \lambda/r'$ , where  $\lambda$  is the wavelength of the resonant radiation, this condition can be written as  $r' \gg \lambda$ .

#### § 4. NORMALIZATION

The condition that the total probability of the system being in all configurations is unity, gives

$$|A_0^\mu|^2 + |A_1^\mu|^2 + \sum |A_i^\mu|^2 = 1 \quad \dots\dots(8)$$

for all values of the root index  $\mu$ . Substituting from (1) gives

$$A_1^\mu = \left\{ \sum_i \frac{H_{11}H_{10}}{\Lambda_\mu - E_1} A_0 + \sum_i \frac{|H_{11}|^2}{\Lambda - E_i} A_1^\mu \right\} \cdot \frac{1}{\Lambda_\mu - E_1}.$$

Making these summations by the method of § 3, and using (7) to evaluate  $\cot \{(\Lambda - E_s)\pi/\Delta E\}$  where necessary, it appears that

$$A_1^\mu = \pm A_0^\mu, \quad \dots\dots(9)$$

where the  $\pm$  sign is to be taken according as the upper or lower set of signs is used in (7). Further, from (1), (3) and (9)

$$\begin{aligned} \sum_i |A_i^\mu|^2 &= |A_0^\mu|^2 \cdot \sum_i |H_{01}|^2 \cdot |1 \pm \exp \{-i(\mathbf{p}_i \cdot \mathbf{r}')\}|^2 / (\Lambda - E_1)^2 \\ &= 2 |A_0^\mu|^2 \cdot |\overline{H_{01}}|^2 \cdot (\pi/\Delta E)^2 \cdot \operatorname{cosec}^2 \{(\Lambda - E_s)\pi/\Delta E\} \\ &\quad \times \{1 \pm [G_1(\Lambda r') \sin(\Lambda r') + G_2(\Lambda r') \cos(\Lambda r')]\}, \quad \dots\dots(10) \end{aligned}$$

provided  $r' \ll L$ , the linear dimension of the enclosing box.

Now it is clear, by using the relation  $\Gamma/2 = (\pi/\Delta E) \cdot |\overline{H_{01}}|^2$ , that in (8) the terms  $|A_0^\mu|^2$ ,  $|A_1^\mu|^2$  are unimportant, as  $\pi/\Delta E$  is very large. The normalization is therefore determined by the photon states. From (10) and (7) it follows that

$$|A_0^\mu|^2 = \frac{1}{2} \cdot \frac{|\overline{H_{01}}|^2 \cdot \{1 \pm [G_1 \sin(\Lambda r') + G_2 \cos(\Lambda r')]\}}{\{\Lambda - E_1 \mp (\Gamma/2)[G_2 \sin(\Lambda r') - G_1 \cos(\Lambda r')]\}^2 + (\Gamma/2)^2 \{1 \pm [G_1 \sin(\Lambda r') + G_2 \cos(\Lambda r')]\}^2} \quad \dots\dots(11)$$

§ 5. THE EXCITATION OF THE ATOMS

It follows from (2) that the probability of the occupation of the state  $\psi_0$  is given by  $|a_0|^2$ , where  $a_0$  is related to the  $A_0^\mu$  through the equation

$$a_0 = \sum_{\mu} c_{\mu} A_0^{\mu} \exp \{ -i(\Lambda_{\mu} - E_0)t \}.$$

For the initial conditions (2')  $c^{\mu} = \bar{A}_0^{\mu}$ , so

$$a_0(t) \exp \{ -iE_0 t \} = \sum_{\mu} |A_0^{\mu}|^2 \exp \{ -i\Lambda^{\mu} t \}, \quad \dots\dots (12)$$

where the summation runs over all the roots of (1). Using (11) it is seen that the summation over the pair of  $\Lambda_{\mu}$  values which lie in each energy interval  $\Delta E$  just cancels out the terms of order  $\lambda/r'$ , leaving a large term, plus terms of order  $(\lambda/r')^2$ . (The slight difference between the two values of  $\Lambda_{\mu}$  give corrections which vanish as  $L \rightarrow \infty$ ). Omitting the terms of order  $(\lambda/r')^2$  the sum of such pairs of  $|A_0^{\mu}|^2$  values is  $(|A_0^{\mu}|^2)' = |H_{01}|^2 / \{ (\Lambda - E_0)^2 + \Gamma^2/4 \}$ ;  $(|A_0^{\mu}|^2)'$  is identical with the term  $|A_0^{\mu}|^2$  which arises in the single atom problem (cf. I). Replacing the summation in (12) by an integration it is readily seen that  $|a_0(t)|^2 = \exp(-\Gamma t)$  as for the single atom.

The behaviour of the probability function  $|a_1|^2$  for the excitation of atom B is quite different. This function is given by

$$a_1(t) \exp(-iE_1 t) = \sum_{\mu} A_1^{\mu} \bar{A}_0^{\mu} \exp(-i\Lambda_{\mu} t). \quad \dots\dots (13)$$

Relation (9) causes a cancellation of the largest term in  $|A_0^{\mu}|^2$ , on adding the contribution from the pair of values within a range  $\Delta E$ . The remaining terms are smaller than  $(|A_0^{\mu}|^2)'$  by a factor of the order  $\lambda/r'$ .

Equation (13) can be written in the form

$$a_1 \exp(-iE_1 t) = \sum_{\mu+} |A_0^{\mu+}|^2 \exp(-i\Lambda_{\mu+} t) - \sum_{\mu-} |A_0^{\mu-}|^2 \exp(-i\Lambda_{\mu-} t), \quad \dots\dots (14)$$

where the  $+$ ,  $-$  indicate the two types of roots corresponding to  $A_1^{\mu} = \pm A_0^{\mu}$ . Also, (11) can be written

$$|A_0^{\mu}|^2 = \frac{\Delta E}{4\pi i} \left\{ \frac{1}{(\Lambda_{\mu} - E_1 - i\Gamma/2) \pm (\Gamma/2)(G_1 - iG_2) \exp(-i\Lambda_{\mu} r')} - \frac{1}{(\Lambda_{\mu} - E_1 + i\Gamma/2) \pm (\Gamma/2)(G_1 + iG_2) \exp(i\Lambda_{\mu} r')} \right\}$$

It can be assumed that  $\Lambda_{\mu+} = \Lambda_{\mu-} = \Lambda$ , as the error introduced thereby is negligible. Replacing the summation in (14) by an integration gives

$$a_1 \exp(-iE_1 t) = \frac{1}{2\pi i} \left( \frac{\Gamma}{2} \right) \left\{ \int_{-\infty}^{+\infty} d\Lambda \frac{(G_1 + iG_2) \exp \{ i\Lambda(r' - t) \}}{(\Lambda - E_1 + i\Gamma/2)^2 - (\Gamma/2)^2 (G_1 + iG_2)^2 \exp(2i\Lambda r')} - \int_{-\infty}^{+\infty} d\Lambda \frac{(G_1 - iG_2) \exp \{ -i\Lambda(r' + t) \}}{(\Lambda - E_1 - i\Gamma/2)^2 - (\Gamma/2)^2 (G_1 - iG_2)^2 \exp(-2i\Lambda r')} \right\} \dots\dots (15)$$

Equation (15) is exact, provided the dimensions of the "periodic box" are great enough; and this equation could be used to calculate  $a_1$  to any power of  $(\lambda/r')$ . Here it will be considered sufficient to find  $a_1$  to the lowest power of  $(\lambda/r')$ . Thus  $G_2$  is neglected. Further, the variation of  $G_1(\Lambda r')$  with  $\Lambda$  is neglected for the range of values of  $\Lambda$  which is important; and from (15) it is clear that this range is of the order of  $\Gamma$ .

With these assumptions the integrals in (15) can be evaluated by contour integration. The circuit consists of the real axis, together with half of the circle at infinity. On the circle at infinity the second integrand takes the form  $\exp\{y(r' + t)\}/(R^2 + C \exp(2yr'))$ , where  $\Lambda = x + iy$ ,  $|\Lambda| = R$ , and  $|C|$  is a constant. On the half circle  $y < 0$  this integrand will give no contribution, provided  $t > -r'$ . Moreover, the poles of the second integrand all lie on the half plane  $y > 0$ . To see this, substitute  $\Lambda' = \Lambda - E_1 - i\Gamma/2$ . The poles are given by

$$\Lambda' = \pm (\Gamma/2) G_1 \exp\{(\Gamma/2)r' - i(E_1 + \Lambda')r'\}.$$

If  $\Lambda' = x' - iy'$ , this gives

$$\sqrt{(x'^2 + y'^2)} = (\Gamma/2) |G_1| \exp\{(\Gamma/2 - y')r'\}.$$

As  $|G_1| \ll 1$ ,  $y' > \Gamma/2$  is impossible, and hence the result. Thus the second integrand gives no contribution to  $a_1$ , provided  $t > -r'$ . Actually it represents the "incoming" wave and plays no part in the solution for  $t > 0$ .

It is readily seen that the roots of the denominator of the first integrand all lie on the half plane  $y < 0$ . On the infinite circle the form of this integrand is  $\exp\{-y(r' - t)\}/\{R^2 + C \exp(-2yr')\}$ . When  $t < r'$  this gives no contribution when integrated over the upper half circle, so  $a_1(t) = 0$  if  $t < r'$ .

For  $t \geq r'$  the value of the integral can be found by noting that, as there are no roots of the denominator on the upper half plane, the integral is equal to

$$-G_1 \int_C d\Lambda \frac{\exp\{i\Lambda(r' - t)\}}{(\Lambda - E_1 + i\Gamma/2)^2 - (\Gamma/2)^2 G_1^2 \exp(2i\Lambda r')},$$

where  $C$  is the upper half circle at infinity. On  $C$  the second term in the denominator can be neglected, giving  $-G_1 \int_C d\Lambda [\exp\{i\Lambda(r' - t)\}]/(\Lambda - E_1 + i\Gamma/2)^2$ . The path  $C$  can be closed by including the lower half circle at infinity which gives no contribution when  $t \geq r'$ . Thus the integral becomes

$$-G_1 \int_O d\Lambda [\exp\{i\Lambda(r' - t)\}]/(\Lambda - E_1 + i\Gamma/2)^2,$$

where  $O$  is any contour surrounding the point  $(E_1 - i\Gamma/2)$ . Hence

$$a_1(t) \exp(-iE_1 t) = iG_1 \cdot (\Gamma/2)(t - r') \exp\{-\Gamma(t - r')/2\} \exp(iE_2 r') \quad (t > r'),$$

and as  $|G_1|^2 = K(\lambda/r')^2$ , where  $K$  is of the order of magnitude unity, the final result is

$$\left. \begin{aligned} |a_1(t)|^2 &= 0 & t \leq r' \\ |a_1(t)|^2 &= K(\lambda/r')^2 \{\Gamma(t - r')/2\}^2 \exp\{-\Gamma(t - r')\} & t > r' \end{aligned} \right\} \dots\dots (16)$$

Thus the atom B remains in its normal state till time  $r'$ , after which it is excited for a time of the order  $1/\Gamma$ . The maximum probability of excitation is of the form  $K(\lambda/r')^2$ , which is in agreement with the usual ideas on electromagnetic propagation.

The resonance phenomenon will arise from the re-emission of radiation by the atom B, and its absorption by A. The excitation amplitude of A will be of the order  $(\lambda/r')^2$ , and therefore does not occur in the approximation used in this section.

#### REFERENCES

- FERRETTI, B., and PEIERLS, R. E., 1947, *Nature, Lond.*, **160**, 531.  
 HAMILTON, J., 1947, *Proc. Phys. Soc.*, **59**, 917.  
 HEITLER, W., and PENG, H. W., 1942, *Proc. Camb. Phil. Soc.*, **38**, 296.  
 KIKUCHI, S., 1930, *Z. Phys.*, **66**, 558.  
 WENTZEL, G., 1933, *Handbuch der Physik* (Berlin: Springer), XXIV/1, 761.

# Continuous $\gamma$ -Emission in Neutron-Proton Collisions

By M. KROOK

Department of Mathematical Physics, University, Birmingham

*Communicated by R. E. Peierls; MS. received 28th May 1948*

**ABSTRACT.** The cross-section for Bremsstrahlung in neutron-proton collisions is calculated with a central exchange-force model and for energies up to 20 mev. Its value is found to lie between  $10^{-28}$  and  $10^{-29}$  cm<sup>2</sup>. This probably is too small to be measured with experimental techniques at present available.

## § 1. INTRODUCTION

THE aim of this paper is to estimate the magnitude of the cross-section for Bremsstrahlung in n-p (neutron-proton) collisions and its sensitivity to variation of the hypotheses concerning the n-p interaction. Neutron and proton will be treated here as point particles interacting by means of a central force of the exchange type. Their interaction with radiation will be supposed to conform to the usual theory for particles in a radiation field. We thus omit refinements which have been included by Pais (1943) in his treatment of the photo-disintegration of the deuteron.

This simple model is inadequate when the incident neutron energies are high (of the order of the meson rest-energy). Our discussion will thus be restricted to a lower energy-range. The relevant energies will then, in general, not be large compared with a suitable average of the potential. In these circumstances, use of the Born approximation may result in appreciable error. For this reason, exact continuum wave functions of the n-p system will be used to calculate the required cross-sections.

## § 2. WAVE FUNCTIONS

Referred to the centre of gravity frame, (C-system), the wave equation for the internal motion of the n-p system is

$$[\nabla^2 + (M/\hbar^2)(E - V)]\psi(\mathbf{r}; m_1, m_2) = 0. \quad \dots\dots(2.1)$$

Here  $\mathbf{r} \equiv (x, y, z)$  is the position-vector of the neutron relative to the proton,  $m_1$  and  $m_2$  are spin-variables of the particles,  $M$  the mass of a nucleon and  $2E$  is the kinetic energy of the incident neutron in the laboratory system. The interaction operator  $V$  will be chosen to represent a mixture of central exchange forces of Majorana and Heisenberg type (cf. Bethe and Bacher 1936, §§ 11, 12, 13).

The wave functions will be required to represent "incoming" or "outgoing" particles which have, at large distances, a definite momentum  $\hbar\mathbf{k}$ . Correspondingly we determine the following types of solution of (2.1):

- (a) To represent incoming particles: solutions which have, for  $r \rightarrow \infty$ , the asymptotic form

$$[\exp \{i(\mathbf{k} \cdot \mathbf{r})\} + \text{diverging spherical wave}] \times (\text{spin function})$$

- (b) To represent outgoing particles we choose, for reasons of symmetry, those solutions which have the asymptotic form

$$[\exp \{i(\mathbf{k} \cdot \mathbf{r})\} + \text{converging spherical wave}] \times (\text{spin function}).$$

The eigenstates can be classified into triplet states with wave functions

$$\psi^{(3)} = U^{(3)}(\mathbf{r}) {}^3\chi_m \quad (m=0, \pm 1), \quad \dots\dots(2.2)$$

and singlet states with wave functions

$$\psi^{(1)} = U^{(1)}(\mathbf{r}) {}^1\chi. \quad \dots\dots(2.3)$$

${}^3\chi_m$ , ( $m=0, \pm 1$ ) and  ${}^1\chi$  are the usual normalized symmetric and antisymmetric spin functions of the two-particle problem. The wave equations for triplet and for singlet states are independent. Also, the space part  $U^{(3)}(\mathbf{r})$  of the triplet wave function (2.2) is independent of  $m$ . On separating out the spin-dependence, the functions  $U^{(3)}$  and  $U^{(1)}$  satisfy equations which may be written together in the form

$$(\hbar^2\Delta/M + E)U(\mathbf{r}) = V(r)U(-\mathbf{r}). \quad \dots\dots(2.4)$$

If  $M(r)$  and  $H(r)$  describe the dependence on distance of the Majorana and Heisenberg potentials, respectively, then

$$V(r) = \begin{cases} M(r) + H(r) & \text{(triplet states)} \\ M(r) - H(r) & \text{(singlet states)} \end{cases}. \quad \dots\dots(2.5)$$

Each wave function will be characterized by an associated wave vector  $\mathbf{k}$  of length  $k = (ME/\hbar^2)^{1/2}$ . This dependence on the parameter  $\mathbf{k}$  will be indicated by the notation  $U(\mathbf{r}; \mathbf{k})$ . Introducing spherical polar coordinates  $(r, \theta, \phi)$  with polar axis in the direction  $\mathbf{k}$ , those wave functions which satisfy conditions (a) or (b) above can be expanded in the form:

$$U_{\pm}(\mathbf{r}; \mathbf{k}) = \sum_{l=0}^{\infty} (2l+1) i^l \exp\{\pm i\eta_l(k)\} \frac{u_l(r; k)}{kr} P_l(\cos\theta) \quad \dots\dots(2.6)$$

(cf. Mott and Massey 1933). The  $P_l(t)$  are non-normalized Legendre polynomials and  $u_l(r; k)$  is that solution of

$$\frac{d^2u}{dr^2} + \left[ k^2 - \frac{l(l+1)}{r^2} - (-1)^l \frac{MV(r)}{\hbar^2} \right] u = 0 \quad \dots\dots(2.7)$$

which vanishes for  $r=0$  and which has, for  $r \rightarrow \infty$ , the asymptotic form

$$u_l(r; k) \sim \sin[kr - \frac{1}{2}l\pi + \eta_l(k)]. \quad \dots\dots(2.8)$$

$U_+$  and  $U_-$  correspond respectively to the cases with diverging and converging spherical waves.

The incident beam will be assumed to be unpolarized and to consist of particles with wave vector  $\mathbf{k}_0$  (in the C-system). There are then four independent initial states of equal weight:

$$\psi_{\text{in}}(\mathbf{r}; \mathbf{k}_0) = \begin{cases} U_+^{(3)}(\mathbf{r}; \mathbf{k}_0) {}^3\chi_m, & (m=0, \pm 1) \\ U_+^{(1)}(\mathbf{r}; \mathbf{k}_0) {}^1\chi \end{cases}. \quad \dots\dots(2.9)$$

$U_+^{(3)}$  and  $U_+^{(1)}$  are given by (2.6) with  $\mathbf{k} = \mathbf{k}_0$ . Similarly, there are four independent wave functions corresponding to final states with wave vector  $\mathbf{k}$ :

$$\psi_{\text{fin}}(\mathbf{r}; \mathbf{k}) = \begin{cases} U_-^{(3)}(\mathbf{r}; \mathbf{k}) {}^3\chi_m, & (m=0, \pm 1) \\ U_-^{(1)}(\mathbf{r}; \mathbf{k}) {}^1\chi \end{cases}, \quad \dots\dots(2.10)$$

$U_-^{(3)}$  and  $U_-^{(1)}$  are given by (2.6) with  $\mathbf{k}$  as polar axis. (Since  $V$  contains no spin-orbit coupling terms, the spin functions in both (2.9) and (2.10) may be referred

to the same coordinate system with  $\mathbf{k}_0$  as  $z$ -axis.) We shall denote coordinates in a system with  $\mathbf{k}_0$  as  $z$ -axis by  $(x, y, z)$  or  $(r, \theta, \phi)$  and polar coordinates in a system with  $\mathbf{k}$  as polar axis by  $(r, \theta', \phi')$ .

Each of the functions in (2.9), (2.10) is normalized per unit volume, i.e.

$$\lim_{v \rightarrow \infty} \frac{1}{v} \int |U|^2 d\tau = 1.$$

### § 3. MATRIX ELEMENTS

We shall consider processes in which the  $n$ - $p$  system (referred to the C-frame), makes a radiative transition from one of the states characterized by wave vector  $\mathbf{k}_0$  (energy  $E_0$ ) to states characterized by wave vector  $\mathbf{k}$  (energy  $E$ ). The circular frequency  $\omega$  of the photon emitted is then given by

$$\hbar\omega = E_0 - E = (\hbar^2/M)(k_0^2 - k^2). \quad \dots\dots(3.1)$$

Strictly speaking, the C-systems appropriate to initial and to final states are not identical. The difference—due to the momentum carried off by the photon—is, however, very small and will be neglected.

Two types of process will be taken into account. These are (Bethe and Bacher 1936, §§ 16, 17): (a) transitions induced by the electric dipole  $\frac{1}{2}e\mathbf{r}$ ; and (b) transitions induced by the magnetic dipole  $\mu_0\mathbf{T} \equiv \mu_0(\mu_p\boldsymbol{\sigma}_p + \mu_n\boldsymbol{\sigma}_n)$ ,  $\boldsymbol{\sigma}_p, \boldsymbol{\sigma}_n$  are the spin operators and  $\mu_p, \mu_n$  the magnitudes of the magnetic moments in units of a nuclear magneton  $\mu_0 = e\hbar/2Mc$ .

Correspondingly, we shall have to evaluate matrix elements of the following two main types:

$$\mathcal{M} = \frac{1}{2}e\mathbf{M} = \frac{1}{2}e \int \psi_{\text{fin}}^*(\mathbf{r}; \mathbf{k}) \mathbf{r} \psi_{\text{in}}(\mathbf{r}; \mathbf{k}_0) d\tau, \quad \dots\dots(3.2)$$

$$\mathcal{N} = \mu_0\mathbf{N} = \mu_0 \int \psi_{\text{fin}}^*(\mathbf{r}; \mathbf{k}) \mathbf{T} \psi_{\text{in}}(\mathbf{r}; \mathbf{k}_0) d\tau. \quad \dots\dots(3.3)$$

The required cross-sections are to be obtained by calculating the eight partial cross-sections with each of the states (2.9) as initial state and then adding them with weight-factor  $\frac{1}{4}$  for each.

Considering first transitions of type (a), the only non-vanishing matrix elements are:

(i) three equal elements:

$$\mathbf{M}^{(3)} = \int U_+^{(3)}(\mathbf{r}; \mathbf{k}_0) \mathbf{r} U_-^{(3)*}(\mathbf{r}; \mathbf{k}) d\tau, \quad \dots\dots(3.4)$$

corresponding to transitions  $U_+^{(3)} \cdot {}^3\chi_m \rightarrow U_-^{(3)} \cdot {}^3\chi_m$ , ( $m = 0, \pm 1$ ), and

(ii) one element:

$$\mathbf{M}^{(1)} = \int U_+^{(1)}(\mathbf{r}; \mathbf{k}_0) \mathbf{r} U_-^{(1)*}(\mathbf{r}; \mathbf{k}) d\tau, \quad \dots\dots(3.5)$$

corresponding to the transition  $U_+^{(1)} \chi \rightarrow U_-^{(1)} \chi$ .

In the sum for the composite cross-section, (3.4) contributes with weight  $\frac{3}{4}$  and (3.5) with weight  $\frac{1}{4}$ .

Let  $(\lambda, \mu)$  be the angular coordinates of  $\mathbf{k}$  in the coordinate system with  $\mathbf{k}_0$  as polar axis. For conciseness we write

$$\eta_l^{(i)} \equiv \eta_l^{(i)}(k), \quad \bar{\eta}_l^{(i)} \equiv \eta_l^{(i)}(k_0), \quad (i = 3 \text{ or } 1) \quad \dots\dots(3.6)$$

and

$$G_{l,n} = \frac{1}{k_0 k} \int_0^\infty u_l(r; k_0) u_n(r; k) r dr. \quad \dots\dots(3.7)$$



In (3.7)  $G_{l,n}^{(3)}$  and  $G_{l,n}^{(1)}$  are to be distinguished according as triplet or singlet wave functions and phases are involved.

As it stands, the integral in (3.7) is divergent. However, it is summable, e.g. by inserting a convergence factor  $e^{-br}$  and then proceeding to the limit  $b \rightarrow 0$  after the integration has been performed. It is in this sense that (3.7) and the analogous divergent integrals in (3.13) have to be interpreted here.

When the wave functions in the form (2.6) are substituted in (3.4) and (3.5) the integrals over angles are easily evaluated by using the spherical harmonic addition theorem. We find (writing  $t = \cos \lambda$ )

$$M_z = 4\pi i \sum_{l=0}^{\infty} (l+1) \{G_{l+1,l} \exp \{i(\bar{\eta}_{l+1} + \eta_l)\} P_l(t) - G_{l,l+1} \exp \{i(\bar{\eta}_l + \eta_{l+1})\} P_{l+1}(t)\}, \quad \dots\dots (3.8)$$

$$M_x \pm iM_y = -4\pi \exp(\pm i\mu) \sum_{l=0}^{\infty} \{G_{l+1,l} \exp \{i(\bar{\eta}_{l+1} + \eta_l)\} P_l^1(t) + G_{l,l+1} \exp \{i(\bar{\eta}_l + \eta_{l+1})\} P_{l+1}^1(t)\}. \quad \dots\dots (3.9)$$

Turning now to the photomagnetic transitions, the only surviving elements  $\mathcal{N}(\mathbf{k}_0; \mathbf{k})$  are of the forms:

$\mathcal{N}^{(3,1)}$  corresponding to transitions triplet  $\rightarrow$  singlet,

$\mathcal{N}^{(1,3)}$  corresponding to transitions singlet  $\rightarrow$  triplet.

Writing

$$A^{(i,j)} = \int U_+^{(i)}(\mathbf{r}; \mathbf{k}_0) U^{(j)*}(\mathbf{r}; \mathbf{k}) d\tau \quad [(i,j) = (3,1) \text{ or } (1,3)], \quad \dots\dots (3.10)$$

we have

$$\sum_{(3)\text{-states}} \{|N_x^{(i,j)}|^2 + |N_y^{(i,j)}|^2\} = 2 \sum_{(3)\text{-states}} |N_z^{(i,j)}|^2 = 2(\mu_p - \mu_n)^2 |A^{(i,j)}|^2. \quad \dots\dots (3.11)$$

The cross-sections obtained from (3.11) with  $(i,j) = (3,1)$  and  $(1,3)$  each contribute with weight  $\frac{1}{2}$  to the final cross-section.

Substituting wave functions of the form (2.6) in (3.10) we find analogously to (3.8), (3.9):

$$A^{(i,j)} = 4\pi \sum_{l=0}^{\infty} (2l+1) K_l^{(i,j)} \exp \{i(\bar{\eta}_l^{(i)} + \eta_l^{(j)})\} P_l(t), \quad \dots\dots (3.12)$$

with

$$K_l^{(i,j)} = \frac{1}{k_0 k} \int_0^{\infty} u_l^{(i)}(r; k_0) u_l^{(j)}(r; k) dr. \quad \dots\dots (3.13)$$

#### § 4. CROSS-SECTION FORMULAE

Each wave function (2.9) for an initial state corresponds to an incident current of  $2\hbar k_0/M$  neutrons/cm<sup>2</sup>/second. Each final wave function (2.10) is normalized per unit volume; there are then  $(Mk/16\pi^3\hbar^2) dE d\Omega$  final states of each type corresponding to motion within  $d\Omega = \sin \lambda d\lambda d\mu$  and with energy in the range  $(E, E+dE)$ . The factor

$$\frac{M^2}{32\pi^3\hbar^3} \left(\frac{E}{E_0}\right)^{\frac{1}{2}} dE d\Omega \quad \dots\dots (4.1)$$

is thus required to translate transition probabilities calculated with the wave functions (2.9), (2.10) into differential cross-sections.

Let  $\sigma(E_0; E, \lambda, \alpha) \sin \lambda \sin \alpha d\lambda d\alpha$  be the cross-section for a process in which (i) the n-p system makes a radiative transition from a state  $(\mathbf{k}_0, E_0)$  to a state with energy in  $(E, E + dE)$  and direction of motion making an angle between  $\lambda$  and  $\lambda + d\lambda$  with  $\mathbf{k}_0$ ; (ii) a photon with circular frequency  $\omega = (E_0 - E)/\hbar$  is emitted in a direction making an angle between  $\alpha$  and  $\alpha + d\alpha$  with  $\mathbf{k}_0$ . Then

$$\sigma(E_0; E, \lambda, \alpha) = \frac{M^2}{32\pi^3 \hbar^3} \left( \frac{E}{E_0} \right)^{\frac{1}{2}} \frac{\omega^3}{\hbar c^3} \{ (|\mathcal{M}_x|^2 + |\mathcal{M}_y|^2)(1 + \cos^2 \alpha) + 2|\mathcal{M}_z|^2 \sin^2 \alpha \}, \quad \dots (4.2)$$

where  $\mathcal{M}$  is to be interpreted as  $\mathcal{M}^{(3)}$  or  $\mathcal{M}^{(1)}$  in the electric dipole case and as  $\mathcal{N}^{(3,1)}$  or  $\mathcal{N}^{(1,3)}$  in the magnetic dipole case. The corresponding cross-sections will be distinguished by affixing the same indices to  $\sigma$ .

Further cross-sections of interest are derived from (4.2) by integration. They may be written in an obvious notation as  $\sigma(E_0; E, \lambda)$ ,  $\sigma(E_0; E; \alpha)$ ,  $\sigma(E_0; E)$  and  $\sigma(E_0)$ . In particular

$$\sigma(E_0; E) = \frac{M^2 \omega^3}{12\pi^2 \hbar^4 c^3} \left( \frac{E}{E_0} \right)^{\frac{1}{2}} \int_0^\pi \sum_{x,y,z} |\mathcal{M}_x|^2 \sin \lambda d\lambda. \quad \dots (4.3)$$

From (4.3) with (3.8), (3.9) and with (3.11), (3.12) we have

$$\sigma_{el}^{(i)}(E_0; E) = \frac{2e^2 M^2 \omega^3}{3\hbar^4 c^3} \left( \frac{E}{E_0} \right)^{\frac{1}{2}} \sum_{l=0}^{\infty} (l+1) \{ (G_{l,l+1}^{(i)})^2 + (G_{l+1,l}^{(i)})^2 \}, \quad \dots (4.4)$$

$$\sigma_{mag}^{(i,j)}(E_0; E) = \frac{8\mu_0^2 (\mu_p - \mu_n)^2 M^2 \omega^3}{\hbar^4 c^3} \left( \frac{E}{E_0} \right)^{\frac{1}{2}} \sum_{l=0}^{\infty} (2l+1) (K_l^{(i,j)})^2. \quad \dots (4.5)$$

## § 5. SHORT RANGE FORCES

For further progress it is necessary to introduce explicit assumptions for the interaction function  $V(r)$  in (2.4), (2.7). In this section we assume only that the forces are of short range, so that we may put effectively

$$V(r) = 0 \quad \text{for } r > a. \quad \dots (5.1)$$

In the range  $r > a$ , the required solution of (2.7) can be expressed in terms of Hankel functions:

$$u_l(r; k) = \frac{1}{2} \left( \frac{\pi k r}{2} \right)^{\frac{1}{2}} \{ \exp(i\eta_l) H_{l+\frac{1}{2}}^{(1)}(kr) + \exp(-i\eta_l) H_{l+\frac{1}{2}}^{(2)}(kr) \}. \quad \dots (5.2)$$

The phase  $\eta_l(k)$  is determined by fitting the interior and exterior solutions smoothly at  $r = a$ ; it depends on the detailed form of  $V(r)$  in  $(0, a)$ . (5.2) can also be represented in the form

$$u_l(r; k) = F_l(kr) \sin(kr + \eta_l) + G_l(kr) \cos(kr + \eta_l). \quad \dots (5.3)$$

$F_l(x)$  and  $G_l(x)$  are polynomials in  $x^{-1}$ , defined through the Bessel functions by  $(\frac{1}{2}\pi x)^{\frac{1}{2}} J_{l+\frac{1}{2}}(x) = F_l(x) \sin x + G_l(x) \cos x$ .

Now, the hypothesis of short-range forces implies that, given  $k$ , there exists an integer  $l_0(k)$  such that for all  $l \geq l_0$ , (i)  $\eta_l(k)$  does not differ appreciably from zero, and (ii) the  $u_l(r; k)$  do not differ appreciably from the unmodified plane-wave components  $(\pi k r / 2)^{\frac{1}{2}} J_{l+\frac{1}{2}}(kr)$  in the whole range  $(0, \infty)$ . It follows that, for  $l, n \geq l_0(k_0)$ , the  $G_{l,n}$  in (3.7) can effectively be taken equal to 0. Similar considerations apply to the  $K_l$ .

We now introduce the approximation of replacing the integrations over  $(0, \infty)$  in (3.7) and (3.13) by integrations over  $(a, \infty)$ . This approximation is valid only for energies which are not too high; this has been checked for the case of a rectangular potential (cf. § 7). For energies much larger than those considered here the contribution from  $(0, a)$  is no longer negligible; the calculated cross-sections would then depend more intimately on the detailed form of  $V(r)$  than in the low-energy case.

The integrals for  $G_{l,l+1}$  and  $K_l$  are now easily evaluated by elementary methods. (The evaluation for higher  $l$  can be simplified by using for the  $u_l$  certain recurrence formulae analogous to, and easily derivable from, those for the Hankel functions.) In particular we have

$$(k_0^2 - k^2)^2 G_{0,1} = \left(\frac{E_0}{E} - 3\right) \bar{c}_0 s_1 + 2 \left(\frac{E_0}{E}\right)^{\frac{1}{2}} \bar{s}_0 c_1 - k_0 a \left(1 - \frac{E}{E_0}\right) \left[ \left(\frac{E_0}{E}\right)^{\frac{1}{2}} \bar{c}_0 c_1 + \bar{s}_0 s_1 \right], \quad \dots (5.4)$$

$$(k_0^2 - k^2) G_{1,0} = \left(\frac{E}{E_0} - 3\right) c_0 s_1 + 2 \left(\frac{E_0}{E}\right)^{\frac{1}{2}} s_0 \bar{c}_1 + k_0 a \left(1 - \frac{E}{E_0}\right) \left[ c_0 \bar{c}_1 + \left(\frac{E_0}{E}\right)^{\frac{1}{2}} s_0 \bar{s}_1 \right], \quad \dots (5.5)$$

where, for conciseness, we have written (cf. (3.6))

$$\bar{s}_l = \bar{s}_l^{(i)} = \sin(k_0 a + \bar{\eta}_l^{(i)}), \quad s_l = s_l^{(i)} = \sin(ka + \eta_l^{(i)}), \text{ etc.} \quad \dots (5.6)$$

Also

$$(k_0^2 - k^2)^{3/2} K_0^{(3,1)} = \left(1 - \frac{E}{E_0}\right)^{\frac{1}{2}} \left[ \left(\frac{E_0}{E}\right)^{\frac{1}{2}} \bar{c}_0^{(3)} s_0^{(1)} - \bar{s}_0^{(3)} c_0^{(1)} \right], \quad \dots (5.7)$$

$$(k_0^2 - k^2)^{3/2} K_0^{(1,3)} = \left(1 - \frac{E}{E_0}\right)^{\frac{1}{2}} \left[ \left(\frac{E_0}{E}\right)^{\frac{1}{2}} \bar{c}_0^{(1)} s_0^{(3)} - \bar{s}_0^{(1)} c_0^{(3)} \right]. \quad \dots (5.8)$$

#### § 6. FORCES OF "ZERO RANGE"

We consider the simple limiting case where the range  $a \rightarrow 0$ . Here  $\eta_l^{(i)} \rightarrow 0$  for all  $l > 0$ . Let  $\epsilon_3$  and  $-\epsilon_1$  be the binding energies of the deuteron for the ground state and for the virtual singlet level respectively. Then

$$ka + \eta_0^{(3)} \rightarrow \frac{1}{2}\pi + \arctan(\epsilon_3/E)^{\frac{1}{2}}; \quad ka + \eta_0^{(1)} \rightarrow \frac{1}{2}\pi - \arctan(\epsilon_1/E)^{\frac{1}{2}}. \quad \dots (6.1)$$

In this case  $G_{l,l+1}$ ,  $G_{l+1,l}$  and the  $K_l$  are zero for all  $l \neq 0$  and

$$(k_0^2 - k^2)^2 G_{0,1} = 2 \left(\frac{E}{\epsilon + E_0}\right)^{\frac{1}{2}}; \quad (k_0^2 - k^2)^2 G_{1,0} = 2 \left(\frac{E_0}{\epsilon + E}\right)^{\frac{1}{2}}, \quad \dots (6.2)$$

$\epsilon$  being taken as  $\epsilon_3$  for the  $G^{(3)}$  and as  $\epsilon_1$  for the  $G^{(1)}$ . Also

$$(k_0^2 - k^2)^{3/2} K_0^{(i,j)} = (\epsilon_3^{\frac{1}{2}} + \epsilon_1^{\frac{1}{2}}) \left[ \frac{E_0 - E}{(\epsilon_i + E_0)(\epsilon_j + E)} \right]^{\frac{1}{2}}. \quad \dots (6.3)$$

The various cross-sections are then given by

$$\sigma_{cl}^{(i)}(E_0; E) = \frac{2.13 \times 10^{-30}}{E_0 - E} \left(\frac{E}{E_0}\right)^{\frac{1}{2}} \left\{ \frac{4E}{\epsilon_i + E_0} + \frac{4E_0}{\epsilon_i + E} \right\}, \quad \dots (6.4)$$

$$\sigma_{mag}^{(i,j)}(E_0; E) = 1.63 \times 10^{-31} \left(\frac{E}{E_0}\right)^{\frac{1}{2}} (\epsilon_3^{\frac{1}{2}} + \epsilon_1^{\frac{1}{2}})^2 \frac{E_0 - E}{(\epsilon_i + E_0)(\epsilon_j + E)}. \quad \dots (6.5)$$

Table 1 lists total cross-sections (integrated over  $E$ ) for the various types of process, and total averaged cross-sections  $\bar{\sigma}(E_0)$ , for a few values of  $E_0$ . The integral for  $\sigma_{el}(E_0)$  diverges logarithmically at  $E_0$ ; we have taken

$$\sigma_{el}(E_0) \equiv \int_0^{f^2 E_0} \sigma(E_0; E) dE.$$

The calculation has been made with  $\epsilon_3 = 2.17$ ,  $\epsilon_1 = 0.05$  mev. in (6.4), (6.5) and with  $f^2 = 0.95$ .

Table 1. Total Cross-sections in Units of  $10^{-23}$  cm<sup>2</sup> for Radiative Scattering by Protons of Neutrons with Energy  $2E_0$  mev.

$E_0$ (mev.)	$\sigma_{el}^{(3)}$	$\sigma_{el}^{(1)}$	$\sigma_{mag}$	$\bar{\sigma}(E_0)$
1	1.19	3.26	0.02	1.7
4	2.64	4.30	0.05	3.1
6	3.07	4.50	0.06	3.5
10	3.56	4.67	0.08	3.9

#### § 7. FINITE RANGE

The cross-sections were also calculated for energy  $E_0 = 10$  mev. using a rectangular potential model with range  $a = 2.5 \times 10^{-13}$  cm.,  $(V)_{r < a} = 25$  mev. (triplet states), 15 mev. (singlet states). By far the largest contribution is again due to the electric dipole transitions  $l=0 \rightarrow l=1$ . The approximation of replacing integrations over  $(0, \infty)$  by ones over  $(a, \infty)$  (cf. § 5) was checked for this case. In no case did the neglected contribution from  $(0, a)$  amount to more than 10% of the total; in general it is considerably less, as also is its averaged contribution. In Table 2 are listed the cross-sections for a number of values of  $E$  (column 2). For comparison,  $\sigma(10, E)$  in the limiting case  $a=0$  are given in column 3.

Table 2. Partial Cross-sections in Units of  $10^{-29}$  cm<sup>2</sup> for Radiative Scattering by Protons of Neutrons with Initial Energy 20 mev.

$E$ (mev.)	$\sigma(10, E)$	$\sigma(10, E), (a=0)$	$\sigma(10, E), (\text{max})$
1	1.7	1.3	26
5	2.7	2.3	18
7	4.7	4.2	29
9	15.0	13.8	

We have noted that the major contributions to the cross-section, for initial energies  $E_0$  up to about 10 mev., arises from the terms in  $G_{0,1}$  and  $G_{1,0}$  of  $\sigma_{el}$ . For such energies  $G_{0,1}$  and  $G_{1,0}$  are closely approximated to by (5.4) and (5.5) irrespective of the detailed form of  $V(r)$  in  $(0, a)$ . We thus obtain an upper limit to these coefficients, and so to the calculated cross-sections, by replacing all sine and cosine factors by unity. Then.

$$\begin{aligned} (k_0^2 - k^2)^2 |G_{0,1}| &\leq \frac{E_0}{E} - 3 + 2 \left( \frac{E}{E_0} \right)^{\frac{1}{2}} + k_0 a \left( 1 - \frac{E}{E_0} \right) \left[ \left( \frac{E_0}{E} \right)^{\frac{1}{2}} + 1 \right], \\ (k_0^2 - k^2)^2 |G_{1,0}| &\leq \frac{E}{E_0} - 3 + 2 \left( \frac{E_0}{E} \right)^{\frac{1}{2}} + k_0 a \left( 1 - \frac{E}{E_0} \right) \left[ \left( \frac{E_0}{E} \right)^{\frac{1}{2}} + 1 \right]. \end{aligned}$$

.....(7.1)

Column 4 of Table 2 gives maximum possible values of the cross-section obtained by using (7.1) with  $E_0 = 10$  mev.

The cross-sections for Bremsstrahlung on the central exchange force model thus come out very small in the energy range considered; in n-p collisions there would be about 10,000 elastic scattering processes for each such inelastic process. The relative probability for a given direction of the proton has also been investigated and found to be of the same order of magnitude. It thus appears that it would not be possible to detect and measure such radiative collisions with experimental techniques at present available. (In view of the smallness of the cross-sections it would be pedantic to discuss here the question of angular distribution of the particles and photons.) For much higher energies the cross-section for Bremsstrahlung would increase appreciably (at least on this model), and might be capable of measurement. The model used in this paper would, however, be inadequate for treating the problem at high energies with any exactness.

#### ACKNOWLEDGMENT

In conclusion I would like to record my thanks to Professor R. E. Peierls for suggesting the problem and for several helpful discussions.

#### REFERENCES

- BETHE, H. A., and BACHER, R. F., 1936, *Rev. Mod. Phys.*, **16**, 82.  
MOTT, N. F., and MASSEY, H. S. W., 1933, *Theory of Atomic Collisions*.  
PAIS, A., 1943, *Det Kgl. Dansk. Vid. Selskab XX*, Nr. 17.

## Resonance Transfer of Electronic Energy in Organic Crystals

By E. J. BOWEN, E. MIKIEWICZ AND F. W. SMITH

Physical Chemistry Laboratory, Oxford

*MS. received 9th June 1948*

**ABSTRACT.** The resonance transfer of energy in crystals of organic compounds when excited by visible or ultra-violet light has been examined by measuring the fluorescence of the systems naphthalene-anthracene, anthracene-naphthacene, naphthacene-pentacene, anthracene-acridine, anthracene-phenazine, and anthracene-di- and hexabromobenzenes. The conditions for "exciton" trapping and the relations of resonance transfer to fluorescence quenching are discussed.

#### § 1. INTRODUCTION

THE transfer of excitation energy by resonance from molecule to molecule in organic crystals is most strikingly shown by the anthracene-naphthacene system (Bowen 1945, Bowen and Mikiewicz 1947). Very small quantities of naphthacene in solid solution in anthracene change the fluorescence from blue to green, the excitation energy travelling by exchange until it is trapped at a naphthacene molecule. This effect disappears when the crystals are dissolved in benzene. The resonance exchange is doubtless assisted by the fact that the flat molecules of anthracene lie nearly parallel in the crystal (Robertson 1932); in the solid solutions the naphthacene molecules are again parallel to them.

For the unambiguous demonstration of the phenomenon it is necessary to use systems where the extinction coefficients show (a) that the exciting light is absorbed by the major constituent, and (b) that the fluorescence of the major constituent is not reduced through secondary absorption by the added substance. For "exciton" trapping to occur the added substance should have a possible transition between energy states associated with a lower energy quantum than a similar transition in the major substance, i.e., should absorb at somewhat longer wavelengths. This implies that the fluorescence band of the latter will almost coincide with the absorption band of the former, but condition (b) will hold if the added substance acts at sufficiently small concentrations. Extinction coefficient measurements are usually wanting for the crystalline state. The crystals are optically highly anisotropic. From the results of Kortum and Finckh (1942) on anthracene, however, it appears that there is little difference between the averaged values for crystals and solutions, except for a shift of about 200 Å. of the band to the red in the case of crystals. Solution values have therefore been used after slight correction.

A very high degree of purity is necessary in this work, and the materials used were subjected to careful purification and checked by absorption or fluorescence examination. Mixtures were prepared by weighing the components into a small tube, evacuating, and fusing together. The crystals were ground up and spread in a thin layer on the flat outer side of the inner part of a specially designed metal Dewar vessel with a silica window for excitation and observation. The fluorescence was excited by a concentrated beam from a small high-pressure mercury arc with filters, and measured through other filters by a photo-electron multiplier unit.

The excitation energy in the crystal may undergo a variety of processes, which may be formally represented by the following scheme, in which the  $k$ 's are velocity constants, the square brackets indicate concentrations and  $A^*$ ,  $B^*$  = molecules of  $A$ ,  $B$  with excitation energy.

Process	Relative Rate	Description of Process
$A + h\nu = A^*$	1	Excitation by light.
$A^* \rightarrow A + h\nu_1$	$k_1[A^*]$	Fluorescence of major constituent.
$A^* = A$	$k_1k_2[A^*]$	Self-quenching of major constituent.
$A^* + A \rightarrow A + A^*$		Exciton transfer.
$A^* + B \rightarrow B^* + A$	$k_1k_3[A^*][B]$	Exciton transfer to added substance.
$B^* \rightarrow B + h\nu_2$	$k_4[B^*]$	Fluorescence of added substance.
$B^* \rightarrow B$	$k_4k_5[B^*]$	
$B^* + B \rightarrow B + B$	$k_4k_6[B^*][B]$	Self-quenching of added substance.
$A^* + B \rightarrow B + A$	$k_1k_7[A^*][B]$	Quenching by added substance.

The quantum efficiencies of fluorescence are then for  $A$ :

$$1/\{1 + k_2 + k_3[B] + k_7[B]\};$$

and for  $B$ :

$$k_3[B]/\{1 + k_2 + k_3[B] + k_7[B]\}\{1 + k_5 + k_6[B]\}.$$

## § 2. RESULTS

The following systems were examined and results are shown graphically in Figure 1. Ordinates are fluorescence efficiencies (quantum yields) and abscissae the concentrations of the minor constituent expressed logarithmically (e.g. 7 indicates  $10^{-7}$  gm/gm.) except in the case of the anthracene-bromobenzene systems, where they are given as gm. per cent. The values of molar extinction

coefficients  $\epsilon$  given below for comparison relate to solutions of the hydrocarbons with a slight correction for band shift in the solid substances.

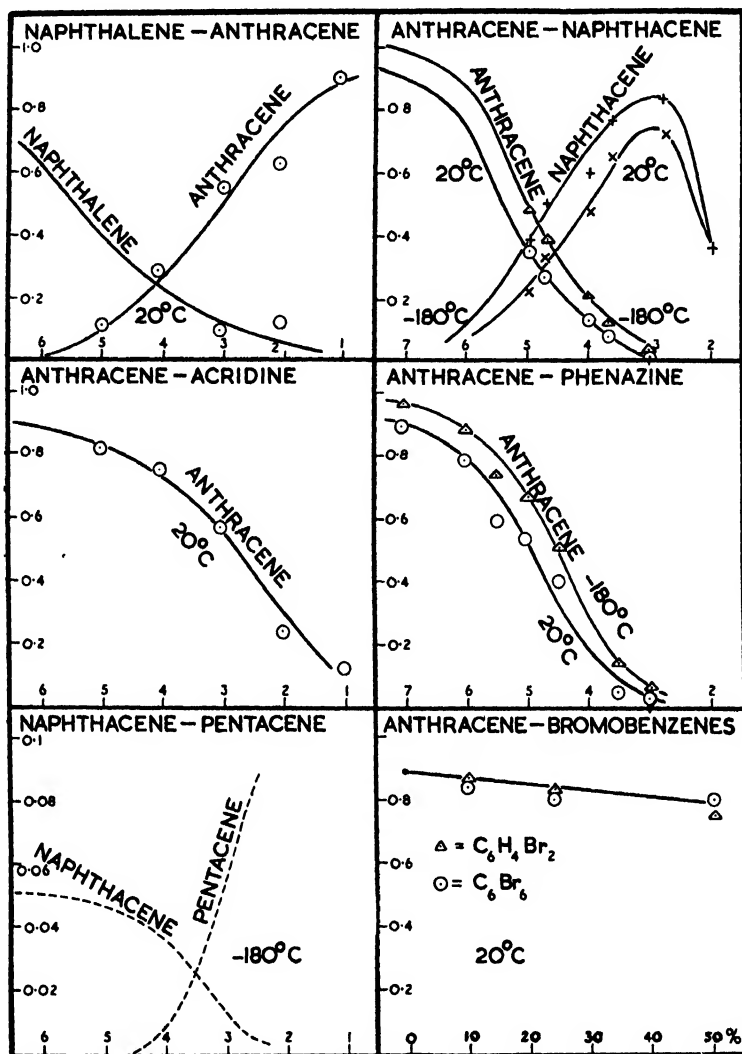
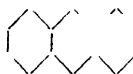


Figure 1. Abscissae: concentration of minor constituent expressed logarithmically (for anthracene-bromobenzene, expressed as a percentage). Ordinates: fluorescence efficiencies.



with anthracene



Exciting light:

2900–3200 Å., filtered by solutions of nickel, cobalt, and copper sulphates.

Absorption: naphthalene 2500–3200 Å.,  $\log \epsilon = 3.5$  at 3000.

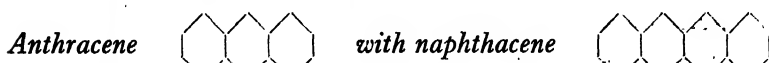
anthracene 3200–4100 Å.,  $\log \epsilon = 2.4$  at 3000, and 3.5 at 3650.

Fluorescence: naphthalene 3130–3720 Å., estimated by amount of fluorescence cut off by an Ilford 805 filter.

anthracene 4020–5020 Å., estimated from total fluorescence less that removed by an Ilford 805 filter.

Crystalline naphthalene has an efficiency of about 0.7 at ordinary temperature, but in the anthracene solid solutions the anthracene fluorescence rises to an

efficiency of 0.9, equal to that of pure anthracene, at a concentration of 10%. At  $-180^{\circ}\text{C}$ . the efficiencies are 0.95 and 1.0 respectively;  $k_2=0.3$ ,  $k_3=5 \times 10^4$  at  $20^{\circ}\text{C}$ .,  $k_2=0.05$ ,  $k_3=1.3 \times 10^4$  at  $-180^{\circ}\text{C}$ . The other constants are zero.

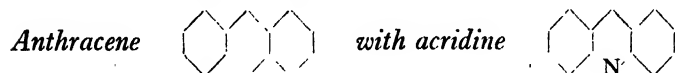


Exciting light: 3650 Å., filtered by Chance's glass OX 1.

Absorption: anthracene 3200–4100 Å.,  $\log \epsilon = 3.5$  at 3650.  
naphthacene 3600–5000 Å.,  $\log \epsilon = 2.4$  at 3650, and 4.0 at 4900.

Fluorescence: anthracene 4020–5020 Å., estimated through Ilford filter 601.  
naphthacene 4900–5750 Å., estimated through Ilford filter 404.

The falling off of the naphthacene fluorescence at concentrations above about 0.1% is attributed to self-quenching effects. The limit of anthracene–naphthacene solid solution formation is unknown, but appears to be much greater than 0.1%, so that it cannot be ascribed to the separation of a different solid phase.  $k_2=0.1$ ,  $k_3=2 \times 10^5$ ,  $k_6=2.5 \times 10^2$  at  $20^{\circ}\text{C}$ .,  $k_2=0$ ,  $k_3=6 \times 10^4$ ,  $k_6=10^2$  at  $-180^{\circ}\text{C}$ .; the other constants are zero.

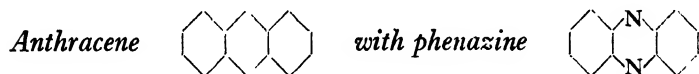


Exciting light: 3650 Å.

Absorption: anthracene 3200–4100 Å.,  $\log \epsilon = 3.5$  at 3650.  
acridine 3000–4300 Å.,  $\log \epsilon = 3.6$  at 3650.

Fluorescence: anthracene 4020–5020 Å.; acridine feeble.

Since the solid solutions containing acridine show practically only anthracene fluorescence the acridine traps and quenches the exciton.  $k_2=0.1$ ,  $k_7=5 \times 10^2$  at  $20^{\circ}\text{C}$ .; the other constants are zero.



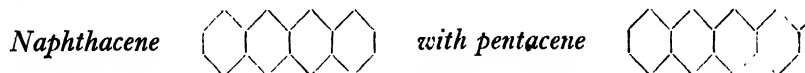
Exciting light: 3650 Å.

Absorption: anthracene 3200–4100 Å.,  $\log \epsilon = 3.5$  at 3650.  
phenazine 3100–5000 Å.,  $\log \epsilon = 4.0$  at 3650.

Fluorescence: anthracene 4020–5020 Å.; phenazine none.

As acridine, phenazine acts as an exciton quencher.  $k_2=0.1$ ,  $k_7=7 \times 10^4$  at  $20^{\circ}\text{C}$ .,  $k_2=0$ ,  $k_7=3 \times 10^4$  at  $-180^{\circ}\text{C}$ .; the other constants are zero.

The naphthalene–quinolene system is closely similar to this one except that its bands lie at shorter wavelengths.



Exciting light: 4358 Å., filtered by solutions of cuprammonium sulphate and sodium nitrite.

Absorption: naphthacene 3600–5100 Å.,  $\log \epsilon = 3.5$  at 4358.  
pentacene 4300–6100 Å.,  $\log \epsilon = 2.6$  at 4358 and 4.3 at 6000.

Fluorescence: naphthacene 5000–5900 Å.; pentacene beyond 6000.

Owing to the feeble fluorescence of this system observations could be made only at liquid air temperatures, and even here it was possible only to make rough visual estimations. The absolute values of the fluorescence efficiencies given are very rough approximations:  $k_2=2 \times 10^2$ ,  $k_3=10^6$ ,  $k_5=3 \times 10^2$  approx. at  $-180^{\circ}\text{C}$ .



*Anthracene with p-dibromobenzene and hexabromobenzene.*

Exciting light 3650 Å.

Though it forms solid solutions with anthracene up to 30% concentration, p-dibromobenzene exerts little quenching effect. Hexabromobenzene behaves similarly. These substances have absorption bands at shorter wavelengths than 3650 Å. and appear unable to act as exciton traps, though they act as quenchers for anthracene fluorescence in liquid solutions (Bowen and Norton 1939). In the latter state van der Waals associations of anthracene molecules with bromo-compounds appear to be responsible for the quenching (Bowen, Barnes and Holliday 1947).

In addition to the above systems the three-component system anthracene with small quantities of both naphthacene and phenazine was examined. The phenazine diminishes the observed fluorescence coming from both the anthracene and the naphthacene. The two-component system constants given above were found to reproduce the fluorescences observed through Ilford filters 601 and 404 (blue anthracene and green naphthacene emissions) within the limits of error. The agreement between observed and calculated results in all the above instances is only approximate, due to the inevitable inaccuracies of fluorescence measurements from crystals. Large errors occur through variations of light diffusion losses in different preparations. The solid solutions also are far from uniform in composition. When a solid solution of naphthacene in anthracene is prepared, for example, either by fusion or by crystallization from a solvent, the first crystals deposited have a higher naphthacene concentration than the liquid, and as deposition proceeds a series of solid solutions of different compositions are formed successively. The only way out of this difficulty would be to prepare specimens by crystallizing a small fraction only from a liquid and to find its composition by subsequent analysis. This would require large quantities of highly purified materials which were beyond our resources.

## § 3. DISCUSSION

A quantity of great interest in relation to these systems is the "life" of an exciton process. The mean lives of anthracene fluorescence in the solid and dissolved states are not accurately known. Wood (1921) found a value of about  $10^{-5}$  sec. for crystalline anthracene, but recent unpublished work indicates that it is really very much smaller. The average life for dissolved anthracene, estimated by the polarization method in glycerol, appears to be  $10^{-7}$  sec., but this is probably too long because the "micro" viscosity of the solvent may be less than the ordinary viscosity. The absorption band areas  $\int \epsilon d\omega$  (Lewis and Kasha 1945) give about  $10^{-8}$  sec. for both solid and liquid anthracene, assuming the accuracy of the curves of Kortum and Finckh (1942). The exciton movement in the crystal does not seem to cause any great lengthening of the period between absorption and radiation. The question then arises, what terminates the resonance transfer process in the absence of any added trapping agent? There are two possibilities: radiation may occur from molecules which are "displaced" in the crystal, or at the surfaces of "mosaic structure", or the removal of excess vibrational energy from the excited molecule may stop transfer. Figure 2 shows potential energy curves for a diatomic molecule.

Absorption is represented by the vertical line BK and fluorescence by GM. The time for passage from K to G is about  $10^{-12}$  sec. It might be assumed that exciton transfer continues while the energy available is represented by point K,

but that when a molecule falls to G it has insufficient energy for an energy exchange chain.

A further matter of interest is the alternative of radiation or quenching in these crystals. Quenching is undoubtedly favoured by polarizability effects (Bowen 1947). The series of solids anthracene, naphthacene and pentacene have fluorescent efficiencies at 20° C. of about 0.9, 0.002, and 0 respectively, probably due to increasing polarizability of the molecules. When embedded in an anthracene crystal naphthacene and pentacene molecules fluoresce with much higher efficiencies. If two polarizable molecules approach closely, their potential-energy curves (see Figure 2) become shifted and less well defined, especially in the region

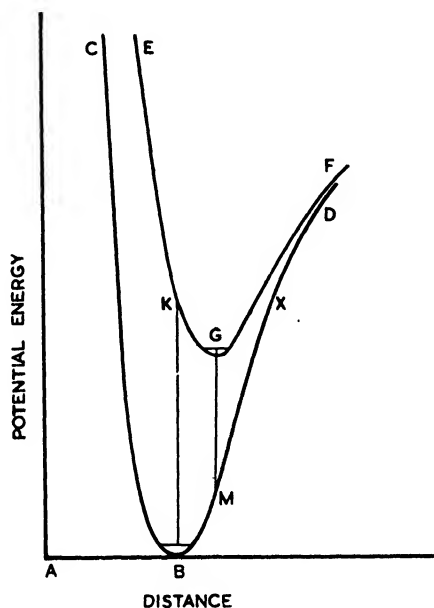


Figure 2.

marked X. Radiationless transition to the ground state is then possible, the excitation energy passing into vibrational energies of the two molecules. Resonance transfer of energy, however, occurs at larger distances, where polarizability has less effect, but where there is sufficient electronic interaction present. Both processes may be visualized as initiated by the transfer of an electron from an unexcited molecule to the vacated orbital of an excited one with transfer of the excited electron in the reverse direction. If the transfers are simultaneous the process gives rise to the exciton, but any check between them may lead to quenching. How these two effects depend on the relative orientations of molecules to each other with ensuing directional effects in the crystal is a matter about which we know little at present.

#### REFERENCES

- BOWEN, E. J., 1945, *J. Chem. Phys.*, **13**, 306; *Quart. Rev. Chem. Soc.*, 1947, **1**, 1.  
 BOWEN, E. J., BARNES, A. W., and HOLLIDAY, P., 1947, *Trans. Faraday Soc.*, **43**, 27.  
 BOWEN, E. J., and MIKIEWICZ, E., 1947, *Nature, Lond.*, **159**, 706.  
 BOWEN, E. J., and NORTON, A., 1939, *Trans. Faraday Soc.*, **35**, 44.  
 KORTUM, G., and FINCKH, B., 1942, *Z. phys. Chem.*, B **52**, 263.  
 LEWIS, G. N., and KASHA, M., 1945, *J. Amer. Chem. Soc.*, **67**, 994.  
 ROBERTSON, J., 1932, *Proc. Roy. Soc. A*, **40**, 79.  
 WOOD, R. W., 1921, *Proc. Roy. Soc. A*, **99**, 362.

## Further Experiments with an Adjustable Geiger-Müller Counter

BY A. G. FENTON AND E. W. FULLER

Physics Department, University of Birmingham

*Communicated by M. L. Oliphant ; MS. received 24th June 1948*

**ABSTRACT.** An adjustable Geiger-Müller counter and special electronic circuits have been used to study the effect of several counter variables on the occurrence of multiple pulses. The results show that the plateau characteristics combine the effects of an increase in efficiency and an increase in the probability of a multiple pulse as the operating potential is raised. It was found that the probability of occurrence of multiple pulses does not depend simply upon the charge per pulse, but that it depends also upon the anode diameter and the total pressure of the filling.

Curves have been drawn showing the charge per pulse as a function of the operating potential. A change of slope occurs in these curves when the charge per pulse is approximately equal to the charge on the active portion of the anode.

The counter was used as an ionization chamber at operating potentials below the Geiger region. It was found that as the potential is raised above the threshold of the proportional region the ionization current varies with potential as  $\log I \propto V$  while at higher potentials the relation is adequately expressed by  $\log \log I \propto V$ . Near the Geiger region a sharp break occurs in the log log curve, which is taken to indicate that the discharge begins to spread at this stage.

### § 1. INTRODUCTION

IN a previous paper (Chaudhri and Fenton 1948, subsequently referred to as I) it was shown that with a given cathode and filling the length and slope of the plateau depend strongly on the anode diameter. The present paper is a report of work primarily intended to extend the investigations to include the effect of pressure on the plateau characteristics.

Previous workers (see for example Korff and Present 1944, Curran and Rae 1947) have attributed the slope of the plateau to spurious pulses and to an increase in the effective anode length as the operating potential is raised. It is convenient to divide the spurious pulses into two classes : (a) those pulses which occur as a result of previous pulses and are separated from them by time intervals of the order of several hundred microseconds; (b) pulses which are not the result of the entry of any ionizing particle into the effective volume of the counter.

Pulses of type (a) may be distinguished by their non random distribution while pulses of type (b) can be distinguished if the rate at which they occur depends on the counter variables. In particular, to affect the plateau slope the rate must vary with operating potential. In view of the observation that the plateaux corrected for spurious pulses of type (a) are the same within experimental fluctuations over the range of pressures and anodes used, we believe that very few pulses of type (b) occur in our counter.

To study the contribution of spurious pulses of type (a) to the plateau characteristics an interval discriminator circuit was used during the measurements. During the course of the work the charge per pulse was measured over the range of operating potentials for each anode and pressure. The counter was also used as an ionization chamber and the results provide interesting information about the threshold of the Geiger region.

For convenience we give below a list of the symbols and definitions used in the report.

- $V_s$  threshold of the Geiger region.
- $M$  number of square waves per second produced by the multivibrator.
- $C$  number of coincidences per second.
- $R$  counting rate in counts/second excluding spurious pulses of type (a).
- $S$  number of spurious pulses of type (a) per second.
- $G$  total counting rate in counts per second.
- $P$  measured probability that any pulse will produce a spurious pulse of type (a).  
 $P = S/G$ .
- $t_d$  dead time, i.e. the time which elapses after the occurrence of a pulse before another Geiger discharge can occur.
- $q$  charge per pulse.

## § 2. APPARATUS AND EXPERIMENTAL METHODS

The adjustable counter described previously (I) was used during the present observations. The counter was set so that the central 5 cm. length of the anode was used, and the filling was 90% of spectroscopically pure argon plus 10% of alcohol. The tungsten anodes used were of 0.05, 0.07, 0.1, 0.15, and 0.20 mm. diameter. The gas pressure could be changed without pumping and refilling (a process which has proved to be not reproducible with our set-up) by adjusting the level of mercury in a 1-litre flask attached to the system. In view of the experiments reported by Korff (1944) no trouble was to be expected due to the small amounts of mercury vapour thus introduced into the counter. Throughout the work to be described the pressure could be set at any value from 7.5 to 19 cm. of mercury, the pressure being read from a U-tube manometer. Relatively low counting rates (of the order of 1,000 per minute) were used because earlier results had shown that high counting rates alter the background (I).

To find the contribution of spurious counts to the plateau characteristics the circuits shown in Figure 1 were used with the triggered multivibrator set to give waves of 1,000  $\mu$ sec. duration, thus dividing the Geiger counts into two groups: group 1, recorded by scaler 1, counts occurring at any time greater than 1,000  $\mu$ sec. after the previous count, group 2 (scaler 2), those occurring less than 1,000  $\mu$ sec. after the previous count.

A small correction was made for the number of random counts in group 2. Because of the dead time of the counter during which no pulses, random or otherwise, can occur, the effective time interval used for the calculation of the number of random pulses likely to occur is 1,000  $\mu$ sec. minus the dead time. The dead times were therefore measured, for each operating potential during the plateau measurements, by decreasing the length of the square wave until no coincidences occurred.

It was shown that all spurious counts occur within 1,000  $\mu$ sec. of the previous pulse by measuring the rate at which spurious counts occurred for a series of values of the multivibrator interval at constant operating voltage. The spurious rate increased rapidly with multivibrator interval at first but ultimately became more constant. This measurement was made at points near the beginning, the middle, and the end of the plateaux for each anode using a pressure of 12 cm. Hg. The time value at which the rate ceases to increase with interval was always found to be less than 1,000  $\mu$ sec. A check was made at other pressures by increasing the interval from 1,000 to 1,360  $\mu$ sec. and as this gave no increase in  $S$  it was concluded that all the spurious counts occur within the 1,000  $\mu$ sec. interval.

For the charge measurements a type 954 acorn valve was used in an electrometer circuit attached to the anode of the counter as shown in Figure 1. In practice the opening of the key K was synchronized with the closing of the scaler counting switch, and the number of counts necessary to alter the potential of the grid of the electrometer valve by 0.5 volts was registered. Hence the average charge per pulse can be calculated, using the measured capacity of the system.

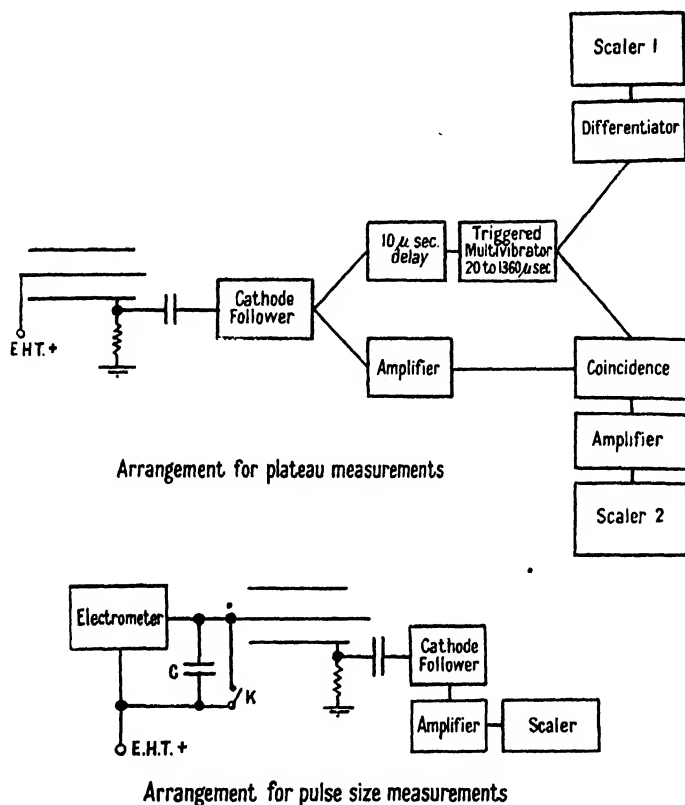


Figure 1.

When the counter was used as an ionization chamber the electrometer was employed to indicate the collection of a predetermined charge in a measured time. By altering the capacity  $C$  it was possible to measure over a large range of ionization currents without having to measure either very short or very long time intervals. The currents measured ranged from about  $2 \times 10^{-13}$  to  $10^{-8}$  amp. when the gamma-ray source was placed close to the counter. An additional factor of about 100 was obtained in two stages by moving the source away from the counter, so that in effect the measurements covered the current range from about  $2 \times 10^{-13}$  to  $10^{-6}$  amp.

### § 3. RESULTS

#### 3.1. Plateau Characteristics

The curves obtained have the general form shown in Figure 2. The corrected plateaux corresponding to the various pressures and anode diameters give the shape of the plateaux that would be obtained if there were no multiple pulses. Graphs of these lie close together when plotted with the same counting rate and

overvoltage coordinates. As there are no observable trends of variation with pressure or anode diameter it appears that the shape of the corrected plateau is, from the practical viewpoint, independent of these variables over the range covered by the present experiments. Eventually, as the potential is raised, the corrected plateau breaks off due to sprays of multiple pulses lasting more than  $1,000 \mu\text{sec}$ .

The curves of  $P$  plotted against operating potential vary considerably with

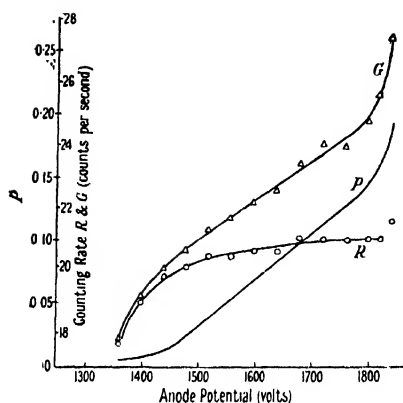


Figure 2. Typical plateau analysis.

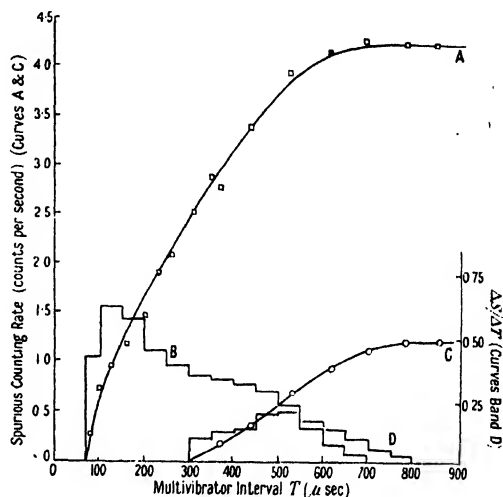


Figure 4.

Counter data: Anode diameter 0.07 mm.

Total pressure 12 cm.

Operating Potential: A and B 1,440 v.

C and D 1,240 v.

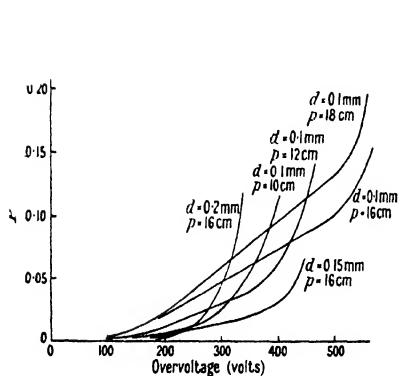


Figure 3. Variation of  $P$  with overvoltage for various anode diameters ( $d$ ) and total pressures ( $p$ ).

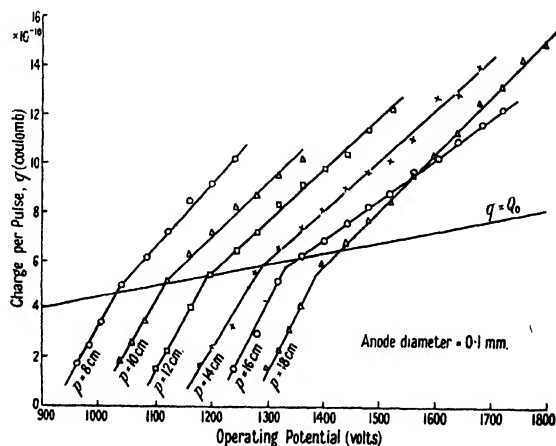


Figure 5.

pressure and with anode diameter (Figure 3). For purposes of comparison it is convenient to plot, as a function of the potential, the probability that a multiple count occurs, instead of the spurious counting rate. The results show that  $P$  increases rapidly at overvoltages corresponding to the upper ends of the Geiger plateaux; the overvoltage at which this rapid increase begins increases as the

anode diameter is reduced from 0.2 mm., passes through a maximum at an anode diameter of about 0.1 mm. and then decreases. The slope of the straight portion of  $P$  curves increases the anode diameter is reduced.

### 3.2. Spurious Count Distribution

The curves obtained by plotting the spurious counting rate against multivibrator interval show that the spurious counts begin to occur immediately after the dead time (Figure 4, curves A and C). As measured above,  $t_d$  is the time after a pulse during which the counter is unable to give a pulse as great as the minimum detectable size. By observing the pulses on a triggered cathode-ray oscillograph it was shown that this minimum size is reached after about 1.1 of the true dead time and that pulses smaller than this minimum detectable size also occur more frequently than the random rate.

The distribution in time of the spurious counts was obtained by taking a histogram of the curves of  $S$  plotted against multivibrator interval. Except at high overvoltages the maxima of these histograms occur at a time approximately equal to that required for the space charge to cross the counter, assuming an ionic mobility intermediate between those given in the International Critical Tables for argon ( $k = 1.66$  cm/sec. per v/cm.) and alcohol ( $k = 0.48$  cm/sec. per v/cm.). Figure 4, curve B, is for a high overvoltage. At overvoltages near the middle of the plateau and below the histograms are nearly symmetrical (Figure 4, curve D).

### 3.3. Pulse Size Measurements

Figure 5 shows the average charge per pulse  $q$  plotted against the operating voltage for a series of pressures using the 0.1-mm. diameter anode. The line  $q = Q_0$  gives the charge on the active length (5 cm.) of the counter wire. With anodes of diameter 0.05, 0.07 and 0.1 mm. and at pressures ranging from 8 cm. to 18 cm. Hg a sharp break occurs in the curves at about  $q = Q_0$  while the ratio of the slopes of the lines on either side of the break ranges from 0.4 to 0.67. For larger anodes (0.15 and 0.2 mm. diameter) and at the higher pressures the break occurs for  $q < Q_0$  and the slope ratio increases.

In Figure 6 the charge obtained at a total pressure of 10 cm. Hg is plotted against overvoltage for four different anode wires. The curves show that the charge at a given overvoltage increases slowly with increasing anode diameter.

The break voltage also increases with increasing wire diameter. The starting voltage, from which these overvoltages are obtained, is defined as the voltage at which the extrapolated  $q \sim V$  curve shows  $q = 0$ . Figure 7 shows that the break voltage increases linearly with pressure for all anodes where the break is clearly defined.

### 3.4. Measurement of Ionization Current

The counter was used as an ionization chamber, connected as shown in Figure 1. As the potential is raised above the proportional starting voltage  $V_p$  the logarithm of the ionization current  $I$  is proportional to the potential at first; then at higher potentials  $\log \log I$  becomes proportional to potential as shown in Figure 8, curves A and B. Sharp breaks occur in the  $\log \log$  curves and when these are matched, as shown in the figure, the curves for different gas pressures converge as the potential is raised. Figure 8, curve C shows  $I$  plotted against potential for the region above the break for 16 cm. pressure. This curve may be

compared with the charge per pulse curves of Figure 5. Figure 8, curve C shows that the value of  $V_s$  as defined in § 3.3 is about 50 v. above the potential given by the break in the log log curve. Figure 9 shows that the value of  $\log \log I$  at the break in the log log curves depends linearly on the pressure.

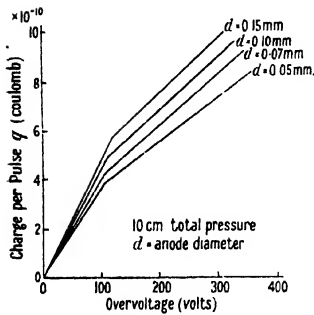


Figure 6.

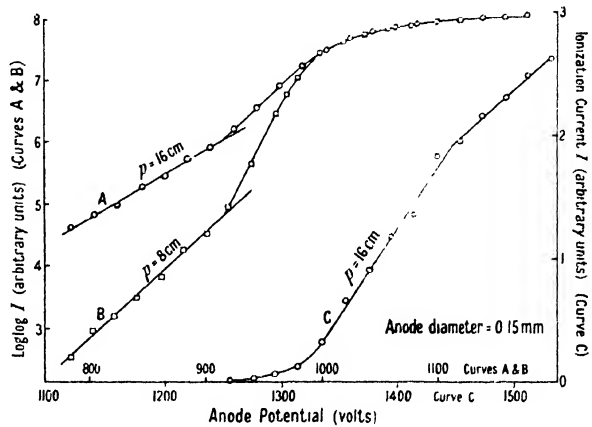


Figure 8.

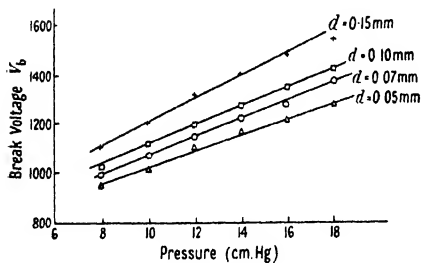


Figure 7.

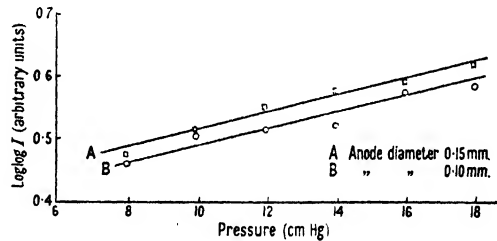


Figure 9.

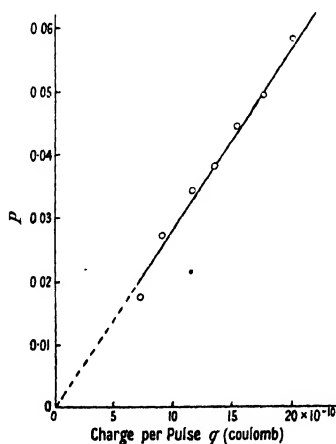


Figure 10.  
Counter data : Total pressure 12 cm.  
Anode diameter 0.1 mm.  
Operating potential 1,400 v.

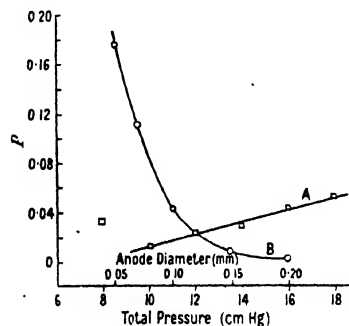


Figure 11. Variation of  $P$  with pressure (A) and with anode diameter (B) when  $q = 8 \times 10^{-10}$  coulombs.



### 3.5. The Dependence of $P$ on $q$

The probability  $P$  of the occurrence of spurious pulses and the charge per pulse  $q$  were obtained as functions of the anode length, and from the resulting straight line relationships the relation between  $P$  and  $q$  was obtained. Figure 10 shows the linear dependence of  $P$  on  $q$  for a 0.1 mm. anode, 10% alcohol, and 12 cm. Hg total pressure, at a fixed operating potential of 1,400 v. This method of varying  $q$  has the advantage that as the operating potential is held constant the discharge mechanism does not alter, the charge increasing with anode length simply because the discharge has further to spread. The possibility that the variation of counting rate with anode length may have some effect on the value of  $P$  was removed by using a fixed anode length and altering the position of the gamma-ray source to cover the range of counting rates obtained during the experiment in which the anode length was varied.  $P$  was found to be independent of  $R$  over this range.

In order to find the dependence of  $P$  on the anode diameter and the pressure of the filling a fixed value of  $q$  was chosen and the corresponding values of  $P$  were taken from the  $P$  vs  $(V - V_s)$  curves, examples of which are shown in Figure 3. The results are shown in Figure 11 where the values of  $P$  corresponding to  $q = 8 \times 10^{-10}$  coulombs are plotted against pressure (curve A) and anode diameter (curve B). This value of  $q$  was chosen because, with the exception of the value at 8 cm. total pressure the corresponding values of  $P$  lie on the early portions of the  $P$  vs  $(V - V_s)$  curves, in the region where the majority of the multiple pulses contain only two individual pulses. The rapid increase of  $P$  corresponding to the upper limit of the plateau is associated with multiple pulses of multiplicity greater than two.

## § 4. DISCUSSION

The corrected plateaux of which an example is given in Figure 2 do not flatten to any extent until the operating potential is appreciably above the threshold. Further, as can be seen with a cathode-ray oscillograph, the pulses are of approximately equal size before the apparatus begins to register counts (minimum detectable pulse size = 1.2 v.). It has also been shown by varying the amplifier gain that the increase in the corrected counting rate with operating potential is not due to small pulses being brought within range of the apparatus. Part of the increase may be due to an increase in the effective length as mentioned in § 1, but because of the method of shielding the anode used in our counter we do not think that end effects can account entirely for the observed increase. On the other hand, plateaux of this form are predicted by Narwijn (1943) and Wilkinson\* who obtain the probability that the discharge begins to spread as a function of overvoltage.

For one electron set free in the counter by the ionizing agency this probability is rather low (0.6) at an overvoltage of about 50 v. (i.e. when counts are first registered) and increases with overvoltage to about unity at 200 v. above the threshold, corresponding to a fairly large slope in the corrected plateau. At a fixed overvoltage the probability of spreading increases as the specific ionization increases, and at 50 v. overvoltage is practically unity when the number of electrons set free by the ionizing particle exceeds five. A gamma-ray photon can only be detected if it releases an electron which then enters the effective volume of the counter. In our case the gamma rays from radium are filtered by 3 cm. of lead so that most of the primary electrons will have energies of 1 mev. or over. Depending

\* We are indebted to Dr. D. H. Wilkinson, Cavendish Laboratory, Cambridge, for this information prior to its publication.

on its path through the counter, from one to about eight secondaries will be produced by an electron of this energy, so that we should not expect the plateau to flatten until appreciable overvoltages are used. From the practical standpoint the corrected plateau curves show that in a counter such as ours the overvoltage used should be of the order of 200 v. This would apply also when the cathode is treated to reduce spurious pulses to a minimum, or when a paralysis circuit is used to prevent their being counted.

It was reported earlier (I) that there is an optimum anode diameter corresponding to a given filling and cathode for which the best Geiger plateau is obtained. This observation is explained in terms of the way in which the spurious counting rate curves vary with anode diameter and the way in which they combine with the corrected plateaux to give the Geiger plateaux. It should also be pointed out that the sum of the corrected plateau and the spurious counting rate curve does not always yield a curve with a really straight portion. This explains the deviation of points sometimes observed from the straight lines usually drawn for the Geiger plateaux, even when a large number of counts are taken in order to reduce the standard deviation.

The sharp breaks in curves A and B of Figure 8 are interpreted as marking the stage at which the discharge begins to spread along the anode. This view is supported by observations with a cathode-ray oscillograph in the neighbourhood of the break. A few volts above the potential corresponding to the break there is a distribution of pulse sizes. The maximum pulse size observed at a given operating potential is halved by halving the effective length of the counter, showing that at quite low overvoltages the discharge can spread to the full length (10 cm.). As the potential is raised the number of pulses reaching the corresponding maximum size increases until at about 20 volts overvoltage all the pulses appear to be of the same size. The starting potential for the Geiger region is generally defined (Korff 1944) as the potential at which all the pulses are of equal size. While this definition is usually adequate for the practical use of counters it simply indicates the potential at which the discharge spreads to the full length of the counter, and because of the statistical nature of the spreading mechanism (Alder *et al.* 1947, Wilkinson, unpublished) its value depends on the counter length. However, when the discharge mechanism is being investigated the potential at which spreading begins is often of importance and this may be determined quite simply by the method described in this paper.

The observed dependence of the probability of occurrence of spurious counts on the charge per pulse is consistent with the view expressed by Korff (1944) that multiple pulses are due to statistical breakdown in the quenching mechanism which occurs when the positive ions reach the cathode. However,  $P$  does not depend only on the number of ions reaching the cathode but, as shown in Figure 11, depends also on the anode diameter and the pressure. These results suggest that the ions which arrive at the cathode are not all of the same type, and that the production of the ions which are more likely to produce spurious pulses is favoured by the use of high pressures and small anode wires. The effect may be due to the increase in the field near the anode when smaller anodes or higher pressures are used. Calculation of the fields at the anode surfaces using the operating potentials corresponding to the points given in Figure 11 yields values of the field strength ranging from 37,000 v/cm. for the 0.2 mm. anode to 110,000 v/cm. for the 0.05 mm. anode. For the 0.1 mm. anode it ranges from 49,000 v/cm. at 8 cm. pressure to 64,000 v/cm. at 18 cm. pressure.

The spurious count distribution curves (e.g. Figure 4) together with the observations with a triggered cathode-ray oscillograph show that some spurious pulses occur as soon as the end of the dead time is reached and that the pulses are distributed over a fairly wide range of times. These curves also provide evidence that the ions formed in the discharge are not all of the same type. The distributions obtained at low voltages are symmetrical, as would be expected if the space charge is regarded as a group of ions moving with a Maxwellian velocity distribution upon which one drift velocity (due to the electric field) is imposed. This applies in the outer part of the counter where the field varies slowly so that focusing is negligible and ions of the one type have approximately constant drift velocity. At high voltages the distribution curves are characterized by a sharp rise to the maximum followed by a very gradual fall. Such a distribution would be given if the space charge contained multiply, as well as singly ionized atoms; the higher drift velocity imposed on the multiply ionized group would give the early maximum and the subsequent arrival of the singly ionized group would explain the very gradual fall. This view is supported by the fact that the asymmetry sets in at points lower on the plateau for the smaller anodes, as here the field strength at the wire is greater. The continuous electron transfer between singly ionized argon atoms and alcohol molecules which, according to Korff (1944), explains the quenching action, does not affect the argument. Such a transfer affects the position of the maximum because of the difference in the mobilities of the ions, but it could not produce the observed asymmetry as the exchange is complete before the ion sheath reaches the cathode.

#### ACKNOWLEDGMENTS

It is with great pleasure that we record our sincere thanks to Professors M. L. Oliphant, F.R.S., and P. B. Moon, F.R.S., for their continued interest and guidance during this work. One of us (A.G.F.) wishes to thank both Messrs. Cadbury-Fry-Pascall Ltd., Claremont, Tasmania, for an Overseas Fellowship, and the University of Tasmania for granting leave of absence. The other (E.W.F.) is grateful to the University of Birmingham for a Research Scholarship which enabled him to take part in this research.

#### REFERENCES

- ALDER, F., BALDINGER, E., HUBER, P., and METZER, F., 1947, *Helv. phys. Acta*, **20**, 73.  
CHAUDHRI, R. M., and FENTON, A. G., 1948, *Proc. Phys. Soc.*, **60**, 183.  
CURRAN, S. C., and RAE, E. R., 1947, *Rev. Sci. Instrum.*, **18**, 871.  
KORFF, S. A., and PRESENT, R. D., 1944, *Phys. Rev.*, **65**, 274.  
NARWIJN, A., 1943, *Het Gasontladings Mechanisme van den Geiger-Müller Teller* (Delft. Drukkerij Hoogland).

## The Steady Non-Uniform State for a Liquid

By R. EISENSCHITZ

University College London

*MS. received 12th August 1948*

**ABSTRACT.** The Smoluchowski equation for the distribution of the relative coordinates of a representative pair of molecules in a liquid is formulated in such a way that the effect of non-uniform velocity or temperature is taken into account. The equation is reduced to an ordinary linear differential equation of the second order. One of the two constants of integration is readily determined whereas the determination of the other constant may lead to inconsistencies. The molecules are assumed to interact with the average potential that is appropriate to thermal equilibrium. If it is assumed that this potential becomes infinite of the first order at distance zero then the problem of viscous flow and the problem of thermal conduction are uniquely soluble. Approximate evaluation of the transport coefficients shows the right kind of temperature effect. The result is in accordance with the previous treatment by means of the cell model.

### § 1. INTRODUCTION

IN a previous paper (1947) referred to as I the author analysed the transport phenomena in liquids by means of extremely simplified assumptions on the liquid state. The "cell model" was employed and the Smoluchowski equation was used for determining the distribution in coordinates of one representative molecule. The influence of the rate of shear or gradient of temperature on the distribution was taken into account only on the surface but not in the interior of the cell. The calculated distribution functions were infinite at the centre of the cell but yielded finite values for the flow of momentum or energy. The marked difference of the temperature effect on viscosity and thermal conductivity was obtained without any additional assumption and in spite of the complete similarity of mathematical operations which lead to the one and to the other transport coefficient.

The author was unaware of a paper by Auluck and Kothari (1944) in which formulae similar to the author's are derived from the well-known "hole" model as given by Fürth (1941); in addition, numerical values of the right order of magnitude are obtained. In their paper the mechanism and the rate of transfer is explicitly assumed to be markedly different for momentum and energy. The author's result shows at least that assumptions of this kind are unnecessary.

In the meantime Born and Green (1947) published the extension of their general kinetic theory of liquids to transport phenomena and made a preliminary calculation of the viscosity; in their result various approximations are involved and the equilibrium distribution of a pair of molecules in a liquid is replaced by the distribution of a pair of isolated molecules. Since thermal conductivity still awaits detailed treatment, and the introduction of the liquid state distribution may affect the result appreciably, it cannot yet be seen to which conclusions the rigorous theory, as developed by these authors, will lead.

The method as employed in paper I is too crude for the actual calculation of the transport coefficients. In addition, its foundations, that is, the cell model and the application of the Smoluchowski equation, are open to criticism.

The cell model is hardly suitable for a quantitative theory since it is impossible to divide the liquid into cells of fixed size and shape without introducing arbitrary and sometimes inconsistent assumptions. The partial success of this model is due to the fact that fundamentally it is an approach to the specification of the liquid state in terms of the distribution of relative coordinates of two representative molecules.

The Smoluchowski equation is at first sight a legitimate approximation to the equation which has been shown by Kirkwood (1946) to be adequate and it is preferable from the point of view of mathematical simplicity. Its application in paper I resulted, however, in distributions which are infinite at one point.

In the present paper an attempt is made to clear the ground for the calculation of transport coefficients by employing the pair distribution instead of the cell model and by admitting only solutions of the Smoluchowski equation which, when interpreted as probability distributions, are in agreement with the physical conditions.

## § 2. THE MODEL OF THE LIQUID STATE

In this paper the liquid state is described in terms of the relative coordinates of two representative molecules. The probability distribution of the relative coordinates of the two molecules is, in the case of monatomic liquids, a probability distribution of the distance  $r$ . The assumption is made that the two molecules interact with a force equal to the negative gradient of an average potential  $\Phi(r)$  which itself is derived from the equilibrium distribution.

The probability density in equilibrium is zero at small distances, has one strong and possibly several weak maxima and tends to a constant value at large distance. It can be derived from experimental x-ray interference patterns or calculated from the intermolecular forces according to the theory of Kirkwood (1935) or Green (1947).

The average potential  $\Phi$  which is essential for the model under consideration is defined by writing the equilibrium distribution  $g_0(r)$  as

$$g_0(r) = (1/V) \exp(-\Phi/kT). \quad \dots\dots (1)$$

$\Phi$  depends according to this definition explicitly on the temperature, but little is known of the amount of this dependence. In equilibrium only the minima of potential are densely occupied; in non-equilibrium distributions all ranges of the potential curve may be of importance. For large distances  $\Phi$  is zero. Where the potential is markedly positive it is not likely to depend very much on the temperature. Near the main minimum at about one molecular diameter distance, the potential varies with temperature so that the minimum becomes flatter when temperature decreases; this variation is an expression of the fact that the molecules have not the tendency to crowd together at the distance of the minimum. At small distances the potential is likely to approach the repulsion potential of a pair of isolated molecules. If overlapping of the electronic clouds is almost complete—the corresponding small distances are practically never reached—the potential becomes infinite of the first order owing to the Coulomb repulsion of the nuclei.

For the model under consideration the Smoluchowski equation has to be modified in order to account for the non-uniform velocity or temperature independently of the boundary conditions.

### § 3. THE DIFFERENTIAL EQUATIONS

If temperature and velocity are uniform, the distribution,  $g$ , of relative coordinates is determined by the Smoluchowski equation

$$\partial g / \partial t = \text{div} [g \text{grad} (kTg / \beta m) + (g \text{grad} \Phi / \beta m)], \quad \dots\dots(2)$$

where  $\beta$  is the "friction constant" having the dimension  $\text{time}^{-1}$ ,  $-\text{grad} \Phi / \beta m$  is the mean displacement,  $kT / \beta m$  is the mean square displacement per time unit; the expression in the bracket is equal to the negative flow vector  $\mathbf{j}$ . In thermal equilibrium  $g = g_0$ ,  $\mathbf{j} = 0$ .

For a steady non-uniform state let  $g = g_0(1 + w)$ . For the specification of viscous flow let the velocity  $\mathbf{c}$  depend in an arbitrary way upon the coordinates subject to the condition  $\text{div} \mathbf{c} = 0$ ;  $\mathbf{c}$  is added to the mean displacement. Neglecting terms of the magnitude  $\mathbf{c} \cdot w$ , the flow is then given by

$$\mathbf{j} = g_0 [\mathbf{c} - (kT / \beta m) \text{grad} w] \quad \dots\dots(3a)$$

and  $w$  is determined by

$$\nabla^2 w - (\text{grad} \Psi, \text{grad} w) = -(\beta m / kT)(\mathbf{c}, \text{grad} \Psi), \quad \dots\dots(4a)$$

where  $\Psi = \Phi / kT$  subject to the boundary condition

$$\text{grad} w = 0 \quad (r = \infty) \quad \dots\dots(5a)$$

so that in infinity the flow is equal to  $g_0 \cdot \mathbf{c}$ .

For specifying thermal conduction let  $T$  be an arbitrary function of the coordinates subject to the condition  $\nabla^2 T = 0$ . Neglecting terms of the magnitude  $w \text{grad} T$ ,  $\text{grad}^2 T$  etc., the flow is given by

$$\mathbf{j} = -(k / \beta m) g_0 [T_0 \text{grad} w + (1 + \Psi) \text{grad} T], \quad \dots\dots(3b)$$

where  $T_0$  is the temperature at the origin and  $w$  is determined by

$$\nabla^2 w - (\text{grad} \Psi, \text{grad} w) = (\Psi / T_0)(\text{grad} \Psi, \text{grad} T), \quad \dots\dots(4b)$$

subject to the boundary condition

$$T_0 \text{grad} w + \text{grad} T = 0 \quad \dots\dots(5b)$$

so that the flow is zero at infinity.

For the purpose of calculating viscosity let the flow be laminar with a rate of shear equal to  $\frac{1}{2}a$  and the velocity be distributed according to  $c_x = c_z = 0$ ;  $c_y = ax$ . Then the right hand side of (4a) is  $-\alpha \Psi' r \sin^2 \theta \sin \phi \cos \phi$ ;  $\alpha = a\beta m / kT$ . Let  $w$  have the form  $w = u(r) \sin^2 \theta \sin \phi \cos \phi$ . The function  $w$  changes sign at  $\phi = 0, \pi/2, \pi, 3\pi/2$ . If one molecule is placed arbitrarily at the centre the probability that the other will be in one pair of quadrants, say 1 and 3, is greater than that it will be in the other quadrants 2 and 4. This means that in the flowing liquid the distribution of molecules is anisotropic. The function  $u$  is determined by

$$u'' + [(2/r) - \Psi']u' - (6u/r^2) = -\alpha \Psi' r, \quad \dots\dots(6a)$$

with the boundary condition

$$du/dr = 0; \quad u/r = 0 \quad (r = \infty). \quad \dots\dots(7a)$$

For the purpose of calculating thermal conductivity let the temperature be distributed according to  $T = T_0(1 + bx)$  so that the gradient is constant:  $\text{grad}_x T = \text{grad}_y T = 0$ ;  $\text{grad}_z T = bT_0$ . Then the right-hand side of (4b) is  $b\Psi\Psi' \cos \theta$ . Let  $w$  have the form  $w = v(r) \cos \theta$ , then  $v$  is determined by

$$v'' + [(2/r) - \Psi']v' - (2v/r^2) = b\Psi\Psi' \quad \dots\dots(6b)$$

with the boundary condition

$$dv/dr = -b; \quad v/r = -b \quad (r = \infty). \quad \dots\dots(7b)$$

The calculation of the transport coefficients is reduced to the integration of the radial differential equations (6 a), (6 b). Which solutions are admissible must be decided by considering how the probability for finding the relative coordinates in a finite volume deviates from the equilibrium distribution. This deviation of probability is proportional to

$$J_a = \int_0^r g_0 u r^2 dr \quad \text{and} \quad J_b = \int_0^r g_0 v r^2 dr$$

respectively. These integrals must be finite for every finite value of the upper limits.

It is known from experiments that laminar flow does not cause any appreciable anisotropy in liquids composed of simple molecules. The integral  $J_a$  to which the probability of preferential distribution in an odd quadrant is proportional, gives a measure of anisotropy, and it follows from what has been said that even if the upper limit becomes infinite the integral  $J_a$  must remain finite. No restriction of this kind is expected to hold for the integral  $J_b$ .

#### § 4. SOLUTIONS NEAR THE SINGULAR POINTS

Integration of equations (6 a), (6 b) near their singular points at the origin and at infinity provides the means for selecting solutions of physical significance.

$\Psi$  has a pole of the first order at the origin; it will alternatively also be assumed that  $\Psi(0)$  is finite.  $\Psi' = 0$  if  $r$  is sufficiently large.

The two arbitrary constants of integration are denoted by  $A_1, A_2$  and  $B_1, B_2$ . Other constants appearing in the solutions are denoted by  $F$  and  $H$  with suitable suffixes.

The homogeneous equation corresponding to (6 a) is

$$u'' + [(2/r) - \Psi']u' - (6u/r^2) = 0. \quad \dots\dots(8a)$$

If the term  $-\Psi'u'$  is omitted an equation results which has the solutions  $u = r^2$  and  $u = 1/r^3$ .

At large values of  $r$  equation (8 a) has accordingly two solutions, one being finite at the origin and of the form

$$u_1 = F_1 r^2 + F_2/r^3 + O(r^{-4}), \quad \dots\dots(9a)$$

the other vanishing at infinity and of the form

$$u_2 = 1/r^3 + O(r^{-4}). \quad \dots\dots(10a)$$

Assuming at first that  $\Psi(0)$  is finite, it is seen that at  $r=0$  the expansion of  $u_1$  commences with the second power of  $r$ ; it can be written as

$$u_1 = r^2 + \frac{1}{3}r^3\Psi'(0) + \dots \quad \dots\dots(11a)$$

The other solution has near the origin the form

$$u_2 = F_3/r^3 + \dots \quad \dots\dots(12a)$$

The general solution of equation (6 a) can be written as

$$u = A_1 u_1 + A_2 u_2 + u_3 \quad \dots\dots(13a)$$

where

$$u_3 = \frac{1}{2}\alpha r^2, \quad \dots\dots(14a)$$

is a particular solution.

If the potential has a pole at the origin so that for  $r < r_0$  it is equal to  $\Psi = C/r$ , this does not affect  $u_3$  and the expressions (9 a), (10 a). In the range  $0 \leq r \leq r_0$ , the appropriate expressions for  $u_1, u_2$  are found to be

$$\left. \begin{aligned} u_1 &= u_1^*; & u_1^* &= 1 + (6r/C) + (12r^2/C^2); \\ u_2 &= F_4 u_1^* + F_5 u_2^*; & u_2^* &= [1 - (6r/C) + (12r^2/C^2)] \exp(C/r) \end{aligned} \right\} \dots\dots (15 a)$$

Equation (6 b) is discussed in a similar way. The corresponding homogeneous equation

$$v'' + [(2r/v - \Psi')v' - (2v/r^2)] = 0 \quad \dots\dots (8 b)$$

has, for large values of  $r$ , solutions of the form

$$v_1 = H_1 r + H_2/r^2 + 0(r^{-3}), \quad \dots\dots (9 b)$$

$$v_2 = 1/r^2 + 0(r^{-3}). \quad \dots\dots (10 b)$$

If  $\Psi(0)$  is finite the expansion of  $v_1$  at  $r=0$  can be written

$$v_1 = r + \frac{1}{2} r^2 \Psi''(0) + \dots\dots (11 b)$$

The other solution has near the origin the form  $v_2 = H_3/r^2 + \dots\dots$

The general solution of (6 b) can be written as

$$v = B_1 v_1 + B_2 v_2 + v_3, \quad \dots\dots (13 b)$$

where the particular solution  $v_3$  is given by

$$v_3(r) = -b \int_0^r \Psi(\xi) \Psi''(\xi) \exp\{-\Psi(\xi)\} \xi^2 [v_2(r) v_1(\xi) - v_1(r) v_2(\xi)] d\xi, \quad \dots\dots (16)$$

and has at large values of  $r$  the form

$$v_3 = b H_6 r + b H_7/r^2 + 0(r^{-3}). \quad \dots\dots (14 b)$$

If the potential has a pole at the origin the appropriate expressions for  $v_1, v_2$  in the region  $0 < r \leq r_0$  are found to be

$$\left. \begin{aligned} v_1 &= v_1^*; & v_1^* &= 1 + (2r/C); \\ v_2 &= H_4 v_1^* + H_5 v_2^*; & v_2^* &= [1 - (2r/C)] \exp(C/r) \end{aligned} \right\} \dots\dots (15 b)$$

and  $v_3^* = b\{[1 + (2r/C)][2(r_0 - r) + C \ln(r/r_0)]$

$$+ [1 - (2r/C)][2r - C \exp(C/r)] \int_{C/r}^{\infty} \exp(-\xi) \xi^{-1} d\xi\}$$

is substituted for  $v_3$ . At the origin the function  $v_2^*$  and its derivative

$$dv_2^*/dr = -[(C/r^2) + (2/r) - (2/C)] \exp(C/r) \quad \dots\dots (17)$$

are exponentially infinite and  $v_3$  is infinite of the order  $\ln r$ .

## § 5. SELECTION OF SIGNIFICANT SOLUTIONS

In determining the constants of integration it is at first assumed that  $\Psi(0)$  is finite.

In the problem of viscous flow the first condition (7 a) is applied to (13 a); considering (9 a), (10 a), (14 a) an equation determining  $A_1$  is derived:

$$A_1 F_1 - \frac{1}{2} \alpha = 0. \quad \dots\dots (18 a)$$

The corresponding choice of  $A_1$  complies with the second condition (7 a). The constant  $A_2$  has to be chosen so that the probability  $J_a$  is finite for infinite  $r$ .



If  $A_2$  is assumed to vanish,  $J_a$  becomes infinite owing to the second term in (9 a). If  $A_2 \neq 0$ , the integral determining  $J_a$  is divergent. No solution of (6 a) is admissible.

In the problem of thermal conduction the first condition (7 b) is applied to (13 b); considering (9 b), (10 b), (14 b) an equation determining  $B_1$  is derived:

$$B_1 H_1 + b H_6 = -b. \quad \dots (18 b)$$

The corresponding choice of  $B_1$  complies with the second condition (7 b). The integral determining  $J_b$  converges independently of any choice of the constant  $B_2$  although the integrand is infinite at the origin if  $B_2 \neq 0$ . The assumption  $B_2 = 0$  is most plausible but not necessary; the distribution and consequently the thermal conductivity remain undetermined.

These difficulties are overcome by letting the potential have a pole at the origin. In the problem of viscous flow  $A_2$  is determined so that  $r^3 u$  vanishes at infinity:

$$A_1 F_2 + A_2 = 0. \quad \dots (19 a)$$

Whereas  $u$  is now exponentially infinite at the origin, the integrand of  $J_a$  is finite and the integral is finite for infinite distance. In the problem of thermal conduction the constant  $B_2$  is not determined by considering  $J_b$ . The integrand of (25 b) determining the flow of energy contains terms which are proportional to  $(r\Psi'' - \Psi')g_0 v' r^2$ . At the origin the expression in the bracket is proportional to  $1/r$  and according to (15 b) and (17)  $v'$  is proportional to  $1/r^2$  if there is any contribution of  $v_2^*$  to  $v$ . In order to prevent the flow of energy becoming infinite it is therefore necessary to let

$$B_2 = 0. \quad \dots (19 b)$$

The necessity of specifying the potential near the origin in detail is due to the limit of validity of the Smoluchowski equation. Near the origin the calculated functions cannot be expected to be good approximations; in the problem of viscous flow the correct probability density is likely to be much smaller than  $g_0 u$ . The contribution of the region near the origin to the flow of momentum or energy is, however, small since the corresponding integrands vanish.

## § 6. APPROXIMATE INTEGRATION

Approximate expressions for the distributions are found by solving differential equations which are distinct from the correct equations by relatively small terms.

If  $\Psi(0)$  is finite and  $\gamma$  is a constant let

$$f_1(r) = \frac{1}{5} r^2 + \gamma r^{-3} \int_0^r [\exp \Psi(\xi) - 1] \xi^4 d\xi. \quad \dots (20 a)$$

This function solves the equation

$$u'' + [(2/r) - \Psi']u' - (6u/r^2) - [3f_1 - (1 - \gamma)r^2](\Psi'u/rf_1) = 0, \quad \dots (21 a)$$

which differs from (8 a) by the last term only. Transformation of (8 a) by means of

$$u = u_0 \exp \frac{1}{2} \Psi, \quad \dots (22 a)$$

gives

$$u_0'' + [(\Psi'/r) + \frac{1}{2} \Psi'' - \frac{1}{4} \Psi'^2 - (6/r^2)]u_0 = 0. \quad \dots (23 a)$$

Substituting (22 a) in (21 a) with  $\gamma = 0$  and  $\gamma = 1$  yields equations differing from (23 a) by  $2\Psi'u_0/r$  and  $-3\Psi'u_0/r$  respectively. They are small compared with

the second term of (23 a), particularly if  $|\Psi'| \gg 1/r$  or  $\Psi' = 0$ .  $f_1$  is therefore an approximation to  $u_1$  and the other solution of (21 a)

$$f_2 = pf_1 \quad p(r) = - \int_r^\infty [\xi f_1(\xi)]^{-2} \exp \Psi(\xi) d\xi, \quad \dots\dots(24 a)$$

is an approximation to  $u_2$ .

A value between 0 and 1 is then assigned to the constant  $\gamma$  in order to obtain the best possible approximation at small values of  $r$ . The first two terms in the expansion of  $f_1$  are accordingly fitted to the corresponding terms in (11 a). It is found that  $\gamma = \frac{2}{3} \exp(-\Psi(0))$ .

In order to account for the pole of  $\Psi$  at the origin,  $f_1$  and  $f_2$  are calculated as appropriate to a modified potential curve which follows the tangent of the real curve at  $r_0$  and has the value  $2C/r_0$  at  $r=0$ . At  $r=r_0$  the functions  $f_1$  and  $u_1^*$  are joined and similarly the functions  $f_2$  and  $u_2^*$ :

for  $r < r_0$ ,  $u_1 = u_1^*$ ,  $u_2 = F_4 u_1^* + F_5 u_2^*$ ; for  $r > r_0$ ,  $u_1 = F_8 f_1 + F_9 f_2$ ,  $u_2 = f_2$ .

The four constants are determined by four equations expressing continuity of the functions and their derivatives at  $r_0$ .

Approximations to the solutions of (8 b) are found similarly by means of the equation

$$v'' + [(2/r) - \Psi']v' - (2v/r^2) - [2h_1 - (1 - \gamma)r](\Psi'v/rh_1) = 0, \quad \dots\dots(21 b)$$

the solutions of which are

$$h_1(r) = \frac{1}{3}r + \gamma r^{-2} \int_0^r [\exp \Psi(\xi) - 1] \xi^2 d\xi, \quad \dots\dots(20 b)$$

$$h_2 = qh_1 \quad q(r) = - \int^\infty [\xi h_1(\xi)]^{-2} \exp \Psi(\xi) d\xi \quad \dots\dots(24 b)$$

with  $\gamma = \frac{1}{2} \exp(-\Psi(0))$ , and the pole is accounted for in the same way as above. The function  $v_3$  is equal to  $v_3^*$  for  $r < r_0$  and is determined by (16) for  $r > r_0$  with  $r_0$  instead of 0 as lower limit of integration.

The present approximations, even without corrections for the pole, are sufficient for estimating the temperature effect. When better approximations are required they can be obtained by substituting the first approximation for the function in the last term of (21 a) and (21 b), adding the modified term to the right hand side and integrating by means of standard formulae.

## § 7. THE TEMPERATURE EFFECT

The coefficient of viscosity  $\eta$  and the coefficient of thermal conductivity  $\lambda$  are determined by expressions corresponding to those given in § 4 of paper I:

$$\eta = -(N^2 k T / a V) \int g_0 \Psi' u r^3 \sin^5 \theta \sin^2 2\phi dr d\theta d\phi, \quad \dots\dots(25 a)$$

$$\lambda = -(N^2 k^2 T / 2 \beta m V) \int \{ (r \Psi' - \Psi) [(v'/b) + \Psi + 1] \cos^2 \theta + (\frac{1}{2} r \Psi' - \Psi) [(v/rb) + \Psi + 1] \sin^2 \theta \} g_0 r^2 \sin \theta dr d\theta d\phi. \quad \dots\dots(25 b)$$

In (25 b)  $T_0$  is replaced by  $T$ .

Viscosity is known to have a factor  $\exp(U/kT)$  where  $U$  is an energy of the magnitude of the potential barrier outside the main minimum and  $\exp(U/kT) \gg 1$ . It is accordingly of interest to find out which solutions of (6 a) and (6 b) are of a magnitude similar to that of the exponential.

The integrand in (20 *a*) and (20 *b*) determining  $f_1$  and  $h_1$  is small at small values of  $r$  but increases exponentially outside the main minimum. Accordingly at large values of  $r$  the integrals are of the same magnitude as  $\exp(U/kT)$ . A lower limit for  $f_1$  is derived from (20 *a*):

$$f_1 > \frac{1}{5}r^2 - \gamma r^{-3} \int_0^r \xi^4 d\xi = \frac{1}{2}(1 - \gamma)r^2 \quad \dots\dots (26)$$

and a similar expression applies to  $h_1$ .

The functions  $f_2$  and  $h_2$  are, according to (24 *a*), (24 *b*) extremely small at distances outside the barrier and reach the magnitude of unity only near the barrier. Their possible increase at the minimum is limited by the lower limit of  $f_1$  and  $h_1$  according to (26), so that their value is of a magnitude smaller than that of the exponential. Only at small values of  $r$  will the functions  $f_2$  and  $h_2$  increase exponentially.

The integrands in expression (16) determining the function  $v_3$  have at no point the magnitude of  $\exp(U/kT)$  so that the integrals do not reach this magnitude;  $v_3$  itself is of the magnitude of the exponential at large values of  $r$  owing to the factor  $h_1(r)$ .

In the integrands of (25 *a*) and (25 *b*) the functions  $u_1$ ,  $v_1$  etc., are multiplied into  $g_0$ . The high values of  $u_2$  and  $v_2$  near the origin and of the functions  $u_1$  and  $v_1$  near the barrier are offset by the negative exponential in  $g_0$ . At large distances the high values of the functions  $u_1$  and  $v_1$  are ineffective because the integrand vanishes with  $\Psi'$ .

The transport coefficients can have accordingly an exponential temperature factor only if a constant of integration is proportional to a factor of this kind. These constants are determined by the constants in (9 *a*), (9 *b*). According to (20 *a*), (20 *b*) and considering the magnitude of the integrals in these expressions, only the constants  $F_2$  and  $H_2$  have the magnitude  $\exp(U/kT)$ . The constants  $F_1$  and  $H_1$  and, according to (14 *b*) and (16), the constant  $H_6$  are of smaller magnitude which by way of comparison may be said to be of magnitude unity. Determination of  $A_1$  according to the boundary condition (18 *a*) and of  $B_1$  according to conditions (18 *b*) shows that these constants have no exponential factor.  $B_2$  vanishes according to (19 *b*). Only the constant  $A_2$  as determined by (19 *a*) has an exponential factor which is peculiar to the viscosity of liquids. The characteristic difference of the temperature effect on the two transport coefficients is seen to be represented by the constants of integration.

## § 8. CONCLUSION

The effect of temperature on the transport coefficients as obtained in this paper is of a similar kind to that derived in paper I. The previous interpretation of the temperature effect is confirmed. In viscous flow the molecules are forced to occupy frequently positions of high potential energy whereas no such necessity is imposed on the molecules in the case of non-uniform temperature. In the first case the distortion of the equilibrium distribution is of higher magnitude than in the second.

The methods applied in this paper and in paper I may be regarded as different approximations to the exact theory. The present method no longer depends on the crude parabolic potential previously employed and can be adapted to the correct potential curve.

# ACKNOWLEDGMENT

The writer wishes to thank Professor E. N. da C. Andrade, F.R.S., for helpful discussions.

# REFERENCES

- AULUCK, F. C., and KOTHARI, D. S., 1944, *Proc. Nat. Inst. Sci. India*, **10**, 397.
- BORN, M., and Green, H. S., 1947, *Proc. Roy. Soc. A*, **190**, 455.
- EISENSCHITZ, R., 1947, *Proc. Phys. Soc.*, **59**, 1030.
- FÜRTH, R., 1941, *Proc. Camb. Phil. Soc.*, **37**, 252, 276, 281.
- GREEN, H. S., 1947, *Proc. Roy. Soc. A*, **189**, 103.
- KIRKWOOD, J. G., 1935, *J. Chem. Phys.*, **3**, 300; 1946, *Ibid.*, **14**, 180.

## Dislocation Theory of Yielding and Strain Ageing of Iron

BY A. H. COTTRELL AND B. A. BILBY

Metallurgy Department, University of Birmingham

*Communicated by N. F. Mott ; MS. received 10th August 1948*

**ABSTRACT.** A theory of yielding and strain ageing of iron, based on the segregation of carbon atoms to form atmospheres round dislocations, is developed. The form of an atmosphere is discussed and the force needed to release a dislocation from its atmosphere is roughly estimated and found to be reasonable. The dependence on temperature of the yield point is explained on the assumption that thermal fluctuations enable small dislocation loops to break away ; these loops subsequently extend and cause yielding to develop catastrophically by helping other dislocations to break away. The predicted form of the relation between yield point and temperature agrees closely with experiment.

Strain ageing is interpreted as the migration of carbon atoms to free dislocations. The rate of ageing depends upon the concentration of carbon in solution and the estimated initial rate agrees with experiment on the assumption that about 0.003% by weight of carbon is present in solution.

## § 1. INTRODUCTION

IT was shown recently (Cottrell 1948) that the relief of stresses round a dislocation by foreign atoms in solid solution can cause an equilibrium "atmosphere" to form, in which large solute atoms are gathered in the dilated part of the dislocation field and small ones in the compressed part. An atom in substitutional solution relieves hydrostatic stresses and its interaction energy with a positive edge dislocation has been given as

$$V = \frac{4}{3} G \epsilon r_a^3 \lambda \frac{1 + \nu}{1 - \nu} \frac{\sin \alpha}{r}, \quad \dots\dots(1)$$

where  $r$  and  $\alpha$  are its coordinates relative to the dislocation,  $\alpha$  being measured from the slip direction,  $G$  and  $\nu$  are the rigidity modulus and Poisson's ratio respectively,  $\lambda$  is the slip distance in the dislocation, and  $r_a$  and  $r_a(1 + \epsilon)$  are the respective atomic radii of solvent and solute. This formula fails at the origin because the elastic continuum theory is not valid in this region. To a first approximation, the dilatation is zero at the centre of a dislocation and it is reasonable to assume that  $V = 0$  when  $r < r_0$ , where  $r_0 \sim \lambda$ , and is otherwise given by equation (1).

In a dilute atmosphere the concentration of solute will be

$$n(r, \alpha) = n_0 \exp \{ - V(r, \alpha) / kT \}, \quad \dots\dots(2)$$

where  $n_0$  is the average concentration expressed as atoms per unit volume, but in a dense atmosphere substantial relaxation of the hydrostatic stresses is possible and an upper (*saturation*) limit of concentration is set by the condition that the local dilatations produced by the solute atoms and the field of the dislocation are everywhere equal and of the same sign.

Dislocations surrounded by atmospheres can produce plastic flow in two ways. If the applied force is small, the dislocations cannot escape from their atmospheres and the solute atoms must migrate with the dislocations. By applying a sufficiently large force, however, the dislocations can be torn from their atmospheres, in which case they then become highly mobile and able to produce rapid flow under smaller forces; a sharp *upper yield point*, followed by flow at a *lower yield point*, occurs. A specimen which is unloaded in this overstrained condition contains free dislocations and, on immediate reloading, shows no yield point, but if it is rested for a sufficient time at not too low a temperature before reloading, solute atoms migrate to the dislocations to form new atmospheres and the yield point returns (*strain ageing*). This type of hardening, caused by the assembly of mobile solute atoms round dislocations, is to be distinguished from the type of hardening considered previously in which dislocations are impeded by the strain fields of immobile irregularities, such as particles of precipitate. It is to be expected that, under suitable conditions, both types of hardening will be present simultaneously in the same material.

The yield phenomenon is particularly marked in mild steel and soft iron, where it is known to be associated with the presence of small amounts of carbon or nitrogen (Edwards, Phillips and Jones 1940, Snoek 1941b, Low and Gensamer 1944). Accordingly, it has been suggested (Cottrell 1948, Nabarro 1948) that the yield point of iron is due to carbon or nitrogen atmospheres. In the present paper this theory is examined by attempting to estimate the yield point and rate of strain ageing associated with carbon atmospheres; carbon is considered rather than nitrogen because it is more commonly present in iron, but the following discussion can be applied with very little modification to the case of nitrogen.

## §2. CARBON ATMOSPHERES IN $\alpha$ -IRON

X-ray studies of martensite show that when carbon dissolves interstitially in  $\alpha$ -iron it causes a marked lattice expansion and distorts the structure from cubic to tetragonal. These large strains must lead to a strong interaction between a carbon atom and a dislocation, which is consistent with the pronounced yield point of iron. In the case of a (positive) edge dislocation a carbon atom can relieve hydrostatic stresses by entering the expanded region below the dislocation centre; also, as was first pointed out by Nabarro (1948), an additional interaction can be expected because the non-symmetrical character of the distortion produced by carbon should enable shear stresses to be relieved. For a screw dislocation, Frank (1948) has suggested that the interaction must be due solely to the relief of shear stresses because hydrostatic stresses do not exist round a pure screw dislocation, so that in this case atmosphere formation can only occur with those solutes which, like carbon, produce a non-symmetrical distortion. The conditions for a given solute to be able to produce the yield phenomenon may thus be more stringent than was previously suggested, and a high mobility and a large degree of misfit, although necessary, may not in themselves be sufficient. However, considering the atomic structure in a screw dislocation in an actual metal lattice,

it seems likely that the stress field will contain a small hydrostatic component, so that a weak interaction may exist with atoms which cause only spherically symmetrical strains.

The interstitial nature of the solution of carbon in iron and the non-symmetrical distortion prevent the use of equation (1) for calculating the interaction energy. Since the axis of the tetragonal distortion produced by a carbon atom is confined to one of the  $\langle 100 \rangle$  directions of the body-centred cubic cell and a dislocation is confined to a slip-plane, with its direction of displacement lying in a slip direction, the system is not free to arrange that the tetragonal axis coincides with the direction of greatest tension in the dislocation field. For a complete analysis, therefore, the orientation and form of a dislocation in the iron lattice must be determined. The problem is much simplified if only the hydrostatic interaction is considered because hydrostatic stress is a scalar and the question of orientation is then avoided. In order merely to examine whether the anchoring force is sufficient to account for the yield point this simplification is justified and, accordingly, the present treatment deals only with the hydrostatic interaction with an edge dislocation. It is hoped to discuss the shear interaction in a later paper.

The interaction energy is determined by evaluating the work done by forces from the dislocation field when a lattice expansion occurs equivalent to the expansion caused by the introduction of a solute atom (Cottrell 1948). Assuming that each carbon atom alters the edges of the cell in which it is from  $a, a, a$ , to  $c, a_1, a_1$ , the mean changes in the lattice parameter produced by dissolving  $n$  carbon atoms in a crystal of  $N$  iron atoms are given by  $\Delta c = 2(c - a)n/N$  and  $\Delta a = 2(a_1 - a)n/N$ . Using the lattice parameter measurements on martensite of Lipson and Parker (1944) and extrapolating to  $n/N = 0.5$ , the volume change caused by the introduction of a carbon atom is given as  $\Delta v = 0.78 \times 10^{-23} \text{ cm}^3$ . Hence, if the stresses due to the dislocation in the surrounding medium remain constant when this local volume change occurs, the interaction energy is

$$V = p\Delta v = -q\Theta\Delta v \quad \dots\dots(3)$$

where  $p$  and  $\Theta$  are the local pressure and dilatation, respectively, caused by the dislocation, and  $q$  is the bulk modulus. Using Koehler's (1941) formulae for the stresses round a positive edge dislocation

$$\Theta = -\frac{\lambda}{2\pi} \frac{1-2\nu}{1-\nu} \frac{\sin \alpha}{r},$$

and assuming that  $\Theta = 0$  when  $r < r_0$  we have

$$V = A \frac{\sin \alpha}{r} = \Delta v \cdot \frac{G\lambda}{3\pi} \frac{1+\nu}{1-\nu} \frac{\sin \alpha}{r} \quad r \geq r_0; \quad V = 0 \quad r < r_0. \quad \dots\dots(4)$$

The assumption that the dislocation stresses, and hence  $\Theta$ , remain unchanged when the carbon atom is introduced implies that the stress field is effectively constant over regions large compared with the size of the carbon atom, a reasonable approximation in regions remote from the dislocation centre. Near the centre, however, the dislocation stresses are rapidly varying functions of position and must be greatly altered by the introduction of the carbon atom. In the part of the crystal below the dislocation (i.e. where  $\Theta$  is positive), which is the region of interest for the case of carbon in iron, the (negative) pressure must relax as the local volume change  $\Delta v$  takes place so that the interaction energy will be less

than is given by equation (4). Very near the dislocation centre equation (4) will grossly overestimate the interaction and can only be used to give a rough indication of the general order of magnitude.

Taking  $G = 8.28 \times 10^{11}$  dyne.cm<sup>-2</sup>,  $\lambda = 2r_a = 2.48 \times 10^{-8}$  cm., and  $\nu = 0.28$ , the constant  $A$  in equation (4) is  $3 \times 10^{-20}$  dyne.cm<sup>2</sup>. At room temperature  $A kT = 76$  A. and, with such a value, the Maxwell-Boltzmann formula (2) gives impossibly large values of  $n/n_0$  in the lower half crystal within about 10 A. of the dislocation centre. The concentration in this region must be limited by other factors. An assembly of carbon atoms can never completely relieve all the dislocation stresses, but, as the atmosphere builds up, the progressive relief of stress will lead to a condition of saturation in which the addition of more atoms to the atmosphere no longer reduces the energy. An estimate of the number of atoms required for saturation can be made by equating the volume changes produced by the atoms and by the dislocation field. Taking a section consisting of one atomic plane threaded by the dislocation line, the radius  $R$  of a semi-circular annulus, in which the total volume change produced by the dislocation is equal to that produced by introducing one carbon atom, is determined by

$$\Delta v = \lambda \int_{r_0}^R \int_{\pi}^{2\pi} \Theta r dr d\alpha.$$

Using the above value for  $\Delta v$  and assuming  $r_0 \sim 2$  A.,  $R$  is about 10 A. It is thus reasonable to assume that in the equilibrium state only one carbon atom per atom plane is contained within 10 A. of the dislocation centre. Since the greatest tensile strain must occur immediately below the dislocation centre and in the atomic plane which constitutes the lower side of the slip plane, the most favourable position for the central carbon atom will be at  $\alpha = 3\pi/2$  and  $r \sim 2$  A., and it seems likely that the central part of the atmosphere consists of a line of carbon atoms, parallel to the dislocation line, in this position. In the annulus between 10–20 A. the total volume change is again about the same as that produced by one carbon atom per atom plane, but this volume change is spread more uniformly over a much larger region of the crystal and, in this case, the carbon atoms could hardly be arranged along a line. The atmosphere is pictured, therefore, as a central row of carbon atoms, situated just below the dislocation centre, which is surrounded in the lower half-crystal by a dilute distribution of the Maxwell-Boltzmann type.

It should be noticed that an extremely small amount of carbon is required to provide atmospheres for all dislocations in a crystal; the actual value depends,

Table 1

Density of dislocation (lines/cm <sup>2</sup> )	..	10 <sup>12</sup>	10 <sup>8</sup>
% of C by weight absorbed	{ Full yield point	.. > 10 <sup>-2</sup>	> 10 <sup>-6</sup>
in dislocations for	{ No yield point	.. < 10 <sup>-3</sup>	< 10 <sup>-7</sup>

of course, on the density of dislocations. Table 1 shows the results of the assumption that a full yield point is obtained when every dislocation has one carbon atom per atom plane and that the yield point is absent at below one-tenth of this amount of carbon.

### § 3. FORCE REQUIRED TO PULL A DISLOCATION FROM ITS ATMOSPHERE

It is clear that the force required to pull a dislocation from its atmosphere is determined almost completely by the interaction with the carbon atoms of

the central row, since (i) these atoms, being so near to the dislocation, interact strongly with it, and (ii) the restraining force due to their interaction must reach its maximum at a very small displacement of the dislocation from its equilibrium position, and at such a small displacement the contribution to the restraining force from carbon atoms further out will still be comparatively small. From the point of view of calculating the yield point this is unfortunate, since it means that the important contribution of force is from atoms near the dislocation centre, where the interaction energy cannot be accurately evaluated, so that only a rough estimate is possible.

In Figure 1 consider a positive edge dislocation lying along the  $Z$  axis (the  $X$  axis is the slip direction) and a line of carbon atoms  $CC'$ , lying parallel to the dislocation, in the most favourable position at a distance  $\rho$  below it. The interaction energy per atom plane, when the dislocation has been displaced a distance  $x$  in the slip direction is

$$V(x) = -A \sin \phi / r = -A\rho / (x^2 + \rho^2) \quad \dots\dots (5)$$

and the corresponding force is  $F(x) = \partial V / \partial x = 2A\rho x / (x^2 + \rho^2)^2$  which has a maximum of  $3\sqrt{3}A/8\rho^2$  dynes per atom plane at  $x = \rho/\sqrt{3}$ .

The critical force for releasing a dislocation is thus  $F_0 = 3\sqrt{3}A/8\lambda\rho^2$  dynes/cm. and, by using the relation  $\tau = F/\lambda$  (Mott and Nabarro 1948) where  $\tau$  is resolved shear stress, this can be converted to an equivalent critical shear stress  $\tau_0 = 3\sqrt{3}A/8\lambda^2\rho^2$  dyne.cm<sup>-2</sup> on the slip plane. Assuming that in the case of a tensile test the active slip planes are inclined at approximately  $\pi/4$  to the tensile axis, the critical tensile stress is

$$\sigma_0 = 3\sqrt{3}A/4\lambda^2\rho^2 \text{ dyne.cm}^{-2}. \quad \dots\dots (6)$$

Table 2 gives the observed values of the yield point of annealed ingot iron at various temperatures, as derived from the graphical results of McAdam and Mebs (1943). The yield shows a strong temperature dependence and it is clear

Table 2

Temperature ( $^{\circ}$ K.)	85	144	195	303	373
Yield point $\sigma$ (dynes/cm <sup>2</sup> $\times 10^9$ )	6.07	4.14	2.83	1.45	1.10
$\sigma/\sigma_0$	0.485	0.330	0.225	0.115	0.090

that  $\sigma_0$  in equation (6) must correspond with the zero point yield stress. If a curve is fitted to these results and extrapolated to  $0^{\circ}$  K., the experimental value of  $\sigma_0$  is about  $1.25 \times 10^{10}$  dynes/cm<sup>2</sup>. Using the precious values of  $A$  and  $\lambda$  the theoretical value of  $\sigma_0$  can be made to agree with this if  $\rho$  is taken to be  $7\text{ \AA}$ ., which shows that the restraining force is strong enough to account for the yield point. If  $\rho$  is taken to be  $2\text{ \AA}$ ., as suggested in §2, the estimated value of  $\sigma_0$  is an order of magnitude higher; however, it must be remembered that the interaction energy is seriously over-estimated near the dislocation centre and the theory can only give a rough indication of the yield stress. Comparison with the experimental value of  $\sigma_0$  suggests that a reasonable value of  $A$  near the dislocation centre is  $3 \times 10^{-21}$  dyne.cm<sup>2</sup>.

Figure 2 shows the variation of interaction energy and stress with position of the dislocation for the cases  $\rho = 2\text{ \AA}$ .,  $A = 3 \times 10^{-20}$  dyne.cm<sup>2</sup>, and  $\rho = 2\text{ \AA}$ .,  $A = 3 \times 10^{-21}$  dyne.cm<sup>2</sup>.



## §4. EFFECT OF THERMAL FLUCTUATIONS ON THE YIELD POINT

At temperatures above  $0^\circ\text{K.}$ , thermal fluctuations help the external forces to tear a dislocation from its atmosphere and yielding occurs before  $\sigma$  reaches  $\sigma_0$ . When a stress  $\sigma = p\sigma_0$  is applied the dislocation moves forward to the position  $x_1$  of stable equilibrium (Figure 2) and can only be released by this stress after it has been taken further forward to the position  $x_2$  of unstable equilibrium, beyond which the external force exceeds the restraining force.

The activation energy per atom plane for the release, by thermal fluctuations, of a dislocation which remains straight is thus the difference  $V(x_2) - V(x_1)$  in

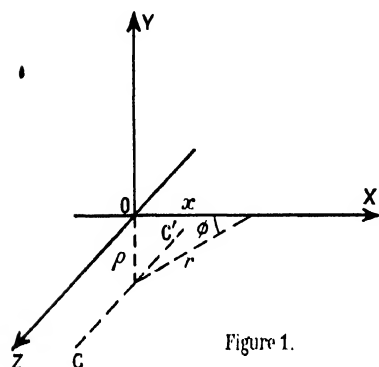
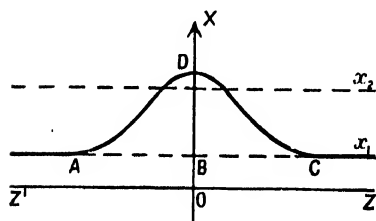
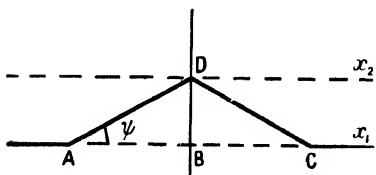


Figure 1.

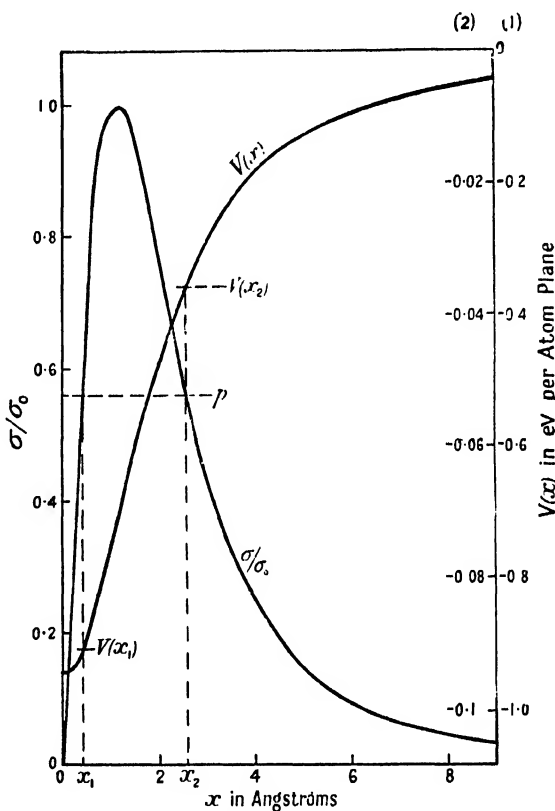


(a)



(b)

Figure 3.

Figure 2. Variation of interaction energy ( $V$ ) and applied stress ( $\sigma/\sigma_0$ ) with dislocation position.

Scale (1)  $A = 3 \times 10^{-20}$  erg.cm.  $\rho = 2 \text{ \AA.}$

Scale (2)  $A = 3 \times 10^{-21}$  erg.cm.  $\rho = 2 \text{ \AA.}$

interaction energy minus the work done by the external force when the dislocation moves from  $x_1$  to  $x_2$ . In calculating the activation energy which thermal fluctuations must supply in order to release the whole dislocation, however, an energy contribution caused by the change in form of the dislocation must be considered.

Let the plane of Figure 3(a) represent the slip plane. When the applied stress is zero the equilibrium position of the dislocation is  $ZZ'$ , vertically above the line of the atmosphere. Under the stress  $\sigma$  the dislocation moves forward to the line  $x_1$ . To produce yielding it is not necessary for the fluctuation to

move the entire dislocation to  $x_2$  as this would require an unnecessarily large energy. If a loop ADC of the dislocation is thrown forward, and this loop is sufficiently large, the force pulling the looped part forward can exceed the restraining force and the dislocation will then be torn from its atmosphere, the centre of the loop moving forward and the sides moving laterally towards the ends of the dislocation. This process depends upon the ability of the dislocation to be bent and extended. The theory of flexible dislocations has been developed by Mott and Nabarro (1948) who have shown that a dislocation behaves like a one-dimensional soap film; it possesses an energy  $WL$ , where  $L$  is its length and  $W = 1 - 5$  ev. per atom plane, which it tries to minimize by becoming as short as possible. Thus to form the loop ADC, an activation energy has to be supplied which is made up of (i) the energy of interaction with the atmosphere, (ii) the length energy associated with the increase in length, ADC - ABC, and (iii) the energy gain due to the work done by the external forces.

To calculate the exact size and shape of the smallest stable loop is difficult, but it is clear that an essential condition is that part of the dislocation has to be brought by the fluctuation to at least the line  $x_2$ , since otherwise there will be no part of the looped dislocation on which the net force acts in the forward direction. Thus consider the simpler model shown in Figure 3(b). Here a triangular loop is formed, of depth BD, reaching to the line  $x_2$  at its apex, and the value of the angle  $\psi$  is chosen to make the activation energy a minimum. This loop is, of course, too small to be stable; however, the true activation energy cannot be very much greater than is given by this model, for calculation shows that about one-half of the energy of the triangular loop arises from the length energy term and much larger loops could be formed with only a small additional increase in the length of the dislocation.

It is assumed that the interaction energy of an element at any point on the portions AD and DC is the same as that of an element with that point as centre and lying parallel to  $ZZ'$ ; this assumption is consistent with the results of the analysis by Mott and Nabarro (1948) of the strains round a zigzag dislocation. Accordingly, when an element  $dz$  of the dislocation moves forward from  $x_1$  to  $x$ , with the formation of the loop, its interaction energy changes by

$$\{V(x) - V(x_1)\} dz = -\cot \psi \{V(x) - V(x_1)\} dx$$

and the contribution of the interaction with the atmosphere to the activation energy is

$$2 \int_{x_1}^{x_2} -\cot \psi \{V(x) - V(x_1)\} dx.$$

Taking  $V(x) = -A\rho/\lambda(x^2 + \rho^2)$  erg/cm. this becomes

$$-\left[ \frac{2A}{\lambda} \{ \tan^{-1}(x_2/\rho) - \tan^{-1}(x_1/\rho) \} + 2(x_2 - x_1)V(x_1) \right] \cot \psi. \quad \dots\dots(7)$$

The increase in length energy is

$$W(\text{ADC} - \text{ABC}) = 2W(x_2 - x_1)(\text{cosec } \psi - \cot \psi) \quad \dots\dots(8)$$

and, if the external force per unit length on the dislocation is  $F$ , the work it does when the loop is formed is

$$F(x_2 - x_1)^2 \cot \psi. \quad \dots\dots(9)$$

Subtracting (9) from the sum of (7) and (8) gives the activation energy,  $U$ , which is of the form  $\propto \operatorname{cosec} \psi - \beta \cot \psi$ ; minimizing  $U$  with respect to  $\psi$  defines  $\psi$  as  $\cos^{-1}(\beta/\alpha)$  and substituting this value then gives the activation energy in terms of  $W$  and  $\sigma/\sigma_0$ . It can be readily shown that  $U$  is of the form

$$U = D(\sigma/\sigma_0)[AE(\sigma/\sigma_0)\{2W\rho - AE(\sigma/\sigma_0)\}]^{\frac{1}{2}},$$

where  $D$  and  $E$  do not depend on the physical parameters  $A$ ,  $W$  and  $\rho$ . Thus, if  $2W\rho \gg AE$ ,  $U/(2AW\rho)^{\frac{1}{2}}$  is essentially a function of  $\sigma/\sigma_0$  only, so that altering  $A$ ,  $W$  and  $\rho$  only alters the curve of  $U$  against  $\sigma/\sigma_0$  by a scale factor, the form of the curve remaining unchanged. For the range of values of  $A$ ,  $W$ ,  $\rho$  and  $\sigma/\sigma_0$  considered,  $AE$  is never greater than about  $W\rho/2$  and in most cases is much less than this, so that the form of the activation energy curve is almost independent of the parameters. Figure 4 shows the curve for various values of  $A$ ,  $W$  and  $\rho$ .

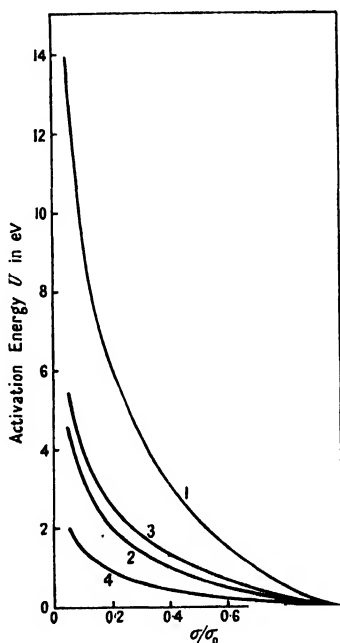


Figure 4. Activation energy for the formation of a loop.

Curve	1	2	3	4
$W$ (ev.) per atom plane	5	5	1	1
$A$ (erg.cm.)	$3 \times 10^{-20}$	$3 \times 10^{-21}$	$3 \times 10^{-20}$	$3 \times 10^{-21}$
$\rho$ (A.)	2	2	2	2

It is to be expected that, as the stress is increased towards  $\sigma_0$ , the first successful attempt to form a loop occurs on a dislocation in a highly stressed region of the specimen. The first stable loop to be formed is subsequently extended by the applied force until the entire dislocation to which it belongs is released from its atmosphere. This dislocation accelerates and enables other dislocations to break away by setting up an elastic disturbance in their midst; in this way yielding develops catastrophically throughout the entire specimen. This description agrees with the well-known observations that yielding starts in highly stressed regions and is propagated, in the form of Luder's bands, from these regions along the specimen. The elementary yielding process—the release of a dislocation from its atmosphere—occurs in both the start and the propagation of yielding; the difference between the upper and lower yield points is that, in the case of the

lower yield, the release of dislocations (at the edges of a Luder's band) is helped by the elastic disturbance caused by nearby plastic flow, whereas in the upper yield this help is not available.

With the above picture the effects of temperature and testing rate on the yield point can be examined. When the stress in the neighbourhood of a dislocation lies in the range  $\sigma/\sigma_0$  to  $(\sigma + d\sigma)/\sigma_0$  the time  $t_1$  before a successful fluctuation occurs is proportional to  $\exp\{U(\sigma/\sigma_0)/kT\}$ . On the other hand, the time  $t_2$  spent in this stress range is inversely proportional to the rate of stressing,  $d\sigma/dt$ . Yielding should occur when  $t_1 \sim t_2$ , i.e. when the quantity

$$S = (d\sigma/dt) \exp\{-U(\sigma/\sigma_0)/kT\} \dots\dots(10)$$

reaches a characteristic, fixed value. Thus, in experiments at constant testing rate, the yield point should vary with temperature in such a manner that  $U/kT$  remains constant, and similarly, at constant temperature  $U$  should depend logarithmically on the testing rate. From McAdam and Mebs' results (Table 2) the temperature dependence can be examined. If the experimental and theoretical values of  $\sigma/\sigma_0$  are equated at one arbitrarily chosen temperature, the value of  $U$  and hence  $U/kT$  can be found from Figure 4. Keeping  $U/kT$  constant the theoretical  $\sigma/\sigma_0$  values can be obtained at various temperatures from Figure 4 and compared with the experimental values. Figure 5 shows the results obtained

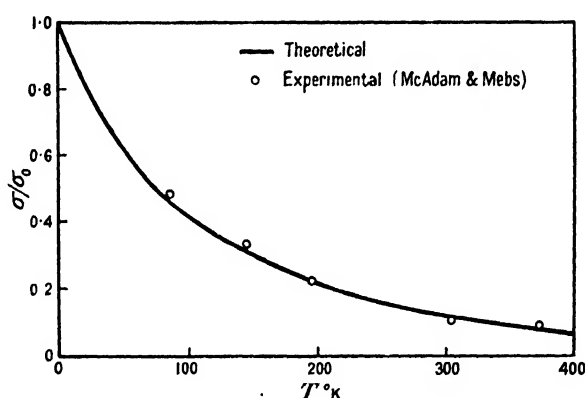


Figure 5. Variation of yield point with temperature.  
The theoretical curve is fitted to the experimental value of  $\sigma/\sigma_0$  at 195° K.

when the  $\sigma/\sigma_0$  values are equated at 195° K. and the activation energy curve 4 of Figure 4 is used. Since the activation energy curves have almost identical forms essentially the same results are obtained when the other curves are used. The good fit obtained over a wide range shows that the activation energy curves

Table 3

Activation energy curve	..	1	2	3	4
$W$ (ev. per atom plane) ..	..	5	5	1	1
$A$ (dyne.cm <sup>2</sup> $\times 10^{-20}$ ) ..	..	3	0.3	3	0.3
$U/kT$ .. ..	..	330	107	140	47

have the correct shape to account for the experimental observations. The values of  $U/kT$  given by equating the  $\sigma/\sigma_0$  values are shown in Table 3. Since  $U/kT$  in practice could hardly exceed about 50, it appears that the most reasonable values of  $W$  and  $A$  are those of curve 4.

In the present theory, the large temperature dependence of the yield point of iron is explained by the narrowness of the potential energy trough associated with an atmosphere of solute atoms (cf. Figure 2), so that only a small displacement of the dislocation, and hence a small activation energy, is required to overcome the restraining force. In a precipitation-hardened alloy, on the other hand, the existence of wide potential energy troughs causes a large activation energy for moving a dislocation, thus giving a small temperature dependence of yield strength (Mott and Nabarro 1948).

### § 5. RATE OF FORMATION OF THE ATMOSPHERE

In the present theory, strain ageing is regarded as the process whereby carbon atoms in solution migrate towards free dislocations, at rest in an overstrained crystal, to form new atmospheres. To examine this process consider a free dislocation at rest in a region where the solute is initially randomly dispersed, with concentration  $n_0$  atoms per  $\text{cm}^3$ . Moving by thermal agitation the solute atoms acquire a drift velocity relative to the dislocation (Cottrell 1948) given by

$$\mathbf{v} = -(D/kT)\nabla V \quad \dots\dots(11)$$

where  $D$  is the diffusion coefficient and  $V$  is given by equation (4). As the atmosphere builds up to equilibrium, both saturation and concentration differences become important in modifying the flow velocity, but in the early stages of atmosphere formation they are negligible. As it is extremely difficult to take account of these factors quantitatively, only the initial stages of ageing, where the drift flow is dominant, will be considered.

Equation (11) shows that the atoms move normally to the equipotential surfaces of  $V$ . It is thus convenient to choose as coordinate lines for the problem an orthogonal, curvilinear set consisting of the families made up from the lines of constant  $V$  and the lines of flow; the problem is, of course, two-dimensional. Since  $V = A \sin \alpha / r$ , the first coordinate may be defined by the parameter  $\eta = r / \sin \alpha$ , so that the equipotential lines are those on which  $\eta$  is constant. The flow lines, conjugate to these, are defined by the coordinate  $\xi = r / \cos \alpha$ . Using the standard transformation formulae, the elements of length along the  $\xi$  and  $\eta$  lines are, respectively,

$$\frac{\xi^2}{\xi^2 + \eta^2} d\eta \quad \text{and} \quad \frac{\eta^2}{\xi^2 + \eta^2} d\xi \quad \dots\dots(12)$$

and  $\nabla V$  is

$$-A \frac{\xi^2 + \eta^2}{\xi^2 \eta^2} \mathbf{i}, \quad \dots\dots(13)$$

where  $\mathbf{i}$  is the unit vector in the  $\eta$  direction. As shown in Figure 6, the  $\xi, \eta$  coordinate system consists of circles centred on the X, Y axes and passing through the origin.

A carbon atom will migrate towards the most favourable position below the dislocation, moving along a line of constant  $\xi$  and eventually come to rest at a position where its  $\eta$  coordinate has a value,  $-\eta_0$ , of a few Angströms. From (11), (12) and (13), the time required for an atom to move an elementary distance in the  $\eta$  direction is

$$dt = \frac{kT}{AD} \frac{\xi^4 \eta^2}{(\xi^2 + \eta^2)^2} d\eta,$$

and hence the time to move from  $(\xi, +\eta_0)$  to  $(\xi, -\eta_0)$  is

$$t = \frac{kT}{AD} \xi^4 \left( \int_{+\eta_0}^{+\infty} \frac{\eta^2 d\eta}{(\xi^2 + \eta^2)^2} + \int_{-\infty}^{-\eta_0} \frac{\eta^2 d\eta}{(\xi^2 + \eta^2)^2} \right) \\ = (kT\xi^3/AD) [\pi/2 - \tan^{-1}(\eta_0/\xi) + \frac{1}{2} \sin \{2 \tan^{-1}(\eta_0/\xi)\}].$$

If  $\eta_0/\xi \ll 1$  this can be approximated to

$$t = \pi kT\xi^3/2AD \quad \dots\dots(14)$$

since  $\tan^{-1}(\eta_0/\xi) \sim \frac{1}{2} \sin \{2 \tan^{-1}(\eta_0/\xi)\} \sim \eta_0/\xi$ . After the time  $t$ , all lines of flow for which  $\xi^3 \leq 2ADt/\pi kT$  will have been drained of carbon atoms and will take no further part in the ageing process. Taking the smallest value of  $\xi$  compatible with the above approximation to be  $10\text{ \AA}$ , and using the value of §2 for  $A/kT$ ,

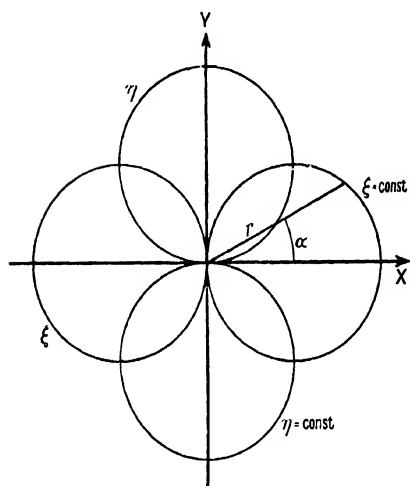


Figure 6.

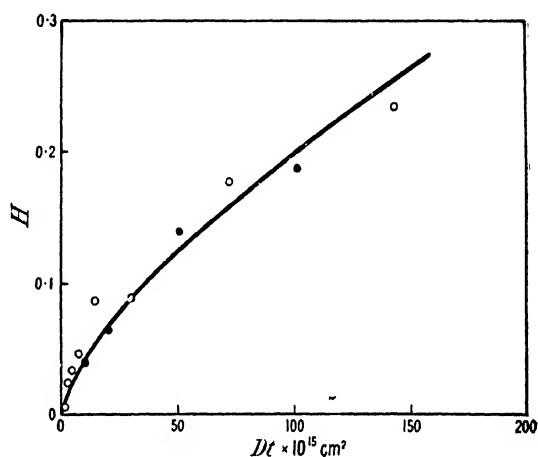


Figure 7. Strain ageing of a low-carbon steel. (From results of Davenport and Bain.)

○ = Ageing at 20 °C.  
● = Ageing at 40 °C.  
— = Equation (16) assuming a carbon concentration of 0.003 % by weight.

it can be seen that this conclusion should be valid for ageing times such that  $Dt > 2 \times 10^{-15} \text{ cm}^2$ . As Figure 7 shows, strain ageing does not become appreciable until much longer ageing times than this have elapsed.

Consider flow along a filament of width  $d\xi$  which is still supplying atoms at the time  $t$ . The time for an atom to move an elementary distance along this filament, in the region where  $\eta = -\eta_0$ , is

$$dt = \frac{kT}{AD} \frac{\xi^4 \eta_0^2}{(\xi^2 + \eta_0^2)^2} d\eta.$$

and the area of the corresponding element of the filament is

$$\frac{\xi^2 \eta_0^2}{(\xi^2 + \eta_0^2)^2} d\eta d\xi = \frac{AD d\xi}{kT \xi^2} dt.$$

Using equation (14) to define the limits of integration, the total area which can supply carbon atoms to the dislocation in the interval of time from  $t$  to  $t + dt$  is

$$\frac{AD}{kT} \left( \int_{+(2ADt/\pi kT)^{\frac{1}{3}}}^{+\infty} \xi^{-2} d\xi + \int_{-\infty}^{-(2ADt/\pi kT)^{\frac{1}{3}}} \xi^{-2} d\xi \right) dt = 2 \left( \frac{\pi}{2} \right)^{\frac{1}{3}} \left( \frac{AD}{kT} \right)^{\frac{1}{3}} \frac{dt}{t^{\frac{1}{3}}}. \quad \dots\dots(15)$$

An important feature is that, in the region of the dislocation field where the relation  $V = A \sin \alpha / r$  holds, and outside the regions defined by equation (14) from which the carbon atoms have been removed, the concentration of carbon remains constant during the drift flow. The hydrodynamical equation of continuity,  $\nabla \cdot (\rho \mathbf{v}) = -\partial \rho / \partial t$ , here takes the form  $\nabla \cdot \{n(D/kT) \nabla V\} = \partial n / \partial t$  where  $n = n(r, \alpha, t)$  is the concentration of solute. Since  $n = n_0 = \text{constant}$  at  $t = 0$ , and since  $\nabla^2 V = (\partial^2 / \partial r^2 + \partial / \partial r \partial r + \partial^2 / r^2 \partial \alpha^2)(A \sin \alpha / r) = 0$  then  $\partial n / \partial t = 0$  and the condition  $n = n_0$  is perpetuated.

If unit length of the dislocation is considered, the number of carbon atoms which arrive within a time  $t$  is, from equation (15),

$$N(t) = n_0 2 \left( \frac{\pi}{2} \right)^{1/2} \left( \frac{AD}{kT} \right)^{1/2} \int_0^t t^{-1/2} dt = n_0 3 \left( \frac{\pi}{2} \right)^{1/2} \left( \frac{ADt}{kT} \right)^{1/2}.$$

The total number,  $N_s$ , of carbon atoms per unit length of the dislocation required to form an atmosphere of one atom per atom plane is  $1/\lambda$ , so that the degree of formation of the atmosphere at time  $t$  is

$$N(t)/N_s = n_0 \lambda 3 (\pi/2)^{1/2} (ADt/kT)^{1/2}. \quad \dots (16)$$

## § 6. RATE OF STRAIN AGEING

An experimental study of strain ageing has been made by Davenport and Bain (1935) who measured the increase in hardness of a low-carbon steel with time of ageing at various temperatures. Nabarro (1948) has shown that several features of strain ageing, shown by their results, are explicable on the basis of the present theory and provide evidence in its support. To compare the ageing rates found by Davenport and Bain with the rate predicted in the previous section the quantity  $H = (H_t - H_0)/(H_m - H_0)$  which is a measure of the degree of strain age-hardening, is first derived from the graphical results given in their Figure 11 (upper block); in this expression,  $H_t$  is the hardness after ageing for a time  $t$ ,  $H_0$  is the value before ageing and  $H_m$  is the maximum produced by prolonged ageing. To assemble results from different temperatures in the same diagram it is convenient to plot  $H$  against  $Dt$  rather than the time  $t$  itself, where  $D = 5.2 \times 10^{-4} e^{-9000/T}$  (Snoek 1941a, Polder 1945) is the diffusion coefficient of carbon in  $\alpha$ -iron, since all the results then lie on the same curve.

Figure 7 shows the experimental and theoretical variation of  $H$  with  $Dt$ . The theoretical curve has been derived from equation (16) by assuming that  $H = N(t)/N_s$ , by using the values of  $\lambda$  and  $A/kT$  given in § 2, and by taking a value of  $n_0$  corresponding to 0.003% carbon by weight. The assumption  $H = N(t)/N_s$  cannot be strictly valid since the first atoms to arrive at a dislocation ought to be more effective in anchoring it than those that arrive later. Equation (16) represents the observed ageing behaviour fairly well up to about  $N(t)/N_s = 0.3$  but beyond this range it gives a rate of ageing which is too high; this is to be expected since the neglect of the effects of saturation and concentration differences, and the assumption  $H = N(t)/N_s$ , will each cause the theoretically estimated rate to be too high in the later stages of ageing.

The carbon concentration determined above by fitting the observed and calculated ageing rates ought to correspond to the value for the residual carbon

in solution in  $\alpha$ -iron at room temperature. Most of the carbon in irons and steels of higher carbon content is, of course, precipitated as cementite and only that which remains in solution takes part in strain ageing. Experimental evidence for the solubility of carbon in iron at room temperature is meagre, but suggests that the above value of 0.003% is reasonable. Thus Yensen (1924) and Dijkstra (1947) have given the upper limit of the residual solubility as 0.006% and 0.001% respectively.

#### §7. OTHER AGEING EFFECTS

The migration of solute atoms into dislocations, causing the latter to become anchored, ought to produce several mechanical and physical effects, which can be divided into two groups: (i) those resulting from the anchoring of the dislocations, and (ii) those resulting from the removal of solute atoms from random solution to form atmospheres.

The most striking effect belonging to the first group is, of course, the return of the yield point. In addition, a reduction of certain "anelastic" effects (Zener 1946) is to be expected, and this is confirmed by experiment. A freshly strained specimen possesses a high internal friction and shows slight plasticity at stresses well below the stress at which extensive plastic flow sets in. Zener has attributed these anelastic effects to local readjustments in position of dislocations in the slip bands of the worked material; this is reasonable since small displacements of free dislocations in a Taylor (1934) array can occur under small stresses, even though a high stress is required to overcome the interaction forces of neighbouring dislocations and so produce extensive flow. Low-temperature annealing, for times which would allow strain ageing to occur, greatly reduces this source of internal friction and causes a true elastic range to return, which is consistent with the suggestion that dislocations become anchored by the ageing process.

Ageing effects belonging to the second group should be provided by properties which are sensitive to the amount of carbon in random solution in  $\alpha$ -iron. Thus we may expect both electrical resistance and magnetic ageing effects. Recent work by Mr. A. T. Churchman and one of us (A. H. C.) has shown that a small decrease in electrical resistance of the right order of magnitude does in fact occur during strain ageing. Another effect has been observed by Snoek (1941a), who found that cold working and low-temperature annealing caused the elimination of a certain type of elastic after-effect known to be caused by mobile carbon (or nitrogen) atoms in solution in  $\alpha$ -iron. Snoek suggested that this treatment probably caused the solute atoms to become bound by internal stress fields created by the cold working. If we interpret the sources of the stress fields as dislocations, this suggestion becomes quite specific, since then the solute atoms cannot produce internal friction by Snoek's mechanism because they are assembled in dislocations.

#### ACKNOWLEDGMENTS

We wish to thank Professor D. Hanson, under whose general supervision this work was carried out, for his interest and support, and Professor N. F. Mott for several valuable discussions during the progress of the work. Financial help has been given by the Department of Scientific and Industrial Research and by the award of a University Fellowship to one of us (B. A. B.).



## REFERENCES

- COTTRELL, A. H., 1948, *Report on the Strength of Solids* (London: Physical Society), p. 30.  
 DAVENPORT, E. S., and BAIN, E. C., 1935, *Trans. Amer. Met. Soc.*, **23**, 1047.  
 DIJKSTRA, L. J., 1947, *Philips Res. Rep.*, **2**, 357.  
 EDWARDS, C. A., PHILLIPS, D. L., and JONES, H. N., 1940, *J. Iron and Steel Inst.*, **142**, 199.  
 FRANK, F. C., 1948, private communication.  
 KOEHLER, J. S., 1941, *Phys. Rev.*, **60**, 397.  
 LIPSON, H., and PARKER, A. M. B., 1944, *J. Iron and Steel Inst.*, **149**, 123.  
 LOW, J. R., and GENSAMER, M., 1944, *Trans. Amer. Inst. Min. Met. Eng.*, **158**, 207.  
 McADAM, D. J., and MEBS, R. W., 1943, *Trans. Amer. Soc. Test Mat.*, **43**, 661.  
 MOTT, N. F., and NABARRO, F. R. N., 1948, *Report on the Strength of Solids* (London: Physical Society), p. 2.  
 NABARRO, F. R. N., 1948, *Report on the Strength of Solids* (London: Physical Society), p. 38.  
 POLDER, D., 1945, *Philips Res. Rep.*, **1**, 5.  
 SNOEK, J. L., 1941 a, *Physica*, **8**, 711; 1941 b, *Ibid.*, **8**, 734.  
 TAYLOR, G. I., 1934, *Proc. Roy. Soc. A*, **145**, 362.  
 YENSEN, C. F. D., 1924, *J. Amer. Inst. Elec. Eng.*, **43**, 455.  
 ZENER, C., 1946, *Met. Tech.*, **13**, Tech. Pub. No. 1992.

## Investigations on the Binding Energy of Heavy Nuclei

By R. HUBY\*

H. H. Wills Physical Laboratory, University of Bristol

\* Now at Department of Theoretical Physics, University of Liverpool

*MS. received 18th May 1948, and in amended form 28th September 1948*

**ABSTRACT.** The binding energy of a heavy nucleus is one of the quantities which a satisfactory nuclear force theory ought to predict correctly. Approximate calculations of this binding energy are performed, taking as nuclear force the static interaction of Møller and Rosenfeld. The parameters appearing in the interaction have been fixed by data on light nuclei.

The Fermi-gas model is taken as basis for the calculations, a first solution being obtained by a first-order perturbation (or variation) method. For refinement, a second-order perturbation calculation is made, and Svartholm's variation-iteration method is attempted. The first-order results yield about 10% of the required energy, and the second-order about 40%; a reasonable prediction of the size of the nucleus is obtained. The reliability of the perturbation results is uncertain; Svartholm's method does not appear to be well suited to the investigation of heavy nuclei.

Two alternative modifications are made to the nuclear force to make it yield the correct binding energy according to the perturbation calculation.

### § 1. INTRODUCTION

IN principle, one of the most important tests of any proposed nuclear force is its compatibility with the observed binding energies of heavy nuclei. By a semi-empirical procedure these can be approximately expressed by a simple function of atomic number  $Z$  and mass number  $A$ , containing a few parameters. One of these parameters, the coefficient of an energy contribution simply proportional to  $A$ , can be taken as representing the major effect of the nuclear forces, and a theory might be tested by the value which it predicts for this parameter. Of the theories which have been put forward, that of Møller and Rosenfeld (Møller and Rosenfeld 1940, Rosenfeld 1945, 1948) is capable of accounting for many of

the properties of light nuclei, and is at the same time relatively easy to handle: this is the theory here considered in relation to heavy nuclei. The parameters appearing in the interaction are fixed by data on light nuclei. The problem posed is the solution of the wave equation for the ground state of a very heavy nucleus. Approximate methods must be employed for this, and in consequence the reliability of the test cannot very well be assessed.

The methods used are based on the Fermi gas model (§ 3.1), a first approximate solution being obtained by a first-order perturbation (or variation) treatment (§ 3.2). Two different possibilities of refinement have then been attempted, viz. a second order perturbation calculation (§ 3.3), similar to that first performed by Euler (1937) for a different form of interaction; and Svartholm's variation-iteration method (§ 5). The former leads to positive results, but it appears that Svartholm's method is not well suited to the investigation of heavy nuclei. The results of the perturbation calculations are presented in § 2, and the calculations are criticized in § 4.

## § 2. FORMULATION OF PROBLEM AND RESULT

### 2.1. Formulation of Problem

The binding energy  $-E$  of a nucleus of atomic number  $Z$  and mass number  $A$  can be represented approximately by the semi-empirical formula (Rosenfeld 1948, Chap. 2)

$$E = -c_1 A \left[ 1 - c_2 \left( \frac{N-Z}{A} \right)^2 \right] + c_3 A^{\frac{2}{3}} + \frac{3}{5} \left( \frac{e^2}{r_0} \right) \frac{Z^2}{A^{\frac{1}{3}}}, \quad \dots\dots (1)$$

where  $c_1, c_2, c_3$  are constants,  $N$  is the number of neutrons,  $A-Z$ , and  $r_0$  is the radius of the sphere whose volume is that occupied by one nucleon, viz.

$$r_0 = (\text{radius of nucleus})/A^{\frac{1}{3}}.$$

$r_0$  is observed to be approximately constant, and is taken to be exactly so in equation (1).

The several terms in the formula have the following significance: The first (if  $c_2$  is neglected) represents the bulk of the "nuclear forces" binding the nucleus. The factor containing  $c_2$  is a correction for disparity in the numbers of neutrons and protons. The second term is a "surface-tension" effect, and the last term represents the electrical energy of repulsion of the protons.

We are chiefly concerned with the parameter  $c_1$ , whose observed value, found by fitting equation (1) to the nuclear energy surface, is to be compared with that predicted theoretically. By extrapolation of equation (1),  $c_1$  may be interpreted as the binding energy per nucleon of an "ideal" nucleus, i.e. an assembly of an infinite number of neutrons and protons in equal proportions, if the electrical repulsion between the protons is removed.  $r_0$  can also be estimated theoretically and compared with the observed value.

For the theoretical analysis the static interaction of Møller and Rosenfeld (Møller and Rosenfeld 1940, Rosenfeld 1945, 1948) is employed. At this point, dimensionless variables, to be used throughout, are introduced, by setting up the following "absolute" units:—

- Unit of mass—mass  $M$  of a nucleon (proton and neutron being assumed equally heavy).
  - Unit of length—range of nuclear force,  $1/\lambda$ ; defined by  $\lambda = \mu c/\hbar$  where  $\mu$  = mass of meson.
  - Unit of angular momentum— $\hbar$ .
- (2)

These yield the derived "absolute" unit:

$$\text{Unit of energy} - Mc^2(\mu/M)^2 = \lambda^2 \hbar^2 / M. \quad \dots (3)$$

Then in these units, any pair of nucleons  $i$  and  $j$  has the mutual potential

$$w_{ij} = (\tau_i \cdot \tau_j) [g^2 + f^2(\sigma_i \cdot \sigma_j)] \exp(-\xi_{ij}) / \xi_{ij}, \quad \dots (4)$$

where  $\sigma_i$  and  $\tau_i$  are the spin and isotopic operators respectively for the  $i$ -th nucleon,  $\xi_{ij}$  is the separation of the nucleons, and  $g$  and  $f$  are interaction constants.

The values of the parameters  $\mu$ ,  $f$  and  $g$  are taken from Fröhlich *et al.* (1947, equation (76)), where they were chosen so as to fit correctly the two lowest energy levels of the neutron-proton system and the ground level of  $H^3$ :

$$\mu = 220 \text{ m.}; \quad f^2 = 0.595; \quad g^2 = 0.258. \quad \dots (5)$$

These make the unit length,  $1/\lambda$ , equal to  $1.75 \times 10^{-13}$  cm.; and the unit of energy equal to 14.4 M.M.U., or 13.4 mev.

The observed values assumed for the quantities  $c_1$  and  $r_0$  of equation (1) are those given by Bethe and Bacher (1936, § 30), viz.  $c_1 = 14.9$  M.M.U. (1.03 in absolute units),  $r_0 = 1.48 \times 10^{-13}$  cm. (0.85 in absolute units).

## 2.2. Results

The "ideal" nucleus is subjected in § 3.2 to a variation treatment, on the basis of the Fermi-gas model. This yields a value of the binding energy per nucleon for each initially arbitrarily assumed size of the nucleus. Minimization of the energy with respect to the size yields estimates of both the actual binding energy and the actual size.

In Figure 1 are plotted the expectation values of the kinetic, potential and total

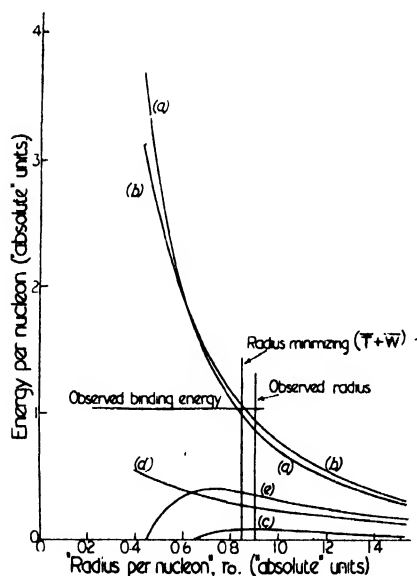


Figure 1. Energies per nucleon calculated on Fermi-gas model, vs  $r_0$ , representing size of nucleus.

(a)  $\bar{T}/A$ ; (b)  $\bar{W}/A$ ; (c)  $(\bar{T} + \bar{W})/A$ ; (d)  $E''/A$ ; (e)  $(\bar{T} + \bar{W} + E'')/A$ .

The kinetic energy  $\bar{T}/A$  (curve (a)) and potential energy  $\bar{W}/A$  (curve (b)) almost cancel. The maximum binding energy  $-(\bar{T} + \bar{W})/A$  by the variation (first order perturbation) method is far below the observed value: the radius  $r_0$  which minimizes  $(\bar{T} + \bar{W})$  is in good agreement with the observed value.

The second order perturbation energy  $E''/A$  (curve (d)), when added to  $(\bar{T} + \bar{W})/A$  (curve (e)), raises the binding energy considerably, but it is still well below the observed value for all  $r_0$ .

energies (curves  $a, b, c$ , respectively) per nucleon as functions of  $r_0$ , the "radius per nucleon". At the minimum of the total energy it is found that the kinetic energy per nucleon  $= \bar{T}/A = 0.97$ , the potential energy per nucleon  $= \bar{W}/A = -1.06$ , and therefore total energy per nucleon  $= -0.09$ . (All energies are expressed in the absolute units of equation (3)). The binding energy is thus of a smaller order of

magnitude than the value 1.03 required, as in the case of similar calculations previously carried out with different forms of interaction (Bethe and Bacher 1936, p. 157, Rosenfeld 1948). The minimizing radius  $r_0$  is equal to 0.90 (in the absolute unit of equations (2)), which compares well with the observed value 0.85.

Although the binding energy obtained is so small, it may be noted that a quite moderate increase in the strength of the potential would increase it rapidly, because the potential and kinetic energies under the assumed conditions almost cancel.

The second order perturbation calculation, which is carried out in §3.3, yields a term  $E''$  to be added to the former energy  $(\bar{T} + \bar{W})$ . The energy is again found for variable size of the nucleus; although perturbation theory does not strictly prescribe what size will give the best prediction for the energy  $(\bar{T} + \bar{W} + E'')$ , the minimum of the latter quantity with respect to size was taken as being probably as good as any. However, there seems no reason in principle why the corresponding minimizing radius  $r_0$  yielded by the second order calculation should be any better as an approximation to the actual radius than that yielded by the variation calculation. The latter has therefore been retained as the theoretical prediction of the radius  $r_0$ .

Graphs of  $E''/A$  and the total energy  $(\bar{T} + \bar{W} + E'')/A$  are shown in Figure 1, curves (d) and (e). It will be seen that  $|E''|$  is much larger than  $|\bar{T} + \bar{W}|$  at all radii, indicating that the variation treatment is extremely poor. The minimal value of the total energy per nucleon is found to be  $-0.41$ . This is much better than before, but still falls far short of the required value  $-1.03$ . This second result, then, indicates that the Møller-Rosenfeld interaction is too weak for the binding of heavy nuclei, but it is not clear how much in error the calculation still may be.

If the second order calculation is tentatively accepted as substantially correct, one may investigate what slight modifications to the nuclear force could yield the observed binding. Two possibilities are considered. Firstly, the interaction effective in heavy nuclei may differ from that in light, owing to "many-body" forces. To represent this effect the magnitude of the potential has been increased, the parameters  $f$  and  $g$  of equation (4) being varied in the same proportion, while the meson mass, and hence  $1/\lambda$ , are left unaltered. The resulting energy per nucleon in an "ideal" nucleus, taken to be the minimum of  $(\bar{T} + \bar{W} + E'')/A$  with respect to variation of size of the nucleus, is plotted against  $f^2$  in Figure 2, curve (a). It will be seen that  $f^2$  requires to be raised from the assumed value of 0.595 to 0.73—approximately 25% increase—to yield the observed binding. The corresponding predicted size of the nucleus, given by the  $r_0$  which minimizes  $(\bar{T} + \bar{W})$ , is plotted against  $f^2$  in Figure 2, curve (b). When  $f^2$  is raised sufficiently to yield the correct binding,  $r_0$  falls to 0.65, only about 75% of the observed value 0.85. Thus if many-body forces are invoked to account for the binding energy, the agreement regarding the size of the nucleus deteriorates.

Secondly, the interaction can be altered so as to yield the correct binding energy per nucleon in an "ideal" nucleus, by making this one of the quantities by which the parameters of the interaction (equation (4)) are fixed. The interaction can then be compatible with only two at most of the three quantities pertaining to light nuclei, by which the parameters were fixed by Fröhlich *et al.* (1947): the two lowest levels of the neutron-proton system have been retained, while the ground-state energy of  $H^3$  was abandoned. By fitting the two former quantities,  $f^2$  and  $g^2$

were calculated approximately for each value of the meson mass  $\mu$ , a method differing only slightly from that of Fröhlich *et al.* (1947, §3) being employed. Then for each meson mass the binding energy per nucleon of an "ideal" nucleus was calculated, as shown in Figure 3, curve (a). Again, the minimum of  $(\bar{T} + \bar{W} + E'')$  with respect to size of the nucleus was taken. It is found that to obtain the observed binding energy the mass of the meson required is  $400m$ . The values of  $f^2$  and  $g^2$  appropriate to this meson mass are  $f^2 = 0.60$ ,  $g^2 = 0.11$ .

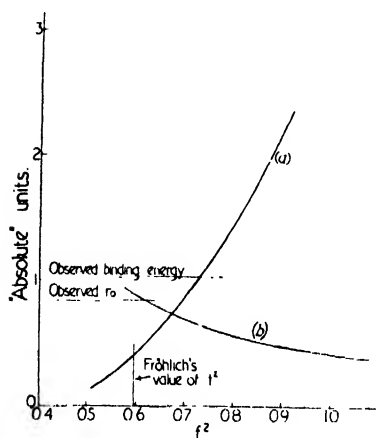


Figure 2. Effect of postulated "many-body" forces: change of binding energy and size of nucleus with effective nuclear-force parameter  $f^2$ . Curve (a): Binding energy per nucleon by second order perturbation calculation, i.e.  $(-1) \times$  minimum of

$$(\bar{T} + \bar{W} + E'')/A.$$

Curve (b): Radius  $r_0$  which minimizes the variation energy  $(\bar{T} + \bar{W})$ .

To obtain observed binding energy,  $f^2$  has to be raised from given value 0.595 to 0.73: the radius  $r_0$  then falls to 0.65 (observed value 0.85).

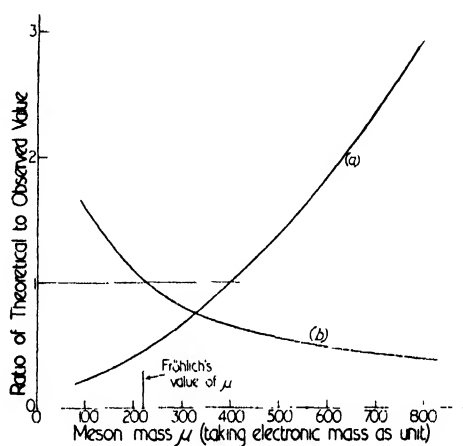


Figure 3. Predictions for heavy nucleus, when meson mass is variable, and interaction parameters are chosen to fit two observed constants of neutron-proton system.

Curve (a): Binding energy per nucleon by second order perturbation calculation, i.e.  $(-1) \times$  minimum of  $(\bar{T} + \bar{W} + E'')/A$ .

Curve (b): Radius  $r_0$  which minimizes the variation energy  $(\bar{T} + \bar{W})$ .

To obtain observed binding energy, mass of meson must be  $400m$ :  $r_0$  then falls to 67% of observed value.

Together with each binding energy is found a prediction of the size of the nucleus (the value of  $r_0$  minimizing  $(\bar{T} + \bar{W})$ ), which is shown plotted in Figure 3, curve (b). When the meson mass is  $400m$ ,  $r_0$  is only 67% of the observed value. Thus, again, fitting of the binding energy is incompatible with correct nuclear size.

### § 3. CALCULATION OF THE BINDING ENERGY

#### 3.1. Use of the Fermi-gas Model

On this model the nucleus is treated in the lowest approximation as an assembly of non-interacting particles, enclosed in a box at zero potential, with high potential walls. If the nucleons—neutrons and protons alike—are described by space, spin and isotopic coordinates, then the exclusion principle requires the wave function to be antisymmetric with respect to interchange of all the coordinates of any pair of particles. Suitable antisymmetric wave functions for the system may be built up in determinantal form from different individual wave functions for single

particles. The composite wave functions so obtained will be approximate eigenfunctions for the system, provided the individual wave functions are given by

$$\Psi_r = \psi_l \omega_\mu. \quad \dots\dots (6)$$

$\psi_p$  is a function of the space coordinates only, zero outside the box, and

$$\psi_l = (8L^3)^{-1/4} \exp(i(\mathbf{k}_l \cdot \boldsymbol{\xi})) \quad \dots\dots (7)$$

inside the box. Here  $2L$  is the length of the sides of the cube constituting the box,  $\boldsymbol{\xi}$  is the space-coordinate of the particle concerned,  $\mathbf{k}_l$  is the dimensionless momentum, quantized by the condition

$$\mathbf{k}_l = \mathbf{n}_l \pi / L, \quad \dots\dots (8)$$

where  $\mathbf{n}_p$  is any vector whose components are all integers.  $\omega_\mu$  in equation (6) is one of the four spin and isotopic wave functions:

$$\omega_1 = \alpha \xi, \quad \omega_2 = \beta \xi, \quad \omega_3 = \alpha \eta, \quad \omega_4 = \beta \eta, \quad \dots\dots (9)$$

where  $\alpha$  and  $\beta$  are the Pauli spin wave functions, and  $\xi$  and  $\eta$  are similar for the isotopic coordinates.

To represent the ground state of the system, the composite wave function is built up of the  $A$  individual wave functions  $\Psi_r$  of lowest momentum  $k_l$ . For the "ideal" nucleus considered, the  $A/4$  spatial wave functions  $\psi_l$  of lowest momentum are associated each in turn with all four  $\omega_\mu$ .

The Fermi-gas model described has now to be used to calculate the ground-state energy of the system of nucleons with nuclear interactions operative.

In §3.2 a variation calculation is performed, using the ground-state wave function of the model, together with the Hamiltonian of the "ideal" nucleus, to find

$$E = \bar{T} + \bar{W}, \quad \dots\dots (10)$$

where  $\bar{T}$  is the expectation kinetic energy, and  $\bar{W}$  the expectation potential energy. This is carried out initially for arbitrary dimension  $L$  of the box.

A perturbation approach is adopted in §3.3. Here the Fermi-gas of non-interacting particles is taken as an unperturbed system and the nuclear interaction  $W$  is applied as perturbation. The unperturbed energy is the kinetic energy  $\bar{T}$ , and the first order perturbation energy is  $\bar{W}$ , both already calculated. The second order approximation adds an energy  $E''$ , given by

$$E'' = - \sum_R' |W_{0R}|^2 / (E_R^0 - E_0^0); \quad \dots\dots (11)$$

where the suffix  $R$  indicates the  $R$ th unperturbed state and the suffix 0 the ground state.  $\sum'$  indicates summation over all states but the ground state, obtained by building the composite wave function from all possible combinations of different individual wave functions. The size chosen for the box is again initially arbitrary. The index 0 on the energy indicates the unperturbed kinetic energy of the state concerned.

### 3.2. Variation Method

The expectation kinetic energy  $\bar{T}$  is first calculated. In the dimensionless variables employed, it is found that

$$\bar{T} = -\frac{1}{2} \int \Phi^* \left( \sum_{s=1}^A \nabla_s^2 \right) \Phi dq = \frac{1}{2} \sum_{\text{states}} k_l^2, \quad \dots\dots (12)$$

where  $\Phi$  is the ground-state wave function of the Fermi-gas model and  $\int dq$  indicates integration or summation over all coordinates. The individual spatial states occupied form a lattice in  $\mathbf{k}$  space, with a spacing  $\pi/L$  (cf. equation (8)). The occupied points, each four times occupied, are all those points falling within a sphere of radius  $a$ , given by

$$a = \frac{A^{\frac{1}{3}}}{2L} \left( \frac{3}{2} \pi^2 \right)^{\frac{1}{3}} = \frac{(9\pi)^{\frac{1}{3}}}{r_0}. \quad \dots\dots(13)$$

The sum in (12) can approximately be replaced by an integral in  $\mathbf{k}$  space, evaluation of which yields

$$\bar{T}/A = 3a^2/10. \quad \dots\dots(14)$$

The expectation potential energy is next found, using for the potential operator  $\sum_{i < j} w_{ij}$ , where  $w_{ij}$  is given by (4), and the same wave function  $\Phi$ . The result is

$$\bar{W} = \frac{1}{2} \sum_{r,s} [(rs|w|rs) - (rs|w|sr)], \quad \dots\dots(15)$$

where, for instance,

$$(rs|w|rs) = \int \Psi_r^*(1) \Psi_s^*(2) w_{12} \Psi_r(1) \Psi_s(2) dq_1 dq_2$$

and the sum takes  $r$  and  $s$  over all occupied individual-nucleon states.

The matrix elements involved may be split into spatial and non-spatial parts if we write (cf. (4))

$$\Gamma_{ij} = (\tau_i \cdot \tau_j) [g^2 + f^2 (\sigma_i \cdot \sigma_j)]; \quad v_{ij} = \{\exp(-\xi_{ij})\}/\xi_{ij}, \quad \dots\dots(16)$$

so that (15) becomes

$$\bar{W} = \frac{1}{2} \left\{ \left[ \sum_{\mu, \nu=1}^4 (\mu\nu | \Gamma | \mu\nu) \right] \left[ \sum_{l,m} (lm | v | lm) \right] - \left[ \sum_{\mu, \nu=1}^4 (\mu\nu | \Gamma | \nu\mu) \right] \left[ \sum_{l,m} (lm | v | ml) \right] \right\}. \quad \dots\dots(17)$$

$\mu, \nu$  are non-spatial, and  $l, m$  are spatial quantum numbers (cf. equation (6)), the latter to be summed over the occupied sphere in  $\mathbf{k}$  space. The first, non-exchange, term vanishes, on account of the non-spatial factor, in conformity with the saturation requirements of nuclear forces (Rosenfeld 1948, chap. XI). Towards the evaluation of the remaining exchange term, it is found that

$$\sum_{\mu, \nu=1}^4 (\mu\nu | \Gamma | \nu\mu) = 12(g^2 + 3f^2), \quad \dots\dots(18)$$

and

$$(lm | v | ml) = \frac{\pi}{2L^3} \frac{1}{1 + |\mathbf{k}_l - \mathbf{k}_m|^2}. \quad \dots\dots(19)$$

The sum over  $l, m$  in (17) is replaced by a double integral in  $\mathbf{k}$  space, leading to the final result

$$\bar{W}/A = -(9/8\pi)(g^2 + 3f^2)\Omega_1(a),$$

where

$$\Omega_1(a) = 2 \left[ \frac{1}{2a} + \frac{1}{3(2a)^3} \right] \ln(1 + (2a)^2) + \left( 2a - \frac{2}{3} \frac{1}{2a} \right) - \frac{8}{3} \tan^{-1}(2a). \quad \dots\dots(20)$$

The kinetic and potential energies of equations (14) and (20) are plotted against  $r_0$  in Figure 1, curves (a) and (b), for the values of  $f^2$  and  $g^2$  given in equation (5).

## 3.3. Second Order Perturbation

The second order contribution to the energy (equation (11)) requires evaluation of the matrix element  $W_{0R}$  for each excited, unperturbed state  $R$ . The only states giving non-zero contributions are those built up from a set of individual wave functions  $\Psi_r$ , and differing only by one or two constituents from the set constituting the ground state; and of these, the only ones which may not be neglected are those obtained from the ground state by replacing two individual wave functions  $\Psi_r, \Psi_s$  by two others  $\Psi_{r'}, \Psi_{s'}$  satisfying a "conservation of momentum" condition

$$\mathbf{k}_l + \mathbf{k}_m = \mathbf{k}_{r'} + \mathbf{k}_{s'}, \quad \dots\dots(21)$$

where  $l, m$  etc. are the spatial quantum numbers pertaining to the individual states  $r, s$ , etc. respectively (cf. equation (6)). Development of (11) then yields

$$E'' = - \sum_{r,s} \sum'_{r',s'} \frac{|(rs|w|r's')|^2 - (rs|w|r's')^*(rs|w|s'r')}{(k_r^2 + k_{m'}^2) - (k_l^2 + k_m^2)}. \quad \dots\dots(22)$$

Here  $\sum$  means double summation over all ground-state constituent individual states  $\Psi_r$  and  $\Psi_s$ , and  $\sum'$  means double summation over all the other individual states  $\Psi_{r'}$  and  $\Psi_{s'}$  conforming to the selection rule (21). The spatial and non-spatial factors in the matrix elements are now separated out, as in the previous subsection. The sum over the non-spatial quantum numbers involved is readily carried out, with the result

$$E'' = - \sum_{l,m} \sum'_{l',m'} \frac{A|(lm|v|l'm')|^2 - B(lm|v|l'm')^*(lm|v|m'l')}{(k_l^2 + k_{m'}^2) - (k_{l'}^2 + k_m^2)}, \quad \dots\dots(23)$$

where  $A = 48(g^4 + 3f^4)$ ,  $B = 12(3f^4 - 6g^2f^2 - g^4)$ . The spatial quantum numbers  $l, m$  are each to be summed over the sphere of radius  $a$  in  $\mathbf{k}$  space; and  $l', m'$  are each to be summed over the space exterior to this sphere, subject to the selection rule (21).

Evaluation of  $(lm|v|l'm')$  yields

$$(lm|v|l'm') = \frac{\pi}{2L^3} \frac{1}{1 + \frac{1}{4}|\mathbf{k}_{l'} - \mathbf{k}_l - \mathbf{k}_{m'} + \mathbf{k}_m|^2}. \quad \dots\dots(24)$$

The sums in (23) may, as usual, be replaced by integrals in  $\mathbf{k}$  space. By an obvious abbreviation, (23) may be written

$$E'' = -(AI - BJ). \quad \dots\dots(25)$$

It has been found possible to evaluate  $I$  but not  $J$ . However, it appears that the intractable term containing  $J$  is negligible; for it readily follows from the form of the integrals that  $I > J > 0$ , and insertion in (23) of the values of  $f^2$  and  $g^2$  given in (5) shows that  $|A| \gg |B|$ , in fact  $A = 217$ ,  $B = 3.6$ .

Thus neglect of the term  $BJ$  introduces an error of less than 2%. The smallness of the error is to some extent due to fortunate given values of  $f^2$  and  $g^2$ : it may be noted, however, that the form of  $A$  and  $B$  is such that the error could not exceed -25% to +50% for any values of  $f^2$  and  $g^2$  whatever.

Evaluation of  $I$  from (23) and (24) then yields finally

$$E''/A = (-9/2\pi^2)(g^4 + 3f^4)\Omega_2(a),$$



where

$$\begin{aligned} \Omega_2 = & \ln(1 + (2a)^2) \cdot \left[ \frac{13}{12} - \frac{4}{3} \ln 2 + \frac{1}{4(2a)^2} \right] - \frac{7}{18} + \frac{49}{18} \ln 2 + \frac{5}{6} \ln 2 \cdot \frac{1}{(2a)^2} \\ & + \cot^{-1}(2a) \left[ 2a - \frac{2}{3} \frac{1}{2a} \right] + \left[ \frac{1}{2}(2a) + \frac{1}{2a} + \frac{1}{2} \frac{1}{(2a)^3} \right] \int_0^{\tan^{-1}(2a)} \ln(2 \cos x) dx \\ & + 2 \left[ 1 + \frac{1}{3} \frac{1}{(2a)^2} \right] \int_0^1 \frac{\ln(1-x^2)}{x^2 + (2a)^2} dx - \frac{8}{3} (2a)^2 \int_0^1 \frac{\tanh^{-1} x}{x(x^2 + (2a)^2)} dx. \quad \dots\dots (26) \end{aligned}$$

This is plotted against  $r_0$  in Figure 1, curve (d), for the  $f^2$  and  $g^2$  of equation (5).

#### § 4. CRITICISM OF CALCULATIONS

The argument has proceeded by the three following stages, each of which requires to be examined: (i) by a semi-empirical approach, based on equation (1), the binding energy per nucleon of an "ideal" nucleus has been determined; (ii) the parameters in the nuclear force employed have been chosen to fit certain properties of light nuclei; (iii) the nuclear force has been used to calculate approximately the binding energy per nucleon of an "ideal" nucleus, for comparison with the result of (i).

The procedure of the first stage is well known, and an extensive literature (e.g. Bethe and Bacher 1936, § 30, Mattauch and Flüge 1942, p. 90, Feenberg 1947) establishes that the results obtained for the "ideal" nucleus can be relied upon to the accuracy relevant here.

Stage (ii) was carried out by Fröhlich *et al.* (1947), and is again probably sufficiently accurate as a basis for the present calculations.

Stage (iii) concerns the accuracy of the approximate solutions of the Schrödinger equation. The inadequacy of the variation calculation is palpable, in view of the relative largeness of the second order perturbation result. As regards the latter, it may be noted that, even if high order perturbation energies were calculated, and if they converged, the Fermi-gas model could only yield the energy of the system of particles when enclosed in a box of the assumed size, with infinitely high walls. The method is thus best considered as an approximation to a solution for the nucleus so immured. For each order of perturbation, the best energy would be taken as the minimum with respect to variation of the size of the box. From this viewpoint, three orders of perturbation energy have been obtained, viz.  $\bar{T}$ ,  $\bar{W}$  and  $E''$ . The only available criterion of the goodness of the approximation is the rate of apparent convergence of these terms; per nucleon, they are in order (for the interaction parameters assumed, and at the radius which minimizes their sum) 1.35, -1.41, -0.35 (sum = -0.41) (in absolute units). These figures might suggest inception of convergence, but only at a slow rate.

#### § 5. SVARTHOLM VARIATION-ITERATION METHOD

The method developed by Svartholm (1945) has been used by him to investigate the ground states of the lightest nuclei, and its application to heavier nuclei seemed worth considering. It is found, however, that the method loses its usual advantage of assured convergence in such an application; and in practice a calculation with the Fermi-gas model has yielded no useful results.

The convergence question will be dealt with first. Reference should be made to Svartholm's thesis (1945) for an account of the method, but it may be remarked

here that by an iteration procedure one may obtain in principle a succession of approximations  $\Lambda_0, \Lambda_1, \dots$  to the eigenvalue  $\Lambda$  of the interaction constant required to yield a given binding energy. A virtue of the method is that, subject to certain conditions, the series of approximations  $\Lambda_0, \Lambda_1, \dots$  decreases monotonically towards the required eigenvalue. One of those conditions, however, is that the potential function  $u$  should be "negative definite", i.e. for any arbitrary wave function  $\Phi$ ,  $\int \Phi^* u \Phi dq \leq 0$ . Now one requirement of a nuclear force suitable for heavier nuclei is that it shall lead to the "saturation" phenomenon (Rosenfeld 1948, chap. XI), and it can be shown very generally that this implies that the potential shall *not* be negative definite. Thus for such a force, there is in general no assurance of the convergence of the series of approximations.

Nevertheless, the author has made a calculation with the method, using as initial wave function the Fermi-gas function of § 3.1. The zero-order calculation yielding  $\Lambda_0$ , is then simply equivalent to the variation treatment of § 3.2.  $\Lambda_1$  was next calculated, only leading terms with respect to powers of  $A$  being retained. The result found was that, quite generally, for any type of saturating short-range potential,  $\Lambda_1$  is identically the same as  $\Lambda_0$ . Thus to this order, the Svartholm treatment gives no improvement over the variation treatment.

#### ACKNOWLEDGMENT

The author is happy to express his sincere thanks to Dr. H. Fröhlich, who suggested this subject, and has been unsparing of advice and encouragement.

#### REFERENCES

- BETHE, H. A., and BACHER, R. F., 1936, *Rev. Mod. Phys.*, **8**, 82.  
 EULER, H., 1937, *Z. Phys.*, **105**, 553.  
 FEENBERG, E., 1947, *Rev. Mod. Phys.*, **19**, 239.  
 FRÖHLICH, H., HUANG, K., and SNEDDON, I. N., 1947, *Proc. Roy. Soc. A*, **191**, 61.  
 MATTAUCH, J., and FLÜGGE, S., 1942, *Kernphysikalische Tabellen* (Berlin : Springer).  
 MØLLER, C., and ROSENFELD, L., 1940, *K. Dansk. Vidensk. Selsk. mat.-fys. Meddel.*, **17**, no. 8.  
 ROSENFELD, L., 1945, *K. Dansk. Vidensk. Selsk. mat.-fys. Meddel.*, **23**, no. 13 ; 1948, *Nuclear Forces* (Amsterdam : North Holland).  
 SVARTHOLM, N., 1945, *Thesis*, Lund.

## REVIEWS OF BOOKS

*Practical Five-figure Mathematical Tables*, by C. ATTWOOD. Pp. v+74. (London : Macmillan and Co. Ltd., 1948.) 3s.

The publication of this set of tables is an event of more importance than would at first meet the eye. The first mathematical tables were naturally of many figures, and then, in the nineteenth century, logarithmic and trigonometric tables settled down to seven figures as the norm. Towards the end of the century, and for the first part of the twentieth, the value of four-figure tables for the scientist was realized, and many a set was issued. With them, were a few six-figure sets and a fair number of five-figure ones. But their compilers followed each other rather monotonously, and seldom introduced real innovations, except for a few impracticable ones. The present reviewer, for example, has (or has lent and lost), more than a dozen different books of four or five figure compilations, most of them indistinguishable from each other.

The difference that marks this, and that ought to make it very widely known and used, is that the author has thought out afresh what functions are wanted, at what intervals they should be tabulated, and the most convenient means for interpolation in them.

His choice of functions does not in fact offer any surprises. There are no transcendental functions such as we find in Dale's five-figure tables, or in Jahnke and Emde, but a generous selection of those likely to be wanted in an all-purpose compilation. Logarithms and anti-logarithms, the six trigonometric functions, both natural and logarithmic, for degrees and minutes, we may take for granted. In addition, Mr. Attwood gives us logarithms of reciprocals (to save subtraction) and trigonometric functions of angles given in radians; he also tabulates squares and square roots, cubes and cube roots, the fourth and fifth roots of integers to 100, and the exact values of powers up to the sixth of integers from 1 to 100, as well as reciprocals. Then there are natural logarithms and exponential functions and (a concession to engineers?) the areas of circles.

Logarithms and trigonometrical functions offer difficulties in places, as we all know, where they change rapidly, and there are many ways in use for turning the difficulty. We may use the reciprocal or the function of the complement of the angle, or we may tabulate some function which varies less rapidly, we may vary the interval of the argument, or we may use the inverse function. Mr. Attwood points out, at the appropriate page, when the former expedients are desirable, but in general he relies on the method of changing the interval. This he has done most judiciously. Related to this matter is the question of the use of proportional parts: some five-figure tables give proportional parts in little marginal tables, leaving the user to form his own differences and to take the appropriate proportional parts (the reviewer's favourite five-figure tables, due to Schlömilch, take them to one extra decimal place and indicate whether the tabular entries are in excess or defect, so that there is no loss of accuracy) whilst others give mean proportional parts applicable to a whole line of the table. These are dangerous when the differences change rapidly, and it is not uncommon to give two lines of mean proportional parts, splitting the tabular entries to share them between the two. In the present volume, this device is widely adopted and somewhat extended, so that as many as four lines of mean proportional parts (m.p.p.) may be given to a line of the table. The m.p.p. have been individually examined to get the best compromise, and are printed in red whenever they have to be subtracted. The author asserts that more than 95% of the 160,533 combinations obtainable with the m.p.p. are in error by 0 or 1 unit, only 0.6% leading to errors of more than 3 units. Where there is a danger of error of five units, the m.p.p. are in italics, so that a user can use proper interpolation methods if needed. There is a table showing the maximum possible error in every table, but here the author is unfair to himself. No one could use m.p.p. to stretch across more than half the tabular interval, but should always take differences from the nearest entry. This would reduce the errors in a number of places. Where m.p.p. are not given, the user is instructed to adopt linear or second-difference interpolation, and is given instruction in this, with a critical table of Bessel coefficients, but second differences are never printed as part of the tables.

To close with a few words on general points. The author has varied in his interpretation of five figures. In some tables, it means five decimal places, as in the cosine of  $89^{\circ} 42'$ , which is 0.00524, and sometimes five significant figures, as in the secant of the same angle, which is 190.99. From the latter, with the aid of the table of reciprocals, we may find that the cosine is really 0.0052359, or from the tables of logarithmic cosines and antilogs, we may find it as 0.0052360. In the table of secants, there is a change at  $45^{\circ}$  from five decimal to five significant figures.

The printing is good, and there is a strong limp cloth cover. If any change in a good book might be suggested, it is a thumb index to enable two tables to be used in conjunction more easily. To find out if there are misprints will call for longer use, or for deliberate and systematic examination of differences.

J. H. A.

*Some Aspects of the Luminescence of Solids*, by F. A. KRÖGER. Pp. xii+310.  
(New York and Amsterdam: Elsevier Publishing Co., 1948.) \$5.50 (30s.).

The luminescence of solids is a subject which has benefited much from the development of theoretical conceptions of the solid state during the last fifteen years; perhaps before long we shall see new theoretical ideas arising as a result of new experimental work. The work of the Lenard School during the early years of the century was the most significant in this field, but, unfortunately, the lack of a satisfactory theoretical picture of the behaviour of electrons in solids robbed much of the work of the value it might otherwise have had,

During the last ten years a great deal of attention has been given to the study and understanding of afterglow or phosphorescence phenomena in solids, and there have been notable advances. While to some extent a reasonably satisfactory picture can now be given of these effects, we know little as yet about the nature of luminescence centres and electron traps in solids. These problems in relation to infra-red sensitive phosphors and their properties are particularly important, and it is in this direction that we may hope for new advances.

Dr. Kröger's volume is of a rather special category, in that it is a research monograph and not a comprehensive review of a wide field of work. The volume is based on experimental work carried out in the physics laboratories of the N. V. Philips Gloeilampenfabrieken, Eindhoven, during the last five years, or it may be assumed that it represents a convenient form of publication of work carried out during, and held up by, the war.

The first chapter contains a useful account of energy levels in pure and perturbed crystals, and an attempt is made to develop a general picture capable of covering all possible luminescent effects. Some of us will think that it is a little early for such attempts, but are nevertheless grateful for the setting out of Dr. Kröger's ideas in coherent form.

In the following four chapters the author discusses new experimental results on tungstates, molybdates and phosphors activated by manganese, titanium and uranium. In the final chapter the effect of temperature on the efficiency of luminescence has been considered. The data presented in these chapters will be of value to other workers in the subject, but can hardly be expected to interest a wider audience. The book ends with 36 pages of tabular matter of the kind only too familiar to readers of Vol. XXIII/1 of the *Handbuch der Experimental Physik*. Is it of much scientific value to be told that the luminescence of magnesium orthosilicate is "violet"? Or that the luminescence is "strong" or "weak" or "faint"? I think not: it is time for workers and writers in this field to rid themselves of these older inexact traditions if the subject is to advance as it should. Dr. Kröger's volume is a useful addition to the research literature of the luminescence of solids, and the work described must, for the most part, have been carried out under appallingly difficult conditions.

J. T. RANDALL.

*Electrons and Nuclear Counters*, by S. A. KORFF. Pp. xi+212. (New York and Toronto: D. Van Nostrand Co. Inc., 1947; British Agents: Macmillan and Co. Ltd., London.) 18s. net.

Until a few years ago, an aura of mystery surrounded the mode of operation of a Geiger-Müller counter and it was regarded as an erratic device which had to be made according to some favourite "cookery-book" recipe. Recent advances in our knowledge of the discharge mechanism in these counters has done much to clarify the situation so that they are now standard tools for work on nuclear physics and are being satisfactorily manufactured commercially. There has been a deeply felt need for a book giving an up-to-date account of the state of the subject and Professor Korff is to be congratulated upon a pioneer effort on these lines.

It should perhaps be stated at the outset that he has produced a survey suitable for the student and general reader rather than a work of reference for the specialist. The book opens with an introductory chapter describing the different modes of operation of an ion counter, that is, its use as an ionization chamber, proportional counter or Geiger-Müller counter. The next three chapters, which form the main body of the book, discuss each of these modes of operation in more detail, the main stress being laid on the Geiger-Müller region. The fundamental principles involved are well brought out and a good general account is given of the discharge which occurs in the gas of the counter and of the various factors which influence it. Unfortunately this account suffers from a rather poor arrangement of the material so that there is a considerable amount of repetition and frequent and very irritating references forward to matters dealt with subsequently.

In chapter five, the author gives a very clear account of the principles and procedure involved in the practical construction of counters. He has dealt only with the cylindrical cathode, axial-wire anode type of counter. Sections dealing with other types, such as point counters and parallel plate ionization chambers would have been valuable additions. There

follows a brief chapter on the errors and corrections involved in counting. The treatment is rather sketchy and can only be regarded as a general introduction to the subject. The final chapter deals with some of the auxiliary electronic circuits employed in conjunction with counters. This constitutes a very extensive subject in itself, so that, in the space at his disposal, the author has been able to give only a very brief outline of the types of circuits which can be employed. The book also includes a fairly comprehensive list of references to original papers on ion counters. Summing up, Professor Korff's book can be recommended to those readers who want a good general introduction to the behaviour of ion counters.

J. L. MICHIELS.

*Theoretical Aerodynamics*, by L. M. MILNE-THOMSON, M.A., F.R.S.E. Pp. xx+363. (London: Macmillan & Co., 1948.) 40s.

The purpose for which this book is written is to give a sound mathematical basis of theoretical aerodynamics on which applications to practical problems of aircraft design and flight must rest and to state clearly the underlying assumptions of the mathematical theory so that there is no uncertainty on what can legitimately be deduced from the assumptions as a first approximation.

The book has 19 chapters. Chapters I and II are introductory and concerned mainly with general features of fluid motion. Chapters III to XII and Chapter XIV deal in a commendable manner with well-known subjects of theoretical aerodynamics, namely two-dimensional motion, rectilinear vortices, the properties of two-dimensional airflow past a circular cylinder, Joukowski's transformation theory of two-dimensional aerofoils, thin aerofoils, induced velocity, aerofoils of finite aspect ratio, lifting-line theory, lifting-surface theory and wind-tunnel corrections. The treatment of the mathematical theorems and of the illustrative applications chosen is made as simple as possible to help a reader whose mathematical knowledge does not extend much beyond the elements of the differential and integral calculus. The appeal which the selected applications make to an aerodynamicist familiar with the subject will depend on the extent to which his needs have been appreciated by the author: but the illustrations chosen give clues for the solution of related applications.

Chapter XV on subsonic and supersonic flow serves as an introduction to a subject on which a great deal of theoretical investigation has been made during recent years. Present knowledge on the mathematical theory of compressible flow is sufficient to provide subject matter for a complete book: it is not to be expected that it could be treated adequately in a single chapter. Chapter XIII and Chapters XVI-XVIII on propellers, simple flight problems, moments and aircraft stability respectively are limited in scope but suffice to give a student an insight into some theoretical problems related to the performance and behaviour of aircraft. Chapter XIX is well worth inclusion for the benefit of a reader who has little or no acquaintance with vector methods of presentation.

Exercises for a student are given at the end of each chapter: lists of references to relevant papers are unfortunately not given. It is perhaps surprising that a chapter on the mathematical theory of boundary-layer flow is not included.

The book fulfils the purpose for which it was written: it can be recommended as a good introduction to theoretical aerodynamics.

A. FAGE.

## CONTENTS FOR SECTION B

	PAGE
Editorial . . . . .	1
Dr. G. D. WASSERMANN and Dr. E. WOLF. On the Theory of Aplanatic Aspheric Systems . . . . .	2
Dr. W. EHRENBERG and Mr. R. E. SIDAY. The Refractive Index in Electron Optics and the Principles of Dynamics . . . . .	8
Dr. H. H. HOPKINS. The Disturbance near the Focus of Waves of Radially Non-Uniform Amplitude . . . . .	22
Dr. R. F. BARROW and Mr. E. F. CALDIN. Some Spectroscopic Observations on Pyrotechnic Flames . . . . .	32
Mr. A. A. JAFFE, Dr. J. D. CRAGGS and Mr. C. BALAKRISHNAN. Some Experiments on Photo-ionization in Gases . . . . .	39
Mr. G. C. WILLIAMS, Dr. J. D. CRAGGS and Mr. W. HOPWOOD. The Excitation and Transport of Metal Vapour in Short Sparks in Air . . . . .	49
Dr. A. VAN ITTERBEEK and Dr. W. VAN DONINCK. Measurements on the Velocity of Sound in Mixtures of Hydrogen, Helium, Oxygen, Nitrogen and Carbon Monoxide at Low Temperatures . . . . .	62
Dr. A. SCHALLAMACH. Ultrasonic Dispersion in Organic Liquids . . . . .	70
Reviews of Books . . . . .	77
Contents for Section A . . . . .	79
Abstracts for Section A . . . . .	79

## ABSTRACTS FOR SECTION B

*On the Theory of Aplanatic Aspheric Systems*, by G. D. WASSERMANN and E. WOLF.

**ABSTRACT.** Methods are described for the design of two aspheric surfaces for any given centred system, so as to achieve exact aplanatism. The practical application of the methods is illustrated by the design of a reflecting microscope.

*The Refractive Index in Electron Optics and the Principles of Dynamics*, by W. EHRENBERG and R. E. SIDAY.

**ABSTRACT.** In view of mis-statements made in the literature, the origin of the refractive index in electron optics is discussed in some detail, and the uniqueness of an expression previously given is demonstrated. On this basis, some general properties of electron optics are investigated.

A relation between ray direction and wave normal is obtained. Whereas the refractive index is unique in terms of the magnetic vector potential  $\mathbf{A}$ , this itself is arbitrary to some extent. It is shown that  $\mathbf{A}$  must, for purposes of electron optics, be chosen so as to satisfy Stokes' theorem and that, if it does, no observable effects result from the arbitrariness of  $\mathbf{A}$ . An expression for the optical path difference is given in terms of the magnetic flux enclosed. The results are applied to a number of questions, viz. the differential equations for trajectories, the focusing properties of an axially symmetric field and the interference pattern produced by two converging bundles of rays which enclose a magnetic flux.

*The Disturbance near the Focus of Waves of Radially Non-Uniform Amplitude*, by H. H. HOPKINS.

**ABSTRACT.** Lommel's problem, the disturbance near the focus of waves of uniform amplitude, is generalized to consider waves of radially non-uniform amplitude. Lommel's numerical results are extended, and his  $U$  and  $V$  functions, tabulated on a new basis, together with some new related functions, are employed to provide extensive intensity distribution curves for the diffracting patterns associated with waves of both uniform and non-uniform amplitude.

*Some Spectroscopic Observations on Pyrotechnic Flames*, by R. F. BARROW and E. F. CALDIN.

**ABSTRACT.** The results of a spectroscopic study of the white or coloured flames from typical pyrotechnic compositions are reported. Most of the visible light from these sources comes from a limited number of atomic or diatomic emitters. The effects of secondary emitters on the dominant wavelength, colorimetric purity and relative intensity are considered in general terms and some suggestions for improving the quality of the flames are put forward.

*Some Experiments on Photo-ionization in Gases*, by A. A. JAFFE, J. D. CRAGGS and C. BALAKRISHNAN.

**ABSTRACT.** From an investigation of the discharge spread in Geiger counters filled with hydrogen, neon, argon or helium, it is possible to show that in certain circumstances the discharge spread is due almost entirely to photo-ionization in the gaseous counter filling. The results enable the absorption coefficients of the operative radiations to be found.

*The Excitation and Transport of Metal Vapour in Short Sparks in Air*, by G. C. WILLIAMS, J. D. CRAGGS and W. HOPWOOD.

**ABSTRACT.** The paper describes a study of the excitation temperature in certain spark discharges of accurately known current characteristics. The excitation temperatures are found by measuring intensity ratios for certain spectral lines where the relevant transition probabilities are known, and are compatible with earlier work by Ornstein and his collaborators on arc discharges.

The excitation temperatures are, as would be expected, higher than those generally found for arc conditions.

Certain peculiarities relating to the evaporation of electrode metal are described. In particular the presence of discontinuous evaporation was noticed, and it was found that different electrode metals showed considerable variations in their behaviour in this respect.

*Measurements on the Velocity of Sound in Mixtures of Hydrogen, Helium, Oxygen, Nitrogen and Carbon Monoxide at Low Temperatures*, by A. VAN ITTERBEEK and W. VAN DONINCK.

**ABSTRACT.** Values of the velocity of sound in  $H_2-N_2$ ,  $H_2-O_2$ ,  $H_2-CO$ ,  $He-N_2$ ,  $He-O_2$  mixtures of varying proportions have been determined by experiment and compared with the theoretical values. Curves showing the variation of sound velocity with the pressure of the mixtures for different temperatures (65° K. to 90° K.) are given.

*Ultrasonic Dispersion in Organic Liquids*, by A. SCHALLAMACH.

**ABSTRACT.** The sound velocities  $v$  have been measured, at frequencies  $f$  between about 700 and 3,000 kc/s., and at temperatures between about  $\pm 15^\circ$  and  $-80^\circ$  C., of the following liquids: geraniol, di-dihydrocitronellyl ether, castor oil and iso-butyl alcohol. There is evidence of a positive dispersion ( $\partial v / \partial f > 0$ ) in the first three liquids at low temperatures. A negative dispersion has been observed in geraniol and di-dihydrocitronellyl ether at higher temperatures, and in iso-butyl alcohol over the whole temperature range.

The positive dispersions are discussed on the basis of the classical hydrodynamic theory, and the implications of a complex viscosity are examined.

# THE PROCEEDINGS OF THE PHYSICAL SOCIETY

## Section A

VOL. 62, PART 2

1 February 1949

No. 350 A

### The Size-Variation of Resistivity for Mercury and Tin

By E. R. ANDREW

Royal Society Mond Laboratory, Cambridge

*Communicated by D. Shoenberg; MS. received 8th September 1948*

**ABSTRACT.** Measurements have been made of the low temperature resistivity of mercury wires down to  $6\mu$  diameter and of rolled tin foils down to  $3\mu$  thickness. A continuous increase of resistivity with decrease of diameter and thickness was found, and it is concluded that this was due to a shortening of the mean free path of the conduction electrons by inelastic collision with the boundary surfaces of the metal. The theory of this effect for a wire is examined; a rigorous theory for a foil already exists (Fuchs 1938). By comparing the experimental results with the theory, values of the product  $lp$  are found for both metals; ( $l$  is the mean free path and  $\rho$  the resistivity for the metal in bulk). These values of  $lp$  are in satisfactory agreement with those obtained from Pippard's measurements on the anomalous skin effect for the two metals.

#### § 1. INTRODUCTION

IN the course of attempts to extend the scope of the investigation on the intermediate state of superconductors (Andrew 1948) to specimens of smaller dimensions, a number of mercury wires down to  $6\mu$  diameter and rolled tin foils down to  $3\mu$  thickness were prepared: in this paper the results of resistance measurements on these specimens in the normal state are described. It had been noticed in the previous work that the normal resistivity increased with decrease of diameter. J. J. Thomson (1901) first suggested that inelastic boundary collisions of conduction electrons in a metal might cause a reduction in mean free path and thus an increase in resistivity; this effect would of course become more pronounced as the dimensions of the conductor are decreased. The effect was found with evaporated metallic films by Hamburger (1931), Lovell (1936) and Appleyard and Lovell (1937), and for wires of small diameter by Eucken and Förster (1934) and Riedel (1937). The lowest temperature used previously was  $14^\circ\text{K.}$ , but at liquid helium temperatures the bulk resistivity of pure metals such as mercury and tin becomes so small that the mean free path is of order  $10^{-2}\text{ cm.}$  and thus the size effects should be noticeable for wires and foils of this order of diameter and thickness. By fitting the experimental results to theoretical relations for the size-dependence, values are obtained for the mean free path of the conduction electrons in the bulk metal.

#### § 2. EXPERIMENTS WITH MERCURY

##### 2.1. *Experimental Details*

The material used was Hilger 11,023, stated by the makers to contain 1 part in  $10^6$  of silver as the only measurable impurity. The wires were made by filling glass capillaries of appropriate bore with liquid metal and freezing them, electrical



connections being made to reservoirs at each end of the capillaries. For diameters greater than  $20\mu$ , a pressure difference of one atmosphere sufficed to overcome surface tension effects, and the specimens were those used for measurements on the intermediate state of superconducting mercury which have already been described (Andrew 1948).

For diameters less than  $20\mu$  additional pressure was applied over one of the reservoirs. A pressurizer designed by A. B. Pippard proved useful for this purpose after various modifications and additions had been made; a section of this pressurizer is shown in Figure 1. Pure mercury was held in the distrene cup F

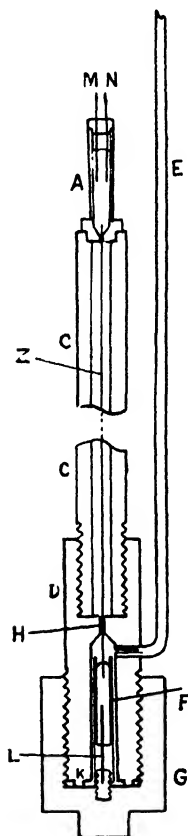


Figure 1.  
Section of pressurizer.

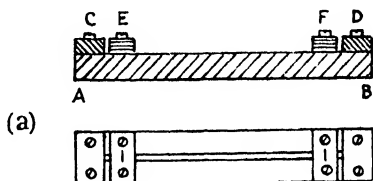


Figure 4.  
(a) Method of mounting tin foils.  
(b) Section of potential clamp.

inside the brass pressure chamber G. The capillary Z, 4–5 cm. in length, was sealed into a fine hole H in the top of the chamber with black wax, its lower end dipping into the mercury. This seal, and also the brass rim K, proved an effective seal up to the highest pressure applied (60 atmospheres). The upper end of the capillary was sealed with distrene cement into a hole in the bottom of another distrene cup A containing mercury. This cup was carried by the hollow cylindrical ebonite spacer C, in which longitudinal slots had been cut to enable ready access of liquid helium to the capillary. Compressed air was applied through the fine bore German silver tube E, by which the pressurizer was suspended in the Dewar flask. The two platinum wires M and N served as current and potential leads to

the mercury in the upper vessel. Only one independent electrical connection could conveniently be made to the lower mercury pool, and was made by the platinum wire L, hard-soldered to the brass, current and potential leads being connected to the outside. The resistance of the mercury in the normal state was sufficiently high for the end effect in the brass to be negligible. The specimens were frozen from the top (low pressure) end first, so that the volume reduction on freezing could be taken up by liquid under pressure, without the thread breaking.

Although the capillary of smallest bore tried,  $2\mu$  diameter, was successfully filled and the thread frozen,  $6\mu$  proved to be the smallest diameter which could be cooled to liquid helium temperatures without the thread breaking. The smaller diameter specimens were annealed for several hours at  $-60^{\circ}\text{C}$ . and cooled slowly thereafter. A sensitive indication of strain is given by the breadth of the temperature transition into the superconducting state which, as the data in Table 1 show, became greater as the diameter was reduced below  $12\mu$ .

The glass capillaries were drawn down from wider tubes and microscope examination showed that the cross-section maintained its circularity after drawing. As the resistivity of the mercury at room temperature is accurately known, resistance served to give the best estimate of wire diameter, provided of course that the specimen cross-section was uniform. As a check, the inside diameter of the capillaries was also examined by immersing them in a liquid of exactly the same refractive index under a cover glass; the correct liquid was found using the mineralogist's Becke line test and box of graded liquids. The inside diameter could then be measured directly at any point along the length of the capillary with a travelling microscope or a calibrated eyepiece.

Resistance was measured with a potentiometer, using the improvements of Kapitza and Milner (1937). Since mercury becomes superconducting, measurements below  $4.17^{\circ}\text{K}$ . were made in a longitudinal field greater than the critical value. The temperature of the liquid helium bath in which the specimens were immersed was determined from the vapour pressure using the 1932 Leiden scale of temperature.

## *2.2. Experimental Results*

The normal resistances of all the wires at  $79^{\circ}\text{K}$ . and at various temperatures in the liquid helium range are given in Table 1, where they are expressed as a fraction of the room temperature (liquid) value. The resistance ratios are plotted in Figures 2 and 3. The full lines are explained in §4. The C series of specimens (Table 1) are those of narrow diameter prepared in the pressurizer, and the B series are those of wider diameter described previously. At  $1.05^{\circ}\text{K}$ . the bulk resistivity was almost entirely independent of temperature and therefore nearly equal to the "residual resistance", while at  $4.2^{\circ}\text{K}$ . it was many times larger and so mostly "ideal resistance". The low value of resistance ratio,  $2.0 \times 10^{-5}$ , for the specimen B6 at  $1.05^{\circ}\text{K}$ . is an indication of the high purity of the material.

Corrections for the magneto-resistance effect and for anisotropy have been made to the measured values before compiling Table 1. For low resistivities such as were obtained with fat specimens at the lowest temperatures, the magneto-resistance effect was quite appreciable, especially as the applied magnetic field required to destroy superconductivity was several hundred gauss; by making measurements over a range of higher fields a fairly accurate extrapolation to zero field could be made.

The resistivity of solid mercury is markedly anisotropic. The ratio of the resistivities parallel and perpendicular to the principal axis is 0.76 (Sckell 1930),

and does not vary appreciably with temperature down to  $82^\circ \text{K}$ ., the lowest temperature investigated by Sckell. At  $79^\circ \text{K}$ ., the ratio of the solid resistivity to the room temperature liquid value is  $5.5 \times 10^{-2}$  for a direction parallel to the principal axis,  $7.2 \times 10^{-2}$  perpendicular, and  $6.6 \times 10^{-2}$  for a random polycrystal. It follows from the figures in Table 1 that the thinnest pressurized specimens are probably monocrystalline with the principal axis approximately perpendicular to the wire axis. In fact, for all but three of the fatter specimens (B1, B2 and the second freezing of B4), the ratio lies between  $7.0$  and  $7.3 \times 10^{-2}$ , suggesting a preference for the crystallites to be oriented with their axes normal to that of the capillary. The three exceptions showed lower ratios, and so presumably had their axes oriented in other directions. Any geometrical effect due to imperfect freezing, such as the formation of cavities, would have produced higher ratios, and hence appears to be absent.

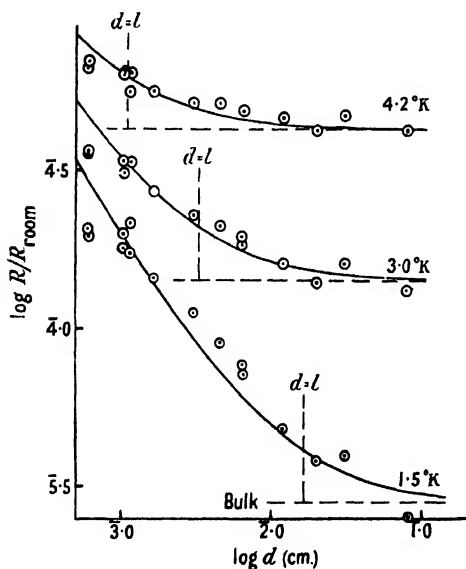


Figure 2.

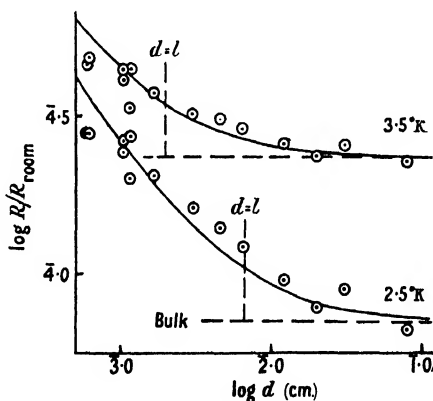


Figure 3.

The resistivity of mercury wires plotted logarithmically against wire diameter  $d$ .

Figure 2, for  $4.2^\circ \text{K}$ .,  $3.0^\circ \text{K}$ ., and  $1.5^\circ \text{K}$ . Figure 3, for  $3.5^\circ \text{K}$ ., and  $2.5^\circ \text{K}$ .

The full lines are the theoretical curves of Fuchs for diffuse scattering (see § 4).

Since all but the three specimens mentioned have approximately the same crystallographic orientation, a correction should be made to bring these three into line. The correction will, however, be necessarily somewhat uncertain since no data are available for the anisotropy of the ideal or the residual resistance of solid mercury at liquid helium temperatures, and moreover, the effect of anisotropy on the extra resistance due to surface collisions is not known. The mean value of the ratio of the resistance at  $79^\circ \text{K}$ . to that at room temperature for all but the three exceptions is  $7.2 \times 10^{-2}$ . For these exceptions the resistances at liquid helium temperatures have been multiplied up in the ratio of  $7.2 \times 10^{-2}$  to the  $79^\circ \text{K}$ . resistance ratio for each specimen. This correction assumes that the anisotropy of resistance is independent of temperature, and in the absence of other information, this is the simplest assumption that can be made. In any case only 3 of the 15 mercury specimens are affected.

The significance of the results is discussed together with those for the thin tin foils in § 4.

Table 1. Resistance Ratios for Mercury Wires. The resistance ratios at liquid helium temperatures have been corrected for anisotropy as explained in the text. This correction has *not* been applied at 79° K.

Specimen (1)	Diam. ( $\mu$ ) (2)	(3)	(4)									
			79	4.2	4.0	3.5	3.0	2.5	2.0	1.5	1.05	
B 6	790	0.013	7.2	4.25	3.60	2.26	1.31	0.67	0.40	0.25	0.20	
B 3	310	0.018	7.1	4.70	4.16	2.60	1.61	0.91	0.53	0.40	0.37	
B 1	200	0.013	6.2	4.20	3.57	2.34	1.39	0.78	0.52	0.38	0.34	
B 2	120	0.013	6.6	4.64	3.98	2.58	1.60	0.96	0.63	0.48	0.42	
B 4*	65	{ 0.020	7.1	4.86	4.22	2.90	1.95	1.25	0.91	0.77	0.73	
		{ 0.016	5.9	4.90	4.15	2.88	1.85	1.22	0.87	0.72	0.69	
C 8	46	0.012	7.3	5.16	4.52	3.10	2.10	1.41	1.06	0.90	0.85	
B 5	30	0.020	7.0	5.18	4.52	3.23	2.29	1.62	1.25	1.12	1.08	
C 7	16.6	0.020	7.0	5.63	5.00	3.72	2.70	2.04	—	1.45	1.43	
C 2	11.6	0.030	7.2	5.60	5.08	3.36	—	2.00	—	1.74	—	
C 4	11.8	0.035	7.0	6.44	5.70	4.40	3.37	2.72	2.30	2.16	2.07	
C 3*	10.5	{ 0.028	7.3	6.50	5.85	4.42	3.39	2.64	2.22	2.00	1.90	
		{ 0.021	7.3	6.38	5.59	4.09	3.10	2.43	1.98	1.80	1.74	
C 5	6.0	0.071	7.3	6.68	6.02	4.62	3.56	2.80	2.30	2.06	1.97	
C 6	6.1	0.047	7.3	6.99	6.35	4.83	3.65	2.79	2.22	1.97	1.81	

(3) Superconducting temperature transition width (° K.) defined as the temperature interval between the 0.1 and 0.9 resistance values.

(4) Resistance expressed as a fraction of room temperature (liquid) value,  $\times 10^2$  at 79° K. and  $\times 10^4$  for 1.05–4.2° K.

\* A second set of measurements was taken on this specimen after melting and refreezing.

## § 3. EXPERIMENTS WITH TIN

3.1. *The Specimens*

The material used was Johnson and Matthey 2,356, stated by the makers to contain less than 0.004% impurity. The ratio of resistance at 3.8° K. to that at 18° C. for the thickest specimen,  $1.8 \times 10^{-4}$ , appears to be the lowest recorded for tin and indicates that the material is of high purity. Foils were rolled out using an accurately ground and carefully cleaned rolling mill; a range of thickness 3–2,000  $\mu$  was covered. The specimens were cut in the form of rectangular strips using a razor blade for the thinner ones and a guillotine for the thicker ones. It was necessary that the width of the strip should be much greater than its thickness in order that the foil should approximate to an infinite plate for the purpose of comparison of the experimental results with the predictions of the theory. For thicknesses of 80  $\mu$  or less the foils were 1 mm. wide and 3–5 cm. long. For foils of thickness 0.1–1 mm. the width was increased to 3 mm. The thickest "foil", 2 mm. thick, was made only 4 mm. wide in order to keep the resistance large enough for accurate measurement at liquid helium temperatures. Since the mean free path turned out to be of the order of 70  $\mu$ , the size effect for this thickness was almost negligible, so that the insufficient ratio of width to thickness was not important.

The method of mounting is illustrated in Figure 4(a), p. 78. The strips were laid flat on the paxolin board AB, and fastened down at the ends with small brass clamps C and D to which current leads were attached. A few millimetres from the ends, small paxolin clamps pressed on the foil bearing the potential leads. A section of one of these clamps is shown in Figure 4(b). A groove was cut in the base of the clamp parallel to the width of the foil, and a loop of 36 s.w.g. copper wire was fastened along the groove so as to protrude slightly below the plane of the paxolin (dotted line). This protrusion was then ground away until the wire presented a plane surface flush with the paxolin. The force used in tightening the clamp was thus distributed over the whole underside and was not applied to the potential wire alone.

The coefficient of thermal expansion of the paxolin in the direction of the tin strip was about two thirds of the value for tin. For the thinnest foils the small relative contraction of the order 0.005 cm. was easily taken up by the slight lack of tautness in mounting; the thicker and therefore more rigid foils dragged slightly under the clamps which had only been screwed up lightly to avoid biting into the metal, as was indicated by the fact that they bowed out slightly on warming up. The sharpness of the temperature transitions into the superconducting state and of the longitudinal magnetic field transitions from the superconducting state to the normal state for all thicknesses of foil, examples of which are given in the next paper, indicated the absence of appreciable strain.

The thickness of the foils was known roughly from the room temperature resistance, and the mean thickness was found with an accuracy of 1% after the experiment by weighing the portion between the potential points.

3.2. *Experimental Results*

Since the Debye temperature is much higher for tin than for mercury, resistance below 4.2° K. is almost entirely residual, the temperature-dependent part being only about 1%. In order to cover a wide range of bulk resistivities, as was possible with mercury in the liquid helium range alone, it was necessary to make

measurements also in the liquid hydrogen range (14–20° K.). Since, however, at 14° K. the resistivity is already about 16 times its value at 4·2° K., it is unfortunate that the interesting range 4–14° K. was not readily accessible.

The normal resistances of the foils at 3·8° K., 13·9° K. and 20·4° K. are given in Table 2, where they are expressed as a fraction of the resistance at 18° C.; these resistance ratios are plotted in Figures 5 and 6. The full lines are explained in § 4.

Table 2. Resistance Ratios for Tin Foils

Specimen (1)	Thickness ( $\mu$ ) (2)	(3)	(4)			
			79	Temperatures (° K.) 20·4      13·9		3·8
E 7	1,950	11·7	0·203	100·0	30·4	1·80
E 10	915	12·0	0·210	98·7	30·7	2·03
E 9	487	12·1	0·206	100·0	30·3	2·22
E 6	255	12·6	0·207	—	—	2·20
E 8	133	12·2	0·205	102·1	30·7	2·61
E 3	77·7	12·3	0·205	—	—	3·02
E 11	53·5	12·0	0·209	103·1	30·8	2·64
E 12	30·7	12·6	0·207	103·1	31·0	3·10
E 13	15·1	11·9	0·206	104·1	33·7	5·33
E 14	9·9	13·2	0·205	—	—	6·75
E 17	7·46	12·3	0·203	115·0	42·9	10·8
E 4	6·94	12·7	0·208	—	—	10·5
E 15	5·15	13·8	—	—	—	14·4
E 5	4·11	13·4	0·205	—	—	19·0
E 2	3·43	13·5	0·204	—	—	18·6
E 18	3·34	13·7	0·204	128·9	55·2	20·1

(3) Resistivity at 18° C. (microhm cm.).

(4) Resistance expressed as a fraction of value at 291° K. ( $\times 10^4$  at 20·4°, 13·9° and 3·8° K.).

Values of the room temperature resistivity are also shown in Table 2. It will be seen that there is a general increase in the resistivity at 18° C. from  $11·7 \times 10^{-6}$  ohm cm. for the thickest specimen to  $13·7 \times 10^{-6}$  ohm cm. for the thinnest. Bridgman (1925) has measured the resistivity of single crystals of tin in various directions at 20° C., and found the values  $14·3$  and  $9·9 \times 10^{-6}$  ohm cm. for directions parallel and perpendicular to the tetrad axis, so that the value for a random polycrystal is  $11·1 \times 10^{-6}$  ohm cm. It seems, therefore, that the process of rolling causes the crystal grains of the polycrystalline material to have a preferred orientation of the tetrad axis towards the direction of rolling.

As the figures in Table 2 show, there was no significant difference from one foil to another in the ratios of resistivity at 79° K. and at 291° K.; the small scatter of values is probably due to variations in the temperature of measurement from the nominal 79° K., due to changes of oxygen content in the liquid air. Since the mean free path of the conduction electrons at 79° K. turns out to be less than  $10^{-5}$  cm., no size effect is to be expected, and therefore the constancy of the resistance ratio may be interpreted as a constancy of anisotropy of resistivity from room temperature down to 79° K.

There are some indications from the data in Table 2 that the anisotropy remains much the same down to 14° K.; if it is still constant down to 3·8° K. (which is rather

uncertain since the resistance is residual), then by plotting resistance ratios rather than absolute resistance, the effects of variations in crystal orientation are eliminated. This procedure has been adopted in Figures 5 and 6.

#### § 4. DISCUSSION

The experimental results show that the resistivity increases for both tin and mercury as the specimen size is decreased, but the possibility must be considered that the effects are due to strain or impurity. The mercury is unlikely to have been appreciably contaminated in handling, particularly in a systematic manner, but strain was indicated by the superconducting properties for wires of diameter less than  $12\mu$ . The increase in resistivity on the other hand was quite appreciable for diameters as large as  $100\mu$ . For tin the superconducting properties indicated no

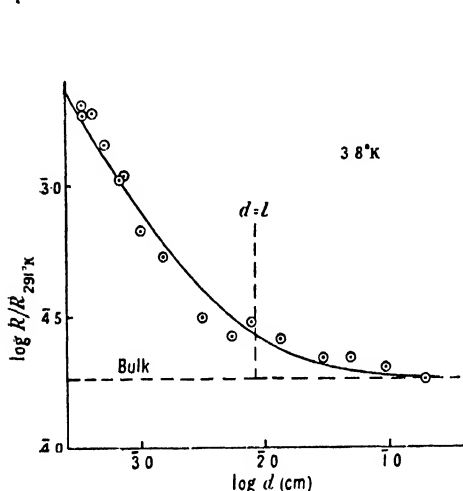


Figure 5.

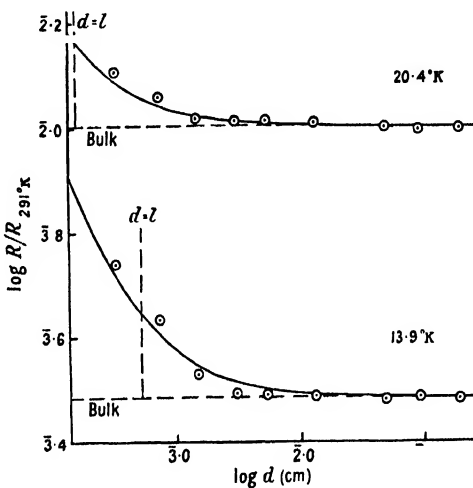


Figure 6.

The resistivity of tin foils plotted logarithmically against foil thickness.

Figure 5, for  $3.8^\circ\text{K}$ . Figure 6, for  $13.9^\circ\text{K}$  and  $20.4^\circ\text{K}$ .

The full lines are the theoretical curve of Fuchs for diffuse scattering ( $\epsilon=0$ ).

appreciable strain, so that only impurity need be seriously considered. While it is true that the thinner foils are likely to pick up more impurity in rolling than the thicker ones, the amount is unlikely to account for the factor of ten increase in resistivity found with the thinnest foils.

A test that may be applied to the hypothesis that the increase in resistivity is due to strain or impurity is to see whether Matthiessen's rule is obeyed. As the temperature approaches  $0^\circ\text{K}$ ., the ideal resistance tends to zero roughly as the fourth power of the temperature (actually a  $4.2$  power law fits the mercury results best). By plotting resistance as a function of temperature, the temperature-independent resistance may be readily found from the experimental results of Table 1, and is in fact very little lower than the value at  $1.05^\circ\text{K}$ . If there is no effect due to electron collisions with the boundaries, then this temperature-independent resistance is the residual value due to strain and impurity alone. Subtraction from the actual resistance at each temperature then gives the ideal resistance as a function of temperature, and if the observed increase of resistance were due to impurity or strain, this ideal resistance should be independent of specimen diameter. The curves obtained after this subtraction are shown in Figure 7 for four mercury

specimens, and it is seen that there is a size variation of this apparent ideal resistance; the increased resistance cannot therefore be explained away as due to strain if Matthiessen's rule is valid, although strain may make a contribution. For the tin foils also, the application of Matthiessen's rule to the data in Table 2 for the foils investigated at the lowest three temperatures, leads to values of apparent ideal resistance which are greater for the thinner foils; the increased resistance cannot therefore be explained away as due to impurity for tin either, although additional impurity may make a contribution. The theory of the increase of resistivity due to inelastic scattering of the conduction electrons at the metal surface does however lead to a size-variation of the apparent ideal resistance in the manner found experimentally.

The variation of the resistivity of thin films due to inelastic scattering at the film boundaries has been the subject of theoretical investigation by Thomson (1901)

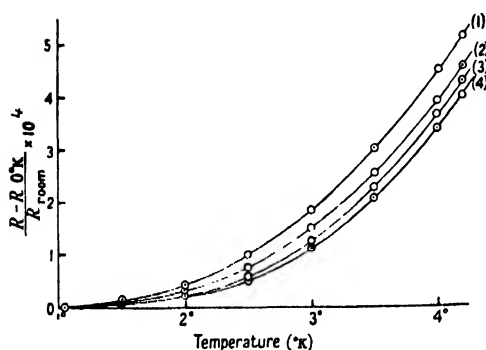


Figure 7. The temperature dependence of the apparent "ideal" resistance of mercury for four wire diameters: (1)  $6\mu$ , (2)  $10.5\mu$ , (3)  $46\mu$ , (4)  $790\mu$ .

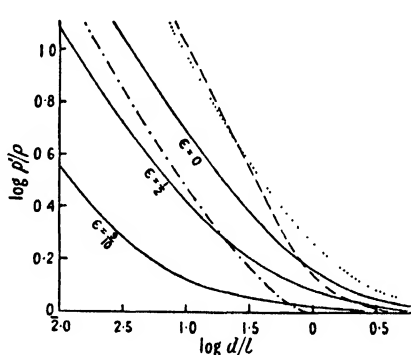


Figure 8. The theoretical variation of resistivity with size of conductor.

$l$  = mean free path in bulk metal,  
 $d$  = plate thickness or wire diameter,  
 $\epsilon$  = proportion of electrons scattered elastically.

— plate, Fuchs (1938).  
 - - - plate, Lovell (1936),  $\epsilon = 0$ .  
 - - - wire, using Lovell's assumptions,  $\epsilon = 0$ .  
 ..... wire, Nordheim's relation,  $\epsilon = 0$ .

who first suggested the possibility, by Lovell (1936) and by Fuchs (1938). Making certain simplifying assumptions, Lovell obtained the following relation between the resistivity  $\rho'$  of the thin film and that of the bulk material  $\rho$ :

$$\rho/\rho' = (d/l)[1 + \ln l/d], \quad \dots (1)$$

where  $d$  is the film thickness and  $l$  is the mean free path of the conduction electrons in the bulk metal. Relation (1) is plotted logarithmically in Figure 8. Fuchs made a more rigorous calculation and solved the problem for the general case when a proportion  $\epsilon$  of the electrons is scattered elastically at the surface (Lovell had assumed  $\epsilon = 0$ ). Curves of Fuchs' solution for  $\epsilon = 0, \frac{1}{2}, \frac{9}{10}$  are also shown in Figure 8.

For the tin foils these theoretical relations of Fuchs should be directly applicable, and the curve for  $\epsilon = 0$  (diffuse scattering) has been fitted as well as possible to the experimental data from Table 2. In the absence of other information the simplest value to assume for  $\epsilon$  is zero. The process of fitting yields



values at each temperature of the bulk mean free path  $l$  and of the ratio of the bulk resistivity  $\rho$  to the room temperature value. The product of these two quantities should be independent of temperature if  $\epsilon$  is independent of temperature. The curves for the three temperatures using a constant product  $l\rho = 2.0 \times 10^{-11}$  ohm cm<sup>2</sup> are shown as the full lines in Figures 5 and 6, and indicate a satisfactory agreement between theory and experiment. The scatter of points is most noticeable at 3.8° K. for the fatter specimens, but since the scale is logarithmic this corresponds to only small differences in (residual) resistivity of the order usually found between various samples of the same material. If the bulk residual resistivity is isotropic, rather than having the same anisotropy as the ideal resistivity as is assumed by the method of plotting, the effect would be to cause the points for the thinnest foils to lie slightly above the theoretical curve in Figure 5.

The accuracy of the product  $l\rho$  for tin is estimated to be about 25% from the scatter of the points. If the scattering coefficient  $\epsilon$  were considerably different from the zero value assumed, the product  $l\rho$  deduced would be greater. Figure 8 shows that the theoretical curve for  $\epsilon = \frac{1}{2}$  is roughly similar to that for  $\epsilon = 0$  but is displaced by a factor 2.5. For  $\epsilon = 9/10$  the factor is about 14.

The rigorous calculation for a wire corresponding to Fuchs' calculation for a film has not been carried out. Eucken and Förster (1934) have used a relation due to Nordheim:

$$\rho'/\rho = 1 + \alpha(l/d), \quad \dots\dots(2)$$

where  $d$  is the wire diameter, and the coefficient  $\alpha$  has a maximum value  $8/3\pi$  for diffuse reflection. The relation is also plotted in Figure 8. Its derivation does not seem to have been published, but appears to be based on a simple geometrical argument involving the assumption that collisions with the boundary may be described by an appropriate relaxation time for the process as for lattice collisions; the validity of this assumption seems doubtful. From the form of relation (2), if  $\alpha$  is independent of temperature, the additional resistance should appear as an increased residual resistance, since  $l\rho$  is independent of temperature; this is not in agreement with the results for mercury illustrated in Figure 7, or the corresponding results for tin. Thus it seems that Nordheim's relation is inadequate. The solution for a wire using Lovell's assumptions has been worked out, as is shown in Figure 8; an outline of the calculation is given in the Appendix.

It will be seen from Figure 8 that the curves for a plate and for a wire, using Lovell's assumptions, are very similar, being laterally displaced along the  $\log d/l$  axis by a roughly constant amount which corresponds to a ratio of about 3 in  $d/l$  for the  $\rho'/\rho$  values dealt with here. Pending the availability of a rigorous solution of the problem for a wire, it therefore seems reasonable to assume that it would yield curves similar to those of Fuchs for a plate, but laterally displaced by the same ratio. Although such a mathematical guess should be treated with caution, it is unlikely to be in error by more than a factor of two. Comparison of the results for the tin foils using Fuchs' curves, which are directly applicable to this case, with some scanty data for tin wires suggests that the ratio 3 is quite reasonable.\*

The curve of Fuchs for  $\epsilon = 0$  has accordingly been fitted as well as possible to the experimental data for mercury from Table 1; the curves for the various temperatures using a constant product  $l\rho = 1.5 \times 10^{-11}$  ohm cm<sup>2</sup> are shown as the full lines in Figures 2 and 3. In view of the uncertainty associated with the factor

\* The thinnest tin wires were made using the pressurizer described in § 2 suitably modified for use in a furnace.

3 which has been applied, an accuracy of better than 50% in  $l\rho$  cannot be assumed.

Values of  $l\rho$  for mercury and tin have been calculated by Pippard from his 1,200-Mc/s. high frequency measurements (1947), using the theoretical treatment of the anomalous skin effect by Reuter and Söndheimer (1948). For mercury he finds the values of the product to be 2.0 and  $3.9 \times 10^{-11}$  ohm cm<sup>2</sup> for diffuse and elastic scattering respectively, while for tin the values are 1.0 and  $1.5 \times 10^{-11}$  ohm cm<sup>2</sup>, each with an estimated accuracy of 50%. The coefficient of elastic scattering  $\epsilon$  in the D.C. case is not necessarily the same as that for the high-frequency case, since in the latter case only electrons moving in directions almost parallel to the surface contribute to the current, while in the D.C. case electrons moving in all directions contribute. Bearing this in mind, and also the limited accuracy of both determinations of the product  $l\rho$ , the agreement is satisfactory, and leaves little doubt that the size-variation of D.C. resistivity is due to inelastic scattering of the conduction electrons at the metal surface; the correlation with the high-frequency measurements suggests that a low value of  $\epsilon$  characterizes the scattering.

Although no theoretical value of the product  $l\rho$  is available for tin or mercury, the formulae for a free electron metal may be used to check that the order of magnitude of the experimental values is correct. Simple considerations show that the resistivity of a free electron metal is given by  $\rho = mv/ne^2l$ , where  $e$  and  $m$  are the electronic charge and mass,  $n$  is the effective number of free electrons per cm<sup>3</sup> and  $v$  is the velocity of the electrons at the top of the Fermi distribution. Quantum theory shows that  $v = (\hbar/m)(3n/8\pi)^{1/3}$ , where  $\hbar$  is Planck's constant. Hence the product  $l\rho$  is given by

$$l\rho = (\hbar/2e^2)(3/\pi n^2)^{1/3}, \quad \dots\dots (3)$$

and rough values of  $n$  may be found by substituting in (3) the values of  $l\rho$  deduced from the present experiments. The values of  $n$  thus obtained correspond to 0.43 electrons per atom for tin and 0.57 electrons per atom for mercury. Such values are quite reasonable, and imply that the experimentally determined values of  $l\rho$  are of the right order of magnitude.

#### ACKNOWLEDGMENTS

I wish to thank Dr. D. Shoenberg, Mr. A. B. Pippard and Mr. R. G. Chambers for useful discussions, Mr. A. B. Pippard for putting his pressurizer at my disposal, and Dr. G. J. van den Berg for drawing my attention to the earlier German work.

#### APPENDIX

The assumptions made by Lovell (1936) in calculating the resistivity of thin films will also be made here for a wire. The diameter of the wire  $d$  is considered sufficiently less than the bulk mean free path  $l$  for all free paths to be taken as starting from the wire surface. The collisions with the surface are considered inelastic, so that there is a uniform density of electrons in all inward directions from the surface.

Consider one point on the wire surface. Path directions from this point will be designated by the polar coordinates  $\theta, \phi$ ;  $\phi$  determines the azimuth in a plane normal to the wire axis through the point, and  $\theta$  is the angle of elevation of the path above the plane. The fraction of paths from the point lying within the element of solid angle defined by  $\theta, \theta + d\theta$  and  $\phi, \phi + d\phi$  is  $\cos\theta d\theta d\phi/2\pi$ . The distance  $r$

along any path to the next intersection with the wire boundary is  $d \cos \phi \sec \theta$ . Again, following Lovell, it is assumed that for  $r < l$  the free path is  $r$ , while for  $r > l$  the free path is  $l$ . Hence the modified mean free path  $l'$  is given by

$$l' = \frac{2}{\pi} \int_0^{\pi/2} \left[ \int_0^{\cos^{-1}(a \cos \phi)} d \cos \phi d\theta + \int_{\cos^{-1}(a \cos \phi)}^{\pi/2} l \cos \theta d\theta \right] d\phi,$$

where  $a = d/l$ . Hence for  $a \leq 1$

$$\frac{\rho}{\rho'} = \frac{l'}{l} = 1 + a - \frac{2}{\pi} \{E(a) + a^2 B(a)\},$$

and for  $a \geq 1$

$$\frac{\rho}{\rho'} = \frac{l'}{l} = 1 + a - \frac{2}{\pi} \left\{ aE\left(\frac{1}{a}\right) + \frac{1}{a} B\left(\frac{1}{a}\right) \right\},$$

where  $E$  and  $B$  are complete elliptic integrals.

The case  $a > 1$  is considered in order to complete the curve although the assumption made above that all paths commence on the wire surface no longer holds. The integrals have been computed graphically for the purpose of drawing the curve in Figure 8.

#### REFERENCES

- ANDREW, E. R., 1948, *Proc. Roy. Soc. A*, **194**, 80 ; 1949, *Proc. Phys. Soc. A*, **62**, 88.  
 APPLEYARD, E. T. S., and LOVELL, A. C. B., 1937, *Proc. Roy. Soc. A*, **158**, 718.  
 BRIDGMAN, P. W., 1925, *Proc. Amer. Acad. Sci.*, **60**, 305.  
 EUCKEN, A., and FÖRSTER, F., 1934, *Göttingen Nachrichten*, **1**, 43, 129.  
 FUCHS, K., 1938, *Proc. Camb. Phil. Soc.*, **34**, 100.  
 HAMBURGER, L., 1931, *Ann. Phys., Lpz.*, **10**, 789.  
 KAPITZA, P., and MILNER, C. J., 1937, *J. Sci. Instrum.*, **14**, 165.  
 LOVELL, A. C. B., 1936, *Proc. Roy. Soc. A*, **157**, 311.  
 PIPPARD, A. B., 1947, *Proc. Roy. Soc. A*, **191**, 385.  
 REUTER, G. E. H., and SONDHEIMER, E. H., 1948, *Proc. Roy. Soc. A*, in the press.  
 RIEDEL, L., 1937, *Ann. Phys., Lpz.*, **28**, 603.  
 SCKELL, O., 1930, *Ann. Phys., Lpz.*, **6**, 932.  
 THOMSON, J. J., 1901, *Proc. Camb. Phil. Soc.*, **11**, 120.

## Critical Field Measurements on Superconducting Tin Foils

By E. R. ANDREW

Royal Society Mond Laboratory, Cambridge

*Communicated by D. Shoenberg ; MS. received 8th September 1948*

**ABSTRACT.** The critical fields of superconducting tin foils have been determined from resistance measurements in a longitudinal magnetic field. Pomeranchuk's relation,  $H_f = H_c(1 + \lambda'/d)$ , between the foil critical field  $H_f$  and the foil thickness  $d$  was verified, and values of the length  $\lambda'$  were found as a function of temperature ; at 0° K. the value of  $\lambda'$  was estimated to be  $1.2 \times 10^{-5}$  cm., rising rapidly close to the transition temperature. It is noticed that  $\lambda'$  is approximately twice the penetration depth  $\lambda$  for tin at all temperatures. Assuming the validity of Ginsburg's interpretation of  $\lambda'$  as the sum of  $\lambda$  and the surface energy parameter  $\beta$ , it is seen that  $\lambda$  and  $\beta$  are approximately equal.

## § 1. INTRODUCTION

It was found by Pontius (1937) that the critical field of thin superconducting lead wires is greater than the value  $H_c$  for the metal in bulk. A more complete investigation of the size-variation of critical field for mercury in the form of evaporated films has been made by Appleyard, Bristow, London and Misener (1939). The present paper describes the results of a similar investigation for tin using thin rolled foils. Since, however, the thinnest foil was much thicker than the penetration depth  $\lambda$  of a magnetic field, the information derived was necessarily less comprehensive than that for mercury obtained by Appleyard *et al.*, who used films of thickness of the order  $\lambda$ . Experiments were also carried out using the thin pressurized mercury wires described in the previous paper (Andrew 1949), but no useful results were obtained since the small changes of critical field were masked by effects due to strain.

Pomeranchuk (1938) has shown that if there is a difference in surface energy  $\lambda' H_c^2/8\pi$  between a plate in the normal and the superconducting states, the critical field for the plate is given by

$$H_f = H_c(1 + \lambda'/d), \quad \dots (1)$$

where  $d$  is the plate thickness, provided that  $d \gg \lambda'$ . Ginsburg (1945) has shown that if the penetration laws of F. and H. London are assumed valid, and the penetration depth is assumed independent of field strength, then  $\lambda' = \lambda + \beta$ , where  $\beta = 8\pi(\alpha_n - \alpha_s)/H_c^2$  and  $\alpha_n, \alpha_s$  are the surface energies per unit area between the normal metal and an insulator, and the superconducting metal and an insulator respectively.

The experiments described here show that the relation between  $H_f$  and  $d$  has in fact the form of equation (1); values of  $\lambda'$  as a function of temperature are deduced, and their interpretation is discussed.

## § 2. EXPERIMENTAL DETAILS

2.1. *The Specimens*

The material used was Johnson and Matthey tin No. 2,356. The report of the maker's spectrographic analysis indicated less than 0.004% impurity. The foils were rolled out using an accurately ground and carefully cleaned rolling mill. The specimens were cut with a razor blade in the form of rectangular strips 1 mm. wide and 3–5 cm. long. The method of mounting is described in the previous paper (Andrew 1949). The sharpness of the temperature transitions, and of the longitudinal magnetic field transitions, for all foil thicknesses, indicated the absence of appreciable strain, as did also the residual resistance measurements given in the previous paper.

The specimens were mounted vertically in the appendage of a Dewar flask at the centre of a Helmholtz pair of coils whose field was uniform within 0.1% over the length of the foil. Resistance was measured by a potentiometer method, using the improvements of Kapitza and Milner (1937). A measuring current of 1 ma. was used for foils 3–4  $\mu$  thickness, while for the thicker foils the measuring current was increased roughly in proportion to the thickness. The magnetic field due to this measuring current could be neglected since it was found that close to the transition temperature, where its effect should be greatest, a current three times as large caused an apparent reduction in critical field of only 0.1 gauss. The thickness of the foils was known roughly from the room temperature resistance, and

the mean thickness was found with an accuracy of about 1% after the experiment by weighing the portion between the potential points.

The temperatures of the specimens were deduced from the vapour pressure of the liquid helium in which they were immersed, using the 1932 Leiden scale of temperature.

## 2.2. *Special Precautions*

For the thinnest foil ( $3\mu$ ) the change in critical field that has to be measured ranges from about 1 gauss when  $H_c$  is 3 gauss to about 8 gauss when  $H_c$  is 240 gauss. While such a change may be readily observed, a reasonable accuracy in the determination of  $\lambda'$  calls for critical field measurements with an accuracy of a few tenths of a gauss, and hence involves a number of precautions. It was not necessary of course to have an absolute accuracy of this order, and in fact one could work entirely in terms of the currents passed through the Helmholtz coils. Since the slope of the threshold curve is about 150 gauss/°K. at the transition temperature, falling off to about 75 gauss/°K. at 1.6° K., very careful temperature control was essential in order to achieve the desired accuracy, and this was conveniently obtained using the automatic device described elsewhere (Andrew 1948 b); the error in critical field measurement due to temperature drift was not more than 0.1 gauss except at the lowest temperature, 1.66° K., where an error of 0.3 gauss was possible.

It was important that the applied field should be accurately parallel to the plane of the foil. The field coils were mounted so that they could be rotated through  $\pm 5^\circ$  about any horizontal axis. The position of the plane of the foil was known within a few degrees beforehand. Longitudinal resistance transitions were measured for several coil directions a few degrees on either side of the position which had been guessed as correct. From the transition at the highest field strengths the correct position of the coils could be found within  $\frac{1}{2}^\circ$ . An error of  $\pm 1^\circ$  caused the transition to be displaced to field values about 0.2% lower, and of  $\pm 2^\circ$  to field values about 0.8% lower.

Since the transition temperatures  $T_c$  for various specimens are never quite the same, a correction for the differences is necessary. Such a correction involves some assumption concerning the functional form of the threshold field curves. For instance, it may be assumed that  $H_c$  is a function of  $(T_c - T)$ , or of  $T/T_c$ . The former implies that the threshold field curves are geometrically similar for different specimens, but subject to small shifts along the temperature axis, while the latter assumes that the values of critical field become equal at 0° K. Near the transition temperature, however, all likely assumptions will lead to the same correction, while at lower temperatures  $H_c$  is much larger and  $dH_c/dT$  is smaller, so that the fractional correction is in any case small. For practical purposes the former assumption was therefore made, and in order to avoid as far as possible the application of a numerical correction to the experimental results, measurements were made at temperatures  $T$  such that  $\Delta T (= T_c - T)$  took certain predetermined values. The small remaining correction that had to be applied, due to the fact that the  $\Delta T$  values were not quite equal to the predetermined values, amounted to only a few tenths of a gauss.

The experimental procedure was therefore as follows: (a) the temperature transition was measured (i.e. resistance against temperature in zero field);

(b) the coil system was exactly aligned at  $\Delta T = 0.53^\circ \text{K}$ .; (c) the specimen was allowed to warm up above the transition temperature; (d) systematic measurements were made of resistance as a function of field at various  $\Delta T$ .

For the measurements of the temperature transition, the earth's vertical field was compensated, but it was uncompensated in the critical field determinations and, therefore, its value, 0.4 gauss, had to be added to the applied fields. The earth's horizontal field (about 0.15 gauss) was not compensated in any of the measurements; its direction was almost in the plane of the specimen, so that no serious error is likely to result from its neglect.

### 2.3. Determination of the Critical Fields

The value of the applied longitudinal field which was taken as the critical field, was the value which restored half the normal resistance. This requires some justification since previous workers have sometimes taken the field which produces the first trace of resistance (e.g. Pontius 1937). It is well known that unstrained single crystals of tin give sharp temperature and longitudinal field transitions, whilst those for polycrystalline material are usually about  $0.02^\circ \text{K}$ . and 3 gauss broad respectively. Since strain is known to affect the temperature and field transitions (Sizoo, de Haas and Onnes 1925), it may be supposed that the crystal grains of which the polycrystalline material is composed are each under stress at low temperatures, due to the anisotropy of thermal expansion coefficient for tin and an inability to anneal at such temperatures. If one assumes a Gaussian distribution of stresses for the crystal grains, then one has a Gaussian distribution of transition temperatures and critical fields, since the effects of stress, being small, may be taken as linear. This information alone, however, does not suffice to determine the shape of the resistance transitions as the geometrical arrangement of the crystal grains is also of importance. If, however, we first consider the fictitious one-dimensional case of a metallic line consisting of a random distribution of elements, some superconducting and some normal, then it is obvious that the fractional resistance will be proportional to the fractional length of normal metal. If the transition temperature and the critical field have a Gaussian distribution, then the fraction  $\alpha$  of normal resistance restored either at a temperature  $T$  in a temperature transition or at a field  $h$  in a field transition will have the form

$$\alpha = \frac{1}{\sqrt{\pi}} \int_{-\infty}^x \exp(-t^2) dt, \quad \dots\dots(2)$$

where, for a temperature transition,  $x = (T - T_c)/\sqrt{2}T_0$  and for a longitudinal field transition  $x = (h - H_c)/\sqrt{2}H_0$ , ( $T_c$  is the critical temperature,  $H_c$  the critical field, and  $T_0$  and  $H_0$  are the standard deviations of the two Gaussian distributions).

Temperature transitions for the four foils, of thickness 3–20  $\mu$ , are shown in Figure 1 and equation (2) has been fitted to them as well as possible (broken lines). It will be seen that the theoretical form for the fictitious one-dimensional model fits the results fairly well. Etching showed that the crystal grains varied in size from 0.1 to 1 mm.: thus for all the foils there was generally not more than one single crystal extending through the thickness of the foil, but there were generally two or three grains across the width. For one foil (6.94  $\mu$ ) there were many large crystal grains, several of which extended over the whole width of the foil (1 mm.). It is satisfactory that for this foil equation (2) fits particularly well (Curve (2),

Figure 1), confirming that it is a good approximation to the one-dimensional model. The slight deviations from equation (2) for the more usual case in which there are several grains across any width may be accounted for qualitatively by simple arguments.

Since the crystal grains extend right through the foil, each affords entry and exit for lines of force in a magnetic field, so that approximately the longitudinal magnetic field transitions should be geometrically similar to the temperature transition. This is in fact the case, as is illustrated for the  $4.11\ \mu$  foil in Figure 2 close to the transition temperature, and continues to be the case with roughly the same width (or slightly narrower) at lower temperatures. The transitions were about 3 gauss wide for all specimens and temperatures.

There will be a family of critical field-temperature curves corresponding to the various values of  $T_c$  and  $H_c$  in the Gaussian distributions. Any member of the family near the mean will serve our purpose since, when plotted as a function of  $\Delta T$ , they will all coincide. The half-resistance point on the resistance-field curves has been chosen to determine the critical field values because this critical field is very close to the mean of the Gaussian distribution, and also because the field value can be determined most precisely at this point since the curves are steepest there.

### § 3. EXPERIMENTAL RESULTS AND DISCUSSION

The foils used had thicknesses 3.43, 4.11, 6.94 and  $19.4\ \mu$ . In order to obtain, in addition, critical field values close to the bulk values, a wire of diameter 0.26 mm. was used rather than a thick foil. A foil of this thickness would have a demagnetization coefficient  $n$  of 0.005, causing an apparent lowering of the critical field by a fraction of this order; the value of  $n$  for the  $19.4\ \mu$  foil, the thickest used for these measurements, was  $4 \times 10^{-4}$ , the effect of which was negligible. For the wire of diameter 0.26 mm. and length 5 cm., the value of  $n$  was  $1.3 \times 10^{-4}$ , and hence its effect also was negligible. The wire was cast in a thin-walled capillary and the glass cracked off; potential leads of pure tin were fixed on with a pinhole flame.

The values of the foil critical fields  $H_c$  are shown in Table 1, and were plotted against the reciprocal of the thickness  $d$ ,\* as is shown for three values of  $\Delta T$  in Figure 3; the fact that the relations are linear is a confirmation of (1). The slope  $\lambda' H_c$ , the intercept  $H_c$ , and their probable errors were calculated by the method of least squares. From these quantities  $\lambda'$  was obtained as a function of  $\Delta T$ ; the values are shown in Table 1 and are plotted in Figure 4, the vertical lines indicating the calculated probable errors. The smooth curve that has been drawn through the points indicates that  $\lambda'$ , like the penetration depth  $\lambda$ , tends to infinity at  $T_c$  and becomes independent of temperature at low temperatures. The calculated values of  $H_c$  are also shown in Table 1, and are in good agreement with other published values (de Haas and Engelkes 1937, Daunt and Mendelssohn 1937, Andrew 1948).

Unfortunately absolute values of  $\lambda$  are not available for comparison with the present values of  $\lambda'$ , but Pippard (1947) has obtained relative values  $(\lambda - \lambda_{2.3^\circ \text{K}})/\lambda_{2.3^\circ \text{K}}$ . Using the relation  $\lambda_{0^\circ \text{K}}^2/\lambda^2 = 1 - (T/T_c)^4$ , which fits the data for mercury well (Daunt, Miller, Pippard and Shoenberg 1948), Pippard's results lead to the value  $\lambda_{2.3^\circ \text{K}} = (0.6 \pm 0.1) \times 10^{-5}$  cm. The measurements of Laurmann and Shoenberg (see Shoenberg 1948) are in good agreement with this estimate. The absolute values of  $\lambda$  thus deduced are shown in Figure 4 (broken line). If Ginsburg's

\* In the case of the wire, the appropriate value is twice the reciprocal of the diameter, as a cylinder has twice the surface area/volume ratio of a plate.

interpretation of  $\lambda'$  is correct, the differences  $\lambda' - \lambda$  give the values of  $\beta$ , and these also are shown in Figure 4 (chain line). Smoothed values of  $\lambda'$ , together with values of  $\lambda$  and  $\beta$ , are given in Table 2.

The interesting feature which emerges, and which is shown clearly by Figure 4, is the near equality of  $\lambda$  and  $\beta$  at all temperatures. The same feature was found for mercury also by Ginsburg (1945), who calculated values of  $\lambda$  and  $\beta$  from the mercury

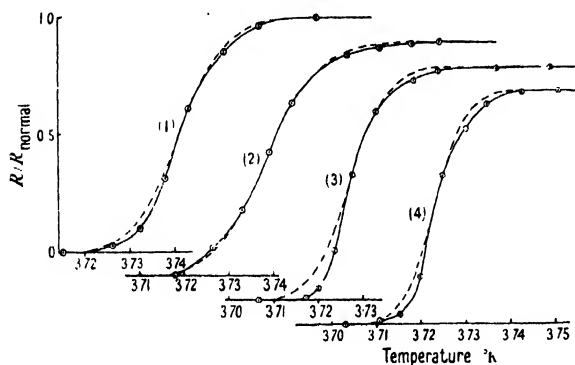


Figure 1. Temperature transitions of four tin foils; thickness (1)  $3.43 \mu$ , (2)  $6.94 \mu$ , (3)  $4.11 \mu$ , (4)  $19.4 \mu$ . The broken lines are given by equation (2).

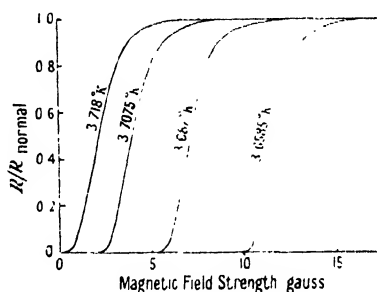


Figure 2. Resistance curves in a longitudinal field for the  $4.11 \mu$  foil. Measuring current 1 ma.;  $T_c = 3.728 \text{ K}$ . The vertical component of the earth's field (0.4 gauss) opposes the applied field.

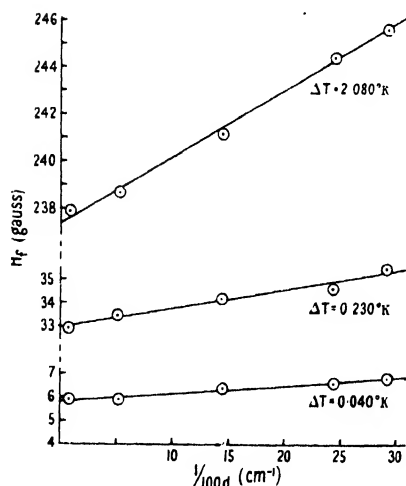


Figure 3. Critical field values  $H_c$  of the foils for three values of  $\Delta T$ , plotted against the reciprocal of the thickness  $d$ .

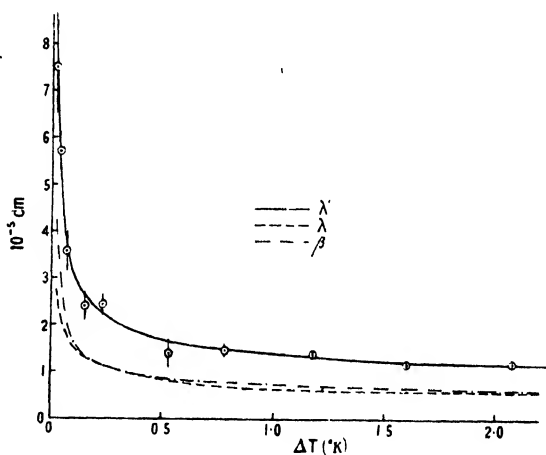


Figure 4. The values of  $\lambda'$  deduced from the experiments, plotted against  $\Delta T (= T_c - T)$ , together with the values of the penetration depth  $\lambda$ , and of  $\beta$  (defined as  $\lambda' - \lambda$ ).

film results of Appleyard *et al.* (1939). The result of this calculation is, however, at variance with that of Désirant and Shoenberg (1948a), who combined the results of their absolute determination of  $\lambda$  for mercury (obtained from susceptibility measurements on colloidal spheres and on thin wires) with the critical field measurements of Appleyard *et al.* Doubt has however been cast on the reliability of the thin wire results (Shoenberg 1948); the discrepancy may therefore prove



unfounded. In any case the interpretation of  $\lambda'$  as  $\lambda + \beta$  assumes, as Ginsburg pointed out, that  $\lambda$  is independent of magnetic field strength; this is an assumption which may well be untrue. The correct interpretation of  $\lambda'$  therefore awaits a more complete theory. It is of interest to note, however, that if Ginsburg's interpretation is adopted, the values of  $\beta$  which have been derived here for tin are

Table 1. Values of  $H_f$ ,  $H_c$  and  $\lambda'$ 

$d(\mu)$ $T_c(^{\circ}\text{K.})$	Values of $H_f$ (gauss)					$H_c$ (gauss)	$\lambda' *$	P.E. in $\lambda' *$
	E 16 260 3.715	E 1 19.4 3.724	E 4 6.94 3.739	E 5 4.11 3.728	E 2 3.43 3.742			
$\Delta T(^{\circ}\text{K.})$								
0.010	1.4	1.5	2.0	1.8	2.1	1.4	15.0	3.9
0.020	3.1	3.0	3.4	3.5	3.7	3.0	7.5	1.0
0.040	5.9	5.9	6.4	6.6	6.8	5.8	5.7	0.4
0.070	10.4	10.4	11.1	11.2	11.4	10.4	3.6	0.4
0.150	21.7	22.4	22.8	23.1	23.4	21.9	2.4	0.3
0.230	32.9	33.5	34.2	34.6	35.5	33.0	2.45	0.20
0.530	73.2	74.9	76.0	76.0	76.7	73.9	1.38	0.26
0.780	105.6	—	108.3	109.2	110.2	105.7	1.47	0.12
1.180	153.1	153.2	155.8	157.4	159.1	152.6	1.40	0.08
1.600	197.1	—	200.4	202.7	203.5	197.0	1.16	0.04
2.080	237.8	238.7	241.2	244.5	245.7	237.4	1.20	0.03

\*  $\lambda'$  in  $10^{-5}$  cm.

Table 2. Values of  $\lambda'$ ,  $\lambda$  and  $\beta$  for Tin

$\Delta T(^{\circ}\text{K.})$	$\lambda'_{\text{(smoothed)}}$ ( $10^{-5}$ cm.)	$\lambda$ ( $10^{-5}$ cm.)	$\beta$ ( $10^{-5}$ cm.)
0.02	8.0	3.0	5.0
0.04	5.4	2.2	3.2
0.07	3.8	1.7	2.1
0.10	3.15	1.5	1.65
0.20	2.40	1.18	1.22
0.50	1.69	0.82	0.87
0.80	1.46	0.69	0.77
1.20	1.33	0.62	0.71
1.60	1.25	0.60	0.65
2.10	1.20	0.58	0.62

of the same order of magnitude as the values of  $\Delta$  obtained from experiments on tin cylinders in the intermediate state (Désirant and Shoenberg 1948 b, Andrew 1948 a), where  $\Delta = 8\pi\alpha_{\text{ns}}/H_c^2$  and  $\alpha_{\text{ns}}$  is the surface energy per unit area at the boundary between normal and superconducting domains of metal. This means that  $\alpha_{\text{ns}}$  and  $(\alpha_n - \alpha_s)$  are of the same order, as one might expect.

## REFERENCES

- ANDREW, E. R., 1948 a, *Proc. Roy. Soc. A*, **194**, 80 ; 1948 b, *J. Sci. Instrum.* (in the press); 1949, *Proc. Phys. Soc. A*, **62**, 77.  
 APPLEYARD, E. T. S., BRISTOW, J. R., LONDON, H., and MISENER, A. D., 1939, *Proc. Roy. Soc. A*, **172**, 540.

- DAUNT, J. G., and MENDELSSOHN, K., 1937, *Proc. Roy. Soc. A*, **160**, 127.  
 DAUNT, J. G., MILLER, A. R., PIPPARD, A. B., and SHOENBERG, D., 1948, *Phys. Rev.* **74**, 842.  
 DÉSIKANT, M., and SHOENBERG, D., 1948 a, *Proc. Phys. Soc.*, **60**, 413 ; 1948 b, *Proc. Roy. Soc. A*, **194**, 63.  
 GINSBURG, V., 1945, *J. Phys. U.S.S.R.*, **9**, 305.  
 DE HAAS, W. J., and ENGELKES, A. D., 1937, *Physica*, **4**, 325.  
 KAPITZA, P., and MILNER, C. J., 1937, *J. Sci. Instrum.*, **14**, 165.  
 LONDON, F. and H., 1935, *Proc. Roy. Soc. A*, **149**, 71.  
 PIPPARD, A. B., 1947, *Proc. Roy. Soc. A*, **191**, 370.  
 POMERANCHUK, I., 1938, see *Superconductivity*, by D. Shoenberg (Cambridge : University Press), p. 98.  
 PONTIUS, R. B., 1937, *Phil. Mag.*, **24**, 787.  
 SHOENBERG, D., 1948, *Amsterdam Conference on Metals*.  
 SIZOO, C. J., DE HAAS, W. J., and ONNES, H. K., 1925, *Leiden Comm.*, 180 c, d.

## On the Radiation from Transient Light Sources

By F. BOOTH

H. H. Wills Physical Laboratory, University of Bristol

*MS. received 2nd February 1948, in amended form 14th August 1948*

**ABSTRACT.** A theoretical treatment is given of the problem of analysing the radiation from transient light sources in the form of clouds of incandescent particles. Recently a method of correlating this radiation with various physical parameters has been suggested by E. F. Caldin. In the present paper a critical examination of this method is made, and exact formulae derived for special models.

Expressions for the radiation emitted by a cloud of incandescent particles, all at the same temperature, are obtained for the following cases : (i) a uniform spherical distribution of equal, perfectly emitting and absorbing particles; (ii) a uniform distribution of particles which are not perfect absorbers, but in which (a) radiation is reflected specularly from the particle surface, and (b) the particles reflect light diffusely; (iii) a uniform distribution of particles in a thin spherical shell.

It is shown that the condition for the radiation from a cloud of black body particles to be equal in intensity to that from a black body of the same size and shape is that  $R^2 a \rho_0 \ll M$ , where  $R$  is the radius of the cloud,  $a$  the particle radius,  $\rho_0$  the particle density and  $M$  the total mass of the cloud. The cooling of clouds by radiation transfer is also examined theoretically.

The bearing of the results on Caldin's method is discussed, and more exact methods of analysing the cooling of this form of light source sketched.

### § 1. INTRODUCTION

THE following paper is a theoretical investigation of some problems suggested by an analysis due to Caldin (1946) of the radiation from transient light sources. The light sources Caldin considers are all of the same general type. A metal is ignited either in oxygen, or in the presence of an oxidizing agent; owing to the large amount of heat liberated, the temperature of the reactants becomes very high and part of the energy is radiated as light. All the sources show the same type of light intensity-time curve—a rapid rise to the maximum intensity, followed by a slower fall in intensity.

A general theory of transient light sources of this kind would be very complicated since three distinct problems would have to be solved: (a) determination of the behaviour with time of the pressure, temperature and velocity of various parts of the system as the reaction proceeds; (b) some knowledge of the kinetics of the

oxidation would be required so that the proportion of metal oxidized at any time and the temperature of the products could be found; (c) evaluation of the radiation reaching an external point from the source.

For practical purposes all we need to know is the quantity and quality of the luminous radiation as found by (c). But although problem (c) is quite distinct from problems (a) and (b), these must first be solved to find the radiation emitted. Unfortunately the two problems cannot be solved independently. For example, the dynamical behaviour will depend upon the reaction kinetics, and the rate of oxidation upon the pressure and temperature of the material of the light source, that is, upon variables determined by (a). At the present stage an exact solution of the whole behaviour seems out of the question; drastic assumptions must be made about the first two problems (a) and (b) and attention concentrated upon the remaining problem (c). This is the procedure proposed by Caldin (1946 a, b).

In Caldin's first paper (1946 a) the cooling of a body by radiation from the surface is considered. It is assumed that initially, and during the subsequent cooling, the body is of uniform temperature. By equating the rate of energy loss from the surface to the rate of reduction of the internal energy, expressions are derived for the total intensity of radiation, brightness and temperature as a function of the time. In the second paper (1946 b) the spectral distribution of the energy is found as a function of the time, and, by integration, the total amount of energy radiated at a given wavelength is obtained as a function of the initial temperature. All the expressions obtained hold only for a "Planckian radiator"—that is, for a radiator whose emissivity is independent of the wavelength and temperature.

Now consider the transient light sources. Suppose that at the maximum intensity of the light emission the chemical reaction is complete, and that the material is of uniform temperature and at rest. Then if we assume that the material behaves as a "Planckian radiator" of uniform temperature, the theory can be used to analyse the decay of the light intensity. For example, from the total energy liberated at any particular wavelength, the initial temperature can be found. The validity of the method rests, however, on whether or not the radiating material can be treated as a uniform temperature "Planckian radiator". From observations on the spectrum and temperature it seems probable that the light radiated after the maximum intensity is due to temperature radiation from incandescent solid particles—very probably oxide particles. If we assume that there is little radial motion, problem (c) is resolved into the determination of the radiation from a roughly spherical cloud of fine particles, each cooling by radiation. The temperature and density are not, in general, uniform. If the problem of cooling is solved by Caldin's method two basic assumptions are implied: (1) the temperature throughout the cloud is initially uniform, and remains so as it cools; (2) the radiation from the cloud is the same as it would be from a solid surface consisting of the radiating material and coincident with the boundary between the outer layers of the cloud and surrounding space.

The second assumption may be restated as two rather simpler assumptions: (2') if each solid particle in the cloud is a perfect absorber and emitter then the radiation from the cloud is that of a solid black body at the same temperature; (2'') if the surface emissivity of each particle is  $\epsilon$  then the radiation from the cloud is that of a solid black body at the same temperature multiplied by  $\epsilon$ .

In the following account, we shall find the conditions which these assumptions impose on the physical properties of the material in the light source.

## § 2. EXAMINATION OF ASSUMPTION (2)

### 2.1. Radiation from a Cloud of black-body Particles (Assumption (2'))

We first consider assumption (2'), assuming (1) to be valid. Let  $R$  be the radius of a spherical cloud composed of spherical particles of radius  $a$ , density  $\rho_0$ , and at temperature  $T$ ; the density distribution is assumed to be spherically symmetrical. If  $N(r)$  is the number of particles per  $\text{cm}^3$  in a small region round a point  $P$ , distant  $r$  from the centre of the cloud, then  $N_0$ , the total number of particles in the cloud is given by

$$N_0 = 4\pi \int_0^R N(r)r^2 dr = 3M/4\pi\rho_0 a^3, \quad \dots\dots(2.1)$$

where  $M$  is the total mass of solid material in the cloud. To examine assumption (2') we require the total amount of light radiated from a cloud of this form in unit time. It is first necessary to derive the fundamental equation for the transfer of radiation.

Let  $I$  denote the total intensity of radiation of all wavelengths at a point  $P$ , in direction  $\mathbf{s}$ . Then if  $dA$  is a small area element at  $P$  in a plane perpendicular to  $\mathbf{s}$ , the amount of radiation which crosses  $dA$  in unit time and spreads into a small solid angle  $d\omega$  containing direction  $\mathbf{s}$  is  $I(\mathbf{P}, \mathbf{s})d\omega dA$ . Let  $P'$  be a point distant  $ds$  from  $P$  along direction  $\mathbf{s}$ . In traversing  $PP'$ , part of the radiation is lost by absorption, but there is also a gain from the radiation emitted by the particles. Assuming that  $(dA)^{\frac{1}{2}}$  and  $ds$  are large compared with  $a$ ,\* the number of particles within the cylinder formed by  $dA$  and  $ds$  will be  $NdA ds$ .

Since each particle is a perfect absorber the amount of light absorbed in unit time by the particles from the light in direction  $d\omega$  will be  $I(\mathbf{P}, \mathbf{s})\pi a^2 N(r) dA ds d\omega$ . The radiation emitted into  $d\omega$  per second will be  $4\pi a^2 N(r) dA ds B(T) d\omega/4\pi$ , where  $B(T)$  is the total energy liberated by unit area of the surface of a black body in unit time at temperature  $T$ . From radiation theory

$$B(T) = \sigma T^4, \quad \dots\dots(2.2)$$

where  $\sigma$  is Stefan's constant.

Hence

$$[I(\mathbf{P}', \mathbf{s}) - I(\mathbf{P}, \mathbf{s})] dA d\omega = \pi a^2 N(\mathbf{P}) dA ds d\omega [(\sigma T^4/\pi) - I(\mathbf{P}, \mathbf{s})],$$

$$\text{or} \quad (\mathbf{P}, \mathbf{s}) dI ds = \pi a^2 N(r) [(\sigma T^4/\pi) - I(\mathbf{P}, \mathbf{s})]. \quad \dots\dots(2.3)$$

Now  $dI/ds = \partial I/\partial s + \partial I/c\partial t$ , where  $c$  is the velocity of light. Since we assume the cloud at rest and  $T$  constant,  $\partial I/\partial t = 0$ , and (2.3) can be written

$$\partial I/\partial \tau = \sigma T^4/\pi - I, \quad \dots\dots(2.4)$$

$$\text{where} \quad \tau = \pi a^2 \int^s N ds. \quad \dots\dots(2.5)$$

Integrating the equation along direction  $\mathbf{s}$  from  $P_1$  ( $s = s_1$  or  $\tau = \tau_1$ ) to  $P_2$  ( $s = s_2$  or  $\tau = \tau_2$ ), we get

$$I(\tau_1, \mathbf{s}) \exp \tau_1 - I(\tau_2, \mathbf{s}) \exp \tau_2 = (\sigma T^4/\pi) (\exp \tau_1 - \exp \tau_2). \quad \dots\dots(2.6)$$

Now apply this equation to determine the radiation from the cloud. We first take  $N(\mathbf{P})$  uniform, but this restriction will be removed later. Thus  $\tau = \alpha s$  where  $\alpha = \pi a^2 N_0$ . Let  $PQ$  denote a small cylindrical volume element of the sphere,

\* The only essential limitation this condition imposes, is that  $a \ll R$ . This is a fairly obvious restriction, for it would seem absurd to analyse the radiation transfer in the manner we intend, if all the material in the flash were concentrated in a few pieces. It transpires, however, that even in this case, the results of the method are correct.

whose axis is parallel to  $\mathbf{s}$  and whose normal cross section is  $dA$  (Figure 1). The total light emitted from the end surface at  $Q$  in  $d\omega$  about direction  $\mathbf{s}$  is  $I(Q, \mathbf{s}) dA d\omega$ . From (2.6),

$$I(P, \mathbf{s}) - I(Q, \mathbf{s}) \exp(\alpha PQ) = (\sigma T^4/\pi) \{1 - \exp(\alpha PQ)\}. \quad \dots\dots(2.7)$$

Clearly  $I(P, \mathbf{s}) = 0$  since we assume no light reaches the sphere from outside, and so

$$I(Q, \mathbf{s}) = (\sigma T^4/\pi) \{1 - \exp(-\alpha PQ)\}. \quad \dots\dots(2.8)$$

If  $z$  is the distance of the axis of  $PQ$  from  $O$ , the centre of the sphere,  $dA = z dz d\theta$  where  $\theta$  is the angle between the normal to  $PQ$  from  $O$ , and a reference line in the plane through  $O$  perpendicular to  $\mathbf{s}$ . Hence from (2.8) the total radiation emitted into  $d\omega$  is

$$H = d\omega (\sigma T^4/\pi) \int_0^R \int_0^{2\pi} z (1 - \exp\{-2\alpha\sqrt{(R^2 - z^2)}\}) dz d\theta, \quad \dots\dots(2.9)$$

which integrates to

$$d\omega \sigma T^4 R^2 \left[ 1 - \frac{1}{2R^2\alpha^2} + \exp(-2R\alpha) \left( \frac{1}{R\alpha} + \frac{1}{2R^2\alpha^2} \right) \right]. \quad \dots\dots(2.10)$$

Integrating over  $d\omega$ , the total radiation emitted becomes

$$\begin{aligned} H &= 4\pi R^2 \sigma T^4 \left[ 1 - \frac{1}{2R^2\alpha^2} + e^{-2R\alpha} \left( \frac{1}{R\alpha} + \frac{1}{2R^2\alpha^2} \right) \right] \\ &= H^* E(R\alpha), \end{aligned} \quad \dots\dots(2.11)$$

where

$$H^* = 4\pi R^2 \sigma T^4, \quad \dots\dots(2.12)$$

that is, the radiation from a solid black body sphere of radius  $R$ , and  $E(x)$  is given by

$$E(x) = 1 - \frac{1}{2x^2} + e^{-2x} \left( \frac{1}{x} + \frac{1}{2x^2} \right). \quad \dots\dots(2.13)$$

Clearly we may call  $E(x)$  the "effective emissivity" of the cloud.

Consider the behaviour of  $E(x)$  as  $x$  varies: (i) as  $x \rightarrow \infty$ ,  $E(x) \rightarrow 1$ ; (ii) as  $x \rightarrow 0$ ,  $E(x) \rightarrow 4x/3$ ; (iii)  $dE(x)/dx = x^{-3}[1 - e^{-2x}(2x^2 + 2x + 1)]$ . Since  $x$  is always positive  $e^{2x} > 1 + 2x + 2x^2$  and so  $dE(x)/dx > 0$ . Hence  $E(x)$  is always positive and increases steadily from  $4x/3$  to 1 as  $x$  moves from small to large values. Therefore the condition that  $H = H^*$  or that assumption (2') is fulfilled, is that  $R\alpha \gg 1$ , or from (2.1),

$$R^2 a \rho_0 \ll 9M/16\pi. \quad \dots\dots(2.14)$$

On the other hand, for  $R\alpha$  small or when

$$R^2 a \rho_0 \gg 9M/16\pi, \quad \dots\dots(2.15)$$

$$H = 4R\alpha H^*/3 = 4\pi a^2 N_0 \sigma T^4. \quad \dots\dots(2.16)$$

The radiation is then simply the sum of the radiations emitted by each particle and none is absorbed.

In subsequent work we shall frequently refer to (2.14) and (2.15) as  $E$  and  $E'$  respectively. For brevity, when a cloud satisfies inequality  $E$ , we shall say it is an "E" state, when inequality  $E'$ , in an "E'" state.

Now let us consider how the results of the analysis are modified if we remove the restriction that  $N(r)$  is constant. Equation (2.9) then becomes

$$H = 4\sigma T^4 \int_0^R \int_0^{2\pi} z (1 - \exp\{-\tau(PQ)\}) dz d\theta, \quad \dots\dots(2.17)$$

where

$$\tau(\text{PQ}) = \pi a^2 \int_{\text{P}}^{\text{Q}} N(r) d(\text{PQ}). \quad \dots (2.18)$$

To evaluate  $H$  accurately, the exact form of  $N(r)$  is required. But it seems very likely that condition (2.14) still applies for assumption (2') to be valid, for it is easily derived for the case of a thin cloud in the form of a spherical shell, which is a probable density distribution for practical cases. Suppose the material is concentrated in a thin spherical shell of thickness  $\Delta$ . Then  $H$  may be written

$$H = 4\sigma T^4 \int_0^{2\pi} \left[ \int_0^{R-\Delta} z(1 - \exp\{-\tau(\text{PQ})\}) dz + \int_{R-\Delta}^R z(1 - \exp\{-\tau(\text{PQ})\}) dz \right] d\theta. \quad \dots (2.19)$$

Since  $\Delta \ll R$ , the second term is small compared with the first and we have very nearly

$$H = 4\sigma T^4 \int_0^{2\pi} \int_0^{R-\Delta} z(1 - \exp\{-\tau(\text{PQ})\}) dz d\theta. \quad \dots (2.20)$$

For  $H = H^*$  then, we must have, for all possible values of PQ,  $\exp\{-\tau(\text{PQ})\} \ll 1$  or

$$\tau(\text{PQ}) \gg 1. \quad \dots (2.21)$$

Now in the range of integration 0 to  $R - \Delta$ ,  $\tau(\text{PQ})$  has its minimum value when PQ lies along the diameter in the direction  $\mathbf{s}$ . Hence (2.21) is satisfied if

$$2\pi a^2 \int_{R-\Delta}^R N dr \gg 1. \quad \dots (2.22)$$

Since  $4\pi R^2 \int_{R-\Delta}^R N dr = N_0$ , (2.22) gives  $R^2 a \rho_0 \ll 3M/8\pi$  which is equivalent to E.

When  $\tau(\text{PQ}) \ll 1$ , it is easy to show that we can derive expression (2.16) for the total radiation emitted for in this case

$$H = 4\sigma T^4 \pi a^2 \int_0^R \int_0^{2\pi} \int_{\text{P}}^{\text{Q}} N(r) z dz d\theta d(\text{PQ}) = 4\pi a^2 \sigma T^4 N_0.$$

Summarizing these results, we see that for a spherical shell of radiating particles we may write

$$H = H^* E_s(\tau_0), \quad \dots (2.23)$$

where

$$\tau_0 = \pi a^2 \int_{R-\Delta}^R N(r) dr \quad \dots (2.24)$$

and  $E_s(x) \simeq E(x)$  for both large and small  $x$ .

Hence the main conclusions reached for the case of a uniform distribution still hold for a spherical shell.

## 2.2. Radiation from a Cloud in which the Particles are not Perfect Absorbers or Perfect Emitters (Assumption (2''))

We shall now examine assumption (2''). Suppose the absorption coefficient of the surface of the particle is independent of the wavelength. Then, by Kirchhoff's law, the absorption coefficient equals the emissivity  $\epsilon$ , where  $\epsilon$  is defined as the ratio of the total energy radiated by unit area of the surface in unit time to the energy radiated by a unit area of black body surface in unit time. To evaluate the radiation from the cloud, it is now necessary to take into account scattering of

radiation by the particles. For, consider a single particle, in the path of a parallel beam. If  $I$  is the intensity of the beam in direction  $\mathbf{s}$  in  $d\omega$ , the total amount of light received from the beam in unit time is clearly  $I\pi a^2 d\omega$ . But the radiation absorbed in unit time is  $\epsilon I\pi a^2 d\omega$ . Hence the amount scattered out of the beam by the particle is  $(1 - \epsilon)I\pi a^2 d\omega$ . Let a fraction

$$\gamma(\mathbf{P}, \mathbf{s}', \mathbf{s}) d\omega' / 4\pi \quad \dots\dots (2.25)$$

of the total light scattered by a particle be scattered into directions within solid angle  $d\omega'$  about the direction  $\mathbf{s}'$ . It follows that

$$\int \gamma(\mathbf{P}, \mathbf{s}', \mathbf{s}) d\omega' = 4\pi, \quad \dots\dots (2.26)$$

where integration is over all directions  $\mathbf{s}'$ . The more general form of equation (2.3), in which account is taken of scattering is

$$\frac{\partial I(\mathbf{P}, \mathbf{s})}{\partial s} = \pi a^2 N \left[ \frac{\epsilon \sigma T^4}{\pi} - I(\mathbf{P}, \mathbf{s}) + \frac{(1 - \epsilon)}{4\pi} \int I(\mathbf{P}, \mathbf{s})' \gamma(\mathbf{P}, \mathbf{s}', \mathbf{s}) d\omega' \right]. \quad \dots\dots (2.27)$$

The first term of the right-hand side represents radiation gained by emission, the second, radiation lost by absorption and scattering, and the third, the contribution due to radiation scattered *into* direction  $\mathbf{s}$ . The integration in the third term is again over all directions  $\mathbf{s}'$ .

If we neglect the light scattered into  $d\omega'$  equation (2.27) becomes

$$\frac{\partial I(\mathbf{P}, \mathbf{s})}{\partial s} = \pi a^2 N \left[ \frac{\epsilon \sigma T^4}{\pi} - I(\mathbf{P}, \mathbf{s}) \right], \quad \dots\dots (2.28)$$

which is equivalent to (2.3) with  $\sigma$  replaced by  $\epsilon \sigma$ . Hence if (2.28) were satisfied, together with the condition E, assumption (2'') would be correct. But it is clearly illegitimate to reject the light scattered *into*  $d\omega$  and retain the light scattered *out* in the derivation of (2.27). Hence (2'') is incorrect and gives too small a value for the emitted radiation.

On the other hand, even if E is satisfied the radiation is *less* than it would be from a solid sphere emitting black-body radiation. For, suppose the cloud is placed in a black-body enclosure whose walls are at temperature  $T$ . Let  $H_m$  be the radiation emitted by the material of the cloud which traverses the outer surface in unit time. Then the total radiation received by the enclosure from the particles is  $H_1 = H_m + H_s$  where  $H_s$  represents the part of the energy from the walls of the enclosure which is scattered back to the walls by the cloud. But  $H_1$  represents the energy emitted by a cloud of black-body material since in this case  $H_s = 0$ . Thus for  $\epsilon < 1$ ,  $H_m < H^*$ . Hence it follows that the total energy radiated per second is

$$H = 4\pi R^2 \epsilon' \sigma T^4, \quad \dots\dots (2.29)$$

where  $\epsilon < \epsilon' < 1$ . To determine  $\epsilon'$ , which we may again call the "effective emissivity" it is first necessary to determine  $\gamma(\mathbf{P}, \mathbf{s}', \mathbf{s})$ . This is, strictly, a matter for experiment. But  $\gamma(\mathbf{P}, \mathbf{s}', \mathbf{s})$  can be calculated for simple cases. For example, if the light scattered is reflected specularly from the particle surface

$$\gamma(\mathbf{P}, \mathbf{s}', \mathbf{s}) = 1. \quad \dots\dots (2.30)$$

For diffuse reflection

$$\gamma(\mathbf{P}, \mathbf{s}', \mathbf{s}) = (8/3\pi)(\sin \phi - \phi \cos \phi), \quad \dots\dots (2.31)$$

where  $\phi$  is the angle between  $\mathbf{s}$  and  $\mathbf{s}'$ . Another law which might be considered is that for "Rayleigh scattering", which is given by

$$\gamma(\mathbf{P}, \mathbf{s}', \mathbf{s}) = 3(1 + \cos^2 \phi)/4. \quad \dots\dots(2.32)$$

But for this law to hold,  $a$  would have to be small compared with the light wavelength and it is unlikely that the particles in the light sources we are considering are so small. The evaluation of the expressions (2.30) and (2.31) is given in Appendix I.

It now remains to calculate  $\epsilon'$  by substituting expressions (2.30) or (2.31) in equation (2.27) and solving for  $I$ . Unfortunately, owing to the last term of equation (2.27), the total radiation from the sphere cannot be evaluated in the same manner as in the case of (2.11). We can, however, give an approximate calculation, the results of which agree quite well with (2.11) in the case of  $\epsilon = 1$ .

Let the angle between the radius vector drawn to any point in the cloud and the direction  $\mathbf{s}$  be  $\theta$ . Then

$$\frac{\partial I}{\partial s} = \cos \theta \frac{\partial I}{\partial r} - \frac{\sin \theta}{r} \frac{\partial I}{\partial \theta}. \quad \dots\dots(2.33)$$

If we again assume  $N$  is constant and write

$$\tau = \pi a^2 N(r), \quad \dots\dots(2.34)$$

then equation (2.27) becomes

$$\cos \theta \frac{\partial I}{\partial \tau} - \frac{\sin \theta}{\tau} \frac{\partial I}{\partial \theta} = \frac{\epsilon \sigma T^4}{\pi} + \frac{(1-\epsilon)}{4\pi} \int I(\tau, \theta') \gamma(\tau, \theta', \theta) d\omega' - I. \quad \dots\dots(2.35)$$

Let  $J$  denote the total intensity of radiation and  $F$  the total flux of radiation in the direction of increasing  $\tau$ , then

$$J(\tau) = \int I d\omega = 2\pi \int_0^\pi I(\tau, \theta) \sin \theta d\theta, \quad \dots\dots(2.36)$$

$$F(\tau) = \int I \cos \theta d\omega = 2\pi \int_0^\pi I(\tau, \theta) \sin \theta \cos \theta d\theta. \quad \dots\dots(2.37)$$

We also define a quantity  $K$  by the relation

$$K(\tau) = \int I \cos^2 \theta d\omega = 2\pi \int_0^\pi I(\tau, \theta) \sin \theta \cos^2 \theta d\theta. \quad \dots\dots(2.38)$$

Multiplying equation (2.35) by  $d\omega$  and integrating over all directions, we have

$$\frac{dF}{d\tau} - \frac{1}{\tau} \int \frac{\partial I}{\partial \theta} \sin \theta d\omega = 4\epsilon \sigma T^4 + \frac{(1-\epsilon)}{4\pi} \int d\omega \int I(\tau, \theta') \gamma(\tau, \theta', \theta) d\omega' - J. \quad \dots\dots(2.39)$$

Using (2.26)

$$\int d\omega \int I(\tau, \theta') \gamma(\tau, \theta', \theta) d\omega' = \int I(\tau, \theta') d\omega' \int \gamma(\tau, \theta', \theta) d\omega = 4\pi J. \quad \dots\dots(2.40)$$

Also

$$\int \frac{\partial I}{\partial \theta} \sin \theta d\omega = 2\pi \int_0^\pi \frac{\partial I}{\partial \theta} \sin^2 \theta d\theta - 2\pi \left[ I \sin^2 \theta \Big|_0^\pi - 2 \int_0^\pi I \sin \theta \cos \theta d\theta \right] = -2F. \quad \dots\dots(2.41)$$

Hence (2.39) becomes

$$dF/d\tau + 2F/\tau = \epsilon(4\sigma T^4 - J). \quad \dots\dots(2.42)$$



Multiplying equation (2.35) by  $\cos \theta d\omega$  and integrating again, we get

$$\frac{dK}{d\tau} - \frac{1}{\tau} \int \frac{\partial I}{\partial \theta} \sin \theta \cos \theta d\omega = \frac{(1-\epsilon)}{4\pi} \int \cos \theta d\omega \int I(\tau, \theta') \gamma(\tau, \theta', \theta) d\omega' - F. \quad \dots\dots(2.43)$$

Reversing the order of integration, we find

$$\int \cos \theta d\omega \int I(\tau, \theta') \gamma(\tau, \theta', \theta) d\omega' = \int I(\tau, \theta') d\omega' \int \gamma(\tau, \theta', \theta) \cos \theta d\omega. \quad \dots\dots(2.44)$$

Let  $\phi$  denote the angle between  $\mathbf{s}$  and  $\mathbf{s}'$ , and  $\psi$  the angle between the plane containing directions  $\mathbf{s}'$  and  $\mathbf{s}$  and the plane containing direction  $\mathbf{s}'$  and the radius vector. Then we can put  $d\omega = \sin \phi d\phi d\psi$ , and since

$$\cos \theta = \cos \phi \cos \theta' + \sin \phi \sin \theta' \cos \psi,$$

we have

$$\begin{aligned} \int \gamma(\tau, \theta', \theta) \cos \theta d\omega &= \int_0^\pi \int_0^{2\pi} \gamma(\phi) (\cos \phi \cos \theta' + \sin \theta' \sin \phi \cos \psi) \sin \phi d\phi d\psi \\ &= -4\pi X \cos \theta', \end{aligned} \quad \dots\dots(2.45)$$

where  $X$  is a constant.  $\gamma(\phi)$  is given by one of the relations (2.30), (2.31) or (2.32).

Integrating (2.45) we find  $X=0$  for regular reflection or Rayleigh scattering, and  $X=4/9$  for diffuse reflection.

We also have

$$\begin{aligned} \int \frac{\partial I}{\partial \theta} \sin \theta \cos \theta d\omega &= 2\pi \int_0^\pi \frac{\partial I}{\partial \theta} \sin^2 \theta \cos \theta d\theta \\ &= 2\pi \left[ I \sin^2 \theta \cos \theta \Big|_0^\pi - \int_0^\pi I (3 \sin \theta \cos^2 \theta - \sin \theta) d\theta \right] = J - 3K. \end{aligned} \quad \dots\dots(2.46)$$

Now the mean value of  $\cos^2 \theta$  over the unit sphere is  $\frac{1}{3}$ . Hence we have, approximately,

$$K = \int I \cos^2 \theta d\omega \simeq \overline{\cos^2 \theta} \int I d\omega = \frac{1}{3}J. \quad \dots\dots(2.47)$$

This approximation is exact if  $I$  could be expanded in odd powers of  $\cos \theta$ . It is a well-known approximation (Eddington 1930) in the theory of radiative equilibrium. Hence (2.43) becomes

$$dK/d\tau = -F[X(1-\epsilon) + 1]. \quad \dots\dots(2.48)$$

From (2.42), (2.47) and (2.48) we have a single differential equation for  $J$ , namely

$$\frac{d^2 J}{d\tau^2} + \frac{2}{\tau} \frac{dJ}{d\tau} = 3\epsilon[X(1-\epsilon) + 1][J - 4\sigma T^4]$$

or

$$d^2(J\tau)/d\tau^2 = \beta^2 \tau (J - 4\sigma T^4), \quad \dots\dots(2.49)$$

if

$$\beta = \sqrt{\{3\epsilon[X(1-\epsilon) + 1]\}}. \quad \dots\dots(2.50)$$

The solution is

$$J(\tau) = 4\sigma T^4 + \tau^{-1}(A e^{-\beta\tau} \beta\tau + B e^{-\beta\tau} \beta\tau), \quad \dots\dots(2.51)$$

where  $A$  and  $B$  are constants of integration.

Since  $J$  must remain finite near  $\tau=0$  we must have

$$A + B = 0. \quad \dots\dots(2.52)$$

To find  $A$ , we observe that, at the boundary  $I(\alpha R, \theta) = 0$  for  $\theta > \pi/2$ . Hence

$$F(\alpha R) = 2\pi \int_0^{\pi/2} I(\alpha R, \theta) \sin \theta \cos \theta d\theta, \quad J(\alpha R) = 2\pi \int_0^{\pi/2} I(\alpha R, \theta) \sin \theta d\theta.$$

Replacing  $\cos \theta$  in the first integral by its mean value from 0 to  $\pi/2$ , we find

$$J(\alpha R) = 2F(\alpha R). \quad \dots\dots(2.53)$$

But from (2.48)

$$F(\alpha R) = -\frac{\epsilon}{\beta^2} \frac{dJ}{d\tau} \bigg|_{\tau=\alpha R} \quad \dots\dots(2.54)$$

Hence from (2.51), (2.53) and (2.54),

$$A = \frac{2\alpha RT^4}{\left[ \frac{\epsilon}{\beta^2 \alpha R} - \frac{\epsilon}{\beta} - \frac{1}{2} \right] \exp(\alpha \beta R) - \left[ \frac{\epsilon}{\beta^2 \alpha R} + \frac{\epsilon}{\beta} - \frac{1}{2} \right] \exp(-\alpha \beta R)}, \quad \dots\dots(2.55)$$

and for the surface flux  $F(\alpha R) = \sigma T^4 E_e(\alpha R)$  where

$$E_e(\alpha R) = \frac{4\epsilon \left[ \left( 1 - \frac{1}{\beta \alpha R} \right) + \left( 1 + \frac{1}{\beta \alpha R} \right) \exp(-2\beta \alpha R) \right]}{\left[ \beta + 2\epsilon \left( 1 - \frac{1}{\beta \alpha R} \right) - \left( \beta - 2\epsilon \left[ 1 + \frac{1}{\beta \alpha R} \right] \right) \exp(-2\beta \alpha R) \right]}. \quad \dots\dots(2.56)$$

Since the surface flux would be  $\sigma T^4$  if the boundary were replaced by a black body,  $E_e(\alpha R)$  represents the effective emissivity. It is clearly a generalization of the formula (2.11) for  $E(\alpha R)$  to the case when  $\epsilon < 1$ .

Consider the value of  $E_e(\alpha R)$  for  $\epsilon = 1$  and  $\alpha R$  large, i.e. condition E satisfied. We find

$$E_e(\infty) = 4\epsilon/(\beta + 2\epsilon). \quad \dots\dots(2.57)$$

Since  $\beta = \sqrt{3\epsilon}$  it follows that  $E_1(\infty) = 1.072$ ; the correct value is, of course, 1. This shows that our approximation is quite close, and suggests that we write, for the effective emissivity,  $\epsilon_e'$

$$\epsilon_e'(\alpha R) = 0.93 E_e(\alpha R), \quad \dots\dots(2.58)$$

instead of the quantity  $E_e(\alpha R)$  defined by equation (2.56).

The following special cases of formula (2.56) are of interest.

1. For  $\epsilon = 1$  we should have, from formulae (2.58) and (2.57)  $\epsilon_1'(\alpha R) = E(\alpha R)$ . In Figure 2, curves 1 and 2 show how these quantities compare. Curve 1 is, of course, exact, and the two curves differ because of the approximations (2.47) and (2.53) which have been introduced to obtain expression (2.56). It will be seen that curve 2 lies just below 1 for most of the range. If  $E_e(\alpha R)$  were plotted it would almost lie on curve 1 except near the origin. The curves show that the approximation (2.58) is only a few per cent out.

2. Suppose E is satisfied, that is  $\alpha R$  is large. Then for uniform and Rayleigh scattering

$$\epsilon_e'(\infty) = 3.72\sqrt{\epsilon}/(2\sqrt{\epsilon} + \sqrt{3}). \quad \dots\dots(2.59)$$

For diffuse reflection

$$\epsilon_e'(\infty) = \frac{3.72\sqrt{\epsilon}}{2\sqrt{\epsilon} + \sqrt{\{(13-4\epsilon)/3\}}}. \quad \dots\dots(2.60)$$

Figure 3 shows how these expressions depend upon  $\epsilon$ .

When E is satisfied, higher degrees of approximation are possible and  $\epsilon'_e(\infty)$  is better expressed by

$$\epsilon'_e(\infty) = 1 - \frac{2(1-\epsilon)}{2\epsilon + \sqrt{(3\epsilon)}} \left[ 1 - \frac{\ln \{1 + \sqrt{(3\epsilon)}\}}{\sqrt{(3\epsilon)}} \right]. \quad \dots\dots (2.61)$$

This approximation gives  $\epsilon' = 1$  when  $\epsilon = 1$ ; it is almost indistinguishable from (2.59) in Figure 3. This expression is derived in Appendix II.

3. When  $\alpha R$  is small, that is, the cloud is in state "E'",  $E_e(\alpha R) = 4\epsilon\alpha R/3$  and

$$H = 4\pi a^2 N_0 \epsilon \sigma T^4. \quad \dots\dots (2.62)$$

As we should expect physically, the radiation is simply the total radiation emitted by each of the particles.

The dependence of  $\epsilon'$  upon  $a$  for a cloud of given size and mass is seen in Figure 2, which is plotted for a cloud of aluminium oxide particles. The curves show several points of interest. There is not very much difference between the curves for diffuse and uniform scattering—the latter lying slightly above the former. For different values of  $\epsilon$ , the curves are of the same general shape, but reduced in scale along both the  $y$  and  $x$  directions. From the shape it will be seen that the radiation is sensitive to  $a$ , the particle size, over a fairly restricted range. For  $\epsilon = 1$  this range is approximately  $10^{-3}$  to  $6 \times 10^{-3}$  cm. When  $\epsilon = 0.1$  and  $0.01$  the corresponding ranges are  $5 \times 10^{-4}$  to  $2 \times 10^{-3}$  cm. and  $10^{-3}$  to  $3 \times 10^{-4}$  cm. respectively.

### 2.3. Radiation from a Cloud of Particles in the Form of a Spherical Shell

Suppose now that  $N$  is constant within the spherical shell of bounding radii  $R'$  and  $R$  but that there is no matter within the sphere of radius  $R'$ . The whole of the analysis of the radiation within the uniform sphere given above applies to the radiation within the shell, except the boundary condition (2.52). This is replaced by a boundary condition at  $r = R'$ . Since there is no matter inside the sphere of radius  $R'$ , there can be no net flow of radiation outwards across the surface. Hence, by symmetry,

$$F(\alpha R') = 0. \quad \dots\dots (2.63)$$

The formulae for the effective emissivity corresponding to equation (2.56) is

$$\begin{aligned} \epsilon'_e(\alpha, R, R') = & 1.86 \left[ 1 - \beta \left\{ \beta + 2\epsilon \left[ 1 - \frac{1}{\alpha\beta R} \right] \right. \right. \\ & + [\exp \{-2\alpha\beta(R - R')\}] \left[ \frac{\alpha\beta R' - 1}{\alpha\beta R' + 1} \right] \left[ \beta - 2\epsilon \left( 1 + \frac{1}{\alpha\beta R} \right) \right] \Big\}^{-1} \\ & - \beta \left\{ \beta - 2\epsilon \left[ 1 + \frac{1}{\alpha\beta R} \right] \right. \\ & + [\exp \{2\alpha\beta(R - R')\}] \left[ \frac{\alpha\beta R' + 1}{\alpha\beta R' - 1} \right] \left[ \beta + 2\epsilon \left( 1 - \frac{1}{\alpha\beta R} \right) \right] \Big\}^{-1} \Big]. \\ & \dots\dots (2.64) \end{aligned}$$

When  $R' = 0$ , it is easy to verify that (2.64) gives formula (2.58).

Suppose  $\alpha(R - R')$  is large. Then *a fortiori*  $\alpha R$  is large and we find (2.64) gives (2.59) or (2.60) for the effective emissivity. For  $\alpha R$  small we again obtain formula (2.62). If  $\alpha$  is fixed, as  $R' \rightarrow R$ ,  $\epsilon'_e(\alpha, R, R') \rightarrow 0$ . But suppose we fix  $a$  and the total mass of material in the cloud but vary  $R'$ . As  $R'$  increases, the

material is compressed more and more into a thin shell between radii  $R'$  and  $R$ . In fact, if  $\alpha_0$  is the value of  $\alpha$  when  $R=0$  the value of  $\alpha$  in the general case is

$$\alpha = \alpha_0 R^3 / (R^3 - R'^3). \quad \dots\dots (2.65)$$

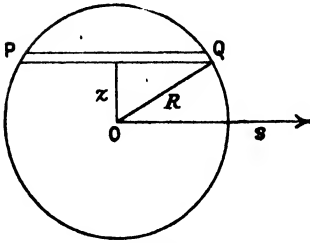


Figure 1.

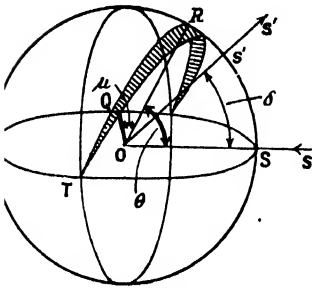


Figure 5.

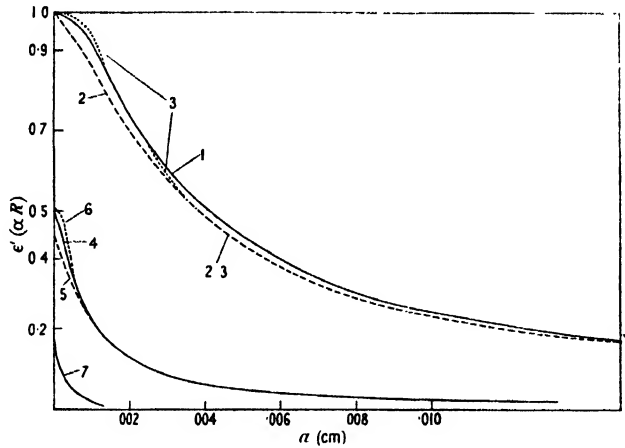


Figure 2. Variation of effective emissivity with particle radius.  $M=3.7$  gm.  $R=1$  ft. 1,  $\epsilon=1$ , exact formula (2.13); 2,  $\epsilon=1$ , approximate formula (2.58); 3,  $\epsilon=1$ , uniform scattering, uniform distribution in thin spherical shell, formula (2.66); 4,  $\epsilon=0.1$ , uniform scattering, formula (2.58); 5,  $\epsilon=0.1$ , diffuse scattering (2.58); 6,  $\epsilon=0.1$ , uniform scattering, thin shell (2.66); 7,  $\epsilon=0.01$ , uniform scattering (2.58).

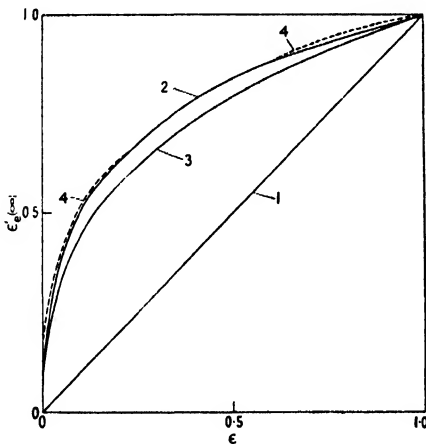


Figure 3. Variation of effective emissivity  $\epsilon'$  with  $\epsilon$  (clouds in E state). 1,  $\epsilon=\epsilon$ ; 2, uniform scattering, first approximation (2.59); 3, diffuse scattering, first approximation (2.60); 4, uniform scattering, second approximation (2.61).

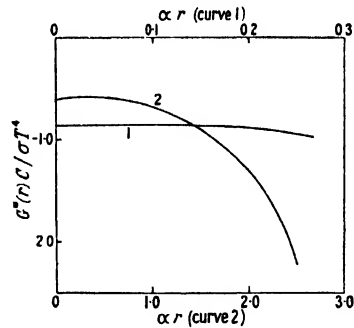


Figure 4. Dependence upon  $\alpha R$  of temperature distribution when cloud is cooling. Curve 1,  $\alpha R=0.3$ . Curve 2,  $\alpha R=3$ .

In the limiting case  $R' \rightarrow R$  we find  $\alpha\beta R = \alpha\beta R' \rightarrow \infty$ ;  $\exp\{-2\alpha\beta(R-R')\} \rightarrow \exp\{-2\alpha_0\beta R/3\}$ . Hence the effective emissivity of a thin spherical shell is given by

$$\epsilon_e'(\alpha, R, R') = \frac{3.72\epsilon(1 - \exp\{-2\alpha_0\beta R/3\})}{\beta + 2\epsilon + (\beta - 2\epsilon)\exp\{-2\alpha_0\beta R/3\}}. \quad \dots\dots (2.66)$$

In Figure 2 we have plotted this expression against the particle size for  $\epsilon = 1$  and 0.1 and regular scattering. The emissivity is not markedly different from that of the uniform spherical distribution. This rather surprising indifference of  $\epsilon'$  to the distribution law is also shown by calculating  $\epsilon_1'(\alpha, R, R')$  as a function of  $R'$ . We have calculated  $\epsilon'$  for particles of 0.004 cm. and a cloud of the same size and mass as for Figure 2. The variation of  $\epsilon'$  as  $R'$  increases from zero to 1 ft. is only about 1%.

The approximations (2.47) and (2.53) may not be very good as  $R'$  approaches  $R$  but the general behaviour of (2.64) suggests that the radiation from the cloud is not affected very much by the density distribution of the particles within it.

### § 3. COOLING OF THE CLOUD. EXAMINATION OF ASSUMPTION (1)

We must now examine the conditions under which assumption (1) is valid; that is, for the temperature to remain uniform as the cloud cools. Suppose that the particles are maintained in some way at a uniform temperature  $T$  for time  $t < t'$ . At  $t = t'$  let the heat supply be discontinued so that the cloud begins to cool. Let  $G(r)$  denote the initial rate of fall in temperature.

$$G(r) = -\partial T(r)/\partial t|_{t'}. \quad \dots (3.1)$$

The condition that the temperature remains uniform in the subsequent cooling is, clearly, that  $G(r)$  is independent of  $r$ .

Heat may be transferred from the inner to the outer layers of the cloud by radiation, conduction or convection. The condition that  $G(r)$  is independent of  $r$  will, in each of the three cases, impose restrictions on the physical quantities involved. We first consider the transfer of heat by radiation.

The total loss of heat from a spherical part of the cloud of radius  $r$  equals the amount of heat emitted from the portion radius  $r$ , less the heat absorbed from the outer shell of thickness  $(R - r)$ . Assuming that the density of the cloud is uniform this gives

$$4\pi C \int_0^r G(r)r^2 dr = 4\pi r^2 \sigma T^4 E(\alpha r) - A, \quad \dots (3.2)$$

where  $A$  denotes the heat absorbed from part  $(R - r)$  and  $C$  the thermal capacity of the cloud per unit volume. To estimate  $A$  we consider as before the heat transfer in a thin cylinder  $SP'Q'T$ , in directions within solid angle  $d\omega$  about  $\mathbf{s}$ . The portion  $P'Q'$  lies in the sphere radius  $r$ , and  $SP'$ ,  $Q'T$  lie in the shell  $(R - r)$ . We have from (2.6)

$$I(P', \mathbf{s}) = (\sigma T^4/\pi) \{1 - \exp(-\alpha SP')\}. \quad \dots (3.3)$$

A fraction  $1 - \exp(-\alpha P'Q')$  of this light is absorbed in  $P'Q'$ . Hence the total amount of light absorbed by the inner sphere from the outer shell is

$$A = 8\pi\sigma T^4 \int_0^R [1 - \exp(-\alpha SP')][1 - \exp(-\alpha P'Q')] z dz, \quad \dots (3.4)$$

where  $z$  is the distance of  $P'Q'$  from the axis. The integral cannot be evaluated, but the maximum value of  $SP$  is  $(R^2 - r^2)^{1/2}$  and the minimum value is  $(R - r)$ . Hence it follows that the heat absorbed lies between the quantities

$$8\pi\sigma T^4 [1 - \exp\{-\alpha(R - r)\}] \int_0^r z [1 - \exp\{-2\alpha(r^2 - z^2)^{1/2}\}] dz$$

and

$$8\pi\sigma T^4 [1 - \exp\{-\alpha(R^2 - r^2)^{1/2}\}] \int_0^r z [1 - \exp\{-2\alpha(r^2 - z^2)^{1/2}\}] dz$$

or

$$4\pi\sigma T^4 r^2 E(\alpha r)[1 - \exp\{-\alpha(R-r)\}] < A < 4\pi\sigma T^4 r^2 E(\alpha r)[1 - \exp\{-\alpha(R^2 - r^2)^{\frac{1}{2}}\}]. \quad \dots\dots(3.5)$$

Substituting the value of  $A$  given by equation (3.2) we find

$$r^2 E(\alpha r) \exp\{-\alpha(R^2 - r^2)^{\frac{1}{2}}\} < \frac{CG}{\sigma T^4} \int_0^r G(r) r^2 dr < r^2 E(\alpha r) \exp\{-\alpha(R-r)\}. \quad \dots\dots(3.6)$$

If  $G(r) = G$ , where  $G$  is independent of  $r$ , we must have, for all values of  $r$ ,

$$r^{-1} E(\alpha r) \exp\{-\alpha(R^2 - r^2)^{\frac{1}{2}}\} < CG/3\sigma T^4 < r^{-1} E(\alpha r) \exp\{-\alpha(R-r)\}. \quad \dots\dots(3.7)$$

The two outer limits  $r \rightarrow 0$  and  $r \rightarrow R$  must converge, hence the condition that  $G(r)$  is independent of  $r$  is

$$\lim_{r \rightarrow 0} r^{-1} E(\alpha r) \exp\{-\alpha(R-r)\} = \lim_{r \rightarrow R} r^{-1} E(\alpha r) \exp\{-\alpha(R-r)\}. \quad \dots\dots(3.8)$$

From (2.13)  $\lim_{r \rightarrow 0} r^{-1} E(\alpha r) = 4\alpha/3$ . Hence (3.8) becomes

$$4\alpha R/3 = \exp(\alpha R) E(\alpha R). \quad \dots\dots(3.9)$$

Now from equation (2.13) for  $E(x)$  we have

$$4\alpha R/3 - \exp(\alpha R) E(\alpha R) = -\sum_2^{\infty} a_n (\alpha R)^n, \quad \dots\dots(3.10)$$

where  $a_n = [(n+3)(n+1)]/(n+2)!$ ,  $n$  odd, and  $a_n = n/(n+1)!$ ,  $n$  even. Hence, since all the coefficients  $a_n$  are greater than 0, condition (3.10) is only satisfied if

$$\alpha R \ll 1, \quad \dots\dots(3.11)$$

that is, if condition  $E'$  holds. This is the reverse of  $E$ , the condition found for the radiation to be equivalent to that of a solid back-body radiator.

Unfortunately relation (3.6) cannot tell us much about the behaviour of  $G(r)$  since it does not follow that

$$\frac{d}{dr} [r^2 E(\alpha r) \exp\{-\alpha(R^2 - r^2)^{\frac{1}{2}}\}] < \frac{Cr^2}{\sigma T^4} G(r) < \frac{d}{dr} [r^2 E(\alpha r) \exp\{-\alpha(R-r)\}]. \quad \dots\dots(3.12)$$

In view of equation (3.6), however, and the fact that the above relation is certainly true near  $r=0$ , it seems reasonable to suppose that the quantity

$$G^*(r) = \frac{\sigma T^4}{2Cr^2} \frac{d}{dr} r^2 E(\alpha r) [\exp\{-\alpha(R-r)\} + \exp\{-\alpha(R^2 - r^2)^{\frac{1}{2}}\}], \quad \dots\dots(3.13)$$

gives a good approximation to the behaviour of  $G(r)$ .

In Figure 4,  $G^*(r)$  is plotted as a function of  $r$  for the two cases  $\alpha R = 0.3$  and  $\alpha R = 3$ . It will be seen that in the first case  $G^*$  is very nearly uniform but this is by no means correct for  $\alpha R = 3$ . It is easy to visualize the physical mechanism in cases  $\alpha R \gg 1$ . Strictly each part of the material radiates the same amount of energy but most of the energy is re-absorbed except near the surface where it can escape into outer space. Hence the temperature of the outer part is lower than that of the interior. The same general considerations will obviously apply to particles for which  $\epsilon$  is less than 1.

We must now examine the possibility of the temperature being maintained uniform in state  $E$  by conduction of heat. Suppose heat is lost from the surface

of the cloud by radiation only, whereas inside it is transferred by conduction only. Let  $k$  be the thermal conductivity of the gas occupying the space between the particles. If  $H$  is the energy radiated by the cloud in unit time

$$H = -4\pi k R^2 (\partial T / \partial r)|_{R}. \quad \dots\dots(3.14)$$

But 
$$H = -4\pi \int_0^R C \frac{\partial T}{\partial t} r^2 dr. \quad \dots\dots(3.15)$$

If the temperature is nearly uniform, we may replace the second integral by

$$4\pi C \frac{\partial \bar{T}}{\partial t} \int_0^R r^2 dr = \frac{4\pi R^3}{3} C \frac{\partial \bar{T}}{\partial t}, \quad \dots\dots(3.16)$$

where  $\partial T / \partial t$  represents the mean value of  $\partial T / \partial t$ . But we also have

$$kr^2 \frac{\partial T}{\partial r} = \int_0^r C \frac{\partial T}{\partial t} r^2 dr \quad \text{or} \quad k \frac{\partial T}{\partial r} = C \frac{\partial \bar{T}}{\partial t} \frac{r}{3}. \quad \dots\dots(3.17)$$

Integrating, we find

$$T(R) - T(0) = (CR^2/6k) (\partial \bar{T} / \partial t) = H/8\pi k R. \quad \dots\dots(3.18)$$

For  $R = 1$  ft. and  $T = 2700^\circ \text{K.}$  and a temperature difference of  $100^\circ \text{C.}$  between the centre and surface of the cloud we should require  $k \simeq 1$  c.g.s. units.

At  $T \sim 2700^\circ \text{K.}$ ,  $k$  for air is about  $4 \times 10^{-4}$  c.g.s. unit; thus it appears that the thermal conductivity is much too low to maintain uniform temperature.

There remains transport of heat by convection or turbulence; this is difficult to deal with quantitatively. But it seems possible that this factor is quite important in view of the high temperatures involved.

Hence we conclude that  $E'$  is a necessary condition for the temperature of the cloud to remain uniform if it were so initially, unless the temperature is maintained uniform by convection.

#### § 4. DISCUSSION

Summarizing our results, we find:

(i) If the transfer of heat by convection may be ignored, uniform temperature during cooling requires condition  $E'$ . When this condition is not satisfied, the cloud is cooler near the surface than in the interior.

(ii) When the temperature is uniform and  $\epsilon = 1$ , the cloud is equivalent to a solid black body if  $E$  holds. Whether or not  $E$  is satisfied for  $\epsilon$  less than 1 the total radiation lies between the value it would have if  $\epsilon$  equalled 1, and this value multiplied by  $\epsilon$ . In other words, if  $\epsilon'$  is the effective emissivity  $\epsilon < \epsilon' < 1$ .

Now let us consider the bearing of these results on Caldin's theory. If transfer of heat by convection is important it follows that this method is legitimate provided that the appropriate expression for the effective emissivity is employed. On the other hand, if transfer of heat takes place through radiation only, it would seem at first sight that our results show that it would be impossible to apply Caldin's theory to transient light sources, for this theory assumes uniform temperatures—which requires condition  $E'$ —and yet assumes  $E$  and that  $\epsilon = \epsilon'$  in the determination of the heat radiated. But one or the other of  $E$  and  $E'$  may be satisfied, not both simultaneously. This is a little too drastic however; for if  $E'$  is satisfied, the theory is still valid provided that for the effective emissivity  $\epsilon'$  of the radiator we use *not* the ordinary solid surface emissivity  $\epsilon$ , but the expression

$$\epsilon' = 3M\epsilon/4\pi R^2 a\rho_0. \quad \dots\dots(4.1)$$

This follows from equation (2.16).

Condition E' imposes a lower limit on the particle size—for example, with a cloud of radius one foot containing 4 grammes of magnesium oxide we require  $a \gg 2.0 \times 10^{-3}$  cm. Magnesium metal burning in air gives small cubic crystals of the oxide with side lengths from  $10^{-5}$  to  $10^{-4}$  cm., so that in this case E' is apparently not satisfied. But experimental evidence must decide the state of the cloud in each particular case.

It is of interest, however, to consider some of the consequences if, both in the formation of the cloud and its subsequent cooling, the cloud is cooler near the surface than in the interior. A necessary condition for this state of affairs would be the non-fulfilment of condition E'. The amount of radiation given off is determined mainly by the temperature of the surface layers. For, owing to absorption, the fraction of the emitted radiation which escapes to outer space decreases as we move from surface to centre; defining the effective temperature  $T_e$  of the cloud by the equation

$$F(0) = \sigma T_e^4, \quad \dots\dots(4.2)$$

then  $T_e < \bar{T}$ .

In certain cases it is possible to find the effective temperature in terms of the temperatures in the interior and at the surface. For, assume E and that  $\epsilon = 1$ ; then equation (2.3) gives the intensity. Suppose the temperature, instead of being constant is given by

$$T^4(\tau) = T_0^4[1 - \mu \exp(-\tau/\tau_0)]. \quad \dots\dots(4.3)$$

This would represent a temperature distribution like that of Figure 4, curve 2, in general shape—nearly uniform temperature in the interior surrounded by a cooler layer.  $\tau_0$  is a rough measure of the thickness of this layer. The surface temperature will be

$$T_s = T_0(1 - \mu)^{\frac{1}{4}} \quad \dots\dots(4.4)$$

if  $T_0$  is the temperature of the interior. The equation for  $I$  is

$$\cos \theta \partial I(\tau, \theta) / \partial \tau = I(\tau, \theta) - (\sigma T_0^4 / \pi) [1 - \mu \exp(-\tau/\tau_0)]. \quad \dots\dots(4.5)$$

Integrating, for  $\theta < \pi/2$ ,

$$I(0, \theta) = (\sigma T_0^4 / \pi) [1 - \mu \tau_0 / (\tau_0 + \cos \theta)]. \quad \dots\dots(4.6)$$

Hence

$$\begin{aligned} F(0) &= \sigma T_e^4 = 2\pi \int_0^{\pi/2} I(0, \theta) \sin \theta \cos \theta d\theta, \\ &= \sigma T_0^4 [1 - 2\mu \tau_0 \{1 - \tau_0 \ln(1 + \tau_0) / \tau_0\}]. \end{aligned} \quad \dots\dots(4.7)$$

For  $\tau_0 \gg 1$ , that is for large optical depth of the cool layer,  $T_e = T_s$ , and for  $\tau_0 \ll 1$ , or for small optical depth of the cool layer,  $T_e = T_0$ . From Figure 4, curve 2, we should expect in practice  $\tau_0 \sim 1$ , i.e. from (4.7)

$$T_e^4 \simeq 0.39 T_0^4 + 0.61 T_s^4. \quad \dots\dots(4.8)$$

This result still holds even if the cool layer is so thin, compared with the radius of the cloud, that the mean temperature is effectively  $T_0$ .

Conditions E and E' have a bearing upon the efficiency of transient light sources. Consider two clouds initially at the same uniform temperature, and of the same thermal capacity, one of which, S, satisfies E, the other, S', E'. Let us also



assume that in S convection is not sufficient to maintain uniform temperature. After a long time both will have ultimately lost all their heat to the surroundings. But whereas S' cools with uniform temperature, S has a cool outer layer and so its radiation escapes more slowly, and at a lower effective temperature than S. In the temperature range which we are concerned, the ratio of the quantity of light energy to total energy in the black body spectrum increases as the temperature increases. Hence, although S and S' ultimately lose the same amount of energy, a greater fraction escapes as light in S' than in S. Thus the efficiency of a cloud as a source of light increases as we pass from state E to state E'.

Another consequence of the cool outer layer is that the emergent radiation will not be black-body radiation for states E. When E is satisfied the intensity of radiation of wavelength  $\lambda$  emerging at  $\theta$  is

$$I_{\lambda}(0, \theta) = \frac{2hc^2}{\lambda^5} \int_0^{\infty} \frac{\exp(-\tau \sec \theta)}{\exp(hc/\lambda kT) - 1} \sec \theta d\tau. \quad \dots (4.9)$$

This will not necessarily correspond to the Planck distribution at temperature  $T_e$  since  $T$  in the integrand is a function of  $\tau$ . The energy distribution of (4.9) for *radiative equilibrium* has been studied by Milne (1900). In this case the spectrum of the total flux corresponds to a temperature 4% higher than  $T_e$ . The spectral distribution is slightly bluer than black-body radiation for the effective temperature  $T_e$ . The deviation from the Planck formula is so slight that it is of little importance in astrophysics. It seems reasonable to conclude that the same applies to light sources.

### § 5. EXACT THEORY OF COOLING

In view of the limitation on Caldin's method it is natural to enquire if a more exact theory is possible in which account is taken of variations of temperature in the light source. The above analysis suggests various possible approximations; for example we might use equation (4.8) to give the radiation lost in unit time assuming  $T_s = 0$ . It is quite easy, however, to set up an exact formal theory of cooling but the equation must eventually be solved numerically.

Consider how the fundamental equation (2.27) is modified, if, instead of being maintained at constant temperature the material cools by radiation. The only change in the equation is that  $T$ , instead of being constant, is a function of  $r$ . We have, also, an additional equation determining the rate of change of temperature at any point.

For a single particle the total radiation absorbed from a beam of intensity  $I$  in directions within solid angle  $d\omega$  about directions  $\mathbf{s}$  in unit time is  $\epsilon\pi a^2 I d\omega$ . Integrating over all directions this becomes  $\epsilon\pi a^2 J$ . The amount of energy radiated if  $T$  is the temperature is  $4\pi a^2 \epsilon \sigma T^4$ , hence the equation to determine  $T$  is

$$\frac{4\pi a^3 \rho_0 h}{3} \frac{\partial T}{\partial t} = \epsilon\pi a^2 J - 4\pi a^2 \epsilon \sigma T^4 \quad \text{or} \quad \frac{4a\rho_0 h}{3} \frac{\partial T}{\partial t} = \epsilon(J - 4\sigma T^4), \quad \dots (5.1)$$

where  $h$  is the specific heat of the solid material.

If we assume a uniform density distribution, (2.27) becomes (2.35). The temperature and radiation intensity are determined for all  $t$  and  $r$  from equations (5.1) and (2.35) provided the initial and boundary conditions are known. (5.1) and (2.35) cannot be solved exactly. The only feasible method seems to be to retain (2.35) unmodified, but to replace (5.1) by a difference equation.

Suppose we know  $T$  as a function of  $r$  at  $t=0$ . Then, solving (2.35) we can determine  $I$  and so  $J$  at  $t=0$ . Suppose  $\Delta t$  is a small time interval, so small that  $J$  and  $T$  are not changed very much at the end of it. Then if  $\Delta T$  denotes the small change in  $T$  in intervals  $\Delta t$ , we have from (5.1)

$$\Delta T = (J - 4\sigma T^4) 3\Delta t / 4\pi \rho_0 h. \quad \dots\dots (5.2)$$

Hence  $T$  is known at  $t = \Delta t$  and, from (2.35),  $I$  and  $J$ . From (5.1) we can find  $T$  at  $2\Delta t$  and so on. Any desired degree of accuracy is obtainable by making the interval  $\Delta t$  sufficiently small, but the process becomes more tedious with smaller intervals.

It only remains to express the solution of (2.35) in a suitable form, when  $T$  is given as an arbitrary function of  $\tau$ . Using the method of §2, (2.35) becomes

$$d^2(J\tau)/d\tau^2 = \beta\tau^2(J - 4\sigma T^4), \quad \dots\dots (5.3)$$

since equation (2.49) is still true if  $T$  is an arbitrary function of  $\tau$ .

$$\text{Writing} \quad J(\tau) = \beta \exp(\beta\tau) \int_0^\tau L d\tau, \quad \dots\dots (5.4)$$

$$(5.3) \text{ becomes} \quad (dL/d\tau) + 2\beta L + 4\beta\sigma T^4\tau \exp(-\beta\tau) = 0. \quad \dots\dots (5.5)$$

Integration gives

$$L(\tau) = L(0) \exp(-2\beta\tau) - 4\beta\sigma \exp(-2\beta\tau) \int_0^\tau x T^4(x) \exp(\beta x) dx, \quad \dots\dots (5.6)$$

and for  $J$

$$\begin{aligned} J(\tau) &= A \exp(\beta\tau) \\ &+ B \exp(-\beta\tau) - 4\beta\sigma \exp(\beta\tau) \int_0^\tau \exp(-2\beta z) dz \int_0^z x T^4(x) \exp(\beta x) dx. \end{aligned} \quad \dots\dots (5.7)$$

$A$  and  $B$  are determined by the boundary condition at  $r=0$  and  $r=R$ , namely  $F=0$  when  $\tau=0$ ,  $F=2J$  when  $\tau=\pi a^2 NR$ . The total radiation from the sphere is

$$H = 8\pi R^2 J(R). \quad \dots\dots (5.8)$$

There is no point in making any calculations by the above method until more is known about the size of the particles.

## APPENDIX I

### (a) Law of scattering for particles with a perfectly reflecting surface

Let the angle the radius vector to any point on the surface makes with  $\mathbf{s}$  be  $\theta$ . The particle is placed in the path of a parallel beam and we require the amount of light scattered into  $d\omega$  about  $\mathbf{s}$  when the surface scatters light according to the law of reflection. Clearly all the light which meets the surface between radii whose angles  $\theta$  lie between  $\phi/2$  and  $\phi/2 + d\phi/2$  is scattered into directions  $\mathbf{s}$  between angles  $\phi$  and  $\phi + d\phi$ .

Hence, using the definition (2.25) of  $\gamma(P, \mathbf{s}', \mathbf{s})$ , we have

$$(1/4\pi)\gamma(P, \mathbf{s}', \mathbf{s}) 2\pi \sin \phi d\phi = (\sin^2(\phi + d\phi)/2 - \sin^2 \phi/2). \quad \dots\dots (6.1)$$

$$\text{Hence} \quad \gamma(P, \mathbf{s}', \mathbf{s}) = 1, \quad \dots\dots (6.2)$$

and the scattering is uniform.

### (b) Law of scattering for particles with a diffusely reflecting surface

Let OT (Figure 5) be normal to the plane containing  $\mathbf{s}$  and  $\mathbf{s}'$ . OR lies in the plane containing  $\mathbf{s}$ ,  $\mathbf{s}'$  and OQ lies in the plane containing OT and OR.

All the points T, Q and R lie on the surface. Put  $\angle ROS = \theta$ ,  $\angle SOS = \delta$ ,  $\angle ROQ = \mu$ . Let  $\psi_1, \psi_2$  be the angles between the normal at Q and the directions  $\mathbf{s}$  and  $\mathbf{s}'$ . Now the element of area at Q is  $a^2 \cos \mu d\mu d\theta$ .

If  $I$  is the intensity of the incident light in directions in  $d\omega$  about  $\mathbf{s}$ , the amount of light falling on this area at Q is  $I \cos \psi_1 d\omega a^2 \cos \mu d\mu d\theta$ . By Lambert's law of diffuse reflection, the amount of light scattered into directions  $d\omega'$  about  $\mathbf{s}'$  is

$$\pi^{-1} d\omega' \cos \psi_2 I \cos \psi_1 d\omega a^2 \cos \mu d\mu d\theta.$$

But  $\cos \psi_1 = \cos \mu \cos \theta$ ,  $\cos \psi_2 = \cos \mu \cos (\theta - \delta)$ . Hence the above expression becomes  $\pi^{-1} d\omega d\omega' a^2 I \cos^3 \mu \cos \theta \cos (\theta - \delta) d\mu d\theta$ . Hence

$$\begin{aligned} \frac{1}{4\pi} \gamma(P, \mathbf{s}', \mathbf{s}) &= \frac{1}{\pi^2} \int_{\varphi-\pi/2}^{\pi/2} \int_{-\pi/2}^{\pi/2} \cos^3 \mu \cos \theta \cos (\theta - \delta) d\theta d\mu \\ &= \frac{2}{3\pi^2} [(\pi - \delta) \cos \delta + \sin \delta]. \end{aligned} \quad \dots\dots (6.3)$$

If we put  $\phi$  equal to the angle between directions  $\mathbf{s}$  and  $\mathbf{s}$ , i.e.  $\phi = \pi - \delta$ , then we have finally from (6.3)

$$\gamma(P, \mathbf{s}', \mathbf{s}) = (8/3\pi)(\sin \phi - \phi \cos \phi). \quad \dots\dots (6.4)$$

## APPENDIX II

*Calculation of the higher approximation to  $\epsilon$  for the case when E is satisfied*

When  $\epsilon = 1$  we have from (2.8)

$$I(\mathbf{S}, \mathbf{s}) = (\sigma T^4 / \pi) [1 - \exp(-\alpha PS)] \quad \dots\dots (7.1)$$

if P is the point where direction  $-\mathbf{s}$  through S cuts the surface of the envelope of the cloud. If condition E holds,  $\alpha PS$  is large except when  $PS \ll R$ . Hence  $I$  is uniform and of magnitude  $\sigma T^4 / \pi$  except in a thin layer near the surface of the sphere. At the surface  $I$  cannot be uniform; for when  $\theta > \pi/2$ ,  $I = 0$ . As the thickness of this layer is reduced, conditions near the surface clearly approximate more and more to those of a plane surface. Hence with E satisfied, the second term of (2.33) is small compared with the first and

$$\partial I / \partial s = \cos \theta (\partial I / \partial r). \quad \dots\dots (7.2)$$

The same kind of behaviour is to be expected for the case  $\epsilon < 1$ . Hence (2.27) becomes

$$\cos \theta \frac{\partial I(r, \theta)}{\partial r} = \pi a^2 N \left[ \frac{\epsilon \sigma T^4}{\pi} - I(r, \theta) + \frac{(1 - \epsilon)}{4\pi} \int I(r, \theta') \gamma(r, \theta', \theta) d\omega \right], \quad \dots\dots (7.3)$$

$$\text{or if} \quad \tau = \pi a^2 \int_R N dr, \quad \dots\dots (7.4)$$

$$\cos \theta \frac{\partial I(\tau, \theta)}{\partial \tau} = I(\tau, \theta) - \frac{(1 - \epsilon)}{4\pi} \int I(\tau, \theta') \gamma(\tau, \theta', \theta) d\omega' - \frac{\epsilon \sigma T^4}{\pi}. \quad \dots\dots (7.5)$$

When  $\tau = 0$ ,  $r = R$  and from (7.4),  $\tau$  is large for points in the interior of the cloud not near the surface.

An exact solution of (7.5) is possible only for the case  $\gamma(r, \theta', \theta) = 1$ , that is, for scattering by specular reflection. Equation (7.5) can then be transformed into an integral equation which is very similar to the fundamental integral equation of

the theory of radiative equilibrium developed by Schwarzschild and others for astrophysical purposes (Milne 1928, Titchmarsh 1937). The solution is complicated, however, and requires extensive computations (Lindblad 1923).

The method of § 2 can, however, be applied (with only slight modifications) to obtain a first approximation for  $\epsilon'$ . From this approximation it is possible to calculate a second approximation in the case  $\gamma=1$ . The method cannot be applied to the more general equation (2.35). For  $J$ , the first approximation is

$$J(\tau) = 4\sigma T^4 + B \exp(-\beta\tau), \quad \dots\dots(7.6)$$

where  $\beta$  is given by (2.50) and

$$B = -4\sigma T^4/(1 + 2\epsilon/\beta). \quad \dots\dots(7.7)$$

Substituting expression (7.6) for  $J$  in (7.5) the equation for  $I$  is

$$\cos\theta \frac{\partial I}{\partial \tau} = I - \frac{\sigma T^4}{\pi} - B \frac{(1-\epsilon)}{4\pi} \exp(-\beta\tau). \quad \dots\dots(7.8)$$

Integrating with respect to  $\tau$  from 0 to  $\infty$ ,

$$I(0, \theta) = \frac{\sigma T^4}{\pi} + \frac{B(1-\epsilon)}{4\pi(1 + \beta \cos\theta)} \quad \text{if } \theta < \pi/2. \quad \dots\dots(7.9)$$

Hence

$$F(0) = 2\pi \int_0^{\pi/2} I(0, \theta) \sin\theta \cos\theta d\theta = \sigma T^4 \left[ 1 - \frac{2(1-\epsilon)}{\beta + 2\epsilon} \left\{ 1 - \frac{\ln(1 + \beta)}{\beta} \right\} \right]. \quad \dots\dots(7.10)$$

It follows that if we denote the second approximation to  $\epsilon'$  by  $[\epsilon'_e(\tau)]_{II}$

$$[\epsilon'_e(\infty)]_{II} = 1 - \frac{2(1-\epsilon)}{2\epsilon + \sqrt{3\epsilon}} \left[ 1 - \frac{\ln\{1 + \sqrt{3\epsilon}\}}{\sqrt{3\epsilon}} \right]. \quad \dots\dots(7.11)$$

For  $\epsilon=1$  we find  $[\epsilon'_e(\infty)]_{II} = 1$ .

In Figure 2 the first and second approximations are plotted. It will be seen that there is very close agreement between the two, suggesting that (2.59) and (2.60) are very near to the correct values. For diffuse scattering the method fails unless further approximations are introduced. It is interesting to note that a more sophisticated method of obtaining successive approximations to the solution of the fundamental equation of radiative equilibrium, which has been developed recently by Chandrasekhar (1944), could also be applied to equation (7.5). Since, however, it is not our aim to obtain very exact estimates of  $\epsilon$  we shall not pursue the matter further.

#### ACKNOWLEDGMENT

The calculations given above are based upon work done in the Theoretical Research Section of the Armament Research Department, Ministry of Supply. The writer wishes to thank the Chief Scientist, Ministry of Supply, for permission to publish this paper.

#### REFERENCES

- CALDIN, E. F., 1946 a, *Proc. Phys. Soc.*, **58**, 342; 1946 b, *Ibid.*, **58**, 350.  
 CHANDRASEKHAR, S., 1944, *Astrophys. J.*, **99**, 180; **100**, 76, 117.  
 EDDINGTON, A. S., 1930, *The Internal Constitution of the Stars* (Cambridge: University Press), p. 322.  
 LINDBLAD, B., 1923, *Nova Acta R. Soc. Upsala*, Ser. 4, **6**, No. 1.  
 MILNE, E. A., 1928, *Handbuch der Astrophysik*, Band III/1, Chapter 2, p. 111, equation (63).  
 TITCHMARSH, E. C., 1937, *Theory of Fourier Integrals* (Oxford: Clarendon Press), p. 344.

# On the Schumann-Runge $O_2$ Bands emitted at Atmospheric Pressure

By M. W. FEAST

Imperial College of Science and Technology, London

*MS. received 26th May 1948*

**ABSTRACT.** The Schumann-Runge bands of  $O_2$ , previously analysed in the region 3100–4200 Å. and photographed below 3100 Å. under small dispersion, with only a tentative analysis, have been obtained from 2000 Å. to 5000 Å. on sufficient dispersion for the vibrational analysis to be extended and for the rotational structure to be clearly resolved. Conditions for their emission are discussed and the probable process, involving dissociation followed by recombination, is outlined. On this basis the results obtained in discharges, ozonizers and high-voltage arcs are explained. Flory's suggestion of predissociation in the upper state is reviewed and the experimental evidence found to be against it. The conclusions reached are applied to considerations regarding the spectrum of the night sky.

## §1. INTRODUCTION

CONSIDERABLE interest is now being taken by spectroscopists in the spectra of the aurorae and the night sky, since from these a great deal of information may be obtained about processes occurring in the upper atmosphere. In connection with this work it is necessary to study the spectra emitted by the atmospheric gases in the laboratory. The present paper describes some new experiments on the emission spectrum of  $O_2$ , and it is convenient to begin with a brief summary of previous investigations.

(a) In the red and infra-red regions of the spectrum absorption bands corresponding to the transition  $A^1\Sigma_g^+ \leftarrow X^3\Sigma_g^-$  have been observed. Near these bands others are found resulting from the transition  ${}^1\Delta_g \leftarrow X^3\Sigma_g^-$ . Recently Kaplan (1947) has obtained some of these bands in emission from an oxygen afterglow.

(b) Absorption bands found by Hopfield and others in the far ultraviolet region have been shown to be due to transitions from the  $O_2$  ground state to various  $O_2^+$  states, forming a Rydberg series of bands.

(c) Hopfield (1930) discovered a number of emission bands near 2000 Å. forming a single  $v$  progression. They are produced in a condensed discharge in a  $O_2$ -He mixture and are attributed to  $O_2$  on experimental evidence only.

(d) Herzberg's ultraviolet absorption system ( ${}^3\Sigma_u^+ \leftarrow X^3\Sigma_g^-$ ) is forbidden and has not yet been obtained in emission in the laboratory, though some strong night-sky bands are thought to belong to this system.

(e) The most readily observed absorption in  $O_2$  is that found by Schumann, which sets the limit to observations in the ultraviolet region with air-filled spectrographs. These bands result from the transition  ${}^3\Sigma_u^- \leftarrow X^3\Sigma_g^-$  and bands observed by Runge in a high voltage arc in the region 4200–3100 Å. are known to be part of the same system in emission.

(f) At very high pressures new absorption bands appear in the oxygen spectrum, and these are thought to be due to the molecule  $O_4$ . Further absorption bands are obtained in solid and liquid oxygen, most of which have been analysed into four systems.

The present paper gives extended data on Runge's bands and discusses the processes involved in their emission. The new results are not consistent with the suggested predissociation of the  $^3\Sigma_u^+$  state at  $v'=2$ , and, therefore, all the relevant experimental evidence is examined in order to settle this question definitely. Finally the conclusions reached in this investigation are reviewed in relation to the work on the night-sky spectrum.

## §2. EXPERIMENTAL

The discovery of the Schumann-Runge bands in emission was published by Runge (1921), and various workers measured and analysed the plates he obtained, the most complete analysis being given by Lochte-Holtgreven and Dieke (1929). This work was confined to the region 3100 Å. to 4200 Å., and no spectra were published. In his experiments Runge used a high voltage D.C. arc in flowing oxygen. Whilst investigating the oxonizer discharge, Wulf and Melvin (1939) compared its spectrum when filled with cylinder oxygen with that given by a high voltage, low current A.C. arc in the same oxygen. They published a small dispersion spectrogram of the two sources; that of the arc showing Schumann-Runge bands extended from 4000 Å. to 2500 Å., whereas that of the ozonizer shows only N<sub>2</sub> Second Positive bands. Millon and Herman (1944) have carried out experiments with discharges in extremely pure oxygen and also report the appearance of some of the bands; this work will be considered in a latter section.

In the present investigation a high voltage, low current A.C. arc was used. A two-litre Pyrex flask contained the source, which consisted of an arc running between two thin (0.03 in. diameter) platinum-rhodium wires. The Pt-Rh wires were supported on the ends of tungsten wires sealed into ground-glass joints which fitted into the flask, so that easy adjustment of the electrodes was possible. A Hyvac pump and a McLeod gauge were provided and the gas was supplied from a cylinder. Pressures between 0.05 mm. and 1 atmosphere were employed. The discharge is a true arc, the electrodes becoming red- or white-hot and presumably maintaining the arc by thermionic emission. Various electrodes were tried, the difficulty being to find a material which can remain red-hot in oxygen without oxidizing. Platinum has been found to work reasonably well, but it is an advantage to use a platinum-rhodium alloy as the melting point is then raised.

The voltage in such a source is determined mainly by the separation of the electrodes, whilst the current can be varied by means of variable resistances in the primary circuit of the transformer used. Usually the arc ran at about 1000 v. and 0.1 amp. These figures are, however, only of qualitative significance since the voltage characteristic is far from sinusoidal. Current and voltage wave-forms were investigated with a Cossor double-beam oscilloscope and showed the form predicted for A.C. arc (Simon 1905, Loeb 1939, figure 286); the current is practically sinusoidal, whereas the voltage shows a sharp breakdown peak at the start of each half-cycle, followed by a period of constant voltage. Higher intensities could presumably be obtained by using higher currents, but the source is convenient in its present form, running extremely steadily and giving sufficient intensity for photographs to be obtained on a Quartz Littrow (Hilger E.1) spectrograph with exposures of about  $\frac{1}{2}$  hour in the more intense regions.

Commercial cylinder oxygen was used and, although this contains various impurities, especially nitrogen, no bands of molecules other than O<sub>2</sub> appeared on the plates taken at 1 atmosphere pressure. The bands are in fact quite strongly

excited in air at atmospheric pressure so long as a continuous flow is maintained to remove the  $\text{NO}_2$  which is formed and which has strong absorption bands in the visible and ultraviolet regions. This should be contrasted with the behaviour of impure oxygen in a normal low pressure discharge, when only impurity bands are readily emitted. The only necessary precaution is the complete drying of the gas with  $\text{P}_2\text{O}_5$ , otherwise the OH bands appear. Experiments showed that as the pressure is reduced from 1 atmosphere the intensity of the bands falls rapidly and that at about  $\frac{1}{2}$  atmosphere they become difficult to photograph, especially as the bands of NO and  $\text{N}_2$  are readily excited at the lower pressures. In consequence of this the reproductions are all from spectra taken at atmospheric pressure. With the Quartz Littrow the region 2000 Å. to 5000 Å. has been investigated, and from 4500 Å. to 9000 Å. spectra have been taken on a prism-grating instrument.

### §3. DESCRIPTION OF THE SPECTRUM

The present investigation shows the Schumann-Runge bands extending from 2000 Å. to 4800 Å. The bands fall into no well-marked sequences, the system having a wide Condon parabola. The heads are weak since the bands are strongly degraded towards the red and the rotational temperature is high ( $\approx 2000$  K.). The region 4200 Å. to 3100 Å. has been measured in detail by Lochte-Holtgreven and Dieke (1929). Their work shows that the transition is  $^3\Sigma_u^- \rightarrow ^3\Sigma_g^-$  and each band has six main branches, three P and three R. On the dispersion used here the spin splitting is unresolved, and hence each band appears simply as consisting of a single P and R branch. In some bands the structure is further simplified by the R and P branches being unresolved from each other.

Identification of new bands cannot conveniently be made from head data since the band heads are very weak. However, extension of the analysis was achieved by calculating from the measurements of Lochte-Holtgreven and Dieke the wavelengths of several of the lines of each band in the  $v' = 0, 1, 2$  progressions. It was found best to calculate P(17), R(21) and P(27), R(31), and these four lines appear, in the majority of cases, as two doublets separated by four other doublets, and hence the rest of the bands may be readily identified. In the plate, in order to avoid the confusion which would result if every line identified were marked, only a few lines of each band are indicated. It is not possible to calculate accurately in this way the rotational structure of bands with  $v' > 2$ ; these were found by inspection. At the short wavelength end of the spectrum it was necessary to use plates with rather large grains, and hence the resolving power was slightly reduced, also (see § 5 (i)) the band lines in this region which correspond to higher  $v'$  values than in the near ultraviolet were somewhat broadened. The far ultraviolet region is not, as yet, very completely analysed, though it seems safe to assume that it consists of bands with  $v' > 2$ .

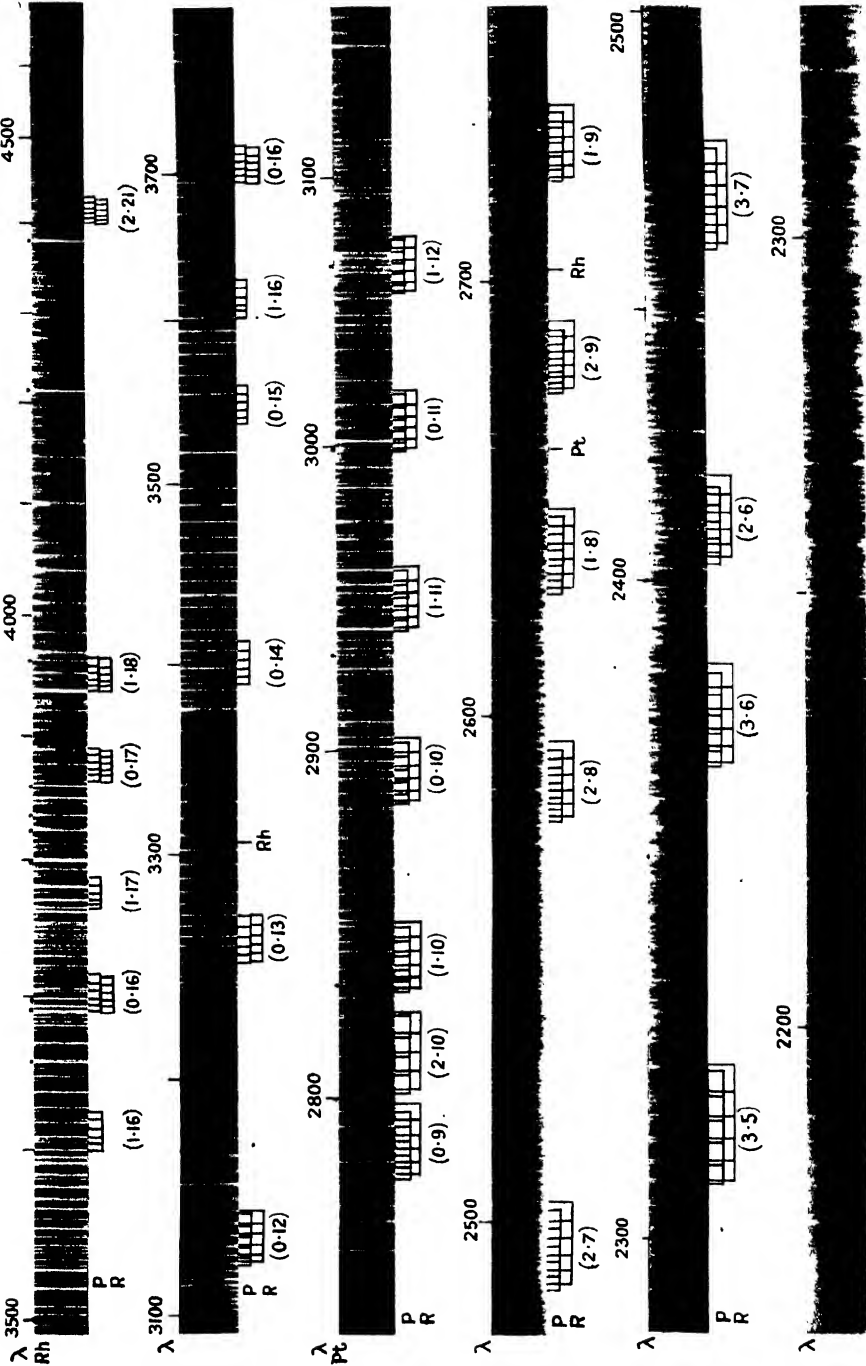
The only atomic lines occurring in the ultraviolet spectrum are due to platinum and rhodium. As will be seen from the plate, these are not of sufficient number or intensity to cause trouble. In the infra-red region a few lines appear, and these have been identified, from the list of Edlén (1943), as due to OI:

$$8446 \text{ Å.} : (4\text{S})3s^3\text{S}_1 - (4\text{S})3p^3\text{P}_{0,1,2};$$

$$7774 \text{ Å.} : (4\text{S})3s^5\text{S}_2 - (4\text{S})3p^5\text{P}_{1,2,3};$$

$$7950 \text{ Å.} : (2\text{D})3s^3\text{D}_{1,2,3} - (2\text{D})3p^3\text{F}_{2,3,4}.$$

These are the strongest lines in Edlén's list, the rest being too weak to be observed in the present work.



The spectra are reproduced from E.1 spectrograms of a high voltage arc in  $O_2$  between Pt-Rh electrodes. A part of the rotational structure of each band found is marked and the vibrational quantum numbers shown. Lines marked with dots are of Pt or Rh (the chemical symbol is given on the left of each strip). An approximate wavelength scale is included.





## §4. THE EMISSION PROCESS

The present experiments show that the intensity of the band system falls rapidly with decrease of pressure in the discharge, so that at  $\frac{1}{2}$  atmosphere it is exceedingly weak. This behaviour is completely different from that of many other gases (for example  $N_2$ ) which emit best in a discharge at low pressure. Hence it becomes necessary to attempt an explanation of this result. The reason for this behaviour may best be discussed in conjunction with the figure, which shows the potential curves of the upper and lower states of the Schumann-Runge system. These curves are drawn to agree with the experimental evidence, absorption, emission and photochemical. As is well known (e.g. Mott and Massey 1933), a collision of an electron with a molecule leading to electronic excitation may be treated according to the Franck-Condon principle. Thus it follows from the

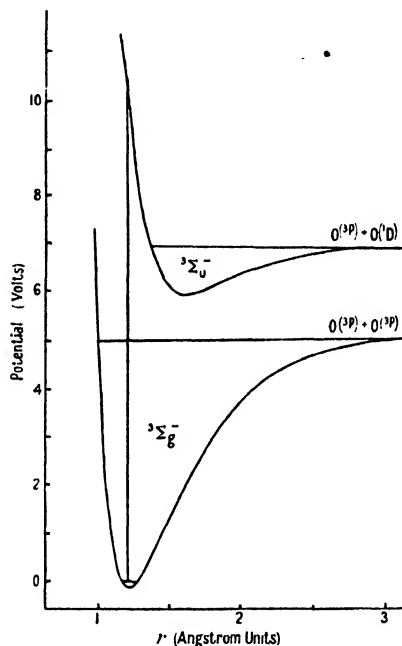


figure that the excitation of  $O_2$  molecules in the ground state will most frequently result in dissociation in the upper state. The experiments of Ladenburg and Van Voorhis (1933) on the absorption coefficient of oxygen in the vacuum ultra-violet region show that the transition of maximum probability (equal instantaneous internuclear distance in the upper and lower states) gives an average kinetic energy of about 1.7 e.v. per atom after dissociation. The action of a discharge on oxygen will thus be to start dissociating it, and various authors have pointed out that atomic oxygen is very reactive, readily combining with gaseous or solid impurities. However, in the high pressure experiments here described there is a much greater probability than in the low pressure discharge that the atoms will recombine again to the upper state of the Schumann-Runge system. This would probably take place by a three-body process, and the molecule would then return to the ground state by emitting the Schumann-Runge bands. It should be noted that the dissociation leads to a normal  $O(^3P)$  atom and an excited  $O(^1D)$  atom. But since the  $^1D$  level is metastable (mean life 100 sec. (Condon 1934)), it will not easily revert to the ground state by radiation, and so prevent the recombination taking place. Furthermore, recent experiments (Vegard and Kvitte 1947) have shown that the

de-activation of metastable oxygen atoms by collisions with other oxygen atoms or molecules has a very low probability. The high rotational temperature of the bands is consistent with these views of the emission process, since the recombination of atoms with high kinetic energy will obviously lead to the formation of molecules of high rotational energy.

It is of interest to apply the above reasoning to the results obtained by Wulf and Melvin (1939) with an ozonizer discharge in commercial cylinder oxygen. At 1 atmosphere pressure they obtained no oxygen bands but only  $N_2$  impurity bands. Here the dissociation phenomenon gives an explanation, since, although in the ozonizer the volume of gas in which excitation takes place is much larger than in the case of the high voltage arc, the amount of energy dissipated may not be very different (Wulf and Melvin used the same transformer for both). Hence to a first approximation the intensity of bands excited by direct collisions in each case will be the same. But in the case of oxygen recombination followed by emission is favoured in the arc with its small volume of highly dissociated gas rather than in the uniformly distributed dissociation of the ozonizer.

Millon and Herman (1944) have run discharges in extremely pure oxygen during investigations on the forbidden red and green lines of oxygen. At a pressure of a few centimetres Hg the Schumann-Runge bands occur with intensity comparable to that of the red and green lines. It is difficult to tell from their short paper the absolute intensity of the bands, but since the lines simultaneously observed are forbidden it seems safe to assume a low intensity. This then falls into line with other results since in any but the purest oxygen impurity bands would obscure the  $O_2$  bands and the oxygen atoms would tend to react with the impurities rather than reform  $O_2$ . Millon and Herman's wavelengths of heads are not of sufficient accuracy for a completely certain vibrational analysis of the bands, but apart from the measurements of Lochte-Holtgreven and Dieke, the assignments (0,11), (1,11), (0,10), (1,10), (0,9) probably agree with the present work. However, the bands they identify as (0,8), (0,7), (0,6), (0,5) are possibly the ones taken here as (2,9), (2,8), (2,7), (2,6), which seems more consistent with the expected Condon parabola. They have also found a band at 2331 Å. which they take as (0,4); no band at this wavelength has been observed in the present investigation. It is hoped that a complete rotational analysis will settle any doubts about the vibrational scheme.

When the major part of this paper had been written a note by Lalji Lal (1948) appeared. He has observed bands from 2450 Å. to 4490 Å. in a high frequency discharge in pure oxygen. Twenty-six heads have been measured on small dispersion, and these bands have been assigned to the Schumann-Runge system. The analysis he gives is quite different from that given here, and no bands at his wavelengths can be found on the present spectra. The two results have been briefly compared by the author (Feast 1948), and further data on Lalji Lal's bands, especially a photograph, are needed before the matter is completely discussed.

## § 5. PREDISSOCIATION

Flory (1936) has suggested that the behaviour of oxygen can only be successfully explained by assuming that the upper state of the Schumann-Runge system is predissociated by a repulsive  $^3\Pi_u$  state at  $v' = 2$  of the  $^3\Sigma_u^-$  state, this leading to the formation of two normal oxygen atoms. This would mean that bands with  $v' > 2$  would not be observed in emission. However, according to the analysis proposed.

here, bands with  $v' = 3$  are found, and it seems difficult to find any other interpretation for the unanalysed region at the short wavelength end of the spectrum than that it is due to bands with  $v' > 2$ . It is therefore important to re-examine Flory's arguments to see if all oxygen phenomena can be explained without assuming predissociation.

#### (i) Emission Bands

Flory suggests that from Lochte-Holtgreven and Dieke's results a Condon parabola may be deduced which indicates that the bands (3,15), (3,16), (3,20), (3,21), (3,22) should have appeared on Runge's plates: in fact these bands are not found. He maintains that collision quenching could not have prevented observation of the bands since he assumes Runge's pressure as less than 0.01 atmosphere.. This can be criticized on two grounds: (a) As has been shown earlier, the bands are only produced with high intensity at high pressures; Runge's pressure would thus probably be near atmospheric, where the collision frequency is about  $10^{10}$  sec., while the radiative lifetime is about  $10^{-8}$  sec. Hence collision broadening is very important at these pressures and explains the tendency to broadening in the short wavelength bands. (b) The intensity of the bands, on the plates published here, indicates a wider Condon parabola than that taken by Flory, so that the bands quoted above do not lie on the line of maximum intensities.

#### (ii) Absorption Bands

Analysis of the absorption Schumann-Runge bands has been carried out by Curry and Herzberg (1934) working at 1 atmosphere pressure and by Knauss and Ballard (1935) at 5–15 mm. Hg. Curry and Herzberg's photograph is thought by Flory to show broadening for  $v' > 2$ , thus bearing out the predissociation theory. The effect must in any case have been small to escape the experimenters, and the fact that in the lower pressure work the bands are clearly resolved, with no trace of diffuseness, suggests that any broadening may be put down to collision quenching.

#### (iii) Fluorescence Experiments

Rasetti (1929) found O<sub>2</sub> fluorescence at atmospheric pressure but none at 8 mm. Hg. This is explainable on a theory of predissociation, but it may also be understood if collision quenching does not fall off more rapidly than the number of molecules excited by fluorescence when the pressure is reduced.

#### (iv) Photochemical Experiments

The pressure decrease when oxygen is exposed to radiation of  $\lambda < 1751$  Å. is due to the reaction of the atoms formed by absorption of the Schumann-Runge continuum with wall impurities (Neujmin and Popov 1934). Flory and Johnston (1935) used 1 cm. of air as a filter and claim that the small pressure decrease, still noted, is due to a predissociation following absorption of radiation of  $\lambda > 1751$  Å. However, since the observed effect is small, there are some other factors worth considering: (a) 1 cm. of air may still allow transmission of a small amount of radiation with  $\lambda < 1751$  Å., thus forming atoms in the normal way; (b) though, as Flory states, the effect of dissociation by a bimolecular collision of an excited and a normal molecule will be small, it may not be completely negligible; (c) absorption of radiation in the region of the Herzberg system continuum is a possible mechanism for dissociation at wavelengths greater than 1751 Å.

## (v) Conclusion

From the above discussion, and from the results on the emission bands, it appears that the experimental evidence is against the predissociation theory. In certain cases the results previously quoted in support of the predissociation are found to have other possible causes.

## §6. APPLICATION TO THE NIGHT-SKY SPECTRUM

Since oxygen is abundant in the upper atmosphere, its presence or absence in the spectrum of the night sky is of great importance. At present there seems a good deal of agreement amongst astrophysicists that the Herzberg oxygen bands occur in emission. The presence of the Schumann-Runge bands is somewhat doubtful, though various authors claim to have identified them. The Herzberg emission bands are calculated from the absorption measurements and from the ground-state differences of the Schumann-Runge bands ( $\Delta v''$ ). At present the  $\Delta v''$  values required have to be extrapolated from the measurements of Lochte-Holtgreven and Dieke. The work described here was started with the object of extending the data on the Schumann-Runge bands so that the Herzberg bands could be calculated without the uncertainty of an extrapolation. Since it appears that the heads are too weak for direct measurement, the necessary information will only be obtained by a complete rotational analysis, and it is hoped to publish this shortly. Various workers (e.g. Pearse 1943) have calculated the wavelengths of bands corresponding to bands of the Schumann-Runge system with  $v' = -1$  and  $-2$  and have noted some good coincidences with night-sky bands. This has led to some speculation as to whether the accepted  $v'$  values are correct. None of these bands can be found on the present spectra, and hence it must be assumed that the  $v'$  assignment is correct. The most conclusive test would be a study of the isotope shifts.

We know that above 100 km. the oxygen is almost completely dissociated by solar radiation during the day (Wulf and Deming 1938). Thus it seems possible that a three-body recombination to the upper state of the Schumann-Runge bands will take place at night, though this would yield low intensities.

Swings (1947) and Nicolet (1948) have advocated that night-sky bands should be identified by first computing the low temperature profiles of the bands. In this connection it should be noted that if the Schumann-Runge bands do occur due to the process outlined above then their rotational temperature may be considerably higher than the accepted night-sky value, and the profile computing method would break down.

Finally, since the pressure is low in the upper atmosphere, collision quenching will not be important and higher  $v'$  values should be expected.

## ACKNOWLEDGMENTS

This work was suggested by Assistant Professor R. W. B. Pearse, and the author is deeply indebted to him for many helpful discussions during its progress. The work was made possible by the award of a D.S.I.R. maintenance grant.

## REFERENCES

- CONDON, E. U., 1934, *Astrophys. J.*, **79**, 217.
- CURRY, J., and HERZBERG, G., 1934, *Ann. Phys., Lpz.*, **19**, 800.
- EDLÉN, B., 1943, *Kungl. Svenska Vetensk. Akad. Handl.*, **20**, No. 10.
- FEAST, M. W., 1948, *Nature, Lond.*, **162**, 214.

- FLORY, P. J., 1936, *J. Chem. Phys.*, **4**, 23.  
 FLORY, P. J., and JOHNSTON, H. L., 1935, *J. Amer. Chem. Soc.*, **57**, 2641.  
 HOPFIELD, J. J., 1930, *Phys. Rev.*, **36**, 789.  
 KAPLAN, J., 1947, *Nature, Lond.*, **159**, 673.  
 KNAUSS, H. P., and BALLARD, S. S., 1935, *Phys. Rev.*, **48**, 796.  
 LADENBURG, R., and VAN VOORHIS, C. C., 1933, *Phys. Rev.*, **43**, 315.  
 LALJI LAL, 1948, *Nature, Lond.*, **161**, 477.  
 LOCHTE-HOLTGREVEN, W., and DIEKE, G. H., 1929, *Ann. Phys., Lpz.*, **3**, 937.  
 LOEB, L. B., 1939, *Fundamental Processes of the Electrical Discharge in Gases* (New York : John Wiley).  
 MILLON, J., and HERMAN, L., 1944, *C.R. Acad. Sci., Paris*, **218**, 152.  
 MOTT, N. F., and MASSEY, H. S. W., 1933, *Theory of Atomic Collisions* (Oxford : Clarendon Press).  
 NEUJMIN, H., and POPOV, B., 1934, *Z. phys. Chem. B*, **27**, 15.  
 NICOLET, M., 1948, Conference on *The Emission Spectra of the Night Sky and Aurorae* (Report from Gassiot Committee) (London : Physical Society), p. 105.  
 PEARSE, R. W. B., 1943, *Rep. Prog. Phys.*, **9**, 42.  
 RASETTI, F., 1929, *Proc. Nat. Acad. Sci.*, **15**, 411.  
 RUNGE, C., 1921, *Physica*, **1**, 254.  
 SIMON, H. T., 1905, *Phys. Z.*, **6**, 297.  
 SWINGS, P., 1947, *Report on the Night Sky and the Aurorae to the Conference on Planetary Atmospheres* (Yerkes Observatory).  
 VEGARD, L., and KVIFTE, G., 1947, *Geofys. Publ., Oslo*, No. 1.  
 WULF, O. R., and DEMING, L. S., 1938, *Terr. Magn. Atmos. Elect.*, **42**, 283.  
 WULF, O. R., and MELVIN, E. H., 1939, *Phys. Rev.*, **55**, 687.

## The CN Tail Bands emitted by the Carbon Arc in Air

By M. W. FEAST

Imperial College of Science and Technology, London

MS. received 16th July 1948

**ABSTRACT.** Wavelengths and intensities of twenty-one CN tail bands, observed in the carbon arc spectrum, are listed and  $v'$ ,  $v''$  values assigned. Nine of the bands have been previously reported as occurring in the nitrogen afterglow excitation. The intensities of the tail bands are shown to be in accordance with the accepted potential curves for this system.

### § 1. INTRODUCTION

As is well known, the CN violet band system ( $^2\Sigma - ^2\Sigma$ ) occurs readily in many laboratory and astrophysical light sources. The system consists of several strong sequences degraded to the shorter wavelengths, together with some weaker bands degraded in the opposite direction and known as the tail bands. The principal sources used by investigators of this system have been the carbon arc in air and the nitrogen afterglow with carbon compounds present. In active nitrogen both the main bands (Jevons 1926) and the tail bands (Jenkins 1928) have been studied. Extensive rotational structure measurements of the main bands as obtained in the arc have also been made (see Jevons (1926) for references). However, there seem to be no data available on the arc excitation of the tail bands. Such data are of importance both for laboratory identification of the bands, the carbon arc being used extensively in analysis, and for identification of astrophysical spectra. The present communication gives wavelengths and

intensities of twenty-one tail bands observed in the arc spectrum: nine of these are bands which have been reported in the afterglow spectrum, whilst the rest correspond to previously unreported transitions. The band intensities are in qualitative agreement with the Condon parabola deduced from the accepted potential curves.

## §2. MEASUREMENTS AND ANALYSIS

The measurements of the band heads were made from Hilger E.1 spectrograms of a 110 v. 5 amp. carbon (graphite) arc in air. To obtain the tail bands with sufficient intensity it was necessary to have the main CN bands considerably over-exposed.

The new data are given in the table.

$v', v''$	$\lambda_c$ (Å.)	$I_c$	$\lambda_n$ (Å.)	$\nu_c$ (cm <sup>-1</sup> )	$\nu_0$ (cm <sup>-1</sup> )	$\nu_c - \nu_0$
15, 15	a		4078.72			
14, 14	4028.38 e	6 ?	4029.33	24817	24779 m	38
13, 13	3984.52 e	9	3984.62	25090	25049 m	41
12, 12	3944.52 e	9	3944.66	25345	25288 m	57
11, 11	3909.90 e	10	b	25569	25498 m	71
10, 10	a		b			
12, 11	a		b			
11, 10	3657.66 e	5	3658.13	27332	27275 m	57
10, 9	3628.53 e	7	b	27552	27477 m	75
9, 8	3602.63 e	7	b	27750	27642 m	108
13, 11	a		b			
12, 10	3465.33	6	b	28849	28818 m	31
11, 9	3432.92	6	3433.00	29126	29080 m	46
10, 8	3404.84	7		29362	29302	60
9, 7	3380.29	6		29575	29494	81
8, 6	3359.06	4		29762	29651	111
7, 5	3340.56	4		29926	29776	150
6, 4	3322.29	4		30091	29868	223
5, 3	3296.29	3		30328	29932	396
10, 7	3203.46	4		31207	31154	53
9, 6	3180.22	4		31436	31371	65
8, 5	3159.89	4		31637	31556	81
7, 4	3142.57	4		31812	31708	104
6, 3	3127.56	3		31964	31827	137
5, 2	3114.34	2		32101	31929	182

$v', v''$ , vibrational quantum numbers;  $\lambda_c$ ,  $I_c$ , wave length, intensity, of band head in arc;  $\lambda_n$ , wavelength of band head in afterglow spectrum (see text);  $\nu_c$ , wave number corresponding to  $\lambda_c$ ;  $\nu_0$ , the wave number of origin ("m" denotes measured values); "a", band obscured by main bands; "b", band, but not head, observed in afterglow; "e", measurement of band made difficult by strong overlapping main bands.

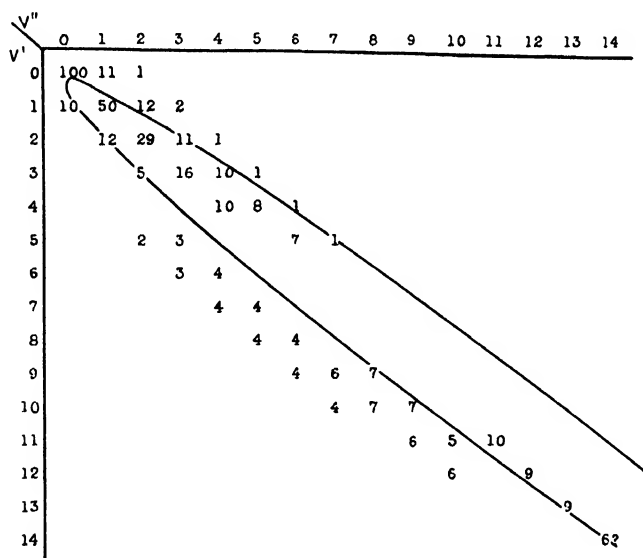
In calculating  $\nu_0$ , the combined data of Jevons and Jenkins have been used; where the experimental values are available they are indicated by "m". For the majority of the bands reported here the values of  $B'$  and  $B''$  are not known with sufficient accuracy for the positions of the band heads to be reliably calculated and compared with the experimental values. However, the values of  $\nu_c - \nu_0$  given in the table are all of the correct order and vary from band to band in the expected manner.

The column  $\lambda_n$  in the table gives the wavelengths of heads measured by Jenkins in the afterglow spectrum and it will be noted that in several cases there is a considerable difference between this value and  $\lambda_c$ . This is partly due to the fact that in the arc many of the tail bands are badly confused with the main CN bands

(those most affected are marked "e" in the table). A second reason for this discrepancy is that  $\lambda_n$  is the wavelength of the last rotational line in the R branch, as measured by Jenkins, the rotational temperature being such that no lines on the returning part of the branch are observed. A consideration of Jenkins' measurements shows that the line taken as forming the band head may be  $0.5\text{ cm}^{-1}$  or more to the long wavelength side of the true head.

### § 3. DISTRIBUTION OF VIBRATIONAL INTENSITIES

The figure shows the distribution of the intensities in the CN main and tail bands as excited in the arc. The band intensities are head estimates, and since  $\nu_c - \nu_0$  is not constant from band to band, these values are not reliable for the overall intensity of the band though they may be used for a qualitative investigation. The main band intensities were obtained by microphotometry of Hilger E.1 spectrograms (Tawde 1936). No attempt has been made to put the two parts of the system on a common intensity scale as the difference of intensities between the main and tail bands is too great to be estimated by eye. The tail band intensities are eye estimates.



The Condon parabola in the figure is drawn from the potential curves calculated by Herzberg (1939, figure 177) and is practically the same as that obtained from the Morse and Rydberg potential curves given by Tawde. It is seen that it fits quite closely to the experimental line of maxima. Bands near the parabola, in the (1, 0) sequence from  $v' = 4$  to 8 and in the (0, 0) sequence from  $v' = 5$  to 10, are not observed since these bands are either headless or fall in regions where the main bands are very strong.

The vibrational intensity distribution in the afterglow (Jenkins 1928) is similar to that given here except that bands with the head far from the origin appear relatively weaker, due to the low intensity of high  $J$  value lines.

### § 4. NOTE ON THE (4,4) MAIN BAND

The wavelength of the (4, 4) band is  $3850.95\text{ \AA}$ ; this measurement does not appear to have been recorded previously.



## ACKNOWLEDGMENTS

The author wishes to express his thanks to Dr. R. W. B. Pearse, who suggested this investigation, for his interest and advice. The work was made possible by a D.S.I.R. grant.

## REFERENCES

- HERZBERG, G., 1939, *Molecular Spectra and Molecular Structure*, Vol. 1 (New York: Prentice-Hall).  
 JENKINS, F. A., 1928, *Phys. Rev.*, **31**, 539.  
 JEVONS, W., 1926, *Proc. Roy. Soc. A*, **112**, 407.  
 TAWDE, N. R., 1936, *Proc. Indian Acad. Sci.*, **3A**, 140.

Ultra-Violet Bands of Na<sub>2</sub>

By S. P. SINHA

Science College, Patna, India \*

MS. received 27th July 1948

**ABSTRACT.** The ultra-violet bands of Na<sub>2</sub> between  $\lambda$  3600 Å. and  $\lambda$  3200 Å. have been photographed in absorption in the first order of a 21 ft. concave grating with a dispersion of about 1.3 Å/mm. and their vibrational analysis carried out. All the bands belong to a single system and can be represented by the equation

$$v = 29342 + 119.33(u') - 0.53(u')^2 - 159.23(u'') + 0.726(u'')^2 + 0.0027(u'')^3,$$

where  $u = v + \frac{1}{2}$ .

The heat of dissociation for the upper state is calculated to be 6510 cm<sup>-2</sup>. The bands are due to transition from the ground  $^1\Sigma_g^+$  state to an excited state which is probably  $^1\Sigma_u^+$  in character. The dissociation products for the upper state are either 3  $^2S$  + 4  $^2P$  or 3  $^2S$  + 3  $^2D$  atoms of sodium.

## § 1. INTRODUCTION

THE ultra-violet bands of Na<sub>2</sub> lie in the region  $\lambda$  3650– $\lambda$  2500 Å. and have been studied by Walter and Barratt (1928), Weizel and Kulp (1930), Kimura and Uchida (1932) and Sinha (1947). In an earlier report (Sinha 1947), it has been considered that the bands belong to seven different systems of which only three appear at all extensive, the remaining ones being merely fragmentary. Two of these systems, reported there as system 1 and system 3, have been found to be strong while system 2 is comparatively weak. The analysis proposed suffers from the defect that the vibrational differences are not quite satisfactory. It was, therefore, considered necessary to photograph the bands at higher dispersion and determine the molecular constants more accurately. This has, however, been done only for the bands lying between  $\lambda$  3500 and 3200 Å., corresponding to the first ultra-violet system mentioned above.

## § 2. EXPERIMENTAL.

The bands have been studied in absorption. The details of the absorption tube used have been described elsewhere (Sinha 1948). Sodium, freed from the oil in which it was stored, was placed at the centre of the tube and was heated electrically from outside. To prevent rapid distillation of the metal to cooler

\* The work described in the present paper was done at Imperial College, London.

parts some nitrogen was introduced inside the chamber. The bands were found to appear most satisfactorily when the temperature inside the tube was about  $750^\circ\text{C}$ . and the pressure of nitrogen was 5 to 10 cm. of mercury. A hydrogen discharge tube of the type described by Hunter and Pearse (1936) was used as a source of continuum and the bands were photographed in the first order of a 21-ft. concave grating with a dispersion of about 1.3 Å. per mm.

### § 3. APPEARANCE OF THE SPECTRUM AND MEASUREMENT

The  $\text{Na}_2$  ultra-violet bands first appear at about  $700^\circ\text{C}$ . when the pressure of nitrogen inside the chamber is about 5 cm. of mercury and lie between  $\lambda 3450$  and  $\lambda 3250$  Å. As the temperature is raised they become stronger and extend up to  $\lambda 3600$  Å. on the long wavelength side and  $\lambda 3200$  Å. on the short wavelength side. With temperature higher than  $850^\circ\text{C}$ ., the absorption in this region becomes almost continuous and quite strong bands begin to appear at wavelengths lower than about  $\lambda 3000$  Å. At still higher temperature ( $1000$  to  $1100^\circ\text{C}$ . or more), the entire region from  $\lambda 3600$  to  $\lambda 2800$  Å. is completely absorbed except for a narrow region at about  $\lambda 3100$  Å. which still continues to be transparent.

The  $\lambda 3600$ – $\lambda 3200$  Å. system of bands which forms the subject of the present investigation appears most satisfactorily when the temperature is about  $750^\circ\text{C}$ . The strong bands lie up to  $\lambda 3550$  Å. while fainter ones extend to even longer than  $\lambda 3600$  Å. Closely spaced lines pertaining to rotational fine structure appear over the entire region, but as the structure of one band overlaps that of the neighbouring band in most cases, it is not possible to separate the structure of each individual band, nor is it possible to see the band origins. A rough calculation with values of  $B$ 's of the two states involved reveals that the head is formed by as low as the third or fourth member of the head forming R branch, and since both  $B'$  and  $B''$  are so small that the low member lines of each branch lie very close together, the individual lines near the band origin cannot be distinctly resolved, with the consequence that the band origin cannot be observed. Even the band head, although quite distinct, was not as prominent as is ordinarily expected in view of the close spacing of the lines near the head. The reason for this is that in the rotational structure of a band there is an intensity maximum which lies at a  $J$  value that is higher the higher the temperature or the smaller  $B$ . In the present case  $B$  is low and the temperature used was high, and therefore the higher members of the branch were stronger than the lower members which formed the heads. The difficulty could probably be overcome by working at a lower temperature and a correspondingly longer absorption path.

Measurements are given in Table 1. The iron arc was used for comparison spectra. The values of  $\lambda$ 's given here differ from those published before (Sinha 1947). Since the heads are formed from relatively weak lines there is difficulty in correctly locating the position of the band-heads in both cases, but since the present measurements are from a plate of much higher dispersion and since the bands were more satisfactorily developed it is considered that the present measurements are definitely the more accurate.

The bands were all degraded to the red and appeared to have single heads suggesting  $^1\Sigma$ – $^1\Sigma$  transition. It may, however, be noted that even if the bands had more than one head, it may not always be possible, under the circumstances described above, to see the different heads distinctly and the band may appear to have just a single head.

Table 1. Na<sub>2</sub> Bands between  $\lambda$ 3600 and  $\lambda$ 3200 Å.

$\lambda_{\text{nir}}$ (Å.)	Int.	$v', v''$	$\nu_{\text{obs}} - \nu_{\text{calc}}$	$\lambda_{\text{nir}}$ (Å.)	Int.	$v', v''$	$\nu_{\text{obs}} - \nu_{\text{calc}}$
3595.2	1	2, 12	2	3400.4	8	3, 2	0
86.7	1	—	—	3395.9	5	2, 1	0
80.2	1	3, 12	2	92.0	4	1, 0	0
77.0	1	2, 11	3	87.1	5	4, 2	0
70.5	1	0, 9	3	82.4	6	3, 1	0
65.4	2	4, 12	2	77.8	4	2, 0	0
62.3	3	3, 11	2	74.1	5	5, 2	0
59.0	2	2, 10	2	69.2	10	4, 1	1
55.5	3	1, 9	4	64.6	4	3, 0	-1
52.0	2	0, 8	2	61.4	5	6, 2	0
47.7	3	4, 11	2	56.5	8	5, 1	-1
44.3	3	3, 10	2	51.5	7	4, 0	0
40.8	3	2, 9	4	48.7	5	7, 2	0
37.3	2	1, 8	2	43.7	6	6, 1	0
33.5	2	0, 7	3	38.8	10	5, 0	-1
30.1	2	4, 10	1	31.4	5	7, 1	-1
26.3	3	3, 9	3	26.3	10	6, 0	-1
22.6	3	2, 8	2	19.2	5	8, 1	-1
19.0	3	1, 7	2	14.0	10	7, 0	-2
15.0	3	0, 6	3	07.3	5	9, 1	-2
12.1	3	4, 9	3	3295.5	5	10, 1	-3
08.3	3	3, 8	1	90.0	9	9, 0	-2
04.5	3	2, 7	3	83.9	5	11, 1	-3
00.6	3	1, 6	2	78.4	8	10, 0	-3
3496.6	3	0, 5	2	72.3	4	12, 1	-2
94.2	3	4, 8	2	66.8	7	11, 0	-2
90.2	3	3, 7	3	66.2	5	14, 2	1
86.3	4	2, 6	2	60.8	4	13, 1	0
82.2	3	1, 5	3	55.5	7	{ 12, 0	-2
78.2	3	0, 4	2			{ 15, 2	-2
72.2	3	3, 6	2	50.2	6	17, 3	-2
68.1	5	2, 5	2	49.6	3	14, 1	0
64.0	3	1, 4	1	44.5	3	16, 2	-2
60.0	3	0, 3	0	39.8	5	18, 3	-3
50.0	7	2, 4	2	38.7	3	15, 1	0
46.0	4	1, 3	0	34.1	3	17, 2	-1
41.6	4	0, 2	0	33.2	5	14, 0	-1
32.2	7	2, 3	0	29.5	5	19, 3	-2
27.7	5	1, 2	0	28.2	3	16, 1	-1
23.2	4	0, 1	0	23.6	3	18, 2	-1
18.5	4	3, 3	-1	19.3	4	20, 3	-3
14.0	5	2, 2	0	17.6	4	17, 1	-2
09.4	4	1, 1	0	13.4	3	19, 2	-2
03.8	5	{ 0, 0	0	09.2	2	21, 3	-2
		{ 3, 4	-1	03.3	2	20, 2	-3

Table 2. Deslandres' Scheme for Na<sub>2</sub> Bands

$v'$	$v''$	0	1	2	3	4	5	6	7	8	9	10	11	12	Mean diff.
0		29362	29204	29048	28893	28742	28591	28441	28292	28145	27999				
1		118	118	118	118	118	118	117	117	117	118				117.7
2		29480	29322	29166	29011	28860	28709	28558	28409	28262	28117				
3		117	117	117	117	117	117	118	118	118	117				117.3
4		29597	29439	29283	29128	28977	28826	28676	28527	28380	28234	28090	27948	27807	
5		116	117	117	116	116	116	116	116	116	116	116	116	116	116.2
6		29713	29556	29400	29244	29088	28932	28776	28620	28464	28308	28152	27996	27840	115.6
7		113	113	113	113	113	113	113	113	113	113	113	113	113	113.0
8		29829	29672	29515	29358	29202	29045	28888	28732	28575	28418	28262	28105	27948	113.3
9		111	111	111	111	111	111	111	111	111	111	111	111	111	111.3
10		30055	29898	29742	29585	29428	29271	29114	28957	28800	28643	28486	28329	28172	110.0
11		108	108	108	108	108	108	108	108	108	108	108	108	108	108.0
12		30166	30009	29854	29697	29540	29383	29226	29069	28912	28755	28598	28441	28284	107.5
13		*	30119	29962	29805	29648	29491	29334	29177	29020	28863	28706	28549	28392	107.5
14		30386	30229	30072	29915	29758	29601	29444	29287	29130	28973	28816	28659	28502	107.0
15		108	108	108	108	108	108	108	108	108	108	108	108	108	108.0
16		30494	30337	30180	30023	29866	29709	29552	29395	29238	29081	28924	28767	28610	107.5
17		107	107	107	107	107	107	107	107	107	107	107	107	107	107.0
18		30602	30445	30288	30131	29974	29817	29660	29503	29346	29189	29032	28875	28718	106.0
19		107	107	107	107	107	107	107	107	107	107	107	107	107	106.0
20		30709	30552	30395	30238	30081	29924	29767	29610	29453	29296	29139	28982	28825	102.0
21		106	106	106	106	106	106	106	106	106	106	106	106	106	101.5
22		30920	30764	30608	30451	30294	30137	29980	29823	29666	29509	29352	29195	29038	101.5
23		103	103	103	103	103	103	103	103	103	103	103	103	103	99.5
24		30968	30811	30654	30497	30340	30183	30026	29869	29712	29555	29398	29241	29084	98.5
25		101	101	101	101	101	101	101	101	101	101	101	101	101	98.0
26		31069	30913	30756	30599	30442	30285	30128	29971	29814	29657	29500	29343	29186	97.0
27		100	100	100	100	100	100	100	100	100	100	100	100	100	
28		31013	30857	30700	30543	30386	30229	30072	29915	29758	29601	29444	29287	29130	
29		98	98	98	98	98	98	98	98	98	98	98	98	98	
30		31111	30956	30800	30643	30486	30329	30172	30015	29858	29701	29544	29387	29230	
31		98	98	98	98	98	98	98	98	98	98	98	98	98	
32		31209	31054	30897	30740	30583	30426	30269	30112	29955	29798	29641	29484	29327	
33		97	97	97	97	97	97	97	97	97	97	97	97	97	
34		31151	30994	30837	30680	30523	30366	30209	30052	29895	29738	29581	29424	29267	
35		157.6	156.2	155.0	153.0	151.0	150.3	149.0	147.0	145.8	144.7	143.0	140.7		
36		158.0	156.0	155.0	153.5	151.5	150.5	149.0	146.5	146.0	144.0	143.0	140.0		

Mean diff.  
From Loomis  
and Nussbaum

## § 4. VIBRATIONAL ANALYSIS AND MOLECULAR CONSTANTS

The vibrational quantum numbers assigned to the bands are given in column 3 of Table 1. Table 2 gives their wave-numbers in vacuum in the usual  $v'$ ,  $v''$  square array. The asterisk denotes the position of the  $\text{Na}_2$  band that was overlapped by the  $\lambda 3303$  Å. line of Na. The mean differences between the vibrational levels for the ground state from the work of Loomis and Nusbaum (1932) are given at the foot of Table 2.

Nearly all the bands measured can be represented by the equation

$$\nu = 29342 + 119.33(u') - 0.53(u')^2 - 159.23(u'') + 0.726(u'')^2 + 0.0027(u'')^3,$$

where  $u = v + \frac{1}{2}$ . The terms in  $u''$  correspond to those given by Loomis (1928). The values for  $\nu_{\text{obs}} - \nu_{\text{calc}}$  given in column 4 of Table 1 have been calculated from the above equation. Although there is not much discrepancy between the observed and the calculated values there seems to be rather a systematic difference for large values of both the quantum numbers  $v'$  and  $v''$ . The discrepancy for large values of  $v''$  seems to be due to fact that the constants in  $v''$  used in the above formula do not refer to the band heads but to the magnetic rotation lines which very nearly represent the band origins, whereas the measurements included in Table 1 refer to the band heads. The difference between  $\nu_{\text{head}}$  and  $\nu_{\text{origin}}$  for bands degraded to the red becomes larger for higher values of the vibrational quantum numbers of the lower state (Jevons 1932), and since for such bands  $\nu_{\text{head}} - \nu_{\text{origin}}$  is positive,  $\nu_{\text{obs}} - \nu_{\text{calc}}$  should also be positive. This agrees with the present observation. The discrepancy for large values of  $v'$  suggests that higher terms in  $v'$  should be included in the above equation. It further indicates, as is often seen with the excited states of such molecules, that the levels are tending to converge more rapidly than is demanded by the linear relationship between  $\omega_v$  and  $v$ . However, the discrepancies are nowhere too large and the arrangement seems satisfactory.

Vibrational constants for the four states of  $\text{Na}_2$  are given in Table 3. The heat of dissociation for the upper state of the present system has been calculated by the method of extrapolation due to Birge and Sponer and would probably be a little higher than the true value. The constants  $\nu_0$ ,  $\omega_0$ ,  $\omega_0 x_0$ ,  $\omega_0 y_0$  are given in  $\text{cm}^{-1}$  and are those in the usual expansion  $\nu(v) = \nu_0 + \omega_0 v - \omega_0 x_0 v^2 + \omega_0 y_0 v^3$ , where  $u = v + \frac{1}{2}$ .

Table 3. Vibrational Constants for the Ground and the Excited States of  $\text{Na}_2$

State	$\nu_0$	$\omega_0$	$\omega_0 x_0$	$\omega_0 y_0$	$D$	Dissociation Products	
$^1\Sigma_g$	0	159.23	0.726	-0.0027	6150	3 $^2\text{S}$	3 $^2\text{S}$
$^1\Sigma_u$	14680.4	117.6	0.38	—	8100	3 $^2\text{S}$	3 $^2\text{P}$
$^1\Pi_u$	20318.9	123.79	0.63	-0.0094	2840	3 $^2\text{S}$	3 $^2\text{P}$
$^1\Sigma_u^+$ (?)	29342	119.33	0.53	—	6510	3 $^2\text{S}$	3 $^2\text{D}$
						or	
						3 $^2\text{S}$	4 $^2\text{P}$

## § 5. DISSOCIATION PRODUCTS

The energy possessed by the dissociated atoms in the upper state of the system can be calculated from the equation  $\nu_{\text{atom}} = \nu_{0,0} + D' - D''$ , where the terms used have the usual significance. Since,  $\nu_{0,0} = 29360 \text{ cm}^{-1}$ ,  $D' = 6510 \text{ cm}^{-1}$  and  $D'' = 6150 \text{ cm}^{-1}$ , we have  $\nu_{\text{atom}} = 29720 \text{ cm}^{-1}$ . Also from the line spectra data it is

known that for sodium  $3^2\text{S} - 3^2\text{D} = 29170 \text{ cm}^{-1}$  and  $3^2\text{S} - 4^2\text{P} = 30270 \text{ cm}^{-1}$ . The above are the nearest atomic states to the calculated  $\nu_{\text{atom}}$ , other states being still farther apart. Since, however, the energy possessed by the dissociated atoms is midway between that corresponding to  $3^2\text{S} - 3^2\text{D}$  and  $3^2\text{S} - 4^2\text{P}$ , it is difficult to decide between these two sets of dissociation products. Of the three terms used in calculating  $\nu_{\text{atom}}$ ,  $D''$ , the heat of dissociation for the ground state, is known correct up to  $\pm 175 \text{ cm}^{-1}$  due to the work of Loomis and Nusbaum (1932). Table 2 giving the  $v' - v''$  scheme indicates that the value of  $\nu_{0,0}$  can be taken to be quite reliable. Hence the only uncertainty lies in the value of  $D'$  employed in the above calculation.  $D'$  has been calculated by Birge and Sponer's extrapolation method. This method is applicable to an electronic state for which the relationship between  $\omega_v$  and  $v$  is linear and has been found to yield fairly satisfactory results for the ground states of non-polar molecules. At any rate, the smaller the range of extrapolation employed the more certain one can be of the calculated value of the heat of dissociation. For the excited states the values calculated by this method are often too high. A critical discussion on the suitability of this method has been provided by Gaydon (1946). Although in the case of the present system of bands, over the range investigated the relationship between  $\omega_v$  and  $v$  seems fairly linear, it is difficult to predict how it would behave for higher values of  $v'$ . Judging from experience of other states of such molecules it can be concluded that, possibly, the true  $D'$  and hence  $\nu_{\text{atom}}$  may be smaller than the value given above. This would lead to the conclusion that the dissociation products are  $3^2\text{S} + 3^2\text{D}$  atoms rather than  $3^2\text{S} + 4^2\text{P}$  atoms, but a definite decision should not be based on this consideration alone.

## § 6. DISCUSSION

The ground state of  $\text{Na}_2$  is a stable  $1^1\Sigma_g^+$  state formed from two atoms of sodium each in the unexcited  $3^2\text{S}$  state. The other state formed from these two atoms is a  $3^1\Sigma_u^+$  state which is regarded as a repulsive one. Since in absorption, transition is to take place from the ground  $1^1\Sigma_g^+$  state, the only excited states that matter are those of the type  $1^1\Sigma_u^+$  and  $1^1\Pi_u$ . The excited states are obtained by considering one of the sodium atoms to be raised from the ground  $3^2\text{S}$  state to higher and higher excited states like the  $3^2\text{P}$ ,  $4^2\text{S}$ ,  $3^2\text{D}$ ,  $4^2\text{P}$  etc. If we consider states resulting from  $3^2\text{S}$  and  $3^2\text{P}$  atoms, there will be as many as eight of them of which only one will be  $1^1\Sigma_u^+$  and only one  $1^1\Pi_u$ . There should thus be two systems of bands  $1^1\Sigma_u^+ \leftarrow 1^1\Sigma_g^+$  and  $1^1\Pi_u \leftarrow 1^1\Sigma_g^+$  whose upper state should dissociate into  $3^2\text{S}$  and  $3^2\text{P}$  atoms of sodium. These correspond respectively to the red system studied notably by Fredrickson and Watson (1927) and Fredrickson and Stannard (1933), and to the green system studied notably by Loomis (1931) and Loomis and Nusbaum (1932).

Let us now consider that one of the sodium atoms is raised to the next excited state i.e. the  $4^2\text{S}$  state. The  $3^2\text{S} + 4^2\text{S}$  atoms of sodium will give four states, out of which there will be one  $1^1\Sigma_u^+$  and no  $1^1\Pi_u$  state. The transition from the ground state to this  $1^1\Sigma_u^+$  state should give rise to a system of bands whose origin should lie at about  $\lambda 3900 \text{ \AA}$ , if we assume that the excited state has nearly the same dissociation energy as the ground state, or at longer or shorter wavelengths according as  $D'$  is greater or smaller than  $D''$ . Experiment does not reveal any band due to  $\text{Na}_2$  near  $\lambda 3900 \text{ \AA}$ . The bands at longer wavelengths are the green system of  $\text{Na}_2$  bands which are definitely known to be due to  $3^2\text{S} + 3^2\text{P}$  atoms. The bands at shorter wavelengths are the bands under present investigation and

lie between  $\lambda 3600$  and  $\lambda 3200$  Å. If we wish to associate this system of bands with  $\text{Na } 3^2\text{S} + 4^2\text{S}$ ,  $D'$  for the upper state should be about  $2500\text{ cm}^{-1}$ . Although this is not an improbable value, the results of analysis do not suggest that  $D'$  could be as low as that. Further from analogy with the known  $\Sigma$  states of  $\text{Na}_2$ ,  $\text{K}_2$  and  $\text{NaK}$ , it is expected that this state should also be fairly deep. This might lead one to conclude that the  $^1\Sigma_u^+(3^2\text{S} + 2^2\text{S}) \leftarrow ^1\Sigma_g^+$  system of bands is not observed.

The next excited states should result from consideration of an unexcited  $3^2\text{S}$  and an excited  $3^2\text{D}$  atom of sodium. This gives twelve molecular states, with only two possible transitions, viz.  $^1\Sigma_u^+$  and  $^1\Pi_u$  from the ground state. Consequently two systems of bands should be obtained whose upper states will dissociate into  $3^2\text{S} + 3^2\text{D}$  atoms. Again, just as two systems of bands are observed due to transitions from the ground state to the excited states resulting from  $3^2\text{S} + 3^2\text{P}$  atoms of sodium, similarly two systems should be observed due to  $^1\Sigma_u^+ \leftarrow ^1\Sigma_g^+$  and  $^1\Pi_u \rightarrow ^1\Sigma_g^+$  transitions whose upper states will dissociate into  $3^2\text{S} + 4^2\text{P}$  atoms. We should thus have four systems of bands, two associated with  $3^2\text{D}$  atoms and two with  $4^2\text{P}$  atoms, all of which should lie close together. Actually, however, only three systems of bands are observed in the corresponding region including the present system (Sinha 1947). Study of the absorption spectrum of  $\text{K}_2$  has also revealed only three systems of bands in the corresponding region (Sinha 1948). Work is in progress to explain this discrepancy and also to understand the absence of bands associated with  $3^2\text{S} + 4^2\text{S}$  atoms.

#### ACKNOWLEDGMENTS

The author wishes to acknowledge his indebtedness to Assistant Professor R. W. B. Pearse, D.Sc., for his kind help and valuable suggestions, and to Patna University, India, for the grant of their Birla scholarship.

#### REFERENCES

- FREDRICKSON, W. R., and STANNARD, C. R., 1933, *Phys. Rev.*, **44**, 633.  
 FREDRICKSON, W. R., and WATSON, W. W., 1927, *Phys. Rev.*, **30**, 429.  
 GAYDON, A. G., 1946, *Proc. Phys. Soc.*, **58**, 525.  
 HUNTER, A., and PEARSE, R. W. B., 1936, *J. Sci. Instrum.*, **13**, 403.  
 JEVONS, W., 1932, *Report on Band Spectra of Diatomic Molecules* (London: Physical Society), p. 55.  
 KIMURA, M., and UCHIDA, Y., 1932, *Sci. Pap. Inst. Phys. Chem. Res. Tokyo*, **18**, 109.  
 LOOMIS, F. W., 1928, *Phys. Rev.*, **31**, 323.  
 LOOMIS, F. W., and NUSBAUM, R. E., 1932, *Phys. Rev.*, **40**, 380.  
 SINHA, S. P., 1947, *Proc. Phys. Soc.*, **59**, 610; 1948, *Ibid.*, **60**, 436.  
 WALTER, J. M., and BARRATT, S., 1928, *Proc. Roy. Soc. A*, **119**, 265.  
 WEIZEL, W., and KULP, M., 1930, *Ann. Phys., Lpz.*, **4**, 971.

# On the Equations of Motion of Crystal Dislocations

By F. C. FRANK

H. H. Wills Physical Laboratory, University of Bristol

*MS. received 25th August 1948, and in amended form 25th November 1948*

**ABSTRACT.** It is shown that when a Burgers screw dislocation moves with velocity  $v$  it suffers a longitudinal contraction by the factor  $(1-v^2/c^2)^{1/2}$ , where  $c$  is the velocity of transverse sound. The total energy of the moving dislocation is given by the formula  $E=E_0/(1-v^2/c^2)^{1/2}$ , where  $E_0$  is the potential energy of the dislocation at rest. Taylor dislocations behave in a qualitatively similar manner, complicated by the fact that both longitudinal and transverse displacements and sound velocities are involved.

## § 1

FRANKEL and Kontorowa (1938), studying the properties of what is essentially a one-dimensional dislocation model, found equations of motion for the dislocation which can be brought into a form strikingly analogous to those of a particle in special relativity. It has a limiting velocity equal to the characteristic velocity of sound in the (actually dispersive) system, suffers a contraction analogous to that of Lorentz as it approaches that velocity, and the ratio of its energy in motion to its energy at rest likewise depends "relativistically" on velocity. This result (which we actually discovered independently) will be discussed more fully, along with other properties of one-dimensional dislocation models, in papers to be published with Mr. J. H. van der Merwe. It has been noted before (Frank 1948) that in the three-dimensional case of crystal dislocations the kinetic energy of a Burgers "screw" dislocation (Burgers 1939), extrapolated by the approximate formula valid at low velocity up to the velocity of transverse sound waves, is equal to half its potential energy. This is equivalent to the relativistic equation  $m_0 = E_0/c^2$ , where  $E_0$  is rest energy and  $m_0$  rest mass. It is shown below that all the elementary relativistic formulae are applicable to a screw dislocation, and that the behaviour of a Taylor "bridge" (or "edge") dislocation (Taylor 1934) may be described as "relativistic with complications": the limiting velocity is that of longitudinal sound waves, but the velocity of transverse sound waves also plays a part.

## § 2

The displacement function  $\mathbf{u}(x, y, z)$  of a resting dislocation according to linear isotropic elastic theory, given by Burgers (1939) for bridge and screw dislocations, is a solution of the three equations ( $1_x, 1_y, 1_z$ ) of elasto-static equilibrium typified by

$$(\lambda + \mu) \frac{\partial}{\partial x} \left( \frac{\partial u_x}{\partial x} + \frac{\partial u_y}{\partial y} + \frac{\partial u_z}{\partial z} \right) + \mu \left( \frac{\partial^2}{\partial x^2} + \frac{\partial^2}{\partial y^2} + \frac{\partial^2}{\partial z^2} \right) u_x = 0. \quad \dots (1_x)$$

Dislocations in motion must be represented by solutions of the three equations of elasto-dynamic equilibrium (wave equations) typified by

$$(\lambda + \mu) \frac{\partial}{\partial x} \left( \frac{\partial u_x}{\partial x} + \frac{\partial u_y}{\partial y} + \frac{\partial u_z}{\partial z} \right) + \mu \left( \frac{\partial^2}{\partial x^2} + \frac{\partial^2}{\partial y^2} + \frac{\partial^2}{\partial z^2} \right) u_x - \rho \frac{\partial^2 u_x}{\partial t^2} = 0. \quad \dots (2_x)$$



In particular, a dislocation in steady motion with velocity  $v$  in the  $x$  direction must be represented by a propagational solution of equations (2), a time-independent function of  $x'$ ,  $y$  and  $z$  where  $x' = (x - vt)$ . With this substitution,  $x$  is replaced by  $x'$  and  $(\partial^2/\partial t^2)$  is replaced by  $v^2(\partial^2/\partial x'^2)$  in equations (2), producing three equations  $(3_x, 3_y, 3_z)$  which are equivalent to equations (1) with  $x$  replaced by  $x'$ , except for the operands of  $(\partial^2/\partial x'^2)$  which are :

$$\text{in } (3_x) : (\lambda + 2\mu - v^2\rho)u_x \text{ in place of } (\lambda + 2\mu)u_x,$$

$$\text{in } (3_y) : (\mu - v^2\rho)u_y \text{ in place of } \mu u_y,$$

$$\text{in } (3_z) : (\mu - v^2\rho)u_z \text{ in place of } \mu u_z.$$

### § 3

Now one of the solutions of (1) is the screw dislocation along the  $z$ -axis, for which (Burgers 1939)

$$u_x = 0, \quad u_y = 0, \quad u_z = (b/2\pi) \arctan(y/x), \quad \dots \dots (4)$$

equations  $(1_x)$  and  $(1_y)$  reducing to  $0=0$  and  $(1_z)$  to  $\mu \partial^2 u_z / \partial x^2 + \mu \partial^2 u_z / \partial y^2 = 0$ . Likewise for a screw dislocation in motion, equations  $(3_x)$  and  $(3_y)$  reduce to  $0=0$  and  $(3_z)$  to  $(\mu - v^2\rho) \partial^2 u_z / \partial x'^2 + \mu \partial^2 u_z / \partial y^2 = 0$ . Hence in this case equations (3) are brought into identical form with equations (1) on introducing

$$x'' = x' / (1 - v^2\rho/\mu)^{\frac{1}{2}} = (x - vt) / (1 - v^2/c^2)^{\frac{1}{2}},$$

where  $c_1 = (\mu/\rho)^{\frac{1}{2}}$  is the velocity of transverse sound waves in the material. Hence the displacement function of a screw dislocation in motion is identical with that of a screw dislocation at rest, apart from a "Lorentz contraction".

### § 4

The potential energy of a resting screw dislocation is

$$E_0 = \frac{1}{2}\mu \int [(\partial u_z / \partial x)^2 + (\partial u_z / \partial y)^2] dx dy dz = (\mu b^2 / 4\pi) \ln(r_1/r_0)$$

per unit length in the  $z$  direction.  $r_0$ , of the order of the interatomic spacing  $b$ , represents the boundary within which linear elastic theory is inapplicable, and  $r_1$  the outer boundary of the material. Moderate changes in the size or form of these boundaries are unimportant. Neglect of strain energy in the non-linear elastic region within  $r_0$  is justified when  $r_1/r_0$  is large; but on the evidence of the one-dimensional model it is likely that the results obtained below will remain true in a higher approximation which takes account of this energy. The potential energy  $E_1$  of a moving screw dislocation is given by the same integral, which on writing  $dx = (1 - \beta^2)^{\frac{1}{2}} dx''$ , where  $\beta = v/c$ , becomes

$$\begin{aligned} E_1 &= \frac{1}{2}\mu \int [(\partial u_z / \partial x'')^2 / (1 - \beta^2) + (\partial u_z / \partial y)^2] (1 - \beta^2)^{\frac{1}{2}} dx'' dy dz \\ &= \frac{1}{2}\mu / (1 - \beta^2)^{\frac{1}{2}} + \frac{1}{2}E_0(1 - \beta^2)^{\frac{1}{2}} = E_0(1 - \frac{1}{2}\beta^2) / (1 - \beta^2)^{\frac{1}{2}}, \end{aligned}$$

since  $u$  is the same function of  $(x'', y, z)$  as it was formerly of  $(x, y, z)$ .

The kinetic energy associated with a moving screw dislocation is

$$\begin{aligned} E_2 &= \frac{1}{2}\rho \int (\partial u_z / \partial t)^2 dx'' dy dz = \frac{1}{2}\rho \int (\partial u_z / \partial x'')^2 [v^2 / (1 - \beta^2)] (1 - \beta^2)^{\frac{1}{2}} dx'' dy dz \\ &= \{v^2 / (1 - \beta^2)^{\frac{1}{2}}\} (\rho/\mu) E_0 / 2 = \frac{1}{2}E_0 \beta^2 / (1 - \beta^2)^{\frac{1}{2}}. \end{aligned}$$

Hence the total energy associated with the moving dislocation is

$$E = E_1 + E_2 = E_0/(1 - \beta^2)^{\frac{1}{2}}.$$

For dislocations moving at low velocity we may define an equivalent mass  $m_0$  by equating the energy of motion  $E - E_0$  to  $\frac{1}{2}m_0v^2$ . Then  $m_0 = E_0/c^2$ .

### § 5

The work done by an applied shear stress  $\sigma$  on the glide plane when the dislocation is translated a distance  $x$  is  $(\sigma \cdot \mathbf{b})x$  per unit length of dislocation. This energy goes partly into kinetic energy and partly into setting up oscillations in the crystal. This latter "radiation damping" of the motion of the dislocation should arise from the acceleration of the dislocation, under the influence of the applied stress and in its interactions with irregularities in the lattice, e.g. other dislocations, and also, at high velocity, from the periodic structure of the lattice itself. Formally we may define the force acting on the dislocation,  $f$ , as  $(\sigma \cdot \mathbf{b})$  diminished by a frictional force arising from the radiation damping. We expect this correction to be small in a reasonably perfect crystal, provided that the velocities or accelerations are not exceedingly high.

We could identify the energy of a moving dislocation by integrating energy in the material. (It should be noted, however, that  $E - E_0$ , which might reasonably be called the kinetic energy of the dislocation, is not quite identical with the kinetic energy in the material, which is  $E_1$ .) The same cannot be done with momentum, but we can define an equivalent momentum,  $p = \int f dt$ , corresponding to  $E - E_0 = \int f dx$ . Then introducing  $v/c = \beta = \sin \phi$  (a substitution which simplifies all the formulae of elementary relativistic mechanics) so that  $E = E_0/\cos \phi$ , we have  $dp/dt = f = dE/dx = (E_0 \sin \phi / \cos^2 \phi) d\phi/dx = (E_0/c \cos^2 \phi) d\phi/dt$ , and hence  $p = \int (E_0/c \cos^2 \phi) d\phi = (E_0/c) \tan \phi = (E/c^2)v$  and  $E^2 = E_0^2 + p^2c^2$  as usual.

A screw dislocation (unlike a bridge dislocation) may move in any plane containing its singular line. The transformations employed above may be performed independently for motions in the  $x$  and  $y$  directions. Hence  $p$  has independent  $x$  and  $y$  components, i.e., is a vector.  $E$  is of course scalar. In view of the "radiation damping" we cannot suppose there is strict conservation of the components of  $p$  unless we are able to assign a corresponding equivalent momentum to oscillations in the crystal.

### § 6

The case of the Taylor bridge dislocation is more complicated, since both longitudinal and transverse displacements occur in its motion. If it lies along the  $z$ -axis, with displacement vector  $\mathbf{b}$  on the  $x$ -axis, which must also be its direction of motion, the displacements  $u_z$  and all derivatives with respect to  $z$  vanish by symmetry. Equations (1) for the dislocation at rest then reduce to

$$(\lambda + 2\mu)\partial^2 u_x / \partial x^2 + \mu\partial^2 u_x / \partial y^2 + (\lambda + \mu)\partial^2 u_y / \partial x \partial y = 0, \quad \dots\dots (5_x)$$

$$(\lambda + 2\mu)\partial^2 u_y / \partial y^2 + \mu\partial^2 u_y / \partial x^2 + (\lambda + \mu)\partial^2 u_x / \partial x \partial y = 0. \quad \dots\dots (5_y)$$

The major displacements are  $u_x$ , parallel to  $\mathbf{b}$ , and to a first approximation satisfy (5<sub>x</sub>) with the final term neglected. Through the final term of (5<sub>y</sub>) the  $x$ -displacements give rise to  $y$ -displacements which react back upon the  $x$ -displacements through the final term of (5<sub>x</sub>). This description is appropriate to a solution of (5) by successive approximations.

The solution of the first approximation is

$$u_{x(1)} = (b/2\pi) \arctan [ \{ (\lambda + 2\mu)\mu \}^{\frac{1}{2}} (y/x) ]. \quad \dots\dots (6_x)$$

The closed solution obtained by Burgers (1939) is

$$u_x = (b/2\pi) [ \theta + \{ (\lambda + \mu)/(\lambda + 2\mu) \} \sin \theta \cos \theta ], \quad \dots\dots (7_x)$$

$$u_y = -(b/2\pi) [ \{ \mu/(\lambda + 2\mu) \} \ln (r/r_0) - \{ (\lambda + \mu)/(\lambda + 2\mu) \} \sin^2 \theta ], \quad \dots\dots (7_y)$$

where  $\tan \theta = y/x$  and  $r = (x^2 + y^2)^{\frac{1}{2}}$ .

The difference between  $u_{x(1)}$  and  $u_x$  as given by (7) is small, being at the worst  $0.014v$  (when  $\theta = \pi/3$ ) in the case  $\lambda = \mu$  (Poisson's ratio  $\sigma = \frac{1}{2}$ ). Thus the first approximation is a not unsatisfactory one.

Equations (3) for the bridge dislocation in motion become

$$(\lambda + 2\mu - v^2\rho)\partial^2 u_x / \partial x'^2 + \mu\partial^2 u_x / \partial y^2 + (\lambda + \mu)\partial^2 u_y / \partial x' \partial y = 0, \quad \dots\dots (8_x)$$

$$(\lambda + 2\mu)\partial^2 u_y / \partial y^2 + (\mu - v^2\rho)\partial^2 u_y / \partial x'^2 + (\lambda + \mu)\partial^2 u_x / \partial x' \partial y = 0. \quad \dots\dots (8_y)$$

To the same first approximation as we have just discussed, taking the first two terms of (8<sub>x</sub>) the problem reduces "relativistically" to the static problem on substituting  $x'' = x'/(1 - v^2/c^2)^{\frac{1}{2}}$  where  $c_1^2 = \{ (\lambda + 2\mu)/\rho \}^{\frac{1}{2}}$ , the speed of longitudinal sound waves.

*Note added in amendment 24th November 1948.*—Further incomplete treatment of the problem (which originally followed here) can be omitted, as a complete solution has now been obtained, and will shortly be published, by Mr. J. D. Eshelby. From his treatment it appears that the requisite differential equations can be satisfied both by an irrotational and a distortional dislocation with displacement vectors in the direction of travel, or by any combination of the two. Both suffer "Lorentz contraction", with limiting velocities equal to the velocities of longitudinal and transverse sound waves respectively. Either motion alone can only be maintained if a force, normal to the direction of motion, is applied at the centre of the dislocation, with counteracting forces on the remote surfaces. These forces do no work, but there is no means of applying the force at the centre. This force vanishes when the irrotational and distortional dislocations are combined in appropriate proportions (dependent on the velocity). This, therefore, gives the only physically important solution. The force at the centre cannot be made to vanish for a dislocation travelling faster than transverse sound.

#### ACKNOWLEDGMENTS

The author wishes to thank Mr. J. D. Eshelby for the above information; he wishes also to thank Mr. F. R. N. Nabarro and Mr. G. Wyllie for valuable critical discussion.

#### REFERENCES

- BURGERS, J. M., 1939, *Proc. Kon. Ned. Akad. v. Wet.*, **42**, 293.  
 FRANK, F. C., 1948, *Report of a Conference on Strength of Solids* (London: Physical Society), p. 48.  
 FRENKEL, J., and KONTOROWA, T., 1938, *Phys. Z. Sowjet*, **13**, 1.  
 TAYLOR, G. I., 1934, *Proc. Roy. Soc. A*, **145**, 362.

## LETTERS TO THE EDITOR

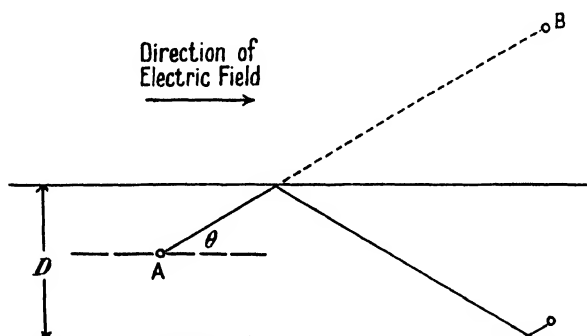
### The Resistivity of Thin Metallic Films

Various formulae have been suggested from time to time to account for the variation of the resistivity of thin metallic films with the thickness of the film. The simplest of these is an empirical expression due to Planck (1914) :

$$\rho = \rho_{\infty}(1 + A/D)$$

where  $\rho$  is the resistivity and  $D$  the thickness of the film, and  $\rho_{\infty}$  the resistivity of the bulk metal;  $A$  is an unspecified constant. This formula accounted satisfactorily for his own experimental results and for Pogány's classical work on the resistivities and optical constants of thin films (1916).

When the thickness of the film is a small multiple or submultiple of the length of the mean free path of the electrons the number of electronic collisions is going to be increased. The Figure illustrates the shortening of the mean free path  $l$  and the corresponding increase



in the collisions.  $AB$  represents the mean free path in the bulk metal, and, in this case, the number of collisions will be  $\nu(1 + kl/D)$  where  $k$  is a numerical factor. As a rough first approximation the latter may be said to be equal to  $4/\pi$  since  $2/\pi$  is the mean of the possible values of  $\sin \theta$ , and there are two surfaces. When  $D$  is larger than  $l$ ,  $k$  will have a different (smaller) value, which can be calculated by suitable averaging. Substituting the above value for the frequency of collision between the atoms and electrons in Drude's classical formula it follows that

$$\sigma = \frac{Ne^2}{2m\nu(1 + kl/D)} \quad \sim \quad \frac{\sigma_{\infty}}{1 + 4l/\pi D} \quad \dots \dots (1)$$

where  $\sigma$  is the conductivity of the film,  $D$  its thickness,  $\sigma_{\infty}$  the conductivity of the bulk metal,  $N$  the number of free electrons per  $\text{cm}^3$ , and  $e$  and  $m$  the electronic mass and charge respectively. From (1) we obtain

$$\rho = \rho_{\infty}(1 + 4l/\pi D) \quad \dots \dots (2)$$

which can be identified with Planck's empirical formula mentioned above.

Considering small temperature changes at about room temperature it is assumed that  $\rho_{\infty}$  and  $l$  experience appreciable, but  $D$  negligible, variations. Then (2) can be written

$$\rho = \rho_0 \rho_{\infty} (\alpha T + a) (1 + 4l_0/\pi D \gamma T). \quad \dots \dots (3)$$

$\alpha$  is the normal temperature coefficient of resistivity,  $\gamma$  the coefficient of the mean free path,  $a$  that part of the resistivity which does not depend on the temperature; the suffix  $(_0)$  refers to values at  $0^\circ \text{C.}$  but  $T$  is measured on the absolute scale.

When (3) is differentiated with respect to  $T$  an expression is obtained for the effective temperature coefficient  $\alpha'$ :

$$\alpha' = \alpha - \frac{1}{T} \left( \frac{1}{1 + \pi D \gamma T / 4l_0} \right) \quad \dots\dots (4)$$

It is readily seen that  $\alpha'$  is zero when

$$1/\alpha = T(1 + \pi D \gamma T / 4l_0), \quad \dots\dots (5)$$

and for correspondingly smaller thicknesses or lower temperatures  $\alpha'$  will be negative. In general,  $\alpha'$  is less than  $\alpha$ .

It follows that when  $l_0$  is large the thickness  $D$  for which  $\alpha' = 0$  will be large for given values of  $\gamma$  and  $T$ . There is evidence suggesting that the mean free path of the electrons in bismuth is exceptionally long. It is thus to be expected that comparatively thick bismuth films will exhibit a negative temperature coefficient (Tulley 1946). In addition, it follows from (5) that the thicker the film the lower the temperature at which  $\alpha' = 0$  (Curtiss 1921). It is not suggested that expression (3) has a general applicability at lower temperatures, indeed, it is known that the resistivity varies at temperatures lower than  $0^\circ \text{C}$ . with a higher power of  $T$  than unity. It is none the less interesting to note that the results of van Itterbeek and De Greve (1945, 1946) on the resistivity of nickel films at comparatively low temperatures are in good agreement with the above expressions. The temperature coefficient of resistivity varies with the thickness, and the minima of resistivity vary with the thickness and the temperature as predicted. These authors quote the results of De Haas and Van den Berg (1937) on gold wires in support of their own. Since gold wires cannot really be compared with thin films a somewhat different explanation is required. This will be dealt with in the near future.

South-West Essex Technical College,

R. A. WEALE.

London E.17.

November 1948.

CURTISS, L. F., 1921, *Phys. Rev.*, **18**, 255.

DE HAAS, W. J., and VAN DEN BERG, G. J., 1937, *Physica*, **4**, 663.

VAN ITTERBEEK, A., and DE GREVE, L., 1945, *Nature, Lond.*, **156**, 63; 1946, *Ibid.*, **158**, 100.

PLANCK, W., 1914, *Phys. Z.*, **15**, 563.

POGÁNY, B., 1916, *Ann. Phys., Lpz.*, **49**, 531.

TULLEY, T. J., 1946, *Nature, Lond.*, **157**, 372.

## Note on the Slowing Down of Mesons

Fermi, Teller and Weisskopf (1947), and Fermi and Teller (1947), have given a formula for the rate of loss of energy of slow mesons passing through a metal, the metal being treated as a degenerate electron gas. The formula is (Fermi and Teller, equation (15))

$$\frac{dW}{dt} = \frac{2}{3\pi} \frac{m^2 e^4 V^2}{\hbar^3} \ln \frac{137v_0}{V} \quad \dots\dots (1)$$

where  $m$ ,  $e$  are the mass and charge of an electron,  $V$  the velocity of the meson,  $W$  its energy and  $v_0$  the maximum velocity of the electrons which form the degenerate Fermi gas in the metal. The formula is derived for the case when  $V \ll v_0$ . Some doubt has been thrown on the validity of this result (cf. for example Fröhlich 1948); the purpose of this note is to confirm the result by showing that it is identical with that obtained in a problem on the electrical resistance of alloys, for which the application of the same methods has given results in agreement with experiment.

If the effect of the lattice field is neglected, the calculations required to obtain the following two quantities are identical: (a) The rate  $dW/dt$  of loss of energy by a heavy charged particle moving with velocity  $V$  through the gas. (b) The rate of loss of energy of an electron gas moving with velocity  $V$  past a stationary charged particle (e.g. a proton). The second problem is the same as that of finding the residual resistance of a metal containing

\* For a treatment of the effect of free electrons when  $V > v_0$  see Kramers (1947).

dissolved hydrogen. For suppose that the resistance of a metal containing  $xN$  stationary protons per unit volume is  $x\rho$ ;  $N$  is here the number of metal atoms per unit volume. Then the rate of loss of energy per unit volume, if a current of density  $j$  is flowing, is

$$x\rho j^2. \quad \dots\dots (2)$$

If the metal is monovalent and thus contains  $N$  electrons per unit volume, we may set  $j=NeV$ , so that (2) becomes  $x\rho N^2e^2V^2$ . The rate of loss of energy due to a single stationary charged particle, which can be equated to  $dW/dt$ , is given by

$$dW/dt = \rho Ne^2V^2. \quad \dots\dots (3)$$

The resistance  $\rho$  due to any type of foreign atom can be calculated by the method originally due to Nordheim (1931) (cf. also Mott and Jones 1936, p. 289). We may write

$$\rho = m v_0 A / e^2, \quad \dots\dots (4)$$

where  $A$  is the area defined by

$$A = \int I(\theta)(1 - \cos \theta) d\omega. \quad \dots\dots (5)$$

$I(\theta)d\omega$  is here the cross-section for scattering of an electron having velocity  $v_0$  by a foreign atom into the solid angle  $d\omega$ . This can be calculated if the field round the foreign atom is known; in Mott and Jones (1936), p. 97, a screened Coulomb field of potential

$$U(r) = \pm (e^2/r) \exp(-qr) \quad \dots\dots (6)$$

is taken, and  $q$  obtained by using the Thomas-Fermi method to find the density of the electron gas round a proton. One finds

$$q = (4\pi e^2/\hbar^2)(3N/\pi)^{1/3}. \quad \dots\dots (7)$$

With this field  $I(\theta)$  can be obtained, using the Born approximation; one finds (using the value given for  $I(\theta)$  by Mott and Jones (1936), p. 294, equation (86))\* from (4), (5), (6), (7).

$$\rho = \frac{2\pi e^2}{m v_0^3} \ln \left( \frac{\pi \hbar v_0}{e^2} \right).$$

Substituting in (2), using the equation  $m v = (3\pi)^{1/3} \hbar / N^{1/3}$ , we obtain the formula

$$\frac{dW}{dt} = \frac{2}{3\pi} \frac{m^2 e^4 V^2}{\hbar^2} \ln \left( \frac{\pi \hbar v_0}{e^2} \right)$$

which differs from that of Fermi and Teller only in the  $\pi$  in the logarithm. Since the Born approximation is strictly valid only if  $\hbar v_0 \gg e^2$ , the change is unimportant.

No experimental results are known for the increase of resistance due to hydrogen in monovalent metals, to which alone this analysis should be applicable; but the theory agrees well with experiment when applied to calculate the increase of resistance due to the addition of 1% of Ni, Zn, Ga, Ge or As to copper (Mott and Jones 1936, p. 293). The resistance is found experimentally to increase in the ratio of the numbers 1, 1, 4, 9, 16 for these metals. This can be explained (Mott and Jones 1936, p. 292) quantitatively on the above theory, taking a field round each foreign atom of potential  $(ze^2/r) \exp(-qr)$ , where  $z$  takes the values  $-1, 1, 2, 3$  etc. It thus appears that, for example, a zinc atom replacing a copper atom behaves like an additional charge  $e$ , and the residual resistance is that due to a screened charge.

H. H. Wills Physical Laboratory,  
University of Bristol.  
23rd November, 1948.

N. F. MOTT.

FERMI, E., and TELLER, E., 1947, *Phys. Rev.*, **72**, 399.

FERMI, E., TELLER, E., and WEISSKOPF, V., 1947, *Phys. Rev.*, **71**, 314.

FRÖHLICH, H., 1948, *Nature, Lond.*, **162**, 450.

KRAMERS, H. A., 1947, *Physica*, **13**, 401.

MOTT, N. F., and JONES, H., 1936, *Theory of the Properties of Metals and Alloys* (Oxford: Clarendon Press).

NORDHEIM, L., 1931, *Ann Phys., Lpz.*, **9**, 641.

\* In this equation we have put  $y \ll 1$ , since only under these conditions is the Born approximation valid.

## REVIEWS OF BOOKS

*Preparation and Characteristics of Solid Luminescent Materials*, by G. R. FONDA and F. SEITZ (Editors). Pp. xv + 459. (New York: John Wiley, 1948.) 30s.

This book comprises twenty-nine papers together with associated discussions which formed the subject matter of a Symposium on Luminescence held at Cornell University in October 1946. It is concerned with recent researches on specific aspects of luminescence in synthesized phosphors, such as sulphides, silicates and tungstates. The papers presented at the Conference have been arranged in five main groups, while a further group contains the final discussions of the Conference.

In the first group of papers a general survey of phosphors, their characteristics and methods of preparation is made. The next group contains four papers which deal with two important aspects of recent research on the storage of energy in phosphors. These aspects are the mechanisms of phosphorescence and thermoluminescence, both of which arise from the thermal ejection of trapped electrons, and the processes involved in the infra-red stimulation of phosphors. The third group of papers is devoted to factors affecting the fluorescence characteristics of phosphors, such as phosphor constitution, nature and intensity of exciting radiation and the phosphor temperature. The next six papers deal in more detail with the storage of energy in phosphors and its release by thermal or optical ejection of trapped electrons.

The last group of papers covers miscellaneous aspects of luminescence, such as photochemical action in phosphors, the function of manganese as a luminescence activator in different solids and the correlation of the structures of different classes of materials. In the last section of the book the present theoretical problems of luminescence and possible future approaches to their solution are discussed. In particular, the need for using luminescent solids in the form of single crystals in experimental studies is emphasized.

This book is not intended to be a comprehensive, up-to-date text-book on luminescence. Its value lies in its accounts of the results of recent studies having a rather specialized nature and in the discussions which may have more general significance. These discussions would probably have been even more valuable if they had been based on abstracts of the papers circulated previous to the Conference. It might also have been better to reduce the number of papers and to include and expand those in which a marked contribution to the knowledge of luminescence processes was evident.

However, there is included in the book an account of studies showing the renewed interest in the release of stored energy in phosphors by infra-red radiation. Quenching and stimulation processes in phosphors due to infra-red irradiation were popular subjects for early workers in luminescence. Although they are intimately connected with trapped electrons, the latest studies show that there is little correlation between the thermal and optical ejection of these electrons. The confusion of ideas with respect to the effects of infra-red radiation in phosphors shown in the appropriate papers serves to indicate the present inadequacy of the theory developed for the interpretation of other processes, such as phosphorescence and thermoluminescence.

Although the book will be of great value to those engaged in research on luminescence, the lack of clarity in some of the individual papers will make it difficult reading for others having a secondary interest in the subject.

G. F. J. GARLICK.

## CONTENTS FOR SECTION B

	PAGE
Dr. H. A. DELL. An Investigation of the Physical Properties of Thin Films used in the Reduction of Surface Reflection . . . . .	81
Mr. L. R. GRIFFIN. An Extended Theory of the Reflection Echelon Grating . . . . .	93
Mr. E. COLIN CHERRY. The Duality between Interlinked Electric and Magnetic Circuits and the Formation of Transformer Equivalent Circuits . . . . .	101
Mr. K. W. HILLIER and Dr. H. KOLSKY. An investigation of the Dynamic Elastic Properties of some High Polymers . . . . .	111
Dr. G. D. YARNOLD and Mr. B. J. MASON. A Theory of the Angle of Contact . . . . .	121
Dr. G. D. YARNOLD and Mr. B. J. MASON. The Angle of Contact between Water and Wax . . . . .	125
Mr. J. M. M. PINKERTON. The Absorption of Ultrasonic Waves in Liquids and its Relation to Molecular Constitution . . . . .	129
Letters to the Editor :	
Dr. R. STREET and Mr. J. C. WOOLLEY. A Note on Magnetic Viscosity in Alnico . . . . .	141
Reviews of Books . . . . .	142
Contents for Section A . . . . .	147
Abstracts for Section A . . . . .	147

## ABSTRACTS FOR SECTION B

### *An Investigation of the Physical Properties of Thin Films used in the Reduction of Surface Reflection, by H. A. DELL.*

**ABSTRACT.** A simple mathematical treatment of reflection from thin films is extended to cover the properties of films likely to be met with in practice. In particular, reflection from multiple films of more than one substance is considered, and the reflection of polarized light from simple films. A photometer used for testing these results is described, and the different types of cryolite films found are enumerated.

Evidence is given suggesting that polished or aged cryolite films behave as if they consisted of a lower stratum of cryolite surmounted by a secondary layer of higher refractive index. Some of the properties of this layer are described.

### *An Extended Theory of the Reflection Echelon Grating, by L. R. GRIFFIN.*

**ABSTRACT.** The single reflection echelon grating has the disadvantage that it is impossible to interpret the fringe pattern without further information about the correct order allocation. The present methods of obtaining this information are briefly reviewed; they are progressively less useful as the wavelength decreases into the ultra-violet. The properties of the grating are investigated theoretically when the light is incident at relatively large angles in two special cases, and the performance of the instrument in these positions compared with that of its normal use. It is shown that the required order allocation could be obtained using a single reflection echelon grating by measuring the fractional order separation with the grating in two positions. This would considerably increase the value of the instrument.

### *The Duality between Interlinked Electric and Magnetic Circuits and the Formation of Transformer Equivalent Circuits, by E. COLIN CHERRY.*

**ABSTRACT.** When making calculations on a circuit, containing both electric impedances and transformers, it is frequently desirable to consider the transformers removed and the constraints they impose replaced by a rearrangement of the impedances connected to their terminals. Such "equivalent circuits" may not always be found; the rules are here established for their formation, and also for checking, by inspection, whether the transformer



constraints are removable in this way in any particular case. It is shown that the equivalent electric circuit of a transformer, having any arrangement of magnetic paths, is derivable from its magnetic circuit by application of the topological principle of duality. This cannot be done if the magnetic circuit is non-planar, as in the case of a transformer possessing four or more winding with leakage couplings; a physically realizable circuit does not then exist.

Under certain conditions the principle may be applied in reverse and the impedances in a given electric circuit may be coupled together by a suitable transformer, so that the various current and voltage constraints are unaltered.

*An Investigation of the Dynamic Elastic Properties of Some High Polymers*, by K. W. HILLIER and H. KOLSKY.

- **ABSTRACT.** An apparatus for the investigation of the transmission of sound along filaments at frequencies between 1,000 and 6,000 cycles per second is described, both for unstrained specimen and whilst they are being elongated at a constant rate of increase of strain. Measurements of the dynamic elasticity and damping factors of filaments of polythene, neoprene and nylon have been obtained, and the correlation of these results with the molecular rearrangements which take place during stretching is discussed.

*A Theory of the Angle of Contact*, by G. D. YARNOLD and B. J. MASON.

**ABSTRACT.** It does not appear to be possible to give a quantitative account of the angle of contact of a continuous liquid in terms of cohesive forces. By using Young's energy relation and making allowance for the effects of adsorbed films on the surface of the solid, expressions are derived for the advancing and receding angles, and a general explanation of the hysteresis of the angle of contact is put forward.

*The Angle of Contact Between Water and Wax*, by G. D. YARNOLD and B. J. MASON.

**ABSTRACT.** The effects (a) of the velocity of the liquid surface, and (b) of the time of immersion, on the angle of contact between clean surfaces of water and wax have been investigated by dynamical method. It is clear that Ablett's measurements are vitiated by the fact that the time of immersion is disregarded. The term "equilibrium angle of contact" appears to be meaningless.

*The Absorption of Ultrasonic Waves in Liquids and its Relation to Molecular Constitution*, by J. M. M. PINKERTON.

**ABSTRACT.** Measurements of the absorption of ultrasonic waves in water and ethyl alcohol were made by the pulse method, and are more accurate than those made by other methods. The absorption coefficient  $\alpha$  in water was found to vary as the square of the frequency  $\nu$  over a wide range of temperatures. The measurements in water were made at frequencies between 7.5 and 67.5 Mc/s. and temperatures between 0 and 95° C. The absorption decreased with increasing temperature by a factor of 8 between freezing and boiling points. The observed absorption was about three times that calculated from Stokes' formula and this ratio was nearly independent of temperature. In ethyl alcohol measurements were made at 52.4 Mc/s., and at temperatures between -50° and +60° C. The absorption decreased by a factor 3 in this range and observed values were about twice those given by Stokes' formula. Values of  $(\alpha/\nu^2)$  at 25° C. are  $22.0 \times 10^{-17}$  sec<sup>2</sup>/cm. for water and  $50.5 \times 10^{-17}$  sec<sup>2</sup>/cm. for ethyl alcohol.

Published values of the absorption coefficients of a wide range of pure liquids and of some mixtures are reviewed, and a classification proposed. The experimental results suggests that the absorption in associated liquids is due to a different mechanism from that in non-associated liquids. In the latter the absorption is probably due to the same phenomenon as in gases: a slow exchange of energy between different degrees of freedom. The relaxation frequencies must be above 200 Mc/s. for most liquids. A simple theory is given to explain the observed variation of the absorption with concentration in mixtures of non-associated liquids. The semi-quantitative agreement of theory with experiment lends support to the relaxation hypothesis.

# THE PROCEEDINGS OF THE PHYSICAL SOCIETY

## Section A

---

VOL. 62, PART 3

1 March 1949

No. 351 A

---

### A Theory of Ultrasonic Absorption in Unassociated Liquids

By E. BAUER

Cavendish Laboratory, Cambridge

*Communicated by Sir Lawrence Bragg; MS. received 28th June 1948*

**ABSTRACT.** In many liquids the absorption of sound waves is very much larger than can be explained classically, in terms of viscosity and heat conduction. It is now fairly well established that different types of liquids behave very differently in this respect, and that the cause of the excess absorption in unassociated, polyatomic liquids like benzene and carbon disulphide lies in the incomplete excitation, by the sound wave, of the vibrational degrees of freedom. It is shown that this effect leads to mean dispersion frequencies in the range  $10^9$  to  $10^{10}$  c/s. at  $300^\circ$  K. This frequency range shows that, as in the case of gases, the efficiency of collisions in producing excitation or de-excitation of vibrational degrees of freedom is fairly low; a theoretical treatment of this effect is outlined. Detailed considerations of temperature coefficients of absorption lead to the conclusion that all the vibrational levels of a liquid do not relax at the same frequency but that high excited levels relax at relatively low frequencies. In the case of carbon disulphide a numerical estimate of these individual dispersion frequencies is made. It is also shown that the variation of absorption with concentration in binary mixtures can be described quite simply in terms of the analysis developed in this paper.

#### § 1. INTRODUCTION

IN most liquids the absorption coefficient of sound waves, measured per unit length of path, varies as the square of the frequency. This frequency dependence agrees with that predicted assuming the absorption to be due to viscosity (Stokes 1845) and thermal conductivity (Kirchhoff 1868) but its magnitude is frequently many times larger than that calculated on these classical theories. It is now reasonably well established that there are at least two distinct mechanisms, additional to viscosity and thermal conductivity, which contribute to the absorption of sound waves in liquids. These are the relaxation of a structural perturbation and of some internal degrees of freedom of the molecules of the liquid.

There is a definite correspondence between the chemical structure of a liquid and its absorption coefficient for sound waves (cf. Pinkerton 1947, 1949). The classical (Stokes-Kirchhoff) value of the absorption is observed in monatomic liquids like mercury and also in highly viscous liquids like glycerol, in which viscosity is the predominating factor. Water and the alcohols are typical of another important class of liquids which are highly associated so that the liquid exhibits a considerable degree of order. Here the observed absorption is up to three times the calculated viscous absorption and their ratio remains remarkably

constant over a wide range of temperature. The excess absorption in these liquids has been explained in terms of their relatively close-bound structure, a comparatively long time being required to re-establish equilibrium after the structure has been distorted (Hall 1948). In acetic acid there is a large fall in the absorption and also a dispersion near 2.5 Mc/s. This is probably due to the perturbation of a chemical equilibrium, possibly the dimerization equilibrium. In chemically simple, unassociated polyatomic liquids like benzene, carbon disulphide, and chloroform the absorption coefficient has many times its classical value and frequently increases with the temperature. It seems likely that this effect is analogous to that observed in polyatomic gases, in which at room temperature a dispersion is observed in the range  $10^3$ – $10^6$  c/s. This has been shown to be due to the fact that equilibrium between internal (vibrational) and external (translational and rotational) degrees of freedom is established relatively slowly (Richards 1939). Consequently, at low frequencies the sound wave is absorbed as a result of incomplete excitation of the vibrational degrees of freedom, while at higher frequencies there is a dispersion. At frequencies well above the dispersion frequency the vibrational modes do not participate in the propagation of the sound wave.

There have been numerous treatments of this relaxation effect for a perfect gas and equivalent results have been obtained by three distinct methods. Herzfeld and Rice (1928) introduced the relaxation process in a phenomenological way which does not indicate its molecular significance. The analysis of Bourgin (1936) is based on considerations of detailed balancing and molecular transport, while Einstein (1920), Kneser (1931) and Rutgers (1933) developed a treatment which depends on thermodynamics, the equation of state of a perfect gas, and on detailed balance.

Herzfeld (1941) showed that it is possible to obtain an expression for the absorption without making use of an equation of state. In the present paper a similar, but rather more detailed, thermodynamical treatment is given, with the aim of indicating the physical processes and assumptions involved.

## § 2. THERMODYNAMICAL ANALYSIS

In order to indicate the method of approach and to show clearly the nature of the basic approximations used, a general outline of the method will be given first. The absorption arises because the passage of the ultrasonic waves disturbs the statistical equilibrium of the vibrational levels, so that the effective vibrational specific heat depends on time. Essentially a perturbation method is used, the velocity of sound in the liquid being considered under conditions of disturbed equilibrium. A convenient way of isolating the perturbation in the expression for the velocity is to consider plane sound waves represented by a complex exponential. The perturbation depends on time, so that time derivatives arise in the calculation: these are imaginary numbers and thus one sees that the absorption depends essentially on the imaginary part of the expression for the velocity of sound.

In transforming the expression for the velocity of sound, thermodynamic results are used. If there is some absorption of the wave, its propagation is not adiabatic or thermodynamically reversible, as is implicitly assumed when thermodynamic relations are applied. This kind of difficulty frequently arises when thermodynamics is applied to actual physical processes which are not quasi-static

and the condition for the results to be valid is that the fractional energy loss per cycle shall be small. Provided this condition is satisfied, the fractional energy loss per cycle is given by  $2\mu$ , where  $\mu$  is the amplitude absorption coefficient per wavelength.  $\mu$  is given by the product of the amplitude absorption coefficient per unit length of path  $\alpha$ , and the wavelength  $\lambda$  in the liquid. For example, in benzene  $2\mu = 1.6\%$  at 10 Mc/s.; as in all liquids of this type,  $\mu$  is proportional to the frequency. The same difficulty occurs in considering gases, but the agreement between observed and calculated absorption is quite good over the whole dispersive range of frequencies.

The velocity of sound,  $\Gamma$ , is expressed by the Euler-Laplace relation

$$\Gamma^2 = (\delta p / \delta \rho)_{\text{adiab.}} \quad \dots\dots(1)$$

where  $p$  is the pressure and  $\rho$  the density of the fluid. For a plane harmonic wave  $\Gamma$  is complex, and if  $\alpha$  is the absorption coefficient per unit length of a wave propagated in the  $x$ -direction, then the wave motion is represented by

$$\exp \{i2\pi\nu(t - x/\Gamma)\} = \exp \{i2\pi\nu(t - x/c)\} \exp \{-\alpha x\}$$

so that 
$$\alpha = -\pi c \nu \mathcal{I} \left[ \frac{1}{\Gamma^2} \right] \quad \dots\dots(2)$$

where  $\nu$  is the frequency,  $c$  the measured velocity of sound which is equal to the real part of  $\Gamma$  and  $\mathcal{I}(z)$  denotes the imaginary part of  $z$ . Because  $\alpha$  is proportional to the square of the frequency, it is usual to consider  $\alpha/\nu^2$  which is independent of frequency.

For an adiabatic change, the first law of thermodynamics is written in terms of the internal energy  $E$  and the enthalpy  $H$

$$\delta E + p\delta V = 0; \quad \delta H - V\delta p = 0 \quad \dots\dots(3)$$

where 
$$E = E' + \sum_j W_j a_j; \quad H = H' + \sum_j W_j a_j, \quad \dots\dots(4)$$

$a_j$  is the fraction of molecules in the  $j$ th excited level of energy  $W_j$ , and primes refer to quantities excluding the contributions of the excited levels. All extensive quantities ( $E$ ,  $H$ ,  $W_j$ ,  $V$ ) are referred to one gram molecule as unit.

It is convenient to take the change in temperature produced at any point in the liquid by the sound wave as independent variable, and thus equations (1) and (3) give

$$\Gamma^2 = \frac{p(\partial H / \partial T)_S}{\rho(\partial E / \partial T)_S}.$$

Using standard thermodynamical relations this gives

$$\Gamma^2 = \frac{p}{\rho} \frac{C_p / lT}{C_v p \kappa / lT}$$

where  $l$  is the coefficient of thermal expansion,  $\kappa$  is the isothermal compressibility, and  $C_p$  and  $C_v$  are the principal specific heats. The division of the thermodynamical functions into the contributions of external and internal degrees of freedom must be made at this stage, because it is assumed that the entropy of the whole assembly,  $S = S' + \sum_j a_j S_j$ , is conserved.\* Thus we have

$$\Gamma^2 = \frac{1}{\rho \kappa} \frac{(C'_p + \sum_j W_j (\delta a_j / \delta T))}{(C'_v + \sum_j W_j (\delta a_j / \delta T))} \quad \dots\dots(5)$$

\* I am indebted to Professor Herzfeld for pointing this out.

The vibrational specific heat,  $\Sigma_j W_j (\delta a_j / \delta T)$ , is the only quantity contributing to  $\Gamma$  which depends on time, so that with the present formulation it is the only complex quantity. Taking the vibrational specific heat to be much smaller than  $C_p'$  and  $C_v'$ , although this is not always the case, equations (2) and (5) give

$$\frac{\alpha}{\nu^2} = -\frac{\pi}{\nu} \frac{c}{c'^2} \frac{\gamma' - 1}{C_p'} \mathcal{J}[\Sigma_j W_j (\delta a_j / \delta T)] \quad \dots\dots(6)$$

where  $\gamma$  is the ratio of the principal specific heats.

### § 3. THE RELAXING SPECIFIC HEAT

Because of the relatively high frequency of the sound wave the specific heat,  $\Sigma_j W_j (\delta a_j / \delta T)$ , differs slightly from its equilibrium value. Its value can be calculated most conveniently by setting up an equation of detailed balance and considering it under conditions of slightly perturbed equilibrium.

First, we shall consider a single excited level,  $j$ , in equilibrium with the ground state which is denoted by the suffix 0. Thus  $a_j$ ,  $a_0$  ( $= 1 - a_j$ ) are the fractions of molecules that are excited and unexcited respectively, and the equation of detailed balance may be written

$$\partial a_j / \partial t = a_0 k_{0j} - a_j k_{j0}, \quad \dots\dots(7)$$

where the  $k_{ij}$  are rate constants. In equilibrium,  $\partial a_j / \partial t = 0$ , and therefore

$$a_j / a_0 = k_{0j} / k_{j0} = \exp(-W_j / RT). \quad \dots\dots(8)$$

The perturbation is produced by plane harmonic sound waves of frequency  $\nu = \omega / 2\pi$ . Thus writing  $i\omega$  for  $\partial / \partial t$  we get, from equations (7) and (8).

$$\delta(\partial a_j / \partial t) = i\omega \delta a_j = \delta(a_0 k_{0j} - a_j k_{j0}) = k_{j0} \delta(a_0 k_{0j} / k_{j0} - a_j)$$

provided the perturbation is small. Taking the temperature as independent variable, we obtain (Rutgers 1933)

$$\frac{\delta a_j}{\delta T} = \frac{W_j}{RT^2} a_j \left[ 1 + i \frac{\omega}{k_{j0} + k_{0j}} \right]^{-1}.$$

If we disregard the excitation of harmonics of the vibration it is consistent to neglect  $\exp(-W_j / RT)$  compared with unity. This gives

$$\frac{\delta a_j}{\delta T} = \frac{W_j}{RT^2} [1 + i\omega / k_{j0}]^{-1} \exp(-W_j / RT) \quad \dots\dots(9)$$

and if the equilibrium value of the vibrational specific heat is denoted by  $C_j$ ,

$$\mathcal{J}[W_j \delta a_j / \delta T] = -(\nu / \nu_j) C_j [1 + (\nu / \nu_j)^2]^{-1} \quad \dots\dots(10)$$

where  $\nu_j = k_{j0} / 2\pi$  is the dispersion frequency of the  $j$ th level.

In the numerical applications which are given later, the Einstein specific heat  $R(W_j / RT)^2 \exp(W_j / RT) [\exp(W_j / RT) - 1]^{-2}$  is used for  $C_j$ . It can be seen that, when  $\exp(-W_j / RT)$  is neglected compared with unity, the Einstein specific heat reduces to the simple form of  $C_j$  given in equations (9) and (10). In the case of polyatomic substances there are always several vibrational levels, and equations corresponding to (7) and (8) can be written down for the case of  $l$  excited levels.

They are

$$a_j = a_0 \exp(-W_j/RT); \quad \partial a_j / \partial t = \sum_{i=0, i \neq j}^l [a_i k_{ij} - a_j k_{ji}] \quad \dots\dots (11)$$

where  $j = 1, 2, \dots l$  and a fraction  $a_j$  of the molecules is excited with energy  $W_j$ ;  $k_{ij}$  is the rate constant corresponding to an  $i \rightarrow j$  transition.

Proceeding as before, we find  $(l+1)$  linear simultaneous equations in the  $(l+1)$  variables  $\delta a_i / \delta T$ ;

$$\left. \begin{aligned} [(\sum_{i \neq j} k_{ji}) + i\omega] \delta a_j / \delta T - \sum_{i \neq j} k_{ij} \delta a_i / \delta T &= \sum_{i \neq j} a_i k_{ij} (W_j - W_i) / RT^2 \\ \sum_{i=0}^l \delta a_i / \delta T &= 0. \end{aligned} \right\} \quad \dots\dots (12)$$

In principle there is no difficulty in solving these equations, but there are  $l(l+1)$  quantities  $k_{ij}$  with  $\frac{1}{2}l(l+1)$  relations of type (8) between them, and as the  $k_{ij}$  are unknown quantities (see § 5), it is not practicable to solve equations (12).

Because there are  $l$  excited levels, the vibrational specific heat can be expressed (Kronig 1938) as a sum of  $l$  terms of the type

$$\sum_{j=1}^l \frac{C_j}{1 + i\nu/\nu_j} = \frac{\Sigma C_j}{1 + i\nu/\nu_m} \quad \dots\dots (13)$$

where the most important contribution to  $\nu_j$  is  $k_{j0}/2\pi$ . Results have generally been expressed in terms of a mean dispersion frequency  $\nu_m$  defined by equation (13); from various considerations it appears very improbable that in liquids like carbon disulphide and benzene all vibrational levels relax at the same frequency, so that  $\nu_m$  has no detailed physical meaning, although it does give the order of magnitude of the dispersive frequency range in a liquid.

From equations (6) and (13), the absorption coefficient is given by

$$\frac{\alpha}{\nu^2} = \pi \frac{c}{c'^2} \frac{\gamma' - 1}{C_p'} \frac{\Sigma C_j}{\nu_m} \frac{1}{1 + (\nu/\nu_m)^2} \quad \dots\dots (14)$$

Equation (9) shows that when  $\nu$  is very much larger than  $\nu_j$ , the effective vibrational specific heat  $\Sigma_j W_j \delta a_j / \delta T$  becomes negligibly small, and so primed quantities, which do not include the contribution of the vibrational levels, correspond to the case  $\nu \gg \nu_m$ .

#### § 4. THE MEAN DISPERSION FREQUENCY

Equation (14) can be used to give values of the mean dispersion frequency for different liquids by substituting experimental values of  $\alpha/\nu^2$ . The results for a number of liquids are recorded in Table 1.

What has actually been calculated is  $\mu_m$ , the absorption coefficient per wavelength at  $\nu = \nu_m$ , which is given by

$$\mu_m = \frac{\pi \gamma}{2 \gamma'} \frac{\gamma' - 1}{C_p'} \Sigma C_j, \quad \dots\dots (15)$$

and the mean dispersion frequency  $\nu_m$  is calculated from the relation

$$\nu_m = (2\mu_m/c)[1/(\alpha/\nu^2)_{\nu \ll \nu_m}] \quad \dots\dots (16)$$

which was given by Kneser (1938) and has been used by Pinkerton (1949) to obtain

approximate estimates for  $\nu_m$ . However, both from experimental results (Rapuano 1947) and from a consideration of temperature coefficients of absorption (§6), as well as of transition probabilities which determine the dispersion frequencies  $\nu_j$  of the individual vibrational levels (§5) it appears that all levels do not in fact relax together, so that while equation (15) defines some quantity  $\mu_m^*$  which, when substituted in (16) gives the correct  $\nu_m$ , yet  $\mu_m^*$  is not the absorption coefficient per wavelength at  $\nu = \nu_m$ . It follows that  $2\mu_m^*$  does not give the fractional energy loss per cycle at dispersion and thus the method used by Pinkerton (1949) in estimating  $\nu_m$ , while interesting and good to an order of magnitude, cannot be regarded as supported in detail by the present considerations.

Table 1. Mean Dispersion Frequencies of some Liquids, calculated from Equation (16). All values refer to 300° K.

Substance	$\alpha/\nu^2$ (1)	$c$ (2)	$c'$ (3)	$C$ (4)	$2\mu_m^*$ (5)	$\nu_m$ (6)
Carbon disulphide	10,800 (a)	1.14 (f)	1.25	4.00	0.644	52.5
Benzene	830 (b)	1.31 (b)	1.53	11.7	1.300	1,200
Carbon tetrachloride	513 (b)	0.910 (b)	1.09	12.3	1.593	3,420
Chloroform	380 (c)	0.987 (c)	1.10	7.84	0.835	2,230
Toluene	84 (c)	1.31 (c)	1.44	(13.0)	0.823	7,500
Acetone	60 (c)	1.17 (c)	1.27	7.50 (e)	0.614	8,720
Ethyl bromide	56 (b)	0.932 (b)	1.07	(8.0)	1.137	21,800

(1) Experimental values of absorption  $\alpha/\nu^2$  ( $\text{sec}^2 \text{ cm}^{-1} \times 10^{-17}$ )†.

(2) Experimental values of velocity  $c$  ( $\text{cm. sec}^{-1} \times 10^5$ ) ( $\nu \ll \nu_m$ ).

(3) Calculated value of  $c'$ , the velocity at frequencies  $\nu \gg \nu_m$  ( $\text{cm. sec}^{-1} \times 10^5$ ).

(4) Vibrational specific heat  $C_j$  (cal/mole deg.) (d).

(5) Values of  $2\mu_m^*$  from equation (15).

(6) Mean dispersion frequency  $\nu_m$  (Mc/s.).

(a) Kneser (1938).

(d) Herzberg (1945).

(b) Pellam and Galt (1946).

(e) Schumann and Aston (1938).

(c) Willard (1941).

(f) Biquard (1935).

† The value of  $\alpha/\nu^2$  due to viscosity and heat conduction has been subtracted.

It may be convenient to give here the formula for the dependence of the velocity on frequency, which is of course the real "dispersion" formula. From equations (4) and (8) we obtain

$$c_v^2 = c'^2 \left[ 1 - \frac{\sum C_j}{1 + (\nu/\nu_m)^2} \frac{\gamma' - 1}{C_p'} \right] \dots\dots (17)$$

since  $\sum_j W_j \delta a_j / \delta T \ll C_p'$ ,  $C_v'$ . This equation shows that  $\lim_{\nu \rightarrow \infty} c_v = c'$ , as has already been inferred from physical considerations.

## § 5. THEORETICAL ESTIMATES OF THE DISPERSION FREQUENCY

From equations (9) and (10) it can be seen that to calculate  $\nu_j$  the essential step is the calculation of  $k_{j0}$ , the rate at which a molecule in the  $j$ th excited vibrational level falls back into the ground state. There is no reason to believe that there exists a potential barrier large compared with  $kT$  to prevent de-excitation

(Eucken and Becker 1934), so that the rate constant  $k_{j0}$  is given by the product of the collision frequency  $\nu_{\text{coll}}$  and the transition probability  $p_{j0}$ . For a gas, the collision frequency can be calculated from the mean free path and mean velocity of the molecules; at room temperature and atmospheric pressure  $\nu_{\text{coll}} \sim 5 \cdot 10^9 \text{ sec}^{-1}$ . For liquids,  $\nu_{\text{coll}} \sim kT/h$  (Glasstone, Laidler and Eyring 1941) which is of the order  $10^{12} \text{ sec}^{-1}$  at  $300^\circ \text{K}$ . The observed dispersion frequencies for gases lie in the range  $10^3$ – $10^6 \text{ c/s.}$ , and predicted values for liquids are of the order  $10^9$ – $10^{10} \text{ c/s.}$  Thus the transition probabilities lie in the ranges  $10^{-6}$  to  $10^{-3}$  for gases and  $10^{-3}$  to  $10^{-2}$  for liquids.

The low value of this transition probability in the case of a gas has been explained by Zener (1931), who showed that it is a consequence of the quantal treatment of collisions between an atom and a vibrating molecule that inelastic collisions are infrequent. Later, Landau and Teller (1936) derived an approximate classical formula for the dispersion frequency, but their result is not applicable at room temperature where the spacing of the vibrational levels is relatively large compared with  $kT$ .

In the case of liquids it is easy to modify Zener's treatment by adding a constant attractive potential  $U_0$ , representing the cohesion, to the Lennard-Jones repulsion between molecules,  $E_0 \exp[-\alpha(r-r_0)]$  which of course depends very strongly on  $r$ , the distance apart of the molecules. Then, if  $\epsilon_j$  is the energy of the  $j$ th level and  $K$  is the kinetic energy of the colliding particles before the impact, the transition probability is given by

$$p_{j0} = \frac{\pi^2 \mu}{16 \mu_m} \frac{E_0}{\epsilon_j} \left( \frac{K + U_0}{K + U_0 + \epsilon_j} \right)^{\sqrt{(E_0)}, 2/2} \dots\dots (18)$$

where all quantities are measured in atomic units, and  $\mu$  and  $\mu_m$  are reduced masses of the system as a whole and the vibrating molecule respectively. An outline of the derivation of (18) is given in the appendix where order of magnitude values for the various quantities are indicated. They give values of  $p_{j0}$  which are of the correct order ( $10^{-3}$  to  $10^{-2}$ ) and in view of the idealizations and approximations of the analysis no detailed deductions can usefully be made; in particular, the difference in the behaviour of different substances cannot be explained because no account is taken of the structure of the colliding particles or of dipole moments which produce an increase in the transition probabilities (Metter 1937). From equation (18) it can be seen that  $p_{j0}$  decreases with increasing energy of excitation  $\epsilon_j$  and, as both  $K$  and  $U_0$  are of the order  $3kT/2$ , the transition probability increases with increasing temperature.

Eucken and Becker (1934) found that the transition probability in gaseous mixtures increases as the third or fourth power of the temperature. In an attempt to explain the inefficiency of collisions they showed that if the efficiency of a collision is inversely proportional to the  $2n$ th power of the closest distance of approach of the molecules, then this transition probability is proportional to  $T^n$ . Exactly the same temperature variation results if one supposes that the efficiency of a collision is proportional to the  $n$ th power of the mutual kinetic energy of the particles before impact. In the case of liquids this picture again has a qualitative significance, but because of the interaction represented by  $U_0$ , the value of  $n$  will be rather smaller, of the order 1 to 2.



## § 6. THE TEMPERATURE COEFFICIENT OF ABSORPTION

We write equation (14) in the form

$$\frac{\alpha}{\nu^2} = \text{const.} \frac{(\gamma' - 1) \Sigma C_j}{c \nu_m} \quad \dots\dots (14 a)$$

where the constant,  $\pi\gamma/\gamma'C_p$ , is approximately independent of temperature, while by a standard thermodynamic result  $(\gamma' - 1)$  is proportional to  $T$ . Now it is convenient to write  $\partial \log C_j / \partial T = D_j / T$  where  $D_j \simeq W_j / RT - 2$  for  $W_j \gg RT$  and  $\partial \log \Sigma C_j / \partial T = \bar{D} / T$ . It has been seen that the transition probability increases with temperature, approximately as  $T^n$ , where  $n$  is of order 1 to 2. The collision frequency,  $kT/h$ , is proportional to  $T$ , and logarithmic differentiation of equation (14 a) gives

$$\frac{1}{\alpha} \frac{\partial \alpha}{\partial T} = -\frac{1}{c} \frac{\partial c}{\partial T} + \frac{1}{T} [\bar{D} - n]. \quad \dots\dots (19)$$

By consideration of Table 2 we see that, for this equation to be satisfied,  $n$  would

Table 2. Temperature Coefficients of Absorption

Substance	$10^{+3} \text{ deg}^{-1}*$ (1)	$10^3 \text{ deg}^{-1}$ (2)	$(D - n)_{\text{eff}}$ (3)	$\bar{D} = T \partial \log \Sigma C_j / \partial T$ (4)
Carbon disulphide	(10)	— (3.5)	+ 1.95	0.874
Benzene	11 (a)	— 3.6 (a)	+ 2.22	1.820
Carbon tetrachloride	(0)	— (3.5)	— 1.05	0.623
Chloroform	(10)	— 3.4 (b)	+ 1.98	0.660
Acetone	(10)	— 3.8 (b)	+ 1.86	1.840
Ethyl bromide	10 (a)	— 3.6 (a)	+ 1.92	(1.0)

(1) Measured values of temperature coefficients of absorption ( $10^3 \text{ deg}^{-1}$ ).

(2) Measured values of temperature coefficients of velocity ( $10^3 \text{ deg}^{-1}$ ).

(3)  $(D - n)_{\text{eff}}$  calculated from equation (19).

(4)  $\bar{D} = T \partial \log \Sigma C_j / \partial T$  (see § 6).

(a) Pellam and Galt (1946).

(b) Willard (1941).

\* Experimental values for temperature coefficients of absorption are rather incomplete, but for unassociated liquids the values are generally near  $(+ )10^{-2} \text{ deg}^{-1}$ ; carbon tetrachloride is an exception, as here the absorption seems to vary very little with temperature (Bazulin 1937).

have to be much less than one or negative in many cases. These values cannot be reconciled with equation (18), or with simple physical considerations like those of Eucken and Becker.

The difficulty can be overcome if we suppose that the individual levels relax one by one, a high excited level having a low probability of de-excitation and thus a low dispersion frequency. Because a high excited level has a low specific heat but a large temperature coefficient of specific heat, the change in weight of the several levels arising from the replacement of

$$\partial[\log(\Sigma C_j / \nu_m)] / \partial T \quad \text{by} \quad \partial[\log(\Sigma C_j / \nu_j)] / \partial T$$

would result in a larger value of  $(D - n)_{\text{eff}}$ .

Unfortunately there are no data available on the values of  $\nu_j$ , but there are several independent results which show that in certain cases different vibrational

levels relax at different frequencies. Acetaldehyde vapour (Alexander and Lambert 1942) shows three distinct dispersion regions, which the authors ascribe to the relative complexity of the molecule.

The behaviour of liquid carbon disulphide is of special interest, because it is the most highly absorbing simple liquid which has been investigated. A study of the absorption coefficients measured at different frequencies shows that multiple dispersions must be assumed to explain the results which are given in Table 3A.

In Table 3B these results are interpreted in the light of the previous discussion and the dispersion frequencies of the three vibrational levels are calculated.

Table 3. Multiple Dispersion in Carbon Disulphide

A: Experimental values of the absorption

$\alpha/\nu^2$ (cm <sup>-1</sup> sec <sup>2</sup> × 10 <sup>-17</sup> )	10,750 ± 1,000	7,400	1,400
Frequency (Mc/s.)	< 1	6.5	75,105
Observer	Claeys, Errera, Sack quoted from Kneser (1938)	Willard (1941)	Rapuanio (1947)

B: Interpretation of these results

Vibrational level frequency (cm <sup>-1</sup> )	Vibrational specific heat, $C_j$ (cal/mole deg.)	Velocity		$2\mu_j$ [cf. eq. (15)]	$\Delta(\alpha/\nu^2)$ (cm <sup>-1</sup> sec <sup>2</sup> × 10 <sup>-17</sup> )	$\nu_j$ (Mc/s)
		$c$ ( $\nu \ll \nu_j$ ) (cm. sec <sup>-1</sup> × 10 <sup>3</sup> )	$c'$ ( $\nu \gg \nu_j$ ) (cm. sec <sup>-1</sup> × 10 <sup>3</sup> )			
1523	0.0724	1.14	1.14	0.00705	3,350	1.85
656.5	0.930	1.14	1.157	0.106	6,000	15.5
397 (doublet)	3.00	1.157	1.245	0.494	1,400	305

It is now possible to evaluate

$$D_{\text{eff}} = \frac{T}{\Sigma C_j / \nu_j} \frac{\partial C_j}{\partial T} \Sigma \frac{1}{\nu_j}$$

for carbon disulphide on the basis of Table 3B. The value obtained is 2.76, so that if  $n$  is taken equal to one,  $(1/\alpha)(\partial\alpha/\partial T) \simeq 9 \cdot 10^{-3} \text{ deg}^{-1}$ .

## § 7. BINARY MIXTURES

It is well known that in the case of gases small traces of impurities may have an extremely large effect on the absorption (Eucken and Becker 1934). A similar effect has been found in a number of liquids like carbon disulphide and benzene where the absorption falls very rapidly when a small quantity of a less absorbing liquid is added to one of high absorption. Pinkerton (1949) has shown that this effect can be explained on a very simple relaxation picture. It is shown here how the same basic ideas, when interpreted in terms of transition probabilities, yield results which are in good agreement with experiment.

Let A be the strongly absorbing liquid and B the other one. Then A has a much smaller dispersion frequency than B, so that an A molecule, once excited, has a much smaller chance of de-excitation than an excited B molecule. For

simplicity in the analysis it will be assumed that only binary collisions need be considered and that collisions between excited molecules may be neglected. Then if A and A\* represent an unexcited and an excited A molecule respectively, and similarly for B, B\*, then an (A\*A) collision is much less efficient than a (B\*B) collision because  $\nu_m^A$  is much smaller than  $\nu_m^B$ . In a mixture of molecules of both species, A and B, there will, in addition to (A\*A) and (B\*B) collisions also be (A\*B) and (B\*A) impacts which have a rather high de-excitation efficiency because it is in general impossible for a quantum of vibrational energy to be transferred from one type of molecule to the other without some loss of energy. Now, following Pinkerton, we make the crucial assumption that (A\*B) and (B\*A) collisions are as efficient in producing excitation and de-excitation as (B\*B) collisions. Thus, as the concentration of B molecules increases, the net efficiency of all collisions tends rapidly to the value corresponding to the liquid B, so that the absorption falls sharply.

In the analysis it is convenient to suppose that each molecular species has only a single excited level of energy  $W_A$  and  $W_B$  for A and B respectively. The generalization for a number of levels proceeds as in §3 for the case of a single liquid, and the same approximation is made.

Consider 1 gm. mol. of the mixture; a fraction  $a$  is made up of A molecules, there being mole fractions  $a_1$ ,  $a_0 (= a - a_1)$  of excited and unexcited molecules, and similarly mole fractions  $b_1$ ,  $b_0$  for the liquid B, where  $a + b_1 + b_0 = 1$ . Introducing  $k, g, l$  and  $h$  respectively as (AA), (AB), (BA) and (BB) transition probabilities, we can write two equations of detailed balance:

$$\begin{aligned} \frac{\partial a_1}{\partial t} &= (k_{01}a_0 + g_{01}b_0)a_0 - (k_{10}a_0 + g_{10}b_0)a_1 = \phi_{01}a_0 - \phi_{10}a_1 \\ \frac{\partial b_1}{\partial t} &= (l_{01}a_0 + h_{01}b_0)b_0 - (l_{10}a_0 + h_{10}b_0)b_1 = \psi_{01}b_0 - \psi_{10}b_1 \end{aligned} \quad \dots\dots (20)$$

Proceeding as in §3, one arrives at the result

$$\left. \begin{aligned} \partial a_1 / \partial T &= (W_A / RT^2) a [1 + i\omega / \phi_{10}]^{-1} \exp(-W_A / RT) \\ \partial b_1 / \partial T &= (W_B / RT^2) (1 - a) [1 + i\omega / \psi_{10}]^{-1} \exp(-W_B / RT) \end{aligned} \right\} \dots\dots (21)$$

and if  $C_A$ ,  $C_B$  denote the vibrational specific heats of A and B, equation (13) becomes

$$\left( \frac{\alpha}{\nu^2} \right)_a = 2\pi \left[ \frac{\pi c}{c'^2} (\gamma' - 1) \frac{1}{C_p'} \right]_a \left[ \frac{a C_A}{\phi_{10}} + \frac{(1 - a) C_B}{\psi_{10}} \right] \dots\dots (22)$$

Now two approximations are introduced:

(i) The crucial assumption that, to a first approximation, (B\*B), (B\*A), (A\*B) collisions are all equally efficient in producing an inelastic transition,  $z$  times ( $z \sim 10$ ) more so than (A\*A) collisions. In mathematical form this is written  $zk_{ij} = g_{ij} = l_{ij} = h_{ij}$  ( $i, j = 0, 1$ ).

(ii) The quantity  $2\pi^2 \frac{c}{c'^2} (\gamma' - 1) \frac{1}{C_p'}$  changes linearly with concentration  $a$ .

This is not a critical assumption because the total variation in this quantity is not large. It will be written  $M_B(1 - fa)$ .

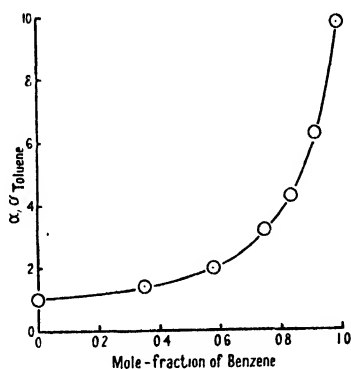
Then equation (22) becomes

$$(\alpha / \nu^2)_a = (M_B / g_{10}) (1 - fa) [(1 - a) C_B + az C_A / \{z - a(z - 1)\}]$$

which can conveniently be compared with experiment in the form

$$\frac{\alpha_A}{\alpha_B} = (1-fa) \left[ (1-a) + \frac{az}{z-a(z-1)} \frac{C_A}{C_B} \right]. \quad \dots\dots(23)$$

Results for a benzene-toluene mixture are given in the Figure. If A specifies.



Ratio of the absorption coefficient of a mixture of benzene and toluene to the absorption coefficient of toluene as a function of the mole fraction of benzene.

Full line : theoretical curve (equation (23)).

Circles : experimental points (Grobe 1938).

benzene and B toluene then, using the values given in Table 1,  $f$  and  $z$  are given by  $f = 1 - \frac{\alpha_A}{\alpha_B} \frac{C_B}{C_A} \frac{1}{z} = -0.743$  and  $z = \nu_m^B / \nu_m^A = 6.28$  since  $C_A / C_B = 0.904$  and  $\alpha_A / \alpha_B = 9.80$ . Pinkerton's (1949) result is recovered by putting  $f=0$  and  $C_A = C_B$  so that  $z = \alpha_A / \alpha_B$ .

## § 8. DISCUSSION

Since the present approach to the problem of vibrational relaxation is based on rather general considerations regarding the perturbation of an equilibrium, the same general method can be applied to a number of different aspects of the problem of incomplete excitation of some internal degree of freedom of the molecules. In particular, the application to the perturbation of a chemical equilibrium by the sound wave is of interest. Such an effect may be the cause of the dispersion observed in acetic acid by Spakovskij (1938) and others. Pinkerton (1948), using his own and Bazulin's (1936) results for the absorption of sound in acetic acid near 2 Mc/s., has estimated by a graphical method that the fall in  $\alpha/\nu^2$  in this frequency range is  $12,000 \times 10^{-17} \text{ cm}^{-1} \text{ sec}^2$  and that the dispersion frequency is 2 Mc/s. at 17° C. From these data a value of the relaxing specific heat can be calculated from equation (14): its value is 1.4 cal/mole degree. This is very large and might correspond to a hindered rotation or similar process.

## § 9. CONCLUSIONS

In the case of simple, unassociated polyatomic liquids like benzene, incomplete excitation of the vibrational degrees of freedom by the sound wave is shown to lead to a dispersion, with mean dispersion frequencies in the range  $10^9$  to  $10^{10}$  c/s. at room temperature. It does not seem probable that all vibrational levels of a liquid relax together: it is possible that some high excited levels have dispersion.

frequencies below  $10^7$  c/s. which have not so far been detected. Carbon disulphide may well be a case in point, for consideration of the available experimental data indicates that its three vibrational levels may have dispersion frequencies of 1.85, 15.5 and 305 Mc/s.

#### ACKNOWLEDGMENTS

I wish to thank Dr. A. R. Miller, who suggested this problem, for his constant interest and detailed advice. I also wish to thank Mr. J. M. M. Pinkerton for many discussions and in particular for making available his experimental results in advance of publication. This work was carried out during the tenure of a maintenance allowance from the Department of Scientific and Industrial Research.

#### APPENDIX

##### *Calculation of Transition Probabilities*

A brief outline of Zener's (1931) treatment is presented here, with a modification to account for the cohesive forces in a liquid. To facilitate reference to the original paper a similar notation is employed and atomic units are used.

Zener considers the one dimensional collision of an atom A of mass  $M_A$  with a vibrating molecule B-C, the two atoms of this having masses  $M_B$  and  $M_C$ . By a suitable choice of coordinates the motion of the centre of mass becomes separable and is eliminated, and the wave equation of the system is written

$$\left[ \frac{1}{\mu_m} \frac{d^2}{dx^2} + \frac{1}{\mu} \frac{d^2}{dr^2} - V(x) - U(x, r) + E \right] \Psi = 0. \quad \dots\dots(24)$$

Here  $r$  is the coordinate describing the position of A relative to the centre of mass BC,  $x$  is the distance BC between the vibrating atoms,  $\mu_m = M_B M_C / (M_B + M_C)$  and  $\mu = M_A (M_B + M_C) / (M_A + M_B + M_C)$  are the reduced masses of the vibrator BC and the whole system respectively;  $E$  is the total energy of the system,  $V(x)$  the potential energy of the vibrator, and  $U(x, r)$  the mutual potential energy of atom A and molecule BC. The modification which has been made to Zener's treatment is that a constant attractive term  $-U_0$  is added to the repulsive term  $V(x, r)$  which depends strongly on distance.  $U_0$  must be present, and rather larger than  $3kT/2$ , for the liquid to maintain its volume.

$$U(x, r) = -U_0 + V(x, r). \quad \dots\dots(25)$$

The vibrational motion of (BC) in its  $i$ th state is described by the wave equation

$$[(1/\mu_m)(d^2/dx^2) - V(x) + E_i] \phi_i(x) = 0 \quad \dots\dots(26)$$

where  $\phi_i(x)$  is the normalized wave function corresponding to the energy  $E_i$ .

Now, define the momentum,  $p_i$ , by

$$p_i = [\mu(E + U_0 - E_i)]^{1/2}. \quad \dots\dots(27)$$

We require a solution of (27) having the asymptotic form

$$\Psi(r \rightarrow \infty) = \frac{e^{ip_i r} + e^{-ip_i r}}{p_i^{1/2}} + \sum_f \gamma_{if} \frac{e^{-ip_f r}}{p_f^{1/2}} \phi_f(x). \quad \dots\dots(28)$$

This solution of course consists of an incident wave which is scattered, in part inelastically: the probability of a change  $i \rightarrow f$  in vibrational quantum number is  $|\gamma_{if}|^2$ .

To obtain  $\gamma_{ij}$ , we must find a solution for (24) of the form (28). The wave function is expanded as  $\Psi = \sum_k Q_k(r) \phi_k(x)$ , the  $Q_k(r)$  being undetermined functions. This is substituted in equation (27) and after multiplying by  $\phi_j(x)$  and integrating over  $x$ , the orthonormality of the  $\phi_j$  leads to

$$\left[ \frac{d^2}{dr^2} - \mu V_{kk} + p_k^2 \right] Q_k(r) = \mu \sum_{j \neq k} Q_j(r) V_{kj}(x) \quad \dots\dots (29)$$

where  $V_{ij}(r) = \int \phi_i(x) V(x, r) \phi_j(x) dx$ .

Born's collision method is now used to obtain approximate solutions of (29); first the right hand side of (29) is put equal to zero and the zero-order solution,  $Q_k^{(0)}(r)$ , corresponding to elastic scattering is found. Then  $Q_k^{(0)}(r)$  is substituted on the right hand side and the equation solved again, to give the first order approximation,  $Q_k^{(1)}(r)$  which is the one used.

The remainder of Zener's treatment is purely mathematical. In order to obtain a relatively simple set of solutions of equation (29), he replaces the potential  $V_{kk} = E_0 \exp \{ -\alpha(r-r_0) \}$  by an inverse square law which fits the exponential function in the critical region where  $r \sim r_0$ . This enables the solution of (29) to be found in terms of Bessel functions and finally gives the transition probability for de-excitation of the first excited state of the  $j$ th level, of energy  $\epsilon_j$ ,

$$p_{j0} = |\gamma_{j0}^{(j)}|^2 = \frac{\pi^2}{16} \frac{\mu}{\mu_m} \frac{E_0}{\epsilon_j} \cdot \left( \frac{p_i}{p_f} \right)^{\sqrt{(uE_0)} \cdot 4/x} \quad \dots\dots (30)$$

If one writes  $E - E_i = K$ , the relative kinetic energy of the atom A relative to the molecule BC before impact, equation (27) gives

$$p_{j0} = \frac{\pi^2}{16} \frac{\mu}{\mu_m} \frac{E_0}{\epsilon_j} \left( \frac{K + U_0}{K + U_0 + \epsilon_j} \right)^{\sqrt{(uE)} \cdot 2/x} \quad \dots\dots (18)$$

Substitution of numerical values shows that this expression gives results which are of the correct order of magnitude. Taking A, B and C to be each of molecular weight 50,  $E_0 = kT$ ,  $K = U_0 = 3kT/2$ ,  $\epsilon_j = 3kT$  at 300° K. ( $\sim 625 \text{ cm}^{-1}$ ) then for  $\alpha$  equal to 2 and 3 in atomic units the corresponding values\* of  $p_{j0}$  are  $6.04 \times 10^{-3}$  and  $3.12 \times 10^{-2}$ .

*Note added in proof (8th January 1949).* The treatment of transition probabilities which is outlined in the appendix cannot be regarded as completely satisfactory in its application to liquids, as it is but a modification of the corresponding analysis for a gas. It would be better to use a quasi-crystalline model of a liquid, and work on this is proceeding.

## REFERENCES

- ALEXANDER, E. A., and LAMBERT, J. D., 1942, *Proc. Roy. Soc. A*, **179**, 499.  
 BAZULIN, P., 1936, *C.R. Acad. Sci. U.R.S.S. (Doklady)*, **3**, 285 ; 1937, *Ibid.*, **14**, 273.  
 BIQUARD, P., 1935, *Thesis*, Paris.  
 BOURGIN, D. G., 1936, *Phys. Rev.*, **50**, 355.  
 EINSTEIN, A., 1920, *Sitz. Ber. preuss. Akad. Wiss.*, 380.  
 EUCKEN, A., and BECKER, R., 1934, *Z. phys. Chem. B*, **27**, 235.  
 GLASSTONE, S., LAIDLER, K. J., and EYRING, H., 1941, *The Theory of Rate Processes* (New York : McGraw-Hill), Chap. I.  
 GROBE, H., 1938, *Phys. Z.*, **39**, 333.

\* Jackson and Mott (1932) have pointed out that there is a factor 4 missing in Zener's equation corresponding to equation (30) of this paper. This factor has been allowed for here.

- HALL, L., 1948, *Phys. Rev.*, **73**, 775.  
 HERZBERG, G., 1945, *Infra-red and Raman Spectra of Polyatomic Molecules* (New York : van Nostrand), Chap. 3.  
 HERZFELD, K. F., 1941, *J. Acoust. Soc. Amer.*, **13**, 33.  
 HERZFELD, K. F., and RICE, F. O., 1928, *Phys. Rev.*, **31**, 691.  
 JACKSON, J. M., and MOTT, N. F., 1932, *Proc. Roy. Soc. A*, **137**, 703.  
 KIRCHHOFF, G., 1868, *Pogg. Ann.*, **134**, 177.  
 KNESER, H. O., 1931, *Ann. Phys., Lpz.*, **11**, 761 ; 1938, *Ibid.*, **32**, 277.  
 KRONIG, R. DE L., 1938, *Phys. Z.*, **39**, 823.  
 LANDAU, L., and TELLER, E., 1936, *Phys. Z. Sowjet*, **10**, 34.  
 METTER, I. M., 1937, *Phys. Z. Sowjet*, **12**, 233.  
 PELLAM, J. R., and GALT, J. K., 1946, *J. Chem. Phys.*, **14**, 608.  
 PINKERTON, J. M. M., 1947, *Nature, Lond.*, **160**, 128 ; 1948, *Ibid.*, **162**, 106 ; 1949, *Proc. Phys. Soc. B*, **62**, 129.  
 RAPUANO, R. A., 1947, *Phys. Rev.*, **72**, 78.  
 RICHARDS, W. T., 1939, *Rev. Mod. Phys.*, **11**, 36.  
 RUTGERS, A. J., 1933, *Ann. Phys., Lpz.*, **16**, 350.  
 SCHUMANN, S. C., and ASTON, J. G., 1938, *J. Chem. Phys.*, **6**, 485.  
 SPAKOVSKIJ, B. J., 1938, *C.R. Acad. Sci. U.R.S.S. (Doklady)*, **18**, 173.  
 STOKES, G. G., 1845, *Trans. Camb. Phil. Soc.*, **8**, 287.  
 WILLARD, G. W., 1941, *J. Acoust. Soc. Amer.*, **12**, 438.  
 ZENER, C., 1931, *Phys. Rev.*, **37**, 556.

## Second Sound and the Behaviour of Helium II

By R. B. DINGLE\*

H. H. Wills Physical Laboratory, Royal Fort, Bristol

*Communicated by N. F. Mott; MS. received 21st August 1948, and in amended form 18th October 1948*

**ABSTRACT.** In this paper some theoretical consequences of the existence of second sound in helium II are discussed. A method is suggested for setting up a quantitative phenomenological description of the thermodynamical behaviour of helium II. It is known that expressions for the velocities of first and second sound may be obtained by using quite general models. The thermodynamical behaviour may be described in terms of the velocities of these two types of sound, so that it becomes possible, in principle, to obtain explicit values of the unknowns by combining the two sets of equations. On the basis of these ideas a discussion is given of the coefficient of thermal expansion of helium, the ordinary thermal conductivity, and the attenuation of second sound.

The paper contains a discussion of the modifications necessary to the Debye theory of specific heats when the sound velocities are temperature-dependent.

### §1. PREVIOUS THEORIES OF THE THERMODYNAMICAL BEHAVIOUR OF HELIUM II

IT is well known that liquid helium at very low temperatures possesses anomalous properties. At 2.19° K., the  $\lambda$ -point, a phase change of the second order takes place, and below this temperature the liquid, known as helium II, possesses properties rather similar in nature to those of superconductors. Details of these properties may be found in Keesom's book on helium (Keesom 1942). A particular property with which we shall be concerned in this paper is that below

\* Now at the Royal Society Mond Laboratory, Cambridge

the  $\lambda$ -point the values of the entropy and the specific heat of the liquid are very much larger than the values to be expected from Debye's theory (Debye 1912), calculated from the known values for the velocity of ordinary sound in the liquid. Theories have been suggested by several authors to account for these properties; we may mention in particular those of London (1938, 1939), Tisza (1938, 1940, 1947), Landau (1941), and Green (1948).

The ideas of London and Tisza are based on the concept of a Bose-Einstein condensation, a phenomenon predicted theoretically for an ideal gas (London 1938, 1939, Fowler and Jones 1938, Dingle 1949). According to this theory, below a certain very low temperature a fraction of the available atoms become condensed into the lowest available state. These authors believe that many of the peculiar properties of this ideal Bose-Einstein gas may be taken over into the theory of liquid helium. However, it must be stressed that the theory is only a qualitative one, since the values of the entropy as a function of temperature given by ideal gas theory are too inaccurate to be of value, the entropy being given as proportional to  $T^{1.5}$  as opposed to the experimental relation  $S \propto T^{5.5}$ . In order to obtain reasonable agreement with experiment, the model must be altered in an empirical manner.

Landau's general theory of helium (Landau 1941) is based on his quantum hydrodynamics, which is an attempt in quantum theory to avoid the difficulties of a complete microscopic theory of fluids in a similar way to that in which they are avoided by classical hydrodynamics. Landau concludes that only discrete values of the curl of the velocity are permitted, and that there will be a gap in the energy spectrum associated with these "roton" excitations. The entropy will be contributed by ordinary Debye waves (phonons) and by these rotons. The phonon contributions are calculated in the usual manner. In order to derive the roton contributions, Landau assumes that only the first gap in the roton energy spectrum is of importance, and the excited levels are replaced by a continuum for which the energy  $\epsilon$  is given by  $\epsilon = \Delta + p^2/2\mu$ , where  $\Delta$  is the energy gap,  $p$  the momentum, and  $\mu$  the effective mass of a roton. Thus in Landau's theory we have still two arbitrary parameters  $\Delta$  and  $\mu$ , which must be fixed by appeal to experiment.\*

The very recent work of Green (1948) is based on the general kinetic theory of liquids developed by himself and Born (Born and Green 1946, 1947a, b, Green 1947, 1948). On quantization it appears that pressure defined thermodynamically is no longer identical with pressure defined by kinetic theory. Green believes that many of the peculiar properties of liquid helium may be explained as due to this difference. Unfortunately, the detailed theory proves too complicated for direct application, and Green's results (e.g. the magnitude of this pressure difference) have in fact to be derived from experiment rather than from theory.

## § 2. QUALITATIVE DISCUSSION OF THE THEORY PROPOSED

The London-Tisza model, based on the concept of Bose-Einstein condensation, and the Landau theory, based on quantum hydrodynamics, agree both between themselves and with experiment in so far as the helium II is considered rather as a mixture of normal fluid and superfluid. On the London-Tisza model, the superfluid is supposed to consist of atoms which have piled up in the ground state, due to

\* In a recent variant of the theory there are three parameters (Landau 1947).



some kind of Bose-Einstein condensation, and the normal fluid to consist of the remaining atoms, i.e. those in the excited states. On the Landau theory, the superfluid is likewise made up of atoms in the ground state, whilst the normal fluid is described by excitations of Debye waves (phonons) and excitations of vortices (rotons). In both theories the entropy of the superfluid is of order zero, since only atoms in the ground state are involved. Tisza and Landau have shown independently that in a fluid of this nature we should expect two types of sound: ordinary "first" sound caused by the movement of the normal and superfluid together, and a new type, "second" sound, caused by relative movement of normal and superfluid. In second sound, owing to the relative movement of normal fluid, which carries entropy, and superfluid, which does not, we obtain a state of the liquid such that alternate layers contain an excess or a deficit of entropy. It follows that these layers are respectively at an effectively higher and lower temperature. The most important difference between the two types of sound is that the dominating feature in first sound is fluctuation in pressure, whilst in second sound it is fluctuation in temperature. Similar conclusions have also been reached by Green (1948).

On two-fluid types of model, the velocity  $u_2$  of second sound is given by  $u_2^2 = TS^2\rho_s/C\rho_n$ , where  $T$  is the temperature,  $S$  the entropy per gramme,  $C$  the specific heat per gramme and  $\rho_s/\rho_n$  the ratio of the densities of superfluid and normal fluid. In previous theories, more specialized models, or empirical formulae, have been used to calculate the values of  $S$ ,  $C$  and  $\rho_s/\rho_n$ , and hence of  $u_2$  as a function of temperature. In this paper we suggest a method by which these special models may be avoided. The argument is that a quantitative thermodynamical description of helium II may be given in terms of the velocities of the two kinds of sound by employing an extension of Debye's theory of specific heat: this gives us the values of  $S$ ,  $C$  and  $\rho_s/\rho_n$  in terms of  $u_2$ , assuming that these two types of sound provide the dominant contributions to the thermal energy. In principle we have only to combine these equations with that giving  $u_2$  in terms of the thermodynamical quantities to enable us to determine all the unknowns. In practice it will be much easier to show that the experimental values of  $u_2$  are consistent with both sets of equations.

We shall encounter three main difficulties. Firstly, we know that there are  $3N$  degrees of freedom per unit volume, where  $N$  is the number of atoms per unit volume. Thus there are  $3N$  normal independent modes of vibration per unit volume: our problem is that of allocating these between first and second sound. A similar difficulty arises in the usual Debye theory, namely the question of the allocation of the available modes between longitudinal and transverse waves. Here some authors have made the arbitrary assumption that the frequency limits of the two types of waves may be taken to be the same; Brillouin (1936) and Lucas (1937) have shown that the assumption of equal wavelength limits is probably preferable. In our case this difficulty is not serious, as we shall find that second sound contributions are of overwhelming importance in the temperature region so far investigated.

Secondly, the usual Debye theory giving the thermodynamical behaviour in terms of the velocities of sound is only valid if these velocities are independent of temperature, the substance being at constant volume. This condition is roughly satisfied for first sound, but not for second sound, particularly near the  $\lambda$ -point. We shall discuss this problem in §§ 8 and 9 of this paper.

The third difficulty is that of determining how to take into account the absorption and dispersion of sound waves, as it is known that these effects become important as the  $\lambda$ -point is approached.

### § 3. THE DEBYE THEORY

Debye (1912) considers that in solids (and liquids) waves of sound will be present continually, the frequencies represented being those up to a certain limit dictated by the atomic structure of the material. This upper limit may be calculated from the fact that a real solid (or liquid) has only a finite number of degrees of freedom, so that we must cut off the upper end of the frequency spectrum to make the theory correspond. Physically, this corresponds to the idea that if the wavelength of the supposed Debye waves were shorter than the interatomic distance, the vibrations of shorter wavelength would not be independent of those of longer wavelength, since it is always possible to represent displacements of a finite number of particles equally well by an infinite number of vibrations of wavelength shorter than the interatomic distance.

For a single sound velocity  $c$ , independent of temperature, the Debye theory yields the following values for the thermodynamical quantities in which we are interested (see § 8):

$$\frac{E}{T} = 9R \left( \frac{T}{\theta} \right)^3 \int_0^{\theta/T} \frac{x^3 dx}{e^x - 1}, \quad \dots\dots(1)$$

$$S = 3R \left[ 4 \left( \frac{T}{\theta} \right)^3 \int_0^{\theta/T} \frac{x^3 dx}{e^x - 1} - \ln(1 - e^{-\theta/T}) \right], \quad \dots\dots(2)$$

$$C = 9R \left[ 4 \left( \frac{T}{\theta} \right)^3 \int_0^{\theta/T} \frac{x^3 dx}{e^x - 1} - \frac{\theta/T}{e^{\theta/T} - 1} \right], \quad \dots\dots(3)$$

where here  $C$  is the specific heat (at constant volume) per molecular volume.  $\theta$  is the Debye characteristic temperature given by the relation

$$k\theta = c(9N\hbar^3/4\pi)^{1/3}. \quad \dots\dots(4)$$

At sufficiently low temperatures,  $T \ll \theta$ , we may use the simpler expressions

$$E/T = 9R(T/\theta)^3 \pi^4/15, \quad \dots\dots(5)$$

$$S = 12R(T/\theta)^3 \pi^4/15, \quad \dots\dots(6)$$

$$C = 36R(T/\theta)^3 \pi^4/15. \quad \dots\dots(7)$$

### § 4. THE APPLICATION OF THE DEBYE THEORY

The formal theory quoted in the last section refers to the case of a single type of sound wave of constant velocity  $c$ . This differs from our case in two respects:

(a) It is an experimental fact that with decrease in temperature below the  $\lambda$ -point the velocity of first sound rises steadily with temperature,\* and that of second sound rises rapidly from zero at the  $\lambda$ -point to a value which may be considered as roughly constant † between 2.0° K. and 1.03° K., the lowest temperature for which it has been measured. For a preliminary discussion we shall apply the results of the Debye theory as given above, replacing the temperature-dependent

\* Since the coefficient of expansion of helium II is both very small and negative, this holds for constant volume as well as for the measured results at constant pressure.

† More accurately, there is a very flat maximum in the curve of velocity against temperature at about 1.6° K. and a minimum at 1.12° K.

sound velocities by mean values. In §§ 8 and 9 of this paper a detailed treatment of this problem will be given; this yields information on the possible shape of the curve of second sound velocity against temperature.

(b) The results of the last section have been given for the case of a single type of sound wave of velocity  $c$ . In our case we have two types of sound: first sound of velocity  $u_1$ , and second sound of velocity  $u_2$ . The question to be decided is that of allocating the  $3N$  modes of vibration available. We may discuss the following simplifying assumptions: (i) The frequency limits are taken to be the same, in which case we may introduce a mean velocity  $c$  defined by the relation  $1/c^3 = 1/u_1^3 + 1/u_2^3$ , and then apply the theory given above without further alteration. We are assuming here that only longitudinal waves may pass through the liquid. (ii) The wavelength limits are taken to be the same, in which case we must take the frequency limits as proportional to the respective velocities. To preserve the total number of normal modes at  $3N$ , we must take the frequency limits as  $\nu_1 = (9N/8\pi)^{1/3}u_1$  and  $\nu_2 = (9N/8\pi)^{1/3}u_2$ . We then consider the contributions from the two types of sound separately. In the known temperature region, where  $u_2 \sim u_1/13$ , the effects of first sound may be neglected, so that assumptions (i) and (ii) give the same result.

There is also a third possibility, which arises in the following way. In first sound our frequency limits are really connected with the point at which the concept of hydrodynamic flow becomes meaningless; this limit will be determined by the condition that the wavelength becomes of the order of magnitude of the interatomic distance. In second sound our frequency limit is determined by the breakdown of the concept of relative hydrodynamic flow between the superfluid and the normal fluid. This breakdown will occur when the wavelength is of the order of magnitude of the mean distance between superfluid atoms if these are in the minority, or between normal atoms if these are in the minority. We may then show that the characteristic temperature must be proportional to  $(\rho_s/\rho)^{1/3}$  or to  $(\rho_n/\rho)^{1/3}$ , whichever is the smaller at the temperature considered. An objection to this argument must be raised. When we speak of a normal or a superfluid atom, we must remember that the chosen atom will remain "normal" or "superfluid" for a time of the order of the relaxation time between different energy states. If the relaxation time involved were much shorter than the reciprocal of the frequency of sound concerned, the above argument breaks down, as superfluid and normal atoms constantly interchange, so that we again become interested in the much more slowly varying mean distance between atoms, regardless of the energy levels which they occupy.

## § 5. COMPARISON WITH EXPERIMENT

A formally complete description of the thermodynamical behaviour of helium II should be given by the combination of the following equations. (The effects of first sound will be neglected, a procedure justified in the temperature region so far investigated.)

(1) The equation  $u_2^2 = TS^2\rho_s/C\rho_n = (1 - \rho/\rho_n)/d(1/S)/dT$ .

(2) Equation (2) of § 3, or more accurately equation (11) of § 9, giving  $S$  in terms of  $u_2$ .

(3) The equation  $\rho_n/\rho = 4E/3u_2^2$  (or more accurately equation (14) of § 9), an extension of an equation due to Landau (1941).

We have now sufficient equations to eliminate the unknowns—at least in principle. However, as has been remarked previously, it is much simpler to take the experimental values of  $u_2$  or, alternatively, trial values, and check that they are consistent with these three equations and with the experimental values of the entropy.

First, it is instructive to calculate the entropy taking only first sound effects into account—i.e. to find the Debye entropy calculated according to previous theories. It is known that the velocity of first sound in helium II is about 240 metres per second, and that the molecular volume is  $27.6 \text{ cm}^3$ . From these we deduce\* the value  $\theta_1 \sim 29^\circ \text{ K.}$  from the relation  $\theta_1 = \hbar v_m / k = \hbar u_1 (9N/4\pi)^{1/3}$ . This value of the Debye characteristic temperature is so much higher than the temperatures in which we are interested that we may use the simple formulae valid in the  $T^3$  region. The value of the entropy derived is  $1.8 \times 10^{-3} T^3 \text{ cal/gm.}$ , which is to be compared with the experimental relation  $S = 0.405 \times (T/T_0)^{5.5} \text{ cal/gm.}$ ,  $T_0$  being the temperature of the  $\lambda$ -point. Thus near the  $\lambda$ -point the experimental value of the specific heat ( $T dS/dT$ ) is roughly 40 times the value calculated from the usual Debye theory, taking only first sound into account.

Let us now introduce second sound. At first sight it might appear that since  $C \sim 1/c^3$  (in the  $T^3$  region) and  $u_2 \sim u_1/13$ , second sound would contribute a specific heat about two thousand times as large as that of first sound. This is not so, because the introduction of second sound effects causes us to pass right out of the  $T^3$  region for all except the very lowest temperatures. This may be seen from the relation  $\theta \propto c$ , showing that  $\theta_2 \sim \theta_1/13 \sim 2.2^\circ \text{ K.}$ , so that  $\theta_2$  is of the same order of magnitude as the temperatures we wish to consider. For instance, to take a very simple case, the energy is proportional to the integral  $\int_0^{\theta/T} x^3 dx / (e^x - 1)$ . When  $\theta/T \gg 1$  (i.e. in the  $T^3$  region), this has the value 6.45, but when  $\theta/T = 1$ , say, it takes the value 0.224. Thus instead of second sound effects giving an energy approximately 2,000 times that previously calculated (assuming only first sound), it provides a contribution approximately 70 times as large. The other thermodynamical quantities are cut down in a similar way.

An experimental fact that is particularly interesting is that the specific heat just above the  $\lambda$ -point is unduly high, so much so that the slope of the curve of specific heat against temperature is negative. This may well imply that it is possible to transmit hypersonic waves of second sound at temperatures just above the  $\lambda$ -point; it may also be possible to transmit waves of attainable frequencies.

## § 6. THE THERMAL EXPANSION OF HELIUM II

Generally speaking, solids and liquids have a positive coefficient of thermal expansion. We wish to explain why the coefficient of thermal expansion of helium II is very small and negative in sign, whilst that of helium I is of normal magnitude and of normal (positive) sign. First we must find a quantitative relation between the coefficient of thermal expansion,  $\alpha$ , say, and  $\theta$ , the characteristic temperature. For the present we shall make the usual assumption that  $\theta$

\* Tisza (1947) has given the value  $18^\circ \text{ K.}$ , but we are unable to see how he arrives at this result. We also cannot agree with his criticism of Pickard and Simon's (1939) experimental value of  $\theta$ , since the formulae for the specific heat, etc., given in terms of  $\theta$  are completely independent of theoretical speculations concerning the existence or non-existence of transverse waves in liquids, these all being collected in the connection between  $\theta$  and the velocity of sound.

depends only on volume—i.e.  $\theta = \theta(V)$ . Referring back to (2), we see that the entropy is a function of  $T/\theta(V)$ . Thus  $S = S(T/\theta(V))$ , so that

$$\left(\frac{\partial S}{\partial T}\right)_V = \frac{S'}{\theta} \quad \text{and} \quad \left(\frac{\partial S}{\partial V}\right)_T = -\frac{S'T}{\theta^2} \left(\frac{\partial \theta}{\partial V}\right)_T,$$

where  $S'$  is the differential coefficient of  $S$  with respect to the variable  $T/\theta$ . Eliminating  $S'$ , we have

$$\left(\frac{\partial S}{\partial V}\right)_T = -\left(\frac{T}{\theta}\right) \left(\frac{\partial \theta}{\partial V}\right)_T \left(\frac{\partial S}{\partial T}\right)_V.$$

Applying the Maxwell thermodynamic relationship  $(\partial S/\partial V)_T = (\partial p/\partial T)_V$  and the relation  $C = T(\partial S/\partial T)_V$  for the specific heat at constant volume, we obtain

$$\left(\frac{\partial p}{\partial T}\right)_V = -\frac{1}{\theta} \left(\frac{\partial \theta}{\partial V}\right)_T C = -\frac{\gamma C}{V},$$

where  $\gamma = (\partial \ln \theta / \partial \ln V)_T$  and  $V$  is the molecular volume. Now since

$$dp = \left(\frac{\partial p}{\partial T}\right)_V dT + \left(\frac{\partial p}{\partial V}\right)_T dV,$$

we see that

$$\left(\frac{\partial p}{\partial T}\right)_V = -\left(\frac{\partial V}{\partial T}\right)_p \left(\frac{\partial p}{\partial V}\right)_T = \frac{\alpha}{\chi},$$

where  $\alpha$  is the coefficient of thermal expansion and  $\chi$  is the isothermal compressibility. Thus  $\alpha = -\gamma C \chi / V$ .

To sufficient accuracy we may treat  $\chi$  and  $V$  as independent of temperature. It is worth noting that since  $\alpha$  is proportional to  $C$ , the coefficient of expansion will have a peak value at the  $\lambda$ -point, and will fall to zero at very low temperatures.

The sign of the coefficient of expansion will be the same as the sign of  $-\gamma$ , i.e. the sign of  $(-\partial c/\partial V)_T$ , where  $c$  is the velocity of the hypersonic waves concerned. Above the  $\lambda$ -point we take  $c = u_1$ , the velocity of first sound; below the  $\lambda$ -point we may take with sufficient accuracy  $c = u_2$ , the velocity of second sound. In order to account for the observed behaviour of the expansion coefficient of helium, we must explain two points: (i) why  $(\partial u_1/\partial V)_T$  above the  $\lambda$ -point is negative; (ii) why  $(\partial u_2/\partial V)_T$  below the  $\lambda$ -point is very small and positive.

To explain (i) we recall the relation  $u_1^2 = \chi^* / \rho$ , where  $\chi^*$  is the adiabatic compressibility and  $\rho$  the density. Assuming the existence of short range forces,  $\chi^*$  must depend on volume much more sensitively than  $\rho$ , so that the ratio will decrease with increase in volume.

To account for (ii), which has recently been checked experimentally, we recall the relation  $u_2^2 = (1 - \rho/\rho_n) d(1/S)/dT$ . It is unlikely that either the fraction of normal fluid  $\rho_n/\rho$  or the entropy per unit mass would be sensitive to volume changes, so that a very small value of  $(\partial u_2/\partial V)_T$  is to be expected. Quantitatively, we may investigate the magnitude of  $(\partial u_2/\partial V)_T$  by finding a relation between the change in velocity due to alterations in volume and the change in velocity due to variations in temperature. Let us write  $f = u_2/T^{\frac{1}{2}} = (S^2 \rho_n / C \rho_n)^{\frac{1}{2}}$ , so that  $f$  depends only on the quantities which will be given by a theory of the Debye type,  $f = f(T/\theta)$ . The  $\lambda$ -point  $T_0$  is given by the condition that all atoms are normal, i.e. by  $\rho_n(T_0) = \rho$ . We have seen that  $\rho_n \propto E/u_2^2$ . Hence  $T_0$  will be given linearly in terms of  $\theta$ , and, therefore,  $f = f(T/T_0)$ . Thus  $(\partial f/\partial T_0) = -(T/T_0)(\partial f/\partial T)$  and hence

$$\left(\frac{\partial f}{\partial V}\right)_T = -\frac{T}{V} \left(\frac{d \ln T_0}{d \ln V}\right)_T \left(\frac{\partial f}{\partial T}\right)_V.$$

The slope of the  $\lambda$ -line in the  $p, T$  diagram of helium is negative, so that  $(d \ln T_0 / d \ln V)_T$  is positive, although very small. The sign of  $(\partial f / \partial T)_v$ , i.e. the slope of the curve of  $u_2 / T^{\frac{1}{2}}$  against temperature, is found to be negative in the temperature region so far investigated. Hence  $(\partial u_2 / \partial V)_T = T^{\frac{1}{2}} (\partial f / \partial V)_T$  will be very small and positive, as required to explain (ii). In principle, this argument might be extended by the methods of § 5, so as to become independent of experimental values of velocity.

#### § 7. THE ORDINARY THERMAL CONDUCTIVITY AND THE ATTENUATION OF SECOND SOUND

Debye (1914) and Brillouin (1914, 1920) have suggested a theory giving the coefficient of thermal conductivity of solids (and liquids) in terms of the velocity and attenuation of the hypersonic waves of sound supposed present. The theory is analogous to the well-known one for the thermal conductivity of a gas, i.e. that leading to the result  $K = \frac{1}{3} m C n l c$ , where  $m$  is the mass of a gas molecule,  $n$  the number of gas molecules per unit volume,  $C$  the specific heat per gramme,  $l$  the mean free path of a molecule and  $c$  the mean velocity of the molecules.  $(m C n \delta T)$  is the heat transported across a temperature difference  $\delta T$  by the molecules contained in a unit volume; the analogous quantity in the wave picture of a solid or liquid will be

$$\frac{\partial}{\partial T} \left( \frac{4\pi\nu^2}{c^3} \frac{h\nu}{\exp(h\nu/kT) - 1} \right) \delta T$$

per unit frequency range, since the bracketed expression is the thermal energy per unit volume at temperature  $T$ . In the wave picture  $l$  will now refer to the mean free path of a wave—i.e. to the reciprocal of the attenuation coefficient of the sound waves concerned, and  $c$  will refer to the mean velocity of these waves. Integrating over all frequencies, we find for the coefficient of thermal conductivity the expression

$$K = \frac{1}{3} c \int_0^{\nu_m} l \frac{\partial}{\partial T} \left( \frac{4\pi\nu^2}{c^3} \frac{h\nu}{\exp(h\nu/kT) - 1} \right) d\nu.$$

For the ideal case in which  $c$ ,  $\nu_m$  and  $l$  are independent of temperature this reduces to

$$K = \frac{1}{3} c l \frac{\partial}{\partial T} \int_0^{\nu_m} \frac{4\pi\nu^2}{c^3} \frac{h\nu}{\exp(h\nu/kT) - 1} d\nu = \frac{1}{3} \rho c l C,$$

where  $C$  is the specific heat per unit mass. This ideal relation is the same for solids, liquids and gases, provided the symbols are interpreted in the appropriate manner.

For the case of liquid helium we have  $K = \frac{1}{3} \rho (l_1 u_1 C_1 + l_2 u_2 C_2)$ , where  $C_1$  and  $C_2$  are the contributions to the specific heat from first and second sound respectively. As we have seen, below the  $\lambda$ -point  $u_2 C_2 \gg u_1 C_1$ , whilst above  $u_2 C_2 = 0$ , so that we have

$$K \simeq \frac{1}{3} \rho l_2 u_2 C(T) \text{ for } 0 < T < \lambda\text{-point}, \quad K = \frac{1}{3} \rho l_1 u_1 C(T) \text{ for } T > \lambda\text{-point}.$$

The value of the product  $u C$  does not vary by more than an order of magnitude for liquid helium over the greater part of its temperature range. This is due to a series of compensating effects. For instance, the large value of the specific heat just below the  $\lambda$ -point is compensated by a fall in the velocity of second sound, and the change over to the value of the velocity of first sound is compensated by the fact that the specific heat just above the  $\lambda$ -point is much smaller than that just below it. Thus any striking variation in  $K$  would be due to a change in the attenuation.

We must stress the fact that  $K$  is the ordinary thermal conductivity, i.e. the heat flux per unit temperature gradient. As has been shown (Dingle 1948), a finite value for  $K$  will result in absorption of second sound by irreversible processes. If we assume that the attenuation due to this cause is of prime importance, we may find  $l$  and  $K$  explicitly by combining the results of this section with a result of the previous paper, i.e.  $l_2 = 2u_2^3 \rho C / K \omega^2$ , where  $u_2$ ,  $\rho$ ,  $C$  and  $K$  refer respectively to the velocity of second sound, the fluid density, the specific heat per unit mass and the ordinary conductivity, and  $\omega/2\pi$  is the frequency. This expression shows that the mean free path is in fact a function of the frequency  $\nu$ . Strictly speaking, therefore, we are unable to use the simplified expressions giving  $K$  in terms of  $l$ , except for rough estimates. We may show very simply that the theory gives reasonable value for  $K$  and  $l$ . The minimum free path  $l_{\min}$  will be that for the waves of highest frequency  $\nu_m$ . Thus

$$l_{\min} \sim 8\pi^2 u_2^3 \rho C / K \nu_m^2 \quad \text{and} \quad K \sim \frac{1}{3} \rho l_{\min} u_2 C$$

giving 
$$K \sim (8\pi^2/3)^{\frac{1}{2}} \rho u_2^2 C / \nu_m = (8\pi^2/3)^{\frac{1}{2}} h \rho u_2^2 C / k \theta,$$

and 
$$l_{\min} \sim (24)^{\frac{1}{2}} \pi u_2 / \nu_m = (24)^{\frac{1}{2}} h u_2 / k \theta.$$

Numerically,  $l_{\min} \sim 7 \times 10^{-7}$  cm. at  $1.5^\circ$  K. This is a satisfactory value, showing that the minimum free path is of the order of twenty interatomic distances. A smaller value would have shown that the maximum frequency of vibration is dictated not by the number of normal modes available, but by absorption effects.

We may proceed further and determine the approximate mean free path of second sound waves of attainable frequencies. Since  $l(\nu) \propto 1/\nu^2$  for a given temperature, we have  $l(\nu) \sim 7 \times 10^{-7} (\nu_m/\nu)^2$  at  $1.5^\circ$  K., where  $\nu_m \sim 4 \times 10^{10}$  cycles per second.

#### § 8. THE DEBYE THEORY AND THE NECESSITY FOR MODIFICATION

In this section we wish to show that the use of the ordinary Debye theory is not justified if the sound velocities (at constant volume) vary with temperature.

The number of independent modes of vibration per unit volume is known to be  $4\pi\nu^2/c^3$  per unit frequency range, where  $c$  is a velocity of sound. We shall find it convenient to rewrite this expression. Let  $p$  be the momentum of a wave, then the energy is given by  $\epsilon = pc = h\nu$ , so that the number of modes per unit volume is given by  $4\pi p^2/h^3$  per unit momentum range. The upper limit to this momentum,  $p_m$  say, is given by the consideration that the number of modes per unit volume is  $3N$ , where  $N$  is the number of atoms per unit volume. Thus  $3N = (4\pi/h^3) \int_0^{p_m} p^2 dp$ , and hence  $p_m = (9N h^3/4\pi)^{\frac{1}{3}}$ . Therefore  $p_m$  is independent of temperature. However, the energy of each wave of given momentum,  $\epsilon = pc$ , may not be constant, since the velocity  $c$  may vary with temperature. Supposing for the present that this variation of the velocity is negligible, we have for the partition function  $Z = \prod_i \{1 - \exp(p_i c/kT)\}^{-1}$ , where  $p_i$  are the allowed momenta, this being the well known result valid for a set of oscillators with no restriction either on the number of quanta allowed per oscillator or the number allowed per energy level.

We may proceed in two ways: either we may work out the free energy  $A = -kT \ln Z$  and from this the thermodynamic quantities, or else we may find the mean occupation numbers  $\bar{n}_i$  from the relation  $\bar{n}_i = x_i \partial \ln Z / \partial x_i$ , where

$z_i = \exp(-p_i c / kT)$ , and from these the mean energy, and hence, by differentiation, the specific heat. Using the former method, and still supposing the temperature variation of the velocity to be negligible, we have

$$A = -kT \ln Z = kT \sum_i \ln \{1 - \exp(-p_i c / kT)\} \\ = kT \frac{4\pi}{h^3} \int_0^{p_m} p^2 dp \ln \{1 - \exp(-pc / kT)\}.$$

Introducing the Debye characteristic temperature  $\theta$  by the relation  $k\theta = p_m c$ , we obtain

$$\frac{A}{T} = 9R \left(\frac{T}{\theta}\right)^3 \int_0^{\theta/T} x^2 dx \ln(1 - e^{-x}) = 3R \left[ \ln(1 - e^{-\theta/T}) - \left(\frac{T}{\theta}\right)^3 \int_0^{\theta/T} \frac{x^3 dx}{e^x - 1} \right] \\ \dots\dots (8)$$

per molecular volume. Using the well-known thermodynamic formulae for the entropy  $S$ , the energy  $E$ , and the specific heat  $C$ , viz.  $S = (E - A)/T = -(\partial A / \partial T)_V$  and  $E = -T^2 [\partial(A/T) / \partial T]_V$  (from the Gibbs-Helmholtz equation), and

$$C = -T(\partial^2 A / \partial T^2)_V = \partial E / \partial T,$$

we deduce equations (1), (2) and (3) of § 3.

Combining (8) with the relationship  $p = -(\partial A / \partial V)_T$ , we find the equation of state

$$p + dW/dV = -E[\partial \ln \theta / \partial V]_T, \quad \dots\dots (9)$$

where  $W$  is the energy at the absolute zero.

Using the second method, that involving occupation numbers, we have

$$\bar{n}_i = z_i \partial \ln Z / \partial z_i = 1 / \{\exp(p_i c / kT) - 1\},$$

so that  $\epsilon_i = p_i c / \{\exp(p_i c / kT) - 1\}$ , and, therefore,

$$E = \frac{4\pi}{h^3} \int_0^{p_m} \frac{(pc)p^2 dp}{\exp(pc / kT) - 1} = 9RT \left(\frac{T}{\theta}\right)^3 \int_0^{\theta/T} \frac{x^3 dx}{e^x - 1},$$

which is the same as the expression deduced by the first method. It is clear, however, that the two methods would yield quite different results if we took into account the variation of the velocity with temperature, for then the value of  $E$  given by the second method would be unchanged, since no differentiations with respect to temperature are involved, whilst the energy derived by the first method would be different.

#### § 9. TEMPERATURE-DEPENDENT DISTRIBUTIONS OF ENERGY LEVELS

The difficulty pointed out in § 8 is caused by the fact that the energy levels which we are considering are themselves functions of temperature. This may be seen from the energy relation  $\epsilon = pc$ , where  $p$  may be considered as independent of temperature, since we must integrate over all values of  $p$  up to a maximum value  $p_m$  which is independent of temperature. The concept of temperature-dependent energy levels arises only because of the difficulties of a complete treatment by the methods of statistical mechanics. If we included in the partition function every possible arrangement of the system, temperature-dependent energy levels would never arise. However, in many problems which are treated approximately, temperature-dependent energy levels are bound to be the rule. It is known in several special cases in classical statistical mechanics (or rather quantum statistical mechanics at higher temperatures) that the correct procedure is to replace the



energies in the exponential terms by free energies. Rushbrooke (1940) has considered this problem in more detail, and has pointed out that we obtain agreement between statistical mechanics and thermodynamics by this procedure in any case in which, in the notation of his paper,  $\bar{N} = \lambda(\partial/\partial\lambda) \ln G(\lambda\theta^e)$  and  $\bar{E} = \theta(\partial/\partial\theta) \ln G(\lambda\theta^e)$ , where  $\ln \theta = -1/kT$  and  $G$  is a generating function:  $\lambda$  is found by equating the sums of terms such as  $\bar{N}$  to the total number of systems in the assembly, and  $\theta$  by equating the sum of terms such as  $\bar{E}$  to the total energy of the assembly. This is equivalent to the statement that the procedure of replacing the energy by the free energy in the exponential terms is justified for all cases in which the method of steepest descents is applicable to the contour integral appearing in the evaluation of the partition function. That the procedure is one of great generality is shown by the following demonstration.

In the customary theory, the partition function is taken to be

$$Z = \sum \exp [-\sum_i n_i \epsilon_i / kT],$$

where the  $\epsilon_i$  designate the energy levels and  $n_i$  the occupation numbers. The outer summation is carried out over all possible configurations (e.g. in the case of a fixed number of particles,  $N$  say, this is subject to the condition that  $\sum_i n_i = N$ ), and the inner summation according to all configurations consistent with the particular statistics employed. Let us replace this formally by  $Z = \sum \exp [-\sum_i n_i f_i / kT]$ . From the Gibbs-Helmholtz equation  $A - E = T(\partial A / \partial T)_V$ , where  $A$  is the free energy, we obtain  $E = -T^2[\partial(A/T) / \partial T]_V$ . By definition,  $A = -kT \ln Z$ , so that

$$E = kT^2 \left( \frac{\partial \ln Z}{\partial T} \right)_V = \frac{\sum [\sum_i n_i \{f_i - T(\partial f_i / \partial T)_V\}] \exp [-\sum_i n_i f_i / kT]}{\sum \exp [-\sum_i n_i f_i / kT]}.$$

Clearly we must have 
$$E = \frac{\sum [\sum_i n_i \epsilon_i] \exp [-\sum_i n_i f_i / kT]}{\sum \exp [-\sum_i n_i f_i / kT]},$$

since  $E$  is merely the energy of each configuration,  $\sum_i n_i \epsilon_i$ , averaged over all possible configurations. Hence, in general,

$$\epsilon_i = f_i - T(\partial f_i / \partial T)_V$$

which is the Gibbs-Helmholtz equation for the energy levels, provided the  $f_i$  are interpreted as free energies.

This result may easily be confirmed for the particular partition function in which we are interested, i.e.  $Z = \prod_i \{1 - \exp(-f_i / kT)\}^{-1}$ .

The effective free energy of a sound wave may be found from the expression  $\epsilon = pc(T)$ . From the Gibbs-Helmholtz equation,  $f - T(\partial f / \partial T)_V = \epsilon$ , we have  $[\partial(f/T) / \partial T]_V = \epsilon / T^2$  and thus  $f = T \int_T^{T_0} (\epsilon / T^2) dT$ , where the upper limit  $T_0$  is left undefined. In the sequel we shall simply write  $c$  for  $[c(T)]_V$ .

We take for the logarithm of the partition function the expression

$$\ln Z = -\frac{4\pi}{h^3} \int_0^{p_m} p^2 dp \ln \left[ 1 - \exp \left\{ -\frac{p}{k} \int_T^{T_0} (c/T^2) dT \right\} \right],$$

where  $p_m = h(9N/4\pi)^{1/3}$ . For convenience we put  $x = (p/k) \int_T^{T_0} (c/T^2) dT$ , so that  $x_m = \frac{h}{k} \left( \frac{9N}{4\pi} \right)^{1/3} \int_T^{T_0} \frac{c}{T^2} dT$ . Then  $\ln Z = -\frac{9N}{x_m^3} \int_0^{x_m} x^2 dx \ln(1 - e^{-x})$  and thus

$$\frac{A}{T} = -k \ln Z = \frac{9R}{x_m^3} \int_0^{x_m} x^2 dx \ln(1 - e^{-x}) = 3R \left[ \ln(1 - e^{-x_m}) - \frac{1}{x_m^3} \int_0^{x_m} \frac{x^3 dx}{e^x - 1} \right] \quad \dots\dots(9)$$

per molecular volume. The energy  $E$  may be obtained either directly, thus

$$E = \frac{4\pi}{h^3} \int_0^{p_m} \frac{(pc)p^2 dp}{\exp[(p/k) \int_T^{T_0} (c/T^2) dT] - 1} = \frac{9Rc}{\int_T^{T_0} (c/T^2) dT} \frac{1}{x_m^3} \int_0^{x_m} \frac{x^3 dx}{e^x - 1}, \quad \dots\dots(10)$$

or from  $A/T$  by differentiation, noting that

$$\frac{1}{x_m} \frac{\partial x_m}{\partial T} = - \frac{c/T^2}{\int_T^{T_0} (c/T^2) dT}.$$

The solutions given by the two methods now agree.

The entropy may be found either by using the thermodynamic definition  $A = E - TS$ , giving

$$\frac{E - A}{T} = 3R \left[ \ln(1 - e^{-x_m}) + \frac{1}{x_m^3} \int_0^{x_m} \frac{x^3 dx}{e^x - 1} \left\{ 1 + \frac{3c}{T \int_T^{T_0} (c/T^2) dT} \right\} \right] \quad \dots\dots(11)$$

or from the thermodynamic formula  $S = -(\partial A / \partial T)_V$ . There is no need to verify that we obtain the same result, since by elimination of  $S$  between these two expressions, i.e.  $S = (E - A)/T = -(\partial A / \partial T)_V$ , we return to the Gibbs-Helmholtz equation which was used in the derivation of the energy: the two values of  $S$  are therefore bound to be identical. Finally, the specific heat  $C$  may be found either by differentiation of the energy, or of the entropy, i.e.  $C = \partial E / \partial T = T(\partial S / \partial T)_V$ . By either method we obtain

$$C = 9R \left[ \frac{1}{x_m^3} \int_0^{x_m} \frac{x^2 dx}{e^x - 1} \left\{ 4 \left( \frac{c}{T \int_T^{T_0} (c/T^2) dT} \right)^2 + \frac{\partial c / \partial T}{\int_T^{T_0} (c/T^2) dT} \right\} - \left( \frac{c}{T \int_T^{T_0} (c/T^2) dT} \right)^2 \left( \frac{x_m}{e^{x_m} - 1} \right) \right] \quad \dots\dots(12)$$

In a similar way, we may show that the equation of state is now

$$p + \frac{dW}{dV} = -E \left( \frac{\partial \ln x_m}{\partial V} \right)_T \frac{T \int_T^{T_0} (c/T^2) dT}{c} \quad \dots\dots(13)$$

and that the equation  $\rho_n / \rho$  should now read

$$\rho_n / \rho = \frac{4}{3} \frac{E}{cT \int_T^{T_0} (c/T^2) dT} \quad \dots\dots(14)$$

The theory given above leaves undetermined the upper limit  $T_0$  of the integrals involved. In our case three choices might be made: (i)  $T_0 = 0^\circ \text{K.}$ ; in this case we must assume that  $c(T)$  varies in such a way that the integrals do not diverge at extremely low temperatures, i.e. near  $T = 0$ ,  $c(T) \propto T^n$ , where  $n > 1$ ; (ii)  $T_0 = 2.19^\circ \text{K.}$ , the  $\lambda$ -point; (iii)  $T_0 = \infty$ .

The second and third give the same result, since  $u_2 = 0$  for  $T \geq 2.19^\circ \text{K.}$  However, the integrals would have a zero value at the  $\lambda$ -point, which would lead

to difficulties—for instance, infinities would appear unless the attenuation of the sound were taken into account in detail. It is therefore probable that  $T_0 = 0^\circ \text{K.}$ , predicting a zero value for the velocity of second sound at the absolute zero.

*Note added in proof. Recent Experimental Work.*

Peshkov (1948a) has recently made measurements of the velocity of second sound at lower temperatures than those used in previous experiments. These show that the velocity again rises at temperatures lower than  $1.12^\circ \text{K.}$ , in accordance with Landau's prediction (Landau 1941, Dingle 1948, §11). Thus the mean value of  $\theta_2$  will be greater than that estimated in §5 of the present paper. As a result, the values of the thermodynamical quantities will be reduced, leading to better agreement between theory and experiment.

Peshkov (1948b) has also measured the velocity of second sound as a function of pressure, i.e.  $(\partial u_2 / \partial p)_T$ . This he finds to be small and negative, so that  $(\partial u_2 / \partial V)_T$  will be small and positive, as predicted theoretically in §6 of this paper. Quantitatively, by similar arguments to those of §6, we obtain

$$\left( \frac{\partial u_2}{\partial p} \right)_T = \frac{T^{3/2}}{T_0} \frac{dT_0}{dp} \cdot \left( \frac{\partial (u_2 / \sqrt{T})}{\partial T} \right)_p.$$

This relation yields values of  $(\partial u_2 / \partial p)_T$  in close agreement with Peshkov's experimental results for temperatures near the  $\lambda$ -point—i.e. in the temperature region in which  $u_2$  varies rapidly with temperature. For temperatures in the neighbourhood of the maximum of  $u_2(T)$  it gives values which are too small by a factor of about four. It follows from the above relation that  $-(\partial u_2 / \partial p)_T$  should again rise in value for temperatures lower than  $1.12^\circ \text{K.}$

#### ACKNOWLEDGMENTS

The author would like to record his acknowledgment of the discussions he has had with Professor N. F. Mott of this Laboratory and with colleagues of the Royal Society Mond Laboratory, Cambridge, in particular with Mr. H. N. V. Temperley, who directed his attention to the work of Rushbrooke. The author is indebted to the Department of Scientific and Industrial Research for a grant.

#### REFERENCES

- BORN, M., and GREEN, H. S., 1946, *Proc. Roy. Soc. A*, **188**, 10; 1947 a, *Ibid.*, **190**, 455; 1947 b, *Ibid.*, **191**, 168.  
 BRILLOUIN, L., 1914, *C.R. Acad. Sci., Paris*, **159**, 27; 1920, *Théorie des solides et les quanta*, *Ann. de l'École Normale*, Supp. 37, 431; 1936, *J. Phys. Radium*, **7**, 153.  
 DEBYE, P., 1912, *Ann. Phys., Lpz.*, **39**, 789; 1914, *Göttinger Vorträge über Kinetische Theorie* (Leipzig: Teubner).  
 DINGLE, R. B., 1948, *Proc. Phys. Soc.*, **61**, 9; 1949, *Proc. Camb. Phil. Soc.* (in the press).  
 FOWLER, R. H., and JONES, H., 1938, *Proc. Camb. Phil. Soc.*, **34**, 573.  
 GREEN, H. S., 1947, *Proc. Roy. Soc. A*, **189**, 103; 1948, *Ibid.*, **194**, 244.  
 KEESOM, W. H., 1942, *Helium* (Amsterdam: Elsevier Publishing Co.).  
 LANDAU, L., 1941, *J. Phys. U.S.S.R.*, **5**, 71; 1947, *Ibid.*, **11**, 91.  
 LONDON, F., 1938, *Phys. Rev.*, **54**, 947; 1939, *J. Phys. Chem.*, **43**, 49.  
 LUCAS, L., 1937, *J. Phys. Radium*, **8**, 410.  
 PESHKOV, V. P., 1948 a, *Exp. Theor. Phys., U.S.S.R.*, **18**, 951; 1948 b, *Ibid.*, **18**, 438.  
 PICKARD, G. L., and SIMON, F., 1939, *Roy. Soc. Abstracts*, S 21.  
 RUSHBROOKE, G. S., 1940, *Trans. Faraday Soc.*, **36**, 1055.  
 TISZA, L., 1938, *C.R. Acad. Sci., Paris*, **207**, 1035, 1186; 1940, *J. Phys. Radium*, **1**, 164, 340; 1947, *Phys. Rev.*, **72**, 838.

# The Surface Energies of Inert-gas and Ionic Crystals

By R. SHUTTLEWORTH

H. H. Wills Physical Laboratory, University of Bristol

*Communicated by N. F. Mott; MS. received 25th July 1948*

**ABSTRACT.** It is shown that the surface energies of inert-gas crystals are proportional to their sublimation energies. The constant of proportionality is evaluated for the {111}, {100} and {110} faces for different assumed forms of the interatomic repulsive forces; to within 15% it is independent of the face, and of the form of the repulsive force. The distance of the outermost plane of atoms from the next at a {100} face is 2.54% greater than normal; this distortion makes a negative contribution of 1% to the surface energy.

The surface energies of sodium and potassium halide crystals are calculated; the ratio of the energies of {110} and {100} faces is about 2.5. The contribution of van der Waals type forces to the surface energy of a {100} face is almost half the total.

Elementary methods are given for the evaluation of lattice sums.

## § 1. INTRODUCTION

THE total free energy of a volume of liquid is the sum of two terms, one proportional to the volume, the other to the surface area; the surface free energy per unit area is defined as the proportionality factor in the second term. The surface free energy per unit area of a crystal face is similarly defined, having regard to the fact that different faces of a crystal have different energies.

Both the surface free energy and the surface "internal" energy are difficult to calculate because they depend on the thermal vibrations. The surface energy at 0° K. is a simpler quantity, for except for zero-point vibrations the molecules are at rest. If the molecules can be regarded as acting upon each other with forces that depend only upon their separation, then the surface energy at 0° K. is the excess potential energy of molecules near the surface.

An increase in area of a given volume of material can occur by its division into two parts by a plane, and the separation of these parts to an infinite distance. This can be supposed to occur in two stages and the energy change of each stage can be calculated. In the first stage the molecules of each part are supposed held in their original relative positions by constraints, so that the energy per unit area needed to separate these two parts to infinity is  $2U'_0$ , where  $-2U'_0$  was the mutual potential per unit area between the two parts before separation. In the second stage the constraints on the molecules are relaxed, the surface molecules are no longer in equilibrium and move to a position of lower energy; this reduces the energy of each surface by an amount  $U''_0$  per unit area. Thus the surface energy per unit area at 0° K. is

$$U_0 = U'_0 - U''_0. \quad \dots\dots(1)$$

$U''_0$  is a small correction to  $U'_0$ .

Numerous authors have attempted to calculate  $U'_0$  for homopolar liquids on the assumptions that the forces between any two molecules act along their line of

centres, are independent of the presence of other molecules, and depend only on their distance apart, i.e. they are central and additive. Using these assumptions Gauss (see for example Rayleigh (1890) or Fowler and Guggenheim (1939)) treated a liquid as a continuum and obtained the expression

$$U'_0 = -\frac{1}{2}\pi n^2 \int_0^\infty r^3 \epsilon(r) dr, \quad \dots\dots (2)$$

where  $\epsilon(r)$  is the potential between two molecules at a distance  $r$  apart and  $n$  is the number of molecules per unit volume. This gives correctly the contribution to  $U'_0$  of those molecules distant from the plane of section.\* It shows that if  $\epsilon(r)$  decreases less rapidly than  $r^{-4}$  the integral does not converge, and then the concept of a constant surface energy per unit area independent of size is not valid. If a volume is so large that gravitational forces between the molecules affect capillary phenomena, they must be estimated independently.

If, however,  $\epsilon(r)$  contains terms that, at  $r=0$ , change more rapidly than  $r^{-4}$ , the integral (2) diverges at the lower limit. Edser (1922), Bakker (1928), Bradley (1931), Kassel and Muscat (1932) and Belton and Evans (1941) have avoided this divergence by using the atomic diameter as the lower limit; this is quite arbitrary and introduces very large and unpredictable errors.

To obtain an accurate estimate of  $U'_0$  it is not sufficient to treat a liquid as a continuum; a knowledge of the molecular arrangement is necessary. Jura (1948) used the experimentally determined radial distribution function of argon and calculated  $U'_{M.P.}$ , the surface potential energy of the liquid at the melting point, from a generalization of equation (2). He assumed that the distribution of atoms near the surface is not altered by the presence of the surface. This procedure is somewhat tedious and demands a knowledge of the radial distribution function.

In this paper it is shown that for a homopolar substance, either liquid or solid, in which the interatomic forces are central and additive,

$$U_0 = K\epsilon_0/a_0^2, \quad \dots\dots (3)$$

where  $\epsilon_0$  is the heat of evaporation and  $a_0$  is a characteristic interatomic distance; both quantities are supposed extrapolated to  $0^\circ \text{K}$ . The value of  $K$  depends on the form of the interatomic force,  $\epsilon(r)$ , and upon the molecular arrangement. Values of  $K$  for {111}, {100}, {110} faces of face-centred-cubic crystals and for different interatomic repulsive forces are calculated by a method of lattice sums devised by Born and Stern (1919) for ionic crystals. The theory is applied to inert-gas atoms, for which the assumptions are most likely to be valid.

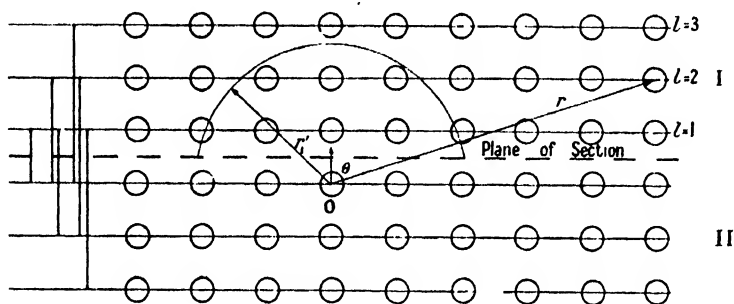
Calculations of the surface energies of the {100} and {110} faces of sodium and potassium halides have been made by Born and Stern (1919), Lennard-Jones and Taylor (1925), and Dent (1929). However, doubt has been thrown on these results because they were less than half the observed value for the liquid. It is shown that this discrepancy is largely due to the neglect of van der Waals attractive forces, which in these ionic salts make a large contribution to the surface energy.

No reliable measurements have been made of the surface energies of solids and it is necessary to compare the theoretical results with the observed values for the liquids. Exact agreement is not to be expected because of the different molecular arrangement in solids and liquids, especially at the surface.

\* The contributions of distant molecules to  $U'_0$  are found by multiplying  $I$  of equation (30) by  $-\frac{1}{2}hn$ ; for a continuum  $h \rightarrow 0$  and the second integral vanishes.

## § 2. THE MUTUAL POTENTIAL BETWEEN TWO PARTS OF A CRYSTAL

It is necessary to calculate the mutual potential per unit area between two parts of a homopolar crystal separated by an imaginary plane of section. Because of the regular crystal structure all atoms can be regarded as lying on planes parallel to the plane of section, and when all lattice points are equivalent the separation  $h$  between all adjacent planes is the same. The mutual potential between the two parts, I and II of the crystals (see Figure), is the sum of the potentials between all planes in



part I and all planes in part II. The potential between any two such parallel planes depends only upon their separation.

From the Figure it is seen that in the expression for the mutual potential the contribution of a pair of planes at separation  $h$  occurs once, at separation  $2h$  twice, and so on. If the planes in part I be enumerated  $l=1, 2, 3, \dots$ , then the mutual potential (per atom in the surface plane)  $-2u'_0$ , is

$$-2u'_0 = \sum_{l=1}^{\infty} l\epsilon(r). \quad \dots\dots(4)$$

Here  $u'_0$  is the surface energy per atom in the surface plane,  $r$  is the distance between an atom O in the surface plane ( $l=0$ ) of part II and an atom in the plane  $l$  of part I; the summation is over all atoms in part I.

This method of calculating the surface energy is based on the assumptions that the interatomic forces are central and additive; these are valid only for inert-gas and ionic crystals. In inert-gas crystals the attractive forces between atoms are van der Waals, which London (1937) showed to be additive. The attractive forces between the ions of ionic crystals are van der Waals and electrostatic forces; the latter are clearly both central and additive. For neither inert-gas nor ionic crystals is it certain that the repulsive forces are additive, but this will be assumed for the inert-gas crystals; for ionic crystals only repulsive forces between nearest and next-nearest neighbour ions will be considered. The form of this assumption is not important because it affects only the interaction between atoms which are not nearest neighbours, and this is small because the forces decrease rapidly with distance.

The method of calculation is not appropriate to metals for which the surface energy is best regarded as arising from the change in kinetic energy of the free electrons due to the presence of the surface (Huang and Wyllie 1949). Nor can it be applied immediately to molecules with a permanent dipole moment, for these will be oriented at the surface of the liquid, and this will give rise to large values of  $U''_0$ . For covalent crystals, such as diamond, the best model is perhaps that of Harkins (1942) who considered only forces between nearest-neighbour atoms; this leads to a simple expression for  $K$ .

## § 3. THE SURFACE ENERGIES OF INERT-GAS CRYSTALS

(i) Calculation of  $U'_0$ 

The force between two atoms is attractive at large distances and repulsive at small distances; at intermediate distances there is an equilibrium separation where the potential energy is a minimum. A simple expression that shows this behaviour is

$$\epsilon(r) = \lambda r^{-s} - \mu r^{-t} \quad s > t, \quad \dots\dots(5)$$

where  $\epsilon(r)$  is the potential between two atoms a distance  $r$  apart;  $-\lambda r^{-(s+1)}$  can be regarded as the short range repulsive force and  $t\mu r^{-(t+1)}$  the longer range attractive force. From a knowledge of  $\epsilon(r)$  both  $u'_0$  and  $u''_0$  can be calculated.

The lattice of inert-gas crystals is face-centred cubic; this may be regarded as a simple cubic lattice, of lattice constant  $a_0$ , in which only alternate sites are occupied. Taking coordinate axes parallel to the cube axes, the coordinates of an atom, with respect to another, are  $(m_1a_0, m_2a_0, m_3a_0)$  where  $m_1, m_2, m_3$  are integers (positive, negative or zero) such that  $m_1 + m_2 + m_3$  is even. Combining equations (4) and (5)

$$-2u'_0 = \lambda a_0^{-s} \left[ \sum_{\substack{l \geq 1 \\ m_1 + m_2 + m_3 \text{ even}}} \frac{l}{(m_1^2 + m_2^2 + m_3^2)^{s/2}} \right] - \mu a_0^{-t} \left[ \sum_{\substack{l \geq 1 \\ m_1 + m_2 + m_3 \text{ even}}} \frac{l}{(m_1^2 + m_2^2 + m_3^2)^{t/2}} \right], \quad \dots\dots(6)$$

$$-2u'_0 = B''_s \lambda a_0^{-s} - B''_t \mu a_0^{-t}. \quad \dots\dots(7)$$

Numerical values of the lattice sums  $B''$  and details of their computation are given in the Appendix for  $\{111\}$ ,  $\{110\}$ , and  $\{100\}$  planes for powers between 6 and 12.

Instead of using explicit values of the force constants  $\lambda$  and  $\mu$  it is possible to express  $u'_0$  in terms of the heat of sublimation of the crystal. The mutual potential of an atom in the centre of a crystal with respect to all the other atoms is

$$-2\epsilon_0 = \Sigma \epsilon(r), \quad \dots\dots(8)$$

where  $\epsilon_0$  is the heat of sublimation per atom at  $0^\circ \text{K}$ . (corrected for zero point vibrations) and the summation is over all the other atoms. The factor 2 occurs because when the sum is repeated for every atom as origin the interaction of each pair is counted twice. Using equation (5)

$$-2\epsilon_0 = \lambda a_0^{-s} \left[ \sum_{m_1 + m_2 + m_3 \text{ even}} \frac{1}{(m_1^2 + m_2^2 + m_3^2)^{s/2}} \right] - \mu a_0^{-t} \left[ \sum_{m_1 + m_2 + m_3 \text{ even}} \frac{1}{(m_1^2 + m_2^2 + m_3^2)^{t/2}} \right], \quad \dots\dots(9)$$

$$-2\epsilon_0 = A''_s \lambda a_0^{-s} - A''_t \mu a_0^{-t}. \quad \dots\dots(10)$$

Lennard-Jones and Ingham (1925) have evaluated  $A''$  for powers between 4 and 30. At  $0^\circ \text{K}$ . the lattice potential energy  $\epsilon_0$  is a minimum with respect to variations in  $a$ .

$$sA''_s \lambda a_0^{-s} = tA''_t \mu a_0^{-t}. \quad \dots\dots(11)$$

Eliminating  $\lambda a_0^{-s}$  and  $\mu a_0^{-t}$  from equations (7), (10), (11),

$$u'_0 = \frac{sB''_t/A''_t - tB''_s/A''_s}{s-t} \epsilon_0 = k(s, t) \epsilon_0. \quad \dots\dots(12)$$

The attractive forces between inert-gas atoms are van der Waals type, for which  $t=6$ . In Table 1,  $k(s, 6)$  for a  $\{111\}$  plane is tabulated for values of  $s$  between 7 and infinity. Increasing values of  $s$  correspond to increasing "hardness" of the atoms; when  $s$  is infinite the atomic model is that of rigid spheres with attractive forces.

Table 1. Variation of  ${}_{111}k$  with "Hardness" of the Atoms

$s$	7	8	9	10	11	12	$\infty$
${}_{111}k(s, 6)$	0.502	0.450	0.418	0.398	0.384	0.374	0.313

If the interaction between atoms that are not nearest neighbours is neglected, then  $B'_l/A'_l$  and  $B''_s/A''_s$  are each equal to the ratio of the number of nearest neighbours in the plane  $l=1$  (3), to the total number of nearest neighbours, (12);  $k$  is then  $\frac{1}{4}$ .

The most significant basis of comparison for the surface energies of different crystal faces is the energy per unit area  $U'_0$

$${}_P U'_0 = {}_P u'_{0i} / \omega_P a_0^2 = {}_P K(s, t) \epsilon_0 / a_0^2, \quad \dots\dots (13)$$

where  $1/\omega_P a_0^2$  is the number of atoms per unit area in the surface plane of crystal face  $\{P\}$ . In Table 2 values of  ${}_P K(s, 6)$  are tabulated for  $\{111\}$ ,  $\{100\}$ , and  $\{110\}$  planes for  $s$  between 7 and infinity.

Table 2. Variation of  $K$  with Crystal Face and "Hardness" of the Atoms

$s$	7	8	9	10	11	12	$\infty$
${}_{111}K(s, 6)$	0.290	0.260	0.242	0.230	0.222	0.216	0.181
${}_{100}K(s, 6)$	0.292	0.264	0.247	0.236	0.229	0.224	0.196
${}_{110}K(s, 6)$	0.301	0.273	0.257	0.247	0.240	0.235	0.206

The variation of surface energy with crystal face arises from the different arrangement of the atoms that are near the surface; the contribution to  ${}_P U'_0$  of atoms distant from the plane of section is the same for all faces. The greater the relative importance of the interaction between neighbouring atoms the greater is the variation of surface energy with crystal face; thus the variation increases with increase of  $s$  and  $t$ . Yamada (1923, 1924) and Frenkel (1945) have shown that the surface energy per unit area of a crystal changes continuously with change of orientation of a crystal face, and that faces with large indices need not necessarily have large energies. This is because faces with large indices can be regarded as a series of steps formed from planes of low indices and of height equal to the interplanar separation. When such steps are few in number the increase in surface energy is only slight. Thus for a homopolar face-centred-cubic crystal the  $\{110\}$  and  $\{111\}$  faces have the absolute maximum and minimum surface energies per unit area; for an inert-gas crystal they do not differ by more than 10%.

From a knowledge of the heat of sublimation and the lattice constant of an inert-gas crystal it is possible to calculate the surface energy to within 15%; a more accurate estimate demands a knowledge of  $s$ . Values of  $s$  are derived from the variation of the second virial coefficient of the gas with temperature; Buckingham (1938) has shown that for inert gases a form of  $\epsilon(r)$  in which  $t=6$ ,  $s=12$  gives good agreement with experiment. Values of  $U'_0$  for the  $\{111\}$ ,  $\{100\}$  and  $\{110\}$  faces of the inert-gas crystals have been calculated from their heat of sublimation,



using  $K(6, 12)$ , and are given in Table 3. They are compared with the value of the surface energies of the liquids extrapolated to  $0^\circ \text{K}$ . (Guggenheim 1945).

Table 3. Surface Energies of Inert-gas Crystals

	$\epsilon_0$ (erg/atom)	$a_0^*$ (Å)	$_{111}U'_0$ (erg/cm <sup>2</sup> )	$_{100}U'_0$ (erg/cm <sup>2</sup> )	$_{110}U'_0$ (erg/cm <sup>2</sup> )	$U_{0 \text{ liq.}}$ (erg/cm <sup>2</sup> )
Ne	$4.08 \times 10^{-14}$	2.26	17.2	17.9	18.7	15.1
A	13.89	2.70	41.1	42.7	44.7	36.3
Kr	19.23	2.79	53.3	55.3	57.9	
Xe	26.87	3.09	60.7	63.0	66.0	

\* The lattice constant is  $\lambda a_0$ .

The heats of sublimation at  $0^\circ \text{K}$ . were calculated by numerical integration from the latent heats at the boiling point, the heats of fusion and the specific heats of the solids and liquids; a correction  $9k\Theta/8$  for the zero point vibrations was made,  $\Theta$  being the Debye temperature. No correction was made for the departure of the gases at atmospheric pressure from the perfect gas law. The experimental data are those of Clusius and his collaborators (1929, 1936, 1937, 1938, 1939).

The surface energies calculated for the crystal are greater than those found by experiment for the liquid. For inert gas crystals  $dU'_0/da$  is negative, but the difference in density of liquid and solid is not quite sufficient to account for the discrepancy.

The effect of zero-point vibrations on the surface energy has been neglected; for while they would invalidate any calculation for helium their effect on the surface energies of crystals formed from the heavier atoms will be small. In (ii) below it is shown that the decrease of energy  $U''_0$  due to surface distortion is less than the uncertainties in the calculation of  $U'_0$ .

### (ii) Contribution of Surface Distortion to Surface Energy

In inert-gas crystals the separation of the atomic planes parallel to the surface is greater near the surface than in the interior of the crystal. The surface energy of the distorted crystal is less than that of the unstable undistorted crystal by  $U''_0$ .

The distortion arises because of the interaction of atoms in non-adjacent planes. In the interior of a crystal (see Figure) the net force between all the atoms above the atomic plane  $l=1$  on all the atoms below the plane is attractive. This is because, in homopolar crystals, the attractive forces decrease more slowly with distance than do the repulsive forces, and the separation of the parts of the crystal above and below  $l=1$  is greater than the equilibrium distance. This attractive force is balanced by net repulsive forces between the atoms in the plane  $l=1$  and the two parts of the crystal above and below  $l=1$ . If the part below  $l=1$  is removed, so that  $l=1$  becomes a surface plane, there is an unbalanced repulsive force which causes the atoms in the plane  $l=1$  to move away from the rest of the crystal until the attractive and repulsive forces again become equal. Similar distortions occur for atoms in successive planes but these are very much smaller and will be neglected. The distortion will be least on crystal faces formed from close-packed planes, for these planes are most widely spaced and the forces between non-adjacent planes smallest. If it is possible to neglect the interaction between atoms that are not nearest neighbours the surface distortion is zero.

$U_0''$  is the decrease of potential energy when the surface plane of atoms moves from the position it occupied when at the centre of the crystal to its equilibrium position of minimum energy. Calculations of distortion and of  $U_0''$  were made for the {100} face of an inert-gas crystal ( $s=12$ ,  $t=6$ ). Distortion occurs by an equal displacement, in a direction perpendicular to the surface, of each atom in the plane  $l=1$ . The potential energy per atom of the surface plane with respect to the remainder of the crystal is:

$$\phi = C_{12}'' \lambda a_0^{-12} - C_6'' \mu a_0^{-6} \quad \dots\dots (14)$$

where 
$$C_i''(c) = \sum_{l \geq 2} (a_0/r)^i, \quad \dots\dots (15)$$

and  $ca_0$  is the distance of the surface plane,  $l=1$ , from the next plane,  $l=2$ . In equation (15)  $r$  is the distance between a particular atom in the surface plane and any atom in the remainder of the crystal; summation is over all atoms in the remainder of the crystal. In Table 9 values of  $C_6''$  and  $C_{12}''$  for a number of values of  $c$  are given. The equilibrium position of the surface plane occurs at the value of  $c$  for which  $\phi$  is a minimum, viz.

$$dC_{12}''/dc = (2A_{12}''/A_6'')(dC_6''/dc). \quad \dots\dots (16)$$

$\lambda a_0^{-12}$  and  $\mu a_0^{-6}$  have been eliminated by equation (11). A solution to equation (16) was found by numerical differentiation:  $c_{\text{equil.}} = 1.0254$ . Thus in an inert-gas crystal the distance between the surface atomic plane and the next is, for a {100} face, 2.5% greater than the distance in the interior of the crystal.

Values of the lattice sums at the equilibrium separation  $c_{\text{equil.}}$  were obtained by interpolation and are included in Table 9. Then

$${}_{100}u_0'' = \Delta\phi = \Delta C_{12}'' \lambda a_0^{-12} - \Delta C_6'' \mu a_0^{-6}, \quad \dots\dots (17)$$

where  $u_0''$  is the decrease of  $\phi$  as  $c$  increases from 1 to 1.0254, and  $\Delta C_{12}''$  and  $\Delta C_6''$  are the corresponding decreases in the lattice sums. As in the derivation of equation (12)

$${}_{100}u_0'' = 2(\Delta C_{12}'', A_{12}'') - 2\Delta C_6''/A_6'' \epsilon_0, \quad \dots\dots (18)$$

$${}_{100}U_0'' = 0.002\epsilon_0/a_0^2, \quad \dots\dots (19)$$

${}_{100}U_0''$  is less than 1% of  ${}_{100}U_0'$  and can be neglected because it is smaller than the inevitable errors in the calculation. Surface distortion will reduce the energy of a {111} face in a somewhat less, and of a {110} face in a somewhat greater proportion, but not sufficiently to affect appreciably the relative magnitudes of different faces.

#### § 4. THE SURFACE ENERGIES OF IONIC CRYSTALS

##### (i) Calculation of $U_0'$

In crystals of the alkali-halides the alkali and halide ions are arranged on alternate points of a simple-cubic lattice. The halide ions have a negative charge of one electron and the alkali ions an equal positive charge. There are also van der Waals attractive forces and short range repulsive forces between the ions. Mayer and his colleagues (Born and Mayer 1932, Mayer and Helmholtz 1932, Mayer 1933, Huggins and Mayer 1933) have considered these forces in detail and given numerical values for the force constants. According to them the potential between two alkali ions at a distance  $r$  apart can be written

$$\epsilon_{++}(r) = e^2 r^{-1} - c_{++} r^{-8} - d_{++} r^{-8} + 1.25b_+^2 \exp(-r/\rho), \quad \dots\dots (20)$$

the potential between two halide ions

$$\epsilon_{--}(r) = e^2 r^{-1} - c_{--} r^{-6} - d_{--} r^{-8} + 0.75b_{--}^2 \exp(-r/\rho), \quad \dots\dots(21)$$

and the potential between an alkali and halide ion

$$\epsilon_{+-}(r) = -e^2 r^{-1} - c_{+-} r^{-6} - d_{+-} r^{-8} + b_{+} b_{-} \exp(-r/\rho). \quad \dots\dots(22)$$

The van der Waals terms proportional to the inverse sixth and inverse eighth power of the distance are referred to as the dipole-dipole and dipole-quadrupole interactions respectively; the latter term is small compared to the first. The repulsive potentials decrease exponentially with distance; in a crystal it is necessary to consider only the repulsion between an ion and its six nearest neighbours, which have opposite charge, and twelve next-nearest neighbours, which have the same charge.

If an ion is selected as origin all ions with the same charge have coordinates for which  $m_1 + m_2 + m_3$  is even, ions with opposite charge have coordinates for which  $m_1 + m_2 + m_3$  is odd. All planes (except {111} planes) contain equal numbers of alkali and halide ions. To find the mutual potential between two parts of an alkali-halide crystal it is necessary to consider the potentials between (a) the alkali ions of part I and the alkali ions of part II, (b) the halide ions of part I and the halide ions of part II, (c) the alkali ions of part I and the halide ions of part II, (d) the halide ions of part I and the alkali ions of part II. The positions of the alkali and halide ions in the lattice are equivalent so that (c) and (d) are equal. The electrostatic contributions if considered separately diverge, and they must be grouped in pairs (a) and (c), (b) and (d), to obtain convergence; these two pairs are equal. As in equation (7) the mutual potential per alkali (or halide) ion in the surface plane is

$$\begin{aligned} -2u'_0 = & -2B''_0 e^2 a_0^{-1} - B''_0 (c_{++} + c_{--}) a_0^{-6} - 2B'_0 c_{+-} a_0^{-6} \\ & - B'_0 (d_{++} + d_{--}) a_0^{-8} - 2B'_0 d_{+-} a_0^{-8} \\ & + N''(1.25b_+^2 + 0.75b_-^2) \exp(-\sqrt{2}a_0/\rho) \\ & + 2N'b_+ b_- \exp(-a_0/\rho), \quad \dots\dots(23) \end{aligned}$$

where  $a_0$  is the alkali-halide ion distance,  $B''_0$  is an electrostatic lattice sum

$$B''_0 = \sum_{\substack{l \geq 1 \\ m_1 + m_2 + m_3 \text{ odd and even}}} \frac{l(-1)^{m_1 + m_2 + m_3}}{(m_1^2 + m_2^2 + m_3^2)^{l/2}}, \quad \dots\dots(24)$$

the factor  $(-1)^{m_1 + m_2 + m_3}$  arising because of the opposite sign of ions at alternate lattice points; the  $B'_l$ 's represent the lattice sums for the van der Waals interaction between alkali and halide ions:

$$B'_l = \sum_{\substack{l \geq 0 \\ m_1 + m_2 + m_3 \text{ odd}}} \frac{l}{(m_1^2 + m_2^2 + m_3^2)^{l/2}}; \quad \dots\dots(25)$$

$N'$  and  $N''$  are respectively the number of nearest and next-nearest bonds per surface ion that cross the plane of section. Values of the lattice sums (divided by  $2\omega_p$ ) for {100} and {110} faces are given in Table 4, and their method of calculation is described in § 5.

The surface energy per unit area,  $U'_0$ , is  $u'_0/\omega_p a_0^2$ , where  $1/\omega_p a_0^2$  is the number of alkali (or halide) ions per unit area in the surface plane. The force constants given by Huggins and Mayer (1933) for sodium and potassium halides were used

to calculate the contributions to  $U'_0$  of the electrostatic, dipole-dipole, dipole-quadrupole and repulsive forces. These contributions and their total are given in Table 5 for a {100} face.

In Table 6 are given the surface energies  ${}_{110}U'_0$  of a {110} face, the ratio  ${}_{110}U'_0/{}_{100}U'_0$  and  $a_0$ . For consistency  $a_0$  was calculated from the force constants.

The electrostatic term is predominant in the lattice energy, and the repulsive and van der Waals terms are only one-tenth and one-thirtieth of the electrostatic term. This is not so for the surface energy: here the electrostatic term (positive) is only a little greater than the repulsive term (negative), so that van der Waals forces give rise to almost half of the net surface energy. This is because  $U'_0$  is the

Table 4. Lattice Sums used to Calculate the Surface Energies of Alkali-halides

	$B''_e/2\omega_P$	$B''_g/2\omega_P$	$B'_g/2\omega_P$	$B''_g/2\omega_P$	$B'_g/2\omega_P$	$N''/2\omega_P$	$N'/2\omega_P$
{100}	0.01631	0.17670	0.33820	0.06920	0.26898	1.00000	0.25000
{110}	0.03174	0.18618	0.43482	0.07353	0.36972	1.06066	0.35355

Table 5. The Contributions of the Different Forces to  $U'_0$  for {100} Faces (erg/cm<sup>2</sup>)

	NaF	NaCl	NaBr	NaI	KF	KCl	KBr	KI
Electrostatic	618.0	345.6	289.7	227.8	396.5	250.3	215.8	175.8
Dipole-dipole	82.8	79.6	77.9	76.2	84.1	69.8	65.0	60.6
Dipole-quadrupole	8.8	8.6	8.4	8.4	8.3	7.2	6.6	6.3
Repulsive	-500.3	245.3	-199.3	-151.9	-294.3	-164.3	-136.2	-106.4
Total	209	189	177	161	195	163	151	136

Table 6. The Surface Energy,  $U'_0$ , of a {110} Face

	NaF	NaCl	NaBr	NaI	KF	KCl	KBr	KI
${}_{110}U'_0$ (erg cm <sup>2</sup> )	640.5	445.3	396.2	337.9	483.1	352.3	316.7	273.6
${}_{110}U'_0/{}_{100}U'_0$	3.06	2.36	2.24	2.11	2.48	2.16	2.09	2.01
$a_0$ (Å.)	2.290	2.780	2.948	3.194	2.655	3.095	3.252	3.482

energy necessary to divide a crystal into two neutral parts, whilst the lattice energy is the energy necessary to divide it into oppositely charged ions. The large ratio of the surface energy of a {110} to a {100} face arises mainly from the difference between the electrostatic terms; this is clear from Table 4.

In the alkali-halide crystals the {111} planes are formed alternately from alkali and halide ions, and there appears no simple method of evaluating the electrostatic contribution to the surface energy of a {111} face.

## (ii) Contribution of Surface Distortion to Surface Energy

Lennard-Jones and Dent (1928a) and Dent (1929) showed that in ionic crystals the most important cause of surface distortion and corresponding decrease of surface energy  $U''_0$  is the polarization of the surface ions in the electrostatic field.

Verwey (1946) has made detailed calculations and shows that, in general, the positive ions at the surface are displaced away from the crystal and the negative surface ions displaced towards the crystal. He shows that for NaBr  $U_0''$  is 32 erg/cm<sup>2</sup>. It is supposed that NaBr is typical, and  ${}_{100}U_0'$  for the other crystals obtained by reducing  ${}_{100}U_0'$  in the same proportion. In Table 7 values of  ${}_{100}U_0'$  are compared with the experimental values of the liquid, which have been extrapolated to 0° K. by Jaeger (1917).

Table 7. Surface Energies  ${}_{100}U_0$  of the {100} Face (erg/cm<sup>2</sup>)

	NaF	NaCl	NaBr	NaI	KF	KCl	KBr	KI
${}_{100}U_0$	171	155	145	132	160	134	124	111
$U_{0(\text{liq.})}$	335	190	178	138	242	173	159	139

Although for alkali-halide crystals  $dU_0'/da$  is positive, the decrease of density on fusion is not sufficient to account for the discrepancy between the two values.

## § 5. THE EVALUATION OF LATTICE SUMS

### (i) Computation of $B_i''$ and $B_i'$

In order to evaluate lattice sums of the form

$$B_i'' = \sum_{\substack{l \geq 1 \\ m_1 + m_2 + m_3 \text{ even}}} \frac{l}{(m_1^2 + m_2^2 + m_3^2)^{3/2}}, \quad \dots\dots (26)$$

it is necessary to express  $l$ , the ordinal of the plane in which an atom lies, in terms of the coordinates of the atom. The relation is different for different planes

$$l_{111} = (m_1 + m_2 + m_3)/2, \quad l_{100} = m_1, \quad l_{110} = m_1 + m_2, \quad \dots\dots (27)$$

where  $m_1, m_2, m_3$  are integers (positive, negative or zero). The values of  $l$  for any value of  $(r/a_0)^2 = m_1^2 + m_2^2 + m_3^2$  are readily enumerated, and the contributions to  $B_i''$  of all atoms (of part I of the crystal) that are within or on a hemisphere centre O and radius  $r_1$  can be found by direct summation. When  $t$  is greater than 10 the sum converges rapidly and an accurate value of  $B_i''$  can be obtained if the contributions of atoms outside a hemisphere radius  $\sqrt{30}a_0$  be neglected. For smaller values of  $t$  the contributions even of those atoms that are outside a hemisphere radius  $\sqrt{50}a_0$  cannot be neglected, and they must be estimated by integration.

Before finding the contributions to  $B_i''$  of those atoms outside a hemisphere radius  $r_1$ , a more general expression that gives the contributions of these atoms to the mutual potential,  $-2U_0'$ , in terms of  $\epsilon(r)$  will be derived. For distant atoms each atomic plane can be regarded as a uniform lamella which extends a distance  $h/2$  above and below the plane; their contribution to  $-2U_0'$  is, by equation (4),

$$I = \frac{n}{h} \iiint z \epsilon(r) dV, \quad \dots\dots (28)$$

$n$  is the number of atoms per unit volume, the element of volume  $dV$  is at a distance  $r$  from O, and  $z$  from the plane  $l=0$  (see Figure). The continuum representing part I of the crystal extends to the plane  $l=\frac{1}{2}$ ; so the region of integration is that

portion of the semi-infinite volume bounded by the plane  $l = \frac{1}{2}$  that is outside the hemisphere radius  $r'_1$ . This region is the difference of two other regions: (a) the semi-infinite volume above the plane  $l = 0$  and outside the hemisphere  $r'_1$ , (b) the portion of the infinite slab lying between the planes  $l = 0$  and  $l = \frac{1}{2}$  that is outside the cylinder radius  $r'_1$ . The integrals over the two regions are written in spherical and cylindrical coordinates respectively, and in the second integral the approximation is made of putting the cylindrical radial coordinate equal to  $r$ , the distance of a volume element from O.

$$r = \frac{n}{h} \int_{r'_1}^{\infty} \int_0^{\pi/2} \int_0^{2\pi} r^3 \epsilon(r) \cos \theta \sin \theta d\phi d\theta dr - \frac{n}{h} \int_{r'_1}^{\infty} \int_0^{h/2} \int_0^{2\pi} r \epsilon(r) z d\phi dz dr, \quad \dots\dots (29)$$

$$I = \pi \frac{n}{h} \int_{r'_1}^{\infty} r^3 \epsilon(r) dr - \frac{n}{4} \int_{r'_1}^{\infty} r \epsilon(r) dr. \quad \dots\dots (30)$$

In a face-centred-cubic lattice

$$n = 1/2a_0^3 \quad \text{and} \quad nh = 1/\omega_P a_0^2, \quad \dots\dots (31)$$

so if  $\epsilon(r)$  contains a term  $\lambda r^{-t}$  the contribution of the integrals to  $B'_t$  is

$$\frac{\pi \omega_P}{4(t-4)(r'_1/a_0)^{t-4}} - \frac{\pi}{4\omega_P(t-2)(r'_1/a_0)^{t-2}}.$$

In order that the contributions to  $B'_t$  of atoms on the surface of the hemisphere  $r_1$  should not be included in both the sum and the integral, the lower limit of integration  $r'_1$  was defined by

$$r'_1/a_0 = (3/2\pi)^{1/3} N^{1/3}, \quad \dots\dots (32)$$

where  $N$  is the number of atoms that are in and on a sphere centre O and radius  $r_1$ , and  $4\pi r_1^3/3$  is the volume of continuum these  $N$  atoms would occupy. To compute  $B''_0$  it was necessary to find by direct summation the contributions of all atoms within a hemisphere radius  $\sqrt{50}a_0$ .  $B'_t$  is tabulated in Table 8 for {111}, {100}, and {110} faces for  $t$  between 6 and 12.

Table 8. The Lattice Sum  $B'_t$

$t$	6	7	8	9	10	11	12
$_{111}B'_t$	0.56593	0.33264	0.21428	0.14391	0.09873	0.068545	0.047914
$_{100}B'_t$	0.70680	0.42387	0.27680	0.18765	0.12960	0.090387	0.063389
$_{110}B'_t$	1.0532	0.63547	0.41596	0.28218	0.19486	0.135863	0.095244

Similar computations were made for  $B'_t$  and the results, in the form  $B'_t/2\omega_P$ , are given in Table 4.

(ii) *Computation of  $C''_0$  and  $C''_{12}$*

In the computation of  $C''_0$  the contributions of all atoms inside and on a cylinder whose radius was  $\sqrt{50}a_0$ , and whose bases were on the planes  $l = 2-7$ , were found by direct summation. The contributions of those atoms in the planes  $l = 2-7$  that are outside this cylinder were found by integrating separately for each

plane; a lower limit of integration given by an equation analogous to (32) was used. The contributions of atoms in the planes  $l > 7$  were found by a single integration; the lower limit of integration was taken as  $l = 7.5$ .  $C_{12}''$  converged so rapidly that it was sufficient merely to sum atoms inside and on a cylinder radius  $\sqrt{14}a_0$  that lay between the planes  $l = 2$  and  $l = 4$ .  $C_6''$  and  $C_{12}''$  are given in Table 9 for values of  $c$  between 1.00 and 1.04.

Table 9. The Lattice Sums  $C_6''$  and  $C_{12}''$  \*

$c$	1.00	1.01	1.02	1.03	1.04	1.0254
$C_6''$	0.612195	0.595823	0.579923	0.564479	0.549472	0.571527
$C_{12}''$	0.063028	0.059367	0.055920	0.052673	0.049616	0.054144

\* Individual values are not accurate to this number of figures but the set is consistent.

### (iii) Computation of $B_c'''$

Previous calculations of  $B_c'''$  for  $\{100\}$  and  $\{110\}$  faces of sodium-chloride type crystals have been made by Born and Stern (1919). The atomic planes parallel to these faces are neutral and their potentials decrease very rapidly in a normal direction. Using Madelung's method (see for example Lennard-Jones and Dent 1928 b), Born and Stern evaluated the potentials of the planes  $l = 1, 2, 3$ , and found they could neglect the others. Their value of  $_{110}B_c'''$  is used in this paper.

It is possible rapidly to evaluate  $_{100}B_c'''$  for a  $\{100\}$  plane by an elementary method of direct summation similar to one suggested by Slater (1939) for the evaluation of Madelung's constant. If the contributions of positive and negative ions to  $B_c'''$  are summed separately, both diverge; convergence is possible only if the net charge on all the ions included in the sum is zero. If rapid convergence is to occur the domain of summation must be such that all ions outside it can be grouped so that every group has zero charge and makes only a small contribution to the potential at O (see Figure).

First, an approximate value of the potential at O due to each of the planes  $l = 1-5$  was found by summing over all the ions of a plane inside and on a square with centre on the normal cube axis through O and sides parallel to the other cube axes. In order that such a square be neutral an ion on a side was treated as only half in the square and an ion at the corner as only a quarter in the square. The potentials of each plane  $l_1e/a_0, l_2e/a_0, l_3e/a_0$  etc. thus calculated, converged somewhat slowly as the size of the square was increased. The errors, which arise because of ions not included in the sum, have opposite signs for adjacent planes, since in adjacent planes positive and negative ions interchange their positions. If the planes are grouped in threes and the middle plane given double weight, the potential of the triplet rapidly converges; this is because the error of the centre sum is almost the mean of the errors of the exterior sums and has opposite sign.

The two triplets,  $l_1 + 2l_2 + l_3$  and  $2(l_3 + 2l_4 + l_5)$ , were evaluated using a square of side  $10a_0$ ; this gave a value of  $B_c'''$  ( $= l_1 + 2l_2 + 3l_3 \dots$ ) equal to 0.06525. The second triplet was only 1% of the first.

### ACKNOWLEDGMENTS

The author wishes to express his indebtedness to his colleagues and especially to Dr. K. Huang for discussions during the preparation of this paper.

REFERENCES

- BAKKER, G., 1928, *Wein-Harms Handb. exp. Phys.*, Vol. 6.  
 BELTON, J. W., and EVANS, M. G., 1941, *Trans. Faraday Soc.*, **37**, 1.  
 BORN, M., and MAYER, J. E., 1932, *Z. Phys.*, **75**, 1.  
 BORN, M., and STERN, O., 1919, *S. B. preuss. Akad. Wiss.*, 901.  
 BRADLEY, R. S., 1931, *Phil. Mag.*, **11**, 846.  
 BUCKINGHAM, R. A., 1938, *Proc. Roy. Soc. A*, **168**, 264.  
 CLUSIUS, K., 1929, *Z. phys. Chem. B* **4**, 1; 1936, *Ibid.*, **31**, 459.  
 CLUSIUS, K., KRUIS, A., and KONNERTZ, F., 1938, *Ann. Phys., Lpz.*, **33**, 642.  
 CLUSIUS, K., and RICCOBONI, L., 1937, *Z. phys. Chem. B* **38**, 81.  
 DENT, B. M., 1929, *Phil. Mag.*, **8**, 530.  
 EDSER, E., 1922, *Fourth Report on Colloid Chemistry* (London: H.M.S.O.), p. 40.  
 FOWLER, R. H., and GUGGENHEIM, E. A., 1939, *Statistical Thermodynamics* (Cambridge: University Press).  
 FRANK, A., and CLUSIUS, K., 1939, *Z. phys. Chem. B* **42**, 395.  
 FRENKEL, J., 1945, *J. Phys., U.S.S.R.*, **9**, 392.  
 GUGGENHEIM, E. A., 1945, *J. Chem. Phys.*, **13**, 253.  
 HARKINS, W. D., 1942, *J. Chem. Phys.*, **10**, 268.  
 HUANG, K., and WYLLIE, G., 1949, *Proc. Phys. Soc. A*, **62**, 180.  
 HUGGINS, M. L., and MAYER, J. E., 1933, *J. Chem. Phys.*, **1**, 643.  
 JAEGER, F. M., 1917, *Z. anorg. Chem.*, **101**, 1.  
 JURA, G., 1948, *J. Phys. Coll. Chem.*, **52**, 40.  
 KASSEL, L. S., and MUSCAT, M., 1932, *Phys. Rev.*, **40**, 627.  
 LENNARD-JONES, J. E., and DENT, B. M., 1928a, *Proc. Roy. Soc. A*, **121**, 247; 1928b, *Trans. Faraday Soc.*, **24**, 92.  
 LENNARD-JONES, J. E., and INGHAM, A. E., 1925, *Proc. Roy. Soc. A*, **107**, 636.  
 LENNARD-JONES, J. E., and TAYLOR, P. A., 1925, *Proc. Roy. Soc. A*, **109**, 476.  
 LONDON, F., 1937, *Trans. Faraday Soc.*, **33**, 8.  
 MAYER, J. E., 1933, *J. Chem. Phys.*, **1**, 270.  
 MAYER, J. E., and HELMHOLTZ, L., 1932, *Z. Phys.*, **75**, 19.  
 RAYLEIGH, LORD, 1890, *Phil. Mag.*, **30**, 285.  
 SLATER, J. C., 1939, *Introduction to Chemical Physics* (New York: McGraw-Hill).  
 STEFAN, J., 1886, *Wied. Ann.*, **29**, 655.  
 VERWEY, E. J. W., 1946, *Rec. des Trav. Chim. Pays-Bas*, **65**, 521.  
 YAMADA, V. M., 1923, *Phys. Z.*, **24**, 364; 1924, *Ibid.*, **25**, 52.



## On the Surface Free Energy of Certain Metals

By K. HUANG \* AND G. WYLLIE

H. H. Wills Physical Laboratory, Bristol University

*Communicated by N. F. Mott; MS. received 26th July 1948*

**ABSTRACT.** For the purpose of calculating the surface energy and surface double layer for a number of monovalent metals, a simple and yet adequate model is proposed, which does not have the disadvantages of models employed by previous authors. In this the valence electrons are treated according to a simple Sommerfeld model, and the positive charge of the ions is distributed uniformly through the metal. It is shown that by a suitable combination of the methods of Thomas-Fermi and of direct wave mechanics, both the surface energy and the strength of the double layer can be calculated. The surface double layers for the metals considered are found to lie in the range 0.1–0.5 ev. The contribution to the surface energy from the electrostatic energy in the double layer is found to be very small. In estimating the surface energy, the electrons in a metal can be considered as moving in a box with finite potential walls of suitably determined height  $\phi$ . A temperature-dependent term in the surface free energy due to the change in lattice vibrations caused by the free surface is also considered. The surface energies obtained from  $\phi$  determined in two independent ways agree closely and are found to agree with the experimental values of the surface tension of the liquid metals to within a factor 1.5.

### § 1. INTRODUCTION

IN spite of the high values of the surface tension exhibited by metals, it is an interesting fact that the ratio of the surface energy per surface atom to the heat of vaporization per atom is for monovalent metals of the order of 1 : 7, for zinc and cadmium about 1 : 3.5 and for mercury about 1 : 2.4, whereas for many other substances the ratio is of the order 1 : 2.

Shuttleworth (1949) has discussed the values of this ratio arising from various simple laws of force, applicable in ionic and molecular crystals, and finds results varying from 1 : 2 to 1 : 4 according to the law of force.

In the present work we show that the peculiarly low values of surface tension in monovalent metals result directly from the properties of the free electron gas. The model used is certainly fairly adequate for the monovalent metals in the solid state, so the surface free energy of the solid at the melting point has been calculated for these substances for comparison with the measured surface tension of the liquid. The calculated values are about 1.5 times the observed.

### § 2. REVIEW OF EARLIER WORK

The surface energy of metals has been treated theoretically by several workers (Frenkel 1917, Gogate and Kothari 1935, Dorfman 1943, Samoilovich 1945, Brager and Schuchowitzky 1946a, b). However, only the last two investigations are relevant to the present article. We shall consider briefly the models and methods employed by these authors before discussing those of the present work.

Samoilovich replaced the lattice of ions by a uniform distribution of positive charge and employed the Thomas-Fermi statistical method, according to which the total energy of the electrons is completely determined by the electron density distribution. The positive surface energy thus obtained, however, arises entirely

\* Now at the Department of Physics, University of Liverpool.

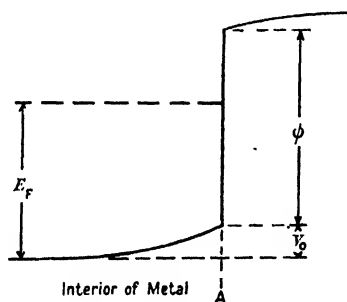
from the use of the Weizsäcker term, which corrects for the kinetic energy associated with the rapid change of electron density at the metal surface. This may easily be seen, since the original Thomas–Fermi method would give zero surface energy for that distribution of electron charge (not a solution of the Thomas–Fermi equation) which is uniform over the region containing the positive cloud and zero elsewhere. The distribution which satisfies the Thomas–Fermi equation, having lower energy (Lenz 1932), then gives a negative value for the surface energy.

Apart from the uncertainty of the Weizsäcker correction, this model makes no allowance for the different ionic fields of different metals, the surface tension being determined entirely by the density of positive charge which depends only on the valency and density of the metal.

In view of Samoilovich's result, that the positive surface energy is due to the increase in kinetic energy of the electrons imposed by the steep potential barrier at the surface, Brager and Schuchowitzky treated this effect by the direct wave-mechanical consideration of free electrons enclosed in a box with impenetrable walls, at which the wave function vanishes. They found that the total energy contained a term proportional to the surface and identified this term as the surface energy. This model neglects the electrical double layer at the surface and, more important, the finite values of the work function of real metals.

### § 3. THE MODEL

It is possible to find for the monovalent metals Li, Na, K, Rb, Cs, Cu, Ag, Au a model which avoids the faults of the two so far considered. Theoretical work on binding energy has shown that in these metals the positions of the conduction electrons are so strongly correlated that we may regard each electron as moving at any instant only in the field of the ion nearest to it, other ions being neutralized by the electrons on them. Then to a good approximation the electrons behave as free electrons at a constant potential  $V$ , where  $-eV$  is the mean potential energy between an electron and its nearest ion. The potential naturally vanishes outside a metal surface so that we have essentially a Sommerfeld picture of the metal. Thus the model we adopt is as follows. The positive charge of the metal ions is supposed to be uniformly distributed over a volume proportional to the number of ions. At the boundary of this volume we imagine a finite discontinuous jump in potential. The variation in potential energy of an electron as it passes through the surface is then as shown in the Figure.



The approximately exponential rise in the potential energy outside the boundary arises from the overlap of the wave functions beyond A. There is thus a distribution of negative charge in this region which may be calculated by wave

mechanics from the electron distribution inside the boundary. The latter is calculated by the Thomas–Fermi statistical method. The conditions that an equal resultant positive charge must remain inside the metal and that the field must vanish in the interior of the metal determine the solution uniquely.

The electronic surface energy is then divided into two terms: (i) that which results from “compressing” the electron gas within the potential well; this gives a smaller term than one would obtain if  $\phi$  were taken to be infinite as in the Russian work; (ii) the electrostatic energy of the double layer: this is found to be small.

### (i) Charge Penetration

We first find the relation between the charge density outside and inside the surface. If we take the  $x$ -axis normal to the surface ( $x=0$ ), the wave function representing a stream of electrons with momentum  $P$  incident on the surface at an angle  $\theta$  from the normal and undergoing reflection is

$$\begin{aligned}\psi_1 &= A(2m\phi)^{1/2} \exp [iP(y \sin \theta + x \cos \theta + \alpha)/\hbar] \\ &\quad + A(2m\phi)^{1/2} \exp [iP(y \sin \theta - x \cos \theta - \alpha)/\hbar], \quad x < 0 \quad \dots\dots(1) \\ \psi_2 &= 2AP \cos \theta \exp [(iPy \sin \theta - \beta x)/\hbar], \quad x > 0\end{aligned}$$

where  $\tan(\alpha P/\hbar) = \beta/P \cos \theta$  and  $\beta = \sqrt{(2m\phi - P^2 \cos^2 \theta)}$ . The density  $\rho(P, \theta)$  of electrons in the incident beam is

$$\rho(P, \theta) = |A|^2 2m\phi. \quad \dots\dots(2)$$

The number of particles per unit area outside the surface is then

$$\int_0^\infty |\psi_2|^2 dx = \hbar \rho(P, \theta) P^2 \cos^2 \theta, m\phi\beta. \quad \dots\dots(3)$$

In the Thomas–Fermi method the particle velocities at any point are random in direction; thus the density of electrons incident on the surface in the range of inclination to the normal from  $\theta$  to  $\theta + d\theta$  and for momentum from  $P$  to  $P + dP$  is given by

$$\rho(P, \theta) dP d\theta = 4\pi \hbar^{-3} P^2 \sin \theta dP d\theta.$$

Thus for the whole Fermi distribution the number  $n_s$  of electrons outside the surface per unit area is given by substituting for  $\rho(P, \theta)$  in (3) and integrating over  $P$  and  $\theta$ ; the result is

$$\begin{aligned}n_s &= \frac{1}{m\phi \hbar^2} \int_0^\infty dP \int_0^\pi \frac{P^4 \cos^2 \theta \sin \theta}{\sqrt{(2m\phi - P^2 \cos^2 \theta)}} d\theta \\ &= \frac{2m\phi}{\hbar^2} \left\{ \left( \frac{3}{4} - \frac{P_m^2}{4m\phi} \right) \sqrt{\left[ \frac{P_m^2}{2m\phi} \left( 1 - \frac{P_m^2}{2m\phi} \right) \right]} - \left( \frac{3}{4} - \frac{P_m^2}{2m\phi} \right) \sin^{-1} \sqrt{\left( \frac{P_m^2}{2m\phi} \right)} \right\}. \\ &\quad \dots\dots(4)\end{aligned}$$

Here  $P_m$  is the maximum momentum in the Thomas–Fermi distribution just inside the surface and the dimensionless quantity  $P_m^2/2m\phi$  is the ratio of the corresponding maximum kinetic energy of the electrons to the potential energy discontinuity  $\phi$ .

### (ii) The Thomas–Fermi Equation

Let  $E_m$  be the maximum electronic energy and  $V$  at any point the electrostatic potential measured from that in the interior of the metal; then having regard to the

constant density of positive charge inside the surface the Thomas-Fermi equation may be set up in the usual way :

$$\frac{d^2V}{dx^2} = -4\pi \left\{ -e \frac{8\pi}{3h^3} [2m(E_m + eV)]^{3/2} + \frac{3e}{4\pi r_0^3} \right\} \quad \dots\dots (5)$$

where  $4\pi r_0^3/3 = v_0$  is the atomic volume. When the dimensionless quantities

$$g = (E_m + eV)/E_F, \quad \xi = x/(r_0^3 E_F/3e^2)^{1/2} \quad \dots\dots (6)$$

where  $E_F = (9\pi/4)^{2/3} h^2/2mr_0^2$  are introduced, (5) becomes

$$d^2g/d\xi^2 = g^{3/2} - 1. \quad \dots\dots (7)$$

We notice that  $V \rightarrow 0$  in the interior of the metal, where  $E_m = E_F$ , so that  $g = 1$  corresponds to the distribution of one electron per atom, as in the interior far from the surface. We shall find the deviation of  $g$  from 1 to be small in the cases to be treated. It is thus for our purpose more convenient and sufficiently accurate to solve (7) approximately to the second order by setting

$$g = 1 - \Delta \quad \dots\dots (8)$$

and treating  $\Delta$  as small compared with unity.

On substituting (8) in (7) and expanding  $g^{3/2}$ , we find

$$d^2\Delta/d\xi^2 = 3\Delta, 2 - 3\Delta^2, 8 \quad \dots\dots (9)$$

when terms of degree higher than the second are neglected.

The asymptotic solution for large negative  $\xi$  (interior of metal) must clearly be of the form

$$\Delta \sim A \exp [\xi \sqrt{(3/2)}] \quad \text{as} \quad \xi \rightarrow -\infty. \quad \dots\dots (10)$$

Thus  $A$  is the only arbitrary constant to be determined. The approximate solution of (9), to the same order of accuracy as (9), which has the asymptotic form (10) is

$$\Delta = A \exp [\xi \sqrt{(3/2)}] - [A^2 \exp (\xi \sqrt{6})] / 12$$

or

$$g = 1 - A \exp [\xi \sqrt{(3/2)}] + [A^2 \exp (\xi \sqrt{6})] / 12. \quad \dots\dots (11)$$

If the electrostatic field is to vanish at large distances, the sum of the resultant charges inside and outside the surface must vanish. This condition determines  $A$ .

The electron density is proportional to  $g^{3/2}$ . Since when  $g = 1$  the density of electrons is  $3/4\pi r_0^3$ , the net charge density for any value of  $g$  is

$$\sigma_1 e = \frac{3e}{4\pi r_0^3} (1 - g^{3/2}) \quad \dots\dots (12)$$

and the total charge  $n_1 e$  per unit area inside the surface is thus given by

$$n_1 e = -\frac{3e}{4\pi r_0^3} \int_{-\infty}^0 (1 - g^{3/2}) dx. \quad \dots\dots (13)$$

Using (7) and (10), we find on integrating

$$n_1 e = -\frac{3e}{4\pi r_0^2} \left( \frac{r_0 E_F}{3e^2} \right)^{1/2} g_0' \quad \dots\dots (14)$$

where  $g_0 = (dg/d\xi)_{\xi=0}$ .

We have now to eliminate  $P_m$  from the expression (4) for the charge outside the surface. Just inside, we have  $P_m^2/2m = E_m + eV = E_F g_0$  where  $g_0 = (g)_{\xi=0}$ , so that  $n_2$  can be expressed as a function of  $g_0$  :

$$n_2 = \frac{2m\phi}{h^2} \left\{ \left( \frac{3}{4} - \frac{g_0}{2\lambda} \right) \sqrt{\left[ \frac{1}{\lambda} \left( 1 - \frac{g_0}{\lambda} \right) \right]} - \left( \frac{3}{4} - \frac{g_0}{\lambda} \right) \sin^{-1} \sqrt{\left( \frac{g_0}{\lambda} \right)} \right\} \quad \dots\dots (15)$$

where  $1/\lambda = E_F/\phi$ . It is possible to express  $g'_0, g_0$  in terms of  $A$

$$g_0 = 1 - A + A^2/12; \quad g'_0 = -[A - A^2/6]\sqrt{3/2} \quad \dots\dots(16)$$

and  $A$  is then determined by the numerical equality of the charges inside and outside the surface,

$$n_1(A) = -n_2(A). \quad \dots\dots(17)$$

Thus knowing  $r_0$  and  $\phi$  we can calculate the charge distribution near the surface. In the cases to be discussed we find that (17) can easily be solved by successive approximations, taking as the first,  $g_0 = 1$  in (15).

#### § 4. THE ELECTRICAL DOUBLE LAYER

The strength of the surface double layer is measured by the total change in electrostatic potential energy of an electron taken through the double layer; it is thus given by

$$-e[V(\infty) - V(-\infty)] = -eV(\infty), \quad \dots\dots(18)$$

since we have taken the potential energy to be zero in the interior of the metal.

To evaluate  $V(\infty)$ , the charge distribution outside the surface may be approximated by an exponential function

$$\sigma_2(x) = C \exp(-qx). \quad \dots\dots(19)$$

The density at  $x=0$  is  $C$ , which should be equal to the density obtained by integrating the wave mechanical solution  $|\psi_2(0)|^2$  as given by (1). Thus we find

$$C = \frac{16\pi}{15} \left( \frac{P_m}{\hbar} \right)^3 \frac{P_m^2}{2m\phi} \quad \dots\dots(20)$$

$q$  is then determined from the total charge :

$$n_1 = |n_2| = \int_0^\infty \sigma_2(x) dx = C/q. \quad \dots\dots(21)$$

The potential  $V(x)$  for  $x > 0$  can then be determined from the Poisson's equation

$$d^2V(x)/dx^2 = 4\pi e\sigma_2(x) = 4\pi eC \exp(-qx). \quad \dots\dots(22)$$

At  $x=0$  the approximate solution must be equal to the potential just within the surface, given by

$$-eV_0 + P_m^2/2m = E_m = E_F \quad \text{or} \quad eV_0 = -E_F(1 - g(0)). \quad \dots\dots(23)$$

The solution satisfying this boundary condition and the condition that the field vanishes at infinity is

$$V = 4\pi eC \{ \exp(-qx) - 1 \} / q^2 - E_F(1 - g(0)) / e. \quad \dots\dots(24)$$

So we find for the strength of the double layer

$$-eV(\infty) = 4\pi e^2 C / q^2 + E_F(1 - g(0)). \quad \dots\dots(25)$$

We may put this into a more convenient form for calculation by substitution from (14), (21) and (22)

$$-eV(\infty) = E_F g_0 [1 + 5g_0^{-5/2} g'_0{}^2 / 2\lambda] \quad \dots\dots(26)$$

where  $g_0, g'_0$  are defined as above. Numerical values for the metals considered are given in Table 1.

## § 5. THE SURFACE ENERGY

The calculation of surface energy on this model must take account of three terms: The effect dealt with by Brager and Schuchowitzky (1946a, b) which assumes impenetrable boundaries, the penetration of the barrier, and the energy of formation of the electrical double layer. The first two terms arise directly from wave-mechanical considerations, and are not really physically separable, but it is mathematically convenient to treat them separately.

(i) *The Term of Brager and Schuchowitzky*

This term is due to the increase of kinetic energy consequent on the impenetrability of the walls. Mathematically this condition is expressed in the requirement that the standing electron waves should have nodes at the walls. If we consider a cubical box of length  $L$ , then in the wave function  $\psi = \sin k_x x \sin k_y y \sin k_z z$  the wave numbers  $k_x, k_y, k_z$  must have respectively the values  $l\pi/L, m\pi/L, n\pi/L$  where  $l, m, n$  are positive integers.

Table 1

Metal	Cu	Ag	Au	Li	Na	K	Rb	Cs
$E_F$ (ev.)	7.05	5.5	5.5	4.7	3.15	2.03	1.77	1.52
$\phi$ (ev.)	15.4	13.7	16.3	9.85	8.13	6.48	6.09	5.62
$S_1 + S_2$ (erg cm <sup>-2</sup> )	2180	1400	1490	960	470	208	165	125
$S_3$ (erg cm <sup>-2</sup> )	8.0	2.3	2.2	4.5	1.3	0.32	0.2	0.12
$-F_s$ (erg cm <sup>-2</sup> )	360	257	240	66	34	25	21	18
$\sigma$ (erg cm <sup>-2</sup> )	1820	1140	1250	890	440	180	140	110
$\sigma$ (exp.) (erg cm <sup>-2</sup> )	1100	800	600-1000	—	290	200-400	—	—
Double layer (ev.)	0.55	0.29	0.28	0.43	0.25	0.12	0.10	0.08

$S_1 + S_2$  is the surface energy arising from the change in kinetic energy of the electron gas due to the presence of the surface.

$F_s$  is the surface free energy arising from the change in thermal vibrations.

$S_3$  is the electrostatic energy of the surface double layer.

$\sigma$  is the surface free energy obtained from these three terms.

These discrete states are conveniently represented as lattice points in the space  $(k_x, k_y, k_z)$  with lattice constant  $\pi/L$ . The number of occupied lattice points, multiplied by a factor 2 to allow for the alternative spin states, must be equal to the number of electrons to be accommodated and the total kinetic energy is the sum of

$$\hbar^2(k_x^2 + k_y^2 + k_z^2)/2m \quad \dots\dots (27)$$

over the occupied states. An energy proportional to  $L^3$  is obtained if we assume that the number of lattice points in a spherical octant of volume  $\pi k_m^3/6$  is just  $L^3 k_m^3/\pi^2$  and that the average energy is simply the integral average of (27) throughout the sphere. Clearly this procedure counts also points on the basal planes, but with weight  $\frac{1}{2}$ . These however do not represent permitted states since the corresponding wave functions vanish everywhere if they are zero on the walls.

These rejected points must be made good by taking just half as many at the surface of the sphere. The total energy corresponding to those points which were wrongly included is

$$\left(\frac{L}{\pi}\right)^3 \frac{2\pi}{4} \int_0^{k_m} \frac{\hbar^2 k^2}{2m} k dk = \frac{3\pi}{16m} \left(\frac{L\hbar}{\pi}\right)^2 k_m^4 \quad \dots\dots (28)$$

The total number of states thus rejected is  $3(L/\pi)^2 \pi k_m^2/4$ . The energy necessary to make them good at the surface of the sphere is

$$\left(\frac{L}{\pi}\right)^2 \frac{\pi k_m^2}{4} \cdot \frac{\hbar^2 k_m^2}{2m} \dots (29)$$

Thus the Brager-Schuchowitzky correction, which is the difference of (29) and (28), becomes  $3\pi(L/\pi)^2 \hbar^2 k_m^4/16m$ . Since the total surface of the cube is  $6L^2$  this is equivalent to a surface energy

$$S_1 = \pi P_m^4/8\hbar^2 m \text{ per unit area.} \dots (30)$$

Brager (1947) has further shown that the same expression is obtained for a spherical mass of material, so that its identification as a surface energy is reasonable.

### (ii) Term due to Barrier Penetration

Since the potential energy step at the surface of the metal is actually finite, electrons penetrate the barrier and their wave functions are not zero at the boundary. In fact each wave function has a definite shift in phase as though it possessed a virtual node a little outside the boundary, and there is a corresponding decrease in the energy of that state. Let us consider a cube of edge  $L$  as in the above section; suppose it to lie entirely in the region  $x < 0$  and let the face  $x = 0$  alone have a finite potential barrier, the others remaining infinite. We see that in equations (1), only the factor dependent on  $x$  is affected by the barrier. If we write  $\hbar^{-1} P \cos \theta = k_x$ , this factor becomes

$$\alpha \sin(k_x x - \delta) \dots (31)$$

where

$$\tan \delta = k_x / \sqrt{(2m\phi/\hbar^2 - k_x^2)}. \dots (32)$$

Thus the wave function has a phase-shift  $\delta$  at the boundary which tends to zero as  $\phi$  increases.

The boundary condition at the opposite wall, i.e. at  $x = -L$ , requires that  $\sin(-k_x L - \delta) = 0$ , whence

$$k_x = l\pi/L - \delta/L, \dots (33)$$

where  $l$  is an integer. Thus the substitution of the finite for the infinite barrier reduces  $k_x$  for each state by  $\delta/L$ , corresponding to an energy change

$$\Delta E = \hbar^2 \Delta(k_x^2 + k_y^2 + k_z^2)/2m = -(\hbar^2/m)k_x(\delta/L). \dots (34)$$

The number of states with  $k_x$  in the range  $dk_x$  is

$$\frac{1}{2}\pi(k_m^2 - k_x^2)(L/\pi)^3 dk_x. \dots (35)$$

Thus when  $L$  is large the energy change per unit surface is given by the integral

$$S_2 = \frac{\Sigma \Delta E}{L^2} = -\frac{\hbar^2}{2\pi^2 m} \int_0^{k_m} (k_m^2 - k_x^2) k_x \tan^{-1} \left[ \frac{k_x}{\sqrt{(2m\phi/\hbar^2 - k_x^2)}} \right] dx. \dots (36)$$

The integral is easily evaluated to give

$$S_2 = -\frac{P_m^4}{16m\hbar^2} \{3(2-\lambda)\sqrt{(\lambda-1)} + [3\lambda^2 - 8\lambda + 8] \sin^{-1} \lambda^{-1}\} \dots (37)$$

where, as before,  $\lambda = \phi/E_F$ .

(iii) *The Energy of Formation of the Electrical Double Layer*

Apart from the changes in kinetic energy, the energy of electrostatic interaction within the system is increased by the formation of the double layer. By some authors the surface energy has been attributed entirely to this source. In fact, however, we shall see that the electrostatic contribution is entirely negligible compared with the kinetic energy terms  $S_1$  and  $S_2$ .

Suppose as before that the surface lies in the plane  $x=0$ , and let the metal occupy the semi-infinite region for which  $x<0$ . It is convenient to consider first only the finite interval  $-L \leq x \leq L$ . The energy of the double layer is the sum of the self energy of the negative charge cloud, that of the positive cloud, and the interaction energy of the two, less the same quantity for a uniform neutral distribution confined to  $x<0$ .

The distribution of positive charge is unaltered and given by

$$\rho_+(x) = \rho_0, \quad x < 0; \quad \rho_+(x) = 0, \quad x > 0. \quad \dots\dots (38)$$

Thus its self energy is invariable and need not be considered. The energy of any arbitrary charge distribution may be referred to a standard state (zero of energy) which may be fixed arbitrarily. We find it most convenient to take the standard state to be that in which all the negative charge is concentrated in a surface layer at  $x=0$ . Then the potential energy between the negative charge in  $(x_1, x_1+dx_1)$  and that in  $(x_2-x_2+dx_2)$  is

$$-2\pi\rho(x_1)\rho(x_2)dx_1dx_2|x_1-x_2| \quad \dots\dots (39)$$

per unit area. For  $\rho(x_1)dx_1$  is the surface density in the infinite layer of thickness  $dx_1$  at  $x_1$ , and so  $2\pi\rho(x_1)dx_1\rho(x_2)dx_2$  is the constant repulsive force exerted on the charge in unit area of the layer between  $x_2$  and  $x_2+dx_2$ , while  $|x_1-x_2|$  gives the distance of separation. Similar reasoning shows that the potential energy due to the interaction of a layer of positive charge in the interval  $(x_1, x_1+dx_1)$  and the negative charge in  $(x_2-x_2+dx_2)$  is

$$-2\pi x_1\rho_+(x_1)\rho(x_2)dx_1dx_2 - 2\pi|x_1-x_2|\rho_+(x_1)\rho(x_2)dx_1dx_2 \quad \dots\dots (40)$$

per unit area. Here the first term gives the work done to bring the negative charge  $\rho(x_2)dx_2$  from  $x=0$  to  $x=x_1$ , which is clearly negative. The second term gives the work done to separate it again from the positive charge by a distance  $|x_1-x_2|$ , which is always positive. The total energy  $\Sigma$  is obtained by combining (39) and (40) and integrating over the various pairs of elements.

$$\Sigma = \pi \int_{-L}^L dx_1 \int_{-L}^L dx_2 \{ |x_1-x_2| [-\rho(x_1)\rho(x_2) - 2\rho_+(x_1)\rho(x_2)] - 2x_1\rho_+(x_1)\rho(x_2) \}. \quad \dots\dots (41)$$

For the uniform distribution we have simply

$$\rho(x) = -\rho_+(x).$$

Let  $\rho'(x) = -\rho_+(x) + \Delta\rho(x)$  be the density of the double layer distribution determined above. The energy of the double layer is then

$$\begin{aligned} S_3 &= \pi \int_{-L}^L dx_1 \int_{-L}^L dx_2 |x_1-x_2| \{ \rho_+(x_1)\Delta\rho(x_2) + \rho_+(x_2)\Delta\rho(x_1) + \rho_+(x_1)\rho_+(x_2) \\ &\quad - 2\rho_+(x_1)\Delta\rho(x_2) - \Delta\rho(x_1)\Delta\rho(x_2) - \rho_+(x_1)\rho_+(x_2) \} \\ &= -\pi \int_{-L}^L dx_1 \int_{-L}^L dx_2 |x_1-x_2| \Delta\rho(x_1)\Delta\rho(x_2). \end{aligned}$$



The second term of (41) drops out directly on forming the difference since the total negative charge  $\int \rho(x_2) dx_2$  is the same in each of the two cases. Since  $\Delta\rho(x)$  diminishes exponentially in both directions we may pass to the limit  $L \rightarrow \infty$  and find

$$S_2 = - \int_{-\infty}^{\infty} dx_1 \int_{-\infty}^{\infty} dx_2 |x_1 - x_2| \Delta\rho(x_1) \Delta\rho(x_2). \quad \dots\dots (42)$$

For  $x > 0$ ,  $\Delta\rho(x)$  is the density of electronic charge which we have called  $-e\sigma_2(x)$ . According to (19), it can be represented approximately by the exponential function  $-eC \exp(-qx)$ . For  $x < 0$ ,  $\Delta\rho(x)$  is the net charge density  $\sigma_1 e$  defined by (12) which may be written

$$\sigma_1 e \simeq \frac{3e}{4\pi r_0^3} \left[ \frac{3}{2} A \exp(\sqrt{\frac{3}{2}} x) \right], \quad \dots\dots (43)$$

where we have neglected the term in  $A^2$ . In the cases considered in the Table the inaccuracy thus introduced is of the order of 1% only. Thus we may write

$$\Delta\rho(x) = Q_2 \exp(-q_2 x), \quad x > 0; \quad \Delta\rho(x) = Q_1 \exp(+q_1 x), \quad x < 0, \quad \dots\dots (44)$$

where

$$Q_2 = - \frac{16\pi e}{15} \left( \frac{P_m}{h} \right)^3 \frac{P_m^2}{2m\phi}, \quad Q_1 = \frac{9e}{8\pi r_0^3} A,$$

$$q_1 = \sqrt{\frac{3}{2}} (r_0 E_F / 3e^2)^{-1/2} r_0^{-1} \quad \text{and} \quad Q_2/q_2 = -Q_1/q_1. \quad \dots\dots (45)$$

The integration in (42) can then be carried out, giving

$$S_3 = \frac{61600 A^2}{V} \left( \frac{0.528}{10^8 r_0} \right)^{3/2} \left( 1 + \frac{15\lambda}{4\sigma_0^{5/2}} A \right) \quad \dots\dots (46)$$

where  $P_m$  is eliminated using the equation  $P_m^2/2m = g_0 E_F$  and  $V$ ,  $r_0$  are respectively the volume per mole and effective atomic radius in the metal.

The total electronic contribution to the surface energy of the metal is thus given by the sum of the three terms  $S = S_1 + S_2 + S_3$  where  $S_1$ ,  $S_2$ ,  $S_3$  are given respectively by (30), (37) and (46).

Only  $S_3$  involves a quantity which cannot be explicitly given, namely  $A$ , which depends on the solution of (17), and determines the value of the electrostatic potential at the boundary, (10), (16). However, we find (see Table 1) that  $S_3$  is only of the order of a few ergs, which is in fact less than the error to be expected from a simple model.

#### (iv) Other Terms

A contribution to the surface energy from the repulsive interaction of the closed electron shells of the metal ions is to be expected.

This interaction, which is well represented by a central force, would according to Shuttleworth contribute about half as much to the surface free energy per atom as to the binding energy. Thus if it contributes a rather small fraction to the cohesion, it will in the monovalent metals contribute between three and four times that fraction of the surface energy. This is negligible both for the bulky alkali metals and for the noble metals with their hard completed d-shells (Fuchs 1936, Huntington and Seitz 1942).

A more important effect is the change in character of the lattice vibrations of the metal in the presence of a free surface. Brager and Schuchowitzky (1946 b) have considered an extension of the Debye model of a crystal to a large thin sheet of material with free boundaries, and obtain a term proportional to the total surface

area in the thermal energy. This surface internal energy due to the lattice vibrations is given by them as

$$E_s = \frac{2 \cdot 15 kT}{v^{2/3}} \frac{1}{x^2} \left[ 2 \int_0^x \frac{u^2 du}{e^u - 1} - \frac{x^3}{e^x - 1} \right] \text{ ergs/cm}^2, \quad \dots\dots (47)$$

where  $x = \Theta/T$  and  $\Theta$  is the Debye characteristic temperature of the material. The corresponding value of the free energy is

$$F_s = E_s - T \int_0^T T^{-1} (dE_s/dT) dT$$

which can be reduced to

$$F_s = -A_m Z(\Theta/T) \quad \dots\dots (48)$$

where  $A_m = 2 \cdot 15 k(\Theta)/v^{2/3}$  and  $Z(x) = x^{-3} \int_0^x \frac{u^2 du}{e^u - 1}$ , so that  $A_m$  is a constant for each metal determined by the Debye characteristic temperature and the atomic volume.

The integral occurring in the function  $Z$  has previously been tabulated (Zanstra 1931), but only for rather large intervals of the argument. Since  $Z(x)$  varies as  $1/x$  for small  $x$ , it was decided to recalculate the integral and  $Z$ . The results are shown in Table 2.

Table 2.  $I(x) = \int_0^x \frac{u^2 du}{e^u - 1}$ ;  $Z(x) = x^{-3} I(x)$

$x$	$I(x)$	$Z(x)$	$x$	$I(x)$	$Z(x)$	$x$	$I(x)$	$Z(x)$
0.1	0.004 835	4.835	0.4	0.069 865	1.092	0.7	0.192 808	0.562
0.12	0.006 916	4.003	0.42	0.076 498	1.033	0.72	0.202 558	0.543
0.14	0.009 351	3.408	0.44	0.083 381	0.979	0.74	0.212 471	0.524
0.16	0.012 131	2.962	0.46	0.090 507	0.930	0.76	0.222 543	0.507
0.18	0.015 250	2.615	0.48	0.097 871	0.885	0.78	0.232 767	0.491
0.2	0.018 700	2.338	0.5	0.105 465	0.844	0.8	0.243 139	0.475
0.22	0.022 474	2.111	0.52	0.113 283	0.806	0.82	0.253 654	0.460
0.24	0.026 565	1.922	0.54	0.121 321	0.771	0.84	0.264 307	0.446
0.26	0.030 966	1.762	0.56	0.129 572	0.738	0.86	0.275 093	0.433
0.28	0.035 670	1.625	0.58	0.138 030	0.707	0.88	0.286 008	0.420
0.3	0.040 668	1.506	0.6	0.146 689	0.679	0.9	0.297 046	0.408
0.32	0.045 956	1.403	0.62	0.155 543	0.653	0.92	0.308 204	0.396
0.34	0.051 527	1.311	0.64	0.164 588	0.628	0.94	0.319 477	0.385
0.36	0.057 373	1.230	0.66	0.173 817	0.605	0.96	0.330 859	0.374
0.38	0.063 488	1.157	0.68	0.183 226	0.583	0.98	0.342 348	0.364

It should be noted that the contribution to the total surface free energy from this source is negative.

This calculation of the surface free energy due to lattice vibrations is, of course, only valid for the crystalline solid. For the liquid, consideration of capillary waves (Frenkel 1946) provides the most reasonable approach, but in the absence of a more detailed theory of liquid structure such considerations cannot be subjected to quantitative test.

We have therefore calculated, for approximate comparison with the experimental results for the surface tension of the liquid metals near their melting points,

the total surface free energies of the solid metals at their melting points, using the expression

$$\begin{aligned}\sigma &\simeq S_1 + S_2 + F_s \\ &= \frac{1.44 \times 10^5}{V^{4/3}} \left\{ \frac{\pi}{8} - \frac{1}{16} \left[ 3(2 - \lambda)\sqrt{(\lambda - 1)} + (3\lambda^2 - 8\lambda + 8) \sin^{-1} \sqrt{\left(\frac{1}{\lambda}\right)} \right] \right\} \\ &\quad - 2.11(\Theta/V^{2/3})Z(\Theta/T_m) \text{ ergs/cm}^2 \quad \dots\dots (49)\end{aligned}$$

where  $V$  is the mole volume in cubic centimetres and  $\Theta$ ,  $T_m$  the Debye characteristic temperature and melting point respectively in degrees absolute.  $\lambda$  is the ratio of the barrier height  $\phi$  to the maximum Fermi energy  $E_F$ .

## § 6. NUMERICAL RESULTS

Theoretical work on the noble and alkali metals has shown that the conduction electrons of these metals behave almost like free electrons. Thus we can use the ordinary electron mass in our calculation, so that the electronic contribution to the surface energy depends only on the height of the potential barrier  $\phi$  and the mole volume  $V$ . The estimate of  $\phi$  most consonant with the model we employ is obtained from the consideration that the binding energy  $W$  of the metal (atomic ionization energy plus heat of sublimation) is related to  $\phi$  by the equation (Huang 1948)

$$-W = \sum_i \left( -\phi + \frac{\hbar^2 k_i^2}{2m} \right) = N \left( \frac{3}{5} E_F - \phi \right). \quad \dots\dots (50)$$

The calculated values of the various terms in the surface energy and the strength of the double layer for the noble and alkali metals are given in Table 1, together with the experimental values used in the calculation. The experimental values of the surface energies of the liquid metals as given in Brager and Schuchowitzky (1946) are given in the Table for comparison.

The agreement with the theoretical values is within a factor of about 1.5, which is as much as can reasonably be expected from this model. The relative values for different metals agree well. There are no definite experimental values for the double layer moments, but the values found are in substantial agreement with more elaborate theoretical calculations obtained (Bardeen 1936) in this theory of the work function.

One might notice that the differences  $(\phi - E_F)$  formed from the values of  $\phi$  and  $E_F$  given in Table 1 are much higher than the experimental values for the work functions of the same metals. This discrepancy is, however, only apparent. It is a consequence of the fact that we have used a single barrier height  $\phi$  for all electrons, whereas in reality different electrons have effectively different barriers owing to the difference in the exchange correlation energy  $-\epsilon(k)$  for electrons with different wave number  $k$  (cf. Seitz 1940). Thus the effective barrier for an electron with wave number  $k$  is higher than that for an electron at the top of the Fermi distribution (wave number  $k_0$ ), by  $\epsilon(k) - \epsilon(k_0)$ . If  $\chi$  is the observed work function, so that the barrier for an electron at the top of the distribution is  $\phi(k_0) = \chi + E_F$ , the effective barrier for an electron with wave number  $k$  is  $\phi(k) = \chi + E_F + \epsilon(k) - \epsilon(k_0)$ . The mean value for all electrons is

$$\bar{\phi} = \chi + E_F + \bar{\epsilon} - \epsilon(k_0) = \chi + E_F + 0.916e^2/r_0 - 0.712e^2/r_0 \quad \dots\dots (51)$$

where the expressions for  $\bar{\epsilon}$ ,  $\epsilon(k_0)$  are from Seitz (1940).

If the mean barrier heights thus determined are used in the calculation, results for the surface energy are obtained which differ only very slightly from those given in Table 1.

#### ACKNOWLEDGMENT

The authors are grateful to Miss Littleton of this Department, who has kindly performed the computations for the integrals  $I(x)$  and  $Z(x)$  given in Table 2.

#### REFERENCES

- ADAM, N. K., 1941, *Physics and Chemistry of Surfaces*, 3rd ed. (Oxford: University Press).  
 BARDEEN, J., 1936, *Phys. Rev.*, **49**, 653.  
 BRAGER, A., 1947, *J. Phys. Chem., U.S.S.R.*, **21**, 623.  
 BRAGER, A., and SCHUCHOWITZKY, A., 1946 a, *Acta Physicochim. (U.R.S.S.)*, **21**, 13; 1946 b, *Ibid.*, **21**, 1001.  
 DORFMAN, S., 1943, *C.R. Acad. Sci., U.R.S.S.*, **41**, 386.  
 FRENKEL, J., 1917, *Phil. Mag.*, **33**, 297; 1946, *Kinetic Theory of Liquids* (Oxford: University Press).  
 FUCHS, K., 1936, *Proc. Roy. Soc. A*, **153**, 622.  
 GOGATE, D. V., and KOTHARI, D. S., 1935, *Phil. Mag.*, **20**, 1136.  
 HUANG, K., 1948, *Proc. Phys. Soc.*, **60**, 161.  
 HUNTINGTON, H. B., and SEITZ, F., 1942, *Phys. Rev.*, **61**, 315.  
 LENZ, W., 1932, *Z. Phys.*, **77**, 713.  
 SAMOILOVICH, H., 1945, *Acta Physicochim. (U.R.S.S.)*, **20**, 97.  
 SEITZ, F., 1940, *Modern Theory of Solids* (London and New York: McGraw-Hill).  
 SHUTTLEWORTH, R., 1949, *Proc. Phys. Soc. A*, **62**, 167.  
 ZANSTRA, J., 1931, *Z. Astrophys.*, **2**, 1.

## The Emission Spectrum of Sodium Hydride

BY R. C. PANKHURST

Imperial College, London \*

*Communicated by R. W. B. Pearse; MS. received 27th July 1948*

**ABSTRACT.** Observations on the spectrum of sodium hydride have been extended to longer wavelengths (from 4600 Å. to 6450 Å.) and photographed under high dispersion. Analysis of the data thus obtained gives values of the vibrational and rotational constants for several new vibrational levels, among which the lowest levels of the excited state are of especial interest.

The intensity distribution has been calculated from the wave functions appropriate to potential energy curves based on the constants derived from the analysis of the band system. The theoretical estimates are found to be in fair agreement with the experimental results.

#### § 1. INTRODUCTION

THE absorption spectrum of sodium hydride was reported by Hori in 1930. The values assigned to  $\nu'$  were subsequently raised by one unit as a result of work on the emission spectrum (Hori 1931), and later by a further three units on the basis of a comparison with the deuteride (Olsson 1934).

No data were available for these lowest three vibrational levels of the excited state. They are of especial interest because the values of  $\omega'_v$  and  $B'_v$  for the hydrides of the alkali metals behave anomalously in that they first increase with

\* Now at the National Physical Laboratory, Teddington.

$v'$  instead of decreasing throughout. The present work was undertaken with a view to determining the missing data; the preliminary results have been reported elsewhere (Pankhurst 1941).

## § 2. EXPERIMENTAL

The spectrum was obtained from a hydrogen discharge tube source of the type described by Pearse and Gaydon (1938), the discharge passing through a quartz constriction containing a pellet of sodium. The tube was cooled by immersion in water, a current of from 0.3 to 1.0 amp. being supplied from a 2,500 v. transformer.

The band system was photographed with 6-m. gratings, using Ilford H.P.2 and hypersensitive panchromatic plates. Between 4600 Å. and 5660 Å. a dispersion of 1.9 Å/mm. was obtained by means of the second order of a grating with 11,000 lines/inch (433 per mm.); further to the red the first order of a grating with 15,000 lines/inch (591 per mm.) was employed, giving a dispersion of 2.6 Å/mm. The whole system was also photographed on a Hilger E2 quartz prism spectrograph.

## § 3. ANALYSIS OF EXPERIMENTAL RESULTS

The system is of the many-line type, with no apparent band-heads. It arises from a  $^1\Sigma-^1\Sigma$  transition and resolves, on analysis, into R- and P- branches. Some 25 new bands were identified, involving transitions from seven vibrational levels. (A copy of the detailed rotational analysis of each band may be seen on application to the author.)

*Rotational and Vibrational Analysis.* Mean values of the observed combination differences, obtained by averaging the values for all the bands obtained from each of the vibrational energy-levels, are set out in Table 1. The rotational analysis was based on the usual power-series representation of the rotational energy, the constants thus derived being given at the foot of the Table. The closeness to which the experimental results are represented is shown by the agreement between the observed combination differences and those calculated from the derived rotational constants: the agreement is everywhere well within the probable error of the observations.

The vibrational analysis is set out in Table 2, which includes Hori's (1931) values for bands involving transitions to the lowest three levels of the ground state. The vibrational energy in each of the two electronic states is represented by the power-series expressions for  $G(v + \frac{1}{2})$  given in the Table. The accuracy to which these expressions fit the experimental data is indicated by the agreement of the calculated band-origins included in Table 2.

*Note on Accuracy.* It is important not to claim high accuracy for the absolute values of constants obtained as coefficients in power-series expansions such as those for  $F(K)$ ,  $B_v(u)$ ,  $D_v(u)$ ,  $H_v(u)$  and  $\omega_v(u)$ , because a substantial alteration to any one of the coefficients can be largely compensated for by appropriate adjustments of the others. It is in fact possible to find several polynomials of the same degree but with corresponding coefficients considerably different, both of which represent the original observations to within the experimental error. Although this may be immaterial if a power series is to be used merely for the purpose of interpolation, it introduces considerable uncertainty when (as in this present case) the coefficients are to be interpreted as physical properties of the system.

Table 1. Rotational Analysis

(a) *Excited State*(i) Mean values of the observed combination differences,  $\Delta'_2(K) = R(K) - P(K)$ 

$K \backslash v'$	1	2	3	4	5	6	7
1	11.85	10.86	11.52	11.69		12.23	
2	18.46	18.68	19.42	19.33		19.77	19.38
3	25.22	26.16	26.87	26.94		27.43	27.17
4	32.66	33.61	34.20	34.57	34.84	34.89	34.68
5	39.47	40.91	41.60	42.17	42.43	42.25	42.37
6	46.84	48.26	49.13	49.68	49.95	50.06	50.02
7	54.00	55.54	56.46	57.15	57.49	57.55	57.43
8	60.94	62.67	63.82	64.57	64.79	64.99	64.91
9	67.76	69.72	71.06	71.81	72.37	72.33	72.25
10	74.54	76.70	78.17	79.10	79.55	79.68	79.56
11	81.21	83.59	85.19	86.14	86.60	86.87	86.72
12	87.82	90.31	92.07	93.16	93.66	93.94	93.87
13	94.23	96.94	98.76	100.03	100.70	100.96	100.85
14	100.63	103.46	105.37	106.80	107.49	107.74	107.67
15	106.88	109.83	112.00	113.41	114.17	114.49	114.38
16	113.00	116.18	118.38	119.90	120.68	120.84	121.06
17	118.97	122.19	124.67	126.29	127.13	127.51	127.56
18	124.84	128.22	130.67	132.46	133.50	133.95	133.83
19	130.65	134.10	136.69	138.44	139.50	140.03	139.97
20	136.42	139.76	142.47	144.24	145.42	145.98	145.97
21	141.75	145.40	148.11	150.21	151.29	151.96	151.78
22	147.12	150.75	153.66	155.63	156.97	158.18	157.42
23	152.28	156.16	159.12	161.15	162.38		162.79
24	157.54	161.37	164.33	166.42	167.71		168.26
25	162.70	166.37	169.31	171.49	172.73		172.95
26	167.60	171.29	174.24	176.46	178.01		
27		176.13	179.06	181.36	182.70		
28		180.80	183.73		187.50		
29		185.32	188.20		191.92		
30		189.33	192.61		196.10		
31			196.90				

(ii) Values derived for the rotational constants (in  $\text{cm}^{-1}$ )

$v'$	1	2	3	4	5	6	7
$B'_v$	1.823	1.875	1.908	1.930	1.938	1.941	1.936
$D'_v \times 10^4$	-2.25	-2.25	-2.20	-2.19	-2.07	-2.01	-1.93
$H'_v \times 10^8$	5.10	3.85	3.04	2.87	2.02	1.5-	1.24

$$F'_v(K) = B'_v K(K+1) + D'_v K^2(K+1)^2 + H'_v K^3(K+1)^3.$$

The above constants may be represented by the equations :

$$B'_v = B'_0 + \alpha'_1 v' + \alpha'_2 v'^2 + \dots \quad (v' = v' + \frac{1}{2})$$

$$D'_v = D'_0 + \beta'_1 v' + \beta'_2 v'^2 + \dots$$

$$H'_v = H'_0 + \gamma'_1 v' + \gamma'_2 v'^2 + \dots$$

with the following values of the coefficients :

$B'_0 = 1.696$ , whence  $I'_0 = 16.31 \times 10^{-40} \text{ gm.cm}^2$  and  $r'_0 = 3.200 \text{ \AA.}$ ;  $\alpha'_1 = 0.1083$ ;  $\alpha'_2 = -0.0175$ ;  $\alpha'_3 = 0.00129$ ;  $\alpha'_4 = 0.000042$ ;  $D'_0 = -2.27 \times 10^{-4}$ ;  $\beta'_1 = -0.01 \times 10^{-4}$ ;  $\beta'_2 = 0.008 \times 10^{-4}$ ;  $H'_0 = 5.7 \times 10^{-8}$ ;  $\gamma'_1 = -0.65 \times 10^{-8}$ .

Table 1 (*cont.*)(b) *Ground State*

(i) Mean values of the observed combination differences,

$$\Delta_2''(K) = R(K-1) - P(K+1)$$

$\begin{smallmatrix} v'' \\ K \end{smallmatrix}$	3	4	5	6	7	8
1	26.45	24.90	25.71			
2	44.33	42.50	42.07	41.33	39.27	
3	61.98	60.22	58.39	56.70	54.70	
4	79.62	77.24	74.96	72.58	70.46	
5	97.13	94.32	91.48	88.60	85.83	83.01
6	114.63	111.15	107.98	104.62	101.14	97.94
7	131.96	128.06	124.30	120.34	116.59	112.66
8	149.24	144.76	140.45	136.12	131.74	127.30
9	166.41	161.37	156.53	151.83	146.94	141.77
10	183.27	177.84	172.50	167.16	161.77	156.45
11	200.10	194.15	188.27	182.41	176.62	170.69
12	216.73	210.35	203.84	197.49	191.27	184.73
13	233.14	226.23	219.32	212.46	205.70	198.74
14	249.40	241.93	234.63	227.20	219.84	212.52
15	265.49	257.57	249.68	241.78	233.93	226.05
16	281.31	272.81	264.49	256.10	247.77	239.36
17	296.76	288.02	278.97	270.19	261.34	252.43
18	312.17	302.78	293.36	284.03	274.71	265.35
19	327.24	317.26	307.60	297.57	287.77	277.99
20	342.03	331.61	321.24	310.93	300.62	290.22
21	356.41	345.52	334.77	—	313.17	
22	370.70	359.40	348.10	336.84	325.35	
23	384.61	372.82	360.98	349.45	337.51	
24	398.25	385.92	373.71	361.15		
25	411.55	398.68	386.02			
26	424.45	411.13	398.07			
27	437.15	423.30	409.65			
28	449.32	435.10	421.00			
29	461.10	447.28	432.01			
30	472.63	—	442.63			
31	483.79	468.72	452.75			

(ii) Values derived for the rotational constants (in  $\text{cm}^{-1}$ )

$v''$	3	4	5	6	7	8
$B_v''$	4.438	4.302	4.180	4.051	3.919	3.790
$D_v'' \times 10^4$	-3.31	-3.13	-3.29	-3.25	-3.05	-3.04
$H_v'' \times 10^8$	2.17	1.13	2.58	2.70	0.69	1.10

$$F_v''(K) = B_v''K(K+1) + D_v''K^2(K+1)^2 + H_v''K^3(K+1)^3.$$

The variation of  $B_v''$  may be represented by the equation  $B_v'' = B_0'' + a_1''v'' + a_2''v''(v''+1)$  with  $B_0'' = 4.886$ , whence  $I_0'' = 5.66 \times 10^{-40} \text{ gm.cm}^2$  and  $r_0'' = 1.885 \text{ \AA.}$ ;  $a_1'' = -0.129$ . Mean value of  $D_v'' = -3.15 \times 10^{-4}$ ; mean value of  $H_v'' = 1.7 \times 10^{-8}$ .

*Energy of Dissociation.* The usual equation

$$D = -\omega_e^2/4x_e\omega_e \quad \dots\dots(1)$$

assumes a regular closing up of the vibrational energy levels. For NaH this condition is satisfied in the ground state but not in the excited state, for which  $\omega_v$  at first increases with  $v$ . The above equation was therefore used only for the ground state; the value for the excited state was obtained from that for the ground state by assuming that the products of dissociation were a normal sodium atom and a normal hydrogen atom from the ground state, and an excited ( $^2P$ ) sodium atom and a normal hydrogen atom from the excited state. The results were:

$$D' = 11,650 \text{ cm}^{-1} = 1.44 \text{ ev.}; \quad D'' = 17,410 \text{ cm}^{-1} = 2.16 \text{ ev.}$$

#### § 4. POTENTIAL ENERGY CURVES, WAVE FUNCTIONS AND INTENSITY DISTRIBUTION

In order to estimate the intensity distribution by the methods of wave mechanics it is first necessary to determine the potential energy curves for the two electronic states and then to calculate the wave functions for all the vibrational levels. If  $\psi'$  and  $\psi''$  denote wave functions for the excited state and the ground state respectively, the intensity of each band ( $v'$ ,  $v''$ ) is obtained from the expression  $\int (\psi' \bar{\psi}'' + \bar{\psi}' \psi'') dr$ , where the bars denote complex conjugates.

*Excited State.* The potential energy in the excited state was written in the form

$$V'(r) = a'_0 \xi'^2 (1 + a'_1 \xi' + a'_2 \xi'^2 + \dots) \quad \dots\dots(2)$$

where

$$\xi' = (r - r'_e)/r'_e \quad \dots\dots(3)$$

with the coefficients evaluated from the vibrational and rotational constants using the expressions given by Dunham (1932) but neglecting the small correction terms of the order  $B_{v'}^2/\omega_{v'}^2$ . The values obtained were:

$$a'_0 = 14,220 \text{ cm}^{-1}; \quad a'_1 = 0.949; \quad a'_2 = 3.25; \quad a'_3 = -7.09.$$

The resulting potential curve lay entirely within the parabola  $a'_0 \xi'^2$  and resembled another parabola of smaller latus rectum. This observation was exploited when calculating the wave functions  $\psi'$  (§ 5). For most molecules the right-hand limb of the potential curve falls below the simple parabola; the irregularity in this instance is associated with the anomalous behaviour of the constants for the excited state.

*Ground State.* In the ground state the potential curve given by a similar power series flattens prematurely, for positive values of  $\xi$ , between  $v''=4$  and  $v''=5$ . As dissociation could not have taken place at these values of  $v''$ , it was concluded that an expression of the form of equation (2) is not suitable for representing the potential energy of NaH in the ground state.

The expression due to Morse (1929) was therefore used instead:

$$V_M(r) = D[1 - e^{-a''(r - r_e)}]^2 \quad \dots\dots(4)$$

with  $D'' = 17,410 \text{ cm}^{-1}$  and  $a'' = 1.070 \text{ \AA}^{-1}$ .

*Intensity Distribution.* The intensity of the band  $v' \rightarrow v''$  is

$$I(v', v'') = C \exp \{ -hcG'(v')/kT \} v_0^4 \left[ \int_0^\infty (\psi' \bar{\psi}'' + \bar{\psi}' \psi'') dr \right]^2 \quad \dots\dots(5)$$

where  $C$  is an arbitrary constant,  $k$  the gas constant per molecule and  $T$  the absolute temperature.



Table 2. Vibrational Scheme

$v''$	0	1	2	3	4	5	6	7	8	Mean $\Delta G'$	$\tau'$
1	—	—	—	—	—	17324-4(948-8)16375-6 [17323-9] [16375-3] (329-9)	—	—	—	—	1
2	—	—	—	19659-8(1021-2)18638-6(984-3)17654-3(948-7)16705-6 [19659-0] [18638-2] [17653-7] [16705-1] (337-1)	—	—	—	—	—	329-9	2
3	23282-8(1132-9)22149-9(1094-5)21055-4(1058-5)19996-9(1021-1)18975-8(984-3)17991-5 [23282-6] [22149-4] [21054-2] [19996-6] [18975-7] [17991-2] (343-8) (343-6) (343-4) (343-9) (343-7) (343-6)	—	—	—	—	—	—	16130-1 [16129-9] (343-6)	—	337-2	3
4	23626-6(1133-1)22493-5(1094-7)21398-8(1058-0)20340-8(1021-3)19319-5 [23626-8] [22493-6] [21398-5] [20340-8] [19319-9] (350-0) (349-4) (349-3) (349-4) (349-9)	—	—	—	—	—	17386-6(912-9)16473-7 [17386-9] [16474-1] (349-6)	—	—	343-7	4
5	23976-0(1133-2)22842-8(1094-6)21748-2(1057-5)20690-7(1021-2)19669-5(984-5)18685-0(948-8)17736-2(912-8)16823-4(877-0)15946-4 [239-765] [22843-3] [21748-1] [20690-5] [19669-6] [18685-1] [17736-6] [16823-8] [15946-6] (353-8) (354-0) (354-0)	—	—	—	—	—	—	—	349-6	349-6	5
6	24329-8(1133-0)23196-8(1094-6)22102-2 [24330-5] [23197-2] [22102-1] (357-4)	—	—	—	—	20023-2(984-4)19038-8 [20023-6] [19039-1] (357-2)	—	—	16300-5 [16300-6] (354-1)	353-9	6
7	24687-2(1132-7)23554-5(1094-9)22459-6 [24687-6] [23554-4] [22459-2] (359-4)	—	—	—	—	20380-4(984-4)19396-0 [20380-7] [19396-2] (357-2)	—	17534-6(876-9)16657-7 [17534-9] [16657-7] (357-2)	357-4	357-4	7
8	25046-6(1133-2)23913-4(1094-5)22818-9 [25046-8] [23913-5] [22818-4] (360-0)	—	—	—	—	—	—	—	359-2	359-2	8
9	25406-6(1132-6)24274-0 [25407-0] [24273-7] (360-2)	—	—	—	—	—	—	—	360-3	360-3	9
10	25766-8(1132-8)24634-0 [25767-2] [24633-9] (359-5)	—	—	—	—	—	—	—	360-1	360-1	10
11	26126-3(1132-8)24993-5 [26126-5] [24993-3] (357-7)	—	—	—	—	—	—	—	359-5	359-5	11
									357-7	357-7	

The entries without brackets are the wave-numbers of the band-origins obtained from the rotational analysis: their differences are given between round brackets. The numbers in square brackets correspond to the equation

$$v = v_0 - G'(u') - G''(u''),$$

with

$$\begin{aligned} G'(u') &= \omega_e u' - x_e' \omega_e u'^2 - y_e' \omega_e u'^3 - \dots \\ &= 310 \cdot 6 u' - 5 \cdot 41 u'^2 - 0 \cdot 197 u'^3 - 0 \cdot 000073 u'^4 - 0 \cdot 000073 u'^5, \\ G''(u'') &= \omega_e'' u'' - x_e'' \omega_e'' u''^2 - y_e'' \omega_e'' u''^3 - \dots \\ &= 1172 \cdot 2 u'' - 19 \cdot 72 u''^2 + 0 \cdot 160 u''^3 - 0 \cdot 005 u''^4 \end{aligned}$$

and

$$v_0 = 22719 \cdot 1 \text{ (cm}^{-1}\text{)}.$$

Table 3 a. Observed Intensity Distribution

$v'$	$v''$	3	4	5	6	7	8
0							
1				3	3		
2			4	4	3		
3		3	6	5		1	
4		5	3			3	
5		3	1	2	3	2	1
6			3	5			3
7			4	3		4	2
8							

Table 3 b. Calculated Intensity Distribution

$v'$	$v''$	3	4	5	6	7	8
0		4	13	31	49	62	90
1		25	60	99	95	71	62
2		61	100	96	50	8	1
3		75	70	32	0	10	16
4		55	21	0	16	20	9
5		15	0	9	9	3	0
6		0	13	9	0	3	3
7		5	11	1	4	6	1
8		7	3	1	5	1	0

12	26484.0 [26484.1] (354.3)	—	12	354.3
13	26838.3 [26839.2] (352.3)	—	13	352.3
14	27190.6(1132.9)26057.7 [27191.1] [26057.8] (348.6) (348.3)		14	348.4
15	27539.2(1133.2)26406.0 [27539.2] [26406.0] (343.6) (344.3)		15	343.9
16	27882.8(1132.5)26750.3 [27883.1] [26749.9] (340.0) (340.0)		16	340.0
17	28222.8(1132.5)27090.3 [28222.5] [27089.3] (334.1) (333.4)		17	333.7
18	28556.9(1133.2)27423.7 [28557.0] [27423.8] (330.1) (330.0)		18	330.0
19	28887.0(1133.3)27753.7 [28886.7] [27753.5] (323.7)		19	323.7
20	29210.7 [29211.6]		20	323.7

Mean $\Delta G''$	1132.9	1094.6	1058.0	1021.2	984.4	948.8	912.8	876.9
-------------------	--------	--------	--------	--------	-------	-------	-------	-------

## § 5. COMPUTATIONAL DETAILS

*Excited State.* As an analytical solution was not available for the wave functions appropriate to a power-series potential curve, they were obtained for the excited state by modifying those for the parabola  $a_0\xi'^2$ , for which the solution may be written  $\psi = bF(v, r)$  where  $b^2 = 2\pi\sqrt{(\mu c\omega_e/\hbar)}$  and

$$F(v, r) = \sqrt{\left(\frac{1}{2^v v! \sqrt{\pi}}\right)} \exp(-s^2/2) H_v(s),$$

$\mu$  being the reduced mass of the molecule, and  $H_v$  denoting successive Hermitian polynomials with  $s = b^2(r - r_e)$ .

The modification consisted simply of adjusting the abscissae so as to "fit" the wave functions to the limbs of the power-series curve instead of to the limbs of the parabola. The ordinates for each vibrational level were then multiplied by a constant factor in order to maintain normalization. This procedure, although somewhat crude, is to some extent justified by the resemblance of the power-series potential curve to another parabola of smaller latus rectum (as already noted in § 4), and might be expected to give results at least as accurate as the eye-estimates of the observed intensity distribution. As a check, a parabola was fitted to the power-series curve by the method of least squares; its wave function was evaluated for one vibrational level ( $v' = 5$ ) and was found to agree reasonably well with that obtained by the arbitrary method indicated above.

*Ground State.* The wave functions corresponding to equation (4) have been derived by Morse (1929) and may be written in the form

$$\psi_M = F_v F_{e,v} F_{e,v,1} \quad \dots\dots (6)$$

where

$$F_v = (ka)^{\frac{1}{2}}, \quad \dots\dots (7)$$

$$F_{e,v} = (N_{v,v})^{-\frac{1}{2}} \frac{\Gamma(k-v)}{v!} \exp\{i\pi(k-v-1)\}, \quad \dots\dots (8)$$

$$F_{e,v,1} = e^{-\frac{1}{2}z^2} \sum_{r=0}^{\infty} \frac{(k-v-1)(k-v-2)\dots(k-v-r)}{2!r!} z^{2r-2} - \dots \quad \dots\dots (9)$$

$$\text{and} \quad k = 4\pi(2\mu D)^{\frac{1}{2}}/a\hbar; \quad z = k \exp\{-a(r-r_e)\}, \quad \dots\dots 10)$$

$$N_{v,v} = [\Gamma(k-v)]^2 \sum_{p=0}^v \Gamma(k-2v+p-1)/\Gamma(p-1). \quad \dots\dots (11)$$

The numerical computation of equations (6) to (11) would involve a prohibitive amount of labour, partly owing to the large number of points needed to define the wave curves for the higher vibrational levels, and partly because each term in equation (9) has to be evaluated to extremely high accuracy in order to obtain relatively few significant figures in the sum, since the positive and negative terms are so nearly equal and opposite. Equation (6) was therefore evaluated for only three of the levels (namely  $v'' = 0, 4$  and  $6$ ) and an approximate method was devised for circumventing the numerical evaluation of equation (6) for the other vibrational levels.

This approximate method is suggested by the observation that if the exponential in equation (4) is expanded in series, the first term is of the form  $a_0\xi'^2$ , for which the wave functions can more readily be obtained. For the remaining levels of the ground state, therefore, wave functions were first calculated for the simple parabola and then modified in a manner similar to that adopted for the

excited state. Normalization was preserved by scaling the ordinates by the constant factor appropriate to each vibrational level. The method was justified by a comparison of the values of  $(\psi'\bar{\psi}'' + \bar{\psi}'\psi'')$  (cf. equation (12) below) with those obtained from the exact solutions for  $v'' = 0, 4$  and  $6$ .

*Intensity Distribution.* With the potential energy curves of equations (2) and (4),

$$\psi'\bar{\psi}'' + \bar{\psi}'\psi'' = \psi'\chi'', \quad \dots\dots(12)$$

where  $\chi'' = F_c'' F_{c,v}'' F_{c,v,r}''$  with  $F_c''$  and  $F_{c,v,r}''$  given by (7) and (9) but with

$$F_{c,v}'' = 2(N_{c,v}'')^{-\frac{1}{2}} \frac{\Gamma(k'' - v'')}{v''!} \cos(k'' - v'' - 1)\pi. \quad \dots\dots(8a)$$

In evaluating equation (5), a temperature of  $680^\circ\text{C}$ . was assumed, corresponding to a value of  $1.5$  for  $hc/kT$ . This assumed temperature may be a little high, but will not materially affect the general comparison with the experimental results. The arbitrary constant  $C$  was so chosen as to give values of intensity on a scale of  $100$  for the strongest band.

#### § 6. THEORETICAL RESULTS

The calculated intensity distribution is compared with the experimental eye-estimates in Table 3 (inset in Table 2). The theoretical values show the three observed loci of maximum intensity indicated by heavy type in the Deslandres array. Moreover, the positions of these loci are given with fair accuracy, despite the high values of  $v'$  and  $v''$  at which the secondary maxima occur, where the approximate wave functions used might be expected to be least reliable. In view of the several approximations introduced in the numerical work, and the various assumptions involved in the basic theory, the general agreement with the observed intensities is surprisingly good.

The trend of the primary (Franck-Condon) locus of maximum intensity for small values of  $v'$  explains completely the drastic extension of the spectrum which had proved to be necessary in order to obtain bands involving transitions from the lower vibrational levels of the excited state.

#### ACKNOWLEDGMENTS

The above investigation was done under the supervision of Dr. R. W. B. Pearse, who has also offered valuable suggestions regarding the preparation of this paper. Acknowledgment is also due to the Board (now Ministry) of Education for the award of a Royal Scholarship, during part of the tenure of which the experimental work was undertaken.

#### REFERENCES

- DUNHAM, J. L., 1932, *Phys. Rev.*, **41**, 721.  
 HORI, T., 1930, *Z. Phys.*, **62**, 352; 1931, *Ibid.*, **71**, 478.  
 MORSE, P. M., 1929, *Phys. Rev.*, **34**, 57.  
 OLSSON, E., 1934, *Z. Phys.*, **93**, 206.  
 PANKHURST, R. C., 1941, *Nature, Lond.*, **147**, 643.  
 PEARSE, R. W. B., and GAYDON, A. G., 1938, *Proc. Phys. Soc.*, **50**, 201.

## Bending Vibrations of a Linear Chain

By L. KELLNER

Imperial College of Science and Technology, London S.W. 7

*MS. received 28th May 1948, and in amended form 12th October 1948*

**ABSTRACT.** The bending frequencies of a linear chain of  $n$  mass points have been calculated using a harmonic potential function involving forces between second neighbours. The proper boundary conditions are introduced and a general formula for the bending frequencies is derived.

THE longitudinal vibrations in a linear chain consisting of equidistant mass points held together by quasi-elastic forces have been known for some time although no attempts have been made to compute the bending frequencies of a linear chain containing a finite number of mass points. In the case of a continuous distribution of mass points, this case passes into the case of the transverse oscillations of an infinitely thin rod.

The linear chain will be assumed to consist of  $n$  equidistant mass points of mass  $m$  which are held together by valence and angle forces, i.e. forces between immediate and second neighbours. The potential function  $V$ , assumed to be harmonic, of such a chain will then be

$$2V = f \sum_{i=1}^{n-1} l_i^2 + a^2 \phi \sum_{i=2}^{n-1} \lambda_i^2, \quad \dots\dots (1)$$

where the  $l_i$  are the variations in the distances between  $P_{i+1}$  and  $P_i$ , the  $\lambda_i$  are the angles between  $P_{i-1}$ ,  $P_i$  and  $P_{i+1}$  produced by the oscillations, and  $a$  is the equilibrium distance between the mass points. If  $u_i$ ,  $v_i$  are the horizontal and vertical displacements respectively of the vibrating mass points, it is easily seen that

$$l_i = u_{i+1} - u_i; \quad \lambda_i = (-1)^i (2v_i - v_{i-1} - v_{i+1})/a, \quad \dots\dots (2)$$

assuming that  $u_i^2$  and  $v_i^2$  are very much less than  $a^2$ . It follows that the vibrations of such a chain split up into two branches, that of the valence vibrations due to the force  $f$  between adjacent masses, and that of the bending frequencies produced by the force  $\phi$  between second neighbours. The valence frequencies arise from the longitudinal displacements of the particles and the bending frequencies from their movements normal to the direction of the chain, in strict analogy to the longitudinal and transverse oscillations of a bar or rod.

The differential equations of the transverse vibrations are, according to (1) and (2)

$$\left. \begin{aligned} -m\ddot{v}_i &= (-1)^i a \phi (2\lambda_i + \lambda_{i-1} + \lambda_{i+1}) \\ \text{or} \quad -m\ddot{v}_i &= \phi (v_{i-2} - 4v_{i-1} + 6v_i - 4v_{i+1} + v_{i+2}). \end{aligned} \right\} \quad \dots\dots (3)$$

If we write  $\Delta^{(1)}v_i = v_{i+1} - v_i$ ;  $\Delta^{(2)}v_i = v_{i+2} - 2v_{i+1} + v_i$  and in general

$$\Delta^{(k)}v_i = \Delta^{(k-1)}v_{i+1} - \Delta^{(k-1)}v_i,$$

the system of equations (3) can be written in the form of difference equations:

$$m\ddot{v}_i = \phi \Delta^{(4)}v_{i+2}, \quad \dots\dots (4)$$

and  $\lambda_i$  becomes  $-(-1)^i \Delta^{(2)}v_{i-1}$ . Equation (4) is analogous to the differential equation determining the transverse vibrations of a bar  $\rho \ddot{y} = -\kappa^2 q (d^4 y / dx^4)$  where  $\rho$  is the density of the material,  $y$  the vertical displacement of the point with the

abscissa  $x$ ,  $\kappa$  the radius of gyration about a line through the axis, and  $q$  Young's modulus (Rayleigh 1929). Using the expression (2), the system (4) transforms into

$$-m\ddot{\lambda}_i = \phi(\lambda_{i-2} + 4\lambda_{i-1} + 6\lambda_i + 4\lambda_{i+1} + \lambda_{i+2}). \quad \dots\dots(5)$$

There are  $n-2$  simultaneous equations corresponding to the  $n-2$  valence angles.

The boundary conditions can now be derived from the equations for the two initial and final angles which have to be evaluated separately from (1) and (2). These equations will be somewhat different from (5) since the points  $P_1$ ,  $P_2$ ,  $P_{n-1}$  and  $P_n$  have not the full complement of second neighbours. There result the equations (6):

$$\left. \begin{aligned} -m\ddot{\lambda}_2 &= \phi(6\lambda_2 + 4\lambda_3 + \lambda_4); & -m\ddot{\lambda}_3 &= \phi(4\lambda_2 + 6\lambda_3 + 4\lambda_4 + \lambda_5); \\ -m\ddot{\lambda}_{n-2} &= \phi(\lambda_{n-4} + 4\lambda_{n-3} + 6\lambda_{n-2} + 4\lambda_{n-1}); & -m\ddot{\lambda}_{n-1} &= \phi(\lambda_{n-3} + 4\lambda_{n-2} + 6\lambda_{n-1}). \end{aligned} \right\} \quad \dots\dots(6)$$

These four equations can be said to have the same form as (5) if it is assumed that

$$\left. \begin{aligned} \lambda_0, \lambda_1, \lambda_n, \lambda_{n+1} &= 0 \\ \Delta^{(2)}v_{-1}, \Delta^{(2)}v_0, \Delta^{(2)}v_{n-1}, \Delta^{(2)}v_n &= 0 \end{aligned} \right\} \quad \dots\dots(6a)$$

The equations (6a) represent the four boundary conditions; they indicate that no force couples act on the two ends of the chain. In the case of the continuous bar they reduce to the conditions that  $d^2y/dx^2=0$  for  $x=0$  and  $x=l$  if the two ends of the bar represented by  $x=0$  and  $x=l$  are free.  $\lambda_r$  is now assumed to be  $\lambda_r = \cos \omega t \{ A e^{ir\alpha} + B e^{-ir\alpha} + (-1)^r C e^{r\beta} + (-1)^r D e^{-r\beta} \}$ . If the first three boundary conditions are applied, the following value obtains for  $\lambda_i$ :

$$\begin{aligned} \lambda_i &= A' \cos \omega t \{ (-1)^{n+i} \sin \alpha \sinh(n-i)\beta - \sin(n-i)\alpha \sinh \beta \\ &\quad + (-1)^n \sin i\alpha \sinh(n-1)\beta + (-1)^n \sin(i-1)\alpha \sinh n\beta \\ &\quad - (-1)^i \sin n\alpha \sinh(i-1)\beta - (-1)^i \sin(n-1)\alpha \sinh i\beta \}. \end{aligned} \quad \dots\dots(7)$$

The last boundary condition leads to

$$\begin{aligned} 0 &= 2 \sin \alpha \sinh \beta + (-1)^n \sin(n+1)\alpha \sinh(n-1)\beta \\ &\quad + (-1)^n \sin(n-1)\alpha \sinh(n+1)\beta + 2(-1)^n \sin n\alpha \sinh n\beta. \end{aligned} \quad \dots\dots(8)$$

The relation between  $\alpha$  and  $\beta$  can be determined in the following way: if equation (5) is solved by a term  $A a^i \cos \omega t$  for  $\lambda_i$ , it follows that  $a$  is a solution of the equation

$$a^4 + 4a^3 + (6\phi - m\omega^2)a^2/\phi + 4a + 1 = 0. \quad \dots\dots(9)$$

If the roots of (9) are  $a_1, a_2, a_3$  and  $a_4$ , we have

$$\sum_{i=1}^4 a_i = -4, \quad \prod_{i=1}^4 a_i = 1, \quad \sum_{i=1}^4 a_i = \sum_{i \neq j \neq k} \sum a_i a_j a_k.$$

These relations are fulfilled if  $a_2 = 1/a_1$ ,  $a_3 = 1/a_4$ . If then  $a_1 = e^{i\alpha}$ ,  $a_2 = e^{-i\alpha}$ , it follows that  $a_3 + 1/a_3 = -4 - 2 \cos \alpha$ . If  $a_3$  is assumed to be  $-e^\beta$ , the relation between  $\alpha$  and  $\beta$  is

$$\cosh \beta = 2 + \cos \alpha. \quad \dots\dots(10)$$

Expression (9) shows that  $6\phi - m\omega^2/\phi = \sum_{i \neq j} a_i a_j = 2(1 - 2 \cos \alpha \cosh \beta)$ , therefore

$\omega = 2\pi\nu$  can be determined, taking (10) into account:

$$m\omega^2 = 4\phi(1 + \cos \alpha)^2; \quad \nu = [(1 + \cos \alpha)/\pi]^{1/2} (\phi/m) \quad 0 < \alpha < \pi. \quad \dots\dots(11)$$

For every value of  $n$ , there are  $n-2$  solutions for  $\cos \alpha$ . All the possible bending

frequencies are contained within the limits  $\nu_{\min}=0$  and  $\nu_{\max}=(2/\pi)\sqrt{(\phi/m)}$ .  $\beta$  can assume values between 0 and 1.76. The bending frequencies of a linear chain are doubly degenerate in the two planes through the axis so that the  $n-2$  frequencies (11) represent  $2n-4$  vibrations. The  $n-1$  valence vibrations are given by the well known formula

$$\nu = \frac{\sin \frac{1}{2}}{\pi} \sqrt{\frac{f}{m}}, \quad \alpha = \pi k n, \quad k = 1, 2, \dots, n-1. \quad \dots\dots (12)$$

The  $3n-5$  possible vibrations of a linear chain consisting of  $n$  mass points are therefore represented by the equations (11) and (12) provided that the particles are subject to valence and angle forces.

#### REFERENCE

RAYLEIGH, LORD, 1929, *Theory of Sound* (London: Macmillan).

## LETTERS TO THE EDITOR

### Sessile Dislocations

Let us consider what would at first sight seem to be the simplest sort of dislocation in a close-packed cubic lattice, made, in imagination, by cleaving the crystal part way between two close-packed (i.e.  $\{111\}$ ) planes and inserting a close-packed half-plane into the cleft. This can be done with maintenance of close-packing of nearest neighbours for all atoms except those at the edge of the half-plane, i.e. along the dislocation line itself. This would appear to be an ordinary Taylor dislocation (Taylor 1934). However, should this dislocation now glide, in the ordinary manner of a Taylor dislocation, in the direction normal to the added plane, it will bring an ever-increasing number of atoms out of the close-packing arrangement into another arrangement of more open packing and consequently of higher energy: so that this glide is prevented by a large restoring force—so large, we may easily conclude, that the glide would not take place under any macroscopically applicable stress. Such a dislocation will be called “sessile”, in contrast with “glissile” dislocations—those which are capable of glide.

The situation may be clarified by considering the displacement vectors—Burgers vectors (Burgers 1939)—of various possible dislocations. The displacement vector of a perfect dislocation is a lattice vector,  $(\frac{1}{2}a, \frac{1}{2}a, 0)$ , with its various permutations, in the close-packed cubic lattice. Besides these perfect dislocations, which transfer atoms from one lattice position to another, there are also imperfect dislocations which transfer atoms from lattice positions to twin-lattice positions. Such are Shockley’s “half-dislocations” (Heidenreich and Shockley 1948) with Burgers vector  $(a/3, a/6, a/6)$  which arise by the dissociation of perfect dislocations in a  $\{111\}$  plane, e.g.

$$(\frac{1}{2}a, \frac{1}{2}a, 0) \rightarrow (a/3, -a/6, -a/6) + (a/6, -a/3, a/6).$$

Such is also the dislocation with Burgers vector  $(a/3, a/3, a/3)$  described in the first paragraph of this letter, and one with Burgers vector  $(-a/3, -a/3, -a/3)$  obtained by removing instead of adding a close-packed half-plane. Unlike perfect dislocations of opposite sign these two are not equivalent to each other.

Now, atoms in twin-lattice positions only fit correctly on the appropriate composition plane (a  $\{111\}$  plane in these cases) of the main lattice. Hence, whereas a perfect dislocation can glide, without changing the amount of misfit in the crystal, in whatever surface contains the line of the dislocation and its Burgers vector, imperfect dislocations increase the misfit unless they glide in a composition plane. Consequently the only kind of imperfect dislocation which can glide freely is one whose Burgers vector lies in the composition plane of the twin relationship to which it belongs. The imperfect dislocations of  $(a/3, a/6, a/6)$  type, lying in  $\{111\}$  planes, are glissile. The imperfect dislocations  $(a/3, a/3, a/3)$ , not lying in  $\{111\}$  planes, and also being incapable of dissociating into glissile partial dislocations, are sessile. The only simple way in which they can move in the lattice is by diffusion processes in which they gain or lose atomic vacancies.

The ways in which these sessile dislocations can be formed (e.g. by the aggregation of vacancies, or by relatively complicated dislocation reactions) will be the subject of a longer communication. It is thought, however, worth while to draw immediate attention to their existence. They have obvious importance in connection with the strength of metals (being fixed sources of stress which exert forces on glissile dislocations) and with crystal growth (Burton, Cabrera and Frank 1949). The sessile Taylor dislocations here described produce the same type of permanent terrace on the {111} faces they intersect as is produced by an  $(a, 0, 0)$  screw dislocation in the {100} face of a simple cubic crystal model.

H. H. WILLS Physical Laboratory,  
University of Bristol.  
22nd December 1948.

F. C. FRANK.

BURGERS, J. M., 1939, *Proc. Kon. Ned. Akad. Wet.*, **42**, 293.  
BURTON, W. K., CABRERA, N., and FRANK, F. C., 1949, *Nature, Lond.* (in the press).  
HEIDENREICH, R. D., and SHOCKLEY, W., 1948, *The Strength of Solids* (London: Physical Society),  
p. 57.  
TAYLOR, G. I., 1934, *Proc. Roy. Soc. A*, **145**, 362.

## CONTENTS FOR SECTION B

	PAGE
Dr. D. BROWN, Mr. C. F. COLEMAN and Mr. J. W. LYTTLETON. A Photoelectric Type of Acoustic Spectrograph using Sound Film . . . . .	149
Dr. K. HOSELITZ and Dr. M. MCCAIG. The Cause of Anisotropy in Permanent Magnet Alloys . . . . .	163
Mr. L. MACKINNON. Magnetic Behaviour of Zinc and Cadmium at Low Temperatures. . . . .	170
Dr. E. E. SALTPETER and Dr. R. E. B. MAKINSON. On the Dielectric Properties of a Gas Discharge. . . . .	180
Mr. D. A. WRIGHT. Thermionic Emission from Oxide Coated Cathodes. . . . .	188
Letters to the Editor :	
Mr. R. W. G. HUNT. Visual Adaptation and the Apparent Saturation of Colours. . . . .	203
Mr. H. H. H. WATSON. Experiments on the Effect of Gas Scattering on Betatron Output. . . . .	206
Reviews of Books . . . . .	208
Contents for Section A . . . . .	211
Abstracts for Section A . . . . .	211

## ABSTRACTS FOR SECTION B

*A Photoelectric Type of Acoustic Spectrograph using Sound Film*, by D. BROWN, C. F. COLEMAN and J. W. LYTTLETON.

**ABSTRACT.** An account is given of an apparatus which analyses non-recurrent wave-forms such as occur in speech, so that frequency-distribution is represented against time in an FT-diagram. From the theory governing such diagrams, no unique representation is possible, the result depending on the analysing convention adopted, but all conventions are governed by the uncertainty relation  $\Delta F \Delta T \geq 1$ . The method employed is an optical one which analyses a continuously moving sound film by means of a frequency-scanning disc, so producing an oscillograph pattern which is photographed on to another moving film. Typical analyses are reproduced and discussed, mainly "speech patterns" which show the composition very clearly. Advantages include the ability to record the amplitude and phase of each component, also the ability to change the analysing convention in any desired manner, for example to give the error-function convention which leads to minimum uncertainty. The paper concludes with considerations of resolving power, spectral line profiles, and amplifier band width requirements.



*The Cause of Anisotropy in Permanent Magnet Alloys*, by K. HOSELITZ and M. McCAIG.

**ABSTRACT.** Measurements of magnetostriction have been made on samples of an anisotropic permanent magnet alloy. From the results it is concluded that the domain magnetization is, in the absence of a field, along that easy crystallographic direction which makes the smallest angle with the axis of anisotropy. This view is supported by measurements of the remanence. The ideal arrangement which obtains after hardening seems to be slightly disturbed during the subsequent tempering operation.

*Magnetic Behaviour of Zinc and Cadmium at Low Temperatures*, by L. MACKINNON.

**ABSTRACT.** Following the recent discovery of the de Haas-van Alphen effect in zinc by Marcus at liquid hydrogen temperatures, the effect has been investigated at liquid helium temperatures using (for the most part) a torsion method similar to that used by Shoenberg in investigating bismuth. The effect in zinc takes the form of a variation of the susceptibility along the hexagonal axis which is periodic in the applied magnetic field. An attempt has been made to correlate the results with Landau's explicit formulae and to derive the various relevant parameters (such as effective masses, and degeneracy temperature) for the electrons causing the effect. Only qualitative agreement has been found, so that too much reliance should not be placed on the physical significance of the figures derived; however, it would appear that, as in the case of bismuth, the effect is caused by only a few times  $10^{-6}$  electrons per atom. In spite of its very similar structure, cadmium did not show the effect; it had, however, at liquid helium temperatures, a magnetic anisotropy some six times that at room temperature.

*On the Dielectric Properties of a Gas Discharge*, by E. E. SALPETER and R. E. B. MAKINSON.

**ABSTRACT.** Formal expressions are derived for the space currents and electrode currents produced by a sinusoidal potential difference of angular frequency  $\omega$  applied between a pair of electrodes at a distance  $d$  apart and immersed in a gas discharge. It is shown that the ionized gas behaves like an isotropic medium of dielectric constant  $\{1 - 4\pi ne^2/m\omega^2\}$  and zero conductivity only in the limiting case of  $\beta = v/\omega d \ll 1$  where  $v$  is the R.M.S. velocity of the free electrons in the gas. The variation of the equivalent dielectric constant and conductivity of the gas with  $\beta$  are sketched. Extensions of Green's reciprocity theorem and of a theorem on induced currents given by W. Shockley are derived in the appendix.

*Thermionic Emission from Oxide Coated Cathodes*, by D. A. WRIGHT.

**ABSTRACT.** It is shown experimentally that with Ba/Sr oxide cathodes, the saturated emission depends on the core material in use, and there is some correlation between total coating resistance and saturated pulsed emission. The steady-state D.C. emission is lower than the pulsed emission, but the D.C. emission measured immediately on application of the anode voltage is similar to the pulsed emission. The difference is due to a decay effect with a time constant in the range 1/1,000–1/10 sec., which is similar in many respects to the decay effect studied in an earlier paper on conductivity measurements. It is shown that the application of semiconductor theory can give a consistent account of coating conductivity and emission, provided the concentration of barium in stoichiometric excess is about  $3 \times 10^{17}$  atoms/cm<sup>3</sup>. This figure has some experimental support. It is shown that the presence of an interface layer of the type actually detected should cause decay phenomena with a time constant less than 1  $\mu$ sec. and in most cases less than 1/10  $\mu$ sec., so that the decay from pulsed to D.C. emission is not due to the capacity effects introduced by the presence of the layer.

With thoria there is little difference thermionically when studied as a coating on tantalum or on tungsten, or as a ceramic tube, and the pulsed emission is about twice the D.C. emission. Experiment and theory indicate that thoria is an excess semiconductor containing a stoichiometric excess of about  $10^{18}$  atoms/cm<sup>3</sup> of thorium. There is very little sensitivity to oxygen, however, at temperatures above 1,850° K.

# THE PROCEEDINGS OF THE PHYSICAL SOCIETY

## Section A

VOL. 62, PART 4

1 April 1949

No. 352 A

### **The Performance of Infra-Red Spectrometers as Limited by Detector Characteristics**

BY E. F. DALY AND G. B. B. M. SUTHERLAND

Pembroke College, Cambridge

*MS. received 11th June 1948*

**ABSTRACT.** The performance of the average infra-red spectrometer is conditioned mainly by the characteristics of the detector employed. Assuming a minimum usable energy level at the exit slit, the square of the minimum frequency band embraced by the exit slit is proportional to the minimum energy level and to the focal length of the collimator, and inversely proportional to the angular dispersion of the prism or grating, the area of the collimator mirror, the energy flux at the entrance slit and the slit length. If, however, the time of response of the detector is taken into account, the inter-relation of spectrum scanning speed, signal-to-noise ratio and resolving power must be considered. For this purpose a simplified model of an infra-red detector has been used, defined by three parameters. This allows the relative merits of detectors to be assessed and the performance of any given spectrometer with a specified detector to be estimated. The inter-relation of resolving power and spectral scanning speed has been examined for "chopped-beam" and "video" presentation.

#### § 1. INTRODUCTION

**D**URING the past ten years several new detectors of infra-red radiation have been developed which are superior to the older ones in speed and sensitivity. The general characteristics of these have been reviewed (Sutherland and Lee 1948, Williams 1948) and some applications have been made in the spectroscopic field, e.g. to achieve cathode-ray presentation of spectra (Daly and Sutherland 1947) or higher resolution of complex spectra (Sutherland, Blackwell and Fellgett 1946), but it is important to enquire into the conditions under which these various detectors may best be used in spectroscopy. If the optimum performance is to be obtained from a spectrometer designed to use one of these detectors it is necessary to investigate carefully the inter-relations between scanning speed, resolving power and detector characteristics. This in turn leads to a consideration of the best way in which to define the characteristics of a detector which is being used for spectroscopic purposes.

In general the resolving power obtainable with an infra-red spectrometer is limited by the performance of the detector and not by the usual optical criteria. We propose therefore to introduce the term "separating power" to indicate the minimum frequency band which can be embraced by the exit slit for a given ratio of the signal produced by the detector to the inherent noise. It will then be the speed with which a spectrum can be scanned for a given separating power which determines the performance of a spectrometer. We start by considering how separating power is related to the optical constants of the spectrometer, working above the limits imposed by aberration and diffraction but employing the specified

minimum usable power input of the detector and ignoring its speed of response. We next consider how this minimum power level is related to the speed of response of the detector, the detector noise and the scanning speed for a given signal-to-noise ratio at the display. In order to do so, however, it is desirable first to define the characteristics of the detector in terms of three parameters, viz.  $\sigma$  the responsivity (say in microvolts per microwatt) when the full signal has been reached,  $\tau$  the time constant (time to reach  $1/e$  of the full signal) and  $\mu$ , inherent noise of the detector. Finally the complex inter-relations between scanning speed and separating power are derived in graphical form for various detectors operating in a spectrometer of specified design.

## §2. MODEL SPECTROMETER

The spectrometer design employed as the basis for discussion is shown in Figure 1. Assuming a small plane black-body source, the power  $W_\nu$  in the

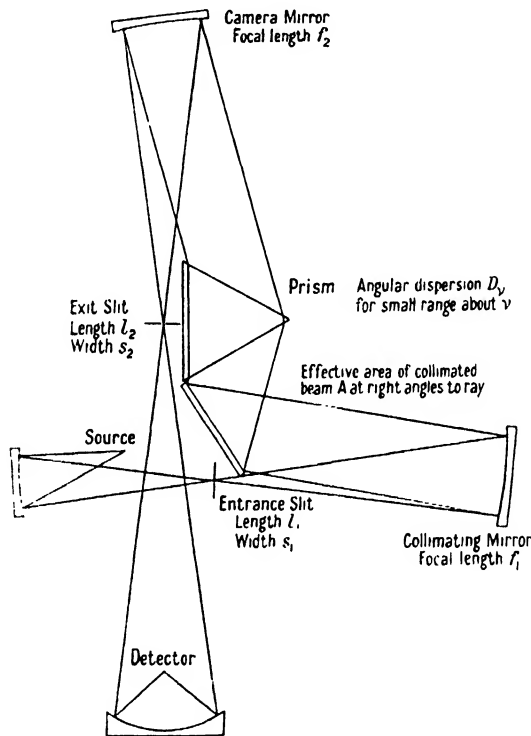


Figure 1. Elementary spectrometer.

spectral range  $\nu$  to  $\nu + \delta\nu$  passing the entrance slit and accepted into the collimated beam is given by

$$W_\nu = \frac{A s_1 l_1}{f_1^2} \frac{1}{\pi} \int_\nu^{\nu + \delta\nu} E_\nu d\nu, \quad \dots (1)$$

where  $A$  is the area of the collimator mirror normal to the ray, and we assume the prism is sufficiently large to take all this radiation,  $s_1$ ,  $l_1$ ,  $f_1$  are the width and length of the entrance slit and the focal length of the collimating mirror respectively, and  $E_\nu$  has its usual value

$$\frac{2\pi\nu^2}{c^2} \frac{h\nu}{\exp(h\nu/kT) - 1}.$$

If it is assumed that the interval  $\delta\nu$  is sufficiently small for  $E_\nu$  to remain constant,  $\int_{\nu}^{\nu+\delta\nu} E_\nu d\nu \simeq E_\nu \delta\nu$ , and the energy passing the entrance slit will be dispersed at the exit slit over an area  $D_\nu f_2 \delta\nu (l_1 f_2 / f_1)$ . In this it is assumed either that  $\delta\nu$  is large compared with one slit width, so that the expression holds regardless of aberration and diffraction, or that  $\delta\nu$  is comparable with a slit width only when this is sufficiently large for aberration and diffraction to be neglected. Here  $D_\nu$  is the angular dispersion, also assumed constant over the range  $\nu$  to  $\nu + \delta\nu$ , and  $f_2$  is the focal length of the camera mirror. The power  $W'_\nu$  passing the exit slit will then be given by the product of the exit slit area and the power per unit area in the dispersed image at the slit. Making the assumption that  $s_2/s_1 = l_2/l_1 = f_2/f_1$ ,

$$W'_\nu = A s_1^2 l_1 E_\nu / D_\nu f_1^3 \pi. \quad \dots\dots(2)$$

In deriving this expression for  $W'_\nu$  no account has been taken of deviations of the source from black-body emissivity, or of energy losses occurring on reflection at mirrors or by passage through windows or through the atmosphere. The effective energy stream available at the detector must therefore be  $W'_\nu$  multiplied by some loss factor,  $\tau$ .

Let  $W_0$  be the minimum energy stream which, falling on the detector, will provide some appropriate minimum signal-to-noise ratio  $M_0$  at the display. To obtain the best resolving power the slits will be closed until the energy stream at the detector,  $\tau W'_\nu$ , becomes equal to  $W_0$ , when the minimum entrance slit width  $s_0$  will be given by

$$s_0^2 = W_0 \pi D_\nu f_1^3 \tau E_\nu A l_1. \quad \dots\dots(3)$$

It will be convenient to express performance in terms of a quantity,  $\Gamma$ , which is the frequency band in  $\text{cm}^{-1}$  embraced by one slit width. (Separating power will then be proportional to  $1/\Gamma$ .) Taking again  $s_2/s_1 = f_2/f_1$ , it appears that  $\Gamma_\nu$  for the frequency range  $\nu$  to  $\nu + \delta\nu$  may be defined, for slit widths at which aberration and diffraction are negligible, as follows:

$$\Gamma_\nu = s_1 / D_\nu f_1. \quad \dots\dots(4)$$

It may be noted at this point that  $l_1$  is normally made as large as is consistent with a reasonable level of aberration (Perry 1938) and that under these conditions  $l_1$  is approximately proportional to  $f_1$ ;  $l_1/f_1 = g$ . Then, using equation (4),

$$\Gamma_\nu = \sqrt{(W_0 \pi / \tau D_\nu A E_\nu g)}. \quad \dots\dots(5)$$

### § 3. SIMPLIFIED MODEL OF INFRA-RED DETECTOR

It is convenient to assume a simplified model of an infra-red detector and then to specify its performance by means of three parameters. In this idealized detector the temperature difference produced in the receiver by the radiation signal is analogous to the voltage produced across a circuit consisting of a resistance and a capacity in parallel fed from a high-impedance constant-current generator. The resistance corresponds to the path along which heat is lost by re-radiation and conduction, and the capacity to the thermal capacity of the receiver. The product of the resistance and capacity values gives the time constant. The output voltage,  $V$ , of such a detector when a step of radiation of height  $W$  is applied may be represented by

$$V = \sigma W \{1 - \exp(-t/\tau)\}, \quad \dots\dots(6)$$

where  $\sigma$  is a steady state sensitivity (say in microvolts per microwatt),  $t$  is time commencing from  $t=0$  when the radiation is applied, and  $\tau$  is the time constant.

In practice, the thermal constants of a receiver are so distributed that for high modulation frequency components of the incident radiation the thermal wavelength in the receiver may be comparable to or smaller than the receiver dimensions, and some form of delay network treatment must be substituted for the simple resistance-capacity circuit postulated in equation (6). Similarly, the heat sink for the receiver may be imperfect, as in some backed bolometers, giving additional time constants greater than  $\tau$  of equation (6). Alternatively, a thermal differentiating circuit may exist, as in the Golay cell (Golay 1947), for which  $V$  after an initial rise returns more slowly to zero instead of remaining constant.

Since, for practical purposes, a detector is used with a radiation modulation frequency appropriate to its time constant, it appears reasonable to accept values of  $\sigma$  and  $\tau$  which make equation (6) most nearly fit the experimental  $V/t$  plot for the detector in question.

A further parameter,  $\mu$ , which is a measure of the total noise arising in the detector, must be introduced. Noise in any detector arises in the first place from random fluctuations in the incident and re-radiated energy streams or in the temperature of the receiver (Daunt 1945, Jones 1947, Lewis 1947, Milatz and van der Velden 1943) and in the second place from electrical fluctuations—Johnson noise, shot noise, current and contact noise of various types. For Johnson noise the mean square fluctuation voltage,  $\bar{V}_n^2$  appearing across a resistance  $R$  at absolute temperature  $T$  for bandwidth  $\Delta f$  is given by

$$\bar{V}_n^2 = 4kTR\Delta f, \quad \dots\dots(7)$$

with correspondingly more general relations for networks having reactance (Nyquist 1928, Johnson 1928).

In a receiver system consisting of detector, amplifier and display, it is in general technically possible to make the noise level at the display dependent only on the detector noise properties and on the effective bandwidth of amplifier and display where, as is usual, this is smaller than the detector bandwidth. Thus it appears desirable to express the observed part of the mean square fluctuation voltage at the detector output as

$$\bar{V}_n^2 = \mu\Delta f, \quad \dots\dots(8)$$

where  $\mu$  is characteristic of the detector alone and  $\Delta f$  is normally characteristic of the amplifier and display alone. It is assumed that  $\mu$  covers detector noise of all types mentioned above. It may therefore vary with the frequency at which the pass-band  $\Delta f$  occurs, particularly in the case of current and contact noise. Since, however, the more fundamental types of noise have a comparatively uniform frequency spectrum over the detector operating ranges considered, we shall assume, for simplicity, that  $\mu$  is constant for any given detector.

#### §4. "CHOPPED-BEAM" AND "VIDEO" SYSTEMS OF PRESENTATION

Using the parameters  $\sigma$ ,  $\tau$ , and  $\mu$  as defined above, it is possible to find an expression for  $W_0$  for a receiver system including a particular detector. The first system to be considered will be that in which the incident radiation is chopped, the radiation pulses having duration  $a$ , the effective bandwidth from the point of view of noise,  $\Delta f$ , being defined as a display bandwidth extending from zero frequency to  $1/a$ . The peak signal voltage,  $V_s$ , reached at the detector output when a pulse of radiation of height  $W_0$  and duration  $a$  is applied is given by

$$V_s = \sigma W_0 \{1 - \exp(-a/\tau)\}. \quad \dots\dots(9)$$

The detector r.m.s. noise voltage observable by means of the amplifier and display is given by  $\bar{V}_n = \sqrt{(\mu\Delta f)} = \sqrt{(\mu/a)}$ , corresponding to a peak-to-peak noise voltage,  $V_p$ , riding on the signal and given by

$$V_p = q\sqrt{(\mu/a)}, \quad \dots\dots(10)$$

where  $q$  has a value of 6 to 8 (Rice 1944). Then for a minimum acceptable signal-to-noise ratio,  $M_0$ , at the display

$$W_0 = \frac{qM_0\sqrt{\mu}}{\sigma\{1 - \exp(-a/\tau)\}\sqrt{a}}. \quad \dots\dots(11)$$

A second system may be considered in which the spectrum traverses the exit slit rapidly, with a scanning speed of  $\Sigma$  cm<sup>-1</sup>/sec., and the detector output contains modulation corresponding to the energy changes of the spectrum. In a system of this type, in which the signal is analogous to a television video signal, the amplifier response must extend from zero, or from some relatively low scan repetition frequency, up to a value which is just greater than the maximum modulation frequency occurring in the detector output.

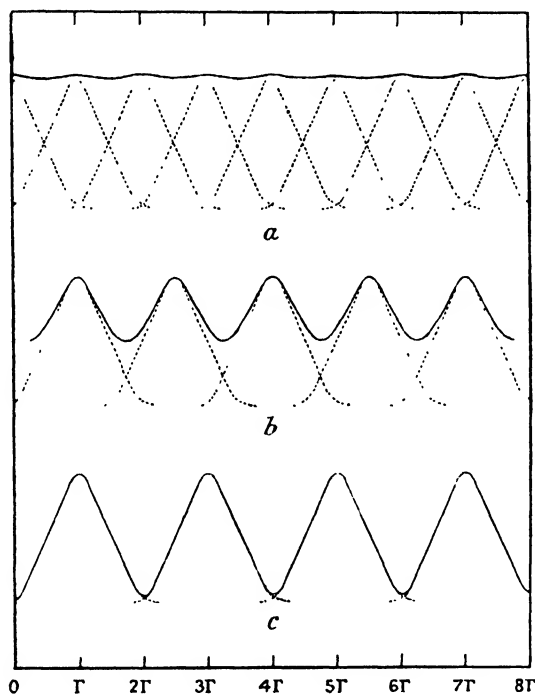


Figure 2. Radiation patterns at spectrometer exit slit on scanning spectra composed of lines at various intervals: (a)  $\Gamma$ , (b)  $3\Gamma/2$ , and (c)  $2\Gamma$ .

The connection between maximum modulation frequency of the radiation and scanning speed may be illustrated as follows. Consider a spectrometer (cf. Figure 1) with equal entrance and exit slit widths and with collimating mirror and camera mirror of equal focal lengths, operating under energy limited conditions. For equal inputs of monochromatic radiation at spectral separations of  $\Gamma$  the radiation pattern appearing at the detector as the spectrum is scanned will have the form plotted in Figure 2(a), while for frequency intervals  $3\Gamma/2$  and  $2\Gamma$  the patterns will resemble those plotted in Figures 2(b) and 2(c) respectively. Thus for separating power  $1/\Gamma$  a signal component of which one cycle corresponds to a wave number range of  $\Gamma$  or greater may be present at the detector. If the scanning speed is  $\Sigma$ ,

then the maximum signal frequency at the detector will be  $\Sigma/\Gamma$ , and this will define the upper limit,  $f_m$ , of the frequency band to which detector, amplifier and display must respond.

For a component of the radiation signal,  $\delta W$ , of angular frequency  $\omega$ , the detector output,  $\delta V_s$ , will be given by

$$\frac{\sigma \delta W}{1 + \omega^2 \tau^2} \quad \dots\dots (12)$$

If  $\omega$  is limited to values less than  $1/\tau$ , and the amplifier-display response is flat, distortion of the spectrum will not be excessive. If, however, no such limitation is placed on the value of  $\omega$ , and distortion must not become unmanageable, the response characteristic of the amplifier-display system must be modified. Peak gain must occur for the highest radiation signal frequency component,  $f_m$ , where  $f_m = \Sigma/\Gamma$ , and be reduced by the factor  $\sqrt{\{1 + \omega_m^2 \tau^2\} (1 + \omega_m^2 \tau^2)}$ , where  $\omega_m = 2\pi f_m$ , for lower values of  $\omega$ . On this basis the signal voltage,  $V_s$ , at the display, integrated over the pass-band, will be given by

$$V_s = \sigma W / \sqrt{1 + \omega_m^2 \tau^2}, \quad \dots\dots (13)$$

and the integrated r.m.s. noise voltage by

$$\bar{V}_n = \sqrt{\left\{ \left( \frac{\mu f_m}{3} \right) \left( 1 + \frac{2}{1 + \omega_m^2 \tau^2} \right) \right\}}, \quad \dots\dots (14)$$

which for  $\omega_m \tau \ll 1$  reduces to  $\bar{V}_n = \sqrt{(\mu f_m)}$  and for  $\omega_m \tau \gg 1$  to  $\bar{V}_n = \sqrt{(\mu f_m / 3)}$ . Thus for a minimum acceptable signal-to-noise ratio,  $M_0$ , at the display

$$W_0 = q M_0 \sqrt{\{ \mu f_m (1 + \omega_m^2 \tau^2 / 3) \}} / \sigma. \quad \dots\dots (15)$$

In the chopped-beam system some suitable number,  $\alpha$ , of radiation pulses should occur while the spectrum traverses one slit width or  $\Gamma \text{ cm}^{-1}$ . Thus the scanning speed is proportional to the number of pulses per second,  $p/a$ , and to the frequency range covered,  $\Gamma$ , per  $\alpha$  pulses:

$$\Sigma = \Gamma(p, \alpha a), \quad \dots\dots (16)$$

where  $p$  is a mark to (mark + space) ratio.

In the video system using an amplifier of flat response within its pass-band the permissible scanning speed is governed by the relation

$$\Sigma = \Gamma / 2\pi\tau, \quad \dots\dots (17)$$

while for an amplifier with response of suitable form, as described above, the corresponding condition is

$$\Sigma = f_m \Gamma. \quad \dots\dots (18)$$

## § 5. INTER-RELATION OF SEPARATING POWER AND SCANNING SPEED

The relations derived above may now be used to discuss the inter-dependence of optimum separation,  $\Gamma_0$ , and scanning speed,  $\Sigma_0$ , in spectroscopic systems. Consider first the chopped-beam system.

For the case in which the energy stream entering the spectrometer is strictly limited the relevant equations are (5), (11) and (16). From these it will be seen that  $\Gamma$  can be plotted as a function of  $a$ , the radiation pulse length, as can  $\Sigma$ . Corresponding values of  $\Gamma$  and  $\Sigma$  for a given system may then be used to yield a curve which represents complete information on the performance of the system. Curves of this type, based on spectrometer and detector data set out in an appendix to this account, are given in Figure 3.

A typical curve of  $\log \Gamma$  against  $\log \Sigma$ , as shown in Figure 3, may be considered to be made up of four distinct sections with fairly well marked inflections between

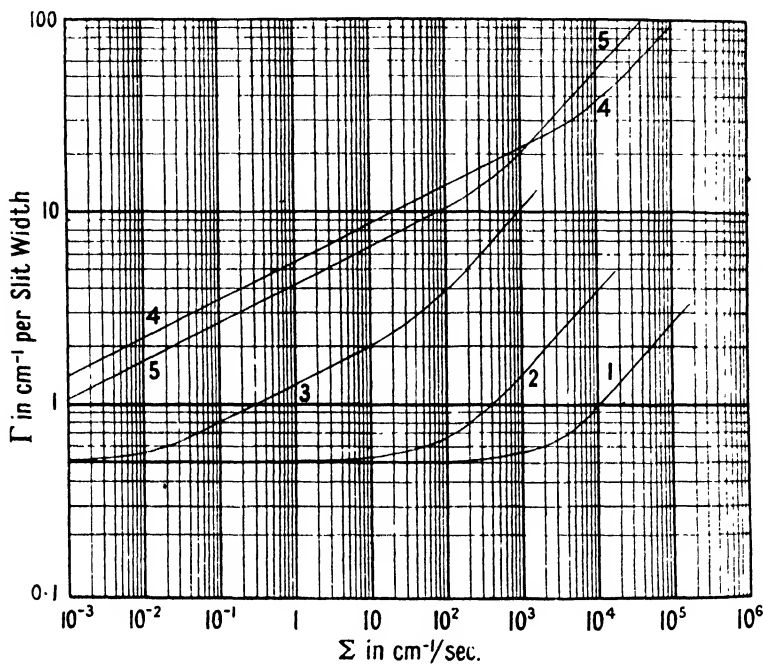


Figure 3. Plot of  $\log \Gamma$  against  $\log \Sigma$  for (1) photoconductive cell, (2) superconducting bolometer, (3) Schwarz type thermopile, (4) Golay cell and (5) thermistor bolometer.

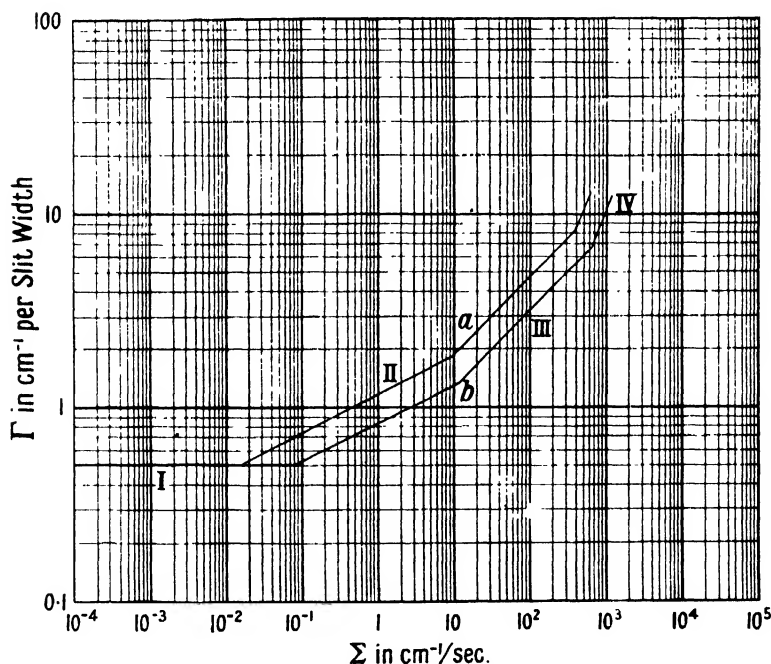


Figure 4. Diagrammatic  $\log \Gamma$   $\log \Sigma$  plot for Schwarz thermopile: (a) "chopped beam" system, (b) "video" system.

them (cf. Figure 4(a)). For very low values of scanning speed the resolving power is limited by optical aberration and diffraction and tends to become approximately



constant, corresponding to section I of the  $\log \Gamma / \log \Sigma$  curve at the left of Figure 4. At higher values of scanning speed, for which the system becomes energy-limited but for which the radiation pulse length remains considerably larger than the detector time constant, the value of  $a/\tau$  is large enough to make  $\exp(-a/\tau)$  negligible in comparison with unity. For this case using equations (5) and (11) and writing  $1 - \exp(-a/\tau) \simeq 1$  and  $\xi = \pi q M_0 \sqrt{\mu/x} D_r A E_r g \sigma$ ,

$$5 \log \Gamma - \log \Sigma = 2 \log \xi + \log \alpha/p. \quad \dots\dots (19)$$

Section II of the  $\log \Gamma / \log \Sigma$  plot, corresponding to this relation, should have a slope of  $1/5$  for any detector.

At still shorter pulse lengths, where  $a$  becomes considerably shorter than  $\tau$ ,  $1 - \exp(-a/\tau) \sim a/\tau$  and a further straight portion of the  $\log \Gamma / \log \Sigma$  plot will occur. Using equations (5) and (11) and writing  $1 - \exp(-a/\tau) = a/\tau$ ,

$$7 \log \Gamma - 3 \log \Sigma = 2 \log \xi + \log \tau^2 x^3 / p^3. \quad \dots\dots (20)$$

Section III of the curve should therefore have a slope of  $3/7$  for any detector. As  $a/\tau$  becomes smaller again, a point will be reached at which the thermal wavelength in the receiver becomes comparable with its dimensions, and a further inflection will occur in the  $\log \Gamma / \log \Sigma$  plot, the slope being subsequently greater than  $3/7$  in section IV.

#### § 6. COMPARISON OF DETECTORS

It is clear that the performance of a detector in a given spectroscopic system may be fairly completely represented by a  $\log \Gamma / \log \Sigma$  curve. One may enquire, however, if there is any way of expressing detector performance by means of a single figure of merit. Such a criterion may be found if the assumption is made that the most valuable detector is one which will give a pulse signal just detectable above noise for an incident radiation pulse of smallest total energy, the overall bandwidth of the amplifier-display system being adjusted to a value appropriate to the radiation pulse length.

An expression may be derived for  $U_0$ , the minimum energy of a radiation pulse of length  $a$  and power  $U_0/a$  which will give an output voltage pulse of height  $qM_0$  times r.m.s. noise voltage. From equation (11), setting  $U_0/a = W_0$  and again taking bandwidth  $1/a$ ,

$$U_0 = qM_0 \left[ \frac{\sqrt{(\mu\tau)}}{\sigma} \right] \frac{\sqrt{(a/\tau)}}{1 - \exp(-a/\tau)}, \quad \dots\dots (21)$$

where the symbols have the same significance as before. This expression may be minimized with respect to  $a/\tau$  to give the minimum detectable pulse energy,  $U_0$ , which occurs when  $a = 1.256\tau$ , giving

$$U_0 = 1.567 q M_0 \sqrt{(\mu\tau)} / \sigma. \quad \dots\dots (22)$$

Thus the factor  $\sqrt{(\mu\tau)} / \sigma$  may be taken as the figure of merit of a detector when sensitivity, speed and noise level have all been taken into account.

#### § 7. HIGH SPEED SCANNING

It will be seen that the optimum pulse length,  $a = 1.256\tau$ , corresponds to the inflection between section II and section III of the  $\log \Gamma / \log \Sigma$  plot of Figure 4, and that at this point

$$W_0 \simeq 1.25 (qM_0/\sigma) \sqrt{(\mu/\tau)}. \quad \dots\dots (23)$$

If the infra-red source brightness is unrestricted, and no limits are placed on  $\Gamma$  or  $\Sigma$ , it appears that equation (23), together with equation (5) and equation (16), specify the best operating conditions.

It is clear that a detector may be operated at radiation chopping frequencies higher than this optimum if a sufficiently high value of  $W_0$  is attainable, and in practice it may be profitable to operate the detector at chopping frequencies up to the inflection between sections III and IV of Figure 4. Beyond this point, in the region where for thermo-detectors the standing-wave pattern in the receiver (and for photo-detectors the duration of the primary photoelectric process) become important, a rapid falling off in detector performance may be expected.

If the video system of presentation is now considered it is seen that again the  $\log \Gamma / \log \Sigma$  plot falls into four distinct sections, as shown in Figure 4(b), the first being determined by purely optical considerations. From equations (5), (15) and (18), for the region in which  $\omega_m^2 \tau^2 \ll 1$ ,

$$5 \log \Gamma - \log \Sigma = 2 \log \xi, \quad \dots\dots(24)$$

and the curve has a slope of  $1/5$ , as in section II of Figure 4(b).

If a flat amplifier response is used, section III of the  $\log \Gamma / \log \Sigma$  plot will be determined, in the region where  $\omega_m^2 \tau^2 \gg 1$ , by equation (17). Thus

$$\log \Gamma - \log \Sigma = \log 2\pi\tau, \quad \dots\dots(25)$$

giving a slope of 1. For the appropriate amplifier-display response characteristic, if it could be realized, the curve would be determined by equations (5), (15) and (18). These give

$$7 \log \Gamma - 3 \log \Sigma = 2 \log \xi + \log 4\pi^2 \tau^2, 3, \quad \dots\dots(26)$$

for which the slope is  $3/7$ . Thus it is seen that  $\log \Gamma / \log \Sigma$  curves for the video system run parallel, in sections II and III to the corresponding curves for the chopped-beam system, but lie below them, indicating that the video method of presentation, if it should prove technically feasible, would use any given detector more efficiently than the chopped-beam method. With the exception of standard D.C. amplification systems, which may be considered as a special case of video presentation, the possibility of constructing amplifiers of suitable phase and amplitude response characteristics has not been fully investigated.

#### ACKNOWLEDGMENT

One of us (E.F.D) is indebted to the Institute of Petroleum for a maintenance grant, during the tenure of which the work was initiated. It was completed during his tenure of an Imperial Chemical Industries Fellowship.

#### REFERENCES

- ANDREWS, D. H., MILTON, R. M., and DE SORBO, W., 1946, *J. Opt. Soc. Amer.*, **36**, 353, and **36**, 518.  
 BARNES, R. B., McDONALD, R. S., WILLIAMS, V. Z., and KINNAIRD, R. F., 1945, *J. Appl. Phys.*, **16**, 77.  
 BECKER, J. A., and MOORE, H. R., 1946, *J. Opt. Soc. Amer.*, **36**, 354.  
 BELL, E. E., BUHL, R. F., NIELSEN, A. H., and NIELSEN, H. H., 1946, *J. Opt. Soc. Amer.*, **36**, 355.  
 BELL TELEPHONE LABORATORIES, 1946, Information supplied by Bell Telephone Laboratories.  
 DALY, E. F., and SUTHERLAND, G. B. B. M., 1947, *Proc. Phys. Soc.*, **59**, 77.

- DAUNT, J. G., 1945, Unpublished report circulated by Admiralty.  
 EPPLEY LABORATORIES, 1947, Information supplied by Eppley Laboratories.  
 GOLAY, M. J. E., 1947, *Rev. Sci. Instrum.*, **18**, 347, and **18**, 357.  
 HILGER, ADAM, 1947, Information supplied by Messrs. Adam Hilger Ltd.  
 JOHNSON, J. B., 1928, *Phys. Rev.*, **32**, 97.  
 JONES, R. C., 1947, *J. Opt. Soc. Amer.*, **37**, 879.  
 LEWIS, W. G., 1947, *Proc. Phys. Soc.*, **59**, 34.  
 MILATZ, J. M. W., and VAN DER VELDEN, H. A., 1943, *Physica*, **10**, 369.  
 MILTON, R. M., 1946, *Chem. Rev.*, **39**, 403.  
 NYQUIST, H., 1928, *Phys. Rev.*, **32**, 110.  
 OXLEY, C. L., 1946, *J. Opt. Soc. Amer.*, **36**, 356.  
 PERKIN ELMER CORPN., 1947, Information supplied by Perkin Elmer Corporation.  
 PERRY, J. W., 1938, *Proc. Phys. Soc.*, **50**, 265.  
 RICE, S. O., 1944, *Bell System Tech. J.*, **23**, 282, also 1945, **24**, 46.  
 SIMPSON, O., SUTHERLAND, G. B. B. M., and BLACKWELL, D. E., 1948, *Nature, Lond.*, **161**, 281.  
 SUTHERLAND, G. B. B. M., BLACKWELL, D. E., and FELLGETT, P. B., 1946, *Nature, Lond.*, **158**, 875.  
 SUTHERLAND, G. B. B. M., and LEE, E., 1948, *Reports on Progress in Physics*, Vol. XI (London: Physical Society), p. 144.  
 WEISS, R. A., 1946, *J. Opt. Soc. Amer.*, **36**, 356.  
 WILLIAMS, V. Z., 1948, *Rev. Sci. Instrum.*, **19**, 135.

## APPENDIX

In computing the  $\log \Gamma / \log \Sigma$  plots given in Figures 3 and 4 the optical system assumed is that of the Perkin Elmer Corporation Model 12B spectrometer (Barnes *et al.* 1945) using a lithium fluoride prism at  $2,000 \text{ cm}^{-1}$ .

$D$	Angular dispersion at $2,000 \text{ cm}^{-1}$	$8.7 \times 10^{-5} \text{ radian/cm}^{-1}$
$A$	Effective prism area	$30 \text{ cm}^2$
$E$	Black-body radiation, $2,000 \text{ cm}^{-1}$	$3 \times 10^{-3} \text{ watt/cm}^{-1} \text{ cm}^2$
$l_1$	Slit length ( $l_1 = l_2$ )	$1.2 \text{ cm.}$
$f_1$	Collimator mirror focal length	$27 \text{ cm.}$
$x$	Loss factor	$0.25$
$M_0$	Min. S/N required at display	$50$
$q$	Peak-to-peak to r.m.s. ratio	$8$
$k$	Boltzmann's constant	$1.37 \times 10^{-23} \text{ joules/deg.}$
$p$	Mark to mark : space ratio	$0.5$
$a$	Number of pulses per slit width	$3$

In obtaining data on the parameters  $\sigma$ ,  $\tau$ , and  $\mu$  for various detectors the Table given below was compiled. It was found that information on  $\mu$  and  $\sigma$  separately was in most cases not available. Where a value of the energy stream,  $W_{M-1}$ , for which the signal voltage equals r.m.s. noise voltage, could be found,  $\sqrt{\mu}/\sigma$  was obtained from this using the relation  $\sqrt{\mu}/\sigma = W_{M-1}/\Delta f$  where  $\Delta f$  is the noise bandwidth.

The quantity  $\sqrt{(\mu\tau)}/\sigma$  is useful as a basis for comparing detectors, and detector performances given in the table are arranged in approximate order of merit in this way. The minimum detectable pulse energy,  $U_0$ , may be obtained by multiplying the value of  $\sqrt{(\mu\tau)}/\sigma$  by the factor  $1.567qM_0$  which, for a pulse just distinguishable above noise, might have a value of 10. From the Table probable values of  $\tau$  and  $\sqrt{\mu}/\sigma$  for the five types of detector considered were obtained and are used in computing the curves of Figures 3 and 4. It may be noted that the value for photoconductive cells is for peak spectral sensitivity, and hence is not strictly applicable when the basis of computation is a spectrometer set at  $2,000 \text{ cm}^{-1}$ .

Values of the constants occurring in equations (19), (20), (24) and (26) are as follows :

$$\begin{aligned} \log \xi &= 10.7014 + \log \sqrt{\mu/\sigma}, & \log \tau^2 \alpha^3 / p^3 &= 2.3343 + 2 \log \tau, \\ \log \alpha / p &= 0.7781, & \log 4\pi^2 \tau^2 / 3 &= 1.1191 + 2 \log \tau. \end{aligned}$$

Values assumed in computing Figure 3 are as follows :

Detector	Curve (Fig. 3)	$\tau$	$\sqrt{\mu/\sigma}$
Photoconductive cell	1	$2 \cdot 10^{-4}$	$2 \cdot 10^{-14}$
Superconducting bolometer	2	$5 \cdot 10^{-4}$	$10^{-12}$
Schwarz type thermopile	3	$10^{-2}$	$5 \cdot 10^{-11}$
Golay cell	4	$5 \cdot 10^{-4}$	$2 \cdot 10^{-9}$
Thermistor bolometer	5	$5 \cdot 10^{-3}$	$10^{-9}$

In computing Figure 4, which is purely diagrammatic, constants for a particular Schwarz thermopile were used, and the effect of distributed thermal capacity in the receiver taken to be of importance at signal frequencies above 100 c/s. In this case  $\tau = 4 \times 10^{-2}$  and  $\sqrt{\mu/\sigma} = 4 \times 10^{-11}$ .

Detector	$\tau$ (sec.)	$\frac{\sqrt{\mu}}{\sigma}$	$\frac{\sqrt{(\mu\tau)}}{\sigma}$	Area (cm <sup>2</sup> )	Res. (ohm)	References and Notes
Photo-conductive cells.	$1.5 \cdot 10^{-4}$	$1.7 \cdot 10^{-14}$	$2.1 \cdot 10^{-16}$	0.01	$7.5 \cdot 10^6$	Simpson <i>et al.</i> 1948, PbTe cell, 2.2 $\mu$ peak at 83° K.
	$10^{-4}$	$3.7 \cdot 10^{-13}$	$3.7 \cdot 10^{-15}$	—	$3 \cdot 10^6$	Sutherland <i>et al.</i> 1946 PbS cell, 2.5 $\mu$ peak, 200° K.
	$10^{-4}$	$2.8 \cdot 10^{-12}$	$2.8 \cdot 10^{-14}$	0.09	—	Oxley 1946, German chemical PbS cell
Super-conducting bolometers	$5 \cdot 10^{-4}$	$8.9 \cdot 10^{-13}$	$2 \cdot 10^{-14}$	0.01	5	Andrews <i>et al.</i> 1946
	$1.8 \cdot 10^{-4}$	$1.8 \cdot 10^{-12}$	$2.4 \cdot 10^{-14}$	0.008	1.6	Milton 1946
	$1.8 \cdot 10^{-3}$	$1.2 \cdot 10^{-11}$	$5 \cdot 10^{-13}$	0.008	0.3	Bell <i>et al.</i> 1946
Schwarz type thermopiles	$8 \cdot 10^{-3}$	$5.7 \cdot 10^{-11}$	$5.1 \cdot 10^{-12}$	0.004	20	Perkin Elmer 1947
	$3.6 \cdot 10^{-2}$	$3.3 \cdot 10^{-11}$	$6.3 \cdot 10^{-12}$	0.004	60	Hilger 1947
Golay cells	$3.4 \cdot 10^{-4}$	$1.6 \cdot 10^{-9}$	$2.9 \cdot 10^{-11}$	—	—	Weiss 1946
	$5 \cdot 10^{-3}$	$7.1 \cdot 10^{-9}$	$5 \cdot 10^{-10}$	0.025	—	Eppley 1947
Thermistor bolometers	$5 \cdot 10^{-3}$	$7.3 \cdot 10^{-10}$	$5.1 \cdot 10^{-11}$	0.006	$2 \cdot 10^6$	Becker & Moore 1946
	$9 \cdot 10^{-3}$	$1.3 \cdot 10^{-9}$	$1.2 \cdot 10^{-10}$	0.004	$2 \cdot 10^6$	Bell Tel. Labs. 1947

## The Luminescence of Wetted Solids

By J. EWLES AND G. C. FARNELL\*

Department of Physics, The University of Leeds

*MS. received 25th July 1948, in amended form 25th November 1948*

**ABSTRACT.** An earlier observation that the association of a non-luminescent pure liquid with a non-luminescent solid produces fluorescence and phosphorescence in the liquid has been confirmed. The luminescent spectra of water, heavy water, and alcohols, as well as some other liquids with different negative radicals when adsorbed by various finely divided ionic solids have been examined and recorded. The positions of the maxima of the main broad band are very similar for all the hydroxy liquids even with different solids (band peaks in the range 4300–4500 Å.) and are different for the same solid with liquids having different negative radicals. Preliminary experiments on the relation between brightness and relative amount of liquid indicate that the phenomena are associated with the active sites on the solid surface, and afford evidence of the existence of these and of their differences on the same solid.

Excitation spectra confirm preliminary observations that the adsorbed molecules have very abnormal absorption regions indicating considerable changes in energy levels. Two suggestions are made to explain the phenomena: (a) the energy changes may be correlated with the heat of adsorption on the active sites; (b) the adsorbed molecules are bonded to the solid by the positive radicals leaving an almost free negative ion.

### § 1. INTRODUCTION

It was observed earlier (Ewles 1930, Ewles and Martin 1939) that many white solids when wetted with water showed, on excitation by the near ultra-violet, a faint blue fluorescence and a phosphorescence lasting for some seconds. On complete drying of the solid the luminescence disappeared. Later observations showed that the spectral distribution of the luminescence was astonishingly similar for different solids. The implication of this effect—that the mere contact of liquid with solid, both separately transparent into the far ultra-violet and both non-luminescent, is sufficient to endow the system with the power of luminescence under excitation by wavelengths which are not normally absorbed—clearly required confirmation.

### § 2. CONFIRMATION OF THE REALITY OF THE PHENOMENON

(a) *The glow might be due to modified scattering.*

In such a case the spectrum would be dependent on the spectral distribution of the exciting light. This was found not to be so. Further, the existence of phosphorescence having the same spectral distribution as the fluorescence makes the scattering hypothesis extremely unlikely since there is so far no evidence for any time lag in the emission of scattered radiation.

(b) *The solid itself might be luminescent, even when dry.*

The earlier investigations referred to above were extended and confirmed. Wetted silica and wetted sodium chloride showing quite a marked blue glow were dried by continued heating *in vacuo*. After three to four hours at 500° C. for silica and half an hour for sodium chloride all traces of the blue glow had

\* Now at the Kodak Research Laboratories, Welldstone, Middx.

disappeared, even under the strongest excitation with light of wavelengths down to 3000 Å. and with the specimen at a temperature of 90° K. Rewetting *in vacuo* restored in large measure the power of glowing under and after excitation.

(c) *The pure liquid might be luminescent.*

Tap water was found to possess a marked luminescence, especially at 90° K. Doubly distilled water, however, showed no trace of glow under the same conditions.

(d) *A soluble impurity in the solid might give a luminescent solution on wetting.*

To test this the silica powder was boiled with doubly distilled water in a carefully cleaned silica flask for some hours. The water remaining was decanted and set aside. Fresh doubly distilled water was added to the silica and the process repeated. After many repetitions the wetted silica in the flask was found to retain undiminished its power of glowing, while none of the decanted samples of water showed any trace of luminescence.

Thus it seems fairly certain that the blue glow is not due to the formation of a luminescent solution on wetting the solid.

(e) *The luminescence might be caused by gases dissolved in the water and adsorbed by the solid on wetting.*

This possibility appears to be eliminated by the facts that (i) rewetting *in vacuo* of the silica dried *in vacuo* by water which has been doubly distilled and then boiled for several minutes produces the same effect as rewetting in air; (ii) after removal of the luminescence by drying *in vacuo* the readmission of dry air causes no restoration of the luminescence even on long standing.

These experiments thus appear to confirm the previous observations and conclusions that the mere contact of a suitable liquid with a white solid confers on the associated system the power of fluorescence and phosphorescence under excitation by light not normally absorbed by either separately.

### § 3. INVESTIGATIONS OF THE LUMINESCENT SPECTRA OF WETTED SOLIDS

A Hilger medium quartz spectrograph was mainly employed, with occasional recourse to the Hilger Constant Deviation glass instrument, and to the larger Hilger instrument ( $f = 170$  cm.). For examination of the spectra excited by the near ultra-violet the excitation was from a Mazda 125 watt Mercra lamp with the outer glass envelope removed. The most satisfactory arrangement of complementary filters available for near ultra-violet excitation was a piece of Wood's glass, 6 mm. thick, on the exciting side and a silica cell containing carbon disulphide, of 2.5 cm. thickness, on the spectrograph side. The latter has a very sharp cut-off at 3750 Å. and negligible absorption above this wavelength. For the far ultra-violet the very useful Bowen filter (Bowen 1935), consisting of a solution of 145 gm. hydrated nickel sulphate and 41.5 gm. hydrated cobalt sulphate in 1,000 ml. of water, was employed (a 10 cm. thickness of this filter was used, in a "stopped-down" silica flask of 10 cm. diameter). This filter has a useful transmission below about 3300 Å. while cutting off between that region and the yellow.

For examination of the fluorescence and phosphorescence at low temperatures the specimens were mounted as shown in Figures 1 and 2.

A cardboard cylinder mounted on a wooden disc attached to the vertical spindle of an electric motor is provided with two horizontal slots JJ of angular aperture just less than the angular distance between the windows W. This

means that when the specimen is just seen by the slit of the spectrograph it is just not illuminated by the exciting light. For fluorescence work an extra aperture is provided in the cardboard cylinder which can be opened or covered as desired. The speed of rotation of the cardboard cylinder (usually a few revolutions a second) could be controlled to give visually the brightest phosphorescence for the sample being investigated. The solids were prepared in the form of very fine powders from A.R. standard substances and were purified by repeated

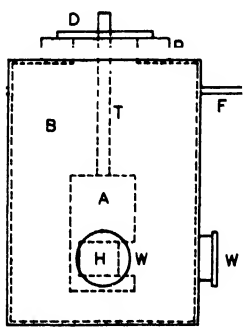


Figure 1. The low temperature specimen mounting. B—vacuum tight brass cylindrical box; FF—side tubes; P—Pyrex annulus; A—brass cylindrical box; H—hemicylindrical gap with flat vertical back for mounting of specimen; T—invar tube; D—brass disc; W—quartz windows.

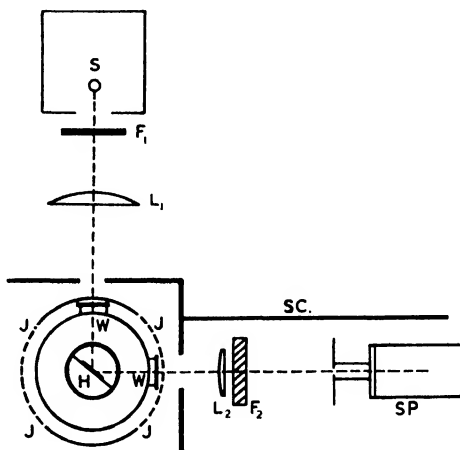


Figure 2. Horizontal section of the general arrangement of apparatus for the recording of emission spectra. S—light source;  $F_1F_2$ —complementary filters;  $L_1L_2$ —quartz focusing lenses; JJ—slots in rotating phosphoroscope cylinder; SP—spectrograph collimator; SC—screening.

re-crystallization or precipitation, except in the case of the silica which had been precipitated from ethyl silicate and needed no further purification except repeated washing with doubly distilled water. Where liquids other than water were employed for activation the solids were freed from water by drying *in vacuo* and rewetted *in vacuo* with the pure, redistilled liquid. In every case the absence of luminescence of the dried solids was checked.

The spectrograms, for the most part, were recorded on Ilford H.P.3. plates and photometered with a Cambridge recording photoelectric photometer, the photometer curves being corrected by the aid of a wavelength-sensitivity graph kindly supplied to us by Messrs. Ilford Limited.

The results are summarized in Tables 1, 2 and 3, and some examples of the photometer curves of the spectra are shown in Figures 3, 4 and 7. In the case of solids wetted with water or alcohols the spectra consist mainly of a broad unresolved band stretching from the blue-green to the violet. In some cases there were indications of weak and ill defined bands with peaks at about 5200 Å. and 5900 Å., but these are doubtful and only the position of the main peak is given in Tables 1 and 2. Attempts to obtain resolution at 90° K. with the large Hilger spectrograph ( $f = 170$  cm.) were unsuccessful.

The features of the spectra to which we now draw attention are:—

- (a) A similarity between different solids wetted by water but a difference in the peak values of the main band which exceed, sometimes considerably, the probable error (20 Å.). (See Table 1)

- (b) The shift of about 4000 Å. to the high frequency side on replacing ordinary water by heavy water. (The heavy water was supplied by I.C.I., Ltd., and was given as 99.77% pure.)
- (c) The similarity between the spectra of the same solid wetted by different hydroxy liquids but with significant differences, exceeding the experimental tolerance, in the main peak values with different positive radicals, e.g.  $\text{SiO}_2\text{-H}_2\text{O}$  4367 Å.,  $\text{SiO}_2\text{-D}_2\text{O}$  3911 Å.,  $\text{SiO}_2\text{-CH}_3\text{OH}$  4266 Å.,  $\text{SiO}_2\text{-C}_2\text{H}_5\text{OH}$  4353 Å. (low temperature fluorescence).
- (d) The agreement, within the experimental tolerance, of the peak values for fluorescence and phosphorescence.
- (e) A shift of the main peak to shorter wavelengths at lower temperatures.

Table 1. Main Band Peaks of Luminescence of Water Wetted Solids

Solid	(1) (Å.)	(2) (Å.)	(3) (Å.)	Solid	(1) (Å.)	(2) (Å.)	(3) (Å.)
$\text{SiO}_2$	4405	4367	4360	KCl	—	4369	—
$\text{SiO}_2(\text{D}_2\text{O})$	3968	3911	—	BcO	4316	—	—
$\text{CaF}_2$	4578	4540	—	$\text{Al}_2\text{O}_3$	4505	4488	—
LiF	4411	4390	—	$\text{CaCO}_3$	—	—	4444
NaF	4426	4392	—	$\text{HgCl}_2$	—	—	4359
NaCl	—	4431	4420				

- (1) Fluorescent emission. Ordinary temperatures.
- (2) Fluorescent emission. Low temperatures.
- (3) Phosphorescent emission. Low temperatures.

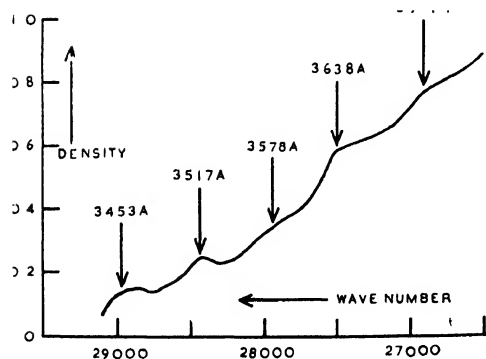


Figure 3. Ultra-violet section of photometer record of fluorescence spectrogram of silica wetted with propylene dichloride (specimen at 90° K.).

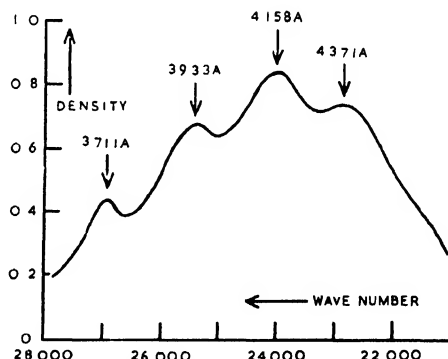


Figure 4. Violet and ultra-violet section of photometer record of fluorescence spectrogram of silica wetted with ethyl bromide (specimen at 90° K.).

Table 2. Main Band Peaks of Luminescence of Solids Wetted by Alcohols

System	(1) (Å.)	(2) (Å.)	(3) (Å.)	System	(1) (Å.)	(2) (Å.)	(3) (Å.)
$\text{SiO}_2(\text{CH}_3\text{OH})$	4289	4266	—	$\text{NaCl}(\text{CH}_3\text{OH})$	—	—	4464
$\text{SiO}_2(\text{C}_2\text{H}_5\text{OH})$	4402	4357	—	$\text{NaCl}(\text{C}_2\text{H}_5\text{OH})$	—	—	4490
$\text{KCl}(\text{C}_2\text{H}_5\text{OH})$	4353	4305	4311				

- (1) Fluorescent emission. Ordinary temperatures.
- (2) Fluorescent emission. Low temperatures.
- (3) Phosphorescent emission. Low temperatures.



Table 3. Luminescence of Silica Wetted by Non-hydroxy Liquids

System	Luminescent Emission	Details of Fluorescent Spectra
$\text{SiO}_2(\text{C}_2\text{H}_4\text{Cl}_2)$	Bluish-violet fluorescence and blue phosphorescence under near and far u-v. excitation.	At 90° K. single broad band with peak at 4274 Å.
$\text{SiO}_2(\text{CH}_3 \cdot \text{CHCl} \cdot \text{CH}_2\text{Cl})$	Bluish white fluorescence and green phosphorescence under near and far u-v. excitation.	At ordinary temperatures a single broad band with peak at 3984 Å. At 90° K. broad band, peak at 4148 Å. with series of narrow bands on u-v. flank at 3453 Å., 3517 Å., 3578 Å., 3638 Å., 3717 Å. (See Plate I, and photometer curve, Figure 3.)
$\text{SiO}_2(\text{C}_2\text{H}_5\text{Br})$	Bluish green fluorescence and green phosphorescence under both near and far u-v. excitation.	At 90° K. four well defined peaks in emission band at 4371 Å., 4158 Å., 3933 Å. and 3711 Å. (See photometer curve, Figure 4.)
$\text{SiO}_2(\text{C}_2\text{H}_5\text{I})$	Bluish white fluorescence and bluish-green phosphorescence under near u-v. excitation. No emission under far u-v. excitation.	At 90° K. a single broad band with peak at 4320 Å.

#### § 4. EXCITATION SPECTRA

In order to investigate the excitation spectra the wetted solid was deposited as a thin uniform layer on a glass plate fitting the plate holder of the spectrograph. The plate so formed was then placed in the plate holder of the spectrograph (with the wetted solid layer facing into the camera) and, using a slit width of 0.5 mm., the spectrum of the source was projected on the wetted solid layer. A photograph of the excitation spectrum so produced was recorded by an external wide field camera. An Ilford "Q" filter was placed in front of the lens of the external camera in order to reduce the effects of the short wavelength exciting light that might leak through the powder layer and plate.

An intense source giving a continuous spectrum of adequate intensity and uniformity over the complete exciting wavelength region was not available. In the end we were forced to employ the discontinuous spectrum of the high pressure mercury vapour lamp and an approximate evaluation of the excitation spectrum was made in the following way. The excitation spectrum, having been excited and photographed as indicated above, was photometered and the densities of the lines appearing thereon compared with the densities of the corresponding mercury lines in the direct spectrum recorded on the same kind of plate and with the same slit width (0.5 mm.). The results for the silica-water system are shown in Figure 5 and examples of the excitation spectra in Plate II.

We are not certain as to the reality of the broad excitation band with peak at about 3650 Å. since the filters were by no means perfect and the emission of the high pressure Hg arc is very strong in this region. The curve indicates with

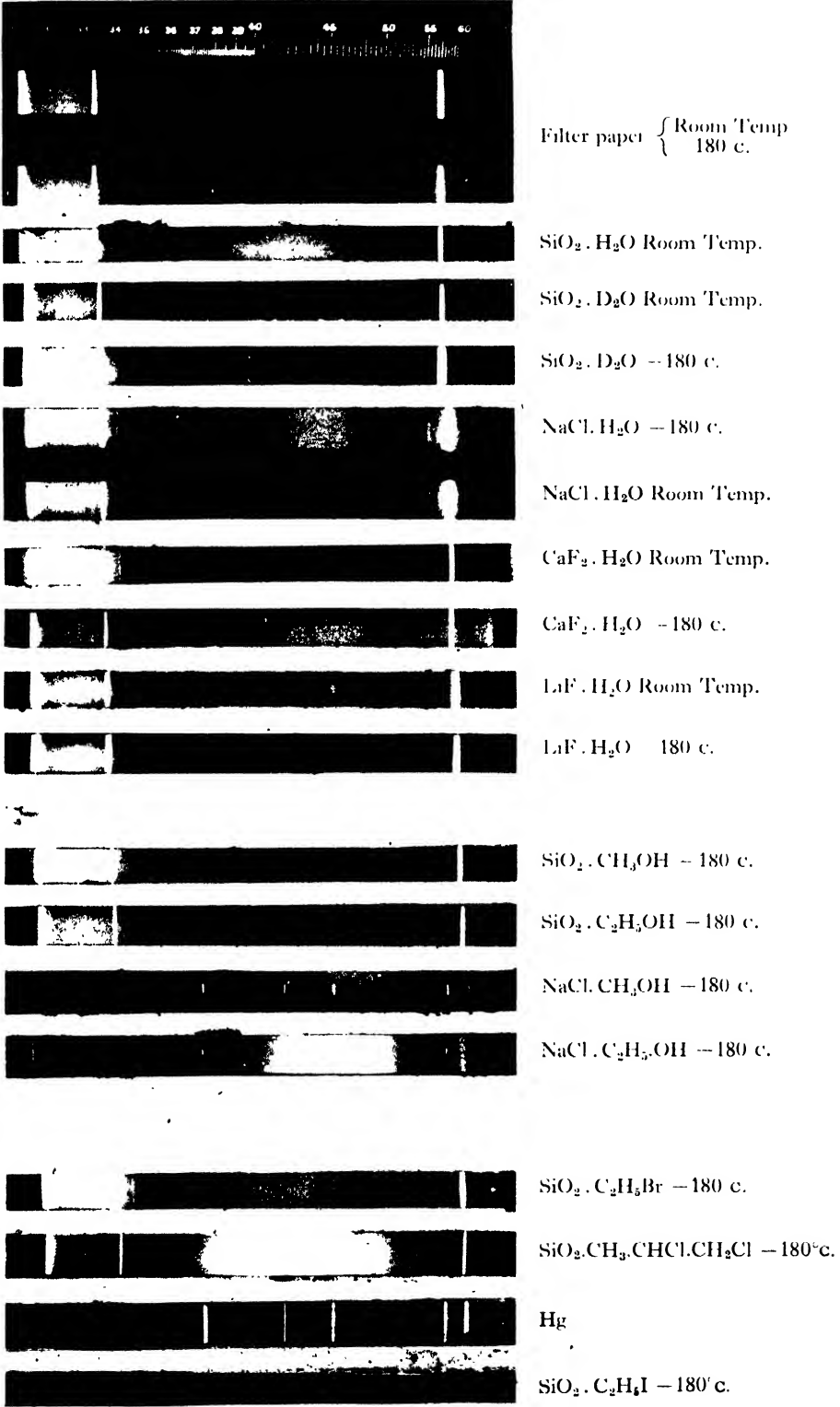


Plate I.

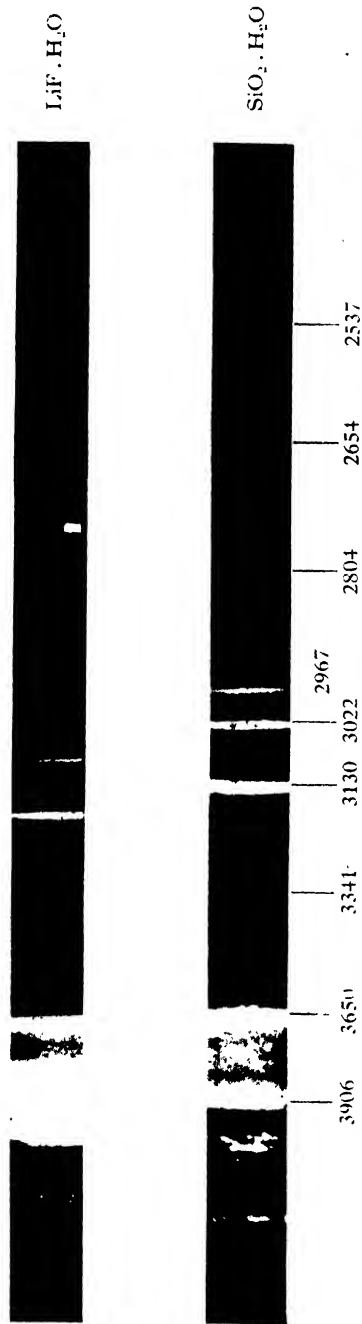


Plate II.  
Excitation spectra with Hg vapour lamp.

some certainty, however, the start of excitation at about 4000 Å., in agreement with the preliminary observations with selective filters referred to above, and indicates a definite strong peak at about 3130 Å. Very similar results were obtained with lithium fluoride wetted with water.

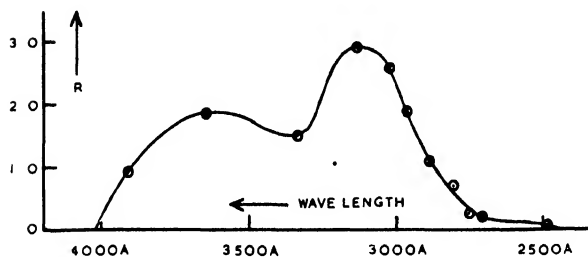


Figure 5. Qualitative representation of excitation spectrum of silica wetted with water.

$$R = \frac{\text{Density of line in excitation spectrum}}{\text{Density of line in direct mercury spectrum}}$$

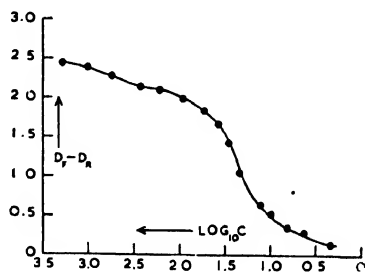


Figure 6. Variation of luminescence brightness with water content of wetted silica.

$D_F - D_R$  = net photographic density produced by image of fluorescent specimen.  
 $C$  = water concentration in molecules  $H_2O : SiO_2 \cdot 10^3$ .

Thus it seems certain that water adsorbed by silica or lithium fluoride is able to absorb radiation of wavelengths not absorbed by the liquid in bulk and, as indicated by the phosphorescence, to possess metastable levels not normally present.

#### § 5. RELATION BETWEEN BRIGHTNESS OF LUMINESCENCE AND LIQUID SOLID RATIO

The exciting light from a high pressure mercury lamp, after filtering through 6 mm. of Wood's glass, was focused on a thoroughly wetted specimen contained as a thin layer in a circular graphite capsule, 21 mm. in diameter, and 3 mm. deep, with thin walls and bottom. The graphite forms a container which is black and non-luminescent, light in weight, relatively inert chemically and relatively non-hygroscopic. A film camera of aperture  $f/2.9$  was set at such a distance from the glowing specimen as to give an image of 2 mm. diameter. A Wratten filter having a reasonable transmission for the peak of the main luminescent band and a carbon bisulphide cell, 2.5 cm. thick, were found to form a fairly efficient complementary filter combination to the Wood's glass. The graphite cell with its specimen of wetted solid was removed for weighing immediately after each photograph and then some liquid removed from the specimen by placing the cell in a glass tube connected to a vacuum pump. For the latter stages of water removal gentle heating was also applied. The cell was replaced in exactly the same position after each weighing and water removal, the camera film moved on 1 cm. and a new photograph of the glowing specimen taken. This procedure was repeated until no further loss of weight could be obtained, even after prolonged heating *in vacuo*. The image spots were photometered on the Cambridge photometer referred to previously. The evaluation of relative brightness cannot of course be carried out from these density measurements alone even if the Schwarzschild law of blackening is assumed to hold strictly.

But putting  $D_f$  = density of image of fluorescent spot,  $D_R$  = density of residual spot due to slight transmission of the exciting radiation by the filter system (i.e. density of spot when fluorescence brightness is reduced to zero, in practice about 0.2), and plotting  $D_f - D_R$  against the liquid-solid ratio, a curve results which appears to possess some interest. Such a plot is shown in Figure 6 for the silica-water system.

It will be observed that there is no indication within the range covered of the existence of an optimum concentration, but that there is first a gradual and relatively small drop of brightness over a large range of liquid content until a point is reached corresponding to about one molecule of water to 25 molecules of silica. There is then a rapid fall in brightness to a region of about one water molecule to 100 silica molecules. Such a result expressed in this manner would not appear to possess any special interest, but it had been noticed in preliminary investigations that the brightness of the luminescence of any wetted powder was clearly connected with the size of the particles; the smaller these were the brighter the luminescence. These observations, taken in conjunction with the spectral indications that the luminescence is related to adsorption, suggested an attempt to correlate the brightness with the specific surface of the solid (surface area per gm.).

The specific surface of the precipitated silica employed in the brightness-concentration experiments was kindly determined for us by Dr. Ashley and Mr. Catchpole of the Fuel and Metallurgy Department of the University of Leeds. They employed the low temperature nitrogen adsorption method of Brunauer, Emmett and Teller (1938). The value of the specific surface so obtained was  $172 \text{ m}^2$ . Using this value together with the value of  $11 \text{ \AA}^2$  for the area of the water molecule (the mean of two values quoted by Brunauer (1944)) it appears that the beginning of the rapid rate of fall of luminescence corresponds to the occupation of about one quarter of the surface by the water molecules. At the moment, we do not wish to assign any particular significance to the actual numbers, for neither the reliability of the underlying assumptions of the Brunauer, Emmett and Teller method nor the accuracy of the brightness determinations warrant this. It does appear reasonably probable, however, that the order is correct, for the size of the particles determined from an x-ray diffraction pattern obtained for us by Dr. G. W. Brindley of the Department of Physics of this University is of the same order as that indicated by the adsorption values. Moreover repetitions of the brightness-concentration curves gave the sudden drop of brightness at about the same point. (Some preliminary results for silica wetted with ethyl alcohol indicate that in this case the onset of the fall in brightness occurs at a coverage corresponding to approximately a monomolecular layer).

#### § 6. GENERAL SURVEY AND DISCUSSION OF RESULTS

Shifts in the spectral absorption of molecules adsorbed by solids have been observed by de Boer and his collaborators (de Boer 1935), but the production of luminescence by the contact of a non-luminescent liquid, such as pure water, with a non-luminescent solid, such as silica, under excitation by radiation not normally absorbed by either, provides evidence from a new angle that the process of adsorption involves energy changes in the adsorbed molecule. The occurrence of phosphorescence visible for some seconds after excitation indicates the introduction of metastable levels not previously existent, or of some measurable probabilities for normally forbidden transitions. The similarity between the

luminescent spectra of the same solid wetted by hydroxy molecules having different positive radicals, and the marked difference introduced by substituting heavy water for ordinary water, or in replacing the  $-OH$  radical by another negative radical, strongly suggest that the change of energy levels resulting in new regions of absorption and in luminescence is associated with energy changes in the negative radical brought about by the interaction of the adsorbed molecule with the solid surface.

The onset of a rapid fall of luminescence with liquid concentration at a point corresponding to only a fraction of a monomolecular layer in the case of silica wetted with water indicates that all the surface is not equally effective in bringing about these energy changes, and provides evidence from this new angle of the existence of active sites. The apparent difference in the number of active sites on the surface of the same solid, as demonstrated by the results of water and alcohol on silica, suggests that the number of active sites depends on the molecule adsorbed. It was observed during these studies that prolonged heating of a solid permanently reduced the brightness of luminescence obtainable by wetting. This result is in keeping with the well-known fact that prolonged heating often partially destroys the adsorptive and catalytic power of solids, presumably by a reduction of the surface area and number of active sites. In this connection it is perhaps worthy of note that of two Kieselguhrs, the more catalytically active was strikingly more luminescent when wetted.

Further evidence that all the active sites on a given solid are not alike is afforded by some observations on the luminescent spectra of wetted silica at three different water concentrations. When the water concentration is reduced to a value corresponding to the occupation of only 1.25 of the solid surface the peak of the main emission band is at 4000 Å. At a concentration corresponding on the above views to the occupation of all the active sites (one quarter of the surface covered) the peak is at 4339 Å., while at a concentration equivalent to five adsorbed layers of water molecules there is only a very slight further shift of the peak (to 4369 Å.). Photometer records of the three spectrograms are shown in Figure 7. If the first occupied sites are the most active, as would be expected, the molecules attached to these would be expected to suffer the greatest energy changes from the normal state. This means that the normal absorption which has been modified by adsorption to give an abnormal absorption at the excitation peak of 3130 Å. must be on the red side. The nearest absorption band of water on the red side appears to be at 5722 Å. (weak) and the so-called rain bands at 5924 Å. and 5952 Å. Assuming that the end state in both cases is the same (e.g. one of pre-dissociation) the shift of absorption would involve an energy change in the water molecule of approximately 42 kgm. calories per mole. The heat of wetting of water on silica is about 15 kg. calories per mole. This, however, is the integrated value, that is, the mean value including molecules added long after all the active sites have been occupied. The heat evolved for the first molecules added at the most active sites is almost certainly much greater, so that although the value of the energy change corresponding to the shift of absorption from the 5924 Å./5952 Å. region to 3130 Å. is nearly three times the integrated heat of wetting, it is not inconceivable that it does represent the heat of adsorption of the molecules adsorbed on the most active sites.

A much simpler interpretation is suggested by the fact that the free  $-OH$  radical has a strong absorption band stretching from 2600 Å. to 3470 Å. with a peak at 3064 Å. The similarity between this peak and the activation peak of

the luminescence of wetted silica suggests that the water molecules first adsorbed may be attached by a hydrogen bridge leaving an almost free  $-OH$  radical. The similarity of the spectra of hydroxy molecules having different positive radicals adsorbed on the same solid indicates that this is the more likely explanation.

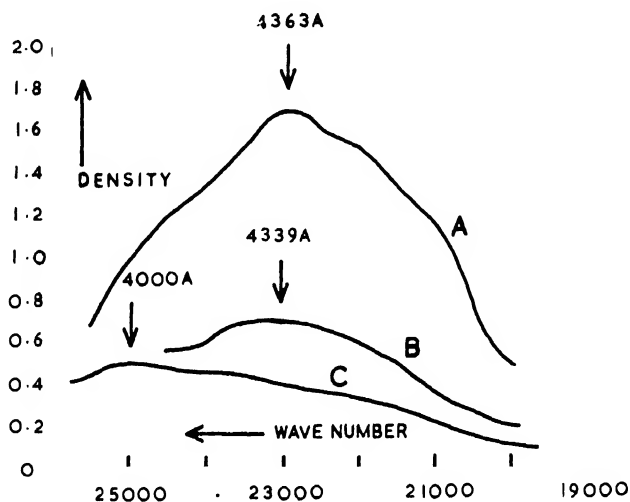


Figure 7. Photometer records of fluorescence spectrograms of silica wetted with water at various surface concentrations (specimen at 90° K.).

Curve A. Surface covered by five layers of water molecules.

Curve B.  $\frac{1}{4}$  of the surface covered by water molecules.

Curve C.  $\frac{1}{25}$  of the surface covered by water molecules.

We can offer no explanation of the phosphorescence, visible in some cases for seconds and even minutes after excitation has ceased. The fact, at least in the case of water on silica, that the phosphorescence is approaching its maximum value at a coverage of the surface corresponding to far less than a monomolecular layer indicates the existence of metastable levels of astonishingly long life in single molecules or ions.

#### ACKNOWLEDGMENTS

It is a pleasure to thank Professor R. Whiddington, F.R.S., C.B.E., for his advice and for the laboratory facilities so freely made available. One of us (G.C.F.) is indebted to the Department of Scientific and Industrial Research for a Research Grant and some of the apparatus was purchased from funds provided by the Government Grant Committee of the Royal Society.

#### REFERENCES

- DE BOER, J. H., 1935, *Electron Emission and Adsorption Phenomena*, p. 181 (Cambridge : University Press).
- BOWEN, E. J., 1935, *J. Chem. Soc.*, 76.
- BRUNAUER, S., 1944, *Physical Adsorption of Gases and Vapours*, p. 274 (Oxford : University Press).
- BRUNAUER, S., EMMETT, P. H., and TELLER, E., 1938, *J. Amer. Chem. Soc.*, **60**, 309.
- EWLES, J., 1930, *Nature, Lond.*, **125**, 706.
- EWLES, J., and MARTIN, W. E., 1939, *Proc. Leeds Phil. Soc.*, **3**, Part X, 557.

# The Resolving Power and Intensity Relationships of the Fabry Perot Interferometer with Silvered Reflecting Surfaces

By R. J. BRIGHT, D. A. JACKSON AND H. KUHN

Clarendon Laboratory, Oxford

*MS. received 30th September 1948*

**ABSTRACT.** By the use of a Fabry Perot etalon with very small spacing, the widths of the interference fringes were measured under conditions where the light could be considered as practically monochromatic. In this way, the resolving power which can be achieved with silver deposits of known optical density was determined for light of five different wavelengths between 6438 and 3610 Å. The results can be used for selecting the most favourable thickness of silvering of etalon plates, namely that which gives the resolving power required for a given purpose without unnecessary loss of intensity. The application of the results to multiple etalons is discussed.

## § 1. INTRODUCTION

THE performance of the Fabry Perot interferometer depends largely on the optical properties of the partially reflecting metal coatings. For an instrument with perfectly plane, parallel and uniform surfaces, the intensity distribution is described by Airy's formula

$$I(\epsilon) = \frac{I_{\max}}{1 + F \sin^2 \pi \epsilon} \quad \dots\dots(1)$$

where  $\epsilon$  is the fraction of a wavelength by which the path difference between two successive rays is in excess of a whole number.

The intensity distribution within the fringes is determined by  $F$ , which depends only on the reflectivity  $R$  according to the relation

$$F = 4R(1 - R)^2 \quad \dots\dots(2)$$

where  $R$  is defined as the intensity of the reflected light relative to that of the incident light. Thus the resolving power of an ideal etalon of given spacing depends only on  $R$ .

The absolute intensity, however, is determined by the factor  $I_{\max}$  in equation (1), which is given by the relationship

$$I_{\max} = T^2(1 - R)^2 \quad \dots\dots(3)$$

and thus depends also on the transmissivity  $T$  of the surface, defined by the ratio of the intensities of transmitted and incident light. It will be assumed throughout that the optical properties of the two reflecting surfaces of the etalon are equal.

In the ideal case of a surface without absorption, for which the relation  $R + T = 1$  holds,  $I_{\max}$  is equal to 1. The intensity at the maxima is then equal to the intensity of illumination which would be observed if the etalon were removed altogether. The degree to which, in actual fact, the sum  $R + T$  approaches unity can serve as a measure of the optical quality of the coating. For highly reflecting surfaces, variation of thickness affects the values of  $R$  and  $T$  in opposite senses; in fact the sum  $R + T$  is found to be approximately constant for films as they are used in practice. If the thickness is made large enough,  $1 - R$  approaches a limiting value while  $T$  continues to decrease. Thus, according to (2) and (3),



increase of the thickness of the metal film may only cause a small increase in  $F$ , and therefore in resolving power, but result in a serious loss in intensity. A correct balance of the two factors is important in most interferometric work, especially when two or more etalons are used in series. Even for silver, which is almost exclusively used in the visible range of the spectrum, very little is known about the reflectivities of partially transparent films.

The measurements described below were made in order to establish the relationship between  $R$  and  $T$  for silver films produced by evaporation, for a range of wavelengths from 6500 to 3400 Å. Since it is easy to control the thickness of the film by measurement of  $T$  during the evaporation, the data thus provided can be used for producing silver films of the required value of  $R$ , after a suitable value of the latter has been chosen as a compromise between resolving power and intensity.

The method of determining  $R$  consisted in measurement of the widths of Fabry Perot fringes produced under such conditions that the radiation could be considered to be practically monochromatic.

## § 2. THE PRODUCTION OF THE SILVER FILMS

The silver films were produced by evaporation *in vacuo*. This method is comparatively simple and reliable and has generally superseded the method of cathodic sputtering, though under carefully chosen conditions this latter also seems to be able to give silver films of high performance. If the target surface is well cleaned and a high vacuum maintained during the evaporation, reproducible and very high values of the reflectivity  $R$  can be achieved for any given transmission  $T$ , i.e. for any given thickness.

The evaporation chamber used in this work was a cylindrical brass tank of length 60 cm. and diameter 20 cm., evacuated by a large aperture mercury diffusion pump fitted with a liquid air trap to freeze out mercury. The vacuum was measured with a Pirani gauge. Three tungsten filaments, each of which carried two beads of pure silver, could be heated independently. This made it possible to stop the heating of each bead before it had completely evaporated. A few turns of fine platinum wire wrapped round the tungsten were used as a well-known method of making the silver adhere to the filaments. A shutter which could be placed between filament and target protected the latter from impurities evaporating from the filament in the early stages of heating. Another shutter, made of mica, prevented the front window from being covered with silver. Both shutters were operated by ground joints passing through the front lid. The vacuum seal between the latter and the chamber was made by means of a sulphur free rubber washer greased with apiezon tap grease.

Windows in the front and back plates allowed light from a lamp behind the tank to pass through the etalon plate *in situ* and to fall on a photocell. Colour filters were used to define the wavelength of the light. In this way the thickness of the silver film could be controlled during the evaporation by means of the measurement of the optical density.

The etalon plates were cleaned with strong nitric acid, rinsed with tap water and dried with pure cotton wool. The final cleaning was done in the tank by ionic bombardment; when a sufficiently good vacuum had been reached, a small amount of air was admitted and a glow discharge was passed through the tank for a few minutes. When a good vacuum had been established again the evaporation was carried out.

## § 3. THE MEASUREMENT OF THE TRANSMISSION

After the etalon plate had been taken out of the evaporation chamber, the transmission was measured more accurately for four narrow ranges of wavelengths in the visible spectrum. The etalon plate, placed face downward over a barrier layer "Eel" photocell, was illuminated by the light from a tungsten filament lamp fitted with suitable filters. The photo-current was measured with a low resistance galvanometer. This arrangement showed linear characteristics, and thus the transmission was given by the ratio of the current with the etalon plate in position to that with the plate removed. The filters used consisted of a copper sulphate filter to cut out all light of wavelength greater than 7000 Å. and transmitting only 10% at 6500 Å., and Wratten filters, according to Table 1.

Table 1

Colour	orange	yellow	green	blue
Catalogue number	27	22 · 58	62	47
Mean wavelength (Å.)	6000	5700	5300	4400

The transmission at 3600 Å. was measured by means of the light from a commercial mercury arc lamp, the bulb of which incorporated a Wratten filter 18a.

For two silverings, measurements of  $T$  were also made at 3380 Å. by photographic photometry. A quartz spectrograph was used and the transmission was measured for the silver line 3380 Å.; for the intensity marks the continuous radiation from a hydrogen discharge was photographed with varying slit widths.

The accuracy of the transmission measurements for visible light was to within about  $\pm 0.005$  in the value of  $T$ , which was sufficient for the present purpose. The measurement of  $T$  was always repeated at least once, after several days or weeks, and never showed any change.

## § 4. INTERFEROMETER AND LIGHT SOURCES

The width of interference fringes generally depends on the actual line width of the incident radiation, caused by Doppler effect, hyperfine structure and other causes of broadening, and on the "instrumental" width, i.e. the width which would be observed with strictly monochromatic light. If an etalon with very small spacing is used, and sufficiently narrow spectral lines are chosen, the width of the fringes is almost entirely due to the instrumental width. This condition was aimed at in the experiments described here.

An etalon with a separation of 1 mm. was used, so that one order corresponded to a wave-number difference of  $5 \text{ cm}^{-1}$ . Three U-shaped loops of tungsten wire were used as spacers. They were arranged so that the ends which were distorted when the wire was cut projected clear of the surface of the etalon plates. The pair of plates which was used throughout was made by Messrs. Adam Hilger Ltd. and consisted of quartz, cut at right angles to the optic axis. Their diameter was 2.5 cm., the thickness 0.7 cm., and the two faces formed an angle of  $2'$ .

The spacers, owing to their small area of contact, responded readily to variations of the pressure of the adjustment springs. This had the advantage that the diameter of the central fringe could be made small enough to allow a very accurate adjustment of the parallelism of the plates. The radius of the central fringe was thus adjusted so that it corresponded to a difference of about  $1/20$  wavelength from that at the centre of the fringe system. Variations in this radius could be

kept down to less than one quarter of its value over the whole area of the etalon illuminated through the stops used (5 to 10 mm. in diameter). The accuracy of the adjustment was thus less than  $1/40$  of a wavelength. This limit was set more by the irregularities in the surfaces of the plates than by the method of adjustment.

With the small distances used, the thermal expansion of the spacers did not present any difficulty. Moreover, the optical system was situated in a room the temperature of which was thermostatically controlled to  $1/10^\circ$  C., while the light sources were in another room, the light being admitted through a small hole in the dividing wall.

The optical system consisted of a Hilger E2 quartz spectrograph ( $f=60$  cm.) and an external etalon mounting. An image of the light source was formed in the plane of the etalon, and a quartz fluorite achromat of focal length 33 cm. formed the interference fringes on the slit of the spectrograph.

The spectrograph, which was slightly astigmatic, was focused for the whole spectral range for horizontal focal lines. The correct setting of the achromat was found by tilting the etalon and finding the best focus for the narrow outer fringes. In the visible spectrum, an alternative method was employed as a check. A telescope fitted with crosswires was focused for "infinity"; the eye piece was then removed and the telescope placed in the position normally occupied by the etalon, with the objective facing towards the quartz-fluorite achromat, so that an image of the crosswire, illuminated by the light source, was formed on the plate. The setting of the achromat giving the best horizontal focus was then chosen. The method is very accurate for etalons of not too large aperture.

Two light sources were used, a commercial cadmium discharge lamp and a water cooled hollow cathode tube, lined with silver foil and operated at a current of about 100 ma. The discharge was carried by helium circulating through charcoal cooled in liquid air.

Table 2 contains a list of the lines used. The second column gives the ratio of wavelength to the half-value width due to Doppler effect, at an estimated temperature of  $250^\circ$  C. in the cadmium lamp and  $50^\circ$  C. in the hollow cathode tube. The last column shows the fraction of an order of an etalon of separation 1 mm. which corresponds to a difference of wavelength equal to this half-value width.

Table 2

Line	$\lambda/d\lambda$	$dn$	Line	$\lambda/d\lambda$	$dn$
Cd 6438	$6 \cdot 10^5$	0.005	Cd 3610	$6 \cdot 10^5$	0.009
Ag 5465	$8 \cdot 10^5$	0.004	Cd 3438	$6 \cdot 10^5$	0.009
Cd 4662	$6 \cdot 10^5$	0.007	Ag 3380	$8 \cdot 10^5$	0.008
He 3888	$1.6 \cdot 10^5$	0.03			

With the exception of He 3888, the Doppler width of all the lines is less than  $1/100$  order. Broadening of the fringes due to this spectral width would therefore be relatively unimportant; only the measurements at 3888 Å. may have been liable to a small systematic error.

The only lines having hyperfine structure are the last three in the table. The ultraviolet Cd lines possess two components on either side of the main lines, but they are too weak to have much effect. The hyperfine structure of the line 3380 of silver is about ten times smaller than the width of the fringes observed at this wavelength.

## § 5. PHOTOMETRIC MEASUREMENT OF THE FRINGES

The tilt of the etalon was so adjusted that the centre of the fringe system was inside the slit image, and that one fringe was visible on both sides of the centre. The half value width was determined from the first fringe and in many cases checked by the use of the second. The scale, near the first fringe, was generally about 7 mm. per order, a half value width of  $1/20$  order corresponding to about 0.3 mm. The grain of the plates (Ilford Astra III and Zenith) and development effects were therefore of no significance.

For the photometric measurements of the plates, the recording microphotometer at the Oxford University Observatory was kindly made available by Professor Plaskett. The resolving power of this instrument is largely determined by the size of the thermocouple, the image of which on the plate is  $1/50$  mm. A ratio of 7:1 of record scale to plate scale was used. Any inaccuracies arising from photographic or photometric effects were therefore well under  $1/100$  of an order.

Intensity marks were made on the same plate, but with a different spectrograph, of focal length 150 cm. The slit was illuminated uniformly with light from a tungsten filament or a hydrogen discharge tube, and exposures of equal duration were made with different widths of the slit.

The somewhat laborious nature of the direct photometric measurement of the widths of the fringes made it difficult to deal with a larger number of plates. A relative method was therefore also employed and proved to be reliable and more convenient.

If a Wollaston prism is interposed between the quartz fluorite achromat and the slit, with its refracting edges horizontal, the fringe system is doubled. Photographs were made with a number of different separations of these doubled fringes, by altering the distance of the Wollaston prism from the slit. (When the Wollaston prism was used, the distance of the achromat was, of course, changed to compensate the change in optical distance.) Visual inspection showed which of these doubled fringes had a separation equal to the half value width, or to some known fraction of it. Measurement of the outer, narrow fringes enabled the splitting caused by the Wollaston prism to be measured accurately.

This visual method was "calibrated" by making a sample plate showing the appearance of double fringes of various degrees of separation. The half value width of the fringes photographed without Wollaston prism was first measured by direct photometry; the Wollaston prism was then inserted and, by variation of its position, a series of double fringes of various known splittings was photographed. The intensity at the minimum, relative to that at the maxima, was calculated by a graphical method and also, as a check, measured photometrically (Table 3).

Table 3

Separation as fraction of half value width	0.63	0.75	0.90	1.1	1.25
Intensity of minimum { calculated	1.0	0.94	0.85	0.75	0.67
{ measured	—	0.93	0.88	0.76	0.65

A separation of 0.75 of the half value width is still observable as resolved, and the greater resolutions are easily recognizable.

By visual comparison with this sample plate, the separation as a fraction of the half value width could be judged with sufficient accuracy from the use of Table 3, and the half value width could thus be calculated. The various fringes in each

exposure and the various exposures taken with different splittings allowed a number of comparisons covering different stages of resolution of these "doublets" with splittings ranging from 0.7 to 1.0 of the half value width. From each "doublet" the half value width was estimated and the average taken.

A difficulty of this double image method arose from the fact that the two fringes of a "doublet" were generally not of equal intensity, owing to polarization effects in the spectrograph. This was overcome by introducing a tilted glass plate causing partial polarization of the incident light. Small inequalities in the intensities were found not to impair the accuracy of the method.

#### § 6 RESULTS OF THE MEASUREMENTS OF TRANSMISSION

Table 4 gives the values of the transmission  $T = I/I_0$  and the optical density  $D = -\log T$  for the five silver coatings used. Each point is the average of two measurements. If an exponential law of absorption holds, the ratio of the optical densities of any two films should be independent of the wavelength. This is, on the whole, confirmed by the approximate agreement of all the values in any one of the last three lines of Table 4, where the suffix refers to the number of the silver

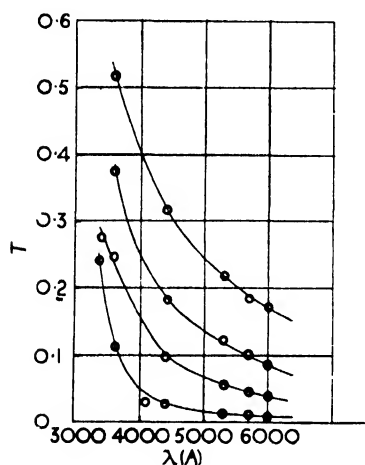


Figure 1.

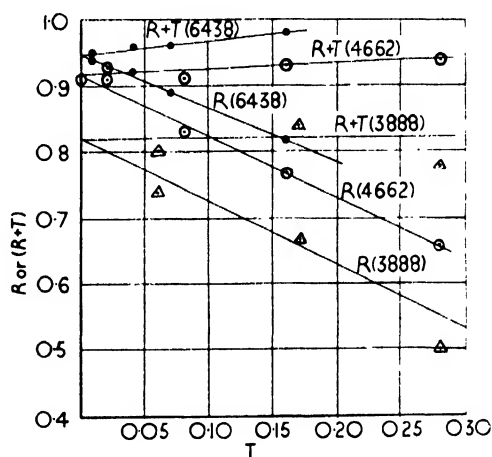


Figure 2.

coating. There seems, however, to be a slight rise of the ratio with increasing frequency. Interference effects inside the silver film might be responsible for these small deviations from Beer's law. The values of  $T$  for the first four films are plotted in Figure 1.

#### § 7. WIDTH OF FRINGES AND REFLECTIVITY

Table 5 contains the half value widths  $\delta$ , expressed as fractions of an order, of the fringes produced by etalons with the five different silverings. The results obtained from each photograph are given separately. The figures in brackets after the half value widths found by the method of the double image, indicate the degree of resolution in the photograph from which this half value width has been deduced; e.g. "0.43 (0.8)" signifies that the degree of resolution was 0.8 of that corresponding to the separation equal to the half value width, and that the value of (separation/0.8) is equal to 0.43.

Table 4

Wavelength (A.)		6000	5700	5300	4400	4100	3600	3380
Film No.								
7	<i>T</i>	0.17	0.19	0.22	0.32		0.52	
	<i>D</i>	0.77	0.72	0.66	0.50		0.28	
3	<i>T</i>	0.086	0.100	0.120	0.182		0.37	
	<i>D</i>	1.065	1.00	0.92	0.74		0.43	
4	<i>T</i>	0.040	0.045	0.053	0.097		0.24	(0.27)
	<i>D</i>	1.40	1.35	1.28	1.01		0.62	(0.57)
5	<i>T</i>	0.008	0.010	0.011	0.027	0.030	0.114	(0.24)
	<i>D</i>	2.10	2.00	1.96	1.57	1.52	0.96	(0.62)
6	<i>T</i>				0.005		0.04	
	<i>D</i>				2.3		1.4	
$D_3 : D_7$		1.39	1.39	1.39	1.48		1.54	
$D_3 : D_3$		1.31	1.35	1.39	1.37		1.44	
$D_5 : D_1$		1.50	1.48	1.53	1.55		1.55	(1.1)

Table 5. Half Value Widths  $\delta$  of Fringes as Fractions of Order

Film No.	Method *	6438	5465	4662	3888	3610	3438	3380 A.
7	D.I.	0.068 (1.0)		0.135 (1.0)	0.25 (1.0)			
		0.064 (0.7)			0.25 (0.7)			
	Ph.	0.065	0.10	0.14				
		0.058		0.14				
3	D.I.	0.039 (0.9)	0.067 (1.0)					
	Ph.	0.036	0.070	0.085	0.20			
4	D.I.	0.028 (0.9)	0.043 (0.8)	0.055 (0.9)		0.18 (0.9)		
		0.028 (0.7)		0.061 (0.7)				
	Ph.	0.023	0.036	0.063	0.13		0.30	
				0.061				
5	D.I.	0.021 (1.0)		0.027 (1.0)	0.10 (1.0)	0.10 (0.9)		0.20 (1.0)
		0.021 (0.8)		0.027 (0.8)	0.10 (0.8)	0.10 (0.7)		0.20 (0.85)
		0.021 (1.0)		0.029 (1.0)	0.10 (0.7)	0.10 (1.0)		0.20 (0.7)
				0.029 (0.8)	0.10 (1.0)	0.12 (0.7)		
				0.029 (0.7)	0.10 (0.9)	0.12 (0.9)		
				0.032 (0.8)	0.10 (0.9)			
				0.032 (1.0)				
				0.030 (1.2)		0.10 (1.0)		
6	D.I.					0.11 (1.1)		
						0.10 (1.0)		
						0.10 (0.7)		
						0.10 (0.9)		

\* D.I.=double image method; Ph.=direct photometric method.

The good agreement between the values obtained by the method of the double image with different degrees of resolution, and the agreement of these values with those found by direct photometric measurement shows that the method of measurement is sufficiently accurate.

The first two lines in each section of Table 6 give the transmissivities  $T$  read from the curves of Figure 1, and the mean values of the half value widths  $\delta$ , as fractions of an order, derived from Table 5.

Table 6

		6438	5465	4662	3888	3610 Å.
7	$T$	0.16	0.21	0.28	0.43	
	$\delta$	0.064	0.10	0.14	0.25	
	$R$	0.82	0.73	0.66	0.46	
	$T \cdot R$	0.98	0.94	0.94	0.89	
3	$T$	0.07	0.11	0.16	0.28	
	$\delta$	0.037	0.068	0.085	0.20	
	$R$	0.89	0.81	0.77	0.50	
	$T \cdot R$	0.96	0.92	0.93	0.78	
4	$T$	0.04	0.05	0.08	0.17	0.24
	$\delta$	0.026	0.039	0.060	0.13	0.18
	$R$	0.92	0.89	0.83	0.67	0.58
	$T \cdot R$	0.96	0.94	0.91	0.84	0.82
5	$T$	0.007		0.02	0.06	0.11
	$\delta$	0.021		0.029	0.10	0.11
	$R$	0.94		0.91	0.74	0.72
	$T \cdot R$	0.95		0.93	0.80	0.83
6	$T$			0.00		0.04
	$\delta$			0.030		0.10
	$R$			0.91		0.74
	$T \cdot R$			0.91		0.78

The formulae (1) and (2) lead to a relation between half value width  $\delta$  and reflectivity  $R$ :

$$\sin \pi \delta / 2 = (1 - R) / (2\sqrt{R}).$$

This relation has been used for calculating the second line of Table 7, and also for calculating the values of  $R$  in the third rows of Table 6 from the measured values of  $\delta$  given in the second rows. Figure 2 shows a plot of these values of  $R$  against  $T$ . To avoid confusion of the graph, the data for 5465 and 3610 Å. have been omitted.

#### § 8. RESOLVING POWER AND INTENSITY

If two monochromatic radiations of equal intensity differ in wavelength by an amount  $d\lambda$  such that the etalon fringes are separated by their half value width, the resulting intensity curve can be derived from Airy's formula. The ratio of the intensity of the maxima to that of the minimum between them is found as

$$1 + \frac{1}{1 + 4R(\sin^2 \pi \delta)(1 - R)^2},$$

where  $\delta$  is the fraction of an order corresponding to the half value width and is the function of  $R$  quoted in § 7. For small values of  $\delta$  this quantity is independent of the value of  $R$  and is equal to 1.20. The dip in the intensity curve is thus very similar to that produced in a prism or grating spectrograph by two lines fulfilling Rayleigh's criterion of resolution, as appears also from the values of Table 3. It is therefore convenient to define the limits of resolution by the condition  $n\lambda = (n - \delta)(\lambda + d\lambda)$  which gives the resolving power  $\lambda/d\lambda = n/\delta = 2t/\lambda\delta$ , where  $n$  is the order of interference and  $t$  the separation between the plates. The value  $1/\delta$  can be considered as "effective number of interfering beams",  $N_{\text{eff}}$ , from which the resolving power is obtained by multiplication with the order of interference. In Figure 3, this value is plotted as a function of  $T$  from the values of Table 5.

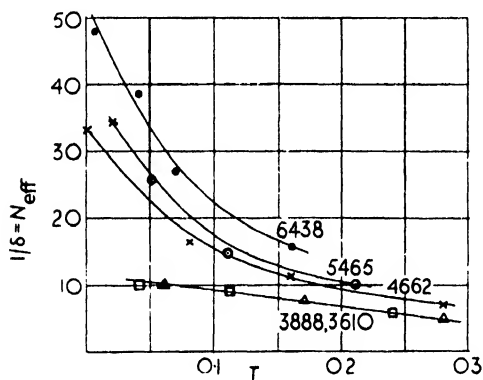


Figure 3.

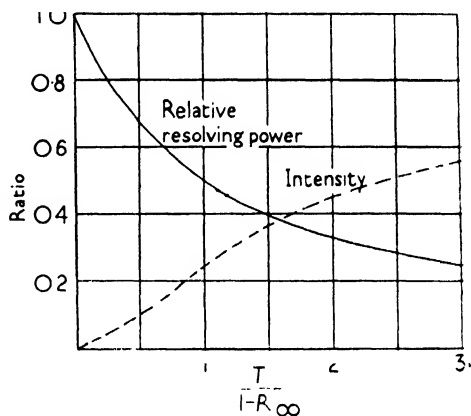


Figure 4.

The "contrast" of the fringes for monochromatic light, i.e. the ratio of the intensity of the maxima to that of the minima (the background at a point midway between two maxima) can be derived from  $R$ :

$$I_{\text{max}}/I_{\text{min}} = (1 + R)^2/(1 - R)^2.$$

This "contrast" factor is also included in Table 7. It is an important factor whenever weak components are to be observed in the presence of strong lines.

The intensity of the maxima, relative to the intensity of illumination in the absence of an etalon depends on both  $R$  and  $T$ , according to equation (3).

Table 7

$R$	0.98	0.975	0.97	0.96	0.95	0.94	0.93	0.92	0.91	0.90	
$1/\delta$	155	134	104	77	62	52	44	38	33	29	
$I_{\max}/I_{\min}$	9800	6200	4300	2400	1500	1000	750	550	450	360	
$R$	0.88	0.86	0.84	0.82	0.80	0.78	0.75	0.70	0.65	0.60	0.50
$1/\delta$	24	20	18	16	14	12	11	9	7	6	5
$I_{\max}/I_{\min}$	240	170	130	100	80	65	50	33	22	16	9

#### § 9. USE OF THE DATA

On the basis of the data contained in Figures 1 and 3, Tables 4 and 6 and equation (3) it is possible (i) to decide upon a value of  $T$  for the silver film which, for the given purpose, provides the best compromise between the requirements of



resolving power and intensity, and (ii) to achieve the required value of  $T$  by controlling, during the evaporation, the optical density measured at any conveniently chosen wavelength.

For example, if a minimum  $N_{\text{eff}}$  (resolving power/order) be required at a given wavelength, Figure 3 gives values of  $T$  for neighbouring wavelengths, and the  $T$  for the required wavelength is found by interpolation from Figure 1. The maximum intensity available is then calculated from equation (3).

The data may be presented in a way in which the parameter wavelength is artificially suppressed, thus reducing the complexity of the numerous curves for different wavelengths. In Figure 2, the sum of  $R$  and  $T$  is plotted against  $T$  for different wavelengths. It appears that for practical purposes  $R + T$  can be assumed to be independent of the thickness of the layer. Actually, the curve for red light shows a drop with decreasing  $T$ , but the accuracy of the values  $R + T$  is probably not better than within 1 or 2%, and it is probable that all or part of the drop is caused by the imperfections of the etalon plates and by the finite spectral width of the lines. These factors might well make it impossible to reach the very high values of resolving power theoretically possible for very low values of  $T$ .

Table 8 gives the values of  $R + T$  interpolated from the results of the measurements.

Table 8

$\lambda$ (A.)	6500	6000	5500	5000	4500	4000	3800	3600	3400
$R_{\infty} - R : T$	0.97	0.96	0.95	0.94	0.92	0.86	0.82	0.78	(0.70)

If  $R + T$  is taken to be constant for any given wavelength, the relation between resolving power and intensity can be graphically represented in the following way (Figure 4): The ordinate of one curve is the intensity of the maxima relative to the intensity in the absence of an etalon, that of the other curve is the resolving power expressed as a fraction of that for a very dense layer with reflectivity  $R_{\infty} = R + T$  (change of wavelength is allowed for by change of the value of  $R_{\infty}$ ). The abscissae of both curves are the values of  $T/(1 - R_{\infty})$ .\*

The curves show, for example, that for  $T = 1 - R_{\infty}$  the resolving power is 50% of the maximum possible with a very dense silvering, and the intensity of the fringes is 25% of that in the absence of an etalon.

#### § 10. APPLICATION OF THE RESULTS TO MULTIPLE ETALONS

In work with the multiple etalon, a quantitative control of the thickness of the reflecting films is almost indispensable. In this instrument, which was first described by Houston (1927), two etalons are used in series, with spacings  $t$  and  $t'$  in an integral ratio. A method of adjustment by means of change of air pressure has been introduced by two of the present authors (Jackson and Kuhn 1938, 1939). The function of the shorter etalon, of spacing  $t'$ , consists mainly in suppressing certain orders of the large etalon and thus extending the spectral range of the latter. The reflectivity of the shorter etalon must therefore be made large enough to cause the subsidiary maxima (the suppressed orders) to be faint compared with the weakest line of the pattern under investigation. The ratio of the intensity of the principal maxima to that of the first, i.e. strongest, subsidiary maxima is

\* The broken curve is the function  $x^2/(x+1)^2$  of the abscissa  $x$ .

given by the relation  $I/I' = 1 + 4R(\sin^2 \pi t'/t)/(1 - R)^2$ . Some typical values of this ratio have been calculated from the data of the preceding paragraphs for a silvering of the shorter etalon with  $T = 0.04$  at 6000 Å. (Table 9).

Table 9

$\lambda$ (Å.)	6500	6000	5500	5000	4500	4000	3800
$t, t'$							
2	1000	750	400	200	140	40	20
4	500	380	200	100	70	20	11
10	100	70	40	20	15	5	4
20	25	18	11	6	4	2	1.5

The compound etalon with both components silvered to this density is very effective; the intensity of the principal maxima is, according to the wavelength, between 0.21 and 0.36 of that in the case of the simple etalon, and between 0.04 and 0.11 of that if the lines were photographed without any etalon. A ratio of the spacings of 10:1 can be used in the red and orange, for most purposes, and 4:1 is satisfactory over most of the visible part of the spectrum.

The small gain in resolving power due to the shorter etalon is of little practical importance, except for very small values of the ratio  $t, t'$ .

If two etalons of equal spacings are used in series, the resolving power of the combination is appreciably larger (by about 60% for equal densities of the silverings) than that of a single etalon. Full use of this fact can only be made if the phases of the two etalons are adjusted very accurately indeed. A more important application of this form of multiple etalon is its use for the detection of very faint components. The ratio of the intensity of the maxima to that at the point midway between them is clearly the product of the corresponding ratios for the individual etalons. If the values in the third line of Table 7 are squared, they give the values  $I_{\max}/I_{\min}$  for the combination of two etalons of equal spacings and equal reflectivities of the silver films.

#### § 11. DISCUSSION AND COMPARISON WITH DIRECT MEASUREMENTS OF REFLECTIVITIES

The intensity relations discussed in the last paragraph are only valid for strictly monochromatic light. If the "spectral" width of the line, which may for instance, be caused by Doppler broadening, is comparable with the instrumental width or even larger, the ratio  $I_{\max}/I_{\min}$  is reduced correspondingly.

When the values of  $R$  derived from widths of etalon fringes are compared with direct measurements of reflectivities, it must be remembered that Airy's formula cannot be expected to hold rigorously, owing to imperfections of the plates and the silver films, and that the value of  $R$  thus derived may differ slightly from the actual reflectivity. This objection does not, of course, affect the relation between transmission and resolving power, both of which have been measured directly. It would, however, affect the intensity relations which then would only have approximate validity. The influence of imperfections on the intensity distribution has been discussed by Dufour and Picca (1945) but the experimental data for the contrast factor  $I_{\max}/I_{\min}$  are too scarce to allow any definite conclusions.

It is fairly obvious that imperfections of the plates or silver films must increase

the half value width for a given reflectivity. The values of  $R$  derived from widths of etalon fringes are therefore likely to be slightly lower than the reflectivities which accurate direct measurements of the same films would have given.

The only direct measurements of reflectivities of vacuum deposited transparent silver films described in the literature appear to be those by Strong and Dibble (1940). But they are relative values only, measured with reference to a thick silver film. For green light, Tolansky (1946) reports some values of  $R$  and  $T$  which are fairly close to our results, but no experimental details are given.

The reflectivity of thick silver films ( $T=0$ ), deposited *in vacuo*, has been measured by Baxter (1937), who finds a value of 0.94 at 6000 Å., and by Strong (1940) who finds 0.95 at the same wavelength. Edwards and Petersen (1936) measure reflectivities of thick films deposited under apparently specially good conditions. Their value of  $R_{\infty}$  for yellow light is 0.985. In view of the mentioned influence of imperfections of the surfaces, this latter value is not incompatible with our results, whereas the values of Baxter and Strong seem to be rather low.

For films produced by cathodic sputtering, some extremely high values of  $R+T$  have been reported by Romanowa, Robzow and Pokrowsky (1934), but it is not clear from the description of their method if infra-red light has been excluded. Measurements by Goos (1936), of reflectivities of sputtered films give considerably lower values, the sum  $R+T$  being about 0.95 for 5780 Å. and 0.92 for 4350 Å.

#### REFERENCES

- BAXTER, A., 1937, *J. Sci. Instrum.*, **14**, 303.  
 DUFOUR, C., and PICCA, P., 1945, *Rev. d'Optique*, **24**, 19.  
 EDWARDS, H. W., and PETERSEN, R. P., 1936, *Phys. Rev.*, **50**, 871.  
 GOOS, F., 1936, *Z. Phys.*, **100**, 95.  
 HOUSTON, W. V., 1927, *Phys. Rev.*, **29**, 475.  
 JACKSON, D. A., and KUHN, H., 1938, *Proc. Roy. Soc. A*, **167**, 205; 1939, *Ibid.*, **173**, 278.  
 ROMANOWA, M., ROBZOW, A., and POKROWSKY, G., 1934, *Phys. Z. Sowjet*, **5**, 46.  
 STRONG, J., 1940, *Mod. Phys. Lab. Practice*, pp. 185 and 375.  
 STRONG, J., and DIBBLE, B., 1940, *J. Opt. Soc. Amer.*, **30**, 431.  
 TOLANSKY, S., 1946, *Physica*, **12**, 650.

# Intensity Distribution for Bands of the $\gamma$ -System of $\text{MgH}^+$

By M. E. PILLOW

Imperial College, London, and Northern Polytechnic, London

*Communicated by R. W. B. Pearse; MS. received 24th May 1948, and in amended form 7th October 1948*

**ABSTRACT.** The intensity distribution for bands of the  $\gamma$ -system of  $\text{MgH}^+$  is deduced theoretically from the wave functions for the various energy states, and is compared with the distribution of the observed bands.

Lines of the (2, 3) band, not previously noted, have been observed.

## § 1. INTRODUCTION

PEARSE (1929) has published particulars of a number of bands in the ultra-violet spectrum produced by a magnesium arc in hydrogen. These bands he attributes to a  $^1\Sigma \rightarrow ^1\Sigma$  transition for  $\text{MgH}^+$ . Guntzsch (1934, 1939) later made further measurements on this system of bands, using as source a hydrogen discharge tube with magnesium electrodes, and also a magnesium-carbon arc, and carrying his investigations to longer wavelengths. His analysis agrees closely with that of Pearse, and he has observed a number of additional bands.

When the bands so measured are set out in the usual vibration table they are found to lie close to one main parabola, with a suggestion of the existence of an inner parabola (Table 1). The positions of these parabolas are indicated by heavy type.

Table 1. Observed Bands

$v''$	0	1	2	3	4	5	6	7	8
$v'$ 0	AB	<b>AB</b>	<b>AB</b>	<b>AB</b>	B				
1	<b>AB</b>	AB		AB	B	<b>B</b>	.		
2	<b>AB</b>			<b>C</b>		B	<b>B</b>	B	
3	<b>AB</b>				<b>B</b>		B	<b>B</b>	<b>B</b>
4	<b>B</b>								<b>B</b>
5	B								
6		<b>B</b>							

A: bands recorded by Pearse; B: bands recorded by Guntzsch; C: band now observed (see § 8).

## § 2. SPECTROSCOPIC DATA AND FORMULAE USED

The vibrational energy terms are expressed in the form

$$G(v) = \omega_e(v + \frac{1}{2}) - x_e \omega_e(v + \frac{1}{2})^2 \dots$$

Pearse's analysis gives, for the two electronic states, initial state  $\omega'_e = 1138.4$ ,  $x'_e \omega'_e = 9.5$ ; final state  $\omega''_e = 1702.2$ ,  $x''_e \omega''_e = 34.2$ .

The rotational terms are expressed in the form

$$F(J) = \{B_e - \alpha(v + \frac{1}{2}) \dots\} J(J+1) + DJ^2(J+1)^2 \dots$$

For these constants, Pearse gives: initial state,  $B'_e = 4.302$ ,  $\alpha' = 0.0492$ ; final state,  $B''_e = 6.378$ ,  $\alpha'' = 0.1854$ . The  $D$ 's are too small to be relevant here. The corresponding values of the constants as calculated by Guntzsch in 1934 from his measurements agree closely with these, except in the case of  $x''_e \omega''_e$ , for which he gives 30.2, and suggests an appreciable term in  $(v'' + \frac{1}{2})^3$ . Pearse's values have been used in the following calculations.\*

### § 3. POTENTIAL ENERGY FUNCTIONS AND DERIVED CONSTANTS

The polynomial expansion in powers of  $(r - r_e)/r_e$ , with coefficients calculated from Dunham's results (1932), was found unsatisfactory for both electronic states, as the coefficients are too large to allow the polynomials to converge suitably. Morse's form of the potential function (1929) has therefore been used,  $U = D(1 - e^{-ax})^2$ , where  $x$  stands for  $(r - r_e)$ . The constants in this equation are derived from the spectroscopic constants:

$$D = \omega_e^2 / 4x_e \omega_e; \quad a = \sqrt{(8\pi^2 c \mu x_e \omega_e / h)}; \quad B'_e = h / 8\pi^2 c \mu r_e^2, \quad \text{giving } r_e;$$

$$\mu = (24.32 / 25.32) \times 1.66 \times 10^{-24} = 1.595 \times 10^{-24} \text{ gm.}$$

$$\text{whence} \quad r'_e = 2.012 \times 10^{-8} \text{ cm.}, \quad r''_e = 1.652 \times 10^{-8} \text{ cm.}; \quad D' = 34,110 \text{ cm}^{-1},$$

$$D'' = 21,180 \text{ cm}^{-1}; \quad a' = 0.7384 \times 10^8 \text{ cm}^{-1}, \quad a'' = 1.401 \times 10^8 \text{ cm}^{-1}.$$

The curves plotted from these data are shown in the Figure, together with the parabolic curves (dotted) obtained by using only the first term,  $D a^2 x^2$ , of the expansion in each case.

Rees (1947) suggests a method of plotting the potential curve directly in terms of the measured constants. This method was applied here, and was found to give curves for both states agreeing very closely with those derived from the Morse function.

[It should be noted that the values  $D'$ ,  $D''$  quoted above give values for the dissociation energies of 4.13 ev. and 2.5 ev., and these are probably high, being derived by extrapolation from the data for a few bands. In particular, the difference  $D'_e - D''_e$  is much greater than that obtained by considering the  $^2P \rightarrow ^2S$  transition for ionized magnesium. But the potential curves are used only over the range covered by the measured bands, and they are presumably reasonably correct within this range.]

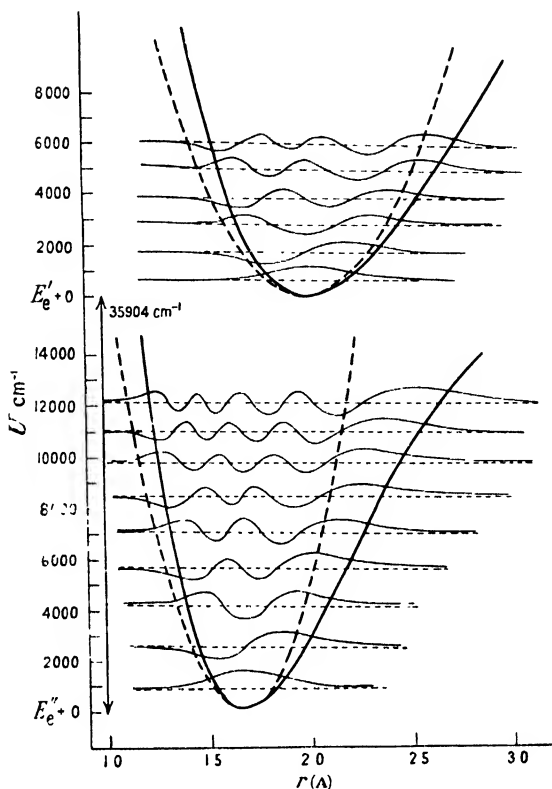
### § 4. WAVE FUNCTIONS FOR VIBRATOR

To avoid the heavy working involved in the calculation of the wave functions from Morse's formula, the curves have been derived by approximation from those for a harmonic oscillator, given by

$$\psi_v = d^{-\frac{1}{2}} (2^v v! \sqrt{\pi})^{-\frac{1}{2}} \exp \left\{ -\frac{1}{2} (x/d)^2 \right\} H_v(x/d),$$

where  $d^2 = h / 4\pi^2 c \mu \omega_e$ . Gaydon and Pearse (1939) give a table of these functions, omitting the initial  $d^{-\frac{1}{2}}$ , for half-integral values of  $x/d$ . For the higher energy levels it has been found necessary to calculate some intermediate values, and the complete scheme used is shown in Table 2.

\* Guntzsch, in his dissertation in 1939, to which the author had access only after making these calculations, introduces a term in  $(v + \frac{1}{2})^3$  in the excited state also, and this necessitates a change in  $x'_e \omega'_e$ , to 6.8. Over the small range of energy levels involved, however, the difference produced by this change of constants is small, and the effect on the calculated intensities negligible.



Potential energy functions and wave functions for vibrations in two electronic states.

Table 2. Wave Functions Corresponding to Parabolic Potential Energy Function

$n$	0	1	2	3	4	5	6	7	8
$x/d$ 0	0.751	0	-0.531	0	0.460	0	-0.420	0	0.393
$\frac{1}{4}$				-0.302	0.336	0.323	-0.261	-0.334	0.128
$\frac{1}{2}$	0.663	0.469	-0.234	-0.478	0.034	0.438	0.096	-0.380	-0.184
$\frac{3}{4}$				-0.460	-0.287	0.279	0.382	-0.102	-0.395
1	0.456	0.644	0.322	-0.263	-0.465	-0.056	0.391	0.263	-0.234
$1\frac{1}{4}$				0.027	-0.420	-0.360	0.124	0.416	0.144
$1\frac{1}{2}$	0.244	0.518	0.604	0.317	-0.187	-0.461	-0.229	0.243	0.397
$1\frac{3}{4}$				0.513	0.125	-0.321	-0.430	-0.106	-0.310
2	0.101	0.287	0.502	0.585	0.393	-0.026	-0.389	-0.393	-0.028
$2\frac{1}{4}$				0.553	0.546	0.282	-0.132	-0.420	-0.349
$2\frac{1}{2}$	0.033	0.117	0.269	0.453	0.567	0.493	0.188	-0.198	-0.428
$2\frac{3}{4}$				0.330	0.493	0.562	0.443	0.130	-0.235
3	0.008	0.035	0.100	0.217	0.373	0.513	0.549	0.405	0.094
$3\frac{1}{4}$						0.401	0.522	0.536	0.366
$3\frac{1}{2}$	0.002	0.008	0.027	0.071	0.153	0.275	0.415	0.522	0.526
$3\frac{3}{4}$									0.542
4	0	0.001	0.005	0.017	0.043	0.093	0.177	0.292	0.418
$4\frac{1}{4}$									
$4\frac{1}{2}$		0	0.001	0.003	0.009	0.022	0.049	0.098	0.174
$4\frac{3}{4}$									
5			0	0	0.001	0.004	0.009	0.022	0.045
$5\frac{1}{4}$									
$5\frac{1}{2}$					0	0	0.001	0.003	0.008
$5\frac{3}{4}$									
6							0	0	0.001

The values of  $d$  in initial state are  $d' = 1.749 \times 10^{-9}$ ;  $d'' = 1.426 \times 10^{-9}$ . Since  $x = r - r_e$ , the function  $\psi_v d^{\frac{1}{2}}$  corresponding to a harmonic oscillator at any one energy level could be plotted from this table.

To each value of  $r$  on the parabolic potential energy curve there corresponds a slightly different value,  $r_M$ , at the same level on the Morse curve. The necessary correction of the wave functions has been made approximately by using  $r_M$  in place of  $r$  for each point plotted. This method of approximation is rapid, gives a smooth curve for the wave function throughout, and seems as well justified as other approximations used for the purpose. No attempt has been made to correct the slight departure from normalization involved, and the factor  $d^{-\frac{1}{2}}$ , being constant, has been omitted throughout. The wave functions plotted in this way are shown in the Figure.

### § 5. CALCULATION OF INTENSITIES OF BANDS

It has been assumed that the intensity of the ( $v', v''$ ) band is proportional to

$$\exp(-E_{v''}/k\theta) \nu^4 \left[ \int_{-\infty}^{\infty} \psi' \psi'' dr \right]^2,$$

where  $\nu_0$  is the wave number of the band-origin and  $\psi', \psi''$  the wave functions for the initial and final vibrational states.

The first factor in the expression is intended to allow for the effect on the distribution of the initial energy states of the absolute temperature  $\theta$ . This is a doubtful quantity, since under the high voltages used the disturbances in the molecular states are not due to thermal movements alone. It will be seen (§7) that the visibility of the measured bands indicates a value of  $\theta$  probably in excess of the temperature actually possible in the tube. The integration has been carried out numerically, using the graphs of the wave functions, as was done by Gaydon and Pearse (1939).

### § 6. TABULATION OF INTENSITIES

Tables 3-6 show the calculated intensities for a series of values of  $\theta$ . The intensity in each case is expressed as a percentage of that of the strongest band, and anything below 1% is omitted. Thick type indicates the parabolas connecting calculated maxima.

No attempt could be made to compare the intensities experimentally, but it is presumed that those bands which have been observed are probably the most intense.

Table 3. Intensity Distribution for  $\theta \rightarrow \infty$

$v''$	0	1	2	3	4	5	6	7	8
$v'$ 0	33 <sup>AB</sup>	85 <sup>AB</sup>	100 <sup>AB</sup>	65 <sup>AB</sup>	33 <sup>B</sup>	7			1
1	71 <sup>AB</sup>	46 <sup>AB</sup>		51 <sup>AB</sup>	87 <sup>B</sup>	69 <sup>B</sup>	24	2	1
2	67 <sup>AB</sup>	12	8	10 <sup>C</sup>	4	78 <sup>B</sup>	85 <sup>B</sup>	46 <sup>B</sup>	5
3	63 <sup>AB</sup>	2	32	1	7 <sup>B</sup>	1	42 <sup>B</sup>	88 <sup>B</sup>	66 <sup>B</sup>
4	19 <sup>B</sup>	21	14	8	23		1	17	73 <sup>B</sup>
5	31 <sup>B</sup>	40		14	1	31	22	3	11

Table 4. Intensity Distribution for  $\theta = 3,000^\circ \text{K.}$

	0	1	2	3	4	5	6	7	8
0	33 <sup>AB</sup>	85 <sup>AB</sup>	100 <sup>AB</sup>	65 <sup>AB</sup>	33	17			1
1	35 <sup>AB</sup>	27 <sup>AB</sup>		30 <sup>AB</sup>	50 <sup>B</sup>	40 <sup>B</sup>	14	1	1
2	22 <sup>AB</sup>	4	3	3 <sup>C</sup>	1	26 <sup>B</sup>	29 <sup>B</sup>	15 <sup>B</sup>	2
3	12 <sup>AB</sup>		6		1 <sup>B</sup>		8 <sup>B</sup>	17 <sup>B</sup>	13 <sup>B</sup>
4	2 <sup>B</sup>	2	2	1	3			2	8 <sup>B</sup>
5	1 <sup>B</sup>	3		1		2	1		

Table 5. Intensity Distribution for  $\theta = 2,000^\circ \text{K.}$

$v''$	0	1	2	3	4	5	6	7	8
0	33 <sup>AB</sup>	85 <sup>AB</sup>	100 <sup>AB</sup>	65 <sup>AB</sup>	33 <sup>B</sup>	7			1
1	27 <sup>AB</sup>	20 <sup>AB</sup>		23 <sup>AB</sup>	38 <sup>B</sup>	30 <sup>B</sup>	11	1	
2	13 <sup>AB</sup>	2	2	2 <sup>C</sup>	1	15 <sup>B</sup>	17 <sup>B</sup>	9 <sup>B</sup>	1
3	5 <sup>AB</sup>		3		1 <sup>B</sup>		4 <sup>B</sup>	8 <sup>B</sup>	6 <sup>B</sup>
4	1 <sup>B</sup>	1			1				3 <sup>B</sup>
5		1							

Table 6. Intensity Distribution for  $\theta = 1,000^\circ \text{K.}$

$v''$	0	1	2	3	4	5	6	7	8
0	33 <sup>AB</sup>	85 <sup>AB</sup>	100 <sup>AB</sup>	65 <sup>AB</sup>	33 <sup>B</sup>	7			1
1	12 <sup>AB</sup>	9 <sup>AB</sup>		10 <sup>AB</sup>	17 <sup>B</sup>	13 <sup>B</sup>	5		
2	2 <sup>AB</sup>					3 <sup>B</sup>	3 <sup>B</sup>	2 <sup>B</sup>	
3								1 <sup>B</sup>	

A : bands observed by Pearse ; B : bands observed by Guntch ; C : band now observed.

## § 7. RESULTS

The calculated intensities at any temperature from  $1,000^\circ \text{K.}$  upwards show maxima lying on a definite outer parabola, with the (0,2) band strongest in every case, and at very high temperatures the inner parabola also appears. The values of  $\theta$  required for all the recorded bands to be intense enough to be seen are very high ; Guntch's bands require at least  $3,000^\circ \text{K.}$ , and Pearse's  $2,000^\circ \text{K.}$  This last is certainly higher than any temperature, in the ordinary sense, that could be attained in the apparatus used by Pearse, and this suggests that the "temperature" in an arc, as indicated by the energy levels of the molecules, may be much higher than the temperature of the electrodes. If this is conceded, it is seen that the distribution of the recorded bands agrees very closely with that deduced from the wave functions.

On Pearse's plates there are many faint lines for which no analysis has yet been published. Measurements have been made on a number of these, and some of them appear to belong to the (2,3) band of the system (Table 7). This band lies on the inner parabola, and the fact that it is just visible is in fair agreement with its calculated intensity.



Table 7. Lines of (2,3) Band

R			P		
(1)	(2)	(3)	(1)	(2)	(3)
8 33106·4	33107·6	33107·1	8 32966·3	32967·2	32968·1
9 33087·3	33088·4	—	9 32930·4	32931·7	32932·1
10 33063·2	33064·3	33065·4	10 32892·0	32892·1	32892·8
11 —	33039·4	33039·5	11 32849·2	32850·8	32851·0
12 33008·8	33009·7	—	12 32805·7	32805·7	32805·1
13 32976·9	32977·9	32978·7	13 32757·1	32758·1	32759·3
14 32942·4	32943·1	32943·5	14 32707·2	32707·6	32708·1
15 32904·2	32905·6	32905·0			
16 32864·2	32865·4	32865·2	(1) $\nu$ calculated from Pearse's data;		
17 32820·4	32821·0	32822·3	(2) $\nu$ calculated from Guntzsch's data;		
18 32774·4	32775·3	—	(3) measured values of $\nu$ .		
19 32725·9	32726·4	32726·6			

There are a few small discrepancies between the calculated intensities and the observed bands :

(1) The calculated intensity of the (3,4) band ( $\nu_0=32805\cdot2$ ) is low at all temperatures. Yet Guntzsch records this band, and even on Pearse's plates a few of the faint lines that have been measured appear to belong to it. Here is apparently a disagreement between calculated and observed intensities.

(2) The (1,6) band ( $\nu_0=27971\cdot4$ ), which at high temperatures should be noticeably intense, has not been observed. This band, however, would lie in the same region as the (2,7) and (3,8) bands, both of which do appear, and Guntzsch states that the lines in this region are crowded, and difficult to identify.

#### § 8. CONCLUSION

Allowing for the approximations made in the calculations, and for the fact that two independent sets of observations have been used, with a consequent slight discrepancy in the derived constants, there is very close agreement between the calculated and observed distributions of the bands in this spectrum.

#### ACKNOWLEDGMENT

The author is indebted to Dr. R. W. B. Pearse for suggesting the subject of this paper, for access to the plates from which his measurements were made, and for help and suggestions throughout.

#### REFERENCES

- DUNHAM, J. L., 1932, *Phys. Rev.*, **41**, 721.  
 GAYDON, A. G., and PEARSE, R. W. B., 1939, *Proc. Roy. Soc. A*, **173**, 37.  
 GUNTZSCH, A., 1934, *Z. Phys.*, **87**, 312; 1939, *Das Bandenspektrum des Magnesium hydrides* (Dissertation).  
 MORSE, P. M., 1929, *Phys. Rev.*, **34**, 57.  
 PEARSE, R. W. B., 1929, *Proc. Roy. Soc. A*, **125**, 157.  
 REES, A. L. G., 1947, *Proc. Phys. Soc.*, **59**, 998.

# Nuclear Disintegrations in Photographic Plates exposed to Cosmic Rays under Lead Absorbers

BY E. P. GEORGE AND A. C. JASON

Birkbeck College, London

*Communicated by G. D. Rochester; MS. received 16th September 1948*

**ABSTRACT.** Ilford Nuclear Research photographic plates have been exposed at the Jungfraujoch, altitude 3,457 metres, under lead screens of various thicknesses up to 28 cm. The intensity of the stars, and its variation with the number of tracks forming them, have been recorded for each thickness of absorber. The absorption curve of the star intensity shows that the range in lead of the radiation causing the stars is  $310 \pm 20$  gm/cm<sup>2</sup>. The size distribution is apparently the same under all absorbers.

The intensity and size distribution have also been recorded in similar plates exposed at sea level. The size distribution is again the same as that found for the high altitude plates, but the range in air of the primaries is  $150 \pm 7$  gm/cm<sup>2</sup>.

These results are consistent with the generally accepted view that the majority of the stars is caused by neutrons.

## § 1. INTRODUCTION

THE intensity of the disintegration stars produced in unscreened photographic plates at various heights in the atmosphere has been measured by Stetter and Wambacher (1939), Zdlanov (1939), Lattes, Occhialini and Powell (1947), and Perkins (1947c). There is general agreement between these authors that the number of stars recorded increases rapidly with altitude. The star intensity is found to vary exponentially with the height according to the relation

$$I = I_0 \exp(-h/R), \quad \dots\dots(1)$$

where  $I$  is the star intensity,  $h$  the depth from the top of the atmosphere expressed in gm/cm<sup>2</sup>, and  $R$ , the range of the primaries causing the stars, is of the order of 140 gm/cm<sup>2</sup>.

Very few observations have been made of the absorption of the star-producing radiation in any other material than air. Thus Heitler, Powell and Fertel (1939) compared the intensity of single proton tracks in unscreened plates and plates screened with 13 cm. lead, left at the Jungfraujoch for 230 days. Later, the complete transition curve for single proton tracks up to 12 cm. lead was obtained by Heitler, Powell and Heitler (1940) at the same altitude. More recently, Perkins (1947c) has recorded the intensity of single proton tracks in photographic plates screened with lead at sea level. All these measurements refer to single tracks and not to stars. The only published paper on the absorption of stars proper is that of Stetter and Wambacher (1944). These authors exposed plates at 2,300 metres altitude, with and without a 10 cm. screen of lead. No significant difference was found either in the number of stars or of single tracks. It seems generally agreed that the absorption of nuclear tracks (single protons or stars) is much less in a given lead absorber than in an equal weight of the atmosphere, though it is apparent that much still remains to be done on the absorption of the star-producing radiation, based on measurements of the stars themselves. We have therefore exposed packets of the new Ilford Nuclear Emulsion plates at the

Jungfraujoch Scientific Station under various lead absorbers up to a maximum of 28 cm. of lead, and under carbon absorbers up to a maximum of 2.5 metres of carbon. Further plates were kept at sea level. In this paper we discuss only the results obtained under the lead absorbers; the results for carbon will be dealt with in a separate communication.

We use the term "intensity of the disintegration stars", or "star intensity" for short, to mean the number of disintegrations recorded in the Nuclear Research plates per cubic centimetre of emulsion per day of exposure. We shall frequently find it necessary to refer to the radiation causing the stars, and for the sake of brevity we shall call it "N-radiation". Finally, by "size distribution" we shall understand a frequency diagram showing the number of stars containing more than  $n$  tracks, plotted as a function of  $n$ .

## § 2. EXPERIMENTAL

The plates used for this experiment were Ilford Nuclear Research, Type C<sub>2</sub>, 50 microns thick, loaded with boron (borax). They were exposed in the aluminium cabin on the roof of the Scientific Station, Jungfraujoch, Switzerland, height 3,457 metres, average barometric pressure 50 cm. Hg. Care was taken to maintain the roof clear of snow, which was never allowed to remain above 3 inches thick. The cabin was maintained between the temperature limits 17° and 24° c. throughout the exposure.

The screening was arranged as follows. The plates were placed on edge with the plane of the emulsion vertical, and a screen,  $t$  cm. thick, built up of lead bricks on the four sides. A roof of lead,  $t$  cm. thick, was then placed on top, as shown in Figure 1. Each packet of plates was provided with its own separate screen. When we refer to plates being exposed under a thickness of  $t$  cm. lead, we refer to plates screened on five sides to  $t$  cm., as shown in Figure 1.

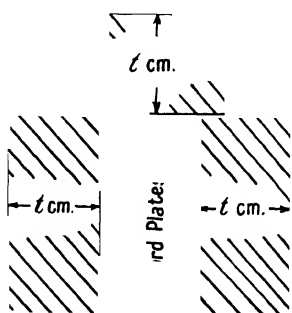


Figure 1. Arrangement of absorbers.

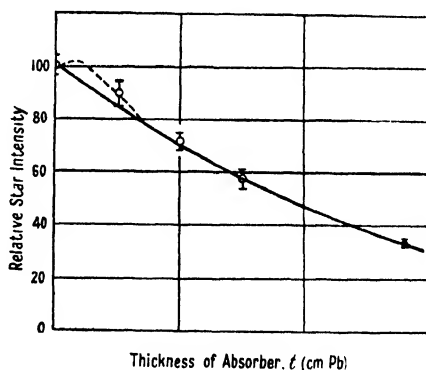


Figure 2. Absorption curve of the star intensity, in lead.

The plates were exposed in two groups. In the first group the exposure was for about 60 days and consisted of plates screened by 0, 15, and 28 cm. of lead. The second was exposed for about 100 days and the plates in it were screened by 0, 5 and 10 cm. of lead. In order to minimize the effects of fading, and any stars that might have been formed while the plates were in transit, they were developed immediately after removal from the lead screen. A further packet of plates was exposed simultaneously in our laboratory on the roof of the Senate House, University of London, for about 100 days.

### § 3. EXPERIMENTAL RESULTS

In recording nuclear disintegration stars in photographic plates care must be taken not to include stars caused by naturally occurring radioactive contamination. To this end we have adopted the definition that a star shall consist of at least three tracks radiating from a common centre, of which at least one track must be longer than 60 microns in the emulsion. From the stars consisting of three tracks we have eliminated those which could be attributed to the scattering of an incident proton in the emulsion.

From the examination of the plates we have obtained (i) the intensity and (ii) the size distribution of the stars formed under lead screens at high altitude, and in unscreened plates at sea level. We discuss the results of these two investigations separately.

#### (i) *Absorption Curve of Stars*

The results showing the relative star intensity under the different absorbers are given in Table 1. A total of 2,032 stars has been recorded in 4.7 cm<sup>3</sup> of emulsion. In each of the two groups of plates that were exposed for about 60 and 100 days respectively, we included an unscreened packet of plates to serve as a control and thus to enable us to allow for any possible effect of fading. The star intensity in the screened plates of each group, expressed as a percentage of the unscreened control plates in the same group, are given in the last column of the Table.

	(1)	(2)	(3)	(4)	(5)	(6)	(7)
First group *	64	0	155	0.775	440	8.8 ± 0.4	100
	66	15	123	0.615	207	5.1 ± 0.35	58 ± 4
	65	28	175	0.875	170	3.0 ± 0.23	34 ± 2.5
Second group †	100	0	118	0.59	481	8.2 ± 0.37	100
	110	5	84	0.42	339	7.4 ± 0.4	90 ± 5
	111	10	89	0.445	293	5.9 ± 0.3	72 ± 3.5
Sea level	110	0	198	0.99	102	0.94 ± 0.10	
Total	..	..	942	4.7	2032		

(1) Exposure (days); (2) thickness of absorber (cm. Pb); (3) area of plate (cm<sup>2</sup>); (4) volume of emulsion (cm<sup>3</sup>); (5) stars >3 tracks; (6) stars/cm<sup>3</sup>/day; (7) star intensity (%).

\* Exposed about 60 days at altitude 3,457 m.

† Exposed about 100 days at altitude 3,457 m.

On comparing the intensities in the unscreened plates exposed for the two different times it will be noticed that the number of stars lost due to fading when the exposure is increased from 64 to 100 days is small, of the order of a few per cent. Thus we feel that the errors in the relative star intensity within one group due to fading will be of the order of 1 to 2%, and hence less than the standard deviations of the individual readings. The points in the last column of the Table are plotted in Figure 2. The points can be fitted to an exponential curve, giving for the mean range in lead of the N-radiation,  $R_{Pb} = 310 \pm 20$  gm/cm<sup>2</sup>. Our present investigations do not allow us to say at this stage whether there is a Rossi maximum in the star curve at about 2 cm. of lead. We are carrying out a further investigation using small thicknesses of lead in order to settle this point.

At the moment it appears probable that if there is a Rossi maximum in the star curve it is small—an increase of not more than 10 to 20%.

From a comparison of the results in the unscreened plates at high altitude and sea level we may also obtain the range in air,  $R_{\text{air}}$  of the N-radiation. The difference in mean pressure between our sea-level laboratory and the Jungfrauoch is 25 cm. Hg or 340 gm/cm<sup>2</sup>. Thus, taking the mean value for the unscreened plates at the high altitude as 8.5 stars per cm<sup>3</sup> per day, and at sea level as 0.94, the range in air is given by

$$\frac{8.5}{0.94} = \exp\left(\frac{340}{R_{\text{air}}}\right), \quad \dots\dots(2)$$

giving  $R_{\text{air}} = 150 \pm 7$  gm/cm<sup>2</sup>, or in other words, the range of the N-radiation in air is almost exactly one half of its range in lead. This result is discussed further below.

### (ii) Size Distribution of Stars

In Figure 3 we show the size distribution of all the 2,032 stars recorded in this investigation. We will call this the mean size distribution of all stars. Plotting

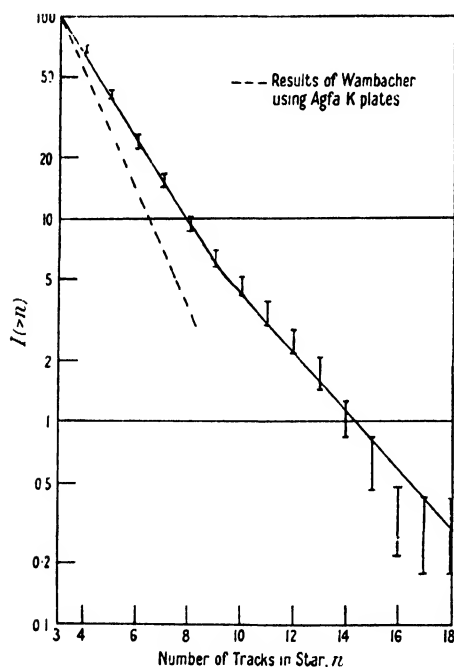


Figure 3. Mean size distribution of all stars.

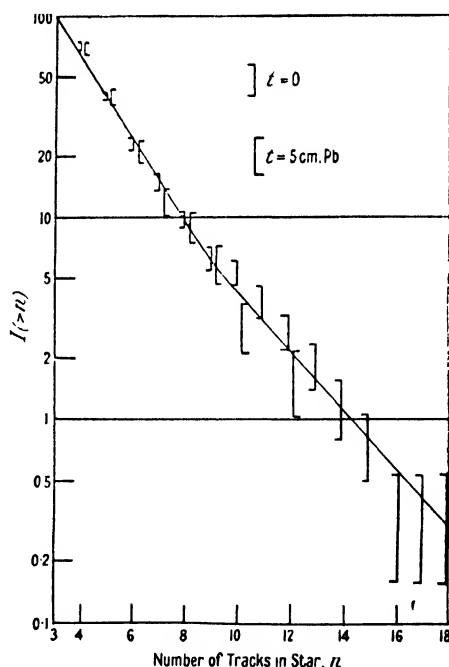


Figure 4(a). Size distribution for  $t=0$  and  $t=5$  cm. Pb.

$\log I(>n)$  against  $n$ , where  $I(>n)$  is the number of stars with more than  $n$  tracks the results appear to lie on a straight line for  $3 < n < 9$ , and on another straight line for  $n > 9$ . For the first part of the curve we have

$$I(>n) = I_0 \exp(-0.48n) \quad 3 < n < 9, \quad \dots\dots(3a)$$

while for the second part we find

$$I(>n) = 0.28 I_0 \exp(-0.33n) \quad n > 9. \quad \dots\dots(3b)$$

We do not attach any great significance to the size distribution given by the empirical relations (3a), (3b), since the distribution must in fact be a very complicated relation, depending on the energy spectrum of the N-radiation, the chemical composition of the emulsion etc. For example, the size distribution given by Bagge (1946) obtained from the work of Wambacher in Agfa K plates is also plotted in Figure 3. These results refer to stars of a similar size range to ours, and were obtained at a comparable height, but the number of stars recorded falls off much more rapidly in the Agfa emulsion than was found with the Ilford emulsion.

What we do feel to be of significance, however, is that within the limits of the errors of measurement we find the same size distribution of the stars under all

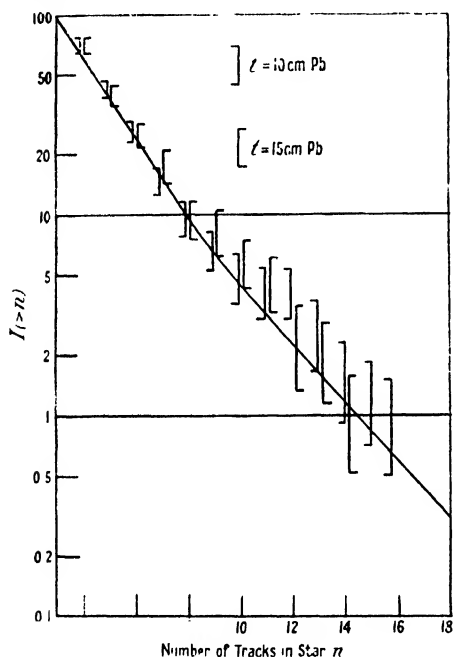


Figure 4 (b). Size distribution for  $t=10$  and 15 cm. Pb.

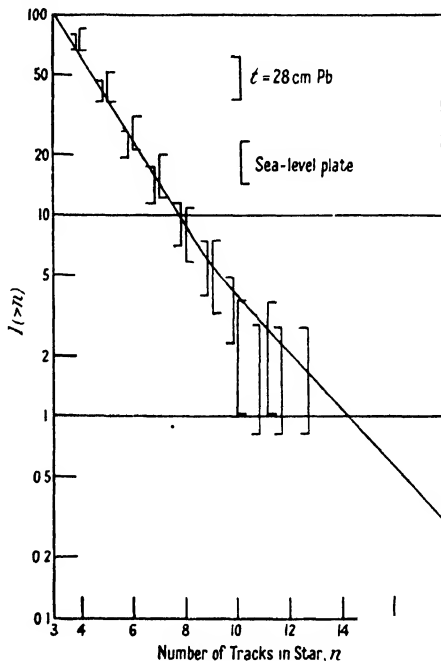


Figure 4 (c). Size distribution for  $t=28$  cm. Pb and for sea-level plate.

thicknesses of lead and at sea level. This is illustrated in Figures 4 (a), (b) and (c), in which we show separately the points for the size distribution measured under 0 and 5 cm. Pb, 10 and 15 cm. Pb, 28 cm. Pb and at sea level respectively. In each case the curve plotted is the mean size distribution, and it is seen that the individual distributions do not differ from the mean to any significant degree.

#### § 4. DISCUSSION OF RESULTS

We may summarize the above results as follows. The range in lead of the N-radiation is found to be  $310 \pm 20$  gm/cm., whereas its range in air is  $150 \pm 7$  gm/cm<sup>2</sup>. No significant difference has been detected in the size distribution in plates exposed under lead screens up to a maximum thickness of 28 cm. at Jungfraujoch, or in plates exposed at sea level. In this discussion we shall show that these results support the prevalent view that most of the stars are due to neutrons.

Concerning the range of energies involved, we estimate that the energy required to produce the average star is about 100 mev., while stars of energies up to and even well above 1,000 mev. have been observed (Leprince-Ringuet *et al.* 1947).

Now, in the first place, the production of stars by neutrons is possible. Thus Lattes and Occhialini (1947) and C. F. Powell and Occhialini (1947) both give examples of stars which, from a consideration of the resultant momentum and the energy of the tracks, may be attributed without doubt to neutrons. Similarly, W. M. Powell (1947) has reported the production of many stars in the gas of a Wilson chamber bombarded by 90 mev. neutrons. A photograph showing two of these events is published by Morrison (1948).

Photons, deuterons, alpha-particles and  $\sigma$ -mesons have also been shown to be capable of causing stars, and their possible contribution to the observed star intensity must be considered. Thus C. F. Powell and Occhialini (1947) have recorded some stars that must be attributed to photons, and stars have also been formed in cloud chambers by 100 mev. photons from the G.E.C. Schenectady betatron (Baldwin and Klaiber 1946, 1948). However, we believe that the shape of the star absorption curve, Figure 2, rules out the possibility that any appreciable fraction of the observed stars can be caused by cosmic-ray photons, and this conclusion is further supported by the cloud chamber observations of stars (Hazen 1944). Using a chamber containing several lead plates, Hazen has shown that most of the low-energy stars are caused by a non-ionizing radiation which is not the photon component, since the stars did not appear to be associated with cascade showers.

Furthermore, the production of stars has been shown to take place when energetic protons, deuterons and alpha-particles are fired into a photographic emulsion (Gardner 1947). Blackett (1937) observed that the number of protons at sea level of momentum less than 500 mev/c. is only about 0.2% of the total corpuscular radiation, and it is exceedingly unlikely that the number of protons with energies less than 1,000 mev. will greatly exceed this figure. The number of other heavy ionizing particles is very much smaller than the number of protons. We show in the next section that the star-producing radiation must constitute about 4% of the total charged corpuscular radiation at sea level, and hence we conclude that not more than about 5% of the stars can be attributed to protons.

Moreover, stars are known to result from the capture of  $\sigma$ -mesons (Perkins 1947 a, Occhialini and Powell 1947). This interaction always appears to occur when the  $\sigma$ -meson has come to the end of its range. Of the 2,032 stars observed, the number with more than three tracks produced by  $\sigma$ -mesons was only 27, or about 1% of the total. After correction for the loss of  $\sigma$ -mesons due to the small thickness of the emulsion (Lattes, Occhialini and Powell 1947), we find that this upper limit becomes 2%. We have not observed any stars that could be attributed to the capture of a  $\sigma$ -meson in flight with an energy less than 10 mev. There remains the possibility that a fraction of the stars may be attributed to  $\sigma$ -mesons (assumed to experience strong nuclear interactions) with an energy greater than 10 mev., in which case they would not leave detectable tracks in the emulsion. We cannot rule out this possibility entirely from the available experimental evidence, but we believe the fraction of stars caused in this manner is probably small, for the following reasons. The energy loss of a  $\sigma$ -meson in traversing our thickest absorber of 28 cm. would be approximately 500 mev. This would result in a considerable hardening of the emergent  $\sigma$ -meson spectrum, which one would expect to observe in the size distribution of the stars. Actually no such change was found. Furthermore, we believe that the number of such  $\sigma$ -mesons that must be assumed to exist is not compatible with the results of cloud chamber investigations at sea level and high altitude.

Let us therefore make the assumption that most of the stars are caused by neutrons with energies within the rough limits indicated above. As a first approximation we make the further assumption that the cross-section for the production of stars is proportional to the nuclear area. In other words, if  $r$  is the effective nuclear radius for a nucleus of mass number  $A$ , then we shall have

$$r = r_0 A^{\frac{1}{3}} \quad \dots\dots (4)$$

with  $r_0 \simeq 10^{-13} \text{ cm.}, \quad \dots\dots (5)$

which value is chosen to fit our own range measurements and is reasonably consistent with the cross-section found for the scattering of energetic neutrons by nucleons and with the current theoretical values.

The total nuclear cross-section will be given simply by  $a = \pi r^2$ , and since the number of nuclei per unit mass,  $n$ , is  $N/A$  where  $N$  is Avogadro's number, the mean free path for these energetic neutrons will be, theoretically,

$$l = 1/n\pi r^2 \text{ gm/cm}^2 \quad \text{or} \quad l = A^{\frac{2}{3}}/N\pi r_0^2 \text{ gm/cm}^2. \quad \dots\dots (6)$$

Substituting the value (5) for  $r_0$ , we obtain  $l_{\text{air}} = 130 \text{ gm/cm}^2$ ,  $l_{\text{Pb}} = 310 \text{ gm/cm}^2$ .

We do not attach much significance to the agreement between these calculated values of the primary range and the observed ones, since the assumed value (5) of  $r_0$  is uncertain to within a factor of two. What perhaps is of more significance is the ratio  $l_{\text{Pb}}/l_{\text{air}}$ , which is independent of the assumed value of  $r_0$  and has the value 2.4, whereas the observed ratio of the ranges of the N-radiation in lead and air has the value  $2.1 \pm 0.2$ .

Thus the difference in the range of the N-radiation in air and lead could be due to the existence of an unstable neutral particle, as has been suggested by Perkins (1947 c), or to a stable neutral particle possessing a collision cross-section which is proportional to the nuclear area.

We can likewise fit in the observed constancy of the star size distribution with the assumption that the stars are produced by neutrons, for any change in the size distribution could only be caused by a change in the energy spectrum of the primaries. If, for example, the neutron collision cross-section decreased rapidly with energy in the energy range considered, then we should expect the neutron energy spectrum to become weighted to higher energies as they passed through an absorbing layer, and hence the stars recorded under absorbers would be expected to show a greater preponderance of large stars. That this is not so is shown by the observed constancy of the size distribution, which we believe to be consistent with the expected constancy of the neutron cross-section for energies in excess of a few hundred mev.

From equation (6) and the known constitution of the Ilford Nuclear Emulsion we obtain a value for the range of the N-radiation in the emulsion :

$$l_E = 1/\Sigma n_A \sigma_A; \quad l_E = 200 \text{ gm/cm}^2 = 50 \text{ cm.}, \quad \dots\dots (7)$$

where  $n_A$  is the number of atoms of atomic number  $A$  per unit mass of emission and  $\sigma_A$  their cross-section,  $\sigma_A = \pi r_0^2 A^{\frac{2}{3}}$ . From this range we have been able to form an estimate of the flux of the N-radiation as follows. Let  $S$  be the number of N-particles from all directions crossing one  $\text{cm}^2$  per day, and  $I$  the number of stars formed in the unscreened emulsion per  $\text{cm}^3$  per day. Then

$$S/l_E = I. \quad \dots\dots (8).$$



This gives, from (7) and the Table,

$$\left. \begin{aligned} S &= 425/\text{cm}^2/\text{day at Jungfrauoch} \\ &= 12\% \text{ of total charged corpuscular radiation,} \end{aligned} \right\} \dots\dots (9a)$$

$$\left. \begin{aligned} S &= 47/\text{cm}^2/\text{day at sea level} \\ &= 4\% \text{ of total charged corpuscular radiation.} \end{aligned} \right\} \dots\dots (9b)$$

These intensities are much greater than the intensities of penetrating neutral radiation recorded by Rossi and Regener (1940) and by Jánossy and Rochester (1943). However, it is likely that these authors were recording neutrons of higher energies than the neutrons responsible for the majority of the stars, and it is reasonable to assume that the neutron energy spectrum would show a decrease with increasing neutron energy.

Attempts have been made to measure the flux of fast neutrons using BF<sub>3</sub>-filled counters (Funfer 1938, Korff and Hamermesh 1946) and photographic plates (Bagge 1946, Morand 1947). We do not feel that the counter measurements are sufficiently developed to enable a useful comparison to be made with our results. The fast neutron fluxes recorded using photographic plates agree reasonably well with the estimates (9). Bagge (1946) calculates the flux of fast neutrons at Jungfrauoch to be about 600 per cm<sup>2</sup> per day, from the experiments of Schopper (1937, 1939) who observed the increase of single proton tracks in plates covered with thin layers of paraffin. An estimate of the fast neutron flux at sea level has recently been made by Morand (1947). His figure is 43 fast neutrons per cm<sup>2</sup> per day at sea level. This figure is based on a measurement of single proton tracks observed to start in the emulsion. They are attributed to protons in the emulsion that recoil from fast neutron collisions.

Further evidence on the nature of the N-radiation is provided by the high altitude cloud chamber studies of W. M. Powell (1946) and Hazen (1944), who used chambers containing several lead plates. In the work of W. M. Powell the cloud chamber was counter-controlled, whereas Hazen's chamber was expanded at random. These authors are in agreement that most stars arise from a non-ionizing component of cosmic radiation, which is not to be identified with the photons of the soft component. Since Hazen used no counter-control, his results are probably the more comparable with our observations of stars in photographic plates. We will therefore attempt to correlate our results further with his, which were obtained at an altitude of 3,300 metres.

Hazen observed fifty-eight stars and 19,000 penetrating particles in the same time. The chamber contained eight 0.7 cm. thick plates of lead separated by 2.5 cm. of air. Of the 58 stars, two small ones originated in the gas of the chamber. The particles constituting these two stars had ranges less than 0.7 cm. Pb. This enables us to form an estimate of the number of stars formed in the lead plates giving rise to particles with ranges less than 0.7 cm. Pb. The relative stopping powers of the lead plates to the air spaces is  $2.6 \times 10^3$  expressed in gm/cm<sup>2</sup>. From our knowledge of the relative ranges of the N-radiation in air and lead ( $= 150/310$ ) we therefore conclude that for every star observed approximately  $2/58 \times 2.6 \times 10^3 \times 15/31$  or 40 stars containing only short range tracks were not observed. Hazen arrives at a figure of 100 for this factor, but had not allowed for the difference in range of the N-radiation in lead and air. Using our value of the range of the N-radiation in lead, 28 cm., we may now form an estimate of the flux of the N-radiation in Hazen's cloud chamber observations. The total thickness of lead

in the chamber was 5.6 cm., and hence the chance of the formation of a star in the chamber by a primary traversing it was 1/5. Since the number of penetrating particles was 19,000, we will relate the N-particles to twice this number of charged particles since at this altitude the proportions of the hard and soft components are just equal. Hence the number of N-particles expressed as a ratio of the total cosmic-ray flux of charged particles is approximately

$$\frac{\text{N-particles} \times 100}{\text{Total charged cosmic rays}} = \frac{58 \times 40 \times 5 \times 100}{2 \times 19,000} = 30\%.$$

This figure is somewhat uncertain owing to the small number of stars originating in the gas of the chamber, and is to be compared with our figure of 12%. It must be borne in mind that our figure will err on the low side because of the number of stars consisting of particles with energies above the limit of detectability in the emulsion. Taken in conjunction with Hazen's conclusion that the initiating particles are predominantly neutrons for the lower energy stars, there seems to be a fair measure of agreement between the conclusions from the cloud chamber and photographic plate observations on stars.

#### § 5. CONCLUSION

The absorption curve of Figure 2 shows that the main bulk of the stars cannot be produced by the soft component, and the rapid increase with height shows that they cannot be caused by the penetrating component ( $\mu$  mesons), since this component only increases by a factor of 1.7 at the altitude of the measurements. This leaves as alternatives the proton, neutron and  $\sigma$ -meson components. From the absorption coefficient we find that the required flux of N-particles at sea level must be about 4% of the total corpuscular radiation. The observed rate of protons at sea level (Blackett 1937) shows that not more than about 5% of the stars can be attributed to protons.

This leaves us therefore with the neutrons or  $\sigma$ -meson components. Our observations on the absorption of the N-radiation in lead and air are consistent with the assumption that the N-particles are neutrons, in agreement with the cloud-chamber evidence, possessing a range proportional to  $A^{1/2}$ , and energies in the rough limits of 100 mev. to greater than 1,000 mev. The size distribution of the stars is found to be the same under all absorbers, and this is again consistent with the prevalent view that the N-rays are neutrons.

The possibility that the stars are also caused to a certain extent by energetic  $\sigma$ -mesons cannot be ruled out, but it appears probable that the contribution from this component must be small.

*Note added in proof.* Since writing the above, figures for the absorption of the N-radiation in lead and air have been published by G. Bernardini and his collaborators (*Phys. Rev.*, 1948, **74**, 1878) which are in close agreement with our values.

#### ACKNOWLEDGMENTS

We wish to thank Professor C. F. Powell and Dr. G. P. S. Occhialini and their group at Bristol for initiating us into the photographic techniques they have perfected. Our thanks are also due to Professor J. D. Bernal for providing us with facilities to do the work and for his continued interest in its progress, and to Professor P. M. S. Blackett for helpful criticism in the preparation of this paper. Many

workers in the Birkbeck Physics Laboratories helped us in the work of scanning the photographic plates, and to these we express our thanks. We are particularly indebted to Mrs. M. H. George for scanning more than half the plates, and to Mr. P. T. Trent for considerable assistance with the scanning technique. We would also like to thank the Director, Professor von Muralt, and the Staff of the Scientific Station, Jungfraujoch, for much assistance during the exposure of the plates. The investigation was made possible by a grant from the Department of Scientific and Industrial Research.

## REFERENCES

- BAGGE, E., 1946, *Cosmic Radiation*, ed. W. Heisenberg (New York : Dover Publications).  
 BALDWIN, G. C., and KLAIBER, G. S., 1946, *Phys. Rev.*, **70**, 259; 1948, *Ibid.*, **73**, 1156.  
 BLACKETT, P. M. S., 1937, *Proc. Roy. Soc. A*, **159**, 1.  
 FUNFER, E., 1938, *Z. Phys.*, **111**, 351.  
 GARDNER, E., 1947, *Phys. Rev.*, **72**, 743A.  
 HAZEN, W. E., 1944, *Phys. Rev.*, **65**, 67.  
 HEITLER, W., POWELL, C. F., and FERTEL, G. E. F., 1939, *Nature, Lond.*, **144**, 283.  
 HEITLER, W., POWELL, C. F., and HEITLER, H., 1940, *Nature, Lond.*, **146**, 65.  
 JÁNOSY, L., and ROCHESTER, G. D., 1943, *Proc. Roy. Soc. A*, **181**, 399.  
 KORFF, S. A., and HAMERMESH, B., 1946, *Phys. Rev.*, **69**, 155.  
 LATTES, C. M., and OCCHIALINI, G. P. S., 1947, *Nature, Lond.*, **159**, 331.  
 LATTES, C. M., OCCHIALINI, G. P. S., and POWELL, C. F., 1947, *Nature, Lond.*, **160**, 486.  
 LEPRINCE-RINGUET, L., *et al.*, 1947, *C.R. Acad. Sci., Paris*, **225**, 1144.  
 MORAND, M., 1947, *C.R. Acad. Sci. Paris*, **225**, 1146.  
 MORRISON, P., 1948, *J. Appl. Phys.*, **19**, 311.  
 OCCHIALINI, G. P. S., and POWELL, C. F., 1947, *Nature, Lond.*, **159**, 186.  
 PERKINS, D. H., 1947 a, *Nature, Lond.*, **159**, 126; 1947 b, *Ibid.*, **160**, 299; 1947 c, *Ibid.*, **160**, 707.  
 POWELL, C. F., and OCCHIALINI, G. P. S., 1947, *Nuclear Physics in Photographs* (Oxford : Clarendon Press).  
 POWELL, W. M., 1946, *Phys. Rev.*, **69**, 385; 1947, *Ibid.*, **72**, 739A.  
 ROSSI, B., and REGENER, V. H., 1940, *Phys. Rev.*, **58**, 837.  
 SCHOPPER, E., 1937, *Naturwissenschaften*, **25**, 557; 1939, *Phys. Z.*, **40**, 22.  
 STETTER, G., and WAMBACHER, H., 1939, *Phys. Z.*, **40**, 702; 1944, *S.B. Akad. Wiss. Wien.*, **152**, 1.  
 ZDHANOV, A. P., 1939, *Akad. Nauk. Otdel. Bull.*, Ser. Phys., **4**, 272.

## Experiments with the Delayed Coincidence Method, including a Search for Short-lived Nuclear Isomers

By D. E. BUNYAN, A. LUNDBY\* AND D. WALKER

Physics Department, University of Birmingham

*Communicated by M. L. Oliphant; MS. received 9th December 1948*

**ABSTRACT.** The delayed coincidence method has been studied in some detail and employed in a search for short-lived isomers in the product nuclei of  $\beta$ -emitters. The influence of counter time-lag fluctuations, which determine the short half-life limit in this method, is discussed in relation to the "differential" procedure for recording the delayed coincidences. It is shown that the time lags exhibited by a Geiger-Müller counter are distributed approximately according to a Gaussian law. A differential delayed coincidence recorder has been constructed in which the overall time-lags in the two input channels due to "rise-time" effects have been stabilized. At the coincidence stage of this recorder the quadratic mean deviation in the time-lag difference between the two channels due to "rise-time" effects has been kept as low as  $\sim 5 \times 10^{-9}$  sec. Details are given of the experimental procedure used in searching for short-lived isomers. The range of possible half-lives most thoroughly investigated extends from about  $3 \times 10^{-7}$  sec. to about  $10^{-3}$  sec. for isomeric transitions giving conversion electron energies greater than about 100 kev. Possible improvements in the range of the experiments are discussed. The short-lived isomers of  $^{181}\text{Tl}$  and  $^{187}\text{Re}$  have been confirmed. The half-life of the metastable state in  $^{187}\text{Re}$  has been found to be  $(5.26 \pm 0.12) \times 10^{-7}$  sec. Negative results are reported for 19 isotopes. In particular the metastable states reported by other authors in  $^{198}\text{Hg}$ ,  $^{111}\text{Pr}$ , and  $^{124}\text{Te}$  are not confirmed.

The half-life of  $^{232}\text{ThC}'$  has been found to be  $(3.04 \pm 0.04) \times 10^{-7}$  sec.

### § 1. INTRODUCTION

SINCE 1946 several nuclear isomers with short decay periods have been discovered by observing delayed coincidences in the radiations from nuclei decaying by  $\beta$ -emission or K-capture.† This method, using Geiger-Müller counters as detectors, is capable of disclosing, in the product nuclei, metastable levels with half-lives from about  $10^{-7}$  to  $10^{-2}$  sec. Most of those so far established have half-lives (from  $5 \times 10^{-8}$  to  $2 \times 10^{-5}$  sec.), transition energies, and internal conversion coefficients consistent with electric octopole or magnetic dipole transitions. This paper discusses delayed coincidence experiments in some detail, including a search for short-lived isomers. Geiger-Müller counters have been used for the detectors.

### § 2. DELAYED COINCIDENCE RECORDERS

The "differential" and "integral" delayed coincidence recorders developed in this laboratory have been described briefly in an earlier paper (Bunyan *et al.* 1948).

#### (i) Integral Recorder

The integral recorder, developed first and intended to have only the best electronic performance readily achievable, does not exhaust the capabilities of Geiger-Müller counters as regards coincidence resolution. The pulse length in

\* Now at the Institutt for Atomenergi, Oslo.

† Bittencourt and Goldhaber (1946), Bowe *et al.* (1948), Bunyan *et al.* (1948), De Benedetti and McGowan (1946, 1947), De Benedetti *et al.* (1948), McGowan and De Benedetti (1948).

channel A (Figure 1) can be varied from approximately  $2 \times 10^{-6}$  sec. upwards, while the pulse length in channel B is fixed at about  $5 \times 10^{-7}$  sec. The count due to instantaneous coincidences can be assessed by use of an anti-coincidence circuit of short resolving time ( $\sim 2 \times 10^{-6}$  sec.), actuated from channel A. This recorder showed no loss of coincidences due to time-lag fluctuations in the Geiger-Müller counters used in our experiments.

### (ii) Differential Recorder

In developing the differential recorder, the objective was an electronic performance such that the coincidence resolution would be limited only by the "intrinsic" (electron-transit) time-lags of the Geiger-Müller counters. Care was taken to minimize effects due to fluctuations in the rise-time of the counter anode pulses and small variations in the sensitivity of subsequent trigger circuits

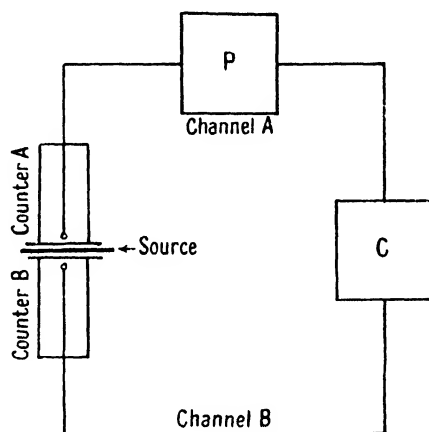


Figure 1. Elements of a delayed coincidence recorder.

P=pulse-delaying circuit (differential recorder) or pulse-lengthening circuit (integral recorder).  
C=coincidence stage.

in the apparatus. For this purpose the counter pulses are amplified sufficiently for the subsequent circuits to trigger at one-tenth of the full pulse amplitude. At the inputs to the coincidence stage (Figure 1) the pulse in each of the two channels is  $2.2 \times 10^{-7}$  sec. in width. The delay introduced in channel A relative to channel B can be varied from  $-10^{-6}$  sec. to  $+10^{-5}$  sec. in steps of  $10^{-7}$  sec.

## § 3. TIME-LAGS IN GEIGER-MÜLLER COUNTERS

### (i) General

The "intrinsic" time-lag in a Geiger-Müller counter, i.e. the time of transit of an electron from the region of primary ionization to the region near the anode where an electron avalanche occurs, depends on the type of gas-filling, the gas pressure and the field strength as well as on the radial distance travelled (Den Hartog *et al.* 1947, Sherwin 1948). The intrinsic time-lag can be reduced only by changes in the counter.

The Geiger-Müller counters used in the experiments with the differential recorder described in § 4 (i), (ii) of this paper are cylindrical end-window counters, of cathode diameter 2.5 cm., anode diameter 0.020 cm., cathode length 5.5 cm., anode length 3 cm., and filled with 9 cm. Hg pressure of argon and 1 cm. Hg pressure

of ethyl alcohol. For such a counter the electron transit time from cathode to anode, according to published results (Bradt and Scherrer 1943a, Den Hartog, Muller and Verster 1947), should be approximately  $2 \times 10^{-7}$  sec. Delays due to electron transit time will be statistically distributed when the ionizing particles pass at random distances from the anode,  $2 \times 10^{-7}$  sec. representing the approximate maximum delay. In practice we observe a small fraction of delays, too large to be explained by free electron transit time alone (see § 4 (i)). Sherwin (1948) observes a similar effect, and suggests that it may be due to fluctuations in the time of formation of the positive ion sheath. There may also possibly be a small contribution from electron attachment to form negative ions (cf. Montgomery and Montgomery 1947).

The time-lag between the start of the first electron avalanche in a Geiger counter and the triggering of the associated electronic circuits is dependent both on the counter itself and on the electronic circuits. The rate of rise of the Geiger anode pulse is probably dependent mainly on the velocity of propagation of the discharge along the anode wire (Hill and Dunworth 1946, Alder *et al.* 1947). For the present counters, on this basis, the pulse once started should rise to its peak in about  $3 \times 10^{-7}$  sec., and reach one tenth of the full pulse amplitude in about  $3 \times 10^{-8}$  sec. (cf. § 2 (ii)).

(ii) *Analysis of Time-lag Effects in the Differential Procedure for Recording Delayed Coincidences*

To determine theoretically the effect of counter time-lags on the coincidence counting rate, we must assume them to follow some distribution law. A Gaussian law, as we shall see, is found to describe the experimental facts closely over a wide range and is used in the following discussion. Bradt and Scherrer (1943a), using a coincidence arrangement with a variable resolving time, have also found agreement with a Gaussian law.

Let us first consider the case in which high energy particles are projected through both Geiger counters or a source which emits radiations in immediate succession is inserted between the counters. Assume a Gaussian distribution of the time lags between the primary ionizing events in a counter and the occurrence of the corresponding pulses at the input of the coincidence stage. Let the Gaussian distribution have a standard deviation  $t_0/\sqrt{2}$  for each counter ( $t_0$  represents the standard deviation of the difference between the time lags of the two counters). Further, let  $\bar{t}_A$  and  $\bar{t}_B$  be the average inherent time lags for the two channels (Figure 1) and let the pulses in channel A suffer an additional deliberate delay  $t_d$ . Let the pulse widths in channels A and B, at the coincidence stage ( $\tau_A, \tau_B$ ), be each equal to  $\tau$  for simplicity. If a particle causes ionization in counter B at a time  $t=0$  the probability of the generated pulse reaching the input of the coincidence stage between  $t$  and  $t+dt$  is assumed to be given by

$$\frac{1}{t_0\sqrt{\pi}} \exp \left\{ - \left( \frac{t - \bar{t}_B}{t_0} \right)^2 \right\} dt,$$

and the probability for counter A, when all pulses in this channel are delayed a time  $t_d$ , is

$$\frac{1}{t_0\sqrt{\pi}} \exp \left\{ - \left( \frac{t - \bar{t}_A - t_d}{t_0} \right)^2 \right\} dt.$$

The probability that radiations causing ionization simultaneously in both counters shall be recorded as being in "delayed coincidence" is then found to be

$$P(t_d) = \frac{1}{2} [\Phi\{(t_d + \tau + \Delta)/t_0\sqrt{2}\} - \Phi\{(t_d - \tau + \Delta)/t_0\sqrt{2}\}], \quad \dots\dots (1)$$

where

$$\Delta = \bar{t}_A - \bar{t}_B, \quad \text{and} \quad \Phi(x) = \frac{2}{\sqrt{\pi}} \int_0^x \exp(-z^2) dz.$$

Let us next consider the case in which the two radiations are delayed "naturally" with respect to each other, i.e. the half-life of the nucleus formed in the first decay is "finite" ( $T_{\frac{1}{2}} \geq 10^{-8}$  sec.). We shall assume that the radiation which is emitted first enters counter A, and the following radiation counter B, and that both give rise to discharges in the counters. The probability that the radiations emitted in the formation and the decay of the intermediate nucleus of decay constant  $\lambda$  shall be recorded as being in delayed coincidence is then given by the expression

$$\begin{aligned} W(\lambda, t_d) = & \frac{1}{2} \left\{ \Phi\left(\frac{t_d + \tau + \Delta}{t_0\sqrt{2}}\right) - \Phi\left(\frac{t_d - \tau + \Delta}{t_0\sqrt{2}}\right) \right\} \\ & + \frac{1}{2} \left[ \left\{ 1 + \Phi\left(\frac{t_d - \tau + \Delta}{t_0\sqrt{2}} - \frac{\lambda t_0}{\sqrt{2}}\right) \right\} \exp(\lambda\tau) \right. \\ & \left. - \left\{ 1 + \Phi\left(\frac{t_d + \tau + \Delta}{t_0\sqrt{2}} - \frac{\lambda t_0}{\sqrt{2}}\right) \right\} \exp(-\lambda\tau) \right] \exp(-\lambda t_d - \lambda\Delta + \frac{1}{2}\lambda^2 t_0^2). \end{aligned}$$

..... (2)

The first term is equal to  $P(t_d)$ , and is important only when

$$-(\tau + t_0\sqrt{2}) \lesssim t_d + \Delta \lesssim \tau + t_0\sqrt{2}.$$

The second term contains two factors, of which the first (the expression in the square brackets) is constant for  $t_d + \Delta \gg \tau + t_0(\sqrt{2} + \lambda t_0)$ . In the latter case the whole expression is equal to Constant  $\times \exp(-\lambda t_d)$ . Figure 2 gives some examples of the functions  $P(t_d)$  and  $W(\lambda, t_d)$  for different values of  $t_0$  and  $\tau$ , with  $\lambda = 2.5 \times 10^6 \text{ sec}^{-1}$ . We have put  $\Delta = 0$  since this transformation results only in a translation of the curves along the  $t_d$  axis.

For a given  $t_0$  it is seen that in order not to lose too many coincidences  $\tau$  must be large compared with  $t_0$ .

#### § 4. PERFORMANCE OF THE DIFFERENTIAL RECORDER

Some measurements made with the differential recorder serve to illustrate both the performance of the recorder and the effects discussed in § 3.

##### (i) *Instantaneous Coincidences*

Using a thin foil coated with  $^{60}\text{Co}$  as a source of instantaneously coincident radiations, the experimental points marked on curve B of Figure 2 were obtained on plotting coincidence rate against the delay of channel A with respect to channel B. (These observed points have all been shifted about  $6 \times 10^{-8}$  sec. to the right in the figure in order to make the centres of the computed and observed curves coincide.) The argon-alcohol counters described in § 3 (i) were used, with a thin lead radiator in front of one to increase the efficiency of  $\gamma$ -detection. The experimental points lie closely along the curve computed from equation (1) with  $\tau = 2.25 \times 10^{-7}$  sec., and  $t_0 = 10^{-7}$  sec.

For comparison we may note that  $(\tau_A + \tau_B)$  as found by random coincidences is equal to  $(4.37 \pm 0.08) \times 10^{-7}$  sec. It should be noted also that, for long delays  $t_d$ , the observed coincidence rate declines towards zero somewhat more slowly than is consistent with the Gaussian distribution. Thus the fraction of counter time-lags which are larger than can be accounted for simply by the transit time of free electrons (cf. § 3 (i)) is actually somewhat greater than that corresponding to a strict Gaussian distribution.

### (ii) Stability

Curve B of Figure 2 can be used to provide a test of the stability of the differential recorder with respect to the time-lag difference between the two channels due to "rise-time" effects. The variation of the coincidence counting rate with

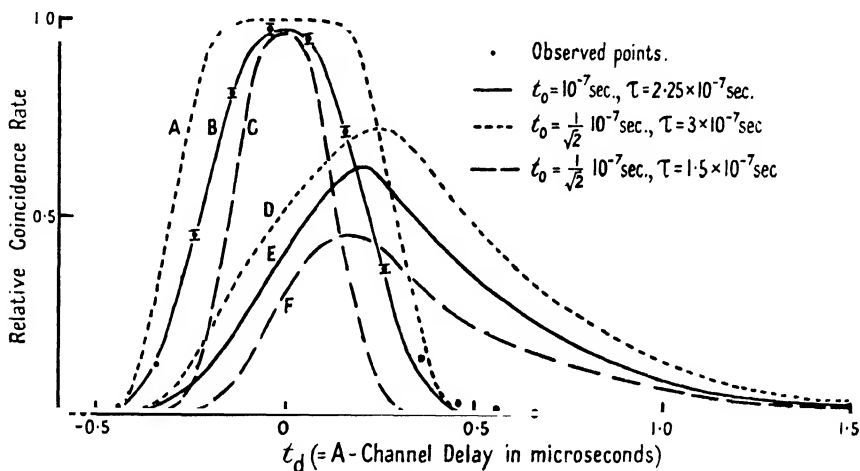


Figure 2. Differential recorder. Variation of coincidence rate with A-channel delay ( $t_d$ ). Curves A, B, C are of  $P(t_d)$  computed from equation (1), and curves D, E, F are of  $W(\lambda, t_d)$  computed from equation (2), using  $\lambda = 2.5 \times 10^6 \text{ sec}^{-1}$  and the indicated values of  $t_0$  and  $\tau$ . For the observed points see § 4 (i).

a change in delay setting ( $t_d$ ) is very rapid at that setting where the rate is reduced to half its maximum (the coincidence rate changes by about 85% for a change of  $10^{-7}$  sec. in  $t_d$ ), and thus the stability of the recorder can be assessed by observing coincidence rate fluctuations in prolonged operation at this setting. The fluctuations observed in a series of readings during a continuous test run of twenty hours corresponded to a quadratic mean deviation in the time-lag difference between the two channels due to "rise-time" effects of approximately  $5 \times 10^{-9}$  sec.

In a test of the stability against fluctuations in the anode voltage of the Geiger-Müller tubes, the change in coincidence counting rate observed for a deliberate change of 25 volts in the working voltage on either tube corresponded to a change in the effective mean time-lag of approximately  $2 \times 10^{-8}$  sec. This is reasonable if one considers the variation with overvoltage of the velocity of propagation of a discharge along the anode wire of a counter (Hill and Dunworth 1946).

### (iii) Half-life of Thorium C'

As a further test of the performance of the differential recorder, the decay period of ThC' was redetermined. The source was an active deposit from radio-thorium (ThB + ThC).



The experimental points on curve A, Figure 3, show the variation of the observed coincidence rate with A-channel delay ( $t_d$ ), using the Th(B + C) source on a platinum foil between the counters. The counter in channel A was a Geiger-Müller  $\beta$ -counter of the type described in § 3 (i). In channel B a proportional counter was used, operated in the high proportional region. This counter was an end-window type, 2.7 cm. in diameter and 5 cm. long. The window was a 2.3 mg/cm<sup>2</sup> Al foil, and the counter was filled with a helium-alcohol mixture at

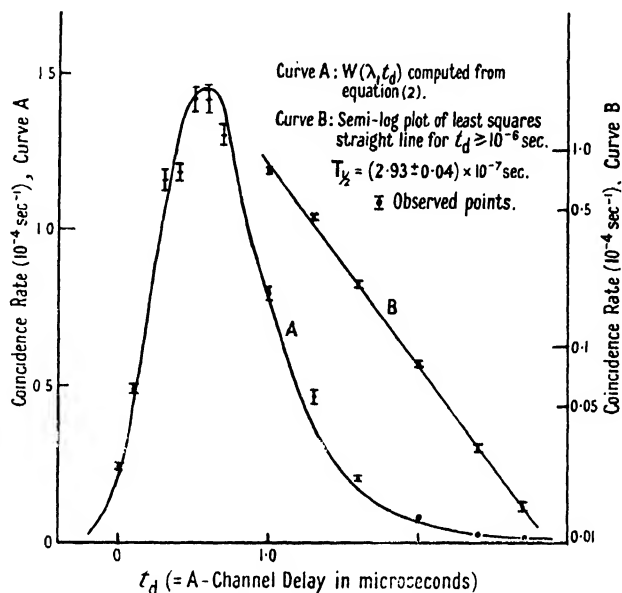


Figure 3. Differential recorder. Decay curve of thorium C'. (The observed coincidence rates have been corrected for the decay of the Th(B + C) source.)

atmospheric pressure, the alcohol pressure being 1 cm. Hg. Owing to the lower electron mobility in this counter as compared with that in channel A the magnitude of the time-lag fluctuations is larger. Curve A (Figure 3) is of the function  $W(\lambda, t_d)$  computed from equation (2) using  $\lambda = 2.37 \times 10^6 \text{ sec}^{-1}$  ( $T_{\frac{1}{2}} = 2.93 \times 10^{-7} \text{ sec.}$ ),  $\tau = 2.25 \times 10^{-7} \text{ sec.}$ , and  $t_0 = 2 \times 10^{-7} \text{ sec.}$

The experimental points on curve B, Figure 3, are for A-channel delays equal to or greater than  $10^{-6} \text{ sec.}$  and fit a half-life for ThC' of  $(2.93 \pm 0.04) \times 10^{-7} \text{ sec.}$  The error in the calibration (only approximate) of the delay lines may be as great as 10%.\* The half-life of ThC' was first estimated by Dunworth (1939) as  $(3 \pm 1) \times 10^{-7} \text{ sec.}$  Recent values are those of Bradt and Scherrer (1943 b),  $T_{\frac{1}{2}} = (2.6 \pm 0.4) \times 10^{-7} \text{ sec.}$ ; and of Hill (1948),  $T_{\frac{1}{2}} = (3.00 \pm 0.15) \times 10^{-7} \text{ sec.}$

## § 5. DETAILS OF EXPERIMENTAL PROCEDURE USED IN SEARCHING FOR SHORT-LIVED ISOMERS

### (i) Preparation of Sources

Substances to be activated have been obtained as fine, chemically pure and chemically stable powders (the element or its oxide) and sealed into silica tubes for neutron irradiation in the small pile at the Atomic Energy Research Establishment, Harwell. Specific activities of the desired  $\beta$ -emitters of  $10^6$  or more disintegrations

\* Footnote added in proof. The delay lines have since been calibrated using a crystal-controlled pulse generator, and we find  $(3.04 \pm 0.04) \times 10^{-7} \text{ sec.}$  for the absolute half-life of ThC'.

per second per gramme have been obtained. In preparing sources for coincidence experiments, some of the irradiated powder of grain size less than approximately  $10\mu$  has been glued, using a layer of cellulose nitrate lacquer of less than  $1\text{ mg/cm}^2$  thickness, to one side of an aluminium foil of about  $2\text{ mg/cm}^2$  thickness. (At  $10\mu$  grain size and a density of  $15\text{ gm/cm}^3$ , self-absorption in the grains would reduce the intensity of a 50 kev. electron component to approximately one-tenth of that in the absence of self-absorption, and the intensity of a 100 kev. component to approximately one-half.)

In mounting the foil between the two counters (Figure 1) the source side faced counter B.

### (ii) Checking the Decay Periods of the $\beta$ -Emitters

The decay in activity of all the irradiated samples has been followed, independently of the delayed coincidence experiments, on a separate counting equipment. This has served both to identify the isotopes involved and to enable the delayed coincidence experiment to be performed at the most favourable time for a given  $\beta$ -emitter, when more than one activity was present in the sample.

### (iii) The Sensitivity of the Delayed Coincidence Experiments

With most of the  $\beta$ -emitters examined it has not been possible to detect a genuine delayed coincidence rate  $C_g$ : that is, the total recorded coincidence rate  $C_t$  has not been significantly different from the computed random coincidence rate  $C_r$ . It is possible to assess, by an approximate argument, the order of magnitude of the minimum fraction  $\phi$  of the  $\beta$ -transitions which, leading to a metastable state of decay constant  $\lambda$  in the product nucleus, would give rise to a detectable  $C_g$ . This smallest detectable  $C_g$  is  $C_g = (\phi N_A) \epsilon_{B2} f$ , where it is assumed that the counting rate  $N_A$  in counter A is due only to  $\beta$ -particles, where  $\epsilon_{B2}$  = net efficiency of counter B for the delayed radiation; and, for the *differential recorder*,  $f \simeq \exp(-\lambda t_1)[1 - \exp\{-\lambda(\tau_A + \tau_B)\}]$ , where  $t_1$  is the maximum intrinsic counter time-lag difference occurring with appreciable frequency. The corresponding minimum delay setting at which no instantaneous coincidences can be recorded through the influence of counter time lags is  $(t_1 + \tau_B)$ . This is the most favourable setting for detecting delayed coincidences.  $\tau_A, \tau_B$  are the pulse lengths in the two channels at the coincidence stage. For the *integral recorder*,  $f = \exp(-\lambda \tau_0) \cdot \exp\{-\lambda(\tau_A - \tau_0)\}$ , where  $\tau_0$  is the length of the anti-coincidence pulse used to suppress instantaneous coincidences ( $t_1 \leq \tau_0 < \tau_A$ , and  $\tau_B \ll \tau_A$ ).

The individual counting rates in counters A and B being  $N_A$  and  $N_B$ , the random coincidence rate is computed from  $C_r = N_A N_B (\tau_A + \tau_B)$ .<sup>\*</sup> The relative error in  $C_r$  is therefore the relative error  $\eta$  in  $(\tau_A + \tau_B)$ <sup>†</sup>, since  $N_A, N_B$  can be measured with a high statistical accuracy. The relative error in the total coincidence rate  $C_t$  is, on simple statistical reasoning,  $1/(C_t t)^{1/2}$ , where  $t$  is the counting time, and this, since  $C_r \simeq C_t$  in the limit of small  $C_g$ , is  $1/(C_r t)^{1/2}$ .

$C_g$  is obtained by subtracting  $C_r$  from  $C_t$ , and hence, to be detected, must exceed the absolute error in either. Thus the minimum detectable  $C_g$  is either  $\eta N_A N_B (\tau_A + \tau_B)$  or  $(C_r/t)^{1/2} = \{N_A N_B (\tau_A + \tau_B)/t\}^{1/2}$ , whichever is greater. Once either error has been reduced to its practical limit, decrease of the other below the

<sup>\*</sup> Strictly for the integral recorder,  $C_r = N_A N_B (\tau_A - \tau_0)$ .

<sup>†</sup> The relative error in  $(\tau_A + \tau_B)$  is determined partly by its stability.

same magnitude brings little improvement, so that at the optimum the error in  $C_r$  should be roughly equal to the error in  $C_i$ . At this limit

$$(C_g)_{\min} = \phi N_A \epsilon_{B2} f \simeq \eta N_A N_B (\tau_A + \tau_B) \simeq \{N_A N_B (\tau_A + \tau_B) / t_c\}^{\frac{1}{2}},$$

where  $t_c$  is the counting time required to reach this condition.

From this

$$\phi = \frac{(N_B/N_A)^{\frac{1}{2}} (\tau_A + \tau_B)^{\frac{1}{2}}}{\epsilon_{B2}} \left( \frac{1}{t_c} \right) \frac{1}{f} \quad \dots\dots (3)$$

at the optimum given by

$$(N_A N_B)^{\frac{1}{2}} t_c^{\frac{1}{2}} = \frac{1}{\eta (\tau_A + \tau_B)^{\frac{1}{2}}} \quad (N_A \sim N_B \text{ in general}).$$

When searching for delayed coincidences, we have at all times observed the conditions for optimum  $\phi$ , using  $t_c \sim 24$  hours.

#### (iv) Quantitative Estimate of Detection Sensitivity $\phi$

In searching for delayed coincidences with the *integral recorder* we have used for counter B a 2.5 cm. diameter Geiger counter with a mica end-window 2.5 mg/cm<sup>2</sup> thick, and filled with helium-alcohol mixture to atmospheric pressure. For a window thickness of 2.5 mg/cm<sup>2</sup> the limiting electron energy is 35 kev.\* The source was less than  $\frac{1}{2}$  cm. from the counter, and  $\epsilon_{B2} > 0.05$  for a sufficiently energetic transition completely internally converted. (Rather strong internal conversion usually accompanies isomeric transitions.) The anti-coincidence resolving time was approximately  $2 \times 10^{-6}$  sec., the A channel pulse length, for a simple test for delayed transitions, set at about  $10^{-5}$  sec. and  $\eta = 0.02$ . Under these conditions, and with  $N_A = N_B$ ,  $\epsilon_{B2} \geq 0.05$  and  $t_c = 24$  hours, equation (3) gives the following maximum values of  $\phi$  for the half-lives indicated:

$T_{\frac{1}{2}}$ (sec.)	$3 \times 10^{-7}$	$5 \times 10^{-7}$	$10^{-6}$	$10^{-5}$	$10^{-4}$	$10^{-3}$	$10^{-2}$
$\phi$	$3 \times 10^{-2}$	$4 \times 10^{-3}$	$9 \times 10^{-1}$	$6 \times 10^{-4}$	$3 \times 10^{-3}$	$3 \times 10^{-2}$	$3 \times 10^{-1}$

$\phi$  will increase inversely as the internal conversion coefficient when this is less than 1. For soft electrons ( $\lesssim 100$  kev.) self-absorption (§ 5 (i)) and window absorption must be also taken into account.

With the *differential recorder* ( $\eta = 0.05$ ), if the helium counters described in the preceding paragraph are used, the simple test of operating at a fixed delay setting ( $t_1 + \tau_B$ ) (§ 5 (iii)) gives no striking gain in sensitivity over the integral recorder for very short half-lives. The intrinsic time-lags of the atmospheric pressure helium counter are excessive, and the window thickness (7 mg/cm<sup>2</sup>) necessary with a reduced pressure argon counter of the type described in § 3 (i) decreases the efficiency of detection of soft electron components. The values of  $\phi$  given in the preceding paragraph may therefore be taken in conjunction with all the negative results listed in § 6 (ii).

A numerical example of the foregoing considerations was obtained by delayed coincidence measurements on tungsten using the integral recorder with  $(\tau_A - \tau_0) = 1.90 \times 10^{-6}$  sec. About 10% of the  $\beta$ -particles from <sup>187</sup>W (half-life 24 hours) are followed by delayed conversion electrons from the decay of a

\* Counter A has been either similar to counter B, or one of the argon-alcohol counters described in § 3 (i) with a window thickness of 7 mg/cm<sup>2</sup> (limiting electron energy 75 kev.).

metastable level in  $^{187}\text{Re}$ , of half-life  $5 \times 10^{-7}$  sec. (De Benedetti and McGowan 1947). No delayed coincidences have been observed in the radiations from  $^{185}\text{W}$  (half-life 77 days). In a source made of neutron-activated tungsten, containing both these isotopes, a genuine delayed coincidence rate  $C_g$  of  $(1.68 \pm 0.78) \times 10^{-4}$  counts per second was still detected when the  $\beta$ -radiation leading to delayed electron emission was only 0.17% of the total  $\beta$ -radiation from the sample. The value of  $\phi$  computed for this case was 0.2%.

#### (v) Improvement of Sensitivity

For half-lives less than approximately  $10^{-7}$  sec. the sensitivity of the differential recorder can be increased by using Geiger-Müller counters with smaller intrinsic time-lags, that is, effectively, argon-alcohol counters of smaller cathode diameter. For half-lives of approximately  $10^{-2}$  to  $10^{-1}$  sec. it is an advantage with the integral recorder to use a correspondingly large  $\tau_A$ . The background counting rates may then become important but could be reduced by lead shielding. With  $\tau_A \sim 10^{-3}$  sec. in the present recorder  $\eta > 0.02$ , and this could be improved. Over the whole range of operation of both recorders the sensitivity of the technique would be improved by careful preparation of very thin sources (e.g. by electro-deposition) to avoid self-absorption of low energy electrons, and by placing the sources inside the counters to eliminate window absorption and improve the geometrical conditions.

For future work the possibilities offered by new methods of particle detection (e.g. scintillation methods employing photo-multipliers) should not be overlooked. Reduced detector time-lags as well as improved efficiency of  $\gamma$ -detection (cf. the effect of  $\epsilon_{\beta\beta}$  in equation (3)) are both important.

### § 6. EXPERIMENTAL RESULTS\*

#### (i) Positive Results

$^{181}_{73}\text{Ta}$ : First found by De Benedetti and McGowan (1946), the metastable level (half-life  $(20.1 \pm 0.7) \times 10^{-6}$  sec.) in  $^{181}_{73}\text{Ta}$  following the  $\beta$ -decay of  $^{181}_{72}\text{Hf}$  (half-life 48 days) was investigated by us and a report on the decay scheme given in an earlier paper (Bunyan *et al.* 1948). Beneš *et al.* (1948) report in their examination of  $^{181}_{72}\text{Hf}$  with a  $\beta$ -ray spectrometer that L-conversion of the soft  $\gamma$ -ray following the metastable level in  $^{181}_{73}\text{Ta}$  is greater than K-conversion. Thus the value of 200 kev. which we gave for the energy of this transition, obtained by adding the K-binding energy (70 kev.) to the energy of the conversion electrons (130 kev.) as found by absorption, is too high. Beneš *et al.* give the energy of the  $\gamma$ -ray as 128 kev. from their spectrograph measurements.

$^{187}_{75}\text{Re}$ :  $\beta$ -decay of  $^{187}_{74}\text{W}$  (24 hours half-life) leads to a metastable level in  $^{187}\text{Re}$ , first reported by De Benedetti and McGowan (1947). Figure 4 shows the results of one of our experimental runs with the differential recorder using a  $^{187}\text{W}$  source. Counter A was one of the 2.5 cm. diameter argon counters and counter B one of the 2.5 cm. diameter atmospheric pressure helium counters (§ 5 (iv)). Curve A, Figure 4, illustrates the type of record obtained when both instantaneous and delayed coincidences originate from the same source. Curve B, Figure 4, is a semi-logarithmic plot of the coincidence rate for A-channel delays  $\geq 7 \times 10^{-7}$  sec.

\* Since the work described here was completed, De Benedetti and McGowan (1948) have published an account of a search for short-lived isomers.

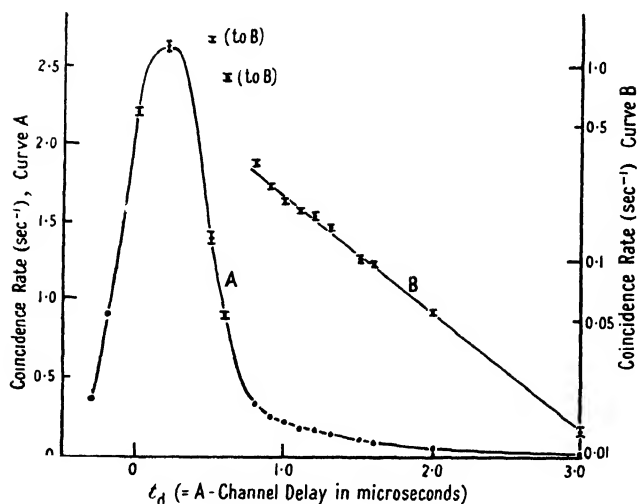


Figure 4. Differential recorder. Decay curve of the metastable state in  $^{187}\text{Re}$ . (The observed coincidence rates have been corrected for the decay of the  $^{187}\text{W}$  source.)

$\beta$ -emitter	Half-life	$\beta$ -emitter	Half-life	$\beta$ -emitter	Half-life
$^{204}_{81}\text{Tl}$	3.5 years	$^{192}_{77}\text{Ir}$	70 days	$^{177}_{71}\text{Lu}$	6.6 days
$^{203}_{80}\text{Hg}$	51.5 days	$^{191}_{76}\text{Os}$	30 hours	$^{143}_{59}\text{Pr}$	13.5 days
$^{198}_{79}\text{Au}$	2.7 days	$^{193}_{76}\text{Os}$	17 days	$^{143}_{58}\text{Ce}$	36 hours
$^{199}_{79}\text{Au}$	3.3 days	$^{188}_{75}\text{Re}$	18 hours	$^{141}_{58}\text{Ce}$	30 days
$^{197}_{78}\text{Pt}$	18 hours	$^{186}_{75}\text{Re}$	90 hours	$^{124}_{51}\text{Sb}$	60 days
$^{187}_{78}\text{Pt}$	3.3 days	$^{185}_{74}\text{V}$	77 days		
$^{194}_{77}\text{Ir}$	20.7 hours	$^{182}_{73}\text{Ta}$	117 days		

#### NOTES

$^{198}\text{Au}$ . Madansky and Wiedenbeck (1947) reported a metastable level in  $^{198}_{80}\text{Hg}$ , following  $\beta$ -decay of  $^{198}\text{Au}$ , whose existence neither Mandeville and Scherb (1948) nor ourselves have been able to confirm.

$^{199}\text{Au}$  was formed by the decay of  $^{199}\text{Pt}$  (31 m.). The sensitivity of our tests in this case is  $\frac{1}{5}$  that implied from § 5 (iii), (iv), since radiation from 3.3 days  $^{197}\text{Pt}$  present in the source tended to mask possible delayed coincidences.

$^{141}\text{Ce}$ . A metastable state of half-life  $(7 \pm 2) \times 10^{-5}$  sec. in  $^{141}\text{Pr}$  following  $\beta$ -decay of  $^{141}\text{Ce}$  was reported by Hirzel *et al.* (1947). In measurements with the integral recorder over a range of integrating pulse lengths ( $\tau_A$ ) up to several times  $10^{-4}$  sec.,\* and with the source deposited on the inside of the window of counter B no delayed coincidences were detected by us.

$^{143}\text{Ce}$  and  $^{143}\text{Pr}$  were also tested in the same fashion as  $^{141}\text{Ce}$ . In the case of  $^{143}\text{Pr}$ , owing to the masking effect from the  $\beta$ -radiations of  $^{141}\text{Ce}$  present in the source, the sensitivity of the test was about  $\frac{1}{5}$  that implied by § 5 (iii), (iv).

$^{124}\text{Sb}$ . Hirzel *et al.* (1947) also reported a metastable state of half-life  $(1.2 \pm 0.4) \times 10^{-3}$  sec. in  $^{124}\text{Te}$  formed by  $\beta$ -decay of  $^{124}\text{Sb}$ . Tests were made over a range of integrating pulse lengths up to several times  $10^{-4}$  sec.,\* but none with the source inside the counter. No delayed coincidences were observed.

$^{185}\text{Re}$  (product nucleus of  $^{185}\text{W}$ ) is possibly of some interest since it possesses the same spin ( $5/2$ ) and the same magnetic moment (3.3 nuclear magnetons) as  $^{187}\text{Re}$ , which has a metastable state. In spite of our negative results,  $^{185}\text{Re}$  may have a metastable state outside the reach of the present method, or any method so far tried with this isotope.

\* The upper limit of detectable isomeric half-lives is about 10 times that for  $\tau_A = 10^{-5}$  sec

The value of the half-life, computed by the method of least squares from the values for A-channel delays  $\geq 10^{-6}$  sec., is  $(5.03 \pm 0.12) \times 10^{-7}$  sec. The probable error given is derived purely from statistical considerations; the error due to the uncertainty in the calibration of the delay lines may be as great as 10%.\*

### (ii) Negative Results

The following  $\beta$ -emitters were examined without evidence being obtained of metastable levels in the product nuclei. Except with the Ce and Pr activities, when the source was placed on the inside of the window of counter B,† radiation entering counter B had to pass through a window 2.5 mg/cm<sup>2</sup> thick (limiting electron energy 35 kev.). The  $\beta$ -counter, counter A, had either a 7 mg. cm<sup>2</sup> or a 2.5 mg/cm<sup>2</sup> window. The sensitivity of our tests is discussed in § 5 (iii), (iv).

### ACKNOWLEDGMENTS

We should like to thank Professor M. L. Oliphant and Professor P. B. Moon for the interest they have shown in this work.

### REFERENCES

- ALDER, F., BALDINGER, E., HUBER, P., and METZGER, F., 1947, *Helv. Phys. Acta*, **20**, 73.  
 BENEŠ, J., GHOSH, A., HEDGRAN, A., and HOLE, N., 1948, *Nature, Lond.*, **162**, 261.  
 BITTENCOURT, P. T., and GOLDBABER, M., 1946, *Phys. Rev.*, **70**, 780.  
 BOWE, J. C., GOLDBABER, M., HILL, R. D., MEYERHOFF, W. E., and SALA, O., 1948, *Phys. Rev.*, **73**, 1219.  
 BRADT, H., and SCHERRER, P., 1943 a, *Helv. Phys. Acta*, **16**, 251; 1943 b, *Ibid.*, 259.  
 BUNYAN, D. E., LUNDBY, A., WARD, A. H., and WALKER, D., 1948, *Proc. Phys. Soc.*, **61**, 300.  
 DE BENEDETTI, S., and MCGOWAN, F. K., 1946, *Phys. Rev.*, **70**, 569; 1947, *Ibid.*, **71**, 380; 1948, *Ibid.*, **74**, 728.  
 DE BENEDETTI, S., MCGOWAN, F. K., and FRANCIS, J. E., 1948, *Phys. Rev.*, **73**, 1404.  
 DEN HARTOG, H., MULLER, F. A., and VERSTER, N. F., 1947, *Physica*, **13**, 251.  
 DUNWORTH, J. V., 1939, *Nature, Lond.*, **144**, 152.  
 HILL, J. M., 1948, *Proc. Camb. Phil. Soc.*, **44**, 440.  
 HILL, J. M., and DUNWORTH, J. V., 1946, *Nature, Lond.*, **158**, 833.  
 HIRZEL, O., STOLL, P., and WÄFFLER, H., 1947, *Helv. Phys. Acta*, **20**, 241.  
 MCGOWAN, F. K., and DE BENEDETTI, S., 1948, *Bull. Amer. Phys. Soc.*, **23**, No. 2, 42.  
 MADANSKY, L., and WIEDENBECK, M. L., 1947, *Phys. Rev.*, **72**, 185.  
 MANDEVILLE, C. E., and SCHERB, M. V., 1948, *Phys. Rev.*, **73**, 634.  
 MONTGOMERY, C. G., and MONTGOMERY, D. D., 1947, *Rev. Sci. Instrum.*, **18**, 411.  
 SHERWIN, C. W., 1948, *Rev. Sci. Instrum.*, **19**, 111.

\* Footnote added in proof. The delay lines have since been calibrated using a crystal-controlled pulse generator, and we find  $(5.26 \pm 0.12) \times 10^{-7}$  sec. for the absolute half-life of the metastable state in <sup>187</sup>Rc.

† The geometrical efficiency of counter B  $\sim 0.5$  in these cases.

## DISCUSSION

on paper by F. C. CHAMPION and R. R. ROY entitled "The Scattering of Fast  $\beta$ -Particles through Large Angles by Nitrogen Nuclei" (*Proc. Phys. Soc.*, 1948, **61**, 532).

Professor N. FEATHER (Edinburgh). Comparison of experiment with theory obviously involves averaging over a finite range of  $\beta$ -particle energy, not only because the theoretical result is energy-dependent, but also because the distribution of scattering points over the chosen scattering volume will be different for particles of different energy (due to differences in extent of magnetic deflection) and because the penetrability of the counters will also be different. Equally obviously, there is a limit to the amount of computation which is profitable. I should like to enquire whether the authors think that their correction terms omit any serious effect of energy-dependence.

Dr. W. T. DAVIES (Clarendon Laboratory, Oxford). It may be of interest to mention some unpublished results by Dr. C. O'Ceallaigh and myself on the nuclear scattering of electrons in air. The work was carried out in Cambridge and London before the war; the conventional cloud chamber method was used, and the energy range investigated was from 1 to nearly 3 mev.

In a measured track length of nearly 90 metres, out of a total length of about 210 metres we found eight cases of elastic scattering through more than  $50^\circ$  where 1 or 2 were to be expected. In view of the smallness of these numbers the significance of our results is open to doubt, although I should point out that the divergence from theory becomes even greater when a correction is applied for the restricted observational solid angle. A fact of possibly greater significance, however, is that scattering with an apparent energy loss exceeding 0.2 of the incident energy was found by us to occur with roughly the same frequency as elastic scattering for angles of scattering greater than  $20^\circ$ , whereas according to an estimate by Mott it should be of order 1/100 as frequent (Mott and Massey, *The Theory of Atomic Collisions* (Oxford: University Press), p. 272).

AUTHORS' reply. We do not consider that our correction terms omit any serious effect arising from energy-dependence. The corrections involved have been the subject of previous examination on several occasions for particles from the same source, and the energy distribution between  $\beta=0.84$  to  $0.94$ , in the scattering volume considered, is well known experimentally. While the penetrability of the counters will be different, as the critic suggests, it will not make a serious contribution over the range of energy considered. Such possible errors and others being taken into account, together with those arising from probability fluctuations, would indicate an accuracy of  $\pm 20\%$ .

We have pointed out that our experimental apparatus is unsuitable in its present form for the examination of inelastic collisions. In earlier experiments with nitrogen and a non-controlled cloud chamber, very few examples of inelastic collisions were found. However, the energy region just below 1 mev., investigated by the authors, is considerably less than that used by Dr. Davies. It is just possible that inelastic collision may increase rapidly with energy above about 1 mev., but the recent results of Van de Graaff *et al.*, which claim extreme accuracy, show no indication of this.

## LETTERS TO THE EDITOR

### Infra-Red Photoconductivity in Layers of Tellurium and Arsenic

Evaporated layers of tellurium have been prepared which exhibit marked photoconductivity at low temperatures when irradiated by wavelengths in the near infra-red, although previous investigators have concluded that this element is not photosensitive (Coblentz 1918, Brown and MacMahon 1929).

The films were deposited on graphite electrodes on the inner walls of small pyrex Dewar flasks. For a tellurium layer, about one milligram of material was inserted into the flask, which was then evacuated to a pressure of less than  $10^{-6}$  mm. of Hg, as recorded on an ionization gauge. The material was distilled on to the outer wall of the vessel and purified by heating just below the evaporation temperature for periods of one to several hours. Finally the layer was distilled on to the electrodes.

Taking the thickness of the films as  $10^{-4}$  cm., specific resistances of about 1 ohm cm. were obtained at room temperature, and 10–20 ohm cm. at liquid oxygen temperature. The response times of the layers (i.e. time required for signal to decay to  $1/e$  after illumination by a pulse of light) were in the range 500 to 1,000 microseconds. The spectral distribution of sensitivity was measured for one layer which was made in an envelope with a thin "bubble" window of pyrex for which the absorption would be negligible over the range of wavelengths concerned. The results are shown in Figure 1, where the relative signal

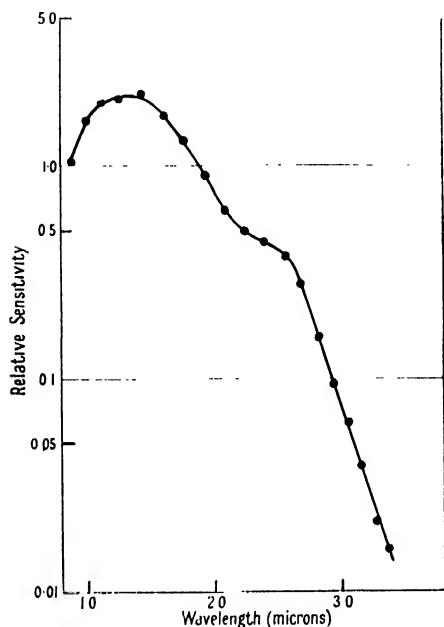


Figure 1. Spectral sensitivity of tellurium layer at  $90^{\circ}$  K.

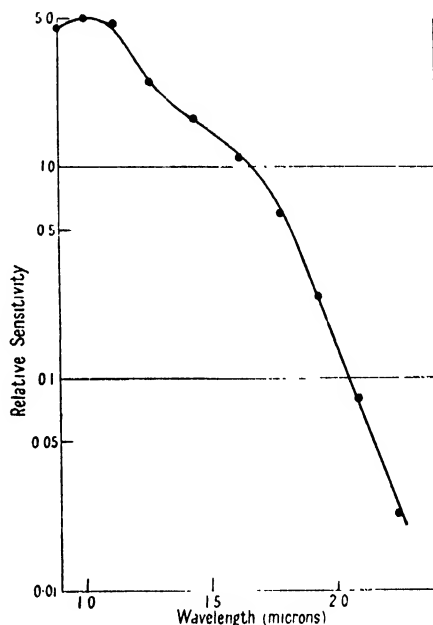


Figure 2. Spectral sensitivity of arsenic layer at room temperature.

output (referred to constant incident energy) is plotted on a logarithmic scale. It may be seen that a rapid exponential fall of sensitivity commences at  $2.7 \mu$ . The most sensitive tellurium cell so far made gave a signal equal to r.m.s. noise in 1 c/s. bandwidth for an incident energy of  $10^{-9}$  watts from a source at roughly 2,000 K., using an interruption rate of 800 c/s.

Banks, Neuman and Schoenfeld, working at the Polytechnic Research and Development Company, Brooklyn, New York, under a contract with the U.S. Office of Naval Research, have independently observed photoconductivity in evaporated and sputtered films of tellurium.

Layers of arsenic showing slight photoconductivity have also been prepared. It is to be noted that whereas for tellurium the effect was appreciable only at low temperatures, for arsenic strong cooling ruined the layer.

Some preliminary measurements have been made on layers of arsenic prepared by techniques similar to those used for tellurium. It is, however, much more difficult to produce mechanically stable layers of this material, and so far only one layer with sensitivity adequate for measuring the spectral response curve has been made. Even in this case very low resolution had to be used in order to get sufficient energy on the layer. The curve is shown in Figure 2. As the wavelength is increased, an exponential fall off begins at about  $1.7 \mu$ .



This layer had a specific resistance of  $10^6$  ohm cm. (approx.) and a response time of  $10^{-3}$  seconds. The arsenic layers had a grey metallic appearance at room temperature, but cooling with liquid oxygen converted them to the red allotropic form, and the photo-sensitivity disappeared.

I am indebted to the Ministry of Supply for permission to carry out this work at Cambridge and to Dr. Banks for communicating to me (through Dr. G. B. B. M. Sutherland) the results referred to above, before publication.

Department of Colloid Science,  
Cambridge.  
5th January 1949.

T. S. Moss.

COBLENTZ, W. W., 1918, *Bull. Nat. Bur. Stand., Wash.*, **14**, 591.

BROWN, F. C., AND MACMAHON, A. M., 1929, *International Critical Tables*, **6** (New York: McGraw-Hill).

## REVIEWS OF BOOKS

*Multiple-Beam Interferometry of Surfaces and Films*, by S. TOLANSKY. Pp. viii + 187. (Oxford: Clarendon Press, 1948.) 18s.

Light interference has always been a useful tool to the scientist and the glass worker. A visitor to a lens factory is impressed by the ease with which lens surfaces are tested in the course of production. A glass gauge embodying the correct spherical surface is applied, with the appropriate skill, to the lens surface and observation in mercury light shows at once the contour of the surface. One interference fringe of regular shape over the surface represents very good quality whereas in an inferior lens the fringes are irregular and are increased in number. In this application of interference and in the usual types of interferometers the variation in brightness produced by the fringes is sinusoidal and consequently the fringes are quite fuzzy in outline. By silvering the surfaces to create multiple interference, sharp line-like fringes can be obtained instead of the broad fuzzy bands. Professor Tolansky and his research workers have pursued vigorously the application of multiple interference to the study of surface markings in crystals, metals etc. This book represents a convenient summary of their work to date.

An immediate result of the sharpened fringes is the increased accuracy with which the topographical features can be measured. In extremely favourable cases an accuracy of 3 Å. is quoted as having been attained. This is indeed remarkable for a system using ordinary light.

The general tone and outlook of the book is that of practical application of this particular optical tool. There is a brief clear theoretical treatment of multiple interference, careful distinction being drawn between the different kinds of fringes and their localization. The bulk of the book, however, is concerned with the examination of surfaces of mica, quartz, metals etc., with results illustrated by numerous photographs. The possibilities of the method will be of interest to those who are concerned in the topography of surfaces, surface finishes etc., and there are also the possible applications to the measurement of small distances and movements of small amplitude.

A chapter is devoted to interference colour filters. This type of filter would be a very useful addition indeed to the customary range of absorbing filters, but at present they remain surprisingly difficult to obtain commercially.

R. D.

## CONTENTS FOR SECTION B

Dr. G. LIEBMANN. Measured Properties of Strong "Unipotential" Electron Lenses . . . . .	213
Dr. A. B. BHATIA. On the Electrical Properties of Cold Worked Iron Carbon Alloys . . . . .	229
Mr. M. K. I. ARAFA. A Calculation of the Solubility Limits of the Copper-Silver System . . . . .	238
Mr. J. P. ROBERTS. Mechanical Breakdown of a Non-Metallic Polycrystalline Material Observed by Reflected Light Microscopy . . . . .	248
Mr. K. GOLDSMITH and Dr. J. IBALL. The Measurement of the Rheological Properties of Visco-plastic Substances . . . . .	251
Mr. J. CRANK and Miss M. E. HENRY. A Comparison of the Rates of Conditioning by Different Methods . . . . .	257
Letter to the Editor :	
Mr. R. B. R.-SHERSBY-HARVIE and Mr. L. B. MULLETT. A Travelling Wave Linear Accelerator with R.F. Power Feedback, and an Observation of R.F. Absorption by Gas in Presence of a Magnetic Field . . . . .	270
Dr. JOHN LAMB and Mr. A. TURNEY. The Dielectric Properties of Ice at 1.25 cm. Wavelength . . . . .	272
Reviews of Books . . . . .	273
Contents for Section A . . . . .	275
Abstracts for Section A . . . . .	275

## ABSTRACTS FOR SECTION B

*Measured Properties of Strong "Unipotential" Electron Lenses*, by G. LIEBMANN.

**ABSTRACT.** The Hartmann test and the "knife-edge" method for the determination of lens constants are described as applied to the investigation of electrostatic "unipotential" lenses. The results of measurements on a number of such lenses are presented graphically.

It is shown that the curvature of the principal surfaces plays an important part and that it is, therefore, necessary to distinguish between longitudinal spherical aberration and difference of zonal focal lengths. Up to about half the lens diameter, primary spherical aberration only is noticeable in most cases. The dimensionless spherical aberration constant  $S$  can be approximately represented, over a wide range of modifications of lens design or lens potentials, by the formula  $S = K_1(f/D)^2$ ,  $f$  being the focal length and  $D$  the internal diameter of the centre electrode of the lens.  $K_1$  is a constant of the order of 10 for the lenses investigated without stops limiting the axial length of the field, and of the order of 20 for lenses incorporating such stops. In the case of one specially constructed lens, good agreement is found with calculations by Ramberg. In an experimental unipotential lens for which the diverging parts of the electrostatic field were removed, the spherical aberration is as low as in magnetic lenses of comparable dimensions.

*On the Electrical Properties of Cold Worked Iron Carbon Alloys*, by A. B. BHATIA.

**ABSTRACT.** The change on "aging" in the electrical properties of cold worked iron-carbon alloys of low concentration is investigated theoretically. During the process of "aging", the carbon atoms diffuse into the dislocations, thus forming rows of atoms. The electrical resistance due to scattering of electrons by these rows of carbon atoms is expressed in terms of the scattering power of a single carbon atom dissolved in the iron lattice, and hence in terms of the resistance of the same number of randomly distributed carbon atoms. It is found that this change depends on the wavelength of the electrons at the Fermi surface. This wavelength is determined by the effective number of free electrons, and with a reasonable value of about 0.6 electrons per atom for iron, the agreement with the observed diminution in resistance is satisfactory.

Alternatively, one can use the calculations to determine both the number of free electrons in iron and the number of dislocations in the specimen at different degrees of hardening, from the observed changes in the electrical resistance and thermoelectric power of the specimen.

*A Calculation of the Solubility Limits of the Copper-Silver System*, by M. K. I. ARAFA.

**ABSTRACT.** A calculation is made of the change in the energy of a monovalent metal when one of its atoms is replaced by an atom of a different monovalent metal, not necessarily of the same atomic volume. From a knowledge of this energy the heat of solution can be determined and thereby, through the usual thermodynamic relations, also the solubility limits. Numerical calculations have been carried out for the copper-silver system and the theory shows in this case the existence of narrow solubility limits, in agreement with the known phase diagram. The theoretical values of the heats of solution are compared with those required to give the observed solubility limits.

*Mechanical Breakdown of a Non-Metallic Polycrystalline Material Observed by Reflected Light Microscopy*, by J. P. ROBERTS.

**ABSTRACT.** A study of fractures in a well-sintered polycrystalline aggregate of corundum crystals has shown that the strengths of the crystals and the crystal-boundaries are approximately equal. Reflected light microscopy was employed and the usefulness of this method of examination has been established.

*The Measurement of the Rheological Properties of Visco-plastic Substances*, by K. GOLDSMITH and J. IBALL.

**ABSTRACT.** A torsion device is described in which a small and decreasing stress is exerted on the visco-plastic substance by means of a blade attached to a torsion wire. A modification of the Scott Blair-Nutting equation is suggested to account for the variation of both stress and strain with time and a "firmness intensity factor" of the substance is calculated, by means of the modified equation, from the observed relation between blade deflection and time. The apparatus has been used to study the properties of milk curds.

*A Comparison of the Rates of Conditioning by Different Methods*, by J. CRANK and M. E. HENRY.

**ABSTRACT.** Four methods of conditioning a sample of material to a prescribed liquid or vapour content are examined mathematically. The "two-stage method" of conditioning leads to considerably shorter conditioning times than the other methods provided it is carried out in a certain way, and information presented in graphical form in this paper shows how to obtain the maximum advantage in practice. The necessary equations are developed for both a plane sheet and a cylinder, and the corresponding problem in heat flow is mentioned.

## CORRIGENDA

"Nuclear Disintegrations in Photographic Plates exposed to Cosmic Rays under Lead Absorbers", by E. P. GEORGE and A. C. JASON (*Proc. Phys. Soc. A*, 1949, **62**, 243).

Pages 250-251, last paragraph of §4. The figures "19,000", occurring three times, should read "9,000".

The percentage stated in the subsequent formula should read "60 per cent" and not "30 per cent".

# THE PROCEEDINGS OF THE PHYSICAL SOCIETY

## Section A

---

VOL. 62, PART 5

1 May 1949

No. 353 A

---

### The Establishment of the Absolute Scale of Temperature below $1^{\circ}\text{K}$ .

By A. H. COOKE

Clarendon Laboratory, Oxford

*Communicated by F. E. Simon; MS. received 12th December 1948*

**ABSTRACT.** Experiments are discussed establishing the relation of the absolute thermodynamic scale of temperature below  $1^{\circ}\text{K}$ . to the magnetic scale obtained by the extrapolation of Curie's law. The experimental results on iron ammonium alum, manganous ammonium sulphate, and chrome potassium alum are compared with the theoretical calculations of Onsager and Van Vleck.

#### § 1. INTRODUCTION

THE range of temperatures below  $1^{\circ}\text{K}$ . forms a distinct region of low temperature technique, in which the temperatures are attained and measured magnetically, in contrast with the methods dependent on the manipulation of gases used at higher temperatures. Temperature measurements below  $1^{\circ}\text{K}$ . are made by determining the magnetic moment of a specimen of paramagnetic salt in a small magnetic field. At high temperatures this is proportional to the magnetic field and inversely proportional to the absolute temperature (Curie's law); the scale of temperature obtained by the extrapolation of this law to the low temperatures reached by the adiabatic demagnetization method is termed the magnetic or Curie scale. Because of demagnetizing effects, the magnetic moment of a given mass of salt at a fixed field and temperature depends on the shape of the specimen. To avoid a multiplicity of magnetic temperature scales, it is the practice to correct the magnetic moment of a specimen to that which would be displayed by a spherical sample (Kurti and Simon 1938, Hull 1947). It is the scale of temperature derived in this way that we shall refer to as the magnetic temperature. It will be denoted by  $T^*$ . Up to the present most of the results obtained in this region of temperature have been expressed in terms of this scale, although it is known that at sufficiently low temperatures departures from Curie's law render it more or less invalid. An extreme case will illustrate this. Adiabatic demagnetization of iron ammonium alum from a field of 15,000 oersted at  $1^{\circ}\text{K}$ . will bring the specimen to a temperature at which its susceptibility is a maximum. Demagnetization from a greater field at  $1^{\circ}\text{K}$ . will bring the specimen to a lower absolute temperature, but to a higher temperature on the magnetic scale, an absurd state of affairs.

In the experiments considered here the relation of the magnetic scale to the absolute scale of temperature has been determined for three different paramagnetic salts. Besides enabling temperature measurements made with these salts to be

corrected to the absolute scale, a comparison of the experimental results with theory enables us to calculate the separation of the energy levels of the magnetic ions in these salts, and to predict to what extent theoretical corrections can safely be applied to magnetic temperature measurements made with other salts. The method used, which was the same in all three cases, was suggested by Keesom (1934) and by Kurti and Simon (1935 a), who first applied it to iron ammonium alum (Kurti and Simon 1935 b). The measurements on manganous ammonium sulphate were made by Dr. R. A. Hull and the writer, and those on potassium chrome alum by Dr. B. Bleaney.

## § 2. EXPERIMENTAL METHOD

The method consists in determining the heat input to the salt and the change in its entropy as functions of the magnetic temperature. Consider a reversible change made at a temperature  $T^*$  on the magnetic scale, involving a small heat input  $dQ$  and a small entropy change  $dS$ . Then the absolute temperature  $T$  corresponding to the magnetic temperature  $T^*$  is given by  $T = dQ/dS$ . Thus if graphs of  $Q$  and  $S$  as functions of the magnetic temperature  $T^*$  are prepared, the ratio of their slopes at a given value of  $T^*$  gives the corresponding absolute temperature  $T$ . Other related quantities, such as the true specific heat,  $dQ/dT$ , can then be evaluated.

The specimens of paramagnetic salt used in the experiments were prepared from "Analar" material. As it is most important that there should be no loss of water of crystallization, the specimens were prepared by selecting large crystals of the salt, grinding them to powder and immediately compressing the powder in a hydraulic press to a pressure of about 2 tons/cm<sup>2</sup>. This process produced cylinders which could be turned in a lathe and finally ground to a spheroidal shape, usually 5 cm. long and 1.25 cm. diameter. As the density of the specimens was within 1% to 2% of the crystalline density, all the calculations of demagnetizing effects used below have been based on the crystalline density.

The entropy curve is determined in a series of experiments in which a specimen of the salt to be examined is magnetized at a known field and temperature, producing a calculable change of entropy, followed by adiabatic demagnetization. The measurement of the resulting temperature on the magnetic scale is made by comparing the magnetic moment of the specimen in a field of a few oersted with its moment in the same field at the known initial temperature. The graph of entropy against magnetic temperature is then obtained by plotting this temperature against the calculated change of entropy occurring during the isothermal magnetization. In principle, this change of entropy could be found experimentally, instead of by calculation, by measuring the heat evolved during magnetization (for example, by measuring the increased evaporation of helium from the cryostat), but in practice it is difficult to secure reversible heat exchange between the specimen and the cryostat, and the entropy change is therefore calculated. At 1° K. the salts used can be considered as ideal paramagnetics in which interaction effects can be ignored.† Tables of entropy of ideal paramagnetics are available (Hull and Hull 1941). The results of two series of such experiments, made on iron ammonium alum and on manganous ammonium sulphate, are shown in Figures 1 and 2. The temperature of magnetization was usually between 0.9° K. and 1.0° K.,

† A correction for interaction effects was in fact applied in the calculations on iron ammonium alum.

and the magnetic fields used ranged between 740 oersted and 40,000 oersted. Values of the (magnetic field)/temperature ratio corresponding to different values of entropy are shown at the right of Figure 2.

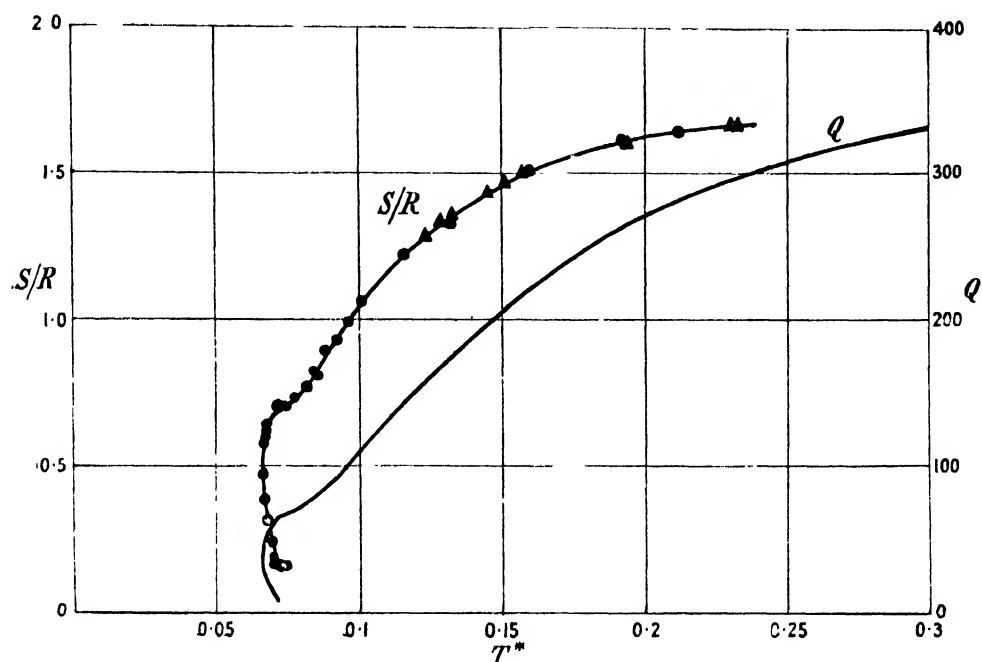


Figure 1. Entropy and heat content of iron ammonium alum, plotted against magnetic temperature. Units of heat content are minutes of  $\gamma$ -ray heating.

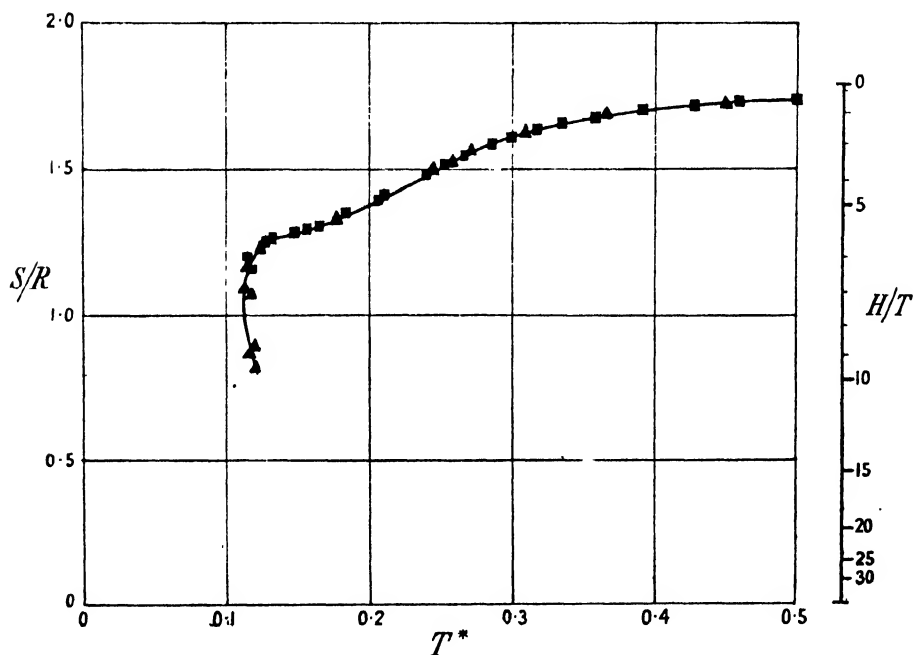


Figure 2. Entropy of manganous ammonium sulphate plotted against magnetic temperature. Right-hand column shows corresponding values of  $H/T$ , in kilo-oersted/degree.

The curve of heat input against magnetic temperature is obtained by demagnetizing the salt to as low a temperature as possible, followed by heating at a uniform rate, with observation of the magnetic temperatures at fixed intervals of time as heating proceeds. The chief experimental difficulty arises from the low thermal conductivity of the salt, which renders uniformly distributed heating essential. In these experiments the salts were heated by gamma ray irradiation, which produces almost uniform heating, as the absorption coefficient is small. It has the disadvantage that the rate of heating, and consequently the thermodynamic temperature scale derived from it, is known only in arbitrary units. To reduce the temperatures to degrees absolute the measurements must extend to sufficiently high temperatures at which the relation of the magnetic scale to the absolute scale is accurately known. Ideally the measurements should be carried up to a point which can be determined from helium vapour pressure measurements. It is, however, a matter of some experimental difficulty to determine the specific heats at temperatures at which the vapour pressure of helium is appreciable, since gas conduction will then impair the thermal insulation (Cooke and Hull 1942). In the three cases discussed here the measurements do not extend to  $1^\circ \text{K}$ . The temperature scales for iron ammonium alum and manganous ammonium sulphate have been adjusted to fit Van Vleck's theoretical formula (discussed below) at  $0.5^\circ \text{K}$ . At this temperature the calculated value of  $T^* - T$  is  $0.010^\circ \text{K}$ . for iron alum and  $0.024^\circ \text{K}$ . for manganous ammonium sulphate, so that the error in  $T$  likely to be involved in using this value is very small and, of course, decreases proportionately to the absolute temperature. The measurements on potassium chrome alum showed that above  $0.5^\circ$  the ratio  $T^*/T$  is constant. It was therefore assumed that at these temperatures the two scales coincide. For this salt the Van Vleck formula gives  $T^* - T = 0.009^\circ \text{K}$ . at  $0.5^\circ \text{K}$ .

Apart from this question of absolute magnitude, the curve of heat input against magnetic temperature can be obtained with great accuracy. For example, the curve for iron ammonium alum shown in Figure 1, obtained by compounding a number of heating experiments, is based on over a thousand experimental points. A large number of points is desirable, because the curve of absolute temperature against magnetic temperature depends on the gradients of the curves. The entropy curve is necessarily based on a smaller number of points, since each one demands a separate demagnetization experiment, but the accuracy of the determination can often be improved by the use of an empirical formula. For example, in the demagnetization of chrome alum from an initial field  $H_i$  and temperature  $T_i$  to a final temperature  $T_f^*$ , it is found that the value of  $H_i T_f^*/T_i$  is practically constant over a range of values of  $T_f^*$  from  $0.1^\circ$  to  $0.3^\circ$ . Over this range interpolation can be made with accuracy, and only a small number of demagnetization experiments need be made. The final results obtained by taking the ratio of the slopes of the heat input and entropy curves are shown in Figures 3, 4 and 5. Figure 3 shows the graph of  $T^*$  against  $T$  for iron ammonium alum, Figure 4 for manganous ammonium sulphate, and Figure 5 shows the relation of  $T^*$  and  $T$  for potassium chrome alum, together with the results of different theoretical calculations of this relation.

### § 3. COMPARISON OF THE RESULTS WITH THEORY

Curie's law will be obeyed by a paramagnetic salt so long as it can be regarded as an assembly of free magnetic dipoles. Two effects will cause departures from

Curie's law, the action on the dipoles of the electric field of the crystalline lattice and the magnetic interaction of the dipoles. Owing to the high magnetic dilution of the salts considered, exchange forces will be neglected. We have to consider the effect of these interactions on the entropy of the salts and on the magnetic susceptibility (i.e. on  $T^*$ ) and also the occurrence of a Curie point, below which ferromagnetism occurs, found near the susceptibility maximum of iron alum or manganous ammonium sulphate.

In iron ammonium alum and manganous ammonium sulphate, for which  $J = \frac{5}{2}$ , there are six energy levels of the magnetic dipoles, giving an entropy

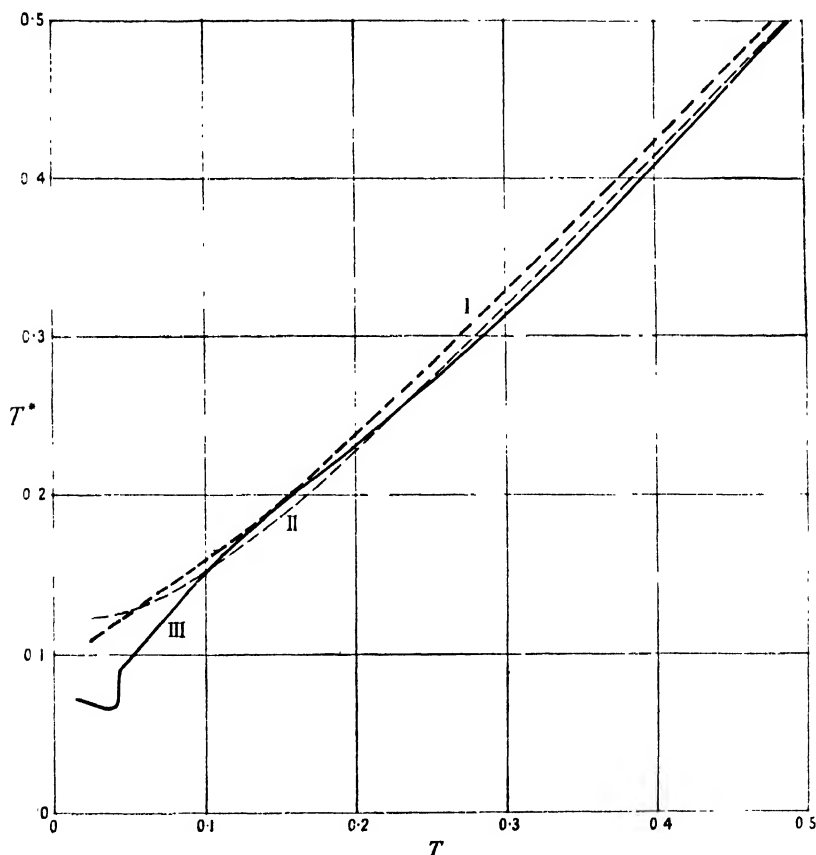


Figure 3. Magnetic temperature against absolute temperature for iron ammonium alum. Curve I, Onsager's theory; Curve II, Van Vleck's theory; Curve III (full line), experimental results.

in zero field of  $R \ln 6$ ,  $(1.792R)$ , per mole. If as a first approximation we assume that the electric field of the crystal lattice possesses cubic symmetry, its effect is to split the levels into two groups, one of two-fold and one of four-fold degeneracy, with an energy separation  $\delta$  (Van Vleck and Penney 1934). The entropy will therefore be reduced at a sufficiently low temperature either to  $R \ln 4$ ,  $(1.386R)$ , or to  $R \ln 2$ ,  $(0.693R)$ , according as the four-fold or the two-fold level possesses the lower energy. The effect of the magnetic interaction will be to remove the remaining degeneracy of the levels, producing a further entropy drop in the neighbourhood of the Curie point. Figures 1 and 2 suggest that these two entropy reductions can be considered to occur in roughly separate stages, and that in iron alum the crystalline field reduces the entropy to  $R \ln 2$ , i.e. the four-fold level.



is uppermost, while in manganous ammonium sulphate the two-fold level is uppermost. Thus, assuming the action of the crystalline field to be independent of the magnetic interaction, its effect is represented by the partition function

$$Z_c = 2\{2 + \exp(-\delta/kT)\},$$

$\delta$  being positive for iron alum and negative for manganous ammonium sulphate.

An electric field of cubic symmetry will not affect the energy levels of chrome alum, for which  $J = \frac{3}{2}$  (Penney and Schlapp 1932), but departures from cubic symmetry will split the levels into two groups of two-fold degeneracy (Schlapp and Penney 1932, Hebb and Purcell 1937). The corresponding partition function is

$$Z_c = 2\{1 + \exp(-\delta/kT)\}.$$

At high temperatures ( $\delta/kT \ll 1$ ) the reduction of entropy due to the crystalline field is then

$$S_0 - S = \frac{1}{9} R(\delta/kT)^2 \text{ for } J = \frac{5}{2}$$

and

$$S_0 - S = \frac{1}{8} R(\delta/kT)^2 \text{ for } J = \frac{3}{2}.$$

These expressions can be used to calculate values of  $\delta$  from the experiments, provided allowance is made for the effect of magnetic interaction. This has been treated by the local field methods of Lorentz (1916) and Onsager (1936), and from a quantum mechanical point of view by Van Vleck, whose method has been applied in detail to paramagnetic salts by Hebb and Purcell (Van Vleck 1937, Hebb and Purcell 1937). Van Vleck obtained an expression for the contribution of magnetic interaction to the partition function, which he expanded in a power series in  $1/T$ . At high temperatures the result is independent of the crystalline interaction, and the reduction of entropy due to magnetic interaction is

$$S_0 - S = Rf\tau^2/T^2,$$

where

$$\tau = ng^2\beta^2 J(J+1)/R.$$

Here  $n$  = number of magnetic ions/cm<sup>3</sup>,  $g$  = Landé factor,  $\beta$  = Bohr magneton.  $\tau/3$  is the Curie constant in the equation for the volume susceptibility at high temperatures,  $\chi = \tau/3T$ . The factor  $f$  depends on the lattice arrangement of the magnetic ions. For a face-centred cubic lattice, as in the alums,  $f = 1.20$ . (Onsager's treatment, which ignores crystal structure, leads to a similar result, except for the factor  $f$ .) Combining the two expressions, we have a formula for the reduction of entropy at high temperatures in which all the quantities save  $\delta$  are known. Comparison with the experimental results gives the following values of  $\delta$ :

Iron ammonium alum	$\tau = 0.0472^\circ$ , $\delta/k = 0.20^\circ$ .
Manganous ammonium sulphate	$\tau = 0.062^\circ$ , $\delta/k = -0.33^\circ$ .
Potassium chrome alum	$\tau = 0.0204^\circ$ , $\delta/k = 0.24^\circ$ .

#### § 4. THE MAGNETIC SUSCEPTIBILITY

Unlike the entropy, the magnetic susceptibility depends on the shape of the specimen. At high temperatures the different methods of calculating magnetic interaction all reduce to the Lorentz local field formula (Lorentz 1916):

$$\frac{T^*}{T} = 1 - \frac{1}{3} \left( \frac{4\pi}{3} - D \right) \frac{\tau}{T},$$

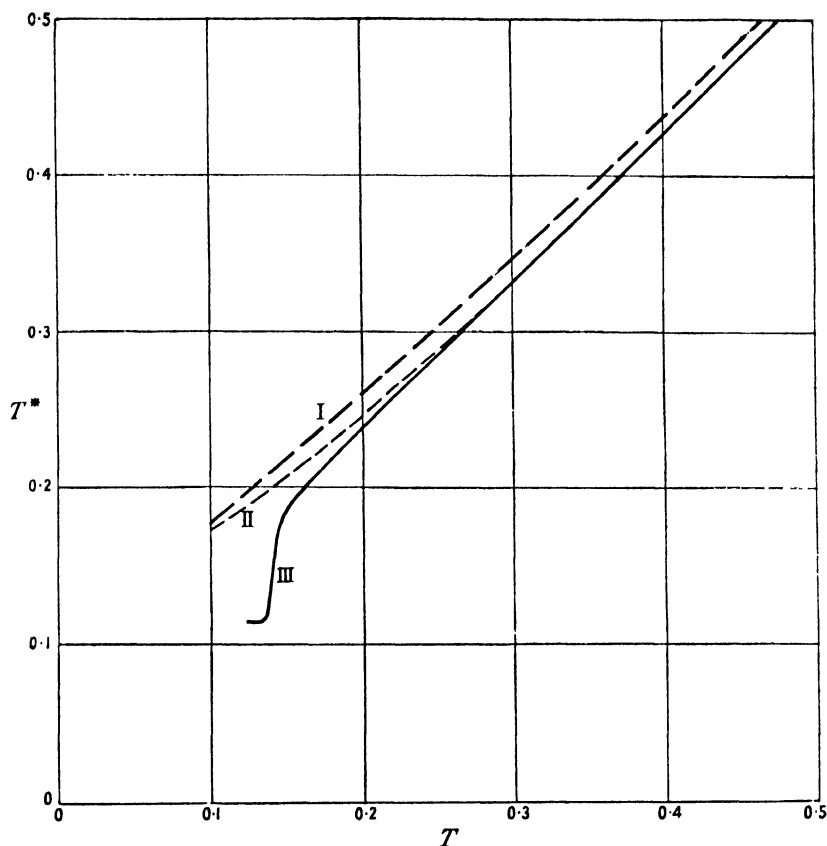


Figure 4. Magnetic temperature against absolute temperature for manganous ammonium sulphate. Curve I, Onsager's theory; Curve II, Van Vleck's theory; Curve III (full line), experimental results.

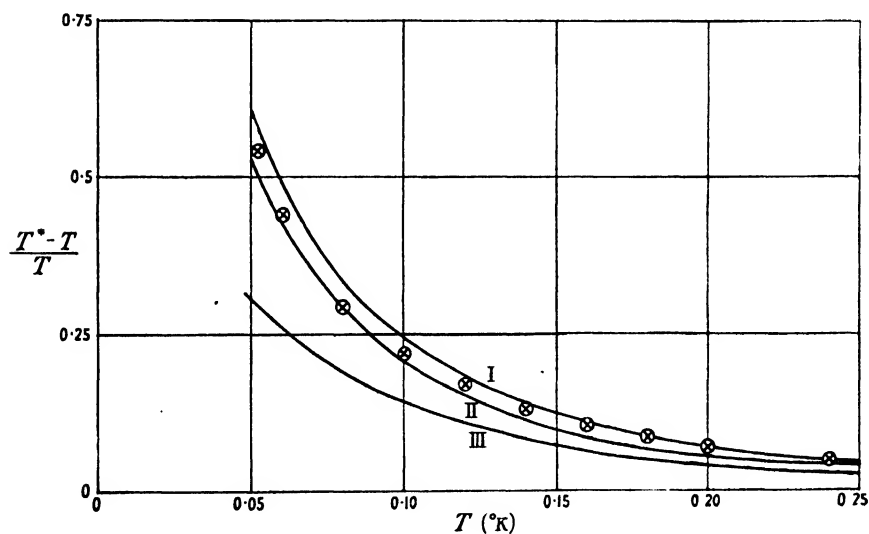


Figure 5. Relation between magnetic temperature and absolute temperature for potassium chrome alum. Curve I, Onsager's theory; Curve II, Van Vleck's theory; Curve III, Lorentz' theory. Crosses are experimental results.

where  $D$  = demagnetizing factor of the specimen. At high temperatures the effect of the crystalline field is negligible, since its lowest order term is  $1/T^2$ . For example, if  $J = \frac{5}{2}$ , the effect of the crystalline field alone is given by the equation

$$\frac{T^*}{T} = 1 + \frac{8}{189} \left( \frac{\delta}{kT} \right)^2.$$

Thus at high temperatures we need only consider the magnetic dipole interaction, which for a spherical specimen, ( $D = 4\pi/3$ ), is cancelled by the demagnetizing field of the sphere, so that  $T^* = T$  to a high degree of approximation.

At the temperatures considered here the effect of the crystalline field can no longer be ignored. Figures 3, 4 and 5, besides showing the experimentally determined curves of  $T^*$  and  $T'$ , give the theoretical relation between these quantities, as calculated by the method of Onsager (Curve I in each diagram) and that of Van Vleck (Curve II). In each case the effect of the crystalline field is first computed. In the notation of Hebb and Purcell (1937) its effect is represented by the introduction of a factor,  $\gamma$ , into the susceptibility formula:

$$\chi_0 = \gamma \tau_i 3T,$$

where

$$\gamma = \frac{2}{21Z_c} \left[ 5 + 32 \frac{kT}{\delta} + \left( 26 - 32 \frac{kT'}{\delta} \right) \exp(-\delta/kT) \right]$$

for iron alum and for manganous ammonium sulphate, and

$$\gamma = \frac{2}{5Z_c} \left[ 3 + 4 \frac{kT'}{\delta} + \left( 3 - 4 \frac{kT'}{\delta} \right) \exp(-\delta/kT') \right]$$

for chrome alum.

In applying these formulae we have used the values of  $\delta$  derived from the entropy curves. The susceptibility  $\chi_0$  so calculated, in which allowance is made for the crystalline field, but not for magnetic interaction, may be considered as the susceptibility at infinite magnetic dilution. In Onsager's theory the magnetic interaction is considered to give rise to a local field. The calculation is purely classical, and takes no account of crystal structure, but it has the advantage of yielding an exact formula. In Van Vleck's theory the contribution of magnetic interaction to the partition function is calculated, and its influence on the magnetic susceptibility is then expressed as a power series in  $1/T$ , of which, unfortunately, we are able to use only the first term. Onsager's formula is

$$\chi = \chi_0 \left[ \frac{3}{4} - \frac{3}{16\pi\chi_0} + \left( \frac{9}{16} + \frac{3}{32\pi\chi_0} + \frac{9}{256\pi^2\chi_0^2} \right)^{\frac{1}{2}} \right].$$

The first term of Van Vleck's formula gives

$$\chi = \chi_0 \left( 1 - \frac{4\pi}{3} \chi_0 + 12\eta\chi_0^2 \right),$$

where

$$\eta = f \left( 1 + \frac{3}{8J(J+1)} \right),$$

Here  $f$  is again the lattice structure factor (1.20 for the alums, 1.4 for the manganese salt).  $T^*$  then follows from either of the formulae for  $\chi$  by the equation

$$T^* = (\tau/3)(1/\chi + 4\pi/3).$$

It will be seen from Figure 5 that either formula fits the experimental results on chrome alum well, over the range of temperatures investigated. The experiments on iron alum and manganous ammonium sulphate (Figures 3 and 4) show, however, that both theories fail at temperatures near the susceptibility maximum (minimum of  $T^*$ ). The Onsager formula predicts no maximum, while the Van Vleck formula, though it predicts a susceptibility maximum, cannot really be considered to be valid at these temperatures owing to the very slow convergence of the power series in  $1/T$  on which it is based. Moreover, neither formula predicts the sudden increase of susceptibility to the maximum value, nor the existence of a Curie point.

#### § 5. THE CURIE POINT

The chief interest in the results obtained at the lowest temperatures is the appearance of a Curie point, below which remanence occurs, at a temperature of  $0.042^\circ\text{K.}$  in the case of iron ammonium alum, and  $0.15^\circ\text{K.}$  in the case of manganous ammonium sulphate. (Both of these temperatures are very near to the values at which the susceptibility maxima occur.) Of the different methods of calculating the magnetic interaction, only the Lorentz method gives a value sufficiently large to produce spontaneous magnetization. Onsager has shown that this method is inexact, but it is useful in that it gives an upper limit for the temperature at which dipole interaction can produce ferromagnetism. According to this theory the Curie point will depend on the shape of the specimen, an infinitely long specimen giving the highest Curie point, while no Curie point occurs for a sphere because of the neutralization of the demagnetizing and interaction fields. This dependence of the Curie point on the shape of the specimen has not been tested experimentally.

The specimens used in the experiments were ellipsoids with axial ratios of 3:1 and 4:1. Following the method of Debye (1938), the Curie points have been computed, using the values of  $\delta$  already calculated. For iron ammonium alum, the calculated Curie point is  $0.032^\circ\text{K.}$  for an infinite cylinder, and  $0.016^\circ\text{K.}$  for a 3:1 ellipsoid. The observed Curie point of a 3:1 ellipsoid is  $0.042^\circ\text{K.}$  For manganous ammonium sulphate the calculated Curie point is  $0.067^\circ\text{K.}$  for an infinite cylinder, and  $0.050^\circ\text{K.}$  for a 4:1 ellipsoid. The observed Curie point for a 4:1 ellipsoid is  $0.15^\circ\text{K.}$  Although it must be emphasized that the determinations of the absolute temperatures are particularly difficult in the neighbourhood of the Curie points, it will be seen that the experimental values of the Curie points are decidedly higher than the calculated values, and in fact exceed the calculated values for infinite cylinders, which are the highest given by any theory of magnetic dipole-dipole interaction. It is clear that though the effect of the crystalline field is successfully treated by the theory, there are further interaction effects which have still to be explained.

#### ACKNOWLEDGMENTS

The author wishes to thank Professor F. Simon, Dr. B. Bleaney, Dr. R. A. Hull and Dr. N. Kurti for their permission to use many unpublished experimental results, and also for many helpful discussions. The measurements on iron alum were made by Dr. Kurti, Professor Simon and Dr. Squire, partly at the Laboratoire du Grand Electroaimant, Bellevue, near Paris, and partly at the Clarendon Laboratory. Those on chrome alum were made by Dr. Bleaney,

and those on manganous ammonium sulphate by Dr. Hull and the writer. Although they were all obtained some years ago, the results have not previously been published, as it was desired to make further measurements in the neighbourhood of the Curie points. It is felt, however, that this review, which was first given as a lecture to the Physical Society Conference in Cambridge in 1946, may be of value in the meantime.

## REFERENCES

- COOKE, A. H., and HULL, R. A., 1942, *Proc. Roy. Soc. A*, **181**, 83.  
 DEBYE, P., 1938, *Ann. Phys., Lpz.*, **32**, 85.  
 HEBB, M. H., and PURCELL, E. M., 1937, *J. Chem. Phys.*, **5**, 338.  
 HULL, J. R., and HULL, R. A., 1941, *J. Chem. Phys.*, **9**, 465.  
 HULL, R. A., 1947, *Report of Cambridge Conference on Low Temperatures* (London: Physical Society), p. 72.  
 KEESOM, W. H., 1934, *J. Phys. Radium*, **5**, 373.  
 KURTI, N., and SIMON, F., 1935 a, *Proc. Roy. Soc. A*, **149**, 161; 1935 b, *Ibid.*, **152**, 21; 1938, *Phil. Mag.*, **26**, 849.  
 LORENTZ, H. A., 1916, *The Theory of Electrons* (Leipzig: Teubner).  
 ONSAGER, L., 1936, *J. Amer. Chem. Soc.*, **58**, 1486.  
 PENNEY, W. G., and SCHLAPP, R., 1932, *Phys. Rev.*, **41**, 194.  
 SCHLAPP, R., and PENNEY, W. G., 1932, *Phys. Rev.*, **42**, 666.  
 VAN VLECK, J. H., 1937, *J. Chem. Phys.*, **5**, 320.  
 VAN VLECK, J. H., and PENNEY, W. G., 1934, *Phil. Mag.*, **17**, 961.

## A Theory of Reflectivity and Emissivity

By D. J. PRICE

Raffles College, Singapore

*MS. received 4th August 1948*

**ABSTRACT.** A general theory of the reflectivity and emissivity of materials is derived in a conveniently tractable form. As an example of the power of the method, it is applied to the Drude-Zener treatment of the optical properties of an ideal metal containing perfectly free electrons only. On this basis it is shown that there should exist a wide region of constant reflectivity and emissivity in the near infra-red. Krönig's theory is shown to be an approximation to the exact expression. The temperature coefficient of reflectivity is investigated and it is seen, on certain general assumptions, that it cannot change sign except in the neighbourhood of a wavelength at which the metal becomes transparent.

Disagreement with experimental observations indicates that the Drude-Zener treatment must be modified, either by a fundamental change in the dispersion formula or, more probably, by assuming that the influence of the bound electron contribution to the optical behaviour of a metal is greater than had been supposed.

### § 1. INTRODUCTION

MANY experimental data on the reflectivity and emissivity of various materials over wide ranges of temperature and of wavelength are available. There is, however, considerable difficulty in interpreting this information theoretically except in the few special cases for which simple approximations can take the place of the more complex expressions derivable from the usual theory. This hindrance has left obscure many controversial points that are of considerable interest.

The theory of reflectivity and emissivity (which are related by Kirchhoff's Law,  $E + R = 1$ ) must be derived from that of the optical constants of materials. This in turn is connected by electromagnetic theory with the study of the dielectric constants and polarizabilities of the media. Quantum-mechanical considerations must be employed to give the dispersion laws for these quantities.

As might be expected from the nature of the steps involved, this chain of reasoning results, for example, in a quite intractable expression for the variation of reflectivity with wavelength, even for the much-simplified model of a metal containing only perfectly free electrons. Such instances of cumbrous expressions have been given by Richardson (1916) and by Weil (1948). The unwieldy structure prohibits physical interpretation and application to experimental data.

An effort is made here to simplify this mathematical machinery so that it may be used to obtain a consistent account of the optical properties of materials. The theory is presented in terms of a complex index of refraction,  $N = n - ik$ . This enables the method to be applied to the important problems arising in the study of absorbing media, in particular, metals.

## § 2. GENERAL THEORY

Dispersion theory is stated in terms of the polarizability of the medium, for it is this quantity which enters into the solutions of the differential equations governing the dispersing oscillators. Classical electromagnetic theory shows that  $N^2 = \epsilon = 1 + 4\pi\alpha$ , where  $\epsilon$  is the complex dielectric constant and  $\alpha$  is the complex polarizability of the medium. For convenience we shall write

$$N^2 - 1 = 4\pi\alpha = 1/(X + iY). \quad \dots\dots(1)$$

Now optical theory gives the well-known result that for normal incidence

$$R = 1 - E = \frac{|N - 1|}{|N + 1|} \quad (2)$$

We may therefore put  $(N - 1)/(N + 1) = R^{\frac{1}{2}}e^{i\theta}$ . Substituting this and (1) in the identity

$$\frac{1}{2}[(N - 1)/(N + 1) + (N + 1)/(N - 1)] = 1 + 2/(N^2 - 1), \quad \dots\dots(3)$$

we obtain on equating the real and the imaginary portions

$$\frac{1}{2}(R^{\frac{1}{2}} + R^{-\frac{1}{2}})\cos\theta = 1 + 2X; \quad \frac{1}{2}(R^{\frac{1}{2}} - R^{-\frac{1}{2}})\sin\theta = 2Y. \quad \dots\dots(4)$$

If we eliminate  $\theta$  and set  $\frac{1}{4}(R^{\frac{1}{2}} - R^{-\frac{1}{2}})^2 = E^2/4R = y$  we obtain the equation

$$y^2 - 4y(Y^2 + X^2 + X) - 4Y^2 = 0. \quad \dots\dots(5)$$

This must always have two real roots of opposite sign. Since however  $R$  must be positive, the negative root is to be rejected. There is therefore a unique solution that can be written explicitly as

$$\frac{1}{2}y = E^2/8R = T + (T^2 + Y^2)^{\frac{1}{2}}, \quad \dots\dots(6)$$

where  $T = Y^2 + X^2 + X$ .

The simple result (6) is completely general and independent of the particular dispersion formula assumed for the medium. It would appear that the quantity  $E^2/R$  is more useful in reflectivity theory than either  $E$  or  $R$ .

## § 3. METAL CONTAINING FREE ELECTRONS ONLY

Modern theories agree that the polarizability of a model metal containing perfectly free electrons only can be represented by

$$-1/4\pi\alpha = (\lambda_0/\lambda)^2 + i(\lambda_r/\lambda), \quad \dots\dots (7)$$

where  $\lambda_0^2 = \pi mc^2 f_0 e^2$  and  $\lambda_r = c/2\sigma$ , while  $f_0$  is the number of free electrons per unit volume and  $\sigma$  is the electrical conductivity for steady currents. On the approximate basis of one free electron per atom,  $\lambda_0$  is of the order of  $0.1 \mu$ , while  $\lambda_r$  is of the order of  $0.001 \mu$  for most metals. We may assume without great danger that  $\lambda_r/\lambda_0$  is small compared with unity.

Substituting the dispersion equation (7) in (1) the use of the above method becomes apparent, for by aid of the artifice the two arbitrary constants are separated, and we find

$$X = -(\lambda_0/\lambda)^2; \quad Y = -(\lambda_r/\lambda). \quad \dots\dots (8)$$

A simple and compact equation for  $E^2/R$  may be obtained by substituting the above values in (6). For the present purposes, however, we substitute in (5) and obtain

$$y^2 - 4y[(\lambda_0/\lambda)^4 - (\lambda_0/\lambda)^2 + (\lambda_r/\lambda)^2] - 4(\lambda_r/\lambda)^2 = 0. \quad \dots\dots (9)$$

From this exact equation it is seen that optical behaviour of such an ideal metal falls naturally into three main regions of the spectrum. In each of these regions useful approximations may be made.

(i) *Region of Transparency*,  $\lambda \ll \lambda_0$ 

For very short wavelengths it is seen from (9) that  $y = 4(\lambda_0/\lambda)^4$ ; under these conditions  $n = 1 - \frac{1}{2}(\lambda_r/\lambda_0)^2$  and  $k = \frac{1}{2}(\lambda_r/\lambda_0)(\lambda/\lambda_0)^3$ , whence  $R = \frac{1}{16}(\lambda/\lambda_0)^4$ .

(ii) *Far Infra-red Region*,  $\lambda \ll \lambda_0^2/\lambda_r$ 

For very long wavelengths the middle term of (9) may be neglected, and  $y = 2(\lambda_r/\lambda)$ . Expressed in the more familiar form,  $E = 2(c/\sigma\lambda)^{\frac{1}{2}}$ , this is seen to be the Hagen-Rubens (or Drude) relation, the validity of which has been the subject of many experimental investigations. Fair agreement with the theory has been found.

(iii) *Intermediate Region*,  $\lambda_0 \ll \lambda \ll \lambda_0^2/\lambda_r$ 

As in the transparent region (i), we neglect the term independent of  $y$  in (9) and obtain the negative solution  $y = -4(\lambda_0/\lambda)^2$ . Since the product of the two roots is  $-4(\lambda_r/\lambda)^2$ , the positive root is  $y = (\lambda_r/\lambda_0)^2 = \text{constant}$ . The constancy of  $y$  in this region is checked by noting that  $k = (\lambda_r/\lambda_0)(\lambda/\lambda_0)^3$  and  $n = \frac{1}{2}(\lambda_r/\lambda_0)(\lambda/\lambda_0)^2$ , giving  $E = 2(\lambda_r/\lambda_0)$ .

(iv) *Transition Regions*

Both the transition regions are rather abrupt. At the upper end we find that for  $\lambda = 2\lambda_0^2/\lambda_r$  the approximations from above and from below both yield  $y = (\lambda_r/\lambda_0)^2$ , whereas the true value is only 0.618 of this. At the lower end the whole transition extends approximately from  $\lambda_0/2$  to  $3\lambda_0/2$ , although there is a central region of width  $\lambda_r$  centred about  $\lambda_0$  over which the main portion of the transition occurs.

The most important result of this section is the appearance of the intermediate region (iii) for the commonly adopted model of an ideal metal. This shows that there exists a wide range of wavelengths, extending from the visible region up to the lower limit of validity of the Hagen-Rubens relationship, over which the emissivity is, to a good approximation, constant and equal to  $2(\lambda_r/\lambda_0)$ .

#### § 4. TEMPERATURE VARIATION

The partial differentiation of (5) gives

$$\frac{\partial y}{\partial X} = \frac{4y^2(2X+1)}{y^2+4Y^2}; \quad \frac{\partial y}{\partial Y} = \frac{8yY(y+1)}{y^2+4Y^2}. \quad \dots\dots(10)$$

It will be observed that except for zero, negative, and infinite values of  $y$  these derivatives can only become zero if  $X = -\frac{1}{2}$  for the first and  $Y = 0$  for the second. This latter case implies that  $N$  is real, and, therefore, that the medium is completely transparent. Now the existence of a stationary point for  $E$  or  $R$  necessitates that  $y$  also be a stationary value. Hence if we assume that  $Y$ , but not  $X$ , is dependent on the temperature  $t$  then  $dy/dt$  can never be zero for wavelengths between zero and infinity, except at a point for which the medium is transparent. This point occurs only at very short ultra-violet wavelengths and, therefore, beyond this the possibility is precluded of the temperature effect ever being in the direction opposite to that predicted from the Hagen-Rubens relation. In the intermediate region of constant emissivity and reflectivity  $y$  is proportional to  $\lambda_r^2$ , whereas in the long-wave region it is proportional to  $\lambda_r$ ; we should therefore expect the temperature dependence to *increase* for decreasing wavelength up to the limit of the transparent region where the variation with temperature becomes suddenly negligible. This is in contradiction to many experimental results for real metals, and we see therefore that more complex assumptions must be made. Either it must be assumed that  $X$  (and hence  $\lambda_0$ ) is temperature dependent, or the dispersion formula must be radically altered. The variation with temperature of  $\lambda_0$  has usually been supposed small in comparison with that of electrical conductivity (i.e.  $\lambda_r$ ). It follows then that the phenomenon of an  $X$ -point (see Price 1947) and the existence of the intermediate region of constant reflectivity demand more experimental attention and perhaps a revision of the present dispersion theory. The contribution of the bound electrons has been neglected in the above treatment, as indeed has almost always been the case in the theoretical investigation of experimental results on the optical properties of metals. Kent (1919) considered the metal as being a combination of a free electron portion with a dielectric portion of constant refractive index, and obtained striking agreement between theory and experiment for a number of molten metals. Incorporation of the bound-electron contribution into (7) might therefore make the difference required to remove the discrepancies stated above. This treatment can only be approximate, and hence precise formulation remains conjectural.

#### § 5. COMPARISON WITH THE THEORY OF KRÖNIG

Equation (6) may be directly compared with a similar one obtained by Krönig (1929, 1931) in his consideration of the optics of a metal containing one class of (free) electrons only. His result, stated in terms of frequency instead of wavelength, is

$$E^2 = 4(\nu/\sigma)[(u^2+1)^{\frac{1}{2}}-u], \quad \dots\dots(11)$$

where  $\sigma$  is the electrical conductivity of the surface layers of the metal and  $u = \nu\sigma/\beta$ , where  $\beta$  is the half-breadth of the resonance line,  $\nu = 0$ , in the equivalent spectrum of the electrons. Comparing the above approximation with the exact expression of (6), we note that Krönig has taken  $R$  to be sensibly equal to unity, so obtaining  $E^2$  instead of  $E^2/R$  on the left-hand side. He also assumes that  $Y^2 = (\nu/2\sigma)^2$  and



that  $T = -\nu^2/2\beta$ . The first of these expressions follows from (8), the second is the first term of the exact form

$$T = -(\lambda_0/\lambda)^2 + (\lambda_0/\lambda)^4 + (\lambda_r/\lambda)^2, \quad \dots\dots(12)$$

provided that we set  $c/\beta = \lambda_0^2/\lambda_r$ . It follows that the half-breadth of the line of

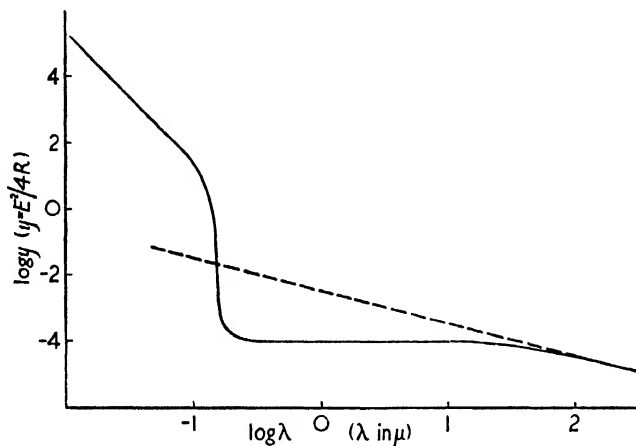


Figure 1. The variation of  $E^2/R$  with wavelength for an ideal metal having constants  $\lambda_0 = 0.16 \mu$  and  $\lambda_r = 0.0016 \mu$ . The dotted line shows the Hagen-Rubens approximation.

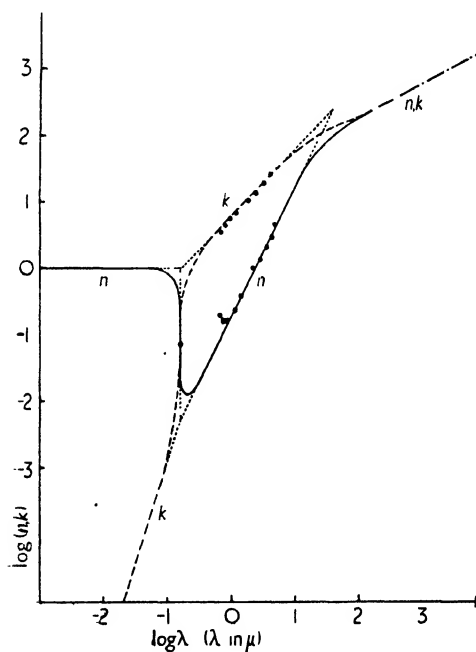


Figure 2. The variation of the optical constants  $n$  and  $k$  with wavelength for the same ideal metal. The dots indicate the experimental observations on silver at room temperature obtained by Försterling and Fréedericksz (1913).

zero frequency is simply half the wavelength that marks the lower limit of validity of the Hagen-Rubens relationship.

From the nature of the approximation to (12) it is seen that the third term may safely be neglected in comparison with the first, since  $(\lambda_r/\lambda_0)$  is very small for most metals. The second term, however, can only be neglected for wavelengths much larger than  $\lambda_0$ .

#### § 6. SPECTRAL VARIATION OF $E^2/4R$ , $n$ , AND $k$

The properties of the intermediate region found by applying the general exact theory to the case of a model metal act as a link between the already well-known properties in the far infra-red region and in the region of short optical wavelengths. Simple graphs of the wavelength variation of the optical properties of an ideal metal are obtainable by the use of the variable  $y = E^2/4R$  and the adoption of logarithmic scales. In Figures 1 and 2 the three main spectral regions are clearly shown to have excellent linear approximations. The form of the transition between the region is also demonstrated; the information may be used to complete the account given by Seitz (1940).

It must be emphasized that equation (6) is perfectly general; all arbitrary assumptions are introduced by (7), and it is this part of the argument that must be modified if the resulting deductions of the presence of a region of constant reflectivity and of the absence of an  $X$ -point are found to be in conflict with experiment.

The general method can be applied equally well to the case of a dielectric containing one class of (bound) electrons only. The modification may be effected by a change in form of  $X$  only,  $Y$  remaining substantially unaltered. We then require  $X = \gamma^2 - (\lambda_0/\lambda)^2$ , where  $\gamma$  is an arbitrary constant depending on the resonance wavelength  $\lambda_0/\gamma$  of the class of electrons responsible for dispersion. Application to the cases of media containing more than one class of electrons is more difficult since  $\alpha$ , but not  $1/\alpha$ , is additive for the different classes.

#### REFERENCES

- FÖRSTERLING, K., and FRÉDERICKSZ, V., 1913, *Ann. Phys., Lpz.*, **40**, 201.  
 KENT, C. V., 1919, *Phys. Rev.*, **14**, 459.  
 KRÖNIG, R. DE L., 1929, *Proc. Roy. Soc. A*, **124**, 409; 1931, *Ibid.*, **133**, 255.  
 PRICE, D. J., 1947, *Proc. Phys. Soc.*, **59**, 131.  
 RICHARDSON, O. W., 1916, *The Electron Theory of Matter* (Cambridge : University Press), p. 179.  
 SEITZ, F., 1940, *Modern Theory of Solids* (New York and London : McGraw-Hill), p. 639.  
 WEIL, R. A., 1948, *Proc. Phys. Soc.*, **60**, 8.

# The Electrical Conductivity of Germanium\*

By E. H. PUTLEY

Queen Mary College, University of London †

**ABSTRACT.** Measurements of the electrical conductivity of germanium are described. The results can be explained by the theoretical calculations of Shifrin (1944). An account is given of the relevant part of Shifrin's work. The experimental results are used to deduce the concentration of impurity centres and of thermally excited electrons and the position of the impurity levels.

## § 1. INTRODUCTION

THE object of this paper is to describe and explain some measurements of the electrical conductivity of germanium made by the writer.

The experimental results are of similar form to those described by Lark-Horovitz and his co-workers (1946), but they are explained here by means of a simpler theoretical model than that used by Lark-Horovitz. The hypothesis of Rutherford scattering by impurity centres has not been used to explain the observed fall in conductivity at liquid air temperatures. A complete explanation of the observed results has been given by Shifrin (1944); but it has been felt necessary to present here the relevant parts of Shifrin's work both for completeness and clarity. It has also been possible to deduce the concentration of impurity centres and the position of the impurity levels. The concentration of electrons in the conduction band may be found at low temperatures.

## § 2. METHOD OF MEASUREMENT AND EXPERIMENTAL RESULTS

Germanium specimens were cast in the form of rods, about 1–2 cm. long and about 0.5 cm. diameter. Their resistances were measured by a potentiometer method. A current of the order of 0.5 amp. was passed through the specimen and the potential difference between two probes was measured with a potentiometer. Chromel-alumel thermocouples were used for the potential leads, so that the temperature of the specimen could also be determined. To eliminate thermoelectric effects the current through the specimen was reversed and the mean was taken of the two results obtained.

Measurements were made over the temperature range 90° K. to 950° K. and on three different specimens. These had all been cast in silica tubes, No. 1 in hydrogen and Nos. 2 and 3 *in vacuo*.

Observations of the sign of the thermoelectric power showed that for all specimens the charge carriers were negative.

The results obtained are shown graphically. In Figure 1 the logarithm of  $\sigma$  the conductivity is plotted against the reciprocal of the absolute temperature  $T$ .

The results for the different specimens have the following features in common. Starting at liquid air temperature,  $\log \sigma$  increases linearly with  $1/T$  until at a temperature around 200–300° K.  $\log \sigma$  passes through a maximum.  $\log \sigma$  then

\* This work formed part of a thesis submitted for the Ph.D. degree of the University of London.

† Now at the Telecommunications Research Establishment, Great Malvern, Worcs.

decreases until at  $T \simeq 500^\circ \text{K}$ . it passes through a minimum. Thereafter  $\log \sigma$  increases very rapidly along a straight line which is the same for all specimens. The results are thus of the same form as reported by Lark-Horovitz.

In Figure 2  $\sigma$  is plotted against  $T$ , using the same results as are used in Figure 1. It is seen that in the region  $300\text{--}500^\circ \text{K}$ .  $\sigma$  falls off approximately linearly with  $T$  for all specimens. This result agrees with the predictions of Shifrin.

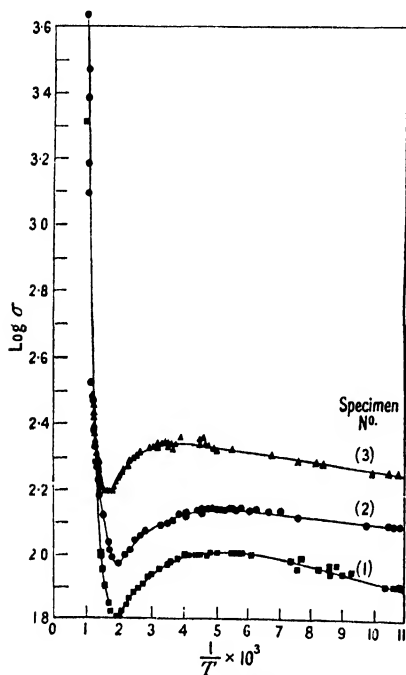


Figure 1.

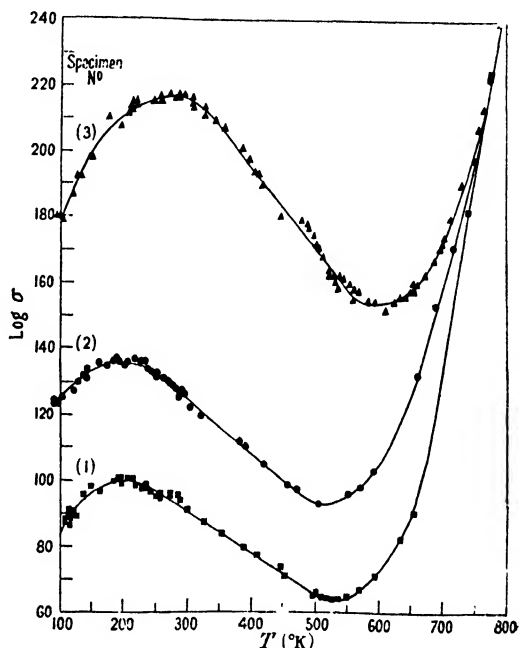


Figure 2.

### § 3. SOME PROPERTIES OF IMPURITY SEMICONDUCTORS CONTAINING A LARGE CONCENTRATION OF IMPURITY CENTRES

The system of energy levels which will be used to explain the behaviour of germanium is shown in Figure 3.  $n_i$  impurity centres per unit volume are situated at a distance  $\epsilon'$  below the bottom of the conduction band. At a temperature  $T$ ,  $n_f$  electrons are excited into the conduction band. It is assumed that at temperatures below  $500^\circ \text{K}$ . all the electrons come from the impurity centres. It will also be assumed that  $\epsilon'$  is of the same order as  $kT$  at room temperature (where  $k$  is Boltzmann's constant) and that the concentration of electrons in the conduction band is so high that Fermi-Dirac statistics must be used to discuss the problem.

Before using this model to calculate the conductivity some general properties of it will be discussed. Most of the conclusions reached were first pointed out by Shifrin (1944) but as detailed accounts of his work are not readily available, it seems desirable to repeat some of his work.

In this section the chemical potential and the concentration of free electrons will be calculated as a function of temperature, and the conditions for which it is necessary to use Fermi statistics will be discussed.

Seitz (1940) has shown that the chemical potential  $\epsilon^*$  is found by solving this equation:

$$n_b = n_b \frac{1}{1 + \exp [-(\epsilon' - \epsilon^*)/kT]} + \frac{4\pi(2m^*)^{\frac{3}{2}}}{h^3} \int_0^\infty \frac{\epsilon^{\frac{1}{2}} d\epsilon}{1 + \exp [(\epsilon - \epsilon^*)/kT]} \quad \dots\dots(1)$$

where  $h$  is Planck's constant,  $m^*$  the effective mass of an electron in the conduction band, and  $\epsilon$  energy, the zero of energy being taken at the bottom of the conduction band. This equation is derived by equating the total number of impurity electrons ( $n_b$ ) to the sum of the number in the conduction band ( $n_f$ ) and the number remaining in the impurity centres.

In equation (1) make the substitutions

$$\epsilon/kT = \eta, \quad \epsilon'/kT = \eta', \quad \epsilon^*/kT = \eta^*$$

and  $A = \frac{\eta_b h^3}{4\pi(2m^* kT)^{\frac{3}{2}}}.$

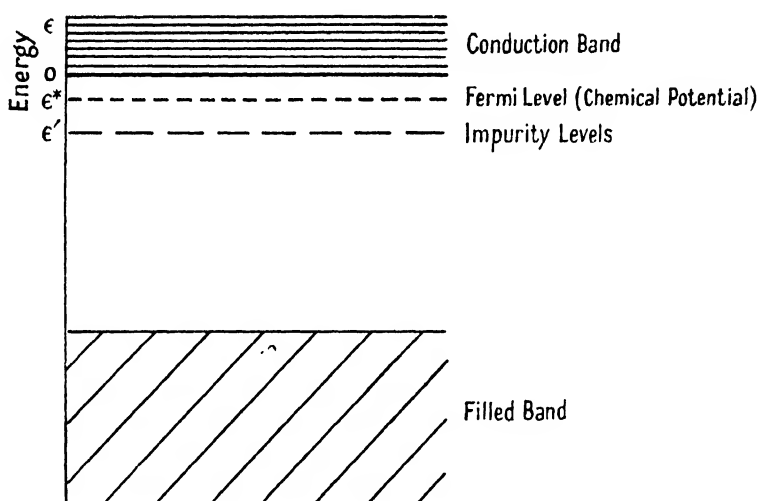


Figure 3.

The equation can then be written

$$\frac{A}{1 + \exp (\eta' + \eta^*)} = \int_0^\infty \frac{\eta^{\frac{1}{2}} d\eta}{1 + \exp (\eta - \eta^*)}; \quad \dots\dots(2)$$

also, from the second term on the right hand side of (1), the following expression for  $n_f$  is obtained

$$n_f = \frac{4\pi(2m^* kT)^{\frac{3}{2}}}{h^3} \int_0^\infty \frac{\eta^{\frac{1}{2}} d\eta}{1 + \exp (\eta - \eta^*)}. \quad \dots\dots(3)$$

Equation (2) was first derived by Shifrin and a similar expression has been derived by Busch (1946). In order to use equations (2) and (3) without making approximations, the integral

$$F_{\frac{1}{2}}(\eta^*) = \int_0^\infty \frac{\eta^{\frac{1}{2}} d\eta}{1 + \exp (\eta - \eta^*)}, \quad \dots\dots(4)$$

must be evaluated. This integral cannot be evaluated directly, but it has been tabulated accurately by McDougall and Stoner (1938).

Neither Shifrin nor Busch seem to be aware of this table because Shifrin tabulates a few values of  $\frac{1}{2}F_{\frac{1}{2}}(\eta^*)$ , some of which are as much as 3% in error and Busch uses Shifrin's values in his paper.

With  $F_{\frac{1}{2}}(\eta^*)$  known, it is possible to determine  $\eta^*$  by solving equation (2) numerically. By this means  $\eta^*$  can be found as accurately as desired in all cases. We wish to consider when this procedure is necessary. When classical statistics can be applied  $F_{\frac{1}{2}}(\eta^*)$  reduces to

$$F_{\frac{1}{2}}(\eta^*) = \frac{1}{2} \sqrt{\pi} \exp \eta^* \quad \dots\dots (5)$$

and equation (3) gives for the chemical potential the semi-classical expression

$$\eta^* = \ln \frac{n_i \hbar^3}{2(2\pi m^* kT)^{\frac{3}{2}}} \quad \dots\dots (6)$$

For  $\eta^* < 0$ ,  $F_{\frac{1}{2}}(\eta^*)$  can be represented by the series

$$F_{\frac{1}{2}}(\eta^*) = \frac{\sqrt{\pi}}{2} \exp \eta^* \sum_{n=0}^{\infty} (-1)^n \frac{\exp n\eta^*}{(1+n)^{\frac{3}{2}}},$$

so that using classical statistics is equivalent to taking only the first term of this series. Therefore the error involved in using classical statistics will be of the same order as the ratio of the first and second terms of the series, i.e. as  $\exp \eta^*/2^{\frac{3}{2}}$ . Thus if  $\eta^* = -2$ , the error is about 5%, and it will become greater as  $\eta^*$  approaches zero. Since 5% is about the accuracy of many experimental measurements, it would seem that in cases where  $\eta^*$  lies between  $-\infty$  and  $-2$  classical statistics may be used with safety, but if  $\eta^*$  is algebraically greater than  $-2$ , then a more exact method of calculation should be used.

To see what this means in terms of the concentration of electrons in the conduction band, put  $\eta^* = -2$  in equation (3). Then  $n_f = 6.1 \times 10^{14} T^{\frac{3}{2}}$  so that for  $T = 290^\circ \text{K.}$ ,  $n_f = 3 \times 10^{18} \text{cm}^{-3}$ . Concentration of conduction electrons of this order are found in specimens of silicon and germanium (Torrey and Whitmer 1948, p. 53 ff), so that the use of classical statistics to discuss these substances does not seem to be adequate.

To illustrate how  $\eta^*$  and  $n_f$  will vary with temperature, the numerical results given in Tables 1 and 2 were calculated. These were calculated for a semiconductor with impurity levels 0.03 ev. below the bottom of the conduction band as this is about the value found in germanium.

Table 1. Variation of Reduced Chemical Potential  $\eta^*$  and Concentration of Conduction Electrons  $n_f$  with the Concentration of Impurity Centres  $n_b$ .

( $T = 290^\circ \text{K.}$  Depth of impurity levels below the conduction band,  $\epsilon' = 0.03 \text{ ev.}$ )

$n_b$ ( $\text{cm}^{-3}$ )	$10^{18}$	$10^{19}$	$10^{20}$	$10^{21}$	$10^{22}$
$n_b$ (as atomic % in Ge)	0.0022	0.022	0.22	2.2	22.0
$\eta^*$	-3.3	-1.4	-0.15	-1.63	+3.26
$n_f$ ( $\text{cm}^{-3}$ )	$8.71 \times 10^{17}$	$5.44 \times 10^{18}$	$2.06 \times 10^{19}$	$5.53 \times 10^{19}$	$1.19 \times 10^{20}$

Table 1 shows how  $\eta^*$  and  $n_f$  vary at room temperature with  $n_b$ , the concentration of impurity centres. It is seen that if  $n_b \geq 10^{19} \text{cm}^{-3}$  the more exact method of calculation should be used. The values of  $\eta^*$  were found by solving equation (2) and  $n_f$  was then found using (3). It will be seen that while  $n_b$  varies by four powers of ten,  $n_f$  varies only by about two, so that the substance is becoming appreciably

degenerate. For germanium, an impurity concentration of  $10^{19} \text{ cm}^{-3}$  corresponds to 0.022 atomic % of impurities. Reference to Torrey and Whitmer (1948) shows that the concentration of impurities used in germanium melts prepared for crystal valves is often considerably greater than this. Therefore these calculations may explain the observation reported by Lark-Horovitz *et al.* (1946) that the number of free electrons at room temperature deduced from Hall effect measurements is appreciably less than the number which would be expected if all the impurity atoms were ionized. This is probably not the complete explanation, because the results of measurements made down to liquid helium temperatures suggest that the simple model is not adequate to account for the behaviour of specimens containing very large concentrations of impurities (Pearson and Shockley 1947).

Table 2 shows how  $\eta^*$  and  $n_f$  vary with temperature for two values of  $n_b$ .

Table 2. Variation of  $\eta^*$  and  $n_f$  with  $T$  for  $\epsilon' = 0.03 \text{ ev}$ .

(a) $n_b = 10^{18} \text{ cm}^{-3}$ .			(b) $n_b = 10^{20} \text{ cm}^{-3}$ .		
$T (^{\circ} \text{K.})$	$\eta^*$	$n_f (\text{cm}^{-3})$	$T (^{\circ} \text{K.})$	$\eta^*$	$n_f (\text{cm}^{-3})$
10	-16.46	$1.09 \times 10^{10}$	10	-14.15	$1.10 \times 10^{11}$
50	-3.75	$4.03 \times 10^{16}$	50	-1.41	$3.86 \times 10^{17}$
100	-2.71	$3.15 \times 10^{17}$	100	-0.12	$3.37 \times 10^{18}$
150	-2.72	$6.73 \times 10^{17}$	150	0.16	$7.71 \times 10^{18}$
200	-2.88	$7.54 \times 10^{17}$	200	+0.25	$1.27 \times 10^{19}$
250	-3.10	$8.49 \times 10^{17}$	250	0.19	$1.70 \times 10^{19}$
290	-3.30	$8.71 \times 10^{17}$	290	0.15	$2.06 \times 10^{19}$
350	-3.57	$8.89 \times 10^{17}$	350	+0.07	$2.57 \times 10^{19}$
400	-3.70	$9.50 \times 10^{17}$	400	0.00	$2.96 \times 10^{19}$

At very low temperatures  $\eta^*$  has a large negative value and  $n_f$  is very small.  $\eta^*$  increases rapidly as the temperature rises and  $n_f$  increases exponentially. Above a certain temperature, the rate of increase of  $\eta^*$  falls off,  $\eta^*$  passes through a maximum, which may be positive, and then starts to decrease. At high temperatures  $\eta^*$  will be negative. Although  $\eta^*$  exhibits a maximum,  $n_f$  increases steadily throughout.

Comparison of the two cases shown in Table 2 shows that when  $n_b = 10^{18} \text{ cm}^{-3}$  the behaviour can be calculated classically and at  $400^{\circ} \text{K}$ . 95% of the impurities are ionized, but with  $n_b = 10^{20}$  there is some evidence of the electron gas becoming degenerate, so that at  $400^{\circ} \text{K}$ . only 30% of the impurities are ionized.

In both the cases described  $\eta^*$  passes through a maximum. It is possible to derive a relation between the maximum value of  $\eta^*$  and the temperature corresponding to it. This relation will be used in examining the experimental results, and a derivation of it will be given in the next section.

#### § 4. DERIVATION OF THE RELATION BETWEEN THE MAXIMUM VALUE OF $\eta^*$ AND TEMPERATURE

To derive the required expression, write the quantity  $A$  in equation (2) in the form:

$$A = a\eta'^{\frac{1}{2}} \quad \text{where} \quad a = n_b \hbar^3 / 4\pi(2m^*\epsilon')^{\frac{1}{2}} \quad \text{and} \quad \eta' = \epsilon' / kT.$$

While  $a$  depends upon the properties of the semiconductor it is independent of temperature. Equation (2) can now be re-written,

$$\eta'^{\frac{1}{2}} a / F_{\frac{1}{2}}(\eta^*) = 1 + \exp(\eta' + \eta^*). \quad \dots\dots(8).$$

Consider some given value of  $\eta^*$ . Then equation (8) can be regarded as an equation to determine the value of  $\eta'$  (and hence  $T$ , since  $\eta' = \epsilon'/kT$ ) corresponding to the value taken for  $\eta^*$ . The nature of the roots of (8) can be seen by considering the curves

$$\left. \begin{aligned} y_1 &= f_1(\eta') = \eta'^{\frac{3}{2}} a / F_{\frac{3}{2}}(\eta^*) \\ y_2 &= f_2(\eta') = 1 + \exp(\eta' + \eta^*) \end{aligned} \right\} \dots\dots(9)$$

It is seen that  $y_2 > y_1$ , both for  $\eta' \sim 0$  and for  $\eta' \rightarrow \infty$ , but for intermediate values of  $\eta'$ ,  $y_2$  may be less than  $y_1$  if the value taken for  $\eta^*$  is not too large; for very large values of  $\eta^*$  the curves will not intersect. Thus, in general, equation (8) will have either two real roots or none. Although, mathematically, two real roots may exist, they are not always both physically realizable, for there is always a maximum temperature at which a substance behaves as an impurity semiconductor; either it will melt or decompose or the number of electrons coming

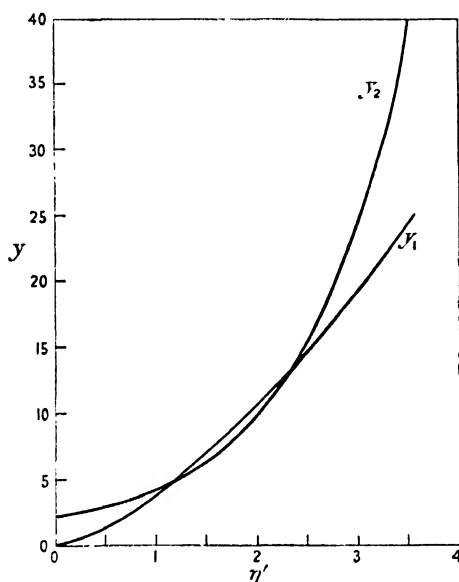


Figure 4.

$$\begin{aligned} \text{Equation (9) } y_1 &= \frac{a}{F_{\frac{3}{2}}(\eta^*)} \eta'^{\frac{3}{2}} ; & y_2 &= 1 + \exp(\eta' + \eta^*) \\ \text{with } \epsilon' &= 0.03 \text{ e.v., } n_0 = 10^{20} \text{ cm}^3, \eta^* = +0.15 \\ \text{giving } y_1 &= 3.70 \eta'^{\frac{3}{2}} ; & y_2 &= 1 + \exp(0.15 + \eta'). \end{aligned}$$

from the full band becomes appreciable. Hence the smaller root of (8) (which corresponds to the higher temperature) may not always be physically significant.

Figure 4 illustrates the behaviour of the curves of equation (9). It has been drawn for the case tabulated in Table 2(b), taking  $\eta^* = 0.15$ . The two points of intersection correspond to temperatures of about 290° K. and 145° K.

While, as we have seen, there are in general two roots to equation (8), there will be a limiting case when the two curves (9) touch. This will give a double root corresponding to a stationary value of  $\eta^*$  with respect to  $T$ . For this case, we have

$$\frac{dy_1}{d\eta'} = \frac{dy_2}{d\eta'}, \quad \text{i.e.} \quad \frac{3}{2} \frac{a}{F_{\frac{3}{2}}(\eta^*)} \eta'^{\frac{1}{2}} = \exp(\eta' + \eta^*).$$



Remembering that this value of  $\eta'$  must satisfy (8), we obtain

$$\frac{2}{3}\eta'_{\max} = 1 + \exp(-\eta'_{\max} - \eta^*_{\max})$$

or

$$\eta^*_{\max} = -\ln(2\epsilon'/3kT_{\max} - 1) - \epsilon'/kT_{\max}. \quad \dots\dots(10)$$

That this equation corresponds to a maximum value of  $\eta^*$  can be seen by considering the behaviour of the curves (9) as  $\eta^*$  is varied. The subscript max is attached to  $\eta'$  and  $T$  to indicate that they have the values for which  $\eta^*$  is a maximum.

The data in Table 2 illustrate how  $\eta^*$  can pass through a maximum, and it is seen that the maximum may be positive or negative and that as the concentration of impurities is increased, both  $\eta^*_{\max}$  and  $T_{\max}$  become larger.

The object of this section has been to derive equation (10). The application of this equation will be discussed later.

#### § 5. DERIVATION OF AN EXPRESSION FOR THE ELECTRICAL CONDUCTIVITY AS A FUNCTION OF $\eta^*$

An expression for the conductivity can be derived by applying the Lorentz-Sommerfeld theory of conductivity. According to Seitz (1940, p. 189) the conductivity  $\sigma$  is given by,

$$\sigma = -\frac{4\pi e^2}{3} \int_0^\infty V^3 l \frac{\partial f_n^0}{\partial x} dV \quad \dots\dots(11)$$

where  $l$  is the mean free path,  $e$  the charge, and  $V$  the scalar speed of the electrons, and  $f_n^0$  the unperturbed velocity distribution function, so that the number of electrons with speeds between  $V$  and  $V + dV$  is  $4\pi f_n^0 V^2 dV$ .

If it is assumed that the mean free path is independent of energy, so that  $l$  can be taken outside the integral, and if  $f_n^0$  is expressed in terms of the Fermi-Dirac function, and the integration variable changed to the reduced energy  $\eta$ , then (11) becomes

$$\sigma = \frac{16\pi}{3} \left( \frac{m^* e^2}{h^3} \right) (lkT) \int_0^\infty \eta \frac{d}{d\eta} \left( \frac{1}{1 + \exp(\eta - \eta^*)} \right) d\eta. \quad \dots\dots(12)$$

This can be integrated to give

$$\sigma = \frac{16\pi}{3} \left( \frac{m^* e^2}{h^3} \right) (lkT) \ln(1 + \exp \eta^*). \quad \dots\dots(13)$$

This expression should hold for all values of  $\eta^*$ , but if  $\eta^*$  is large and negative (i.e. the classical case), then the logarithm in (13) can be expanded. If only the first term is retained, the resulting expression for  $\sigma$  will be found to be identical with that derived by Seitz (1940) for a simple semiconductor.

If we now assume that the principal source of scattering which determines the mean free path is the interaction of electrons with the crystal lattice vibrations, then  $l$  will vary as  $1/T$ , as has been shown by Wilson (1936, p. 211), Sommerfeld and Bethe (1933, p. 560) and Seitz (1948).

We can now write  $l = l_0/kT$  and (13) becomes

$$\sigma = \sigma_0 \ln(1 + \exp \eta^*) \quad \dots\dots(14)$$

where  $\sigma_0 = \frac{16\pi}{3} \left( \frac{m^* e^2}{h^3} \right) l_0$ . Thus  $\sigma_0$  is independent of temperature.

### § 6. DISCUSSION OF RESULTS

If the variation of  $\eta^*$  with  $T$  is known, then the variation of  $\sigma$  can be found at once. From our knowledge of the behaviour of  $\eta^*$  the behaviour of  $\sigma$  can be seen. Starting at very low temperatures,  $\sigma$  will increase exponentially since at low enough temperatures the simpler formula will apply. Thus a plot of  $\log \sigma$  against  $1/T$  will be a straight line at low temperatures. At higher temperatures  $\eta^*$  will pass through a maximum and then decrease. Since  $\ln(1 + \exp \eta^*)$  is a monotonic function of  $\eta^*$ ,  $\sigma$  will be a maximum at the same temperature at which  $\eta^*$  is maximum. As the temperature is raised further,  $\eta^*$  will decrease and  $\sigma$  will decrease with it. Shifrin has stated that  $\sigma$  would be expected to decrease approximately linearly with temperature in this region.

Examination of the experimental results (Figures 1 and 2) shows that up to  $T = 500^\circ \text{K.}$ , the conductivity behaves as predicted by this simple model. At very low temperature, the exponential variation is obtained. The conductivity passes through a maximum at about  $200^\circ \text{K.}$  and thereafter decreases linearly with  $T$ . At about  $500^\circ \text{K.}$  the conductivity passes through a minimum and then begins to vary exponentially again. Thus above  $500^\circ \text{K.}$  the specimens no longer behave as impurity semiconductors. The conductivity at high temperatures has the same value for all specimens and is associated with the excitation of electrons from the filled band, so that at high temperatures germanium behaves as an intrinsic semiconductor.

Thus the model of an impurity semiconductor as discussed here explains the observed results. In the next section an attempt will be made to obtain quantitative data for the specimens measured.

### § 7. APPLICATION OF THEORY

The concentration of free electrons, impurity centres and the position of the impurity energy levels were calculated by applying the following arguments.

In the low temperature region where  $\sigma \propto \exp \eta^*$  write  $\eta^* = -K/T$  where  $K$  is a positive constant.

From the slope of the straight line of  $\log \sigma$  plotted against  $1/T$ , the value of  $K$  is found. This is then used to calculate  $\eta^*$  and hence  $\ln(1 + \exp \eta^*)$  over the low temperature range.

Recalling the fundamental equation (14)

$$\sigma = \sigma_0 \ln(1 + \exp \eta^*)$$

we can now use the measured values of  $\sigma$  to determine  $\sigma_0$ .

Since we are assuming  $\sigma_0$  to be independent of temperature we can now find  $\eta^*$  at any temperature from the conductivity equation.

When  $\eta^*$  is known, the concentration of free electrons can at once be determined, for the equation (3) for  $n_f$  can be expressed

$$n_f = 5.47 \times 10^{15} T^{3/2} F_{1/2}(\eta^*). \quad \dots\dots(15)$$

The values for  $F_{1/2}(\eta^*)$  were obtained from the table of McDougall and Stoner referred to above.

To determine the depth of the impurity centres below the bottom of the conduction band we use the maximum value of the conductivity  $\sigma_{\max}$  to calculate  $\eta_{\max}^*$ .

This is then substituted in equation (10) and  $\epsilon'$  is found by solving this equation, since  $T_{\max}$  is the temperature of maximum conductivity.

Finally we can calculate the density of impurities. Equation (2) can be written

$$n_b = 5.47 \times 10^{15} [1 + \exp(\eta' + \eta^*)] T^{\frac{3}{2}} F_{\frac{1}{2}}(\eta^*). \quad \dots (16)$$

Since all the quantities on the right hand side are known  $n_b$  can be calculated. These calculations were applied to the three specimens measured and the results are given in Table 3.

Table 3.

Specimen	(cm <sup>-3</sup> )	$n_b$ (atomic %)	$n_f$ (cm <sup>-3</sup> ) at 290° K.	$\epsilon'$	$\sigma_0$ (ohm <sup>-1</sup> cm <sup>-1</sup> )
1	$4.4 \times 10^{19}$	0.097	$1.41 \times 10^{19}$	0.0297	174
2	$6.4 \times 10^{19}$	0.141	$1.61 \times 10^{19}$	0.0306	208
3	$8.9 \times 10^{19}$	0.196	$1.66 \times 10^{19}$	0.0383	350

The approximations involved in these calculations are of the order of 10%, and the accuracy of the experimental measurements is somewhat better than this.

### § 8. CONCLUSION

The experimental measurements of the electrical conductivity of germanium can be explained by using a simple model of a semiconductor and applying Shifrin's theory to it.

It is possible to determine the concentration of impurity centres, the position of their energy levels and the concentration of conduction electrons by means of this theory.

### ACKNOWLEDGMENTS

The writer wishes to thank Professor H. R. Robinson, for allowing this work to be carried out in his laboratory, and for the interest he has shown in it. The writer also wishes to acknowledge the receipt of financial assistance from the Department of Scientific and Industrial Research.

### REFERENCES

- BUSCH, G., 1946, *Helv. Phys. Acta*, **19**, 463.  
 LARK-HOROVITZ, K., MIDDLETON, A. E., MILLER, E. P., and WALTERSTEIN, I., 1946, *Phys. Rev.*, **69**, 258.  
 McDougall, J., and Stoner, E. C., 1938, *Phil. Trans. Roy. Soc.*, **237**, 67.  
 PEARSON, G. L., and SHOCKLEY, W., 1947, *Phys. Rev.*, **71**, 141.  
 SEITZ, F., 1940, *Modern Theory of Solids* (New York and London: McGraw-Hill); 1948, *Phys. Rev.*, **73**, 549.  
 SHIFRIN, K., 1944, *J. Phys. U.S.S.R.*, **8**, 242.  
 SOMMERFELD, A., and BETHE, H. A., 1933, *Handbuch der Physik* XXIV/2 (Berlin: Springer).  
 TORREY, H. C., and WHITMER, C. A., 1948, *Crystal Rectifiers, Radiation Laboratory Series* No. 15, (New York and London: McGraw-Hill).  
 WILSON, A. H., 1936, *The Theory of Metals* (Cambridge: University Press).

## Measurement of the Half-Life of ${}^6\text{He}$

By J. E. R. HOLMES

Physics Department, University of Birmingham

*Communicated by P. B. Moon; MS. received 9th December 1948*

**ABSTRACT.** The half-life of  ${}^6\text{He}$  is found to be  $0.823 \pm 0.013$  sec. by a rotating wheel method. The statistical accuracy is considerably higher than that of previous measurements, though all results agree to within their limits of error.

### § 1. INTRODUCTION

**B**ERGE (1936) was the first to identify  ${}^6\text{He}$ , which is formed when beryllium is bombarded by fast neutrons; by a continuous gas-flow method he estimated the half-life of the beta-activity to be of the order of 1 second. Later, Nahmias and Walen (1937) gave a value of  $0.80 \pm 0.04$  sec.; in their method the sample was mounted on a "pendulum" swinging between a neutron source and a G-M counter, the process of alternate irradiation and recording of the activity being repeated many times. More recently two measurements have been made using neutrons generated by a cyclotron. Sommers and Sherr (1946) obtained a value of  $0.85 \pm 0.05$  sec. using a discontinuous flow method, the activity being transported from the cyclotron by hydrogen under pressure through a pipe 120 feet long to the counting chamber. Cassels and Latham (1947) used a pulsed cyclotron in conjunction with electronic gating circuits and obtained a value  $0.87 \pm 0.06$  sec.

### § 2. EXPERIMENTAL ARRANGEMENT

The apparatus used for this experiment was constructed by the author and Mr. R. S. Turgel for a search for short-lived isomers. It consisted essentially

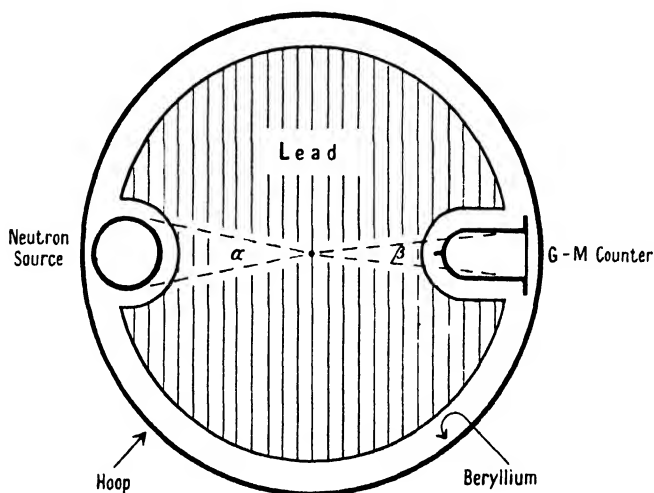


Figure 1. Schematic diagram of the apparatus.

of a steel hoop 45 cm. in diameter carrying 50 gm. of powdered beryllium metal held in position by cellophane tape in a shallow groove running round the interior

surface. The hoop was rotated continuously past a Ra-Be neutron source containing 230 mg. Ra and then in front of an end-on type  $\beta$ -counter. The arrangement is shown schematically in Figure 1. The whole apparatus was heavily shielded with lead to screen the G-M counter from the  $\gamma$ -radiation emitted by the neutron source. This principle has been used previously by Nahmias and Walen (1937) to measure the half-life of short-lived  $\beta$ -activities.

When the hoop has been rotating at a constant speed for some time, the counter will record a constant counting rate due to the activity produced in the beryllium when irradiated with fast neutrons, allowing continuous counting over an extended period of time.

### § 3. THEORY OF THE METHOD

As shown by Nahmias and Walen (1937), the equilibrium counting rate  $C$  is given by

$$C = K \frac{\omega}{\lambda} \{1 - \exp(-\lambda\alpha/\omega)\} \{1 - \exp(-\lambda\beta/\omega)\} \frac{\exp(-\lambda\phi/\omega)}{1 - \exp(-2\lambda\pi/\omega)}, \quad \dots\dots(1)$$

where

$\lambda$  = transformation constant of the activity,  
 $\omega$  = angular velocity of the hoop,  
 $\alpha$  = effective angular width of the source,  
 $\beta$  = effective angular width of the counter,  
 $\phi = \pi - (\alpha + \beta)/2$ ,  
 $K$  = constant.

If  $\lambda\alpha \ll \omega$ ,  $\lambda\beta \ll \omega$  and  $\phi \sim \pi$ , this may be simplified to

$$C = C_0 x / \sinh x, \quad \dots\dots(2)$$

where  $x = \lambda\pi/\omega = 0.347t/T$ ,  $t$  is the period of rotation of the hoop, and  $T$  the half-life of the activity.

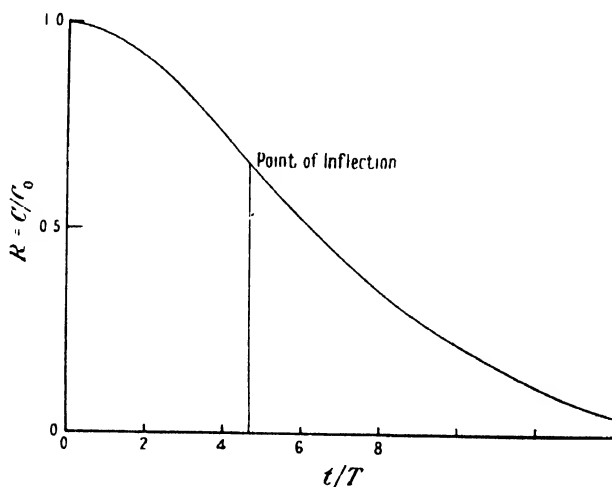


Figure 2. Variation of the counting rate with the period of rotation of the hoop.

The ratio  $R = C/C_0$  is plotted against  $t/T$  in Figure 2, from which it will be seen that  $R$  differs little from 1 when  $t = T$ , and falls to half only when  $t = 6.3T$ . Quite short-lived activities can therefore be investigated with relatively slow rotations of the hoop.

The ratio of the counting rates at any two periods of rotation will in principle enable  $T$  to be determined. In practice, one of the periods is made short enough to make  $R$  approach unity to high accuracy; then not only is the counting rate a maximum, but it is independent of the exact period of rotation. The slower period of rotation should of course be chosen so that  $R$  falls well below unity, and in a region where  $R$  varies most rapidly with  $t/T$ . More confidence will be felt if a number of different "long" periods are used and are found to lead to a statistically consistent value for  $T$ , but the weighting of the values obtained is a complicated matter. If, however, the chosen values of  $t/T$  are restricted to the practically straight portion about the point of inflection of the curve of Figure 2, corresponding values of  $R$  and  $t$  may be fitted to a straight line by the usual "least squares" method. Since the point of intersection of this line with the  $R$  axis can be calculated from equation (2), there is no loss of accuracy due to the restricted range of the experimental points; the most probable value of  $T$  and its statistical error can then be readily obtained.

#### § 4. EXPERIMENTAL DETAILS

A period of rotation of 0.1 sec/rev. was used to measure the maximum counting rate  $C_0$  due to the  ${}^6\text{He}$  activity, which was then within 0.1% of the maximum value. The observed value of  $C_0$  was 60 counts per minute, and the background due to the radiation from the source was 80 counts per minute.

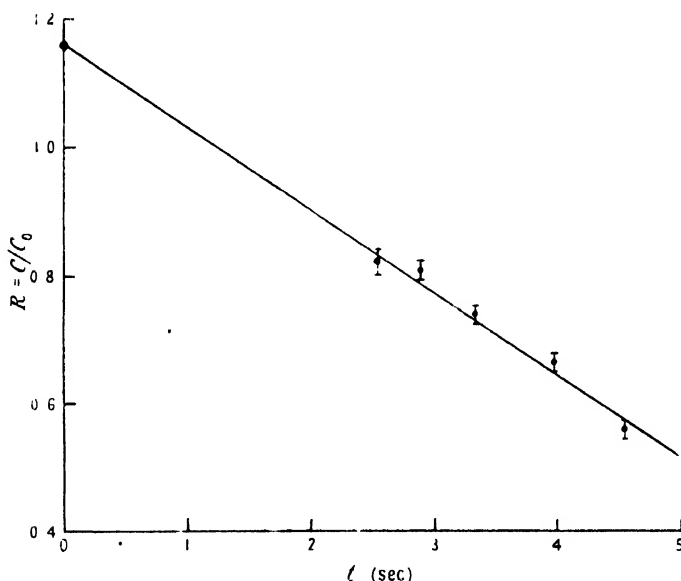


Figure 3. Experimental results with  ${}^6\text{He}$ .

The ratio  $R$  was measured for five periods of rotation of the hoop between 2.5 and 4.6 sec/rev. The direction of rotation of the hoop was reversed for each measurement of  $R$ , to reduce any error due to lack of symmetry in the apparatus. The counting rate for each particular period of rotation was taken over a ten-minute interval. Ten measurements of  $R$  were made for each of the five values of  $t$ , giving fifty independent observations of  $R$ , from which an accuracy rather better than 2% was anticipated for the half-life.

The difference between the linear approximation and equation (2) over the range of  $t$  used was not greater than 0.25%; this error was allowed for in the estimated error of the final value for  $T$ . The simplification of the equation for the counting rate (eqn. (1)) does not introduce an error greater than 0.1%; this was checked by using estimated values of  $\alpha$  and  $\beta$ , the effective angles subtended by the source and the counter respectively.

#### § 5. CONCLUSION

The results obtained are shown graphically in Figure 3. The half-life of  ${}^6\text{He}$  obtained by the "least squares" method from the experimental results is  $T = 0.823 \pm 0.013$  sec.

The statistical accuracy of this result is considerably higher than that of previous determinations, which agree within their limits of error.

#### ACKNOWLEDGMENT

The author is indebted to the Department of Scientific and Industrial Research for a maintenance grant.

#### REFERENCES

- BJERGE, T., 1936, *Nature, Lond.*, **137**, 400.  
 CASSELS, J. M., and LATHAM, R., 1947, *Nature, Lond.*, **159**, 367.  
 NAHMIAS, M. E., and WALLEN, R. J., 1937, *J. Phys. Radium*, **8**, 153.  
 SOMMERS, H. S., and SHERR, R., 1946, *Phys. Rev.*, **69**, 21.

## The Disintegration of Carbon by Fast Neutrons

By L. L. GREEN and W. M. GIBSON

Cavendish Laboratory, Cambridge

*Communicated by O. R. Frisch; MS. received 13th December 1948*

**ABSTRACT.** The disintegration of  ${}^{12}\text{C}$  into three  $\alpha$ -particles by inelastic scattering of fast neutrons has been studied by the photographic plate method. Measurements made on 168 of the stars formed by this disintegration have been used to identify the reaction and to obtain values of the cross-section for the process at neutron energies between 10.8 Mev. and 14.5 Mev. No evidence was found for anisotropic scattering of the neutrons.

#### § 1. INTRODUCTION

IN a cloud chamber containing methane, Chadwick, Feather and Davies (1934) found among the tracks of protons projected forwards by radium-beryllium neutrons a single small star consisting of three short tracks. They attributed this to the reaction  ${}^{12}_6\text{C} + {}^1_0\text{n} \rightarrow 3 {}^4_2\text{He} + {}^1_0\text{n}$  in which a  ${}^{12}\text{C}$  nucleus is split into three  $\alpha$ -particles by a neutron which is itself inelastically scattered.

Nine similar three-pronged stars were found by Aoki (1938), who was using a cloud-chamber containing methane to investigate the neutrons produced in the bombardment of lithium by deuterons. He calculated the total energy for the three particles producing each star, assuming them to be  $\alpha$ -particles, and obtained values which were consistent with the known maximum energy of the  $\text{Li} + \text{D}$  neutrons and the masses of the  ${}^{12}\text{C}$  nucleus and the  $\alpha$ -particle.





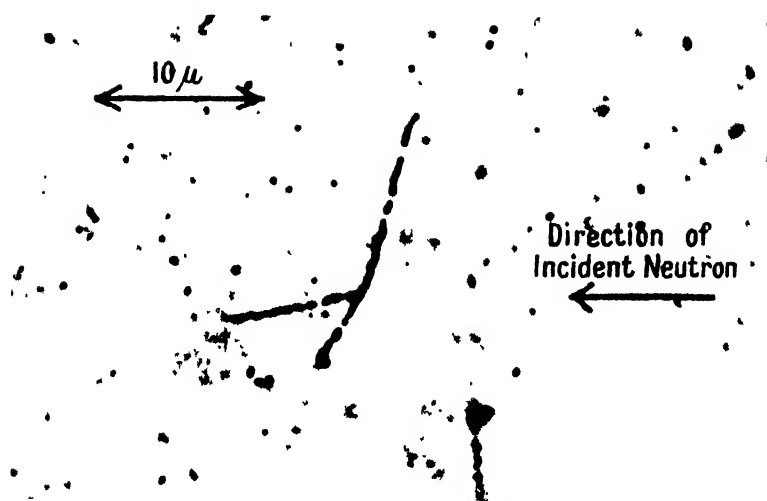
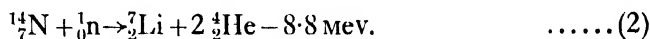
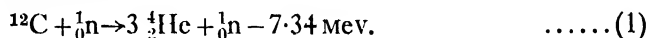


Figure 1. Photomicrograph of  $^{12}\text{C} \rightarrow 3\alpha$  disintegration.

## § 2. DISINTEGRATIONS IN PHOTOGRAPHIC PLATES

We have observed a total of 168 stars, each consisting of three short tracks, while studying by the photographic plate method the spectrum of the neutrons emitted in the bombardment of a lithium target with deuterons of energy 0.93 mev. (Green and Gibson 1949). A photomicrograph of one of these stars is shown in Figure 1. The fact that similar stars appeared in plates exposed to  $^{11}\text{B} + \text{D}$  neutrons, but not in plates exposed to  $\text{D} + \text{D}$ ,  $\text{N} + \text{D}$  or  $^{10}\text{B} + \text{D}$  neutrons, indicated that they were due to disintegrations of nuclei already present in the emulsion by neutrons of energy greater than 7 mev. This fits with the  $Q$ -values of the only two possible reactions:



It is known (Williams, Shepherd and Haxby 1937) that the lifetime of  $^5\text{He}$  is too short for a nucleus formed during reaction (1) to make a track before breaking up into a neutron and an  $\alpha$ -particle.

The  $^7\text{Li}$  nucleus formed in reaction (2) would give a short track indistinguishable from that of an  $\alpha$ -particle; but this reaction was in fact ruled out in the majority of cases by a detailed examination of the energies and the momenta of the particles.

## § 3. MEASUREMENTS AND CALCULATIONS

Detailed measurements were made on 66 of the 80 stars observed in plates exposed to the neutrons emerging from the lithium target in the direction of the incident deuterons, and on 38 of the 88 stars produced by neutrons emerging

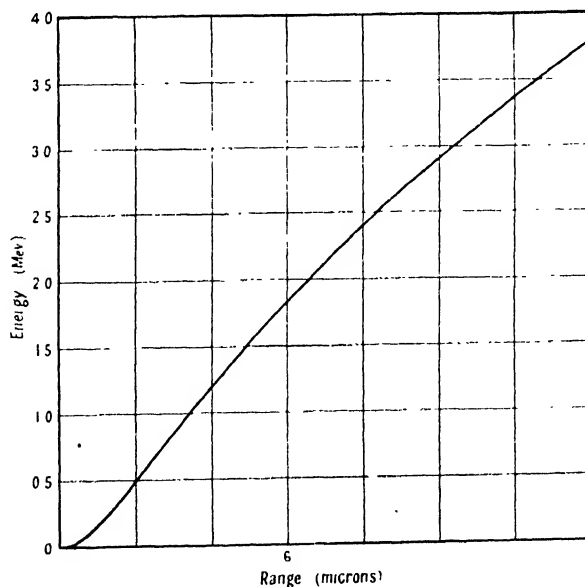


Figure 2. Range-energy relation for  $\alpha$ -particles in Ilford C2 emulsion.

from the target at  $120^\circ$  to this direction. The length of each track and its direction relative to that of the incident neutrons in both vertical and horizontal planes were measured under a magnification of 1,800. The corresponding energy was obtained from an  $\alpha$ -particle range-energy relation constructed from the data

of Holloway and Livingston (1938) for air and of Lattes, Fowler and Cier (1947) for emulsion. The curves published by the latter workers are accurate only at energies above 2 mev., and for lower energies it was necessary to use Holloway and Livingston's curve; the stopping-power at each energy was estimated from the values above 2 mev., on the principles indicated by Rutherford, Chadwick and Ellis (1930). The range-energy relation used is shown in Figure 2.

From the directions and energies of the  $\alpha$ -particles their total momentum was computed and taken to be equal to the (vector) difference of the momenta of the incident and scattered neutron. On the other hand the difference of the energies of the neutron was taken to be  $E+Q$ , where  $E$  is the total energy of the three  $\alpha$ -particles and  $Q$  is 7.34 mev., the energy required to split a  $^{12}\text{C}$  nucleus into three  $\alpha$ -particles (Mattauch 1942). In this way it was possible to obtain the energies of the incident and scattered neutrons and the direction of the scattered neutron relative to the known direction of the incident neutron. The method of calculation may be made clearer by an example.

The lengths ( $a$ ) of the tracks, projected on a horizontal plane, were	9.7 $\mu$ ,	4.0 $\mu$ ,	4.75 $\mu$
The dips ( $h$ ), corrected for the shrinkage of the emulsion, were	1 $\mu$ ,	-2 $\mu$ ,	0
The angles in a horizontal plane relative to the incident neutron direction were	1 ,	- 86 ,	70
The true lengths in space of the tracks ( $L = \sqrt{(a^2 + h^2)}$ ) were	10.2 $\mu$ ,	4.47 $\mu$ ,	4.75 $\mu$
These gave energies ( $E_2$ ) of	3.00,	1.30,	1.38 mev.
	with a total of $E$ 5.68 mev.		
The momenta in arbitrary units ( $M = \sqrt{(AE)}$ for mass number $A$ and energy $E$ ) were	3.46,	2.28,	2.35

These were resolved into three components,  $M_x$  parallel to the incident neutron direction,  $M_y$  perpendicular to this in the plane of the emulsion, and  $M_z$  vertical. The components of the total momentum were  $X = +4.32$ ,  $Y = +0.23$ ,  $Z = -1.36$ .

The energy relation is

$$E + Q = E_{\text{incident}} - E_{\text{scattered}}. \quad \dots\dots (3)$$

The components of the scattered neutron momentum are  $X' = \{\sqrt{(E_{\text{incident}})} - X\}$ ,  $-Y$ , and  $-Z$ , since the momentum of the incident neutron is simply  $\sqrt{(E_{\text{incident}})}$  in the  $X$  direction. The energy of the scattered neutron is therefore

$$E_{\text{scattered}} = X'^2 + Y^2 + Z^2, \quad \dots\dots (4)$$

where  $X' = \sqrt{(E_{\text{incident}})} - X$ .

Equating the expressions for  $E_{\text{scattered}}$ , we get

$$X'^2 + Y^2 + Z^2 = E_{\text{incident}} - (E + Q).$$

With  $E_{\text{incident}} = (X + X')^2$ , this becomes

$$X'^2 + Y^2 + Z^2 = X^2 + 2XX' + X'^2 - (E + Q),$$

from which we get

$$X' = \frac{(E + Q + Y^2 + Z^2) - X^2}{2X}. \quad \dots\dots (5)$$

When  $X'$  is obtained, equation (4) gives  $E_{\text{scattered}}$  and equation (3) then gives  $E_{\text{incident}}$ . In the above example, the values of  $X$ ,  $Y$ ,  $Z$ ,  $E$  and  $Q$  gave  $X' = -0.35$ ; from this, equations (3) and (4) gave 15.0 mev. and 2.0 mev. respectively for the energies of the incident and scattered neutrons. The

direction  $\phi$  of the scattered neutron was found to be  $104^\circ$ , from the relation  $\tan \phi = \{\sqrt{(Y^2 + Z^2)}\}/X'$ .

The number of cases in which the neutron was scattered forwards was compared with the number in which the scattering angle was more than  $90^\circ$  in centre-of-mass space. The ratio obtained was  $1.5 \pm 0.5$ , and this cannot be taken as evidence for a departure from isotropy.

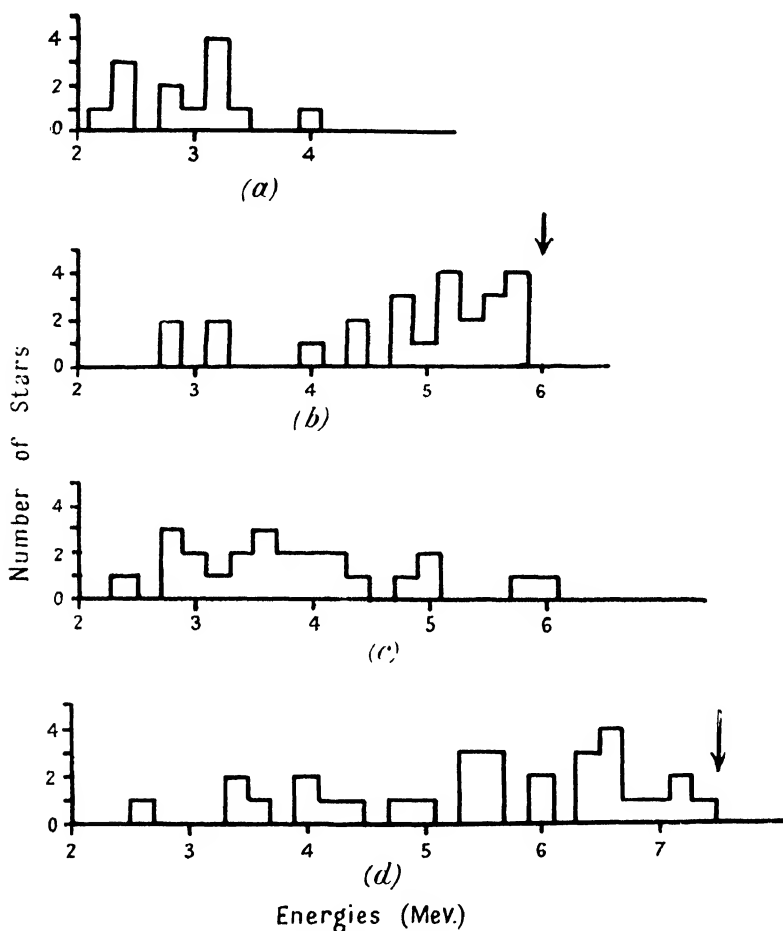


Figure 3. (a) refers to the stars attributed to the 10.8 Mev. group of neutrons in the  $120^\circ$  direction, (b) to the 13.2 Mev. group in the  $120^\circ$  direction, (c) to the 12 Mev. group in the forward direction, and (d) to the 14.5 Mev. group in the forward direction.

The arrows indicate the maximum possible values of the energy.

It is difficult to measure the angle of dip accurately for such short tracks, and this led to some uncertainty in the incident neutron energy, but it was usually possible to attribute the stars definitely to one or other of the two high-energy groups of the Li + D neutron spectrum. The measurements were not sufficiently accurate to yield any definite information about the energy levels of intermediate nuclei (especially  $^8\text{Be}$  and  $^5\text{He}$ ) which might be formed during the reaction. They were, however, accurate enough to show that if the alternative reaction (2) were assumed, no reasonable range-energy relation for  $^7\text{Li}$  nuclei would make it possible to satisfy the laws of conservation of energy and momentum in more than about 10% of the cases.

In Figure 3 are shown, in histogram form, the distributions of the quantity  $E$ , the sum of the energies of the three  $\alpha$ -particles, for the stars of each group. Also shown are the maximum possible values of  $E$ , obtained from the excess of the known maximum incident neutron energy at each angle over the  $Q$ -value of 7.34 mev. which is given by the masses. The maximum observed values of  $E$  fall just below these limits, as expected.

#### § 4. CROSS-SECTION

The number of stars observed and attributed to each of the two neutron groups at each of the two angles relative to the deuteron beam was compared with the number of tracks of protons projected forwards by the neutrons of the same group, allowance being made for the ratio of the areas of plate searched for stars and for proton tracks. To obtain the value for the cross-section for production of stars at each energy, three further multiplying factors were needed: the total neutron-proton scattering cross-section at that energy (Sleator 1947), the fraction of the total number of proton tracks which would be expected to lie within the angular limits chosen and to remain entirely within the emulsion (Gibson and Livesey 1948), and the ratio of the numbers of hydrogen and carbon atoms in the emulsion. The last-mentioned quantity had the value 2.03, and the values of the first two for each neutron energy are shown in the Table below. Also shown in the Table are the numbers of stars and proton tracks on which each value for the cross-section is based, the ratio of these numbers corrected for the difference in areas searched, and the final values for the cross-section for the disintegration of  $^{12}\text{C}$  into three  $\alpha$ -particles. The probable error of each value is of the order of 20%.

Neutron energy (mev.)	10.8	12.0	13.2	14.5
Number of stars	13	27	24	23
Number of proton tracks	46	37	25	12
Number of stars per unit area				
Number of proton tracks per unit area	0.37	0.65	2.34	5.25
Number of measurable proton tracks per unit area				
Total number of proton tracks produced per unit area	0.038	0.032	0.0275	0.023
Neutron-proton scattering cross-section ( $10^{-21} \text{ cm}^2$ )	0.79	0.73	0.69	0.64
Cross-section for disintegration of $^{12}\text{C}$ ( $10^{-26} \text{ cm}^2$ )	2.3	3.1	9.0	15.7

#### ACKNOWLEDGMENTS

The authors wish to express their thanks to Professor O. R. Frisch and Dr. W. E. Burcham for advice and assistance, and to the Department of Scientific and Industrial Research for financial support.

#### REFERENCES

- AOKI, H., 1938, *Proc. Mat.-Phys. Soc., Japan*, **20**, 755.  
 CHADWICK, J., FEATHER, N., and DAVIES, W. T., 1934, *Proc. Camb. Phil. Soc.*, **30**, 357.  
 GIBSON, W. M., and LIVESSEY, D. L., 1948, *Proc. Phys. Soc.*, **60**, 523.  
 GREEN, L. L., and GIBSON, W. M., 1949, to be published.  
 HOLLOWAY, M. G., and LIVINGSTON, M. S., 1938, *Phys. Rev.*, **54**, 18.  
 LATTES, C. M. G., FOWLER, P. H., and CUER, P., 1947, *Proc. Phys. Soc.*, **58**, 883.  
 MATTAUCH, J., 1942, *Kernphysikalische Tabellen* (Berlin: Springer).  
 RUTHERFORD, E., CHADWICK, J., and ELLIS, C. D., 1930, *Radiations from Radioactive Substances* (Cambridge: University Press).  
 SLEATOR, W., 1947, *Phys. Rev.*, **72**, 207.  
 WILLIAMS, J. H., SHEPHERD, W. G., and HAXBY, R. O., 1937, *Phys. Rev.*, **52**, 390.

# A Direct Method of Measuring Nuclear Spin-Lattice Relaxation Times

By L. E. DRAIN

Clarendon Laboratory, Oxford

*Communicated by F. E. Simon; MS. received 27th November 1948; read at the Physical Society Conference, Oxford, July 1948.*

**ABSTRACT.** This direct method of measuring nuclear spin-lattice relaxation times is based on Bloch's nuclear induction experiment in which the material investigated is subjected to a magnetic field that is varied several times per second through the value for nuclear resonance. Under certain conditions a simple calculation may be made of the relation between the magnitude of the nuclear induction effect, the relaxation time, and the time intervals between successive passages through resonance. Experimental observation of this relation then determines the relaxation time directly.

## § 1. INTRODUCTION

THIS direct method of measuring nuclear spin-lattice relaxation times is based on Bloch's nuclear induction experiment (Bloch 1946). In this experiment a strong magnetic field (hereafter called the main field  $H$ ) produces a resultant nuclear magnetic moment in a specimen containing the nuclei under investigation. In addition, a radio-frequency magnetic field is applied perpendicular to the main field. When the applied frequency is close to the Larmor precession frequency for the nuclei in the field a resonance effect occurs.

Usually the frequency of the oscillator is kept constant and the main magnetic field varied. The value of the main field  $H_r$  required for resonance is given by

$$|\gamma| H_r = 2\pi\nu,$$

where  $\gamma$  is the gyromagnetic ratio for the nuclei and  $\nu$  is the frequency of the applied radio-frequency field. The main field is varied over a range including the resonant value by means of an audio-frequency "sweep" field (of, say, 50 cycles/second) superimposed on a steady field. The resonant value is thus passed twice per cycle.

Bloch's nuclear induction experiment differs from most other nuclear resonance experiments in that a comparatively large radio-frequency field is applied, sufficient in fact to cause a considerable change in the nuclear magnetization in one passage through the resonant region, though still small compared with the main field. It can in fact be shown that, if the radio-frequency field is large enough, the nuclear magnetization is actually reversed, or turned over completely, in varying the main field through the resonant value. For this to be true it is necessary to have the following condition satisfied (Bloch's adiabatic condition) :

$$dH/dt \ll |\gamma| H_1^2, \quad \dots\dots (1)$$

where  $2H_1$  is the amplitude of the radio-frequency field and  $dH/dt$  the rate of change of the main field. In this case, when the main field is near the resonant value, the nuclear magnetization precesses about the main field with the applied frequency and there exists a rotating transverse component of the magnetic moment  $M_t$  given by

$$M_t = M(1 + \delta^2)^{-1/2} \quad \text{where} \quad \delta = (H - H_r)/H_1, \quad \dots\dots (2)$$

where  $M$  is the magnitude of the nuclear moment which remains constant during the passage through resonance if relaxation effects can be neglected. ( $M$  is the vector sum of the instantaneous values of the individual nuclear moments, and is in general not equal to the equilibrium value  $M_0$ ). The rotating transverse magnetization induces a radio-frequency E.M.F. in a secondary coil. This E.M.F.,

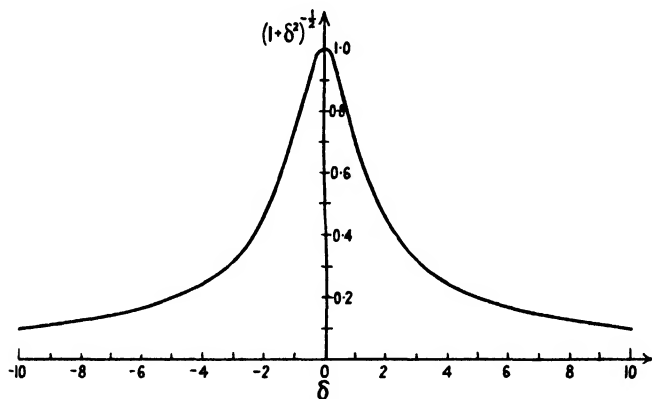


Figure 1. Shape of nuclear induction signal in the case of rapid passage.

after detection and amplification, is put on the Y-plates of a cathode-ray oscillograph. To the X-plates is applied a voltage which is proportional to, and in phase with, the alternating component of the main field. The shape of the signal obtained when the main field passes through its resonant value is shown in Figure 1, which is a plot of the rotating transverse magnetization against the main field.

## § 2. RELAXATION EFFECTS

The relaxation times affecting nuclear magnetism are that for spin-spin equilibrium (Bloch's transverse relaxation time) and that for spin-lattice equilibrium (Bloch's longitudinal relaxation time). In the cases we shall consider, the relaxation times are long compared with the time taken to pass through the resonant region (i.e. the case of rapid passage (Bloch 1946)). In this case the shape of the signals is not altered appreciably by relaxation effects, and if the time spent in resonance is small compared with the period of the audio-frequency alternating field, or sweep, the relaxation effects can be considered as taking place only outside resonance. This is a great simplification and means that only the longitudinal or spin-lattice relaxation time has to be considered, for it will be seen that transverse relaxation can only be effective in the resonant region, for it is only then that there exists a transverse magnetization. In what follows, the term "relaxation time" will refer to the ordinary longitudinal or spin-lattice relaxation time. We may distinguish between two cases: (i) relaxation time long compared with the period of sweep; (ii) relaxation time of the same order as the period of sweep.

In the first case the magnitude and sign of the signals when equilibrium has been attained depends on the relative times spent above and below resonance: the nuclear magnetization will be in the direction of the field during whichever of the two parts of the cycle is greater. The dependence of the size of the signal on its position on the trace of the cathode-ray oscillograph (i.e. on the position of the resonant field with respect to the range of variation of the main field) is shown in Figure 2. It will be seen that the forward and backward traces are

practically the same, since the magnetization has not time to alter appreciably during the time between successive passages through resonance. If the relaxation time is longer than about 1 second, the time taken for the system to adjust itself to new conditions, e.g. to a change in the mean value of the main field, can be seen visually on the cathode-ray tube screen, and the relaxation time obtained easily with the aid of a stop-watch.

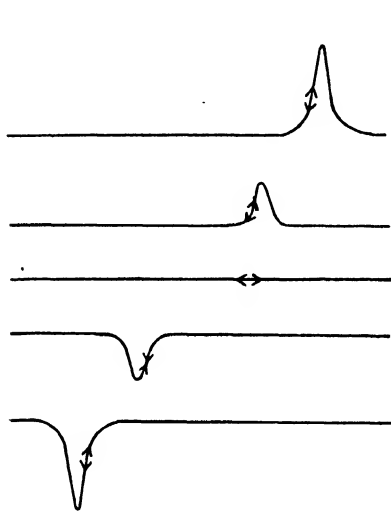


Figure 2. Variation of size of signal with position on trace. Long relaxation time.

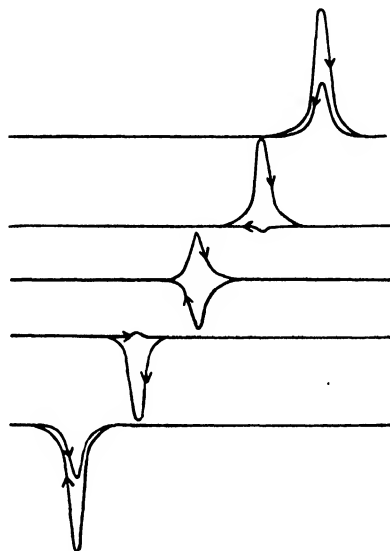


Figure 3. Variation of size of signal with position on trace. Relaxation time equal to the period of sweep.

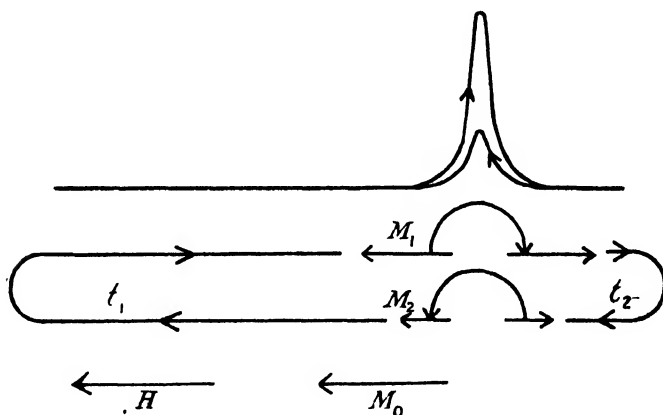


Figure 4. Diagram showing behaviour of the nuclear magnetization during one cycle of the sweep.  $M_0$  is equilibrium value of the nuclear magnetization in a steady field.

In the second case, that is with the relaxation time comparable with the period of sweep, there is time for the magnetization to change during the intervals below and above resonance. The variation of the signal with its position on the trace may be as in Figure 3, which illustrates the case of the relaxation time and period of sweep equal.

In Figure 4 the behaviour of the nuclear magnetic moment during a cycle of the audio-frequency sweep field is illustrated diagrammatically. On the



assumption that the nuclear magnetization tends always to approach its equilibrium value exponentially, a calculation may be made of the signals to be expected. It is evident that the size of the signal in a passage through resonance is directly proportional to the magnetic moment existing just before the passage. For convenience, the nuclear magnetization  $M$  is considered positive if it is parallel to the field below resonance and antiparallel above resonance; thus the sign of the signal is always that of the moment turned over, and the nuclear magnetization does not change sign on passing through resonance. Below resonance we have  $M \rightarrow M_0$  exponentially, and above,  $M \rightarrow -M_0$  exponentially, where  $M_0$  is the equilibrium magnetization with no sweep. (Strictly, as  $M_0$  is proportional to the main field, its value will differ at different points of the sweep, but as the sweep amplitude is always very much smaller than the main field, this difference can be ignored.)

Let  $M_1$  and  $M_2$  be the moments turned over in going through resonance from below to above and above to below respectively; then if  $M_1/M_0 = m_1$  and  $M_2/M_0 = m_2$ , we have

$$\left. \begin{aligned} 1 - m_1 &= (1 - m_2) \exp(-t_1/\tau) \\ -1 - m_2 &= (-1 - m_1) \exp(-t_2/\tau) \end{aligned} \right\} \dots\dots (3)$$

$t_1$  and  $t_2$  are times spent below and above resonance respectively,  $\tau$  is the relaxation time, and  $T (= t_1 + t_2)$ , the period of sweep. Hence

$$\left. \begin{aligned} m_1 &= -1 + [2(1 - \exp\{-t_1/\tau\})]/[1 - \exp\{-T/\tau\}], \\ m_2 &= 1 - [2(1 - \exp\{-t_2/\tau\})]/[1 - \exp\{-T/\tau\}]. \end{aligned} \right\} \dots\dots (4)$$

In Figure 5  $m_1$  and  $m_2$  are plotted for various positions on the trace assuming a sinusoidal sweep. The graph shows how the signal size varies with the position on the trace for various values of the ratio period of sweep-relaxation time.

### § 3. DETERMINATION OF RELAXATION TIMES

By comparison of experimental results with the curves we can determine the relaxation time. A very useful method is to observe the point at which one signal vanishes, and from this the relaxation time follows directly. In this way variations of relaxation time with temperature can be rapidly followed in a substance as it warms or cools. The relation between the point of disappearance and the relaxation time is simply given by putting, say,  $m_2 = 0$ . We get

$$\exp(-t_2/\tau) = \frac{1}{2}[1 + \exp(-T/\tau)]. \dots\dots (5)$$

Relaxation times measured include those for protons in the following substances at 8 Mc/s.:

Paraffin wax at room temperature, 0.02 sec.

Glycerine over the range  $-20^\circ$  to  $+50^\circ$  c., 0.2 sec. ( $54^\circ$  c.), 0.005 sec. ( $-12^\circ$  c.).

Liquid hydrogen at boiling point, 0.2-0.5 sec.

Distilled water at room temperature, 2.7 sec. (stop-watch method).

The results for glycerine agree fairly well with those obtained by Bloembergen, Purcell and Pound (1947) by the saturation method in nuclear resonance absorption. Below  $-20^\circ$  c. the method failed, for the signals became smaller and the results were not independent of the amplitude of sweep. Possibly the reason

for this was that the transverse relaxation time was becoming comparable with the time spent in resonance. The results for glycerine are shown in Figure 6,

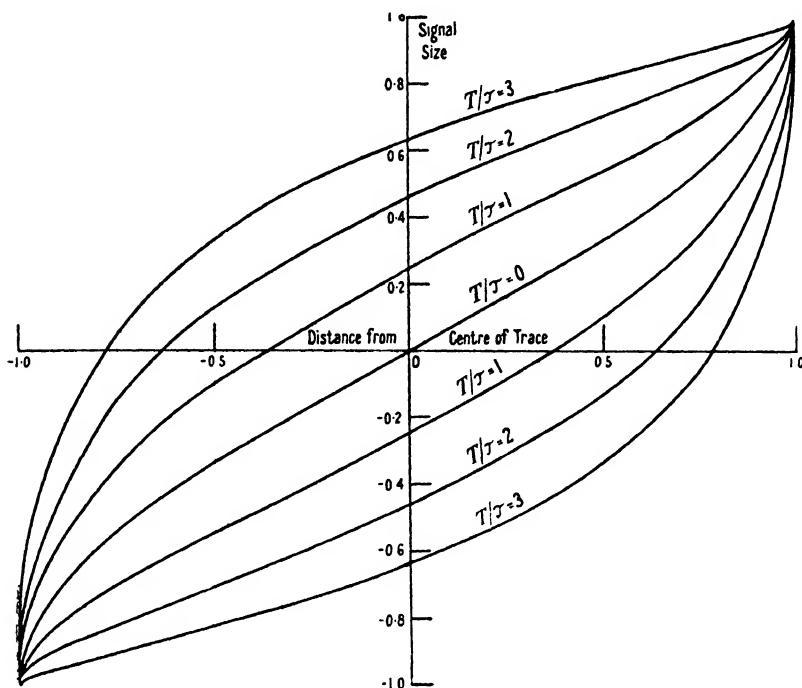


Figure 5. Nuclear induction experiment.  
Dependence of signal size on position of signal on trace.  
 $T$  = Period of modulating field.  $\tau$  = Relaxation time of specimen.

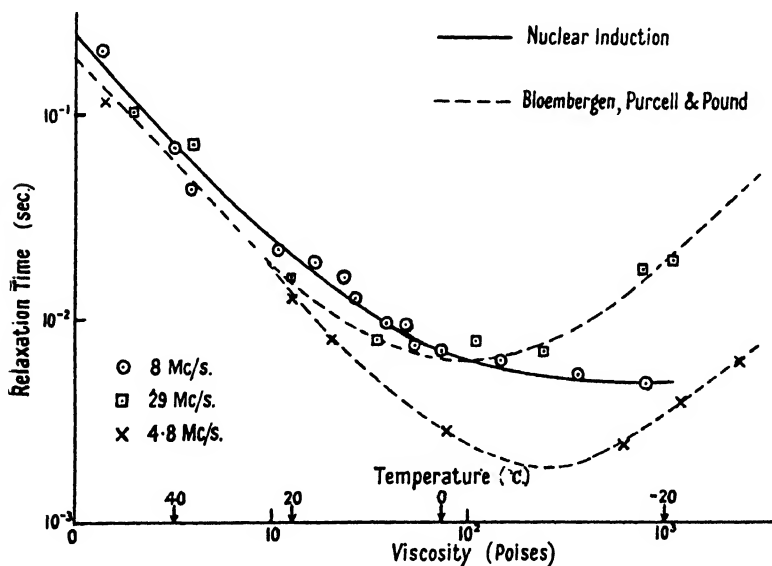


Figure 6. Graph showing variation of the nuclear spin-lattice relaxation time for protons in glycerine. Relaxation time is plotted against viscosity.

in which relaxation time is plotted against viscosity, following Bloembergen, Purcell and Pound. Their results are given for comparison.

The value given for liquid hydrogen is only approximate as the relaxation time is too long for measurement by the method given, with a 50-cycle sweep, but too short for visual observation. Either a lower frequency of sweep is required or a rapid direct method of observation.

#### § 4. CONCLUSION

The range of relaxation times which can be measured with a 50-cycle sweep is from about 0.1 sec. to 0.005 sec. By using lower frequencies it should be possible to extend the range to connect up with the direct timing method. To determine shorter relaxation times it would be necessary to use a higher frequency of sweep but, owing to the adiabatic condition (1), the radio-frequency field would have to be increased too. This, besides entailing a larger oscillator and more heating of the coil, increases the trouble from microphonics and other sources of interference.

It will be seen that the method is not subject to large systematic errors, but to ensure good results we must be sure that the conditions specified are in fact obeyed, that is, that (a) the radio-frequency field is large enough for adiabatic conditions; (b) the transverse relaxation time is long compared with the time spent in resonance.

It is useful to observe the effect of varying the radio-frequency field and the amplitude of sweep in order to be sure that (a) and (b) are obeyed. Under the correct conditions the changing of these variables by quite considerable amounts should not affect the results.

#### ACKNOWLEDGMENTS

This work was carried out with the assistance of a grant from the Department of Scientific and Industrial Research. The author wishes to thank Dr. A. H. Cooke for the great interest taken in the work, and Dr. R. A. Hull and Mr. R. J. Benzie for many helpful suggestions.

#### REFERENCES

BLOCH, F., 1946, *Phys. Rev.*, **70**, 460.

BLOEMBERGEN, N., PURCELL, E. M., and POUND, R. V., 1947, *Nature, Lond.*, **160**, 475.

## Uniformly Moving Dislocations

By J. D. ESHELBY

H. H. Wills Physical Laboratory, University of Bristol

*Communicated by N. F. Mott; MS. received 2nd December 1948*

**ABSTRACT.** An expression is derived for the displacements in an isotropic elastic medium which contains an edge dislocation moving with uniform velocity  $c$ . When  $c=0$  the solution reduces to that given by Burgers for a stationary edge dislocation. The energy density in the medium becomes infinite as  $c$  approaches  $c_2$ , the velocity of shear waves in the medium; this velocity therefore sets a limit beyond which the dislocation cannot be accelerated by applied stresses. The atomic structure of the medium is next partly taken into account, following the method already used by Peierls and Nabarro for the stationary dislocation. The solution found in this way differs from the one in which the atomic structure is neglected only within a region of width  $\zeta$  which extends not more than a few atomic distances from the centre.  $\zeta$  varies with  $c$  and vanishes when  $c=c_1$ , the velocity of Rayleigh waves. It becomes negative when  $c_1 < c < c_2$ . Thus  $c_1$  rather than  $c_2$  appears to be the limiting velocity when the atomic nature of the medium is taken into account. Since  $c_1 \approx 0.9c_2$  the difference is not of much importance.

The same method applied to a screw dislocation gives, in the purely elastic case, the expression already derived by Frank. The corresponding Peierls-Nabarro calculation shows that the width  $\zeta$  is proportional to  $(1-c^2/c_2^2)^{1/2}$ . This "relativistic" behaviour is analogous to Frenkel and Kontorowa's results for their one-dimensional dislocation model.

### § 1. INTRODUCTION

FRANK (1949) has discussed the motion of screw dislocations: he shows that the displacement system suffers a contraction in the direction of motion as  $(1-c^2/c_2^2)^{1/2}$  where  $c$  is the velocity of motion and  $c_2$  is the velocity of shear waves in the medium. He has also discussed the case of edge dislocations approximately. In the present paper an exact solution within the limits of isotropic elasticity theory is given for the motion of an edge dislocation. The material is supposed to be cut at the slip plane, and the displacements due to uniformly moving distributions of force on the cut surfaces are derived. These travelling displacements may be so chosen that the two surfaces can be stuck together again leaving a moving dislocation in the material. This method lends itself (§ 3) to an extension of the calculation of Peierls (1940) and Nabarro (1947) in which the shape of the dislocation near its centre is determined by considering the balance between the elastic forces and the interatomic forces acting across the slip plane. In § 4 the same method is applied to the screw dislocation. Frank's results are reproduced and in addition the Peierls-Nabarro calculation for this case shows that the width of the screw dislocation behaves relativistically just as it does in the one-dimensional model of Frenkel and Kontorowa.

### § 2. MOVING EDGE DISLOCATION

Imagine the infinite unstressed elastic body of Figure 1 to be cut in two along the plane  $y=0$  and the two halves slightly separated. Let tangential forces  $p(x)$  per unit area be applied to the surface AB, independent of  $z$  and everywhere parallel to the  $x$ -axis, and producing horizontal and vertical displacements  $u$ ,  $v$

at the surface. Now let exactly equal opposite forces  $-p(x)$  be applied at corresponding points on CD producing displacements  $\bar{u} = -u$ ,  $\bar{v} = v$ . The two halves can be welded together and the forces  $p$  removed, leaving the body in a "self-stressed" state. A knowledge of  $u$  along the  $x$ -axis is sufficient to determine  $u$  and  $v$  throughout the solid.

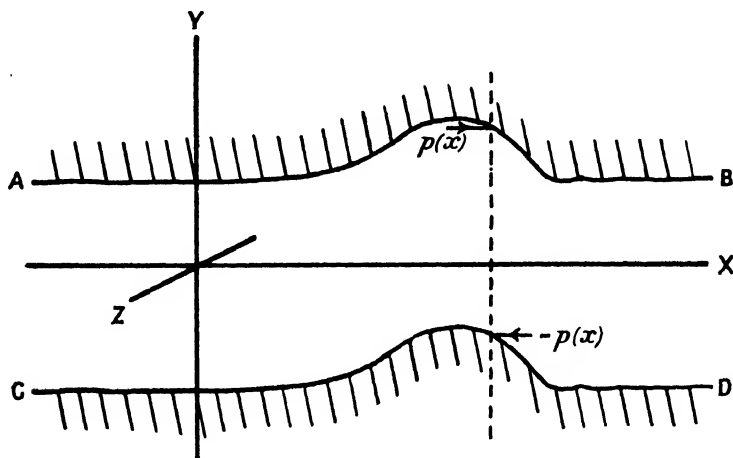


Figure 1.

The particular choice

$$u = -\bar{u} = 0, \quad x > 0; \quad u = -\bar{u} = \lambda_0/2, \quad x < 0 \quad \dots\dots(1)$$

for the surface displacements gives the edge-type dislocation of Burgers (1939) for which

$$\left. \begin{aligned} u &= \frac{\lambda_0}{2\pi} \tan^{-1} \frac{y}{x} + \frac{\lambda_0}{2\pi} \frac{\lambda + \mu}{\lambda + 2\mu} \frac{xy}{x^2 + y^2}, \\ v &= -\frac{\lambda_0}{2\pi} \frac{\mu}{\lambda + 2\mu} \ln(x^2 + y^2)^{\frac{1}{2}} + \frac{\lambda_0}{2\pi} \frac{\lambda + \mu}{\lambda + 2\mu} \frac{y^2}{x^2 + y^2}, \end{aligned} \right\} \quad \dots\dots(2)$$

where  $\lambda$  and  $\mu$  are the Lamé constants and  $\lambda_0$  is the "strength" of the dislocation.  $u$  increases by  $\lambda_0$  on describing a circuit around the origin.

Suppose now that the distributions of force  $p$  and  $-p$  are moving uniformly along the  $x$ -axis with velocity  $c$ , so that they depend on  $x$  and  $t$  only through  $x' = x - ct$ . The corresponding displacements will be of the form  $u(x', y)$ ,  $v(x', y)$ ; their connection with each other and with  $p(x')$  can be found by an extension of the analysis used in discussing Rayleigh surface waves (Love 1944).

Consider the displacements

$$\begin{aligned} u_1 &= A e^{-\gamma s y} \sin s x', & v_1 &= A \gamma e^{-\gamma s y} \cos s x', \\ u_2 &= B \beta e^{-\beta s y} \sin s x', & v_2 &= B e^{-\beta s y} \cos s x', \end{aligned}$$

where

$$\beta = (1 - c^2/c_2^2)^{\frac{1}{2}}, \quad \gamma = (1 - c^2/c_1^2)^{\frac{1}{2}}, \quad x' = x - ct,$$

and  $c_1 = \{(\lambda + 2\mu)/\rho\}^{\frac{1}{2}}$ ,  $c_2 = (\mu/\rho)^{\frac{1}{2}}$  are the velocities of longitudinal and shear waves in the medium, whose density is  $\rho$ .  $u_1$  and  $v_1$  correspond to an irrotational disturbance and satisfy

$$(c_1^2 \nabla^2 - \partial^2/\partial t^2)(u_1, v_1) = 0, \quad \partial u_1/\partial y - \partial v_1/\partial x = 0, \quad \dots\dots(3)$$

while  $u_2$  and  $v_2$  correspond to a distortional disturbance and satisfy

$$(c_2^2 \nabla^2 - \partial^2 / \partial t^2)(u_2, v_2) = 0, \quad \partial u_2 / \partial x + \partial v_2 / \partial y = 0,$$

and consequently the combination  $u = u_1 + u_2$ ,  $v = v_1 + v_2$  satisfies the equations governing the motion of an elastic solid, namely

$$(\lambda + \mu) \frac{\partial}{\partial x} \left( \frac{\partial u}{\partial x} + \frac{\partial v}{\partial y} \right) + \mu \nabla^2 u - \rho \frac{\partial^2 u}{\partial t^2} = 0$$

and a similar equation for  $v$ . The condition that the normal stress

$$p_{yy} = \lambda \partial u / \partial x + (\lambda + 2\mu) \partial v / \partial y$$

should vanish at the surface  $y=0$  is easily found to be  $B/A = -\alpha^2/\beta$ , where  $\alpha = (1 - c^2/2c_2^2)^{1/2}$ . Corresponding  $u$  and  $v$  are then

$$u = (2c_2^2/c^2)(e^{-\gamma sy} - \alpha^2 e^{-\beta sy}) \sin sx', \quad \dots\dots(4)$$

$$v = (2c_2^2/c^2)(\gamma e^{-\gamma sy} - \alpha^2 e^{-\beta sy}/\beta) \cos sx', \quad \dots\dots(5)$$

the amplitude of  $u$  being chosen to be unity for  $y=0$ . The shear stress at the surface must be equal to the applied force  $p(x')$ ; it is easily found to be

$$p_{xy}(x', 0) = p(x') = D(c)s \sin sx', \quad \dots\dots(6)$$

where  $D(c) = -2\mu(2c_2^2/c^2)(\gamma - \alpha^4/\beta)$ . Solving  $D(c)=0$  gives the velocity of Rayleigh waves.

If a more general travelling surface wave is built up in the form

$$u(x', 0) = \int_0^\infty f(s) \sin sx' ds,$$

then

$$u(x', y) = (2c_2^2/c^2) \int_0^\infty (e^{-\gamma sy} - \alpha^2 e^{-\beta sy}) f(s) \sin sx' ds, \quad \dots\dots(7)$$

$$v(x', y) = (2c_2^2/c^2) \int_0^\infty (\gamma e^{-\gamma sy} - \alpha^2 e^{-\beta sy}/\beta) f(s) \cos sx' ds, \quad \dots\dots(8)$$

$$p(x')/D(c) = \int_0^\infty f(s)s \sin sx' ds. \quad \dots\dots(9)$$

If  $u$ ,  $v$  are split up into  $u_1$ ,  $v_1$  and  $u_2$ ,  $v_2$ , the suffix 1 referring to the parts containing  $\gamma$  and 2 to those containing  $\beta$ , then  $\gamma u_1$ ,  $v_1$  are Hilbert transforms (Titchmarsh 1937) and so are  $u_2$ ,  $\beta v_2$ . A more useful relation between them is the following. Equations (3), (4) and (5) give

$$\left( \frac{\partial^2}{\partial x'^2} + \frac{\partial^2}{\partial (\gamma y)^2} \right) (\gamma u_1, v_1) = 0, \quad -\frac{\partial (\gamma u_1)}{\partial x'} = \frac{\partial v_1}{\partial (\gamma y)}, \quad \frac{\partial (\gamma u_1)}{\partial (\gamma y)} = \frac{\partial v_1}{\partial x'},$$

and this will continue to hold for the more general  $u_1$ ,  $v_1$ . By the usual theory of conjugate functions it follows that if

$$\gamma u_1 = \text{Im } P(x + i\gamma y) \quad \text{then} \quad v_1 = \text{Re } P(x + i\gamma y), \quad \dots\dots(10)$$

and similarly if

$$u_2 = \text{Im } Q(x + i\beta y) \quad \text{then} \quad \beta v_2 = \text{Re } Q(x + i\beta y), \quad \dots\dots(11)$$

where  $P$  and  $Q$  are analytic functions. (The relation between Fourier transforms, Hilbert transforms and the complex variable are fully discussed by Titchmarsh).

Suppose that at the surfaces AB and CD  $u$  and  $\bar{u}$  are given by (1) with  $x$  replaced by  $x'$ . This may be written

$$u = -\bar{u} = \frac{\lambda_0}{4} - \frac{\lambda_0}{4\pi} \int_0^\infty \sin sx' ds.$$

The first term clearly represents a constant displacement for all  $x', y$ . Thus by (7) for  $y > 0$

$$\begin{aligned} u(x', y) &= \frac{\lambda_0}{4} - \frac{\lambda_0}{2\pi} \left( \frac{2c_2^2}{c^2} \right) \int_0^\infty (e^{-\gamma sy} - \alpha^2 e^{-\beta sy}) \frac{\sin sx'}{s} ds \\ &= \frac{\lambda_0}{2\pi} \frac{2c_2^2}{c^2} \left[ \tan^{-1} \frac{\gamma y}{x'} - \alpha^2 \tan^{-1} \frac{\beta y}{x'} \right]. \end{aligned} \quad \dots\dots (12)$$

Since

$$\ln(x + iy) = \ln(x^2 + y^2)^{\frac{1}{2}} + i \tan^{-1}(y/x),$$

it follows from (10) and (11) that

$$v(x', y) = \frac{\lambda_0}{2\pi} \frac{2c_2^2}{c^2} \left[ \gamma \ln(x'^2 + y^2)^{\frac{1}{2}} - \frac{\alpha^2}{\beta} \ln(x'^2 + \beta^2 y^2)^{\frac{1}{2}} \right]. \quad \dots\dots (13)$$

There is a corresponding expression for  $(u, v)$  when  $y < 0$  derived from  $\bar{u}$ . Except at the singularity at  $x = 0$  there is no relative motion between the planes AB and CD and they can be imagined to be welded together. It is easy to see that (12) and (13) give the displacements for  $y < 0$  as well as for  $y > 0$ .

On passing to the limit  $c = 0$ , (12) and (13) become (2). Independently of the method of derivation the displacements (12) and (13) have the following properties: (i) they satisfy the wave equation; (ii)  $u$  increases by  $\lambda_0$  on describing any circuit round the point  $x' = x - ct = 0$ ; (iii) they reduce to the expressions for a stationary edge dislocation when  $c = 0$ .

The irrotational and distortional terms behave relativistically with respective limiting velocities  $c_1$  and  $c_2$ , but the proportion between them also alters with velocity. On account of the factor  $1/\beta$  in the second term of  $v$  the energy becomes infinite as  $c$  approaches  $c_2$  even if the singularities at  $x' = 0$  and infinity are excluded in the usual way. If solutions exist for  $c > c_2$  it would be difficult to connect them continuously with the solution for  $c < c_2$  and so identify them as moving edge dislocations;  $c_2$  is thus the limiting velocity.

If (1) is replaced by

$$u = -\bar{u} = \frac{\lambda_0}{4} \left( 1 + \frac{2}{\pi} \tan^{-1} \frac{x'}{\zeta} \right), \quad \dots\dots (14)$$

to which it reduces when  $\zeta \rightarrow 0$ , a corresponding calculation shows that  $u$  and  $v$  in the body of the material are given by (12) and (13) on replacing  $y$  by  $y \pm \zeta$ , the sign of  $\zeta$  to be chosen to be the same as that of  $y$ . Formally this "spread" dislocation is equivalent to a distribution of elementary dislocation of the type (12), (13), the total strength between  $x'$  and  $x' + dx'$  being

$$d\lambda_1 = \frac{\lambda_0}{\pi} \frac{\zeta}{x'^2 + \zeta^2} dx'. \quad \dots\dots (15)$$

The change of  $u$  round a circuit depends on the size and position of the circuit but approaches  $\lambda_0$  for a large circuit surrounding  $x' = 0$ .

At first sight it is surprising that the method used should lead to a moving form of the Burgers expression (2) rather than to a moving form of the original Taylor expression

$$u = \frac{\lambda_0}{2\pi} \tan^{-1} \frac{y}{x}, \quad v = \frac{\lambda_0}{2\pi} \ln(x^2 + y^2)^{\frac{1}{2}}, \quad \dots\dots(16)$$

or something similar. This behaviour can be traced to the condition  $B/A = -\alpha^2/\beta$  imposed to make  $p_{yy}$  vanish over the plane  $y=0$ . The actual condition used was that the Fourier transform of  $p_{yy}(x', 0)$  should vanish for all  $x'$ . Strictly this implies (Doetsch 1937) that  $p_{yy}(x', 0)$  vanishes "almost everywhere" and that any singularities are of such a feeble kind that  $\int_0^X p_{yy}(x', 0) dx' = 0$  for any  $X$ .

A singularity of the type of a Dirac  $\delta$ -function is thus excluded. The last equation implies that  $\int_{-\infty}^{\infty} p_{yy}(x', 0) dx = 0$  which in turn means that

$$\int_{-\infty}^{\infty} p_{yy}(x', y) dx = 0, \quad \dots\dots(17)$$

as can be seen by considering the equilibrium of a slab bounded by the planes  $y=0$  and  $y=\text{const.}$ , or analytically by the method of Love (1944, § 117). As is well-known (16) does not satisfy (17), which accounts for its non-appearance in the previous analysis.

The whole argument could in fact be repeated without requiring that  $p_{yy}(x', 0)=0$  everywhere, and the two halves of the material could be welded together as before and would be in equilibrium provided suitable external forces could be applied to the junction plane. Among other solutions (12), or the corresponding form with  $y$  replaced by  $y \pm \zeta$ , would reappear but with the coefficients of the inverse tangents arbitrary. The first or second terms of (12) and (13) taken separately do in fact satisfy the wave equation and give rise to the two following types of dislocations which could exist with suitable forces applied to the plane  $y=0$ :

$$u = \frac{\lambda_0}{2\pi} \tan^{-1} \frac{\gamma(y \pm \zeta)}{x'}, \quad v = \frac{\lambda_0}{2\pi} \ln \{x'^2 + \gamma^2(y \pm \zeta)^2\}^{\frac{1}{2}} \quad \dots\dots(18)$$

and

$$u = \frac{\lambda_0}{2\pi} \tan^{-1} \frac{\beta(y \pm \zeta)}{x'}, \quad v = \frac{\lambda_0}{2\pi} \frac{1}{\beta} \ln \{x'^2 + \beta^2(y \pm \zeta)^2\}^{\frac{1}{2}}. \quad \dots\dots(19)$$

Their limiting velocities are  $c_1$  and  $c_2$  respectively. For (18)

$$p_{yy} = \pm \frac{\lambda_0}{\pi} \mu \gamma \alpha^2 \frac{\zeta}{x'^2 + \zeta^2}$$

on the surfaces AB and BC (Figure 1) respectively. Thus to support it the dislocation requires a total external force

$$F_1 = 2 \int_{-\infty}^{\infty} p_{yy} dx = 2\lambda_0 \mu \alpha^2$$

parallel to the  $y$ -axis distributed over a distance of the order  $\zeta$  along the  $x$ -axis. When  $\zeta=0$  the force is concentrated at the origin. For a velocity  $c = \sqrt{2c_2}$ ,  $F_1$  vanishes and the dislocation could exist without external forces provided  $\sqrt{2c_2}$  is less than the limiting velocity  $c_1$ : the condition for this is  $\lambda > 0$ , which is satisfied



in normal physical cases. This agrees with (12) and (13) on putting  $c = \sqrt{2}c_2$ . This isolated solution cannot be reached from the solutions for  $c < c_2$ . On the other hand (19) requires a total force  $F_2 = 2\lambda_0\mu\beta$  which does not vanish below the limiting velocity. At any velocity less than  $c_2$  a linear combination of (18) and (19) can exist provided the proportion between them is such that the external forces required to support each separately are equal and opposite. This is equivalent to the condition  $B/A = -\alpha^2/\beta$  and leads back to (12) and (13).

When  $c = 0$  and  $\zeta = 0$  both (18) and (19) reduce to (16). The Taylor expression is thus both irrotational and dilatationless and requires for its maintenance a distribution of force along the  $x$ -axis of linear density  $2\lambda_0\mu$  directed parallel to the  $y$ -axis. If it is to be in equilibrium in the slab defined by the planes  $y = \pm Y$  there must be a normal pressure of total amount  $\lambda_0\mu$  suitably distributed over the surface  $Y$  and a corresponding normal tension of total amount  $\lambda_0\mu$  distributed over the surface  $-Y$ .

### § 3. THE WIDTH OF A MOVING EDGE DISLOCATION

By considering the surfaces AB and CD of Figure 1 not as welded together but as kept in place by interatomic forces across the slip-plane, Peierls (1940) and Nabarro (1947) were led to an expression of the form (14) (with  $x$  replacing  $x'$ ) for a stationary edge dislocation with a width  $\zeta = \lambda_0/2(1-\sigma)$  depending on  $\sigma$ , Poisson's ratio. Briefly their argument was the following. Starting from the relation

$$u = \sin sx, \quad p_{xy} = -\{\mu/(1-\sigma)\}s \sin sx, \quad \dots\dots (20)$$

connecting a sinusoidal displacement of the surface AB with the tangential force necessary to produce it, and from an assumed law

$$p_{xy} = -(\mu/2\pi) \sin 2\pi(u - \bar{u})/\lambda_0, \quad \dots\dots (21)$$

giving the atomic forces arising from the relative horizontal displacement of AB and CD at any point, they reach an integral equation for  $u$  which has (18) as a solution. The atomic nature of the medium only enters the problem through the periodicity of (21) and so the origin of  $x$  in (14) is arbitrary.

In so far as (21) is a good approximation in the stationary case it will also be nearly correct if  $du/dt$  is small compared with the natural velocity of vibration of the atoms, i.e. if the velocity of the dislocation is small compared with  $c_2$ . Even if  $c$  is of this order  $du/dt$  will only approach  $c$  near the centre of the dislocation where (21) is least accurate even in the static case. A repetition of the Peierls-Nabarro calculation for the moving dislocation may therefore have some significance. According to (4) and (6)

$$u = \sin sx', \quad p_{xy} = D(c)s \sin sx' \quad \dots\dots (22)$$

replaces (20), to which it reduces when  $c = 0$ . This leads to (14) (with  $x$  replaced by  $x'$ ) where now

$$\zeta = \delta\lambda_0/2(1-\sigma), \quad \delta = D(c)/D(0).$$

In Figure 2,  $\delta$  is shown for  $\sigma = \frac{1}{3}$ , compared with the simple relativistic contraction factor  $\beta$  occurring in the case of the screw dislocation (§ 4).  $\delta$  vanishes when  $c = c_r$ , the Rayleigh wave velocity.

According to the present model the isolated solution of § 2 with  $c = \sqrt{2}c_2$  would have a complex  $\zeta$  unless  $\lambda = 0$ . In that case  $\zeta = 0$  and  $\gamma = \alpha = 0$  so that it

would exist in the completely contracted form  $v=0$ ,  $u=0$ ,  $x'>0$ ;  $u=\lambda_0/2$ ,  $x'<0$ ,  $y>0$ ;  $u=-\lambda_0/2$ ,  $x'<0$ ,  $y<0$ .

It is hardly worth while discussing what happens when  $c_r < c < c_2$  since the approximations made will be very poor in that region. The statement at the end of §2 should be qualified by saying that the limiting velocity is of the order of  $0.9c_2$ .\*

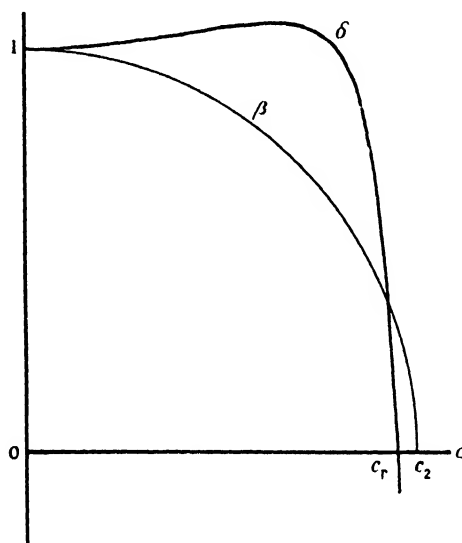


Figure 2.  $\beta$  and  $\delta$  for  $\sigma=\frac{1}{2}$  as functions of  $c$ .

Apart from any considerations of interatomic forces the dislocation of this section when  $\zeta$  is any function of  $c$  which vanishes for  $c=0$  could be considered as the moving form of (1). However, if it is required that the change of  $u$  shall be the same for any circuit surrounding  $x'=0$  the form (12), (13) is unique.

#### § 4. MOVING SCREW DISLOCATION

The screw dislocation already discussed by Frank may be treated in the same way, or more briefly by the following equivalent method.

If  $\phi(x, y)$  satisfies  $(\partial^2\phi/\partial x^2) + (\partial^2\phi/\partial y^2) = 0$  then (Jeffreys and Jeffreys 1946, Titchmarsh 1937)

$$\phi(x, y) = \frac{1}{\pi} \int_{-\infty}^{\infty} d\xi \int_0^{\infty} \phi(\xi, 0) e^{-sy} \cos s(x - \xi) ds.$$

A purely distortional elastic disturbance in which the displacement  $w$  is everywhere in the  $x$ -direction must satisfy

$$\frac{\partial^2 w}{\partial x^2} + \frac{\partial^2 w}{\partial y^2} - \frac{1}{c_2^2} \frac{\partial^2 w}{\partial t^2} = 0.$$

If it is of the form  $w(x', y)$  this becomes

$$\frac{\partial^2 w}{\partial x'^2} + \frac{\partial^2 w}{\partial (\beta y)^2} = 0,$$

\* Note added in proof. The limiting velocity is exactly  $c_r$  only because we have confined the departure from linear elasticity to a plane.

so that if  $w(x', 0) = \int_0^\infty f(s) \sin sx' ds$ , ..... (23)

then  $w(x', y) = \int_0^\infty f(s) e^{-\beta sy} \sin sx' ds$

and  $p_{yz}(x', 0) = \mu \frac{\partial w}{\partial y} = -\mu \beta \int_0^\infty f(s) s \sin sx' ds$ . ..... (24)

If  $w(x', 0)$  is given by the right hand side of (1) (with  $x$  replaced by  $x'$ ) then

$$w(x', y) = \frac{\lambda_0}{2\pi} \tan^{-1} \frac{\beta y}{x'} \quad \text{..... (25)}$$

in agreement with Frank.

If the law

$$p_{yz} = -(\mu/2\pi) \sin 2\pi(w - \bar{w})\lambda_0 \quad \text{..... (26)}$$

is assumed for the interatomic forces across the slip-plane a repetition of the Peierls-Nabarro calculation using (23), (24) and (26) in place of (22) and (21) gives  $w = -\bar{w} = (\lambda_0/2\pi) \tan^{-1}(\beta\zeta/x')$  where now  $\zeta = \lambda_0/2$  is the width of the stationary dislocation which is thus less than the width of the edge dislocation by the factor  $(1 - \sigma) \simeq 2/3$ . The displacement is obtained by replacing  $y$  by  $y \pm \zeta$  in (25), the sign of  $\zeta$  being the same as that of  $y$ , i. e.

$$w = (\lambda_0/2\pi) \tan^{-1} \beta y (1 + \zeta/|y|)/x'. \quad \text{..... (27)}$$

It corresponds to a distribution of dislocations of the type (25) along the  $x$ -axis according to the law (19). (23) can be obtained from (25) by cutting out the material between the planes  $y = \pm \zeta$  and sticking together the remainder.

According to (27) the width of a screw dislocation suffers a simple relativistic contraction (with limiting velocity  $c_2$ ) in complete analogy with the one-dimensional model of Frenkel and Kontorowa (1938).

The calculation leading to (27) is not very significant for a cubic material since there is not a unique slip-plane as there is for the edge dislocation. However (27) may be considered as a crude approximation to the case of a screw dislocation in a hexagonal material. Here there is a unique slip-plane perpendicular to the hexagonal axis. The problem should, of course, be solved using the equations of non-isotropic elastic theory.

#### ACKNOWLEDGMENTS

The author wishes to thank Dr. F. C. Frank and Mr. F. R. N. Nabarro for helpful discussion and suggestions.

#### REFERENCES

- BURGERS, J. M., 1939, *Proc. Kon. Ned. Akad. v. Wet.*, **42**, 293.  
 DOETSCH, G., 1937, *Laplace-Transformation* (Berlin: Springer), p. 102.  
 FRANK, F. C., 1949, *Proc. Phys. Soc. A*, **62**, 131.  
 FRENKEL, J., and KONTOROWA, T., 1938, *Phys. Z. Sowjet*, **13**, 1.  
 JEFFREYS, H. and B. S., 1946, *Methods of Mathematical Physics* (Cambridge: University Press), p. 426.  
 LOVE, A. E. H., 1944, *Elasticity* (Cambridge: University Press), p. 309.  
 NABARRO, F. R. N., 1947, *Proc. Phys. Soc.*, **59**, 256.  
 PEIERLS, R., 1940, *Proc. Phys. Soc.*, **52**, 34.  
 TITCHMARSH, B. C., 1937, *Fourier Integrals* (Oxford: University Press), Chap. V.

## LETTERS TO THE EDITOR

### Misfitting Monolayers

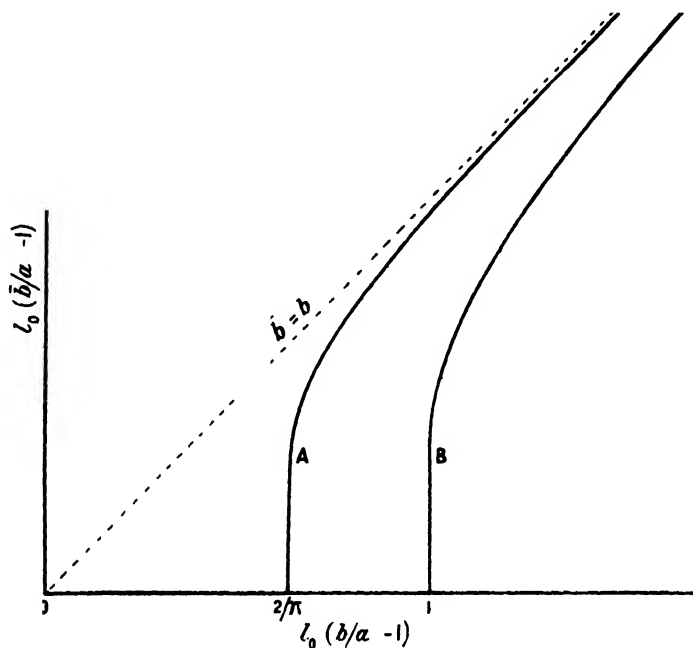
An atom of a certain substance, when deposited at absolute zero on a crystalline substrate, will be adsorbed in the corresponding potential troughs of the substrate. To move to an adjacent trough (at a distance  $a$ ), the atom has to pass a potential barrier of amount  $W$  (say), which will in general be large when there is strong adsorption, and small in the converse case. When more atoms are deposited to form a continuous monolayer, having a natural equilibrium atomic spacing  $b$ , neighbouring atoms will interact with each other. When, say, 99 or 101 atoms in a row are spaced over 100 potential troughs, the majority of atoms lie close to the bottoms of their troughs, while the number lying close to and riding over a potential crest, so as to miss a trough or squeeze an extra atom in, is small. The corresponding small region may be called a "surface dislocation", in analogy with "crystal dislocations". When there are no surface dislocations, the corresponding monolayer is said to "fit" on the substrate. Considering deposition as a process of putting down atom after atom, it is possible for the monolayer, under the influence of the substrate, to go down so as to fit on it, even when  $a$  and  $b$  are unequal.

A theory has been developed (Frank and van der Merwe, to be published) to investigate the conditions under which a monolayer would go down so as to fit the substrate. The theory is developed for a one-dimensional model and then shown to be applicable to a two-dimensional case. The model consists of a row of identical balls (natural spacing  $b$ ) connected by identical springs (force constant  $\mu$ ), the balls at the same time being acted on by a force which varies periodically with distance along the row. The corresponding periodic potential field, wavelength  $a$ , was taken to be sinusoidal with amplitude  $\frac{1}{2}W$ . The actual shape of the potential curve was shown to be of secondary importance as compared with its maximum variation  $W$ , which is the deciding factor.

The mathematical analysis shows that, up to a critical amount of natural misfit defined by  $(b/a - 1)_{\text{critical}} = 2/\pi l_0$ , where  $l_0 = (\mu a^2/2W)^{\frac{1}{2}}$ , the state with no dislocations (a monolayer fitting the substrate), is the one of lowest energy. Assuming, for an average case, the interaction between a substrate and deposit atom (expressed in terms of  $W$ ) to be identical with the interaction of deposit atoms on each other (expressed in terms of  $\mu$ ), calculations with Lennard-Jones forces show that  $l_0$  is about 7, thus making  $2/\pi l_0$  about 9%. Beyond this critical value, however, there still remains an activation energy for the formation of dislocations, and this only falls to zero at a larger critical misfit, defined by  $(b/a - 1)_{\text{critical}} = 1/l_0$ , which is about 14% for  $l_0 = 7$ . Below this critical misfit it is therefore also possible for a monolayer, at low temperatures, to go down so as to fit the substrate. The smaller critical value is presumably important at high temperatures and the larger value at low temperatures. Of course, in practice there will be wide variations about these average values; they will be large when  $W$  is large and  $\mu$  is small, and small in the converse case. Because surface dislocations do not interact until they are close together, there is an abrupt increase in the dislocation density  $\bar{b}/a - 1$  ( $\bar{b}$  is the average spacing of deposit atoms) corresponding to both these states, on passing their critical values, as shown in the graph. Thereafter  $\bar{b}/a - 1$  is almost equal to  $b/a - 1$ , whence  $\bar{b} \simeq b$ .

This theory finds an important application in the phenomenon of oriented overgrowth. Crystal orientations are not in general determined by long range forces, but by influences relayed from one monolayer to the next. Hence in order that there shall be a definite orientation in a crystalline overgrowth on a crystalline substrate, there must be formed, as the initial stage, an immobile monolayer of regular atomic pattern, to be called an "embryo". This is exactly the state of the first monolayer if it goes down so as to fit the substrate. Once completed over any flat region of the substrate, an embryo constitutes a suitable substrate, for the formation of another embryo on it. If the atomic pattern of the first monolayer resembles that in a plane of the natural lattice of the deposit, it is possible, by repetition of embryo formation, for a stable strained oriented overgrowth to grow on the substrate. On the other hand the graph shows that, if the critical conditions are exceeded and there are dislocations, their density will be high; the corresponding monolayer, and hence the subsequent growth, will have no significantly preferred location on the

substrate. The strains, permissible in thin layers, cannot, of course, persist in overgrowths of indefinite thickness, since the strain energy involved is much greater. Therefore, at



Graph of  $l_0(\bar{b}/a - 1)$  against  $l_0(b/a - 1)$ .

A. Lowest energy state; B. State of spontaneous dislocation.

some stage, the abnormal strain energy must be released. At this state the initial orientation may be retained, may be changed, or may be completely lost with the formation of a random orientation. Hence it is likely that the orientations observed in some overgrowths are not the same as those of the corresponding initial embryos. These theoretical ideas are shown (van der Merwe 1949) to be in good general agreement with experimental observations.

We have to thank Professor N. F. Mott for suggesting this problem, and one of us (J. H. van der Merwe) has to thank the South African Council for Scientific and Industrial Research for a grant and special leave, which rendered it possible to perform this research.

H. H. Wills Physical Laboratory,  
University of Bristol.  
17th February 1949.

J. H. VAN DER MERWE.  
F. C. FRANK.

FRANK, F. C., and VAN DER MERWE, J. H., to be published.

VAN DER MERWE, J. H., 1949, *Trans. Faraday Soc.*, Discussion on Crystal Growth, April 1949 (in press).

## The Electron Trap Mechanism of Luminescence in Sulphide and Silicate Phosphors

In a recent publication Garlick and Gibson (1948) report and interpret thermoluminescent measurements on several phosphors. The purpose of this note \* is to correlate their experimental methods and conclusions with data independently reported and theoretically analysed by Williams and Eyring (1947). Both papers report and interpret "glow" data on the ZnS-Cu phosphor. Assuming the two samples to be closely similar, a comparison of the experimental and theoretical methods used by the respective investigators can be made.

From their Figure 9 (b) showing the variation of thermoluminescence after different times of phosphorescence decay at 291° K., they reasonably conclude from the shift of the single glow peak observed that a distribution of electron trap depths, rather than traps of uniform depth, are active. The uniform heating rate of 2.5 K°/sec., earlier used by Randall and Wilkins (1945) was used. Williams and Eyring reported glow data on the same phosphor but used linear heating rates of 0.0310 K°/sec. and 0.0895 K°/sec. At such slow heating rates, the electron traps of different depths become clearly resolved as reproduced in Figure 1 (Williams and Eyring 1947, Figure 13).

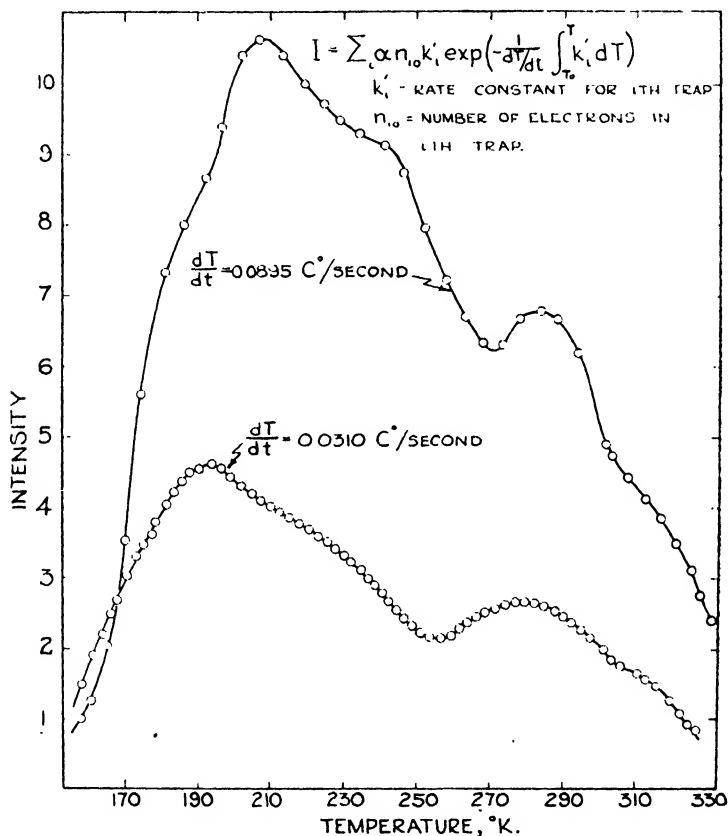


Figure 1. Experimental curve.

By a detailed graphical analysis of the thermoluminescence observed at slow heating rates, Williams and Eyring computed the relative numbers of filled electron traps of different depths and the explicit expressions for the specific rate constants. The analysis can be tested and the experimental results of the two investigators can be correlated by using the relative trap numbers and rate constants obtained from the data of Williams and Eyring to calculate the thermoluminescence data of Garlick and Gibson, substituting, of course,

\* Calculations reported in this note were supported by the Office of Naval Research through Contract N7onr-284, T.O.I.

the heating rate and the period of phosphorescence of the latter. At the heating rate of  $2.5\text{ K}^\circ/\text{sec.}$  and for all phosphorescence periods, all evidence of the fine structure of Figure 1 disappears. This is shown, for example, in Figure 2 for the 20-second phosphorescence period and may be compared with curve *f* of Figure 9 (*b*) of Garlick and Gibson. Differences in peak positions and band width may be attributed to the greater effect at the faster rate heating of competing radiationless processes as evidenced by the dependence of the light sum on heating rates (Cornell 1948), as well as from possible differences in phosphor samples.

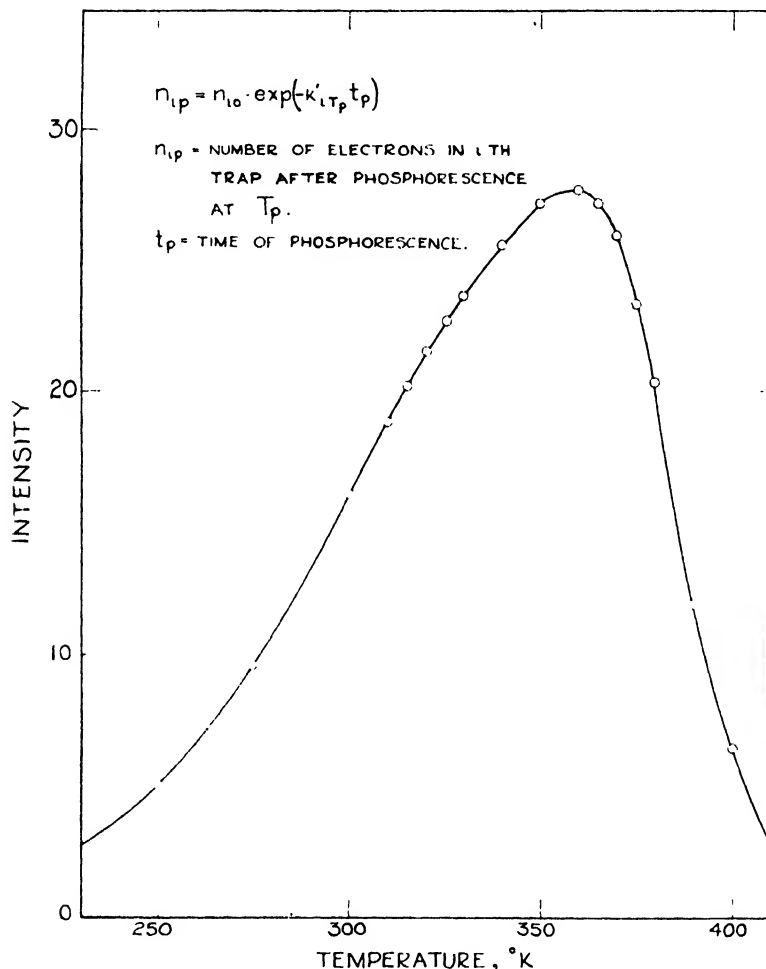


Figure 2. Calculated curve,  $\sim 2.5\text{ C}^\circ/\text{sec.}$

It is reassuring that the investigators agree, although for different reasons, on the significant conclusion, namely, that there are often traps of different depths in a single glow peak, that retrapping is usually negligible, and that monomolecular kinetics dominate thermoluminescence phenomena.

Department of Chemistry,  
 University of North Carolina,  
 Chapel Hill, North Carolina, U.S.A.  
 13th January 1949.

J. S. JOHNSON.  
 F. E. WILLIAMS.

CORNELL SYMPOSIUM, 1948, *Solid Luminescent Materials* (New York and London: Wiley), p. 345.  
 GARLICK, G. F. J., and GIBSON, A. F., 1948, *Proc. Phys. Soc.*, **60**, 574.  
 RANDALL, J. T., and WILKINS, M. H. F., 1945, *Proc. Roy. Soc. A*, **184**, 347, 366, 390.  
 WILLIAMS, F. E., and EYRING, H., 1947, *J. Chem. Phys.*, **15**, 289.

The significant contribution made by the above letter is contained in the second paragraph. The increase in detailed structure revealed by reducing the warming rate in the

thermoluminescence experiments follows from equation (2) of our paper and the curves of Figure 2 (a) since a decrease in the warming rate  $\beta$  produces the same sharpening of the curves as an increase in the constant  $s$ .

It is impossible to compare two copper activated zinc sulphide phosphors as suggested in the beginning of the letter. The "glow" curve of such phosphors is markedly dependent on the method of phosphor preparation (cf. glow curve of ZnS-Cu phosphor given by Garlick and Wilkins (1948)). We have "glow" curves for other ZnS-Cu phosphors measured at a warming rate of 2.5°/sec. which show as much detailed structure as those given in Figure 1 above for much smaller warming rates.

The different peak positions of curve (f) of our Figure 9 (b) and of Figure 2 above may not be correlated since the specimens are different. Even so, we do not think the explanation involving different effects of radiationless processes\* for different warming rates can be accepted since, over the relevant temperature range (300–450° K.), there is little change in the luminescence efficiency of such specimens. It is of interest to note that the half width of the curve of Figure 2 is 95° K., although the warming rate is much slower than in our experiments in which the half width of curve (f) of Figure 9 (b) is 45° K. We suggest that thermoluminescence characteristics need to be studied for very many different specimens of the same type before typical behaviour can be established.

Physics Department,  
The University,  
Edgbaston, Birmingham.  
16th February 1949.

G. F. J. GARLICK.

GARLICK, G. F. J., and GIBSON, A. F., 1948, *Nature, Lond.*, **161**, 359.

GARLICK, G. F. J., and WILKINS, M. H. F., 1948, *Nature, Lond.*, **161**, 565.

## REVIEWS OF BOOKS

*Cosmic Rays*, by L. JÁNOSSY. First Edition. Pp. xiii + 424. (Oxford: University Press, 1947). 35s.

The subject of cosmic rays has a remarkable history, from its inconspicuous beginnings as the study of an unwanted leak in gold foil electroscopes to its present position as a disquietingly generous source of supply of new kinds of fundamental particles. The complexity of the phenomena contributing to the composition of cosmic radiation at various places in the earth's atmosphere, and the difficulty of detection or analysis of some of the effects involved, make progress in this field dependent to a particularly large degree on the improvement of experimental technique. The investigation of atomic and nuclear phenomena in the laboratories led to the design of more and more sensitive apparatus, responding in various ways to the individual particles involved in such processes; and it may be said that each new device or improvement of this type immediately opened up a new field in the study of cosmic radiation and each time disclosed an unsuspected wealth of new phenomena. In fact, cosmic radiation research leads us into a domain of energies which we are only just beginning to reach by means of the largest generators; it has thus been, and still is to a large extent, a most valuable complement to laboratory work on the fundamental properties and the constitution of matter. Its contribution is not restricted to the more spectacular discoveries of new particles and nuclear explosions, but comprises also a considerable amount of quantitative data on the elementary processes concerned, which afford important tests of the validity, under extreme circumstances, of our theoretical treatment of those processes.

One drawback of cosmic-ray study as a source of information on fundamental problems, which applies to all natural phenomena occurring on too large a scale to be under our control, is that we are primarily concerned with the observation of the effects of the impinging radiation without being able to influence their production or essentially to reduce their overwhelming complexity. The most we can do is to try by devious and cumbrous devices to achieve some degree of selection and to disentangle to some extent the maze of atomic and nuclear reactions which build up the radiation as it proceeds through the atmosphere and to great depths underground with continually varying composition. As

\* Part of the theory of Eyring and Williams for non-radiative processes in phosphors has been initiated by experimental facts already given by us (Garlick and Gibson 1948).



a result of this situation, the task facing the author of a monograph on cosmic rays is of disheartening difficulty, even if this author happens to combine, as does Prof. Jánossy, a first hand knowledge of the experimental techniques and a firm mastery of the theoretical methods and results, with a clear and all-embracing view of the vast and steadily growing accumulation of empirical facts and data. From the start he must give up any hope of producing an entirely up-to-date survey; in fact, our author candidly confesses that he has not even been able to harmonize entirely all sections of the book. This last short-coming, however, is not seriously disturbing; and even though the book fails to give an adequate account of the latest discoveries about mesons, it will undoubtedly render invaluable and lasting services as an authoritative introduction to a subject which is of paramount interest not only to those directly engaged in research in it, but also to all workers in the larger field of nuclear physics.

The book under review covers all the main aspects of the subject, and seems to me on the whole to be well-balanced. It opens with an historical survey, in which the broad outlines of the subject are very aptly presented (the account of the high altitude effects, however, is too sketchy to be of any use). The next chapters are of auxiliary character: they treat the experimental technique and the theoretical background (theory of fast collisions). In this connection one must also mention Appendix I, in which a useful account of the statistical treatment of observations is given. The two following chapters contain a discussion of the phenomena observed at sea-level and underground, and of those connected with the instability of the mesons. Next come a thorough treatment of the cascade theory of the soft component and a comprehensive survey of the geomagnetic effects. The last two chapters are devoted to extensive air showers, and to the origin of the meson component (including an account of penetrating showers). A feature of the book which strikes the outsider on the most casual perusal is the pleasingly moderate size of the list of references: in view of the bewildering and apparently unquenchable flow of publications of the subject, this restraint is an indication of a wholesome critical approach. It is just a little perplexing to find that Prof. Rossi's recent contribution in *Reviews of Modern Physics*, which has the same characteristic, does not present quite the same selection.

It certainly cannot be said of this extensive treatise that it makes easy reading; but I should not like to put the blame for this on the author. He has obviously made strenuous and largely successful efforts to bring a most rebellious subject matter into a well-ordered picture. It is true that the formulation of facts and ideas too often shows less care than one would wish, but these stylistic blemishes, which may easily be remedied in a second edition, do not in general impair the clarity of the account. After all, if the multitude of facts to be kept in mind when following a particular line of argument often strains the memory of the untrained reader, it must be realized that this complexity is an unavoidable feature of the phenomena discussed; and it is nobody's fault if even the best evidence, in spite of the ingenuity of the experimental arrangements, only yields relevant information after being subjected to a subtle and intricate analysis.

In the composition of his book, Prof. Jánossy has paid special attention to the practical needs of research workers: his above-mentioned accounts of experimental techniques, and of the statistical treatment of observations, as well as the numerous diagrams and tables throughout the book will be especially welcome. I would like to present a suggestion in this respect: although the exposition of cascade theory given in the book is very complete, it remains a little difficult, especially for one who does not make daily use of it, to find his way in the maze of formulae and pick out ready answers to specific questions. It would therefore be a great help if a brief treatment of a series of typical cases were added, including the most current applications of the theory with the appropriate references to the relevant formulae.

As to the accuracy and reliability of the information conveyed, a very high standard is maintained almost everywhere; the weakest parts are those concerned with meson theory, which would seem to be in need of a serious overhaul. It was somewhat disturbing to me to find the chapter on the soft component opening with a discussion of the soft component allegedly contained in the primary cosmic radiation. From a didactic point of view, it does not seem advisable to start with such a hazardous illustration of the general theory; altogether, too little emphasis is placed in the book on the controversial character of this particular issue. Dissenting views should certainly have been mentioned and a clear summary of the conflicting arguments given. But we may reasonably hope that no occasion for such a criticism will arise in the next edition!

L. ROSENFELD.

*Theoretical Chemistry*, by S. GLASSTONE. Pp. viii+515. (New York: Van Nostrand, 1946.) Third Edition. No price.

Dr. Glasstone's text-book of theoretical chemistry contains chapters which review successively quantum mechanics and the theory of valence, molecular spectra and structure, statistical mechanics and thermodynamics, and intermolecular forces. His object is "to provide an introduction to certain aspects of these subjects that have a bearing on chemical problems", without claiming to give a comprehensive or completely rigorous treatment; he expects any graduate in chemistry to be able to understand the book. It is to some extent a summary of a number of more specialized works, but some references to original papers are also given. On the whole the treatment is formal and there is only the necessary minimum of reference to experimental work. Students will be grateful to Dr. Glasstone for bringing between these two covers so vast and complex a mass of information, competently arranged and making no undue demands on their mathematical abilities. On the other hand the effect is somewhat forbidding, and the pedestrian style does not attract. The book will be useful to those who already have an interest in these matters, but seems unlikely to excite it.

E. F. CALDIN.

*Electronics*, by F. G. SPREADBURY. Pp. x+698. (London: Sir Isaac Pitman & Sons, Ltd.) 55s.

This is an ambitious book. Mr. Spreadbury has attempted in 698 pages to cover all aspects of the subject. There are twenty chapters, the early ones dealing with the fundamentals of the subject—atomic theory, x rays, electron optics, luminescence, electrical conduction in gases and the like. The author presupposes that the reader has a knowledge of elementary physics and mathematics, including the calculus, and the presentation, so far as it goes, is reasonably clear and accurate.

The later sections of the book deal with applied electronics. The subjects discussed include diodes, triodes, multi-electrode valves, valve amplifiers, oscillators, rectifiers, frequency changers, cathode-ray tubes and applications of these devices in practical circuits. There are chapters dealing with electric discharge lamps, photoelectric tubes, electrical measurements and discussion of various miscellaneous matters including cyclotrons, betatrons and electron microscopes. The book represents a great amount of work in collecting and arranging materials from many sources.

The standard of scholarship varies greatly throughout the book. The chapter on electric discharge lamps is well written and informative, whereas the chapter on electrical measurements is only mediocre. The reviewer has no very clear idea of the type of student Mr. Spreadbury had in mind when he wrote this book. Clearly the latter part of the book is suitable for engineering students taking electronics, although the mathematical approach adopted in the early chapters of the book is, perhaps, not very appropriate to such courses. Nevertheless there is much in the book that engineers will find of value. It is not likely to appeal to physicists. The book is well illustrated and printed and appears to contain few printing errors, although the reviewer noted several errors in the circuit diagrams.

DENIS TAYLOR.

*Electromagnetism*, by J. C. SLATER and N. H. FRANK. First Edition. Pp. xiii+240. (New York and London: McGraw-Hill Book Co., 1947.) \$3.50.

One's first reaction on seeing a new book on electromagnetism is to wonder whether it is really called for. However, in this instance one's doubts are soon set at rest; this book is certain of a welcome from many students and teachers for its lucidity and for the unusually broad view of the subject that it gives in a volume of fairly small compass. It starts from first principles and covers the whole ground from electrostatics to optics, including electron theory and dispersion, waveguides, cavity resonators, and diffraction, and this in a manner that no one can dismiss as merely superficial. The book is, however, purely theoretical; the very first equation stated is that for the force on a point charge  $\mathbf{F} = q(\mathbf{E} + \mathbf{v} \times \mathbf{B})$ , and the necessity of swallowing this at the first gulp must leave a conscientious student

with a feeling of mental discomfort. However, he subsequently finds his path smoothed as much as possible, and provided he is prepared to take for granted the physical significance of all the quantities, he has every reason to be well satisfied with the comprehensive view that he gets of theory of electromagnetism as it stands today. The authors have written a companion volume on Mechanics, and others are promised; their aim is to bring out the unity of the various branches of theoretical physics; one can only wish the enterprise every success.

It is a sign of the times that the authors, who have previously published a work in the same field in terms of Gaussian units, now use M.K.S. units, and state their conviction that they have advantages even for theoretical work. The movement in this direction, after having been almost imperceptible for nearly 50 years, is now unmistakable, and gives good grounds for hope that the one single system will soon be universally employed and the others allowed to fade away.

L. HARTSHORN.

*About Cosmic Rays*, by JOHN G. WILSON. First Edition. Pp. 144. (London: Sigma Books Ltd., 1948.) 8s. 6d.

This book is one of the Sigma "Introduction to Science" series, and is meant in the first place for the general reader, though it could also be read with profit by students about to work in the field of cosmic ray physics.

The main criticism is that, through no fault of the author, it is out of date. It is to be hoped that paper can be made available immediately for a revised edition which would include the results obtained, mainly at Bristol, using photographic plates, and an account of the Berkeley experiments on the production of mesons.

This book is logically developed from the Introduction to the apparatus used in cosmic-ray research, to the particles found in cosmic rays in the order of their identification. Included here is a good account of the meson and its connection with the problem of nuclear forces, one of the outstanding topics of physics today.

The last chapter—on Cosmic Rays in Space—could almost equally well have appeared at the beginning. It is so interesting that a shortened version might perhaps have been included in the Introduction.

The drawings and photographs are excellent.

E. P. GEORGE.

*Tables of Physical and Chemical Constants*, by G. W. C. KAYE and T. H. LABY. Pp. vii + 194. (London, New York and Toronto: Longmans, Green & Co., 1948.) 21s. net.

This tenth edition of 'Kaye and Laby' was prepared in Melbourne, presumably on account of the death of Dr. Kaye during the preparation of the ninth edition. It has thus lost some of its associations with the National Physical Laboratory, but it has been fortunate in gaining new assistance in its compilation.

Considerable revision has been undertaken, and in particular the fundamental constants have been corrected in the light of recent determinations and derived constants have been accordingly re-calculated. Similarly, the astronomical constants have been revised, and the Astronomer Royal's determination of the solar parallax is adopted. A useful section on the properties and constants of optical glasses has been added.

A glance at selected tables failed to disclose any misprints, and the general standard of production of the book is very high.

H. H. HOPKINS.

*Les Théories moléculaires du Pouvoir rotatoire naturel*, by JEAN PAUL MATHIEU. Pp. 243. Conférences Rapports sur les Recherches récentes en Physique—Premier Volume. (Paris: Gauthier-Villars, 1946.) 8s.

M. Mathieu comments that although his countrymen have made great contributions to the study of optical rotation a collected account of the modern theoretical work on the subject has not previously been available to them. The book is divided as follows: (i) a survey of the early work, (ii) accounts of the general theoretical treatments, (iii) details of the methods of applying the general theories. In general the active substance is assumed to be liquid or gaseous.

It is shown that optical rotation can be explained macroscopically by rewriting the electric displacement equation so as to contain a term in curl  $\mathcal{E}$ . The coefficient of this term—the “coefficient of rotation”—must be of the nature of a scalar triple product. Microscopically it requires at least four atoms in the molecule to give such a coefficient.

The section on general theory deals with the classical treatment due to Born and de Mallemann; and the wave mechanical method of Condon, rather than the matrix treatment of Rosenfeld. Classically the molecule is assumed to contain a number of coupled vibrating charges. The incident radiation produces the polarization together with a small effect due to the variation of the phase over the molecule. This latter, after averaging over all orientations of the molecule, gives rise to the coefficient of rotation.

In the quantum theory treatment the perturbation of the eigenstates of the molecule is found, and a similar phase effect gives rise to a perturbation term involving the magnetic moment of the molecule. The addition to the displacement vector depends on a product of the electric and magnetic moments, and a similar effect arises from magnetic dipole radiation coupled with an electric dipole perturbation term. The author has neglected the latter effect in the classical treatment, though his argument for doing so is not convincing.

The third section contains a study of the various methods of applying the theory. In order to get a sufficiently great magnetic moment only electronic transitions, or vibrations, are considered. Thus in the quantum theory methods nuclear repulsions, and consequently exchange forces, can be neglected without serious error. Experimental evidence suggests studying the behaviour of radicals, which, though not active by themselves, may become active under the perturbing influence of surrounding radicals.

The molecule of secondary butyl alcohol ( $C_4H_{10}O$ ) is studied in detail. The classical theory method of Boys treats the molecule as being composed of four isotropic dipoles, and considers their mutual interactions. The quantum theory method of Kirkwood, which computes the matrix elements under a dipole-dipole interaction between certain radicals, gives a result which is comparable with that of Boys. Kuhn regards the active part of the molecule as composed of two anisotropic dipoles. He is led to deduce a configuration of the molecule which is the mirror image of that given by Boys and Kirkwood.

Finally, there is the mono-electronic method of Condon, Eyring and their co-workers. They consider a single electron of the OH radical and enumerate its possible transitions under the influence of the radiation, allowing for the effect of the surrounding atoms. Their result shows that the rotatory power varies greatly, and may even change sign, when small changes are made in the configuration of the molecule, or when different types of perturbing forces are used.

It seems that, in spite of the beauty of the general theories, their application is in a very primitive stage of development, due chiefly to the serious mathematical difficulties. M. Mathieu's book should, however, be of considerable value to workers in optical activity; and it should also be of interest to a wider public, partly because the methods of attacking the problem have much wider fields of usefulness, and partly because the development of the theory is an interesting commentary on the growth of modern atomic theories.

J. HAMILTON.

*Bulletin Analytique*. Vol. VIII, No. 11–12, Parts I and II. (Paris: Hermann et Cie, 1947.) Part I, pp. 2577–2964; Part II, pp. 2025–2345.

What *Science Abstracts* attempts to do for Physics, and *Chemical Abstracts* for Chemistry, the *Bulletin Analytique* undertakes for the whole range of Science—Physical and Biological, Pure and Applied. It takes nothing less than the whole of scientific literature for its domain. This colossal venture is in the hands of a sub-section of the *Centre National de la Recherche scientifique* known as the *Centre de Documentation*, a special branch of which carries out the actual editorial duties. The cover also bears the imprint of the *Ministère de l'Éducation Nationale*.

Of the two volumes of the double number which have come to hand, the first (*1<sup>re</sup> Partie*) deals with the physical sciences and their applications, the second with the biological sciences and their ancillary techniques. One imagines, from the pagination, that each “Partie” is intended to form its own separate volume at the end of the year. The two parts together comprise rather more than 700 pages, and include more than 8,000 abstracts

in all. It is a sobering thought that, on the evidence of this journal, scientific papers are being turned out at the rate of one every ten minutes, night and day, day in and day out!

In style and length the individual abstracts are similar to those with which we are familiar in *Science Abstracts*: adequate to indicate the scope of the publication, but not to absolve the reader from the necessity of consulting it. In this connection, however, the Centre de Documentation offers to supply readers with a microfilm reproduction of any of the papers abstracted, a scheme which may be commended to the attention of the learned Societies responsible for the publication of our own *Science Abstracts*.

One gathers that the *Bulletin Analytique* culls its extracts from a rather wider field than our own abstracting journals, and that, in addition to the standard scientific journals, technical, semi-popular and even trade journals are scanned for matter worthy of note. One learns, for example, of the part played by amateur radio fans during the Texas disasters; that geologists have made an excursion to Reading; that Plastics has been looking at Brewing, and that, in view of the recent drought, Valparaiso is to accelerate its plans for a new water supply.

A very valuable addition to the normal abstracting service is the list of new books of scientific and semi-scientific interest which appears at the end of each Part of the *Bulletin*. An author index is also included with each part. Our French colleagues have no cause to complain of the efficiency of their abstracting service.

J. A. CROWTHER.

*Heat*, by A. G. WORTHING and D. HALLIDAY. Pp. xii+522. New York: John Wiley; London: Chapman & Hall, 1948.) \$6.00.

In recent years there has been a big output of books dealing with atomic physics, electronics and cognate subjects, but comparatively few on the older branches of physics such as Heat. The volume under review helps to restore the balance and will probably give the same pleasure to many readers as the appearance of Preston's *Heat* did to their fathers and grandfathers about half a century ago.

One of the authors, Professor Worthing, has an international reputation for his contributions in the high temperature field, and in the present comprehensive treatise he and his co-author give an admirable survey of the present state of our knowledge as regards temperature measurement, expansion, calorimetry, specific heat, thermal conduction, properties of gases, thermodynamics, change of phase, heat engines, refrigerators, convection and radiation.

It is a textbook intended for graduate courses in American universities, but it is also certain of a hearty welcome on this side of the Atlantic.

The authors have searched the literature for new experimental methods and have thereby helped the student, and also the research worker, by providing a first reference to modern methods.

It might be remarked that the authors have taken great care to be precise and consistent in their definitions and in the use of terms and symbols. It will be interesting to see what reception is given to their attempt to eliminate much of the uncertainty in students' minds as to the distinction between mass and weight. They propose the verb "to mass" to apply to the action when the analytical balance is used, and the verb "to weight" is reserved as appropriate for the action involving the spring balance.

A few words will cause mild surprise, for example the statement "there has been much *revamping* of old concepts since the introduction of Planck's quantum concept in 1900", and later, in connection with the porous plug experiment, to be told expansion does work on the gas at the lower pressure in *shoving* it out of the way. The italics are the reviewer's.

That the authors are up to date in their subject is evident throughout the book. One instance may be quoted: in a footnote to a table giving melting points and freezing points, they indicate the change of melting points of certain metals which will result if a new value is decided upon for the second radiation constant  $c_2$ . The Consultative Committee on Thermometry of the International Bureau of Weights and Measures which met in Paris in 1948 has decided on a new value for  $c_2$ , particulars of which will be published shortly.

In a work of this magnitude it is inevitable that a few errors should creep in, and they are minor blemishes, noted here to enable the reader to correct his copy of the book and perhaps help the authors in the preparation of a new edition.

The optical lever method described for measuring coefficients of expansion was devised by Roberts whilst at the N.P.L., not the Cavendish Laboratory.

In the diagram on page 306 the heating coil is shown extending on to the area of the bulb in contact with vapour which might result in superheating.

The apparatus shown on page 174 for the determination of the thermal conductivity of a metal in rod form gives inaccurate results when applied to good conductors; it may, however, be used for carbon rods. Consequently the curve on page 176 giving the variation of thermal conductivity of nickel with temperature is incorrect, as in the case of nickel the conductivity increases with temperature from the change-point.

Two additions might be suggested in future editions. On page 41 one would like to see the simplest form of thermoelectric potentiometer described as an introduction to the more complicated circuits.

On page 72, in connection with the linear expansion apparatus, it would be helpful to mention the dial gauge which is so much used nowadays in this form of apparatus.

The volume can be recommended to students as an excellent treatise on Heat, and the authors are to be congratulated on performing a very useful service to both British as well as American students of the subject.

EZER GRIFFITHS.

*Colloid Chemistry*, by R. J. HARTMAN. Second Edition. Pp. xxxii+572. (London: Sir Isaac Pitman & Sons, 1948). 55s.

The chapters in this volume are conveniently grouped into sections. After a brief introduction, six chapters are devoted to the subject of surface chemistry, then follow ten chapters on lyophobic and four chapters on lyophilic colloidal systems. The last six chapters describe the biocolloids and some colloidal aspects of organisms.

In the first section where the author discusses the scope of colloid chemistry and the subdivision of mass, attention is drawn to the solubility relationships of small crystals. It is a pity that the difficulties which arise in this somewhat naive picture of crystal equilibrium are not even noted. Quite recently, problems of crystal growth have aroused great interest and whilst reference to the Gibbs vapour pressure surface tension equation is justified, attention should likewise be drawn at the same time to Gibbs' discussion on crystal equilibrium.

In the chapters dealing with adsorption, whilst the early work of Freundlich and Langmuir are given, as well as a note on the B.M.T. and the Harkins-Jura method of treatment, the more recent developments, such as the contrast between immobile (Langmuir) and mobile monolayers (Volmer) or monolayers with inter-attractive or repulsive forces are nowhere referred to. A very readable account of Langmuir's work is given; some of the more recent work of English workers in the field of friction and lubrication, e.g. of Bowden, might well have been included. This section concludes with a brief and general account of contact catalyses.

The author adopts the convenient classification of W. Ostwald and of von Buzagh in classifying colloidal systems according to their phase and dimensional characteristics, and in this section gives a very readable account of the various methods, both physical and chemical, of preparing colloidal dispersions.

In discussing the physical properties of colloidal suspensions the work of Odén on settling, of Perrin on Brownian movement and of Svedberg on the ultracentrifuge, are mentioned, as well as a useful section on Debye's extension of the work of Tyndall and Rayleigh. Only the early work on the electrokinetic properties of suspensions is given. This section concludes with a general descriptive treatment of dialysis mainly technical in character, of aerosols, emulsions and foams.

The section on lyophilic colloids and the gels is introduced by a consideration of methods for determining the surface tension of solutions; dynamic methods are not included.

The lack of preciseness in thought, which some years ago was characteristic of the subject of colloids as a whole, is nowhere so well exemplified as in our present ideas regarding

the structure of gels. Chapters 19, 20 and 21 contain a large volume of descriptive matter brought within small compass and it is evident that much more work must be carried out on these systems to clarify our ideas.

The author has chosen an excellent structure for a book on colloid chemistry. It is well printed and contains a great deal of information of value to those who are particularly interested in the technical aspects of colloid chemistry.

ERIC K. RIDEAL.

*The Optical Principles of the Diffraction of X Rays*, by R. W. JAMES. Pp. xv + 623. (London: G. Bell & Sons, Ltd., 1948.) 80s. net.

When the study of the diffraction of x rays by crystals was initiated in 1912 by the Laue - Friedrich - Knipping experiment, it was the physicists who were principally interested: experimental and mathematical physicists - and for a very good reason. X-ray diffraction is a branch of optics; and none but physicists were properly trained to appreciate and overcome all the initial difficulties. The first few simple structures that were determined showed clearly that both crystallographers and chemists would benefit greatly by the knowledge acquired through these experiments. But it was really not until some fifteen years or more had passed that the experimental difficulties had become sufficiently well understood and techniques standardized for the real research interest to move towards the field of structural chemistry.

It is perhaps surprising therefore that the first textbook in English dealing comprehensively with the optical principles of the diffraction of x rays should not appear until more than a third of a century after that auspicious beginning. For a great deal of the experimental spadework was carried out in England, especially in the school of Physics at Manchester, under the leadership of Professor W. L. Bragg. No doubt one reason for the delay has been that those who were capable of writing such a book, and they are not many, were more interested in continuing with their research work. Yet there comes a point when, for the sake of succeeding research students who have not had that early important training (some, indeed, of whom have had far too little training in optics) it is very desirable that a rigorous and yet readable exposition of fundamental principles should be made available in book form.

Professor R. W. James was one of the earliest and most active workers in the field of x-ray optics and, in spite of the difficulties of war-time isolation in South Africa and of heavy teaching and administrative duties, he has maintained an unbroken personal interest in experimental crystallography. No one could be better fitted to write such a textbook, and no one could have written it better.

This volume is not concerned with actual experimental techniques as such, nor with the results of structural research; but the general optical principles with which it deals are well illustrated by reference to experiment in a way that only an experimental physicist could have achieved. At the same time the sound mathematical presentation will provide excellent material for study by students who want to get down to fundamentals. Experienced research workers are sure to refer to it constantly.

The main subjects considered are the geometrical theory of diffraction by space-lattices, both simple and subject to various perturbations; the intensity of reflection of x rays by perfect and by mosaic crystals; Ewald's dynamical theory; the atomic scattering factor; anomalous scattering and dispersion of x rays; the influence of temperature on diffraction; experimental problems of primary and secondary extinction; the use of Fourier series (including Patterson's series) in crystal analysis, and the Fourier projection considered as an optical image; Laue's development of the dynamical theory and its application to Kossel lines; the scattering of x rays by gases, liquids, amorphous solids; diffraction by small crystals, effect of crystal size and of certain kinds of faults and imperfections.

Since the vector notation is used throughout the book, a summary of vector formulae is given in an appendix. Other appendices give a brief account of the geometry of the reciprocal lattice, tables for estimating the corrections for dispersion which must be applied to the atomic scattering factor, and one example of the derivation of a Fourier integral.

Perhaps in a book of this extent it is unreasonable to ask for more, but it would be useful to have, in a second edition, an account of the phenomenon known first as "unweganregung",

sometimes called the "Renninger effect", which is of particular importance in connection with the intensity of the "forbidden" 222 reflection from diamond. (Incidentally, Renninger's name is misspelt in all the places in which it occurs in the book.) It would be helpful also to have some consideration given to the case where multiple reflection occurs within a mosaic crystal in which the individual blocks, although too small to show primary extinction, are in fact parallel; such cases do occur quite frequently in practice and lead to a relative diminution of the secondary extinction in the case of the stronger spectra. The section dealing with the optics of diffraction by lattices in which the arrangement of scattering material is only statistically periodic may need some enlargement in a later edition also, especially for the case of single crystals large enough to give oscillation or Weissenberg photographs.

It only remains to be added that the book is excellently produced and that there is a detailed Table of Contents as well as a subject and an author index. K. LONSDALE.

*Kinematic Relativity*, by E. A. MILNE. Pp. vii+238. (Oxford: University Press, 1948). 25s.

Professor Milne's new book is called a sequel to *Relativity, Gravitation, and World Structure*. It is, however, intended to present the case *ab initio*, and the reader can follow it without necessarily being familiar with the earlier book or the intermediate papers.

The fundamental idea is the comparison of distant clocks by means of light signals, observers on different particles being able to observe each other's clocks. If a signal leaves A and is reflected from B back to A, A can set up a correspondence between the two times on A's clock and the time shown on B's clock at the moment of reflection. A and B can, it is shown, graduate their clocks so that the relations are symmetrical between A and B. The time of travel is interpreted as a distance in terms of a conventional velocity of light. A set of observers is then considered such that if a ray from A to B, say, would meet C on the way, then the return ray would also meet C. This evidently postulates a relation between the motions of A, B and C. Collinear sets in different directions are compared, and it is found that the results correspond to a set of particles expanding symmetrically from a common origin, and that coordinates can be introduced for each particle, those used by different observers being connected by Lorentz transformations. Distance is not supposed measured by a separate scale but defined in terms of travel times. It is then found that a further regraduation of clocks is possible such that the time  $t$  of each observer is replaced by  $\tau$ , where

$$\tau = t_0 \log (t/t_0) + t_0.$$

With a corresponding rescaling of distance, the interval between neighbouring events  $ds$  can be expressed in terms of coordinates with the same values for all observers on fundamental particles. In this form it represents a hyperbolic space.

Milne then considers the distribution in a substratum composed of fundamental particles, and assumes that every observer will find the same law of density about himself. This leads to a density law for the particles and to an infinite mass for the substratum as a whole. He proceeds to a discussion of a free particle, that is, one whose velocity is not the same as that of a fundamental particle at the same place. Dimensional considerations lead to a considerable restriction on the possible forms of the acceleration. By an indirect argument that Milne himself seems to find obscure he finds a definite answer in Lorentz-invariant form, which becomes in  $\tau$  measure an inverse square law of gravitation. An energy function is found, which is conserved, has the same value for all observers, and is not simply the  $t$  component of a 4-vector. The main result is that  $\tau$  measure corresponds to Newtonian time, but is less fundamental than  $t$  measure because it contains the arbitrary constant  $t_0$ .

Applications are made to spiral nebulae, electromagnetism, and classical atomic theory. Modifications of Maxwell's theory lead to a force law between two point charges that involves the classical radius of the electron explicitly, and to a change in the magnetic interaction, which does not depend on interpretation by spin. An adaptation to Bohr's theory gives two distinct sets of circular orbits, one of which suggests the neutron.

The theory invites comparison with that of Eddington, though the results differ greatly. The important question with both, I think, is how much good physics is buried under the bad epistemology. Milne is certainly the more intelligible, but then he does not tackle modern quantum theory.



In the first place, what are the fundamental particles? Milne emphasizes (p. 10) that the process is akin to the construction of an abstract geometry, and makes no appeal to experience; it is sufficient that the structure is self-consistent and free from contradiction. (The distinction is too delicate for me.) Then the fundamental particles can be imaginary points carrying imaginary clocks, and we are at liberty to make them move in any way we like. All that Milne shows about them is that it is self-consistent to suppose that they all move uniformly in straight lines from a single origin. But he later identifies them with the nuclei of extra-galactic nebulae (and presumably the clocks with Cepheid variables), and then the rule that A, C, B, once collinear, remain collinear, becomes an empirical postulate. With some forms of the law of gravitation it would clearly be false. Suppose that gravitation is Newtonian but has no effect on light; that the mass is mainly concentrated near the centre; that there are outlying particles at A, B; and that the normal to AB from the centre meets AB at C between A and B. Then the acceleration of a particle at C would differ from that of any point on AB. But such a scheme is certainly self-consistent. Again, there is no objection to a set of ideal points being distributed so that the distribution appears the same from every point; but ideal points have no mass, and the argument for the infinite mass of the universe breaks down for them. Milne is sure that the mass of the real universe is infinite, this being one point where his system differs seriously from general relativity, but this is an empirical hypothesis and not an abstract rule.

The argument for the inverse square law is dimensional. The problem is to construct out of position and velocity a 4-vector that will have the dimensions of another 4-vector that depends on the acceleration. It is assumed that the only invariants concerned are those already found in the theory. If there are others, the argument breaks down. For instance, if there is anywhere a standard metre bar, a characteristic time could be determined, and could appear in the dimensional formula, which therefore begs the question. The consequences of this type of dimensional argument were fully exposed by N. R. Campbell many years ago, but it continues to be taught and to work havoc in physics. It is conceivable, as for the square law of resistance in hydrodynamics, that the argument may give approximately correct results over a certain range of values of the variables, but it should never be taken as more than a suggestion.

Mach's principle, several times appealed to by Milne, has never, so far as I know, been stated in such a form as to be of any use. In practice, like the dimensional argument, it is made to say that nothing matters except what the investigator is taking into account, and hence that any guess is certain on "philosophical" grounds; hence the number of mutually inconsistent theories of the expanding universe now current.

The most disappointing feature of the book is that, though an exact form of the law of gravitation on Milne's theory is given, its consequences are still not worked out. If it provides explanations of the motion of the perihelion of Mercury, the eclipse displacement, and the spectral shift in the Sun and the companion of Sirius, then it is consistent with Einstein's on the solar system scale; if not, it is physically wrong. I have often found in conversation with physicists that they think that the verification has been carried out because it is so obvious that it ought to be.

On the other hand it is satisfactory that Milne has found equations of motion consistent with the special theory of relativity, which may be useful in problems where gravitation can be neglected, and his modifications of Maxwell's equations and the law of magnetic interaction certainly deserve further examination.

HAROLD JEFFREYS.

*Fourier Technique in X-Ray Organic Structure Analysis*, by A. D. BOOTH.  
Pp. viii + 106. (Cambridge: University Press, 1948.) 12s. 6d.

Structure determination is an important, rapidly advancing, complex art, and Dr. Booth sets out to guide the uninitiated along the tortuous paths that lead from a table of experimental structure amplitudes to a complete knowledge of the atomic arrangement within the unit cell. The attempt is timely, as there is no modern critical account of the many methods that have been devised, developed, modified or abandoned in the last twenty years. The considerable delay between the completion of a manuscript and the appearance of the printed book has, however, left its trace, so that direct methods of phase

determination and the method of steepest descents receive only a mention in the preface. For those with a fair acquaintance with the subject Dr. Booth is a good guide. Nearly every development in Fourier technique is mentioned, and the comments on their relative usefulness are just. Particularly welcome is a connected account of Dr. Booth's own contributions to the subject.

The main chapters of the book are: Methods of obtaining approximate structures, The refinement of atomic coordinates, Methods of computation, and Mechanical computation. There is a certain lack of balance in the treatment; over seven pages are devoted to the theory of the "fly's eye", and less than four to the use of the Beevers and Lipson strips. There is very little about the practice of the fly's eye, and only an exceptional research student would feel no need to seek further guidance on the use of the strips. In execution, moreover, the book leaves much to be desired. Perhaps the least satisfactory part is the first chapter, The interaction of x rays with matter. Dr. Booth assumes from the beginning that the reader has a basic knowledge of classical crystallography and x-ray diffraction. Even so, this chapter suffers from a terseness that will make it difficult for those not already well acquainted with the subject, and also from a certain sloppiness in notation. In equation (1.2) a single prime is simply a distinguishing mark, but a double prime denotes the second derivative with respect to the time. In equation (1.12) the letter  $A$  is used with two meanings, one defined only by implication, and later  $N$  is used with two meanings in successive equations. Such examples could be multiplied, each trivial, but the cumulative effect is irritating. Orthogonal axes are tacitly assumed, and the physical meaning of the mathematical device used to evaluate the integrated intensity of reflection is left obscure.

The book can be thoroughly recommended to the experienced crystallographer. The research student will have to look elsewhere for physical background and practical details of certain techniques, and would be well advised to leave the perusal of this book to a late stage in his training.

A. J. C. WILSON.

*Wave Mechanics and its Applications*, by N. F. MOTT and I. N. SNEDDON.  
Pp. xii + 393. (Oxford: University Press, 1948.) 30s.

This book will be a welcome addition to the library of the student of physics or chemistry, covering as it does many applications of wave mechanics of great importance which are normally only found in specialist monographs or original papers and not in the textbooks on wave mechanics. The authors' aim has been to write a book for those who want to use quantum mechanics. They therefore deal only briefly with the foundations of the subject and devote most of the book to techniques of application and results. The book is nevertheless self-contained and develops logically from its first chapters. The treatment is everywhere concise, and the reader is in no danger of being bogged down by detail. There are copious references to the original papers for anyone wishing to study further. The emphasis, as the title implies, is on wave-mechanical methods, but matrix methods are also used where appropriate, and a chapter at the end of the book is devoted to the historical development of matrix mechanics, thus rounding off the logical form of the exposition.

The book covers such applications as chemical binding, interatomic and intermolecular forces, the theory of solids, collision problems, relativistic wave mechanics and the interaction of radiation with matter. It also gives a brief account of modern developments in the still open fields of the theory of elementary particles and quantum electrodynamics: this is of necessity so superficial that one may doubt whether it was worth doing. Among the useful and unusual features is a chapter on perturbation methods, in which not only the usual straightforward developments in power series are given, but also more refined methods which have been found useful in applications and which are less generally known. The section dealing with the self-consistent field methods of Hartree and Fock, and the Thomas-Fermi model, should also prove welcome.

In the attempt to be concise some misleading statements have crept in. For instance, in the section on magnetism the term in the wave equation which is quadratic in the magnetic field is neglected. This is the term which gives rise to diamagnetism. Paramagnetism

is fairly fully discussed but diamagnetism is ignored ; later, however, evidence on agreement between calculations based on Hartree and Fock wave functions and observed diamagnetic susceptibilities is quoted, which might well puzzle a reader not familiar with this aspect of the subject. The reviewer also found the section on the relativistic treatment of the motion of an electron in a magnetic field confusing, giving as it does a particular solution of the wave equation whose physical context is not discussed. These, however, are minor blemishes. The book is surely one of the most useful published recently. M. H. L. P.

*Micromeritics*, by J. M. DALLAVALLE. Second Edition. Pp. xxviii + 555. (New York: Pitman Publishing Corporation, 1948). 42s. 6d.

The author suggests a new word, *Micromeritics*, to mean the science and technology of fine particles, and gives his suggestion weight by using the new word as the title of a very fine book. No one could quarrel with the Greek employed in this synthesis but, on the other hand, the sub-title, "The Technology of Fine Particles", is plain English and describes the book exactly.

Expensive scientific books are not usually set out to catch the eye. This one, like other books from the same publishers, is different. The bright red, white and black dust cover and the cream boards will inevitably stimulate curiosity in a laboratory or scientific library. The agreeable appearance is backed up by excellent paper, printing and diagrams. Perhaps partly in fun, but none the less with sound business judgment, the printers and publishers have subjected the scientists to the powers of modern advertising, and they have done this with good taste. The book is as smart as a new chromium desk lamp.

As for the contents of the book, they resemble an encyclopaedia. The twenty-three chapters are distinct and each covers a wide field. Broadly speaking, the arrangement is as follows. First comes the dynamics of a single particle in a viscous medium, including applications such as the centrifuge. The next seven chapters deal with the shapes of particles distribution functions, the methods of particle size measurement, the theory of sieving and grading, packing, voids and the behaviour of aggregates under pressure, diffusion of particles and the electrical and sonic properties of particles in a carrying fluid. The following six chapters describe the heat conductivity of packings, the relationships between surface energy, heats of wetting and the like, special aspects of the physical chemistry and chemistry of small particles such as crystal growth and oxidation, the flow of fluids through packings, particle-moisture relationships and capillarity. Chapter 16 describes methods of measuring particle surface. Chapter 17 is about muds and slurries. Chapter 18 summarizes work on the transport of silt in rivers and of muds and slurries through pipes and nozzles. The following three chapters are about dust storms, dust in the atmosphere and industrial dust, and the methods of separating dust from air. Chapter 22 is a short account of fine grinding. The last chapter discusses the application of statistics to sampling as well as giving a critical commentary on the experimental procedure. Finally, there is a bibliography containing a list of over 400 papers, seven appendices, an author index and a subject index.

The author has spared no pains to make the book comprehensive and quickly usable. The list of contents gives chapter headings and paragraph headings. There is a four-page list of the principal symbols and the dimensions of the quantity symbolized. The indexes are excellent, and the bibliography quotes all titles in full in their original language (sometimes with a translation) and the exact reference details. Each chapter is concluded with about half a dozen problems. Some are merely numerical substitutions in formulae given in the text; others are more general and do illustrate and amplify the text. The reader is also helped, where necessary, by the inclusion of sections summarizing fundamental ideas lying at the fringe of the main subject. For example, ten pages are given to the theory of diffusion by turbulence; several pages are given to the various corrections to Stokes' law; and the theory of the coagulation of smokes receives a section on its own. Enough is said to make clear to the reader that if he has a special interest in these matters, a study of the original literature is unavoidable.

The book contains a very large number of equations, and about twenty per chapter are considered sufficiently important to justify a number. Sometimes the equations are derived from commonly known laws, but frequently they are quoted from original papers as representing the best fit to experimental results. The more academic reader might feel a little

uneasy at finding on the one hand equations with a sound fundamental basis, such as the Rayleigh scattering formula, and on the other hand empirical equations, such as Gilbert's, for the amount of silt moved by a stream. The scope of the book, however, unavoidably reaches into regions of science where progress depends more on experiment than on abstract contemplation. The author often does what he can to indicate the reliability and range of the empirical formulae, and sometimes makes a short but valuable criticism. The monumental effort that he has made in reading and summarizing a voluminous and scattered literature deserves our thanks and praise.

The book is highly recommended for all scientific libraries used by chemists, physicists, mathematicians and civil engineers. Physiologists also will find sections of the book informative. Industrial research laboratories encountering problems of dust hazards will probably already have the works and technical side covered comprehensively, and the value of the book to them will lie in its description of scientific fundamentals.

W. G. P.

## CONTENTS FOR SECTION B

	PAGE
Dr. MARY D. WALLER. Vibrations of Free Rectangular Plates . . . . .	277
Mr. J. M. M. PINKERTON. On the Pulse Method of Measuring Ultrasonic Absorption in Liquids . . . . .	286
Mr. J. W. GARDNER. The Confinement of Slow Charged Particles to a Toroidal Tube . . . . .	300
Lt.-Col. A. B. WHATMAN. Observations made on the Ionosphere during Operations in Spitsbergen in 1942-43 . . . . .	307
Dr. B. H. CRAWFORD. The Scotopic Visibility Function . . . . .	321
Letters to the Editor :	
Mr. D. A. BELL. Retarding-Field Current in a Cylindrical Diode . . . . .	334
Reviews of Books . . . . .	335
Contents for Section A . . . . .	339
Abstracts for Section A . . . . .	339

## ABSTRACTS FOR SECTION B

### *Vibrations of Free Rectangular Plates*, by MARY D. WALLER.

**ABSTRACT.** Records are given of the normal vibrating modes and frequencies of free rectangular plates between the limiting shapes of the bar and the square. The nodal systems, which in general consist of straight lines parallel to the sides, are, from considerations of symmetry, divided into four classes. Combined modes, for which the nodal patterns are less simple, are not uncommon. The constituent modes belong to the same class, but their uncombined periods may be appreciably different. The combination of modes belonging to different classes is extremely rare, the uncombined periods differing very little in frequency. As the mirror symmetry of the nodal design is lost in such combinations, it may be questioned whether they are ideally possible even for modes of exactly equal period.

### *On the Pulse Method of Measuring Ultrasonic Absorption in Liquids*, by J. M. M. PINKERTON.

**ABSTRACT.** This paper deals with the experimental problems involved in accurate measurement of the absorption of ultrasonic waves in liquids. Reasons are given for preferring a method employing pulses of ultrasonic energy. The errors likely to be introduced by diffraction are discussed and it is shown that reliable measurements may be

made in both the Fresnel and Fraunhofer regions. An account is given of a convenient method of correcting for divergence of the beam in the Fraunhofer region. The choice of the optimum conditions for accuracy is discussed and illustrated by practical examples. A description is given of the essential features of an apparatus working on six frequencies between 7.5 and 67.5 Mc/s. using the pulse technique.

*The Confinement of Slow Charged Particles to a Toroidal Tube* by J. W. GARDNER.

**ABSTRACT.** In the magnetic field of an infinite straight filament current a slow charged particle is confined near the current but drifts parallel to it. This suggests the field of a circular loop of current as a means of confining a particle within a toroidal tube, and it is found that a particle is so confined in such a field if its velocity is sufficiently small in relation to the field. The results obtained are used to examine briefly the possibility of a magnetic self-constricting effect in electric sparks and arcs.

*Observations made on the Ionosphere during Operations in Spitsbergen in 1942-43,* by A. B. WHATMAN.

**ABSTRACT.** Observations on the ionosphere were made in Spitsbergen (latitude  $78^{\circ}$  N., longitude  $15^{\circ}$  E.) in 1942-43 on behalf of the Admiralty. Observations in such a high latitude have seldom been made. The salient features of the equipment and site are described, the equipment proving excellent except for the magnetograph.

Each region of the ionosphere is then considered in turn; the same main regions are found in Spitsbergen as elsewhere, but there are many abnormalities, of which the "Polar Spur" is perhaps the most interesting. Ionization often changes with great rapidity. The effects of magnetic storms are also described.

*The Scotopic Visibility Function,* by B. H. CRAWFORD.

**ABSTRACT.** The scotopic (dark-adaptation) visibility of radiation through the spectrum has been determined for fifty observers under 30 years of age. A modified photometric matching method was used at a very low brightness ( $3 \times 10^{-6}$  candles/ft<sup>2</sup> or  $3.2 \times 10^{-6}$  stilbs). A subsidiary investigation showed that the ultimate scotopic curve was approximated closely. Another demonstrated the effect of age, showing a progressive decrease in sensitivity at the blue end of the spectrum with increasing age, the effect first becoming noticeable at about 30 years of age. A detailed comparison of the present results with those of previous workers is made and reasons for discrepancies are discussed.

# THE PROCEEDINGS OF THE PHYSICAL SOCIETY

## Section A

---

VOL. 62, PART 6

1 June 1949

No. 354 A

---

### **The Structure and Electrical Properties of Surfaces of Semiconductors.—Part I. Silicon Carbide**

By T. K. JONES, R. A. SCOTT\* AND R. W. SILLARS

Research Department, Metropolitan-Vickers Electrical Co. Ltd.

*MS. received 14th January 1949; read at Science Meeting at Manchester 9th December 1948*

**ABSTRACT.** Electrical contacts with faces of silicon carbide and of many other semiconductors do not obey Ohm's law. This property of silicon carbide has been attributed to an amorphous film known to occur on faces of the crystal. Theoretical work relating to such contacts is hampered by lack of knowledge of the essential physical features of the model. In this paper a study is made of the manner in which the surface texture of the crystal affects the electrical properties of the contact. The electrical characteristics of a contact between a rounded metal point and the demonstrably smooth face of a crystal were shown to vary only slowly across the surface. A series of observations was made of the electrical properties and of the electron diffraction patterns of a basal plane of a crystal as the overlying film of amorphous material was removed.

The results show that the presence of the amorphous film is not essential to the exhibition of the special electrical properties of the contact.

#### § 1. INTRODUCTION

IT is well known that the contact between the surface of some semiconductors, such as silicon carbide, and either a metal probe or a second piece of the semiconductor, has unusual electrical properties. A large fall of potential exists in the neighbourhood of the surface when current is flowing, and this potential difference rises much more slowly than in proportion to the increase of current through the contact; the resistance at the contact does not obey Ohm's law, and such a contact resistance is usually described as non-ohmic. The contact also exhibits rectification.

Various mechanisms have been postulated to give a general explanation of these phenomena. Reduced to the simplest terms, these involve assumptions on the one hand of "tunneling" of electrons through a thin insulating surface layer or, on the other hand, of thermal excitation across the potential barrier formed by a (thicker) insulating layer or formed by a space-charge region at the contact with a material of different work-function. Combinations and elaborations of these mechanisms are possible, and in order to limit the field for speculation there is a great need for direct physical evidence about the structure of the surface. It is the purpose of this paper to provide more detailed information about the physical nature of the contact in the case of contacts with silicon carbide. The work is confined primarily to contacts between a rounded metal point and the

\* Now at Messrs. Henry Simon Ltd., Cheadle Heath, Stockport.

smoothest parts of naturally occurring 0001 crystal faces of hexagonal silicon carbide. Some of the theories which have been suggested involve the assumption that some layer of foreign material is present at the face, and this work was undertaken in an attempt to decide whether the peculiar electrical properties are associated with a gross detectable layer of contaminating material overlying the face.

## § 2. THE HYPOTHESIS OF THE INSULATING LAYER

There is in the literature a considerable amount of evidence to suggest that an overlying layer of foreign material is commonly present at the face of silicon carbide crystals. Sand is one of the principal raw materials used in the preparation of carborundum, and the presence of films of silica on the silicon carbide crystal faces cannot be regarded as unlikely. Many of the crystal faces show interference colours. Finch and Wilman (1937) have investigated the 0001 faces by electron diffraction and have shown that layers, probably of silica and upwards of 50 Å. in thickness, do exist on some crystals. Finch and Wilman showed that such layers can be removed by chemical action and by abrasion.

E. W. J. Mitchell has shown that a crystal heated to 1,800–2,000° C. for a few minutes in a bell-jar containing air at very low pressure ( $10^{-5}$  mm. Hg) possesses on cooling an ohmic contact resistance.

This experiment has been regarded as consistent with the assumption that an initial silica layer has been evaporated from the crystal plane. It has also been shown that subsequent slow heating in air to temperatures above that at which carbon rapidly combines with oxygen (800° C.) leads to a reversion to a non-linear voltage-current characteristic. This experiment has been interpreted as the removal of carbon atoms from the surface of the lattice by oxidation and the conversion of the freed silicon ions to silica.

The electron diffraction evidence of existence of contaminating layers is quite definite, but it must not be implied that such layers are always present; on the contrary, Germer (1936) has indicated that some crystals show electron diffraction patterns characteristic of a clean crystal face. It is clearly important that direct correlation be made between the known "cleanliness" of the surface as determined by electron diffraction and the electrical behaviour of the contact.

A series of experiments was therefore made to determine:

- (i) whether the average electrical characteristics are consistently different between two groups of crystals, one group being formed of crystals with demonstrably obscured 0001 faces and the other with relatively uncontaminated faces;
- (ii) whether crystal faces covered with amorphous layers lose their non-ohmic contact resistance when cleaned of contaminating layers so as to leave demonstrably clean single crystal patterns;
- (iii) whether electron diffraction investigations of the surface of crystals which have been heated to 1,800° C. *in vacuo* show the single-crystal patterns of silicon carbide required by the hypothesis that the cause of the change in electrical properties is evaporation of silica from the crystal face;
- (iv) whether the electrical properties of a face showing demonstrably clean single crystal patterns vary substantially when the face is covered with known thicknesses of evaporated silica.

Finally, a careful attempt was made to estimate the effectiveness of the electron diffraction criterion of cleanliness of surface by determining the minimum thickness of a silica layer superposed on a clean face which would be detectable in terms of perceptible obscuration of the electron diffraction pattern. This determination has made it possible to say that if the basic mechanism is to involve a surface layer physically distinct from the bulk semiconductor, the mechanism must be effective for a layer no thicker than that just perceptible by electron diffraction.

### § 3. APPARATUS

The main apparatus consists on the one hand of an electron diffraction camera and on the other of the electrical contact assembly. The electron diffraction camera is of conventional design and is of the variety supplied commercially by Metropolitan-Vickers Electrical Co. Ltd. The camera is continuously pumped by an oil-diffusion pump; the electron gun is of the thermionic type with biased Wehnelt-cylinder. The acceleration voltage is roughly 56 kv. and is stabilized electronically. An auxiliary gun is fitted and its accelerating voltage and filament current chosen so as to prevent any accumulation of charge which might otherwise collect on the crystal face because of the departure from unity of the secondary-electron coefficient of the silicon carbide face. A camera distance of 21 cm. was normally used during the experiment and the diffraction patterns were recorded on Ilford Photomechanical Plates. The apparatus is shown in cross-section in Figure 1. The contact assembly consists of a cup-shaped metal

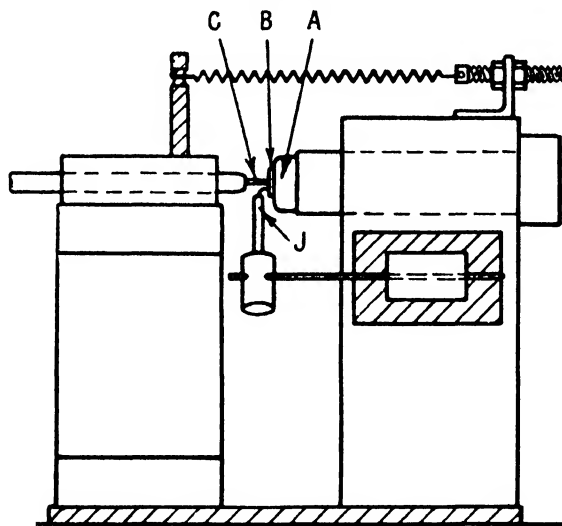


Figure 1. Contact assembly.

holder A supporting the crystal B and secured to the general framework of the apparatus, together with a metal electrode C held with a known pressure in contact with the crystal face by means of a tension spring. It is carefully designed to allow the complete removal and replacement of the crystal from the assembly without disturbing the fixity of location of the contact. It is considered that the location is held to within a few microns. The crystal cup is arranged so as to fit the specimen holder of the electron diffraction camera and the crystal is sufficiently rigidly attached by Wood's metal to the cup to allow the surface of the crystal to be abraded with metallurgical polishing papers.





magma and therefore had not been subjected to the severe chemical cleaning which is customary in the late stages of the preparation of silicon carbide for industrial purposes. As a result of preliminary investigation it was found that the crystal faces could be effectively cleaned of grease by immersion in pure chloroform and careful drying with clean filter paper.

A typical crystal used in the experiment was crushed, and examined by x rays in a powder camera. The results showed evidence of the presence of SiC in the following hexagonal forms: I, II, III, and IV (for nomenclature see Thibault 1944).

The electrical characteristics of each particular contact were obtained by recording voltage across the crystal face for given currents for a complete cycle of increasing and decreasing current in each direction of flow of current. Preliminary tests showed a tendency for the characteristics measured immediately after forming the contact to be occasionally a little unstable (voltage high for a given current). The voltage-current curve becomes more stable after a few cycles and a standard practice was therefore adopted of completing with fair rapidity half a dozen cycles before recording the readings. When care is taken to control the location of the probe and the pressure at the contact, the voltage-current characteristics of a given smooth crystal face prove to be reasonably stable. Graphs are shown in Figure 3 of characteristics of four consecutive points spaced at 0.5 mm. along the arc of a circle in a smooth crystal face, and these curves are seen to be of very similar, but decided non-ohmic, shape and of closely similar slope at any one current.

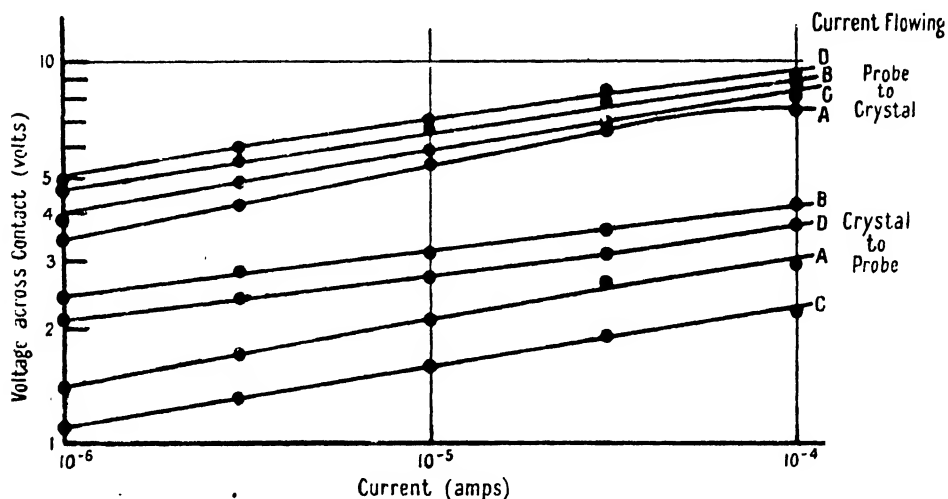


Figure 3. Change in contact characteristic with translation of probe.

#### § 4. EXPERIMENTAL RESULTS

##### (i) Behaviour of Untouched Crystals

An inspection of degreased faces of crystals chosen at random showed a wide variety in the degree of obscuration of the single-crystal pattern known to be typical of 0001 faces of hexagonal silicon carbide (Germer 1936, Finch and Wilman 1937). Some faces showed clear patterns of Kikuchi lines; others showed little but the "halo-pattern" typical of a non-crystalline layer. A batch

of crystals exhibiting fairly clean single crystal patterns and a second batch showing extensive halo-patterns were selected from a group of otherwise apparently similar crystals; the electrical characteristics of the contacts formed between a constant metal probe and each crystal face in turn are shown in Figure 4. The following is the order of decreasing obscurity of crystal face: 21, 11, 19; 12, 17, 14.

#### (ii) *Effect of Abrasion*

A second experiment of similar type was then proceeded with. A second set of six crystals showing some degree of obscuration of the single-crystal pattern was chosen. The electrical characteristics of the definitely located contact between the gramophone needle and the face were determined for the face in its initial (degreased) state. The surface was then lightly abraded with metalurgical polishing paper (Naylor & Co. Stockport No. 0), and the electron diffraction pattern redetermined. The abrasion was repeated until the surface film was so thin that the silicon carbide Kikuchi pattern appeared imperceptibly obscured. Plates 1 and 2 show the corresponding electron diffractions typical of the surface before and after abrasion. The electrical characteristics were then redetermined. The experiment was carried out carefully for each of the crystals and the typical results are shown for two such crystals in Figures 5 and 6. The electrical characteristics are little changed in slope or position after the abrasion and show the typical failure of Ohm's law for such contacts. It was found that black and green crystals behaved in similar fashion in the experiment.

#### (iii) *Effect of Etching with Hydrofluoric Acid*

The above experiment was repeated using, instead of abrasion, treatment with hydrofluoric acid to clean the surface of the crystal. This method proved equally effective as evidenced by electron diffraction. Here again the electrical characteristic showed no significant change.

#### (iv) *Effect of Heating Crystals in Vacuo*

Three crystals were chosen which showed some evidence at least of single crystal pattern. These crystals were heated *in vacuo* ( $10^{-5}$  mm. Hg), the temperature being momentarily raised to  $2,000^{\circ}$  C. On cooling in the vacuum the crystals were found, as was expected, to have ohmic contact resistances. The crystal faces were then investigated in the electron diffraction camera and were found to be heavily contaminated, usually with a polycrystalline layer of material of such thickness that many abrasions were quite ineffective in restoring to view the Kikuchi pattern typical of the unobscured crystal lattice of silicon carbide. A typical pattern taken after heating in the vacuum is shown in Plate 3.

#### (v) *Effect of an Artificial Layer of Silica*

Crystals were selected and cleaned by abrasion so as to yield clean single-crystal patterns. The contact characteristics were determined for this condition of the surface and for successive cases in which the crystal was covered by evaporation with increasing known thicknesses of silica. The depth of the film of silica on the crystal face was determined in the following manner. A small length (2 mm.) of fused silica rod  $\frac{1}{2}$  mm. in diameter is supported by means of two closely spaced parallel tungsten wires (0.4 mm. diam.). The crystal is mounted, face

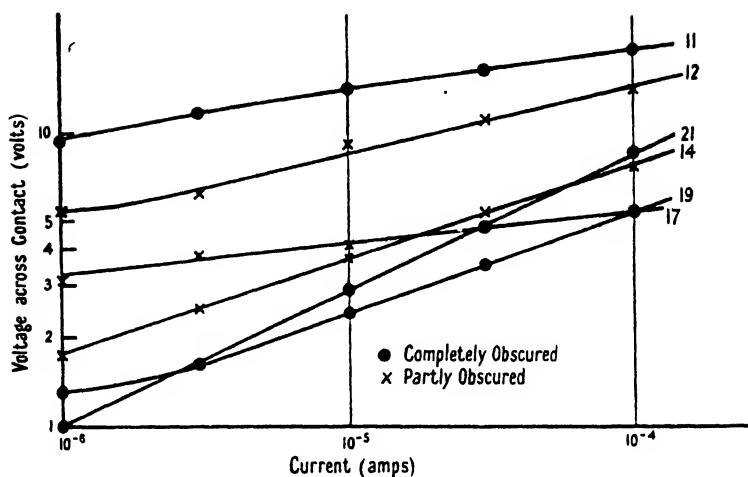


Figure 4. Voltage-current characteristics for various untreated crystals.

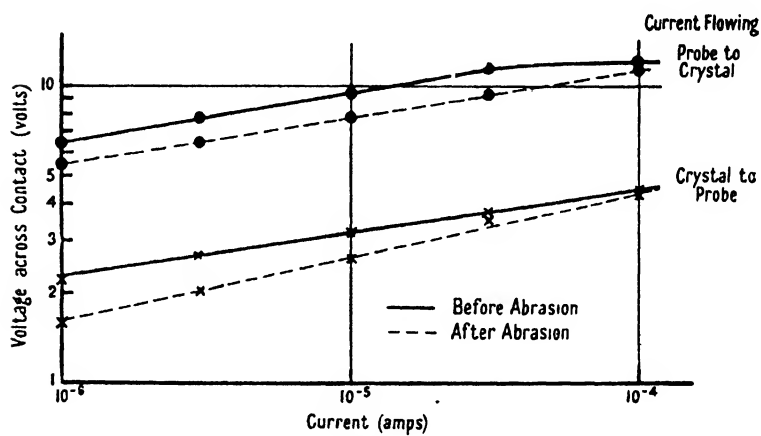


Figure 5.

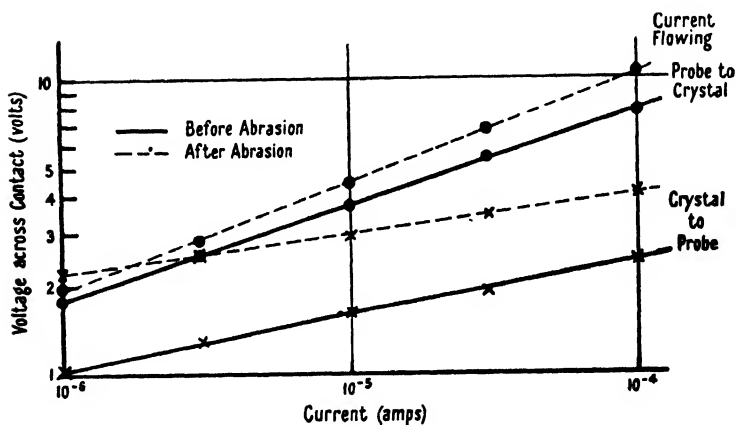


Figure 6.

downwards, on a support 15 cm. above the silica. A square piece of glass cut from photographic plate is mounted horizontally at about a third of the distance of the crystal away from the silica. Half the lower surface of the glass is screened from the source by fixing a piece of thin brass foil closely in contact with the glass. The air-pressure in the space surrounding the apparatus is then reduced to about  $10^{-5}$  mm. of mercury and the silica evaporated by passing a suitable current through the filament. Silica from the filament falls on the glass plate as well as on the specimen and coats the unobscured parts of the plate. Since the source is small, the depth of the film on the plate is proportionately greater than that at the specimen by a factor equal to the inverse of the square of their corresponding distances from the source, provided that the test plate lies closely in the same direction as the specimen relative to the source. After the evaporation

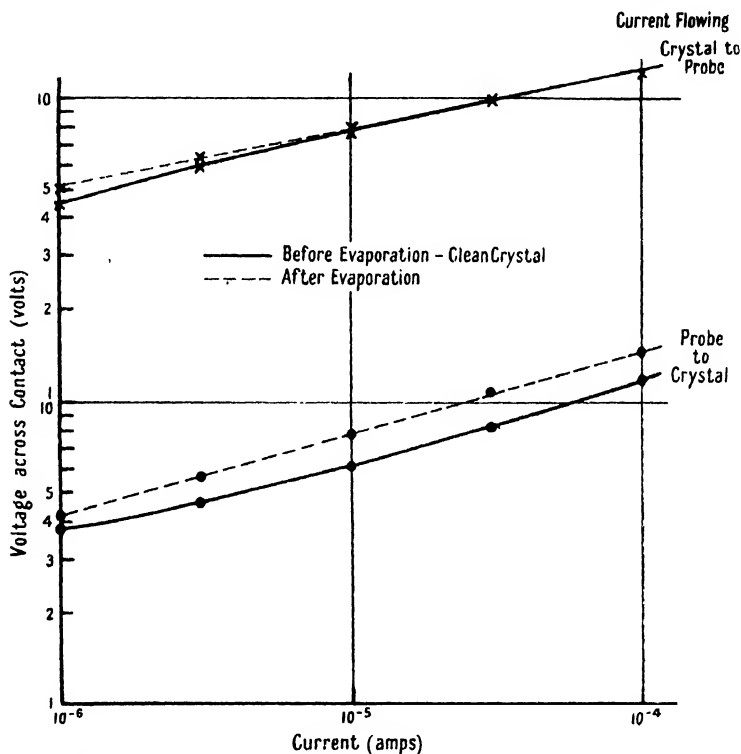


Figure 7. Effect of a thick layer (90 Å.) on contact characteristic.

process the glass test-plate is removed from the system and silvered by evaporation to a depth of about 500 Å. By this process a step is reproduced in the top surface of the silver film of depth equal to the thickness of the silica. This plate is then used in conjunction with a similarly silvered blank plate in a multiple-beam interferometer arrangement of the type used by Tolansky (1948), and from photographs of the fringe system the height of the step is determined. Since measurements can be made by the interference technique to within, say, 10 Å., it is possible to deduce the depth of films deposited on the crystal when the film is no more than 1 Å. thick.

The results of the electrical measurements are shown in Figure 7 for the clean face and for the face when covered with the thickest layer used in the experiment (90 Å.). The characteristics are very little modified by the presence of the silica film.

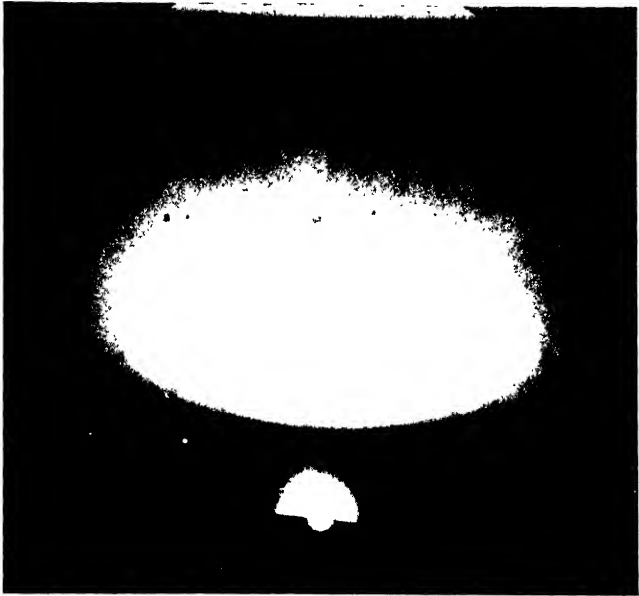


Plate 1.



Plate 2.

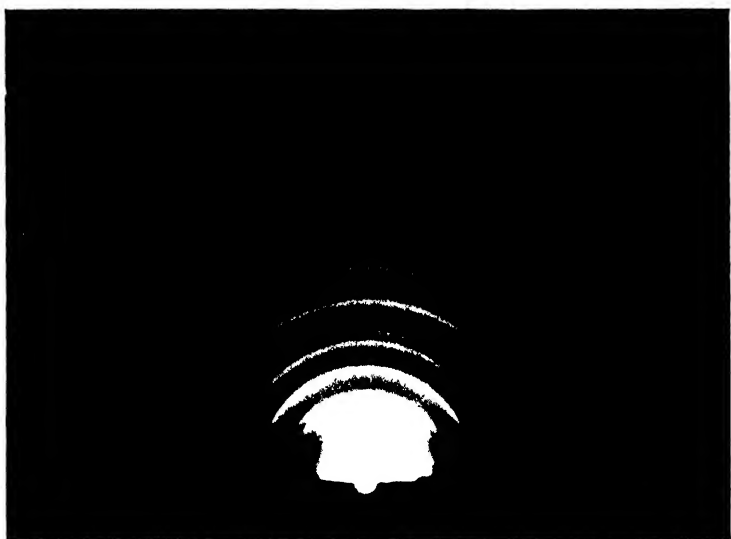


Plate 3.

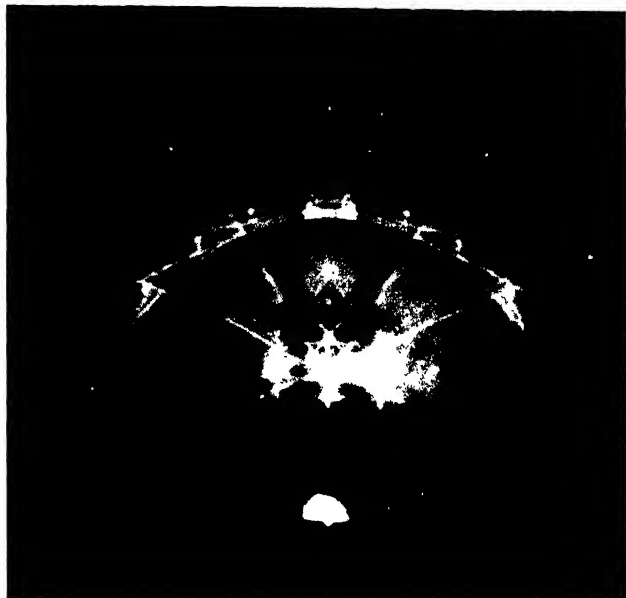


Plate 4.

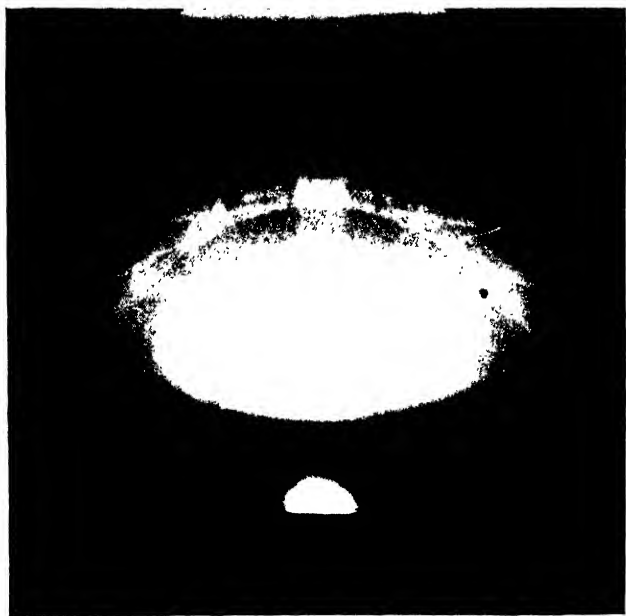


Plate 5.





(vi) *Sensitivity of the Electron Diffraction Test*

The results of the experiments described above show that the non-ohmic contact resistance of silicon carbide faces is not of necessity associated with the thick amorphous layer. In particular, a crystal face from which the amorphous material has been removed to a sufficient extent for the face to yield a clear-cut single-crystal pattern is not appreciably modified in its electrical characteristics by the process. In assessing the importance of this conclusion it is necessary to know how sensitive is the electron diffraction test for the presence of the amorphous film, for it is conceivable that the non-ohmic characteristic of the contact resistance is due to a residual film too thin to be detected by electron diffraction.

Finch and Wilman (1937) have already shown that a monolayer of a paraffin  $C_{32}H_{66}$  of depth known from the geometry of the molecule to be 43 Å. is just sufficient to obscure the crystal pattern. In this work it was more desirable to determine the thickness of the amorphous material that would lead to just perceptible obscuration of the single-crystal pattern. To this end a crystal which showed a sharply defined single-crystal pattern was selected and its surface lightly abraded so as to make sure that any overlying layer had been reduced to a minimum. An electron diffraction pattern of the face in this condition is shown in Plate 4. Thin amorphous films of silica of measured thickness were then evaporated on to the crystal face and after each evaporation a diffraction pattern was recorded. The diffraction patterns were taken for a fixed orientation of the crystal relative to the beam; the beam was incident on the crystal surface at an angle of about 2 degrees. The operating conditions of the camera were carefully controlled. Plates 4 and 5 show patterns taken with a clean face, and with a thickness of 10 Å. of silica on the face. Control patterns were taken at various stages in the experiment to confirm that the pattern of the fully abraded crystal had not deteriorated. Clear evidence can be seen in the original negatives of increased diffuseness, particularly in the central region of the pattern, even in the case of a 3 Å. layer.

## § 5. CONCLUSION

The main conclusion to be drawn from our experimental work is that the occurrence of non-ohmic contact resistances at the interface between a rounded metal probe and a smooth crystal face of silicon carbide does not depend on the presence of a detectable film of foreign material on the surface of the crystal. The principal evidence comes from the close similarity in electrical characteristics of a contact successively made under otherwise identical conditions with a naturally obscured crystal surface, and with the same surface after removal of the foreign material by abrasion. The subsidiary experiments suggest that the surface is certainly that of a lattice plane not covered by more than a few molecules of foreign material; any layer of silica-like material could not be more than 5 Å. thick and is probably less than 3 Å. It may well be remarked in this connection that such a surface is as clean as one might expect a surface to be in the light of the evidence that solids in general acquire layers of absorbed gas atoms when exposed to a gaseous atmosphere.

The fact that no foreign surface layer is necessary to produce non-ohmic behaviour is not surprising, and plausible explanation in terms of space-charge barrier layers is possible. It is, however, a little unexpected to find that a layer

of evaporated silica 90 Å. thick produces no significant change in electrical characteristics. Possible explanations of this observation are:

- (1) The film is mechanically displaced or damaged by the steel probe.
- (2) The film has suffered electrical breakdown before any readings of current were taken.
- (3) The film offers no appreciable resistance to the passage of electrons.

Such experimental evidence on thin  $\text{SiO}_2$  films as is available (Plessner 1948) suggests that explanations (2) and (3) are unlikely, without at least some contribution due to mechanical damage.

Little significance can be attached to the evidence that comes from the ohmic behaviour of crystal faces that have been heated *in vacuo* to  $2,000^\circ\text{C}$ . This evidence appeared to suggest that the ohmic behaviour might be associated with a clean lattice face exposed by evaporation of silica, or similar material, from the face of the crystal; the electron diffraction evidence clearly shows that, far from possessing a clean face, the crystal is covered with a thick tenacious film of polycrystalline material after the heat-treatment.

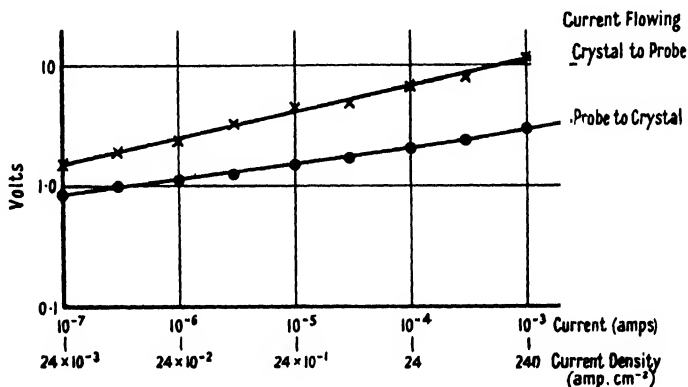


Figure 8.

The numerical value of the ohmic contact resistance in one typical case of a crystal heated to about  $2,000^\circ\text{C}$ . was about  $10^4$  ohms for a contact area which from the flattening of the contact point was estimated to be about  $4 \times 10^{-5}\text{ cm}^2$ . This contact resistance is much too high to be accounted for by the "spreading resistance" at the contact with a material of bulk conductivity equal to that of silicon carbide, and must be attributable to contact with a contaminating layer of much lower conductivity.

The absence of an appreciable non-ohmic contribution from the silicon carbide crystal face is due to the smallness of this component consequent upon the wide distribution of current at the interface between the crystal and the contaminating layer. Moreover the wide distribution of the current at the silicon carbide face implies a low current density at the surface, and measurements on the contacts of all types indicate that the electrical characteristic of silicon carbide is essentially ohmic when the current density is small enough.

The electrical measurements of contact resistance which form one part of the evidence of the investigation are themselves interesting, since measurements refer to contacts of definable geometry for which the area of contact can be estimated with fair accuracy. The electrical characteristics are stable and repeatable to

within a few tens per cent for any assigned position of the initially rounded (but necessarily flattened) steel probe when held with a definite force against a surface which is atomically smooth over the area of contact. Translation of the probe in the face of the crystal leads to relatively small changes in the shape and position of the voltage-current curve, provided care is taken to keep to smooth areas of the face. The change in characteristic from crystal to crystal is usually rather less than one order of magnitude in voltage provided that the force is held at a constant value and that the crystal surface is devoid of pits and scratches. Figure 8 shows a typical characteristic taken for a long range of current; the lower of the two abscissa scales gives the current density at the contact on the assumption that the area of contact is  $4.1 \times 10^{-5} \text{ cm}^2$ . This value for area of contact is that of the visibly flattened portion of the tip and is presumably an underestimate. The area of contact calculated from Hertz's analysis of elastic deformation at the conjunction of a sphere and a plane is  $1.6 \times 10^{-6} \text{ cm}^2$ , but the assumption of perfect elasticity is not acceptable for these stresses.

## ACKNOWLEDGMENTS

The authors wish to acknowledge the assistance of Mr. E. W. J. Mitchell for his co-operation in many points of the work, and of Mr. A. W. Agar for his help in the early part of the investigation. We wish to express our thanks to Mr. F. R. Perry for his interest and encouragement, and to Mr. B. G. Churcher, Manager of the Research Department, and Sir Arthur P. M. Fleming, Director of Research and Education, Metropolitan-Vickers Electrical Co. Ltd. for permission to publish this paper.

## REFERENCES

- FINCH, G. I., and WILMAN, H., 1937, *Trans. Faraday Soc.*, **33**, 337.  
GERMER, L. H., 1936, *Phys. Rev.*, **49**, 163.  
HERTZ, H., 1896, *Theory of Hardness and Area of Contacts* (London: Macmillan).  
MITCHELL, E. W. J., and SILLARS, R. W., 1949, *Phys. Soc. Proc. B*, **62** (in press).  
PLESSNER, K. W., 1948, *Proc. Phys. Soc.*, **60**, 243.  
THIBAUT, N. W., 1944, *Amer. Mineralogist*, **29**, 327.  
TOLANSKY, S., 1948, *Multiple-Beam Interferometry of Surfaces and Films* (Oxford: Clarendon Press).

## The Structure and Epitaxy of Lead Chloride Deposits Formed from Lead Sulphide and Sodium Chloride

By A. J. ELLEMAN AND H. WILMAN

Applied Physical Chemistry Laboratories, Imperial College, London

*MS. received 17th December 1948 ; read at Science Meeting at  
Manchester 9th December 1948*

**ABSTRACT.** Electron diffraction shows that  $\text{PbCl}_2$  is formed instead of  $\text{PbO} \cdot \text{PbSO}_4$  when mosaic single-crystal PbS layers a few hundred Å. thick are heated on their NaCl substrates in air at 200–300° C. The structure and orientation of these  $\text{PbCl}_2$  layers are described. This example of epitaxial crystal growth is particularly interesting because the  $\text{PbCl}_2$  atoms adjacent to the, at least initially, atomically smooth PbS surface do not lie exactly in a single close-packed plane atomic sheet, but the atomic arrangement closely matches that of the PbS substrate in a series of parallel bands. When the composite  $\text{PbCl}_2$ -PbS layers were isolated from their NaCl substrate the transmission patterns showed that they must have partly broken up, leading to curvature about remarkably well-defined axes parallel to the film plane and PbS cube-face diagonals.

### § 1. INTRODUCTION

WHEN lead sulphide layers on single-crystal rocksalt substrates are heated *in vacuo* there is an increase in crystal size and in certain cases a preferential growth of crystals in different orientations from those initially predominant in the layer, these changes taking place to an extent which depends on the temperature and duration of heating (Elleman and Wilman 1948). On the other hand when lead sulphide layers are heated in air at 350° to 500° C. after dissolving away the sodium chloride substrate crystal and drying, they are converted into the cxsulphate, lanarkite,  $\text{PbO} \cdot \text{PbSO}_4$  (Wilman 1948).

Experiments to determine the orientation of the  $\text{PbO} \cdot \text{PbSO}_4$  crystals relative to the PbS crystals from which they are formed have now shown that when "single-crystal" PbS layers are heated in air at 200° to 300° C. on their rocksalt substrates no  $\text{PbO} \cdot \text{PbSO}_4$  appears but a layer of lead chloride,  $\text{PbCl}_2$  (cotunnite), is quickly formed on their upper surface, even when the PbS layer is 250 Å. thick and is made up of crystals at least 500 Å. in lateral diameter, with atomically smooth cube-face surfaces. The structure and orientation of these  $\text{PbCl}_2$  layers are described below and lead to lattice constants and diffraction intensities which agree closely with previous crystallographic and x-ray data. The details of the epitaxial orientations and atomic fitting of the  $\text{PbCl}_2$  with respect to the PbS crystals are particularly interesting because the substrate surface was known (Elleman and Wilman 1948) to be almost atomically smooth initially and the deposit atoms adjacent to the substrate surface do not lie in a close-packed plane atomic sheet. The atomic arrangement, however, is found to match closely that of the substrate in a series of parallel strips.

### § 2. EXPERIMENTAL

The PbS deposits on NaCl cleavage faces were prepared as already described (Elleman and Wilman 1948) so as to obtain untwinned deposits with highly smooth surface. They were heated in atmospheric air in the laboratory and were examined

by electron diffraction immediately after preparation. A Finch type electron-diffraction camera was used (Finch and Wilman 1937a) with 50–60 kv. electrons and a camera length about 50 cm. Transmission specimens were prepared by dissolving away the NaCl so as to leave the PbS film floating on the water surface, and without further washing they were lifted off and dried *in vacuo* so as to leave a trace of NaCl thus remaining on the PbS film. Eight deposits were examined by reflection after heating in air at between 200 and 300° c., and Table 3 (p. 348) shows the relation of the surface composition to the thickness and orientation of the initial PbS deposit.

### § 3. THE STRUCTURE AND ORIENTATION OF THE $\text{PbCl}_2$ DEPOSITS

#### (i) *Random Transmission Specimens; Identification as $\text{PbCl}_2$*

Figure 1 shows the ring pattern from randomly disposed crystals of the reaction product, together with the stronger arcs and some rings due to the remaining PbS, which was evidently much distorted or bent because of break-up and sagging in the meshes of the supporting nickel gauze. Table 1 gives the intensities and the net-plane spacings, calculated on a basis of  $a = 5.929$  Å. for the PbS cubic axis (Wilman 1948, Elleman and Wilman 1948). The x-ray data for  $\text{PbCl}_2$  powder patterns are also given in Table 1 and show that the reaction product was lead chloride with axial lengths of the rhombic lattice close to those found by x rays. Further confirmation of this identification was supplied by transmission patterns (Table 1) from  $\text{PbCl}_2$  (random crystals approximately 500 Å. in diameter) precipitated from hot aqueous solution and sublimed *in vacuo* on to collodion films. Table 2 gives the axial lengths and ratios previously estimated for  $\text{PbCl}_2$ .

The electron-diffraction spacings in Table 1 are mostly slightly higher than the recent x-ray values. A mean value of  $c = 9.035$  Å. was obtained from the pairs of spacings for 101 and 103, 101 and 105, 111 and 113, 111 and 115, 020 and 023, and 031 and 032. The value of  $a$  calculated independently from 012 and 212, 002 and 202, 200 and 111 and 311, 022 and 222, and 122 and 222, was 4.530 Å. For  $b$  a mean value 7.611 Å. was obtained from the pairs of spacings 111 and 121, 111 and 131, 121 and 131, 011 (and 022/2) and 031, 031 and 041, 012 and 032, and from 020 and 040. By assuming the  $a$  and  $c$  values to be reliable, a slightly more representative mean value of  $b$  was obtained from the spacings of the diffractions 012, 110, 020, 111, 120, 022, 121, 122, 031, 023, 130, 032, 131, 132, 221 and 041, the mean being 7.614 Å. The axial lengths are thus  $a = 4.530$ ,  $b = 7.614$ ,  $c = 9.035$  Å. and  $a : b : c = 0.5950 : 1 : 1.187$ . For the sublimed  $\text{PbCl}_2$  also (Table 1)  $a : b : c = 0.5950 : 1 : 1.187$ .

The electron-diffraction spacings and estimates of the axial ratios thus correspond well with those found in x-ray powder patterns, apart from a small difference in axial lengths. It may be noted that since Straumanis and Sauka (1942) did not state the wavelength they attributed to their x rays it is impossible to determine whether or not their axial lengths are in kx. units, requiring a multiplying factor of 1.00202 (Bragg 1947) to convert them to ångströms. The electron-diffraction ring intensities also show mainly a similarity with those of the x-ray patterns, and the differences are presumably partly due to different crystal shape and size, leading to different degrees of absorption in the various diffractions (cf. Wilman 1948).

No trace of any other compound was found. If  $\text{Na}_2\text{S}$  is formed in the reaction it would be attacked by moisture and oxygen in the air, forming compounds which would be easily volatilized.

Table 1. Plane Spacings,  $d$ , and Ring Intensities,  $I$ , from random  $\text{PbCl}_2$  Crystals

Indices		Electron diffraction					x-ray diffraction		
$\text{PbCl}_2$ (rings)	$\text{PbS}$ (arcs)	$\text{PbCl}_2 + \text{PbS}$ (Figure 1)			$\text{PbCl}_2$ sublimed		Powdered $\text{PbCl}_2$		
		$d^*$ (Å.)	$I^\dagger$	$d_{\text{calc.}}^\ddagger$	$d$	$I^\dagger$	$d_{\text{calc.}}^\S$	$d_{\text{ASTM.}}^  $	$I_{\text{ASTM.}}^  $
011	—	5.83	F	5.821	—	—	5.815	—	—
002	—	4.51	MF	4.517	4.52	MF	4.513	4.49	0.4 B
101	—	4.053	M	4.048	4.062	M	4.045	4.03	0.4 B
012	}	3.888	M	3.883	3.890	M	3.880	3.88	0.7
110				3.892			3.888		
020	—	3.795	MF	3.807	3.816	M	3.802	3.79	0.6 B
111	—	3.579	MS	3.574	3.580	MS	3.571	3.57	1.0
—	111	3.418	M	—	—	—	—	—	—
112	200	2.964	S	2.948	2.944	MF	2.945	—	—
120	}	2.916	M	2.914	2.919	MF	2.911	2.91	0.6 B, 0.2 D
022				2.911			2.907		
121	—	2.779	MS	2.773	2.779	S	2.770	2.76	0.8
103	—	2.508	M	2.507	2.511	MS	2.505	2.50	0.8
122	}	2.445	M	2.448	2.446	F	2.446	2.43	0.2 D
031				2.443			2.441		
113	—	2.380	MF	2.381	2.380	F	2.379	2.37	0.3
023	—	2.362	MF	2.362	2.364	F	2.359		
200	}	2.268	M	2.265	2.265	S	2.262	2.26	0.7
004				2.259			2.256		
130	}	2.213	M	2.214	2.213	MF	2.212	2.21	0.6
032				2.212			2.211		
131	—	2.155	M	2.150	2.156	M	2.149	2.15	0.8
123	220	2.096	S	2.094	2.096	M	2.092	2.09	0.8
202	}	2.025	MF	2.024	2.025	F	2.022	—	—
104				2.021			2.019		
132	—	1.994	F	1.988	—	—	1.987	—	—
212	}	1.953	M	1.956	1.951	M	1.955	1.98	0.2 B
114				1.953			1.952		
221	—	1.901	F	1.907	1.902	VF	1.901	—	—
041	—	1.859	F	1.863	1.860	VF	1.860	—	—
222	}	1.787	MS	1.787	1.787	F	1.786	—	—
133				1.784			1.782		
124				1.785			1.783		
213				1.760			1.759		
015	}	1.760	F	1.758	1.760	F	1.756	—	—
140				1.755			1.753		
042				1.754			1.752		
141	222	1.711	MF	1.722	1.719	VF	1.720	—	—
105	—	1.682	F	1.678	1.682	MF	1.676	—	—
231	—	1.662	F	1.661	—	—	1.660	—	—
115	}	1.636	M	1.639	1.638	M	1.637	—	—
142				1.636			1.634		
223				1.634			1.633		
025				1.632			1.630		
204	—	1.600	F	1.599	1.600	F	1.598	—	—
134	—	1.582	MF	1.581	1.582	MS	1.580	—	—
214	—	1.567	F	1.565	—	—	1.563	—	—
125	—	1.537	VF	1.535	—	—	1.534	—	—
143	—	1.518	VF	1.516	1.517	F	1.514	—	—

Table 1 (cont.)

Indices		Electron diffraction				x-ray diffraction				
PbCl <sub>2</sub> (rings)	PbS (arcs)	PbCl <sub>2</sub> +PbS (Figure 1)			PbCl <sub>2</sub> sublimed		Powdered PbCl <sub>2</sub>			
		d* (Å.)	I†	d <sub>calc.</sub> †	d	I†	d <sub>calc.</sub> §	d <sub>ASTM.</sub>	I <sub>ASTM.</sub>	
016	400	1.482	S	1.477	1.476	F	1.476	—	—	
224				1.474			1.473			
233				1.473			1.472			1.471
035				1.472			1.460			
311	—	1.460	MF	1.461	1.460	M	1.460	—	—	
240				1.457			1.455			1.455
044				1.455			1.442			1.437
241				1.442			1.438			1.437
151	—	1.426	MF	1.425	1.427	MF	1.424	1.423	0.6 D	
106				1.429			1.429			1.429
116				1.404			1.403			1.403
320				1.403			1.402			1.402
026	—	1.403	M	1.400	1.402	M	1.399	1.399	0.8 D	
321				1.386			1.385			1.385
144				1.386			1.384			1.384
234				1.353			1.352			1.352
303	331	1.356	MF	1.349	1.350	MF	1.348	1.348	0.6 D	
—	420	1.326	MS	—	—	—	—	—	—	

\* Relative to  $a_{\text{PbS}} = 5.929$  Å. (5.917 kx.) (Wilman 1948, Elleman and Wilman 1948).

† S=strong, M=medium, F=faint, V=very.

‡ Using  $a=4.530$ ,  $b=7.614$ ,  $c=9.035$  Å.

§ Using  $a=4.52476$ ,  $b=7.60446$ ,  $c=9.02666$  (Straumanis and Sauka 1942, 18° C.)

|| Supplement File of x-ray powder-pattern data, 1945, published by the American Society for Testing Materials. B and D refer to intensity estimates by Bräkken (1932) and Döll and Klemm (1939) respectively.

Table 2. Axial Lengths and Axial Ratios of  $\text{PbCl}_2$ 

Axial lengths			Axial ratios			Reference
<i>a</i>	<i>b</i>	<i>c</i>	<i>a</i>	: <i>b</i> :	<i>c</i>	
<i>Optical Goniometer</i>						
—	—	—	0.5951	: 1 :	1.1882	Schabus (1850) (reoriented)
			0.5952	: 1 :	1.1872	Groth (1906) from Stöber (1895)
			0.5947	: 1 :	1.1855	Zambonini (1910)
<i>X-ray Diffraction</i>						
4.496	7.667	9.153	0.5864	: 1 :	1.193	Bräkken and Harang (1928)
4.523	7.618	9.037	0.5938	: 1 :	1.186	Miles (1931)
4.525	7.608	9.030	0.5947	: 1 :	1.187	Bräkken (1932)
4.520	7.605	9.027	0.5947	: 1 :	1.188	Döll and Klemm (1939)
4.52476	7.60446	9.02666	0.594501	: 1 :	1.18702	Straumanis and Sauka (1942)*
4.52583	7.60648	9.02772	0.59499	: 1 :	1.18684	Straumanis and Sauka (1942)†
<i>Present Electron Diffraction Results</i>						
4.530‡	7.614‡	9.035‡	0.5950	: 1 :	1.187	Present results

\* At 18° C. † At 25° C. ‡ Values in Å. relative to  $\text{PbS}$ ,  $a=5.929$  Å. (5.917 kx.)



(ii) *Reflection Specimens*

Table 3 describes eight PbS specimens examined by reflection, with their thickness, orientation, duration of heating at 200° c., and whether or not the patterns contained PbS as well as PbCl<sub>2</sub> diffractions. In all cases the PbCl<sub>2</sub> was in the same two-degree orientations relative to the {001}-orientated PbS crystals, whose axes were parallel to those of the NaCl substrate crystal. The orientations shown by the patterns are of three types: (i) {010}, (ii) {012}, and (iii) {110} parallel to the {001} PbS surface plane. In (i) and (ii) *a*, and in (iii) *c*, of the PbCl<sub>2</sub> was parallel to  $\langle 110 \rangle$ ,  $\langle \bar{1}\bar{1}0 \rangle$ ,  $\langle \bar{1}10 \rangle$  or  $\langle 1\bar{1}0 \rangle$  of the PbS.

Figure 2 is the pattern obtained with the electron beam directed along the PbS cube-face diagonal in its (001) surface. The directions of the PbCl<sub>2</sub> axes as seen when looking along the cube-face diagonals of the PbS are shown in Figure 6 for the above orientations which, as just indicated, fall into three groups with four in each group corresponding to the four-fold symmetry of the (001)

Table 3. Results of Heating PbS on {001} NaCl Substrates in Air at 200–300° c.

PbS Thickness	PbS Orientation on {001} NaCl	Time of heating (min.)	Substances observed by diffraction *
50 A.	{001}	5	PbCl <sub>2</sub>
	{001} + {111}	10	{001} + {111} PbS
250 A.	{001}	5	{001} PbS + PbCl <sub>2</sub>
	{001}	5	PbCl <sub>2</sub>
	{001}	5	{001} PbS + PbCl <sub>2</sub>
	{001}	20	PbCl <sub>2</sub>
	{001} + {111}	45	{001} + {111} PbS + PbCl <sub>2</sub>
1000 A.	{001}	10	{001} PbS

\* The PbCl<sub>2</sub> was in each case in the same orientations with respect to the {001} orientated PbS crystals. The orientations are given in the text.

PbS surface plane. The composite diffraction pattern at this azimuth, resulting from PbCl<sub>2</sub> in these orientations (in the region within about 3 cm. from the undeflected beam spot), accounts for all but a few of the spots visible in Figure 2, with good agreement of the relative intensities with those recorded for the corresponding x-ray diffractions. Figure 6 is an enlarged diagram showing the spot positions in this central part of the pattern and the unit parallelograms of the spot patterns associated with the different PbCl<sub>2</sub> orientations. The spots due to the {010}-orientated PbCl<sub>2</sub> crystals are laterally sharp but are slightly elongated towards the shadow edge, indicating crystals about 500 Å. in lateral diameter with (010) faces as their upper surfaces, parallel to the smooth PbS substrate. The sharp spots due to the other orientations are hardly elongated at all normal to the shadow edge but those due to the {012}-orientated PbCl<sub>2</sub> are arced by about 2° rotation about the undeflected-beam spot. This arcing is more apparent in Figure 4, obtained at an azimuth 1½° displaced from that of Figure 2. The positions and intensities of the remaining spots show that the {010}-orientated crystals were strongly twinned on {012} planes. Measurement of the spot separations in the reflection patterns gave axial ratios  $c/b = 1.186$  and  $c \simeq 2a$ .



Figure 1. PbS (arcs) + PbCl<sub>2</sub> (rings); normal transmission.

Figure 2. PbCl<sub>2</sub> on PbS; beam along [110] PbS.

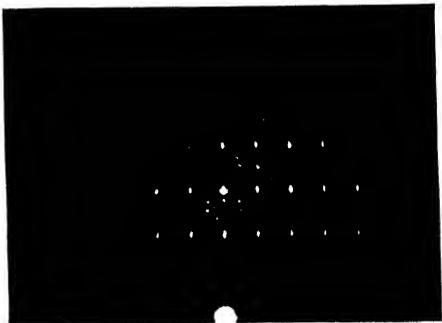


Figure 3. PbCl<sub>2</sub> (spots) + PbS (streaks); beam along [100] PbS.

Figure 4. PbCl<sub>2</sub> on PbS; azimuth 1½° from Figure 2.

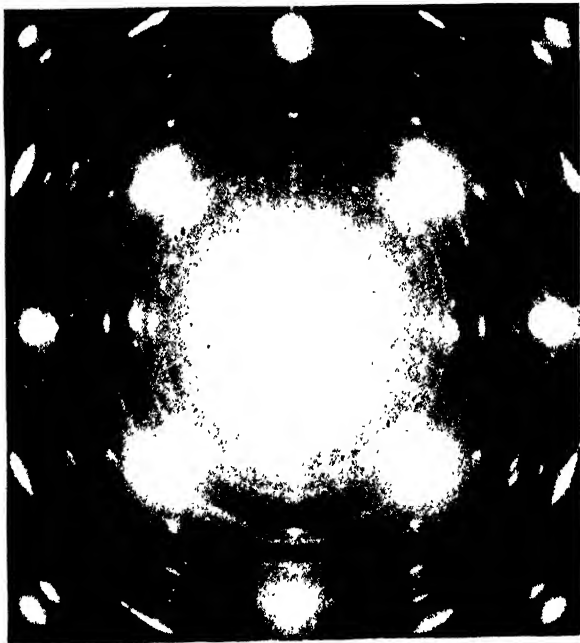


Figure 5. PbS (strong arcs) + PbCl<sub>2</sub> (short arcs and rings); normal transmission from partially broken-up film.



Figure 3 shows the pattern obtained with the beam along a  $\text{PbS}$  cube edge in the  $\text{PbS}$  substrate surface. Most of the strong spots of this pattern correspond to the  $\{010\}$ -orientated  $\text{PbCl}_2$  which was the most preferred orientation shown in Figure 2, thus in Figure 3 the beam was along a  $[201]$   $\text{PbCl}_2$  lattice row of the  $(010)$  plane, and the  $[\bar{2}01]$  row was therefore practically normal to the beam (and parallel to the specimen surface).

The following diffractions (of type  $h, k, 2h$ ) were observed above the rather high shadow edge with strong or medium intensity:—020, 040, 060 080, 0.10.0, 0.12.0, 0.14.0; 122, 142, 162; 224, 244, 264, 284.

### (iii) Transmission Patterns from the Orientated $\text{PbCl}_2$

The patterns obtained at normal transmission from the less distorted films of the  $\text{PbS}$  partially converted to  $\text{PbCl}_2$  are shown diagrammatically in Figure 7 (a). They contain only a few but sharp spots from the  $\text{PbCl}_2$  in addition to the strong  $\text{PbS}$  ones. Figure 7 (a) shows the main features near the centre

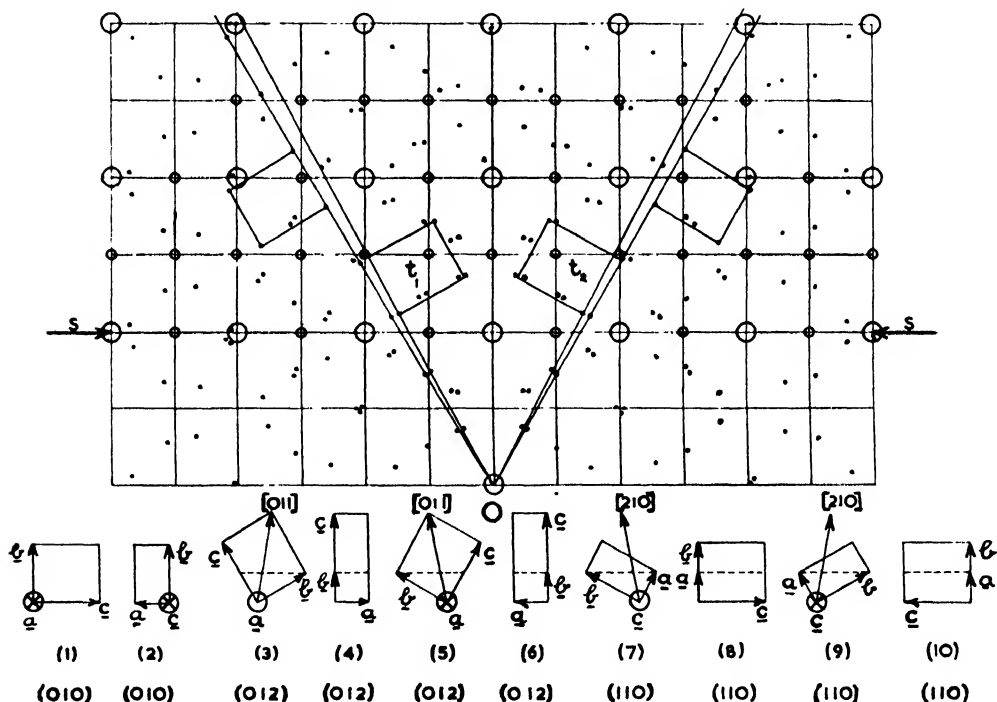


Figure 6. Spot positions in Figure 2, and their origin from the various  $(010)$ ,  $(012)$  and  $(110)$  orientations. The strong spots and weaker ones associated with the main orientations  $(010)$ , (1) and (2), are distinguished by circles;  $t_1$  and  $t_2$  show the rectangular units of the spot patterns from the  $\{012\}$  twins of the  $\{010\}$  orientated crystals (orientations (3) and (5)). S-S indicates the shadow-edge region in Figure 2.

of the pattern, together with the typical indices assigned to the diffractions. The strongest  $\text{PbCl}_2$  diffractions occurring are groups of four spots of 111 and 121 type surrounding the strong  $\text{PbS}$  200 spots; and also the spots of 200 and 032 types close within the  $\text{PbS}$  220 spots along the same radius, those of 204 type close within the  $\text{PbS}$  400 spots, and the spots of 131 type.

The occurrence, positions and relative intensities of the observed diffractions are consistent with the  $\text{PbCl}_2$  orientations established by the reflection patterns provided it is assumed that parts of the composite  $\text{PbS}$ - $\text{PbCl}_2$  film are cylindrically

curved about well-defined axes parallel to the PbS cube-face diagonals in the plane of the film. Such curvature of the remaining PbS substrate layer is shown by the occurrence and positions of PbS diffractions of  $hk1$  type, for example, in Figure 5. The amounts of curvature necessary for the appearance of diffractions of types  $h11$ ,  $h22$ ,  $h21$ , and  $h32$  from  $\{012\}$ -orientated  $\text{PbCl}_2$  and  $11l$ ,  $12l$ ,  $13l$ ,  $14l$ ,  $22l$ ,  $23l$ , and  $24l$  from  $\{110\}$ -orientated  $\text{PbCl}_2$  are shown in Figures 8 (a), (b), (c). The  $h0l$  diffractions near the central spot can arise from the  $\{010\}$ -orientated  $\text{PbCl}_2$  crystals without the need of assuming any curvature. Typical of the agreement of the intensities with those of the x-ray patterns are, for example, the absence of 100, 102, 122, the faintness of 002, 110, 011, 022, 101 and 103 and the relatively high intensity of 200, 204, 012, 032, 111, 121 and 131.

The patterns from more distorted films were as shown in Figure 5 and show even more clearly the curvature about the above well-defined axes. Figure 7 (b) shows the spot positions and intensities diagrammatically on a larger scale. The straight lines and hyperbolae represent construction lines on which the spots lie in agreement with the interpretation of Figure 5 as a superposition of rotation patterns about the two PbS cube face diagonals in the plane of the film.

The hyperbolae correspond to the loci of the intersections of the densely populated  $[001]^*$  rows in the reciprocal lattice with the sphere of reflection, which approximates to a plane normal to the beam near to the central spot, the crystals being initially in  $(012)$  orientation and rotated about the  $[02\bar{1}]$   $\text{PbCl}_2$  axis. The positions of the hyperbolae were calculated as described by Finch and Wilman (1936a) and by Goche and Wilman (1939). If  $\{012\}$ -orientated  $\text{PbCl}_2$  crystals with azimuthal orientation as in number 3 below Figure 7, are rotated about the axis OA in Figure 7 (a), then the hyperbolic loci associated with the  $[001]^*$  rows through the points  $[[hk0]]^*$  have their centres at

$$(0, \lambda Lk(4b^2 + c^2)/2b^2), \text{ i.e. } (0, 0.1511k\lambda L)$$

relative to the rectangular axes OX, OY of Figure 7 (a). Relative to the parallel axes through this centre as origin, the equations of the hyperbolae are

$$x^2c^2 - 4y^2b^2 = (\lambda L)^2 h^2 c^2 / a^2;$$

the vertices are at  $(\pm \lambda Lha^*, 0)$ , i.e.  $(\pm \lambda Lh/a, 0)$ , and the asymptotes have the equation  $y = \pm (c/2b)x = \pm 0.593x$ .

#### § 4. SUMMARY AND DISCUSSION

The main results are: (i) a reaction occurs between mosaic single-crystal PbS layers about 250 Å thick and their single-crystal NaCl substrates in presence of air at 200 to 300° C., to form  $\text{PbCl}_2$ ; (ii) no other product besides  $\text{PbCl}_2$  was observed, and in particular no formation of  $\text{PbO}$ .  $\text{PbSO}_4$  was detected; (iii) the resulting  $\text{PbCl}_2$  took up definite two-degree orientations of  $\{010\}$ ,  $\{012\}$  and  $\{110\}$  types relative to the  $\{001\}$  PbS substrate surface plane; (iv) the  $\{010\}$ -orientated  $\text{PbCl}_2$  crystals were strongly twinned on  $\{012\}$  planes and had relatively smooth  $\{010\}$  faces parallel to the substrate; (v) the  $\text{PbCl}_2$  lattice constants and relative diffraction intensities agreed closely with those found previously by x-ray diffraction; (vi) parts of the initial PbS layers and of the composite  $\text{PbS-PbCl}_2$  layers, when the layers were isolated from the NaCl substrates, became cylindrically curved about remarkably well-defined axes which were parallel to the film plane and to the PbS cube-face diagonals; (vii) this example illustrates

the fact that reflection patterns from such deposits *in situ* on their single-crystal substrates are the most reliable for determining the types of net-plane orientated

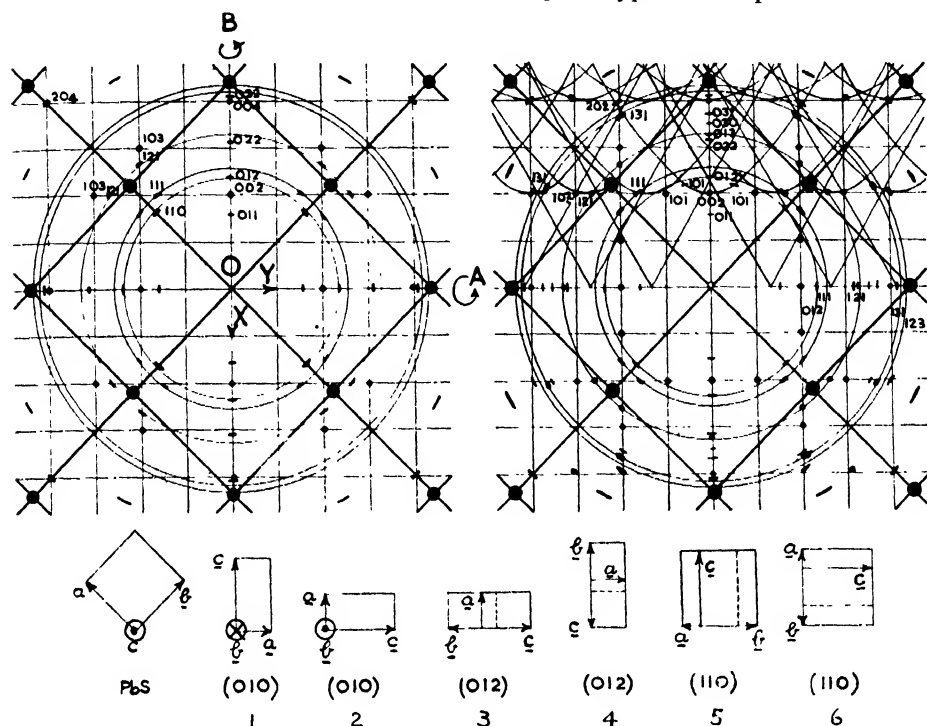


Figure 7. The main features of Figure 5; the  $\text{PbS}$  spot positions are represented by large black circles and long arcs, and the remaining spots and rings are  $\text{PbCl}_2$  diffractions. The  $\text{PbCl}_2$  spots lie either on straight layer lines or the hyperbolic loci whose asymptotes are also shown.

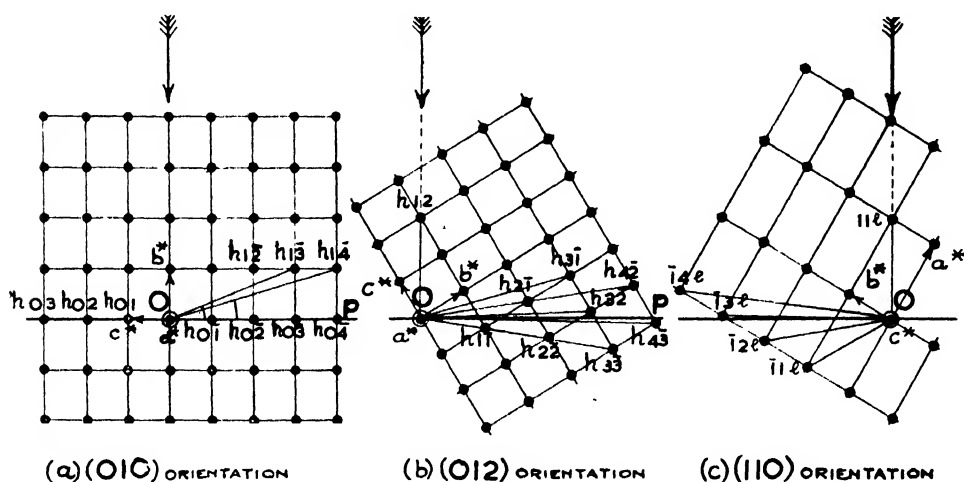


Figure 8. Reciprocal-lattice planes normal to the axes of curvature in the case of the (010), (012) and (110) orientations, showing the angles of rotation required to cause the various diffraction spots to appear.

parallel to the substrate surface, and that transmission patterns, though generally affected by break-up and curvature of the film, can then provide a still more sensitive definition of the azimuthal orientations present.

(i) and (ii). *The Nature of the Reaction*

Results (i) and (ii) are in strong contrast to the observation that  $\text{PbO} \cdot \text{PbSO}_4$  is rapidly formed in air at  $350^\circ \text{C}$ . in absence of  $\text{NaCl}$  (Wilman 1948), and that neither  $\text{PbCl}_2$  nor  $\text{PbO} \cdot \text{PbSO}_4$  is observed when  $\text{PbS}$  is heated on  $\text{NaCl}$  *in vacuo* under similar conditions (Elleman and Wilman 1948). With thicker deposits and those with mixed orientations of the  $\text{PbS}$  the  $\text{PbCl}_2$  was not observed until after a longer time of heating (Table 3), which appears to indicate that the  $\text{Cl}$  ions migrate through the deposit and react on the surface to form  $\text{PbCl}_2$ , and the excess  $\text{S}$  ions are oxidized there to form gaseous  $\text{SO}_2$  which diffuses away. It may be noted that Thomson (1930) sputtered lead on to rocksalt in an argon atmosphere, and the rocksalt became appreciably heated by the discharge so that the deposit was converted to a compound which he tentatively identified from its diffraction pattern as  $\text{PbCl}_2$ .

(iii) *The  $\text{PbCl}_2$  Orientations*

The present example of  $\text{PbCl}_2$  on  $\text{PbS}$  is a relatively clear-cut case illustrating well not only the usual high degree of fitting of the lattice periodicities in substrate and deposit, but also that the observed orientations correspond to an approximate ionic fitting, notwithstanding the low symmetry of one of the materials. This ionic fitting on to the substrate approximates to that of a continued growth of the substrate crystal. The orientations observed conform to the general observation that when strong epitaxial orientation occurs there are at least one and usually two or more lattice row types which are parallel in the substrate and overgrowth crystals, with nearly equal lattice spacings along parallel directions. In this case, for the  $\{010\}$ -orientated  $\text{PbCl}_2$ ,  $a$  (4.530 Å.) or  $c$  (9.035 Å.) was parallel to  $\text{PbS}$   $[110]$  (8.385 Å.) and the differences of  $2a$  and  $c$  from the  $\text{PbS}$ -spacing are 8.0 and 7.7% of the  $\text{PbS}$   $[110]$  periodicity respectively. In the  $\{012\}$ -orientation  $a$  is again parallel to  $\text{PbS}$   $[110]$ , and  $[021]$  ( $T = 17.70$  Å.) parallel to  $\text{PbS}$   $[1\bar{1}0]$ , with differences of 8.0 and 5.5% respectively (for  $2a$  and  $T_{021}/2$ ).

In the  $\{110\}$ -orientated  $\text{PbCl}_2$ ,  $c$  is again parallel to  $\text{PbS}$   $[110]$  and  $[1\bar{1}0]$  ( $T_{110} = 8.859$  Å.) is parallel to  $\text{PbS}$   $[1\bar{1}0]$ , with differences of 7.7 and 5.7% respectively.

Figure 9 shows the atomic positions in the unit cell of  $\text{PbCl}_2$ , estimated by Bräkken (1932). The atoms are all in four-fold positions ( $\frac{3}{4}, \frac{3}{4} + u, v$ ), ( $\frac{1}{4}, \frac{1}{4} - u, \bar{v}$ ), ( $\frac{3}{4}, \frac{1}{4} + u, \frac{1}{2} - v$ ), and ( $\frac{1}{4}, \frac{3}{4} - u, \frac{1}{2} + v$ ), with  $u = 0.004$ ,  $v = 0.095$  for  $\text{Pb}$ ;  $u = 0.40$ ,  $v = 0.07$  for  $\text{Cl}_1$ , and  $u = 0.30$ ,  $v = 0.67$  for  $\text{Cl}_2$ , the cell having an inversion centre at its corners and centre. Miles (1931) had earlier estimated practically the same positions for the  $\text{Pb}$  atoms. Figure 10 was constructed from Figure 9 to show the arrangement of the atoms in and close to  $(010)$ ,  $(012)$  and  $(110)$  planes, superposed above the  $(001)$   $\text{PbS}$  net-plane so that positively charged  $\text{Pb}$  ions lie as nearly as possible above negative  $\text{S}$  ions, and  $\text{Cl}$  ions above  $\text{Pb}$  ions, or nearly so, analogous to the continued growth of  $\text{PbS}$  on the  $\text{PbS}$  crystal. The  $\text{Pb}$  and  $\text{Cl}$  ions are joined by lines merely to show differently situated groups. It will be seen that in the  $\{010\}$  and  $\{012\}$  orientations there are chains of  $\text{Cl}$  and  $\text{Pb}$  ions parallel to the  $\text{PbCl}_2$   $a$  axis, approximating more or less closely in size and positions to the square  $\text{PbS}$  ionic arrangement, with intermediate bands where the  $\text{Pb}$  and  $\text{Cl}$  ions lie (above and) between two pairs of  $\text{PbS}$  ions in less firmly bound positions. In the  $\{110\}$ -orientation there are again  $\text{Cl-Pb-Cl}$  groups in similar positions of

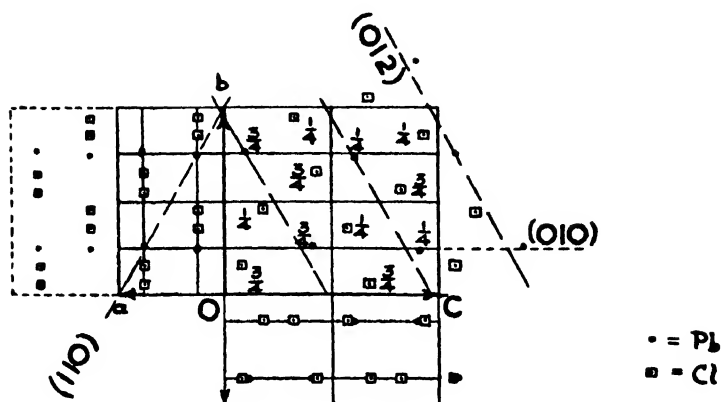


Figure 9. Projections of the atomic positions of  $\text{PbCl}_2$  on the unit cell faces, according to Bräkken (1932), drawn to the same scale as Figure 10.

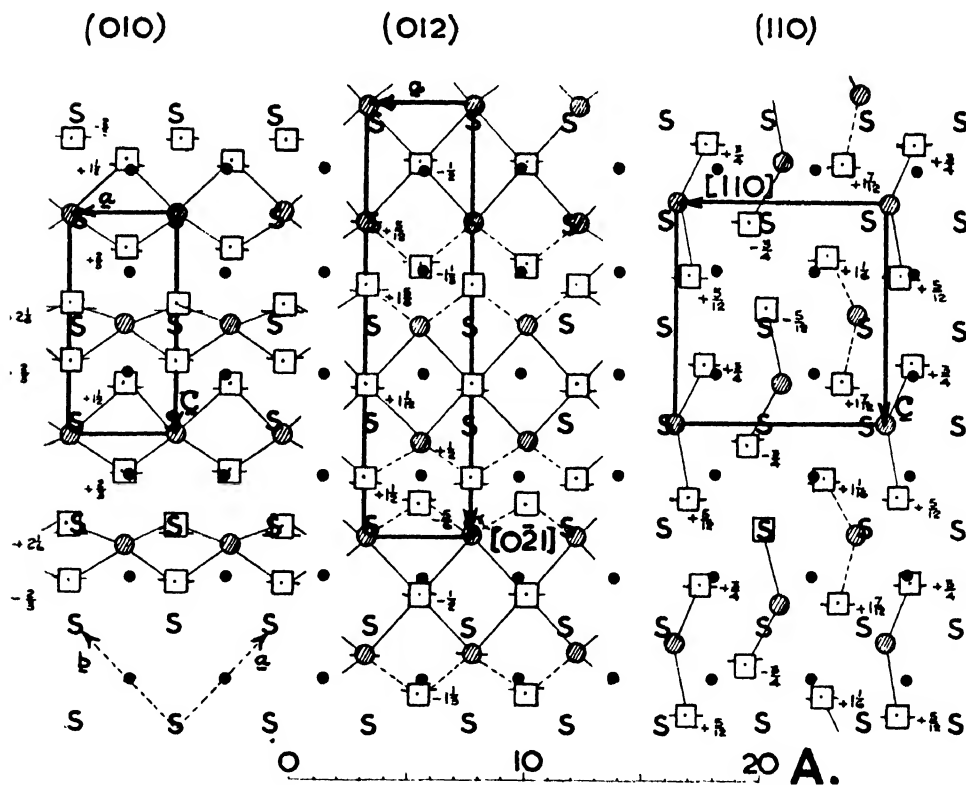


Figure 10. The epitaxial fitting of  $\text{PbCl}_2$  in (010), (012) and (110) orientations on the (001)  $\text{PbS}$  surface.

● = Pb and S = S in  $\text{PbS}$  (001) surface.

/// = Pb and □ = Cl in adjacent  $\text{PbCl}_2$ .

The approximate heights of the Pb and Cl ions of the  $\text{PbCl}_2$  are in Å, and these heights of the ions above the (010), (012) and (110) planes shown in Figure 9 are also represented as fractions of the (002)  $\text{PbS}$  net-plane spacings by the positions of the short horizontal lines at each side of the symbol where the radius of the symbol represents the (002)  $\text{PbS}$  net-plane spacing.



correspondence to the charge distribution in the PbS ion arrangement, but this time not in continuous chains.

The observed orientations are almost certainly in this case characteristic of the growth of the PbCl<sub>2</sub> reaction product on nearly atomically smooth PbS cube-faces. Such smooth PbS faces were demonstrated by vertically elongated PbS diffractions from both the initial PbS deposits and the partially converted layers; thus, either the rougher parts of the PbS crystals were attacked first before the large atomically smooth surfaces, or else the reaction proceeds at first at a nearly plane interface between the PbCl<sub>2</sub> crystals and the still unattacked lower parts of the PbS crystals. The slight imperfection of the orientation of the {012}-orientated PbCl<sub>2</sub> crystals may possibly be associated with the twinning which occurred on these planes in these crystals; or it may be a consequence of the Pb and Cl ion distribution in the neighbourhood of (012) planes, as shown in Figures 9 and 10. It is not due to any larger difference of periodicities from those of the parallel PbS rows since the fit is as good as in the {010} and {110} orientations. Indeed, the occurrence of the three types together, with such equally close correspondence in the lattice periodicities of the parallel PbS and PbCl<sub>2</sub> rows and of the angles between them, is a striking example of the way in which these conditions determine epitaxial orientation.

In comparison with these orientations, which were developed at about 250° c., it is noted that Becke (1885) observed the epitaxial growth of PbCl<sub>2</sub> in what appears to have been the above {110} orientations on fresh PbS cleavage faces when these were attacked by hot concentrated HCl-PbCl<sub>2</sub> solutions (for 24–36 hours) or dilute HCl at 70° c. (30 seconds or more). Becke measured the angles between the small crystal facets by reflected light beams and identified and indexed these facets in terms of the rhombic axes deduced by Schabus (1850), who estimated the axial ratios to be 0.5941:1:0.5951, which evidently corresponds to the now accepted axial ratios  $c/2:b:a$ .

#### (iv) *Twinning of the PbCl<sub>2</sub>*

The {012}-twinning together with trillings on {012} were seen to be abundant by Stöber (1895) in crystals grown from concentrated HCl solution.

#### (v) *Lattice Constants of PbCl<sub>2</sub>*

The close agreement between the two sets of plane spacings in Table 1, from PbCl<sub>2</sub>, suggests that both materials were relatively pure.

One possible explanation of the lattice constants being slightly larger than those obtained by x-rays may be that owing to the high absorption of the electron beam in this compound the coherent diffraction pattern is mainly due to crystals which are only of the order of 100 Å. thick though approximately 500 Å. in lateral diameter, this severe lattice limitation being associated with a slight change of lattice dimensions. Lennard-Jones (1930) showed theoretically that such a change of lattice-dimensions was in general to be expected in the outermost two or three atomic layers of crystals, an expansion or contraction of a few per cent occurring according to the type of binding and surface-plane direction. However, no clear evidence of such a change of dimensions has yet been found in electron diffraction. The relative lattice dimensions of materials of large crystal diameter but of widely different absorbing powers, as with gold and graphite

(Finch and Fordham 1936, Finch and Wilman 1937a), and silver,  $\text{AgCl}$ ,  $\text{AgBr}$  and  $\text{NaCl}$  relative to graphite (Wilman 1940), are practically identical with those of the most reliable x-ray values (for graphite see Trzebiatowski 1937, and Nelson and Riley 1945). The axial ratios of the  $\text{PbCl}_2$  are effectively identical with those found by x-rays, as was the case with graphite (Finch and Wilman 1936b),  $\text{MoS}_2$  (Finch and Wilman 1936a) and  $\text{CdI}_2$  (Finch and Wilman 1937b). An explanation on the above lines would thus appear to be impracticable.

(vi) *The Nature of the Breaking-up and Curvature of the Composite  $\text{PbS-PbCl}_2$  Layer*

The curvatures of the  $\text{PbS}$  and the composite  $\text{PbS-PbCl}_2$  layers about definite axes is similar to the case described by Goche and Wilman (1939) of silver deposits on rock-salt cleavage faces, the axes of bending in both cases being mainly about the cube-face diagonals, and originating from the stepped structure of the rock-salt cleavage faces.

#### § 5. ACKNOWLEDGMENTS

This investigation forms part of a series of studies of crystal growth being carried out in this laboratory, and the authors thank Professor G. I. Finch, for his valued interest. They also thank the Department of Scientific and Industrial Research for a grant to Professor Finch which enabled one of the authors (A. J. E.) to carry out this work.

#### REFERENCES

- American Society for Testing Materials, First Supplement File of X-ray Powder-Pattern Diffraction Data, 1945.
- BECKE, F., 1885, *Tsch. min. Mitt.*, **6**, 240, 270.
- BRAGG, W. L., 1947, *J. Sci. Instrum.*, **24**, 27; 1948, *Acta Crystallographica*, **1**, 46.
- BRÄKKEN, H., 1932, *Z. Kristallogr.*, **83**, 222.
- BRÄKKEN, H., and HARANG, L., 1928, *Z. Kristallogr.*, **68**, 123.
- DÖLL, W., and KLEMM, W., 1939, *Z. anorg. allg. Chem.*, **241**, 246.
- ELLEMAN, A. J., and WILMAN, H., 1948, *Proc. Phys. Soc.*, **61**, 164.
- FINCH, G. I., and FORDHAM, S., 1936, *Proc. Phys. Soc.*, **48**, 85.
- FINCH, G. I., and WILMAN, H., 1936a, *Trans. Faraday Soc.*, **32**, 1539; 1936b, *Proc. Roy. Soc. A*, **155**, 345; 1937a, *Ergebn. exakt. Naturw.*, **16**, 353; 1937b, *Trans. Faraday Soc.*, **33**, 1435.
- GOCHÉ, O., and WILMAN, H., 1939, *Proc. Phys. Soc.*, **51**, 625.
- GROTH, P., 1906-1919, *Chemische Krystallographie*, **1**, 219 (Leipzig: Engelmann).
- LENNARD-JONES, J. E., 1930, *Z. Kristallogr.*, **75**, 215.
- LENNARD-JONES, J. E., and DENT, B. M., 1928, *Proc. Roy. Soc. A*, **121**, 247.
- MILES, F. D., 1931, *Proc. Roy. Soc. A*, **132**, 266.
- NELSON, J. B., and RILEY, D. P., 1945, *Proc. Phys. Soc.*, **57**, 477.
- SCHABUS, C., 1850, *Sitzb. d. Akad. Wiss. Wien*, **4**, 456.
- STÖBER, G., 1895, *Bull. Acad. Belg.*, **30**, 345; *Groth's Zeits.*, **28**, 108.
- STRAUMANIS, M., and SAUKA, J., 1942, *Z. phys. Chem.*, **B**, **51**, 219.
- THOMSON, G. P., 1930, *The Wave Mechanics of Free Electrons* (New York and London: McGraw-Hill), p. 77.
- TRZEBIATOWSKI, W., 1937, *Rocz. Chem.*, **17**, 73.
- WILMAN, H., 1940, *Proc. Phys. Soc.*, **52**, 323; 1948, *Ibid.*, **60**, 117.
- ZAMBONINI, F., 1910, *Min. Vesuv.*, p. 45.

## On the Absorption Spectrum of Cosmic Rays

By E. W. KELLERMANN AND K. WESTERMAN

The Physical Laboratories, The University, Manchester

*Communicated by P. M. S. Blackett; MS. received 10th November 1948*

**ABSTRACT.** Attempts at the measurement of the absorption spectrum of cosmic rays by means of counter telescopes have been made by many authors. It is pointed out here that none of the usual methods, i.e. the determination of the number of coincidences as a function of the absorber thickness, can be satisfactory unless the influence of the geometry through scattering is known. Only then can this (integral) absorption curve be used for the determination of the momentum spectrum.

A method of determining directly the differential absorption curve is described which avoids largely the influence of scattering. This method has been used for the investigation of some specific effects which have been observed by some and denied by other authors. In particular, the region of 12 cm. Pb has been investigated, and it is found that the change of absorption observed here is due solely to the overlapping of the high momenta end of the electron spectrum and of the meson spectrum. Although the present investigation cannot confirm it, it does not exclude the possibility of a specific change of the absorption coefficient in the 22 cm. Pb region.

### §1. INTRODUCTION

CLOUD chamber measurements by Blackett and others (cf. Williams 1939) of the momentum spectrum of cosmic rays confirm—within their limits of accuracy—the picture of the composition of cosmic rays at sea level generally assumed: up to a momentum of 200 mev. electrons are preponderant in the cosmic-ray spectrum; in the low momentum region there are few mesons, as must be assumed considering their decay. The meson differential spectrum curve rises steadily to a maximum at about 700 mev. Meson absorption, except in the low momentum region, is due to ionization loss.

Attempts have been made to interpret the integral absorption curve, i.e. coincidences per unit time plotted against varying thicknesses of absorber, as a monotonic function of the momentum spectrum. In general, the picture of the composition of the spectrum given above is confirmed. On the other hand, none of these integral absorption measurements has a claim to any great accuracy: the slopes of the absorption curves measured by various investigators differ, and the absorption coefficients show variations of up to 100%. A rough calculation shows that variations of this kind can be due to scattering conditioned by the geometry of the arrangement. This has been confirmed by Trumphy and Orlin (1943), who investigated the effect of scattering experimentally.

In addition, some authors have claimed recently to have observed specific deviations from the generally accepted course of the absorption curve. The absorption curve shows a region of relatively rapid absorption to a thickness of 10 cm. Pb, and then a lesser absorption. The first region of absorption is ascribed to the electronic component, and the second to the meson component. Now George in London and Appapillai in Ceylon (George and Appapillai 1945) consider that the integral absorption curve shows a region of zero absorption between 10 and 15 cm. Pb, and in the 23 cm. Pb region Swann and Morris (1947) find a pronounced decrease of the integral absorption at a latitude of 7° S., and they conclude that the effect in the 23 cm. Pb region is latitude dependent. It should

be mentioned that in this region other authors, in particular Chandrashekhar Aiya (1944), have observed specific effects. The effect found by George and Appapillai lies just outside the limits of the single standard deviation, while Chandrashekhar Aiya's discontinuity is still within the standard deviation. None of these authors take account of the influence of scattering. Here, attention must be drawn to the work of Clay, Venema and Jonker (1940), who observe maxima of the absorption curve in the 15 and 25 cm. Pb region when lead is placed above the counters of their telescope, yet no maximum with lead placed between the counters.

Effects of this kind, if definitely established, would, of course, require a modification of the simple picture of cosmic radiation which ascribes the two regions of absorption, one to the electron component and one to the penetrating component. In particular, one would have to introduce special assumptions in order to interpret the absence of mesons of a momentum of 250 to 300 mev., corresponding to a "plateau" between 10 and 15 cm. Pb.

Our experiment has been concerned mainly with the investigation of the 10 to 15 cm. Pb region by means of a counter telescope. We have determined not only the integral absorption curve, but simultaneously have observed the differential absorption curve. Using this latter method, the influence of scattering is greatly diminished, and we have been able to investigate the absorption under conditions when the interpretation of the measurements is less in doubt.

## § 2. EXPERIMENTAL METHOD

A diagram of the counter arrangement is given in Figure 1. The counter trays *t*, *m* and *b* each consisted of two counters connected in parallel, and the three pairs constituted a threefold coincidence arrangement. In addition, *t*, *m* and *b* were also connected in a fourfold coincidence circuit with the side counters *S* and the bottom counters *B*, all of which were in parallel.

The counters *t*, *m*, *b* and *S* were 30 cm. long, the counters *B* 60 cm. in length. The outside diameter of all the counters was 3.7 cm. They were pyrex Geiger-Müller counters filled with argon and alcohol. Lead could be placed between the counters *t* and *m*, and also between *m* and *b*. The counters rested on a light framework, and the lead consisted of plates about 1 cm. in thickness and 8 cm. in width. Thus the counters *m* and *b* were covered by lead, but not the anti-coincidence counters *S*. Between the counters *b* and the bottom counters *B* there was a space sufficient for four lead plates, each of 1 cm. thickness.

The opening angles of the telescope,  $21^\circ$  and  $71^\circ$  respectively, were large enough to give a threefold rate of about 550 counts per hour with 10 cm. Pb between the counters. The telescope gave the following information: Particles setting off *t*, *m*, *b* and *B* were recorded separately as threefold and fourfold coincidences. Particles setting off *t*, *m* and *b*, but unable to penetrate the additional 4 cm. of lead between *b* and *B*, were recorded as threefold coincidences only. Side showers might set off *t*, *m*, *b* and one of the *S* counters and thus give rise to simultaneously recorded threefold and fourfold coincidences. Particles penetrating *t*, *m* and *b*, but scattered so that they did not penetrate the 4 cm. lead, might nevertheless set off one of the counters *B* and thus give rise to a fourfold coincidence. Hence a separate registration of anti-coincidences, i.e. threefold coincidences unaccompanied by fourfold coincidences, gave the number of particles penetrating (say)  $x$  cm. Pb between the counters *t*, *m* and *b*, but not

penetrating  $(x+4)$  cm. Pb. This registration would then also exclude some effects due to side showers and discriminate against the influence of scattering. The recorded threefold coincidences gave the integral absorption curve when plotted against different thicknesses of lead, but did not differentiate against side showers nor any bias introduced by scattering.

The counter pairs *t*, *m* and *b* were each connected to the grids of pentodes in a threefold Rossi circuit triggering a thyratron which in its turn operated two telephone counters in series. The counter pairs were connected also to three other pentodes each, and the counters *S* and *B* to a seventh pentode. The latter four pentodes were again connected in a fourfold Rossi circuit triggering a

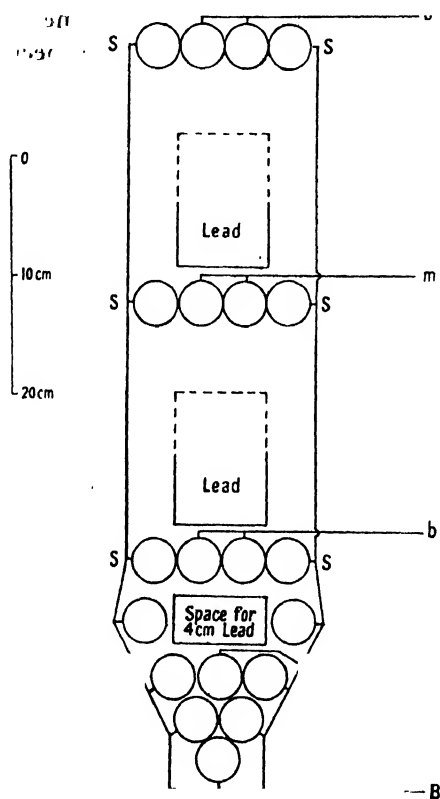


Figure 1. Counter arrangement.

thyratron which operated a telephone counter and a relay in series. The relay when operating short-circuited the second telephone counter of the threefold circuit so that this counter operated only when there was a threefold coincidence unaccompanied by a fourfold and, therefore, registered anti-coincidences.

The relay system was carefully tested, and the counters were checked daily. The resolving time was  $10^{-5}$  sec. All readings were reduced to a barometric pressure of 30 in. Hg (cf. Duperier 1944). An equal number of lead plates was placed between *t* and *m*, and *m* and *b* respectively, and 4 cm. lead was placed between *b* and *B*, always after the background, i.e. the number of anti-coincidences with  $x$  cm. lead between *t*, *m* and *b* and no lead between *b* and *B*, had been determined. The background remained constant at  $2.5 \pm 0.25$  counts per hour throughout the experiment.

## § 3. RESULTS

(i) *The Integral Spectrum*

Coincidence counts were taken for thicknesses  $x$  of lead varying from 0 to 26.3 cm. No point on the curve was determined with a standard deviation of less than  $\pm 0.5\%$ . The results are tabulated in Table 1. Figure 2 shows the

Table 1

(1)	(2)	(3)	(4)	(5)
cm.	hr. min.			
0.0	209 08	162,853	778	2.0
1.9	190 41	115,906	608	2.0
3.9	192 18	113,286	590	2.0
8.0	165 30	93,764	566	2.0
10.3	162 48	90,798	558	2.0
12.2	230 01	128,099	558	1.5
14.2	100 33	55,407	550	$\pm 2.5$
16.2	91 30	48,969	535	2.5
18.2	94 49	49,782	525	$\pm 2.5$
20.2	140 38	70,635	503	$\pm 2.0$
22.3	94 11	47,031	499	$\pm 2.5$
24.3	95 06	46,760	492	$\pm 2.5$
26.3	70 59	33,861	477	$\pm 2.5$

(1) Total thickness of lead in layers 1 and 2. (2) Total time. (3) Total number of counts reduced to 30 in. Hg pressure. (4) Rate per hour. (5) Standard deviation.

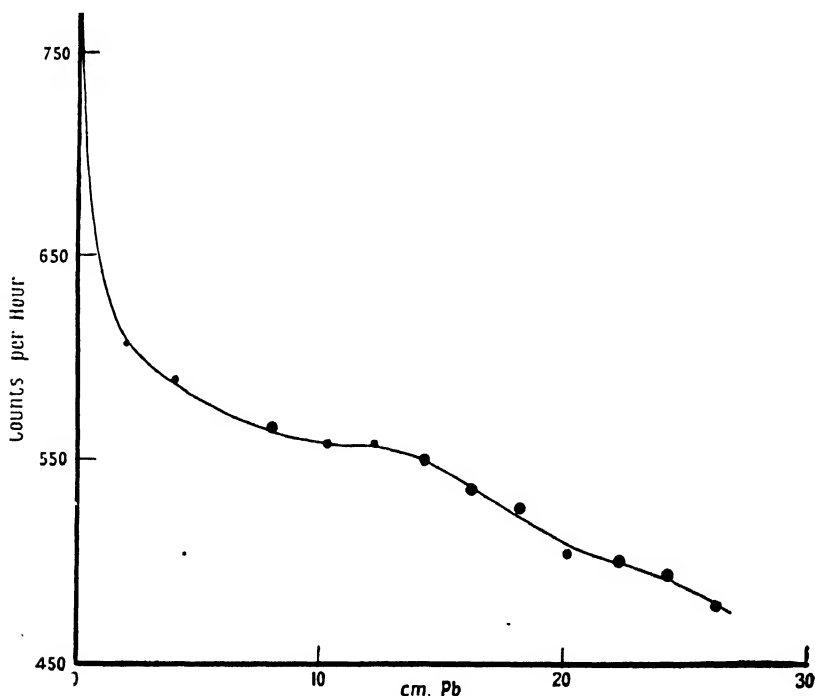


Figure. 2. Integral absorption.  
Radius of circle indicates standard deviation.

number of threefold coincidences per hour as a function of the thickness of the lead absorber. It is seen that there is a rapid decrease to 10 cm. Pb, and thence

a slow drop to 30 cm. Pb. From 10 to 13 cm. the graph shows distinctly an almost horizontal stretch similar to that found by George and Appapillai. Furthermore, it can be seen that there may be another change of slope at 22 cm. Pb, but the statistical error is too great for this to be certain; the change of slope suggested here, however, is of a different character from that described by Chandrashekhar Aiya.

It will be seen that, in spite of small standard deviations (cf. Table 1), our measurement of the integral spectrum alone does not contribute much to the elucidation of the information already available from the work of other authors.

As already described, the general shape of the integral curve is similar to those obtained by George and Appapillai and by other authors, in so far as they all show a region of rapid absorption up to about 9 cm. Pb, very little absorption between 9 and 13 cm. Pb, and then again more rapid absorption (though less than that up to 9 cm. Pb). There are, however, notable differences which appear if the slopes of the integral curves from say 20 cm. Pb onwards, as determined by various

Table 2

(1)	(2)	(3)	(4)	(5)
cm.	hr. min.			
3.9	46 00	603	13.10	$\pm 0.54$
6.1	128 00	1480	11.58	$\pm 0.30$
8.0	236 00	2520	10.69	$\pm 0.21$
8.8	402 43	4235	10.51	$\pm 0.16$
10.3	159 53	1716	10.74	$\pm 0.26$
12.2	209 53	2355	11.22	$\pm 0.23$
14.2	280 50	3281	11.68	$\pm 0.20$
14.8	430 39	5051	11.74	$\pm 0.17$
16.2	160 24	1861	11.60	$\pm 0.27$

(1) Total thickness of lead in layers 1 and 2. (2) Total time. (3) Number of counts with 4 cm. Pb in layer 3 reduced to 30 in. Hg. (4) Rate per hour. (5) Standard deviation.

authors, are compared (Figure 3). These slopes show very large variations, and it is probable that the whole difference arises from the way in which scattering affects the result with various geometrical arrangements.

The experiments of Trumpy and Orlin (1943) show that the value of the apparent absorption coefficient can vary by about 100% according to the geometry of the arrangement employed, and the same result may be reached from our comparison of the results of various authors in Figure 3. We conclude, therefore, that before comparing and interpreting integral absorption curves obtained by direct measurements, a much more thorough investigation must be made of the geometry of the actual arrangements.

### (ii) *The Differential Spectrum*

We determined the differential spectrum by recording the anti-coincidences, i.e. the number of particles penetrating  $x$  cm. of lead, but not  $(x+4)$  cm., and plotting it against  $x$ . Particles setting off the counter rays  $t$ ,  $m$  and  $b$ , but not penetrating the additional 4 cm. lead below the tray  $b$ , were recorded as anti-coincidences, provided no other counters were set off. It has been explained above how our arrangement discriminated against scattered particles, so that our determination of the differential spectrum is largely independent of the influence

of the geometry in that respect. Hence our differential spectrum is not subject to the same criticism which must be made in the case of methods employed in measuring directly the integral absorption curve.

The differential spectrum is plotted in Figure 4. It will be seen at once that in spite of the larger standard deviation as compared with the integral curve we can extract more definite information from the differential than from the integral curve.

Consider in particular the minimum at  $x=9$ . This value of the abscissa corresponds to the interval of 9 to 13 cm. Pb of the abscissa of the integral curve. Whereas in the case of the integral curve we are unable to decide whether the

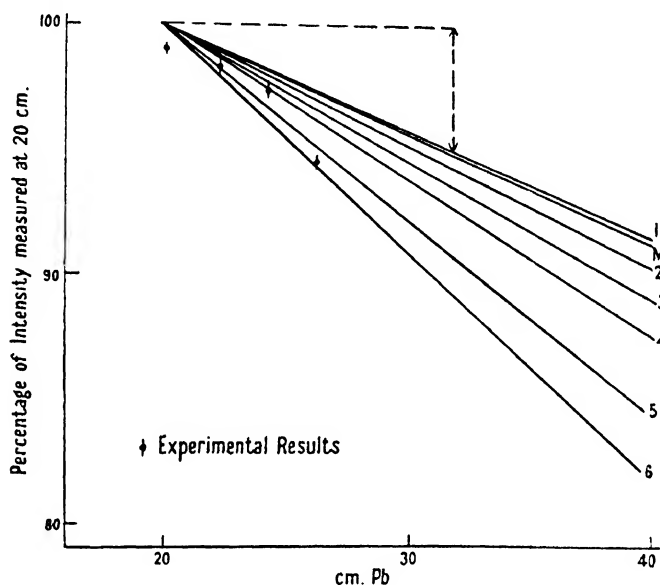


Figure 3. Slopes of integral absorption curves.

M. Determined from meson spectrum (cf. Wilson 1946).

1. Clay and van Gemert (1939).
2. Chandrasekhar Aiyar (1944).
3. George and Appapillai (1945).
4. Rossi (1933).
5. Auger, Leprince-Ringuet, and Ehrenfest (1936).
6. Clay (1936).

The experimental results are those of the present authors.

curve in this region shows a real horizontal "plateau", i.e. a region of zero absorption, we can gain decisive information from the differential curve: here we can see quite clearly that the minimum does not touch the  $x$  axis, but that even the lowest ordinate is still 8 particles per hour.

Hence we conclude that the corresponding part of the integral curve is not a real plateau, but signifies a change of slope only. Therefore, after consideration of the differential curve, there is no need to make special assumptions in order to interpret the existence of particular effects of that kind.

The differential curve can be considered as a superposition of two curves, one decreasing from high values for  $x=0$  to almost zero at about  $x=9$ , and another increasing from zero at  $x=0$  to 9 at  $x=14$ . These two component curves, making up our differential curve, can be interpreted as due to the electron spectrum and to the meson spectrum respectively: the contribution of the electrons will decrease with increasing  $x$ , and at  $x=9$  we find only the contribution of cascades



containing few high momentum electrons. The meson component contains few particles of low momentum, due to the decay of slow mesons in the atmosphere.

We can compare our results with the meson spectrum determined by Wilson (1946) by means of cloud-chamber experiments. Wilson's results have been confirmed by the counter experiments of Shamos and Levy (1948). These authors have determined three points, namely, at 11.2 cm. Pb, at 31.6 cm Pb, and at 31 cm. Pb + 25.4 cm. Fe, and their points lie on Wilson's curve within the limits of error.

In the part of our differential curve due to the meson component, the interval from  $x=9$  up to about  $x=16$  corresponds to a range in lead from 9 cm. Pb up

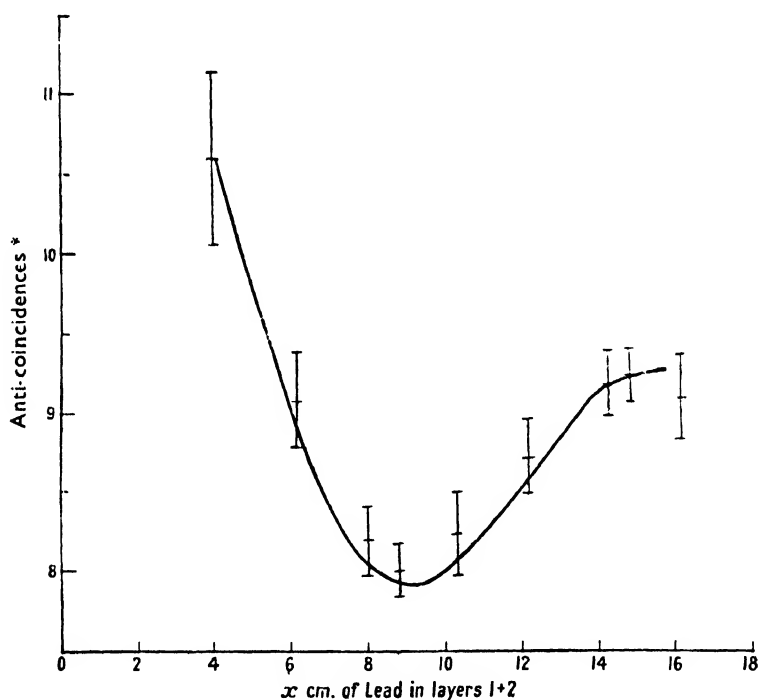


Figure 4. Differential absorption curve.

\* Number of particles per hour penetrating  $x$ , but not  $x+4$  cm. Pb.  
(Background of 2.5 per hr. subtracted.)

to  $16+4=20$  cm. Pb. Using the well-known Rossi-Greisen curves, this corresponds to a momentum interval ranging from 220 to 360 mev. approximately. The momentum range investigated by us covers, therefore, only a small part of the range investigated by Wilson. However, we have sufficient data to represent our results on Wilson's curve by a point, namely the number of mesons between 220 and 320 mev., and also to compare the slope of the meson part of our differential curve in the neighbourhood of this interval with the slope of Wilson's curve near the corresponding point.

Wilson gives his results as numbers per momentum interval per 1,000 mesons of a momentum  $>1,000$  mev. Our telescope gives the number of particles penetrating 30 cm. Pb, i.e. of momentum  $\geq 500$  mev., as about 450 particles per hour, and we can therefore relate our results to Wilson's without difficulty. Relating both results to a total of 1,000 particles in the range  $\geq 500$  mev., we obtain from our curve in the interval 220 to 320 mev., for example,  $(16 \pm 0.8) \times 1,000/450 = 36 \pm 2$  particles per hour.

Relating similarly the slopes of the two curves, we are making no allowance for the possibility that at  $x = 15$ , i.e. in the 350 mev. region, our curve might flatten out slightly. A small change of slope here would not show up on Wilson's curve.

In Figure 5 we have plotted Wilson's spectrum as a dotted line as well as the point and slope determined by us in the corresponding momentum region. It is seen that there is good agreement.

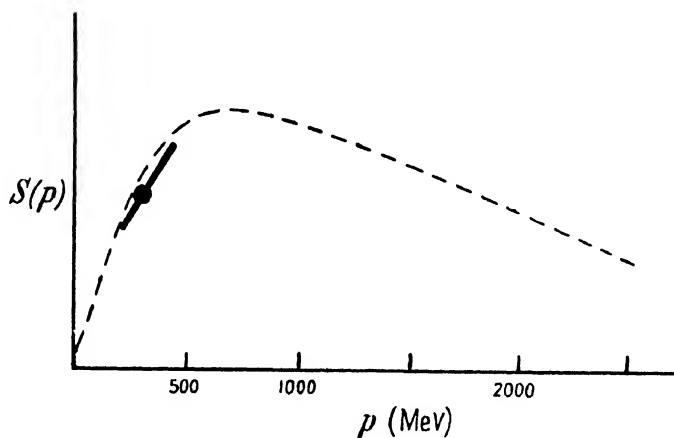


Figure 5. Point and slope of meson spectrum determined from meson part of differential absorption curve.  
Dotted line: ---Wilson's meson spectrum 1946.

One should expect a slight change of slope in our differential curve in the  $x = 15$  region, if the change of slope of the integral curve in the corresponding region of 20 cm. is real. However, we hope to examine this point more closely in a further experiment.

#### ACKNOWLEDGMENTS

One of us (E. W. K.) wishes to acknowledge his indebtedness to Professor A. M. Taylor, University College, Southampton, where this work was begun. Both authors wish to thank Professor P. M. S. Blackett for his continuous interest in this investigation, Professor L. Jánossy for introducing us to these problems and for his advice, and Dr. J. G. Wilson for many helpful discussions.

#### REFERENCES

- AUGER, P., LEPRINCE-RINGUET, L., and EHRENFEST, P., 1936, *J. Phys. Radium*, **7**, 58.  
 CHANDRASHEKHAR AIYAR S. V., 1944, *Nature, Lond.*, **153**, 375.  
 CLAY, J., 1936, *Physica*, **3**, 332.  
 CLAY, J., and v. GEMERT, A., cf. Clay, 1939, *Rev. Mod. Phys.*, **11**, 128.  
 CLAY, J., VENEMA, A., and JONKER, K. J. H., 1940, *Physica*, **7**, 673.  
 DUPERIER, A., 1944, *Nature, Lond.*, **153**, 529.  
 GEORGE, E. P., and APPAPILLAI, V., 1945, *Nature, Lond.*, **155**, 726.  
 ROSSI, B., 1933, *Z. Phys.*, **82**, 151.  
 SHAMOS, M. H., and LEVY, M. G., 1948, *Phys. Rev.*, **73**, 1396.  
 SWANN, W. F. G., and MORRIS, P. F., 1947, *Phys. Rev.*, **72**, 1262.  
 TRUMPY, B., and ORLIN, J., 1943, *Bergens Museums Arbok (N)*, Nr. 7.  
 WILLIAMS, E. J., 1939, *Proc. Roy. Soc. A*, **172**, 194.  
 WILSON, J. G., 1946, *Nature, Lond.*, **158**, 414.

## Momentum Spectrum of the Particles in Extensive Air Showers

BY S. M. MITRA AND W. G. V. ROSSER

The University, Manchester

*Communicated by P. M. S. Blackett; MS. received 11th February 1949*

**ABSTRACT.** An account is given of experiments on the momentum spectrum of the particles in extensive air showers at sea-level. The results are consistent with an integral spectrum of the form  $N(>E) \propto (E + E_c)^{-(1.1 \pm 0.3)}$ , where  $E_c$  is the critical energy in air. Penetrating particles are found in some of the denser showers, the ratio of penetrating particles to electrons being  $(0.8 \pm 0.4)\%$ .

### § 1. INTRODUCTION

THE electronic component of the cosmic radiation at sea-level is due partly to the secondary effects of mesons and partly to the extensive air showers which are initiated by high-energy electrons or photons in the upper atmosphere. In this paper we shall be concerned with the part of the electronic component associated with extensive air showers. The main part of the paper is an account of the determination of the momentum spectrum of the particles in extensive air showers, and of a small number of ionizing penetrating particles which were found in some of the denser showers.

If it is assumed that the electrons or photons which give rise to the extensive showers have an integral energy spectrum of the form

$$N(>E) = K_1 E^{-\gamma}, \quad \dots\dots(1)$$

it is possible in principle to calculate from the cascade theory the form of the spectrum to be expected at sea-level. It has been shown by Rossi and Greisen (1941) that if ionization loss and scattering are neglected, the spectrum retains, at all depths in the atmosphere, the form given in equation (1). Bhabha and Chakrabarty (1943) have shown that if the ionization loss of the particles is taken into account the spectrum is again of the form given in equation (1), but the factor  $E + E_c$  (where  $E_c$  is the critical energy in air) must be used in place of  $E$ . The best theoretical value of the exponent  $\gamma$  appears to be given by

$$\gamma = 1.5. \quad \dots\dots(2)$$

A possible way of testing the validity of this expression might appear to be the random operation of a cloud chamber with very thin walls. Such an experiment would, however, fail to distinguish between that part of the electronic component at sea-level which comes from knock-on and decay electrons and the part arising from extensive showers. Though it is necessary to control the cloud chamber with a counter arrangement sensitive to extensive showers, it is important that no significant bias should be imposed on the spectrum by the control system. The most important bias introduced by every counter system is the imposition of a "cut-off" for showers of less than a certain minimum density. The effect of this type of bias is twofold: (i) to cut off showers of low average density, i.e. showers initiated by low energy primaries, and (ii) to cut off the low density



Photo 2. A dense shower containing one penetrating particle, denoted p p. The momentum of the particle above the lead plate is  $2.1 \times 10^3$  eV c.; the particle is positive.  $H = 7,200$  gauss.



Photo 1. A dense extensive air shower in which the momenta of the particles above the lead plate range from  $1.4 \times 10^8$  to  $4.9 \times 10^9$  eV c. This photograph is an example of a Hoffman burst.  $H = 5,500$  gauss.

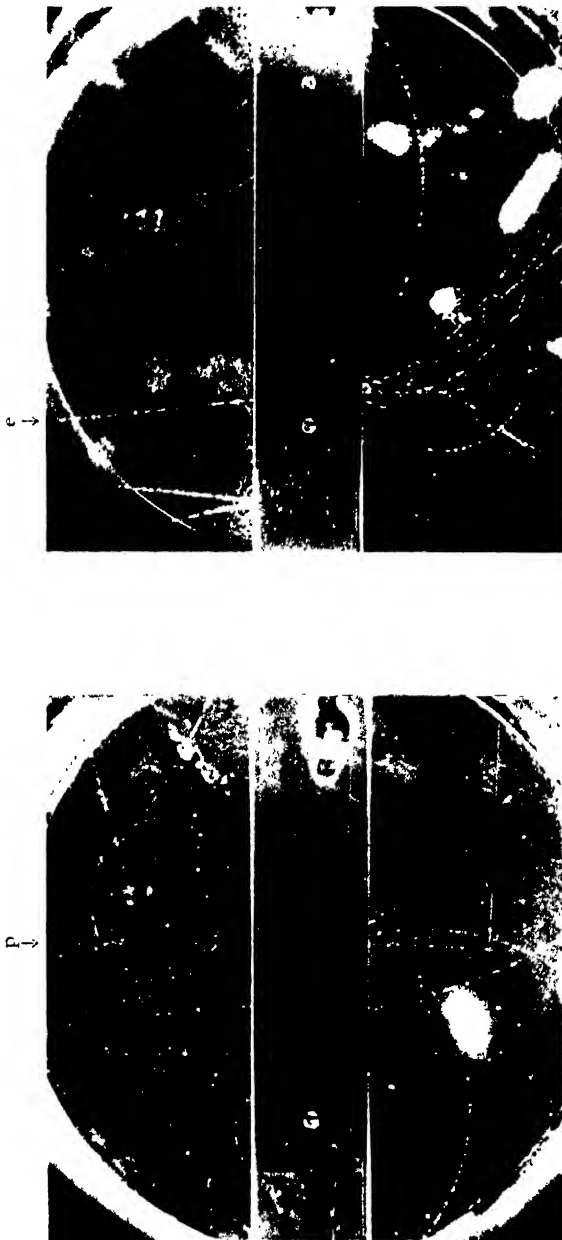


Photo 3. A dense extensive air shower with one negative penetrating particle (p,p) of momentum  $1.2 \times 10^9$  ev c. above the lead plate.  $H=7,100$  gauss.

Photo 4. This photograph shows an incident electron (e) of momentum  $1.5 \times 10^9$  ev c. which produces a small cascade shower in the lead plate. The penetrating track on the right-hand side of the photograph is too fine to be contemporary with the extensive air shower, and was not included in the analysis.  $H=7,100$  gauss.

region of large showers. In each case the effect on the energy spectrum is to decrease the number of low energy electrons recorded relative to the number of high energy electrons and, therefore, to decrease the average value of  $\gamma$ . The minimum density of the showers recorded with the counter arrangement used in the present experiment was 50 particles per square metre.

Another important form of bias is introduced by the presence of solid material above the apparatus. Great care was taken in the present experiments to reduce this effect as much as possible. The thickness of solid material above the chamber was not more than 3 gm/cm<sup>2</sup> made up of light elements, and no particle in the chamber was accepted for measurement which had come through more than this thickness of matter. This criterion necessitated rejecting particles which made more than 60° with the vertical in one plane and 25° with the vertical in the other plane.

Experimental evidence that a fair sample of the particles in extensive air showers has been taken will be given in § 3, where it is shown that the observed distribution of the number of tracks in the cloud chamber agrees closely with the distribution calculated from the counter experiments of Daudin (1943) and Cocconi, Loverdo and Tongiorgi (1946 a, b).

## § 2. EXPERIMENTAL ARRANGEMENT

The general arrangement of the apparatus was essentially the same as that used by Rochester and Butler (1948) to study penetrating showers, except that no lead was placed above the chamber (see Figure 2 of their paper). It consisted of an electromagnet (Blackett 1936) and a counter-controlled cloud chamber. The chamber had an effective collecting area of 150 cm<sup>2</sup> and it was triggered by the five-fold coincidence of an array of counters consisting of three trays above and two trays below the chamber. Another tray of counters of area 1,700 cm<sup>2</sup> was placed one metre away and coincidences between this tray and the five-fold set were indicated by the flash of a small indicator lamp placed in front of the chamber, the resolving time of the control circuit being  $2 \times 10^{-6}$  sec.

In order to distinguish between soft and penetrating particles, a lead plate 3.4 cm. thick was placed across the chamber. The chamber, together with the small indicator lamp, was photographed through the hollow core of the electromagnet, and only the photographs taken with the indicator lamp on were considered in the present experiment. The positions of the tracks above the lead plate in the chamber were carefully determined by reprojection. The minimum track length for measurements was 6 cm.

The curvatures of the high energy tracks were measured by the null method devised by Blackett (1937), viz. by compensating the curvature with a prism; and those of the low energy tracks were measured by comparison with a family of circles of known curvatures. With a field of 7,500 gauss the maximum detectable momentum was  $8.4 \times 10^9$  ev/c. (Rochester and Butler 1948).

## § 3. DENSITY DISTRIBUTION OF THE PARTICLES IN THE SHOWERS

The work of Cocconi, Loverdo and Tongiorgi (1946 a), Daudin (1943), Clay (1943) and Chaudhuri (1948) has shown that the distribution of shower densities follows a power law of the form

$$R(>D) = \text{const. } D^{-1.5}, \quad \dots\dots(3)$$

where  $R(>D)$  is the rate of showers with a density exceeding  $D$ .

Following Chaudhuri (1948), the density distribution obtained in the present experiment can be compared with the results of Cocconi, Loverdo and Tongiorgi by comparing the observed rate of occurrence of showers showing  $n$  tracks above the lead plate with the rate calculated according to the formula

$$R(n) \propto \int_0^\infty (1 - e^{-S_1 D})(1 - e^{-S_3 D})(1 - e^{-S_4 D})(1 - e^{-S_5 D}) \\ \times (1 - e^{-S_E D}) e^{-S_0 D} \cdot \frac{(S_0 D)^n}{n!} \cdot \frac{dD}{D^{(\beta+1)}}, \quad \dots\dots (4)$$

where  $R(n)$  is the fraction of photographs with  $n$  tracks,  $\beta = 1.5$ ,  $S_0$  is the collecting area of the cloud chamber and  $S_E$  is the area of the extension tray. Two of the trays of the five-fold overlapped completely, and as most of the showers at sea-level are nearly vertical, the two trays were considered as one. Only four trays of the counter set ( $S_1$ ,  $S_3$ ,  $S_4$ ,  $S_5$ ) were therefore used in the above expression.

The observed rates are shown in row 2 of Table 1, and the calculated values are shown in row 3. It is seen that the observed and calculated values are in good agreement. The lead plate introduced a slight bias towards particles which

Table 1. Density Distribution of Particles in Extensive Air Showers

No. of particles * . . . .	0	1	2	3	>3
No. of showers { Observed	697	245	75	11	20
{ Calculated	726	220	64	20	18

\* Number of particles above the plate in the photograph.

multiplied in the plate. However, since the rate of occurrence of particles of sufficient energy to multiply in the plate was comparatively low, and since the area of the lead plate was small compared with the areas of the bottom counter trays, the bias towards events penetrating the lead plate was small.

### *The Momentum Spectrum of the Particles*

A total of 474 tracks were selected from 1,048 photographs of extensive air showers taken with high and low magnetic fields. While the chamber was run with a high field (7,500 gauss) there was a stray field of several hundred gauss above the chamber which caused an appreciable loss of low energy particles. In order to find what proportion of these particles was lost, an equal number of photographs was taken at a lower magnetic field (1,500 gauss) when the stray field was negligible. The results are shown in Table 2. It was found that for 62 particles obtained in the range  $1 \times 10^7$  to  $5 \times 10^7$  ev/c. with the high field 109 were obtained with the low field, the numbers above  $p = 5 \times 10^7$  ev/c. being approximately equal (147 and 156 respectively).

The corrected momentum distribution of the particles in the extensive air showers is shown in Table 2, row 4, where the results with low field and high field are added together, the number below  $p = 5 \times 10^7$  ev/c. being calculated, however, from the low field results only.

Of the 60 particles with momenta greater than  $8 \times 10^8$  ev/c., 22 particles were in the range 8 to  $10 \times 10^8$  ev/c., and 38 particles had momenta greater than  $10^9$  ev/c.

The momentum spectrum has been plotted on a log-log scale in Figure 1. The results are consistent with an integral spectrum of the form  $N(>E) \propto (E+E_0)^{-\gamma}$  with  $\gamma = 1.1 \pm 0.3$ , if  $E_0$  is assumed to have the value  $1.14 \times 10^8$  ev., which is the theoretical critical energy in air. This result is consistent with the predictions

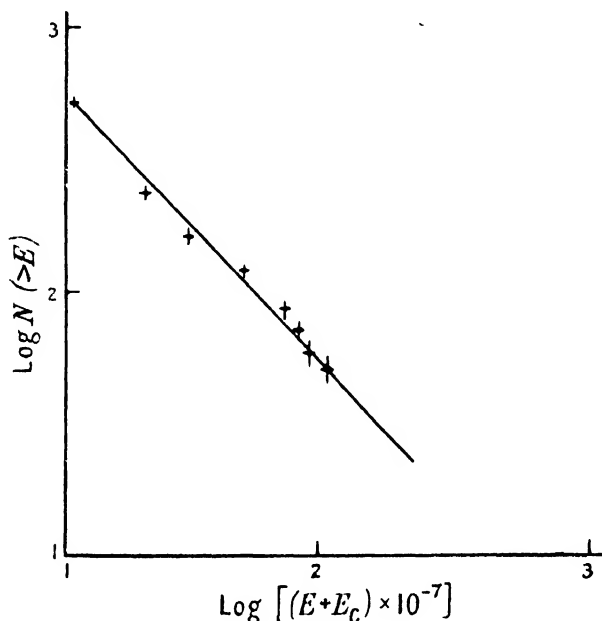


Figure 1.

Table 2. Momentum Distribution of the Particles in Extensive Air Showers

Momentum ( $10^8$ ev/c.)	0-5	5-10	10-15	15-20	20-30	30-40	40-50	50-60	60-70	70-80	>80
Distribution with high field	62	38	21	9	10	12	10	7	7	7	26
Distribution with low field	109	34	20	17	12	6	8	10	8	7	34
Corrected distribution	285		67		22	18	18	17	15	14	60

of cascade theory. The observed value of  $\gamma$  was less than the value of 1.5 given in equation (2), due probably to the effects of the angular scattering of the particles and the selection of high density showers by the counter arrangement.

#### *Ratio of the Penetrating Component to the Soft Component in Extensive Air Showers*

It is known that there are penetrating particles associated with extensive air showers (e.g. Rogozinski 1944, Cocconi, Loverdo and Tongiorgi 1946 b, Broadbent and Jánossy 1948, Cocconi and Greisen 1948, Fretter 1948).



During the present experiment, eight penetrating particles were obtained, and of these, three were single, one was accompanied by a single particle in the chamber, and the other four were accompanied by a number of electrons. Some of these penetrating particles were probably non-associated mesons, since all tracks entering the chamber over a time interval of approximately 0.02 second after the expansion appeared contemporary with the counter-controlled tracks. The meson flux through the chamber, within the solid angle defined in §1, during 0.02 second was 0.005. Thus the mean flux corresponding to all the photographs containing no tracks (697) was 3.5; it was therefore concluded that all the penetrating particles not accompanied by other particles in the chamber could be accounted for as non-associated mesons. Similarly, since 245 photographs contained one track only, the one penetrating particle accompanied by one other particle could also be accounted for as a non-associated meson. The other four penetrating particles were, however, accompanied by a large number of soft particles. Since only 20 photographs contained more than three tracks, these four penetrating particles could not be accounted for as non-associated mesons. The momenta of these penetrating particles above and below the plate are given in Table 3.

Table 3

Momentum of penetrating particle ( $\times 10^8$ ev/c.)	Above plate	8.0	12	19	21
	Below plate	7.4	11	17	19
Sign of charge of penetrating particle		+	-	+	+

It is seen that the loss of energy of each of the particles whilst traversing the plate is less than 10%. If the particles were electrons they would have been unlikely to have emerged from the plate unaccompanied by secondaries. Moreover, even if they did so, the probability of the energy loss being less than 10% was negligible (Heitler 1944). Furthermore, the penetrating particles all travelled in the same direction as the shower.

It was therefore concluded that non-electronic particles were present in the showers, the number observed being  $(0.8 \pm 0.4)\%$  of the total number of particles. This value is consistent with the estimates of other workers. On no occasion was more than one penetrating particle observed on a photograph. The fact that one of the penetrating particles was negative indicates that some at least of the penetrating particles were not protons. This conclusion is consistent with the suggestion of Cocconi, Cocconi and Greisen (1949) that there are  $\mu$ -mesons present in extensive air showers in air.

#### ACKNOWLEDGMENTS

In conclusion, the authors wish to record their sincere thanks to Professor P. M. S. Blackett, Dr. C. C. Butler, Dr. J. G. Wilson and Professor L. Jánossy for their encouragement and great help in all possible ways, and to Dr. G. D. Rochester for his kind guidance.

#### REFERENCES

- GHABHA, H. J., and CHAKRABARTY, S. K., 1943, *Proc. Roy. Soc. A*, **181**, 267.  
 BLACKETT, P. M. S., 1936, *Proc. Roy. Soc. A*, **154**, 504; 1937, *Ibid.*, **159**, 1.  
 BROADBENT, D., and JÁNOSY, L., 1948, *Proc. Roy. Soc. A*, **191**, 517; **192**, 364.  
 CHAUDHURI, B., 1948, *Nature, Lond.*, **161**, 680.

- CLAY, J., 1943, *Physica*, **9**, 897.  
COCCONI, G., COCCONI, V. O., and GREISEN, K., 1949, *Phys. Rev.*, **75**, 1063.  
COCCONI, G., and GREISEN, K., 1948, *Phys. Rev.*, **74**, 62.  
COCCONI, G., LOVERDO, A., and TONGIORGI, V., 1946 a, *Phys. Rev.*, **70**, 841; 1946 b, *Ibid.*, **70**, 852.  
DAUDIN, J., 1943, *Ann. Phys., Paris*, **18**, 145, 217.  
FRETTER, W. B., 1948, *Phys. Rev.*, **73**, 41.  
HEITLER, W., 1944, *Quantum Theory of Radiation* (Oxford: University Press), p. 226.  
ROCHESTER, G. D., and BUTLER, C. C., 1948, *Proc. Phys. Soc.*, **61**, 307.  
ROGOZINSKI, A., 1944, *Phys. Rev.*, **65**, 291.  
ROSSI, B., and GREISEN, K., 1941, *Rev. Mod. Phys.*, **13**, 276.

## The Effect of External Quenching on the Life of Argon-Alcohol Counters

By H. ELLIOT

The University, Manchester

*Communicated by P. M. S. Blackett; MS. received 18th February 1949*

**ABSTRACT.** A simple multivibrator for eliminating multiple discharges in argon-alcohol counters is described. This circuit has been used successfully in cosmic-ray intensity recording equipment requiring a high degree of stability. It is shown that the increase in counter life which is observed when a multivibrator of this kind is used is probably due to quenching of the discharge before it has spread the full length of the counter wire.

### § 1. INTRODUCTION

IN the course of experiments using large numbers of commercially produced argon-alcohol counters, difficulty was experienced because of the large percentage of multiple discharges and a tendency towards instability which developed after a few months of continuous operation. In addition, the life of the counters was very short, amounting on the average to about six months' operation, after which it was necessary to refill them with fresh argon and alcohol.

These counters had an effective length of 60 cm. and a diameter of 4 cm.; the cathodes were of copper foil and the anodes of tungsten wire. They were filled with a mixture of argon (11 cm. Hg) and alcohol (1.5 cm. Hg). The background counting rate was about 15 per second.

In an effort to improve the performance of these counters a single-stroke multivibrator was used for suppressing the multiple discharges. A multivibrator has also been used by Putman (1948) for this purpose. In addition to an improvement in plateau slope and stability, it soon became evident that there was an appreciable increase in counter life, and it therefore seemed worth while to investigate the action of the multivibrator more thoroughly.

### § 2. EXPERIMENTAL PROCEDURE

Multivibrator circuits of varying degrees of complexity have been used by many workers for quenching the discharge in non-self-quenching counters and are described in the literature (Getting 1938, Lewis 1942, Maier Leibnitz 1948).

The circuit of the multivibrator used here is shown in Figure 1. When an ionizing particle produces a discharge in the counter a negative voltage pulse appears across the 220 k $\Omega$  resistance which initiates the usual trigger action

This operation drops the voltage across the counter by about 200 volts. This fall in potential reduces the field below threshold and the discharge ceases. The time constants of the circuit are such that the potential of the counter anode is held below threshold for 1.5 milliseconds, which allows the positive ions to reach the cathode before the anode potential rises again. Any secondary electrons which may be produced cannot therefore cause any further discharge.

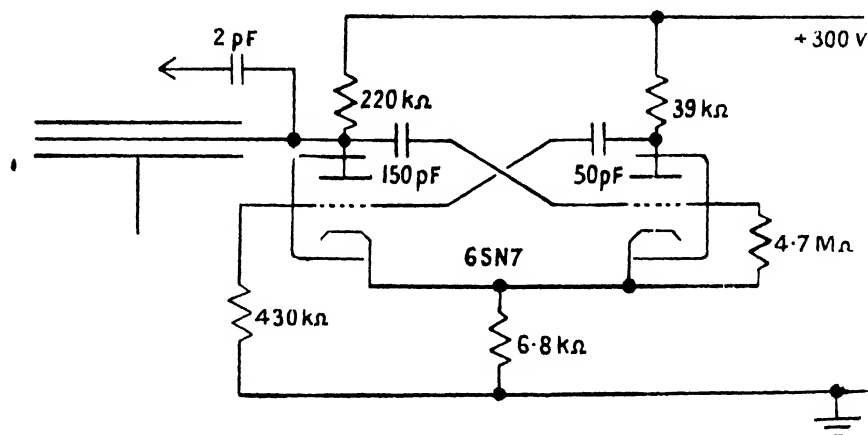


Figure 1.

Since it seemed likely that the increase in life was connected with a decrease in the extent of the discharge, due to the quenching action of the multivibrator, measurements were made of the quantity of electricity  $Q$  passing through the counter during a discharge. These measurements were made by partially discharging a  $0.96 \mu\text{F}$ . condenser through the counter and recording the number of pulses for a given fall in potential across the condenser, correction being made for the finite leakage resistance of the condenser itself.

### § 3. EXPERIMENTAL RESULTS

Measurements of  $Q$  were made for two counters of the same type (60 cm.  $\times$  4 cm.). Figure 2(A) shows  $Q$  plotted against counter voltage for one of these counters, which was operated with a 200,000-ohm series resistance but no multivibrator. Figure 2(B) shows  $Q$  as a function of voltage for the same counter but operated with a multivibrator.

The multivibrator shown in Figure 1 was developed for use in a cosmic-ray intensity recorder which incorporated trays of ten counters connected in parallel, each counter being connected to its own multivibrator. In order to prevent mutual interaction, the multivibrators were not adjusted for maximum sensitivity. Figure 2(C) shows the effect of increasing the sensitivity of the multivibrator (by reducing the cathode bias resistance from 6.8 kΩ to 4.0 kΩ). Similar results were obtained for the second counter.

It is clear from the results of these measurements that  $Q$  is reduced when the counter is externally quenched, the reduction being greater for the more sensitive multivibrator.

### § 4. DISCUSSION OF RESULTS

Hodson (1948) has used a multivibrator for decreasing the dead time of a counter by reversing the anode potential. At the time, this decrease in dead time

was interpreted as being due to positive ion collection at the anode, but later measurements showed that a reduction in effective dead time was still observed if a 250-volt negative pulse of 10 microsecond duration was applied to the counter wire. Positive ion collection could not occur under these conditions, and it was suggested by Sherwin that the application of a negative pulse prevented the discharge from spreading the full length of the counter. Further measurements by Hodson (unpublished) and by Smith (1948) have confirmed this interpretation.

The reduction in  $Q$  when the counter is used with a multivibrator is a further indication that the discharge is being limited in this way. The reduction in  $Q$  as shown in Figure 2 indicates that the discharge is limited to roughly a quarter of the total length of the counter, depending on the sensitivity of the multivibrator and the counter voltage. It should be possible to reduce the extent of the discharge still further by quenching with a more sensitive multivibrator, using two pentodes. A double triode valve has been used here in order to economize in valves and components.

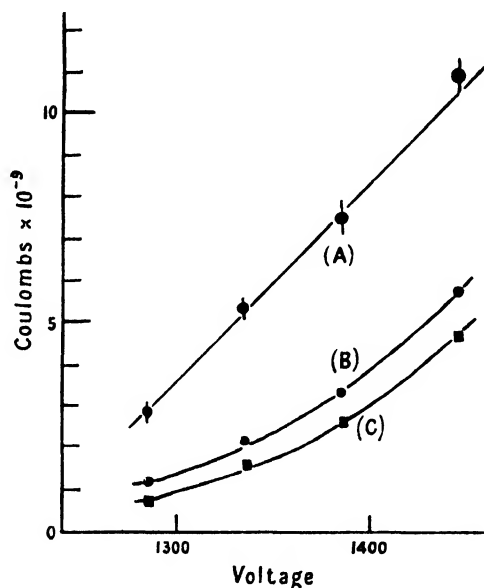


Figure 2.

It is not clear what factors determine the life of a counter, but whether it be dissociation of the alcohol molecules or some surface effect on the cathode or anode it is clear that, if the discharge is confined to part of the counter only, there should be an increase in counter life. Measurements of the velocity of spread of the discharge along counter wires (Hill and Dunworth 1946) give values of the order of 10 cm. per microsecond. If, for example, the anode potential of a 60-cm. counter is reduced to threshold in 1 microsecond, then the discharge will have spread some distance which will be less than 20 cm. (10 cm. in each direction) before being extinguished. Under these conditions it seems reasonable to expect the counter life to be increased by a factor of at least three.

As a further check on this interpretation  $Q$  was measured when the counter was stimulated by  $\gamma$ -rays passing through (a) the middle of the counter, (b) the end of the counter. Under conditions (a) the discharge can spread along the

wire in both directions, whereas in (b) it can spread in one direction only. When the counter operates without a quenching pulse the discharge will spread to the full length of the counter for both (a) and (b) and  $Q$  should be the same for both conditions. When a quenching pulse is applied, however, the discharge will spread further under condition (a) than under condition (b), and consequently  $Q$  should be greater when  $\gamma$ -rays pass through the middle than when they pass through the end.

Measurements were made on two counters with quenching pulses applied to their anodes, and in each case a significant decrease in  $Q$  was observed when the  $\gamma$ -rays passed through the end of the counter. Measurements were also made on the counters when operated without quenching and, as expected, there was no significant difference in  $Q$  as measured under conditions (a) and (b). The results of these measurements are given in the Table.

Values of  $Q$  for Different Operating Conditions

		Counter 1		Counter 2	
		No external quenching	External quenching	No external quenching	External quenching
$\gamma$ -rays through middle	$\left. \begin{array}{l} \gamma\text{-rays} \\ \text{through} \\ \text{middle} \end{array} \right\}$	$3.17 \pm 0.06 \times 10^{-9}$	$1.47 \pm 0.01 \times 10^{-9}$	$4.51 \pm 0.03 \times 10^{-9}$	$1.04 \pm 0.02 \times 10^{-9}$
$\gamma$ -rays through end	$\left. \begin{array}{l} \gamma\text{-rays} \\ \text{through} \\ \text{end} \end{array} \right\}$	$3.22 \pm 0.04 \times 10^{-9}$	$0.87 \pm 0.02 \times 10^{-9}$	$4.51 \pm 0.03 \times 10^{-9}$	$0.63 \pm 0.01 \times 10^{-9}$

Multivibrators of the type described above have been used in cosmic-ray intensity recording equipment in these laboratories since the middle of 1947 and have brought about a marked improvement in the stability and life of the argon-alcohol counters used in the recorder. In order to obtain information, in a reasonable time, about the performance of counters operated in this way for prolonged periods, one counter, selected at random, was stimulated by means of a  $\gamma$ -ray source so that it counted at a rate of 520 per second. This is about 35 times its normal background rate of 15 per second. The counter was operated at 75 volts above threshold. Initially the plateau slope of this counter was 0.02% per volt, but this gradually increased to 0.10% per volt after approximately  $3 \times 10^9$  counts.

The length of the plateau remained very nearly the same (200 v.) during this period, but the background rate rose sharply after  $2.7 \times 10^9$  counts, and the useful life of this counter was therefore approximately  $2.7 \times 10^9$  counts, which corresponds to approximately 6 years' operation at the normal background rate. Assuming that the life of a counter depends on the total number of particles counted, we might expect a counter of this type to last for approximately 6 years without suffering any serious deterioration when used for counting cosmic rays.

This increase in life appears to be greater than might be expected from the measurements of  $Q$ , but it must be remembered that the elimination of multiple discharges alone will increase the life since each ionizing particle passing through the counter produces one discharge only. In addition, a counter which is unusable without external quenching because of multiple discharges will often operate quite satisfactorily with a multivibrator. Because of this a counter

which would normally be supposed to have reached the end of its life can continue to perform satisfactorily if used with a quenching multivibrator. The observed increase in life must be due to a combination of these three effects.

#### § 5. CONCLUSION

The increase in life of argon-alcohol counters which has been observed when these counters have been used with a single-stroke multivibrator appears to be due to the extinction of the discharge before it has spread the full length of the counter and to the suppression of multiple discharges. Under the most favourable conditions described the discharge appears to be limited to about one-quarter of the total length. Measurements made on a counter of length 60 cm. and diameter 4 cm. indicate that such a counter has a life of about  $2.7 \times 10^9$  counts.

In addition to this increase in lifetime, further advantages in using a simple multivibrator of this kind are: (a) the slope of the counter plateau is reduced because of the suppression of multiple discharges; (b) the counter dead time is determined by the time constants of the multivibrator and is, therefore, virtually independent of counter voltage.

#### ACKNOWLEDGMENTS

The writer is indebted to Mr. D. W. N. Dolbear for much valuable help and advice, to Mr. A. L. Hodson for many stimulating discussions and to Professor P. M. S. Blackett for continued interest and encouragement.

#### REFERENCES

- GETTING, I. A., 1938, *Phys. Rev.*, **53**, 103.  
HILL, J. M., and DUNWORTH, J. V., 1946, *Nature, Lond.*, **158**, 833.  
HODSON, A. L., 1948, *J. Sci. Instrum.*, **25**, 11.  
LEWIS, W. B., 1942, *Electrical Counting* (Cambridge: University Press), p. 111.  
MAIER LEIBNITZ, H., 1948, *Rev. Sci. Instrum.*, **19**, 500.  
PUTMAN, J. L., 1948, *Proc. Phys. Soc.*, **61**, 312.  
SMITH, P. B., 1948, *Rev. Sci. Instrum.*, **19**, 453.

## On the Absorption of Meson-producing Nucleons

BY W. HEITLER AND L. JÁNOSSY

Dublin Institute for Advanced Studies

*MS. received 23rd January 1949*

**ABSTRACT.** The absorption of nucleons passing through any number of nuclei is calculated with due consideration of all fluctuations of energy loss. For the probability  $w(\epsilon, E) d\epsilon$  for an energy loss  $\epsilon$  by a nucleon with energy  $E$  hitting a nucleon at rest, a law of the form  $w d\epsilon = w(\epsilon/E) d\epsilon/E$  is assumed, a law suggested by meson theory and Bremsstrahlung. It is shown that, with a primary spectrum, following a power law, the absorption is strictly exponential for any thickness of the absorber and for all energies of the nucleons, apart from small deviations at low energies due to the latitude cut-off. This agrees well with recent experimental results. The experiments also permit some conclusions about the shape of the function  $w$ , and it is shown that  $w$  must be a fairly broad distribution extending up to  $\epsilon/E = 1$ , possibly favouring, but not to a very large extent, low values of  $\epsilon/E$ . The average energy loss of a fast nucleon hitting a nucleon at rest is determined by the experiments within very narrow limits. The conclusions that can be drawn about  $w$ , the total cross-section for meson production and the average energy loss are all compatible with the theory of Hamilton, Heitler and Peng, in its later version.

### § 1. INTRODUCTION

THE absorption of the fast cosmic ray nucleons which are capable of producing small or large penetrating showers has recently been measured throughout the whole atmosphere by various authors using various experimental arrangements for recording different sized showers. It has been found (Braddick and Hodson (private communication), Wataghin 1947, George and Jason 1947, 1948, Tatel and Van Allen 1948, Tinlot 1948 a, b, Rossi 1948, Bernardini, Cortini and Manfredini 1948), that the absorption is exponential with the same absorption coefficient of about  $100 \text{ gm/cm}^2$ , independent of the thickness of the absorber (up to a thickness of  $1,000 \text{ gm/cm}^2 = \text{whole atmosphere}$ ) and of the arrangement. The effective mean free path of  $100 \text{ gm/cm}^2$  in air is twice that to be expected if the cross-section for absorption per nucleus is the geometrical one.

At first sight one is tempted to interpret these findings as follows: (i) the absorption is catastrophic: the nucleons lose so much energy in a single nuclear hit that they are no longer capable of producing further mesons; (ii) the cross-section for such a hit is half the geometrical cross-section; one might, indeed, expect exponential absorption only, if the nucleons are absorbed in a single hit.

However, the comparatively small cross-section of only half the geometrical one is not very likely to be true. The transition curve of penetrating showers favours a larger cross-section, and cases have been observed where one nucleon creates two penetrating showers in succession. So we conclude that the primary nucleons are capable of penetrating on the average through two air nuclei, and the question arises whether we can then account for the purely exponential absorption.

We shall consider the problem here in a fairly general way, taking into consideration all the fluctuations of energy loss. These are due to the following

causes: (i) In passing through a nucleus the length of path (and therefore the number of nucleons hit) can range from 0 to  $d_A$ , where  $d_A$  is the diameter of the nuclei, and there will be a certain probability for a length of path between these two limits. (ii) The nucleon may pass through any number of nuclei and there will be a probability for hitting a specified number of nuclei. (iii) In hitting a single nucleon the primary nucleon with energy  $E$  may lose any energy  $\epsilon = 0 \dots E$  through meson production, and there will be a certain probability  $w(\epsilon, E)d\epsilon$  for a specified energy loss.

While the fluctuations (i) and (ii) are due to statistical and geometrical causes,  $w(\epsilon, E)$  should be taken from a theory of meson production. Since, however, any such theory suffers from many uncertainties, we investigate the problem here in a more phenomenological way: in the present paper we shall assume a simple model for  $w$  and assume that  $w$  depends on  $\epsilon/E$  only:

$$w(\epsilon, E) = w\left(\frac{\epsilon}{E}\right) \frac{\epsilon}{E}. \quad \dots\dots(1)$$

A consequence of (1) is that the total cross-section for meson production is independent of  $E$  and the average energy loss proportional to  $E$ :

$$\int_0^E w\left(\frac{\epsilon}{E}\right) \frac{d\epsilon}{E} = \text{const.}; \quad \int_0^E \epsilon w\left(\frac{\epsilon}{E}\right) \frac{d\epsilon}{E} \sim \text{const. } E. \quad \dots\dots(1')$$

In a later paper we hope to investigate also other cases, for instance  $w = w(\epsilon)$ , independent of  $E$ , etc.

A theory of meson production has been put forward by Hamilton, Heitler and Peng (1943) and improved by Jánosy (1943) and Heitler and Walsh (1945). The result is that the most essential parts of the cross-section fall into the class (1), (1'), and the constants in (1') could be determined within certain limits, the uncertainty being a factor 4 or so (see §4). We shall be able to determine the constants from experiment to some extent, and it will be seen that they are compatible with the predictions of the theory. Moreover, something can also be concluded about the shape of  $w(\epsilon/E)$ ; further, this conclusion agrees qualitatively with the theory.

The original theory was developed before the discovery of the  $\pi$ -meson. It is now clear that the theory should be applied to  $\pi$ -mesons, but not to  $\mu$ -mesons, and also probably to  $\tau$ -mesons (mass 700–1,000). Furthermore, it has been assumed that there occur "transverse" mesons with a short life whose decay is responsible for the soft component. The rôle of this type of meson may be taken over by any short-lived meson that decays into photons or electrons.  $\epsilon$  in (1), (1') includes, of course, all types of meson produced, charged and neutral, whether long- or short-lived.

Furthermore, we shall assume a power law for the primary spectrum of nucleons. This is well justified on many experimental grounds. We shall then show that this spectrum is reproduced after passage through any thickness of material while the total intensity decreases exponentially. This is true for all energies above the latitude cut-off, while for smaller energies certain deviations from the power spectrum and the exponential absorption arise. These deviations are of no importance for European or American latitudes because nucleons which are capable of producing mesons in appreciable numbers must anyhow possess energies close to or larger than the European cut-off energy.



## § 2. THE FLUCTUATIONS OF THE LENGTH OF NUCLEAR PATH

We assume the nuclei to be spheres of diameter

$$d_A = 3 \times 10^{-13} A^{\frac{1}{3}} \text{ cm.} \quad \dots\dots (2)$$

For oxygen  $d_0 = 7.5 \times 10^{-13} \text{ cm.}$ , and the geometrical cross-section is

$$\Phi_0 = 4.4 \times 10^{-25} \text{ cm}^2. \quad \dots\dots (2')$$

This corresponds to a mean free path of  $50 \text{ gm/cm}^2$ . The average number of collisions with nuclei when passing through a thickness  $\theta \text{ gm/cm}^2$  is

$$\bar{p} = \theta n \Phi_A, \quad \dots\dots (2'')$$

where  $n$  is the number of nuclei per gram.

We denote by  $X d_A$  the total length of path which the fast nucleon passes through *nuclear* matter.  $X$  is thus the length of path in units of the nuclear diameter. We require the probability  $P(\theta, X) dX$  for  $X$  to lie in the interval  $dX$  when the nucleon traverses  $\theta \text{ gm/cm}^2$  of material.

The probability for hitting altogether  $p$  nuclei is  $\{\exp(-\bar{p})\} \bar{p}^p / p!$ . Thus, writing  $P_p(\theta, X)$  for the probability of a length of path  $X$  when it is known that actually  $p$  nuclei are hit, we have

$$P(\theta, X) = \sum_{p=0}^{\infty} \{\exp(-\bar{p})\} \frac{\bar{p}^p}{p!} P_p(X). \quad \dots\dots (3)$$

Consider now the  $k$ th collision with a nucleus. The probability that the length of path through the nucleus is  $x_k$  is evidently, on purely geometrical grounds,  $2x_k dx_k$ . Thus,

$$\left. \begin{aligned} P_p(X) dX &= \int \dots \int 2^p x_1 x_2 \dots x_p dx_1 dx_2 \dots dx_p, \\ 0 \leq x_k \leq 1, \quad X \leq x_1 + x_2 + \dots x_p \leq X + dX. \end{aligned} \right\} \quad \dots\dots (4)$$

The integral can be worked out in terms of polynomials, but this is very cumbersome, and the result appears in different analytical forms according to the intervals in which  $X$  lies. Instead we introduce the Laplace-transform of  $P_p$ :

$$L_\lambda(P_p) = \int_0^\infty e^{-\lambda X} P_p(X) dX = 2^p \left( \int_0^1 x e^{-\lambda x} dx \right)^p. \quad \dots\dots (5)$$

Actually only values  $X \leq p$  contribute to the integral. Introducing (5) into (3), we obtain for the Laplace-transform of  $P(\theta, X)$ :

$$L_\lambda(P) \equiv \int_0^\infty e^{-\lambda X} P(\theta, X) dX = \exp \{ -\bar{p} f(\lambda) \}. \quad \dots\dots (6)$$

$$f(\lambda) = 1 - 2 \int_0^1 x e^{-\lambda x} dx = 1 - 2 \frac{1 - (1 + \lambda) e^{-\lambda}}{\lambda^2}. \quad \dots\dots (6')$$

$f(\lambda)$  has no singularity at  $\lambda = 0$ ; the expansion is

$$f(\lambda) = \frac{2}{3} \lambda - \frac{\lambda^2}{4} + \dots \quad \dots\dots (6'')$$

Thus  $f(0) = 0$  and  $\int_0^\infty P(\theta, X) dX = 1$ .  $P(\theta, X)$  is therefore properly normalized.

$f(\lambda)$ , together with its first and second derivatives, is given in the Table.

$\lambda$	$f(\lambda)$	$f'(\lambda)$	$f''(\lambda)$	$\lambda$	$f(\lambda)$	$f'(\lambda)$	$f''(\lambda)$
-1.0	-1.00000	1.43656	-1.1269	-0.5	-0.40511	0.97443	-0.7483
-0.9	-0.86183	1.32839	-1.0378	-0.4	-0.31131	0.90255	-0.6900
-0.8	-0.73404	1.22876	-0.9560	-0.3	-0.22442	0.83627	-0.6364
-0.7	-0.61581	1.13697	-0.8809	-0.2	-0.14389	0.77518	-0.5866
-0.6	-0.50640	1.05239	-0.8118	-0.1	-0.06924	0.71880	-0.5400
0.0	0.00000	0.66667	-0.5000	0.5	0.27837	0.46041	-0.3363
0.1	0.06424	0.61860	-0.4600	0.6	0.32277	0.42806	-0.3109
0.2	0.12385	0.57425	-0.4265	0.7	0.36406	0.39815	-0.2876
0.3	0.17919	0.53326	-0.3938	0.8	0.40248	0.37049	-0.2660
0.4	0.23060	0.49540	-0.3639	0.9	0.43823	0.34489	-0.2462
1.0	0.47152	0.32121	-0.2279	1.6	0.62885	0.21156	-0.1443
1.1	0.50253	0.29927	-0.2110	1.7	0.64930	0.19766	-0.1339
1.2	0.53143	0.27897	-0.1954	1.8	0.66842	0.18476	-0.1219
1.3	0.55837	0.26015	-0.1811	1.9	0.68629	0.17278	-0.1154
1.4	0.58350	0.24271	-0.1678	2.0	0.70300	0.16166	-0.1072
1.5	0.60696	0.22655	-0.1556				

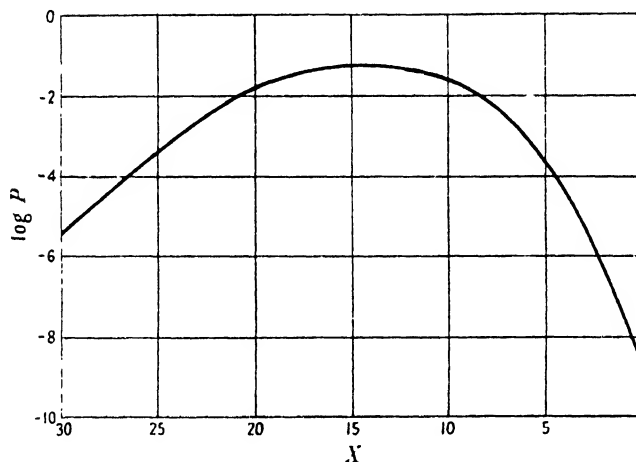


Figure 1. The probability  $P(\theta, X)$  for a path length  $X$  in nuclear matter.  $\bar{p}=20$  (sea level).

Although, for the actual calculation of the absorption, we shall only require the Laplace-transform  $L_{\lambda}(P)$ , the distribution  $P(\theta, X)$  is also of some interest. We have, according to the theory of Laplace transformations,

$$P(\theta, X) = \frac{1}{2\pi i} \int_{\lambda' - i\infty}^{\lambda' + i\infty} \exp \{ \lambda X - \bar{p}f(\lambda) \} d\lambda. \quad \dots (7)$$

Since  $f(\lambda)$  has no singularity except at infinity,  $\lambda'$  can be chosen arbitrarily. Equation (7) can be worked out approximately by the saddle-point method. The position of the saddle-point  $\lambda_0$  is given by

$$\frac{\partial}{\partial \lambda} \{ \lambda X - \bar{p}f(\lambda) \} = 0 \quad \text{or} \quad X = \bar{p}f'(\lambda_0). \quad \dots (8a)$$

Expanding the exponent in (7) up to the order of  $(\lambda - \lambda_0)^2$  and using (8a) we may identify  $\lambda'$  with  $\lambda_0$  and obtain

$$P(\theta, X) = \frac{1}{[2\pi \bar{p}f''(\lambda_0)]^{1/2}} \exp [ \bar{p} \{ \lambda_0 f'(\lambda_0) - f(\lambda_0) \} ]. \quad \dots (8b)$$

$E_0$  is the latitude cut-off energy. The value of  $\gamma$ , derived from the latitude effect of energy flow, is about 1.5. This gives, by (18),

$$M_s(0) = \frac{\gamma}{\gamma - s + 1} E_0^{s-1} \quad \text{Re}(s) < \gamma + 1. \quad \dots\dots (21)$$

The condition  $\text{Re}(s) < \gamma + 1$  is required to make (19) convergent and is compatible with  $\text{Re}(s) > 1$ . Applying the inverse Mellin transformation to (17), we find

$$S(E, X) = \frac{1}{2\pi i E_0} \int_{s_0 - i\infty}^{s_0 + i\infty} \frac{\gamma}{\gamma - s + 1} \left(\frac{E_0}{E}\right)^s \exp\{-(a - W_s)X\} ds. \quad \dots\dots (22)$$

$$1 < s_0 < \gamma + 1.$$

The limits for  $s_0$  are taken so as to conform with the above conditions for  $\text{Re}(s)$ .

We first consider the case  $E > E_0$ , i.e. energies larger than the cut-off energy. The quantity  $a - W_s$  has now always a positive real part. Hence, for  $E > E_0$ , the integrand of (21) vanishes sufficiently rapidly for  $s \rightarrow \infty$  and the path of integration can be completed and deformed into a circle round the pole  $s = \gamma + 1$ . Then

$$S(E, X) = \frac{E\gamma_0^\gamma}{E^{\gamma+1}} \exp\{-(a - W_{\gamma+1})X\} = S(E, 0) \exp\{-(a - W_{\gamma+1})X\}. \quad \dots\dots (23)$$

$$E > E_0.$$

That (23) is the solution of (14) can also be checked directly, by insertion. We see that (i) the primary spectrum is reproduced at any depth, and (ii) the absorption is exponential.

So far (23) refers to a passage through homogeneous nuclear matter. To find  $S(E, \theta)$  for a given thickness of the absorber we have to apply (12), using for  $P$  the results of § 2. Since  $S(E, X)$  varies exponentially, it is just the Laplace-transform of  $P(\theta, X)$  which occurs. From (6), (6'), (12) we get

$$S(E, \theta) = S(E, 0) L_\lambda(P) \quad \dots\dots (23a)$$

$$\text{or} \quad S(E, \theta) = S(E, 0) \exp\{-\theta n \Phi_A f(\lambda)\}, \quad \lambda = a - W_{\gamma+1}, \quad \dots\dots (23b)$$

$$W_{\gamma+1} = \int_0^1 w(z)(1-z)^\gamma dz, \quad a = \int_0^1 w(z) dz. \quad \dots\dots (23c)$$

$f(\lambda)$  is given by (6'). For  $E > E_0$  the problem is now completely solved, as soon as  $S(E, 0)$ , i.e.  $\gamma$  and  $w(\epsilon/E)$  are given. We see that also  $S(E, \theta)$  decreases exponentially with an effective absorption coefficient  $n\Phi_A f(\lambda)$  and that the power spectrum  $\sim E^{-(\gamma+1)} dE$  is reproduced at any depth.

The physical meaning of  $f(\lambda)$  is now also clear: it is the reciprocal of the effective number of nuclear collisions, before the nucleon disappears (i.e. becomes ineffective for meson production).

#### § 4. COMPARISON WITH EXPERIMENTS AND THE THEORY OF MESON PRODUCTION

According to the experimental findings the effective mean free path is  $\sim 100 \text{ gm/cm}^2$  in air and, since  $n\Phi_A \sim 50 \text{ gm/cm}^2$ , the experimental value of  $f(\lambda)$  is  $f(\lambda)_{\text{exp}} = 0.5$ .

From the Table we find that

$$\lambda_{\text{exp}} = (a - W_{\gamma+1})_{\text{exp}} = 1.1. \quad \dots\dots (24)$$

To interpret this result we express the cross-section in natural meson units  $(\hbar/\mu c)^2$ . For a meson mass  $\mu = 286m$ , which corresponds to the mass of the  $\pi$ -meson  $(\hbar/\mu c)^2 = 1.8 \times 10^{-26} \text{ cm}^2$ , thus:

$$\Phi(\epsilon, E) d\epsilon = \left(\frac{\hbar}{\mu c}\right)^2 \phi\left(\frac{\epsilon}{E}\right) d\left(\frac{\epsilon}{E}\right).$$

In  $a$  and  $W_{\gamma+1}$  we can then split off the factor

$$Nd_A \left(\frac{\hbar}{\mu c}\right)^2 = 0.95 \text{ for oxygen.} \quad \dots\dots (25)$$

(24) is therefore equivalent to

$$\int_0^1 \phi(z)[1 - (1-z)^\gamma] dz = 1.15 \quad (z = \epsilon/E). \quad \dots\dots (26)$$

From this relation we can now draw some conclusions about the shape of  $\phi(\epsilon/E)$ . We can best do that by considering a variety of shapes of the type

$$\phi(z) = \alpha(1-z)^\beta. \quad \dots\dots (27)$$

Varying  $\alpha$  and  $\beta$ , all sorts of possible, and reasonable, curves are obtained, favouring either small (large  $\beta$ ) or large (small  $\beta$ ) energy losses, and the true law, if it can be at all represented by a function of  $\epsilon/E$  only, can probably well be approximated by (27). The case  $\beta \leq -1$  must be excluded, otherwise the total cross-section would diverge. Even the case  $\beta < 0$  is unlikely, because so far no known law of energy loss favours high energy losses so strongly. The total cross-section (in units  $(\hbar/\mu c)^2$ ) is

$$\int_0^1 \phi(z) dz = \frac{\alpha}{\beta+1} = k \quad \text{and} \quad \int_0^1 \phi(z)(1-z)^\gamma dz = \frac{\alpha}{\beta+\gamma+1}. \quad \dots\dots (28)$$

Now it is inconceivable, on physical grounds, that  $k$  is much larger than the cross-section corresponding to the range of nuclear forces, i.e.  $\pi(\hbar/\mu c)^2$ . We can therefore say that  $\alpha/(\beta+1) < 4$ , approximately. Now the experimental relation (26) gives

$$(\beta+1)(\beta+\gamma+1) = 1.15, \quad \dots\dots (29)$$

$$\text{or, inserting } \gamma = 1.5, \quad \frac{1.5}{\beta+2.5} > \frac{1.15}{4} \quad \text{or} \quad \beta < 2.7. \quad \dots\dots (29')$$

Thus  $\beta$  cannot be too large, and this means that although small energy losses are favoured (as they are in all cases where the law of energy loss is known), *high energy losses are comparatively frequent*, roughly as in the case of Bremsstrahlung. The numerical figures in (29') must, of course, not be taken too literally, but it is safe to say that  $\beta$  cannot be larger than 3, and is probably less.

The average energy loss follows also from (28):

$$\bar{\epsilon} = \left(\frac{\hbar}{\mu c}\right)^2 E \int_0^1 \phi(z) z dz = \left(\frac{\hbar}{\mu c}\right)^2 E \sigma, \quad \dots\dots (30)$$

$$\sigma = \frac{1}{(\beta+1)(\beta+2)}.$$

Comparing this with (29), we see that

$$\sigma = \frac{1.15}{1.5} \frac{\beta+2.5}{\beta+2} = 0.96 - 0.77,$$

as  $\beta$  ranges from 0 to  $\infty$ . Thus the *mean energy loss is practically determined within narrow limits from the experiments alone*. This can be seen also directly from (26), because  $1 - (1 - z)^\beta$  is not very different from  $z$ .

The unit  $(h/\mu c)^2$  was introduced for dimensional reasons only; what follows from the experiment is, of course, the numerical value of the energy loss. This, as derived from the experiment, can be stated as being (per collision with one nucleon)

$$\bar{\epsilon} = \int_0^E \Phi(\epsilon, E) \epsilon d\epsilon = E(1.6 \pm 0.3) 10^{-26} \text{ cm}^2. \quad \dots\dots (30')$$

This result, of course, holds only if the assumed law  $w = w(\epsilon/E)$  is valid.

Finally we compare our more phenomenological results with the theory of meson production (Heitler 1945, Heitler and Walsh 1945). The main contribution to meson production follows indeed a cross-section of the form  $\phi(\epsilon/E) d(\epsilon/E)$ , with less important contributions of the form  $\phi(\epsilon) d\epsilon$  independent of  $E$ . When the more complicated formulae (Heitler 1945) are plotted, it is seen that they agree fairly well with a form (27) with  $\beta \sim 2$ . (Indeed, the most important terms of  $\phi$  are  $(1 - \epsilon/E)^2$ .) This agrees with the condition (30). The total cross-section and the average energy loss are given by Heitler (1949) for a meson mass 315 : \*

$$\begin{aligned} \int_0^E \phi(\epsilon, E) d\epsilon &\sim \left(\frac{h}{\mu c}\right)^2 k, & k &= 4 - 18, \\ \int_0^E \epsilon \phi(\epsilon, E) d\epsilon &= \left(\frac{h}{\mu c}\right)^2 E \sigma, & \sigma &= 0.9 - 4. \end{aligned} \quad \dots\dots (31)$$

The rather wide range for the constants is due to an uncertainty of the lower limit of the impact parameter, but obviously, from what was said above, the lower, rather than the upper, figure must be accepted if the total cross-section is not to be unphysically large. It is clear that all this is well compatible with the conclusions derived from experiment, and in particular the value for  $\sigma$ , which could be determined from experiments directly, agrees well with the theoretical prediction. The value of  $k$ , however, does not follow from the experiments alone but requires a knowledge of  $\beta$ . If we accept for instance  $\beta = 2$ , it is clear that we should also get the theoretical value for  $k$ , because the theoretical formulae are close to  $\beta = 2$ . In fact (29) gives  $k \sim 3.5$ .

All the above conclusions hold only with the provision that a law  $\phi(\epsilon/E) d(\epsilon/E)$  is valid. The validity of such a law can hardly be deduced yet from the experiments, and it remains to be seen whether different laws for the energy loss can also account for the experiments.

## § 5. EFFECTS FROM THE LATITUDE CUT-OFF

The results of the previous sections (§§ 3 and 4) hold only for  $E > E_0$ . For European latitudes  $E_0 = 3 \cdot 10^9$  e.v., and energies less than this limit are probably of little importance for meson production. This will not be so for the equator, and we therefore investigate now the solution (21) for  $E < E_0$ . We assume, as before,

\* The constant  $k$  refers to charged mesons only, whereas  $\sigma$  includes, of course, neutrettos.  $k$  should therefore be multiplied by 3/2. On the other hand, for the total cross-section some contribution from low energy mesons is included which does not follow the  $w(\epsilon/E) d(\epsilon/E)$  law, and which contributes to the energy loss only in a lower order in  $E$ , but makes  $k$  bigger by a factor 2. For a fair comparison with the assumed  $\alpha(1 - \epsilon/E)^\beta$  law we should therefore multiply  $k$  by a factor 3/4, which is evidently of no importance.

$w(z) = \alpha(1-z)^\beta$ ,  $W_s = \alpha/(\beta+s)$ ,  $k = \alpha/(\beta+1)$ .  $S(E, X)$  is thus given by (22) and  $s_0$  can be chosen in the interval  $-\beta < s_0 < \gamma+1$ . As  $E < E_0$ , the integrand vanishes for  $s \rightarrow -\infty$  and, therefore, the path of integration can be completed to the left and deformed to a small circle round  $s = -\beta$ . This procedure gives for  $S(E, X)$  a series in terms of Bessel functions of imaginary argument. However, the series converges only slowly, and as we are primarily interested in  $S(E, \theta)$  rather than in  $S(E, X)$ , we do not give the explicit expression.

We obtain  $S(E, \theta)$  by introducing (22) into (12), thus

$$S(E, \theta) = \frac{1}{2\pi i E_0} \int_0^\infty P(\theta, X) dX \int_{s_0-i\infty}^{s_0+i\infty} \left(\frac{E_0}{E}\right)^s \frac{\gamma}{\gamma-s+1} \exp\{-(a-W_s)X\} ds. \quad \dots\dots (32)$$

Reversing the order of integration in (32) we obtain with the help of (6),

$$S(E, \theta) = \frac{1}{2\pi i E_0} \int_{s_0-i\infty}^{s_0+i\infty} \left(\frac{E_0}{E}\right)^s \exp\{-\bar{p}f(a-W_s)\} \frac{\gamma}{\gamma-s+1} ds, \quad \dots\dots (33)$$

$$-\beta < s_0 < \gamma+1; \quad \bar{p} = n\Phi_0\theta.$$

The integrand of (37) tends towards  $\infty$  when  $s$  approaches either  $-\beta$  or  $\gamma+1$  from the inside of this interval. Therefore the integrand must have a minimum on the real axis in the interval  $-\beta < s < \gamma+1$ , and thus the integral can be approximated by the saddle-point method. To do this, we write in the usual way

$$\Xi(s) \equiv s \ln \frac{E_0}{E} - \bar{p}f(a-W_s) - \ln(\gamma+1-s)$$

and

$$S(E, \theta) = \frac{\gamma}{2\pi i E_0} \int_{s_0-i\infty}^{s_0+i\infty} \exp\{\Xi(s)\} ds.$$

We choose  $s_0$  so as to make  $\Xi(s_0)$  a minimum on the real axis; this gives

$$\ln \frac{E_0}{E} = -\bar{p} \frac{dW_s}{ds} f'(a-W_s) - \frac{1}{\gamma+1-s}, \quad s=s_0 \quad \dots\dots (34)$$

$$-\beta < s_0 < \gamma+1$$

and

$$S(E, \theta) \simeq \frac{\gamma}{E_0} \frac{\exp\{\Xi(s_0)\}}{\{-2\pi\Xi''(s_0)\}^{1/2}}. \quad \dots\dots (34')$$

The equations (34) and (35) give a parametric representation of  $S(E, \theta)$ .

We note that for a given ratio  $E_0/E > 1$ , for sufficiently large  $\bar{p}$  ( $dW_s/ds < 0$ ),

$$\ln \frac{E_0}{E} \ll -\bar{p} \frac{dW_s}{ds} f'(a-W_s). \quad \dots\dots (35)$$

For such large values of  $\bar{p}$  (34) can only be satisfied by values of  $s_0$  approaching  $\gamma+1$ . Introducing  $\gamma+1-s_0=s'$ , we see that  $s'$  will be small for sufficiently large  $\bar{p}$ . Developing in powers of  $s'$ , we find as the result of a short calculation

$$S(E, \theta) = \gamma \left(\frac{E_0}{E}\right)^{\gamma+1} \frac{e}{\sqrt{(2\pi)}} (1 + \text{terms of order } s'^3). \quad \dots\dots (36)$$

The factor  $e/\sqrt{(2\pi)} = 1.08$  is nearly unity, and thus we see that for values of  $E$  and  $\bar{p}$  such that (35) with  $s = \gamma+1$  is satisfied, the spectrum is simply a continuation of the power spectrum which is exactly valid above  $E_0$ .

For  $\beta=2$ ,  $\gamma=1.5$  the condition for (36) to be valid is  $\ln(E_0/E) \ll 0.15\bar{p}$ . Thus at  $\bar{p}=20$  (sea level), the power spectrum just starts to extend below  $E_0$ .

That the power spectrum should extend below  $E_0$  for very large values of  $\bar{p}$  is obvious, as the primaries below the cut-off  $E_0$  must cease to be effective at sufficiently large depth. Thus (36) can be regarded as a test for the accuracy of the saddle-point method. It appears thus that the error of this method for large  $\bar{p}$  amounts to the deviation of  $e/\sqrt{(2\pi)}$  from unity, i.e. to about  $8\%$ .

We have evaluated the integral spectrum

$$T(E, \theta) = \int_E^{\infty} S(E, \theta) dE$$

by the saddle-point method for  $\beta=1, 2$  and  $\bar{p}=10, 20, 30$ . The results for  $\beta=2$  are shown in a double logarithmic plot in Figure 2.

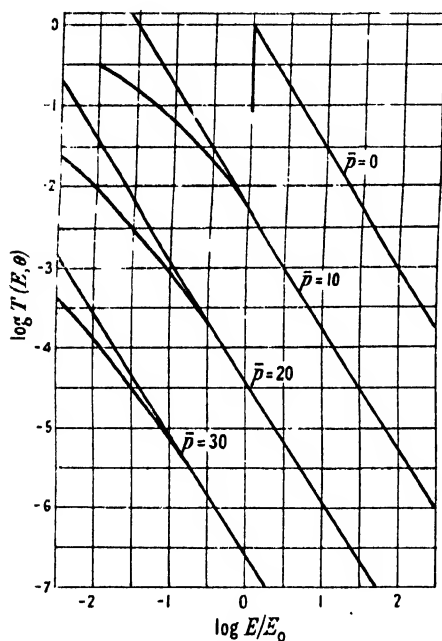


Figure 2. Latitude effect of nucleons at various depths.  $T(E, \theta)$  is the total number of nucleons with energy above  $E$ ,  $T_0(E, \theta)$  (straight lines) is the intensity when no latitude cut-off exists.  $\beta=2$ .  $\bar{p}=0$  is the primary spectrum.

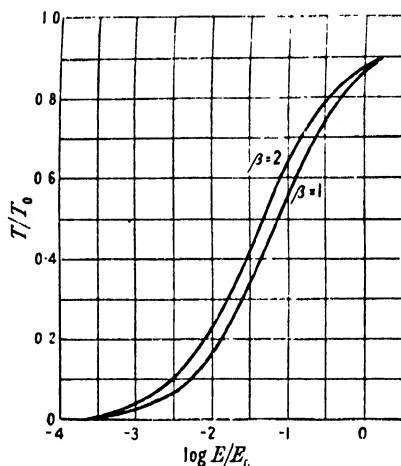


Figure 3. Latitude effect. Ratio of intensities  $T/T_0$  for  $\bar{p}=20$  (sea level) and  $\beta=1, 2$ .

In order to show more clearly the effect of the cut-off energy  $E_0$  we have also plotted  $T(E, \theta)/T_0(E, \theta)$  in Figure 3 for  $\bar{p}=20$ ,  $\beta=1, 2$ .

$$T_0(E, \theta) = (E_0/E)^\gamma \exp \{ -\bar{p}f(\lambda) \}$$

is the extended integral power spectrum.

We see from the graphs that  $T(E, \theta)/T_0(E, \theta) = 0.9$  if evaluated by the saddle-point method for  $E=E_0$ . Thus the method involves an error of about 10%, just as in the case considered above. For  $E=\frac{1}{5}E_0$  (e.g.  $E_0=15 \times 10^9$ ,  $E=3 \times 10^9$ ), we find

$$T(E, \theta)/T_0(E, \theta) = \begin{cases} 0.76 & \beta=2 \\ 0.69 & \beta=1 \end{cases}$$

Allowing for the error of the method, we conclude that the decrease of intensity should be about 15% for  $\beta=2$  and 23% for  $\beta=1$ .

The effect is expected to increase with height quite considerably, as seen from Figure 2.

The only experimental data so far available on the latitude effect of penetrating showers are those of Appapillai and Mailvaganam (1948). These workers do not find an effect, but their observations are not incompatible with an effect of the order of magnitude predicted by the theory.

*Note added in proof.* In the above treatment, contributions to the nucleon intensity arising from the possible production of secondary (recoil) nucleons in the process of meson emission have been neglected. If the production of secondary nucleons also follows a law of the form (1) this contribution can easily be taken into account by adding a further term to the diffusion equation (11). Nothing changes then, except the numerical value of  $W_{\gamma+1}$ . If, for instance, the probability of an energy loss  $\epsilon$ , accompanied by the production of a secondary nucleon of energy  $\epsilon'$  is of the form

$$\propto \left(1 - \frac{\epsilon}{E}\right)^{\beta} \left(1 - \frac{\epsilon'}{E}\right)^{\beta_1},$$

$$\text{then} \quad W_{\gamma+1} \rightarrow W_{\gamma+1} \left(1 - \frac{\gamma}{\beta + \beta_1 + \gamma + 2}\right) + W_1 \frac{\gamma! (\beta + \beta_1 + 1)!}{(\beta + \beta_1 + \gamma + 1)!}.$$

For reasonable values of  $\beta$  and  $\beta_1$  the change is quite small, certainly smaller than the uncertainty of the constants  $\beta$ ,  $\gamma$ , etc. At any rate, whatever change occurs, it will make the determination of  $\bar{\epsilon}$  in § 4 change slightly in favour of a higher value, because the effective absorption coefficient is fixed by experiment.

#### REFERENCES

- APPAPILLAI, V., and MAILVAGANAM, A. W., 1948, *Nature, Lond.*, **162**, 887.  
 BERNARDINI, G., CORTINI, G., and MANFREDINI, M., 1948, *Phys. Rev.*, **74**, 1878.  
 GEORGE, E. P., and JASON, A. C., 1947, *Nature, Lond.*, **160**, 327; 1948, *Ibid.*, **161**, 248.  
 HAMILTON, J., HEITLER, W., and PENG, H. W., 1943, *Phys. Rev.*, **64**, 78.  
 HEITLER, W., 1945, *Proc. Roy. Irish Acad.*, **50**, 155; 1949, *Rev. Mod. Phys.*, in the press.  
 HEITLER, W., and WALSH, P., 1945, *Rev. Mod. Phys.*, **17**, 252.  
 JÁNOSY, L., 1943, *Phys. Rev.*, **64**, 345.  
 ROSSI, B., 1948, *Rev. Mod. Phys.*, **20**, 537.  
 TATEL, H. E., and VAN ALLEN, J. A., 1948, *Phys. Rev.*, **73**, 87.  
 TINLOT, J., 1948, *Phys. Rev.*, **73**, 1476; 1948, *Ibid.*, **74**, 1197.  
 WATAGHIN, G., 1947, Cracow Conference (communication by Gross).



## Some Cut-off Methods for the Electron Self-Energy

By J. RZEWUSKI

Department of Mathematical Physics, University of Birmingham

*Communicated by R. E. Peierls; MS. received 4th February 1949*

**ABSTRACT.** Some Lorentz-invariant cut-off procedures for the electron self-energy are investigated. Expressions for the self-energy are obtained as expansions in inverse powers of the cut-off constant  $K$ . The first term, logarithmic in  $K$ , has the correct transformation properties for all the cut-offs. The second term, independent of  $K$ , is covariant only for one of the procedures. The remaining terms have not the correct properties in any of the procedures, but contain negative powers of  $K$  and, therefore, vanish for  $K \rightarrow \infty$ . The one cut-off procedure which gives a covariant constant term can therefore be used for an unambiguous subtraction of the electron self-energy provided that in the final results one proceeds to the limit  $K \rightarrow \infty$ .

THE electron self-energy in hole theory was first calculated by Weisskopf (1934, 1939). He showed that while the self-energy is still infinitely large, the divergence is only logarithmic owing to the partial cancellation of terms referring to "holes" and real electrons. If the integrations are cut off at some finite wave vector  $K$  the self-energy is, of course, finite and quite small unless  $K$  is chosen extremely large. In Weisskopf's result even the leading term, logarithmic in  $K$ , is not Lorentz invariant, so that the self-mass would appear to depend on the velocity.

Lamb (1947) corrected some numerical errors in Weisskopf's paper and found that the sum of the static and dynamic self-energies (which Weisskopf had given separately), the total self-energy, has the form

$$W = \frac{3}{2} \frac{e^2}{\pi} \frac{m_0^2}{E_0} \ln \frac{K}{m_0} + \text{finite terms.} \quad \dots\dots(1)$$

Here  $E_0$ ,  $m_0$  are energy and mechanical rest mass of the electron,  $K$  is the upper limit in the integrals over the energy  $k$  of the virtual photon which can be emitted by the electron. We have chosen units in which  $\hbar = c = 1$ . The first term of (1) diverges logarithmically as  $K \rightarrow \infty$ . One would, of course, obtain finite answers if one could keep the upper limit  $K$  of integration finite instead of making it tend to infinity.

For physically consistent results the total rest mass of the particle must be constant, so that the energy for a given momentum is  $E_{\text{total}} = \sqrt{(m^2 + p^2)}$ , and if, as perturbation theory implies, the electromagnetic self-mass  $\Delta m$  is small compared to the mechanical mass  $m_0$ ,

$$E_{\text{total}} = E_0 + m_0 \Delta m / E_0. \quad \dots\dots(2)$$

This shows that for Lorentz invariance the self-energy  $W$  should be inversely proportional to  $E_0$ .

This is true of the first term in (1). However, the next term in the expansion, which is independent of  $K$ , has a different behaviour. This was pointed out by Lennox (1948), who obtains the following expression for these terms:

$$W = \frac{e^2}{2\pi} \frac{m_0^2}{E_0} \left\{ 3 \ln \frac{2K}{m_0} - \frac{1}{2} + \frac{4}{9} \left( \frac{p_0}{m_0} \right)^2 \right\}. \quad \dots\dots(3)$$

The lack of covariance can be due to two circumstances. First of all, putting a constant upper limit for  $k$  in the momentum integrals means that the domain of integration is a sphere of radius  $K$  in momentum space. Such a sphere is

obviously not invariant. The second case might be in the foundations of quantum mechanical perturbation theory. The concept of a virtual state is certainly not invariant. To see this it is only necessary to consider the four-vector  $\Delta\mathbf{p}, \Delta E$  corresponding to the change of total momentum and energy in a transition from a real to a virtual state. Conservation of momentum requires  $\Delta\mathbf{p}=0$ , but  $\Delta E$  is arbitrary since in transitions to virtual states the unperturbed energy is not conserved. Transformation to another Lorentz-frame gives  $\Delta\mathbf{p}\neq 0$ . Conservation of momentum is therefore satisfied only in one particular frame of reference.

It is easy to remove the first cause of non-invariance by introducing an invariant cut-off function. The second cause cannot be removed in general without abandoning altogether the perturbation method.

It is, however, interesting to know what improvements can be achieved by retaining the usual perturbation method and eliminating only the first source of non-invariance.

In the case of one electron in interaction with the radiation field, the four-vector  $\Delta\mathbf{p}, \Delta E$  is a sum of two four-vectors corresponding to the change of momentum and energy of the particle  $\Delta\mathbf{p}_{el}, \Delta E_{el}$  and the field  $\Delta\mathbf{p}_f, \Delta E_f$ . There are two independent invariants which can be constructed out of these four-vectors:

$$\Delta\mathbf{p}_{el}^2 - \Delta E_{el}^2 \quad \dots\dots(4)$$

and

$$\Delta\mathbf{p}_{el}\Delta\mathbf{p}_f - \Delta E_{el}\Delta E_f \quad \dots\dots(5)$$

The other obvious combination,  $\Delta\mathbf{p}_f^2 - \Delta E_f^2$ , vanishes for the processes we are considering, and all other invariants can be expressed in terms of (4) and (5).

Wataghin (1934) has suggested cutting off the integrals by means of a weight factor depending on the first invariant (4). Professor Peierls suggested using a function of (5) instead. Both procedures are investigated in this paper. In the limiting case  $K \rightarrow \infty$  the second procedure will be shown to give invariant results whereas the first one does not.

As cut-off function any scalar function  $f(x)$  of the invariants (4) or (5) can be used. The most convenient way is to take a rectangular function:  $f(x)=1$  for  $|x|<C$ ,  $f(x)=0$  for  $|x|>C$ . (The symbol  $x$  stands here for the expressions (4) or (5)). This means that we allow only such virtual states which satisfy the restriction  $|x|<C$ . This is, as we shall see later, essentially a restriction on the energy  $k$  of the virtual quantum. For the cut-off constant  $C$  we choose  $2Km$  in the case of the invariant (4) and  $2K^2$  in case (5). The reasons for this definition will be apparent when we consider the behaviour of the invariants for large  $k$  (see below).

There are two kinds of transitions which contribute to the electron self-energy:

1. Transitions between two states with positive energy ((+) transitions) in which the electron in a state of momentum  $\mathbf{p}_0$  energy  $E_0$  goes over to a state  $\mathbf{p}$ ,  $E$  emitting a light quantum  $-\mathbf{k}, k$ , or the reverse process. In both cases  $E_0>0$ ,  $E>0$ ,  $\mathbf{p}=\mathbf{p}_0+\mathbf{k}$ ,  $\Delta\mathbf{p}_{el}=\mathbf{k}$ ,  $\Delta E_{el}=E-E_0$ ,  $\Delta\mathbf{p}_f=-\mathbf{k}$ ,  $\Delta E_f=k$ . Energy and momentum of the free electron satisfy, of course, the relation  $E^2=p^2+m^2$  (we use energy units for momentum). In this case the invariants (4) and (5) become

$$k^2 - (E - E_0)^2, \quad \dots\dots(6)$$

$$k(k + E - E_0), \quad \dots\dots(7)$$

where  $E = +\sqrt{(E_0^2 + k^2 + 2p_0k \cos \theta)}$ . With this choice of sign they are both positive.  $\theta$  is the angle between  $\mathbf{p}_0$  and  $\mathbf{k}$ .

2. Transitions from negative to positive energy states ((- +) transitions) in which the electron in a negative energy state  $\mathbf{p}$ ,  $E < 0$  emits a quantum  $\mathbf{k}$ ,  $k$  and goes over to a state of positive energy  $\mathbf{p}_0$ ,  $E_0 > 0$ . In this case  $\mathbf{p} = \mathbf{p}_0 + \mathbf{k}$ ,  $\Delta \mathbf{p}_e = -\mathbf{k}$ ,  $\Delta E_e = E_0 - E$ ,  $\Delta \mathbf{p}_f = \mathbf{k}$ ,  $\Delta E_f = k$ . The invariants (4) and (5) become now

$$-k^2 + (E_0 - E)^2, \quad \dots\dots(6')$$

$$k(k - E + E_0), \quad \dots\dots(7')$$

where  $E = -\sqrt{(E_0^2 + k^2 + 2p_0k \cos \theta)}$ . Here again the sign is chosen in such a way as to make both invariants positive.

To obtain the invariant upper limits for the momentum integrals we have therefore to solve the following equations:

$$k^2 - (\sqrt{(E_0^2 + k^2 + 2p_0k \cos \theta)} \mp E_0)^2 = \pm 2Km_0, \quad \dots\dots(6'')$$

$$k(k + \sqrt{(E_0^2 + k^2 + 2p_0k \cos \theta)} \mp E_0) = 2K^2, \quad \dots\dots(7'')$$

where the upper sign corresponds to (+ +), the lower to (- +) transitions. The exact solution of (6'') is

$$\left. \begin{aligned} k^+(x) &= Km_0 \frac{p_0x + E_0\sqrt{(1+\epsilon)}}{E_0^2 - p_0^2x^2}, & k^-(x) &= Km_0 \frac{-p_0x + E_0\sqrt{(1-\epsilon)}}{E_0^2 - p_0^2x^2}, \\ \epsilon &= 2 \frac{E_0^2 - p_0^2x^2}{Km_0}, & x &= \cos \theta. \end{aligned} \right\} \dots\dots(8)$$

$k^+(x)$  is the upper limit for (+ +),  $k^-(x)$  for (- +) transitions. Equation (7'') is cubic in  $k$ , but it is sufficient for our purpose to solve it approximately for large  $K$ . The solution is

$$\left. \begin{aligned} k^+(x) &= \frac{1}{4}(E_0 - p_0x) + K\sqrt{(1-\epsilon_1)}, & k^-(x) &= \frac{-1}{4}(E_0 + p_0x) + K\sqrt{(1-\epsilon_2)}, \\ \epsilon_1 &= \frac{1}{16K^2}(E_0 - p_0x)(3E_0 + 5p_0x), & \epsilon_2 &= \frac{1}{16K^2}(E_0 + p_0x)(3E_0 - 5p_0x). \end{aligned} \right\} \dots\dots(9)$$

To calculate the self-energy we use Weisskopf's (1934, 1939) method for the static part and the usual perturbation method for the dynamic part. The results are

$$W_{\text{static}} = \frac{e^2}{4\pi} \int_{-1}^{+1} dx \int_0^\infty dk \sum_{\sigma_a}^{1,2} \left\{ \sum_{\sigma}^{1,2} - \sum_{\sigma}^{3,4} \right\} (u_0^* u)(u^* u_0), \quad \dots\dots(10)$$

$$W_{\text{dyn}} = \frac{e^2}{4\pi} \int_{-1}^{+1} dx \int_0^\infty k dk \sum_{\pi} \sum_{\sigma_a}^{1,2} \left\{ \frac{\sum_{\sigma} (u_0^* \alpha_a u)(u^* \alpha_a u_0)}{E_0 - |E(\mathbf{k})| - k} - \frac{\sum_{\sigma}^{3,4} (u_0^* \alpha_a u)(u^* \alpha_a u_0)}{-E_0 - |E(\mathbf{k})| - k} \right\}. \quad \dots\dots(11)$$

Here  $u_0$  and  $u$  are the Dirac spinors for free electrons with energy  $E_0$  and  $E$  respectively.  $\alpha_a$  is the component of the Dirac matrix-vector  $\alpha$  in the direction of polarization of the emitted quantum.  $\sum_{\sigma}^{1,2}$  and  $\sum_{\sigma}^{3,4}$  denote summations over the two spin states with positive or negative energy respectively.  $\sigma_a$  corresponds

to energy  $E_0$ ;  $\sum_{\pi}$  is the summation over both directions of polarization of the emitted quantum. Carrying out the summations in the usual way, taking  $k^+(x)$  or  $k^-(x)$  as upper limit in the integrals over  $k$  according to the kind of transitions they concern, and adding the two results (10) and (11) together, we get for the total self-energy the following expression :

$$W = W_{\text{static}} + W_{\text{dynamic}}$$

$$= \frac{e^2}{2\pi} \int_{-1}^{+1} dx \left\{ \int_0^{k^+(x)} dk \left[ \frac{1}{2} \frac{E_0^2 + E_0|E| + p_0 kx}{E_0|E|} + \frac{k}{E_0|E|} \cdot \frac{E_0|E| - m_0^2 - p_0 kx - p_0^2 x^2}{E_0 - |E| - k} \right] \right.$$

$$\left. + \int_0^{k^-(x)} dk \left[ \frac{1}{2} \frac{E_0^2 - E_0|E| + p_0 kx}{E_0|E|} + \frac{k}{E_0|E|} \cdot \frac{E_0|E| + m_0^2 + p_0 kx + p_0^2 x^2}{E_0 + |E| + k} \right] \right\} .$$

.....(12)

Here the first terms are the contributions to the static and dynamic self-energy from the  $(++)$  transitions and the second two terms are the corresponding contributions from the  $(-+)$  transitions.

It is difficult to carry out the integrations in (12) exactly. We shall, therefore, use an approximate method which, as we shall see, will yield the most important features of the procedure.

We split up the integrals over  $k$  in the following way :

$$\int_0^{k(x)} = \int_0^{\kappa} + \int_{\kappa}^{k(x)} ,$$

.....(13)

where  $\kappa$  is an arbitrary constant, equal for both kinds of transitions, which we can choose so large as to ensure convergence of an expansion of the integrand in the second integral in powers of  $1/k$ . Both integrals on the right-hand side of (13) have one non-invariant limit, viz.  $\kappa$ . We may, however, hope that in the sum, which has invariant limits, the non-invariant terms will cancel. The first of the two integrals must, of course, be calculated exactly. Its value for  $k = \kappa$  can then eventually be expanded in powers of  $1/\kappa$ .

The calculation of (12) for  $k^+(x) = k^-(x) = \kappa$  is straightforward. The result is

$$W_0^{\kappa} = \frac{e^2}{2\pi p_0 E_0} \left[ \frac{3}{2} p_0 m_0^2 \ln(k + p_0 + \sqrt{(+)})(k - p_0 + \sqrt{(-)}) + m_0^2 k \ln \frac{\sqrt{(+)} + k + p_0}{\sqrt{(-)} + k - p_0} \right.$$

$$\left. + p_0 k^2 - \frac{1}{6} (2E_0^2 + 2k^2 - 3p_0^2 + 6m_0^2)(\sqrt{(+)} - \sqrt{(-)}) - \frac{1}{6} p_0 k (\sqrt{(+)} + \sqrt{(-)}) \right]_0^{\kappa} ,$$

.....(14)

where  $\sqrt{(+)} = \sqrt{(E_0^2 + k^2 + p_0 k)}$ ,  $\sqrt{(-)} = \sqrt{(E_0^2 + k^2 - p_0 k)}$ .

Expanding the value of the bracket for  $k = \kappa$  in powers of  $1/\kappa$ , and using the exact value for  $k = 0$ , we get, up to terms of the order  $1/\kappa$ ,

$$W_0^{\kappa} = \frac{e^2}{2\pi} \frac{m_0^2}{E_0} \left\{ 3 \ln \frac{2\kappa}{m_0} - \frac{1}{2} + \frac{1}{3} \left( \frac{p_0}{m_0} \right)^2 \right\} .$$

.....(15)

This is, with  $\kappa = K$ , the result of a constant cut-off. It confirms the result (3) of Lennox\* that, in this case, even the constant term has wrong transformation properties.

\* The numerical factor in the term dependent on  $p_0$  appears to differ from that of Lennox as quoted by Bethe (1948).

Now we proceed to the calculation of the contribution of the second integral in (13). Here we first expand the integrand in powers of  $1/k$  and then integrate the series over  $k$  between the limits  $\kappa$  and  $k^+(x)$  or  $k^-(x)$ . The result is, up to terms of the order  $1/k(x)$  or  $1/\kappa$ ,

$$W_{\kappa}^K = \frac{e^2}{4\pi E_0} \int_{-1}^{+1} dx \left\{ 2p_0 x (k^+(x) + k^-(x) - 2\kappa) + \frac{1}{2}(E_0 + 2m_0^2 - 3p_0^2 x^2) \ln \frac{k^+(x)k^-(x)}{\kappa^2} + E_0 p_0 x \ln \frac{k^+(x)}{k^-(x)} \right\}. \quad (16)$$

Before further integration we must put in (16) the explicit expressions for  $k^+(x)$  and  $k^-(x)$ . Expanding these functions also in powers of  $1/K$ , we get the following results for the logarithmic and constant terms:

(1) For the Wataghin cut-off (4, 6, 8)

$$W_{\kappa}^K = \frac{e^2}{2\pi} \frac{m_0^2}{E_0} \left\{ 3 \ln \frac{K}{\kappa} + 3 + \frac{2}{3} \left( \frac{p_0}{m_0} \right)^2 - \frac{3}{2} \frac{E_0}{p_0} \ln \frac{E_0 + p_0}{E_0 - p_0} \right\}. \quad (17)$$

(2) For the scalar product cut-off (5, 7, 9)

$$W_{\kappa}^K = \frac{e^2}{2\pi} \frac{m_0^2}{E_0} \left\{ 3 \ln \frac{K}{\kappa} - \frac{1}{3} \left( \frac{p_0}{m_0} \right)^2 \right\}. \quad (18)$$

To obtain the self-energy corresponding to the invariant cut-off we must add the expression (15) to either (17) or (18). In the case of the Wataghin cut-off (4) the constant term is still not invariant. In the case of the scalar product cut-off, however, the non-invariant terms cancel:

$$W = W_0^K + W_{\kappa}^K = \frac{e^2}{2\pi} \frac{m_0^2}{E_0} \left\{ 3 \ln \frac{2K}{m_0} - \frac{1}{2} \right\}. \quad (19)$$

Of the simple cut-off expressions the scalar product seems to be the only one with this property. For example, if we take the expression

$$(\Delta E)^2 = (\Delta E_{cl} + \Delta E_f)^2 = (\Delta E_{cl} + \Delta E_f)^2 - (\Delta \mathbf{p}_{cl} + \Delta \mathbf{p}_f)^2, \quad (20)$$

which is a linear combination of the two invariants (4) and (5), we obtain

$$W = \frac{e^2}{2\pi} \frac{m_0^2}{E_0} \left\{ 3 \ln \frac{2K}{m_0} - \frac{1}{2} - \frac{1}{3} \left( \frac{p_0}{m_0} \right)^2 \right\}, \quad (21)$$

which is not invariant.

Obviously the next step is to calculate (12) exactly using the scalar product (5), which gives the only promising cut-off. This has been carried out, reversing in (12) the order of integrations. The result is

$$W = \frac{e^2}{2\pi E_0} \left\{ F_1(E_0, k) \Big|_{k=k^+(1)}^{k=k^+(-1)} + F_1(-E_0, k) \Big|_{k=k^-(1)}^{k=k^-(-1)} + F_2(E_0, k^+(1)) + F_2(-E_0, k^-(1)) + F_3(E_0, k^+(-1)) + F_3(-E_0, k^-(-1)) - 3m_0^2 \ln m_0 \right\}, \quad (22)$$

where the  $F_i (i=1, 2, 3)$  are rather complicated functions of  $k$  which we shall not write down explicitly, and where  $k^+(1)$ ,  $k^+(-1)$ ,  $k^-(1)$ ,  $k^-(-1)$  are the roots of the two cubics (7') for  $\cos \theta = 1$  and  $\cos \theta = -1$  respectively.

If (22) is to transform like  $1/E_0$ , the expression in the braces must be invariant (independent of  $p_0$ ). This, however, is not the case. To see this we note that

the quantities  $F_i$  contain logarithmic terms, the remainder being rational. Since the solutions  $k^\pm (\pm 1)$  of the cubic equations are algebraic functions of the parameters  $K$ ,  $E_0$ ,  $m_0$ , the whole expression cannot be constant unless the logarithmic terms by themselves are constant. These can be shown to be

$$\begin{aligned} \frac{e^2}{2\pi} \frac{m_0^2}{E_0} \left\{ \frac{3}{4} \left( 1 - \frac{E_0}{p_0} \right) \ln \left| \left( \frac{2K^2}{k^+(1)} + E_0 + p_0 \right) \left( \frac{2K^2}{k^-(-1)} - E_0 - p_0 \right) \right| \right. \\ \left. + \frac{3}{4} \left( 1 + \frac{E_0}{p_0} \right) \ln \left| \left( \frac{2K^2}{k^+(-1)} + E_0 - p_0 \right) \left( \frac{2K^2}{k^-(1)} - E_0 + p_0 \right) \right| \right. \\ \left. + 2 \frac{E_0}{p_0} \frac{K^2}{m_0^2} \ln \frac{k^+(-1)k^-(-1)}{k^+(1)k^-(1)} - 3 \ln m_0 \right\}. \quad \dots\dots (23) \end{aligned}$$

In order to obtain some information about the dependence of (23) on  $p_0$  we consider the limiting case of large energies:  $E_0 \gg m_0$ , and expand (23) in a series in powers of  $m_0/E_0$ , expanding also the roots  $k^\pm (\pm 1)$  of the cubic equations as series in  $m_0/E_0$ . The coefficient of every power of  $m_0/E_0$  in (23) is a sum of a logarithmic term and a rational function of  $K$ ,  $E_0$ ,  $\sqrt{(K^2 + \frac{1}{4}E_0^2)}$ . Since  $E_0/K$  is arbitrary it is necessary for constancy of every coefficient that each of these terms separately be constant. However, the logarithmic part of the series is

$$\frac{e^2}{2\pi} \frac{m_0^2}{E_0} \left\{ 3 \ln \frac{2K}{m_0} + \frac{3}{8} \frac{m_0^2}{E_0^2} \ln \frac{K^2}{K^2 - E_0^2} + \dots \right\}. \quad \dots\dots (24)$$

The expansion used here converges certainly for sufficiently large  $E_0$ . In (24) the second term is not constant, which proves the non-covariance of (23) and, therefore, also of (22). This result is not in contradiction with (19) since if we assume that  $K$  is large, the leading non-covariant terms are of the order  $E_0^2/K^2$ .

It is therefore impossible by use of the scalar product cut-off to make the electron self-energy finite and covariant. The important property of this cut-off, however, is that for any subtraction procedure of the kind used in the calculation of the energy level shift (Bethe 1948) in which the diverging terms cancel and it is possible in the result to go over to the limit  $K \rightarrow \infty$ , the scalar product cut-off must yield unambiguous results because in this case only the first two terms (19) matter. It could be used, therefore, as a basis for any calculation of this type, and may sometimes be more convenient than the equivalent devices of Weisskopf (Bethe 1948) and Feynman (1948), or the more elaborate theory of Schwinger (Bethe 1948, Schwinger 1948).

#### ACKNOWLEDGMENTS

It is a pleasure to thank Professor R. E. Peierls for suggesting this problem and for helpful advice, and Dr. E. E. Salpeter for useful discussions. I should also like to thank the Polish Central Planning Institute for the award of a research scholarship.

#### REFERENCES

- BETHE, H. A., 1948, *Report to the Solvay Conference*, Sept. 1948.  
 FEYNMAN, R. P., 1948, *Phys. Rev.*, **74**, 1430.  
 LAMB, W. E., 1947, Paper given at the Cosmic Ray Conference at the Brookhaven National Laboratory, September 1947, as quoted by Bethe (1948).  
 LENNOX, E., 1948, *Cornell University Thesis*, as quoted by Bethe (1948).  
 SCHWINGER, J., 1948, *Phys. Rev.*, **74**, 1439.  
 WATAGHIN, G., 1934, *Z. Phys.*, **88**, 92, and **92**, 547.  
 WEISSKOPF, V., 1934, *Z. Phys.*, **89**, 27, and **90**, 817; 1939, *Phys. Rev.*, **56**, 72.

## LETTERS TO THE EDITOR

**The Use of Liquid Helium in Magnetic Cooling Experiments \***

It is well known that vessels containing liquid helium and cooled below the lambda point are subject to a large heat influx due to the helium film in the connecting tube between the vessel and the warmer parts of the apparatus (Rollin and Simon 1939). It seemed to us that, in order to make use of liquid helium in experiments involving the magnetic method of cooling, it was important to devise means of minimizing this effect, for in such experiments it is frequently desired to cool down such a vessel to a very low temperature and to maintain the temperature in that region for a period of time sufficiently long to permit one to make a series of measurements. For example, the properties of liquid helium II have hitherto mainly been investigated down to  $1^{\circ}$  K. only and, as has already been emphasized (Kurti and Simon 1938), it is desirable to extend these measurements—especially those on the anomalous transport phenomena—to temperatures where the vapour pressure of helium is negligibly small. Again, liquid helium might be used as an agent for heat transfer at very low temperatures; whilst it is true that its heat conductivity is very small at such temperatures (Kurti and Simon 1938, de Klerk 1946), it can be estimated that the heat transmittance of thin layers of liquid helium would be sufficiently good to be of practical value; e.g. at  $0.05^{\circ}$  K. a layer 0.1 mm. thick would transmit 100 ergs per minute per  $\text{cm}^2$  for a temperature difference of  $0.001^{\circ}$  K., the contact resistance on the liquid-solid boundary (Kapitza 1941) being probably comparatively small. Liquid helium could be used, therefore, to improve heat transfer between solid surfaces, and "make-and-break" thermal contacts at very low temperatures would thus become feasible.

To eliminate the large heat influx sealed capsules have been used successfully in the past (Kurti, Rollin and Simon 1936, Shire and Allen 1938). This technique, in doing away with the connecting tube and thus eliminating "creep", makes good thermal insulation possible, but it has obvious drawbacks from the practical point of view.

The ideal solution would be to insert a valve at the low temperature end of the filling tube, but a valve that is tight to liquid helium II is hard to make. Experiments in Leyden (de Klerk 1946) with such a valve resulted in a heat influx of several thousand ergs per minute. A simpler solution seemed to us to be offered by the use of a long capillary as filling tube. In such an arrangement the rate of film flow, which is roughly proportional to the circumference of the tube (Rollin and Simon 1939) would be reduced. As, moreover, the capillary offers considerable flow resistance to the re-descending helium vapour, one could hope to prevent most of it from re-condensing by connecting the top of the capillary to a pumping system.

Figure 1 shows the experimental arrangement. The thin-walled German silver vessel A containing about 4 gm. of iron ammonium alum was suspended by means of the German silver capillary C (0.2 mm. inside diameter, 0.5 mm. outside diameter, 7 cm. long) the upper end of which was at the temperature of the helium in the surrounding cryostat (about  $0.9^{\circ}$  K.) and was connected to a diffusion pump of a speed of a few litres per second. About  $1\text{ cm}^3$  of liquid helium was introduced into A by condensation below the lambda point. The demagnetization procedure was as for a salt specimen except that it was found necessary to have a reasonably good vacuum— $10^{-5}$  mm. Hg—round A, which is probably explained by a less efficient "clean-up" of the residual gas by the metallic container than by a salt specimen.

\* A brief account of some of this work was given at the Langevin-Perrin Colloquium, Paris, November 1948.

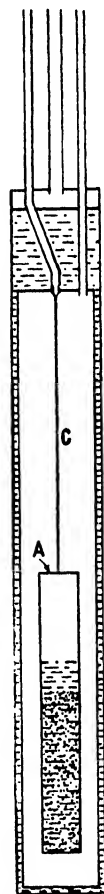


Figure 1.



Figure 1(a).

Figure 2 shows the heating-up curve after demagnetization from 12 kG. and  $1.0^{\circ}\text{K}$  (In order to improve the vacuum the temperature of the cryostat was reduced to  $0.9^{\circ}$  immediately before demagnetization.) From the specific heat of iron alum (that of liquid helium being negligible below  $0.5^{\circ}\text{K}$ .) the initial heat influx was calculated as 300 ergs/min., increasing to about 1000 ergs/min. at higher temperatures. The time of heating-up to  $0.9^{\circ}$  was about  $1\frac{1}{2}$  hours and this could easily be increased by the use of larger quantities of salt.

For experiments requiring higher thermal insulation or better temperature constancy a double container assembly as shown in Figure 1(a) may be used with advantage. In our experimental arrangement the thin walled German silver vessels A and B, each containing

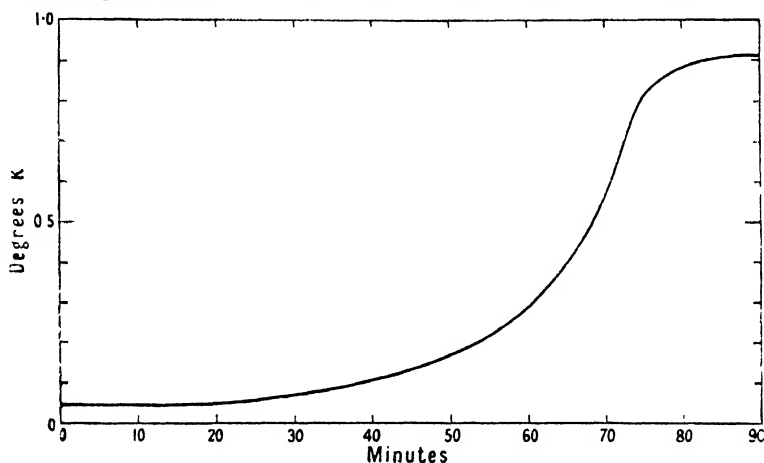


Figure 2.

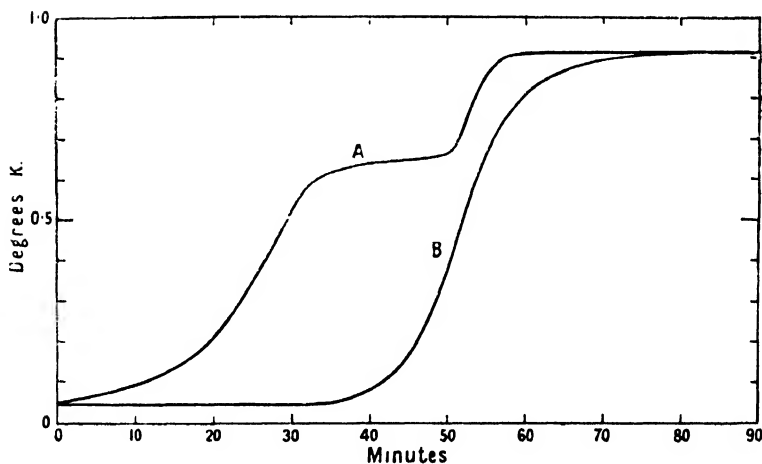


Figure 3.

2.5 gm. of iron alum, were connected by the 3 cm. long capillary C' (0.2 mm. inside diameter), A being connected to the pumping line through another 3.5 cm. long capillary C. The assembly could be filled with liquid helium to any desired level. One would then expect that owing to the small heat transfer through helium, whether bulk or film, below  $0.5^{\circ}\text{K}$ . (Kurti and Simon 1938) container B would receive only a small heat influx from A as long as the latter's temperature was less than  $0.5^{\circ}\text{K}$ . (Heat conduction along the German silver capillary C' was estimated to be negligible at these temperatures.)

Figure 3 gives the heating-up curves of A and B, with B and the capillary C' filled with helium. The heating-up rate of A was higher than in the single container experiment, partly because of the smaller heat capacity and partly because of the shorter length of capillary C. The heating-up rate of the lower vessel B on the other hand was very small



indeed until A reached about  $0.5^{\circ}$  K. (The same general characteristics were found by de Klerk (1946) in his experiments where a column of liquid helium was used to provide thermal contact between two salt specimens.) The temperature of B increased by less than  $0.001^{\circ}$  K. in half an hour and the heat influx was found to be 50 ergs/min. By increasing the heat capacity of A and thus delaying its rise of temperature to  $0.5^{\circ}$  K. it would be possible to prolong the time during which the temperature of B remained sensibly constant.

This arrangement seems to offer a relatively simple means of realizing constant temperature baths below  $0.5^{\circ}$  K. and it can be easily adapted for measurements of heat conductivity, specific heats, etc. and for two-stage demagnetization experiments.

Clarendon Laboratory,  
Oxford.  
2nd May 1949.

R. P. HUDSON,  
B. HUNT,  
N. KURTI.

- KAPITZA, P. L., 1941, *J. Phys. U.S.S.R.*, **4**, 181.  
DE KLERK, D., 1946, *Physica*, **12**, 513.  
KURTI, N., ROLLIN, B. V., AND SIMON, F. E., 1936, *Physica*, **3**, 266.  
KURTI, N., AND SIMON, F. E., 1938, *Nature*, Lond., **142**, 207.  
ROLLIN, B. V., AND SIMON, F. E., 1939, *Physica*, **6**, 219.  
SHIRE E. S., AND ALLEN, J. F., 1938, *Proc. Camb. Phil. Soc.*, **34**, 301.

### A Lantern Model to Illustrate Dislocations in Crystal Structure

For some years I have been accustomed to illustrate roughly the nature of dislocations in a perfect crystal lattice by means of a lantern slide in which a single layer of small spheres is retained between two glass plates. Having been asked from time to time how the slide is made, I think that interest may be sufficient to warrant the following brief description.

As spheres I use carbon shot of about 1 mm. diameter, as supplied for telephone microphones by Messrs. Le Carbone, Ltd. These are enclosed between two ordinary lantern-slide cover glasses, bound with cellophane tape. If this assembly is shaken or tapped, spheres settle down into regions of close packing, separated by lines along which the fit is imperfect, which show white in projection. Occasional holes also appear in the lattice. Figure 1 illustrates a typical appearance (see Plate opposite).

The carbon spheres show variations of diameter up to  $\pm 0.05$  mm. This variation seems favourable for the production of the desired appearance. I have also tried a layer of steel ball-bearing spheres, of  $1/16$  inch diameter, which are very uniform. These tend to show larger regions of close packing, but also exhibit dislocations and holes. Figure 2 is a typical appearance. On the whole, the steel spheres seem to be less satisfactory and are certainly more expensive.

University College,  
London, W.C. 1.  
30th March 1949.

E. N. DA C. ANDRADE.

### Viscosity and Superfluidity in Liquid Helium

The anomalous transport phenomena exhibited by liquid helium below  $2.19^{\circ}$  K. are clearly manifestations of a new physical state into which the liquid passes at this temperature. While as yet there exists no generally accepted theory of this state, it is evident that its establishment is accompanied by a rapid decrease in entropy. The shape of the specific heat curve (Keesom and Keesom 1935) shows, however, that the anomalous drop in the entropy of the liquid begins at a considerably higher temperature ( $\sim 2.6^{\circ}$  K.) and that at  $2.19^{\circ}$  K. about 8% of the total entropy has already disappeared.

The question therefore arises whether this initial drop in entropy will show itself in the transport properties of liquid helium I below  $2.6^{\circ}$  K. The available data show little indication of such a behaviour. Super-flow, the thermo-mechanical effect and the film transfer all seem to approach the value zero as, on warming, the temperature of  $2.19^{\circ}$  K. is reached. The viscosity has been measured by the oscillation method (Wilhelm *et al.*

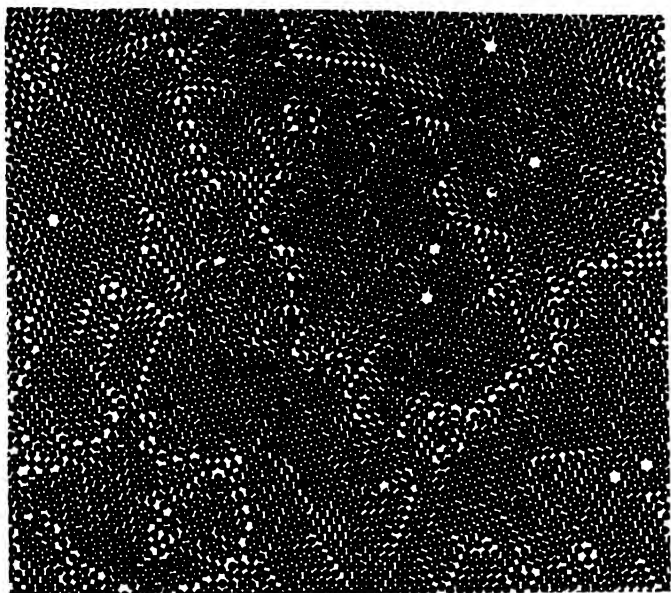


Figure 1.

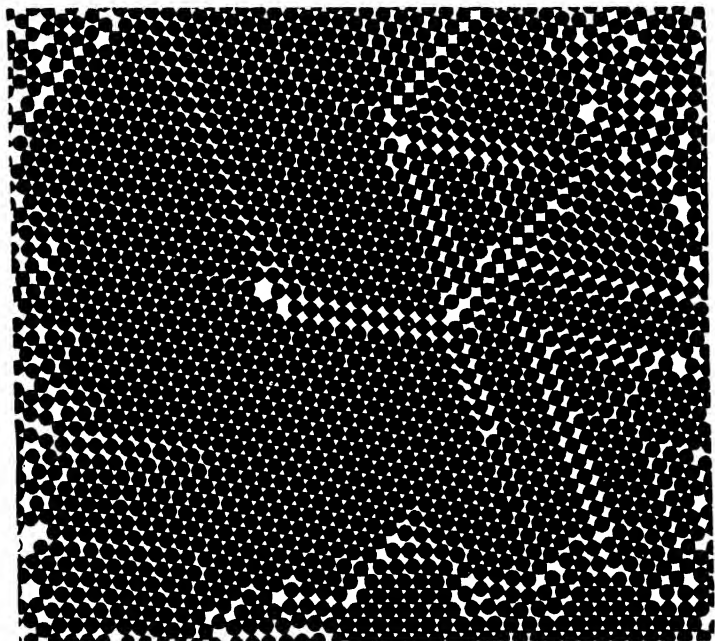
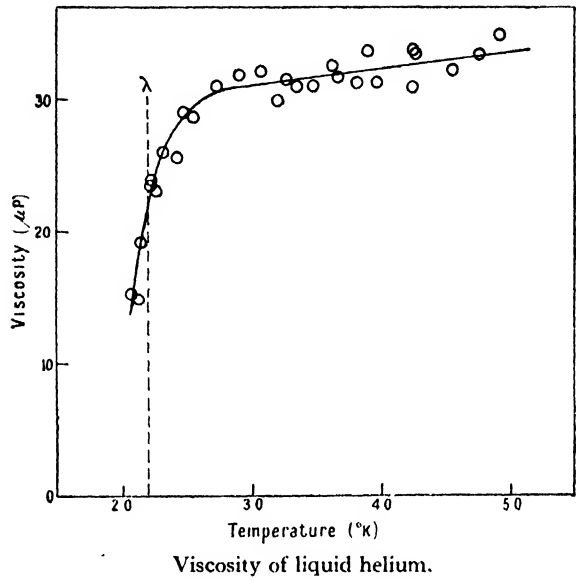
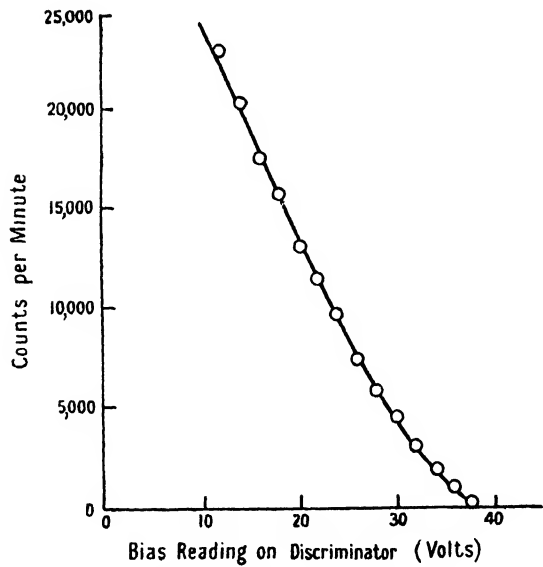


Figure 2.

(R. BOWERS AND K. MENDELSSOHN)



(L. E. BEGHIAN AND H. H. HALBAN)



Pulse height distribution for methane chamber filled to 35 atmospheres using D- $\frac{1}{2}$  D neutrons.

1935, Keesom and MacWood 1938, Keesom and Keesom 1941). The results are not very consistent, but the most recent of these measurements indicate that the viscosity drops gradually in the helium I region and then shows a sharp decrease at  $2.19^{\circ}\text{K}$ . The one existing determination of the viscosity of helium I by a flow method (Johns *et al.* 1939) also indicates a drop, but there is, unfortunately, only one point measured (at  $3.4^{\circ}\text{K}$ .) between the boiling point and the lambda point. It was therefore decided to determine the viscosity of helium I by means of a flow method in some detail.

The apparatus used consisted of a glass capillary of  $4 \times 10^{-3}\text{ cm}$ . radius and 2.5 cm. length, one end of which was attached to a glass reservoir while the other opened into the helium bath. The results given in the accompanying figure\* show that between  $5^{\circ}\text{K}$ . and  $2.7^{\circ}\text{K}$ . the viscosity falls slightly, from about  $33\mu\text{P}$ . to  $30\mu\text{P}$ . This is followed by a sharp drop to about  $23\mu\text{P}$ . at  $2.19^{\circ}\text{K}$ . Although below the lambda point the flow becomes increasingly non-classical, our value at  $2.14^{\circ}\text{K}$ . does not indicate a sharp break in the curve such as was observed with the oscillation methods. One may be inclined to ascribe this anomalous decrease in the viscosity of helium I to the first appearance of superfluidity. However, the observation of flow in this region gave no indication of a non-classical term. In order to decide the question by a more sensitive method, the glass capillary was replaced by a metal tube containing 900 wires of 46 s.w.g. This tube was drawn down until its Poiseuille constant was of the same order as that of the glass capillary. In the helium I region, between  $3^{\circ}\text{K}$ . and  $2.19^{\circ}\text{K}$ ., the flow rate in this tube did not increase more than in the glass capillary. On the other hand, just below the lambda point, at  $2.13^{\circ}\text{K}$ ., the flow through this tube was increased more than six times.

Comparison between the results with the capillary and the wire tube thus shows that the rapid fall in viscosity observed by us above  $2.19^{\circ}\text{K}$ . cannot be interpreted as the appearance of superflow similar to that in helium II. We are, therefore, clearly faced with a decrease in the true viscosity of helium I accompanying the decrease in entropy in a temperature interval of about half a degree above the lambda point. The size of this interval, amounting to about one-fifth of the absolute temperature, also makes it unlikely that the viscosity change is due to fluctuations, i.e. the appearance of small regions of helium II. Phenomenologically, the anomaly above the lambda point corresponds to the appearance of short range order in an order-disorder transformation which at  $2.19^{\circ}\text{K}$ . is followed by the establishment of long range order. All evidence so far indicates that in the case of helium the increase of order with falling temperature occurs in momentum space and not with regard to positions. Consequently we are inclined to ascribe the sharp drop in viscosity above the lambda point to a re-distribution in the velocity spectrum of the liquid preceding the actual condensation phenomenon. It is to be hoped that further investigation of this gradual transition to the state of velocity condensation will lead to a clearer understanding of the latter, and experiments on other physical properties (heat conduction, diffusion etc.) are now in progress. A more detailed account of the present experiments will be given at a later date.

\* See opposite page.

Clarendon Laboratory,  
Oxford.  
6th April 1949.

R. BOWERS.  
K. MENDELSSOHN.

- JOHNS, H. F., WILHELM, J. O., and GRAYSON SMITH, H., 1939, *Canad. J. Res.*, **17A**, 149.  
KEESOM, W. H., and KEESOM, A. P., 1935, *Physica*, **2**, 557.  
KEESOM, W. H., and KEESOM, P. H., 1941, *Physica*, **8**, 65.  
KEESOM, W. H., and MACWOOD, G. E., 1938, *Physica*, **5**, 737.  
WILHELM, J. O., MISENER, A. D., and CLARK, A. R., 1935, *Proc. Roy. Soc. A.*, **151**, 342.

## Electron Collection in High Pressure Methane Ionization Chambers

It was pointed out by Klema and Barschall (1943) that to achieve electron collection in an ionization chamber filled to high pressure with gases such as hydrogen, nitrogen and argon, it is necessary to remove the last traces of electronegative impurities, principally oxygen.

Where an ionization chamber is used for single-particle counting instead of continuous current operation, it is important for many purposes to keep the pulse-rise time as short as possible, and consequently it is desirable to use electron collection. Recently, by filtering hydrogen through a palladium leak, Stafford (1948) has obtained electron collection up to 90 atmospheres pressure; Wilson, Collie and Halban (1948) have employed electrolytically made deuterium up to 30 atmospheres pressure for photodisintegration experiments.

Hydrogen by itself, however, has comparatively small stopping power, and is, therefore, unsuitable for the measurement of proton recoils caused by high energy neutrons; in such cases it has been customary to use hydrogen argon mixtures (Staub and Nicodemus 1946). Alternatively, we have found that carefully purified methane will also give electron collection at high pressure. The high hydrogen content of methane makes it especially useful for proton recoil work, and its stopping power is only slightly less than that of argon.

Investigations were made using a cylindrical chamber of phosphor bronze, 4 cm. diameter, 12 cm. long, with a wall thickness of 2 mm. The collecting electrode consists of a length of Kovar wire 1 mm. in diameter, and is fitted with a guard ring.

The purification of the methane was carried out in a packed fractionating column consisting of thirty equivalent plates. The column was immersed in liquid oxygen and the methane distilled off at this temperature. This was done by Drs. Kronberger and London at A.E.R.E., Harwell.

To avoid contamination of the pure gas, both the storage cylinder and chamber were thoroughly outgassed.

Measurements of proton recoil from neutrons from a D+D source (see Figure \*) show that not more than 15% loss of pulse height occurs up to 35 atmospheres, the highest pressure used. At this pressure, the saturation voltage is 15,000 volts, and the collection time as measured on a triggered oscilloscope is 1  $\mu$ sec.

According to Snyder (1946), the collection time in a cylindrical chamber is given by the formula

$$t = \frac{b-a}{\alpha} \frac{\beta V}{\alpha^2 p \ln(b/a)} \ln \left\{ \left[ b + \frac{\beta V}{\alpha p \ln(b/a)} \right] / \left[ a + \frac{\beta V}{\alpha p \ln(b/a)} \right] \right\},$$

where  $a$  and  $b$  are the wire and outer cylinder radii,  $V$  the applied voltage, and  $p$  the pressure. For methane Snyder quotes  $\alpha = 15 \times 10^5$  cm/sec. and  $\beta = 7.5 \times 10^5$  cm<sup>2</sup> cm. Hg/sec. Using these constants,  $t = 0.7 \mu$ sec., which is in fair agreement with our result.

The efficiency of counting 2.3 mev. neutrons from a D+D source which pass through the whole length of the chamber is 12% at 35 atmospheres pressure, and the maximum range of a proton recoil at this energy is 2.5 mm.

We are very grateful to Drs. Kronberger and London, of A.E.R.E., Harwell, for purifying the methane, to Messrs. R. Wilson and G. Bishop for their helpful advice, and to Lord Cherwell for his interest in this work.

\* Opposite p. 395.

Clarendon Laboratory,  
Oxford.  
5th April 1949.

L. E. BEGHIAN.  
H. H. HALBAN.

KLEMA, E. D., and BARSCHALL, H. H., 1943, *Phys. Rev.*, **63**, 18.

STAFFORD, G. H., 1948, *Nature, Lond.*, **162**, 771.

STAUB, H., and NICODEMUS, D., 1946, Report on an investigation of the behaviour of Argon-Hydrogen Mixtures and Isobutane in a Spherical chamber, *Manhattan District Publication*, P.B. 49, 577.

SNYDER, T., 1946, "High Efficiency Neutron Counter for Fast Coincidence Measurement", *Manhattan District Publication*, P.B. 52,800.

WILSON, R., COLLIE, C. H., and HALBAN, H., 1948, *Nature, Lond.*, **162**, 771.

## REVIEWS OF BOOKS

*Theoretical Structural Metallurgy*, by A. H. COTTRELL. Pp. viii + 256.  
(E. Arnold & Co., 1948.) 21s.

The rapid progress of the physics and mechanics of solids in recent years has placed the majority of metallurgists in a difficult position : with the slender fundamental knowledge dispensed in most University metallurgy degree courses (Dr. Cottrell's University, Birmingham, is a praiseworthy exception) they can hardly follow recent scientific developments in their own field, let alone take an active part in them. Most of the pioneers in the science of metals have been physicists, chemists, or engineers by training; the activity of the professional metallurgist is usually confined to the application of available scientific results to particular metals and alloys, unless he is capable of acquiring the necessary fundamental knowledge by home study. In this difficult situation the appearance of Hume-Rothery's brilliant non-mathematical *Atomic Theory for Students of Metallurgy* in 1946 was an event of great importance, and Dr. Cottrell's new book represents a further welcome addition to the means by which the metallurgist can get acquainted with the modern aspects of the science of metals.

Dr. Cottrell's book falls into two parts of rather different character. The first six chapters give a good elementary account of the electron theory of metals, with a brief sketch of the Bohr theory and of the basic conceptions of wave mechanics; the remaining eight chapters deal with statistical thermodynamics, heterogeneous equilibria, thermodynamical properties of metals and alloy systems, order-disorder transformations, diffusion, and the kinetics of phase changes. These eight chapters treat their subject on a University science standard; in fact, the amount of mathematics used is sometimes above the minimum necessary for the purpose.

Physicists may question whether a useful purpose is served by a mainly descriptive treatment of a mathematical subject such as is the electron theory of metals. In the reviewer's opinion the answer is definitely in the affirmative. A recent text-book entitled *Modern Metallurgy for Engineers* (New York : Pitman, 1941) gives a list of references to literature on metals, with brief commentaries on each item, and here Mott and Jones' book receives the following remark : " For enthusiasts on quantum mechanics. A few engineers may be interested in the mental calisthenics ". Since the author of this revealing utterance is an influential metallurgist, and since the future of metallurgical education depends very much on influential metallurgists, little progress can be expected before these are convinced, by means of clear elementary reviews, that the physics of metals is no more mental calisthenics unworthy of a he-metallurgist.

No doubt many metallurgists will take advantage of Dr. Cottrell's excellent book, and a new edition may have to be printed in due course. This would give an opportunity to increase the accuracy of expression in many passages which, although usually correct from a legalistic point of view, appear likely to be misunderstood by a beginner. One of the first examples of this is found on page 5, where the uncertainty principle might seem to have preceded quantum mechanics, in which " it has become necessary, however, to specify four quantum numbers instead of the single one used in the original formulation of the Bohr theory ".

On page 34 the law of rational intercepts is thought to govern the positions, not of the natural crystal faces, but of lattice planes (for which the statement of the law would be partly trivial, partly—in its emphasis on *small* integers—wrong).

On page 43 we read : " There is some evidence, particularly from the study of crystals by x-ray diffraction, suggesting that a real crystal is not of perfectly uniform orientation, but is composed of a mosaic of small crystals, or crystallites." This seemed a possibility until 1934, when Renninger, using the double-crystal spectrometer, found that a synthetic NaCl crystal was ideally perfect in the sense of the Darwin-Ewald theory; recently Guinier, by means of another x-ray method, came to a substantially identical conclusion for recrystallized aluminium. Thus, a " mosaic " imperfection is characteristic of a *bad* crystal, not of a *real* crystal; the early x-ray workers found most crystals imperfect because they did not know how to obtain perfect ones.

It is a pity that the last chapter, "Phase precipitation by nucleation and growth", does not include strain transformations (martensitic transformations), which are of the very greatest fundamental and practical importance in metallurgy. In this chapter Widmanstätten structures are attributed to oriented nucleation and growth governed by the condition of minimum interface energy. That the typical Widmanstätten pattern does not arise by such a process can be recognized from the very frequent occurrence of lamellae penetrating one another; the absence of isothermal growth, the reversibility of some strain transformations (e.g. the transformation of metastable  $\beta$ -brass by cooling), and many other phenomena show sufficiently that there can be no question of an explanation on the basis of oriented growth. Readers of this chapter will do well to follow it up by consulting Chapter XXII in Barrett's *Structure of Metals*, where a balanced view of the subject is given.

These remarks, however, should not obscure the fact that Dr. Cottrell's book is a most useful contribution to metallurgical literature; it deserves to be present in the library of every metallurgist, and it would certainly have deserved a more attractive paper and binding.

E. OROWAN.

---

## CORRIGENDUM

"Experiments with the Delayed Coincidence Method, including a Search for Short-lived Nuclear Isomers", by D. E. BUNYAN, A. LUNDBY and D. WALKER (*Proc. Phys. Soc. A*, 1949, **62**, 253).

It has been pointed out that pp. 261–263 are difficult to follow. The whole of p. 262 constitutes a table which follows the second paragraph of p. 263. The actual text runs from the bottom of p. 261 to the top of p. 263.

P. 256, line 8. " $T_1 \geq 10^{-8}$  sec." *should read* " $T_1 \gtrsim 10^{-8}$  sec."

## CONTENTS FOR SECTION B

	PAGE
Mr. W. H. WALTON and Mr. W. C. PREWETT. The Production of Sprays and Mists of Uniform Drop Size by Means of Spinning Disc Type Sprayers . . . . .	341
Mr. P. B. FELLGETT. Dynamic Impedance and Sensitivity of Radiation Thermocouples . . . . .	351
Mr. F. W. CUCKOW and Mr. J. TROTTER. Some Experiences in the Application of the Electron Microscope to the Study of Steels . . . . .	360
Prof. F. LLEWELLYN JONES. Electrode Ionization Processes and Spark Initiation .	366
Dr. G. F. HODSMAN, Dr. G. EICHHOLZ and Mr. R. MILLERSHIP. Magnetic Dispersion at Microwave Frequencies . . . . .	377
Dr. J. W. LEECH. The Measurement of the Specific Heats of some Organic Liquids using the Cooling Method . . . . .	390
Letters to the Editor :	
Mr. D. A. WRIGHT. D.C. and Pulsed Emission from Oxide Cathodes . . . . .	398
Reviews of Books . . . . .	400
Corrigendum . . . . .	402
Contents for Section A . . . . .	403
Abstracts for Section A . . . . .	403

## ABSTRACTS FOR SECTION B

### *The Production of Sprays and Mists of Uniform Drop Size by Means of Spinning Disc Type Sprayers, by W. H. WALTON and W. C. PREWETT.*

**ABSTRACT.** Spray of almost uniform drop size is formed when liquid is fed under suitable conditions on to the centre of a rotating disc and centrifuged off the edge. This method of spraying has been studied over a wide range of variables and homogeneous clouds have been produced in the drop-size range from 3 mm. to 15  $\mu$  diameter. The size of the spray drops is given approximately by the equation  $d=3.8 (T/D\rho)^{1/2}/\omega$  where  $d$ =drop diameter,  $D$ =disc diameter,  $\omega$ =angular velocity of disc,  $T$ =surface tension of liquid,  $\rho$ =density of liquid. The spray thus formed also contains a proportion of fine satellite drops, but their smaller distance of projection from the disc enables them to be removed from the cloud when their presence is undesirable. Relatively coarse sprays are easily produced by means of a simple electric motor-driven disc. The finer spray sizes require rotor speeds up to several thousands of revolutions per second and high speed air driven "tops" have been used for this purpose. Suitable designs of apparatus are described.

### *Dynamic Impedance and Sensitivity of Radiation Thermocouples, by P. B. FELLGETT.*

**ABSTRACT.** The concept of dynamic impedance is applied to radiation thermocouples. An equivalent circuit is derived, in terms of which the working of a thermocouple and the factors leading to high sensitivity can be visualized. Methods are given for measuring the dynamic impedance and it is shown that these measurements lead to values for thermoelectric power, heat loss from the receiver, and time constant of the thermocouple. Expressions are given, in terms of the dynamic impedance, for the important properties of radiation thermocouples, namely the signal-to-noise sensitivity, ultimate sensitivity, noise factor and power efficiency. These properties are thus obtained in terms of parameters that can be predicted from the design, or measured in the finished instrument. The



sensitivity is found without recourse to micro-measurements and therefore independent of limitations set by the thermocouple amplifier. The expression for sensitivity differs from those previously published, and the discrepancy is discussed. The way in which the ultimate sensitivity might be approached in practice is indicated. The efficiency is shown to depend on the amount of radiation falling on the receiver of the thermocouple, but to be a constant fraction of the thermodynamic limit  $\Delta T/T$ . For an ideal thermocouple the fraction is one-half, for an actual thermocouple it is less by a factor which we call the relative efficiency.

*Some Experiences in the Application of the Electron Microscope to the Study of Steels*, by F. W. CUCKOW and J. TROTTER.

**ABSTRACT.** Steel specimens have been examined in the light and electron microscopes. The replica technique has been used for the electron microscope work, and all the specimens have been studied with both "Formvar" plastic and polystyrene-silica replicas. The micrographs are critically examined and compared.

There is an obvious gain in picture sharpness in the electron micrographs, particularly in those from silica replicas. It is found, however, that interpretation of the micrographs from plastic replicas in terms of the geometry of the specimen surfaces is more straightforward.

*Electrode Ionization Processes and Spark Initiation*, by F. LLEWELLYN JONES.

**ABSTRACT.** Spark time lags in short gaps with tungsten electrodes were measured for different degrees of oxidation and activation, and the distributions of lags examined and compared. The results, which showed a reduction of mean lag and a narrowing of distribution following oxidation and activation, are discussed in relation to the mechanism of electron emission from oxidized cathodes for impulse and static conditions, and also for the Geiger counter.

*Magnetic Dispersion at Microwave Frequencies*, by G. F. HODSMAN, G. EICHHOLZ and R. MILLERSHIP.

**ABSTRACT.** A method is described which has been developed for the measurement of initial permeabilities of ferromagnetic wires in the microwave region and successfully applied over the range from 3 to 13 cm. wavelength to a variety of materials. The measurements are carried out by comparing the attenuations of coaxial transmission lines with the ferromagnetic specimen and with a non-ferromagnetic reference material as inner conductors. The attenuation constants are derived from observations on the input impedance of the line for different terminations as embodied in a circle diagram of impedance. The results are interpreted in the light of modern theories of magnetic dispersion and an estimate of domain sizes is made. The limitations of the theoretical treatments are indicated.

*The Measurement of the Specific Heats of some Organic Liquids using the Cooling Method*, by J. W. LEECH.

**ABSTRACT.** The cooling method for the determination of the specific heats of liquids is further developed. The power law of cooling  $d\theta/dt = k\theta^n$ , is shown to hold only approximately, and a new method for deducing values of  $d\theta/dt$  is described. The specific heats of a number of liquid carbinols are measured over the approximate range 40–70° C.

# THE PROCEEDINGS OF THE PHYSICAL SOCIETY

## Section A

---

---

VOL. 62, PART 7

1 July 1949

No. 355 A

---

---

### A Recording Spectrometer for Raman Spectroscopy

By C. H. MILLER, D. A. LONG, L. A. WOODWARD  
AND H. W. THOMPSON

Physical Chemistry Laboratory, Oxford

*MS. received 10th January 1949*

**ABSTRACT.** A description is given of a photoelectric recording spectrometer for Raman spectroscopy incorporating a high-intensity excitation system and a novel amplification device. Operation of the exciting mercury arc lamps from 50 c/s. mains imparts to the light signal, and consequently to the current from the photo-multiplier tube, a 100 c/s. periodicity. After amplification by a narrow band-pass amplifier, rectification is achieved in a push-pull phase-sensitive (homodyne) rectifier, by "mixing" the signal with a fixed voltage of identical periodicity. The rectified signal is fed through a filter to a cathode follower valve which provides the power to operate a recording milliammeter. This method of rectification, in conjunction with appropriate filter, effectively reduces the bandwidth of the amplifier, with consequent great improvement in the signal/noise ratio. With this arrangement cooling of the photo-multiplier is unnecessary for normal work. Using a spectrometer of small aperture and resolution and a Raman tube of 35 ml. capacity, traces of the Raman spectrum of carbon tetrachloride show no appreciable background noise.

#### §1. INTRODUCTION

THE difficulties involved in the accurate determination of the intensities of Raman lines by microphotometry from photographic plates are well known. The direct recording of Raman spectra using photoelectric cells has been achieved by Rank and his collaborators (Rank, Pfister and Coleman 1942, Rank, Pfister and Grimm 1943, Rank and Wiegand 1946) and also by Chien and Bender (1947). The present paper describes an instrument we have recently built for this purpose, using a different method of electronic amplification. Our results suggest that the electrical circuits which we have used possess definite advantages over those previously described, particularly as regards the attainment of high gain with low noise. The spectrometer hitherto available to us for this purpose falls far short in resolving power of that which would be justified by the performance of the electrical part of the instrument. In spite of this, excellent records have been obtained. Therefore, although it is hoped eventually to employ a better spectrometer, it seems desirable to describe the arrangement now, and on the basis of our results to indicate changes which may lead to further improvement.

## § 2. THE OPTICAL SYSTEM

Preliminary work showed that high-pressure mercury arcs such as Osira tubes were less satisfactory than Hanovia lamps, the latter having less continuous background and being free from "foreign" lines.

Two arrangements for exciting the Raman spectra have been used. In the first a horizontal Raman vessel, of the Wood's tube form with rear-blackened horn, was placed at one focus of an elliptical chromium-plated reflector. This tube, which was fitted with a jacket for water-cooling or for a filter solution, had a total volume of about 60 ml., of which only about 40 ml. were irradiated. A 500-watt cylindrical Hanovia lamp was placed at the other focus of the reflector, only about half its length being effective for the irradiation of the liquid under investigation. Adjusting devices were provided so that the Raman tube could be accurately aimed relative to the spectrometer collimator, and suitable stops were also used between the tube and the slit so that only light scattered by the liquid entered the spectrometer.

With this arrangement good records of the Raman spectrum of carbon tetrachloride were obtained, the background noise being inappreciable even though the photo-multiplier tube was not cooled below room temperature.

A considerable advantage was obtained, however, by adopting a more intense method of excitation based upon an arrangement due to Dr. A. C. Menzies. A vertical water-cooled Raman tube without horn (volume 35 ml.) is placed with two vertical 500-watt Hanovia mercury lamps inside a water-cooled enclosure. The inner surface of the enclosure is coated with magnesium oxide, which has a high reflectivity for the exciting light. The scattered light passes out through the lower plane end of the Raman tube and is reflected into the spectrometer through a condenser lens, whose focal length is chosen so as to ensure most efficient gathering of the light scattered by the liquid (see Nielsen 1930). The whole is carefully aimed so that only such light enters the spectrometer. With this arrangement the intensity of scattering is so great that the Stokes-Raman lines of carbon tetrachloride can be seen by placing the eye at the position of the photocell.

The spectrometer is a small Hilger constant-deviation glass monochromator in which both lenses are 3.15 cm. in diameter and 18.5 cm. focal length. The small prism gives relatively poor resolution: using slits 0.02 mm. wide it is not possible to separate lines less than about  $20\text{ cm}^{-1}$  apart in the region of 4358 Å. Also, in order to obviate curvature of the spectrum lines, short slits are used (only 0.35 cm. in height). These are severe limitations on the amount of light entering the spectrometer, and the fact that Raman lines can be recorded using lower gain than would give rise to a significant level of noise is highly satisfactory. The prism is caused to rotate by a synchro-motor and gear, so that the spectrum traverses the exit slit. In the region of 4358 Å. the speed of scanning is about 0.1 Å. per second.

The photo-multiplier tube (R.C.A. type 1.P.21) is placed behind the exit slit in a cylindrical housing having a glass window at the front, the whole being surrounded by a metal can into which solid carbon dioxide or a freezing mixture can be placed. The photo-multiplier tube is kept dry by closing the top of its housing by a cap sealed with Apiezon wax, and placing a little calcium chloride at the bottom of the housing. Small electrical heaters near the window and near the cap carrying the leads prevent condensation of moisture when the tube is cooled. The photo-multiplier is protected from stray light by suitable stops,

particularly between the exit slit of the spectrometer and the window. Although good records can be made without cooling, considerable reduction of noise can be achieved by surrounding the photo-multiplier tube with solid carbon dioxide.

### § 3. THE ELECTRICAL SYSTEM

The detection and recording of the Raman spectrum is carried out as follows. The mercury arc lamps are operated from the 50 c/s. mains supply and so produce a pulsating light signal of 100 c/s. periodicity. Thus the photo-multiplier gives a pulsating current of the same periodicity. The voltage developed by this signal across a 1 megohm wire-wound load resistor is increased by an amplifier tuned flat between about 95 and 105 c/s., so as to produce a voltage having a peak value  $S$ . This latter is fed into a phase-sensitive (homodyne) rectifier, which produces a D.C. output voltage proportional to the entrant signal. The operation of the rectifier is as follows. The signal  $S$  is fed into one side of the circuit in phase with a constant voltage  $B$  of identical periodicity obtained from the mains supply, producing a resultant  $(B + S)$ . Into the other side of the circuit the signal  $S$  is fed out of phase with the constant voltage  $B$ , producing a resultant  $(B - S)$ . The two resultants are then coupled in opposition, so that a final D.C. output voltage proportional to  $2S$  is obtained. The latter is then fed through a resistance-capacity filter to a cathode follower valve which supplies the necessary power to drive the pen recorder, a Tinsley recording milliammeter.

The advantage of the homodyne compared with a conventional amplifier is that any entrant voltages due to noise or such extraneous causes, which are not identical in frequency with the 100 c/s. voltage  $B$ , will produce beat voltages which can be removed by the filter preceding the cathode follower tube. The tuning is therefore sharp, and the reduction of noise in the amplifier is determined by the effectiveness of the filter following the homodyne rectifier. This filter can easily be adjusted for various speeds of response. There is no need for the main amplifier preceding the rectifier to be sharply tuned to the 100 c/s. signal, although a reasonably narrow bandwidth is desirable in order to avoid overloading of the later stages of the amplifier by the noise. Further, no difficulties arise from any variation in the mains frequency since it will have an identical effect upon both signal and beat voltage  $B$ .

An alternative method of amplification would be to use a very high load resistor of, say,  $10^{10}$  ohms for the photo-multiplier output, followed by an electrometer triode and one or two stages of D.C. amplification. Such a load resistor cannot in practice be wire-wound, however, and will act as a semiconductor at the frequencies concerned, and thus, when carrying the signal current, will have an inherent noise greater than the Johnson noise. Using a  $10^6$  ohm wire-wound load resistor as in the system now described, with amplification at 100 c/s. there should be no fluctuations in the load resistor other than Johnson noise. The resistor is also sufficiently high in value to be well above the equivalent noise resistance of the first valve in the amplifier.

The details of the amplifier are as follows.

#### (a) *Main amplifier* (Figure 1).

Current from the photo-multiplier is first fed through a screened cable to the wire-wound load resistor (1 megohm), and the voltage drop is applied through a condenser to the grid of the first valve V1 which is a triode connected for least

internal noise, and having its cathode earthed, so that there is minimum pick-up from the heater circuit. The anode load resistors of V1 and V2 are wire-wound so as to minimize noise. V2 is a conventional voltage amplifier stage stabilized by negative feedback and followed by the gain control S1. Stage V3 has feedback applied through the network F1, which results in the response of V3 being that of a high-pass filter with cut-off frequency at about 95 c/s. Additional negative feedback is provided by the non-bypass cathode resistor, so as to improve stability. Stage V4 is similar to V3 except that feedback through F2 leads to the frequency response of a low-pass filter with cut-off frequency about 105 c/s. V5 is an additional voltage amplifier stage preceded by the gain controls S2 and P1.

In order to eliminate interference and pick-up, extensive screening is used in the early stages. All earth connections are made to the cathode of V1, which is also connected to an external earth. The whole amplifier is placed in a screening box, and all cables to the power supply are screened. The box is mounted on rubber shock absorbers to eliminate microphony.

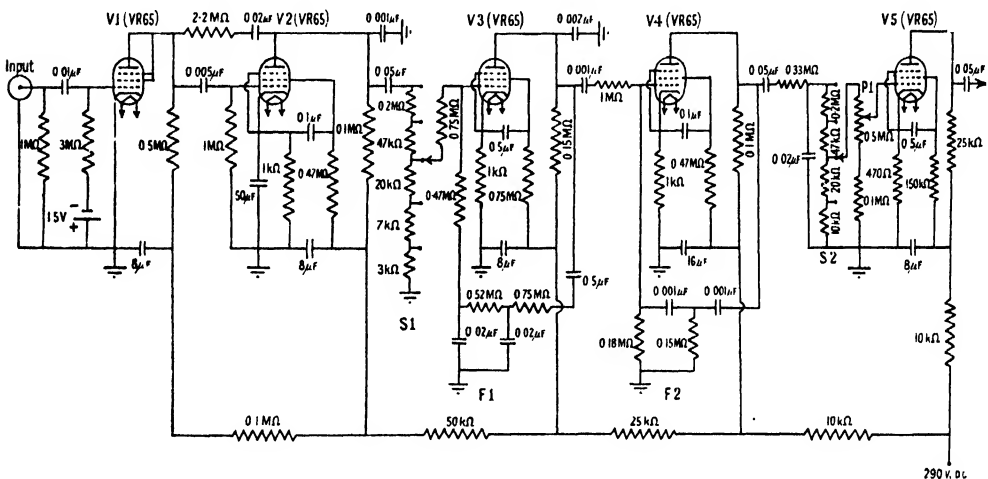


Figure 1.

(b) *Homodyne and output stages (Figure 2).*

In a normal rectifier noise voltages are rectified together with the signal voltage and produce their own fluctuating D.C. component in the output, this being superimposed upon the true D.C. signal. These noise fluctuations can be smoothed out, but their mean amplitude will remain as a residual D.C. voltage superimposed upon the signal. In the homodyne the mean value of such smoothed noise fluctuations is zero, so that the effect of filtering after rectification is similar to a narrowing of the bandwidth of the amplifier as a whole, in so far as reduction of noise is concerned.

In Figure 2 the valves V7 and V8 have the signal voltages fed in push-pull from the phase splitter V6 to their first set of control grids. The potentiometer P2 is preset for exact balance of V7 and V8. The 100 c/s. voltage for mixing with the signal is obtained by full-wave rectification of the mains in V10; and following the phase splitter V11, it is possible to vary the relative phase of the output by means of S4 and P3. Hence a synchronized voltage of variable phase is supplied to the second grids of V7 and V8 connected in parallel.

A smoothing filter of variable time-constant (S3A and S3B) is connected between the anodes of V7 and V8 and the control grids of the cathode follower V9, which drives the recorder. The potentiometer P4 controls the balance of the grids of V9 and acts as a zero-control. By means of S3A and S3B the effective bandwidth of the whole amplifier is variable in five steps.

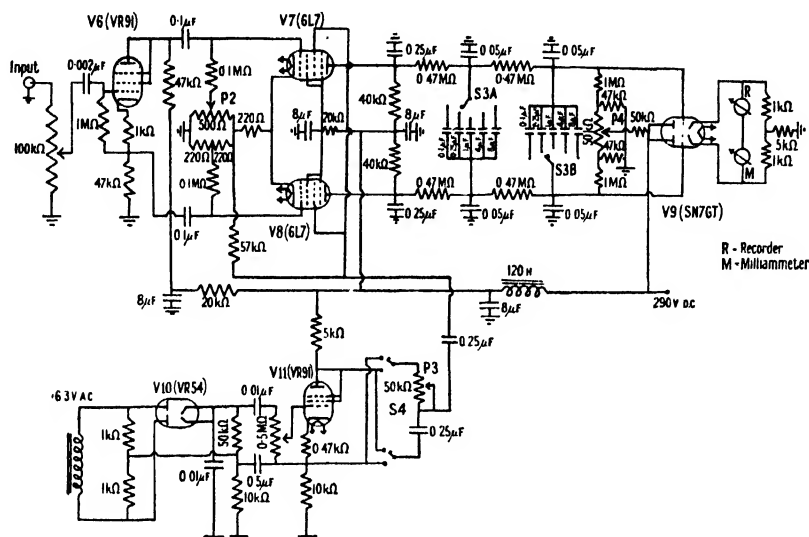
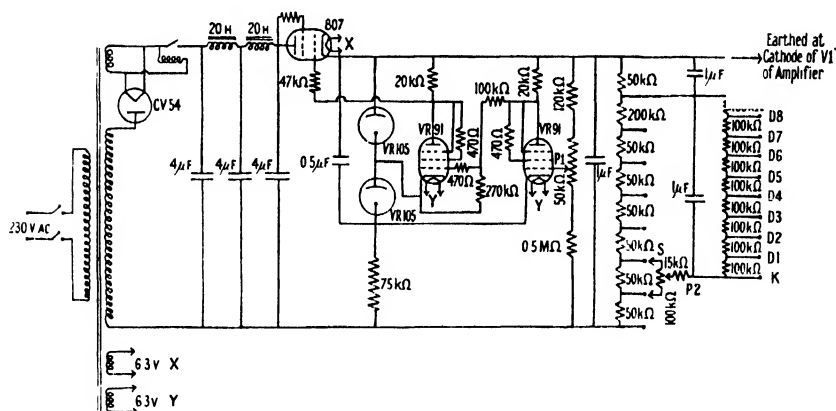


Figure 2.



**Figure 3.**

(c) *Power supplies.*

The high voltage for the photo-multiplier dynodes is obtained from a smoothed power supply derived from the A.C. mains (Figure 3). A step-up transformer provides a voltage of about 1,000, which is then subjected to half-wave rectification and smoothing in the usual way. Regulation is achieved by means of degenerative feedback. Voltage variations in the output are applied to the grid of a VR91 tube and fed back through another VR91 to the grid of the regulator valve 807 in the correct phase, to offset changes in the output. The control grid resistor of the 807 valve is large in order to damp tendencies to oscillation. The potentiometer P1 is preset to determine the voltage at which the circuit regulates. This

final voltage is applied across a series of resistors and by means of the switch S and potentiometer P2 different total voltages can be taken off before final smoothing and division for the dynode stages. The ripple voltage is less than 0.002 volt, and total voltages between 400 and 800 (45 to 90 volts per stage) can be obtained.

The high voltage for the amplifier is provided by a regulator circuit similar to that just described. Regulation is excellent over the range 190 to 260 volts and the 290-volt output used has a ripple of about 0.03 volt. For the earlier stages of the amplifier this ripple is further reduced by smoothing to about 0.001 volt. All earth connections in this circuit are isolated from the chassis and made to the negative side of the H.T. line, which is earthed at the cathode of V1 in the amplifier.

The heaters for the cathodes in the main amplifier are supplied from accumulators (6.3 volts) through short heavy leads.

#### § 4. GENERAL PERFORMANCE

The optimum voltage for the dynodes of the photo-multiplier was found to be about 66 volts per stage, the loss in gain by the use of this relatively low voltage being regained in the amplifier. Using this dynode voltage supply, the specifications of the manufacturers give a current gain in the photo-multiplier of  $5 \times 10^4$ . With the photo-multiplier cooled in solid carbon dioxide the minimum detectable voltage across the load resistor is  $10^{-7}$  volt for a signal/noise ratio of about unity, and the experiments showed that the Johnson noise in the load resistor (1 megohm) is much less than this. Thus the input current to the amplifier is about  $10^{-13}$  amp., the time-constant being sufficiently low to permit the scanning rate already quoted. The minimum detectable primary current is then  $2 \times 10^{-18}$  amp.

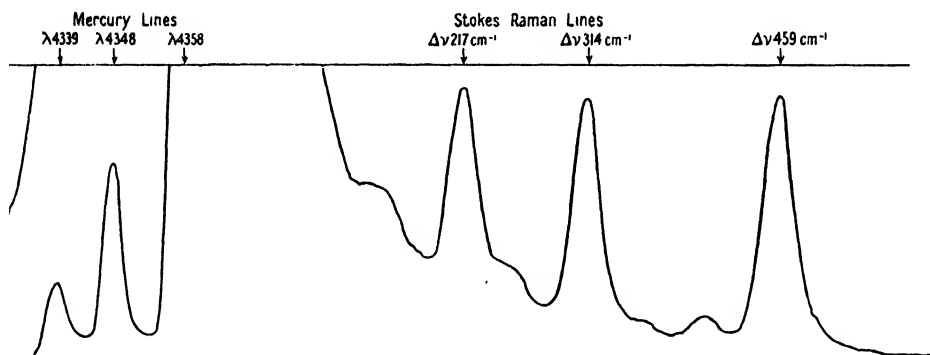


Figure 4.

Figure 4 shows part of a typical record of the Stokes-Raman spectrum of carbon tetrachloride obtained with the vertical Raman tube of 35 ml. capacity (see above). This record was taken with the photo-multiplier at room temperature and with an amplifier gain of only about one-fifth of the maximum practicable under these conditions. The performance indicates that a Raman tube of considerably smaller volume could be satisfactorily used with a spectrometer of greater resolution, particularly where wider slits might be possible.

Figure 4 also shows the exciting mercury line 4358 Å. and its accompanying mercury lines 4348 and 4339 Å., recorded with much lower amplification than that used for the Raman spectrum.

# § 5. FURTHER IMPROVEMENT OF THE SYSTEM

A number of improvements of the instrument are planned, and some have already been carried out. The lack of sharpness of the recorded lines in Figure 4 arises from the poor resolving power of the spectrometer. It is proposed to replace this by an instrument of greater aperture and resolution.

Another alteration is the use of a double recorder. When lines are so strong as to drive the first pen off the paper, the second pen, operated by a less sensitive ammeter, records them. Both the pens record on the same chart.

## ACKNOWLEDGMENTS

We are indebted to Dr. A. C. Menzies for showing one of us a magnesium oxide-coated excitation arrangement similar to that described above. We also wish to express our thanks to the Hydrocarbon Research Group of the Institute of Petroleum for a grant covering part of the cost of the apparatus. One of us (D.A.L.) is indebted to the Department of Scientific and Industrial Research for a maintenance allowance, and another (C.H.M.) to the Rhodes Trustees for a scholarship, enabling them to take part in the work.

## REFERENCES

- CHIEN, J. Y., and BENDER, P., 1947, *J. Chem. Phys.*, **15**, 376.  
 NIELSEN, J. R., 1930, *J. Opt. Soc. Amer.*, **20**, 701.  
 RANK, D. H., PFISTER, R. J., and COLEMAN, P. D., 1942, *J. Opt. Soc. Amer.*, **32**, 390  
 RANK, D. H., PFISTER, R. J., and GRIMM, H. H., 1943, *J. Opt. Soc. Amer.*, **33**, 31.  
 RANK, D. H., and WIEGAND, R. V., 1946, *J. Opt. Soc. Amer.*, **36**, 325.

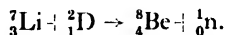
## The Neutrons Emitted in the Disintegration of Lithium by Deuterons

BY L. L. GREEN AND W. M. GIBSON

Cavendish Laboratory, Cambridge

*Communicated by O. R. Frisch ; MS. received 21st January 1949*

**ABSTRACT.** The photographic plate method has been used in an investigation of the neutrons from the reaction

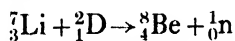


The results are in general agreement with those of Richards, but show the structure of the neutron groups more clearly. In particular, the shape of the broad group attributed by Richards to a level in  ${}^8\text{Be}$  at  $3.0 \pm 0.4$  mev. is discussed in detail.

The total energy release is  $15.0 \pm 0.15$  mev., and evidence is put forward for the existence of energy levels in  ${}^8\text{Be}$  at 2.8 mev., 4.05 mev., 4.9 mev., and 7.5 mev.

## § 1. INTRODUCTION

THE neutrons from the reaction

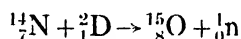


have been studied by Richards (1941). He used the photographic plate technique to obtain the energy distribution of the neutrons emitted at right angles to the direction of the incident deuteron beam. He obtained evidence for a group at 14 mev., corresponding to the formation of  ${}^8\text{Be}$  in its ground state, as well as evidence for a broad level in  ${}^8\text{Be}$  at 3 mev. and another at 7.5 mev.



This reaction is of considerable interest, mainly because of the information which it can give about energy levels in  $^8\text{Be}$ . There is much evidence available about these levels, and Wheeler (1941) has discussed the subject theoretically on the assumption that the  $^8\text{Be}$  nucleus can be considered made up of two separate  $\alpha$ -particles comparatively loosely bound together. The neutrons themselves are useful for experiments in which energies up to 15 mev. are required.

The application of the photographic plate technique to the study of neutron spectra has been described by Powell (1940, 1943) and Richards (1941). Since then the accuracy of the method has been increased by the introduction of concentrated emulsions (Demers 1946, Powell, Occhialini, Livesey and Chilton 1946); the use of Ilford concentrated emulsions for the investigation of the neutrons from the reaction



has been described by Gibson and Livesey (1948). The technique of "temperature development", outlined by Dilworth, Occhialini and Payne (1948), now makes it possible to develop uniformly emulsions of thickness  $300\mu$  or more. With  $300\mu$  emulsions there is a greater chance that a long proton track will remain within the layer, and they are therefore more satisfactory than  $100\mu$  emulsions for the investigation of neutron spectra which extend to energies much above 5 mev.

In view of these improvements in the photographic plate technique, it was thought that a further study of the  $\text{Li} + \text{D}$  neutron spectrum would be profitable.

## § 2. EXPERIMENTAL TECHNIQUE

Ilford C.2 Nuclear Research plates, with emulsion thicknesses ranging from  $100\mu$  to  $300\mu$ , were exposed to the neutrons emitted from a thick lithium hydroxide target. The target was bombarded by a deuteron beam of mean energy 930 kev. from the Cavendish Laboratory 1 mv. set, an average irradiation lasting for 45 minutes with a deuteron beam of 80 microamperes. The plates were held in two positions at a distance of 17 cm. from the target; one set was arranged to receive, at glancing incidence, the neutrons leaving the target at an angle of  $120^\circ$  with respect to the direction of the deuteron beam (" $120^\circ$  neutrons"), while the other set of plates received the neutrons leaving the target at  $0^\circ$  (" $0^\circ$  neutrons").

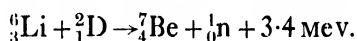
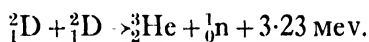
The plates with  $100\mu$  emulsions were developed in the usual way, by soaking for 45 minutes in I.D.19 developer diluted to 1 in 10. Thicker emulsions were processed by the method outlined by Dilworth, Occhialini and Payne (1948): the plates are first soaked in water at  $5^\circ\text{C}$ . for 30 minutes, and then in equally cold developer (I.D.19 diluted to 1 in 5) for 90 minutes. This impregnates the emulsion with developer while allowing little actual development to take place. The main development occurs when the plates are immersed for 30 minutes in developer at  $18^\circ\text{C}$ ., and is uniform throughout the depth of the emulsion. Development is arrested by immersion of the plates in a stop-bath at  $5^\circ\text{C}$ .

## § 3. MEASUREMENTS

The plates were examined on a microscope built specially for nuclear research by Cooke, Troughton and Simms, with two different combinations of objectives and eyepieces which gave overall magnifications of 750 and 1,225. Measurements

of the length, the angle of dip, and the horizontal direction were made for each proton track which started within a definite area of the emulsion; the energy of the neutron responsible for the track was calculated by the method described by Gibson and Livesey (1948).

First, 1,000 tracks were measured in  $100\mu$  emulsions exposed to the  $0^\circ$  neutrons, and a similar number for the  $120^\circ$  neutrons. Only tracks of protons recoiling forwards at angles of less than  $19.5^\circ$  from the direction of the neutron were accepted. Tracks corresponding to neutrons of energy less than 4.5 mev. were also neglected, as it was expected that many of these would be due to the reactions



In the  $120^\circ$  plates an extra 230 tracks corresponding to neutrons of over 7.5 mev. were measured.

In  $300\mu$  emulsions 480 tracks were measured for  $120^\circ$  neutrons and 300 for  $0^\circ$  neutrons; the lower limits of neutron energy were 6 mev. and 7 mev. respectively, and the upper limit of scattering angle was reduced to  $9.5^\circ$ . As changes in angle of dip due to collisions caused appreciable inaccuracies in the measured lengths, the angle of dip was measured at intervals of  $100\mu$  along the projected length of each track, instead of just at the beginning; the total length was then obtained by calculating the actual length in space of each section of the track and adding the results.

#### § 4. NEUTRON SPECTRA

For each set of measurements the number of observed tracks was tabulated as a function of the calculated neutron energy, which for this purpose was taken to the nearest 0.1 mev. In order to reduce the effects of statistical fluctuations, the numbers were later regrouped at 0.3 mev. energy intervals.

To obtain from the observed spectra correct distributions of the numbers of neutrons, it was necessary to multiply the number of tracks corresponding to each neutron energy by a factor proportional to the neutron-proton scattering cross-section at this energy (Sleator 1947) and inversely proportional to the fraction of such tracks which would be expected not to escape from the surfaces of the emulsion; this fraction depends on the neutron energy, the emulsion thickness, and the maximum scattering angle for which tracks are recorded; it was obtained from the equation given by Gibson and Livesey (1948), except at energies above 7.5 mev. in the  $100\mu$  emulsions, where the equation had to be replaced by arithmetical and graphical approximations. The low statistical accuracy of our results at the higher energies did not justify a detailed investigation of the bending of tracks and its effect on the escape correction. The arbitrary constant in the multiplying factor was chosen so as to make the latter equal to unity for a neutron energy of 11 mev.

Figures 1 to 6 show the final results of the observations. Each ordinate is proportional to the number of neutrons in an energy interval of 0.3 mev., and in the region of 11 mev. is equal to the actual number of proton tracks observed in such an interval. The standard deviation of each point is indicated by a vertical line.

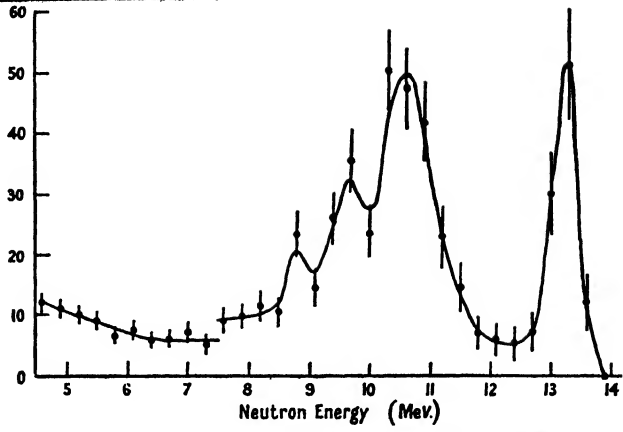


Figure 1. 120° neutron spectrum, from measurements in 100  $\mu$  emulsions.

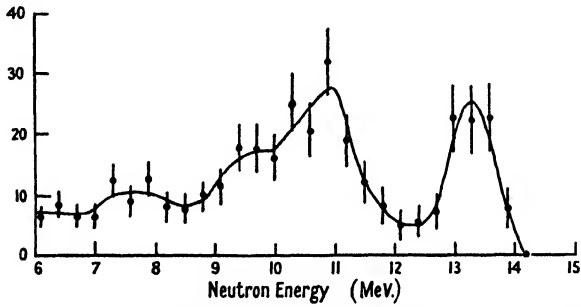


Figure 2. 120° neutron spectrum, from measurements in 300  $\mu$  emulsions.

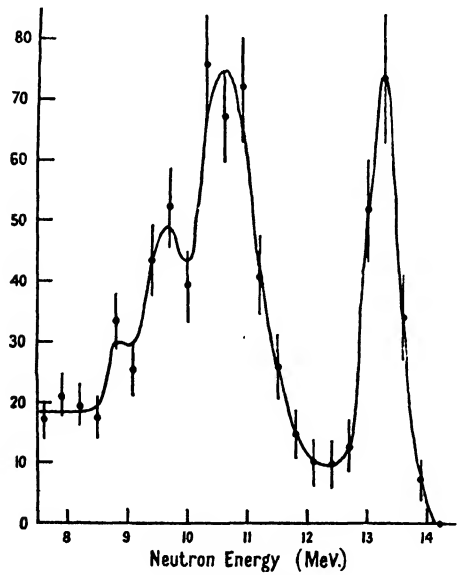


Figure 3. 120° neutron spectrum, from all measurements combined.

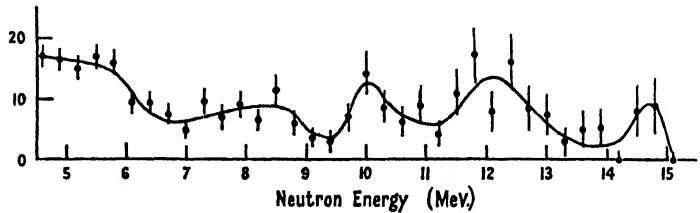


Figure 4. 0° neutron spectrum, from measurements in 100  $\mu$  emulsions.

Figure 1 is the spectrum obtained from the 1,230 tracks measured in  $100\mu$  emulsions exposed to the  $120^\circ$  neutrons. There is a discontinuity at 7.5 mev., as tracks corresponding to lower energies were neglected during part of the observations. Figure 2 shows the results of measurements of tracks in the  $300\mu$  emulsions exposed to the same neutrons, and Figure 3 shows the combined results of all measurements on tracks due to  $120^\circ$  neutrons of energy greater than 7.5 mev.

Figure 4 represents the spectrum of the  $0^\circ$  neutrons, between 4.5 mev. and 15 mev., obtained from 1,000 tracks measured in  $100\mu$  emulsions. Figure 5 shows the results of measurements in  $300\mu$  emulsions, the lower limit of energy being 7 mev., and Figure 6 gives the complete results for  $0^\circ$  neutrons of energies greater than 7 mev.

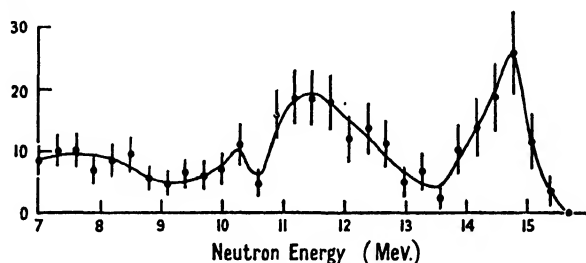


Figure 5.  $0^\circ$  neutron spectrum, from measurements in  $300\mu$  emulsions.

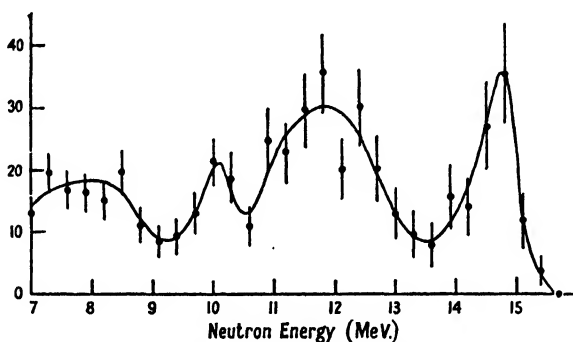


Figure 6.  $0^\circ$  neutron spectrum, from all measurements combined.

(Note.—In Figures 1 to 6, and Figure 9, each ordinate is proportional to the number of neutrons in an energy interval of 0.3 mev., and in the region of 11 mev. is equal to the actual number of proton tracks observed in such an interval.)

Considering first the  $120^\circ$  results, we find a sharp peak at 13.3 mev. in each spectrum. There is also, extending from 9 mev. to 11.5 mev., a very broad group which appears to be composed of a main peak at 10.6 mev. and a subsidiary peak at 9.65 mev. There is a continuous distribution down to 4.5 mev., showing a marked increase at the lower energies. In the results for the  $300\mu$  emulsions there are indications of a possible peak between 7 and 8 mev., but this group does not show up in the  $100\mu$  emulsion results. There is, on the other hand, an indication of a peak at 8.8 mev. in the  $100\mu$  results which does not appear in the  $300\mu$  spectrum.

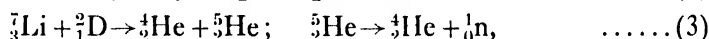
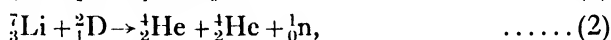
The results for the  $0^\circ$  neutrons have not the same statistical accuracy as those for the  $120^\circ$  neutrons since, although the number of tracks measured was nearly as large, it was spread over a wider energy range. However, the results show similar features: in all spectra there is a high-energy group with a peak at about 14.8 mev., and again there is a broad group at a lower energy. In this case it extends from 10.8 mev. to 13.0 mev. A fairly well

defined group with a peak at 10.15 mev. appears in the results for both 100  $\mu$  and 300  $\mu$  emulsions, and there are indications of a broad group between 7.0 mev. and 8.6 mev. This is superimposed on the continuous background which again extends down to 4.5 mev. with greater intensity at the lower energies.

## § 5. DISCUSSION OF RESULTS

### (i) Possible Reactions

The neutrons emitted by lithium under deuteron bombardment may be due to the reactions:



Reaction (2) involves a three-body disintegration and cannot give rise to homogeneous neutron groups. The reactions (3) similarly cannot give homogeneous groups, and if the  ${}^5_2\text{He}$  nucleus is formed in its ground state, the maximum possible energy of a neutron emitted at 0° is about 4.8 mev. The masses (Bethe 1947) of  ${}^7_3\text{Li}$ ,  ${}^2_1\text{D}$ ,  ${}^7_4\text{Be}$  and  ${}^1_0\text{n}$  give a value of 3.4 mev. for the energy release in reaction (4), which cannot therefore give neutrons of energy greater than 4.5 mev., the lower limit of measurement; a separate investigation of the neutrons from this reaction has been made (Green and Gibson, to be published).

It follows from the above considerations that all groups of neutrons above 4.5 mev. must be due to reaction (1).

### (ii) High-energy Group, Total Energy Release

The high-energy group observed in all spectra corresponds to the formation of  ${}^8\text{Be}$  in the ground state. Wheeler's analysis (1941), of the results of Laaf and Fink indicates that this is a  ${}^1\text{S}_0$  level of width 100 ev., unstable to the extent of about 125 kev. when compared with two  $\alpha$ -particles. Also Walker and McDaniel (1948) have found that the observed width of the 17 mev.  $\gamma$ -ray line produced by bombarding lithium with protons is consistent with the existence of a similar sharp level in  ${}^8\text{Be}$ . The observed widths of our groups, whose shapes are shown in detail in Figures 7 and 8, should therefore be determined entirely by the thick-target and range-straggling effects.

The straggling of proton ranges in concentrated emulsions is known (Lattes, Fowler and Cier 1947) to be about 0.3 mev. at these energies. The effect of the thickness of the target was obtained from the excitation function measured by Bennett, Bonner, Richards and Watt (1947) and the equation

$$8.008 Q = 9.017 E_N - 2\sqrt{(2.033 E_D E_N)} \cos \theta - 5.993 E_D.$$

This equation follows from the kinematics of the reaction, and connects the neutron energy  $E_N$  with the deuteron energy  $E_D$  for particular values of  $Q$  and of the angle of emission  $\theta$ . The excitation function was used to give the yield expected from the deuterons which had been slowed down to a particular energy  $E_D$  in the target, and the equation to give the energy of the resulting neutrons.

The width of the group in the 120° spectrum should be about 0.4 mev. This is mainly due to straggling, since at this angle  $E_N$  does not vary much with  $E_D$ . The term "width" is used here and throughout this paper to mean the interval between the two energies for which the intensity is half that at the peak. The

observed width is 0.6 mev. and the peak is at 13.22 mev.; this gives a  $Q$ -value of  $15.0 \pm 0.1$  mev.

The thick-target effect causes greater broadening in the corresponding group of  $0^\circ$  neutrons. The width for half-intensity should be 0.7 mev., but there will

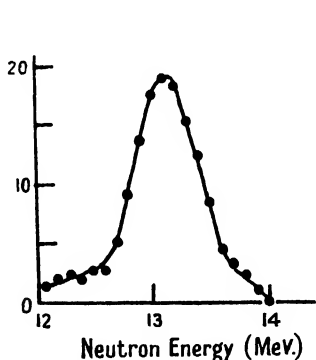


Figure 7.  
Shape of high-energy group in  
 $120^\circ$  spectrum.

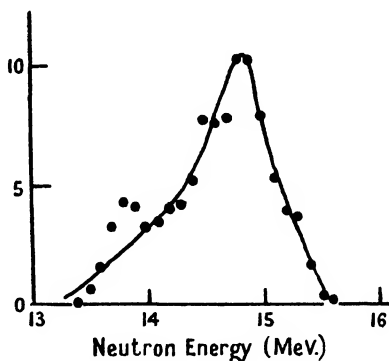


Figure 8.  
Shape of high-energy group in  
 $0^\circ$  spectrum.

(Note.—Ordinates in Figures 7 and 8 are proportional to the numbers of neutrons in energy intervals of 0.1 mev., smoothed by adding to each the mean of its neighbours.)

also be a tail on the low-energy side which may extend as far as 1.3 mev. below the peak. The experimental width is 0.8 mev. and the maximum intensity is at 14.8 mev.; this again gives  $Q = 15.0 \pm 0.1$  mev.

Allowing for the uncertainty of  $\pm 0.08$  mev. in the range-energy relation between 13 and 15 mev., we may give as a final value  $Q = 15.0 \pm 0.15$  mev. This agrees well with the value of 15.04 mev. given by the mass values quoted by Bethe (1947).

### (iii) Other Groups, Excited Levels in $^8\text{Be}$ .

The broad group occurring about 3 mev. below the high-energy group requires more careful discussion. There is a considerable amount of evidence on levels occurring in  $^8\text{Be}$  in the neighbourhood of 3 mev. above the ground state. Wheeler (1941) shows that the main results of experiments on  $\alpha$ - $\alpha$  scattering are accounted for by an excited state of zero angular momentum and energy 2.8 mev. Dee and Gilbert (1936) have attributed the continuum in the  $\alpha$ -particle energy distribution observed in the reaction  $^{11}\text{B}(\alpha)^8\text{Be}$  to an excited state of width 0.8 mev. and energy 3.0 mev. A re-examination of these results by Bethe (1937) indicated that a level at 2.8 mev. and width 0.8 mev. was consistent with the observations. Smith and Murrell (1939) attributed a group of  $\alpha$ -particles from the reaction  $^{10}\text{B}(\text{d}\alpha)^8\text{Be}$  to the formation of  $^8\text{Be}$  in a level at 3 mev.

Wheeler identifies the 2.8 mev.  $\alpha$ - $\alpha$  scattering level with the first vibrational state on the two- $\alpha$ -particle model, and it is reasonable to identify this with the 3 mev. level observed in the boron disintegrations.

Bonner, Evans, Malich and Risser (1948) have reported that the energy distribution of the  $\alpha$ -particles associated with the  $\beta$ -disintegration of  $^8\text{Li}$  may be explained by the assumption of a level in  $^8\text{Be}$  at  $3.4 \pm 0.4$  mev., with  $J=2$ , and a further broad level at 7–9 mev.

Recently, Walker and McDaniel (1948) have confirmed the long-suspected existence of a 14.8 mev.  $\gamma$ -ray from the reaction  $^7\text{Li}(\text{p}\gamma)^8\text{Be}$ , as well as the well-known 17.6 mev.  $\gamma$ -ray. The latter corresponds to the formation of  $^8\text{Be}$  in its

ground state and the former to an excitation of 2.8 mev. This level is probably the same as that observed in boron reactions and in  $\alpha$ - $\alpha$  scattering, but the  $\gamma$ -ray line is found to have a breadth of about 2.1 mev. instead of 0.8 mev. This might indicate the presence of two unresolved lines.

Richards (1941), in an investigation of the reaction  ${}^7\text{Li}(\text{dn}){}^8\text{Be}$ , observed a very broad neutron group which he considered to be composed of two unresolved groups, due respectively to the 2.8 mev. level of width 0.8 mev. and to a level at 4.9 mev. The existence of this 4.9 mev. level was suggested by the observation of a 4.9 mev.  $\gamma$ -ray by Bennett, Bonner, Richards and Watt (1941).

Our results clearly indicate the presence of a broad group of width about 2.0 mev. As in the results of Richards and of Walker and McDaniel, this is considerably greater than the 0.8 mev. width of the 2.8 mev. level. The group due to the 4.9 mev. level would be at too low an energy to account for the width of our group, and has in fact been separately resolved in the  $0^\circ$  spectra. The main group itself appears to be complex and is probably composed of two partially resolved groups. For convenience the spectra shown in Figures 3 and 6 are shown again in Figure 9, with the neutron energy scale replaced by a scale of the corresponding  ${}^8\text{Be}$  excitation energy.

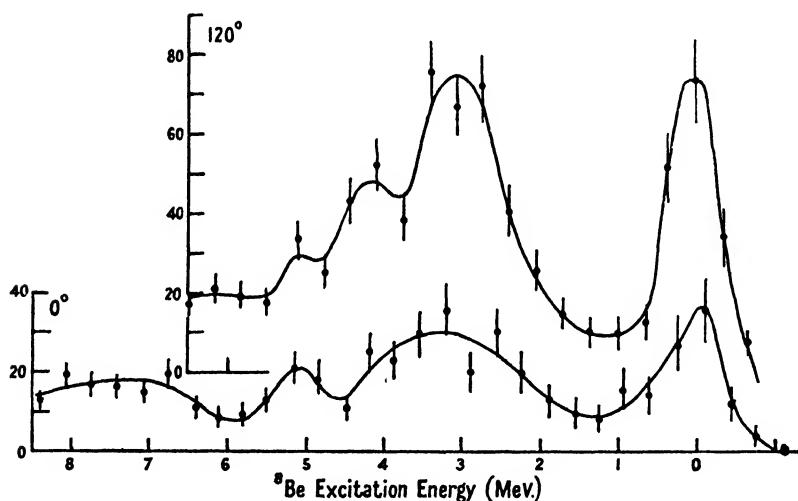


Figure 9. Neutron spectra, from Figures 3 and 6, plotted against  ${}^8\text{Be}$  excitation energy.

The  $120^\circ$  spectra consistently show a partially resolved group at a neutron energy of 9.65 mev. The main group has a maximum at 10.6 mev., corresponding to a  $Q$ -value of 11.9 mev. and an excited state in  ${}^8\text{Be}$  at 3.0 mev. The experimental width of this group is approximately 1.4 mev.; when allowance has been made for straggling and the thick-target effect, this would indicate a width of approximately 0.8 mev. for the 3.0 mev. level.

The subsidiary peak at 9.65 mev. corresponds to a  $Q$ -value of 10.85 mev., and would require a level at 4.05 mev. in the  ${}^8\text{Be}$  nucleus. We cannot draw any conclusions about the width of this level, as the group is only partially resolved. An excited state at 4.05 mev. would be consistent with the results of Walker and McDaniel, and of Richards; it may also be noted that Bonner, Evans, Malich and Risser (1948) have interpreted their results for the energy distribution of the  $\alpha$ -particles from the  $\beta$ -decay of  ${}^8\text{Li}$  by assuming a level in  ${}^8\text{Be}$  at  $3.4 \pm 0.4$  mev.

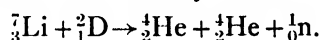
The corresponding group in the  $0^\circ$  spectra may be complex, but the peak due to the 4.05 mev. level is not resolved. The width of the group is 2.0 mev., which

is greater than the value of 1.6 mev. which the straggling and thick-target effects would give with a 3.0 mev. level of width 0.8 mev.

There is a well-defined peak in these spectra at 10.15 mev., corresponding to a  $Q$ -value of 10.0 mev. and requiring a level in  ${}^8\text{Be}$  at 5.0 mev. Smith and Murrell (1939) observed a group of  $\alpha$ -particles from the reaction  ${}^{10}\text{B}(\text{d}\alpha){}^8\text{Be}$  which would have required an excited state of  ${}^8\text{Be}$  at 4.8 mev.; this group could, however, have been attributed to contamination of their target with lithium. It has already been mentioned that Bennett, Bonner, Richards and Watt (1941) have observed the emission of a 4.9 mev.  $\gamma$ -ray from lithium bombarded with deuterons. This  $\gamma$ -ray was attributed to a level in  ${}^8\text{Be}$  at 4.9 mev., which was assumed to have odd angular momentum or odd parity or both, so that the ordinary break-up into two  $\alpha$ -particles was forbidden. It is reasonable to ascribe our group of neutrons to the same level. There are also indications of the presence of a corresponding group of neutrons in the  $120^\circ$  spectra; the lower intensity in this direction may be connected with the odd angular momentum of the state.

The  $0^\circ$  spectra indicate the presence of a broad group of neutrons with a mean energy of 7.9 mev. and width about 2.0 mev. This would require a level in  ${}^8\text{Be}$  at 7.4 mev. and 2.0 mev. wide. Richards has observed a neutron group in the  $90^\circ$  direction requiring a level at 7.5 mev., approximately 1.7 mev. wide. There are indications of a greater neutron intensity between 6.5 mev. and 8.5 mev. in our  $120^\circ$  spectra, but this group is not statistically significant.

In both the  $0^\circ$  and  $120^\circ$  spectra the continuous background of neutrons shows a pronounced increase at the lower energies. This may be another neutron group due, for instance, to the broad level at 10.0 mev. suggested by Richards, or it may be a genuine rise in the intensity of the neutrons due to the reaction



#### ACKNOWLEDGMENTS

The authors wish to express their thanks to Professor O. R. Frisch and Dr. W. E. Burcham for advice and assistance, and to the Department of Scientific and Industrial Research for financial support.

#### REFERENCES

- BENNETT, W. E., BONNER, T. W., RICHARDS, H. T., and WATT, B. E., 1941, *Phys. Rev.*, **59**, 904; 1947, *Ibid.*, **71**, 11.  
 BETHE, H., 1937, *Rev. Mod. Phys.*, **9**, 217; 1947, *Elementary Nuclear Theory* (New York: John Wiley & Son), p. 124.  
 BONNER, T. W., EVANS, J. E., MALICH, C. W., and RISSE, J. R., 1948, *Phys. Rev.*, **73**, 885.  
 DEE, P. I., and GILBERT, C. W., 1936, *Proc. Roy. Soc. A*, **154**, 279.  
 DEMERS, P., 1946, *Phys. Rev.*, **70**, 86.  
 DILWORTH, C. C., OCCHIALINI, G. P. S., and PAYNE, R. M., 1948, *Nature, Lond.*, **162**, 102.  
 GIBSON, W. M., and LIVESEY, D. L., 1948, *Proc. Phys. Soc.*, **60**, 523.  
 GREEN, L. L., and GIBSON, W. M., 1949, to be published.  
 LATTES, C. M. G., FOWLER, P. H., and CUER, P., 1947, *Proc. Phys. Soc.*, **59**, 883.  
 POWELL, C. F., 1940, *Nature, Lond.*, **145**, 155; 1943, *Proc. Roy. Soc. A*, **181**, 344.  
 POWELL, C. F., OCCHIALINI, G. P. S., LIVESEY, D. L., and CHILTON, L. V., 1946, *J. Sci. Instrum.*, **23**, 102.  
 RICHARDS, H. T., 1941, *Phys. Rev.*, **59**, 796.  
 SLEATOR, W., 1947, *Phys. Rev.*, **72**, 207.  
 SMITH, C. L., and MURRELL, E. B. M., 1939, *Proc. Camb. Phil. Soc.*, **35**, 298.  
 WALKER, R. L., and MCDANIEL, B. D., 1948, *Phys. Rev.*, **74**, 315.  
 WHEELER, J. A., 1941, *Phys. Rev.*, **59**, 27.



## The Basis of the Electron Theory of Metals, with Special Reference to the Transition Metals

By N. F. MOTT

H. H. Wills Physical Laboratory, University of Bristol

*MS. received 25th April 1949*

**ABSTRACT.** It is shown that the collective electron and London-Heitler models are not to be regarded as different approximations to the same exact wave function for solids in which, according to the former model, there is a partially filled zone of energy levels. It can thus be shown why nickel oxide in the pure state is a non-conductor, although it contains an incomplete zone. The properties of the metals nickel, palladium and platinum are discussed in the light of these results; platinum differs from nickel in that the orbital contribution to the moment of the elementary magnets is not quenched. A discussion is given of x-ray absorption edges, and it is shown why exciton lines are absent for metals.

### § 1. THE COLLECTIVE ELECTRON AND LONDON-HEITLER METHODS

**I**N discussing the cohesive forces in metals, or their electrical or magnetic properties, it is first necessary to set up an approximate electronic wave function. In doing this, all investigators have used one or other of two approximations; these are:

(a) The London-Heitler or Heisenberg approximation, in which one starts from atomic wave functions, such as that in which  $\psi_a(\mathbf{r}_n)$  describes the space coordinate of the  $n$ th electron in the atom  $a$ . One then forms products of the type

$$\psi_a(\mathbf{r}_1)\psi_b(\mathbf{r}_2) \dots,$$

multiplied by appropriate spin functions, and from these an anti-symmetrical determinant or sum of anti-symmetrical determinants can be set up. This method, though convenient for insulators such as NaCl, where each atom or ion is in a singlet state, has not been applied with much success to metals, owing to the mathematical difficulties introduced by the spin degeneracy. The only exact result deduced by this method is that of Bloch (1930), who treated the case where the exchange integral between neighbours is positive, so that in the lowest state all spins are parallel (ferromagnetism); he showed that if  $I$ ,  $I_0$  are the values of the intrinsic magnetic intensity at temperatures  $T$  and zero,

$$I - I_0 = \text{const. } T^{3/2}. \quad \dots\dots(1)$$

The same argument shows that the electronic specific heat with this model varies as  $T^{3/2}$ . The case where the exchange integral is negative is much more difficult and has not been used to obtain successfully the electronic specific heat. For a discussion of the paramagnetism in this case, cf. Hulthén (1936).

(b) The collective electron treatment, also first used in a quantitative way by Bloch (1928). This is the same as the molecular orbital method of quantum chemistry. Wilson (1931) first showed how convenient the model was for explaining the sharp division of pure solids at low temperatures into metals and non-conductors; the former are those with a partially filled "zone" of electronic states, the latter those in which all zones are either quite full or quite empty.

Stoner\* has recently applied the model to ferromagnetics, and obtained a form for  $I_0 - I$  which, though surprisingly similar to the  $T^{3/2}$  law mentioned above, is derived in quite a different way. The experimental results are certainly not good enough to decide between them.

The main purpose of this paper is to suggest that these two models are *not*, as is usually believed, different approximations to the same exact wave function. We believe, on the other hand, that crystalline solids, which in model (b) have incomplete zones, fall quite sharply into two classes: those for which model (b) is a good approximation (metals), and those for which model (a) is a good approximation.

Let us consider first the physical properties of a substance which we believe to belong to the class (a), namely NiO. This has the simple cubic structure, and may be thought of as being made up of nickel ions  $\text{Ni}^{++}$  and oxygen ions  $\text{O}^{--}$ . It is paramagnetic (Batnagar and Bal 1934), the nickel ions being the paramagnetic elements. The nickel ion has the electronic configuration  $(3d)^8$ ; the 3d state should give rise to a zone containing 10 electrons which may be split by a cubic field into sub-zones containing 4 and 6; thus, using model (b), at least one of these sub-zones is partly empty. Thus, according to model (b), NiO should show metallic conductivity, increasing as the temperature is lowered. But this is not in accordance with the facts. Pure nickel oxide is an insulator, and is transparent to visible light, being pale greenish yellow. And this is what we should expect, starting from model (a). In order that NiO should conduct, there must be present some  $\text{Ni}^{+++}$  ions and some  $\text{Ni}^+$  ions, which can move about by electron transfer. But a definite amount of energy,  $E$  say, is required to remove an electron from one ion (leaving  $\text{Ni}^{+++}$ ) and to put it on a *distant* ion, forming  $\text{Ni}^+$ . Therefore, unless the crystal of NiO as a whole is in an excited electronic state (e.g. at a high temperature), no such pairs are present. Nickel oxide can actually be made to behave as a semiconductor by introducing  $\text{Ni}^{+++}$  ions into the lattice, e.g. by replacing some of the nickel ions by  $\text{Li}^+$  ions, an electron being removed from another ion to secure electrical neutrality (Verwey, Haayman and Romeyn 1948); clearly, then, electrons are not impeded by the rather large interionic distance (*c.* 7 Å.) from jumping from ion to ion.

It has, of course, been noticed by many authors (e.g. Schubin and Wonsowski 1934) that the London-Heitler approximation does not allow for any electric current, and it has been suggested that, in the exact wave function, there will be present *ionized* states—i.e. some atoms having one extra electron and an equal number having one missing; these we may call positive holes. We suggest that this is not quite correct, and that, starting from the London-Heitler approximation, there will either be no pairs (electrons and holes) which have separated *many* atomic distances, or else, as one goes to higher approximations, the number of completely separated pairs will increase indefinitely, so that the whole approximation breaks down and one has to start with the collective electron treatment.

The evidence for this view is as follows:

(i) The facts about NiO quoted above and similar facts about oxides of other transition metals.

(ii) The difficulty in believing that a state with a *small* number of pairs can ever have lower energy than a state with no pairs. One will always have to do work to separate the electron and hole constituting the first pair to be formed,

\* In a series of papers; for references cf. Stoner (1948).

because the electron and positive hole attract each other with a force derived from a potential energy  $-e^2/\kappa r$ , where  $\kappa$  is a dielectric constant. It is known from Schrödinger's equation that two particles which attract each other with a force of this type are capable of existing in a number of stationary states in which they are bound to each other. On the other hand, if some pairs already exist, it no longer follows that work must necessarily be done to form some more. This is because the material is now in a state where a current can be carried; therefore (Mott and Jones 1936, p. 87), the field between the electron and hole is now screened, and is of the form to be derived from a potential  $-(e^2/\kappa r) \exp(-qr)$ . The constant  $q$  increases with the number of electrons and holes present. In a field of this sort, if  $q$  is large enough, there are no bound stationary states. It no longer follows, then, that work must be done when the number of pairs is increased; it is possible that energy may be gained, owing to the negative energy of particles with collective electron orbitals.

We suggest tentatively, then, that the energy  $E$  of a crystalline array of  $N$  atoms—e.g. an array of Na atoms or  $\text{Ni}^{++}$  ions, may be as shown in Figure 1.  $E$  is here the energy corresponding to a wave function containing  $n$  pairs of electrons and holes and is plotted against  $n$ .  $E$  may be supposed to be the minimum (and hence most accurate) energy value obtainable from a wave function of London-Heitler type with ionized states.  $E$ , as we have shown, will always rise first as  $n$  increases. We suggest that it will then decrease. It may or may not drop below

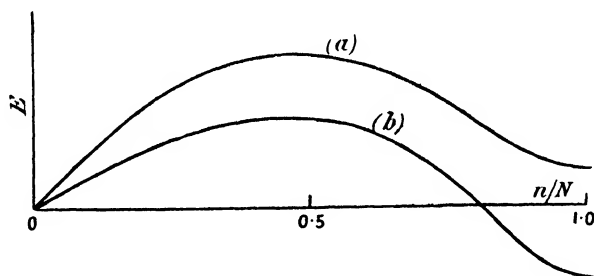


Figure 1. Hypothetical plot of energy  $E$  against number  $n$  of pairs, (a) for large separations between atoms as in NiO, (b) for small separations as in metals.

the value for  $n=0$ . Presumably it will not if the interatomic distance is large (case of NiO), but will otherwise (case of metals). If it does, the number of holes becomes large (comparable with  $N$ ), the approximation breaks down, and we go over to the collective electron treatment.

Some further evidence that the view is correct may perhaps be provided by a recent theoretical paper on the wave functions of the hydrogen molecule (Coulson and Fischer 1949). These authors write the wave function in the unsymmetrical form

$$\{\psi_a(1) + \lambda\psi_b(2)\}\{\psi_b(1) + \lambda\psi_a(2)\},$$

where  $\psi_a, \psi_b$  are atomic wave functions for electrons in the atoms  $a, b$ , and  $\lambda$  is a parameter. By minimizing the energy calculated with this wave function,  $\lambda$  is determined as a function of the distance  $R$  between the nuclei of the two atoms. In  $\text{H}_2$  this is actually 1.4 Å.; the calculations show that  $\lambda=1$  gives the best approximation up to  $R=2.3$  Å., but thereafter  $\lambda$  tends rapidly to zero. In our view the abrupt transition only occurs for infinite chains or lattices.

On the view explained above, therefore, if a substance such as NiO were subjected to very high pressure it should suddenly show metallic conduction for some value of the pressure, and the effective number of free electrons would suddenly jump to about one per atom. This view seems to be in accord with the observed fact that no metals show a very small effective number of free electrons except bismuth and similar elements (Mott and Jones 1936, p. 210). We believe that at the absolute zero of temperature a very small number of free electrons free to take part in a current is impossible, because the electrons and holes would attract each other and form bound pairs, i.e. electrons trapped in the field of holes. A metal substance is only a conductor at  $T=0$  if there are enough electrons and holes to screen the field round any one of them sufficiently to prevent pair formation. Bismuth, of course, proves the rule because, although the number of free electrons is very small, their effective mass is also very small (Mott and Jones 1936, Chap. VI), and hence much less screening (smaller  $q$ ) is necessary to prevent pair formation.

Experiments on the conductivity of cupric salts would be of great interest. One cannot say *a priori* whether or not they should show metallic conduction. According to Hilsch and Brunner (1947), CuS is a superconductor.

## § 2. THE TRANSITION METALS Ni, Pd AND Pt

Turning now to a metal such as nickel, we see that it can be represented as follows. Suppose that a London-Heitler type of wave function were set up representing nickel atoms in the singlet state  $(3d)^{10}$ ; if a few electrons are removed and put into the 4s conduction band, leaving mobile holes in the 3d band, the energy will at first rise. But it seems very plausible that it will fall again, as in Figure 1, as the number is increased, owing to the bonding effect of the 4s conduction electrons—described of course by wave functions of the collective electron type. All the experimental evidence from the magnetic properties of these metals and their alloys goes to show that a minimum in the energy is reached when 0.6 holes per atom have been formed, giving 0.6 conduction electrons.

We thus consider that nickel contains 0.6 conduction electrons described by periodic wave functions and 0.6 holes; these must also be described by periodic wave functions extending through the lattice, quite independently of how big the interatomic distance may be. This is because the number of holes is non-integral; one could not set up a London-Heitler wave function with no ionized states for this case, and it seems certain that these holes can move through the lattice and contribute to a current. The model is essentially the same as the overlapping band model first introduced by Mott (1935), though we would now stress the applicability of the collective electron treatment for the holes rather than for the electrons of the d band.

The large electronic specific heats shown by Ni, Pd and Pt at liquid helium temperatures is known to be due to the holes, which can be treated in the usual way as a degenerate gas of particles with large effective mass. It is at first sight surprising that these metals do not all show an electronic specific heat at high temperatures given by

$$(C_v)_{el} = 0.6 \times \frac{3}{2}R = 1.8 \text{ cal/gm. atom.}$$

For nickel the position is complicated by the transition at the Curie point, though some  $30^\circ$  above it the effect dies out and the specific heat seems in good agreement with theory (Wohlfarth 1949); but Pd and Pt certainly do not show so large a term. For Pd a careful analysis has been given by Clusius and Schachinger

(1947), showing at  $1,000^\circ\text{K}$ . an electronic term of about  $0.9\text{ cal/gm. atom}$ . The probable reason is the form of the d band, shown by Jones and Mott (1937) for small overlap between the wave functions to be as seen in Figure 2 (see also Slater 1936); the calculations of Jones and Mott were for a simple cubic lattice). If, as is quite possible, the d zone in Pd is full up to near the top of the first maximum,

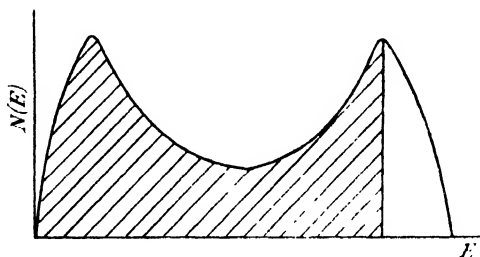


Figure 2. Plot of  $N(E)$  as a function of  $E$  for a d band.

it is clear that the specific heat of the holes will not tend to the classical value but to a lower one. Calculations of the electronic specific heat with various band forms could easily be carried out and would be of interest. The reason for the difference between Ni and Pd is not known.

It has been suggested (Mott and Jones 1936, p. 222, Pauling 1949) that the magnetic carriers in nickel are not single holes, as stated here, but double holes, that is to say, ions in the triplet state of configuration  $(3d)^8$ . This suggestion was made in order to account for the paramagnetic behaviour of nickel above the Curie point, the slope of the line  $(1/\chi \text{ versus } T)$  agreeing with the hypothesis that the elementary magnets have  $j=1$  instead of  $j=\frac{1}{2}$ ,  $g$  of course remaining equal to 2. But it is clear now that this hypothesis is inadmissible, because coupled spins would obey Einstein-Bose rather than Fermi-Dirac statistics, and thus would give an electronic specific heat proportional to  $T^{3/2}$  instead of the observed  $T$ . Wohlfarth (1949) has shown that the observed paramagnetic behaviour can be explained in terms of the collective electron treatment without making any assumptions about coupled spins; one would have to go to higher temperatures than are actually possible to obtain a true paramagnetic magneton number.

In nickel, of course, the  $g$ -value for the holes is 2, there being no orbital contribution. Probably this is not the case for platinum, the orbital motion and spin remaining coupled to give  $j=5/2$  and  $g=6/5$ ; spectroscopic data for the free atom shows that the interval between the terms of the spin doublet of the ion in the state  $5d^9$  is of the order 1 ev. for Pt, while the corresponding interval for Ni is 0.25 ev. There is no difficulty whatever in describing mathematically, through periodic wave functions of the collective electron type, the motion through the lattice of the configuration  $5d^9$  with coupled spin and orbit.

The strongest evidence that in metallic platinum the spin-orbit coupling is not broken down comes from the measurements of Cauchois and Manescu (1940) and Coster and de Lang (1949) on the  $L$  absorption edges of the x-ray spectra. For the  $L_1$  edge one neither expects, nor finds, any sharp line at the edge due to transitions into the empty d states, because the initial  $L$  state is s. For  $L_2$  and  $L_3$ , on the other hand, the initial state is p. For the free atom the empty state in the 5d shell has the  $j$  value  $5/2$ ; one would therefore expect a transition from  $L_3$  ( $j=3/2$ ) but not from  $L_2$  ( $j=1/2$ ). This is in fact what one finds in the

metal, showing that the spin-orbit coupling is not broken down. If it were broken down, the empty d states in the metal would be a mixture of the atomic states with  $j=3/2$  and  $j=5/2$ , and both edges would give lines of comparable strength at the edge. If it is possible to observe the lines for nickel, they should appear both for the  $L_2$  and  $L_3$  absorption edges.

A further application of these ideas to x-ray absorption spectra may be made. One expects that the x-ray absorption edge of an insulator will consist of a series of lines, more or less broadened by lattice vibrations, leading up to a series limit. This is because the ejection of an electron from an inner shell leaves behind a positive charge; there is thus in the insulator a field of potential  $-e^2/\kappa r$ , and for the excited electron a series of stationary states must exist in this field *below* the conduction band. If  $\kappa$  is large, these states will be close together and difficult to observe; they seem however to have been observed in manganate ions (Sunnar 1941) for the K absorption edge of manganese.

In metals no such "exciton" lines have been observed. The reason seems to us to be the following: the field round the positive charge left when the electron is ejected is screened, and of the form  $-(e^2/r) \exp(-qr)$ . Now if  $q$  were not big enough to prevent the formation of bound states in this field, then, according to the argument given above, the atoms from which an electron is missing and those with an extra electron would join together to form pairs, and the material could no longer be a conductor.

Turning now to Bloch's law (1) for  $I_0 - I$  in ferromagnetics, we see that the original derivation is valid only for non-conducting materials (e.g. ferrites). Döring (1949) has, however, shown that for low temperatures it can be derived more generally, from the assumption that the energy  $E$  of a small volume containing a large number of elementary magnets depends on the three components of magnetization  $I_x, I_y, I_z$  through a formula of the type

$$E = A[(\text{grad } I_x)^2 + (\text{grad } I_y)^2 + (\text{grad } I_z)^2],$$

giving its local dependence on the direction of magnetization. The derivation does not, therefore, depend on the use of one model or the other. Thus the  $T^{3/2}$  must be regarded as correct at low temperatures, regardless of any special model; it is analogous to the Debye  $T^3$  law for the specific heat. Stoner's treatment is analogous rather to the Einstein treatment, and should be a good approximation only for higher temperatures, where the "spin waves" have short wavelength.

For non-conducting paramagnetics we have no theoretical or experimental information about the electronic specific heat as  $T$  tends to zero. A theoretical treatment, owing to the difficulty of handling the spin degeneracy, has not been given (cf. Bethe 1931).

#### REFERENCES

- BATNAGAR, S. S., and BAL, G. S., 1934, *J. Ind. Chem. Soc.*, **11**, 603.  
 BETHE, H., 1931, *Z. Phys.*, **71**, 205.  
 BLOCH, F., 1928, *Z. Phys.*, **52**, 553; 1930, *Ibid.*, **61**, 206.  
 CAUCHOIS, Y., and MANESCU, I., 1940, *C.R. Acad. Sci., Paris*, **211**, 172.  
 CLUSIUS, K., and SCHACHINGER, L., 1947, *Z. Naturforschung*, **2a**, 90.  
 COSTER, D., and DE LANG, H., 1949, *Physica*, in the press.  
 COULSON, C. A., and FISCHER, I., 1949, *Phil. Mag.*, **40**, 386.  
 DÖRING, W., 1949, *Z. Phys.*, in the press.  
 HILSCH, R., and BRUNNER, H., 1947, quoted by E. Justi, *Leitfähigkeit und Leitungsmechanismus fester Stoffe* (Göttingen, 1948).

- HULTHÉN, L., 1936, *Proc. Amst. Acad.*, **39**, 190.  
 JONES, H., and MOTT, N. F., 1937, *Proc. Roy. Soc. A*, **162**, 49.  
 MOTT, N. F., 1935, *Proc. Phys. Soc.*, **47**, 571.  
 MOTT, N. F., and JONES, H., 1936, *Theory of the Properties of Metals and Alloys* (Oxford : Clarendon Press).  
 PAULING, L., 1949, *Report of Paris Conference on Chemical Bonds*.  
 SCHUBIN, S., and WONSOWSKI, S., 1934, *Proc. Roy. Soc. A*, **145**, 159.  
 SLATER, J. C., 1936, *Phys. Rev.*, **49**, 537.  
 STONER, E. C., 1948, *Rep. Prog. Phys.*, **11**, 43 (London : Physical Society).  
 SUNNER, V. H., 1941, *Thesis*, Upsala.  
 VERWEY, E. J. W., HAAYMAN, P. W., and ROMEYN, F. C., 1948, *Chemisch. Weekblad*, **44**, 705.  
 WILSON, A. H., 1931, *Proc. Roy. Soc. A*, **133**, 458.  
 WOHLFARTH, E. P., 1949, *Proc. Roy. Soc. A*, **195**, 434.

## The Experimental Basis of Electromagnetism— Part III: The Magnetic Field

BY N. R. CAMPBELL AND L. HARTSHORN

*MS. received 3rd March 1949*

**ABSTRACT.** The principles outlined in previous parts, published in the *Proceedings of the Physical Society* in 1946 and 1948 respectively, which dealt with the direct current circuit and with electrostatics, are here applied to magnetism, with the object of showing how the basic concepts are defined in terms of the operations actually performed in measuring them. This part is confined to a discussion of the vector  $\mathbf{B}$ , which is shown to be measurable independently of a knowledge of any other magnitude. It is solenoidal, and can therefore be determined at all points, even those within solid bodies.

### § 1. INTRODUCTION

THE general purpose of this work, as stated in the abstract of Part I (Campbell and Hartshorn 1946)\*, was "to show to what extent the working principles of electromagnetism can be soundly based on real experimental facts, as distinct from the imaginary experiments which are common to most expositions of the subject". The general principles by which magnitudes are established in terms of experimental operations were described in § 2 of that paper, and at the outset we were optimistic enough to believe that by systematically applying these principles to operations that would be generally admitted as established practice, we should be able to derive the working laws of the experimentalist and a coherent outline of the whole subject in a form free from "mathematical fictions", that is to say, concepts like point charges that are so remote from real experiment that they must be classed as auxiliary devices invented by the human mind rather than anything encountered in nature.

We had some success in treating in this way the direct current circuit (Part I, 1946) and electrostatics (Part II, 1948), though it must be confessed that in Part II the jump from experiment to general law was not always so obvious as to leave no doubt in the mind of the reader about the wisdom of dispensing with the auxiliary devices. We have in the present part applied the same treatment to magnetism, and we have to admit that our early optimism has not been altogether justified. The laws that we have been able to base directly on real experiments can scarcely be regarded as forming a coherent structure, and it therefore seems

\* For references seen end of Part IV, p. 000.

likely that theoretical magnitudes having no direct reference to real experiment form a necessary part of the subject as it is practised today. But though the magnitudes that arise directly from real experiments may not be sufficient, it is at least important that we shall know which they are, and their precise significance in terms of the operations that we actually perform. This part is therefore devoted to a consideration of the most characteristic experimental methods employed in the investigation of magnetic materials and of the magnitudes and laws which arise directly from them. These, in our view, constitute the experimental basis of the subject.

## § 2. THE FLUXMETER

In accordance with our general principles, our first step must be to seek among the instruments used in modern magnetic measurements one whose operations define a magnitude that can be measured independently of any other magnitude. Such an instrument is to be found in the fluxmeter. At first sight it may seem surprising that so complicated an instrument should be accepted as fundamental. The principle is, however, very similar to that which leads us to accept operations performed with balances and clocks, which are quite as complicated as fluxmeters, as the basis of our ideas of mass and time.

By a fluxmeter we mean the familiar combination of a search coil and ballistic galvanometer, the coil having its terminals close together, and being connected to the galvanometer, which is direction-sensitive, by long, flexible, twisted or concentric leads. (The term fluxmeter is often confined to an instrument in which the ballistic galvanometer is of a special kind, but we think it less objectionable to extend this meaning somewhat than to coin a new term.) If the search coil, after having been at rest for a long time in the neighbourhood of a magnet, is moved suddenly relative to it and is then brought to rest again, the galvanometer gives a characteristic response in the form of a transient deflection passing through one or more maximum values. We shall apply the term magnet to any system that produces such responses, so that it includes, not only permanent magnets and electromagnets in the conventional sense, but also current circuits not associated with any magnetic material. Similar responses can be produced by changes in the magnet, and in particular by changes in the current in a circuit forming part of the magnet without any relative motion of coil and magnet. The laws we are about to state in this section are true by whichever method the response is produced: it is convenient therefore to use terms that are equally applicable to either. We shall use the term "the system" to denote the whole combination of search coil, leads, galvanometer and magnet; and the "state of the system", that complex of conditions, sudden \* change in any one of which may produce a response. Thus a change in the state of the system may include a change in the size or shape of the search coil, a displacement of the coil relative to the magnet, or a change in the state of the magnet, such as a change of current in a stationary coil or the displacement of a piece of magnetic material relative to neighbouring circuits.

So long as the changes of the state of the system are always sufficiently sudden and the galvanometer always starts from the same zero, such a system obeys two qualitative laws: (a) If two responses agree in one feature, e.g. the first maximum,

\* By terms such as "sudden", "close together", "long time", we mean *so* sudden, *so* close, *so* long, etc., that the statements in which the terms are used are true. The fact involved in any such statement is that it can be made true by making the motion sudden *enough*, or by placing the terminals close *enough*, and so on. In this, of course, we are only following the practice of many other writers.



they agree in all; accordingly, each response can be completely characterized by a single parameter, say this first maximum. (b) The response is determined wholly by the terminal states between which the change occurs; it is unaffected by the intermediate states traversed in the passage from one terminal state to the other and by the period occupied by the traverse, so long as it is short enough. The system is therefore characterized by pairs of states for which an unambiguous definition of equality can be given, namely that one pair of states is equal to another pair when a change between one pair produces the same response as the change between the other. If we can associate a definition of addition with this definition of equality, we shall arrive at a magnitude, say  $A_{xy}$ , characteristic of the pair of states,  $(x, y)$ , and measurable independently of the measurement of any other magnitude, and which thus resembles direct current, direct voltage, resistance and capacitance, which are fundamental in the discussions of the previous Parts.

Let us adopt then, as the definition of addition,

$$A_{xz} = A_{xy} + A_{yz}, \quad \dots\dots(2.1)$$

or, in words, the value of  $A$  to be associated with a change of state from  $x$  to  $z$  is the sum of the values to be associated with the changes from  $x$  to  $y$  and from  $y$  to  $z$ , where  $y$  is any third state, not necessarily intermediate between  $x$  and  $z$ . (It is just worth noting that (2.1) is *not* a consequence of the law that  $A_{xz}$  is determined only by the terminal states; for a change from  $x$  to  $y$  that halts at  $z$  long enough to observe, the deflection is not "sudden".) We can now calibrate the scale of the galvanometer for  $A_{xy}$  by the standard procedure for independently measurable magnitudes. We choose arbitrarily some pair of states  $(a, b)$ , and assign to  $A_{ab}$  the value unity. We find by experiment other states  $c, d, e \dots$  such that, according to the definition of equality,

$$A_{ab} = A_{bc} = A_{cd} = A_{de} \dots\dots(2.2)$$

Then, according to the definition of addition, the numerals 2, 3, 4 . . . must be assigned to  $A_{ac}$ ,  $A_{ad}$ ,  $A_{ae}$  etc. Tests must now be applied to establish that the rules of arithmetic are obeyed consistently; thus we must enquire whether in fact  $A_{bd}$ ,  $A_{ce}$ , . . . are all 2 (i.e. that changes of state from  $b$  to  $d$ , from  $c$  to  $e$  . . . all give the value 2 on the calibrated scale), that  $A_{be}$  is 3, and so on. Since  $A_{xx} = 0$  (i.e. no change produces no deflection), we must have from (2.1)  $A_{yx} = -A_{xy}$ , and one of our tests must be to ascertain whether this is so. The necessity for this test is one reason why it was specified that the ballistic galvanometer should be direction-sensitive; of course it is not necessary that it should be such that the calibrated scale turns out to be symmetrical about the zero.  $A_{xy}$  in this general form, and without the limitations that will be imposed on it in the following sections, is not an important magnitude. It has no recognized name or symbol; no instrument is ever calibrated to read  $A_{xy}$  by this independent method, and no systematic tests are usually made to establish that (2.1) is actually true for fluxmeters calibrated in other ways. But it would be as wrong to dismiss as unimportant the fact that any satisfactory fluxmeter could be so calibrated as it would be to dismiss similarly the corresponding fact about D.C. ammeters, which also are never in practice calibrated by addition. The reasons are the same in both cases. The laws in virtue of which fluxmeters could be calibrated independently are often assumed to be true in using measurements made by fluxmeters calibrated in other ways; if a fluxmeter calibrated by some conventional method failed to

obey those laws, then that calibration would have to be judged wrong and "an explanation" would be sought in some defect of the method or the instrument; the independent method provides a criterion whereby all other methods can be judged.

### § 3. FLAT SEARCH COILS: $B_n$ AND $B$

We shall now proceed to derive from this magnitude  $A_{xy}$  characteristics of pairs of states of a system including a magnet and a fluxmeter, first a magnitude  $X_x$  characteristic of a single state of the system, magnet and search coil, and then a magnitude  $B$  dependent only on the state of the magnet and position relative to it.

Change of the ballistic galvanometer or of the leads (if they provide any appreciable part of the resistance of the fluxmeter circuit) will change the deflection associated with any given change of the state of the system; but if the same change of state is always taken as the unit, and the scale calibrated in terms of that unit, then the value to be associated with any given change of state is independent of both the ballistic galvanometer and the leads; that is an experimental fact. If it were similarly independent of the search coil,  $A_{xy}$  would depend only on the state of the magnet and of the positions of the search coil relative to it; but the mention of "position" shows at once that complete independence of the search coil is impossible. For the position of the search coil relative to the magnet, which enters into the definition of the unit of  $A_{xy}$ , has no meaning unless limits are placed on the form that the coil may take; apart from some geometrical convention, it would be meaningless to say that the position of a long helix relative to some system was the same as that of a flat coil.

Let us therefore place limits on the form of the search coil and adopt the convention that all are to be "flat" and rigid, though they may differ in area and in the number of turns, and are to have one "marked" face. Then the position of any search coil relative to any coordinate frame fixed in the magnet is perfectly determinate when the position of its centre and the direction of the normal to the marked face are given; and we can inquire whether, if some particular state of the magnet and positions of the search coil are always used to define the unit, the value of  $A_{xy}$  is independent of the search coil used in measuring it and characteristic of the states of the magnet and positions relative to it. We find that it is so characteristic so long as the area of each coil is small enough, and that the permissible upper limit depends upon the magnet (i.e. on the uniformity of its field, in ordinary terms); so we adopt the further convention that, in measurements on any particular magnet, the area of the search coil must not exceed this limit. We thus arrive at a magnitude (in spite of the added conventions, it will still be denoted by  $A_{xy}$ ), measurable independently of the measurement of any other magnitude, characteristic (for any given magnet) of pairs of positions around it, each position being defined by the situation of a point and the direction of a line drawn from that point.

The form of the law (2.1) on which the measurement of  $A_{xy}$  depends shows that, given any distribution of  $A_{xy}$ , it must be possible to find a set of magnitudes  $X_x, X_y$  each characteristic of a single position (not, like  $A_{xy}$ , of a pair of positions) such that

$$A_{xy} = k(X_x - X_y). \quad \dots\dots(3.1)$$

But, unless something is added, the  $X$ 's, unlike normal magnitudes, would involve an arbitrary additive constant, as well as the arbitrary scale factor  $k$ . This

difference would vanish if we could find facts or laws that distinguish one choice of the additive constant from all others, and thus make it no longer arbitrary, and especially if we could find a reason for attributing the value 0 to  $X_0$ , characteristic of some position or set of positions denoted by suffix 0.

Such a reason can be found. Suppose that the flat search coil is symmetrical about an axis lying in its own plane, so that on rotation through  $180^\circ$  about the axis the winding of the coil occupies the same space as before, but the normal to the unmarked face replaces that to the marked face; such a rotation will be called "reversal". Then experiment shows that, in general, reversal produces a response of the galvanometer, as does any other motion of the coil; but that for each point near the magnet there is a plane such that, if the marked normal originally lies in that plane, reversal produces no response; when this condition is fulfilled, the coil will be said to be in a "zero" position characterized by  $X_0$ . The plane and the zero position are, in general, different for different points, but if the coil is suddenly transferred from one zero position to another, no response occurs, and none occurs if it is suddenly transferred from one of these zero positions near the magnet to a point very distant from it, where any magnitude determined by the magnet would be expected to be zero.\* All these facts support the idea that the value 0 should be assigned to every  $X_0$ , so that  $X_x$  characteristic of any non-zero position  $x$  will be  $A_{x0}/k$ , where  $A_{x0}$  is the reading on the calibrated scale when the search coil is suddenly transferred from  $x$  to a zero position.

The reader will no doubt have realized already that  $X_x$ , apart from a scale factor, is the familiar quantity that might be written  $(B_n)_x$ , i.e. the component of the flux-density normal to the small flat search coil when its centre is located at the point and its marked normal is turned in the direction characteristic of the position denoted by  $x$ ; when  $B_n$  has been measured for all positions  $x$ , the fact that it is the normal component of a vector  $\mathbf{B}$  will appear from a study of the measurements, and the complete distribution of  $\mathbf{B}$  will be determined. Accordingly the final result of this discussion is to show that  $\mathbf{B}$ , the flux-density (or magnetic induction), can be measured by methods that do not involve any measurement of any other magnitude (and, in particular, of any other magnetic magnitude), methods that involve only laws of equality and of addition together with conventions (namely the limitation to small flat coils) that are based upon real and definite experiments.

#### § 4. FLUX-LINKAGE

The distribution of  $\mathbf{B}$  round magnets of various kinds can therefore be determined by direct measurement, and it can be established that  $\mathbf{B}$ , wherever it can be measured, is solenoidal, i.e. that the surface integral of its normal component over any closed surface is zero. It cannot be measured at all inside solid bodies, for small flat coils cannot be introduced into, or rotated within, solid bodies. It is tempting to assume that  $\mathbf{B}$  is solenoidal, even where it cannot be directly measured, and if that assumption is made,  $\mathbf{B}$  can be determined everywhere; for the distribution, within a closed surface, of a vector known to be everywhere solenoidal can be determined by calculation from values of the vector measured at appropriate points outside the surface. However, in Part II, § 16, we had an example of a vector that is solenoidal in some regions but not in others; the general assumption must therefore not be made without adequate reason. Good reason for making the assumption so far as non-magnetic bodies are concerned

\* The neglect of the earth's field here and elsewhere (e.g. § 6) is justifiable because the experiments described could really be conducted in a space where the earth's field is neutralized.

(bodies that are air-equivalent in the sense of Part I, § 15) is immediately found; for direct experiment shows that if we take any system in air, for which  $\mathbf{B}$  has been shown to be solenoidal, the mere insertion of non-magnetic bodies into any region of the system makes no difference to any response of the fluxmeter; in other words, bodies that are air-equivalent with respect to compass needles are also air-equivalent with respect to fluxmeters. Thus  $\mathbf{B}$  is established as solenoidal and measurable throughout any system which is composed of non-magnetic materials only. In systems which include magnetic material, it is measurable and solenoidal in the air spaces, but we have as yet no evidence concerning points inside magnetic solids.

The further consideration of this matter is facilitated by the removal of the limitation to small flat search coils that was imposed in order to establish  $\mathbf{B}$  as a measurable property. We therefore examine search coils of various shapes and sizes, and seek a law connecting the response of the fluxmeter with the magnitude  $\mathbf{B}$  and the shape and size of the search coil. Experiment shows that a simple law can be found provided we limit it to search coils that satisfy the following conditions: (a) the wire must be so thin and the terminals so close together that the geometrical properties of the coil are completely represented by a single closed curve; (b) the resistance of the whole fluxmeter circuit shall remain unaltered when any change of coil is made. It is scarcely necessary to add that the coil must be constructed entirely of non-magnetic material, for this condition has been assumed throughout, any magnetic material included in the system always being regarded as part of the magnet. (This condition is of course always satisfied in practice.) We have already seen that the responses of a fluxmeter which includes such a search coil serve to determine a magnitude  $X$  characteristic of the state  $x$  of the system under examination. We can now establish a relation between  $X$ , the field of  $\mathbf{B}$ , and the geometrical properties of the search coil. In practice, systems which are found to possess a uniform field of  $\mathbf{B}$  throughout some particular region are of outstanding importance. It is found that the value of  $X$  for a search coil that lies wholly within such a region is determined only by the magnitude of  $\mathbf{B}$  and the total projected area  $A$  of the search coil on a plane perpendicular to  $\mathbf{B}$  (i.e.,  $A$  is the area enclosed by the curve traced out on the specified plane by the projection of a point  $P$  on the coil as this point travels once completely round the winding from one terminal to the other). The law may be written

$$X = kBA, \quad \dots\dots(4.1)$$

where the proportionality factor  $k$  is independent of the size, shape and orientation of the coil and of the field of  $\mathbf{B}$  so long as the stipulated conditions are satisfied. This simple relation suggests the more general law, which is implied by calling  $\mathbf{B}$  the flux-density at a specified point and  $X$  the flux-linkage of the search coil for the particular state of the system, that  $X$  is proportional to the surface integral  $\Phi$  of the normal component of  $\mathbf{B}$  over any continuous surface bounded by the closed curve along which the winding of the search coil lies. It must be noted that this surface integral only has a unique value for the closed curve if the distribution of  $\mathbf{B}$  is solenoidal throughout the whole field. The application of the law to systems containing magnetic material therefore involves the assumption that  $\mathbf{B}$  is solenoidal within magnetic materials. Now  $X$  can certainly be measured for many systems that include magnetic material, and the values are always uniquely associated with particular distributions of such values of  $\mathbf{B}$  as can be measured, and they are, moreover, consistent in every way with a solenoidal distribution of

$\mathbf{B}$  throughout the system. The conception of  $\mathbf{B}$  as a magnitude that is solenoidal throughout all magnetic systems whatever their composition is, therefore, fully justified by experiment, and since values of  $\mathbf{B}$  inside a magnetic solid can, with this conception, be determined from measured values of  $X$ , we may legitimately regard  $\mathbf{B}$  as measurable everywhere. The general law may be written

$$X = \Phi = \int B_n dS, \quad \dots\dots(4.2)$$

the scale factor being omitted since the units of  $\mathbf{B}$  and  $X$  are always chosen so as to make it unity. We shall therefore henceforward regard  $X$  and  $\Phi$  as the same magnitude and use the same symbol  $\Phi$  for both.

We may note here that  $\Phi$  can be measured for search coils of any size and shape, but that for the measurement of  $\mathbf{B}$  the coil must be small enough to lie wholly within a region throughout which  $\mathbf{B}$  can be shown to be sensibly uniform; it must also possess a definite axis rigidly fixed with respect to the winding, and a determinate „effective area”  $A$ , which is its projected area on a plane perpendicular to this axis. Measurements of  $\mathbf{B}$  can then be made in accordance with the law

$$\Phi = B_n A, \quad \dots\dots(4.3)$$

where  $B_n$  denotes the component of  $\mathbf{B}$  in the direction of the axis of the search coil.

#### § 5. INDUCED E.M.F.: FARADAY'S LAW

At this stage it becomes practicable to establish Faraday's law of induction in the familiar form

$$e = k d\Phi/dt, \quad \dots\dots(5.1)$$

i.e. the instantaneous E.M.F. generated in any search coil by a change of state of the system is proportional to the rate of change of flux-linkage of the coil. Instantaneous E.M.F. is of course a generalization of the magnitude  $E$  established in Part I, consistent with the instantaneous voltage and current of Part II. Thus  $e$  is defined as instantaneous open-circuit voltage and (5.1) can be considered as an experimental law that can be established by means of experiments with, say, a cathode-ray oscillograph calibrated as a voltmeter.

It is natural at this point to see whether  $e$ , like  $E$ , satisfies Kirchhoff's second law, and therefore accounts for the transient currents indicated by the galvanometer of the fluxmeter. However, it is sufficient to note here that Kirchhoff's law can only be applied to circuits of varying current if terms involving self-inductance and capacitance are included in addition to the  $\Sigma IR$  of the D.C. circuit. The detailed consideration of these matters is more appropriate to the laws of alternating current circuits than to magnetism, and we shall therefore not pursue them here.

Sometimes (5.1) is quoted as a definition of  $\Phi$ , and not a true experimental law: we would therefore emphasize that we have some knowledge of  $\Phi$  independent of this relation. It must also be remembered that (5.1) is not a complete statement of the relation between  $e$  and  $\Phi$  for any circuit. If the circuit is not wholly filamentary, but passes through an extended conductor which is in motion, as in the Faraday wheel and Lorentz apparatus, an E.M.F. can be measured even when  $d\Phi/dt = 0$ . The complete law must be written

$$e = - \left\{ \frac{\partial \Phi}{\partial t} + \int_e (\mathbf{B} \times \mathbf{v}) dl \right\}, \quad \dots\dots(5.2)$$

where  $\partial\Phi/\partial t$  represents the rate of change in the absence of motion, and  $\mathbf{v}$  is the velocity of the element  $dl$  of the material in the circuit relative to the field  $\mathbf{B}$ : that is to say, the complete law must include *both* "change of linkage" and "flux-cutting". The Lorenz method for the absolute determination of the ohm constitutes an accurate verification of (5.2), which, therefore, we also regard as an established experimental law. In (5.2) the proportionality factor  $k$  of (5.1) has been made  $-1$ , which is of course the usual choice, and serves the very important practical purpose of defining the unit of  $E$  by reference to the units of  $\Phi$  and  $\mathbf{B}$ . It would be tedious to trace in detail the reason for the negative sign, but it may be worth noting that it is determined solely by conventions laid down in connection with other laws, e.g. that fixing the sense in which circulations are linked positively, and that prescribing that in any circuit an E.M.F. and the current it drives shall have the same sign.

The next problem is to decide by what the field of  $\mathbf{B}$  is determined. Here we meet the conception of "magnetic materials", and some difficulties rather different in kind from those we have discussed so far. These are dealt with in the following paper.

## The Experimental Basis of Electromagnetism— Part IV: Magnetic Materials

By L. HARTSHORN

National Physical Laboratory, Teddington

*MS. received 3rd March 1949*

**ABSTRACT.** This paper concludes the inquiry which was undertaken by N. R. Campbell and the author with the object of elucidating the connection between the concepts and principles of electromagnetism and the experimental operations actually performed in the laboratory that constitute their factual basis. In Part III the vector  $\mathbf{B}$  was established as measurable everywhere, even within solid bodies. The vector  $\mathbf{H}$  and the scalar  $\mu \equiv \mathbf{B}/\mathbf{H}$  are now shown to be measurable in special circumstances by means of the magnetometer and permeameter, but in general their values depend on a hypothesis, which is stated. The significant facts concerning the magnetic properties of real materials are briefly reviewed, and the two-fold aspect of the science is emphasized: the self-consistent mathematical theories based on postulates, on the one hand, and the complex of experimental laws on the other. It is important that the relation between the two shall be clearly established, and not merely assumed as self-evident.

### § 6. NON-MAGNETIC MEDIA\*

**I**N Part III of this inquiry we reached the stage at which  $\mathbf{B}$  was established as a vector magnitude measurable independently of any other magnitude and characteristic of the states of certain systems, which we called magnets, and of position in and around them. We now proceed to consider what determines the distribution of  $\mathbf{B}$ , and for simplicity we shall restrict ourselves in the first instance to systems in which all the materials are non-magnetic. Since  $\mathbf{B}$  is everywhere solenoidal, it can be determined experimentally at every point of the system. We can also readily show that  $\mathbf{B}_0$  at any point (we shall use the suffix 0

\* Section headings continue in sequence from Part III.

to indicate the limitation to non-magnetic media) is a linear function of the currents in the circuits of the system, and falls to zero when they all become zero. More generally, we observe that there is a very close connection between  $\mathbf{B}_0$  and the magnitude  $\mathbf{H}_0$ , which was defined in Part I by the equation

$$\mathbf{H}_0 = S \cdot I \cdot \oint \frac{d\mathbf{l} \times \mathbf{r}_1}{r^2} = S \cdot \mathbf{G} \cdot I, \quad \dots\dots (6.1)$$

and which therefore satisfies the equation

$$\oint \mathbf{H}_0 dl = 4\pi S n I. \quad \dots\dots (6.2)$$

Separate measurements of  $\mathbf{B}_0$  and  $\mathbf{H}_0$  enable us to establish with high accuracy the experimental law

$$\mathbf{B}_0 = \mu_0 \mathbf{H}_0. \quad \dots\dots (6.3)$$

In (6.3)  $\mu_0$  is a scale-factor without associated derived magnitude, since it has the same value for all non-magnetic materials. It plays the same part in (6.3) as does  $S$  in (6.1) and (6.2) and  $k$  in (5.1). By assigning convenient arbitrary values to each of these scale-factors, three units are defined in terms of other units. For example, in the M.K.S. system we assign to  $S$  the value  $1/4\pi$ , thereby defining the "ampere-turn per metre" as the unit of  $\mathbf{H}_0$ ; we then assign to  $\mu_0$  the value  $4\pi \times 10^{-7}$ , thus defining the unit of  $B$  by reference to the ampere-turn and metre, and then give  $k$  the value  $-1$ , thereby defining the volt by reference to the ampere-turn, metre, and second. The ohm is of course defined by reference to the volt and ampere by making the scale-factor in Ohm's law unity. A different choice of scale factors gives a different system of units, but all are on the same footing.

This use of the experimental law (6.3) to obtain a unit of  $\mathbf{B}$  is clearly of the greatest practical importance, for apart from some such law, the independent method of measuring  $\mathbf{B}$  would demand frequent reference to one or more fixed positions near some standard magnet in order to re-calibrate fluxmeters every time a change of search coil became necessary. In virtue of this law, every "air-cored" circuit that is accurately measurable in its linear dimensions and current becomes a standard magnet, i.e. a standard field of  $\mathbf{B}$ .

There is some evidence that a law of the form (6.3) remains true, but with some other constant replacing  $\mu_0$ , if the medium surrounding the coils and filling the whole space in which  $\mathbf{B}$  is distributed is uniform but not air-equivalent. Experiments of this kind are, however, only practicable in fluids at ordinary temperatures, and these are so similar magnetically to air that the differences in the measured quantities for different media are not usually much greater than the experimental error. The question of the existence of a derived magnitude characteristic of feebly magnetic materials is therefore best considered in relation to experiments of a different kind, which will be discussed later.

## § 7. MAGNETIC MATERIALS: PERMEABILITY

We pass now to a consideration of the systems for which (6.3) is not even approximately true, i.e. systems which include materials that are markedly not equivalent to air in their effect on fluxmeters and compass needles, the strongly magnetic solids. The evidence which showed  $\mathbf{H}_0$  as defined by (6.1) to be a significant property of non-magnetic systems now no longer applies, but it is

convenient to denote by  $H_I$  the value of  $S \cdot G \cdot I$  of (6.1) for such a system. Very simple experiments with a fluxmeter show that  $B$ , far from being completely determined by  $H_I$  in accordance with (6.3), is frequently large when  $H_I$  is zero. For a given system it is, however, associated with  $H_I$  in the sense that they invariably change together, though  $\Delta B / \Delta H_I$  is usually much greater than  $\mu_0$ , and not obviously characteristic of any part of the system. Useful results have however been obtained by adopting the hypothesis that the vector  $B$  is always associated with a vector  $H$ , which in the special case of a non-magnetic medium reduces to  $H_0$ , and which is such that the ratio  $B/H = \mu$  is a scalar magnitude characteristic of the material at the point to which  $B$  and  $H$  refer. The fact that values of  $\mu$  characteristic of various materials have been obtained provides some justification for the hypothesis. We must now examine the operation by which these values of  $\mu$  and  $H$  are obtained, for according to our principles it is to these experiments that we must look for the meaning of these quantities.

Examination of the methods actually used for measuring  $\mu$  shows that the one to which all others are referred consists in the use of the familiar uniformly wound long solenoid (or an equivalent toroid) and fluxmeter—the permeameter, for short. For simplicity we shall consider only the ideal form, a circuit in the form of an infinitely long solenoid, uniformly wound with  $N$  turns per unit length, and enclosing a search coil of effective area  $A_s$ , which forms part of a fluxmeter. The material to be measured takes the form of an infinitely long cylindrical core of cross-sectional area  $A_m$ ; it is placed in the solenoid so that it is embraced by the search coil and so that its axis is parallel to that of the solenoid. Measurements are made by changing the steady current through the solenoid from a value  $I$  to a value  $I + \Delta I$  and measuring the corresponding change of flux linkage of the search coil  $\Delta\phi$  by means of the fluxmeter. The ideal is of course never completely attained, but since permeameters are only recognized as satisfactory when the inevitable departure from the ideal is concealed by the experimental error, it is unnecessary to consider such departures here.

It follows from (6.1) that  $H_I$  is zero outside the solenoid for all values of  $I$ , and inside it is everywhere  $4\pi SNI$  and parallel to the axis; the solenoid is essentially a device for producing a uniform field of  $H_I$ . For simplicity we will adopt M.K.S. units so that this field is given by  $NI$ . Experiment shows that so long as the whole coil system is free from magnetic material, and the core is absent,

$$\Delta\phi = \mu_0 A_s N \Delta I. \quad \dots\dots (7.1)$$

Indeed, it was mainly on evidence of this kind that (6.3) was based. When the magnetic core is introduced and the measurement repeated,  $\Delta\phi$  is often greatly increased. Observations usually suggest a law of the form

$$\Delta\phi = \{\mu A_m + \mu_0(A_s - A_m)\} N \Delta I, \quad \dots\dots (7.2)$$

where  $\mu$  is much greater than  $\mu_0$ , and depends on the nature of the core. For a class of material which is severely limited, but which includes some of technical importance (“constant-permeability alloys”),  $\mu$  is found to be characteristic of the material and independent of  $A_m$ ,  $NI$  and  $\Delta I$  over a useful range of values. The law (7.2) shows that in a permeameter such materials have an effect which is exactly equivalent to an increase in  $B$ , throughout the space which they occupy, from the original value  $\mu_0 H_I$  to  $\mu H_I$ . This  $\mu$  is the magnitude which is called the permeability of the material, and by analogy  $\mu_0$  is often called the permeability



of free space. (It is convenient in practice to record the relative permeability  $\mu/\mu_0 = \mu_r$  since this ratio has the same value in all the ordinary systems of units.) We conclude that the general vector  $\mathbf{H}$ , whatever else it may be, is identical with  $H_I$  at all points in an ideal permeameter.

### § 8. THE MAGNETIC CIRCUIT

We must now consider how  $H$  is affected when there is a departure from the conditions of the permeameter, and for simplicity we shall, in the first instance, restrict ourselves to materials of constant  $\mu$ . Let the material take the form of a solid ring which completely fills both the uniform toroidal winding and search coil:  $\mu$  can be measured as  $B/H_I$ . Let now a narrow gap be cut in the material. Its effect is well known: the ratio  $\Delta\phi/\Delta H_I$  is greatly reduced, but so long as the length of the gap  $l_0$  is very small compared with the total length of the toroid  $l$  (both measured circumferentially) it remains independent of the position of the search coil, and we therefore conclude that  $\mathbf{B}$  has the same value in the gap where the permeability is  $\mu_0$  and in the material where it is  $\mu$ . If this value is  $B_2$ , then  $\mathbf{H}$  must have the value  $B_2/\mu$  in the material and  $B_2/\mu_0$  in the gap, and neither of these values is  $H_I$ . Thus  $\mathbf{H}$  no longer satisfies (6.1): it is natural to see if it still satisfies (6.2). For this simple system (6.2) becomes

$$\frac{B_2}{\mu}(l-l_0) + \frac{B_2}{\mu_0}l_0 = lNI. \quad \dots\dots(8.1)$$

This law for the toroid with a small gap has been established experimentally, but it must be admitted that the experimental error is usually rather large.

Slightly more general formulae of this kind find useful application in electrical practice, and may therefore be considered as experimentally established. They are, however, limited to systems that can be described as magnetic circuits, i.e. systems in which the field of  $B$  is confined to a closed path of measurable length and cross section, the flux-linkage being constant for all cross sections, but  $\mathbf{B}$  varying with change of cross section along the path. The circuit may be built up of various materials so that  $\mu$  may change discontinuously from point to point along it, but  $\mu$  must be uniform over any section that is everywhere perpendicular to  $\mathbf{B}$ . In the simplest case, the cross section of the circuit is everywhere small enough to justify the neglect of the variation of  $\mathbf{B}$  over it; then at any point where the cross-sectional area is  $A$ ,  $B$  is given by  $\phi/A$  and  $H$  by  $\phi/\mu A$ , and both are directed along the circuit. If the circuit can be divided into portions of length  $l_1, l_2, l_3 \dots l_p$ , each of uniform permeability throughout, the values being  $\mu_1, \mu_2 \dots \mu_p$ , and the cross sections of the several portions  $A_1, A_2 \dots A_p$ , then application of (6.2) yields the formula

$$\phi\{\sum_p l_p/(A_p \mu_p)\} = \sum_r n_r I_r, \quad \dots\dots(8.2)$$

where  $I_r$  denotes the current in the  $r$ th current circuit linked with the magnetic circuit and  $n_r$  is the "number of turns" in this linkage. By analogy with Kirchhoff's second law,  $\sum_r n_r I_r$  is called the magnetomotive force of the system, and the quantity in brackets the reluctance of the magnetic circuit, which is given as the sum of the reluctances of the several portions which are in series-connection in the circuit. Systems of large cross section can often be dealt with by applying (8.2) to elementary tubes of flux of small cross section into which the circuit can be divided. The details need not concern us;  $\mathbf{H}$  is seen as a useful conception in making calculations of this kind, and they are certainly

important in practice; but it will be noted that  $\mathbf{H}$  is only used as an auxiliary variable which does not appear in the result: we must therefore look further for evidence of its significance in terms of experimental operations.

### § 9. THE $B$ - $H$ HYPOTHESIS

The existence of two vectors  $\mathbf{B}$  and  $\mathbf{H}$ , each having a determinate value for points inside solid bodies, cannot be considered as completely established by experiment. Examination of the methods usually employed for determining  $\mathbf{B}$  and  $\mathbf{H}$  suggest that they depend on a hypothesis that we shall call the  $B$ - $H$  hypothesis, and shall state in a general form as follows:

Any point in a system of current circuits and material bodies is characterized by the following magnitudes:

- (a) The vector  $\mathbf{B}$  determined by measurements with a fluxmeter and the equation

$$\text{div } \mathbf{B} = 0. \quad \dots\dots(9.1)$$

- (b) A scalar  $\mu$  and a vector  $\mathbf{H}$  which are uniquely determined by the equations

$$\mathbf{B} = \mu \mathbf{H} \quad \dots\dots(9.2)$$

and

$$\oint \mathbf{H} d\mathbf{l} = \Sigma_r n_r I_r, \quad \dots\dots(9.3)$$

where  $I_r$  is the steady current circulating in the  $r$ th circuit, and  $n_r$  is the number of times which the path around which the integral is taken is linked in the positive sense with the  $r$ th circuit.

It is to be noted that the experimental laws that are well established, viz. those for non-magnetic media, for the permeameter and for the toroid with a narrow gap are merely the results obtained when this hypothesis is applied to specially simple cases. This hypothesis therefore constitutes the definition of the general vector  $\mathbf{H}$ .

The question what limitations are necessary and sufficient to ensure that the above three equations determine a unique distribution of the three magnitudes  $\mathbf{B}$ ,  $\mu$ ,  $\mathbf{H}$  is of purely mathematical interest and therefore outside the scope of this paper.

### § 10. THE MEASUREMENT OF $\mathbf{H}$

We have seen that  $\mathbf{B}$  is (in principle) measurable everywhere. Can the same be said of  $\mathbf{H}$ ? In the special cases of (a) the system that contains no magnetic material and (b) the permeameter,  $\mathbf{H}$  becomes equal to  $\mathbf{H}_l$  and is therefore measurable in terms of current. In the more general case  $\mathbf{H}$ , unlike  $\mathbf{H}_l$ , is not solenoidal and therefore cannot be obtained from the values of current. If the permeability is known  $\mathbf{H}$  can of course be calculated as  $\mathbf{B}/\mu$ , but unless this ratio has some other significance nothing is gained by giving it a special name: indeed,  $\mathbf{H}$  becomes no more than an auxiliary mathematical variable.

A possible method of measuring  $\mathbf{H}$  directly is suggested by the experiments which originally led to the definition of  $\mathbf{H}_0$  by (6.1), viz. experiments concerning the torque  $T$  on a small compass needle in air. Within the experimental error it is given by

$$T = SIG \times m = \mathbf{H}_0 \times m, \quad \dots\dots(10.1)$$

where  $m$  (the moment) is a derived magnitude characteristic of the needle. The suggestion is that we can measure  $\mathbf{H}$  at any point by observing the torque on a compass needle of known moment at that point, in virtue of a law

$$T = \mathbf{m} \times \mathbf{H}. \quad \dots\dots(10.2)$$

Measurements of this kind are certainly made in practice, but they are necessarily severely limited in scope, for compass needles cannot be inserted into solid bodies. In actual practice  $\mathbf{H}$  can only be measured by this method at points in air, and for most magnets the range of  $\mathbf{H}$  over which  $m$  in (10.2) proves to be a constant for the particular magnet is very small. Nevertheless the method can be used for the measurement of  $\mathbf{H}$  over a very wide range if  $m$  in (10.2) is treated, not as a constant, but as a function of  $\mathbf{H}$  characteristic of the particular magnet. Special magnets have been made for which this function is single-valued over a very great range of  $\mathbf{H}$ , so that the value of  $m$  in (10.2) corresponding to any observed value of  $T$  can be determined by an auxiliary measurement in a standard solenoid. In practice the instrument is calibrated in this way to indicate  $\mathbf{H}$  directly.

Thus  $\mathbf{H}$  can be determined by such operations at points in an air space, even one included in a system of strongly magnetic bodies, and provided the small suspended magnet is not allowed to approach too closely to the surface of a strongly magnetic body the values are always found to be equal to  $B/\mu_0$ , and to be consistent with the  $B$ - $H$  hypothesis.

It is interesting to note that these instruments for measuring  $\mathbf{H}$  are usually called fluxmeters, a term normally associated with  $\mathbf{B}$  rather than  $\mathbf{H}$ . This has arisen because they are always used in air-spaces where  $B = \mu_0 H$ , and are generally calibrated in the system of units for which  $\mu_0 = 1$ . The use of this system often leads to the notion that in any air-space  $B$  and  $H$  are identical. The facts are, that they are different in the sense that the operations by which they are measured are different, but they are "the same magnitude" in the sense in which this term was used in Part I.

The well-known methods of measuring  $\mathbf{H}$  at points near the surface of solid bodies by means of very narrow search coils closely fitting the surface, or by means of the magnetic potentiometer, are equivalent to measurements of  $\mathbf{B}$  at points in air near the surface by means of a fluxmeter, and therefore call for no special comment.

Our general conclusion is that  $\mathbf{H}$  is directly measurable in air-spaces, but since it is not in general solenoidal such measurements alone are not sufficient to determine values for points inside magnetic materials. Such values depend on the  $B$ - $H$  hypothesis.

#### § 11. MAGNETIZATION CURVES: HYSTERESIS

We have so far assumed that the materials under discussion all have a definite permeability  $\mu$ , which is independent of  $\mathbf{H}$  or  $\mathbf{B}$ . It is, however, well known that most strongly magnetic materials are so complicated in their behaviour that no single value of  $\mu$  will give any adequate account of it. The permeameter is still the most generally satisfactory instrument for dealing with such materials, the law (7.2) being applied in the form

$$\Delta\phi = A_m \Delta B + \mu_0 (A_s - A_m) \Delta H, \quad \dots\dots(11.1)$$

and values of  $\Delta B$  corresponding to the values  $\Delta H$  being deduced from the observations of  $A$ ,  $\phi$  and  $\Delta I$ . Summations of the values of these increments (i.e.  $\Sigma \Delta B$  and  $\Sigma \Delta H$ ) in a manner too familiar to be detailed here enable us to assign a value

of  $\mathbf{B}$  to each value of  $\mathbf{H}$ , provided one such pair of values is known. A conventional procedure is usually followed in deriving these values, e.g. there is a preliminary "demagnetizing" treatment which general experience suggests will justify the assumption  $\mathbf{B}=0$  when  $\mathbf{H}=0$ , and then the values of  $\mathbf{H}$  follow a regular sequence between certain limits. It is an experimental fact that when such a procedure is followed, the relation between  $B$  and  $H$  can often be represented by a definite "magnetization curve" or a "hysteresis loop" that is characteristic of the material in the permeameter, that is to say, independent of the size and shape of the sample within the limits imposed by the permeameter, and dependent only on the composition and physical condition of the material. Thus the properties of strongly magnetic materials are represented, not by a constant  $\mu$ , but by a characteristic function.

The details of the procedure need not concern us, but we must note that no law that purports to represent the magnetic behaviour of a material by a definite permeability  $\mu$  is generally applicable to real magnetic materials. Such simple laws are applicable only to the relatively few "constant-permeability" materials. Nevertheless engineers often find it convenient to apply the simple formulae to their materials when they are used within a narrow range of magnetic conditions, and in such cases they adopt the simple expedient of interpreting  $\mu$  as  $\Delta B/\Delta H$  for changes of  $B$  and  $H$  which have been found empirically to represent the working conditions. Thus we meet the terms incremental permeability, initial permeability, reversible permeability, differential permeability, representing  $\Delta B/\Delta H$  in accordance with various conventions. Such quantities cannot however be expected to have any wider significance.

It now becomes obvious that the determination of the distribution of  $\mathbf{B}$ ,  $\mathbf{H}$  and  $\mu$  by the application of the  $B$ - $H$  hypothesis to a real system including strongly magnetic materials, is necessarily a very complicated matter. Instead of the constant  $\mu$  first considered, we have now a function represented by a curve or a table of values, and not even a single-valued function of  $H$  in most cases. In such cases the application must be made by numerical computation, and  $\mu$  must be interpreted as the value of the permeability ( $=B/H$ ) given by the characteristic curve for the material occupying the point in question, for the particular value of  $\mathbf{B}$  which satisfies equations (9.1), (9.2), (9.3). When the characteristic curve includes an appreciable hysteresis loop it gives more than one value of  $\mu$  for each value of  $B$ , except at saturation, and computation is then only possible if the previous magnetic history of the system is known sufficiently well to indicate clearly which of the values is appropriate. A preliminary demagnetization (or magnetization to saturation) will often provide the necessary information, but the general problem is one of great complexity and a detailed solution for many actual systems is impracticable, although relaxation methods (Southwell 1946) would probably enable a wider range of conditions to be investigated than has so far been done. The direct evidence for the  $B$ - $H$  hypothesis is obviously meagre, being limited to the simple cases already mentioned. It does however provide satisfactory coordination for a great amount of experimental work, and this constitutes its chief justification.

## § 12. SATURATION: INTENSITY OF MAGNETIZATION

There remains however an important experimental law that gives  $\mathbf{H}$  a significance that is more than mathematical; it is the one suggested by the term saturation, mentioned in the last section. If in the permeameter the current

is steadily increased, then for the large class of strongly magnetic materials of § 11, provided the value of  $\mathbf{H}$  exceeds some particular value which is different for different materials and can only be found by experiment, the relation between  $\Delta B$  and  $\Delta H$  satisfies the law (7.1), which can be written  $\Delta B = \mu_0 \Delta H$ ; in other words, in this region the increments of  $\Delta B$  and  $\Delta H$  obey the same law as if the material were absent. Thus, beyond the particular value of  $\mathbf{H}$ , the value of  $B - \mu_0 H$  remains constant however much  $\mathbf{H}$  is increased, and within this range of values  $\mathbf{H}$  has the same significance within the magnetic material as it does within a non-magnetic material or air. Moreover, for many materials the stationary value of  $B - \mu_0 H$  is found to be more accurately characteristic of the material than  $\mu$ .

The most obvious interpretation of this law is that the material is an open structure of some kind in space, and that the total flux-density  $B$  when the material is present always includes a component  $\mu_0 H$ , which is the flux-density in that portion of space whether the material is present or not, so that  $\mathbf{B} - \mu_0 \mathbf{H} = \mathbf{J}$ , say, represents the contribution of the structure itself, and this contribution cannot exceed some limiting value  $J_s$ , which is characteristic of the structure. The whole idea necessarily implies that  $B$ ,  $H$ ,  $\mu$  and  $J$  only represent properties of the system on a scale that is macroscopic relative to the microscopic scale of the structure itself, but we have no reason for not accepting such a limitation to the significance of our measurements.  $J$  is of course the intensity of magnetization, and  $J_s$  the saturation magnetization. The general definition of  $J$  is the equation

$$\mathbf{B} - \mu_0 \mathbf{H} = S \mathbf{J}. \quad \dots\dots(12.1)$$

The scale factor,  $S_J$ , is frequently chosen to be  $4\pi$  instead of unity, but this is purely a matter of convention. The ratio  $J/\mu_0 H$  is defined as the susceptibility,  $\kappa$ , of the material, and we have therefore

$$\mu_r - 1 = S_J \kappa. \quad \dots\dots(12.2)$$

The susceptibility  $\kappa$  is therefore characteristic of the material to the same extent as  $\mu_r$ , but  $J_s$  is often more accurately representative of the material than either. The fact that  $J$  has this significance in terms of experiment implies that the conception of  $\mathbf{H}$  within a magnetic solid, on which it partly depends, is also not without physical significance.

### § 13. THE MEASUREMENT OF SMALL SUSCEPTIBILITY

The susceptibility of a non-magnetic material is zero by definition. It is well known that there is a very large class of materials that are nearly but not quite non-magnetic, and susceptibility provides a very convenient measure of the magnetic behaviour of these materials. In accordance with our principles we must examine the methods by which  $\kappa$  is determined for such materials in actual practice. The Gouy apparatus may be taken as typical. The material to be measured takes the form of a long straight rod of cross section  $A$ , permeability  $\mu$ , and susceptibility  $\kappa$ , suspended vertically from the beam of a balance in a medium of permeability  $\mu_0$ . Its lower end lies in a strong uniform magnetic field  $H_l$  (generally, but not necessarily horizontal); its upper end in a much weaker field  $H_u$ , which, if appreciable, must also be uniform. The field  $H_l$  can be removed and established at will, and the force  $F$  on the specimen associated with the field  $H_l$  is determined by observation of the increase of weight indicated by the balance

when the field is established. The law established for the method may be written,

$$F = A(\mu - \mu_0)(H_1^2 - H_0^2) \quad \dots\dots(13.1)$$

or

$$F = S_J \kappa \mu_0 A(H_1^2 - H_0^2). \quad \dots\dots(13.2)$$

Thus the measured force is proportional to  $\kappa$ , other things being equal, which is no doubt why the method is usually regarded as one for determining susceptibility rather than permeability. The materials for which the law has been accurately established fall into two classes: the paramagnetic materials for which  $\kappa$  is positive and the diamagnetic materials for which it is negative. For both classes it is usually much smaller than unity, and it is for this reason that  $\mu_r (= 1 + 4\pi\kappa)$  is an inconvenient magnitude for discriminating between materials in these classes.

In writing (13.1) and (13.2) we have tacitly assumed that  $\mu$  and  $H$  are the magnitudes that we have already defined in terms of the permeameter and the  $B$ - $H$  hypothesis and that the scale factor in (13.1) is unity for the units already chosen. All the available evidence is consistent with this law, and it is fairly convincing, because a slight modification of the permeameter technique, described previously, enables us to measure  $(\mu - \mu_0)$  with accuracy for specimens of the same form as are required for the Gouy method. A long solenoid and a search coil of many turns are employed; a large current giving an intense field in the solenoid is established; the fluxmeter circuit, previously open, is then closed, and the specimen suddenly withdrawn from the search coil. In these circumstances the change of flux-linkage  $\phi$  measured is given by

$$\Delta\phi = A_s(\mu - \mu_0)H_I, \quad \dots\dots(13.3)$$

and since both  $A_s$  and  $H_I$  are very large  $(\mu - \mu_0)$  can be accurately determined although it is very small. This is indeed another standard method for the measurement of  $\kappa$ , and one that is of great importance in enabling us to establish that  $\kappa$ , as measured by the Gouy and Faraday methods and their variants, is "the same magnitude", in the sense in which we employ that term, as  $\mu_r - 1$  measured by the permeameter or determined by the  $B$ - $H$  hypothesis.

#### § 14. ENERGY OF THE MAGNETIC FIELD

The law of the Gouy method calls for some consideration of the conception of the energy associated with the magnetic field. When the field is wholly due to currents in a non-magnetic medium, it follows from (4.1), (6.1) and (6.3) that the magnetic flux through the  $r$ th circuit due to the currents in the others is given by

$$\phi_r = \sum_s M_{rs} I_s, \quad \dots\dots(14.1)$$

where

$$M_{rs} = (\mu_0/4\pi)N \quad \dots\dots(14.2)$$

and  $N$  is Neumann's integral for the  $r$ th and  $s$ th circuits. Here and in what follows we insert the scale factor appropriate to M.K.S. units unless the contrary is stated.

It now follows from (5.1) that if  $e_r$  is the instantaneous E.M.F. induced in the  $r$ th circuit

$$e_r = \sum_s M_{rs} dI_s/dt \quad \dots\dots(14.3)$$

and

$$\int -(\sum_r e_r I_r) dt = \frac{1}{2} \sum_r \sum_s M_{rs} I_r I_s = W, \quad \dots\dots(14.4)$$

and if this E.M.F. has all the properties of direct E.M.F. the quantity  $W$  will be the energy that must be expended in order to start the currents, apart from that required to maintain them, and also the energy that will appear as heat or in some other form when the currents are stopped. There is strong experimental evidence for these laws taken together;  $M_{rs}$  proves to be accurately measurable in virtue of (14.3) and the values are consistent with (14.2) to a very high order of accuracy; also Ampère's law is obtained by taking the appropriate derivative of  $W$ , which may therefore be accepted as a "force function" for such systems.

If now the system includes magnetic material of constant permeability, and if  $M_{rs}$  now means the quantity defined by (14.3)—the mutual inductance, which is accurately measurable by, say, A.C. technique—then we find that (14.2) is no longer true. The experimental evidence suggests that for uniform media of constant permeability  $\mu$  the law becomes

$$M_{rs} = (\mu/4\pi)N. \quad \dots\dots(14.5)$$

It follows from the  $B$ - $H$  hypothesis that for systems which include such materials we have

$$W = \frac{1}{2} \sum_r \sum_s M_{rs} I_r I_s = \frac{1}{2} \int \mu H^2 d\tau, \quad \dots\dots(14.6)$$

where  $d\tau$  is an element of volume and the integration is taken throughout the whole region where the integrand is non-zero. All the experimental evidence supports the conclusion that  $W$  is a force function and that  $F_q = \partial W_F / \partial q$  gives not only the forces tending to move and distort circuits, but also those tending to move magnetic material in their field. The Gouy method is one example. When we turn to the more complicated magnetic materials, we find hysteresis effects; the systems can no longer be considered as conservative and no force function can be regarded as established. A familiar argument shows that the energy that must be expended in order to change the magnetic induction from  $B_0$  to  $B$  is given by

$$W = \int d\tau \int_{B_0}^B H dB, \quad \dots\dots(14.7)$$

and this leads to the conclusion that during cyclic magnetization the energy lost per cycle per unit volume of material is determined by the area of the hysteresis loop. This conclusion is supported by the experimental evidence obtained by measuring the power loss by calorimeter and other methods, but the accuracy is not very high since power arising from other causes is nearly always a disturbing factor. The position is that the concept of a distribution of energy throughout materials finds little application in experiments on real magnetic material magnetic apart from those that have a constant permeability.

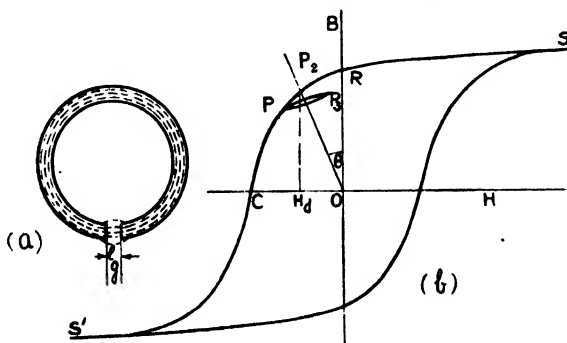
In order to complete our survey of the methods in general use for the measurement of magnetic properties, it will be necessary to consider the use of the magnetometer for this purpose. The term magnetometer is commonly applied to any instrument the use of which involves a measurement of the torque  $T$  exerted on a suitably suspended permanent magnet. We have already considered the use of such instruments for the measurement of  $H$  in air: the Schuster magnetometer was mentioned as an important instrument of high precision in Part I, and the "fluxmeters" mentioned in § 10 above can also be regarded as magnetometers. The historic Kew magnetometer and the magnetometers employed for measurements of  $\mu$  or  $\kappa$  involve an additional law, that concerning the torque exerted

by one magnet on another, and it is this law that we must consider. But before doing so it will be well to consider the properties of “permanent magnets”, using this term in the sense in which it is used in magnetometry.

### § 15. PERMANENT MAGNETS

The historical development of magnetism was based on the conception of the permanent magnet characterized by a definite axis and constant moment. We have employed the conception so far as to refer to compass needles, for which a derived vector magnitude  $\mathbf{m}$  can be established in restricted conditions; indeed, “magnetometer needles” having this property are familiar enough to all physicists, but as we have already mentioned, the experimental evidence contradicts any idea that  $\mathbf{m}$  can be regarded as constant for any given magnet; in particular, it must be expected to vary with  $\mathbf{H}$  and  $\mu$  in its immediate vicinity. It was no doubt for this reason that the magnetometer gave place to the fluxmeter as the standard instrument in this field of work. (It is interesting to note that even as late as 1902 the fluxmeter, although its principle had long been known, was treated in the *Handbuch der Physik* as entirely subsidiary to the magnetometer.) Instruments of the “moving magnet” type are however still of practical, as well as historical, importance, and the properties of the magnets actually employed must therefore be considered.

The most detailed information is that provided by the technicians who design and make such magnets, and we find that the results of their work, which naturally proceeds on empirical lines, can be summarized as follows. Permanent magnets of all forms, including the needle, are most conveniently regarded as magnetic circuits composed of two elements in series, one of a material specially chosen because its characteristic hysteresis loop is of large area and suitable shape, and the other an air path which may be of any form, from a narrow gap in a circular magnet to the air return path from one end of a needle to the other. The term magnet is commonly applied to the circuit-element of strongly marked hysteresis, but the air path is an essential feature. The properties of the magnet can best be understood by considering the procedure followed in making it, and for simplicity we will consider the case of a circular magnet of small and uniform cross section, with a narrow air-gap (see Figure). The gap is first completely filled



with material of very high permeability (soft iron), and the ring, having been provided with a suitable winding, is magnetized to saturation by passing a heavy current through the winding. If now the current is varied cyclically between this saturation value and an equal but oppositely directed one, the behaviour of the material can be represented by the hysteresis loop shown in the Figure.  $B$  and



$H$  will not be quite uniform over any cross section of the magnet, but we may suppose them to be the values for the material within a central tube of flux of small cross section. The curve can be determined by the methods previously discussed, and we find that by first switching on the current corresponding to  $S$  and then reducing it to zero (switching off) we bring the material into the condition represented by  $R$ . If now we remove the soft iron from the gap we find that there is a reduction of flux corresponding to the attainment of a condition represented by  $P$ . The magnet is now complete: the winding can be removed, and experiment shows that the flux  $\phi = BA$  of the magnet remains constant so long as the magnet is not disturbed. The value is, however, liable to change with change of temperature, mechanical shock, and especially with the application of any field of  $H$  or any change in the reluctance of the air gap of the magnet, e.g. the introduction of any material not air-equivalent. An applied negative  $H$  brings the material down the loop to  $P_2$ ; a positive  $H$  takes it along a branch curve to  $P_3$ , while cyclic variations of  $H$  take it round a succession of subsidiary loops, each successive member being slightly lower than its predecessor, until a stable condition is reached. The final state is always represented by some point on or within such a subsidiary loop, and this state may be regarded as the working condition of a magnet in practice. For a good magnet the subsidiary loop is thin and only slightly tilted with respect to the  $H$ -axis, so that  $\phi$ , although not strictly constant, is, to the accuracy that is possible in much experimental work, a single-valued function of  $H$ .

The hysteresis loop is characteristic of the material from which the magnet is made, and is the same for magnets of all sizes and shapes, although in using it one must allow for any variation of  $B$  from point to point in magnets, which, unlike the simple example quoted, do not possess an approximately uniform distribution of  $B$ .

The position of the point  $P$  may be calculated as follows. Let  $l$  denote the length of the magnet along the central tube of flux and  $l_g$  that of the gap. When the magnetizing current is reduced to zero we have by the  $B$ - $H$  hypothesis

$$Hl + Bl_g/\mu_g = 0; \quad \dots\dots (15.1)$$

thus

$$H = -(l_g/l\mu_g)B. \quad \dots\dots (15.2)$$

When the gap is filled with soft iron  $\mu_g$  is very large and, therefore,  $H = 0$ , corresponding to the point  $R$ . When the iron is removed,  $\mu_g$  becomes  $\mu_0$ , and equation (15.2) can be represented by the line  $OP$  in the Figure, where  $\tan \theta = l_g/l\mu_0$ . Thus the wider the gap, the lower down the curve is  $P$ . As the gap widens the flux  $\phi$  spreads over a larger area, i.e. the sectional area of the magnetic circuit increases as we enter the gap. The effect may be represented by dividing  $B$  in (15.2) by a leakage factor  $\alpha$  which is greater than unity and can be determined from fluxmeter measurements. The important point is that the properties of actual magnets can be predicted by such considerations from the characteristic curves of the material and the dimensions of the magnet and its air path. The principles are therefore established as affording a description of the properties of real magnets that is consistent with all the known facts. High accuracy is impossible except in very limited conditions.

#### § 16. THE MAGNETOMETER: MAGNETIC DIPOLES

A magnetometer is essentially a permanent magnet supported so as to be capable of rotation about an axis of symmetry that is perpendicular to the axis of its air path. Such magnets have already been taken for granted as familiar

objects adequately described by the term “compass needle”, and we have shown that they can be used to measure  $H$  in air spaces in virtue of an experimental law,

$$T = \mathbf{m} \times \mathbf{H}, \quad \dots\dots(16.1)$$

valid over a range of  $\mathbf{H}$  that must be found by experiment for the particular magnet used. It can now be added that the deviations from the law that are observed in conditions that are beyond the range established for the instrument are consistent with the laws of permanent magnets described in the previous section.

The magnetometer “needle” may take the form of the ring with a narrow air gap there discussed: it is only necessary that the axis of suspension shall pass symmetrically between the walls of the gap. It is then found that the moment of the magnet  $\mathbf{m}$  is given by

$$\mathbf{m} = BAl_0, \quad \dots\dots(16.2)$$

and that the conditions under which  $\mathbf{m}$  can be treated as constant can therefore be obtained from the  $B$ - $H$  curve for the magnet.

Alternatively, the magnet may be literally of needle form, or rather a straight bar of uniform cross section  $A$  and of length  $l$ , which is large compared with the dimensions of the cross section. Such magnets are prepared by a process analogous to that described for the circular magnet; the magnetizing winding takes the form of a long solenoid instead of a toroid and the closed magnetic circuit may consist of two such bars, each with its own solenoid, and with their ends linked by pieces of soft iron. Again we magnetize the circuit to saturation, switch off the current, and remove the soft iron links; the changes in the value of  $B$  are exactly similar to those for the ring, and can be represented in the same way by the portion RPC of the hysteresis loop, though in this case the calculation of the point P, which represents the working condition of the magnet, is not so simple. It is found, however, that magnets made from a given material can be usefully represented by a single curve RPC, and values of  $\tan \theta$  characteristic of the shape of the magnet, increasing, for example, consistently as the magnet becomes shorter, other factors remaining constant. Similarly magnets of a given shape but different materials have properties which are consistent with a constant value of  $\tan \theta$  applied to the “demagnetization curves” characteristic of the several materials. A magnet in its working condition is therefore regarded as characterized by the demagnetization curve for the material; and a demagnetizing factor  $D = \tan \theta$ , dependent on the shape of the magnet, and determining a demagnetizing field  $H_d = -DB$ , which is identified with  $H$  defined by the  $B$ - $H$  hypothesis. The long thin needle and the ring with the narrow gap are the two forms for which  $D$  is small and  $B$  nearly uniform throughout the material.  $D$  increases as the needle becomes shorter and as the gap in the ring becomes wider; and in both cases the distribution of  $B$  at the same time departs from uniformity, the lines of flux opening out, with a consequent diminution of  $B$ , as they pass from the material into the air path. Thus in any permanent magnet made according to the standard procedure  $B$  increases as we pass along the magnet from the air path and reaches a maximum value in a central region, which is larger the longer the magnet or the narrower the air gap. The values of  $B$  and of  $\phi = BA$  for this central region can be measured accurately by slipping the search coil of a fluxmeter off the magnet, and it can be shown by experiment that long needle magnets conform to the law

$$\mathbf{m} = BAl. \quad \dots\dots(16.3)$$

For these magnets,  $D=0$  and  $H_d=0$ , so that in the working condition  $B=J$ , and we may also write  $\mathbf{m}=J\mathbf{A}l$ . The same argument applied to the ring magnet with a narrow gap leads to  $\mathbf{m}=J\mathbf{A}l_0$ . These two equations show clearly that we must not define  $J$  as "magnetic moment per unit volume" if we are thinking of quantities that are actually measurable, for the relevant volume in the latter case is that of the air gap and in the former that of the magnet.

Another law established by means of the magnetometer is that concerning the torque exerted by one magnet on another. It is most conveniently expressed by the following experimental law for magnets of needle form: A permanent magnet of moment  $\mathbf{m}$  is associated with a field of  $\mathbf{H}$  in the space surrounding it, the value at any point  $P$  being given by

$$\mathbf{H}=S \operatorname{grad} \{(\mathbf{m} \cdot \mathbf{r}/r^3)f(l, r)\}, \quad \dots\dots(16.4)$$

where  $\mathbf{r}$  is the radius vector  $OP$ ,  $O$  being the centre of the axis  $\mathbf{l}$  of the magnet, and  $f$  a function that is known, but need not be considered beyond saying that it tends to 1 as  $l/r \rightarrow 0$ . This field is superposed on any field that may exist at  $P$  in the absence of the magnet. (It would be well to note at this point that  $\mathbf{H}$  in (16.1) is the value at the point in question in the absence of the magnet.)

It is scarcely necessary to trace in detail the experiments required to justify this law. Every physicist will recognize that the standard procedure associated with the Kew magnetometer will provide much of the evidence required. The well-known use of the magnetometer method for determining magnetization curves and hysteresis loops is also to the point. We must note that the law holds good for long solenoids, either with or without cores of magnetic material, as well as for permanent magnets, if we apply (16.3) to such solenoids. Results obtained in this way are consistent with those obtained with the permeameter, and this agreement also provides some support for the conception of magnetic moment as an important quantity. The theoretical conception of the magnetic dipole is derived directly from this conception and (16.4) in the limiting case when  $f(l, r)=1$ . The dipole is indeed defined as an entity of very small dimensions which obeys the equation

$$\mathbf{H}=S \operatorname{grad} \{(\mathbf{m} \cdot \mathbf{r}/r^3)\}, \quad \dots\dots(16.5)$$

where  $\mathbf{m}$  is constant. This is exactly the same equation as was obtained for a current  $I$  circulating in a small circuit of area  $A$  surrounding the point  $O$  in a vacuous medium if  $\mathbf{m}=IA$ , and has the direction of the normal to the surface  $A$  (Part I, § 15). It follows that the magnetic dipole can be conceived as either a minute current whirl or a minute permanent magnet in a vacuous medium. In either case we must assume that the dipole differs from the corresponding real object not only in the smallness of its dimensions, but also in freedom from resistance in the case of the current whirl, and freedom from all changes of moment in the other case. The magnetic field of a real circuit can be shown to be the same as that of a surface distribution of such dipoles, which is the "magnetic shell" of the old treatises. It is scarcely necessary to point out that the shell has by definition properties entirely different from those of real permanent magnets.

It is well known that the law of the torque between dipoles is mathematically equivalent to a law for point poles of the same form as those for point masses and point electric charges, and this has led to the development of mathematical theories in which the point pole with this law of force is the basic postulate. Such theories are quite divorced from the experimental basis of the subject as

we understand it, but the law is so frequently quoted as the fundamental experimental law of magnetism that it is impossible to ignore it completely. The most curious thing about the law is that even today, after generations of experiment, there is no general agreement about its exact form. There are two schools of thought: one stating the law in the form

$$F = Sq_1q_2/d^2, \quad \dots\dots(16.6)$$

where  $S$  is a mere scale-factor or universal constant, the same for all materials, and the other in the form

$$F = Sq_1q_2/\mu d^2, \quad \dots\dots(16.7)$$

where  $\mu$ , the permeability, varies from one medium to another. Self-consistent theories can be built up from either law by making the assumptions necessary to secure some sort of correspondence with the known experimental facts. One law requires the recognition of "induced charges" in the medium, also subject to the law, while the other does not. Livens (1947) has recently discussed the matter in detail and has decided in favour of (16.6) on the grounds of the simplicity, scope, and generality of the resulting theory, which is essentially the original theory of Poisson, Kelvin and Maxwell. It is no part of our purpose to question his decision; we would only point out that the other law has been so widely quoted as fundamental in recent years that one can only make sense of the situation by recognizing that these are not experimental laws at all.

#### § 17. CONCLUSION

We have now completed our survey of the operations which are most widely employed in experimental investigations of magnetism, and which therefore give the basic concepts of the science their meaning. The further development of the subject depends largely on mathematical theory, the form of which is dictated by mathematical operations rather than experimental operations. The theory takes the form of a self-consistent body of mathematical doctrine which, proceeding from certain postulates, is found to contain relations of the same form as the experimental laws. The theory is therefore accepted as a working mathematical model of the world of the experimenter, certain of the mathematical concepts being identified with the corresponding physical concepts. It is not to be expected that the basic postulates of the theory will correspond with the experimenter's basic concepts, and we have shown that they do not; the magnetic dipole or the point pole which forms the starting point of many theories is remote from the experimental basis of the subject and, provided the fact is recognized, there can be no objection to the procedure. We should, however, not confuse the laws of force between poles or dipoles with experimental laws; neither should we assume that because certain parts of the theoretical model correspond with the real thing that all its parts necessarily have their counterparts in the real world. It is from this point of view that our work should be considered. We believe that the actual correspondence between the experimental laws and the theoretical concepts requires a much closer scrutiny than is usually given to it. The self-consistency of a theory, although of great importance, affords no evidence whatever of its relevance to experiment; that evidence must be sought independently by actual examination of experiments. Self-consistency of the theories has always been examined with great care: consistency among the experimental concepts and the actual correspondence between those of theory and experiment

are too frequently taken for granted. It is sometimes said that these things are known by "physical intuition", a quality that can be cultivated by practice but not described. To us it seems to be only a cloak for a certain mistiness of thought which is out of place in physics, and which it is our chief aim to dispel.

#### REFERENCES

- CAMPBELL, N. R., and HARTSHORN, L., 1946, *Proc. Phys. Soc.*, **58**, 634 ; 1948, *Ibid.*, **60**, 27.  
 LIVENS, G. H., 1947, *Phil. Mag.*, Ser. 7, **38**, 453.  
 SOUTHWELL, R. V., 1946, *Relaxation Methods in Theoretical Physics* (Oxford : University Press), Sec. 85.

#### DISCUSSION

Dr. N. R. CAMPBELL. The fundamental difference between Dr. Hartshorn and myself which has prevented my sharing with him the authorship of his last paper (IV), as I have that of our earlier papers I, II, III, concerns the significance of his "general vector"  $\mathbf{H}$  ; we are perfectly agreed concerning  $\mathbf{B}$  and  $\mathbf{H}_I$ .

1. I do not think it desirable to denote by  $\mathbf{H}$  the vector, measured by the torque on a compass needle, that is the subject of IV, § 10. When it is measured in an air space it is the same "magnitude" as  $\mathbf{B}$  in the sense of I, § 10, this being the only sense in which that term seems to me useful. Theorists have discussed\* elaborately what the vector would be if it could be measured in a space filled with appreciably magnetic matter, and have usually concluded that it would differ from  $\mathbf{B}$  by a factor involving  $\mu$  for that matter ; it has been suggested that its relation to  $\mathbf{B}$  would differ according as the field was due to currents or to permanent magnets. None of these speculations have any experimental support ; it seems to me foolish to introduce a special symbol in order to express them. I should therefore denote the magnitudes of IV, § 10 (in suitable units), by  $\mathbf{B}$  and call it flux density.

2. If this were done,  $\mathbf{H}$  would always mean the auxiliary variable characteristic of the  $B$ - $H$  hypothesis, which I should prefer to state thus :—It is possible to calculate the distribution of  $\mathbf{B}$  about any collection of current circuits and magnetic bodies by assuming (a) that  $\mathbf{B}$  is everywhere solenoidal, (b) that it is associated at each point with a vector  $\mathbf{H}$ , of which it is true (c) that

$$\oint \mathbf{H} d\mathbf{l} = \sum n_r I_r$$

and (d) that it is related to  $\mathbf{B}$  at each point in the same way as  $\mathbf{H}_I$  is related to  $\mathbf{B}$  in a permeameter whose core consists of the material occupying that point.

3. The appearance of  $\mathbf{H}$  in a proposition would then be an indication that the  $B$ - $H$  hypothesis was involved in it. This would justify some unexpected appearances. Thus in IV, § 13, the field is usually measured by a fluxmeter (in the sense of III, § 2) ; it might seem therefore that  $\mathbf{B}$  would be more appropriate than  $\mathbf{H}$  in IV, (13.1). But the flux density is measured in the absence of the magnetic material. Now it is a consequence of the  $B$ - $H$  hypothesis, not often stated explicitly, that, if a *small* quantity of magnetic material is introduced into an air-space in which  $\mathbf{B}$  has been measured, then, though the introduction will in general change both  $\mathbf{B}$  and  $\mathbf{H}$  everywhere, in the neighbourhood of the material introduced, the change of  $\mathbf{H}$  will be much less than the change of  $\mathbf{B}$ . Accordingly, by expressing IV, (13.1) in terms of  $\mathbf{H}$ , not  $\mathbf{B}$ , we make sure that the unknown error, due to making no allowance for the effect of the material on the field, is as small as possible.

4. Research during the last generation, by revealing the existence of "domains", has shown that no piece of ferromagnetic material as large as a permeameter core can be homogeneous ; it cannot be truly characterized by a single parameter or function ; the  $B$ - $H$  hypothesis cannot really be true of it. Since  $\mathbf{H}$  derives its significance from the  $B$ - $H$  hypothesis, it cannot really be applicable to bulk material.

5. The best that can be said of the hypothesis and the magnitude dependent on it is that they are valid over the whole of some practically important range of experiment, so long as no methods of measurement are used more precise than those normally employed in such

\* See e.g., H. Chipart, *C.R. Acad. Sci. Paris*, 1921, **172**, 589-591, 750-753; L. R. Wilberforce, *Proc. Phys. Soc.*, 1933, **44**, 82-86; L. Page, *Phys. Rev.*, 1933, **45**, 112-115.

These authors, though all professing to expound the same classical theory, differ notably in their conclusions.

experiment. But I submit that even this is not true. The  $B$ - $H$  hypothesis is of no practical use unless some subsidiary simplifying hypothesis is made about the  $B$ - $H$  relation. Thus the conception of a magnetic circuit, having reluctance and containing M.M.F., is valueless unless it is assumed that  $B/H$  is constant; that can almost always be shown to be false by the very experiments used to determine the constant value or by some slightly modified variant. Again, the assumption of constant  $\mu$ , involved in attributing a definite inductance to a coil with a dust-core, is almost always accompanied by the contradictory assumption that the core material has "hysteresis loss". Again, in Evershed's theory of permanent magnets (which theorists conspire to neglect, although it is much more important practically than propositions to which they devote reams of paper, and at least equally nearly true), the  $B$ - $H$  relation is identified with the demagnetizing branch of the hysteresis curve; this, of course, is true only for very small changes.

6. I admire the gallantry and ingenuity of Dr. Hartshorn's attempt to base the significance of  $\mathbf{H}$  on constant-permeability alloys and the extension of the hysteresis curve beyond saturation. But he will hardly convince anyone who remembers that the facts on which his defence rests were unknown until his  $\mathbf{H}$ , and the "classical theory" on which it rests, had been established for at least two generations, and even now are not usually recorded in textbooks. The real position, I suggest, is that the theory has been taken seriously only because it was propounded before any of the important facts about ferromagnetism were known, and because, by the time that those facts were discovered, Maxwell's reputation was so firmly based on other work that anything he said had become (and has remained for most physicists) outside the range of dispassionate examination.

7. The analogy between magnetic materials and dielectrics, which was undoubtedly one of the foundation stones of the classical theory, is invalid in respect of the matters considered here. The concept of permittivity has survived the discovery that all dielectrics are imperfect, because their imperfection can be represented by the substitution of a complex for a real permittivity; there is no analogous way of representing the fact that  $B/H_I$  is not single-valued.

8. If, as I maintain, the sole use of  $\mathbf{H}$  is to make statements about magnetic materials that are either definitely false or unsupported by any evidence, it is particularly out of place in a theory that explains away magnetic materials as the electron theory explains away dielectrics. The essence of the modern theory of magnetic materials is that certain atoms are dipoles of zero dimensions, having magnetic moments independent of the field in which they find themselves; their behaviour is governed by equations of the form of IV, (15.1), (15.4)—the latter expressed in quantum-theory terms—by which it is possible, in the Kew magnetometer, to measure both of the vectors  $\mathbf{m}$ ,  $\mathbf{H}$  without measuring any other magnetic magnitude.  $\mathbf{H}$  so measured turns out to be the same magnitude as  $\mathbf{B}$ ; for in the presence of magnetic materials the equations cease to be true and  $\mathbf{H}$  to be measurable by this method. Since the theory which explains magnetic materials cannot suppose that there is magnetic material in the field of the dipoles representing magnetic material, the vector  $\mathbf{H}$  concerned in it cannot fail to be the same as  $\mathbf{B}$ ; nowadays it is sheer perversity, based on the accidents of history, to represent it otherwise.

I do not say that all propositions about theoretical dipoles to be found in current literature remain true if  $\mathbf{B}$  is substituted for the usual  $\mathbf{H}$ . But if they do not, then there must be some error or ambiguity that requires the attention of experts.

Dr. L. HARTSHORN (in reply). In view of the lamentable death of Dr. Campbell before these notes have appeared in print I think it more appropriate to outline the circumstances in which they were written than to attempt to reply in detail. The two papers III and IV were originally drafted by me as a single paper based on earlier drafts prepared by Dr. Campbell and extensive discussions with him. My expectation was that the whole would be published as a joint paper after Dr. Campbell had made whatever amendments he found necessary. This was his own idea also at first, but after a careful study of the matter he came to the conclusion that although he had little objection to anything actually stated in the paper, it showed that our views were essentially divergent. He therefore abandoned the attempt to produce an amended version on which we could be unanimous, and suggested that the form in which the papers now appear should be adopted. The difficulties raised by Dr. Campbell seem to me either unimportant or adequately covered by Part IV, but I am glad that it has been possible to state them in his own words, so that points that I may have missed are faithfully recorded.

## Temperature Variation of the Electrical Properties of Nickel Oxide

By R. W. WRIGHT AND J. P. ANDREWS

Queen Mary College, London

*MS. received 17th January 1949*

**ABSTRACT.** An experimental method of preparing specimens of NiO in the form of coherent strips is described. Simultaneous measurements of electrical conductivity  $\sigma$  and Hall effect  $R$  are then made at various temperatures up to about 700° C. and the thermo-electric power  $dE/dT$  measured immediately afterwards, all on one sample. The experiments are then repeated on different samples, and they show that  $\log \sigma$ ,  $\log R$ , and  $dE/dT$  are linear functions of  $1/T$ , where  $T$  is the mean absolute temperature of the specimen. The graphs for  $\log \sigma$  and  $\log |R|$  against  $1/T$  each consist of two rectilinear portions, one covering the high, the other the low temperature results. Thermo-electric measurements yielded results only for the high temperature part.

The theory of impurity semiconductors is developed and found adequate to explain the variation, at any rate at higher temperatures. It is found that an activation energy of about 2 e.v. at high temperatures, and from 0.3 to 0.64 e.v. at low temperatures, is required for excitation of electrons to the conduction band. The concentration of impurity centres operative in the high temperature range is about  $8.6 \times 10^{20}$ , the electrons having a mean free path of about  $10^{-6}$  cm. The concentration of free "carriers" varies from  $10^{11}$  to  $10^{13}$  as the temperature rises. NiO behaves like a defect semiconductor, "hole" conduction predominating. The significance of these results is discussed.

### § 1. INTRODUCTION

EXPERIMENTS on semiconductors are generally designed either to study the common characteristics of a whole group of materials or else to probe in detail the behaviour of a single substance—or even of a single specimen. The virtue of the second method, of which our work is an example, is the elimination of at least some of the confusing complications which befog the study of the electrical properties of solids, particularly of semiconductors. Small differences of impurity content or heat treatment of different samples of the same material, or obscure differences in the structure of different substances believed to be of the same type, make generalization difficult. If, however, simultaneous measurements of electrical conductivity and Hall effect, or of conductivity and thermo-electric power, are made on one sample, quite definite conclusions can often be arrived at about the internal behaviour of a sample, and thus a good deal of light can sometimes be thrown on the general theory of solids.

In nickel oxide we have selected a substance which seems specially well adapted to this kind of detailed study. Hitherto most work on semiconductors—of which NiO is an example—has been performed on samples of compressed powders, although a few investigations have been carried out with single crystals, e.g. SiC (Busch and Labhardt 1946), or with coherent specimens, as in  $\text{Cu}_2\text{O}$ , formed by oxidizing a strip of copper (Mönch 1933). One of our reasons for choosing NiO was the possibility of forming a suitable specimen by direct oxidation of the metal, thus avoiding, it may be hoped, some of the objections which may be urged against the use of powders. A second reason was the special interest attaching to the ionic structure of solid NiO. It is known that in the crystal lattice the  $\text{Ni}^{++}$  ions have an incomplete 3d electron-shell, and this suggests the

possibility of free electron movement which might be expected to produce metallic conduction. NiO, however, is by no means a metallic conductor. This interesting dilemma is found in certain other substances in which the 3d shell is incomplete, and de Boer and Verwey (1937) have proposed a theory of these materials. We refer later to the bearing of this theory on our results.

Some measurements of electrical conductivity  $\sigma$  of NiO at different temperatures are already available in the work of Baumbach and Wagner (1934), and the effect on  $\sigma$  and  $dE/dt$  (the thermo-electric power) of changes in the pressure of oxygen in the surrounding atmosphere has been measured by Hogarth (1948) in this laboratory with specimens of compressed powders, but no detailed simultaneous study of more than one of the properties is known to us.

## § 2. PREPARATION OF THE SPECIMEN

From the purest obtainable nickel foil a strip of dimensions  $7 \times 1.1 \times 0.0067$  cm. was cut. According to the suppliers, the impurities in this material consisted of traces of Fe, Cu, Mn, Co, to a total of 0.4%. The strip was first rolled flat and two small holes were made, one near each end. From these holes the strip was suspended under tension along the axis of a vertical tube furnace so that a current of air flowed constantly past the specimen and the strip was prevented from buckling. While in this position it was maintained at a temperature of

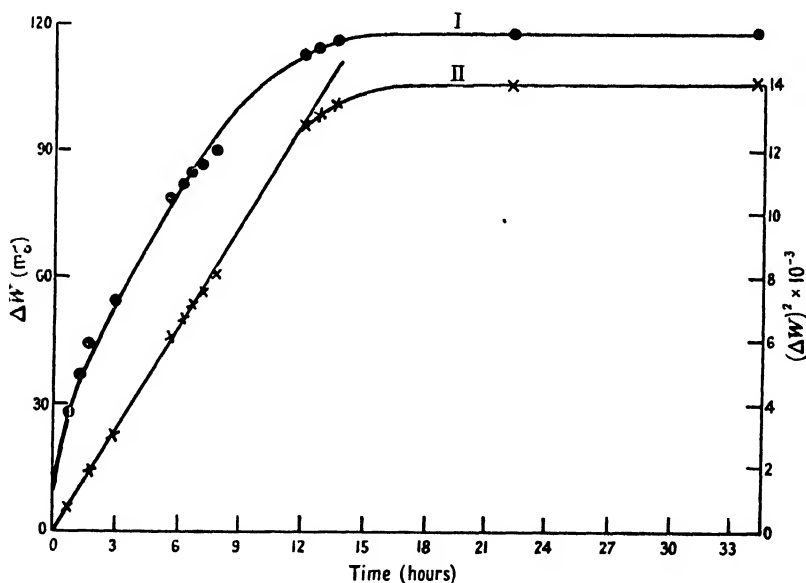


Figure 1. Increase in weight of the specimen due to oxidation as a function of the time. Curve I shows the increase in weight as a function of the time. Curve II shows the square of the increase in weight as a function of the time.

1,000° c. for a period up to 30 hours, after which oxidation was considered to be complete. For our investigation it is naturally most important that we should be sure of the completeness of the oxidation, and to this end one specimen was removed from the furnace from time to time and weighed. Figure 1 shows how the weight increased, the constancy after about 20 hours indicating completion. (The observations show that the square of the gain in weight is proportional to the time, as curve II of Figure 1 illustrates.) Examination of the broken section after about 30 hours' heating revealed no sign of unoxidized core.



Upon this very fragile specimen it was next necessary to prepare electrical contacts. These were made by evaporating silver *in vacuo* on to the specimen over the small regions required, namely one region at each end for the entrance and exit of the main current and for the attachment of potential leads, and another pair at the middle of the two long edges for the attachment of the Hall effect electrodes.

### §3. APPARATUS FOR HALL EFFECT AND CONDUCTIVITY, AND METHOD OF MEASUREMENT

The strip specimen prepared in this manner was mounted, together with a heating element of nichrome ribbon, as illustrated in Figure 2, within a framework of "syndanio" or asbestos slate, the heater being carefully insulated from the specimen by means of mica. When the framework was assembled, spring

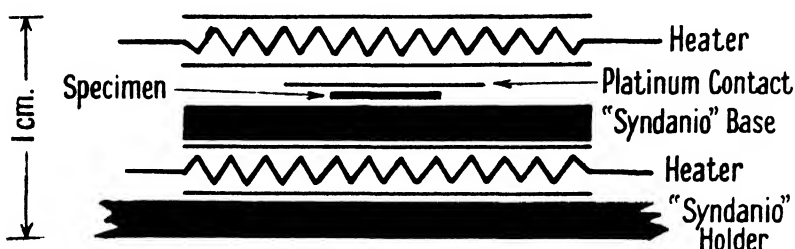


Figure 2. A diagrammatic representation of an end section of the apparatus used for measuring the Hall effect and conductivity.

contacts of platinum pressed against each of the silvered regions with sufficient pressure to ensure firm connection. By careful designing it was found possible to keep the thickness of the whole device, including framework, specimen, heater, contacts, and thermocouples for measuring the temperature of the specimen, rather less than one centimetre. The device was then inserted between the poles of an electromagnet with which a maximum magnetic field of 11,500 oersted was obtainable, varying by less than 1% over a region 3 cm. wide between the pole-pieces. A potential difference of about 500 volts D.C. sufficed to drive a very small current longitudinally through the specimen and through a fixed resistance placed in series, so that the current could be measured by observing the potential drop across the resistance. The potential drop across the specimen was measured through potential leads taken to an electrostatic voltmeter, the resistance of the specimen being then calculated from this potential drop and the current.

The resistance was measured in this manner after air currents had been excluded from the apparatus as far as possible, and after sufficient time had elapsed to ensure thermal equilibrium; the Hall effect was then measured. For this purpose the lateral contacts were connected, via a quadrant electrometer or sensitive galvanometer, to a thermocouple-type potentiometer, the magnetic field was switched on, and the transverse potential difference between the Hall electrodes balanced out. This potential difference is generally the sum of two parts, due respectively to the Hall effect and to the small departure from exact symmetry which it is generally impossible to avoid in placing the Hall electrodes. If the magnetic field is now reversed, the contribution from the Hall effect is reversed, while the other contribution remains unaffected. The difference between the readings of the potentiometer is then twice the Hall E.M.F.

## § 4. ARRANGEMENT FOR THERMO-ELECTRIC EFFECT

For measurement of the thermo-electric effect the specimen in its framework was removed from the magnet after the completion of the conductivity and Hall effect measurements, and arranged in an electric furnace so that the temperature of one of its ends differed by  $40^\circ$  or  $50^\circ$  C. from that of the other, the greatest care being taken to exclude draughts, which are liable to set up uncontrollable temperature fluctuations. Experiments making use of larger and of smaller temperature differences were found to lead to practically the same results. Against the two ends were pressed pieces of platinum to form the hot and cold junctions, and the thermo-E.M.F. was measured with the potentiometer, using a sensitive galvanometer as indicator at higher temperatures, and a quadrant electrometer at low temperatures. The temperatures of the ends were measured with the aid of thermocouples, and the mean temperature  $T$  used as the temperature of the specimen in plotting the results. Below  $300^\circ$  C. mean temperature the results were erratic, probably because of a distinct thermo-electric effect in the syndanio holder.

## § 5. RESULTS

Preliminary experiments were first performed to verify that the conduction was completely electronic. Ohm's law was found to be obeyed over the range of currents used. Moreover, supplementary experiments designed to detect any transport of ions gave an entirely negative result. The possible interference of the Ettingshausen effect on the measured Hall E.M.F.s was also examined. No measurable lateral temperature difference that reversed with the reversal of the applied magnetic field could be detected. In order that E.M.F.s of magnitude similar to that of the Hall E.M.F.s should be produced, a temperature difference of the order of  $100^\circ$  C. would be required. Furthermore, reversal of the applied magnetic field produced immediate reversal of the lateral E.M.F., which remained

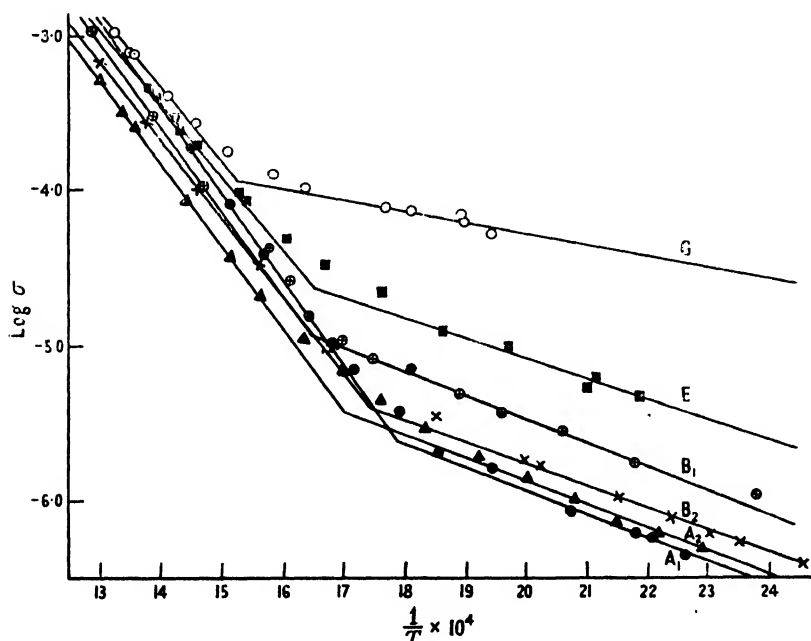


Figure 3. Log of the conductivity as a function of the reciprocal of the absolute temperature for various specimens as indicated.

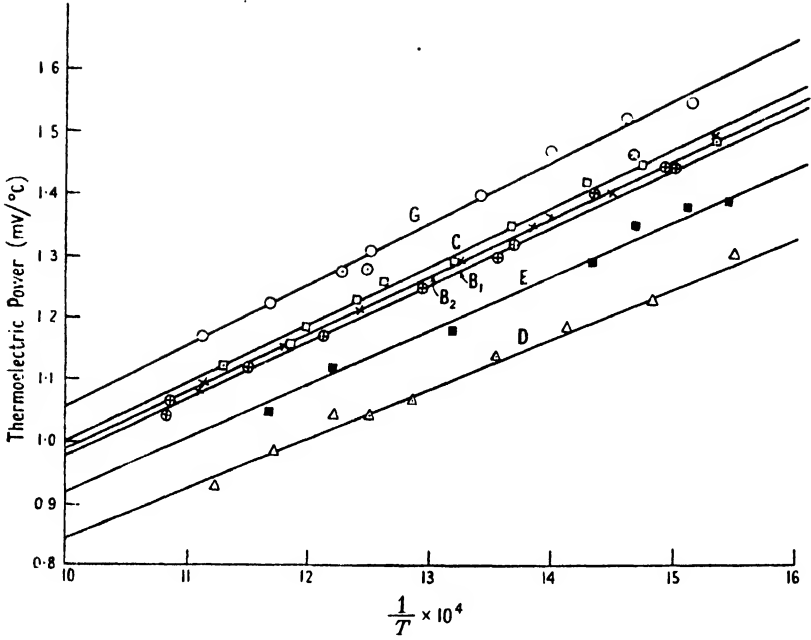


Figure 4. The thermo-electric power as a function of the reciprocal of the absolute temperature for various specimens as indicated.

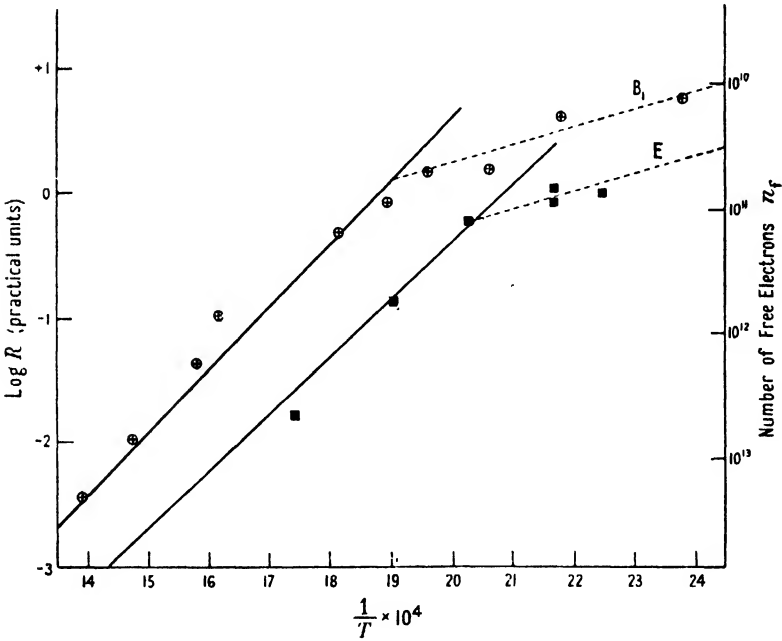


Figure 5. Log of the Hall constant as a function of the reciprocal of the absolute temperature for the two specimens as indicated.

The points shown are the experimental points. The full lines indicate the values predicted by the theory from the experimental values of the conductivity and thermo-electric power.

constant thereafter. We considered, therefore, that the contribution due to the Ettingshausen effect must have been less than 1% of the total E.M.F. measured.

Experiments were carried out on many specimens, but because of their extreme fragility several failed to survive for the complete series of observations. In the graphs of Figures 3, 4 and 5 results for different samples are indicated by letters. Thus B, for example, indicates the simultaneous results for conductivity  $\sigma$  and Hall effect  $R$ , and for the subsequent measurements of thermo-electric power  $dE/dT$ , made on the same sample. For reasons discussed in the next section, the abscissae in all the graphs are in units of  $10^4/T$ , where  $T$  is the mean temperature of the specimen, so that high temperature results appear to the left of the diagrams. It will be seen that when  $\log \sigma$ ,  $\log R$ , or  $dE/dT$  is plotted as ordinate, the results appear to lie on sets of straight lines, and the reasons for this regularity will now be discussed.

## § 6. THEORY

We suppose that the chief energy levels in the semiconductor consist of a lower band completely filled with electrons at absolute zero of temperature, together with a higher band completely empty at absolute zero, the two bands being separated by a forbidden energy step, in which no energy levels exist except for a narrow range of levels due to the presence of impurities. If the semiconductor is of the "excess" or "normal" type, these impurity levels are to be found near the bottom of the upper or conduction band, and at absolute zero are considered to be completely filled with electrons. In a "defect" or "abnormal" semiconductor, the impurity levels are near the top of the lower filled band, and are considered to be empty at absolute zero. With minor changes the theory is the same in both cases, and it is customary to develop it for excess semiconductors. In what follows this procedure is adhered to. Developments of the theory already made by various authors show a rather distressing variety of notations, and we have decided therefore to follow that of Putley (1949) for the sake of uniform treatment of rather similar problems.

As in Putley's account, then, we suppose there are  $n_i$  impurity centres per unit volume, each having an energy level  $\epsilon'$  below the bottom of the conduction band. At absolute temperature  $T$  we assume that  $n_t$  electrons per unit volume from these centres are excited into the conduction band. Let  $\epsilon^*$  be the chemical potential, then by expressing in terms of Fermi-Dirac statistics the condition that the sum of the electrons excited to the conduction band, and the number left unexcited in the impurity centres, must be equal to the number,  $n_i$ , of impurity levels, it is not difficult to show that

$$n_i \frac{1}{1 + \exp \{(\epsilon' + \epsilon^*)/kT\}} = \frac{4\pi(2m^*)^{3/2}}{h^3} \int_0^\infty \frac{\epsilon^{1/2} d\epsilon}{1 + \exp \{(\epsilon - \epsilon^*)/kT\}}, \quad \dots (1)$$

where  $h$  is Planck's constant,  $m^*$  is the effective mass of the electron in the conduction band, and  $\epsilon$  denotes energy. If we now write  $\epsilon/kT = \eta$ ,  $\epsilon'/kT = \eta'$ ,  $\epsilon^*/kT = \eta^*$ , equation (1) becomes

$$n_i \frac{1}{1 + \exp (\eta' + \eta^*)} = \frac{4\pi(2m^*kT)^{3/2}}{h^3} \int_0^\infty \frac{\eta^{1/2} d\eta}{1 + \exp (\eta - \eta^*)}. \quad \dots (2)$$

In the same notation  $n_f$  is given by

$$n_f = \frac{4\pi(2m^*kT)^{3/2}}{h^3} \int_0^\infty \frac{\eta^{1/2} d\eta}{1 + \exp(\eta - \eta^*)} \quad \dots\dots (3)$$

In these expressions the reduced chemical potential  $\eta^*$ , which is a function of the concentration of electrons, may be considered as a parameter indicating the degree of degeneracy of the electron gas—a device used extensively by Shifrin (1944). Now Shifrin has shown that if  $n_f < 10^{18.5}$ , so that the degree of degeneracy is very small, and  $-\eta^* \gg 1$ , then to an accuracy of better than 5%, we may write

$$\frac{1}{2} \int_0^\infty \frac{\eta^{1/2} d\eta}{1 + \exp(\eta - \eta^*)} = \frac{\sqrt{\pi}}{4} \exp \eta^*$$

We shall present evidence to show that in NiO the concentration of charge carriers is probably very much less than  $10^{18.5}$  per  $\text{cm}^3$ , so that the approximation may be used with confidence in our case, and we may write  $n_f = K \exp \eta^*$ , where  $K = 2(2\pi m^* kT/h^2)^{3/2}$ , and it then follows from equation (2) that

$$n_b = n_f + K \exp(\eta' + 2\eta^*).$$

If the number of carriers excited is only a very small fraction of  $n_b$ , as it appears to be in NiO, the second of these equations may be written approximately as

$$n_b = K \exp(\eta' + 2\eta^*),$$

so that

$$n_f = \sqrt{(Kn_b)} \exp(-\eta'/2),$$

and

$$\eta^* = \ln n_f / K = \ln \sqrt{(n_b/K)} - \eta'/2.$$

The expressions for the Hall effect  $R$ , conductivity  $\sigma$  and thermo-electric effect  $dE/dT$ , derived by several authors (see Seitz 1940, p. 192) for this model, may now be expressed as follows:

$R = \pm 3\pi/8n_f e$ , where  $e$  is the electronic charge in E.M.U. Hence

$$\ln |R| = \ln \{3\pi/8e \sqrt{(n_b/K)}\} + \epsilon'/2kT.$$

$\sigma = 4n_f l_0 e^2/3 \sqrt{(2m^* kT)}$ , where the mean free path  $l_0$  of electrons is assumed to be constant over the relevant range of electron energies.

$$\ln \sigma = \ln \left[ \sqrt{n_b l_0} \frac{4}{3} e^2 \sqrt{\left( \frac{K^2}{2\pi m^* kT} \right)} \right] - \frac{\epsilon'}{2kT},$$

$$dE/dT = \pm \frac{k}{e} (2 - \eta^*) = \pm \frac{k}{e} \left( 2 - \ln \sqrt{\left( \frac{n_b}{K} \right)} + \frac{\epsilon'}{2kT} \right) \quad \dagger$$

In these expressions the main variation with temperature is due to the term  $\epsilon'/2kT$ , and over the range of temperature used in our experiments the deviation from constancy of the remaining terms is small and produces a negligibly small change in the value of the whole expression. Consequently  $\log |R|$ ,  $\log \sigma$  and  $|dE/dT|$  all differ from linear functions of  $1/T$  by negligible amounts. It follows that from the gradients and intercepts of appropriate graphs  $n_b$ ,  $\epsilon'$  and  $l_0$  may all be found. From  $n_b$  and  $\epsilon'$  a value of  $\eta^*$  can be calculated, and hence  $n_f$ . It is of course implied that the values of  $R$ ,  $\sigma$  and  $dE/dT$  used in this computation should have been measured simultaneously on the same specimen.

<sup>†</sup> Seitz (1940, p. 191) gives a formula for the Thomson coefficient from which our formula may be derived.

In order to facilitate the calculation, numerical values of  $k$ ,  $e$  etc. may be inserted—taking  $m^*$  to be the electronic mass and  $T = 625^\circ \text{A.}$  in the nearly constant term of the expression for  $\sigma$ . We then have

$$\log |R| = \frac{\epsilon'}{3.96} \frac{10^4}{T} - \log \sqrt{n_b} + 0.9325,$$

$$\log \sigma = -\frac{\epsilon'}{3.96} \frac{10^4}{T} + \log (l_0 n_b^{\frac{1}{2}}) - 0.948,$$

$$|dE/dT| = \frac{\epsilon' 10^4}{2T} + \frac{1}{11.7} (24.78 - \ln \sqrt{n_b}) \text{ mv/deg.}$$

Making use of these equations, the constants shown in the Table are obtained for the different specimens. In this list  $B_1$  and  $B_2$  refer to a single sample in which the conductivity and Hall effect are first determined as usual ( $B_1$ ), then the thermo-electric power is measured, and finally the conductivity is measured a second time ( $B_2$ ). The small difference between these two sets of results is no doubt due to the intervening heat treatment. In most of the specimens the most elusive quantity was  $R$ , the Hall effect. In most cases the true Hall E.M.F. was obscured by sudden and uncontrollable fluctuations, which may, perhaps, have been caused by imperfections in the necessarily delicate contacts, but which generally could not

Specimen	Conductivity measurements				Thermo-electric measurements		
	High temp.		Low temp.		High temp.		
	(1)	(2)	(3)	(4)	(5)	(6)	(7)
A <sub>1</sub>	2.16	4.90	0.61	-1.91			$3.4 \times 10^{-6}$
A <sub>2</sub>	2.09	4.65	0.61	-1.85			$1.9 \times 10^{-6}$
B <sub>1</sub>	2.15	4.75	0.64	-1.18	1.84	20.7	$2.4 \times 10^{-6}$
B <sub>2</sub>	2.04	4.42	0.64	-1.94	1.85	20.7	$1.12 \times 10^{-6}$
C					1.86	20.6	
D					1.67	20.9	
E	1.88	4.10	0.52	-1.49	1.74	20.8	$0.54 \times 10^{-6}$
G	1.92	4.48	0.30	-1.85	1.94	20.7	$1.3 \times 10^{-6}$

(1), (3), (5)  $\epsilon'$  (ev.); (2), (4)  $\log (l_0 \sqrt{n_b})$ ; (6)  $\log n_b$ ; (7) calculated values of  $l_0$  ( $n_b = 5.37 \times 10^{20}$ ).

be eliminated. In two samples only (B and E) steady results were consistently obtained, and these are shown in Figure 5. At the lower temperatures, measurements of thermo-electric power were also found difficult to make with any degree of certainty, and we therefore include only the much more dependable results obtained at temperatures above  $370^\circ \text{C.}$  Now it will be observed from the diagrams that the graphs of  $\log \sigma$  and  $\log R$  each consists of two straight lines, a low temperature and a high temperature section. The results we give for  $dE/dT$  correspond only to the high temperature parts of the other graphs. It may be that a determination of  $dE/dT$  at low temperatures will eventually show a similar division of results into two parts, at high and low temperatures, but at present our low temperature results would not justify a definite statement about it.

In these results it is worth noticing that the figures obtained from the thermo-electric measurements agree rather better among themselves than do the conductivity results.\* In particular the satisfactory constancy of  $\log n_b$ , as calculated

\* The values for  $\epsilon'$  obtained from the conductivity measurements are in good agreement with those obtained by Baumbach and Wagner (1934). Their results, however, showed no special low temperature region. This probably indicates that their specimens were freer from foreign impurities.

from these measurements justifies the use of the mean value of  $\log n_b$  in the calculation of the mean free path from the values of  $\log l_0 \sqrt{n_b}$  in the third (high temperature) column of the Table. Results for  $l_0$ , calculated in this way, are shown in the last column of the Table, and indicate an extreme variation of mean free path of about 5 to 1 between the specimens. The order of magnitude of  $l_0$  ( $10^{-6}$  cm.) does not appear to be unreasonably large—it compares well, for example, with the mean free path estimated for cuprous oxide (Mott and Gurney 1940, p. 168).

We are now in a position to see how far the Hall effect results fall into line with the others. From values of  $\epsilon'$  and  $n_b$ ,  $\log |R|$  at any temperature can be calculated from the formula already quoted. For the low temperature range we have no independent value of  $n_b$ , but over the high temperature region we have the values of  $\log n_b$  given in the Table. For the same range we have also two separate values of  $\epsilon'$  for each specimen, and we have taken the mean of these in calculating  $R$ . In Figure 5, showing the variation of  $\log R$ , the continuous line passes through points calculated in this manner. The agreement therefore seems to be very satisfactory. Moreover, since  $R = (3\pi/8ln_f)$ , the numbers of free carriers in the two specimens may now be calculated at different temperatures. These numbers are given on the right-hand scale of Figure 5, and are seen to vary between about  $10^{11}$  and  $10^{13}$  per  $\text{cm}^3$  over the high temperature range. The average number of impurity centres,  $n_b$ , is about  $8.6 \times 10^{20}$  per  $\text{cm}^3$ .

In the thermo-electric experiments the cold end of the specimen was positive, as would be expected if the carriers were positively charged. This indicates that conduction takes place by "positive holes"—or in other words that NiO is a defect or "abnormal" semiconductor, and this was confirmed by the direction of the Hall E.M.F.

## § 7. DISCUSSION

It seems quite clear from these results that in the higher temperature range NiO is an impurity semiconductor of the kind already considered in the theory. It may be presumed that through the low temperature range the main action is of the same character, but that at these temperatures the contribution due to those impurity centres which are active at high temperatures is small, another set of impurity centres with lower activation energy then dominating the action. At this point the experiments of Jusé and Kurtschatow (1932) on cuprous oxide may be recalled. Their results for conductivity bear a striking resemblance to ours for NiO, and for the high temperature parts of their graphs they offer the suggestion of intrinsic conduction, that is, the conduction is supposed to be due to the direct excitation of electrons from the lower band of energy levels (supposed all filled at  $T=0$ ) to the conduction band. Since the transference of an electron in this fashion creates at the same time a positive hole in the lower band, conduction must be due to the combined effect of free electron and free hole. The theory of conduction differs in this case from ours. Some aspects of it have been worked out by Fowler (1933). It is easy to see that changes introduced by a theory of intrinsic conduction would differ according to the electrical property being considered. Thus changes in the predicted variations of Hall effect and thermo-electric power, which depend on the first power of the carrier charge, would be very unlikely to resemble the changes in the variation of conductivity, which depends on the second power of the charge. The convincing agreement of the

results for  $\sigma$  and  $dE/dT$  with those for  $R$  in NiO, as interpreted by the theory of impurity conduction, seems to show that intrinsic conduction cannot play the main, or even an important, part in our experiments.

On the nature of the impurity centres evidence at present is not conclusive. From experiments in this laboratory Hogarth has shown that the thermo-electric power of NiO is a linear function of  $\log P_0$ , where  $P_0$  is the pressure of oxygen in the surrounding atmosphere. On certain hypotheses it is possible to account for this kind of variation in terms of the quasi-chemical equilibrium of oxygen in the crystal lattice, but reasonable assumptions about the underlying mechanism do not seem to lead to good numerical agreement when the variation is calculated. It is, however, generally assumed that the extra oxygen absorbed is to be found in correct lattice positions, so that a number of vacant Ni sites remain. If we take the crystal density of NiO to be  $7.45 \text{ gm/cm}^3$ , unit volume will contain about  $6.9 \times 10^{22}$  atoms of Ni or of O, the total number of atoms of both kinds being therefore about  $1.38 \times 10^{23}$  per  $\text{cm}^3$ . The  $8.6 \times 10^{20}$  impurity centres per  $\text{cm}^3$  therefore represent about 0.62 atomic per cent. This is also generally considered to be about the percentage of excess oxygen in black NiO obtained by oxidizing green-grey NiO. Our specimens, although dark, were not black, however. While it may be assumed that the impurities in the higher temperature range are due to this excess oxygen, there still remains the problem of the centres of lower activation energy which predominate at low temperatures. In one particular the hypothesis introduced by de Boer and Verwey, primarily to explain the lack of metallic conduction in NiO, finds some corroboration in our results. This is the existence of an internal potential barrier requiring an activation energy of about 2 e.v. to surmount. We do in fact find an activation energy of that magnitude (see Table).

#### ACKNOWLEDGMENTS

We should like to express our gratitude to Professor H. R. Robinson, in whose laboratory these experiments were performed, for facilities and advice. The work was carried out with the assistance of a grant from the Department of Scientific and Industrial Research.

#### REFERENCES

- BAUMBACH, H. H., and WAGNER, C., 1934, *Z. Phys. Chem.*, **24**, 59.  
DE BOER, J. H., and VERWEY, E. J. W., 1937, *Proc. Phys. Soc.*, **49**, extra part, 59.  
BUSCH, G., and LABHARDT, H., 1946, *Helv. Phys. Acta*, **19**, 643.  
FOWLER, R. H., 1933, *Proc. Roy. Soc. A*, **141**, 56.  
HOGARTH, C. A., 1948, *Thesis*, London.  
JUSÉ, W., and KURTSCHATOW, B. W., 1932, *Phys. Z. Sowjet*, **2**, 453.  
MÖNCH, G., 1933, *Z. Phys.*, **83**, 247.  
MOTT, N. F., and GURNEY, R. W., 1940, *Electronic Processes in Ionic Crystals* (Oxford : University Press), p. 168.  
PUTLEY, E. H., 1949, *Proc. Phys. Soc. A*, **62**, 284.  
SEITZ, F., 1940, *Modern Theory of Solids* (New York and London : McGraw-Hill Book Co., Inc.).  
SHIFRIN, K., 1944, *J. Phys., U.S.S.R.*, **8**, 242.

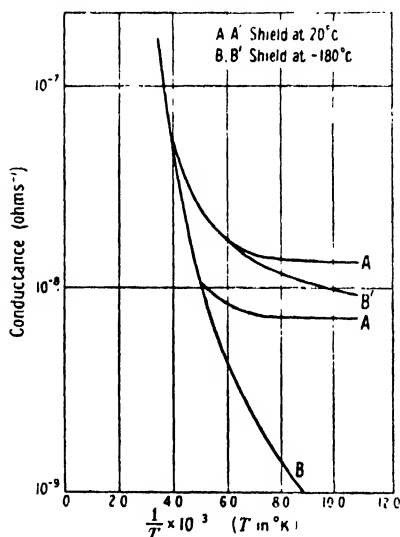


## LETTERS TO THE EDITOR

## Increased Sensitivity of Infra-red Photoconductive Receivers

A number of investigators have observed the anomalous dependence on temperature of the conductance of infra-red sensitive photoconductive films. The conductance is found to decrease rapidly on first lowering the temperature, whereas, on further cooling, the conductance tends to a steady state or may even increase again. Several hypotheses regarding the constitution of the layer (Macfarlane 1948) have been advanced to account for this behaviour; however, Simpson (1948) recently demonstrated that for films of lead telluride, with photo-sensitivity at wavelengths up to  $5.5\ \mu$ , this effect may be attributed entirely to radiation from the surroundings falling on the photoconductive surface. It has now been shown, firstly, that the same explanation holds for films of lead sulphide sensitive only up to  $3.8\ \mu$ , and secondly, that by removal of this background irradiation a large increase in sensitivity can be obtained.

In the present investigation a highly sensitive chemical type lead sulphide cell, B.T.H. type C, in the form of a small Dewar flask, was completely enclosed in a metal shield. On immersion in liquid air, the case cooled immediately to  $-183^\circ\text{C}$ , while the sensitive surface took about 20 minutes to reach this temperature. This allowed the conductivity of the layer to be determined at various temperatures, the shield being maintained at liquid air temperature. Similarly, by allowing liquid air to evaporate completely from the inside of the Dewar flask, the film slowly warmed and conductivity measurements were made over the same temperature range, the shield being maintained at room temperature. These results are shown in curves A and B of the Figure, where the logarithm of the conductance is



plotted against the reciprocal of the absolute temperature. It will be seen that the effect of excluding the room temperature radiation is to produce a continuous decrease in conductance with decrease in temperature.

If a small constant amount of radiation is allowed to fall on the sensitive surface through a small aperture in the shield, curve A is displaced to A' and curve B to B'. Defining sensitivity as  $(\sigma_1 - \sigma_D)/\sigma_D$  where  $\sigma_D$  and  $\sigma_1$  are the conductivities of the layer in the dark and when irradiated, respectively, the vertical interval between the curves A and A', or B and B' is a measure of the sensitivity. It will be observed that the exclusion of the background room temperature irradiation greatly increases the sensitivity of strongly cooled layers.

Modern techniques, using modulated radiation, have made the signal-to-noise ratio of far greater importance than the sensitivity as defined above. It is well known that the signal-to-noise ratio of chemically deposited lead sulphide cells can be increased by a factor of 10 by cooling to  $-80^\circ\text{C}$ . On further cooling to liquid air temperatures the improvement for the higher sensitivity cells is, however, small; in some cases even a deterioration of signal-to-noise ratio occurs. It has now been found that if the sensitive layer is shielded from the

constant irradiation of its surroundings, the signal-to-noise ratio increases continuously with decrease in temperature. By cooling the cell with liquid air and maintaining the shield at the same temperature, both the resistance and the signal-to-noise ratio are increased to over 1,000 times their value at room temperature. Measurements have demonstrated a detection limit of  $2 \times 10^{-8}$  watt.cm<sup>-2</sup> for 85° c. black-body radiation, and  $2 \times 10^{-13}$  watt.cm<sup>-2</sup> at the peak of its spectral response for 1 c/s. bandwidth.

If full advantage is to be taken of this greatly increased sensitivity, great care must be exercised in the design of the first stage of the amplifier. The high values of the resistance reached by these cells, when cooled and shielded, may well require the use of an electrometer type of valve in the pre-amplifier. It has been widely recognized that the response time of this type of cell increases with resistance; in the case illustrated above, the time constant increased from about 40 microseconds at room temperature to a value of 10–20 milliseconds when the cell was cooled and screened at liquid air temperatures. Therefore it is necessary to use much lower interruption frequencies than those normally employed with this type of receiver. The above measurements were made with an interruption frequency of  $16\frac{2}{3}$  c/s.

It was considered possible that the increase in sensitivity might be accompanied by an extension of the spectral response curve to longer wavelengths, similar to that already found on cooling (Moss 1947). However, preliminary spectral response measurements do not indicate any such extension. It can be shown that loss of the maximum sensitivity is not solely associated with long wavelengths (room-temperature radiation). When the resistance of a cooled and shielded cell was reduced to a similar extent by a constant irradiation at short wavelengths (tungsten lamp), the signal-to-noise ratio for a small superimposed modulated irradiation was also greatly reduced.

I desire to thank Mr. L. J. Davies, Director of Research, The British Thomson-Houston Co. Ltd., for permission to publish this note, and Dr. C. J. Milner for many helpful discussions.

British Thomson-Houston Co. Ltd.,  
Rugby.  
14th May 1949.

B. N. WATTS.

MACFARLANE, G. G., 1948, *M.I.T. Conference on Physical Electronics*, April 1948.  
MOSS, T. S., 1947, *Nature Lond.*, **159**, 476.  
SIMPSON, O., 1948, *Proc. Phys. Soc.*, **61**, 487.

## The Decay Constant of Radio-Sodium, <sup>24</sup>Na

The accurate determination of decay constants is a tedious measurement not altogether free from the danger of systematic errors which can be troublesome to detect and eliminate. For this reason the number of radioactive substances for which the decay constant is known with precision is quite small, careful measurements usually being made only when an accurate value is required for a special purpose.

During the course of some work using radio-sodium as a calibrated source of monochromatic  $\gamma$ -rays, the decay constant was redetermined with the object of enabling accurate estimates of the activity to be made, even after the lapse of several half periods. A good knowledge of the decay constant was essential as the absolute determination\* of the activity of the radio-sodium could only be made on an aliquot fraction some considerable time after the irradiated sodium carbonate had been withdrawn from the pile.

The method adopted was to measure the ionization produced by the  $\gamma$ -radiation in a large shallow chamber 50 cm. diameter and 6 cm. total depth. The source was placed on a stand 6 cm. above the chamber. The advantage of a chamber of this type, which is similar to that used by Madame Curie (1912) in her work on the  $\gamma$ -rays of radium, is that errors due to location of the source are quite negligible. The ionization current was compared directly with that produced by a 200 mc. radio-thorium standard. This eliminates, or greatly reduces, the two main sources of error in work of this type, namely, changes

\* The absolute determination was made by J. L. Putman and R. Wilment at A.E.R.E., Harwell using a  $\beta$ - $\gamma$  coincidence method.

in the sensitivity of the electrometer and changes in the efficiency of the chamber such as are due to changes in barometric pressure and humidity. The time was measured to the nearest 10 seconds with a chronometer which had been compared with the laboratory crystal-controlled clock.

The ionization currents were compared using a selected 954 valve as an electrometer valve.

The circuit used is shown in Figure 1. The electrometer is used only as a null instrument, the measurement consisting of a comparison of the voltage produced by the ionization current passing down a fixed grid resistance  $R^\dagger$  with that obtained with a low-voltage potentiometer. The method is alternative to that described by Ward (1939), and enables quicker measurements to be made with strong sources.

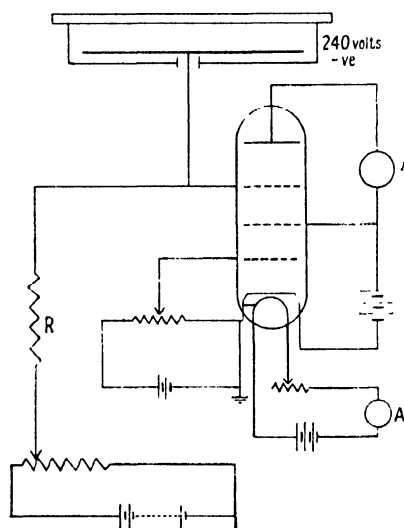


Figure 1. Circuit diagram of ionization chamber and electrometer valve.  
Resistance  $R$  is 10,000 megohms.

It was found that in this way the two sources could be compared accurately with a time interval of only a few minutes between the measurements, thus greatly reducing errors due to drift in the characteristic of the electrometer valve and grid leak.

The results obtained are shown in the Table.

Series I		Series II		Series III	
Time (hours)	Resistance ratio	Time (hours)	Resistance ratio	Time (hours)	Resistance ratio
0	3.75139	0	2.43170	0	3.60647
6.51667	5.04451	2.96667	2.81181	0.21667	3.59673
19.05000	8.93435	6.25000	3.27573	2.76667	4.12194
22.70000	10.72052	10.63333	4.01195	2.95000	4.11092
27.41667	13.34078	22.30000	6.88563	6.90000	4.94828
42.70000	27.43638	27.30000	8.68861	6.96667	4.93040
44.16667	29.26085	29.90000	9.85738	18.91667	8.62175
				19.03333	8.64929
				23.36667	10.56491
				23.43333	10.20523
				27.05000	12.57298
				27.16667	12.52778

† For Series I an S.S. White resistor was used, and for Series II and III a Welwyn resistor.

The decay constant was calculated from the linear logarithmic plot (Figure 2) by Gauss' method of least squares. This assumes that all the readings have equal weight, but this is not the case since the experimental quantities which may be assumed to have equal weights are the actual ionization currents.

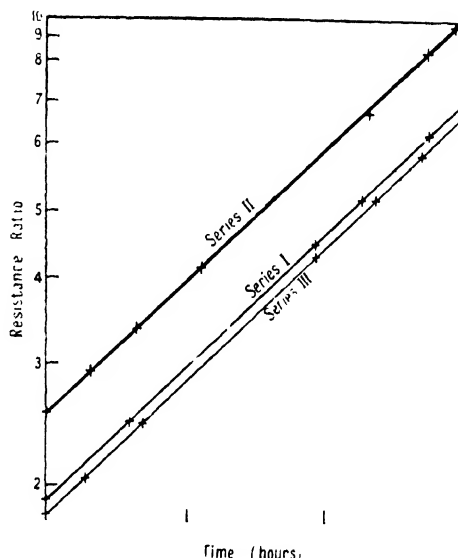


Figure 2. Linear logarithmic plot of resistance ratio against time in hours. For series I and III the ordinate is divided by 2.

Thus, if the activity  $A$  has an error  $\epsilon$  so that the ionization current is  $(A \pm \epsilon) = A(1 \pm \epsilon/A)$ , then the ordinate  $y$  in the logarithmic plot is given by  $y = \log A + \log(1 \pm \epsilon/A) = \log A \pm \epsilon/A$ . Thus the points on the logarithmic plot must be weighted according to the square of the measured activity. The results obtained from the three series of measurements are as follows. A correction was made for the decay of the radio-thorium source.

Series I	$14.8878 \pm 0.02$ hrs.	$(14.89 \pm 0.03)$
Series II	$14.8952 \pm 0.02$ hrs.	$(14.89 \pm 0.036)$
Series III	$14.9170 \pm 0.03$ hrs.	$(14.94 \pm 0.038)$

Average  $= 14.90 \pm 0.02$  hrs.

Decay constant  $= 0.04652 \pm 0.000062$  hr $^{-1}$ .

The figures in brackets are those obtained by a simple graphical treatment in which the slope is calculated from every combination of these points and the average taken. The mean value stated lies within the limits of error quoted by van Voorhis (1936). The three decay constants calculated by Gauss' method agree within the estimated error. The small differences from the value (in brackets) obtained graphically from the logarithmic plot shows that the observed ionizations are well represented throughout the measurement by an exponential decay, so that there is no reason to suppose that any errors due to changes in the high resistance units have not been eliminated.

We have to thank A.E.R.E., Harwell, for the radioactive sodium and Messrs. Putman and Wilment for work on this, the Department of Scientific and Industrial Research for maintenance grants, and Mr. C. H. Collie for his interest and advice.

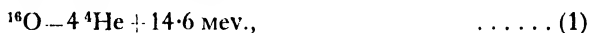
Clarendon Laboratory,  
Oxford.  
23rd February 1949.

R. WILSON.  
G. R. BISHOP.

CURIE, E., 1912, *J. Phys. Radium*, **2**, 795.  
VAN VOORHIS, S. N., 1936, *Phys. Rev.*, **49**, 889 A.  
WARD, A. G., 1939, *Proc. Camb. Phil. Soc.*, **35**, 523.

## The Photo-Disintegration of Oxygen into Four Alpha-Particles

The Atomic Energy Research Establishment synchrotron has been used to irradiate unloaded Ilford Nuclear Research Plates with a continuous spectrum of gamma-rays extending to 23 mev. Many "stars" were observed, consisting of three or four charged particles, in some of which unobserved neutrons may have been present; such stars were expected from cloud-chamber studies by Baldwin and Klaiber (1946). Among the stars observed, thirteen have consisted of four alpha-particles and may be identified as oxygen disintegrating. A typical star of this type is shown in Figure 1 (see Plate), and a histogram showing the total energy,  $E_T$ , released in the four alpha-particles of each star is shown in Figure 2. If it is assumed that the reaction occurring is



then a scale of the energy,  $E_\gamma$ , of the gamma-ray producing a particular star may be added as shown (upper scale). The fact that the spectral limit of the radiation and the limit of the energy released differ by 14.6 mev. (within the limits to which the spectral limit has been determined, namely,  $\pm 0.5$  mev.) is perhaps the surest indication that the reaction occurring is that of equation (1). Further evidence, and also an indication that neutrons are not involved in the reaction, is afforded by the momentum balance in the stars. The balance agrees with equation (1), assuming that the range of the alpha-tracks may be subject to an error of  $0.5\ \mu$ .

The number of stars observed is too small to give evidence of the detailed mechanism of equation (1) by an analysis of the distribution of energy amongst the individual alpha particles. It is unlikely, from the work of Hänni *et al.* (1948) on the disintegration of carbon that oxygen would disintegrate directly into four alpha-particles; more probably the disintegration will involve an excited level of  $^{16}\text{O}$  as an intermediate stage (with or without  $^{12}\text{C}$  as a further intermediary). Such mechanisms would be consistent with the form of the stars observed and would also account for the fact that no small stars (with  $E_T$  less than 6 mev.) have been detected.

The cross section of the reaction may be estimated from the known composition of the plate, a measurement of the ionization produced in a chamber with thick graphite walls, and a spectrum calculated theoretically (Heitler 1944). The mean value of the cross section thus obtained, for quanta between 20.5 and 23 mev., is  $2 \times 10^{-29}\text{ cm}^2$ ; this value may be in error by a factor of two, due to deviations of the spectrum from the theoretical value, particularly near the threshold, and also due to poor statistics.

This letter is published with the approval of the Director of the Atomic Energy Research Establishment.

Atomic Energy Research Establishment,  
Harwell, Didcot, Berks.  
25th May 1949.

F. K. GOWARD,  
E. W. TITTERTON,  
J. J. WILKINS.

BALDWIN, G. C., and KLAIBER, G. S., 1946, *Phys. Rev.*, **70**, 259.  
HÄNNI, H., TELEGI, V. L., and ZUNTI, W., 1948, *Helv. Phys. Acta*, **21**, 203. (Several hundred carbon disintegrations have also been observed in plates irradiated by the synchrotron, and are being analysed at A.E.R.E. and at E.T.H., Zürich.)  
HEITLER, W., 1944, *Quantum Theory of Radiation* (Oxford: University Press).

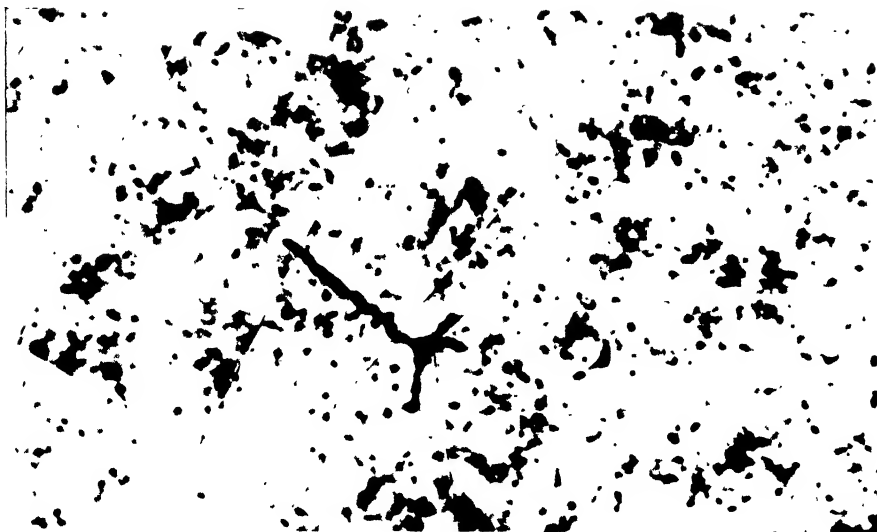


Figure 1.  $^{18}\text{O}$  ( $\lambda$ , 4a) Event. Observer Mrs. B. D. Mathieson. Ilford type  $\text{C}_2$  Emulsion. The  $\alpha$ -particle ranges are 3.3, 3.3, 4.4 and 15.7  $\mu$  respectively, representing an energy release of 7.3 MeV.

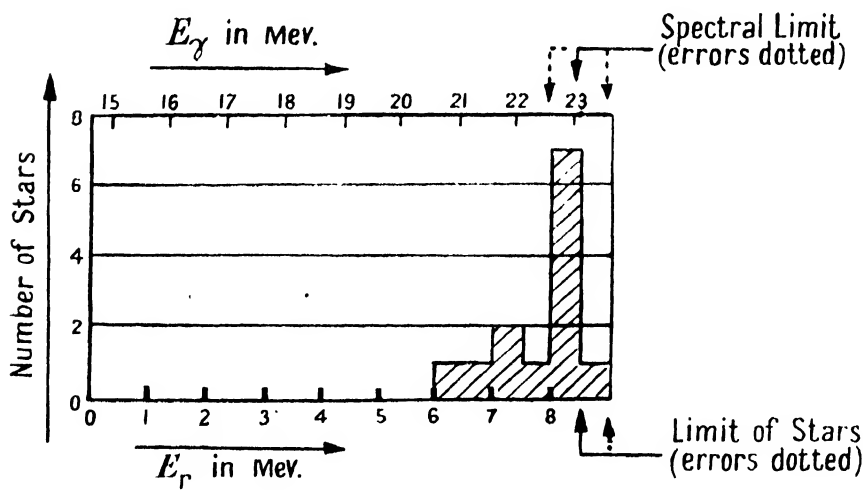


Figure 2. Histogram of oxygen stars.



## REVIEWS OF BOOKS

*Chambers' Six-figure Mathematical Tables*, by L. J. COMRIE. Volume 1, Logarithmic Values, pp. xxii+576; Volume 2, Natural Values, pp. xxxvi+576. (Edinburgh and London: W. & R. Chambers Ltd., 1948.) 42s. each volume.

Chambers' *Mathematical Tables* is probably the best known set of tables (with the possible exception of the Board of Education's four-figure set), and the present two volumes are in some sense the successor to it, for it appears that in 1944, the centenary of their publication, Dr. Comrie was asked to report on that work with a view to bringing it thoroughly abreast of modern requirements, and that the new work is the outcome.

The bulk of the old book was a 200-page table of seven-figure logarithms and just over 130 pages of natural and logarithmic trigonometric functions; the remainder of its 454 pages were occupied with a miscellany of geodetic and navigational tables. The new work, even if a successor to the old, is in no sense a revision of it. Dr. Comrie has considered first the requirements of the present-day physicist and statistician and provided the tables he is likely to need, to an accuracy which seems adequate for most work. The logarithms are now to six figures, and occupy 180 pages, but data for obtaining eight-figure logarithms are also provided (the old book gave ten figures for argument 1 to 1.06 at intervals of 0.0005).

In volume 2, the more interesting of the two, we have, for  $x=1$  to 1,000, the square, cube and fourth power (fifth power up to 100), the reciprocal, the factorial and the prime factors, as well as  $\log x!$  and  $x^{\frac{1}{2}}$  ( $10x$ ) $^{\frac{1}{2}}$ ,  $x^{\frac{1}{3}}$ , ( $10x$ ) $^{\frac{1}{3}}$  and ( $100x$ ) $^{\frac{1}{3}}$  and some powers of the reciprocals. The factorials above 200 are here published for the first time. From 1,000 to 3,400 we have the square, cube and prime factors. There is also a table of the first 1,540 primes, the largest of which is 12,919; evidently this table is in no sense a competitor with the specialist tables for the use of those interested in properties of numbers. There are three sets of tables of the circular functions, with arguments respectively in degrees and minutes, in radians, and in degrees and decimals of a degree. In each case the cot and cosec for small angles are given at a reduced interval, and the usual auxiliary functions are provided for the functions where they become excessively large. There is a table for conversion from rectangular to polar coordinates.

The hyperbolic functions are well tabulated, as well as natural logarithms, the inverse hyperbolic (and circular) functions and the Gudermannian with its inverse.

Beyond these elementary functions, a selection of transcendents has been made, the choice falling on the gamma function and the probability integral in its two main forms. Here the range has been most carefully considered so that the danger of a user wanting values beyond the arguments tabulated is very small. Where so much is provided it is ungenerous to complain, but I think many a physicist would have welcomed some tabulation of elliptic functions, if only in the form of the elliptic integrals  $E$  and  $F$ .

This very short account of the volume, which does not do justice to the care taken in the arrangement of the tables to make interpolation easy and to ensure the maximum convenience in use, also fails to mention another very valuable feature—the little treatise on numerical differentiation and differential equations, which comes near the end. There is also a great deal of really valuable information in the introduction, and a very helpful bibliography of larger tables at the end.

In volume two, the 6- and 8-figure logarithms have been mentioned. There is also a table of antilogarithms, a function for which tables to more than four figures have been remarkably scarce up to the present. Naturally, too, there are tables of the logarithms of trigonometric functions, which, as in volume 1, are given for angles expressed in degrees and minutes, or in degrees and decimals, or in radians. The  $S$  and  $T$  functions are also given for all these arguments and for seconds of time as well. There are tables of  $\log \Gamma(x)$  and of the logarithms of the hyperbolic functions.

Taking the two volumes together, it seems reasonable to suppose that they will suffice for the everyday needs of most workers who have calculations to do, though each will supplement them with tables for his own special work; perhaps he will want a selection of tables



for statisticians, or tables of Bessel functions, or maybe of factors. From this point of view the collection is not the successor to Chambers' Tables, but to such collections as those of Hoüel or Potin, Barlow, Hutton, Dale or Dwight. Certainly, with Barlow's tables on one side of the new book and Jahnke and Emde on the other, any worker would have a fine collection of tables at hand.

From a footnote to the preface, it appears that there is also an abridged edition of these 6-figure tables, in one volume, but the exact contents are not known to the reviewer. There is also a suggestion that the 64-page book of four-figure tables prepared by the same compiler for Messrs. Chambers is a miniature version of the present two volumes. It is certainly a very handy volume, but to the present writer it would have seemed that a nearer analogue is *Standard Mathematical Tables* by Milne-Thomson and Comrie.

J. H. A.

*Five-Figure Tables of Mathematical Functions*, by J. B. DALE. Second Edition. Pp. viii + 121. (London: Edward Arnold & Co., 1949). Price 6s.

The first edition of this book must be familiar to most readers of this review. Since 1903 it has been one of the few convenient single-volume sets of miscellaneous tables compiled with the physicist and applied mathematician in mind. In addition to logs, antilogs and trigonometrical functions, it contained Bessel functions, gamma functions, elliptic integrals and Legendre functions, which are all of value at times to the ordinary physicist.

In the present edition the contents have hardly been altered: the table of logarithms is somewhat improved and there is now a table of the logarithms of hyperbolic functions. The old edition gave logs for the range  $1.00(0.01)9.99$ , and the new gives, in addition,  $1.000(0.001)2.999$ , which is a definite improvement. In the old edition the amount to be added for the next figure of the argument was given in the way that is usual with four-figure logarithms—columns for 1, 2, . . . 9, based on the mean differences of the line, were given opposite the entries. In the new edition this plan is retained for the first table, but for the second the actual differences are to be used, and there is a proper table of proportional parts, but, unfortunately, it is not on the same page as the logs themselves.

The whole book has been re-set, with modern "heads and tails" type, instead of the old, uniform-height type, and on paper which is very pleasant to handle.

J. H. A.

*The Theory and Use of the Complex Variable*, by S. L. GREEN. Second Edition. Pp. viii + 136. (London: Sir Isaac Pitman and Sons Ltd., 1949). 12s. 6d

This excellent little book may not find the favour it deserves, among mathematicians at least, because of the lack of rigour. Among physicists this will be less of an impediment, although the fact that the basic ideas are introduced non-rigorously should have been emphasized. For many it is indeed a considerable advantage to know what a subject is about first, and then to consider it rigorously.

Complex numbers are introduced by means of the elementary theory of equations, it being *assumed* that they obey the ordinary laws of algebra. The Argand diagram, de Moivre's theorem, infinite series and the exponential, logarithmic, circular and hyperbolic functions are treated in chapters I, II and III.

Chapter IV is devoted to the consideration of functions of a complex variable. Oddly enough the Cauchy-Riemann equations are left unnamed in the text. A curvilinear integral is defined, but neither its existence nor its uniqueness are discussed. This is followed by Cauchy's theorem, Taylor and Laurent expansions and contour integration by means of the residues theorem. It is a little surprising to find the contour integral representations of a function and its  $n$ th derivative omitted.

Chapter V deals with conformal transformations, the important Schwarz-Christoffel transformation has a separate chapter. The last two chapters are devoted to applications in potential and alternating current theory.

The text is admirably written; and, for the student who does not expect rigour, it will form an excellent introduction to a branch of mathematics of considerable importance to physicists.

H. H. H.

## CONTENTS FOR SECTION B

	PAGE
Mr. J. HOLDEN. Multiple-Beam Interferometry: Intensity Distribution in the Reflected System . . . . .	405
Dr. F. D. STOTT. Optical Transmission of a Colloidal Solution in a Magnetic Field . . . . .	418
Mr. B. MELTZER. Electron Flow in Curved Paths under Space-Charge Conditions . . . . .	431
Mr. W. WEST. The Accuracy of Measurements by Rayleigh Disc . . . . .	437
Mr. R. L. G. GILBERT. A Dynamic Gravimeter of Novel Design . . . . .	445
Dr. C. DODD and Mr. HU PAK MI. Viscosity and Density in the Supercooled Liquid State . . . . .	454
Letters to the Editor :	
Professor G. TORALDO DI FRANZIA. The Radiation Pattern of Retinal Receptors . . . . .	461
Reviews of Books . . . . .	463
Contents for Section A . . . . .	467
Abstracts for Section A . . . . .	467

## ABSTRACTS FOR SECTION B

*Multiple-Beam Interferometry: Intensity Distribution in the Reflected System*, by J. HOLDEN.

**ABSTRACT.** The intensity distribution within the reflected fringe system from a multiple-beam interferometer employing silvered reflecting surfaces is discussed in its dependence upon the reflectivities and phase conditions at the reflecting surfaces. Using the Fizeau fringes of equal thickness localized on the zero order Feussner surface, the reflected intensity distribution is examined experimentally as the reflection coefficients of the interferometer surfaces vary between 4% and 90%. In the range of low reflectivities, when the silverings used showed marked colours, the changes in the reflected system lead to the measurement of a phase quantity related to the optical constants of the silver in the form of the thin film. Also in this range, the reflected fringes have a symmetrical form which is of use in the examination of sources of low intensity. In the range of high reflectivities, the conditions for the use of the reflected fringes in topographical investigation are discussed. The findings apply to fringes of equal chromatic order as well as to Fizeau fringes in reflection.

*Optical Transmission of a Colloidal Solution in a Magnetic Field*, by F. D. STOTT.

**ABSTRACT.** The change in optical transmission of a solution of colloidal graphite in a magnetic field has been measured as a function of a field strength and of concentration, and the results obtained compared with those to be expected from theory.

It is found that the experimental results agree closely with the hypothesis that the change in transmission is due to the change in projected area of the plate-like particles when these are aligned by the magnetic field.

By comparison of theoretical and experimental curves the particle volume is found. The rate of decay, after removal of the field, of the change in transmission produced by the field has also been measured.

An approximate theory is given to connect this rate with the diameter of the particles, and from this the size of the particles has been calculated. The dimensions so found agree satisfactorily with evidence from other sources.

*Electron Flow in Curved Paths under Space-Charge Conditions*, by B. MELTZER.

**ABSTRACT.** A general, synthetic method of obtaining rigorous solutions of steady electron flow subject to space-charge forces is presented. The solutions are not obtained for given boundary conditions, but the boundary conditions are deduced from the solutions. Two examples of such solutions, involving strongly curved two-dimensional electron trajectories, are given; the method is in principle capable of giving the solutions of all possible electron flow patterns in three dimensions except perhaps those involving inter-crossing trajectories. It is suggested that the subject offers scope for applied mathematical research at least on the same scale as potential theory.

*The Accuracy of Measurements by Rayleigh Disc*, by W. WEST.

**ABSTRACT.** A review of proposals made for altering the formula due to König, on which are based measurements of air-particle velocity by Rayleigh disc, leads to the conclusion that there is insufficient evidence for altering the numerical constant in the formula. Comparisons between Rayleigh disc and other methods of calibration of individual microphones are discussed, and the possibility of difference due to reaction on the sound pressure by the vibration of the diaphragm is considered.

*A Dynamic Gravimeter of Novel Design*, by R. L. G. GILBERT.

**ABSTRACT.** A new type of gravimeter is described, which depends for its operation on the change of frequency of the natural vibration of a vertical wire stretched by a weight. The advantages of such an instrument are presented, and a description given of the design which has so far been evolved. The results of laboratory tests and of trials carried out at sea in H.M. Submarine *Talent* are given.

*Viscosity and Density in the Supercooled Liquid State*, by C. DODD and HU PAK MI.

**ABSTRACT.** In order to determine whether any structural change takes place when a liquid is supercooled, measurements have been made on the viscosity of pure phenyl ether, which by its melting point ( $26.85^{\circ}\text{C.}$ ) is suitable for accurate work. It has been found that in both the ordinary and the supercooled state the liquid obeys a formula of the type  $\eta = A \exp(b/T)$ , but that the value of  $b$  in the supercooled state, which was investigated down to  $17^{\circ}\text{C.}$  below the melting point, is significantly larger than the value of  $b$  for liquid above the melting point. It is shown that an accurate value for the melting point can be obtained from viscosity measurements without the liquid ever becoming solid. The temperature coefficient of density shows no detectable change in passing through the melting point.





PROFESSOR G. I. FINCH, M.B.E., D.Sc., F.R.S.,  
*President of the Physical Society, 1947-1949.*

# THE PROCEEDINGS OF THE PHYSICAL SOCIETY

## Section A

---

---

VOL. 62, PART 8

1 August 1949

No. 356 A

---

---

### Steam in the Ring Discharge

By G. I. FINCH\*

*Presidential Address, delivered 6th May 1949*

**ABSTRACT.** The behaviour of steam and its decomposition products in the ring discharge has been examined.

Dry hydrogen is not dissociated. The production of atomic hydrogen is dependent upon the presence of steam which dissociates into hydroxyl and atomic hydrogen. A secondary source of atomic hydrogen is then afforded by the interaction of hydroxyl with molecular hydrogen.

The escape from the discharge of atomic hydrogen, a long-lived species, favours the dissociation of steam. Mercury vapour, on the other hand, inhibits the formation of atomic hydrogen and thus leads to a high equilibrium steam concentration.

Unlike dry hydrogen, dry oxygen is dissociated into atoms, but these have a short life as such and recombine in the discharge to form molecular oxygen and ozone.

The reaction mechanisms occurring in the discharge are discussed in the light of spectrographic results.

#### § 1. INTRODUCTION

BETWEEN 1926 and 1935 my collaborators and I carried out a systematic study of the combustion of hydrogen and carbon monoxide by oxygen in the cathode glow of the electric discharge maintained between metallic electrodes. Our object was to elucidate the nature of the mechanisms of these combustion processes, and the results and conclusions drawn therefrom were summarized in the *Journal of the Chemical Society* (Finch 1935). It may be remarked that, during the progress of this work, it became apparent that the results were also of practical interest, in that they threw fresh light on the chemistry of the thermionic valve, particularly in relation to the electron emissivity of the cathode.

Whilst certain phenomena arising out of the use of metallic electrodes in our experiments had helped towards an understanding of some aspects of the general mechanism of combustion, it became evident that, in other directions, they tended to obscure the issues. Indeed, as regards the undoubtedly complex mechanism of the homogeneous combustion of hydrogen by oxygen to steam, we could, in 1935, say no more than that, when the combustible mixture was rigidly dried, the initial step was the formation of the hydroxyl radical and that, in the undried mixture, steam was first dissociated into atomic hydrogen and hydroxyl, whereupon the hydroxyl somehow acted as a powerful promoter in the succeeding stages, leading ultimately to the formation of steam. No positive rôle in the combustion

\* The Presidential Address will also appear in *Proc. Phys. Soc.* for September 1949, Section B.

process could be assigned to atomic hydrogen. This was remarkable since, under the conditions of our experiments, atomic hydrogen was known to be produced in considerable quantities. Accordingly it was decided to examine the equilibrium between steam and its dissociation products in the electrodeless discharge under conditions which would eliminate surface effects, or at least permit of an adequate appreciation of the part played by them.

## § 2. APPARATUS AND GENERAL PROCEDURE

The gas (steam,  $2\text{H}_2 + \text{O}_2$ ,  $\text{H}_2$ ,  $\text{O}_2$  or rare gas, or various mixtures thereof) was contained in the closed circulation system shown in Figure 1. This was assembled from the cleaned components using a dry, filtered, glass-blowing air supply, and was so constructed that the circulating gas came into contact only with glass, mercury or quartz, thus avoiding the contaminations introduced by

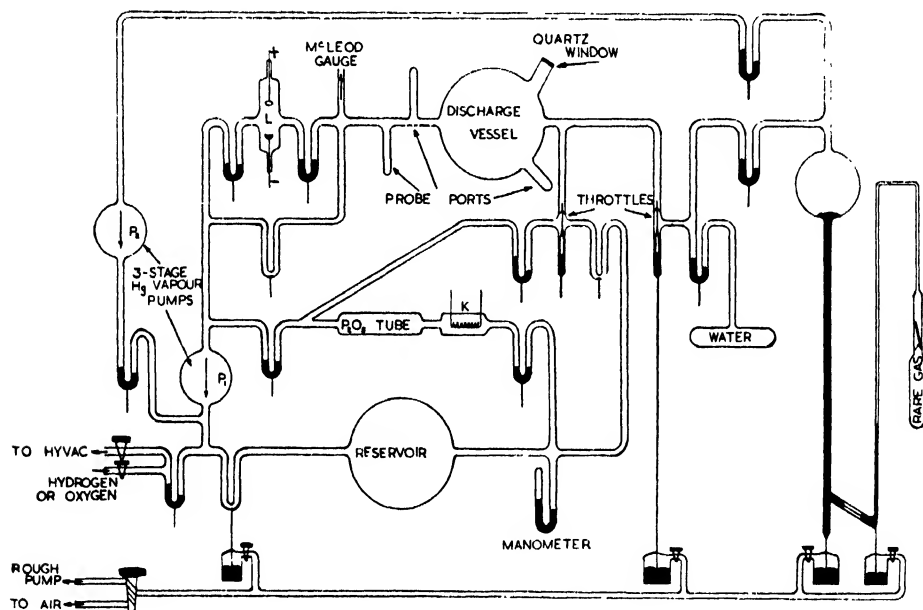


Figure 1.

lubricated stopcocks and rubber joints which have in the past so often vitiated the results of work on the combustion of hydrogen. The glass and quartz components were cleaned with chromic acid and distilled water; the mercury, previously washed in the usual manner and distilled, was redistilled into the appropriate vessels; and the phosphoric oxide was redistilled in oxygen until free from the lower oxides (Finch and Fraser 1926). The major remaining sources of impurity (other than mercury vapour) were the gases, chiefly carbon monoxide and nitrogen, dissolved in the glass of the discharge vessel. As will be seen later, getting rid of these gases presented no difficulty.

In Figure 1 the apparatus is shown with the barometric cut-offs and throttles set for the passage of the gas through the main circulation system consisting of the discharge vessel (10 cm. diameter), the three-stage mercury vapour pump, P<sub>1</sub>, and the reservoir (10 cm. diameter). In L a high-tension arc could be maintained between a nickel anode and a molten lithium cathode for the purification of the rare gas admitted to the system. By a suitable setting of the

appropriate cut-offs, the vessel K and the phosphoric oxide tube could be inserted into the circulation system between the reservoir and discharge vessels for the purpose of the quantitative analysis of steam-hydrogen-oxygen mixtures. Thus, with the platinum wire coil in K cold, the steam was removed with a corresponding change in the manometer level. Next, with the coil heated, hydrogen and oxygen in their combining proportions were removed, with a further change in the manometer level, the remaining gas being excess hydrogen, oxygen or known added inert diluent such as, for example, neon. The gaseous contents of the discharge vessel-reservoir circulation system could be well dried by circulation through the interposed phosphoric oxide tube, though that degree of rigid drying which exerts a marked effect in increasing the resistance of hydrogen to ignition could not be achieved. It is well known to workers in this field that, despite all precautions, the use of mercury seals and cut-offs invariably introduces traces of moisture.

The normal working pressure of gas in the reservoir during circulation was between about 7 and 10 mm., whilst that in the discharge vessel was maintained at between 0.026 and 0.03 mm. Hg by means of the pump,  $P_1$ , and the appropriate throttle. The rate of circulation through the discharge vessel was rather over 200 cm<sup>3</sup> per second; this was measured in a manner which will be obvious from Figure 1. Owing to the fall in pressure at the throttle, the partial pressure of mercury vapour in the discharge vessel could not exceed  $3 \times 10^{-6}$  mm., the rate of circulation being more than sufficient to prevent diffusion of mercury from the McLeod gauge, cut-offs or pump towards the discharge vessel.

Short sealed-off tubes were fused, as shown, into the discharge vessel and the 1.2 cm. bore tube, nearly 1 metre long, between the discharge vessel and the McLeod gauge entry tube. These tubes served for the sealing in of probes projecting into the discharge or gas stream. Three probe tubes, two of which are shown in Figure 1, were situated at 5, 20 and 50 cm. respectively beyond the discharge vessel outlet. In all other respects Figure 1 is self-explanatory.

The discharge was maintained by means of a high-frequency current in a solenoid, 13 cm. in length and internal diameter, mounted coaxially with the discharge vessel, and consisting of seven turns of 4 mm. diameter copper tubing. The current was obtained from a valve (Mullard S.W.9) oscillator in a modified Hartley circuit. The valve filament was run at its rated value and, unless otherwise stated, the input to the oscillator was 160 watts. The frequency was 26 Mc/s. as measured by a Southworth-Lecher (Southworth 1920) wire system. Further, the gas pressure in the discharge vessel was maintained at between about 0.026 and 0.03 mm. Hg, preferably nearer the former, the McLeod gauge readings being corrected for the experimentally determined equilibrium steam contents when moist gaseous mixtures were in use.

Under these conditions the discharge in steam consisted of a bright rose-pink annulus coaxial with the discharge vessel, from the cool walls of which it was separated by a dark sheath about 2 or 3 mm. thick. In cross section the diameter of the bright core of the annulus was about 4 cm., the intensity of the glow decreasing considerably near the centre of the discharge tube. It will be evident that this was a ring discharge, the theory of which was outlined in the 13th Guthrie Lecture by J. J. Thomson (1928). In such a discharge the currents form closed circuits in the gas, though it is possible that, under the conditions of these experiments, the actual initiation of the discharge was effected by the electrostatic field across



the ends of the solenoid (Mackinnon 1929, Esclangen 1934). It will be appreciated that conditions in this ring discharge closely resemble those in the positive column.

The evacuated discharge vessel was finally cleansed and gases absorbed in its walls sufficiently removed, first by prolonged baking at about  $350^{\circ}\text{C}$ . and then by maintaining the discharge in a stream of steam drawn from the vessel containing  $\text{CO}_2$ -free water, past the appropriate throttle, through the cool discharge vessel and the pump  $P_1$  backed by the 'Hyvac' pump. This also served to free the water in its storage vessel from dissolved air. After evacuation following upon such cleansing, the main circulation route was restored and the system filled with the appropriate gas to the desired pressures in the discharge and reservoir vessels.

A mixture of hydrogen and oxygen in combining proportions was frequently used in the experiments to be described below. It was conveniently prepared in a high state of purity by drawing pure steam through the discharge and drying the products accumulated in the reservoir by subsequent circulation through the phosphoric oxide tube. Oxygen was obtained by heating recrystallized potassium permanganate and then washing with a caustic potash solution. Hydrogen was prepared by electrolysis of a saturated recrystallized baryta solution and, when necessary, was subsequently freed from oxygen and hydrogen oxides by circulation past the heated platinum spiral K and through the phosphoric oxide tube.

### § 3. EXPERIMENTAL RESULTS AND CONCLUSIONS

*Series 1—Dry and moist hydrogen.* A puzzling feature of our work on the cathodic combustion of hydrogen was that, as has already been remarked, no evidence was found to justify the assigning of a direct rôle in combustion to the atomic hydrogen, which was known to be produced in considerable quantities. Accordingly it was decided to examine first the behaviour of hydrogen, dried as well as possible by circulation over phosphoric oxide, in the electrodeless discharge.

After a preliminary drying of the discharge tube walls by means of a prolonged circulation of dry hydrogen with the phosphoric oxide tube in the circuit, the filament K glowing and the discharge in action, the apparatus was evacuated and charged with dried hydrogen. It was then found that the hydrogen could be circulated through the discharge for long periods without any change in pressure and that, in the early stages of circulation, the spectrum (Figure 2\*) of the bluish-white discharge consisted mainly of the secondary spectrum due to neutral molecular hydrogen. The hydroxyl bands (2808 and 3064 Å.) and the more intense lines ( $\text{H}_{\alpha}$  6563,  $\text{H}_{\beta}$  4861 and  $\text{H}_{\gamma}$  4350 Å.) of the Balmer series, due to neutral atomic hydrogen, were visible but, with the exception of  $\text{H}_{\alpha}$ , were feeble compared with those of the secondary series. Also in evidence were a few mercury lines, in particular 2536, 3650 and 4358 Å. With increasing time of circulation and drying, during which precautions were taken to avoid shaking or otherwise disturbing the mercury in the McLeod gauge and the cut-offs associated with the main circulation system, the degree of dryness of the gas evidently improved until, except for the brilliant secondary series and the few mercury lines mentioned above, only the 3064 Å. hydroxyl band-head region and the red  $\text{H}_{\alpha}$  line still remained.

\* For Figures 2 to 6 see Plates.

visible. Thus it seems likely that, had it been possible to achieve a rigid drying of the hydrogen, the Balmer series and hydroxyl bands would have been eliminated.

These results confirm, in all essential respects, the experimental findings of Wood (1920, 1921, 1922 a, b), Copeland (1930), Poole (1937) and other workers. Wood concluded that atomic hydrogen was copiously formed in the discharge passing through dry hydrogen and attributed the virtual non-appearance of the Balmer series to a catalytic recombination of the atomic hydrogen to the molecular form at the dry walls of the vessel. Other workers have since accepted this hypothesis.

For the three following reasons, however, I have not been able to subscribe to this view without submitting it to the test of further experiment. In the first place, Wood and others worked with gas pressures of the order of 1 mm. ; it seems improbable, therefore, that any considerable proportion of hydrogen atoms formed in the discharge could arrive at the walls of the vessel without being excited and radiating, and thus giving rise to the Balmer series. Next, the catalytic inertness of cool, clean dry glass is well known, particularly to workers in the field of gaseous reactions in closed vessels. Thus Strutt (1911) found that the greenish glow of active nitrogen in a clean glass vessel persisted for several minutes after excitation, although it was extinguished almost instantaneously on introducing into the vessel a superficially oxidized copper wire. Finally, although the quantum theory indicates the possibility of the dissociation of the hydrogen molecule by electron impact, the necessary excitation energy would be 18 ev. (Mott and Massey 1933), and it is doubtful if such high energies were available in the ring discharge maintained under the conditions set forth above. The matter is one which was put to the test of crucial experiment as follows.

The pointed end of a glass needle was wetted to a length of about 3 mm. with diluted waterglass, dusted with yellow mercuric oxide powder, dried *in vacuo* and sealed into the discharge vessel probe port. The tip of the needle was about level with the contour of the discharge vessel so that, if any hydrogen atoms were formed in the discharge, some would reach the mercuric oxide-coated needle tip directly. The circulation system with the phosphoric oxide tube in circuit and the wire K at red heat was then filled with hydrogen which was circulated for 26 hours. The discharge was then started in the, by this time, relatively well-dried, oxygen-free hydrogen, and the circulation continued. At first no change could be seen in the appearance of the mercuric oxide ; it was not until after 20 minutes that the first signs of reduction, consisting in a blackening due to the formation of mercurous oxide, could be detected. The drying tube was then by-passed out of the circulation system and a little oxygen admitted to the reservoir contents, whereupon, within a few seconds, the yellow changed to black oxide and this, in turn, was quickly further reduced to minute droplets of mercury which slowly evaporated. In another experiment a similar procedure was followed, except that instead of oxygen about 2 per cent by volume of steam was added to the reservoir vessel contents. Here again the same remarkable acceleration in the rate of reduction of the mercuric oxide occurred. As will be shown later, the agent responsible for the reduction of both mercury oxides was atomic hydrogen.

It is difficult to resist drawing from these experimental results the conclusion that, apart from traces due to imperfect drying and revealed spectrographically, atomic hydrogen is not formed when an electrodeless discharge passes through dry hydrogen. Hence, the hitherto generally accepted view that the hydrogen

molecule is atomized by the discharge in dry hydrogen and that the absence of the Balmer spectrum is to be accounted for by a recombination to the molecular state at the surface of the discharge vessel is untenable. These experiments, of course, afford no information as to the relative activities of dry and moist glass surfaces in causing the recombination of hydrogen atoms to molecules; but they do show that dry hydrogen is not dissociated by the discharge, and that the minute amount of atomic hydrogen formed is attributable to that trace of moisture which can hardly be eliminated in an experiment of this kind carried out in an apparatus equipped with barometric mercury cut-offs.

*Series 2—The steam equilibrium.* Preliminary experiments in which steam had been circulated through the discharge, primarily with a view to outgassing the discharge vessel, had shown that much of the steam was decomposed and that the only other products received into the reservoir vessel consisted of hydrogen and oxygen in their combining proportions. In further such experiments steam was drawn through the discharge, and the products accumulated to a pressure of about 10 mm. in the previously evacuated reservoir, the cut-off between this and the discharge vessel being closed. On interrupting the steam supply and restoring the main circuit, no further change in pressure occurred, even after several hours' circulation. Analyses immediately before resumption of, or after, prolonged circulation revealed no change in the steam concentration, the remaining products always consisting of hydrogen and oxygen in their combining proportions. It is clear, therefore, that the steam dissociation equilibrium was attained in a single passage of the steam through the discharge and, further, that no gas was lost by, for example, combination with mercury.

In the course of these and other exploratory experiments it was also found that the extent of this dissociation was much affected by the state of the surface of the walls of the discharge vessel. For example, with clean walls and starting with either steam or the equivalent mixture of hydrogen and oxygen, the products at equilibrium contained between 16.5 and 19 per cent by volume of steam. On repeating such an experiment, but with a fine (37 s.w.g.) copper wire protruding into the discharge through the appropriate port, the wire glowed and the equilibrium steam concentration rose progressively in the course of five two-hour runs to between 38 and 40 per cent. By this time the walls of the discharge vessel near the wire were faintly discoloured, presumably by evaporated copper which may or may not have been oxidized. The glowing of the wire was due to some energetic surface reaction, and not merely to eddy-current heating, as was shown by the fact that on reducing the pressure in the discharge vessel, by closing the throttle and thus extinguishing the gas discharge, the wire at once ceased to glow. The wire was then removed and the port sealed off, whereupon further runs, in which equilibrium was approached sometimes from one side and sometimes from the other, continued to yield equilibrium steam concentrations approaching 40 per cent as before. Thus there was no tendency for this concentration to increase, as had been the case when the copper wire protruded into the discharge.

The discharge vessel was now cut out of the apparatus, cleaned with fuming nitric acid followed by chromic acid, washed with distilled water and finally dried with warm filtered air. The vessel was then re-sealed into the circulation apparatus, using dry filtered air for glass-blowing purposes. It was then found that this cleaning had restored the discharge vessel to its original state, equilibrium steam concentrations of about 18 per cent being once more obtained.

These results point to a promotion, by the copper stain on the discharge vessel walls, of some surface reaction or reactions which, either directly or through the products formed, favoured the formation of steam.

The reactants concerned must be relatively long-lived, because they survive passage from the discharge region to the vessel walls across the intervening discharge-free dark zone. Further, bearing in mind the evidence afforded by the glowing copper wire of the highly energetic nature of the reaction, and the testimony of the mercuric oxide probe experiments with moist hydrogen to the arrival of atomic hydrogen at the discharge vessel walls, it seems likely that the surface reaction is the recombination of atomic to molecular hydrogen, and that this may be, indeed, the dominating reaction increasing the equilibrium steam concentration. In other words, the formation of atomic hydrogen seems, somehow or other, to hinder the formation of steam.

Further light was thrown on these matters by the spectrograms (Figure 3) of the discharge in steam and its decomposition products. These are striking in that, apart from the relatively weak mercury spectrum, they consist of the Balmer series (3771, 3797, 3835, 3890, 3970, 4102, 4340, 4861 and 6562 Å.), the hydroxyl bands with heads at 2808 and 3064 Å., and the rather weak lines, 3947 and 4368 Å., due to atomic oxygen. The secondary molecular hydrogen spectrum is absent. Further, the presence or otherwise of copper deposited on the discharge vessel walls had no appreciable effect on the appearance of the spectrograms or on the relative intensities of the hydroxyl band and Balmer spectra, despite the profound effect exerted by the copper stain in the equilibrium steam concentration.

Wood and other workers have obtained spectra under conditions comparable to those outlined above, except that, instead of pure steam, they used moist hydrogen, the steam concentration being in general about 2½ per cent. Apart from the absence of all atomic oxygen lines, their spectra are essentially similar to those obtained in the present experiments. Thus, while Wood and others have shown that copious supplies of long-lived atomic hydrogen are obtained from the discharge in moist hydrogen, the above experiments demonstrate that atomic hydrogen is also freely produced when steam alone is fed to the discharge.

*Series 3---Steam-hydrogen mixtures.* In order to gain further insight into the mechanism of the formation of atomic hydrogen, experiments were now carried out in which a wide range of mixtures of hydrogen with steam, or with hydrogen and oxygen in their combining proportions, were circulated through the discharge. Before each such experiment, however, the circulation system was prepared in the following manner. Glass needles, the points of which had been coated with ash (mainly tin oxide and lime) by calcining a thin smear of sealing wax, were sealed into the three ports with their tips projecting into the tube between the discharge vessel and the McLeod gauge. Another ash-coated probe was sealed into the discharge tube port with its tip level with the contour of the vessel. Dry oxygen was then circulated under standard pressure conditions through the discharge. The reaction product reacted with mercury vapour to deposit in a few minutes broad rings or, rather, bands of yellow mercuric oxide about the openings leading to the McLeod gauge and the rare gas purifier, and just above the entry to the pump,  $P_1$ . The apparatus was then evacuated and the circulation system, with the phosphoric oxide tube in circuit, swept out and finally charged with roughly dried hydrogen, which was then still further dried by prolonged circulation during which the platinum spiral, K, was glowing. Throughout

these operations the mercuric oxide films remained unchanged. The discharge was now started and spectrographed. Apart from the strong secondary molecular spectrum and the usual lines due to traces of mercury, only the  $H_{\alpha}$  (moderate to weak),  $H_{\beta}$  (weak) and  $H_{\gamma}$  (very weak) lines of the Balmer series and the hydroxyl 3064 Å. band-head region were visible. The circulating gas had no visible effect on any of the probes coated with sealing-wax ash; likewise, the mercuric oxide films near the McLeod gauge and the pump were unchanged, even after two hours' circulation.

The apparatus was now evacuated, and the normal circulation route restored and filled to the usual pressures with the required mixture of hydrogen and steam. After a sufficiently prolonged circulation to ensure thorough mixing of the gases, the discharge was started. The range of mixtures examined extended from steam alone to steam (or the equivalent hydrogen-oxygen mixture) diluted with up to 95 per cent of hydrogen. Spectrograms were obtained in each case under uniform conditions of exposure and development. The sealing-wax ash probe inserted through the discharge vessel port was withdrawn after the first experiment and was not replaced.

The results of this series are illuminating. In the first experiment, carried out with steam alone, the mercuric oxide films, including that near the mercury vapour pump inlet, about  $1\frac{1}{2}$  metres beyond the discharge vessel, were completely reduced within a few minutes of starting the discharge. The progress of such reduction could, however, be immediately arrested by interrupting the discharge. Further, the particles of ash on the discharge vessel probe and on the two probes nearest to the discharge vessel flashed into incandescence immediately the discharge was started, but ceased to glow when this was interrupted. From time to time glowing fragments of ash would fly off the probes, particularly that in the discharge vessel, and these continued to incandesce after lodging on the wall of the vessel or in the tube beyond it. Indeed, owing to this stripping-off of the ash, the section of tubing carrying the first two ports beyond the discharge vessel had to be removed for cleaning after each experiment and fresh ash-coated probes inserted in preparation for the next. As stated above, the discharge vessel probe was removed and not replaced after the first experiment.

The incandescence of the ash on the second probe beyond the discharge vessel was less brilliant than that of the first probe and, in the case of the third probe some 50 cm. beyond the discharge vessel, an ash particle would sometimes glow, but only in mixtures containing initially between about 30 and 60 per cent of hydrogen.

The spectrograms were similar to those obtained with pure steam (Figure 3), except that the atomic oxygen lines, 3947 and 4368 Å., seemed to weaken with increasing hydrogen concentration; they no longer appeared in a spectrogram from the discharge in a mixture of steam and hydrogen in equal volumes. Visual comparison of the spectrograms, more particularly of the hydroxyl band 2808 Å. with H 3797 and H 3835 Å., and of the hydroxyl band 3064 Å. with H 3890 and H 3970 Å., revealed no change with increasing hydrogen concentration in the relative intensities of the hydroxyl band and Balmer series spectra.

Finally, it was found that the steam equilibrium constant decreased with increasing dilution of the mixture by hydrogen. For example, with steam alone the constant  $K = (H_2O)^2 / [(H_2)^2 \cdot (O_2)] = 0.46$ , but was 0.38 and 0.25 in the case of mixtures diluted with 55 and 69 per cent of hydrogen respectively. Thus,



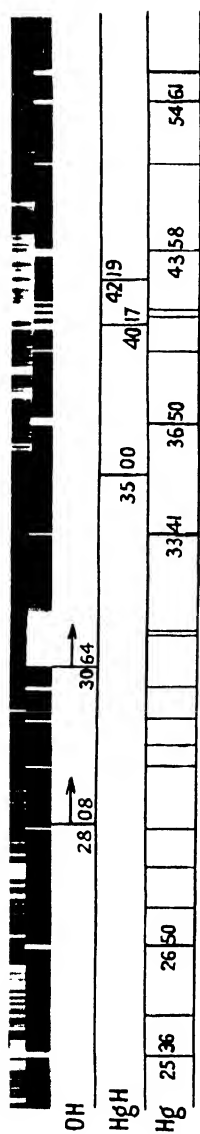


Figure 4. Steam and mercury vapour.

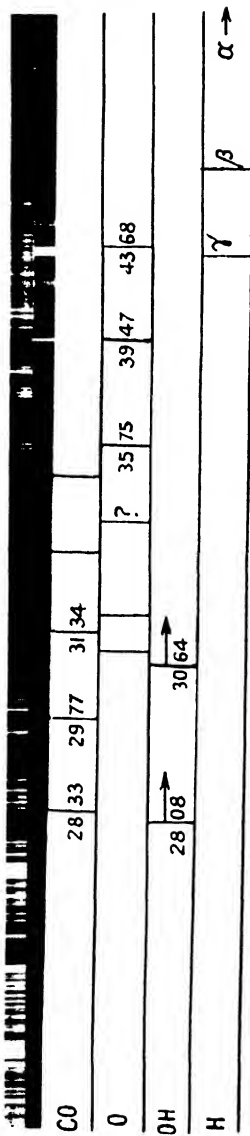


Figure 5. Roughly dried oxygen.

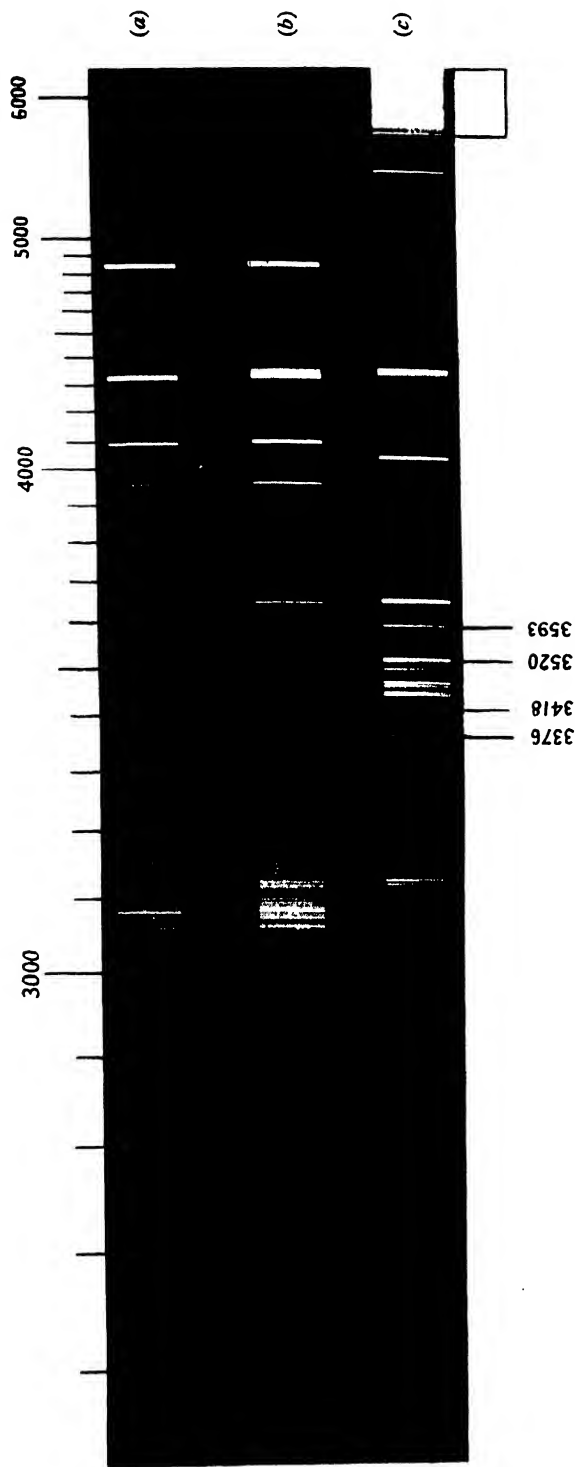


Figure 6. (a) Steam; (b) 50% steam and 50% neon; (c) neon.





although dilution with hydrogen did, in fact, greatly reduce the dissociation of the steam by the discharge, it did not do so to the extent required by the law of mass action.

The reason is not far to seek. The results of these experiments as a whole now afford overwhelming evidence that the first step towards equilibrium in steam or in a steam-hydrogen mixture is the direct dissociation of the steam into hydroxyl and atomic hydrogen. The molecular hydrogen as such is not dissociated by the discharge and, when steam is present in adequate supply (which may possibly be considerably less than 5 per cent), either the hydrogen is not excited or it reacts in some way before it can radiate. This dissociation of steam must be practically irreversible in the gaseous phase, because quantum energy considerations forbid the reverse reaction by which atomic hydrogen and hydroxyl might recombine to form steam, except as a result of necessarily infrequent three-body collisions. Similar considerations apply in the case of the union of hydrogen atoms to the molecular state. On the other hand, the life of the hydroxyl radical (Bonhoeffer and Pearson 1931, Geib and Harteck 1934, Oldenberg 1937) can be terminated by two-body collision processes such as, for example,  $2\text{OH} = \text{H}_2\text{O} + \text{O}$ , and  $\text{OH} + \text{H}_2 = \text{H}_2\text{O} + \text{H}$ . Thus the fall in the steam dissociation equilibrium constant with increasing dilution by hydrogen is to be accounted for by the practically irreversible formation, and hence escape, of atomic hydrogen from the reaction zone.

There is evidence from the above experiments that the hydroxyl reacted in the discharge in both the ways suggested. That the first reaction occurred is supported by the appearance of oxygen atom lines in the spectrograms from the discharge in steam, and by their weakening and final disappearance on progressive dilution with hydrogen. As for the second reaction, in which hydroxyl interacts with hydrogen, the likelihood of its occurrence is supported by the following facts and considerations. In the first place, the relative intensities of the hydroxyl and Balmer spectra (Figure 3) were independent of hydrogen dilution of steam over a wide range. This strongly supports the previous conclusion, that the sole primary source of atomic hydrogen is the direct dissociation of steam in the discharge. Next, the fact that the third sealing-wax ash probe glowed only in mixtures of steam diluted by a roughly equal proportion of hydrogen shows that the yield of atomic hydrogen was increased by such dilution. Hence the diluent hydrogen must itself contribute in some way to the ultimate yield of atomic hydrogen. Since, as has already been shown, atomic hydrogen cannot have been produced by direct dissociation of molecular hydrogen, the probable source of this contribution lies in the interaction in the discharge of hydroxyl and molecular hydrogen, whereby atomic hydrogen and steam are formed. This view received strong support from the results, which showed that the recombination of atomic hydrogen at the copper-stained walls of the discharge vessel increased the steam equilibrium concentration by returning molecular hydrogen to the discharge and thus reducing the amount escaping in the atomic state from the reaction zone. The possibility of a surface reaction between hydroxyl and atomic hydrogen in similarly affecting the steam equilibrium will be considered later.

The results of this series of experiments furnish ample evidence of the significance to be attached to the probe and mercuric oxide reactions. Thus, when the discharge was fed with steam, steam diluted with hydrogen, or the equivalent hydrogen-oxygen mixtures, the mercuric oxide films were rapidly reduced, and

the sealing-wax ash probes incandesced with a brilliancy which increased as the discharge vessel was approached. Further, all these phenomena ceased immediately the discharge was interrupted, irrespective of whether the circulating gas was steam (or the equivalent hydrogen-oxygen mixture) alone or diluted with hydrogen. Therefore the agent reducing the mercuric oxide could not have been molecular hydrogen, nor could the reaction catalysed by the ash have been the union of hydrogen and oxygen to steam. In addition to the normal equilibrium products entering the reservoir vessel, the only other products for which there is evidence of formation in the discharge are atomic hydrogen, hydroxyl and hydrogen peroxide (Finch and Mahler 1931). Atomic oxygen can be excluded because, although revealed spectrographically in the case of steam traversing the discharge, it was eliminated by sufficient dilution of the reaction mixture with hydrogen. Hence, whereas the reduction of the mercuric oxide films can only be attributed to atomic hydrogen, the incandescence of the ash-coated probes might be ascribed either to the formation of molecular hydrogen or to the interaction of atomic hydrogen with hydroxyl to form steam. The heat evolutions of these reactions are similar, being about 103,000 kcal/gm. mol (see Steacie 1946). Whilst there is no doubt about the longevity of atomic hydrogen, the situation in regard to the life of hydroxyl, though known to be much shorter than that of atomic hydrogen, is less clear. Thus, while Bonhoeffer and Pearson (1931) were unable to find the radical in the gas flowing from a discharge through water vapour, Frost and Oldenberg (1936), using a 21-foot grating, detected hydroxyl for as long as  $\frac{1}{3}$  second after their discharge in steam was interrupted. Thermal conditions may, however, have contributed to this result. The reduction of the mercuric oxide probe in the discharge vessel port, when the discharge took place in moist hydrogen, would be difficult to explain if hydroxyl arrived at the probe, and hence also at the surface of the vessel, at a rate comparable with that of the atomic hydrogen. Thus the evidence so far supports the view that the incandescence of the ash-coated probes was due to the recombination of atomic hydrogen. This issue was further tested in the next series of experiments.

Of the three ash-coated probes, all of which were much nearer to the discharge vessel than were the mercuric oxide films, the first two incandesced regularly, whilst the third did so spasmodically, and then only under the most favourable conditions. It would seem that, whilst the reduction of the mercuric oxide film formed a sensitive test for the presence of atomic hydrogen, the sealing-wax ash probes could respond only to a relatively high concentration.

*Series 4—Further probe experiments.* In the first experiment of this series a closely wound spiral nearly 1 cm. in diameter, of 28 s.w.g. copper wire, was inserted into the exhaust tube leading from the discharge vessel. The spiral, previously cleaned and reduced by hot hydrogen, extended from near the second port, which was fitted with a mercuric oxide-coated probe, to within 0.5 cm. from the discharge vessel. The equilibrium steam concentration was then determined, starting with steam or the equivalent hydrogen-oxygen mixture. The mean steam yield from eight such runs was 19.2 per cent, a value which did not differ significantly from that (18.9 per cent) afforded by a similar series of runs carried out before inserting the spiral. The presence of the copper spiral, however, practically inhibited the reduction of the mercuric oxide, thus showing that the bulk of the atomic hydrogen leaving the discharge vessel was, on passing through the spiral, transformed to the molecular state. This, together with the fact that the steam yield was virtually unaffected by the presence or otherwise of

the spiral, proves conclusively that hydroxyl could not have survived long enough after leaving the discharge to reach the spiral in appreciable quantities ; otherwise the equilibrium steam concentration must have increased, which it did not do. Hence these results confirm that the ash incandescence observed in the previous experiments was due solely to recombination of atomic hydrogen.

The spiral was now removed and the corresponding tube section cleaned and re-fused into the apparatus. The glass pinch of a tungsten filament lamp was then sealed into the first probe port beyond the discharge vessel, the lamp filament having been replaced by a 2.5 cm. long fine (37 s.w.g.) platinum wire and the current-carrying posts shrouded with quill tubing. The wire projected in the form of a hoop into the path of the gas stream from the discharge vessel.

In the next experiment a mixture of hydrogen and oxygen was circulated under normal conditions but without the discharge, the phosphoric oxide tube being included in the circulation path. After drying the gas in this manner until the manometer readings were steady, the platinum filament was brought to a bright red heat and circulation continued. The McLeod gauge readings then fell from the steady value of 0.027 mm., obtained before heating the filament, to 0.019 mm., thus clearly indicating that steam was being formed as a result of a surface union of hydrogen and oxygen on the heated platinum wire. This was further confirmed by a progressive fall in the reservoir manometer readings as circulation proceeded. On interrupting the heating current, the wire immediately cooled and the McLeod gauge reading rose to its previous steady value of 0.027 mm. Evidently the rate of heat evolution during the formation of steam at this low pressure was not sufficient to compensate for the heat losses from the wire, which in consequence cooled and ceased to catalyse the reaction. Immediately the discharge was started, however, the platinum filament began to glow brightly, but cooled at once when the discharge was switched off. That the heating of the wire must have been due solely to the recombination of atomic hydrogen, and not to heating of the filament by the high-frequency field exciting the discharge, was shown by the fact that the wire cooled immediately the discharge was interrupted by closing the throttle admitting gas into the discharge vessel.

The difference in behaviour of the platinum wire in atomic hydrogen and in a mixture of hydrogen and oxygen in equivalent proportions finds a natural explanation in the heat evolution of the appropriate reactions, the heat of formation of molecular hydrogen being 103,000 kcal/gm. mol, while that of steam is only about 59,000.

Further experiments were carried out with, in place of the platinum filament, a probe consisting of a straight length of either 36 s.w.g. tungsten or 37 s.w.g. copper wire protruding into the gas stream from a glass rod sealed into the port adjacent to the discharge vessel. When steam was fed to the discharge, these wires glowed dull red. With a mixture of steam and hydrogen in equal proportions, the copper wire became bright red and the tungsten wire was even hotter.

Wood (1922a) also found that a tungsten wire glowed in atomic hydrogen ; he did not however obtain such an effect with a platinum wire. This may have been due to the state of the surface of his wire. It is a common experience that catalysing the combustion of a mixture of hydrogen and oxygen at a bright red heat not only cleans and activates a platinum surface but also roughens it.

*Series 5—Steam-mercury vapour mixtures.* At the conclusion of the experiments of Series 3 the question was left open as to whether or not the effect of the copper-staining of the discharge vessel walls in promoting a high yield of

steam might be due, not only to the returning of molecular hydrogen to the reaction zone, but also to a surface reaction between atomic hydrogen and hydroxyl. In previous work on cathodic combustion (Finch 1935) it had been suspected that mercury vapour facilitated the combustion of hydrogen. This, and the fact that mercury vapour can play an important rôle in photosynthesized reactions involving hydrogen (Taylor and Bates 1926, Rieke 1936, Olsen 1938), suggested that its use might throw light on the present problem. Accordingly arrangements were made to examine the effect of mercury vapour additions to steam passing through the ring discharge.

About 0.5 cm<sup>3</sup> of mercury was distilled into the discharge vessel port tube through a branch tube, which was then sealed off close to the port tube. A few turns of resistance wire wrapped round the port tube and immersed in an oil-filled jacket enabled the mercury to be warmed. An ash-coated probe was inserted through the first port beyond the discharge vessel. Mercuric oxide films were then formed, in the manner previously described, at the usual places where the circulating gas stream came in contact with stagnant mercury vapour. A similar deposit also formed about the entry to the discharge-vessel port tube.

Steam (or the equivalent hydrogen-oxygen mixture) was then circulated along the usual path under the normal pressure distribution of 0.026 mm. in the discharge vessel and 7 or 10 mm. in the reservoir, according to the nature of the gas mixture used. The mercury in the discharge port vessel was then gently heated and maintained at between 40 and 45°C. When steady conditions had been attained, the discharge was started. Instead of a rose-pink ring, it now formed an apparently uniform bluish-green sphere. A rough estimate afforded by the increased damping of the oscillation circuit suggested that the partial pressure of mercury vapour was between 0.005 and 0.012 mm., probably nearer the former. Despite this, no condensation occurred anywhere between the discharge vessel and the pump though, with time, a barely perceptible brownish band formed on the discharge vessel walls coaxial with the solenoid.

The mercury vapour exerted a profound effect on the results. The ash-coated probe did not incandesce and, although the mercuric oxide film near the discharge vessel port had disappeared within five minutes of starting the discharge, the more remote films were only very slowly reduced. Also, the equilibrium steam concentration, which previously had been between 18 and 19.4 per cent, was now practically 100 per cent, irrespective of the direction of approach to equilibrium. Finally, the spectrogram (Figure 4) of the discharge differs strikingly from that obtained with steam or steam-hydrogen mixtures (Figure 3). Apart from the strong, well-developed mercury line spectrum, its main features are the 2808 and 3064 Å. hydroxyl bands, the latter being intense, and the three mercurous hydride line groups 3500, 4017 and 4219 Å. Neither the secondary hydrogen nor the Balmer spectra appear.

These results show that the effect of the mercury vapour was largely to suppress the formation of atomic hydrogen, thereby shifting the equilibrium so far towards the steam side that the reaction products consisted almost wholly of steam. Thus the evidence suggests that steam is reduced, reversibly, by mercury to mercurous hydride and hydroxyl. In view of the high intensity of the 2536 Å. mercury line [ $\text{Hg}(6^3\text{P}_1)$ ] the reduction of mercury by hydrogen to mercurous hydride and atomic hydrogen is also likely to occur. Again, since mercury is

oxidized by ozone to mercuric oxide, and this in turn is reduced in the cold by atomic hydrogen and by molecular hydrogen at about 120°c. (Manchot and Kampschulte 1907, 1910), further probable reactions are the oxidation of mercurous hydride to mercuric oxide and hydroxyl, and the reduction of mercuric oxide by atomic or molecular hydrogen to mercury and hydroxyl or steam respectively. In addition, the short life of hydroxyl is terminated in the manner set forth in Series 3 and 4 of the above experiments.

The question is still left open as to whether the survival life of hydroxyl is sufficient for it to interact with atomic hydrogen at the walls of the discharge vessel; the results of Series 4 show, however, that this reaction does not occur at surfaces beyond the discharge vessel.

*Series 6—Dry and moist oxygen mixtures.* The behaviour of oxygen, both dry and moist (or diluted with hydrogen), in various types of discharges, including the ring discharge, has been the subject of much experimental work. In general, a broad measure of agreement has been reached as to findings and conclusions. In one respect, however, a conflict of views does exist. Harteck and Kopsch (1931), Geib and Harteck (1934), Geib (1938) and others incline to the belief that, like atomic hydrogen, atomic oxygen has a relatively long life. On the other hand, Strutt (1910) and Finch and Bradford (1934) froze out ozone from the gas issuing from a discharge fed with dry oxygen, but found no evidence of the survival of atomic oxygen. All these workers appear to have used discharges between electrodes. Copeland (1930), however, used an electrodeless discharge, and concluded that atomic oxygen not only has a life comparable with that of atomic hydrogen but is also formed in the discharge by a mechanism similar to that postulated by Wood, whereby a poisoning of the discharge vessel walls by moisture was supposed to be necessary for the survival of the atomic species. It has, however, already been mentioned above that mercuric oxide films were formed after a brief circulation of oxygen through the discharge. These films were as readily obtained with dry as with moist oxygen. Thus if, as Copeland held, they were due to the interaction of mercury vapour and atomic oxygen, their formation with dry oxygen conflicted with his hypothesis. It was therefore decided to examine the matter further.

Owing to the difficulty of removing stains, caused by the experiments of Series 5, from the discharge vessel without etching the glass and thus impairing its smooth surface, a new vessel was fitted. It had previously been cleaned in the usual way but not baked out or degassed by circulating steam through the discharge. After fitting the first port beyond the discharge vessel with an ash-coated probe and the discharge vessel port with a 36 s.w.g. tungsten wire protruding into the discharge region, the normal circulation system was filled with oxygen previously washed with concentrated caustic potash and roughly dried by a single passage over phosphoric oxide. The gas was then circulated through the discharge under the normal conditions of pressure.

Rapid formation of the mercuric oxide films again occurred and was followed more slowly by a "tailing" of the mercury in the pump boiler. Neither the ash-coated nor the tungsten probe showed any signs of incandescence. The "tailing" and mercuric oxide films were easily removed by reduction, in the manner previously described, with atomic hydrogen formed from a hydrogen-steam mixture in equal proportions. A spectrogram, taken about half an hour after

starting the discharge, is reproduced in Figure 5. It reveals, *inter alia*, a fairly strong atomic oxygen spectrum, faint hydroxyl bands, the first three lines of the Balmer series, and prominent bands due to carbon monoxide.

On repeating this experiment, a spectrogram similar to Figure 5 was obtained, but without the carbon monoxide spectrum. It would appear, therefore, that in the first experiment of this series the circulation of oxygen through the discharge had effectively out-gassed the discharge vessel walls. A fresh charge of oxygen was circulated for several hours past the heated spiral K and through the drying tube before starting the discharge, and a further spectrogram taken. This was again similar to Figure 5, except that, in addition to the absence of the carbon monoxide spectrum, the 3064, but not the 2808 Å., hydroxyl band-head region was visible.  $H_\beta$  of the Balmer spectrum was very faint.

It will be evident at once that, in affording the primary (atomic) spectrum, the behaviour of dry oxygen in the ring discharge differed radically from that of dry hydrogen which, in the main, yielded the secondary spectrum, with weak hydroxyl bands and a few faint lines of the Balmer series attributable to traces of moisture.

It is noteworthy that, despite the spectrographic evidence of the production of atomic oxygen in the discharge, the tungsten and ash-coated probes remained cool throughout. Since the heat of formation of molecular oxygen ( $>117,000$  kcal/gm. mol.) is greater than that of hydrogen, it is plain that little or no atomic oxygen survived to reach the ash probe, only 5 cm. beyond the discharge vessel, or even the tungsten wire probe. It is most unlikely, therefore, that the mercuric oxide films, which had formed so rapidly, could have been due to the interaction of mercury vapour and atomic oxygen, as Copeland has supposed. Rather must this phenomenon be ascribed to some other active modification of oxygen.

In the next experiments the effect of the dilution of oxygen by steam was examined. A wide range of mixtures was used containing between 5 and 96 per cent steam, the remainder being oxygen. The results have so much in common that it will suffice to summarize them as follows:

(i) Mercuric oxide films were formed, as with dry oxygen, at the usual sites, and "tailing" in the pump also occurred. The rate of formation of the mercuric oxide, as estimated from the growth in density of the film near the McLeod gauge, was roughly proportional to the oxygen concentration.

(ii) The ash-coated probe incandesced to some extent in all cases, but did so most vigorously in mixtures rich in steam. The tungsten wire probe glowed brightly in all cases.

(iii) The spectrograms reveal a progressive weakening of the atomic oxygen spectrum with increasing steam concentration, but a few lines, notably 3947 and 4368 Å., remain, even in the case of pure steam. The hydroxyl band and Balmer spectra are prominent throughout.

It has already been shown in the case of dry oxygen that the formation of the mercuric oxide films was due to some active form of oxygen, other than atomic oxygen, which was incapable of exciting either the ash-coated or tungsten wire probe to incandescence. Hence, the fact that this oxidation process was slowed down by progressive dilution of the oxygen with steam strongly suggests that in the cases of both dry and moist oxygen the same agent was responsible for the oxidation of mercury. The results obtained by Strutt (1911) and Finch and Bradford (1934), taken into consideration with the fact that ozone is known to form

yellow mercuric oxide with mercury (Manchot and Kampschulte 1907, 1910), justify the assumption that ozone was the long-lived, active form of oxygen produced in these experiments.

Since the ash probe and, to a lesser extent, the tungsten wire incandesced more brightly with increasing dilution with steam, it is evident that this could only have been due to recombination of atomic hydrogen. That the phenomena of the probe incandescence and mercuric oxide formation occurred simultaneously, even in mixtures containing as little as 5 per cent of oxygen, suggests that atomic hydrogen and ozone interact in the gas phase only relatively slowly, if at all, under the conditions of our experiments.

In the light of these results we are forced to conclude that, unlike atomic hydrogen, atomic oxygen does not survive as such on escaping from the discharge. There is a ready explanation for this. Thomson and Thomson (1928) point out that, unlike hydrogen, the oxygen molecule readily captures an electron to form a negative ion. It is to be expected that the oxygen atom is even more efficient in this respect. There is ample opportunity for such capture to occur within the discharge, where the electron population is of the same order as that of the molecules present (Thomson 1928). Under these circumstances, two-body collision reactions, such as the recombination of oxygen atoms to molecular oxygen, or of oxygen atoms with molecules to form ozone, are no longer subject to quantum-mechanical restrictions, provided one or both of the reactants is a negative ion.

*Series 7—Neon-steam mixtures.* This series of experiments forms, in a sense, a continuation of Series 6, the oxygen component being, however, replaced by a rare gas. It was hoped that a comparison of the results of the two sets of experiments would throw further light on, *inter alia*, the apparent strange reluctance of atomic hydrogen and ozone to interact. The experiments were carried out with mixtures covering a range from well-dried neon to pure steam.

The essential results can be summarized briefly by stating that (i) the intensity of the incandescence of the ash and tungsten wire probes increased with increasing steam concentration in a manner which closely paralleled that observed in the case of the corresponding oxygen-steam mixtures and, (ii) unlike the case of steam-diluted oxygen, the spectrograms (Figure 6) show that on increasing the steam concentration the neon spectrum was quickly suppressed. For instance, in a mixture of neon and steam in equal proportions only the hydroxyl and Balmer series spectra are visible.

The parallel behaviour of the probes in the two series supports the conclusion that in the case of both oxygen and neon-steam mixtures incandescence of the probes was caused solely by atomic hydrogen and, further, that atomic hydrogen and ozone are, for some unknown reason, slow to react with each other. It is also not difficult to see that, except for the formation or otherwise of mercuric oxide, the experimental results which led Copeland to suppose that atomic oxygen of long life is formed by the action of the electrodeless discharge on moist oxygen could equally well have been obtained with moist neon.

#### § 4. SUMMARIZED FINDINGS AND CONCLUSIONS

The behaviour of steam or a mixture of hydrogen and oxygen in combining proportions, and their mixtures with hydrogen or oxygen, ranging from dry hydrogen to dry oxygen, have been studied in the ring discharge. The effect of mercury vapour and of neon on the steam equilibrium was also examined.



The principal facts established were as follows :

(i) *Dry hydrogen.* The secondary hydrogen spectrum was strongly emitted. The hydroxyl-band and Balmer spectra were weak and tended to disappear with progressive drying. Apart from traces attributable to incomplete drying, no agent capable of reducing yellow mercuric oxide at room temperature reached the walls of the discharge vessel.

(ii) *Moist hydrogen.* On adding to dry hydrogen about 1 per cent of oxygen or 2 per cent of steam (and possibly much less) the spectrum changed radically, the secondary hydrogen spectrum being replaced by the hydroxyl-band and Balmer spectra. Mercuric oxide at the wall of the discharge vessel was rapidly reduced.

(iii) *Steam.* The emission consisted mainly of the hydroxyl-band and Balmer spectra, together with a few lines due to atomic oxygen.

The stable end-products obtained from steam (or the equivalent hydrogen-oxygen mixture) consisted of steam, hydrogen and oxygen, the last two in their combining proportions. With a clean discharge vessel, the final steam concentration was between 16.5 and 19 per cent, but partial contamination of the vessel's walls by a barely visible film of copper sufficed to more than double the steam yield, which, however, returned to its previous value after removal of the copper film.

Glass needles, coated with sealing-wax ash ( $\text{SnO}$  and  $\text{CaO}$ ) and inserted into the exhaust tube through ports situated 5 and 20 cm. beyond the discharge vessel, incandesced brightly. Films of yellow mercuric oxide deposited in the exhaust tube were rapidly reduced to metallic mercury. Copper, tungsten or platinum wire probes in the discharge vessel or in the exhaust tube glowed. The insertion of a copper wire spiral into the exhaust tube between the discharge vessel and an ash-coated probe suppressed the incandescence of the probe and practically stopped the reduction of the mercuric oxide films. The spiral did not appreciably affect the equilibrium steam concentration. With the ring discharge interrupted, an electrically heated platinum wire probe, situated in the exhaust tube near the discharge vessel, catalysed the formation of steam from the equivalent hydrogen-oxygen mixture, but ceased to do so and cooled when the heating current was stopped. The wire glowed spontaneously, however, immediately the ring discharge was restored.

(iv) *Steam-hydrogen and the equivalent hydrogen-oxygen mixtures.* The hydroxyl-band and Balmer spectra were prominent in all mixtures containing up to 95 per cent (and possibly more) diluent hydrogen, and their relative intensities appeared to be independent of such dilution. On increasing dilution with hydrogen, the atomic oxygen lines observed with steam alone weakened and eventually disappeared.

Dilution with hydrogen reduced the dissociation of steam, but not to the extent required by the law of mass action.

The ash-coated probes incandesced and the mercuric oxide films were reduced in all mixtures examined, incandescence being most pronounced in the case of mixtures containing hydrogen and steam in roughly equal proportions.

(v) *Steam-mercury vapour.* Apart from an intense mercury spectrum, the emission from the ring discharge in a mixture of steam (or the equivalent hydrogen-oxygen mixture) with roughly one-third its volume of mercury vapour consisted chiefly of the hydroxyl-band and mercurous-hydride spectra. The Balmer and secondary hydrogen spectra were absent. The ash probes did not incandesce.

The mercuric oxide films in the exhaust tube were only slowly reduced. In contrast to the steam yield of about 18 per cent obtained with pure steam, the equilibrium steam concentration rose to nearly 100 per cent.

(vi) *Dry oxygen.* The emission consisted mainly of the atomic oxygen spectrum, with faint hydroxyl-bands and a few faint lines of the Balmer series attributable to traces of moisture.

Yellow mercuric oxide was formed in the exhaust tube at all those sites where the gas stream issuing from the discharge came into contact with stagnant mercury vapour. The wire and ash-coated probes remained cool.

(vii) *Oxygen-steam.* The atomic oxygen spectrum weakened with increasing dilution by steam, but a few lines remained even with pure steam. The hydroxyl-band and Balmer spectra were prominent throughout.

Mercuric oxide films were formed, as with dry oxygen, even in mixtures containing only 5 per cent of oxygen. The ash-coated probes incandescenced in all mixtures containing up to 95 per cent oxygen, but were brightest in steam-rich mixtures.

(viii) *Neon-steam.* The hydroxyl-band and Balmer spectra only gave way to the neon spectrum as the neon concentration approached 100 per cent. The behaviour of the ash-coated and wire probes was similar to that observed in the case of the corresponding oxygen-steam mixtures, in that the incandescence effect increased with increasing steam concentration.

The following conclusions have been drawn :

Dry molecular hydrogen is not dissociated but only excited in the ring discharge. The generally accepted view, according to which atomic hydrogen is formed and the absence of the Balmer spectrum is due to recombination of the atoms on the walls of the discharge vessel, is therefore untenable.

Atomic hydrogen issues in considerable quantity from the discharge in steam, hydrogen-steam or hydrogen-oxygen mixtures. The incandescence of ash-coated probes, and the spontaneous glowing of copper, tungsten, or platinum wires in the gases drawn from the discharge testify to a high concentration of atomic hydrogen, whilst the reduction of mercuric oxide films serves as a more sensitive test. It is unlikely that moisture adsorbed on the walls of the discharge vessel materially affects the yield of atomic hydrogen ; for, if it did, it should also cloak the catalytic activity of a thin copper film, which it does not do.

The following reactions take place in hydrogen-steam and the equivalent hydrogen-oxygen mixtures. Steam is dissociated into hydroxyl and atomic hydrogen. The reverse reaction cannot proceed except through three-body collisions, and is therefore practically excluded. The same is true of the union of hydrogen atoms to molecules ; consequently atomic hydrogen has a long survival life. On the other hand, the life of hydroxyl is short and is terminated by reacting with molecular hydrogen to form steam and atomic hydrogen, and with hydroxyl to form steam and atomic oxygen. Owing to the ease with which oxygen atoms form negative ions, they revert quickly to the molecular state. Finally, hydrogen reacts with oxygen to form steam and atomic oxygen. Some hydrogen peroxide may also be formed, but mainly at surfaces.

Dry oxygen, unlike dry hydrogen, is dissociated directly into atomic oxygen, which has a short life and quickly reacts within the discharge to form molecular oxygen and ozone. With stagnant mercury vapour, ozone forms films of yellow mercuric oxide. All the reactions occurring in oxygen and in hydrogen-steam mixtures also take place in oxygen-steam and the equivalent oxygen-hydrogen

mixtures ; thus ozone and atomic hydrogen appear together in the effluent gases and interact, if at all, very slowly. The phenomena of the formation of mercuric oxide and the heating of ash-coated probes and wires in oxygen-steam mixtures are due to ozone and atomic hydrogen respectively, and are not evidence, as hitherto supposed, of a long life of oxygen in the atomic state.

The products leaving the ring discharge fed with a mixture of steam (or the equivalent hydrogen-oxygen mixture) and sufficient mercury vapour consist almost wholly of steam ; only traces of atomic hydrogen are present. In this case the steam is no longer directly dissociated into hydroxyl and atomic hydrogen, but reacts with mercury to form hydroxyl and mercurous hydride. Other reactions occurring are the oxidation of mercurous hydride to form mercuric oxide and hydroxyl, the reduction of mercuric oxide by atomic (or molecular) hydrogen to mercury and hydroxyl (or steam), the reduction of mercury by molecular hydrogen to mercurous hydride and atomic hydrogen, and the formation of steam and atomic oxygen from hydroxyl.

In neon-steam and the equivalent neon-hydrogen-oxygen mixtures, the reactions are similar to those occurring in steam.

#### ACKNOWLEDGMENTS

I have received much help in this study and wish to thank in particular Dr. E. E. Thompson and Dr. A. E. W. Austen, who carried out much of the experimental work, and Dr. R. W. B. Pearse, who checked the analyses of the spectrograms. My thanks are also due to Messrs. Ferranti for financial support of the work.

#### REFERENCES

- BONHOEFFER, K. F., and PEARSON, T. G., 1931, *Z. phys. Chem.* **B14**, 1.  
 COPELAND, L. C., 1930, *Phys. Rev.*, **36**, 1221.  
 ESCLANGEN, F., 1934, *Ann. Phys., Paris*, **11**, 267.  
 FINCH, G. I., 1935, *J. Chem. Soc.*, 32.  
 FINCH, G. I., and BRADFORD, B. W., 1934, *J. Chem. Soc.*, 360.  
 FINCH, G. I., and FRASER, R. P., 1926, *J. Chem. Soc.*, 117.  
 FINCH, G. I., and MAHLER, E. A. J., 1931, *Proc. Roy. Soc. A*, **133**, 173.  
 FROST, A. A., and OLDENBERG, O., 1936, *J. Chem. Phys.*, **4**, 642.  
 GEIB, K. H., 1938, *Z. Elektrochem.*, **44**, 81.  
 GEIB, K. H., and HARTECK, P., 1934, *Trans. Faraday Soc.*, **30**, 134.  
 HARTECK, P., and KOPSCH, U., 1931, *Z. phys. Chem.*, **B12**, 327.  
 MACKINNON, K. A., 1929, *Phil. Mag.*, **3**, 605.  
 MANCHOT, W., and KAMPSCHULTE, W., 1907, *Chem. Ber.*, **40**, 2891; 1910, *Ibid.*, **43**, 750.  
 MOTT, N. F., and MASSEY, H. S. W., 1933, *Atomic Theory of Collisions* (Oxford : Clarendon Press), p. 214.  
 OLDENBERG, O., 1937, *J. Phys. Chem.*, **41**, 293.  
 OLSEN, L. O., 1938, *J. Chem. Phys.*, **6**, 307.  
 POOLE, H. G., 1937, *Proc. Roy. Soc. A*, **163**, 404.  
 RIEKE, F. F., 1936, *J. Chem. Phys.*, **4**, 513.  
 SOUTHWORTH, G. C., 1920, *Radio Rev.*, **1**, 583.  
 STEACIE, E. W. R., 1946, *Atomic and Free Radical Reactions* (New York : Reinhold).  
 STRUTT, R. J., 1910, *Proc. Phys. Soc.*, **23**, 66; 1911, *Proc. Roy. Soc. A*, **85**, 226.  
 TAYLOR, H. S., and BATES, J. R., 1926, *Proc. Nat. Acad. Sci., Wash.*, **12**, 714.  
 THOMSON, J. J., 1928, *Proc. Phys. Soc.*, **40**, 79.  
 THOMSON, J. J., and THOMSON, G. P., 1928, *Conduction of Electricity through Gases* (Cambridge : University Press), 3rd ed., p. 242.  
 WOOD, R. W., 1920, *Proc. Roy. Soc. A*, **97**, 455; 1921, *Phil. Mag.*, **42**, 729; 1922 a, *Ibid.*, **44**, 538; 1922 b, *Proc. Roy. Soc. A*, **102**, 1.

# The Significance of the Observation of Intense Radio-Frequency Emission from the Sun

By M. RYLE

Cavendish Laboratory, Cambridge

*Communicated by Sir Lawrence Bragg ; MS. received 7th April 1949*

**ABSTRACT.** A summarizing account is given of possible mechanisms which have been proposed to account for the emission of intense radio waves from the sun. Whilst most authors agree that the radiation from the undisturbed sun is due to an electron temperature of a million degrees in the solar corona, the greater intensity emitted from sunspots has led some authors to propose non-thermal mechanisms, based on the coherent oscillation of a large number of electrons in the solar corona above the sunspot. The mechanisms proposed for the maintenance of coherent oscillations are examined in detail in this paper and it is concluded that whilst they give adequate explanations for the oscillation observed in discharge tubes, no satisfactory mechanism has yet been suggested for the maintenance of electron oscillations in the solar corona.

It is therefore concluded that the observations can only be accounted for by the occurrence, in the solar corona near sunspots, of electron temperatures of up to  $10^{10}$  deg. K.

The problem of maintaining an electron temperature of  $10^6$  deg. K. in the normal corona, and  $10^{10}$  deg. K. in the corona near a large sunspot, has been considered in an earlier paper ; it was there shown that by the action of the general magnetic field of the sun and the non-uniform rotation of the solar surface, a potential difference is developed between the poles and the equator which is capable of maintaining an adequate electron temperature in both regions.

## §1. INTRODUCTION

RECENT experimental work has shown that the sun emits radio waves of great intensity. For wavelengths between 1 metre and 5 metres, the intensity corresponds to black-body emission at temperatures of about  $10^6$  deg. K. for the undisturbed sun and up to  $10^{10}$  deg. K. for regions near sunspots. There is general agreement that the radiation from the undisturbed sun is due to a genuine electron temperature of about a million degrees in the solar corona.

Some authors have suggested that the more intense radiation from regions near sunspots is produced by the coherent oscillation of a large number of electrons by some mechanism similar to that which produces plasma oscillations. If this were the true explanation it would not be necessary to assume that, near sunspots, the electrons had a mean energy corresponding to a temperature of  $10^{10}$  deg. K.

The main object of this paper is to examine in detail the mechanisms which have been proposed for the coherent oscillation of electrons in the solar corona. It is shown that although it is a simple matter to demonstrate the occurrence in the solar corona of a natural "plasma" frequency of the electron gas, it is much more difficult to suggest any mechanism which would maintain the plasma oscillations, or any mechanism by which radio waves could be emitted from the plasma even if it did oscillate. All the mechanisms proposed to explain the oscillations in discharge tubes require sharp gradients of electron density and electron beams having a highly ordered motion ; it is difficult to see how either of these conditions could occur in the solar corona. The conclusion is therefore reached that no

satisfactory mechanism has yet been suggested. It is therefore concluded that the radiation emitted from near sunspots must be produced by the non-coherent acceleration of electrons, so that its observation implies the occurrence of genuine electron temperatures of  $10^{10}$  deg. K. in these regions. A mechanism for the maintenance of such a great electron temperature in the neighbourhood of sunspots has been considered in an earlier paper. It was there suggested that by the action of the general magnetic field of the sun and the non-uniform rotation of the solar surface, a large potential difference is developed between the poles and the equator, which is capable of maintaining a mean electron energy in the undisturbed corona corresponding to a temperature of at least  $10^8$  deg. K. The distortion of the general magnetic field by the magnetic field of a sunspot allows the maintenance of still greater electric fields in the corona near the sunspot, and mean electron energies corresponding to a temperature of  $10^{10}$  deg. K. are likely to occur near large sunspots.

## § 2. THE EXPERIMENTAL OBSERVATIONS

The earliest deductions that the sun occasionally emits radio waves whose intensity greatly exceeds that expected from a source at  $6,000^\circ$  K. were made by Appleton (1945) and Hey (1946) from observations on frequencies of about 70 Mc/s. Since that time a large amount of experimental work has been carried out on frequencies between 60 Mc/s. and 3,000 Mc/s. It has been found that for frequencies between 60 Mc/s. and 200 Mc/s. the intensity from the undisturbed sun corresponds to what would be emitted if the whole solar disc were at a temperature of about a million degrees (Pawsey 1946, Ryle and Vonberg 1948).

At times of sunspot activity much greater intensities have been observed (Appleton 1945, Hey 1946, Pawsey, Payne-Scott and McCready 1946, Ryle and Vonberg 1946); the radiation at frequencies of about 200 Mc/s. then corresponds to what would be emitted if the whole solar disc were at a temperature of about  $10^8$  deg. K.

Experiments have also been made to determine the position and size of the source of the intense radiation (Ryle and Vonberg 1946, McCready, Pawsey and Payne-Scott 1947). The results obtained have shown that the radiation is emitted from a comparatively small region in the neighbourhood of the sunspot. The observed intensities of radiation therefore correspond to a still greater effective temperature, and it must be concluded that regions near sunspots are capable of emitting radiation whose intensity corresponds to the emission from a black-body source at a temperature exceeding  $10^{10}$  deg. K.

The intense radiation from sunspots has been found to be circularly polarized, but the radiation from the undisturbed sun is apparently unpolarized (Martyn 1946 a, Appleton and Hey 1946, Ryle and Vonberg 1946, 1948).

## § 3. EQUILIBRIUM MECHANISMS LEADING TO THE DEDUCTION OF VERY HIGH TEMPERATURES

Some theories of radio-frequency emission from the sun have been based upon "equilibrium mechanisms", in which the intensity of the radiation tends to the value associated with the mean electron energy. The radiation from an infinite heated ionized gas of low density would correspond to that from a black-body, although in practical cases the total "optical depth" may be insufficient for the full intensity to be established. It is clear that such theories cannot account

for radiation of intensity greater than that emitted by a black-body having the same temperature as that of the electrons; an explanation of solar radiation by these theories therefore requires the existence of very high electron temperatures.

(i) *Undisturbed Sun*

In a previous communication (Ryle 1948) a mechanism for the generation of radio-frequency radiation in the solar atmosphere was developed. By an application of Appleton's magneto-ionic theory to the propagation of metre waves in the solar atmosphere, it was shown that radiation could only escape to the earth from a source situated at or above the level at which the refractive index vanished (about  $5 \times 10^9$  cm. above the photosphere for a wave of frequency 200 Mc/s.). It was further shown that the absorption of an incoming wave was negligible except near the level at which the refractive index vanished, but that the total absorption in this region was considerable. It was therefore concluded that each region in the solar atmosphere would radiate at a particular frequency with an intensity which might approach that corresponding to a black-body radiator having the same temperature as the electrons in the region. It was therefore suggested that the observed intensity of the radiation from the undisturbed sun was the result of an electron temperature of at least a million degrees in the corona.

It was suggested that the maintenance of such an electron temperature could be accounted for by the existence of a potential difference between the poles and equator of the sun, the potential difference being developed by the action of the general solar magnetic field on the non-uniform rotation of the photosphere.

Martyn (1946 b, 1948) has also developed a "thermal" theory of the radiation from the undisturbed sun, and whilst not suggesting a mechanism for the maintenance of the electron temperature, he considers that the observations can be accounted for by assuming a temperature of a million degrees in the corona. Waldmeier (1948) and Shklovsky (1947) have also developed theories involving a comparable coronal temperature. Moreover, the observation of lines of very highly ionized atoms in the coronal spectrum leaves little doubt that the radiation from the undisturbed sun is due to purely "thermal" processes in the corona.

(ii) *Sunspot Radiation*

In the previous paper (Ryle 1948) the theory was extended to the case of sunspot radiation. It was shown that in the solar corona above a sunspot appreciable absorption could occur at two levels (about  $10^9$  cm. and  $10^{10}$  cm. above the photosphere for a frequency of 200 Mc/s. and a sunspot magnetic field of 3,000 gauss); each region would absorb one of the circularly polarized components. It was therefore suggested that circularly polarized radiation would be generated in each of these regions; the intensities of the two waves would approach the values associated with the electron temperatures in the two regions.

It was further shown that the distortion of the general solar magnetic field by the magnetic field of the sunspot could give rise to a very much greater electric field in the corona above a sunspot than in the undisturbed corona. It was shown that if the non-uniform rotation of the sun produced a potential difference between poles and equator which was capable of maintaining a normal electron temperature of  $10^6$  deg. K., then the distortion of the magnetic field near a large sunspot might be expected to lead to temperatures of the order of  $10^{10}$  deg. K.

#### § 4. MECHANISMS INVOLVING THE COHERENT OSCILLATION OF ELECTRONS

##### (i) *Non-thermal Theories of Sunspot Radiation*

The extremely great electron temperatures which are required to account for the observed intensity of the radiation from sunspots have led other authors to propose non-thermal mechanisms. In order to produce an intense radiated field by electrons of comparatively low energy, it seems necessary to develop a mechanism for maintaining the coherent oscillation of a large number of electrons.

Martyn (1947) and Shklovsky (1947) have both suggested that the coherent oscillation of electrons in the corona could be produced by a mechanism analogous to the plasma oscillations familiar in gas discharge tubes. If such a process were to occur, the intensity of the radiation emitted could be very much greater than that associated with the thermal motion of the electrons in the corona. It is therefore important to examine whether oscillations of this kind could occur under the conditions likely to exist in the solar corona.

##### (ii) *Existing Theories of the Mechanism of Plasma Oscillations*

Before attempting to consider the possibility that plasma oscillations could account for the intense emission from the solar corona it is important to understand the precise mechanisms which are envisaged in such theories. Unfortunately, the literature of plasma oscillations is notable for the small amount of detailed theoretical study as compared with the quantity of careful experimental results which have been obtained in the study of gas discharges.

In the original theory of Tonks and Langmuir (1929) it was shown that the electrons in an ionized gas had a natural frequency of oscillation given by  $(Ne^2/\pi m)^{1/2}$ , where  $N$  is the electron density and  $e$  and  $m$  the charge and mass of the electron. (They also showed the existence of ionic oscillations having much lower frequencies, but it will be seen later that such oscillations cannot account for the emission of radio-frequency radiation from the sun.) It should be noted that although this theory provided natural periods of oscillation of the same order as those observed in experiments on gas discharges, no definite mechanism was proposed for the excitation of such oscillations. Without some additional mechanism, a plasma is not capable of generating oscillations, and has merely the characteristics of a tuned circuit. If some feedback mechanism or "negative resistance" is introduced, however, a plasma will then become capable of generating oscillations.

A further difficulty arises in accounting for the detection of the oscillations. This difficulty is due to the fact that the group velocity in the plasma is zero (Tonks and Langmuir 1929, Tonks 1929); it is therefore impossible for energy to be propagated by an electromagnetic field from the oscillating region to the measuring probe, unless the gradient of electron density or magnetic field is sufficiently great to allow appreciable transfer by way of the evanescent wave.

The original theory has since been extended to account both for the excitation of plasma oscillations and for the escape of energy from the oscillating region.

##### (a) *The excitation of plasma oscillations.*

Later work by Merrill and Webb (1939) suggested that the oscillation of a thin layer near the cathode was responsible for velocity modulation of the primary electron stream from the cathode, a conclusion which has been confirmed by

Armstrong (1947). Recently Neill (1949) has shown that it is possible to account for the experimental observations by a feedback mechanism analogous to that by which a diode can maintain oscillations in virtue of transit-time effects. He supposes that electrons emitted by the cathode are subject to an accelerating field which depends on the space-charge in the plasma-sheath; if this space-charge is varying, the electron stream will be velocity-modulated, and if the distance to the plasma is suitable it will produce a bunching of the electrons which in turn can affect the space-charge. In this way part of the energy from the cathode fall of potential is converted into energy of oscillation of the plasma. Neill has shown that the theory provides good quantitative agreement with many of the related observed phenomena.

A more elaborate mechanism for the generation of oscillations in vacuum tubes has recently been suggested by Haeff (1949), which depends upon the interaction of two coherent beams of electrons.\* Haeff has shown that under certain conditions a region containing two interpenetrating electron beams is capable of amplifying an initial disturbance having a frequency related to the plasma frequencies of the two beams. Whilst insufficient detail has been given of the precise mechanism, it appears that it is analogous to that of the travelling-wave tube, in that the disturbance is guided along the moving electron beams, and that the wave frequency to an observer moving with the electron beam is related to the plasma frequency.

This brief survey shows that all the detailed mechanisms so far proposed for the maintenance of oscillations in a gas discharge tube depend on the velocity modulation of an incident electron beam. It will be necessary to examine (in §4(iii)) whether such a mechanism could provide excitation for the coherent oscillation of electrons in the solar corona.

*(b) The escape of energy from the oscillating region.*

Tonks and Langmuir (1929) considered that even in the small-scale conditions of the discharge tube, where the entire plasma occupies a thickness considerably less than a vacuum wavelength, it might be necessary to account for the detection of the oscillations by virtue of the escape of accelerated electrons from the plasma region. Merrill and Webb (1939) concluded that the alternating voltage observed on the measuring probe in their experiments was due to the periodic fluctuations of the space-charge in the incident electron stream. Later experiments by Armstrong (1947) and Neill (1949) have shown that the oscillating plasma will cause velocity modulation of the incident electron stream; they have also confirmed the earlier conclusion that the voltage observed on the measuring probe is caused by the bunching of such an incident electron stream.

Velocity modulation of the incident stream of electrons could also account for the escape of energy from a region which was oscillating by the mechanism suggested by Haeff (1949). The possibility that electromagnetic radiation could escape from such an oscillating region cannot be excluded until a more precise physical picture of the mechanism has been given; since, however, the emission of an electromagnetic wave relative to a coordinate system moving with the stream of electrons corresponds closely to the escape of radiation from a normal plasma, it seems probable that the escape of energy by electromagnetic radiation presents considerable difficulty.

\* A mechanism somewhat analogous to that proposed by Pierce (1948) to account for low-frequency oscillations in an electron stream passing through a stationary ion cloud.



In the absence of further information it therefore appears that energy is only likely to escape from an oscillating plasma by virtue of the velocity modulation imposed on an electron stream which has passed through the region.

It is clear that in the large-scale conditions of the solar corona, the escape of energy from an oscillating plasma presents even more serious difficulties than for the case of the discharge tube; the application of the theories outlined above to the solar corona will be discussed in the next section.

### (iii) *The Possibility of Electronic Plasma Oscillations in the Solar Corona*

It is first important to note that the existing experimental and theoretical work on plasma oscillations in gas discharge tubes relates to conditions in which the dimensions of the plasma are small compared with the vacuum wavelength of the oscillation. In the solar corona it is probable that the electron density and magnetic field will be virtually constant over a volume of many cubic wavelengths.

#### (a) *The excitation of plasma oscillations in the corona.*

In a gas discharge tube containing a cathode at a low temperature, the initial velocities of the electrons are small compared with the velocity produced by the applied electric field. Under the influence of a steady applied field, the stream of electrons will therefore travel a distance of the order of one mean free path before the motion becomes disordered. If now an alternating field is superimposed on the steady field near the cathode, the electrons will be velocity-modulated and, if the mean free path is sufficient, will become bunched at some distance from the cathode. Neill (1949) has shown that the variation of the space-charge resulting from this bunching can then provide excitation to the oscillating plasma.

If now the temperature of the cathode is increased, the initial distribution of the velocities of the electrons may become comparable with the velocity produced by the applied field; although the superimposition of an alternating field will still result in the acceleration of each electron, the spread in the initial velocities of the electrons will prevent effective bunching. An alternating density of space-charge will therefore no longer be produced, and the oscillations of the plasma cannot be maintained.

In the solar corona the initial random velocities of the electrons in any particular region will be of the same order as the velocities gained during a mean free path, and the conditions therefore correspond to those in a discharge tube having a cathode at a very high temperature. The superimposition of an alternating field will not produce appreciable bunching in such circumstances; the mechanism suggested by Neill (1949) cannot therefore account for the maintenance of plasma oscillations in the solar corona.

Although Haefl (1949) has given no detailed description of the conditions which are necessary for the generation of oscillations by the interaction of two electron beams, it seems likely that here also the distribution of velocities in the primary electron beams must initially be small compared with the ordered velocity.

It appears that any mechanism which involves velocity modulation of an incident electron stream is equally unlikely to be effective in maintaining the coherent oscillation of electrons in the conditions of the solar corona.

*(b) The escape of the energy.*

Even if it is assumed that the coherent oscillation of electrons could be maintained in the solar corona, it is doubtful whether any energy so generated could escape to the earth. It is clearly more difficult to account for leakage of the evanescent wave in a region where the gradient of electron density and magnetic field will be very much smaller than those in a discharge tube. It is therefore necessary to examine the possibility that energy might be transferred from the oscillating region by the passage of electrons through the region. A stream of electrons undergoing velocity modulation in this way might pass into an overlying region from which radiation could escape; such a stream is unlikely to be an efficient radiator, but some of the energy imposed by the oscillating plasma might be able to escape. It is, however, necessary that the electron stream shall still be effectively bunched when it emerges into the region from which the radiation can be propagated. Unless there are very considerable gradients of electron density or magnetic field, the electron stream must travel a distance corresponding to a very large number of wavelengths. The accurate collimation of a velocity-modulated electron stream which has traversed such a distance can only occur if the random velocity of the electrons is negligible compared with their ordered motion. It has already been shown that such a condition is unlikely in the solar corona.

It therefore appears that although the electrons in the solar corona may have a suitable natural period of oscillation, there are serious difficulties in accounting for the intense radiation at radio frequencies by mechanisms involving plasma oscillations. Satisfactory theories have been developed to account for both the driving mechanism and the mechanism of energy transfer for plasma oscillations in discharge tubes; these theories are not applicable in the large-scale conditions of the solar corona unless very large gradients of electron density or magnetic field are assumed. The maintenance of such gradients in a region where the mean free path for an electron is many kilometres does not appear possible.

*(iv) The Possibility of Ionic Plasma Oscillations in the Solar Corona*

So far attention has only been given to the coherent oscillation of electrons. If positive ions are also present, they will be capable of oscillating with a natural frequency of  $(Ne^2/\pi M)^{1/2}$ , where  $N$  and  $M$  are the number density and mass of the ion and  $e$  is the electronic charge (Tonks and Langmuir 1929). In a region containing an equal number of ions and electrons, the natural frequency of the ionic oscillations will be very much less than that of the electronic oscillations; the refractive index for a wave having the frequency of the ionic oscillations is therefore imaginary, and ionic oscillations cannot generate radio-frequency radiation which can escape through the overlying layers.

Tonks and Langmuir (1929) have, however, also shown that oscillations of very low frequency can be generated in an ionized gas, and that these oscillations may be propagated in a manner analogous to the propagation of sound waves. It is possible that such oscillations might occur in the solar corona; the passage of such a wave through a region which was emitting radio-frequency radiation would produce variations in the mean energy or density of the particles, and might cause fluctuations in the intensity of the emission. Thus, whilst ionic plasma oscillations cannot account for the great intensity of the radio-frequency radiation emitted by the corona, it is possible that they might produce low-frequency

fluctuations in the intensity of the emitted radiation. Such waves might be responsible for the "bursts" of radiation associated with the emission from sunspot regions.

### § 5. CONCLUSIONS

A detailed consideration of theories of plasma oscillations has not revealed a satisfactory explanation for the maintenance of coherent electronic oscillations in the solar corona. It is therefore concluded that the observed radio-frequency radiation arises from purely random motion of the electrons in the corona. It has previously been shown (Ryle 1948) that each region of the corona is absorbing to a certain radio frequency, and thus each region will radiate at a particular frequency with an intensity depending upon the electron temperature and the total absorption coefficient. If the absorption is sufficient, the intensity will equal that of black-body radiation corresponding to the electron temperature in the region.

If these conclusions are accepted, the observations show that the electron temperature in the normal corona is at least a million degrees (a figure assumed in many theories of the radiation from the undisturbed sun), whilst in the corona above large sunspots the electron temperature may reach  $10^{10}$  deg. K. The existence of such electron temperatures in the solar corona is clearly of great significance; observations over a range of radio frequencies may allow a detailed study to be made of the distribution of electron temperature throughout the corona.

A mechanism for the maintenance of a large electron temperature in the solar corona has already been suggested (Ryle 1948). It was shown that the non-uniform rotation of the solar surface, together with the general magnetic field of the sun, will produce a potential difference of about  $5 \times 10^8$  volts between poles and equator. A potential difference of this order is sufficient to maintain not only a normal electron temperature in the corona of about a million degrees, but also an increased electron temperature in the corona above sunspots. For a large sunspot the potential gradient is sufficient to maintain in the regions responsible for the emission of radio-frequency radiation a mean electron energy corresponding to a temperature of  $10^{10}$  deg. K.

The application of similar mechanisms to account for the discrete sources of radio waves in the galaxy, and the possible relation between these sources and the origin of cosmic rays, will be considered in another paper (Ryle 1949).

### ACKNOWLEDGMENTS

I am indebted to Mr. J. A. Ratcliffe for his advice and helpful criticism throughout this work. I also had the advantage of useful discussions with Professor K. G. Emel  us and Professor J. Sayers on the mechanism of plasma oscillations.

### REFERENCES

- APPLETON, E. V., 1945, *Nature, Lond.*, **156**, 534.  
 APPLETON, E. V., and HEY, J. S., 1946, *Nature, Lond.*, **158**, 339.  
 ARMSTRONG, E. B., 1947, *Nature, Lond.*, **160**, 713.  
 HAEFF, A. V., 1949, *Proc. Inst. Radio Engrs.*, **37**, 4.  
 HEY, J. S., 1946, *Nature, Lond.*, **157**, 47.  
 MCCREADY, L. L., PAWSEY, J. L., and PAYNE-SCOTT, R., 1947, *Proc. Roy. Soc. A*, **190**, 357.  
 MARTYN, D. F., 1946 a, *Nature, Lond.*, **158**, 308; 1946 b, *Ibid.*, **158**, 632; 1947, *Ibid.*, **159**, 26; 1948, *Proc. Roy. Soc. A*, **193**, 44.  
 MERRILL, H. J., and WEBB, H. W., 1939, *Phys. Rev.*, **55**, 1191.

- NEILL, T. R., 1949, *Nature, Lond.*, **163**, 59.  
 PAWSEY, J. L., 1946, *Nature, Lond.*, **158**, 633.  
 PAWSEY, J. L., PAYNE-SCOTT, R., and MCCREADY, L. L., 1946, *Nature, Lond.*, **157**, 158.  
 PIERCE, J. R., 1948, *J. Appl. Phys.*, **19**, 231.  
 RYLE, M., 1948, *Proc. Roy. Soc. A*, **195**, 82 ; 1949, *Proc. Phys. Soc. A*, **62**, 491.  
 RYLE, M., and VONBERG, D. D., 1946, *Nature, Lond.*, **158**, 339 ; 1948, *Proc. Roy. Soc. A*, **193**, 98.  
 SHKLOVSKY, J. S., 1947, *Nature, Lond.*, **159**, 752.  
 TONKS, L., 1929, *Phys. Rev.*, **33**, 239.  
 TONKS, L., and LANGMUIR, I., 1929, *Phys. Rev.*, **33**, 195.  
 WALDMEIER, M., 1948, *Experientia*, **4**, 64.

## Evidence for the Stellar Origin of Cosmic Rays

By M. RYLE

Cavendish Laboratory, Cambridge

*Communicated by Sir Lawrence Bragg ; MS. received 7th April 1949*

**ABSTRACT.** Several authors have suggested the possibility that cosmic rays are due to the acceleration of charged particles in the atmospheres of certain stars. Recent observations at radio frequencies have provided some evidence in support of this hypothesis which is reviewed in this paper.

The observations have shown that at least part of the radio-frequency radiation from the galaxy is emitted by discrete sources of small angular diameter. Measurements of the intensity of the radiation from these sources, and of the time variations of the intensity, indicate that the sources emit radio waves as if they were at a temperature of more than  $10^{14}$  deg. K. It is concluded that this intense radiation cannot be caused by the coherent oscillation of a large number of electrons, but must be due to a genuine electron temperature of about  $10^{14}$  deg. K. (corresponding to a mean electron energy of  $10^{10}$  electron volts). The existence of this electron temperature indicates that in certain stellar bodies there are mechanisms capable of accelerating particles to cosmic ray energies.

A previous theory of the emission of radio waves from the sun is extended to other stellar bodies. It is concluded that a star having a surface magnetic field strength and a peripheral velocity somewhat greater than those which have so far been observed could emit radio waves having the observed intensity. A star of this type could also accelerate charged particles to cosmic ray energies.

The small visual brightness of the sources of radio waves suggests that these bodies may be characterized by small visual opacity or small photospheric temperature.

It is suggested that the difference between the angular distribution of cosmic rays and of the radio waves from the galaxy is due to the deflection of cosmic ray particles by magnetic fields. In addition to previous theories of a general magnetic field in the galaxy, it is shown that the scattering produced by the magnetic fields of the distributed sources themselves should be sufficient to produce an isotropic distribution of cosmic rays at the earth even though the sources may show a marked concentration near the galactic equator.

### § 1. INTRODUCTION

SEVERAL authors have proposed mechanisms for the generation of cosmic rays by the acceleration of charged particles in the atmospheres of certain stars. Swann (1933) demonstrated that the growth of the magnetic field of a sunspot could give rise to potentials of the order of  $10^9$  volts in a region where little energy would be lost by collisions. He suggested that similar disturbances in other stars might give rise to particles having an energy of more than  $10^{10}$  electron volts. Alfvén (1937) showed that even in the absence of sunspots a comparable potential could be developed by the non-uniform rotation of the solar

surface. Davis (1947) deduced that the star BD-18°-3789, which recent measurements (Babcock 1947b) have shown to have a magnetic field strength at the poles of about 5,500 gauss, would produce, relative to a stationary observer, a potential difference of about  $10^{14}$  volts. He showed, however, that owing to the formation of a space-charge this potential difference was not available for the acceleration of charged particles. Babcock (1948) has considered this process in relation to magnetically variable stars, and he has shown that the periodic reversal of the magnetic field would allow the escape of particles of high energy during a certain fraction of the magnetic cycle.

Recent measurements (Hey, Parsons and Phillips 1946, Bolton and Stanley 1948, Ryle and Smith 1948) on the emission of radio-frequency radiation from the galaxy have provided independent evidence for the existence of such sources; it is the purpose of this paper to examine this evidence and to make certain deductions concerning the nature of the sources.

The observations have shown that at least part of the radio-frequency radiation from the galaxy is emitted by discrete sources, whose angular diameters are smaller than the resolving power of the apparatus (about eight minutes of arc). It has also been found that the intensity from some of the sources fluctuates rapidly and that sometimes "bursts" of radiation are observed, in which the intensity is doubled for a period of about 20 seconds. Providing that these fluctuations represent genuine variations of the emission from the source, it is possible to fix an upper limit to the dimensions of the source. Extended measurements of the positions of the two intense sources have suggested that they are not part of the solar system; if it is assumed that they are situated at the distance of the nearest fixed star, the deduced diameter and the observed intensity would correspond to the emission from a black-body source at a temperature of more than  $10^{14}$  deg. K.

It is possible that some special radiating process might be responsible for the emission of radiation having an intensity greater than that corresponding to the electron temperature; in the absence of such a process, the radiation can only be accounted for by assuming that the electrons have a random energy corresponding to the thermal energy at a temperature of  $10^{14}$  deg. K. (the mean energy of an electron is then about  $10^{10}$  electron volts).

The maintenance of this electron energy implies the existence of mechanisms capable of accelerating particles to cosmic ray energies. It is therefore suggested that the sources of intense radio-frequency radiation may also be responsible for the emission of cosmic rays.

The assumptions made in the development of this theory are analysed in detail in the following sections. A mechanism is suggested by which intense radio waves (and cosmic ray particles) could be emitted from the atmospheres of certain stars having a large rotational velocity and surface magnetic field. It is further shown that the scattering effect caused by the magnetic fields of such stars would be expected to lead to an isotropic distribution of cosmic rays at the earth, independent of the distribution of the sources in the galaxy.

## § 2. THE EXPERIMENTAL EVIDENCE

Hey, Parsons and Phillips (1946) first observed that the intensity of the radio-frequency radiation from the constellation of Cygnus showed fluctuations in a period of a few minutes; they therefore concluded that at least part of the radiation

from the galaxy was due to the emission from discrete sources. More refined experiments by Bolton and Stanley (1948) and Bolton (1948) enabled the source to be located more precisely, and showed that its angular diameter was less than the resolving power of the apparatus (about eight minutes of arc). Similar observations by Ryle and Smith (1948) showed a second, more intense, source in the constellation of Cassiopeia, and extended observations showed that whilst the intensity from the source in Cygnus frequently showed sudden increases, that from the source in Cassiopeia was notably constant. They also found that the radiation from both sources appeared to be randomly polarized.

The intensity of the 80 Mc/s. radiation from the sources in Cygnus and Cassiopeia has been found to be of the order of  $2 \times 10^{-22} \text{ w.m}^{-2} (\text{c/s.})^{-1}$ . Both Bolton (1948) and Ryle and Smith (1948) have detected other discrete sources of smaller intensity, and some of these have also shown fluctuations of intensity. None of the sources appears to coincide with an outstanding visual star.

### §3. DETERMINATION OF THE EQUIVALENT TEMPERATURE OF A SOURCE

The intensity of the radiation emitted by a distant source may be compared with that from a black-body source which subtends an equal solid angle. If the intensity corresponds to that produced by the black-body at a temperature  $T$ , the source may be said to have an "equivalent temperature"  $T$ . The significance of this temperature will be discussed in §4, and it will be used now merely as a convenient unit with which to express the emission from the source.

In order to determine the equivalent temperature of a galactic source of radio-frequency radiation, it is necessary to observe both the intensity of the radiation at the earth and the solid angle subtended by the source. Unfortunately it has not been possible to achieve a sufficiently large resolving power to measure the solid angle directly. Observations of the source in Cygnus have, however, shown sudden fluctuations in which the intensity is doubled in a period of 20 seconds. This variation might represent variations in emission, or might be caused by refraction in an intervening medium; it will first be shown that a refraction process is unlikely.

The observation that the intensity from the source in Cygnus exhibits rapid fluctuations, whilst that from the source in Cassiopeia remains noticeably constant, suggests that the fluctuations are not produced by general refraction in interstellar matter. Since the observations were made when the sources were nearly vertically overhead, it seems unlikely that refraction in the ionosphere could affect one source and not the other (the angles of incidence during observation are about  $12^\circ$  for the source in Cygnus and  $6^\circ$  for the source in Cassiopeia). Whilst the possibility still remains that the intensity from the source in Cygnus is affected by refraction in some localized region of interstellar matter, it seems most probable that the observed fluctuations represent a true variation of the emission.

The total intensity of the radiation received from a source may be considered as being due to the addition of the radiation emitted by a large number of small elements of the source. If the radiation from each of these small elements exhibits sudden increases of intensity, the total intensity will only show such increases if the fluctuations from different elements arrive simultaneously. If large increases are observed it is therefore necessary that the different elements of the source shall be separated by a distance not greater than the distance travelled by an

electromagnetic wave in the duration of the fluctuations. In the absence of any special orientation of the emitting surfaces relative to the earth it is therefore possible to deduce a maximum dimension of the source by determining the duration of the sudden fluctuations.

Observations of the source in Cygnus have provided records showing a doubling of the intensity in a time of 20 seconds. It is therefore deduced that the source of the variable component of the radiation occupies a volume whose linear dimensions do not greatly exceed the distance travelled by electromagnetic waves in 20 seconds (about  $10^{12}$  cm.).

There is, as yet, insufficient information on the distance of the sources. Parallax measurements at radio frequencies are unlikely to be of sufficient accuracy to determine the distances, although preliminary measurements by Ryle and Smith (unpublished) have shown that the sources in Cygnus and Cassiopeia are at distances greater than  $2 \times 10^{18}$  cm. Improvements in the angular accuracy of the measuring apparatus are unlikely to lead to a significant extension of parallax measurements by radio methods, although they may allow the sources to be identified with known stellar bodies, in which case parallax measurements by visual methods may be possible. The existing measurements indicate that it is unlikely that the sources are part of the solar system, and in the absence of further experimental evidence it will be assumed that they are not nearer than the nearest known fixed star (about  $3 \times 10^{18}$  cm.).

With this assumption, and for the deduced maximum diameter of  $10^{12}$  cm., it is found that the source in Cygnus emits radiation at a frequency of 80 Mc/s. as if it were a black-body at a temperature of  $10^{14}$  deg. K.

#### § 4. THE EVIDENCE FOR THE EXISTENCE OF HIGH-ENERGY PARTICLES IN THE SOURCE

The occurrence in the source of a true temperature of  $10^{14}$  deg. K. would involve collisions by electrons having a mean energy of about  $10^{10}$  electron volts. It is necessary to examine the possibility that special mechanisms may be responsible for the emission of intense radio waves by electrons of comparatively low energy.

The coherent oscillation of a large number of electrons might produce intense radio waves; both Martyn (1947) and Shklovsky (1947) have suggested that plasma oscillations in the solar corona could, in this way, account for the intense radiation associated with sunspots. This mechanism has been examined in some detail in a previous communication (Ryle 1949) which will be referred to as Paper 2. It was there concluded that the mechanism could not account for the emission of intense radio waves from the sun. It is now necessary to apply the arguments then used to determine whether plasma oscillations could account for the intense radiation from galactic sources.

When considering the possibility of plasma oscillations in the solar corona the range of electron density and magnetic field likely to occur in the region of the source were known from well-established observations. For the case of the galactic sources there is no information on the magnitude of the electron density or the magnetic field except that obtained from the radio-frequency observations.

It is first important to note that the radiation will only be able to reach the earth if the refractive index remains real at all points between the source and the

earth. In the absence of a magnetic field the refractive index for a wave having a frequency of 80 Mc/s. vanishes at an electron density of about  $8 \times 10^7 \text{ cm}^{-3}$ . In the presence of an intense magnetic field the propagation of one circularly polarized component becomes possible for an appreciably greater electron density. If the source were situated in a region of great electron density and an intense magnetic field permitted the escape of one component, the radiation observed at the earth would, however, appear circularly polarized, a result which is not confirmed by experiment (Ryle and Smith 1948).

It is therefore concluded that the presence of an intense magnetic field is not essential to the emission of radio waves from the type of galactic source which has been described. (The variable component of the radiation from some galactic sources is suggestive of the radiation associated with sunspots, although preliminary experiments have suggested that this component is also randomly polarized.)

It might be suggested that circularly polarized radiation emitted from the two hemispheres of a star would be of opposite polarity and approximately equal intensity for an observer situated near the equatorial plane of the star. The observer would therefore deduce that the radiation was randomly polarized. Detailed observations of the polarization from both the intense galactic sources have, however, shown that the polarized component appears to be less than 5% of the total intensity; it is unlikely that both sources would be orientated with such precision as to give this kind of signal at the earth if the radiation were comprised of two circularly polarized waves of opposite polarity. It is therefore concluded that the observed random polarization is genuine; both components can therefore escape from the region of the source.

In the absence of an intense magnetic field in the region of generation, the radiation must be emitted at or above the level at which the electron density is about  $8 \times 10^7 \text{ cm}^{-3}$ . Unless the temperature is less than about  $10,000^\circ \text{ K.}$ , ionization will be complete and the total particle density will not greatly exceed  $1.6 \times 10^8 \text{ cm}^{-3}$ .

It is thus apparent that the observed radiation can only be generated in regions where the electron density and magnetic field are similar to those in the solar corona. In Paper 2 reasons were given for supposing that plasma oscillations could not occur under the conditions of the solar corona, and it was suggested that the observed intensity of radio waves was due to the random motion of electrons having a mean energy corresponding to a temperature of  $10^6 \text{ deg. K.}$  in the normal corona and up to  $10^{10} \text{ deg. K.}$  near sunspots. The same arguments may now be applied to the radiation from galactic sources; in the absence of coherent electronic oscillations the observed intensity can only be accounted for by an electron temperature of at least  $10^{14} \text{ deg. K.}$

The emission of radio waves from an electron gas and the maintenance of a large electron temperature in the solar corona by an electric field have been considered in an earlier paper (Ryle 1948); this paper will be referred to as Paper 1. It seems probable that similar mechanisms occur in the sources of intense galactic radiation; if an electric field is responsible for the maintenance of an electron temperature of  $10^{14} \text{ deg. K.}$ , it is necessary that the energy gained by an electron between collisions shall be equal to the mean energy of thermal agitation of a gas at a temperature of  $10^{14} \text{ deg. K.}$  The electron density in the region of generation has been deduced from a determination of the refractive index at a frequency of



80 Mc/s.; the mean free path of an electron (for appreciable loss of energy) is then about  $10^{10}$  cm. It may therefore be seen that an electric field of  $1 \text{ volt cm}^{-1}$  would be sufficient to maintain a mean electron energy of  $10^{10}$  volts (corresponding to an electron temperature of  $10^{14}$  deg. K.).

The existence of an electric field of this magnitude would be capable of accelerating charges of either sign to a very great energy and, as has been shown for the case of the solar corona (Paper 1), some of these particles would be able to escape from the stellar atmosphere with a large energy.

It is therefore suggested that the observed galactic sources are also capable of emitting particles having an energy corresponding to a potential of at least  $10^{10}$  electron volts and that the total emission of particles from these bodies may be the origin of the primary cosmic rays.

The application of a theory of Alfvén (1937) to account for the maintenance of a large electron temperature in the solar corona has already been considered in Paper 1; the extension of these mechanisms to account for greater electron temperatures in the envelopes of other stellar bodies will now be considered.

#### § 5. THE PRODUCTION OF HIGH-ENERGY PARTICLES IN A STELLAR ENVELOPE

Alfvén (1937) has shown that the potential developed between the poles and equator of a star of radius  $R_0$  and polar field strength  $H_0$  is of the order of  $H_0 R_0^2 (\omega - \omega')$  where  $\omega$  and  $\omega'$  represent the angular velocities at the equator and the poles. For a star embedded in a region containing a large density of interstellar matter, the available potential may be significantly greater and is given by  $H_0 R_0^2 \omega$ . The recent observation (Babcock 1947a) of stars having magnetic field strengths and rotational velocities very much greater than those of the sun therefore suggests that in certain stars a very large potential difference may be developed.

It was shown in Paper 1 that the intensity of radio waves emitted at any frequency by a stellar envelope depends on the mean electron energy in the region where the refractive index for that frequency vanishes. This energy depends on (a) the electric field and (b) the electron density, and the latter is determined by the frequency of the wave,\* so that the intensity at a given frequency is determined solely by the magnitude of the electric field.

For a star in which the available potential is given by  $H_0 R_0^2 \omega$ , the electric field in the envelope will be of the order  $H_0 R_0 \omega$ . Observations by Babcock (1947b) have shown that certain stars are likely to have, at the photosphere, a polar field strength of 5,000 gauss and a peripheral velocity ( $R_0 \omega$ ) of  $2 \times 10^7 \text{ cm. sec}^{-1}$ . The product of these two quantities is about  $10^4$  times the corresponding figure for the sun; a star having these characteristics might therefore be expected to emit radio waves corresponding to a temperature about  $10^4$  times that observed for the sun. It is possible that stars having somewhat greater magnetic fields and rotational velocities may exist, and it is suggested that the mechanism described would be adequate to account for the maintenance of an electron temperature as great as  $10^{14}$  deg. K. in the envelopes of certain stars.

#### § 6. THE ANGULAR DISTRIBUTION OF THE SOURCES

Observations by Reber (1944) and Hey, Phillips and Parsons (1946) have shown that the intensity of radio waves is greatest from directions near the galactic

\* This statement assumes that the emitted wave is unpolarized.

equator, whereas the distribution of cosmic rays at the earth is highly isotropic. If the hypothesis put forward in this paper is correct, it is necessary to show how the observed isotropic distribution of cosmic rays could be produced during their passage from remote sources to the earth; it will be suggested that the important controlling factor is the magnetic fields of those stellar bodies which themselves produce the particles.

Babcock (1948) has shown that the magnetic field of certain stars could deflect a cosmic ray particle at a considerable distance; it is possible to calculate the "effective radius for large-angle scattering" for particles of different energies. If it is assumed that the stars responsible for scattering cosmic ray particles have, for particles of energy  $10^{10}$  electron volts, an "effective scattering radius"  $R$ , and are distributed through the galaxy with density  $\Delta$ , then if  $\rho$  is the effective radius of the galaxy, the probability  $P$  that a particle is deflected through a large angle as it traverses the galaxy is given by

$$P = \pi R^2 \Delta \rho. \quad \dots\dots(1)$$

If now it is assumed that certain stellar bodies are responsible for the production of the radio waves from the galaxy (and of the cosmic ray particles), and that these bodies also cause the deflection of the particles, it is possible to use the knowledge derived from the radio measurements to make an estimate of  $P$ .

The average radius of these stellar bodies for the emission of radio waves will be of the same order as the "photospheric" radius  $R_0$ ; they will therefore subtend a total solid angle  $\pi R_0^2 \Delta \rho$  at the earth.

It has already been shown that the emission of radio waves at a frequency of 80 Mc/s. corresponds to an effective temperature of  $10^{14}$  deg. K. at the source, so that if all the sources subtend a total solid angle  $\pi R_0^2 \Delta \rho$ , the effective mean temperature measured at this frequency will be  $\pi R_0^2 \Delta \rho \times 10^{14}$  deg. K. Measurements at 80 Mc/s. have shown that the mean temperature of the galaxy is about  $10^4$  deg. K., and so it is deduced that  $\pi R_0^2 \Delta \rho \simeq 10^{-10}$ .

Substitution from equation (1) now gives:

$$P = 10^{-10} (R/R_0)^2. \quad \dots\dots(2)$$

It would therefore be possible to deduce a value for  $P$  without a knowledge of  $\Delta$  or  $\rho$ , providing  $(R/R_0)^2$  were known.

From calculations based on Babcock's theory (1948), it can be shown that for a cosmic ray particle having an energy of  $10^{10}$  electron volts,  $(R/R_0)^2 = 3 \times 10^{-8} H_0 R_0$  (where electromagnetic c.g.s. units are used). Reasons have already been given (§ 5) for supposing that galactic radio waves are produced in bodies for which  $H_0 R_0 \omega$  is about  $10^8$  times the corresponding quantity for the sun. On the assumption that their angular velocity is the same as that of the sun,  $H_0 R_0 \simeq 3 \times 10^{20}$  and  $(R/R_0)^2 \simeq 10^{13}$ .

The probability that a cosmic ray particle of energy  $10^{10}$  electron volts will be deflected through a large angle in passing through the galaxy would therefore be 1,000 (from equation (2)). Even if the angular velocities of the stellar bodies were 1,000 times as great as that of the sun, the probability of a violent deflection would be unity and the distribution of cosmic rays at the earth would still be isotropic.

It is therefore concluded that even in the absence of a general galactic magnetic field (Alfvén 1938, Babcock 1947 b) considerable scattering would be produced

by the magnetic fields of the distributed sources themselves; the difference in angular distribution of cosmic rays and the radio waves from the galaxy is therefore not regarded as an argument against their generation in a common source.

### § 7. CONCLUSIONS

Observations of intense sources of radio-frequency radiation have suggested that certain stellar bodies are responsible for the emission, at metre wavelengths, of radiation whose intensity corresponds to the radiation from a black-body source at a temperature of  $10^{14}$  deg. K. This estimate is based on deductions made from the intensity and its time fluctuations and on the assumption that the source is not nearer than the nearest known fixed star. So far it has not been possible to identify any of the sources with known stars, but it seems unlikely that a body having the characteristics deduced from the radio observations could pass unnoticed if it were at a comparatively small distance.

The possibility that intense radio waves could be emitted by the coherent motion of electrons of comparatively low energy has been examined, but the necessary conditions seem improbable in a stellar envelope. It is therefore concluded that the observations indicate the existence of regions in which the mean electron energy is of the order of  $10^{10}$  electron volts. These regions would, under certain conditions, be capable of emitting particles having energies of this order of magnitude, and it is suggested that they are responsible for the production of primary cosmic rays.

The difficulty of identifying sources of such outstanding characteristics with those of visual observations may imply the existence of a type of star in which a high temperature corona is associated with a comparatively small visual temperature or opacity. This condition might arise in rapidly rotating stars having a large magnetic field.

The observations which have already been made on discrete sources of radio-frequency radiation suggest that it may be possible to explain the total radiation from the galaxy on the basis of a number of such sources. It therefore appears that a type of star which has so far not been classified in astronomy at visual wavelengths may be responsible for two major astrophysical phenomena—the origin of cosmic rays and of the intense radio waves from the galaxy.

The difference in the angular distribution of the radio waves and cosmic rays is accounted for by the deflecting effects of magnetic fields in the galaxy. In addition to previous theories of interstellar magnetic fields it is shown that the magnetic fields of the sources themselves are likely to cause an isotropic distribution of cosmic rays at the earth.

### ACKNOWLEDGMENTS

I wish to acknowledge the great assistance provided by my colleagues at the Cavendish Laboratory, particularly by Mr. F. G. Smith, who has in addition carried out most of the analysis of our experimental records. I also owe much to stimulating discussions with Professor H. Alfvén.

The work was carried out as part of a programme supported at the Cavendish Laboratory by the Department of Scientific and Industrial Research.

### REFERENCES

- ALFVÉN, H., 1937, *Z. Phys.*, **105**, 633 ; 1938, *Phys. Rev.*, **54**, 97.  
 BABCOCK, H. W., 1947 a, *Astrophys. J.*, **105**, 105 ; 1947 b, *Phys. Rev.*, **72**, 83 ; 1948, *Ibid.*, **74**, 480.

- BOLTON, J. G., 1948, *Nature, Lond.*, **162**, 141.  
 BOLTON, J. G., and STANLEY, G. J., 1948, *Nature, Lond.*, **161**, 312.  
 DAVIS, L., 1947, *Phys. Rev.*, **72**, 632.  
 HEY, J. S., PARSONS, S. J., and PHILLIPS, J. W., 1946, *Nature, Lond.*, **158**, 234.  
 HEY, J. S., PHILLIPS, J. W., and PARSONS, S. J., 1946, *Nature, Lond.*, **157**, 296.  
 MARTYN, D. F., 1947, *Nature, Lond.*, **159**, 26.  
 REBER, G., 1944, *Astrophys. J.*, **100**, 279.  
 RYLE, M., 1948, *Proc. Roy. Soc. A*, **195**, 82 (referred to as Paper 1) ; 1949, *Proc. Phys. Soc. A*, **62**, (referred to as Paper 2).  
 RYLE, M., and SMITH, F. G., 1948, *Nature, Lond.*, **162**, 462.  
 SHKLOVSKY, J. S., 1947, *Nature, Lond.*, **159**, 752.  
 SWANN, W. F. G., 1933, *Phys. Rev.*, **43**, 217.

## Pair-Production in Different Elements by $\gamma$ -Rays

By R. R. ROY

Wheatstone Physics Laboratory, King's College, University of London

*Communicated by J. T. Randall ; MS. received 5th October 1948, and in amended form 6th April 1949*

**ABSTRACT.** The production of electron pairs on bombardment of Pb, Pt, Sn, Ag and Cu by  $\gamma$ -rays from 200 mg. of Ra and its equilibrium products has been investigated. 1,200 photographs were taken for each element and the yield was 100 pairs in Pb, 85 in Pt, 72 in Sn, 63 in Ag and 50 in Cu. The distribution of energy of the positrons in Pb and Pt follows the shape of the theoretical curve of Bethe and Heitler, but the position of the maximum of the energy distribution curves in Sn, Ag and Cu shows a discrepancy with that to be expected theoretically. The theoretical difference between the average energies of the positrons and electrons in the elements studied, when plotted against  $Z$ , is consistently higher than the experimental, though both can be approximately represented by straight lines. The angular distribution of the positrons and electrons with respect to the incident  $\gamma$ -rays agrees with the theory.

### § 1. INTRODUCTION

THE creation of a pair of electrons of opposite charge in the Coulomb field of the nucleus by  $\gamma$ -rays of energy greater than  $2m_0c^2$  is a well-known phenomenon, and the cross section of this process has been calculated by Bethe and Heitler (1934) and by Jaeger and Hulme (1936). The experimental cross section for pair-production in Pb has also been studied, in particular by Chadwick, Blackett and Occhialini (1934), and it was found to agree quite well with the theoretical cross section as given by Bethe and Heitler. The present experiments were undertaken to investigate (i) the energy spectra of the positrons of the pairs created in Pb, Pt, Sn, Ag and Cu, (ii) the difference between the average energy of the positrons and electrons as a function of the atomic number of the elements studied, (iii) the angle between the positron and electron and the angles of emission with respect to the direction of the incident  $\gamma$ -rays.

### § 2. EXPERIMENTAL ARRANGEMENTS

The experiments were carried out in a rubber-piston type cloud-chamber 16.5 cm. in diameter and 4 cm. in height; the standard source of illumination, viz. five 100-volt, 100-watt lamps, flashed across 200 volts, was used. A magnetic field of 400 gauss, supplied by a pair of Helmholtz coils, was used to determine the

energy of the tracks. The measurements of the angles and curvatures of the tracks were taken after re-projecting the images from the two cameras. To reduce inaccuracy arising from multiple scattering, only those tracks whose radius of curvature lay between certain limits were taken into account. The source used was  $\gamma$ -rays from 200 mg. of Ra in equilibrium with its products, and, although the  $\gamma$ -rays from Ra have several lines above 1 mev., in these experiments observations were restricted by energy consideration to those  $\gamma$ -rays the energy of which was 2.2 mev. The foil of the element to be studied was placed in the cloud-chamber, against the glass ring; facing the side where the foil was situated was a lead block 45 cm. in length, 12 cm. in width, and 10 cm. in height, through which a hole 5 mm. in diameter had been drilled. This lead was necessary to prevent continuous ionization in the chamber due to  $\gamma$ -rays. At the other end of the block, away from the cloud-chamber, there was placed on one side of the hole a thin-walled iron container with the source inside it; on the other side, an electromagnet. When the expansion took place, the container was drawn towards the magnet; hence the source was in line with the hole and the  $\gamma$ -rays could pass through and bombard the element.

### § 3. RESULTS AND DISCUSSION

The results are given in Table 1.

Table 1

Element studied	Pb	Pt	Sn	Ag	Cu
Thickness of foil ( $\mu$ )	15	15	20	20	25
No. of photographs taken	1200	1200	1200	1200	1200
No. of pairs found	100	85	72	63	50

Taking into account the density and thickness of the material, the yield of pairs bears out, approximately, the theoretical predictions.

#### (i) *The Energy Spectrum of the Positrons in Pb, Pt, Sn, Ag and Cu*

As mentioned above, the energy of the incident  $\gamma$ -rays was 2.2 mev., and hence the energy available for the pair is 1.2 mev. From the experimental results it was found that the energyspectra for Pb and Pt, and for Ag and Sn, were essentially the same; therefore, only the energy distribution curves for Pb and Sn (Figures 1 (a) and 1 (b)), and that for Cu (Figure 1 (c)), are given. They are plotted against the theoretical curve of Bethe and Heitler.

The abscissa in each figure represents the total energy of the positrons, that is, the sum of the kinetic and rest energies; the ordinate gives the ratio of the number of positrons at a particular energy to that of the total number of positrons observed from a given element. Examination of these curves shows that in the case of Pb and Pt the maximum lies at about 1.38 mev., in the case of Sn and Ag at 1.25 mev. and in the case of Cu at 1.15 mev. It will be seen that for 2.2 mev. incident  $\gamma$ -rays the energy distribution curve for Pb and Pt agrees in shape with the theoretical curve. However, whereas the energy at which the maximum of the theoretical curve occurs remains the same for all elements, the experimental results show a variation in the maximum from higher to lower values according as the element studied is heavier or lighter. In addition, it may be noted that the curve of Pb and Pt falls very rapidly above 1.4 mev. and there are more particles at the higher

than at the lower energies. The curve of Cu is almost symmetrical and the energy of the  $\gamma$ -quantum after the creation of a pair is more or less equally distributed between the positron and electron.

In order to calculate the energy of the positrons the curvatures of the tracks have to be measured. This measurement involves an inaccuracy at low energies, because of multiple scattering and the difficulty in ascertaining the small radii of curvature. At high energies inaccuracies are also liable to occur because of the large radius of curvature. The maximum error here was not more than 8%

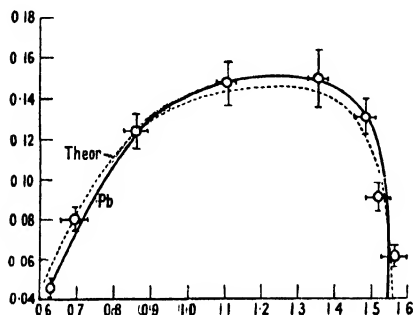


Figure 1 (a).

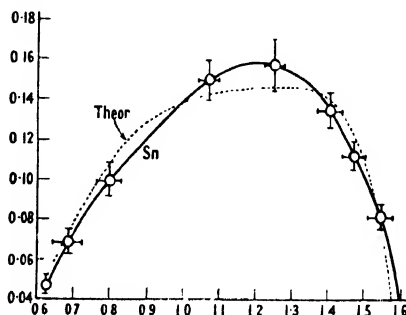


Figure 1 (b).

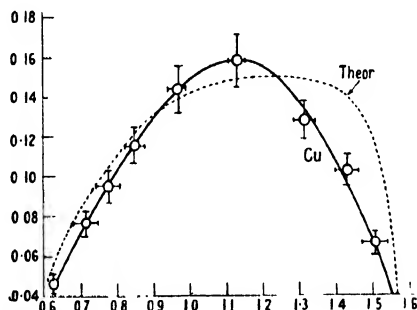


Figure 1 (c).

in the extreme cases. However, at those energies where the curves indicate the maximum yield, the measurement of the curvatures was accurate to within 4%. The discrepancy between experiment and theory noted in this region for lighter elements therefore seems real.

In one aspect the present experiment confirms that of Alichanow, Alichanian and Kosodaew (1936), who observed the pair-formation in Pb by 2.2 mev.  $\gamma$ -rays from RaC and found that the maximum of the energy distribution curve of the positrons was at about 1.38 mev.

### (ii) *The Difference of Energy of Positron and Electron*

Approximate theoretical values for  $\bar{E}_+ - \bar{E}_-$  can be calculated from the formula given by Bethe and Heitler :

$$\bar{E}_+ - \bar{E}_- = \frac{2m_0c^2Z}{137},$$

where  $Z$  is the atomic number.

Table 2 sets out the experimental results together with those given by the theory.

Table 2.  $\bar{E}_+ - \bar{E}_-$

Element	Pb	Pt	Sn	Ag	Cu
Theory	0.6	0.57	0.36	0.34	0.21
Experiment	$0.41 \pm 0.06$	$0.38 \pm 0.06$	$0.21 \pm 0.05$	$0.19 \pm 0.05$	$0.10 \pm 0.04$

The experimental results appear to be consistently lower than the theoretical values, but whether this discrepancy is real or whether it arises from approximation in the theory for the energy under consideration is not clear. The above formula is precise in requiring that the difference of the average energy should be proportional to the atomic number.

A graph has been plotted to show the variation of  $E_+ - \bar{E}_-$  against  $Z$ .

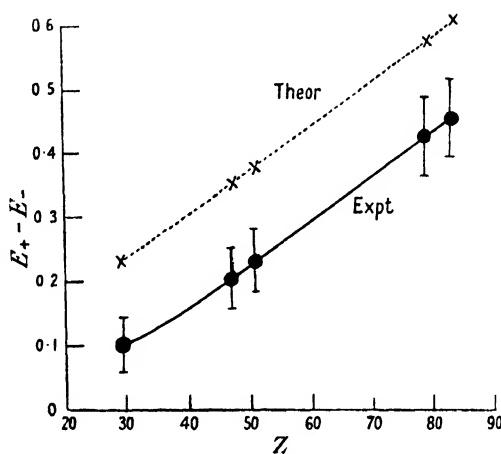


Figure 2.

Figure 2 shows the graphs of both theoretical and experimental results. The theoretical results show a straight line with a slope  $h = 0.0073$ . The experimental curve is almost a straight line having a slope  $h = 0.0063 \pm 0.001$ .

### (iii) The Angular Distribution

According to Bethe and Heitler, the fraction of the particles projected between the angles  $\theta$  and  $\theta + d\theta$  to the incident photon is given by

$$\frac{\theta d\theta}{(\Theta^2 + \theta^2)^2}$$

where  $\Theta = m_0 c^2 / E$ , where  $E$  is the total energy of either of the projected particles, i.e. the sum of the kinetic and rest energies. The maximum of the theoretical distribution of either positrons or electrons for  $\gamma$ -rays of 2.2 mev. when plotted against the direction of the incident photon lies at about  $15^\circ$ . From the experimental data it is found that the angular distribution of both positrons and electrons is the same in each element, and that the maximum of the curves of Pb, Pt, Sn, Ag and Cu lies at about  $18^\circ$ . Therefore only one curve has been used to illustrate the results.

Figure 3 shows the angular distribution for the positrons in Pb together with theoretical curve, given by the dotted line. The experimental curve follows the general shape of the theoretical distribution, and to this extent indicates fair agreement between the theoretical and experimental results.

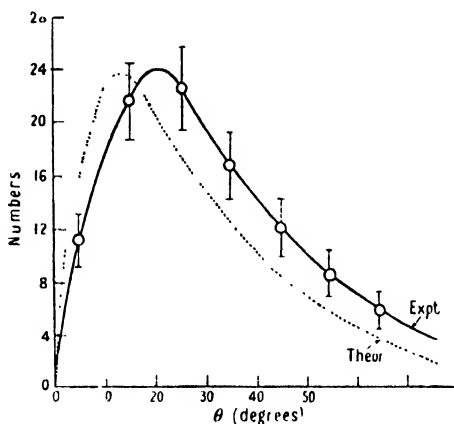


Figure 3.

The measurements of the angles between the directions of emission of the positrons and electrons are given in Table 3.

Table 3

Element	Pb	Pt	Sn	Ag	Cu
Average angle ( $^{\circ}$ ) between positron and electron	31	30	30	28	28
Average angle ( $^{\circ}$ ) between positron and $\gamma$ -ray	13	13	14	13	13
Average angle ( $^{\circ}$ ) between electron and $\gamma$ -ray	18	17	16	15	15

The Table shows that the average angle between the positron and electron in the different elements is approximately the same, and is about  $30^{\circ}$ . The measurements of the angles are accurate to within  $3^{\circ}$ . The mean of the average angles between the electron and  $\gamma$ -ray is  $16^{\circ}$ , and that of the positron and  $\gamma$ -ray is  $13^{\circ}$ .

Klarman and Bothe (1936) investigated the problem of pair-production in krypton and xenon by  $\text{ThC}''$   $\gamma$ -rays of energy 2.6 mev. and found that the average angle between the positron and electron increased with the atomic number. Thus for krypton it was  $19^{\circ}$  and for xenon  $42^{\circ}$ , but the number of pairs studied was only 13. The present observation does not confirm this, but agrees with Simons and Zuber (1937), who found that the average angle in argon was  $30^{\circ}$  and in iodine  $32^{\circ}$ . The photograph (see Plate) shows the formation of a pair in copper by a  $\gamma$ -ray of energy 2.2 mev.

#### § 4. CONCLUSION

Lawson (1949) has discussed the limitations of the theory of Bethe and Heitler, and it appears that this theory is not suitable for precise comparison with the present experimental results. For  $\gamma$ -rays of energy less than 3 mev. Lawson states that the calculation of Jaeger and Hulme gives a correction of opposite sign to that required when comparing the experimental results with the theory of Bethe and Heitler. Since with heavy elements, however, the lack of agreement between theory and experiment possibly arises from the inapplicability of the Born approximation, while for light elements it may arise from the use of the



Fermi-Thomas atom, satisfactory comparison between experiment and any present theory is hardly possible. Bethe and Heitler's theory predicts that the angular distribution should be the same for both electrons and positrons. The experimental results show that the angle between the direction of emission of positron and incident  $\gamma$ -ray is smaller than the angle between the electron and  $\gamma$ -ray, but the difference observed falls within the error involved in the measurements and hence the agreement between the theory and experiment in this connection may be satisfactory. However, the most probable angle of ejection of either positron or electron for all elements is somewhat higher, as shown in Figure 3, than the theory indicates. In addition, the difference of average energy between the positron and electron is consistently lower than that to be expected from the theory. The change in the position of the maximum of the energy spectrum of the positrons with the element studied is quite distinct, and cannot be explained within the limits of probable error.

#### ACKNOWLEDGMENT

The author wishes to express his thanks to Dr. F. C. Champion for his continued interest in the progress of the experiment and for his helpful discussions.

#### REFERENCES

- ALICHANOW, A. I., ALICHANIAN, A. E., and KOSODAEW, M. S., 1936, *J. Phys. Radium*, **7**, 163.  
BETHE, H., and HEITLER, W., 1934, *Proc. Roy. Soc. A*, **146**, 83.  
CHADWICK, J., BLACKETT, P. M. S., and OCCHIALINI, G. P. S., 1934, *Proc. Roy. Soc. A*, **144**, 235.  
JAEGER, J. C., and HULME, H. R., 1936, *Proc. Roy. Soc. A*, **153**, 443.  
KLARMANN, H., and BOTHE, W., 1936, *Z. Phys.*, **101**, 489.  
LAWSON, J. L., 1949, *Phys. Rev.*, **75**, 433.  
SIMONS, L., and ZUBER, K., 1937, *Proc. Roy. Soc. A*, **159**, 383.





## Structure and Diamagnetic Anisotropy of P-Benzoquinodimethane in Connection with those of P-Benzoquinone

BY M. G. EVANS\*, J. DE HEER† AND J. GERGELY‡,

*Communicated by C. A. Coulson ; MS. received 1st February 1949*

**ABSTRACT.** The interest in the diamagnetic properties of quinodimethane lies in the fact that this molecule can be considered as a prototype for quinone. The diamagnetic anisotropy,  $\Delta\chi$ , of p-benzoquinodimethane has been calculated by the molecular orbital method following the treatment given by F. London in 1937. We find :

$$\Delta\chi_{\text{p-benzoquinodimethane}} \sim 0.3\Delta\chi_{\text{benzene}}$$

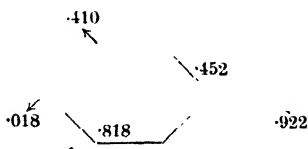
Calculations of the diamagnetic anisotropy of quinone itself fail because the perturbation used here breaks down in this case, in which all the centres in the molecule are not identical.

The result obtained for the quinodimethane can be discussed in connection with the observations by K. Lonsdale and K. S. Krishnan on quinone. We conclude that although  $\Delta\chi$  of quinone is much reduced compared with that for benzene, we need not postulate, to account for this observation, a complete or nearly complete localization of the  $\pi$ -electrons in this structure.

THOUGH Szwarc (1947) has only recently shown the presence of p-quinodimethane,



in the products of the pyrolysis of p-xylene, this compound has been, for several reasons, studied theoretically since 1945 (Diatkina, Namiot, Syrkin 1945, Coulson, Craig, Maccoll, Pullman 1947, Pullman, Berthier, Pullman 1948). In the diagram below we show the free valencies and bond-orders§ as calculated by Pullman *et al.* (1948) by means of the molecular orbital method :



For reasons which will be discussed below, we were interested in the diamagnetic anisotropy,  $\Delta\chi$ , of this compound. A theoretical approach is the only possible one at present. Unfortunately so far no well-established general theory of diamagnetic anisotropy has been put forward. F. London, in 1937, developed a method for calculating  $\Delta\chi$  in certain aromatic systems with reference to  $\Delta\chi$  for benzene as standard. This method is essentially equivalent to a molecular

\* Department of Chemistry, The University, Manchester.

† Department of Chemistry, The University, Manchester; Ramsay Memorial Fellow, the Netherlands.

‡ Laboratory of Physical Biology, National Institute of Health, Bethesda, U.S.A.

§ For the definition of these quantities see e.g. Coulson (1947).

orbital treatment of the mobile  $\pi$ -electrons in these systems with the usual L.C.A.O. approximation.<sup>†</sup> By choosing variation functions of a suitable type, the energies  $\epsilon^1$  of the molecular orbitals, in a magnetic field of strength  $H$  in the direction perpendicular to the plane of the molecule, are obtained as the solutions of a secular equation of the general form

$$|\mathcal{H}_{kl} - \epsilon^1 \delta_{kl}| = 0. \quad \dots\dots(1)$$

$\mathcal{H}_{kl}$  reduces to the ordinary Coulomb integral,  $\alpha$ , for  $k = l$ .  $\mathcal{H}_{kl} = \beta \exp(2\pi i f_{kl}) = \beta \eta_{kl}$  if  $k$  and  $l$  are adjacent atoms ( $\beta$  is the ordinary resonance integral) and  $\mathcal{H}_{kl}$  is zero otherwise.  $\delta_{kl}$  is the Kronecker symbol and the quantity  $f_{kl}$  above expresses in suitable units the magnetic flux through the triangle formed by the centre of the molecule and the bond between the two atoms  $k$  and  $l$ . In the case of the p-quinodimethane molecule an eighth-order equation is obtained, which can be reduced by means of group-theory (the only symmetry operation allowed in the presence of the magnetic field being an inversion with respect to the centre of the molecule) to the following two:

$$\begin{vmatrix} x & \beta & 0 & 0 \\ \beta & x & \eta_s & \eta_s^* \\ 0 & \eta_s^* & x & \eta_d \\ 0 & \eta_s & \eta_d^* & x \end{vmatrix} = 0 \quad \dots\dots(2a) \quad \text{and} \quad \begin{vmatrix} x & \beta & 0 & 0 \\ \beta & x & \eta_s & -\eta_s^* \\ 0 & \eta_s^* & x & \eta_d \\ 0 & -\eta_s & \eta_d^* & x \end{vmatrix} = 0, \quad \dots\dots(2b)$$

where  $x$  is written for  $(\alpha - \epsilon^1)/\beta$ , the  $\eta^*$ s are the complex conjugates of the  $\eta$ s, and the suffixes  $s$  and  $d$  indicate a "single" and a "double" bond in the ring of the molecule. Write

$$\eta_s^2 \eta_d = \exp(\pi i f), \quad \dots\dots(3)$$

where  $f[(e/\hbar c)H]^{-1}$  is put equal to the area of the benzene ring. In this approximate treatment we can neglect the small difference between the areas of the benzene and the "quinoid" ring in quinodimethane. As  $f$  is a small quantity, we obtain from (2a), (2b):

$$x^4 - 4x^2 + 2x + 1 = (\pi f)^2 x, \quad \dots\dots(4a)$$

$$x^4 - 4x^2 - 2x + 1 = -(\pi f)^2 x. \quad \dots\dots(4b)$$

These equations, the solutions of which we will call  $x^1$ , reduce to the ones we would have obtained from the ordinary secular equations for p-benzoquinodimethane if  $f$  were zero ( $H$  is zero). The solutions of the latter, which we will call  $x_0$ , are known (Pullman, Berthier, Pullman 1948) and as  $f$  is a small quantity we obtain from (4a), (4b)

$$(x^1 - x_0)/(\pi f)^2 = \frac{x_0}{4x_0^3 - 8x_0 + 2}, \quad \dots\dots(5a)$$

$$(x^1 - x_0)/(\pi f)^2 = \frac{-x_0}{4x_0^3 - 8x_0 - 2}. \quad \dots\dots(5b)$$

From (5a), (5b) the  $x^1$ s and so the  $\epsilon^1$ s are readily calculated, and by summing these over all the occupied orbitals we obtain the total mobile energy  $E^1$  in the presence of the magnetic field in terms of  $(\pi f)^2$ . Finally, following London (1937), the

<sup>†</sup> A summary of the approximations involved in this method is given by Coulson and Dewar (1947).

diamagnetic anisotropy,  $\Delta\chi$ , is assumed to be equal to the diamagnetic susceptibility due to the "motion" of the mobile electrons in the plane of the molecule, and thus is given by

$$\Delta\chi = -\frac{1}{H} \frac{\partial E}{\partial H} \quad \dots\dots (6)$$

The result of our calculation (which is expressed most simply in terms of  $\Delta\chi_{\text{benzene}}$ ), is  $\Delta\chi_{\text{p-benzoquinodimethane}} = 0.27\Delta\chi_{\text{benzene}}$ .

This value is surprisingly low if we compare it with the experimental data for p-benzoquinone (such data lacking for the quinodimethane itself). Lonsdale (1939, see also Lonsdale and Krishnan 1936) reported a value for  $\Delta\chi_{\text{p-benzoquinone}}$  of 40.6 compared with 61.9 for benzene. This relatively low diamagnetic anisotropy has been put forward by one of us (Evans 1946) as an argument to approximate a quinone as a molecule in which the  $\pi$ -electrons are completely localized in the "double" bonds. On the other hand McMurry's investigations of the spectra of C=O compounds (1941) indicate that in a quinone  $\pi$ -electrons must occupy molecular orbitals extending all through the molecule just as in the quinodimethanes. Recently the authors have confirmed the latter point of view (Evans, Gergely, de Heer 1949). We have shown that there still is an appreciable delocalization of  $\pi$ -electrons in a quinone structure even when we introduce in the secular equations appropriate parameters to take into account the extra binding energy of the C=O bond as compared with the C-C bond and the extra electronegativity of the O-atom as compared with that of the C-atom. But now the problem remained to account theoretically for the low diamagnetic anisotropy of these structures. We tried to calculate the  $\Delta\chi$  for p-benzoquinone by introducing similar parameters to those mentioned above in the secular equations (2). In this way, however, we found a "negative diamagnetic anisotropy" (or a "paramagnetic contribution" of the  $\pi$ -electrons), which of course has no meaning at all and at present only seems to show the limitations of the London method.

The fact that this method breaks down for quinones is not surprising, as here a second-order effect is calculated by means of a first-order perturbation calculus. The fairly good results nevertheless obtained by London might be correlated with the fact that he only considered molecules which were described as "crossable hydrocarbons" by Coulson and Rushbrooke (1940) and as "alternant hydrocarbons" by Coulson and Longuet-Higgins (1947). These authors showed that only for these hydrocarbons is the molecular orbital method in its simplest form self-consistent. So, while this method is still useful to calculate quantities such as mobile energy, bond-orders and free valencies in both non-crossable hydrocarbons and hetero molecules (in the absence of an external field), it might easily give completely wrong results if used to calculate a second-order effect such as the diamagnetic anisotropy.

As a result of this difficulty we had to confine ourselves to the calculation of  $\Delta\chi$  for p-benzoquinodimethane and to consider this molecule as the prototype of a quinone (as has been done before (Pullman, Berthier and Pullman 1948, Diatkina and Syrkin 1946)). As we saw, this computation gave us a very low  $\Delta\chi$ , though the relatively high resonance energy of  $1.924\beta$  indicates an appreciable delocalization, and the bond-orders shown in the diagram above indicate that the ring in this molecule approaches more closely to a benzene ring than to a completely localized quinonoid structure.

Although, remembering the approximate character of the London method, we do not attach any undue importance to the numerical value we have found, we tentatively suggest that a relatively small perturbation of the "pure benzene structure" in an aromatic compound can cause a rapid decrease in the diamagnetic anisotropy. While a satisfactory explanation of this fact cannot be given at present, we may conclude conversely that the low diamagnetic anisotropy found experimentally in p-benzoquinone need not be correlated at all with a complete, or nearly complete, localization of the double bonds in this molecule.

*Note added in proof.* It is easy to modify our calculations so as to include the effect of an overlap integral  $S$  between the atomic wave functions on adjacent atoms. As is well known, the inclusion of this integral modifies the solutions,  $x_0$ , of the unperturbed secular equation by a factor  $1/(1 - Sx_0)$ . Brooks (1940) has shown that in a magnetic field the solutions ( $x^1 - x_0$ ) of equations (5 *a, b*) above have to be "normalized" by  $1/(1 - Sx_0)^2$ , the diamagnetic properties being far more sensitive to this non-orthogonality correction than the energy. Although with  $S=0.25$  the contributions of the individual electrons,  $\epsilon^1$ , change appreciably, the total mobile energy  $E^1$  remains practically unchanged.

Our final result now becomes

$$\Delta\chi_{\text{p-benzoquinodimethane}} = 0.25\Delta\chi_{\text{benzene}}$$

#### ACKNOWLEDGMENT

We wish to thank Professor C. A. Coulson for many helpful discussions.

#### REFERENCES

- BROOKS, HARVEY., 1941, *J. Chem. Phys.*, **9**, 463.  
 COULSON, C. A., 1947, *The Labile Molecule*: Discussion of the Faraday Soc., p. 9.  
 COULSON, C. A., CRAIG, D. P., MACCOLL, A., and PULLMAN, A., 1947, *The Labile Molecule*: Discussion of the Faraday Soc., p. 36.  
 COULSON, C. A., and DEWAR, M. J. S., 1947, *The Labile Molecule*: Discussion of the Faraday Soc., p. 54.  
 COULSON, C. A., and LONGUET-HIGGINS, H. C., 1947, *Proc. Roy. Soc. A*, **192**, 16.  
 COULSON, C. A., and RUSHBROOKE, G. S., 1940, *Proc. Camb. Phil. Soc.*, **36**, 193.  
 DIATKINA, M., NAMIOT, A. J., and SYRKIN, J., 1945, *C.R. Acad. Sci. U.R.S.S.*, **48**, 233.  
 DIATKINA, M., and SYRKIN, J., 1946, *Acta Phys. Chem. U.R.S.S.*, **XXI**, **5**, 921.  
 EVANS, M. G., 1946, *Trans. Faraday Soc.*, **42**, 113.  
 EVANS, M. G., GERGELY, J., and DE HEER, J., 1949, *Trans. Faraday Soc.*, **45**, 312.  
 LONDON, F., 1937, *J. Phys. Radium*, **8**, 397.  
 LONSDALE, K., 1939, *Proc. Roy. Soc. A*, **171**, 559.  
 LONSDALE, K., and KRISHNAN, K. S., 1936, *Proc. Roy. Soc. A*, **156**, 597.  
 McMURRY, H. L., 1941, *J. Chem. Phys.*, **9**, 241.  
 PULLMAN, A., BERTHIER, G., and PULLMAN, B., 1948, *Bull. Soc. Chim. France*, 5<sup>e</sup> ser., **15**, 450.  
 SZWARC, M., 1947, *The Labile Molecule*: Discussion of the Faraday Soc., p. 46.

# The Computation of Wave Functions in Momentum Space— I: The Helium Atom

BY R. McWEENY\* AND C. A. COULSON†

*MS. received 19th April 1949*

**ABSTRACT.** The possibilities of obtaining precise momentum wave functions for atoms by direct solution of the wave equation in momentum space are examined in some detail. An iterative method of approximating to the wave function is employed in computing the momentum distribution function for the helium atom. Although in this instance considerable accuracy is achieved, formidable difficulties arise in extending the calculations to more complicated atoms.

## §1. INTRODUCTION

FOR some time the importance of momentum wave functions has been appreciated: in particular, such functions are fundamental to any discussion of the Compton scattering of x rays (DuMond 1933) and the inelastic scattering of fast electrons (Hughes and Mann 1938).

Hitherto the possibility of computing momentum wave functions directly, by solving the eigenvalue equation in the momentum representation, has usually been dismissed as impracticable and the required functions have been obtained by an application of transformation theory to the more familiar coordinate space wave functions (Duncanson and Coulson 1945). Although this procedure is satisfactory when the approximate solution is built up solely from hydrogen-like orbitals with appropriate screening constants, it proves impossible to transform to momentum space the most accurate wave functions in which electron correlation is adequately represented, the integrals involved being quite insuperable. This difficulty has prompted a further examination of the possibilities of a direct solution in momentum space. The methods of calculation are essentially those employed by Svartholm (1945) in the momentum space treatment of nuclear systems: a distinction arises, however, in that emphasis will be placed upon the computation of the wave functions themselves rather than the associated energies; for this purpose the iterative method is particularly suitable. In the present paper, the  $n$ -electron problem is formulated in momentum space and in the case of the helium atom the iterative method of solution is applied with considerable success. In more general problems the "screening constant" wave functions of Slater and others may be improved to some extent by iteration but there appears to be little prospect, at present, of obtaining from such improved functions the necessary momentum distribution function.

## §2. FORMULATION OF THE PROBLEM

For generality we consider a system of  $N$  particles, the first  $N-1$  being electrons of mass  $m$  and charge  $-e$ , while the  $N$ th is a nucleus of mass  $M$  and charge  $+Ze$ . Since it is impossible to avoid a certain amount of transformation theory a notation for matrix elements and transformation functions must be introduced: the Dirac notation seems most convenient for the formal derivation of the eigenvalue

\* University College, Oxford, now at King's College, University of Durham.

† Wheatstone Physics Laboratory, King's College, London.



equation. For practical purposes however, a familiarity with representation theory is not essential since we may begin our calculations starting with equation (8). In what follows we shall use either of the following equivalent notations for the momentum wave function and its complex conjugate :

$$\begin{aligned}\langle p_{1x} p_{1y} \dots p_{Nx} | &\equiv \Phi(p_{1x} \dots p_{Nx}), \\ | p_{1x} p_{1y} \dots p_{Nx} \rangle &\equiv \Phi^*(p_{1x} \dots p_{Nx}).\end{aligned}$$

The set of commuting observables  $p_{1x}, \dots, p_{Nx}$  may suggest that  $\Phi$  is essentially a function of the Cartesian components of momentum : the choice of coordinates in which the wave function is expressed is, of course, arbitrary and the dependence of  $\Phi$  on the momenta may be abbreviated to  $\Phi = \Phi(\mathbf{p}_1 \dots \mathbf{p}_N)$  i.e. a function of  $N$  momenta, each momentum being dependent upon three variables. In many cases the spherical polar coordinates  $(p, \theta, \phi)$  of each momentum prove most convenient. Often the whole set of momenta will be abbreviated to  $\mathbf{p}$ . The formalism should be clear from the following equivalences :

$$\begin{aligned}\langle \mathbf{p} | &\equiv \Phi(\mathbf{p}) \equiv \Phi(\mathbf{p}_1 \mathbf{p}_2 \dots \mathbf{p}_N) \equiv \Phi(p_1, \theta_1, \phi_1, p_2, \theta_2, \phi_2, \dots, \phi_N), \\ d\mathbf{p} &\equiv d\mathbf{p}_1 d\mathbf{p}_2 \dots d\mathbf{p}_N \equiv p_1^2 \sin \theta_1 dp_1 d\theta_1 d\phi_1 p_2^2 \dots d\phi_N.\end{aligned}$$

In momentum space the eigenvalue equation for the energy becomes

$$\left[ \frac{1}{2M} \mathbf{p}_N^2 + \frac{1}{2m} \sum_{j=1}^{N-1} \mathbf{p}_j^2 \right] \langle \mathbf{p} | + \int \langle \mathbf{p} | V | \mathbf{p}' \rangle d\mathbf{p}' \langle \mathbf{p}' | \rangle = E \langle \mathbf{p} |. \quad \dots (1)$$

The representative  $\langle \mathbf{p} | V | \mathbf{p}' \rangle$  of the potential energy operator is most expediently found by transformation theory. In coordinate space

$$V = \sum_{j=1}^{N-1} V_{jN}(|\mathbf{r}_{jN}|) + \sum_{j < k}^{N-1} V_{jk}(|\mathbf{r}_{jk}|), \quad \dots (2)$$

$\mathbf{r}_{jk}, \mathbf{r}_{jN}$  being the vector separations of particles  $(j, k), (j, N)$ . A single term may be transformed to momentum space according to

$$\begin{aligned}\langle \mathbf{p}_1 \dots \mathbf{p}_N | V_{jk} | \mathbf{p}'_1 \dots \mathbf{p}'_N \rangle &= \int \dots \int \langle \mathbf{p}_1 | \mathbf{r}_1 \rangle \dots \langle \mathbf{p}_N | \mathbf{r}_N \rangle V(|\mathbf{r}_j - \mathbf{r}_k|) \\ &\times d\mathbf{r}_1 \dots d\mathbf{r}_N \langle \mathbf{r}_1 | \mathbf{p}'_1 \rangle \dots \langle \mathbf{r}_N | \mathbf{p}'_N \rangle, \quad \dots (3)\end{aligned}$$

where  $\mathbf{r}_1 \dots \mathbf{r}_N$  are the position vectors of the  $N$  particles, and  $d\mathbf{r}_1 \dots d\mathbf{r}_N$  are volume elements in three dimensions. The transformation functions are

$$\langle \mathbf{p} | \mathbf{r} \rangle = h^{-3/2} \exp \{ -i \mathbf{p} \cdot \mathbf{r} / \hbar \}, \quad \langle \mathbf{r} | \mathbf{p} \rangle = h^{-3/2} \exp \{ i \mathbf{p} \cdot \mathbf{r} / \hbar \}.$$

The multiple integral (3) may be separated into a product of integrals over the 3-dimensional subspaces and finally an introduction of relative coordinates gives (cf. Svartholm 1945)

$$\begin{aligned}\langle \mathbf{p}_1 \dots \mathbf{p}_N | V_{jk} | \mathbf{p}'_1 \dots \mathbf{p}'_N \rangle \\ = \delta(\mathbf{p}_j - \mathbf{p}'_j + \mathbf{p}_k - \mathbf{p}'_k) \prod_{r \neq j \neq k} \delta(\mathbf{p}_r - \mathbf{p}'_r) \cdot \langle \mathbf{p}_j | V_{jk} | \mathbf{p}'_j \rangle, \quad \dots (4)\end{aligned}$$

$$\text{where} \quad \langle \mathbf{p}_j | V_{jk} | \mathbf{p}'_j \rangle = h^{-3} \int \exp \{ -i \mathbf{p}_j - \mathbf{p}'_j \cdot \mathbf{r} / \hbar \} V_{jk}(|\mathbf{r}|) d\mathbf{r}. \quad \dots (5)$$

With attractions of Coulombic form the appropriate integral is easily evaluated \*, giving

$$\langle \mathbf{p}_j | \frac{1}{|\mathbf{r}|} | \mathbf{p}'_j \rangle = \frac{1}{2\pi^2 \hbar} \cdot \frac{1}{|\mathbf{p}_j - \mathbf{p}'_j|^2}. \quad \dots (6)$$

\* A convergence factor must be employed.

Substitution of this result in (1) gives an integral equation for the eigenvalues and eigenfunctions. We confine ourselves to solutions in which there is no resultant translatory motion of the whole system by setting

$$\langle \mathbf{p}_1, \mathbf{p}_2, \dots, \mathbf{p}_N | \rangle = \delta(\mathbf{p}_1 + \mathbf{p}_2 + \dots + \mathbf{p}_N) \langle \mathbf{p}_1 \mathbf{p}_2 \dots \mathbf{p}_{N-1} | \rangle.$$

Putting  $p_0^2 = -2mE$ ,  $R = m/M$ ,  $\lambda = m/\pi^2\hbar$  we find finally

$$\begin{aligned} & \left[ p_0^2 + 2R \sum_{j < k}^{N-1} \mathbf{p}_j \cdot \mathbf{p}_k + (1+R) \sum_{j=1}^{N-1} p_j^2 \right] \langle \mathbf{p}_1 \dots \mathbf{p}_{N-1} | \rangle \\ &= -\lambda \left[ \sum_{j=1}^{N-1} \int \langle \mathbf{p}_j | V_{jN} | \mathbf{p}'_j \rangle d\mathbf{p}'_j \langle \mathbf{p}_1 \dots \mathbf{p}'_j \dots \mathbf{p}_{N-1} | \rangle \right. \\ & \quad \left. + \sum_{j < k}^{N-1} \int \langle \mathbf{p}_j | V_{jk} | \mathbf{p}'_j \rangle d\mathbf{p}'_j \langle \mathbf{p}_1 \dots \mathbf{p}'_j \dots \overline{\mathbf{p}_j + \mathbf{p}_k - \mathbf{p}'_j} \dots \mathbf{p}_{N-1} | \rangle \right]. \end{aligned} \quad \dots (7)$$

The accuracy of solution does not, in most cases, warrant the inclusion of  $R$ : iteration with a finite value of  $R$  would introduce a correction for the motion of the nucleus. We shall regard  $R$  as vanishingly small, and, with a slight change of variables, write the eigenvalue equation for an atomic system, for which the forces are Coulombic, in the following form, where  $n = N - 1$  is the number of electrons in the atom:

$$\begin{aligned} \sum_0^n p_j^2 \langle \mathbf{p}_1 \dots \mathbf{p}_n | \rangle &= \lambda \left[ Z \sum_{j=1}^n \int \frac{d\mathbf{p}}{|\mathbf{p}|^2} \langle \mathbf{p}_1 \dots \overline{\mathbf{p}_j - \mathbf{p}} \dots \mathbf{p}_n | \rangle \right. \\ & \quad \left. - \sum_{j < k}^n \int \frac{d\mathbf{p}}{|\mathbf{p}|^2} \langle \mathbf{p}_1 \dots \overline{\mathbf{p}_j - \mathbf{p}} \dots \overline{\mathbf{p}_k + \mathbf{p}} \dots \mathbf{p}_n | \rangle \right]. \end{aligned} \quad \dots (8)$$

### § 3. METHOD OF SOLUTION

The integral equation (8) may be written quite generally as

$$T(\mathbf{p}) \langle \mathbf{p} | \rangle = \lambda \int \langle \mathbf{p} | V | \mathbf{p}' \rangle d\mathbf{p}' \langle \mathbf{p}' | \rangle. \quad \dots (9)$$

In momentum space  $T(\mathbf{p})$  is always algebraic, being in fact a homogeneous quadratic form in the momenta,

$$T(\mathbf{p}_1 \mathbf{p}_2 \dots \mathbf{p}_n) = (p_0^2 + p_1^2 + p_2^2 + \dots + p_n^2).$$

Solutions of (9) usually exist for a discrete set of negative values of  $E$  (positive values of  $p_0^2$ ): we are primarily interested in the (algebraically) least of these. For the purposes of solution it is convenient to regard  $\lambda$  as the eigenvalue parameter: ultimately we determine an expression for an upper bound to the least eigenvalue  $\lambda^0$  in terms of the constants of the problem and the unknown  $p_0^2$ : on giving  $\lambda$  its true value  $1/\pi^2 a$  a corresponding value of  $p_0^2$  may be calculated. It is easily seen that the value of  $E$  obtained in this way is an upper bound to the least energy eigenvalue.

The most powerful method of obtaining approximate solutions of an equation of this kind appears to be that contained in a theorem originally due to Kellogg (1922). A simple proof is given by Svartholm (1945), who shows that the solution of (9) may be approached by iteration in the following way.

Choosing an arbitrary initial function  $\langle \mathbf{p} | \rangle^0$  form the iterated functions  $\langle \mathbf{p} | \rangle^1, \langle \mathbf{p} | \rangle^2, \dots$  according to the rule  $\langle \mathbf{p} | \rangle^{j+1} = \frac{1}{T(\mathbf{p})} \int \langle \mathbf{p} | V | \mathbf{p}' \rangle d\mathbf{p}' \langle \mathbf{p}' | \rangle^j$ , and the integrals

$$\begin{aligned} T_j &= \int^j \langle \mathbf{p} | T(\mathbf{p}) d\mathbf{p} \langle \mathbf{p} | \rangle^j, \\ W_j &= \int^j \langle \mathbf{p} | d\mathbf{p} \langle \mathbf{p} | V | \mathbf{p}' \rangle d\mathbf{p}' \langle \mathbf{p}' | \rangle^j. \end{aligned}$$

Next form the ratios  $\lambda_j = T_j/W_j$ ,  $\lambda_{j+1} = W_j/T_{j+1}$  ( $j=0, 1, \dots$ ). Then the sequence  $\lambda_0 > \lambda_1 > \lambda_2 > \dots$  converges monotonically to the numerically least eigenvalue ( $\lambda^0$ ) of (9). This result is dependent on the positive definiteness of the operators  $T$  and  $V$ .

For our purposes the trend of the iterated functions themselves is more important. It is not difficult to show that

$$\langle \mathbf{p} | \rangle^j \rightarrow \frac{\text{const.}}{(\lambda^0)^j} \langle \mathbf{p} | 0 \rangle, \quad j \rightarrow \infty,$$

where  $\langle \mathbf{p} | 0 \rangle$  is the eigenfunction corresponding to the eigenvalue  $\lambda^0$ .

For, writing  $\langle \mathbf{p} | \rangle^0 = \sum_s \langle \mathbf{p} | s \rangle \langle s | \rangle^0$ , where  $|s\rangle$  is the  $s$ th eigenstate of (9), and making use of the definition  $T(\mathbf{p})\langle \mathbf{p} | s \rangle = \lambda^s \int \langle \mathbf{p} | V | \mathbf{p}' \rangle d\mathbf{p}' \langle \mathbf{p}' | s \rangle$ , we have

$$\langle \mathbf{p} | \rangle^1 = \sum_s \frac{1}{T(\mathbf{p})} \int \langle \mathbf{p} | V | \mathbf{p}' \rangle d\mathbf{p}' \langle \mathbf{p}' | s \rangle \langle s | \rangle^0 = \sum_s \frac{1}{\lambda^s} \langle \mathbf{p} | s \rangle \langle s | \rangle^0.$$

Repetition then yields  $\langle \mathbf{p} | \rangle^j = \sum_s \left( \frac{1}{\lambda^s} \right)^j \langle \mathbf{p} | s \rangle \langle s | \rangle^0$ , and since  $\lambda^0$  is by hypothesis the numerically least eigenvalue, the desired result follows immediately.

The rapidity of convergence of the process thus depends essentially on the separation of the eigenvalues  $\lambda^0, \lambda^1, \dots, \lambda^s, \dots$  (higher eigenvalues of  $\lambda$  corresponding to excited states of a hypothetical system rather than of the actual one) and is difficult to assess precisely. It appears, however, that with a carefully chosen initial function one iteration is often sufficient to produce a rather accurate approximation to the eigenfunction.

Even at this stage an advantage peculiar to the iterative method is evident. Although in many cases neither  $T_1$  nor  $W_1$  is calculable, the formal expression for the eigenfunction with which they are associated, i.e. the eigenfunction corresponding to the third approximation,  $\lambda_1$ , to the eigenvalue, has already occurred in the calculation of  $W_0$ . The superiority of this approach over a variational method, in which the approximate eigenvalue must first be evaluated and secondly minimized in order to assess the best values of the parameters, is apparent.

#### §4. APPLICATION TO THE HELIUM ATOM

##### (i) Choice of Initial Function.

With  $n=2$  the eigenvalue equation becomes, using atomic units,

$$(p_0^2 + p_1^2 + p_2^2) \Phi(\mathbf{p}_1 \mathbf{p}_2) = \lambda [Z(I_1(\mathbf{p}_1 \mathbf{p}_2) + I_2(\mathbf{p}_1 \mathbf{p}_2)) - I_{12}(\mathbf{p}_1 \mathbf{p}_2)], \quad \dots \dots (10)$$

where

$$\left. \begin{aligned} I_1 &= \int \frac{d\mathbf{p}}{|\mathbf{p}|^2} \Phi(\overline{\mathbf{p}_1 - \mathbf{p}}, \mathbf{p}_2), \quad I_2 = \int \frac{d\mathbf{p}}{|\mathbf{p}|^2} \Phi(\mathbf{p}_1, \overline{\mathbf{p}_2 - \mathbf{p}}) \\ I_{12} &= \int \frac{d\mathbf{p}}{|\mathbf{p}|^2} \Phi(\overline{\mathbf{p}_1 - \mathbf{p}}, \overline{\mathbf{p}_2 + \mathbf{p}}), \quad \lambda = 1/\pi^2. \end{aligned} \right\} \quad (11)$$

In constructing a first approximation to the wave function for an atom it is customary to regard the mutual interaction of the electrons as a negligible perturbation. Neglect of all integrals such as  $I_{12}$  then permits a separation of (10), or more generally (8), and indicates an approximate solution of the product

form analogous to the Hartree type solution in coordinate space. When spin functions are included and the required antisymmetry is introduced  $\Phi$  is most generally a linear superposition of determinantal functions such as

$$\Phi_1 = \begin{vmatrix} \phi_1(\mathbf{p}_1)\alpha(1) & \phi_1(\mathbf{p}_1)\beta(1) & \phi_2(\mathbf{p}_1)\alpha(1) & \dots \\ \phi_1(\mathbf{p}_2)\alpha(2) & \phi_1(\mathbf{p}_2)\beta(2) & \phi_2(\mathbf{p}_2)\alpha(2) & \dots \end{vmatrix} \dots \quad (12)$$

where  $\phi_1(\mathbf{p})$ ,  $\phi_2(\mathbf{p})$ , ... are the various possible wave functions for one electron in the field of the nucleus.

In the ground state problem at present under consideration

$$\phi_1(\mathbf{p}) = \phi_2(\mathbf{p}) = \phi_{1s}(\mathbf{p})$$

and for a Hamiltonian not including spin variables, the antisymmetric spin factor in the wave function may, of course, be omitted. We may then write

$$\Phi^0(\mathbf{p}_1\mathbf{p}_2) = \phi_{1s}(\mathbf{p}_1) \cdot \phi_{1s}(\mathbf{p}_2).$$

As in coordinate space the single particle functions are of simple analytical form: in order to introduce some flexibility into the functions we admit a variable parameter and write

$$\Phi^0(\mathbf{p}_1\mathbf{p}_2) = \frac{1}{(p_1^2 + a^2)^2(p_2^2 + a^2)^2}, \quad \dots\dots (13)$$

where, using atomic units,  $a$  is numerically equal to an "effective" nuclear charge. There is no need to normalize the function at this stage.

Since this function is simply the Fourier transform of the screening constant wave function in coordinate space, we expect, and in fact obtain, an identical variational value of the energy from a calculation of  $\lambda_0$ . The evaluation of the integrals  $T_0$ ,  $W_0$  (or their equivalents), has been carried through independently by Copson (1943): it is worth noting that the calculation is not appreciably more difficult than the corresponding calculation in coordinate space.

In view of our previous observations as to the relative merits of variation and iteration, (13) appears to be the most suitable initial function, further refinement being most conveniently introduced by iteration.

## (ii) The Iterated Function and Variation Treatment.

Using the initial function (13) the first iterated function is given by

$$(p_0^2 + p_1^2 + p_2^2)\Phi^1(\mathbf{p}_1\mathbf{p}_2) = [Z(I_1(\mathbf{p}_1\mathbf{p}_2) + I_2(\mathbf{p}_1\mathbf{p}_2) - I_{12}(\mathbf{p}_1\mathbf{p}_2)], \quad \dots\dots (14)$$

where, from (11), we find easily

$$I_1(\mathbf{p}_1\mathbf{p}_2) = \frac{\pi^2}{a} \frac{1}{(p_1^2 + a^2)(p_2^2 + a^2)^2}, \quad I_2(\mathbf{p}_1\mathbf{p}_2) = \frac{\pi^2}{a} \frac{1}{(p_1^2 + a^2)^2(p_2^2 + a^2)},$$

$$I_{12}(\mathbf{p}_1\mathbf{p}_2) = \int \frac{d\mathbf{p}}{|\mathbf{p}|^2} \frac{1}{\{(\mathbf{p}_1 - \mathbf{p})^2 + a^2\}^2 \{(\mathbf{p}_2 + \mathbf{p})^2 + a^2\}^2}. \quad \dots\dots (15)$$

$W_0$  may now be calculated:

$$W_0 = \iint \Phi^{0*}(p_0^2 + p_1^2 + p_2^2)\Phi^1 d\mathbf{p}_1 d\mathbf{p}_2.$$

By performing the integrations over  $\mathbf{p}_1$  and  $\mathbf{p}_2$  first the direct evaluation of  $I_{12}$  is circumvented and we obtain

$$W_0 = \frac{\pi^6}{16a^9}(Z-5/16). \quad \dots\dots(16)$$

The calculation of  $T_0$  is straightforward

$$T_0 = \frac{\pi^4}{64a^8} \left( 2 + \frac{p_0^2}{a^2} \right). \quad \dots\dots(17)$$

So  $\lambda_0 = \frac{1}{4a\pi^2} \cdot \frac{2a^2 + p_0^2}{Z-5/16}$  possesses a least value  $\frac{p_0}{\pi^2\sqrt{2}} \frac{1}{(Z-5/16)}$  when  $a^2 = p_0^2/2$ .

Now, according to (11) we must put this minimum value equal to  $1/\pi^2$ . This gives

$$p_0^2 = 2(Z-5/16)^2 \text{A.U.}, \quad E = 2(Z-5/16)^2 W_H. \quad \dots\dots(18)$$

In this way the most suitable value of  $a$  is obtained. In the actual computation of the iterated function we shall therefore take  $a = 2 - 5/16 = 1.6875 \text{A.U.}$

Before proceeding with the computation a further remark upon the choice of numerical parameters is necessary, for (16) involves not only  $a$  but  $p_0^2$ .

Now in practice we cannot make an infinite number of iterations and so are never able to compute exactly the appropriate  $\lambda$  in the relation  $\lambda = \lambda(p_0^2)$ . This implies that we can never exactly infer the inverse relation  $p_0^2 = p_0^2(\lambda)$  and consequently can never compute the true value of  $p_0^2$  in the case of interest where  $\lambda = 1/\pi^2$ . Fortunately, however, the iterated wave function shows only a weak dependence upon  $p_0^2$  and the use of a nearly correct  $p_0^2$  instead of the completely correct one has no significant effect on the resultant wave function. In the present case we shall use the accurately known value  $p_0^2 = 5.8074 \text{A.U.}$

The significance of the various members of the iterated function becomes apparent on giving  $p_0^2$  its variational value,  $a^2/2$ . With this somewhat inferior choice we find

$$\frac{I_1(\mathbf{p}_1\mathbf{p}_2) + I_2(\mathbf{p}_1\mathbf{p}_2)}{(p_0^2 + p_1^2 + p_2^2)} \rightarrow \frac{\pi^2}{a} \frac{1}{(p_1^2 + a^2)^2 (p_2^2 + a^2)^2},$$

which is simply a multiple of the initial function. Accordingly we rewrite (14) in the form

$$\Phi^1(\mathbf{p}_1\mathbf{p}_2) = I'(\mathbf{p}_1\mathbf{p}_2) - I'_{12}(\mathbf{p}_1\mathbf{p}_2), \quad \dots\dots(19)$$

where

$$I'(\mathbf{p}_1\mathbf{p}_2) = \frac{Z(I_1(\mathbf{p}_1\mathbf{p}_2) + I_2(\mathbf{p}_1\mathbf{p}_2))}{(p_0^2 + p_1^2 + p_2^2)}$$

$$I'_{12}(\mathbf{p}_1\mathbf{p}_2) = \frac{I_{12}(\mathbf{p}_1\mathbf{p}_2)}{(p_0^2 + p_1^2 + p_2^2)}.$$

Here  $I'(\mathbf{p}_1\mathbf{p}_2)$  in itself represents a slightly improved wave function when  $p_0^2$  is given its true value: in this case

$$I'(\mathbf{p}_1\mathbf{p}_2) = \frac{Z\pi^2}{a} \frac{p_1^2 + p_2^2 + 2a^2}{(p_0^2 + p_1^2 + p_2^2)(p_1^2 + a^2)^2 (p_2^2 + a^2)^2}, \quad \dots\dots(20)$$

which is no longer a simple product,  $f(\mathbf{p}_1) \cdot f(\mathbf{p}_2)$ . In this way the probability distribution of  $\mathbf{p}_1$  is made to depend on the instantaneous value of  $|\mathbf{p}_2|$ : a similar small correction arises from  $I'_{12}$ , as may be verified by expanding the denominator of the integrand in terms of  $\cos(\mathbf{p}_1, \mathbf{p})$ ,  $\cos(\mathbf{p}_2, \mathbf{p})$ : all terms beyond the first are dependent on the mutual inclination of the electron momenta as well as on their magnitudes.

(iii) *The Momentum Distribution Function.*

Although the function  $\Phi^1(\mathbf{p}_1\mathbf{p}_2)$  is of some intrinsic interest it is of little practical value: since the electrons are indistinguishable the only observable quantity is the probability of any electron having a given momentum  $\mathbf{p}$ . This latter function is obtained by integrating the probability density over the momentum coordinates of all electrons but one. In the present case it is accordingly

$$P^1(\mathbf{p}_1) = \int \Phi^{1*}(\mathbf{p}_1\mathbf{p}_2) \Phi^1(\mathbf{p}_1\mathbf{p}_2) d\mathbf{p}_2. \quad \dots\dots(21)$$

Moreover, since we invariably conduct our experiments on an array of randomly oriented atoms or molecules rather than on a single system, a further integration over the solid angle  $\omega_1$  about  $\mathbf{p}_1$  is necessary. The quantity of greatest importance in the present case is thus

$$P(p_1) = \int \int \Phi'^*(\mathbf{p}_1\mathbf{p}_2) \Phi'(\mathbf{p}_1\mathbf{p}_2) d\mathbf{p}_2 p_1^2 d\omega_1. \quad \dots\dots(22)$$

$P(p_1) dp_1$  then measures the probability of observing a momentum with magnitude between  $p_1$  and  $p_1 + dp_1$ .

When simple product wave functions are employed the integrations are easily performed since the integrals separate into a product of "one-electron" integrals (cf. Duncanson and Coulson 1945). In particular, we record the normalized probability distribution corresponding to the initial variation function:

$$P^0(p) = \frac{32a^5 p^2}{\pi(p^2 + a^2)^4}$$

With a better wave function, however, such as  $\Phi^1(\mathbf{p}_1\mathbf{p}_2)$ , a separation of this kind is not possible and the integration over all  $\mathbf{p}_2$ -space may constitute a major difficulty.

Neglecting terms which are of the second order of small quantities

$$P'(\mathbf{p}_1) = \int (I'^2 - 2I'' I'_{12}) d\mathbf{p}_2, \quad \dots\dots(23)$$

where  $I''$  denotes the approximation to  $I'$  which results on taking  $\mathbf{p}_0^2 = a^2/2$ ; this choice of  $\mathbf{p}_0^2$  in  $I'$  makes a quite negligible change in the small correction term  $2I' I'_{12}$  and at the same time greatly simplifies the computation.

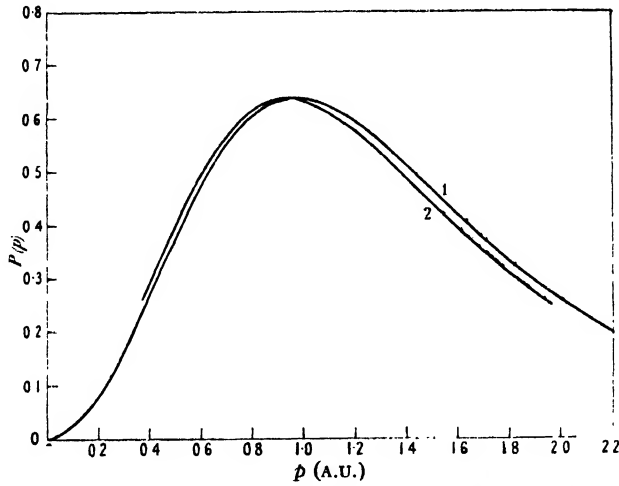
It is of interest to plot the corrected distribution retaining only the major term in the integral. We find easily

$$\int I'^2 d\mathbf{p}_2 = \frac{2\pi^5 Z^2}{a^2} \left[ \frac{I(2/22, p_1)}{(p_1^2 + a^2)^4} + \frac{2I(2/32, p_1)}{(p_1^2 + a^2)^3} + \frac{I(2/42, p_1)}{(p_1^2 + a^2)^2} \right], \quad \dots\dots(24)$$

where

$$I(2/r2, p_1) = \int_{-\infty}^{+\infty} \frac{z^2 dz}{(z^2 + a^2)^r (z^2 + p_0^2 + p_1^2)^2}.$$

The various integrals have been tabulated as functions of  $p_1$  and the modified distribution curve plotted: to the scale adopted in the Figure the curve is, however,



1. Initial approximation  $P^0(p)$ . 2. Corrected function  $P^1(p)$ .

almost indistinguishable from the first approximation.

The contribution of the second term in the integrand of (23) is

$$2 \int I'' I'_{12} d\mathbf{p}_2 = \frac{2\pi^2 Z}{a} \iint \frac{1}{(p_1^2 + a^2)^2 (p_2^2 + a^2)^2} \cdot \frac{1}{(p_0^2 + p_1^2 + p_2^2)} \cdot \frac{d\mathbf{p} d\mathbf{p}_2}{|\mathbf{p}|^2 \{(\mathbf{p}_1 + \mathbf{p})^2 + a^2\}^2 \{(\mathbf{p}_2 - \mathbf{p})^2 + a^2\}^2}.$$

We may write

$$\int I'' I'_{12} d\mathbf{p}_2 = \frac{\pi^2 Z}{a} \frac{1}{(p_1^2 + a^2)^2} \int \frac{K'(\mathbf{p}) d\mathbf{p}}{|\mathbf{p}|^2 \{(\mathbf{p}_1 + \mathbf{p})^2 + a^2\}^2}, \quad \dots (25)$$

where

$$K'(\mathbf{p}) = \int \frac{1}{(p_2^2 + c^2)(p_2^2 + b^2)} \frac{1}{(p_2^2 + a^2)} \frac{d\mathbf{p}_2}{\{(\mathbf{p}_2 - \mathbf{p})^2 + a^2\}^2}.$$

It is convenient to evaluate first

$$K(\mathbf{p}) = \int \frac{1}{(p_2^2 + c^2)(p_2^2 + b^2)} \frac{d\mathbf{p}_2}{\{(\mathbf{p}_2 - \mathbf{p})^2 + a^2\}^2}, [b^2 = p_0^2 + p_1^2], \quad \dots (26)$$

from which  $K'(\mathbf{p})$  may be obtained by differentiating with respect to  $c$  and subsequently letting  $c \rightarrow a$ .

Taking polar coordinates about  $\mathbf{p}$

$$K(\mathbf{p}) = \int_0^{2\pi} \int_0^\pi \int_0^\infty \frac{p_2^2 dp_2 \sin \theta d\theta d\phi}{(p_2^2 + c^2)(p_2^2 + b^2)(p_2^2 + a^2 - 2pp_2 \cos \theta)^2}.$$

The angle integrations are easily accomplished and the denominator of the resultant integral may be factorized to give

$$K(\mathbf{p}) = 4\pi \int_0^\infty \frac{z^2 dz}{(z + ic)(z - ic)(z + ib)(z - ib)(z - p + ia)(z - p - ia)(z + p + ia)(z + p - ia)} \quad \dots (27)$$

By symmetry it is sufficient to evaluate the integral between the limits  $\pm\infty$ , this being accomplished by calculus of residues on completing the contour by an infinite semicircle in the upper half-plane.

We proceed directly to the calculation of  $K'(\mathbf{p})$ , writing down the residues, differentiating with respect to  $c$ , and letting  $c \rightarrow a$ . After some reduction we obtain

$$K'(\mathbf{p}) = \frac{\pi^2}{a(a^2 - b^2)^2} \left[ \frac{Ap^4 + Bp^2 + C}{(p^2 + 4a^2)^2(p^4 + 2Pp^2 + Q^2)} \right], \quad \dots\dots (28)$$

where

$$\begin{aligned} A &= (a-b)^2, \quad B = (11a^4 - 16a^3b + 2a^2b^2 + 3b^4), \\ C &= (10a^6 - 32a^5b + 30a^4b^2 - 10a^2b^4 + 2b^6), \\ P &= (a^2 + b^2), \quad Q = (a^2 - b^2). \end{aligned}$$

The second integration, that indicated in (25), is rather more involved: it may be similarly reduced to a contour integral resembling (27) but with additional poles. The final result is

$$\int I'' I'_{12} d\mathbf{p}_2 = \frac{\pi^4}{2a^2(p_1^2 + a^2)^2} [R_1 + R_2 + R_3], \quad \dots\dots (29)$$

where

$$R_1 = \frac{2(B - Aa^2)}{LM} + \frac{4(16Aa^4 - 4Ba^2 + C)(a^2 - p_1^2)}{LM^2} \\ + \frac{(16Aa^4 - 4Ba^2 + C)(p_1^4 - 26a^2p_1^2 + 57a^4)}{4a^2 L^2 M}$$

$$R_2 = \frac{AX + BY + CZ}{2L^2(p_1^2 + a^2)^5}$$

$$R_3 = (a+b)[2ab(p_1^2 + a^2) - (a^4 - b^4)],$$

and

$$L = p_1^4 + 10a^2p_1^2 + 9a^4,$$

$$M = p_1^4 - 6a^2p_1^2 - 7a^4,$$

$$X = (p_1^2 + a^2)^3(p_1^6 + 7a^2p_1^4 + 27a^4p_1^2 + 21a^6),$$

$$Y = (p_1^2 + a^2)^2(p_1^6 - a^2p_1^4 - 5a^4p_1^2 - 3a^6),$$

$$Z = (p_1^8 - 12a^2p_1^6 - 42a^4p_1^4 - 44a^6p_1^2 - 15a^8).$$

Remembering  $b = \sqrt{(p_0^2 + p_1^2)} \approx \sqrt{(2a^2 + p_1^2)}$  to the present approximation, we may tabulate the above expressions as functions of  $p_1$ . Since the result is angle independent the integration over the solid angle  $\omega_1$  yields only a factor  $4\pi$ . The final momentum distribution including this further correction is illustrated in the Figure. The curve indicates a considerable decrease in the mean momentum, as would be expected from the virial theorem. For in momentum space

$$T = \frac{1}{2m} \int_0^\infty P(p) p^2 dp$$

and a shift of the peak of  $P(p)$  towards regions of lower momentum implies a shift of weight from large to small values of  $p$ , with a consequent reduction in  $\bar{T}$ . Normalization is not easily effected analytically and for purposes of comparison the curve is plotted to the same peak height as with the first approximation.



(iv) *Possibilities of Further Applications.*

We conclude with an enquiry into the possibilities of extending the analysis just developed for helium to other atomic systems. Since the eigenvalue equation whose solution we are seeking refers essentially to a monatomic system, and association of any kind is known to have a profound effect on the momentum distribution, the next simplest atom to be dealt with should, logically, be neon, intervening atoms in the periodic table being incapable of sustained independent existence.

It is essential that the initial function should possess the completely anti-symmetric form demanded by the Pauli Principle, for otherwise iteration would lead to a "collapse" of the initial functions into the lowest available orbitals. This naturally introduces enormous complications but there is still no formal difficulty in writing down an iterated function. Thus we find

$$\Phi^1(\mathbf{p}_1 \dots \mathbf{p}_n) = \frac{S}{(p_0^2 + p_1^2 + \dots + p_n^2)} \frac{S_{rs}}{(p_0^2 + p_1^2 + \dots + p_n^2)},$$

where  $S$  denotes the appropriate antisymmetric sum of a number of terms containing only one-electron integrals (every one of which is integrable with a screening constant initial function) and  $S_{rs}$  denotes a similar sum of "correlation integrals" (such as  $I_{12}$  of the last section).

As already noted, the leading term in the expansion of each correlation integral could be evaluated and with the inclusion of such terms a rather accurate wave function might be obtained.

In this way correlation effects would be represented to a considerable extent, and the corrected wave function would no longer be a simple product of one-electron functions. Unfortunately, however, a serious difficulty is simultaneously introduced. No function is of very great practical utility unless it permits the computation of  $P(p)$ : the suggested function after iteration does not lend itself to such a computation, the task of integrating over all the momenta but one proving a formidable obstacle to further progress. For that reason we have not proceeded with the calculation of the iterated function.

## REFERENCES

- COPSON, E. T., 1943, *Proc. Roy. Soc. Edinb.*, **61**, 260.  
 DU MOND, J. W. M., 1933, *Rev. Mod. Phys.*, **5**, 1.  
 DUNCANSON, W. E., and COULSON, C. A., 1945, *Proc. Phys. Soc.*, **57**, 190.  
 HUGHES, A. L., and MANN, M. M., 1938, *Phys. Rev.*, **53**, 50.  
 KELLOGG, O. D., 1922, *Math. Ann.*, **86**, 14.  
 SVARTHOLM, N. V., 1945, *The Binding Energies of the Lightest Atomic Nuclei* (Stockholm: Lund).

# The Computation of Wave Functions in Momentum Space— II: The Hydrogen Molecule Ion

BY R. McWEENY\*  
University College, Oxford

*Communicated by C. A. Coulson ; MS. received 19th April 1949*

**ABSTRACT.** A new approach is made to the problem of computing accurate momentum distribution functions for electrons in molecules. The usual molecular orbital wave function (linear combination of atomic orbitals) has already been employed for this purpose but has proved inadequate in attempts to explain the width of the Compton profile. Using the method of a previous paper, the l.c.a.o. type of molecular orbital is formally corrected by iteration. In most cases it seems likely that the corrected orbital will be associated with a greater spread of the momentum distribution and will thus lead to a broader Compton profile: the broadening should become more marked with increasing delocalization of the electron and may apparently be very considerable. A complete calculation has confirmed these conclusions in the case of the hydrogen molecule ion: a preliminary treatment of the neutral molecule is given.

## § 1. INTRODUCTION

IN Part I† of this work the distribution of momentum in a simple monatomic system was computed directly by approximate solution of the eigenvalue integral equation in momentum space; certain features of the iterative method employed were found particularly suited to this purpose.

The object of the present investigation is to determine whether similar methods may be employed in computing the momentum distribution of electrons in molecules. A complete calculation is at present confined to the simplest of all diatomic molecules, the hydrogen molecule ion, but certain general effects of aggregation upon individual atomic orbitals are predicted. Results suggest that the use of more accurate wave functions might give very much better agreement than hitherto between the computed and observed profiles for Compton scattering from molecules and solid scatterers.

## § 2. THE MOTION OF AN ELECTRON ABOUT $n$ CENTRES OF FORCE

### (i) *Formulation of the Problem*

For generality let us consider the motion of an electron about  $n$  centres of force located at points with position vectors  $\mathbf{R}_1, \mathbf{R}_2, \dots, \mathbf{R}_n$ . Let the position vector of the electron be  $\mathbf{r}$ . We shall require the momentum space representative of the potential energy operator: this may be obtained using the methods and notation of I. If  $V_s$  be the potential function for the  $s$ th centre

$$V = \sum_s V_s(|\mathbf{r} - \mathbf{R}_s|).$$

A single term is transformed to momentum space according to

$$\langle \mathbf{p} | V_s(|\mathbf{r} - \mathbf{R}_s|) | \mathbf{p}' \rangle = \hbar^{-3} \int \exp \{ -i \overline{\mathbf{p} - \mathbf{p}'} \cdot \mathbf{r} / \hbar \} \cdot V_s(|\mathbf{r} - \mathbf{R}_s|) d\mathbf{r}.$$

\* Now at King's College, University of Durham.

† Page 509 of this Journal: hereafter referred to as I.

With a change of variable we easily find, using atomic units as in I,

$$\langle \mathbf{p} | V_s(|\mathbf{r} - \mathbf{R}_s|) | \mathbf{p}' \rangle = \exp \{ -i \overline{\mathbf{p} - \mathbf{p}' \cdot \mathbf{R}_s} \} \cdot \langle \mathbf{p} | V_s(|\mathbf{r}|) | \mathbf{p}' \rangle, \quad \dots (1)$$

where  $\langle \mathbf{p} | V_s(|\mathbf{r}|) | \mathbf{p}' \rangle$  is simply the momentum space transform of  $V_s$  with the  $s$ th centre regarded as origin.

The eigenvalue equation may thus be written

$$(p_0^2 + p^2)\phi(\mathbf{p}) = -2m \sum_{s=1}^n \int \exp \{ -i \overline{\mathbf{p} - \mathbf{p}' \cdot \mathbf{R}_s} \} \cdot \langle \mathbf{p} | V_s | \mathbf{p}' \rangle d\mathbf{p}' \phi(\mathbf{p}'). \quad \dots (2)$$

If we suppose the electron to be in the vicinity of one particular nucleus and assume that all other terms in the potential function are therefore negligible compared with, say,  $V_s$ , it is easily verified that

$$\phi(\mathbf{p}) = \exp(-i\mathbf{p} \cdot \mathbf{R}_s) \cdot \phi_s(\mathbf{p}) \quad \dots (3)$$

is a solution of (2) provided  $\phi_s(\mathbf{p})$  satisfies

$$(p_0^2 + p^2)\phi_s(\mathbf{p}) = -2m \int \langle \mathbf{p} | V_s | \mathbf{p}' \rangle d\mathbf{p}' \phi_s(\mathbf{p}').$$

The function  $\phi_s(\mathbf{p})$  is thus simply an eigenfunction for the motion of the electron about the  $s$ th nucleus alone, situated at the origin. We may therefore call  $\exp(-i\mathbf{p} \cdot \mathbf{R}_s)$  a "displacement operator". Putting

$$D_s(\mathbf{p}) = \exp(-i\mathbf{p} \cdot \mathbf{R}_s), \quad D_s^{-1}(\mathbf{p}) = \exp(+i\mathbf{p} \cdot \mathbf{R}_s),$$

the displacement of a physical system from  $\mathbf{0}$  to  $\mathbf{R}$  induces the following transformation of associated operators and wave function

$$\begin{aligned} \langle \mathbf{p} | V | \mathbf{p}' \rangle &\rightarrow D_s(\mathbf{p}) \langle \mathbf{p} | V | \mathbf{p}' \rangle D_s^{-1}(\mathbf{p}'), \\ \phi(\mathbf{p}) &\rightarrow D_s(\mathbf{p}) \cdot \phi(\mathbf{p}). \end{aligned}$$

The eigenvalue equation (2) may thus be written

$$(p_0^2 + p^2)\phi(\mathbf{p}) = -2m \sum_{s=1}^n \int D_s(\mathbf{p}) \langle \mathbf{p} | V_s | \mathbf{p}' \rangle D_s^{-1}(\mathbf{p}') d\mathbf{p}' \phi(\mathbf{p}'). \quad \dots (2')$$

A superposition wave function precisely equivalent to the molecular orbital in coordinate space may be formed from terms such as (3). We shall call such a function  $\phi^0(\mathbf{p})$  and take it as our initial function, namely

$$\phi^0(\mathbf{p}) = \sigma_1 D_1(\mathbf{p}) \cdot \phi_1(\mathbf{p}) + \sigma_2 D_2(\mathbf{p}) \cdot \phi_2(\mathbf{p}) + \dots \sigma_n D_n(\mathbf{p}) \cdot \phi_n(\mathbf{p}). \quad \dots (4)$$

$\phi_1(\mathbf{p}) \dots \phi_n(\mathbf{p})$  are the momentum space transforms of atomic orbitals about centres 1, ...  $n$ , and will in general be approximated by hydrogen-like wave functions.  $\sigma_1 \dots \sigma_n$  are best assessed by the usual molecular orbital treatment.

### (ii) The Iterative Correction

Taking (4) as the starting point of our treatment the first iterated function  $\phi^1(\mathbf{p})$  may immediately be written down. From (2')

$$\begin{aligned} \phi^1(\mathbf{p}) &= \frac{-2m}{(p_0^2 + p^2)} \sum_s \sigma_s \int D_s(\mathbf{p}) \langle \mathbf{p} | V_s | \mathbf{p}' \rangle D_s^{-1}(\mathbf{p}') d\mathbf{p}' D_s(\mathbf{p}') \phi_s(\mathbf{p}') \\ &= \frac{-2m}{(p_0^2 + p^2)} \sum_s \sigma_s I^{st} D_s(\mathbf{p}), \end{aligned} \quad \dots (5)$$

where

$$I^{st} = \int \langle \mathbf{p} | V_s | \mathbf{p}' \rangle \exp \{ -i \overline{\mathbf{p}' \cdot \mathbf{R}_t - \mathbf{R}_s} \} d\mathbf{p}' \phi_t(\mathbf{p}'). \quad \dots (6)$$

Even at this stage inferences as to the nature of the corrections may be made. A typical term,  $I^s D_s(\mathbf{p})$ , of the summand in (5) may be said to represent the perturbing influence of the  $s$ th nucleus on the momentum distribution of an electron moving in the field of the  $t$ th nucleus alone. Even with neglect of all terms except those for which  $s = t$  a correction results, for, to this approximation

$$\phi^1(\mathbf{p}) = \frac{-2m}{(p_0^2 + p^2)} \sum_{t=1}^n \sigma_t D_t(\mathbf{p}) \int \langle \mathbf{p} | V_t | \mathbf{p}' \rangle d\mathbf{p}' \phi_t(\mathbf{p}'). \quad \dots\dots (7)$$

But, by definition of the atomic orbital  $\phi_t(\mathbf{p})$

$$[(p_0^2)_t + p^2] \phi_t(\mathbf{p}) = -2m \int \langle \mathbf{p} | V_t | \mathbf{p}' \rangle d\mathbf{p}' \phi_t(\mathbf{p}'), \quad \dots\dots (8)$$

so that

$$\phi^1(\mathbf{p}) = \sum_{t=1}^n \sigma_t D_t(\mathbf{p}) \frac{(p_0^2)_t + p^2}{p_0^2 + p^2} \phi_t(\mathbf{p}). \quad \dots\dots (9)$$

Now (9) is simply a linear superposition molecular orbital in which the individual atomic orbitals have been modified by a factor which is an angle-independent function of  $\mathbf{p}$ . Moreover, we can at once predict the effect of this correction on the momentum distribution function, for  $(p_0^2)_t$  and  $p_0^2$  may be regarded as, at least, approximately known quantities. Quite generally we may suppose  $p_0^2 > (p_0^2)_t$  since we are concerned solely with the ground state in which the electron occupies a bonding molecular orbital. Each atomic orbital in (9) is thus multiplied by a monotonically increasing function of  $p$ : consequently the resultant momentum distribution is a less rapidly decreasing function of  $p$  than the initial approximation would suggest. To a first approximation the half-width of the momentum distribution function is in this way always increased by the perturbing effect of neighbouring nuclei. Since, generally speaking, the difference between  $(p_0^2)_t$  and  $p_0^2$  becomes more marked as the binding of the electron to the  $t$ th centre becomes less, we may say that the increase in half-width of the distribution function over that predicted on a simple l.c.a.o. treatment (Coulson 1941) will become greater as localization of the electron at a particular centre decreases. This result is in agreement with experimental results on Compton scattering. Although the width of the Compton profile is not simply proportional to the width of the momentum distribution there is always a marked similarity between the two curves and it may at least be shown that an increase in width of one implies an increase in width of the other. The computed profile agrees very well with experimental curves for monatomic scatterers but for molecular and solid scatterers the computed width, using the l.c.a.o. approximation to the wave function, falls far short of the observed width (Duncanson and Coulson 1941, p. 417). Assuming the approximate additivity of one-electron distributions (Coulson 1941), these considerations suggest that refinement of the wave functions may lead to much closer agreement. This result is substantiated in a subsequent section.

The modification of the initial wave function so far discussed may be described as a spherically symmetrical distortion of each atomic orbital in the initial linear combination. The modifications imposed by those terms so far neglected are generally smaller and introduce an angle-dependent distortion, or polarization, of each atomic orbital, together with a "mixing" of the orbitals. Reference to (5) shows that we may still regard the molecular orbital as a linear combination of atomic orbitals provided  $\sum_t \sigma_t I^s$  be interpreted as a distorted atomic orbital about the  $s$ th centre. In addition to the dominant correction already discussed there will then be a contribution from every other centre,  $t$ , dependent on three factors: (i) the

form of the orbital about the  $t$ th centre, (ii) the relative importance of this orbital, measured by  $\sigma_t$ , (iii) the magnitude and direction of the position vector of  $t$  relative to  $s$ .

In this way each atomic orbital takes up, on correction, the symmetry of the whole molecule. It is difficult to assess generally the effect of this correction on the momentum distribution function; calculation shows that in the case of the hydrogen molecule ion it is to oppose the correction first discussed. The polarization effect will, however, become less marked with increasing nuclear separation and with increasing symmetry of the configuration, features characteristic of the solid state.

### § 3. THE HYDROGEN MOLECULE ION

<sup>†</sup> For a homonuclear system such as  $\text{H}_2^+$  with nuclei 1 and 2 at  $-\mathbf{R}$  and  $+\mathbf{R}$ , (2) and (4) assume particularly simple forms. With a nuclear charge  $Z$  and attractions of Coulombic form we find, using atomic units

$$(\dot{p}_0^2 + \dot{p}^2)\phi(\mathbf{p}) = \frac{2Z}{\pi^2} \int \frac{\cos(\overline{\mathbf{p} - \mathbf{p}'} \cdot \mathbf{R})}{|\mathbf{p} - \mathbf{p}'|^2} d\mathbf{p}' \phi(\mathbf{p}'), \quad \dots\dots(10)$$

$$\phi^0(\mathbf{p}) = 2 \cos(\mathbf{p} \cdot \mathbf{R}) \cdot \phi_1(\mathbf{p}), \quad \dots\dots(11)$$

where  $\phi_1(\mathbf{p})$  is an atomic orbital for motion about either centre and symmetry has imposed the condition  $\sigma_1 = \sigma_2$ .

The momentum distribution corresponding to a wave function (11) has been obtained elsewhere (Coulson 1941). For purposes of comparison the normalized curve is plotted in Figure 1 as  $P^0(p)$ .

As we have already noted (I) a variational method of approximating to the wave function, using a linear function system such as

$$\phi_r(\mathbf{p}) = \sum_{m,n} \frac{P_m(\cos \theta)}{(\dot{p}^2 + a^2)^n},$$

is often precluded by the fact that it necessitates a computation of the energy eigenvalue and this may be vastly more difficult in momentum space than in coordinate space. For this reason we adopt the iterative approach.

The first iterated function, corresponding to (5), is most conveniently written

$$\phi^1(\mathbf{p}) = \frac{1}{\dot{p}_0^2 + \dot{p}^2} [I_s(\mathbf{p}) + I_p(\mathbf{p})], \quad \dots\dots(12)$$

$$\text{where } I_s(\mathbf{p}) = 2 \cos(\mathbf{p} \cdot \mathbf{R}) \int \frac{d\mathbf{p}'}{|\mathbf{p} - \mathbf{p}'|^2} \phi_1(\mathbf{p}'), \quad \dots\dots(13)$$

$$\text{and } I_p(\mathbf{p}) = 2 \text{Re} [\exp(i\mathbf{p} \cdot \mathbf{R})] \int \frac{d\mathbf{p}'}{|\mathbf{p} - \mathbf{p}'|^2} \exp(-2i\mathbf{p}' \cdot \mathbf{R}) \cdot \phi_1(\mathbf{p}'). \quad \dots\dots(14)$$

$I_s(\mathbf{p})$  and  $I_p(\mathbf{p})$  then introduce, respectively, the angle-independent and the angle-dependent corrections to the initial atomic orbitals.

Since  $\phi_1(\mathbf{p})$  satisfies, by definition, an equation

$$[(\dot{p}_0^2)_1 + \dot{p}^2]\phi_1(\mathbf{p}) = \frac{Z'}{\pi^2} \int \frac{d\mathbf{p}'}{|\mathbf{p} - \mathbf{p}'|^2} \phi_1(\mathbf{p}'), \quad \dots\dots(15)$$

where  $Z'$  is an effective nuclear charge and  $(\dot{p}_0^2)_1$  the associated value of  $\dot{p}_0^2$ , the dominant term in (12) is

$$\frac{2\pi^2}{Z'} \cos(\mathbf{p} \cdot \mathbf{R}) \frac{[(\dot{p}_0^2)_1 + \dot{p}^2]}{(\dot{p}_0^2 + \dot{p}^2)} \phi_1(\mathbf{p}). \quad \dots\dots(16)$$

In the present case, guided by the screening constant calculation in coordinate space, we shall take  $Z' = 1.228$ . The corresponding exact solution of (15) for the  $1s$  state is

$$\phi_1(\mathbf{p}) = \frac{1}{(p^2 + a^2)^2}, \quad \text{with } a = (p_0)_1 = Z', \quad \dots\dots(17)$$

(16) may therefore be written

$$\frac{2\pi^2}{a} \cos(\mathbf{p} \cdot \mathbf{R}) \frac{1}{(p^2 + a^2)(p^2 + b^2)}, \quad (b = p_0).$$

Comparison with (11) shows that the principal modification introduced by iteration is the replacement of the simple  $1s$  atomic orbital by the function

$$\phi'_1(\mathbf{p}) = \frac{1}{(p^2 + a^2)(p^2 + b^2)}. \quad \dots\dots(18)$$

In coordinate space a more satisfactory molecular orbital might therefore be a superposition of atomic orbitals such as

$$\frac{\exp(-ar) - \exp(-br)}{\quad} \quad \left( \text{or } \frac{2 \sinh \frac{1}{2}(b-a)r}{\quad} \cdot \exp\left\{-\frac{1}{2}(a+b)r\right\} \right).$$

this being the Fourier transform of (18), rather than of the simple  $1s$  orbitals,  $\exp(-ar)$ .

Since (18) is not appreciably more complicated than (17) we shall accommodate this result in our treatment at the outset by employing  $\phi'_1(\mathbf{p})$  rather than  $\phi_1(\mathbf{p})$  as an initial atomic orbital. A further complete iteration will now be carried through with the inclusion of angle-dependent corrections. As in I we shall take the best available values of the parameters, namely  $p_0^2 = 2.20523$  A.U.;  $R = 1.000$  A.U.

### (i) Spherically Symmetrical Correction

We deal first with the angle-dependent part of the iterated function. With the new initial orbital,  $\phi'_1(\mathbf{p})$ , it is possible to evaluate  $I_s(\mathbf{p})$  by standard methods of the calculus of residues. We find

$$I_s(\mathbf{p}) = 2 \cos(\mathbf{p} \cdot \mathbf{R}) \frac{2\pi^2}{(a^2 - b^2)p} \tan^{-1} \left\{ \frac{(a-b)p}{ab + p^2} \right\}. \quad \dots\dots(19)$$

The numerical magnitudes involved allow us to replace the  $\tan^{-1}$  by the first term in its expansion with a maximum error of the order  $\frac{1}{3}\%$ . Since it would be presumptuous to regard this as significant we take simply

$$I_s(\mathbf{p}) = \cos(\mathbf{p} \cdot \mathbf{R}) \frac{4\pi^2}{(a+b)(ab + p^2)}. \quad \dots\dots(20)$$

Ultimately, as already noted, the momentum distribution function  $P(p)$  is required. From (12)

$$P(p) = \int \frac{p^2 d\omega}{(p_0^2 + p^2)^2} [I_s^2 + 2I_s I_p + I_p^2]. \quad \dots\dots(21)$$

The term in  $I_s^2$  arises, as we have seen, from the partially corrected initial function; the second term in the integrand introduces a further correction whose

order of magnitude justifies the neglect of the remaining, second order, term. We are here concerned with the angle-independent term: a simple integration gives

$$P_s(p) = \int_0^{2\pi} \int_0^\pi \frac{p^2 [I_s(\mathbf{p})]^2}{(p_0^2 + p^2)^2} \sin \theta \, d\theta \, d\phi = \frac{2\pi p^2}{(p_0^2 + p^2)^2} \left[ \frac{4\pi^2}{(a+b)(ab+p^2)} \right]^2 \left[ \frac{\sin 2pR}{2pR} + 1 \right]. \quad \dots\dots (22)$$

This curve is compared with the screening constant approximation in Figure 1, where it is scaled to the same peak height.

### (ii) Polarization Correction

Before the correction due to polarization of the initial atomic orbitals can be computed it is necessary to obtain a series expansion of the integral  $I_p(\mathbf{p})$  which cannot be evaluated in closed form. Writing (14) as

$$I_\nu(\mathbf{p}) = 2 \operatorname{Re} \exp(i\mathbf{p} \cdot \mathbf{R}) \cdot I(\mathbf{p}),$$

we may take polar coordinates about  $\mathbf{p}$  as axis and, with  $\mathbf{R} = (R, \theta, 0)$ ,  $\mathbf{p}' = (p', \theta', \phi')$ , write

$$I(\mathbf{p}) = \int_0^{2\pi} \int_0^\pi \int_0^\infty \frac{\exp \{-2ip'R(\sin \theta \sin \theta' \cos \phi' + \cos \theta \cos \theta')\} p'^2 dp' \sin \theta' d\theta' d\phi'}{(p^2 + p'^2 - 2pp' \cos \theta') (p'^2 + a^2) (p'^2 + b^2)}.$$

The  $\phi'$  integration is easily accomplished (Sommerfeld's Integral), giving

$$I(\mathbf{p}) = 2\pi \int_0^\pi \int_0^\infty \frac{\exp \{-2ip'R \cos \theta' \cos \theta\} \cdot J_0(2p'R \sin \theta' \sin \theta) p'^2 dp' \sin \theta' d\theta'}{(p^2 + p'^2 - 2pp' \cos \theta') (p'^2 + a^2) (p'^2 + b^2)} \quad \dots\dots (23)$$

The remaining angle integration is awkward but may be performed term by term on making the expansion

$$\frac{1}{(p^2 + p'^2 - 2pp' \cos \theta')} = \frac{1}{(p^2 + p'^2)} \{P_0(\cos \theta') + \mu_1 P_1(\cos \theta') + \dots\}, \quad \dots\dots (24)$$

which is obtained from a binomial expansion by expressing the powers of  $\cos \theta'$  in terms of the Legendre functions. The  $\mu$ 's are, of course, functions of  $p$  and  $p'$ .

Subsequently the following result, due to Gegenbauer (1874) may be employed

$$\begin{aligned} \int_0^\pi \exp(iz \cos \theta \cos \psi) \cdot J_{\nu-\frac{1}{2}}(z \sin \theta \sin \psi) \cdot C_r^\nu(\cos \theta) \cdot \sin^{\nu+\frac{1}{2}} \theta \, d\theta \\ = \left(\frac{2\pi}{z}\right)^{\frac{1}{2}} (i)^r \sin^{\nu-\frac{1}{2}} \psi \cdot C_r^\nu(\cos \psi) \cdot J_{\nu+r}(z). \end{aligned}$$

Assuming the validity of (24) and remembering  $P_r(\cos \theta') = C_r^{\frac{1}{2}}(\cos \theta')$ , an application of this result with  $\nu = \frac{1}{2}$  gives finally

$$I(\mathbf{p}) = 4\pi \int_0^\infty \left(\frac{\pi}{p'R}\right)^{\frac{1}{2}} \frac{[A \cos(\mathbf{p} \cdot \mathbf{R}) - B \sin(\mathbf{p} \cdot \mathbf{R})] p'^2 dp'}{(p'^2 + a^2)(p'^2 + b^2)(p'^2 + p^2)}, \quad \dots\dots (25)$$

where

$$A = P_0(\cos \theta) \cdot J_{\frac{1}{2}}(2p'R) - \mu_2 P_2(\cos \theta) \cdot J_{\frac{5}{2}}(2p'R) + \mu_4 P_4(\cos \theta) \cdot J_{\frac{9}{2}}(2p'R) - \dots$$

and

$$\begin{aligned} B = -\mu_1 P_1(\cos \theta) \cdot J_{\frac{3}{2}}(2p'R) + \mu_3 P_3(\cos \theta) \cdot J_{\frac{7}{2}}(2p'R) \\ - \mu_5 P_5(\cos \theta) \cdot J_{\frac{11}{2}}(2p'R) + \dots \end{aligned}$$

Expressing the  $\mu$ 's explicitly as functions of  $p$  and  $p'$ , and the Bessel functions in terms of elementary functions we might complete the integration expressed in (25). Since we require ultimately  $P(p)$  this would not be a very profitable course; instead we compute directly

$$P_p(p) = \frac{2p^2}{(p_0^2 + p^2)^2} \int_0^{2\pi} \int_0^\pi I_s(\mathbf{p}) I_p(\mathbf{p}) \sin \theta d\theta d\phi,$$

with  $\mathbf{R}$  as polar axis. The  $\phi$  integration is trivial on account of axial symmetry and we find finally

$$P_p(p) = \frac{16\pi^2 p^2}{(p_0^2 + p^2)^2} \left[ \frac{4\pi^2}{(a+b)(ab+p^2)} \right] [C(p) - D(p)], \quad \dots\dots (26)$$

where

$$C(p) = \sum_n C_{\theta n} C_{Rn}, \quad n \text{ even},$$

$$D(p) = \sum_n C_{\theta n} C_{Rn}, \quad n \text{ odd},$$

and

$$C_{\theta n} = \int_{-1}^{+1} \cos^2(pRx) \cdot P_n(x) dx, \quad n \text{ even},$$

$$= \int_{-1}^{+1} \cos(pRx) \sin(pRx) \cdot P_n(x) dx, \quad n \text{ odd},$$

$$C_{Rn} = (-1)^{n/2} \int_0^\infty \left( \frac{\pi}{p'R} \right)^{\frac{1}{2}} \frac{\mu_n(p') \cdot J_{n+\frac{1}{2}}(2p'R) p'^2 dp'}{(p'^2 + a^2)(p'^2 + b^2)(p'^2 + p^2)}, \quad n \text{ even},$$

$$= (-1)^{(n+1)/2} \int_0^\infty \left( \frac{\pi}{p'R} \right)^{\frac{1}{2}} \frac{\mu_n(p') J_{n+\frac{1}{2}}(2p'R) p'^2 dp'}{(p'^2 + a^2)(p'^2 + b^2)(p'^2 + p^2)}, \quad n \text{ odd}.$$

The functions  $C_{\theta n}$  are most easily built up from

$$I_{\theta n} = \int_0^1 \cos(2pRx) \cdot x^n dx, \quad n \text{ even}, \quad = \int_0^1 \sin(2pRx) \cdot x^n dx, \quad n \text{ odd},$$

which may all be derived from  $I_{\theta 0}$  by the recurrence relations

$$(2pR)I_{\theta, n+1} = (n+1)I_{\theta n} - \cos(2pR), \quad n \text{ even},$$

$$(2pR)I_{\theta, n+1} = \sin(2pR) - (n+1)I_{\theta, n}, \quad n \text{ odd}.$$

The integrals  $C_{Rn}$  involve the  $\mu$ 's: these are easily obtained explicitly by a power series expansion of  $(p^2 + p'^2 - 2pp' \cos \theta')^{-1}$  in  $a \cos \theta'$  where  $a = 2pp'/(p^2 + p'^2) (\leq 1)$ . The cosines may be written in terms of the Legendre functions by recursion. All the integrals are ultimately reducible to sums of integrals of the type

$$\left. \begin{aligned} I(rS/s, p) &= \int_{-\infty}^{+\infty} \frac{p'r \sin(2p'R) dp'}{(p'^2 + a^2)(p'^2 + b^2)(p'^2 + p^2)^s}, & r \text{ odd}, \\ I(rC/s, p) &= \int_{-\infty}^{+\infty} \frac{p'r \cos(2p'R) dp'}{(p'^2 + a^2)(p'^2 + b^2)(p'^2 + p^2)^s}, & r \text{ even}. \end{aligned} \right\} \quad \dots\dots (27)$$

Since a rather large number of these integrals must be computed as functions of  $p$  it is gratifying to find that for values of  $s > 2$  numerical differentiation of  $I(rS/2)$ ,  $I(rC/2)$  affords a convenient method of tabulation: higher integrals rapidly become smaller and this treatment gives adequate accuracy. The basic integrals  $I(rS/2)$ ,  $I(rC/2)$  may be evaluated by calculus of residues and have been tabulated for  $r = 1, 2, \dots 5$ . A five-point rule proves adequate for subsequent differentiation.



The results of the complete calculation appear in Figure 1. Comparison of the final curve with that obtained by Duncanson (1941) by transformation of the

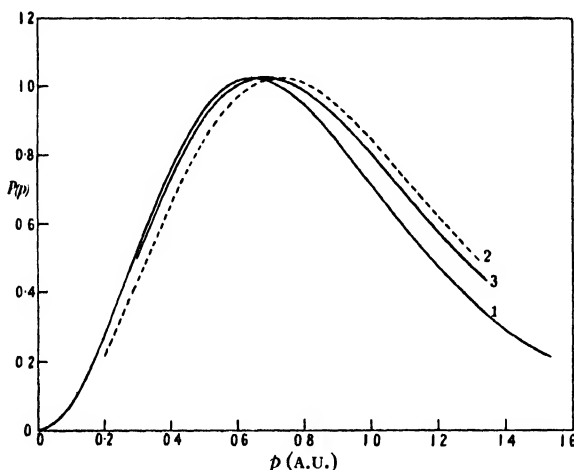


Figure 1. 1. Initial approximation  $P^0(p)$ . 2. Partially corrected function  $P_s(p)$ . 3. Corrected function  $P(p)$ .

coordinate space function due to James (1935) shows that the trend towards regions of higher momentum is maintained with increasing accuracy of the wave function.

#### § 4. EXTENSION TO THE NORMAL MOLECULE

In view of the preceding results it seems likely that even in the case of the normal molecule a preliminary correction of the initial function might be achieved by taking account of the angle-independent distortion of the atomic orbitals. Some progress along these lines has been made and will now be indicated very briefly.

The eigenvalue equation for the normal molecule is found to be

$$\begin{aligned} (p_0^2 + p_1^2 + p_2^2)\Phi(\mathbf{p}_1\mathbf{p}_2) = \frac{1}{\pi^2} \left[ 2Z \left\{ \int \frac{\cos \overline{\mathbf{p}_1 - \mathbf{p}'_1} \cdot \mathbf{R}}{|\mathbf{p}_1 - \mathbf{p}'_1|^2} d\mathbf{p}'_1 \Phi(\mathbf{p}'_1\mathbf{p}_2) \right. \right. \\ \left. \left. + \int \frac{\cos \overline{\mathbf{p}_2 - \mathbf{p}'_2} \cdot \mathbf{R}}{|\mathbf{p}_2 - \mathbf{p}'_2|^2} d\mathbf{p}'_2 \Phi(\mathbf{p}_1\mathbf{p}'_2) \right\} - \int \frac{d\mathbf{p}}{|\mathbf{p}|^2} \Phi(\overline{\mathbf{p}_1 - \mathbf{p}}, \overline{\mathbf{p}_2 + \mathbf{p}}) \right]. \end{aligned} \quad \dots\dots(28)$$

As in coordinate space, two types of initial function suggest themselves. Taking the product of two molecular orbitals such as

$$\phi^0(\mathbf{p}) = \exp(i\mathbf{p} \cdot \mathbf{R}) \cdot \phi_1(\mathbf{p}) + \exp(-i\mathbf{p} \cdot \mathbf{R}) \cdot \phi_1(\mathbf{p}),$$

and omitting terms corresponding to ionic states gives the "electron-pair" function

$$\Phi^0(\mathbf{p}_1\mathbf{p}_2) = 2\phi_1(\mathbf{p}_1)\phi_1(\mathbf{p}_2)\cos \overline{\mathbf{p}_1 - \mathbf{p}_2} \cdot \mathbf{R}. \quad \dots\dots(29)$$

This function is known to be slightly superior to the complete product function and will be made the starting point of our treatment. The momentum distribution corresponding to (29) is easily calculated (Coulson 1941). With hydrogen-like 1s functions (17) we adopt Wang's value of the effective nuclear charge

$Z' = a = 1.166$  but accept more accurate values of  $R$  and  $p_0^2$ , namely  $R = 0.7000$  A.U.,  $p_0^2 = 3.7774$  A.U., since we wish to compute the wave function for the known configuration of the system.

The iterated function  $\Phi^1(\mathbf{p}_1\mathbf{p}_2)$  may be written

$$\Phi^1(\mathbf{p}_1\mathbf{p}_2) = \frac{1}{(p_0^2 + p_1^2 + p_2^2)} [\{I_1^s \phi_1(\mathbf{p}_2) + I_2^s \phi_1(\mathbf{p}_1)\} + \{I_1^p \phi_1(\mathbf{p}_2) + I_2^p \phi_1(\mathbf{p}_1)\} - I_{12}], \quad \dots\dots(30)$$

where 
$$I_1^s = 2 \cos \overline{\mathbf{p}_1 - \mathbf{p}_2} \cdot \mathbf{R} \int \frac{d\mathbf{p}'_1}{|\mathbf{p}_1 - \mathbf{p}'_1|^2} \phi_1(\mathbf{p}'_1)$$

$$I_1^p = 2 \operatorname{Re} [\exp(i\overline{\mathbf{p}_1 + \mathbf{p}_2} \cdot \mathbf{R})] \int \frac{\exp(-2i\mathbf{p}'_1 \cdot \mathbf{R})}{|\mathbf{p}_1 - \mathbf{p}'_1|^2} d\mathbf{p}'_1 \phi_1(\mathbf{p}'_1),$$

interchange of suffixes yielding  $I_2^s$ ,  $I_2^p$ , and

$$I_{12} = 2 \operatorname{Re} [\exp(i\overline{\mathbf{p}_1 - \mathbf{p}_2} \cdot \mathbf{R})] \int \frac{\exp(-2i\mathbf{p} \cdot \mathbf{R})}{|\mathbf{p}|^2} d\mathbf{p} \cdot \phi_1(\overline{\mathbf{p}_1 - \mathbf{p}}) \cdot \phi_1(\overline{\mathbf{p}_2 + \mathbf{p}}).$$

To compute  $P(p_1)$  it is necessary to square the expression (30), integrate over all  $\mathbf{p}_2$ -space and finally over all directions in  $\mathbf{p}_1$ -space. Denoting the three terms in

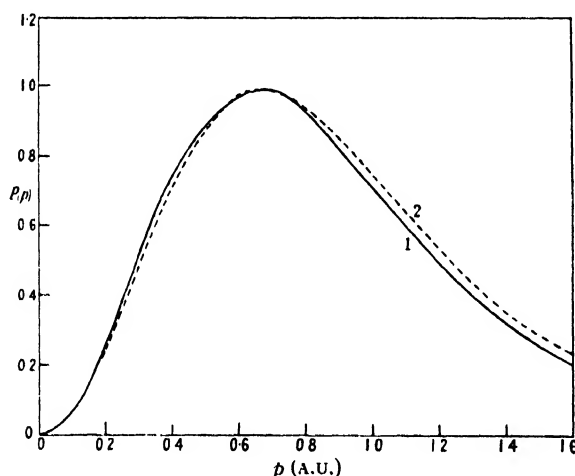


Figure 2. 1. Initial approximation  $P^0(p)$ . 2. Partially corrected function  $P_s(p)$ .

(30) by  $E^s$ ,  $E^p$  and  $E_{12}$ , and remembering  $E^p$  and  $E_{12}$  are small compared with  $E^s$  it is sufficient to compute

$$P(p_1) = \int \int \frac{d\mathbf{p}_2 p_1^2 d\omega_1}{(p_0^2 + p_1^2 + p_2^2)^2} [E^{s2} + 2E^s E^p - 2E^s E_{12}]. \quad \dots\dots(31)$$

The second and final terms in the integrand contain finer details of the corrections due to polarization and to electron correlation respectively: it is, however, noteworthy that the first and dominant term, in itself, is parametrically related to these corrections through  $p_0^2$ . For the present we shall evaluate only the major contribution to the momentum distribution, retaining the first term of the integrand alone. In terms of the integrals

$$I(1S/r2, p) = \int_{-\infty}^{+\infty} \frac{p' \sin 2p'R dp'}{(p'^2 + a^2)^r (p'^2 + b^2)^2}, \quad I(2/r2, p) = \int_{-\infty}^{+\infty} \frac{p'^2 dp'}{(p'^2 + a^2)^r (p'^2 + b^2)^2},$$

where  $b^2 = p_0^2 + p^2$ , a closed analytical expression for  $P(p_1)$  is obtained:

$$P(p_1) = \frac{8\pi^5 p_1^2}{a^2} \left[ \frac{\sin(2p_1 R)}{2R \cdot (2p_1 R)} \left\{ \frac{I(1S/42, p_1)}{(p_1^2 + a^2)^2} + \frac{2I(1S/32, p_1)}{(p_1^2 + a^2)^3} + \frac{I(1S/22, p_1)}{(p_1^2 + a^2)^4} \right\} + \left\{ \frac{I(2/42, p_1)}{(p_1^2 + a^2)^2} + \frac{2I(2/32, p_1)}{(p_1^2 + a^2)^3} + \frac{I(2/22, p_1)}{(p_1^2 + a^2)^4} \right\} \right].$$

The integrals have been tabulated as functions of  $p_1$  and the result of this first correction of the momentum distribution appears in Figure 2. The broadening of the curve is not so marked as in the cases of the ion: that is, however, a natural consequence of electron correlation since the mutual repulsion of the electrons tends to localize each of them in the vicinity of its own nucleus, making the molecular orbitals of the last section a less appropriate description of the behaviour of each electron.

A more complete treatment of the problem would involve a rather comprehensive tabulation of integrals of the form (14), and is perhaps not easily justified.

## § 5. CONCLUSION

The analysis in this paper makes it clear that the method of iteration is not very conveniently applied to any specific molecule: when it is remembered that our aim has been to construct really precise wave functions this is hardly surprising. Nevertheless iteration does appear to be of some value in indicating the *type* of correction which must be made in order to approach more closely the exact solution of a problem. Unpublished calculations show that the method may be applied with some success to problems having a more qualitative significance, in particular to the correlation of electron velocities by interaction. Only in this type of investigation does there appear to be any prospect of making any further useful progress.

## ACKNOWLEDGMENTS

It is a pleasure to record my thanks to Professor C. A. Coulson for his encouragement in this work. The writer is also indebted to the Department of Scientific and Industrial Research and to the Covenantors Educational Trust for Research Grants.

## REFERENCES

- COULSON, C. A., 1941, *Proc. Camb. Phil. Soc.*, **37**, 55.  
 DUNCANSON, W. E., 1941, *Proc. Camb. Phil. Soc.*, **37**, 397.  
 DUNCANSON, W. E., and COULSON, C. A., 1941, *Proc. Camb. Phil. Soc.*, **37**, 406.  
 GEGENBAUER, L., 1877, *Wiener Sitzungsberichte*, **75**, 221; see also WATSON, G. N., *Theory of Bessel Functions* (Cambridge, 1922).  
 JAMES, H. M., 1935, *J. Chem. Phys.*, **3**, 9.

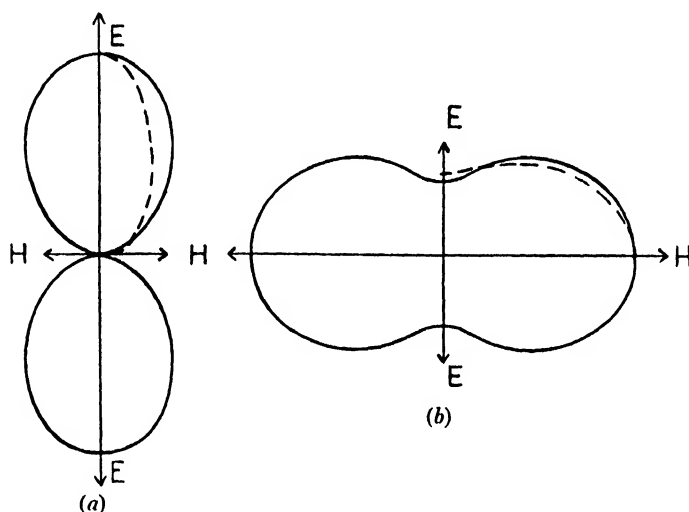
## LETTERS TO THE EDITOR

## Electrons Ejected by Polarized Radiation

It is well known that, theoretically, the azimuthal angular distribution of photoelectrons ejected by plane polarized radiation follows the "cosine-squared" law (Auger and Perrin 1927). The number of electrons ejected with components between  $\chi$  and  $\chi + d\chi$  is

$$N(\chi) d\chi \sim \cos^2 \chi d\chi, \quad \dots (1)$$

where  $\chi$  is the azimuthal angle with respect to the electric vector  $\mathbf{E}$ . ( $\chi$  is the component of angle measured in the plane perpendicular to the original photon.) The electron intensity shown in polar form in Figure (a) is thus greatest in the direction of  $\mathbf{E}$ . Kirchner's



mean experimental results (Kirchner 1926, 1927), shown by the dotted curve, are in close agreement with theory.

Comparatively little attention has been given to the azimuthal distribution of recoil electrons ejected by plane polarized radiation. It is, however, known that in this case the emission is greatest in the longitudinal plane containing the magnetic vector  $\mathbf{H}$  ( $\chi = \pi/2$ ) and not in that containing  $\mathbf{E}$ . The reason for this is that the scattered radiation intensity is greatest for  $\chi = \pi/2$  or  $3\pi/2$ , and on Compton's theory it is assumed that momentum is conserved in a collision between an incident photon and a free electron. The azimuthal angles of a recoil electron and scattered photon thus always differ by  $\pi$ , whatever their longitudinal angles may be. If the further assumption is made, that to each scattered photon there corresponds one, and only one, recoil electron, the azimuthal distributions of recoil electrons and scattered photons will be identical, although of course the longitudinal distributions will be quite different.

According to the Klein-Nishina theory (Heitler 1944) the number of photons scattered at a longitudinal angle  $\theta$  into the element  $d\Omega$ , and with a given polarization, is

$$N(\theta)_X d\Omega \sim \left( \frac{\nu_\theta}{\nu_0} \right)^2 \left( \frac{\nu_\theta}{\nu_0} + \frac{\nu_0}{\nu_\theta} - 2 + 4 \cos^2 X \right) d\Omega, \quad \dots (2)$$

where  $X$  is the angle between the electric vectors of the incident and scattered radiations. Following Heitler (1944), consider the scattered radiation as composed of two components, with polarizations  $\mathbf{E}'$  at right angles. For the first,  $\mathbf{E}'$  is perpendicular to  $\mathbf{E}$ , so that  $\cos X = 0$ . For the second,  $\mathbf{E}'$  is in a plane parallel to that containing the direction of the primary photon

and its electric vector  $\mathbf{E}$ . In this case,  $\cos^2 \chi = 1 - \cos^2 \theta \sin^2 \theta$ . Taking the mean of these components, the number of photons ejected in the direction  $(\chi, \theta)$  becomes, from (2)

$$N(\chi, \theta) d\Omega \sim \left(\frac{\nu_\theta}{\nu_0}\right)^2 \left(\frac{\nu_\theta}{\nu_0} + \frac{\nu_0}{\nu_0} - 2 \cos^2 \chi \sin^2 \theta\right) d\Omega. \quad \dots (3)$$

In (2) and (3),  $\nu_\theta = \nu_0/[1 + \alpha(1 - \cos \theta)]$ , and  $\alpha = h\nu_0/mc^2$ , the energy of the radiation in terms of  $mc^2$ .

The azimuthal distribution of the recoil electrons, which is the same as that of the scattered photons, is now obtained by integrating (3) over  $\theta$

$$n(\chi) d\chi \sim d\chi \int_0^\pi \left(\frac{\nu_\theta}{\nu_0}\right)^2 \left(\frac{\nu_\theta}{\nu_0} + \frac{\nu_0}{\nu_0} - 2 \cos^2 \chi \sin^2 \theta\right) \sin \theta d\theta. \quad \dots (4)$$

This can be put in the form

$$n(\chi) d\chi \sim (1 - A \cos^2 \chi) d\chi. \quad \dots (5)$$

The value of  $A$  in (5) can be determined analytically from (4) for the case of  $\alpha = 0$  ( $\nu_\theta = \nu_0$ ). Its value is then  $2/3$ . This means that the ratio of the electron emission in the direction  $\mathbf{H}$  to that in the direction  $\mathbf{E}$  is 3 to 1. Graphical integration for other cases shows that, as  $\alpha$  increases, the value of  $A$  diminishes. For  $\alpha = 1$ ,  $A = 0.52$ ; for  $\alpha = 10$ ,  $A = 0.16$ . At very high energies the electrons are emitted with azimuthal symmetry by *polarized* radiation. The polar distribution is shown in Figure (b) for  $\alpha = 0.274$  (140 kev.). The dotted curve, which is in close agreement with the theoretical, represents Kirchner's mean results for recoil electrons ejected in air and argon by radiation of this energy.

17 Parkfield Avenue,  
Headstone Lane,  
Harrow, Middx.  
8th June 1949.

K. H. SPRING.

AUGER, P., and PERRIN, F., 1927, *J. Phys. Radium*, **8**, 93.

KIRCHNER, 1926, *Phys. Z.*, **27**, 385 and 799; 1927, *Ann. Phys.*, **83**, 521.

HEITLER, W., 1944, *The Quantum Theory of Radiation* (Oxford: University Press), p. 154 (equation 47 et seq.).

## Theory of Photoconductivity of Layers of Semiconducting Substances

In a previous paper (Schwarz 1948) it has been suggested that adsorption of oxygen ions during the evaporation of semiconducting substances and after the deposit has been formed is an essential condition for the production of photoconductive layers. Based on the experimental results, a qualitative theory of the photoconductivity of these substances is proposed.

During the evaporation of the substance in an electric discharge, several types of adsorption forces are probably active: (i) Van der Waals forces. (ii) Electrostatic forces between the positively charged evaporating particles and the negatively charged oxygen ions. Both kinds of ions are produced by electron bombardment in the electric discharge. (iii) Forces arising from the surface energy of the evaporating particles. (iv) Forces involving valency due to unsaturated valencies or to a small excess of the metallic constituent of the compound as a consequence of slight dissociation during the evaporation.

Each particle when deposited is thus surrounded by an insulating layer of oxygen ions which form a coherent film round the semiconductor particles. This intercrystalline layer fulfils three functions: (a) it prevents the coagulation of the particles; (b) by the formation of a double layer with the negative side away from the particle it constitutes a potential barrier for the exit of electrons from the particle into the neighbouring particles; (c) it is the source and carrier of electrons which by thermal excitation and/or radiation are liberated, accelerated by the external field and form a part of the current.

The transport of electrons along a continuous layer of adsorbed oxygen ions may be visualized as hole conductivity; a doubly charged oxygen ion loses one electron to a neighbouring singly charged oxygen ion, thus becoming singly charged, and in turn takes up another electron,

A cataphoretic migration of the oxygen ions in an applied electric field, especially at higher temperatures, is also possible.

There are many observations on semiconductors which indicate the presence of a surface layer with special properties and there is strong evidence for a conductivity along the surface different from the bulk conductivity (Leo 1931, 1932, Dubar 1938). It is tentatively suggested that the hole conductivity as discussed above is at least partly responsible for the observed surface conductivity and that the surface levels introduced by Tamm (1932) and investigated by others are, in the case of photoconductive layers, occupied by oxygen ions, adsorbed on the internal surfaces of the semiconductor particles.

The magnitude of hole conductivity will depend on the number of holes and on their activation energy, and these in turn depend on the thickness of the adsorbed layer, on the bond strength between the semiconductor particles and the oxygen ions and on the metal excess within the particle, as will be discussed later.

The adsorption of gas on the particles *during* the evaporation, or in general before the bond between the particles can be established, is essential for the formation of a barrier layer. No heat treatment will produce a sensitive layer if the substance is perfectly free from oxygen and if no oxygen is admitted and adsorbed by the substance while the bond between neighbouring particles is interrupted.

For the formation of an effective barrier layer and a photosensitive deposit it is furthermore essential that a small metal excess within the particle is produced either during the evaporation or after formation of the deposit by a suitable heat treatment. If by unsuitable heat treatment the oxygen ions are removed by desorption, diffusion into the lattice or oxide formation, the photoconductivity is destroyed.

The sensitive layer then possesses at the same time an excess of metal and non-metal. This small metal excess fulfils the following functions: (i) By producing a positive charge of the particle it facilitates the adsorption of negatively charged oxygen ions. (ii) It acts as a donor of electrons producing electrical conductivity of the particle. The activation energy will decrease with increasing metal excess and may even become negative. (iii) The work function may decrease with increasing metal excess. (iv) New absorption bands may be produced. Further experiments have to be made to clarify points (iii) and (iv).

The final barrier layer has most likely a complex structure consisting of a chemisorbed layer near the surface of the particle and physically adsorbed layers on top of it.

The bond strength between the oxygen ions and the particle decreases with increasing layer thickness so that the ions of the outermost layer approach the state of free oxygen ions for which the electron affinity for the second electron is negative. Although this state is not reached for adsorbed oxygen ions it indicates that the activation energy for the production of holes will decrease with increasing barrier layer thickness. With increasing metal excess and increasing barrier layer thickness the wavelength threshold for the same substance should therefore shift to longer wavelengths.

Under the influence of radiation absorbed in the insulating layer positive holes are created which render this layer conductive and exert attraction on the electrons within the particle. At the same time radiation absorbed by the semiconductor particle causes an increase of the number and the energy of these electrons, thus increasing the pressure on the barrier layer. The potential barrier breaks down, and electrons can pass between the particles, constituting the photocurrent. It follows that any quantum yield greater than unity is possible, and that under illumination the ratio of excess to defect conductivity should increase.

The electrical and optical properties of the photosensitive deposit will consequently depend on the distribution, size and properties of the semiconductor particles, on the properties of the adsorbed layer and on the interaction between them.

It follows from the foregoing that the photoconductive layer represents a state of non-equilibrium for the ionic and electronic constituents and may be considered as a disperse system. The similarity in colour for layers of different substances and the kind of colour suggest that the size of the particles is fairly uniform for different substances and within the colloidal range.

If adsorption is the essential factor in the production of these films one should expect to find these layers catalytically active. The high catalytic activity of many sulphides and oxides is well known, and the activating treatment of these catalysts closely resembles the

heat treatment of the photoconductive layers aiming at the appearance of a new phase—the small metal excess in the case of the photoconductive layer—without making it the predominant component (Hütting 1935). Rectifier plates of  $\text{Cu}_2\text{O}$  showed catalytic activity (Ostwald and Erbring 1931) and the efficiency of rectification increased with the activity, indicating that adsorption of oxygen ions may be essential for rectification of  $\text{Cu}_2\text{O}$  plates.

My thanks are due to Hilger and Watts Ltd. for permission to publish this letter.

Hilger and Watts Ltd.,  
98 St. Pancras Way,  
Camden Road,  
London, N.W. 1.  
22nd June 1949.

E. SCHWARZ.

- DUBAR, L., 1938, *Ann. Phys., Paris*, **9**, 5.  
HÜTTIG, G. F., 1935, *Z. Elektrochem.*, **41**, 527.  
LEO, W., 1932, *Ann. Phys., Lpz.*, **9**, 347; 1932, *Ibid.*, **15**, 129.  
OSTWALD, W., and ERBRING, H., 1931, *Colloid Z.*, **57**, 7.  
SCHWARZ, E., 1948, *Nature, Lond.*, **162**, 614.  
TAMM, T., 1932, *Phys. Z. Sowjet*, **1**, 733.

## REVIEWS OF BOOKS

*A Text Book of Heat*, by LEROY D. WELD. 1st Edition. Pp. x+436. (New York: The Macmillan Co., 1948). 25s.

This is described as a book for upper classmen, and has been based on the material used for 35 years as lecture notes in a junior-senior course in heat. This does not mean that it is old-fashioned, for modern work has been incorporated wherever it is needed. The properties of liquid helium receive due attention, the totally enclosed absorption type of refrigerator is described, and the International Temperature Scale properly treated.

The general outlook of the book is good. It aims evidently at presenting the student with principles rather than with practice, and many teachers may feel that it gives too little of experimental details; whether he is telling the student how to measure heat quantities or temperatures, or describing the evidence which led to the acceptance of the first law of thermodynamics, the author gives clear explanations of the principles of the experiment, but very little about the practical dodges adopted or required.

The scope of the book includes thermodynamics and statistical mechanics, but the latter suffers because quantum theory is always treated as something outside, to be superimposed on the classical theory. Apart from this, it is an excellent treatment.

The chapters are all accompanied with well selected sets of exercises, and with references for further reading. These show a distinctly American bias, which is, indeed, evident throughout the book. The attribution of the theory of light darts to Epstein may be an example of this, or may be a misprint.

As a whole, the book is very sound, and may give some very useful ideas and hints to those engaged in teaching this subject at the intermediate or pass degree level. J. H. A.

*The Theory of Solutions of High Polymers*, by A. R. MILLER. Pp. vii+118. (Oxford: University Press, 1948). 12s. 6d.

This book summarizes, in a short space, modern ideas on the properties and behaviour of long molecules in solution. It can be said immediately that, so far as chemists are concerned, only those with an unusual flair for the mathematical approach will find the subject matter readily comprehensible. This is by no means the fault of the author's presentation, which is extremely good, but is due solely to the method of approach necessary in dealing with a difficult subject. Physicists and mathematicians cannot do otherwise than benefit greatly from having recent work brought together in this volume.

The author discusses first the classical theories of solution developed by van't Hoff, van Laer, Gibbs and Lewis, and outlines the assumptions necessary for the derivation of such expressions as Raoult's Law. He then explains the nature of an eigenfunction and of the grand partition function, and their application, first to general cases and then to more specific solutions.

The second chapter is concerned with a description of long chain molecules and the connection between structure and configurational energy. Consideration is then given to the evaluation of the "combinatory factor", using Bethe's method and modifications thereof. The method involves a statistical examination of sites occupied by molecules in a quasi-crystalline array. It is treated in detail for dimer and trimer molecules. There follows a discussion of free energy of mixing of polymer molecules and the derivation of general formulae.

The section having perhaps greatest interest, at any rate from a practical standpoint, is that which compares theory with experimental findings, e.g. vapour pressure, molar free energies of mixing and heats of dilution of such materials as polystyrene and natural rubber. Because of the nature of the initial assumptions, absolute agreement is not to be expected, but it is interesting that theory and practice are sufficiently related to justify confidence in the postulated ideas. Even for mixtures having non-zero energy of mixing, the relationships are sufficiently close, although the general impression given is that much planned experimental work remains to be done.

The last chapter provides illuminating criticisms of the theory, and shows how the relative sizes of the polymer segments and solvent molecules, and the self-coiling of polymers may affect results. Comments are also made on the validity of the quasi-crystalline model adopted, and it is suggested that further advances may be made by devising a somewhat more satisfactory physical model.

As stated above, the mathematical character of the book will make reading difficult for all except specialists in the field. To these, the matter summarized can only be of the greatest value; other workers interested in high polymers generally will be stimulated by the new concepts discussed by the author. The style is logical throughout, the format is of the highest quality, and the absence of minor errors provides an excellent example of the care taken by the author in compiling this work.

N. J. L. MEGSON.

*Radiology Physics*, by JOHN K. ROBERTSON. Pp. xvii + 323. Second Edition. (London: Macmillan, 1948.) 22s.

During the last few years Professor Robertson's *Radiology Physics* has been widely recognized and used as a valuable introductory course for medical and pre-medical students and for those studying the physical principles underlying Medical Radiology.

The first edition, published in 1940, has been amplified very effectively by the addition of sections on Transmutation of matter and neutrons, Artificial radioactivity, mass and energy, and Uranium fission and atomic piles. In addition, the opportunity has been taken to meet previous criticism by the inclusion of a good deal of further information on ultra-violet and infra-red radiations and their applications in medicine.

In accordance with the trend of events Professor Robertson has also included some discussion of the absolute energy systems of dosimetry, which seem destined to play a more important rôle in the correlation of physical phenomena with biological implications. The book does, therefore, provide an admirable introduction to the more recent developments of pure physics and their applications to Medical Radiology, and will continue to be of great service to those commencing a study of the subject.

W. V. M.

*X-Ray Optics*, by A. J. C. WILSON. Pp. vii + 127. Methuen's Monographs on Physical Subjects. 1st Edition. (London: Methuen, 1949.) 6s.

The subject matter of this monograph is best indicated by its subtitle, "The diffraction of x-rays by finite and imperfect crystals". An opening chapter deals with crystal structure and the Laue diffraction theory and is followed by a discussion of the reciprocal lattice. This is used in the main part of the book, which is devoted to the structure of the diffraction



pattern from crystals with various types of imperfections, e.g. layer lattices with planes of a "wrong" type, alloys in a "disordered" state, distorted crystals.

The mathematical treatment is kept as simple as possible. The complex form for a wave is avoided throughout most of the book, and the reciprocal lattice is treated without vector algebra. It seems to the reviewer that the author is unduly pessimistic as to the mathematical equipment of those physics students who are likely to want to read his book. It is, however, a welcome sign that the need for the reciprocal lattice has at last been conceded by English writers on x-ray diffraction. It is to be hoped that the use of vectors will follow in the not too distant future.

A somewhat disturbing feature in a lively and otherwise well written book is the curious terminology employed. No one will deny that physics is more important than phraseology, but is there really any need for the clumsy, misshapen and misleading expression "three dimensional mistakes", or, for that matter, for "frozen side bands"—another term favoured by the Cambridge School?

M. BLACKMAN.

## CORRIGENDUM

"The Establishment of the Absolute Scale of Temperature below 1°K.", by  
A. H. COOKE (*Proc. Phys. Soc. A*, 1949, **62**, 269).

Line 4, p. 274, should read

$$Z_c = 2\{1 + 2 \exp(-\delta/kT)\} \quad \text{instead of} \\ Z_c = 2\{2 + \exp(-\delta/kT)\}.$$

Line 32, p. 276, should read

$$\chi = \chi_0 \left( 1 - \frac{4\pi}{3} \chi_0 + 12\eta \chi_0^2 \right)^{-1} \quad \text{instead of} \\ \chi = \chi_0 \left( 1 - \frac{4\pi}{3} \chi_0 + 12\eta \chi_0^2 \right).$$

## CONTENTS FOR SECTION B

	PAGE
Mr. C. GURNEY and Dr. S. PEARSON. The Effect of the Surrounding Atmosphere on the Delayed Fracture of Glass . . . . .	469
Mr. R. MANSFIELD. The Electrical Properties of Bismuth Oxide . . . . .	476
Prof. E. N. DA C. ANDRADE and Mr. J. W. FOX. The Mechanism of Dilatancy . . . . .	483
Mr. A. J. KENNEDY. The Effect of Instantaneous Pre-Strain on the Character of Creep in Lead Polycrystals . . . . .	501
Mr. E. W. J. MITCHELL and Dr. R. W. SILLARS. Observations of the Electrical Behaviour of Silicon Carbide Contacts . . . . .	509
Dr. H. G. WOLFARD and Dr. W. G. PARKER. Temperature Measurements of Flames containing Incandescent Particles. . . . .	523
Letters to the Editor :	
Dr. D. WALKER. Graphical Representation of a Continuous Noise Spectrum. . . . .	530
Contents for Section A. . . . .	530
Abstracts for Section A . . . . .	531

## ABSTRACTS FOR SECTION B

### *The Effect of the Surrounding Atmosphere on the Delayed Fracture of Glass*, by C. GURNEY and S. PEARSON.

**ABSTRACT.** Round soda-lime-silica glass rods were subjected to a series of given bending moments, and times to fracture were recorded. Experiments were made in air and *in vacuo* of  $10^{-1}$  and  $10^{-5}$  mm. of mercury; and the effects of heating *in vacuo* to drive off absorbed atmospheric constituents were also investigated. For the same prior heat treatment the slopes of the curves of stress against time to fracture decrease with decrease of pressure. At  $10^{-5}$  mm. Hg, after heat treatment, the curve was very flat. It is evident that the main cause of delayed fracture is attack of the glass by atmospheric constituents. Experiments in which glass was subjected to air from which water vapour and carbon dioxide were removed separately and together showed that both these substances cause delayed fracture. Other constituents of the atmosphere seem relatively ineffective. These conclusions are in agreement with the work of Preston and his collaborators. It is further concluded that these atmospheric constituents can be supplied by capillary liquid contained in surface cracks and by migration from surface layers as well as by direct attack from the gaseous phase.

### *The Electrical Properties of Bismuth Oxide*, by R. MANSFIELD.

**ABSTRACT.** The conductivity  $\sigma$  and thermo-electric power  $dE/dT$  of bismuth oxide is measured over a temperature range of  $680^\circ$  to  $150^\circ$  C., and for variations of oxygen pressures from 76 to  $10^{-4}$  cm. Hg. The results above  $340^\circ$  C. and at atmospheric pressure are well represented by the formulae  $\sigma = A_1 \exp(-\alpha/2T)$  and below  $340^\circ$  C. by  $\sigma = A_2 \exp(-\alpha/T)$ , in which the values of the constants  $A_1$ ,  $A_2$  and  $\alpha$  are very similar for two different specimens. The variation of  $\sigma$  with oxygen pressure above  $500^\circ$  C. and for pressures down to 1 mm. Hg obeys the formula  $\sigma = k(P_{O_2})^{\frac{1}{2}}$ . The thermo-electric power results may be summarized by the equation  $dE/dT = a + b/T$ , where  $a$  and  $b$  are constants, the positive sign of  $dE/dT$  indicating that  $\text{Bi}_2\text{O}_3$  is a defect semiconductor. The variations of  $dE/dT$  with oxygen pressure are small, less than 10%, except at pressures less than  $10^{-3}$  cm. Hg, when the sign of  $dE/dT$  changes at temperatures greater than  $550^\circ$  C. Under these conditions it is suggested that  $\text{Bi}_2\text{O}_3$  becomes an excess or intrinsic semiconductor. The results are discussed and good agreement is obtained between theory and experiment if it is assumed that normal Wagner and Schottky lattice defects become of importance at low temperatures when the concentration of free electrons is small.

*The Mechanism of Dilatancy*, by E. N. DA C. ANDRADE and J. W. FOX.

**ABSTRACT.** The dilatancy in question is the change of overall volume produced by strain in an assembly of particles. This has been demonstrated in the case of a mixture of sand and water by a photoelectric method of measuring the wetness of the surface. The general phenomenon has been experimentally studied in detail with a two-dimensional hexagonal array of uniform cylinders, part of the free surface of which is loaded with a rigid piston. An alternate increase and decrease of overall volume as the piston descends has been demonstrated and the mechanism of slip by which it comes about has been established. The elastic stress distribution in the array before slipping takes place has been calculated and shown to be a determining factor. The effect of friction between the component units has been studied. Experiments have also been carried out on three-dimensional irregular arrays of carbon shot and of sand.

*The Effect of Instantaneous Pre-Strain on the Character of Creep in Lead Polycrystals*, by A. J. KENNEDY.

**ABSTRACT.** The extension-against-time curves of lead wires that have been subjected to rapid strain just before the experiment may be expressed by the Andrade creep equation  $l = l_0(1 + \beta t^{\frac{1}{4}}) \exp(\kappa t)$ , using the same constants as those which satisfy the creep of the metal under the same constant stress, but with the  $t$  value associated with  $\beta$  replaced by  $(t + t_0)$ , where  $t_0$  is a constant for a given experiment, its value increasing with increasing pre-strain. While for pre-strains less than 10% the value of  $\kappa$  is unchanged by the pre-strain, for greater pre-strains the  $\kappa$ -flow is also modified and appears to approach more nearly to a linear variation with stress.

*Observations of the Electrical Behaviour of Silicon Carbide Contacts*, by E. W. J. MITCHELL and R. W. SILLARS.

**ABSTRACT.** The electrical behaviour of individual silicon carbide contacts has been examined using probes and high resistance electrometer circuits to measure the potential drop across a contact. Voltage-current curves were obtained and the well-known departures from Ohm's law at the contact were confirmed. Attempts were made to fit these experimental results and other data to the theoretical expressions for tunnelling through an insulating film, a hypothesis which does not appear to fit the facts very satisfactorily. Observations were made of the effect of heating the material to high temperatures *in vacuo*, of the properties of a newly formed surface and of the capacitance across the barrier layer. These indicate that the "barrier" has complicated properties which are not consistent with a simple tunnelling model. An alternative model is suggested.

*Temperature Measurements of Flames containing Incandescent Particles*, by H. G. WOLFARD and W. G. PARKER.

**ABSTRACT.** Colour temperatures measured on photoflash powders are higher than expected from theoretical calculations. Determinations of the true temperature of stationary flames of aluminium flakes suspended in air have been made (a) by a line reversal method and (b) by measuring the absolute light intensity. The experimental values obtained were very close to the theoretical flame temperature of about 3,000° C., that is, the boiling point of the oxide. An explanation is offered for the difference between the true temperature and colour temperature for flames containing incandescent particles, the reason being the small size of the radiant particles, which introduce optical anomalies. It is concluded therefore to be unprofitable to measure the colour temperature at all as this has no relation to the true temperature. Magnesium behaved very similarly, the true temperature being the melting point of MgO, near 2,800° C., whereas the colour temperature is above 3,900° K. The two-colour method of Hottel and Broughton for temperature measurements in hydrocarbon flames is examined in the light of this experience,

# THE PROCEEDINGS OF THE PHYSICAL SOCIETY

## Section A

---

VOL. 62, PART 9

1 September 1949

No. 357 A

---

### The Physical Basis of Life\*

By J. D. BERNAL†

Birkbeck College, London

*32nd Guthrie Lecture, delivered 21st November 1947; MS. received 18th May 1949*

Mr. Chairman, Ladies and Gentlemen,

I feel deeply honoured at being asked to join the very distinguished series of Guthrie lecturers. I have chosen a subject which at first sight seems rather far removed from the work of Professor Guthrie. However, physics has changed much since his time, and even then the foundations were being laid for its transition towards biology. I only know two persons who were students of Professor Guthrie, men of almost completely contrasting temperaments, H. G. Wells and Professor Tutton. The first, as a man of imagination and of qualitative views, did not take kindly to the intensely practical nature of Professor Guthrie's physics course, and has left an amusing account of it in his *Experiment in Autobiography*—“ . . . Now when I came into the physics laboratory I was given a blowpipe, a piece of glass tubing, a slab of wood which required planing and some bits of paper and brass, and I was told I had to make a barometer. So instead of a student I became an amateur glass worker and carpenter.

“ After breaking a fair amount of glass and burning my fingers severely several times, I succeeded in sealing a yard's length tube, bending it, opening out the other end, tacking it on to the plank, filling it with mercury, attaching a scale to it and producing the most inelegant and untruthful barometer the world has ever seen. In the course of some days of heated and uncongenial effort, I had learnt

\* The title of this lecture is an unconscious echo of the once celebrated lecture of T. H. Huxley (1901) delivered in Edinburgh in 1868. I did not read that lecture till long after I gave this one, but it is interesting to note the changes that eighty years have brought since it was first clearly stated that life had *one* physical basis. Huxley had a word for it—Protoplasm. He was concerned with stressing that it was functionally, formally and substantially the same over the whole range of living things. In function all organisms showed metabolism, movement, growth and reproduction; in form they were all composed of nucleated cells; in substance they were all made of protein, a compound of carbon, hydrogen, oxygen and nitrogen. Not only was life one, but it was linked materially with the non-living, by the capacity of converting inorganic gases and minerals into protoplasm.

The latter half of the lecture was spent in defending the thesis of the former from the charge of rank materialism on the grounds that we did not know any more what matter was than what spirit was, and it was reasonable to accept our ultimate ignorance, however laudable our efforts at understanding. This was the basis of his famous attitude of *Agnosticism*.

The positive part of his lecture stands as firm today as it did when he first put it forward. What is curious, however, is that he nowhere attempted, great evolutionist as he was, to explain the unity of all life in terms of a common history. The developments of physiology and biochemistry have filled in the details of Huxley's picture but they add nothing fundamentally new to it unless they leave the field of describing structures and mechanism and enter into that of searching for origins. It is here, if anywhere, that lies the excuse for making a new attempt at understanding the physical basis of life.

† This article will also appear in *Proc. Phys. Soc. B* for October.

nothing about the barometer, atmospheric pressure, or the science of physics that I had not known thoroughly before I left Midhurst, unless it was the blistering truth that glass can still be intensely hot after it has ceased to glow red.

"I was then given a slip of glass on which to etch a millimetre scale with fluorine. Never had millimetre intervals greater individuality than I gave to mine. Again I added nothing to my knowledge—and I stained my only pair of trousers badly with acid."

Professor Tutton, on the other hand, one of the most precise of physicists and crystallographers, rather overdid it in the other direction. Apparently the barometer he produced was not only perfect in every detail but was varnished to boot; and legend has it that Professor Guthrie proceeded to smash it up on the grounds that he was training physicists and not instrument makers.

In one particular respect Professor Guthrie's work does touch the subject of this lecture. He was one of the first to examine the properties of the cryohydrates, those salts in which a large amount of water is held in fixed positions similar to those they occupy in ice. As I shall show, cryohydrates are a significant feature in the crystallography of the proteins and may have had an important part to play in the origin of large molecules adsorbed on clay particles.

I have chosen a very general subject for this lecture mainly because, owing to the events of recent years, I have been unemployed as an experimental physicist for longer than I like to think, and have not been long enough back at work to be able to produce new material on the detailed study of any physical field. Instead, I want to discuss in a general way one of the aspects of physics that is coming more and more into prominence at this time—its relation to the processes of life. At present there are two really exciting fields in physics: one of them is at the outer edge of physics—nuclear physics, and the even more short-period and energetic processes of cosmic rays—and the other at the inner edge—where physics touches biology, a field in which the interest lies in complexity rather than in intrinsic energy. In saying this I am treating physics in its modern and more extensive connotation as including chemistry, because, although chemical manipulation and the logical structural analyses of the older chemistry still remain, and the direct study of material substances and transformations will continue as a source of knowledge, chemistry and physics are now embedded in one common theory and are in future bound to become one integral discipline. Accordingly biophysics and biochemistry, to make any sense, must be considered together.

What I am trying to put before you is the first crude attempt at stating the problems of the origin and function of life from a physical standpoint. In doing so I am fully aware of my inadequacy. It is probable that even a formulation of this problem is beyond the reach of any one scientist, for such a scientist would have to be at the same time a competent mathematician, physicist, and experienced organic chemist, he should have a very extensive knowledge of geology, geophysics and geochemistry and, besides all this, be absolutely at home in all biological disciplines. Sooner or later this task will have to be given to groups representing all these faculties and working closely together theoretically as well as experimentally. The most I can do is to indicate some of the fields in which the key problems exist and provide some preliminary guesses as to the direction in which to look for solutions.

\* The approach I am choosing is the broadest one possible, and deliberately so. I am not here concerned with the task of elucidating this or that physical structure

or mechanism underlying particular functions of existing organisms, but rather with the whole range of the phenomena which we commonly call life. But my emphasis will be on one particular aspect of life, on the problem of *origin* rather than that of structure, metabolism and behaviour. I have chosen this emphasis on origin in biological systems because it is far more important than in physical systems. Until recently discussions on the origins of systems were considered in some way improper to science, but now even in physics itself the questions of origins are coming into discussion, as, for example, those of the origin of the nebulae, the solar system and the elements themselves. Most of what I say will not be new, it is largely based on the writings of other workers, notably Haldane (1928), Lwoff (1943), Oparin (1938) and Dauvillier (1947). What I have done is to correlate these different contributions and add some speculations of my own on the actual conditions under which life originated. My aim is by such a broad sketch to bring out in sharp relief the critical points of difficulty, not in order to evade them by pious allusions to mysteries beyond human comprehension, but as a guide to practical research in the future.

The first obvious step in the discussion should be to define the terms. But life is an extremely difficult term to define. In fact Dr. Pirie (1937) in his paper on "The meaninglessness of the terms 'Life' and 'Living'" has practically proved that it is incapable of definition:

"We have now examined destructively the various qualities which might be used to define the word 'life' and we have found that they are individually inadequate for even an approximate definition. There is not space here to discuss what might be done with all the permutations of these qualities; it may be said however, that combinations of two or three qualities, though they might easily be drawn up to exclude all obviously non-living systems, will also exclude some which are, if not typically living, at least generally included in that category.

"Until a valid definition has been framed it seems prudent to avoid the use of the word 'life' in any discussion about border-line systems and to refrain from saying that certain observations on a system have proved that it is or is not 'alive'."

By taking every quality, such as respiration or movement, usually considered characteristic of life, he is able to show that there are many things called "alive" which do not possess any of them, and equally many possessing some of them that we do not call "alive".

I wish to avoid these troubles by not attempting to give a definition of any particular form of life or living organism, but rather by treating the common word "life" as referring particularly to the totality of processes accessible to our observation on this earth: to what Goldschmidt has called the biosphere, consisting materially of the group of complex organic compounds found almost exclusively in the watery layer on the surface of the earth, the hydrosphere, or in the adjoining regions of the atmosphere or parts of the lithosphere clearly derived from it. If we limit it in this way we can for the moment find one common material characteristic, the presence of protein molecules, and at the same time one common physico-chemical process, the stepwise catalysis of organic compounds carried out practically isothermally by quantum jumps of between 3 and 16 kilocalories, small compared with the usual jumps of 300 in laboratory chemistry.

These terrestrial limitations obviously beg the question of whether there is any more generalized activity that we can call life. Biology in this respect is on a different basis from physics and chemistry in that it deals less with universals

and more with contingents. It belongs to the kind of descriptive and interpretative studies we might more properly call "graphies", including observational astronomy and geography. Whether there are some general characteristics which would apply not only to life on this planet with its very special set of physical conditions, but to life of any kind, is an interesting but so far purely theoretical question. I once discussed it with Einstein, and he concluded that any generalized description of life would have to include many things that we only call life in a somewhat poetical fashion. Any self-subsisting and dynamically stable entity transforming energy from any source, or, as Haldane put it, "any self-perpetuating pattern of chemical reactions"; might be called "alive" in this sense. The value of distinguishing it as an individual system or organism would only exist if the total phenomena persisted for a time appreciably longer than the periods or characteristic times of any internal processes it might contain. In this sense a galaxy or a star is alive, or, on a more terrestrial scale, a flame. Passing to a degree of complication greater than the biological, we might talk of the life of a human culture or civilization. All are characterized by birth, persistence and death.

These considerations, however, are all very abstract. Their only immediate value is to indicate that though there may be a number of kinds of life in this sense, these kinds of life are quite distinct, and each has a very limited sphere of existence. All must satisfy two necessary criteria. The first is that they must be functional, in the sense that the processes that comprise them must have a certain dynamic stability\*.

Now this leads us back again to the method of tackling the problem as one at the same time historical and physiological. The actual material structures which build up our terrestrial life, with which we shall be exclusively concerned from now on, are to be considered at the same time under both aspects, those of their function and of their origin. An object such as a galaxy or an apple carries its whole significance only if we consider the stages of its development as well as its instantaneous activity. The ostensible purpose of biology in unravelling the processes that occur in living things is at the same time the elucidation of the necessary stages by which they arrived at their actual structures. Present study throws light on past history and vice versa. Every existing organism is in this sense a fossil. It carries in it by inference all the evidence of its predecessors;† and this remains the case even if we cannot read it clearly or at all. Naturally the study of the past, which cannot be directly determined, can provide no positive proof to set against immediate observation of the present; but it can do something equally important. It can give indications as to where to look in the present to find significant things.

The history of science affords many remarkable examples of this process. The chief of them of course is Darwin's statement of natural selection as a mechanism for evolution. Undoubtedly evolution is a hypothesis, natural selection is

\* The meaning of this first criterion has been made much clearer by the work of Prigogine (1947) on the thermodynamics of "open systems". Such a system can take in and pass out matter as well as energy and is not subject to the second law of thermodynamics, that is, its entropy may remain constant or even decrease, the condition of stability of such a system being that the rate of change of entropy is a minimum; and secondly, they must originate and develop out of some pre-existing system, or, in plain English, they must work and they must have got there in the first place.

† Professor Haldane says "No, it doesn't. Gene segregation is a trick for halving the amount of the 'evidence' once per metazoan life cycle. It may carry enough evidence." It would have been better perhaps to have phrased the statement conversely as "everything an organism contains is evidence of its predecessors".

an observational fact: but it was from the hypothesis of evolution, that is, from the need to provide an explanation of present forms of life in terms of older ones, that Darwin was driven to use the natural selection argument which he borrowed from Malthus. As a result he not only put into order the chaos of the accumulating biological observations of his time, but led to the fertile and useful experimental studies of ecology, morphology and heredity.

Darwin himself, curiously enough, was opposed to any generalization of his own methods. In a letter to Sir J. Hooker (see Darwin 1887) he said: "It is mere rubbish thinking at present of the origin of life; one might as well think of the origin of matter." We are now almost in a position to take him at his word. For the origin of matter, at least the origin of the forms in which matter presents itself on this earth, is at last becoming clear. The chemical elements, in their ordered multiplicity, and with their apparently arbitrary and enormous variations of abundance, are seen now as perfectly logical products of a process going on in some primordial hyperstar or concentrated universe some four billion years ago. In fact, the physicists have reconstructed, somewhat provisionally, the temperatures and pressures of that time from the relative abundances of different elements, and in the process have discovered anomalies which would not have been discovered without some such hypothesis as to origin.

This does not mean that we should accept wild hypotheses of the origin of life or of matter which simply conceal ignorance, but rather that we should attempt almost from the outset to produce careful and logical sequences in which we can hope to demonstrate that certain stages must have preceded certain others, and from these partial sequences gradually build up one coherent history. There are bound to be gaps where this cannot be done, but until the process is attempted these gaps cannot be located, nor can the attempt be made to fill them. The process is not dissimilar, though on a vastly greater scale, to the attempts of the geologists two hundred years ago to determine the history of the crust of our globe, which, once theological preoccupations had been overcome, led to the ordered logical sequences of Hutton and Lyell.

There are a certain number of general considerations which we can employ in building these sequences. In the first place we may know that we can expect gaps where processes are particularly rapid. In any sequence which passes through a number of phases the occurrence of any phase will be proportional to its duration. Unstable elements are the least abundant. Rapidly evolving forms leave the fewest fossils. What we observe easily are the stable stages, and they may form a very small fraction of the whole process, giving a much greater impression of discontinuity than really exists. Life as we know it consists of only a relatively small number of kinds of simple molecules—sugars, amino acids, purines—molecules out of which are composed the far more complicated macro-molecules of the proteins and nucleic acids and microscopically visible structures such as membranes and fibres. We now know, particularly through the use of tracer elements, that there exist as well a large number of intermediate molecules which are changed so quickly that they cannot be observed by ordinary methods. But we may further infer that in the history of life there have been formed a still larger number of molecules that have played a decisive rôle in its chemical evolution, but which can be reconstructed now only from the traces they have left in the structure of existing molecules.



Another very general consideration for all developing systems is the way in which processes occurring for the first time react on those already established. One of the perennial arguments in biology has been the question of spontaneous generation. Ceaselessly put forward to explain otherwise obscure phenomena, it has always been disproved whenever careful work has been carried out, and we are apt to think that Pasteur has settled it for all time. But those who demonstrated that spontaneous generation did not normally occur under existing conditions usually went further and claimed that they had also proved that it could never have occurred at all by natural means, and, therefore, only substituted an original miracle for a series of continuing ones (see Engels 1940). Now one obvious weakness of this argument is that the conditions in which life originated do not exist any more on this earth. It is not necessary, to prove this, to assume any gross change in the external physical conditions, surface temperature or solar energy, etc. It is sufficient to know, as Haldane (1928) has pointed out, that the very existence of life itself radically changed the initial conditions, principally by producing molecular oxygen. Similarly, at almost every stage in the evolution of life, successful new forms interfered with all that had gone before. There is no guarantee, of course, that life itself will not so interfere with the universe into which it has intruded itself as to wipe itself out. All it has done so far is to block possibilities of development other than those actually taken. This implies, of course, a potentiality for life much more extensive than the actuality.

There is a definite and limited range of potentiality fixed at a lower level of complication by the physical and chemical properties of molecules. This corresponds to what Henderson spoke of in his remarkable book of forty years ago, *The Fitness of the Environment*. He pointed out that the peculiar properties of water and carbon dioxide, for instance, were as suitable for life as life was adapted to them. But though life in its terrestrial form depended on these properties, we now see that this is about equivalent to saying that life depends on the laws of arithmetic or geometry, because the peculiar properties of water and carbon dioxide are implicit in the number of electrons contained in their atoms, and that the abundance of atoms with these numbers and their presence on the surface of the earth follows logically from their nuclear composition. When these interactions, however, become as complicated as they have done in life, we can no longer be sure that the only absolutely possible track has been taken. Indeed, from the very variety of life on this earth, in past as in present times, we know what a great range of possibility there has been and what apparently small accidents, some of them outside the range of life altogether, such as those of geography or climate, have determined the success or failure of this or that form.

We can if we like call these possibilities the Aristotelian entelechies, and this can be done without any mystical invocations. Any arrangement of atoms or molecules necessarily carries with it complex possibilities of order and function, and those are *immanent* in the structure of the molecules themselves. Which appear and which do not appear are, however, immanent not in any particular combinations themselves but in the total play of universal forces, and, therefore, for the consideration of the system, may be considered as *contingent* or accidental. It is a convenience for us to separate the immanent and contingent elements, attributing the first to science and the second to cosmic history, but their interaction must always be taken into account. Deepening our knowledge of the behaviour of material systems helps us to detect and to understand historical

changes. Conversely, knowledge of the origin and history of life gives a clue to the understanding of biochemistry and microbiology.

The new interest in the physical nature of biological systems has coincided necessarily with the development of new physical tools, theoretical and practical. Of the former, by far the most important is the development of the quantum theory and its extension to cover at least in principle the theories of chemistry and to give precious indications of the far more complex phenomena of biochemistry and biophysics. Without exaggeration it can be said that the conception of quantum energy changes in chemical reactions is the most illuminating and the most effective new idea in modern biology. We begin to see now that the material aspects of a living system are but the struts and levers of a machine, the particular function of which is to effect energy interchanges, and that growth and assimilation are but means of achieving a metabolism consisting of enzyme promoted energy changes. Thus in a very physical sense process takes precedence over structure. The developments of other aspects of physical science also have theoretical applications to biology, particularly the theory of solids and liquids, which may help to explain the apparently mysterious activities which go on inside living cells. On the other side our new knowledge of soil science and of geochemistry, as well as that of physical geography and oceanography, throw light on the medium from which life evolved and which still supports it.

With these advances in understanding has come a much greater armoury of experimental methods. On every level of organization, both of structure and of energy change, new physical and chemical instruments are offering the biologist a range of opportunity unequalled since the first use of the microscope and of the balance in the seventeenth century. On the chemical level the introduction of radioactive tracers is likely so to revolutionize the unravelling of reactions in both organic and biochemistry as to make what we think we know now obsolete in a matter of a few years. For the determination of molecular structure, the use of spectroscopy, particularly infra-red spectroscopy, and of x-ray crystallography combined, gives us a picture of atomic arrangements limited in its accuracy and extent only by the number of workers in the field and the slowness of the computations involved; and this limitation itself is likely to be removed in a few years by the further development of electronic calculating machines which will enable some years' work to be done in a few hours. Chemical methods themselves have enormously increased their range and accuracy, owing to the development of industrial polymer chemistry. Differential chromatography, which enables the simple and complex constituents of proteins and other organic substances to be analysed and labelled with ease and certainty, provides a bridge between the chemistry and the physics of large molecules.

It is, however, in the intermediate zone, the zone between the chemical molecule of some tens of Ångströms in dimensions, and the old limit of microscopy at 2000 Ångströms, that the most significant advances have been made. Indirect methods of great beauty and interest we have had for some time—the use of the ultra-centrifuge by Svedberg, of electrophoresis by Tiselius, of viscosity by Staudinger, and more recently of light scattering by Doty. These provided the first really quantitative picture of the approximate size and shape of the large molecules of biological and industrial origin. Now, however, we have far more precise and accurate methods. X-ray analysis can be extended to deal with molecules of hundreds of Ångströms in dimensions, and although it cannot as

yet give the precise details of their atomic constitution, it has already led to significant information as to their general nature, particularly of their constancy under different physical conditions.

Far more spectacular in recent years, however, has been the development of the electron microscope, making visible in an immediately understandable form structures from those containing a few score atoms to the limits of microscopic vision and beyond. We are certainly now in a Galilean phase of observational biology. Until the advent of the electron microscope, a great blank existed between the knowledge of atomic combinations provided by chemistry and that of histological structures observable with the microscope. This gap was filled with the mystic word "colloid", which served to explain the very real but very obscure properties depending on the existence of structures of magnitudes between ten and ten thousand Ångströms. Now the colloid world is open for inspection, and the term itself will probably vanish or acquire a precise and limited meaning. The coming of the electron microscope, as has often happened in the history of science, has stirred the optical microscopists into exertions which their sole possession of the field did not provoke. The microscope had, in fact, stood virtually still between 1880 and 1940, but now, with the rival in the field, it was found that it could be improved in many ways, and the new phase microscopes, and the ultra-violet, infra-red, polarizing and reflecting microscopes provide an armoury which, though they cannot rival the electron microscope in resolving power, have, in the hands of such workers as Caspersen, shown a power of chemical interpretation of structure greater than any other method, and having the additional enormous advantage that they can be used on living material. With all these new methods simultaneously available it is not surprising that the present picture of biological research should be one of exciting but somewhat disordered advance—an advance so rapid that attempts to assess the position will be out of date almost as soon as, if not before, they are written.

In the account which follows an attempt is made to present the main outlines and the critical stages in the development of life from its inorganic origins. It is based essentially on two kinds of data—the geochemistry and physico-chemistry of the cooling planet, and the organic chemical composition common to all existing living organisms. Such an attempt reveals at once the large gaps that still exist, but it also reveals the lack of perfectly feasible research which is bound to help to reduce these gaps and to bring out others that may now be unsuspected.

The process is one which we can imagine as taking the form of a play divided into a prologue and three acts. The prologue introduces the scene on the surface of the primitive earth, and the first group of actors of an entirely inorganic kind which must start the play. The first act deals with the accumulation of chemical substances and the appearance of a stable process of conversion between them, which we call life; the second with the almost equally important stabilization of that process and its freeing from energy dependence on anything but sunlight. It is a stage of further synthesis and of the appearance of molecular oxygen and respiration. The third act is that of the development of specific organisms, cells, animals and plants from these beginnings. All we have hitherto studied in biology is really summed up in the last few lines of this act, and from this and the stage set we have to infer the rest of the play.

Our knowledge of the nature of the surface of the primitive earth is derived from the spectroscopic evidence as to the abundance of the elements in the stars, and the much more meagre information we have about them in the atmospheres

of the planets on the one hand, and on the other the knowledge of geochemistry and geophysics. This field of study has been entirely transformed in recent years through the application of x-ray crystallography in the hands particularly of the Braggs and Goldschmidt. In the latter's great work, *Verteilungsgesetz der Elemente* (1923-37), are traced the processes by which the primitively mixed elements of the original solar filament sorted themselves out in the first place under simple gravity, and at the latter stages by crystallization according to the laws of ionic combination, which he discovered and Pauling later refined. It is still an open question whether the first sorting process was ever complete, whether the still liquid interior of the earth consists of iron or of unconsolidated solar matter, mostly of hydrogen, as Kuhn (1946) has recently proposed.

The outer layers, however, in their melted form, must have contained in addition to silicates—predominantly basic silicates—much water and carbonate in solution, the whole being originally surrounded by an atmosphere of hydrogen and hydrides,  $\text{CH}_4$ ,  $\text{NH}_3$ ,  $\text{H}_2\text{S}$ , and  $\text{H}_2\text{O}$  though in far less quantities than now. This original atmosphere must have been modified in two particular ways. The actual crystallization of the crust must have forced into the atmosphere vast quantities of water vapour and carbon dioxide. At the same time hydrogen was being steadily lost at the top of the atmosphere, the gravitational pull not being strong enough to hold it. The result is bound to have been a steady oxidation, methane turning to  $\text{CO}_2$  and water through intermediate compounds such as aldehydes, alcohols and acids which may have had a rôle in the formation of life; ammonia oxidized to nitrogen and  $\text{H}_2\text{S}$  to sulphur. Further oxidation seems most unlikely at the pre-organic stage. Some must have occurred at the very top of the atmosphere in the dissociation of water to hydroxyl and free hydrogen, but the small amount of hydroxyl formed would be used up on oxidizing compounds in the lower atmosphere, and there remained an enormous residue of reducing material in the ferrous iron of the then exposed primitive rocks.

By the time the earth had cooled sufficiently for the water to condense, the atmosphere may have been largely one of nitrogen with a gradually decreasing concentration of carbon dioxide as its partition coefficient in the cooling sea became less and less. The seas would contain primarily ammonia, carbon dioxide and hydrogen sulphide in solution. Whether they also contained salt in anything like the present concentration is still an open question, though there are enough minerals containing chloride to provide for present concentration if sufficient rock had been worked over in the course of geological history by weathering processes; but on the other hand it is possible that vapourized halides formed parts of the original atmosphere, came down molten, solidified and were dissolved in the primitive seas (Dauvillier 1947).

The surface of the world at this stage must not have been very different from what it is now, except for the bareness of the rocks and consequently greater speed of weathering. We still do not understand the mechanism of continent and mountain formation, but there is no reason to believe that it was dependent on organic processes. We may therefore assume most of the geographical features which we now observe, with the exception of coral islands, though inorganic calcium carbonate precipitation may have occurred. In particular there must have been, as now, extensive areas of mud in deltas and on continental shelves, some of which would be exposed to the tides. Correspondingly on the land a kind of soil would be formed wherever the run-off was not sufficient to remove weathered material or where it was deposited in rivers, and this soil would also contain clay.

At first sight there might be no reason why the world should not have continued in this state indefinitely, but there was an active agent operating at that time which is no longer in operation, namely the influx of solar radiation out to the far ultra-violet of 2000 Å. or less. If we put to a physical chemist the problem of the reactions occurring in a weak solution of ammonium carbonate and sulphide under such radiation, he would agree that although it was not possible without experiment to determine exactly what compounds would be formed, a process of polymerization and condensation leading to the formation of nitrogenous organic compounds such as the amino acids is almost certain, and would proceed until an equilibrium was reached where breakdown was equal to formation. It would be of the utmost importance to make these vague remarks more precise, and researches in ultra-violet photosynthesis would certainly be of interest, and might be of practical use.

Equilibrium, moreover, could be reached in two ways. One would be the straight photochemical process of absorption and emission; the other might well be a dark breakdown through a number of intermediate compounds liberating energies corresponding to smaller quantum steps and longer wavelengths. Life from the purely physico-chemical point of view is simply a denotation of the complex mechanism of this latter process. We may give a schematic picture of this in the form of a graph showing purely qualitatively the effective utilization of sunlight at different periods of world history. At first the absorption is determined only by the original constituents of CO<sub>2</sub> and ammonia. Later the more complex forms give rise to greater absorption. When life appears, and these forms are broken down, the absorption decreases. The subsequent hypothetical changes due to the appearance of organic photosynthesis and respiration will be discussed later.

The stage is now set for the appearance of life itself. In Moleschott's classic phase, "It is woven out of air by light". It is here that organic chemistry first begins. Condensations and dehydrogenations are bound to lead to increasingly unsaturated substances, and ultimately to simple and possibly even to condensed ring structures, almost certainly containing nitrogen, such as the pyrimidines and purines. The appearance of such molecules makes possible still further syntheses. The primary difficulty, however, of imagining processes going thus far is the extreme dilution of the system if it is supposed to take place in the free ocean. The concentration of products is an absolute necessity for any further evolution. One method of concentration would of course take place in lagoons and pools which are bound to have fringed all early coastlines, produced by the same physical factors of wind and wave that produce them today. It has occurred to me, however, that a much more favourable condition for concentration, and one which must certainly have taken place on a very large scale, is that of adsorption in fine clay deposits, marine and fresh water. Our recent knowledge of the structures of clays has shown what an enormous rôle they still play in living processes. There is probably today more living matter that is protein in the soil and in the estuarine and sea-bed clays than above the surface or in the waters. Now the effective part of this fine-grained clay is known, particularly through the electron microscope studies of Hast (1947), to consist of what might reasonably be called clay molecules, single layers of aluminium silicate some ten Ångströms thick and a hundred and forty across, covered on both surfaces with hydroxyl groups and capable of adhering with a larger or smaller number of water molecules.

into small pseudo-crystals like piles of coins. Such a small clay particle has an enormous effective adsorptive surface. It has already been shown, particularly by MacEwan (1948), that organic chemicals of a wide variety are preferentially adsorbed on such surfaces in a regular way. It is therefore certain that the primary photochemical products would be so adsorbed, and during the movement of the clay might easily be held blocked from further possibly destructive transformations. In this way relatively large concentrations of molecules could be formed.

This formation is impossible nowadays for two reasons: firstly the cutting off of the ultra-violet by the ozone layer, and secondly the almost universal presence of life, which would destroy such molecules if they were formed in any other way. The very absence of life ensures an accumulation of material containing available energy for indefinite periods: the original world was sterile. Now the clay molecules have another property besides adsorption. Small molecules attached to them are not fixed at random, but in definite positions relative not only to the clay but to each other, and held in such positions they can interact and form more complex compounds, especially if energy can be supplied in the form of light. Clays are now one of the most important of industrial catalysts\*. Polymerization would take place particularly easily with unsaturated compounds, with relatively free electrons. It is in this way that we may imagine that simpler molecular compounds could be made to undergo complex polymerization, polymerization to such an extent that the macromolecules produced might be able to persist in a colloidal form even without clay, and become catalysts or, as we should now call them, enzymes in their turn.

Clay is not the only material on which adsorption may take place. Quartz is another very active material which, as sand, would occur separately or together with clay. The importance of quartz in the formation of primitive molecules out of which life is constructed may be a crucial one in that quartz is the only common mineral possessing asymmetrical structure, some crystals having a right-handed twist and others a left. The characteristic of molecules occurring in living organisms, first brought out by Pasteur a hundred years ago, is that they are also asymmetric, and it has always been a very great difficulty to explain life originating with such molecules, as normal chemical processes produce right- and left-handed molecules with equal facility. It may be, of course, as Pasteur himself thought, that some general feature in the environment favours one rather than the other type, for example, the rotary polarization of moonlight or the magnetic moment of the earth; but to me it seems more plausible that the particular twist was given at one time by the preferential adsorption of a pair of asymmetric molecules on quartz, and, as Mills has shown, once one asymmetric isomer was produced, even locally, it would produce a situation in which ultimately only one kind could be formed.

So far we have followed the track from the inorganic world by steps which, though they cannot be indicated in detail for the lack of necessary research, most

\* The mechanism of catalysis and enzyme action is now becoming much clearer. It seems to depend to a very large extent on movement of hydrogen ions or protons for the most mobile of all chemical species. The most illuminating experiment carried out by Turkevich and Smith (1946) on phosphoric acid translocation of double bonds in butenes, using tritium as a tracer, shows that the actual process consists of a simultaneous transfer of a proton from one part of the molecule to the phosphate, and simultaneously one from the phosphate to another part of the molecule, thus effecting a proton transfer from one part of the molecule to the other, and leaving the phosphate without any net change. They point out, however, that most known crystals, either of a metallic kind or of an ionic kind, such as silicates, sulphates etc., can effect such transfers, and it seems highly probable that protein enzymes act in a similar way.

of which is quite feasible, nevertheless are not only plausible, but, with our present knowledge, inevitable. However, to get any significant information we must look at the other end of the play and try to draw deductions from the inner chemical structure of actual organisms. Now here we are met at the outset with a remarkable set of facts, which call for explanation in terms of origin. The overwhelming majority of living organisms, from the lowest bacteria to trees and men, are all built of a relatively small number (about thirty in all) of types of chemical molecules containing between four and forty atoms in each. Every chemical molecule has its origin in some previous combination, as certainly as every atom of every element. More complex forms, particularly in this or that organism, can be derived from those simple types, and the few cases which have been studied have been shown to be so derived.

From this it follows that there is only one predominating life, derived from one common chemical basis\*. This is exactly the same logic that shows, for example, that all so-called Indo-European languages have a common set of root words, however much they have deviated afterwards. It would be wrong, however, to assume that the common molecules, the amino acids, the sugars and the purines which are the joint stock of existing life are necessarily the first organic chemicals, because there are to be found some aberrant bacteria: the purple and green sulphur bacteria which do not contain some of these molecules, in particular free sugar. It may be that modern life, as we may call it, represents a second stage, and we may have to reconstruct the first stage from these particularly primitive survivals. But all life, including these, contains one group of compounds of a far more complex nature which does seem to be of crucial importance, namely the proteins.

A hundred years ago Engels referred to life as the "mode of action of albuminous or protein substances", and biochemical advances have only confirmed this dictum and made it more precise. The work of the last fifty years has shown something both of their function and of their structure. So many of the chemical reactions occurring in living systems have been shown to be catalytic processes occurring isothermally on the surface of specific proteins, referred to as enzymes, that it seems fairly safe to assume that all are of this nature and that the proteins are the necessary basis for carrying out the processes that we call life. Now although since the great work of Fischer we know that the proteins consist of various combinations of some twenty amino acids, we still do not know the precise structure of any of them. But we do know that they have a precise structure, and we have reasonable hope of determining it in the not so very distant future. It is perhaps significant that though the number of different proteins may be counted in tens of thousands, this represents an insignificant proportion of the possible combination of twenty amino acids. The most likely explanation is that certain sub-units containing the same amino acids in the same order must occur over and over again.

The work of the physico-chemists, particularly of Svedberg, has shown that active proteins exist in the form of molecules of definite molecular weight, and more recently x-ray structure analysis has shown that they are perfectly definite chemical compounds with identical molecules which persist unchanged through various grades of crystal hydration and into solution. We possess already much information as to the actual molecular arrangement, but unfortunately its full

\* This was the major conclusion of T. H. Huxley's *The Physical Basis of Life*, see footnote, p. 537.

interpretation is a task for the future. The situation at the moment is extremely similar to that of an archaeological expedition that has discovered large quantities of rock inscriptions in an unreadable script. They may not know what the inscriptions mean, but they do know they mean something, and they may reasonably hope to decipher them.

The first hints at the deciphering come from the structures of degraded proteins, those used for structural purposes in the animals themselves, such as skin and hair, and those produced by violent chemical action, such as in boiling an egg. Here Astbury (1933) has shown that polymerization must occur to form long chains, and that these chains may be straight or curved or folded in a definite plane. As far as the straight chains are concerned this has been confirmed by the artificial polypeptides synthesized by Woodward giving similar x-ray pictures to the natural ones. More recent work by Perutz (1949), Crowfoot (1941) and their pupils has shown that a similar arrangement must hold in the crystalline proteins, and there seems to be emerging a general picture of the primitive protein molecule, such as that derived by Crowfoot for gramicidin-s, or by Kendrew for myoglobin, indicating the existence of parallel groups of chains making up flat layers of about ten Ångströms thick and from thirty to sixty Ångströms wide. The primitive protein may therefore have a resemblance which is more than coincidental to that of the clay particle. More complex proteins are built by agglutination of the simpler groups. Haemoglobin, for instance, studied in detail by Perutz, seems to consist of four of the myoglobin layers held firmly together. In the crystal the molecules may further be separated by layers of water, just as in the clay particles. The complication goes further with the building up of even larger protein molecules, right up to the size of the viruses whose internally crystalline nature, identical in the solid gel and solution, I was able to establish ten years ago with Bawden, Pirie and Fankuchen (1936).

Now the electron microscope has shown the absolute continuity between the external structure of protein molecules and viruses. I am stating this without any idea of claiming that viruses are a primitive form of life. All the evidence points in the opposite direction. The activity of viruses is absolutely dependent on that of other organisms, and they are probably some of the most complex and sophisticated forms of life, though they seem to lack all the structures and most of the enzymes that normal organisms possess. They would appear to be degenerate parasitic forms, having cut everything down to essential characteristic nucleo-protein, rather than primitive forms evolved independently of higher organisms.

Their significance here is that they illustrate the effects on physical structure of the existence of large regular molecules. Once the size of 100 Ångströms or so is surpassed, new kinds of interactions, imperceptible against the thermal background at smaller sizes, become apparent. These are the long range forces assumed to account for many colloidal phenomena, such as gel formation and coacervation. Tobacco mosaic virus provided the first quantitative pictures of such forces, because it showed that the identical rod-shaped particles of the virus maintained themselves at equilibrium distances which are dependent on the pH and salt concentration. The physical nature of these forces, though almost certainly connected with ionic atmospheres, is still in dispute. Langmuir, Levine, and Verwey and Overbeek (1948) have produced theories which account for them qualitatively, but of their real existence there can be no doubt.



This statement of course does not exclude the possibility that no physical forces exist, but instead that thermodynamic equilibria are satisfied for particles maintaining certain distances from each other. What is important for biology is that such distances can be maintained in media such as those of cells.

The moment, therefore, that macro-molecules of this type are produced they must interact in the liquid and give rise to the physical unity which characterizes the individual living organism. Because of the vagueness of the terms, it is difficult to say whether we should count the origin of life from the first moment that steady interactions occurred between complex molecules in a general medium, or from the point when a section of this medium was separated out, sufficiently large to contain a self-maintaining system of reactions with the medium. We might, if we wish to be precise, qualify the first with the origin of *life*, the second with the origin of *organisms* or living things. The first stage is difficult for us to grasp. The idea of life without living things may seem a contradiction in terms, and yet the evidence, as far as it goes, indicates that such a stage must have occurred because simple molecules must have preceded complex ones, and because definite organisms cannot be formed without the pre-existence of complex molecules\*.

For the purposes of understanding the early stages of development of life it is, however, not absolutely necessary to stipulate the colloidal state of the system. For one thing that is becoming increasingly clear of recent years is that the chemical reactions and the modifications of these reactions are the most characteristic features of vital activity. We must therefore infer a long stage of chemical evolution, of what might be called the internal economy of life, long before we need consider the external shape or forms of function of living things. There is work now to be done on the chemical evolution of life more difficult but also far more fundamental and useful than that which Darwin did on the evolution of the higher forms. The key to the understanding of this chemical evolution of life lies in the junction between observational biochemistry on the one hand and quantum theory on the other.

The basic chemical problem of all vital transformations is the achievement of chemical changes in an isothermal medium, by which large amounts of energy can be made use of in the small steps which alone are permissible in such a system. It is found, for instance, that in the linked enzyme systems which occur in all vital chemical transformations, the individual steps are never more than some sixteen calories and are often much less, down to three calories, hardly more than that of a hydrogen bond, whereas the total exchanges of energy may be several hundred calories, equivalent to the complete combustion which, without these enzyme mechanisms, could only occur at high temperatures. In providing these small quantum jumps, the existence of particularly labile inorganic reactions is obviously of the most critical importance. Two of these, on account of their extreme abundance, are known to be specially important—the oxidation and reduction of ferrous to ferric iron, and of sulphydryl,  $-SH$ , to disulphide,  $-S-S-$ . Early life, in the absence of atmospheric oxygen, must have proceeded almost entirely by the enzymic utilization of these transformations.

The processes of life have a close analogy to those of a chemical factory, only here, instead of the materials being poured from one reaction vessel to another, the individual molecules diffuse from one enzyme to the next, the rates are fixed,

\* I owe this example of such a system to Haldane. The bacterium *Haemophilus caris* cannot synthesize hematin and *H. influenzae* cannot synthesize coenzymes I and II. Neither can grow alone on peptone, but a mixed culture grows well.

and a number of them circulate in these cycles, making use of a certain fraction of the available energy of the reaction, to reverse the entropy gain. As Schroedinger has said, life consumes not food, but negative entropy, and it is able to do so by the existence of what are effectively solid structures in the protein molecules themselves. It is with the establishment of any one such chain of reactions where complex molecules can be fed in at one end and simple ones liberated at the other, with a net energy gain, that we may imagine that living processes started.

We have seen that the complex molecules themselves may have been produced by straight light absorption, but on the other hand the environment did not contain any large sinks of energy such as are provided by the existence of free oxygen molecules in the present atmosphere. The first life processes, therefore, must have been extremely inefficient, similar to those that exist at the moment in anaerobic fermentation, where only 10 per cent of the available free energy is made use of. Nevertheless, once a process of this sort gets started, it is bound to spread. We know at the present day a number of bacteria which are called autotrophic, that is, which can nourish themselves entirely on inorganic ions, nitrate, phosphate, sulphhydryl etc. These, however, cannot be representative of the primitive organisms, because they contain all the most complex enzymic systems.

It is certain that life in its first stages was entirely dependent on the pre-existence of organic molecules. But, correspondingly, as life spread, these organic molecules must have been consumed, and if no other process had supervened, early life must have burnt itself out. This, indeed, may have happened over and over again, because such burning, i.e. the decomposition of all complex molecules, must have restored the original state of affairs and started the whole process all over again, without leaving any notable traces. However, we know by our own existence that they did not all burn themselves out.

It seems most probable that the first crisis of primitive life was resolved by some organism chancing on another mode of collecting energy for chemical reactions, namely one which made use of the current input of solar light. At what stage this happened depends on whether the first organisms were adapted to work in the light or the dark. The latter seems more probable, especially as most of the reactions that we now know of in biochemistry are stopped by short-wave ultra-violet light. It is still, however, quite possible, either in the sea or, more probably, in a mud-bank, for the surface to be exposed to the full flux of sunlight, while the interior is carrying on with much reduced light intensity or in virtual darkness. Life creeping up towards the light might in this case find itself involved in the processes in which the absorption of medium ultra-violet or even visible light might assist the cyclic transformations and make them capable of utilizing less highly formed molecules. This is apparently what happens in the purple sulphur bacteria of today, which utilize simultaneously the energy of absorbed light and that derived from oxidations and reductions of iron and sulphur compounds.

Effectively such a process is likely to occur the moment coloured substances capable of acting as sensitizers, as in photography, are synthesized. One group of these which seems to be especially favoured, possibly on account of their easy production, are the *porphyrins*, formed by condensing four pyridene derivatives around a metal ion. It is extremely suggestive that these porphyrins are found acting simultaneously as light receivers in the chlorophyll of all plants, and as respiratory pigments in cells, as oxygen carriers in many animals, and finally,

and most strangely, associated with nitrogen absorption in the root nodules of peas. This points to all life being derived from a light-absorbing intermediate form—essentially a plant.

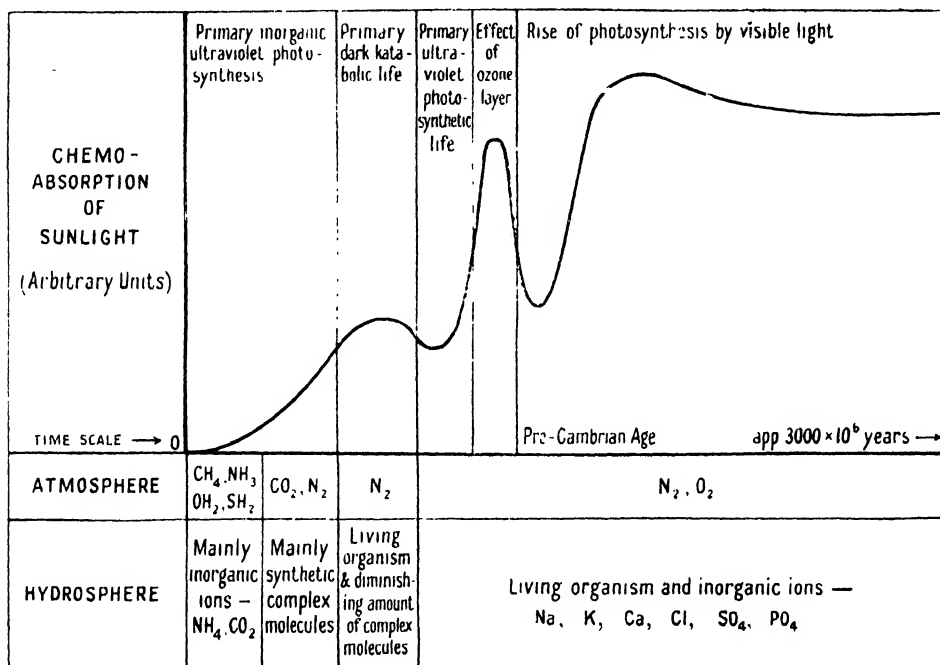
From the light-assisted metabolism of the purple bacteria to the full photosynthesis may not be a very wide step, but once the latter process is achieved, the future of life is assured. Modern research on synthesis shows that it is far from the simple reaction  $\text{CO}_2 + \text{H}_2\text{O} = \text{CH}_2\text{O} + \text{O}_2$ ; that in fact the three processes of light absorption, carbon dioxide absorption and the liberation of free oxygen occur quite separately and may not all have been evolved at the same time. However, once photosynthesis started it made its mark on all subsequent living things, and was undoubtedly so successful that it wiped out earlier forms of life, except in very obscure holes and corners. One characteristic product of photosynthesis is sugar, and the universal prevalence of sugar is only less marked than that of protein in the organic world, though all indications point to it as a much later derivative. Combined either with phosphorus or with purine bodies, or with both, sugars take part in an enormous number of enzyme systems, and particularly in nucleic acid, with its close associations with growth and reproduction.

The processes of respiration are so closely attached to those of photosynthesis that it seems probable that both occurred together in the first place, and only later became separated, when organisms developed predominantly one or the other process. Respiration, as already indicated, is a very much more efficient process than fermentation, and immediately increases the activity and range of living things. But full-scale respiration cannot have occurred until photosynthesis had been going on for some time and had produced the necessary oxygen. Once this happened there were two other direct consequences. In the first place, as already indicated, the oxygen drifting into the upper atmosphere interacted with the ultra-violet to produce an ozone layer which effectively blocked all the original syntheses on which life existed. But the very nature of photosynthesis prevented this having any serious effect on the production of organic from inorganic material. The danger may well have been in the other direction, a relatively unchecked building-up of carbon into cellulose and other sugar products. But the simultaneous existence of oxygen and combustible hydrocarbons put a premium on mechanisms of the reverse kind, and organisms specializing in respiration: bacteria, fungi and animals, tended to restore the balance. This is indicated in the diagram by a second maximum in the effective utilization of sunlight brought about by the reversal of the upsurge due to photosynthesis, by the increase of catabolic processes leading ultimately to the equilibrium in which we now live.

From the moment of the existence of an oxygen-rich atmosphere, the physical environmental conditions of life became essentially what they are now. This is as far as it is possible to go, at least at present, on the basis of purely physical and chemical knowledge, even assisted by what we know of biochemistry. For understanding development in the third act, that of organized life, we must rely on the ever deeper study of living organisms, both in structure and function, and use physical and chemical knowledge to interpret what is observed. A hundred years ago the discovery that the cell was the unit of life seemed to explain the common origin of the large observable organisms and tissues which were then studied in terms of some biological atom. In one sense this is still true. With the exception of the viruses, and possibly of some bacteria and the mycetozoa, all animals and plants are composed of cells; but the structure of the cell is likely to

prove as complicated in terms of its constituents as that of the organism in terms of cells. The first fact which makes a science of cytology possible is that of cells reconstructed on the same basic pattern and developed, and particularly reproduced, by a set of complicated phenomena identical over the whole living kingdom.

The evolution of organisms must have been preceded by a period of the evolution of the cell. But the story of that evolution is certainly the most difficult part of the whole unravelling of biological processes, because it is at the same time the furthest removed from synthetic chemistry and analytical biology. Nevertheless in recent years, thanks to the new methods described above, much deeper understanding of the cell is becoming possible. The most striking general feature is the dual construction. The cell consists, inside a membranous envelope, of two parts, a nucleus itself provided with a membrane, and an external cytoplasm.



This figure is entirely hypothetical except as to the sequence of the stages. The relative heights of the maxima may have been different and the stages may have overlapped much more than is shown, even to the extent of blotting out the maxima and minima.

Each of these volumes in turn contain other finer parts. The nucleus contains filamentous processes of varying number, the chromosomes, together with the associated nucleoli and centromeres, while the cytoplasm contains a world of particles of varying dimensions, particularly the mitochondria, the golgi bodies and a number of the smaller plastids, including the chloroplasts in the plants and the microplastids and other so-called organelles.

Many, if not all, these constituents appear to be self-reproducing. Therefore even in single-celled organisms there is considerable differentiation. Protoplasm is therefore far from a structureless substance, and to its microscopic complexity must correspond an even greater diversity of chemical and physico-chemical function, all pointing to an equally complicated history. I will not attempt to discuss the former of these, the cell equilibrium brought about through enzymes

which seem to be attached to the mitochondria, and to the apparently dominating rôle of desoxyribose and ribose nucleic acids, the former being synthesized in the nucleus and its amount determining growth and division.

The cell, chemically speaking, may be considered as a little world, if not two little worlds, in which the whole set of chemical reactions characterizing some large volume of pre-organic life is concentrated. The essential feature of the chemical life of the cell is its extreme persistence along established lines of chemical reaction, and the way in which these characteristic reactions are reproduced over and over again in daughter cells. Schroedinger has pointed out that this exact reproduction is a quantum phenomenon in itself, and has attached the possibility of overcoming the entropy-increasing effect of normal diffusion by the quasi-solid (solid at least in one dimension) structures of the chromosomes themselves. Actually this uniformity of chemical action is by no means absolute, particularly in bacteria. The actual biochemistry of the cell can in fact be very violently varied by changes in the environment, and even the nucleus itself and the genetic processes are, as we now know, capable of random modification and of directed modification by specific chemicals. Their isolation in the past depended largely on the difficulty of getting the chemicals to the places where they could act.

Where physical methods can be of use is in interpreting the structures visible in the cell and in inferring others. Protoplasm is by no means a uniform substance. Electron microscope and x-ray researches show that it contains, quite apart from the relatively large structures previously referred to, others of intermediate size which, on account of their greater surface, are probably the seat of the greatest activities. The viscosity of the cell contents shows that it contains an appreciable amount of fibrous molecules. These are almost certainly of protein nature. One of the most interesting discoveries in this field is the extreme ability of the so-called globular, but more probably plate-like, proteins to aggregate in the form of fibres. This aggregation, if carried out without drastic conditions of temperature or acid, seems to be perfectly reversible. At least it has been observed to be so in the cases of insulin, actin, tropomyosin and fibrin. It would appear indeed that practically all fibres found in biological systems are made in this way from particulate proteins, for example paramyosin, where the particles can be seen in the electron microscope, collagen and keratin. Conversion of particulate to fibrous proteins is probably some form of chain-ring polymerization, but in the more labile forms this can only affect a small number of the available bonds. These fine fibres, running from 100 to 200 Ångströms in diameter, have of course very large surface areas and are capable, therefore, of carrying on almost as active chemical interchanges as free molecules. Indeed, it seems very probable that all the enzymes in cells are attached in this way, the most notable being the adenosin triphosphatase, which seems to be bound by myosin and to play an important part in muscle contraction.

An analogous phenomenon follows necessarily from the very existence of such fibrous molecules. Zocher and Bernstein (1929) first showed that in dilute clay suspensions the particles tend to arrange themselves in parallel sheets at regular intervals, which may be as great as 5000 Å. I was able to study some phenomena in tobacco mosaic virus, as mentioned above, and in fact we can say now that all such fibrous molecules are attached to each other by long range forces, the range of which is dependent on the conditions of the medium, which may impose coagulation into microscopically visible fibres when the distances are small to a practically fluid and orientated gel when they are large.

The variability of the degree of fibrous nature of the cell contents is nowhere better shown than in the phenomenon of cell division, a complicated pattern which, however, is substantially the same for all cellular organisms. Some ten years ago I put forward a theory of mitosis based on the observation of these long range forces, and particularly on the analysis of the structure of the spindle-shaped tactoids (Bernal 1940). These were first observed by Zocher in iron oxide sols and later studied in more detail in tobacco mosaic virus. When a uniformly diffused area of rod-shaped particles is caused to aggregate, the forms taken by the aggregation are no longer spherical drops, but, on account of the long range forces, particles tend to remain in parallel orientation, giving rise to anisotropic surface forces and leading to an equilibrium in the form of a tactoid with a geometrical surface obeying the formula  $\sigma_1/r_1 + \sigma_2/r_2 = \text{const.}$ , where  $\sigma_1$  and  $\sigma_2$  are the principal surface tensions and  $r_1$  and  $r_2$  the principal radii of curvature. Exactly the same form is taken by inclusions of clear solution in a concentrated aggregate of long molecules. These, analogous to bubbles, are called negative tactoids. Such tactoids undoubtedly exist in dividing cells (see Bernal and Fankuchen 1941).

It would appear that the mechanism of their formation is somewhat as follows : at the instant of division, spontaneously or, perhaps, stimulated by changes going on in the nucleus, a small particle in the cytoplasm, the centrosome, causes a ring-chain polymerization of the proteins, proceeding as in insulin and forming a spherulite assembly of fibres radiating from a point. The centrosome divides and the spherulite correspondingly becomes a tactoid, or spindle. That this is the case has been shown very beautifully by the photographs of mitosis in polarized light. The existence of the tactoid produces an effective long range forces field. In such a field particles which do not mix with the system, such as the chromosomes, will tend to be driven to the equator where the particles are most parallel. This is the stage known as the metaphase.

The next stage marks the reversal of this process, but this appears to originate in a special section of each chromosome, the centromere. The centromeres of each paired chromosome, for the chromosomal division occurs at an earlier stage, proceed to separate, but in such a way as strongly suggests that each pair are the poles of a negative tactoid, and are in fact centres of disaggregation of the protein fibres. Thus they, so to speak, eat their way away from the equator towards the poles. That considerable forces are involved is shown by the fact that anomalous chromosomes which have not fully divided are literally torn in two. Much more research is needed to show whether this hypothesis is the correct one, but it has at least the merit of not invoking any forces other than those that can be demonstrated in other organic and even in inorganic systems such as ferric hydroxide and vanadium pentoxide gels.

Similar explanations based on the knowledge of long range forces may go far to explain the mechanics of chromosome pairing itself. In reproduction the chromosomes belonging to the father and mother nuclei are together in identical pairs. These must, in fact, seek each other out and arrange themselves mutually with extraordinary accuracy. The variation of nucleic acid material along the chromosomes, with its complicated pattern and the corresponding variation in long range forces, may serve to explain this process. Full interaction can only occur if there is a proper opposition of parts, and the difference between a good fit and a bad may insure that after a number of trials a fit is achieved in one place and then proceeds by zipper action over the rest of the chromosomes. We are only

at the beginning of these studies, and far greater complexities will probably be revealed by further observation. But these complexities will act as a spur to further physical researches leading to their explanation.

So far I have spoken only of the interior of the cell. But for the survival of evolution of life, the relation of the cell to its environment seems now no such great mystery as it seemed to Henderson, considering, if our view is correct, that it was blocked out of that environment and represents simply a selective enclave of balanced chemical processes. The pre-condition of the existence of a cell is that it can maintain the concentration of its elements in a medium of very much lower concentration. This involves work, but it is a kind of work that the protein enzyme systems in the cells are particularly suited for, and for which the properties of lipid membranes provide the necessary physical scaffolding.

In the further evolution of organisms we can distinguish size as the major conditioning factor. The uni-cellular organisms of a few microns in dimension must necessarily live in a world in which molecular forces rather than hydrodynamic ones are of prime importance. Small molecules on which nutrition and respiration depend must enter freely by diffusion. But diffusion is absolutely limited by size, and the larger an organism is, the smaller its effective surface, and the smaller the effective volume from which it can draw its nourishment. There are two ways out of this dilemma, and both have been followed by different organisms. The first is to grow only in one or two dimensions, to produce filamentous or leafy forms keeping a large surface. The second is motility, not the directed motility of the larger organisms, but simply moving for moving's sake, out of the comparative starvation of the immediate neighbourhood. The ceaseless motion of bacteria and protozoa had originally no other point, but once a controllable motile mechanism is evolved from such simple protein molecules as cilia, hardly more than a bundle of some eight or sixteen macro-molecules, future evolution towards directed motion becomes almost a necessity.

At this stage there are two directions open to organisms. One is to improve their biochemical mechanisms and be able to make use of a very dilute environment, and the other to move into a better environment; that is the basic distinction between plants and animals. The first remain absorbers of individual molecules, and their motility is limited to extending their surfaces and arranging for the slow and steady flow of an internal environment. The motile forms, however, sooner or later are bound to bump into each other, and from that contact arises the possibility of digestion and, therefore, the possibility of acquiring new material in prefabricated pieces rather than molecularly. Motility in itself may fluctuate between total motility, in which the organism moves through the environment, and relative motility, in which the organism stays still and pushes the environment past it, as in the ciliates, sponges, oysters or barnacles. In the first case the essential new feature is direction, a movement along a chemical and thermal gradient. This involves the production of some kind of sensitive element at the head end, and some link between this and the motility. From these simple beginnings follows the evolution of the necessarily linked triad—sense organ, nerve system and effector.

The actual evolution of the higher organisms, using cell division to create a larger organism than is possible with single cells, may have been really only a mechanical necessity. Once the very small dimensions of the single cell are surpassed, forces utterly inappreciable on the micro-scale become important, such

as turbulence of the medium and gravity. To resist these, greater strength than is provided by the protoplasmic framework is needed, and this is available by using the mechanical strength inherent in cell walls, either simply or strengthened by protein fibres or by cellulose. Where additional strength is required, mineral deposits like shell and bone can be added. Multi-cell organisms can afford to specialize, and our understanding of the physical nature of these specializations, such as the passing of nerve currents, the contraction of muscles or the secretion of chemicals, seem to show that they all use rather specially selected aspects of mechanisms common to all protein systems.

But now the particular function of the organ is no longer self-determining and absolute. It is part of a larger coordination. Modern mathematical analysis is showing us that the very fact of coordination, the very linkage mechanism itself, introduces new complexities and new possibilities of a very specific kind. Take, for example, one of the most complicated, the mechanism of vision. It is relatively straightforward to arrange a one-to-one connection between a single receptor in the retina and a single effector in the visual cortex. But this is only the beginning of the story. Such a system could see, but it could neither recognize nor follow. Three layers of cells are involved in grouping and sorting out the impulses of the cortex and creating the percepts of objects which are the basis of sensual experience of the higher animals. The arrangements of these layers of cells, as Weiner has shown, are essentially similar to the arrangements in modern electronic calculating machines with similar functions. An even higher complexity is required if we have to move from percept to concept, a process which in its fullness has only occurred in man, or possibly in some other social animals. Here the mutual relations of organisms originating in reproductive links have led to a still higher order of mutual interaction and corresponding permanency of cultural tradition.

This brief survey of the field of life does show that we are now beginning to see the possibility of accounting for it in terms that fit in with our intellectual and manipulative control of the non-living parts of environment. It is certain that this account will appear as absurd to those who come after us as did those of Borelli or of the early corpuscular mechanists of the seventeenth century. Yet even then this approach to rationality did make possible further advances of biology at that time, and so we may hope from the present analysis to achieve corresponding advances in biophysics. This does not mean any reduction of biology to simple physics. The complexity of the successive evolutionary levels mark definite orders of advance each with its own laws and each with its own internal unbalance leading forward to new levels. However, by elucidating structures, by following out mechanisms, we may at least clear the air of mystical interpretations which serve simply to conceal ignorance. Instead of concealing ignorance we may hope to reveal it, to find the places where the explanations will not fit, and sooner or later to find the means for studying just these points. In such a study we may reasonably expect to discover further and further points of ignorance and difficulty. But even if the task were endless it would still be worth while. Every new relation gained is an achievement of order, giving confidence and direction to future work, and at the same time providing for new controls over our biological environment, including our own bodies. The profundity of physics should not blind us to its relative simplicity in the scheme of human knowledge. Here in biophysics we have something so complex that it will require not only more industry but more intelligence than went into the



earlier stages either of biology or of physics. Man has, in the past, used his knowledge to effect gross changes in his environment, first mechanical and then chemical. Only an understanding of the biological and social sciences can show how to make those changes of real benefit to man, and how to balance power with intelligence.

## REFERENCES

- ASTBURY, W. T., 1933, *Fundamentals of Fibre Structure* (Oxford : University Press).
- BERNAL, J. D., 1940, *The Cell and Protoplasm*, ed. F. R. Moulton, (Washington : Amer. Assoc. Adv. Sci.), p. 199.
- BERNAL, J. D., BAWDEN, F. C., PIRIE, N. W., and FANKUCHEN, I., 1936, *Nature, Lond.*, **138**, 1051.
- BERNAL, J. D., and FANKUCHEN, I., 1941, *J. Gen. Physiol.*, **25**, 111.
- CROWFOOT, D., 1941, *Chem. Rev.*, **28**, 215.
- DARWIN, F., ed., 1887, *The Life and Letters of Charles Darwin*, vol. 3, p. 18.
- DAUVILLIER, A., 1947, *Genèse nature et évolution des planètes* (Paris : Hermann), pp. 169 ff.
- ENGELS, F., 1940, *Dialectics of Nature* (London : Lawrence and Wishart), p. 194 ff.
- GOLDSCHMIDT, V. M., 1923-1937, *Skriften Norske Vidensk. Akad. K.*, **1**.
- HALDANE, J. B. S., 1928, *Rationalist Annual*, "The Origin of Life", pp. 148-153.
- HAST N., 1947, *Nature, Lond.*, **159**, 354.
- HUXLEY, T. H., 1901, *Collected Essays*, "On the Physical Basis of Life", vol. 1 (London : Macmillan).
- KUHN, W., 1946, *Experientia*, **2**, 10.
- LWOFF, A., 1943, *L'Évolution Physiologique* (Paris : Hermann).
- MACEWAN, D. M. C., 1948, *Trans. Faraday Soc.*, **306**, 349.
- OPARIN, A. I., 1938, *The Origin of Life* (New York : Macmillan).
- PERUTZ, M. F., 1949, *Proc. Roy. Soc. A*, **195**, 474.
- PIRIE, N. W., 1937, *Perspectives in Biochemistry*, eds. J. Needham, and D. R. Green, *The Meaninglessness of the Terms 'Life' and 'Living'* (Cambridge : University Press), pp. 21 ff.
- PRIGOGINE, I., 1947, *Étude thermodynamique des phénomènes irréversibles* (Paris : Dunod).
- TURKEVICH, J., and SMITH, R. K., 1946, *Nature, Lond.*, **157**, 874.
- VERWEY, E. J. W., and OVERBEEK, J. Th. G., 1948, *Theory of the Stability of Lyophobic Colloids* (Leyden : Elsevier).
- ZOCHER, H., and BIRNSTEIN, V., 1929, *Z. Phys. Chem. A*, **142**, 113.

## A Stereographic Projector

By A. E. DE BARR

G.K.N. Research Laboratories, Wolverhampton

*MS. received 26th April 1949*

**ABSTRACT.** An optical device is described by which the effect of rotation on the stereographic projection of a crystal can be observed directly. The application of the device to the construction of pole figures from x-ray data is described.

### § 1. INTRODUCTION

MANY crystallographic problems are most readily discussed and solved by the use of the stereographic projection. Measurements of the angular relationships in and between crystals and calculations of the angular relations involved in tilting or cutting crystals are readily carried out in this way. The most general type of problem involves the determination or the description of the movement of a plane or set of planes when the crystal is moved in a prescribed manner. With a stereographic projection and stereographic and polar nets rotations of any pole about axes normal to or in the plane of the projection may easily be made. Rotations about other axes are not so simple, but can always be resolved into components about axes normal to or in the plane of the projection (De Barr 1948). However, when several rotations are involved and it is required to follow the movements of many poles, the graphical work involved becomes laborious. The principle to be described in this note enables the effect of any rotation on any number of poles to be observed immediately.

### § 2. PRINCIPLE

Referring to Figure 1, P is the pole to be projected, P' is its stereographic projection and O is the centre of the reference sphere. X'OX is the plane of

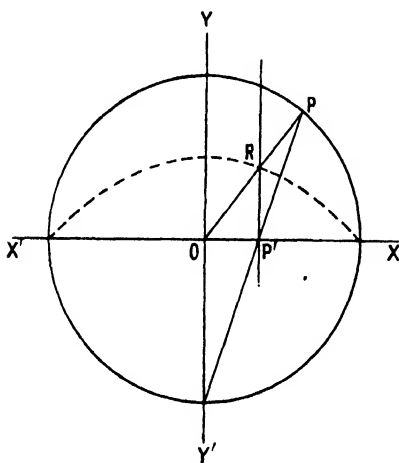


Figure 1.

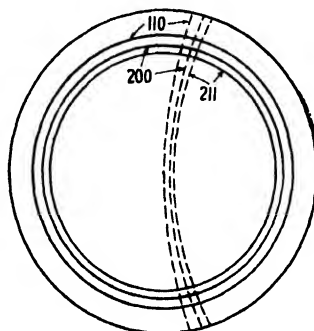


Figure 2. Reflection circles for iron using MoK $\alpha$  radiation

— X-ray beam normal to the plane of projection.  
 - - - X-ray beam at 10° to the plane of projection.

projection. If now the normal to the plane to be projected is represented by a small pencil of light directed along OP and a screen is placed surrounding O and so

situated that the pencil of light intersects the screen at R where R lies on the perpendicular to the projection plane through P, then, viewed normal to the projection plane, the spot of light on the screen appears in the position of the stereographic projection of P. The screen is a surface formed by revolution about YOY' of the locus of all such points as R. It may easily be shown that, referred to axes OXY as shown, the equation to this locus is  $x^2 = r^2 - 2ry$ , where  $r$  is the radius of the projection sphere. The form required for the screen is therefore that of a paraboloid of revolution.

If now a screen of this form is correctly placed over a projection system such that the normals to the planes to be projected are represented by pencils of light, then each such pencil will produce on the screen a spot which, viewed normally to the plane of projection, corresponds with the stereographic projections of the planes. The projection system may be rotated in any manner and, provided that the pencils of light always proceed from the centre of the reference sphere, the spots of light on the screen represent the stereographic projections of the poles, if viewed normally.

### § 3. APPARATUS

Figure 3 shows a convenient arrangement for a stereographic projector using the principle outlined above. The projection system consists of a small source of light A mounted at the centre of an opaque, hollow hemisphere B which is pierced with small holes representing the poles to be projected. (It is convenient to drill in one hemisphere all the holes likely to be required and to fill in with wax those not needed at any one time.) This system is supported with the light source at the centre of a large, hollow hemisphere C resting on ball bearings in the frame D in the manner of a universal joint. The screen E is supported from the frame so that its centre is vertically above the light source by an amount  $r/2$ .

A suitable parabolic screen can be made from  $\frac{1}{16}$  in. Perspex, softened in hot water and pressed to shape in a wooden mould. The two portions of the mould can be made on a lathe from a template constructed to the required screen profile. Allowance must be made for the thickness of the Perspex when making the mould. The screen can be given a ground surface with grinding paste.

### § 4. APPLICATION TO THE CONSTRUCTION OF POLE FIGURES

In the construction of pole figures from x-ray diffraction photographs, the number of photographs required can be considerably reduced if all the diffraction data recorded on the photograph are used (Wood 1948). Thus diffraction photographs of iron with Mo K $\alpha$  radiation show diffraction arcs from 110, 200 and 211 reflections and all this information can be used to construct, say, a 100-pole figure. To use it it is necessary to know, e.g., the positions of the 100 poles when a particular 110 or 211 pole is in a reflecting position. This information is readily obtained from the stereographic projector if a plane transparent screen F carrying the reflection circles (Barrett 1943) for all the planes involved is placed over the projector as in Figure 3. Such a screen is shown in Figure 2. The projector is rotated until, say, a 110 pole lies on the 110 reflection circle in a position corresponding to that of a 110 diffraction arc on the x-ray photograph. The corresponding positions of the 100 poles can then be observed directly on the screen and plotted on the pole figure. The actual rotation of the projector as described above must be adjusted until the results from all the poles are consistent.

If the small light bulb is replaced by a Pointolite source and the lower surface of the screen is coated with fluorescent paint (luminescent powder E(P), supplied by G.E.C. Ltd., has been found suitable for use with a 30 c.p. Pointolite bulb), actual pole figures can be depicted on the screen by moving the projection system around as desired for several seconds. On switching off the lamp, the luminescent pattern remaining represents the pole figure. A model of the stereographic projection showing this feature was exhibited at the Physical Society Exhibition in 1948.

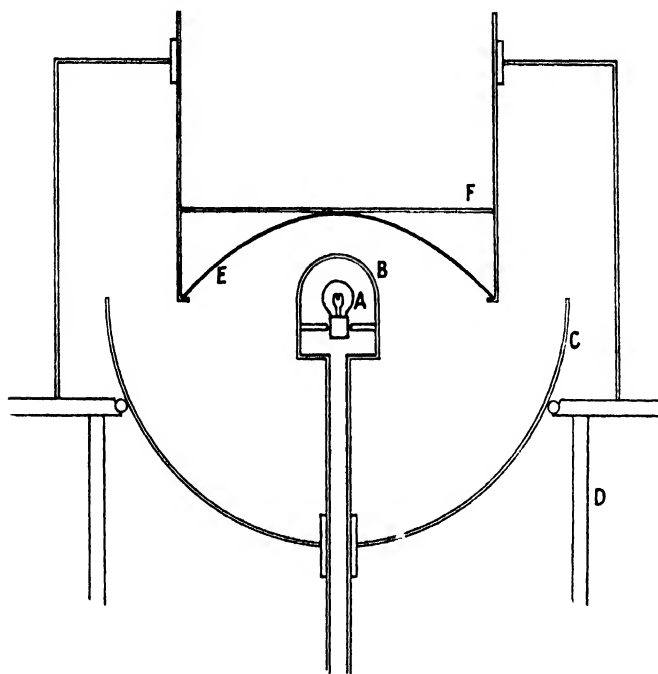


Figure 3. A stereographic projector.

#### ACKNOWLEDGMENTS

The author wishes to thank the Director of Research, Mr. N. F. Astbury, and the Research Board of Guest, Keen and Nettlefolds for permission to publish.

#### REFERENCES

- BARRETT, C. S., 1943, *Structure of Metals* (New York : McGraw-Hill).  
DE BARR, A. E., 1948, *J. Sci. Instrum.*, **25**, 102.  
WOOD, J. K., 1948, *J. Appl. Phys.*, **19**, 784.

## A Study of Magnetic Viscosity

BY R. STREET AND J. C. WOOLLEY

The University, Nottingham

*Communicated by L. F. Bates ; MS. received 11th May 1949*

**ABSTRACT.** A general analysis of magnetic viscosity based on activation energy concepts is given. A particular case is considered of the application of the theory to the phenomenon occurring in materials in which bulk magnetization proceeds by the rotational movement of the vectors of single domains, which process, according to a recent theory of Stoner and Wohlfarth, may occur in certain high coercivity alloys. Experiments have been made, using a magnetometer method, with specimens of alnico maintained at various temperatures within the range  $-187^{\circ}\text{C.}$  to  $250^{\circ}\text{C.}$  The results obtained are found to be in good agreement with the theoretical analysis.

### §1. INTRODUCTION

IF the magnitude of an external magnetic field applied to a ferromagnetic specimen is suddenly increased then, in general, the consequent change of the intensity of magnetization is not correspondingly rapid. For most ferromagnetic substances there is a time lag between the magnetic field and the magnetization which may be accounted for almost completely in terms of the production of eddy currents within the specimen. However, with certain materials the persistence and magnitude of the change of magnetization are much too great to be accounted for by eddy current formation and this phenomenon is now generally called "magnetic viscosity". Previous investigations of the phenomenon have been summarized by Becker and Döring (1939) and the following qualitative observations have been made. The effect (i) is most noticeable on the steepest part of the magnetization curve, (ii) is temperature sensitive, (iii) as far as soft iron specimens are concerned, is influenced by the presence of small quantities of impurities such as carbon and nitrogen, and (iv) closely resembles analogous mechanical and dielectric phenomena.

Becker and Döring have pointed out that no comprehensive theory of magnetic viscosity exists. They have therefore developed the analogy between dielectric and magnetic "after effect"; this involves assigning relaxation times to the ferromagnetic domain processes which give rise to magnetic viscosity. Under certain conditions, they predict that the change in the intensity of magnetization is a logarithmic function of time. Again, Snoek (1938) has developed a theory which accounts successfully for the phenomenon known as the time decrease of permeability which he has shown to be closely connected with magnetic viscosity; owing to certain limitations in this theory it is, however, not possible to compare its predictions with experimental observations on magnetic viscosity.

In the theory given below the problem is approached by considering that magnetic viscosity is an activation-energy process. Physical mechanisms which involve such activation energies can be visualized, and it is shown that, in at least one case, namely that of a high coercivity alloy, the required mechanism is already implicit in a recent theory of heterogeneous alloys (Stoner and Wohlfarth 1948.)

## §2. THEORY

The analysis given in this section is essentially formal and follows that already given by Smith (1948) in his theory of transient creep in metals; consideration of the physical principles underlying the assumptions made here will be deferred until §6.

It is first supposed that at some stage during the magnetization of a ferromagnetic substance, following upon a sudden increase in the applied magnetic field, a certain number of the domains have their magnetization vectors in positions which may be described as "metastable". Thus, a small increase in domain energy makes little difference to the vector orientation, but a larger energy change initiates a transition to stable equilibrium which involves a discontinuous change of orientation. The mechanism envisaged is therefore, in essentials, an activation process.

At a time  $t$  after the sudden increase in applied magnetic field let the number  $N$  of domains characterized by activation energies lying between  $E$  and  $E + dE$  be  $f(E)dE$ . Then the time rate of change of  $N$  due to thermal activation with the specimen maintained at constant absolute temperature  $T$  will be given by

$$\frac{dN}{dt} = -Cf(E)dE \exp(-E/kT) \quad \dots\dots(1)$$

assuming that successful activations do not produce additional metastable states with activation energies in the range from  $E$  to  $E + dE$ . Equation (1) is satisfied by

$$f = f_0 \exp(-\lambda t) \quad \text{where} \quad \lambda = C \exp(-E/kT). \quad \dots\dots(2)$$

$C$  is a constant and  $f_0$  denotes the value of the function  $f$  at time  $t = 0$ .

If each activation contributes an average amount  $\bar{i}$  to the resolved part of the magnetization along the direction of the applied field, then the activation of  $dN$  domains gives a mean increase of the intensity of magnetization of the specimen of

$$\bar{i}Cf_0 \exp(-\lambda t) \exp(-E/kT) dE dt.$$

Taking into account all values of activation energy, the time rate of increase of the intensity of magnetization is

$$\frac{dI}{dt} = \bar{i}C \int_{E_{\min}}^{E_{\max}} f_0 \exp(-\lambda t) \exp(-E/kT) dE \quad \dots\dots(3)$$

and this integral may be evaluated only if the limits and the form of the function  $f_0$  are known. Consequently three simple cases which are relevant to the present problem will be considered below.

(i) Let us assume that  $f_0$  is independent of  $E$  and has a constant value  $p$ . (This is the case considered by Smith (1948).) Then

$$\frac{dI}{dt} = \bar{i}Cp \int_0^{\infty} \exp(-\lambda t) \exp(-E/kT) dE, \quad \dots\dots(4)$$

taking all values of activation energy between 0 and  $\infty$ , as a first approximation. From equation (2)

$$d\lambda = -(C/kT) \exp(-E/kT) dE$$

and substituting in equation (4)

$$\frac{dI}{dt} = \bar{i}p kT \left[ \frac{1}{t} \exp(-\lambda t) \right]_{\lambda=C}^{\lambda=0} \quad \dots\dots(5)$$

$$\frac{dI}{dt} = \frac{\bar{i}p\mathbf{k}T}{t} \{1 - \exp(-Ct)\}.$$

If  $Ct \ll 1$

$$\Delta I = \bar{i}p\mathbf{k}T(Ct) + \text{const.} \quad \dots\dots(6)$$

and if  $Ct \gg 1$

$$\Delta I = \bar{i}p\mathbf{k}T \log t + \text{const.} \quad \dots\dots(7)$$

In these expressions the symbol  $\Delta I$  denotes the contribution to the total intensity of magnetization by the thermal activation of the domains, measured at a time  $t$  after the increase in applied field.

Which of the assumptions made in equations (6) and (7) is more nearly correct in any given case may best be decided by experiment. In the experimental work described below it is shown that the observed variation of  $\Delta I$  is a linear function of  $\log t$  as predicted in equation (7). Consequently, in the other theoretical considerations in this section it will be assumed that  $Ct \gg 1$  for the values of time involved in the experimental studies.

(ii) Equation (7) predicts that the intensity of magnetization of the specimen increases indefinitely (proportional to  $\log t$ ) although in practice the magnetization must eventually reach some finite value. This difficulty is a necessary consequence of the assumption that  $f_0 = p$  for all values of activation energy from 0 to  $\infty$ ; this also implies that, if  $p \neq 0$ , an infinite number of domains may be activated. Physical considerations suggest that a better approximation for the distribution function  $f_0$  is

$$\left. \begin{aligned} f_0(E) &= p & \text{for } 0 < E < E_0 \\ f_0(E) &= 0 & \text{for } E > E_0 \end{aligned} \right\} \quad \dots\dots(8)$$

where  $E_0$  is some limiting upper value of the activation energy. The total number of domains which may be activated,  $N_0$ , is, from equation (8),  $pE_0$ .

Equation (5) now becomes

$$\begin{aligned} \frac{dI}{dt} &= \bar{i}p\mathbf{k}T \left[ \frac{1}{t} \exp(-\lambda t) \right]_{\lambda=\lambda_0}^{\lambda=\infty} \\ &= \frac{\bar{i}p\mathbf{k}T}{t} \{ \exp(-\lambda_0 t) - \exp(-Ct) \}, \quad \dots\dots(9) \end{aligned}$$

where  $\lambda_0 = C \exp(-E_0/\mathbf{k}T)$ .

The experimental work referred to in (i) above shows that in practice equation (7) represents the observed behaviour with some accuracy and thus, in any modifications such as those of equation (8), the upper limit of the integration must be of the form  $\lambda \rightarrow 0$ , and this is so if  $E_0 \gg \mathbf{k}T$ . Hence equation (9) may be reduced to

$$\Delta I = \bar{i}p\mathbf{k}T \int_{t_C}^t \frac{1}{t} \exp(-\lambda_0 t) dt + I_C, \quad \dots\dots(10)$$

where  $I_C$  is the value of  $\Delta I$  at a time  $t_C$  after the change in the applied magnetic field when the term  $\exp(-Ct)$  becomes negligible with respect to  $\exp(-\lambda_0 t)$ ; and  $t_C \ll 1$  since  $E_0$  is assumed  $\gg \mathbf{k}T$ . For the present purposes only an indication of the function  $(I, t)$  is required and this is given as follows.

Expanding

$$\begin{aligned} t^{-1} \exp(-\lambda_0 t) &= t^{-1} - \lambda_0 + \lambda_0^2 t + \dots \\ &\simeq t^{-1} - \lambda_0, \text{ if } t \ll 1/\lambda_0, \end{aligned}$$

then

$$\Delta I \simeq \tau p\mathbf{k}T \{ (\log t) - \lambda_0 t + \text{const.} \}. \quad \dots\dots(11)$$

Equation (11) shows that to the order of approximation assumed, i.e.  $t \ll 1/\lambda_0$ , the value of  $\Delta I$  is reduced from the value predicted by the simple  $\log t$  function by an amount  $\lambda_0 t$ . In the experiments described below this correction term became significant only for large values of  $t$ , and, in the period of time usually considered here, was negligible.

The final steady value attained by  $\Delta I$  is found by taking the upper limit of the integral of equation (10) equal to  $\infty$ . Standard tables of this integral,  $-\text{Ei}(-t_c)$ , (Jahnke and Emde 1938), show that it is finite for integration between the required limits,  $t_c$  and  $\infty$ . Consequently, the distribution function assumed, equation (8), leads to a final constant value of  $\Delta I$  at  $t = \infty$ .

(iii) A particularly simple form of distribution function is obtained by considering that all the domains capable of activation after a sudden increase in the applied field are exactly similar and are characterized by the same activation energy  $E_s$ . Then

$$dI/dt = iN_0\lambda_s \exp(-\lambda_s t)$$

where

$$\lambda_s = C \exp(-E_s/kT)$$

and

$$\Delta I = -iN_0 \{ \exp(-\lambda_s t) + \text{const.} \}. \quad \dots\dots (12)$$

This result is formally equivalent to that obtained by Snoek (1938).

The experimental work described below has been directed towards the determination of the form of the  $(\Delta I, t)$  function and also to the quantitative examination of the influence of temperature on magnetic viscosity.

### § 3. SPECIMENS

The specimens used in the investigations described here were rods of alnico having the following approximate percentage composition: Al 10, Ni 18, Co 12, Cu 6, Fe 54, and dimensions 30 cm. long and 0.65 cm. diameter. Two such rods were available, one as cast or untreated, and the other heat-treated by maintaining it at a temperature of 1250°C. for 20 minutes, allowing it to cool at a rate of about 2°C. per second and then annealing it at 600°C. for about 2 hours. These rods were chosen for the experimental work since, of the various high coercivity materials available, it was known from a previous investigation (Street and Woolley 1949) that the phenomenon of magnetic viscosity was considerably more marked in these specimens than in soft iron. The results given below were all obtained with the untreated specimen, but the behaviour observed with the heat-treated specimen was essentially similar.

### § 4. METHOD AND APPARATUS

The specimens were mounted in either an electrically heated tubular oven (the heater of which was wound non-inductively and fed with D.C.) when temperatures up to 250°C. were required, or a Dewar vessel containing either liquid air or "dry ice" moistened with alcohol as required. External magnetic fields were applied by means of a surrounding water-cooled solenoid of length 60 cm. capable of producing a maximum field intensity of about 800 oersted. The required stability of the magnetic field could only be obtained by supplying the current to the solenoid from a 280 v. battery of high capacity accumulators.

Measurements of the intensity of magnetization of the specimens were made magnetometrically, the magnetometer being set in the "broadside-on" position with respect to the solenoid. The magnetometer consisted of a small bar magnet



of approximate dimensions  $1 \times 0.1 \times 0.1$  cm. and a small concave mirror waxed to a damping vane of mica supported by a single phosphor bronze strip ( $21.5 \times 0.012 \times 0.0012$  cm.) soldered at its upper end to a tensioning spring and at the lower end to a torsion head. The usual coils to neutralize the magnetic field produced by the solenoid alone at the magnetometer needle and to calibrate the instrument were incorporated in the apparatus. In addition, the sensitivity of the magnetometer could be decreased by a large factor by passing a current through another subsidiary coil which augmented the horizontal component of the earth's magnetic field at the magnetometer needle. This coil was only energized when large variations of the intensity of magnetization were produced, e.g. when the specimen was being brought into a cyclic condition; the actual measurements were made with no current flowing in this coil. It was checked that under normal working conditions the deflection of the magnetometer needle was a linear function of the deflecting field. The change in magnetometer deflection was 1.00 cm. when the deflecting field changed by 0.00107 oersted and this field change was produced by a variation of 3.45 gauss in the intensity of magnetization of the specimen.

Temperature measurements during the magnetic experiments were made by a calibrated thermocouple having one junction attached to the mid-point of the specimen. It was shown by means of this thermocouple that the temperature of the specimens could be maintained almost indefinitely at any constant temperature between  $15^\circ\text{C.}$  and  $250^\circ\text{C.}$  to within about  $2^\circ\text{C.}$ ; with solid carbon dioxide in the Dewar vessel the temperature was  $-78 \pm 1^\circ\text{C.}$  for approximately 40 minutes, and when liquid air was used the temperature was maintained at  $-187 \pm 1^\circ\text{C.}$  for 30 minutes.

When measurements of magnetic viscosity were made at a point on the hysteresis cycle of a specimen corresponding to a final steady applied field  $H$  the following procedure was adopted. The specimen was brought into a cyclic state and then the whole apparatus was allowed to reach thermal equilibrium with an applied field  $H$ . If observations were to be made with  $H$  not equal to the coercive field,  $H_c$ , i.e. the intensity of magnetization of the specimen was not zero, then the deflection of the magnetometer was made equal to zero by passing the appropriate current through the calibration coil of the instrument. The specimen was taken through an almost complete hysteresis cycle so that the applied field now was less than the original value,  $H$ , by an amount  $\Delta H$ . After an interval of time the field was suddenly increased by  $\Delta H$  and observations were made of the magnetometer deflection, and hence the change of intensity of magnetization of the specimen, as a function of the time which had elapsed since the sudden increase in applied field. During the measurements the solenoid current varied by not more than  $\frac{1}{4}\%$  and no changes in the calibrating coil current, when used, could be detected.

## §5. RESULTS

A typical set of measurements is shown in Figure 1 in which  $\Delta I$  is plotted directly against  $t$ ; these measurements were made with the alnico rod maintained at room temperature and the final value of the applied field was approximately the coercive field. This figure also includes two curves which have been calculated from equations (7) and (12) respectively and fitted, as far as possible, to the experimental points. Over the time range involved it is obvious that equation (7) gives the better fit. Also the experimental results appear to lie below

the curve of equation (7) at larger values of  $t$  and thus some degree of support for the modified equation (11) is forthcoming. The usual way of presenting these results was in the form of curves of  $(\Delta I, \log t)$  and examples of these are shown in Figure 3; the slopes of such lines will be denoted by  $S$ .

Before it was possible to investigate the variation of  $S$  as a function of the absolute temperature of the specimen it was necessary to determine how  $S$  was affected by variation of the experimental conditions. This preliminary work was carried out at a constant temperature of  $15^\circ \text{C.}$ , and the final magnetic field after the discontinuous change was always the coercive field.  $S$  was found to be independent (i) of the magnitude of the discontinuous field change provided that this was greater than 10 oersteds, and (ii) of the time the specimen was maintained under a steady applied field immediately before the measurements

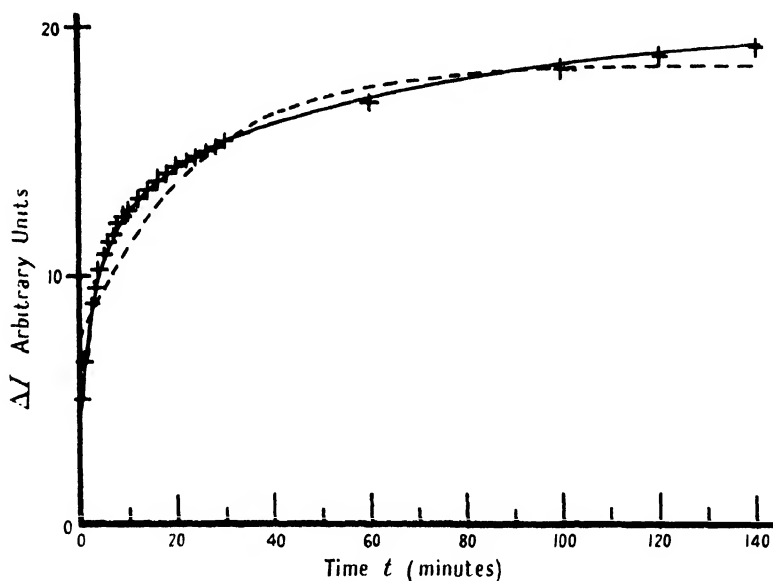


Figure 1. Variation of magnetization as a function of the time after a sudden increase in the applied magnetic field.

- Theoretical curve calculated from  $\Delta I = S \log t + \text{const.}$
- - - Theoretical curve calculated from  $\Delta I = I_0 + I' \{1 - \exp(-t/\tau)\}$ .
- + + + Experimental points for untreated alnico specimen at  $15^\circ \text{C.}$  with coercive field applied.

Note. The zero of the ordinate scale is arbitrary.

were begun if this time was greater than 2 minutes. The behaviour observed in (i) is similar to that of Heaps (1938); result (ii) may be compared with the analysis of Ewing's results for a soft iron specimen (1889), for if these are plotted as  $\Delta I$  against  $\log t$  they show that the  $S$  value found when the waiting period was 3 minutes is greater than its value for a waiting period of 60 minutes. Actually, Ewing's work was confined to the examination of magnetic viscosity over the virgin curve of magnetization of the specimen.

The magnitude of  $S$  was found to be a function of the intensity of magnetization of the specimen at which the observations were made and, as far as the hysteresis cycle was concerned, no appreciable changes of the magnetization were observed in steady applied fields except near the coercive field point. The variation of  $S$  as function of the magnetization  $I$  and the final steady field  $H$  is shown in

Figures 2(a) and (b) respectively. (In these measurements the discontinuous changes in applied magnetic field were of such a magnitude that the intensity of magnetization changed by approximately 200 gauss in each case, and the waiting period, described in the previous paragraph, was about 5 minutes.) The slope of the hysteresis loop  $dI/dH$  is also plotted on these figures as a function of  $I$  and  $H$ , and it will be seen that the maximum value of  $S$  occurred when  $dI/dH$  had the greatest value. In similar measurements carried out over the virgin curve of magnetization a smaller maximum value of  $S$  was observed and again this maximum value was found in the region of maximum  $dI/dH$ .

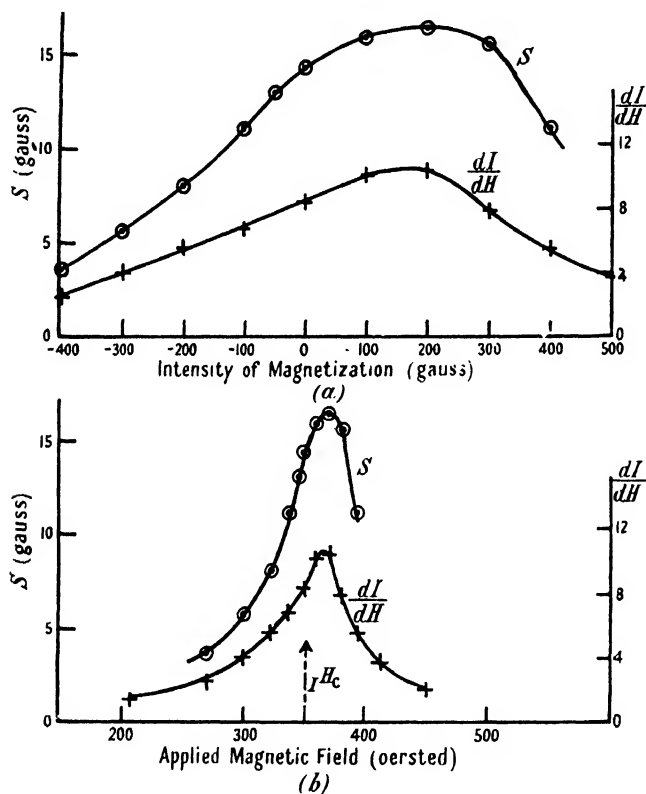


Figure 2. Variation of  $S$  and  $dI/dH$  as a function of both the intensity of magnetization and the applied magnetic field intensity.

The experiments to determine the temperature dependence of  $S$  were simplified by having the final applied field equal to the coercive field; the discontinuous change in intensity was approximately 200 gauss after a waiting period of 5 minutes. The results obtained at different temperatures between  $-187^{\circ}\text{C}$ . and  $250^{\circ}\text{C}$ . are plotted in Figure 3 in the form of curves of  $(\Delta I, \log t)$  and Figure 4 is a plot of  $S$  as a function of the absolute temperature  $T$ . The straight line of Figure 4 shows that  $S$  was a linear function of the absolute temperature and this indicates that  $\dot{\mu}$  (equation (7)) was independent of temperature and had a value of  $3.6 \times 10^{14}$  gauss per erg.

In addition to the magnetometer method described above, other ways of demonstrating magnetic viscosity in these alnico specimens have been used and one will now be described briefly.

(i) The amplitude of magnetostrictive oscillations set up in a ferromagnetic specimen is critically dependent on the magnetization near the coercive field. Any changes in magnetization due to magnetic viscosity may thus be detected by variation of the amplitude of the oscillation and this phenomenon has already been described (Street and Woolley 1948).

(ii) The specimen was placed inside a search coil of 8,000 turns wound in the form of a solenoid. This search coil was connected to a sensitive galvanometer after a discontinuous change in the field applied to the specimen had taken place, when the rate of change of magnetization due to magnetic viscosity induced in the search coil an E.M.F. which gave a detectable galvanometer deflection. The experimental results showed that the galvanometer current was inversely proportional to the time  $t$  after the change in field, over the time period during which measurable deflections were obtained, about 300 seconds. Simple

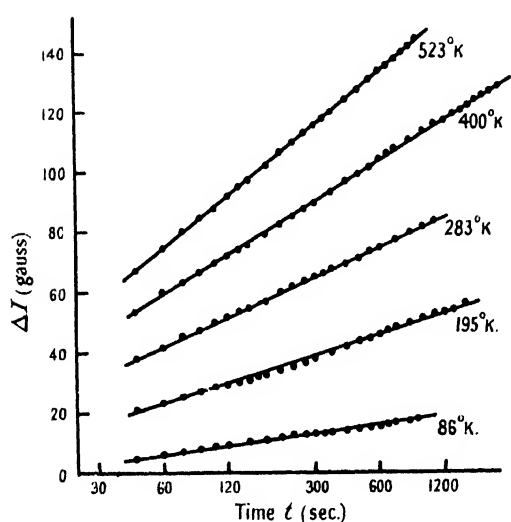


Figure 3. Variation of magnetization as a logarithmic function of time  $t$  after a sudden increase in applied magnetic field. The temperatures at which the experiments were made are indicated on the curves.

Note: The zero of the scale of ordinates is arbitrary and the relative positions of the graphs have been chosen for convenience in drawing.

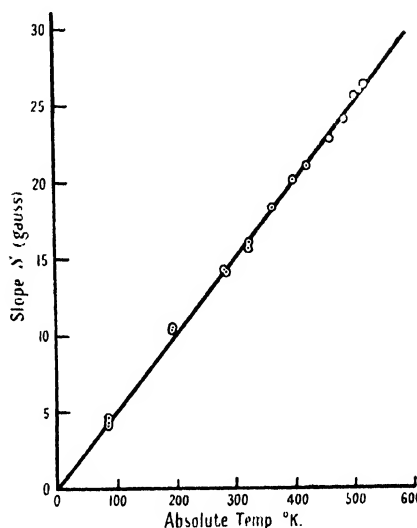


Figure 4. Variation of  $S$ , the slope of  $(\Delta I, \log t)$  curves, as a function of absolute temperature.

analysis of the experimental arrangement showed that this result would be expected if  $\Delta I = S \log t$  as indicated by equation (7). The experiment was carried out at room temperature and the value of  $S$  was found to be 15.1 gauss, which compared satisfactorily with the corresponding value of 14.7 gauss obtained by the magnetometric method.

(iii) If the intensity of magnetization of a specimen lags behind the applied field due to magnetic viscosity then it would be expected that different magnetization curves would be obtained by using first a magnetometer method, during which the magnetization was allowed to approach its steady value, and secondly, a ballistic method. Figures 5(a) and (b) respectively show two sets of magnetization curves obtained by magnetometric and ballistic methods; in the former case measurements of magnetization were made at times up to 30 minutes after

the field change to allow for magnetic viscosity effects. In Figure 5(a) the virgin curve lies almost completely within the hysteresis loop whereas in Figure 5(b) the virgin curve lies significantly above the loop; moreover, the maximum intensity of magnetization is greater in (a) than in (b). The reasons for these differences are that appreciable magnetic viscosity occurs over some regions of the hysteresis cycle and there is a smaller viscosity effect for the virgin curve. The area of the hysteresis loop in (a) is larger than that shown in (b) by about 7%.

(iv) The alnico specimen was mounted in an apparatus for the examination of magnetostriction and it was shown that near the coercive point the magnetostrictive change in the length of the rod, produced by a sudden increase in the applied

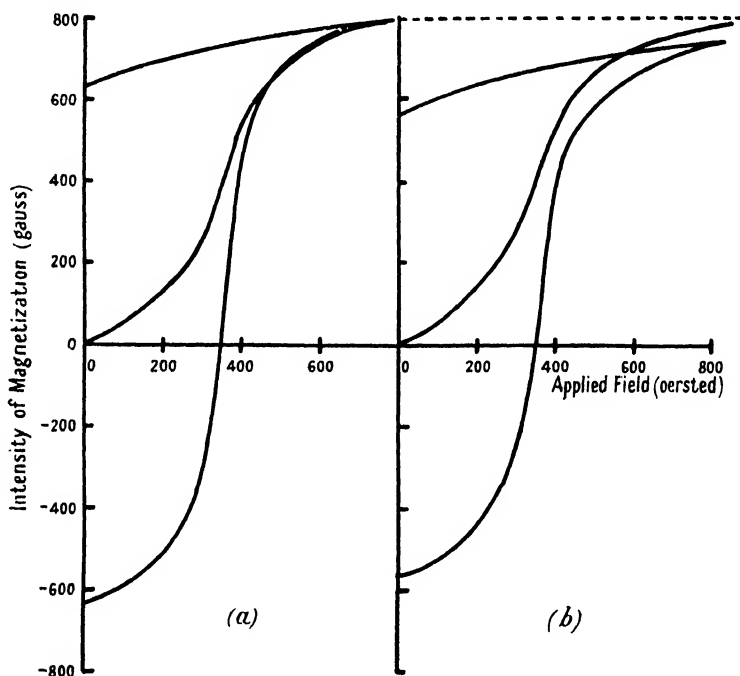


Figure 5. Magnetization curves for alnico.

(a) Obtained magnetometrically.

(b) Obtained ballistically.

field, was not instantaneous but that an appreciable interval of time elapsed before a final value was reached. The coefficient of magnetostriction of the alnico for a maximum field of 850 oersteds was  $+9.0 \times 10^{-6}$  which, with the experimental arrangement adopted, was represented by a scale deflection of 23 mm. Consequently, it was not possible to make accurate measurements of the viscosity effect, but it would appear that such measurements could be made with apparatus of greater sensitivity.

## § 6. DISCUSSION

By assuming that over certain ranges of magnetization the directions of the magnetization vectors of ferromagnetic domains may be influenced by thermal activation, it is possible to formulate a theory of magnetic viscosity which is consistent with experimental observation. The relation between  $\Delta I$  and  $t$  given in equation (7) has been shown to represent the experimental results obtained

with the alnico specimens used here, and it also adequately describes, within limits, other results for soft iron specimens described by Ewing (1889) and by Richter (1937). Certain assumptions have been made in the derivation of equation (7) and the justification of these assumptions must be implicit in any proposed physical mechanism of the phenomenon. Snoek (1939) has already shown that magnetic viscosity cannot be detected in extremely pure soft iron, but as little as 0.01% of carbon and nitrogen impurity does produce pronounced magnetic viscosity. If, as analysis of the results appears to indicate, the activation energy hypothesis given above applies in the case of soft iron, the metastable states involved must be associated with the presence of small amounts of carbon etc. In Snoek's hypothesis it is assumed that magnetic viscosity is due to the diffusion of the impurity atoms into the Bloch zones or boundaries between domains. In view of the description of diffusion in solids given by Glasstone *et al.* (1941), it seems probable that such diffusion of impurity atoms is an activation energy process. A similar diffusion mechanism might account for magnetic viscosity in the alnico specimens. However, Richter's measurements seem to indicate that the variation of  $S$  (the slope of the  $(\Delta I, \log t)$  curve) with temperature in the case of soft iron is essentially different from that shown in Figure 4. In the latter case  $S$  is a linear function of absolute temperature whereas for soft iron  $S$  appears to be substantially independent of temperature. This indicates that Snoek's explanation may not be appropriate in the case of alnico and that here a different mechanism may be involved. Such a mechanism is suggested by the theoretical treatment of heterogeneous alloys given by Stoner and Wohlfarth (1948).

In their theory it is suggested that in high coercivity alloys there are particles, the dimensions of which are smaller than the critical values necessary for the formation of ferromagnetic domain boundaries; these particles are embedded in a less ferromagnetic matrix. Magnetization processes, as far as these single domains are concerned, are therefore confined entirely to rotation of the magnetization vectors, and it has been shown that over certain regions of the hysteresis loop the directions of the domain vectors suffer discontinuous changes. In the theoretical case considered by Stoner which is most nearly appropriate to the present problem of a polycrystalline alnico specimen, these discontinuous changes of orientation occur over a range of the hysteresis loop near the coercive force point. The free energy of a domain has a minimum value both before and after a discontinuous change of orientation, and transition from the initial to the final state may only occur if sufficient energy to overcome the intervening potential barrier is supplied. This transition may therefore be achieved either by an increase in the applied magnetic field or by a change in the strain energy of the domain, and thus stress fluctuation due to thermal agitation may provide the activation energy required. Thus Stoner's analysis accounts naturally for the potential barriers which may be overcome by thermal activation energy. In addition, for any single domain, only one discontinuous change in orientation is possible on the descending branch of the magnetization curve, i.e. a discontinuous change in orientation does not produce domain states which may undergo further activation; this is an assumption which was made in the derivation of equation (7). Evidence for the similarity between the effects of applied magnetic field and stress due to thermal agitation is given in Figure 2(a) of  $(S, I)$  and  $(dI/dH, I)$ . Within the limits of experimental error the maxima of the curves occur at the same value of  $I$ .

The variation of  $S$  as a function of absolute temperature (Figure 4) shows that under the conditions described (i.e. measurements at the coercive force point in the temperature range from  $86^{\circ}\text{K.}$  to  $523^{\circ}\text{K.}$ ) the product  $ip$  is independent of temperature. This result might be expected from Stoner's theory of single domains for, at temperatures well below the Curie point (i.e. where the specific saturation intensity of the domains is constant) the theory does not involve temperature. Also at these temperatures there is no possibility of large scale migration of atoms, and thus the size of the ferromagnetic particles is independent of temperature.

Hence the theory of Stoner and Wohlfarth appears to justify the assumptions made in the analysis given in §2 above. Since the experimental results are in good agreement with this analysis, the work described here provides some experimental evidence for the validity of the single domain concept.

#### ACKNOWLEDGMENTS

The authors wish to record their indebtedness to Professor L. F. Bates for his interest and encouragement during this work and to Mr. E. W. Lee for making the measurements of magnetostriction. Their thanks are also due to Dr. K. Hoselitz for providing the alnico specimens used in the investigation.

#### REFERENCES

- BECKER, R., and DÖRING, W., 1939, *Ferromagnetismus* (Berlin : Springer).  
 EWING, J. A., 1889, *Proc. Roy. Soc. A*, **46**, 269.  
 GLASSTONE, S., LAIDLIER, K. J., and EYRING, H., 1941, *Theory of Rate Processes* (New York : McGraw-Hill).  
 HEAPS, C. W., 1938, *Phys. Rev.*, **54**, 288.  
 JAHNKE, E., and EMDE, F., 1938, *Funktionentafeln*, 3rd Edition (Berlin).  
 RICHTER, G., 1937, *Ann. Phys., Lpz.*, **29**, 605.  
 SMITH, C. L., 1948, *Proc. Phys. Soc.*, **61**, 201.  
 SNOEK, J. L., 1938, *Physica*, **5**, 663 ; 1939, *Ibid.*, **6**, 161.  
 STONER, E. C., and WOHLFARTH, E. P., 1948, *Phil. Trans. Roy. Soc.*, **240**, 599.  
 STREET, R. and WOOLLEY, J. C., 1948, *Proc. Phys. Soc.*, **61**, 391 ; 1949, *Proc. Phys. Soc. B*, **62**, 141.

# The Decay of $^{170}\text{Tm}$ and $^{186}\text{Re}$

By P. J. GRANT AND R. RICHMOND

Cavendish Laboratory, Cambridge

*Communicated by E. S. Shire; MS. received 14th March 1949*

**ABSTRACT.** The radiations from the active isotopes  $^{170}\text{Tm}$  and  $^{186}\text{Re}$  have been investigated.  $^{170}\text{Tm}$  is found to have a  $\beta$ -ray end-point of  $1.00 \pm 0.005$  mev. with possible lower-energy groups at  $0.90 \pm 0.015$ ,  $0.79 \pm 0.025$ ,  $0.45 \pm 0.05$  mev.  $\gamma$ -rays with energies  $82.6 \pm 0.5$ ,  $205 \pm 10$ ,  $430 \pm 20$  kev. were observed. The 430 kev. radiation is thought to be complex.  $^{186}\text{Re}$  is found to have a  $\beta$ -ray end-point of  $1.090 \pm 0.005$  mev. with other groups at  $0.95 \pm 0.015$  and  $0.64 \pm 0.03$  mev. Three  $\gamma$ -rays were observed, having energies  $700 \pm 50$ ,  $275 \pm 8$  and  $133 \pm 1$  kev. The last is assumed to be a mean energy-value of the three low-energy  $\gamma$ -rays found by Cork, Shreffler and Fowler. Decay schemes are suggested for both isotopes.

## § 1 INTRODUCTION

As a result of measurements made with a short magnetic lens  $\beta$ -ray spectrometer and by the use of absorption and coincidence techniques we have been able to suggest decay schemes for the radioactive isotope of thulium,  $^{170}\text{Tm}$ , and the longer-lived active isotope of rhenium,  $^{186}\text{Re}$ . The active samples were prepared in the low-energy pile at the Atomic Energy Research Establishment, Harwell, by slow neutron irradiation of thulium oxide ( $\text{Tm}_2\text{O}_3$ ) for periods of one month and of metallic rhenium for periods of one week.

## § 2. $^{170}\text{Tm}$

This isotope decays by  $\beta$ -emission to the ytterbium isotope  $^{170}\text{Yb}$  with a half-life of approximately 127 days. It has previously been investigated by Bothe (1946), who obtained a value of 1 mev. for the upper limit of the  $\beta$ -ray energy by absorption in aluminium and who stated that no  $\gamma$ -rays were emitted.

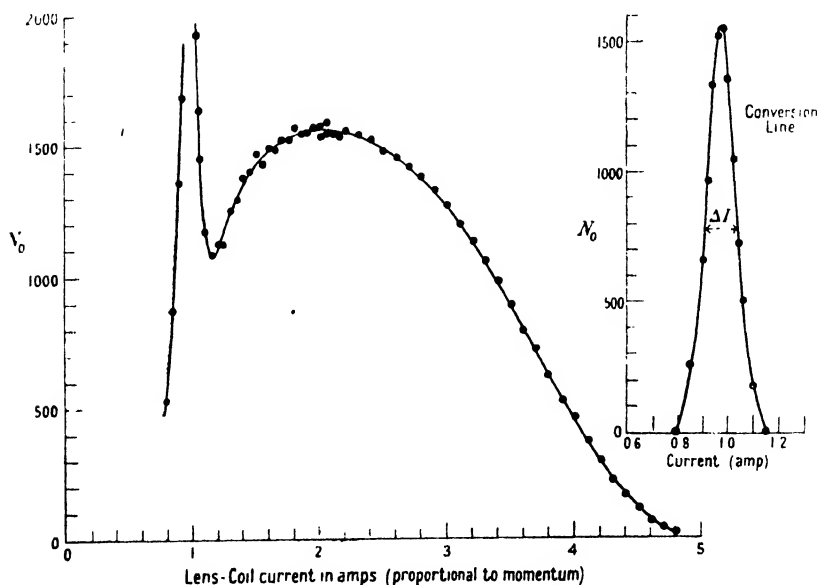


Figure 1.  $^{170}\text{Tm}$   $\beta$ -spectrum (counting rate normalized for equal momentum intervals).

Figure 1 shows a typical  $\beta$ -spectrum obtained with the spectrometer. A strong conversion line is apparent, corresponding to an electron energy of



$72.1 \pm 0.5$  kev. The resolving power of the spectrometer is low.  $\Delta I/I$  at half maximum on the conversion line is about 8%. Figure 2 is a curve showing the absorption of the  $\gamma$ -radiation in lead. It may be resolved to give  $\gamma$ -rays of energies  $430 \pm 20$  kev. and  $205 \pm 10$  kev., and an additional softer radiation whose energy lies below that of the K absorption edge of lead. Absorption measurements using brass absorbers (Figure 3) gave a value of  $83 \pm 2$  kev. for the energy of this  $\gamma$ -ray. There seems little doubt that the conversion line (Figure 1) corresponds to this energy transition, and is due to the conversion in the L electron shell of ytterbium of a  $\gamma$ -ray of energy  $82.6 \pm 0.5$  kev.

Figure 4 shows a Kurie plot of the continuous  $\beta$ -spectrum and gives a value for the upper limit of the  $\beta$ -ray energy of  $1.00 \pm 0.005$  mev. The shape of the Kurie plot indicates that the  $\beta$ -spectrum is complex and, as shown in Figure 4,

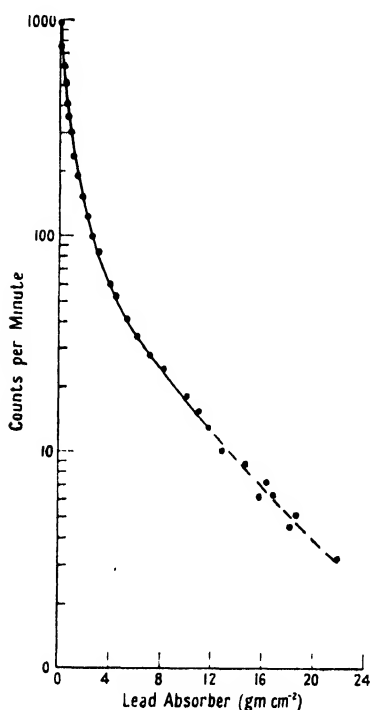


Figure 2.  $^{170}\text{Tm}$  absorption of  $\gamma$ -radiation in lead.

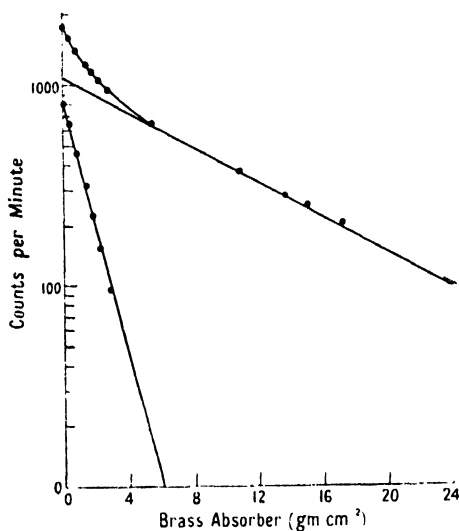


Figure 3.  $^{170}\text{Tm}$  absorption of  $\gamma$ -radiation in brass.

it is possible to resolve it into four components giving additional  $\beta$ -spectra with end-points  $0.90 \pm 0.015$  mev.,  $0.79 \pm 0.025$  mev.,  $0.45 \pm 0.05$  mev. This procedure is, in general, untrustworthy, but in the present instance it seems justified since these energy values are consistent with the values obtained for the  $\gamma$ -ray energies. If correct, these  $\beta$ -ray energies show the possible existence of  $\gamma$ -rays of approximate energies 120, 350, 450 and 550 kev. in addition to the 82.6 and 205 kev.  $\gamma$ -rays. The first of these has not been found and, owing to the low intensity of the  $\gamma$ -radiation from the available sources, that part of the absorption curve corresponding to the three harder  $\gamma$ -rays could not be obtained with sufficient accuracy to determine whether the 430 kev.  $\gamma$ -ray was, in fact, complex.

From direct examination of the  $\beta$ -spectrum the number of L-conversion electrons was estimated as  $4.2 \pm 0.7\%$  of the total disintegrations. When an

approximate correction is made for absorption in the window of the Geiger counter the value  $5.6 \pm 1\%$  is obtained. An estimate of this quantity was also made by observation of coincidences between  $\beta$ -rays and conversion electrons, the value obtained being  $6.1 \pm 0.5\%$ . The two results are therefore in satisfactory agreement. An estimate of the number of K-conversion electrons was made by determining the K x-ray intensity, using an x-ray counter calibrated by means of a samarium source ( $^{153}\text{Sm}$ ), where the ratio of x-ray intensity to  $\beta$ -particle

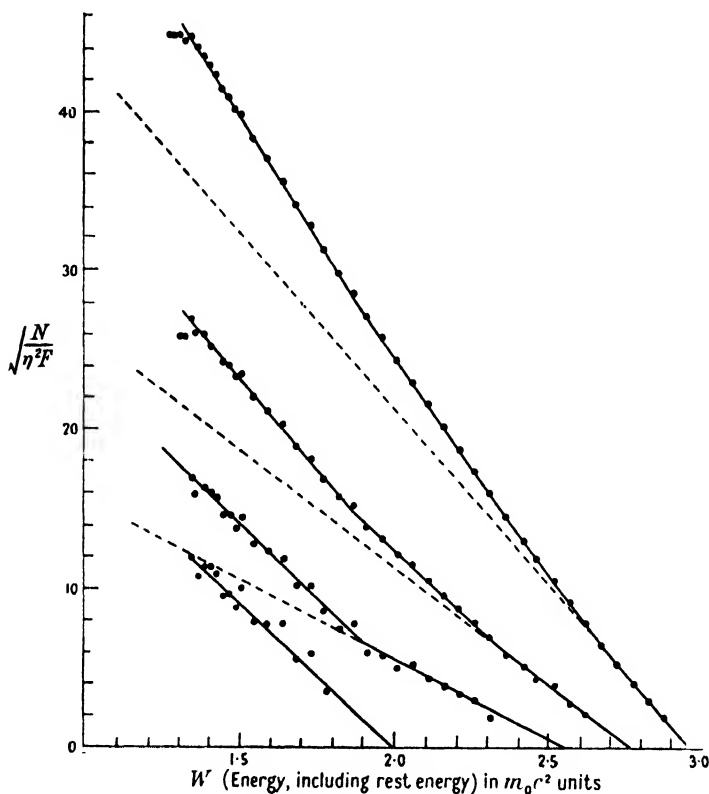


Figure 4.  $^{170}\text{Tm}$  Kurie plot of continuous  $\beta$ -spectrum showing resolution into four possible components.

intensity is known (Hill and Shepherd, private communication). This gave the number of K-conversion electrons as  $5 \pm 1\%$  of the total disintegrations.

By the use of  $\beta$ - and  $\gamma$ -counters of known efficiency (Dunworth 1940), and by comparison of the  $\beta$ - and  $\gamma$ -counting rates given by the Tm source with those obtained using a  $\text{ThC}''$  source, the following values were obtained for the intensities of the  $\gamma$ -rays. In each case the intensity is expressed as a percentage of the total number of disintegrations.

$\gamma$ -ray (kev.)	82.6	205	430
Intensity (%)	$25 \pm 5$	$3.4 \pm 0.3$	$0.6 \pm 0.1$

(The figure for the 82.6 kev.  $\gamma$ -ray includes the percentage of conversion electrons.) These values are satisfactorily confirmed by estimates of the intensities of the partial  $\beta$ -spectra obtained by the Kurie plot analysis. This is further evidence that the analysis is justified.

The proposed decay scheme is shown in Figure 5. As stated above, it was not possible to carry out a further resolution of the hard component of the  $\gamma$ -radiation. However, by absorption of  $\gamma$ - $\gamma$  coincidences it has been shown that the 82.6 kev. and 205 kev.  $\gamma$ -rays are not in coincidence but that each is in coincidence with a harder  $\gamma$ -radiation. The possible harder  $\gamma$ -rays are therefore included in the scheme.

By comparison of the ratios of the numbers of K- and L-conversion electrons,  $N_K/N_L$ , and of L-conversion electrons and  $\gamma$ -quanta,  $N_L/N_Q$ , with the values calculated by Hebb and Nelson (1940) it seems likely that the 82.6 kev. transition may be assigned to electric quadrupole radiation. It might, however, be magnetic dipole radiation. The following table shows the experimental values, the calculated values for electric multipole radiation with  $l=1, 2, 3$ , and also the calculated values for magnetic dipole radiation.

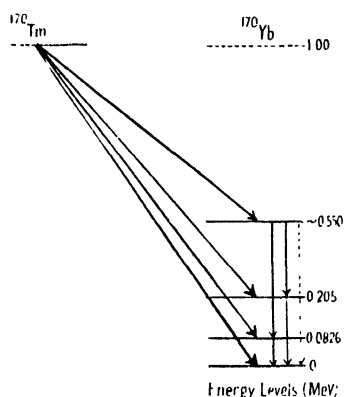


Figure 5. Suggested decay scheme for  $^{170}\text{Tm}$ .

	Electric			Magnetic	Observed
$l$	1	2	3	1	
$N_K/N_L$	9	1.0	0.2	2.5	$0.9 \pm 0.25$
$N_L/N_Q$	0.025	2.1	70	0.22	$0.40 \pm 0.15$

Since  $^{170}\text{Yb}$  is a stable even-even nucleus, the spin of its ground state is zero. Therefore it is presumed that the 82.6 kev. level has a spin of 2.

### § 3. $^{186}\text{Re}$

This isotope has been investigated by Goodman and Pool (1947) and, more recently, by Cork, Shreffler and Fowler (1948). Previously it was reported that no  $\gamma$ -rays were emitted in the disintegration, but this has been disproved by our results and by those of Cork *et al.* Using a  $180^\circ$ -type spectrometer in conjunction with a photographic plate, they observed conversion-electron lines from two, and possibly three, low-energy  $\gamma$ -rays. They also showed the presence of a harder  $\gamma$ -radiation by absorption measurements.

Slow neutron irradiation of rhenium gives rise to two activities. The shorter, which has a half-life of approximately 18 hours, has been assigned to  $^{188}\text{Re}$ . This activity was allowed to decay before measurements were taken. The  $^{186}\text{Re}$  activity was found to decay with a half-life of 91 hours, in good agreement with the results of Cork.

Figure 6 shows a typical  $\beta$ -spectrum with two groups of conversion electrons, one strong and one very weak. Measurements of the absorption in lead of the  $\gamma$ -radiation, Figure 7, demonstrate the presence of three components of energies :

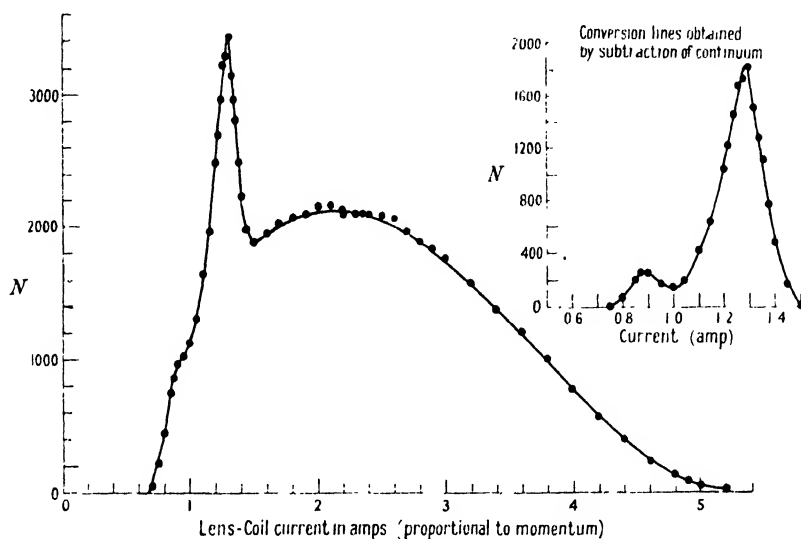


Figure 6.  $^{186}\text{Re}$   $\beta$ -spectrum (counting rate normalized for equal momentum intervals).

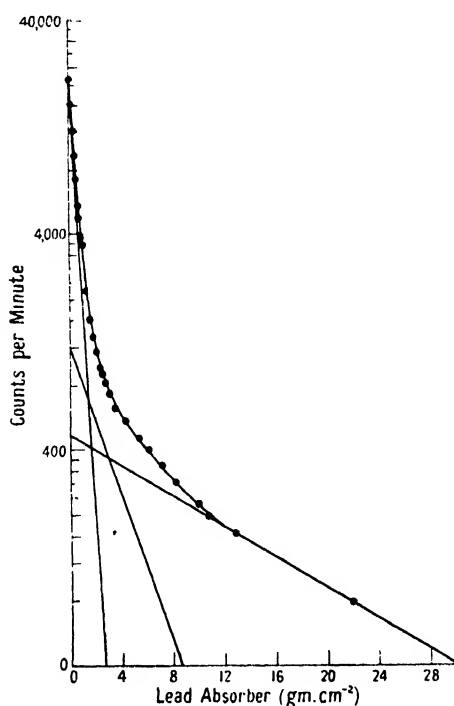


Figure. 7  $^{186}\text{Re}$  absorption of  $\gamma$ -radiation in lead.

$700 \pm 50$  kev.,  $275 \pm 8$  kev.,  $131 \pm 2$  kev. The presence of the 275 kev.  $\gamma$ -ray was confirmed by spectrometer measurements of the energies of Compton electrons ejected from a  $160 \text{ gm.cm}^{-2}$  lead radiator.

A Kurie plot of the continuous  $\beta$ -spectrum is shown in Figure 8. It is possible to resolve this into three partial spectra and to estimate their energies and intensities as follows :

Energy (mev.)	$1.090 \pm 0.005$	$0.95 \pm 0.015$	$0.64 \pm 0.03$
Intensity (%)	$67 \pm 1$	$30 \pm 3$	$3 \pm 4$

The low energy  $\beta$ -transition corresponding to the 700 kev.  $\gamma$ -ray was not observed owing to the low intensity.

The conversion electron groups were at first assigned to the conversions in the K- and L-shells of osmium of a  $\gamma$ -ray of energy  $133 \pm 1$  kev. However, Cork, Shreffler and Fowler have since shown, by observation of K-, L- and M-conversion.

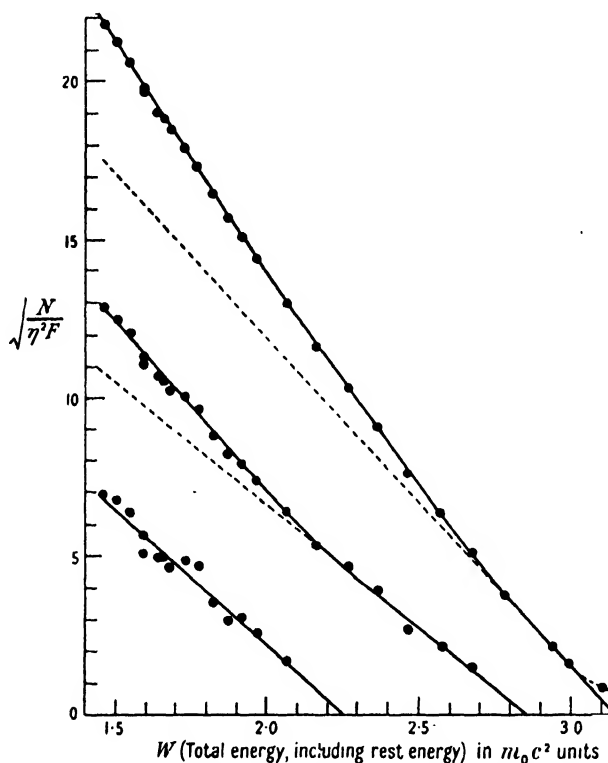


Figure 8.  $^{186}\text{Re}$  Kurie plot of  $\beta$ -spectrum showing resolution into three components.

groups, that there exist  $\gamma$ -rays having energies 122.7, 135.8 and, possibly, 137.5 kev. The resolving power of our spectrometer was not sufficiently high to permit the resolution of these conversion groups, nor, of course, was it possible by absorption measurements to resolve the corresponding  $\gamma$ -rays.

By inspection of the  $\beta$ -spectrum plot, the number of L-conversion electrons was estimated to be  $6.5 \pm 1\%$  of the total number of disintegrations. This is in agreement with the figure of  $5.0 \pm 0.5\%$  obtained by coincidence experiments.

Experiments with calibrated counters gave the  $\gamma$ -ray intensities as

$\gamma$ -ray (kev.)	133	275	700
Intensity (%)	$37 \pm 6$	$2.3 \pm 0.2$	$0.7 \pm 0.1$

(The figure for the 133 kev. transition includes the percentage of conversion electrons.)

## § 4. DECAY SCHEME

Any decay scheme has to satisfy several conditions which are to some extent conflicting :

1. The relative intensities of the 122.7, 135.8 and 137.5 kev.  $\gamma$ -rays found by Cork must be such as to give a mean value for the energy which is consistent with our estimate.
2. Cork does not list the 137.5 kev.  $\gamma$ -ray as definite, but only "possible". This implies that, if it exists, it must be of very low intensity, very little converted, or both.
3. Any scheme must give values for the  $\beta$ -ray branching ratios which are not widely different from the values obtained by the Kurie plot analysis. In addition, the scheme must, of course, agree with all the energy values obtained.

The first possibility (Figure 9(a)) leads to the following conclusions :

- (a) Total intensity of 122.7 kev. transition  $\simeq 7\%$  of the total disintegrations.
- (b) Total intensity of 135.8 kev. transition  $\simeq 25\%$  of the total disintegrations.

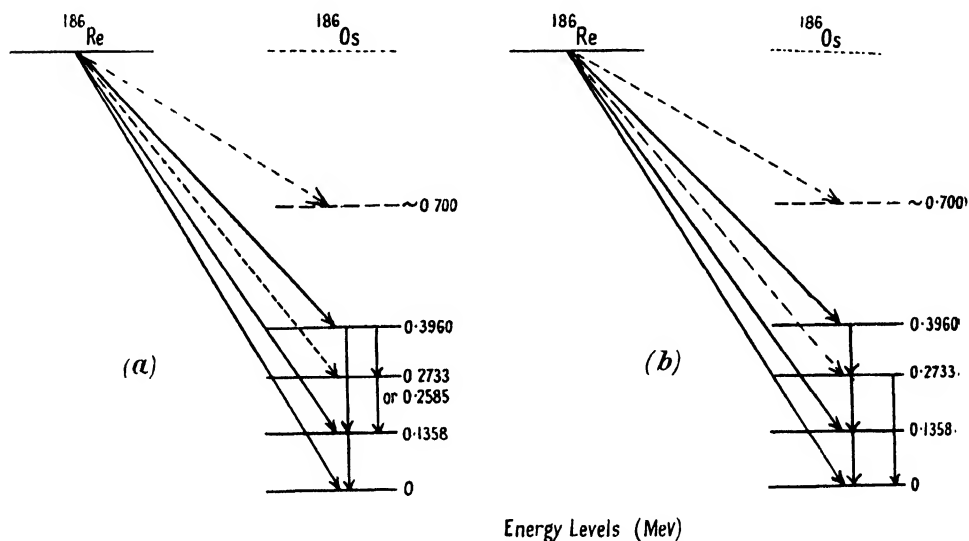


Figure 9. Possible decay schemes for  $^{186}\text{Re}$ .

The  $\beta$ -ray branching ratios are thus 9% : 16% : 75%, which are to be compared with the experimental values of 3% : 30% : 67%. In addition, the scheme gives a value of 260 kev. for the  $\gamma$ -ray energy measured as  $275 \pm 8$  kev. This seems unlikely, though possible.

The second scheme (Figure 9(b)), although not leading to perfect agreement, fits the facts more satisfactorily than the first. Calculations carried out as above lead to the results :

- (a) Total intensity of 122.7 kev. transition 6.5% of total disintegrations.
- (b) Total intensity of 135.8 kev. transition 28.5% of total disintegrations.
- (c) Total intensity of 137.5 kev. transition 4% of total disintegrations.

We therefore obtain  $\beta$ -ray branching ratios of 6.5% : 24.5% : 69%. These are in considerably better agreement with the experimental values. Furthermore, the value given by the scheme for the  $\gamma$ -ray energy measured as  $275 \pm 8$  kev. is now 273.3 kev.

It seems impossible by coincidence measurements to decide between these two schemes. The only deciding factor would be an accurate determination of the energy of the 275 kev.  $\gamma$ -ray. On the general grounds stated above it appears likely that Figure 9(b) gives the true representation of the decay scheme.

## REFERENCES

- BOTHE, W., 1946, *Z. Naturforsch.*, **1**, 173.  
 CORK, J. M., SHREFFLER, R. G., and FOWLER, C. M., 1948, *Phys. Rev.*, **74**, 1657.  
 DUNWORTH, J. V., 1940, *Rev. Sci. Instrum.*, **11**, 167.  
 GOODMAN, L. J., and POOL, M. L., 1947, *Phys. Rev.*, **71**, 288.  
 HEBB, M. H. and NELSON, E., 1940, *Phys. Rev.*, **58**, 486.

A Note on the  $^{10}\text{B}(n, \alpha)^7\text{Li}$  Reaction

By S. DEVONS

Cavendish Laboratory, Cambridge

*Communicated by O. R. Frisch; MS. received 16th May 1949*

**ABSTRACT.** It is difficult to explain the observed preponderance of transitions to the excited state of  $^7\text{Li}$  in the reaction  $^{10}\text{B}(n, \alpha)^7\text{Li}$  in terms of the usual assumption that the ground state and first excited state of  $^7\text{Li}$  form a  $^2\text{P}_{3/2, 1/2}$  doublet. In addition the doublet separation (0.48 mev.) would be much larger than expected theoretically. If the excited state of  $^7\text{Li}$  has total angular momentum other than 1.2, one would expect to find, in general, some angular correlation between the direction of emission of the  $\alpha$ -particle, that of the subsequent  $\gamma$ -radiation and the polarization of the radiation. The correlations to be expected have been calculated on the assumption that the ground state of  $^7\text{Li}$  is (3/2, odd), that of  $^{10}\text{B}$  (3, odd), or (3, even), and that the compound nucleus  $^{11}\text{B}$  has definite  $J = 5/2$  or  $7/2$ . Results are given for excited states of  $^7\text{Li}$  with total angular momentum 1/2, 3/2, 5/2 and 7/2 and both even and odd parities.

## § 1.

It is well established that in the disintegration of  $^{10}\text{B}$  by slow neutrons two alpha-particle groups are emitted corresponding to the production of  $^7\text{Li}$  in the ground state and in an excited state of energy between 0.45 and 0.50 mev., the lower energy group being at least ten times as intense as the other (Bøggild 1945, Gilbert 1948). An excited level of  $^7\text{Li}$  of about the same energy has been observed in numerous reactions in which the  $^7\text{Li}$  nucleus is the end product and it seems likely that the same level with an energy of  $0.479 \pm 0.002$  mev. according to the best measurements is involved in all cases\*. On the assumption that there is in fact a single level of  $^7\text{Li}$  in the region 0.45–0.50 mev., it is tempting to suppose that this level together with the ground state form an “inverted” P doublet,  $^2\text{P}_{3/2}$  (ground state) and  $^2\text{P}_{1/2}$  (0.479 mev. level), as predicted theoretically (Wigner and Feenberg 1941). This interpretation gains support from the recent experimental determination by Elliott and Bell (1948) of the upper limit for the life-time of this excited state of  $^7\text{Li}$  (produced in  $^{10}\text{B}(n, \alpha)$  reaction) as  $2 \times 10^{-13}$  sec., which is consistent with a magnetic dipole transition between the two states in which the transition is attributed to the single odd 2p proton.

\* A complete list of the experimental results (up to 1947) is given by Rosenfeld (1948).

There are, however, serious theoretical difficulties in interpreting the large energy difference of 0.48 mev. as a doublet splitting, and these difficulties have prompted the suggestion by Inglis (1948) that the actual doublet splitting is very much smaller than the observed energy difference between the  $^7\text{Li}$  levels and that the ground state and the excited level each comprise closely spaced doublets, the former  $^2\text{P}_{1/2, 3/2}$  and the latter  $^2\text{F}_{5/2, 7/2}$ . Evidence in favour of such a hypothesis comes from the recent measurements of the spin of  $^{10}\text{B}$  (Gordy, Ring and Burg 1948) as 3 rather than 1 as previously supposed. The capture of a slow neutron by  $^{10}\text{B}$  results, then, in a state of  $^{11}\text{B}$  with spin 5/2 or 7/2 (or possibly, but unlikely,

Table 1. Angular Momentum Relations in the Reaction  $^{11}\text{B}(p, \alpha)^7\text{Li}$ .

$^7\text{Li}$ state Spin Parity	Lowest radiation multipole to ground state (3/2, --)	$^{10}\text{B}$ , even parity (--)		$^{10}\text{B}$ , odd parity (-)	
		$^{11}\text{B}^*: 7/2, +$	$^{11}\text{B}^*: 5/2, +$	$^{11}\text{B}^*: 7/2, -$	$^{11}\text{B}^*: 5/2, -$
1/2	+	4	2	3	3
	-	3	3	4	2
3/2	+	2, 4	2, 4	3, 5	1, 3
	-	3, 5	1, 3	2, 4	2, 4
5/2	+	2, 4, 6	0, 2, 4	1, 3, 5	1, 3, 5
	-	1, 3, 5	1, 3, 5	2, 4, 6	0, 2, 4
7/2	+	0, 2, 4, 6	2, 4, 6	1, 3, 5, 7	1, 3, 5
	-	1, 3, 5, 7	1, 3, 5	0, 2, 4, 6	2, 4, 6

The last four columns give the orbital angular momenta possible in the break up of the compound  $^{11}\text{B}$  nucleus, to leave  $^7\text{Li}$  in the state specified in the first two columns. The smallest angular momentum, shown in heavy type, has been used in the calculations. The fourth line (3/2, -) gives the values for the transition to the ground state of  $^7\text{Li}$ .

a mixture of states with appreciable components of each type), and the dissociation of the compound nucleus  $^{11}\text{B}$  into  $^7\text{Li}$  and an alpha-particle may take place to the F levels of  $^7\text{Li}$  with smaller angular momentum for the alpha-particle than would be possible for transitions to the P levels. One could, in this way, interpret the observed preponderance of alpha-particles of lower energy, i.e. transitions to the excited state(s), since the energy available in the dissociation of  $^{11}\text{B}$  is only 3.2 mev. and one would expect the probability of dissociation to be quite sensitive to the magnitude of the angular momentum with which the alpha-particle is ejected. Table 1 shows the *lowest* angular momentum with which

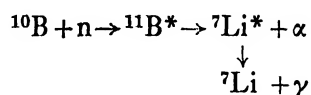


the alpha-particle can be ejected, as determined by the conservation laws of total angular momentum and parity, for different assumed properties of the levels of  ${}^7\text{Li}$  and for  ${}^{10}\text{B}$  having either even or odd parity. (Theoretically even parity is more likely (Wigner and Feenberg 1941).) It should be noticed that in a particular case, if the state of  ${}^{11}\text{B}$  is assumed to have definite  $J$ , the possible angular momenta of the components differ by two units so that the assumption that the lowest angular momentum component predominates should be fairly reliable with alpha-particles of such low energy.

The main objections to the assumption of close doublets for both levels is that, although estimates of the level position as derived from observation of different nuclear processes do range from 0.425 to 0.50 Mev.\*, there is no indication of fine-structure of the levels in any single experiment. In particular, the high resolution available in the measurements of the gamma-radiation (of the order 1% in the experiments of Elliott and Bell (1948) and of Siegbahn (1946)) should be ample to reveal the smallest doublet splitting to be expected on theoretical grounds (of the order 0.01 Mev. for axial-dipole coupling and 0.1 Mev. for "Thomas" precession (Rosenfeld 1948)). It might be argued that transitions from or to *both* members of a doublet are unlikely in one particular mode of exciting the levels. Such an argument could be used, for example, if the excited state of  ${}^7\text{Li}$  produced in a particular process was  ${}^2\text{F}_{7/2}$ , which could then radiate to the ground state  ${}^2\text{P}_{3/2}$  by emission of electric quadrupole radiation, but for the transition to the  ${}^2\text{P}_{1/2}$  member of the doublet, the lowest multipole would be magnetic octupole ( $2^3$ ) or electric  $2^4$ -pole, both of which would probably be of negligible intensity in comparison with the competing electric quadrupole. It would still remain difficult to understand why the  ${}^2\text{F}_{5/2}$  state is not excited in some of the reactions, and for this state the two transitions to the  ${}^2\text{P}_{3/2}$  and  ${}^2\text{P}_{1/2}$  states would be mixed electric quadrupole plus magnetic dipole and electric quadrupole, respectively, which two should be of the same order of probability.

## § 2.

Apart then from any specific assumptions about the multiplet structure and precise spectral identification of the levels of  ${}^7\text{Li}$  it is apparent that the assignment of spin 1/2 to the observed level (or levels) of  ${}^7\text{Li}$  at about 480 keV. presents difficulties in relation both to the present limited theory and to the experimental data. One of the consequences of assuming that the spin of  ${}^7\text{Li}$  is *not* 1/2 is that one would expect, in general, some angular correlation between alpha-particle and gamma-quantum in the process:



both in relative intensity and in polarization. The magnitudes of such correlations have been calculated on the basis of the following simplifying approximations:—

(i) It has been assumed that  $J$ , the total angular momentum of the compound  ${}^{11}\text{B}$  nucleus, is a good quantum number. In view of the low density of levels in such a light nucleus it seems reasonable to assume that the effect of a single level of the compound nucleus predominates and that therefore  $J$  is well defined.

\* Recent measurements by Rasmussen, Lauritsen and Lauritsen (1949) indicate the same energy in all cases.

(ii) The spins of both neutrons and  $^{10}\text{B}$  nuclei are assumed to be randomly oriented. This represents the normal experimental conditions.

(iii) In the emission of the alpha-particles from the compound state it is assumed that the angular momentum of these particles is the lowest value consistent with conservation of angular momentum and parity (see Table 1).

(iv) The gamma-radiation is assumed to be of multipolarity not higher than electric quadrupole, in view of the observed upper limit for the life-time. When both magnetic dipole and electric quadrupole transitions between two states can occur, the possibility that the two effects are of comparable amplitude has been considered, and the transition is treated in such cases as a mixed one, with an unknown complex coefficient introduced to represent the relative magnitude and phase of the two components. The possible radiation multipoles that can arise are, as shown in Table 1, electric dipole, electric quadrupole, and mixed electric quadrupole with magnetic dipole. The radiation multipoles shown are all based on the assumption of  $J=3/2$  and odd parity for the ground state of  $^7\text{Li}$ .

(v) All the results are given for a frame of references in which the centre of gravity of the system ( $^7\text{Li} + \alpha$ ) is at rest. Corrections to allow for the motion of the radiating  $^7\text{Li}$  nucleus would, in part, depend on the variation of efficiency with energy of the gamma-detecting apparatus, and have not therefore been included (cf. Devons and Hine 1949).

### § 3.

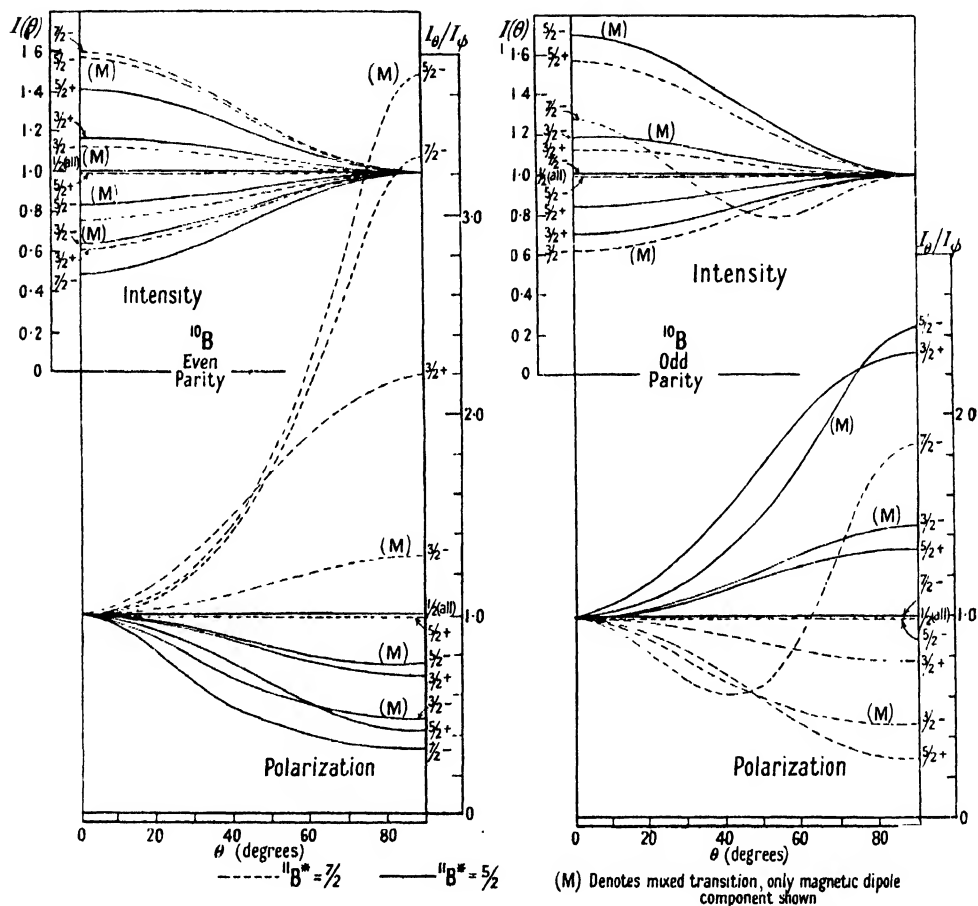
Calculations have been made for the following cases :

- (a) The ground state of  $^{10}\text{B}$  having either even or odd parity.
- (b) The compound  $^{11}\text{B}$  nucleus having  $J = 5/2$  or  $7/2$ .
- (c) States of  $^7\text{Li}$  with spin up to  $7/2$  and odd parity and up to  $5/2$  and even parity. Higher spin values lead to higher multipole transitions than specified in (iv) above.

The results of the calculations are given in Table 2, and illustrated in the accompanying diagram. The intensity of the radiation  $I(\theta)$  is given as a function of the angle between the directions of observation of the emitted gamma-radiation and the preceding alpha-particle.  $\theta = 0$  corresponds to the direction of emission of the latter. The degree of polarization, which is of course a function of the angle  $\theta$ , is expressed as a ratio of the intensity,  $I_\theta$ , of the components polarized (i.e. electric vector) in the plane containing the directions of the observed alpha-particle and gamma-quantum, and the intensity,  $I_\phi$ , in the perpendicular direction. This ratio does not exhaust all the possible information that may be obtained about the polarization, since, in general, the radiation is an incoherent mixture of some linearly and some elliptically polarized components. If however, as is normally the practice (see, e.g., Deutsch and Metzger 1948) the polarization is measured using a device which has no specified axial vector, such as a magnetic field, associated with it, only the ratio  $I_\theta/I_\phi$  will be significant in interpreting the observations.

It is apparent from Table 2 that if the excited state of  $^7\text{Li}$  has spin other than  $1/2$ , then in general the angular correlation of intensity and polarization will be quite marked, and probably of the form  $1 + a \cos^2 \theta$ . The main ambiguity in a detailed theoretical interpretation of an observed angular correlation is due to

the approximate constancy of the correlation functions if one makes the change from even to odd parity of  $^{10}\text{B}$ , together with the change from one of the values  $5/2$  or  $7/2$  for  $^{11}\text{B}$  to the other. It should also be noticed that if the gamma-radiation is observed to be isotropic with respect to the direction of emission of the alpha-particle, this does not provide conclusive evidence for a value  $1/2$  for the spin of the excited state. Whilst the isotropy in other cases is only approximate (due to neglect of higher angular momentum components of the ejected alpha-particle), the departures from isotropy may well be too small to be detected.



$\alpha$ -particle,  $\gamma$ -quantum correlation in the  $^{10}\text{B}$  ( $n, \alpha$ )  $^7\text{Li}^*$  reaction.

*Note added in proof.* Since the paper was written, calculations of a similar nature, though covering a different range of possibilities, have been published by B. T. Feld (*Phys. Rev.*, 1949, **75**, 1618). Feld considers intensity correlation only, and assumes that the alpha-particle is emitted with one unit of orbital angular momentum. Explicit mention is not made of the parity of  $^{10}\text{B}$ , although it appears to have been assumed even. Mixed electric-magnetic transitions are not considered. In two cases where comparison is possible, the calculations are in agreement. A note has also been published recently by S. S. Hanna and D. R. Inglis (*Phys. Rev.*, 1949, **75**, 1767) in which the levels of  $^7\text{Li}$  are discussed in terms of possible coupling schemes.

Table 2. Angular Correlation and Polarization in the Reaction  $^{10}\text{B}(p, \alpha)^7\text{Li}^*$ .

Excited state of $^7\text{Li}$	$^{10}\text{B}$ even parity (+)	$^{10}\text{B}$ odd parity (-)
	$^{11}\text{B}^*, 7/2, +$	$^{11}\text{B}^*, 7/2, -$
	$^{11}\text{B}^*, 5/2, +$	$^{11}\text{B}^*, 5/2, -$
Isotropic in all cases		
1/2	$1 + 2/11 \cos^2 \theta$ [1 - 4/13 $\sin^2 \theta$ ]	$1 - 5/17 \cos^2 \theta$ [1 + 1/32 $\sin^2 \theta$ ]
3/2	$1 - \cos^2 \theta \frac{6(1+\gamma)}{(17+36\alpha+12\gamma)}$ [ $\frac{11+36\alpha+24\gamma-48\gamma \cos^2 \theta}{23+36\alpha-12 \cos^2 \theta(1+2\gamma)}$ ]	$1 + \cos^2 \theta \frac{2(1+6\gamma)}{(11+28\alpha-4\gamma)}$ [ $\frac{13-28\alpha-8\gamma(1-2 \cos^2 \theta)}{9+28\alpha+4 \cos^2 \theta(1+2\gamma)}$ ]
5/2	$1 + 17/41 \cos^2 \theta$ [1 - 17/29 $\sin^2 \theta$ ] $1 - \cos^2 \theta \frac{(1-0.4\alpha-9/2\gamma)}{(7+5.1\alpha-3/2\gamma)}$ [ $\frac{3(1+0.92\alpha-1/2\gamma+\gamma \cos^2 \theta)}{4+2.36\alpha-\cos^2 \theta(1-0.4\alpha-3/2\gamma)}$ ]	$1 - 1/7 \cos^2 \theta$ [1 - 1/3 $\sin^2 \theta$ ] $1 + \cos^2 \theta \left( \frac{1+0.61\alpha-4.5\gamma-1.18\alpha \cos^2 \theta}{1.43+2.78\alpha+1.5\gamma} \right)$ [ $\frac{1+0.66\alpha-0.18\alpha \cos^2 \theta-0.9\gamma \cos 2\theta}{0.41+0.82\alpha+\cos^2 \theta(0.59-0.34\alpha-0.9\gamma)}$ ]
7/2	$1 - 1/2 \cos^2 \theta$ [(3.08 - 2.08 $\cos^2 \theta$ ) $^{-1}$ ]	Isotropic $1 - 1.06 \cos^2 \theta + 1.35 \cos^4 \theta$ [ $\frac{1-2.12 \cos^2 \theta+2.12 \cos^4 \theta}{0.54+0.46 \cos^2 \theta}$ ]

The first line in each case represents the intensity correlation; the second line in square brackets, the polarization ratio  $I_{\theta}/I_{\phi}$ .  $\alpha = \beta^2$  and  $\gamma = \beta \sin \delta$  where  $\beta e^{i\delta}$  is used to denote the relative amplitude and phase of magnetic dipole to electric quadrupole components in a mixed transition. The results plotted in the figure are obtained by putting  $\alpha = \gamma = 0$  (pure magnetic dipole). The case of pure quadrupole radiation is obtained by retaining only the terms containing  $\alpha$ .

## REFERENCES

- BOGGILD, J., 1945, *Det. Kgl. Dansk. Vid. Sels. Math-Fys. Medd.*, **23**, 4.  
 DEVONS, S., and HINE, M. G. N., 1949, *Proc. Roy. Soc. A*, in the press.  
 DEUTSCH, M., and METZGER, F., 1948, *Phys. Rev.*, **74**, 1542.  
 ELLIOTT, L. G., and BELL, R. E., 1948, *Phys. Rev.*, **74**, 1869.  
 GILBERT, C. W., 1948, *Proc. Camb. Phil. Soc.*, **44**, 447.  
 GORDY, W., RING, H., and BURG, A. B., 1948, *Phys. Rev.*, **74**, 1191.  
 INGLIS, D. R., 1948, *Phys. Rev.*, **74**, 1876.  
 ROSENFELD, L., 1948, *Nuclear Forces* (Amsterdam : North Holland Publ. Co.), § 17.5.  
 RASMUSSEN, V. K., LAURITSEN, C. C. and LAURITSEN, T., 1949, *Phys. Rev.*, **75**, 199.  
 SIEGBAHN, K., 1946, *Ark. Mat. Astr. Fys.*, **34B**, No. 6.  
 WIGNER, E. P., and FEENBERG, E., 1941, *Rep. Prog. Phys.*, **8**, 274 (London : Physical Society).

## The Neutrons emitted in the Bombardment of $^{10}\text{B}$ and $^{11}\text{B}$ by Deuterons

BY W. M. GIBSON

Cavendish Laboratory, Cambridge

*Communicated by O. R. Frisch; MS. received 5th May 1949*

**ABSTRACT.** The photographic plate method has been used in an investigation of the neutrons from the (dn) reactions in  $^{10}\text{B}$  and  $^{11}\text{B}$ , separated isotopes being used in the targets.

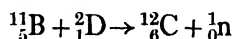
The reaction  $^{10}\text{B}(\text{dn})^{11}\text{C}$  gives neutron groups at 6.70 mev. and 4.85 mev. ; these give an energy release for the transition to the ground state of  $6.59 \pm 0.10$  mev., and show the existence of a level in  $^{11}\text{C}$  at  $2.02 \pm 0.10$  mev.

The reaction  $^{11}\text{B}(\text{dn})^{12}\text{C}$  gives well-defined neutron groups at 13.51 mev., 9.40 mev. and 4.55 mev., with a continuous distribution up to 6 mev. and a small peak at 6.4 mev. The 13.51 mev. group gives an energy release of  $13.92 \pm 0.15$  mev. for the transition to the ground state ; the other groups confirm the existence of levels in  $^{12}\text{C}$  at  $4.47 \pm 0.10$  mev.,  $9.72 \pm 0.15$  mev. and less certainly 7.7 mev., while the continuous distribution is due to the reaction  $^{11}\text{B}(\text{dn})3\alpha$ .

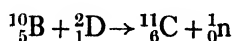
### § 1. INTRODUCTION

THE energy spectrum of the neutrons produced by the bombardment of boron with deuterons has been studied by Powell (1943). He showed that the greater number of neutrons emitted were in two groups, of energies 4 mev. and 9 mev. ; there were also some neutrons in groups at 13 mev. and 6 mev.

Normal boron contains 80% of the isotope  $^{11}\text{B}$  and 20% of the isotope  $^{10}\text{B}$ . The energy release in the reaction



is 13.78 mev. according to the mass-values quoted by Bethe (1947), while that for the reaction



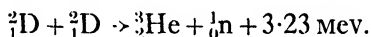
is 6.53 mev. Powell's 13 mev. and 9 mev. groups are therefore attributed to the disintegration of  $^{11}\text{B}$ , the  $^{12}\text{C}$  nucleus being formed in its ground state and in an excited state at 4 mev., respectively. The 6 mev. and 4 mev. groups might be due to further excited states of  $^{12}\text{C}$ , for which there is some evidence, or they might be due to the disintegration of the less abundant isotope  $^{10}\text{B}$ .

In order to obtain more definite evidence about the excited states of  $^{12}\text{C}$  and  $^{11}\text{C}$ , studies of the neutron spectra from deuteron bombardment of the separated boron isotopes have been made and compared with that from a normal boron target. The photographic plate technique has been applied to the study of neutron spectra by Powell (1940, 1943), Richards (1941), Peck (1948) and others; it has been used in the work discussed here, the procedure being similar to that described by Green and Gibson (1949).

## § 2. EXPERIMENTAL TECHNIQUE

The specimens of the separated isotopes were in the form of thin deposits on the copper sheet which had been used as collector in the electromagnetic separator. The thicknesses were such that the energy loss of a deuteron passing through the  $^{11}\text{B}$  layer was of the order of 120 kev., and through the  $^{10}\text{B}$  layer 30 kev.; the separation of the isotopes was practically complete. The specimens were mounted on water-cooled brass plates to form targets 14 mm. in diameter, and were bombarded with a  $70\text{ }\mu\text{a.}$  deuteron beam of mean energy 930 kev., from the Cavendish Laboratory 1mv. equipment. A thick target of unseparated boron was bombarded under similar conditions.

Ilford C.2 plates, with emulsion thicknesses varying from  $250\mu$  to  $290\mu$ , were held in light-tight boxes so that they received at grazing incidence the neutrons emitted from the target at right angles to the direction of the deuteron beam. In the investigation of (dn) reactions some neutrons from the reaction



(Livesey and Wilkinson 1948) are always found, because of deuteron contamination of the target. Neutrons emitted at  $90^\circ$  to the beam were chosen because at this angle the target thickness has little effect, and the separation of the D + D group from the 4 mev. B + D group is better than in the forward direction.

The distance of the plates from the target, and the exposure time, were chosen for each target to give a convenient number of tracks per unit area of emulsion. This was made much easier, and trial irradiations were made unnecessary, by the use of a high-pressure hydrogen ionization chamber; with this it was possible to estimate the neutron flux from each target at the beginning of the irradiation. The exposure times varied between 1 and 2 hours and the distances between 6 and 20 cm.

The plates were processed by the method due to Dilworth, Occhialini and Payne (1948), and were examined under a magnification of 1,100. Proton tracks forming "knock-on" angles of less than  $19.5^\circ$  with the neutron beam were measured, and the corresponding neutron energies calculated in the way described by Gibson and Livesey (1948). Tracks corresponding to neutrons of energy less than 4.0 mev. were neglected for all but about a tenth of the area searched in each plate.

## § 3. NEUTRON SPECTRA

For each of the three spectra, the number of observed tracks in each energy interval of 0.2 mev. was plotted as a function of neutron energy. To obtain the actual distribution of neutron number with energy, it was necessary to correct these spectra for two effects: the variation of neutron-proton scattering cross section with energy (Sleator 1947), and the variation with energy of the fraction of the proton tracks which would be expected to remain within the emulsion.

This fraction was calculated for each neutron energy by the formula of Gibson and Livesey (1948), the appropriate values of the emulsion thickness and the maximum allowed knock-on angle being used. The combined correction factor for cross section and escape is shown in Figure 1, for an emulsion thickness of  $250\mu$  and a knock-on angle limit of  $19.5^\circ$ . The factor is normalized to unity at 7 Mev., so that in the corrected spectra of Figures 2, 3 and 4 the ordinates around this energy represent actual numbers of tracks measured, while being proportional to neutron numbers at all energies. The effect of the variation of the correction factor is shown by the standard deviations indicated on the corrected spectra.

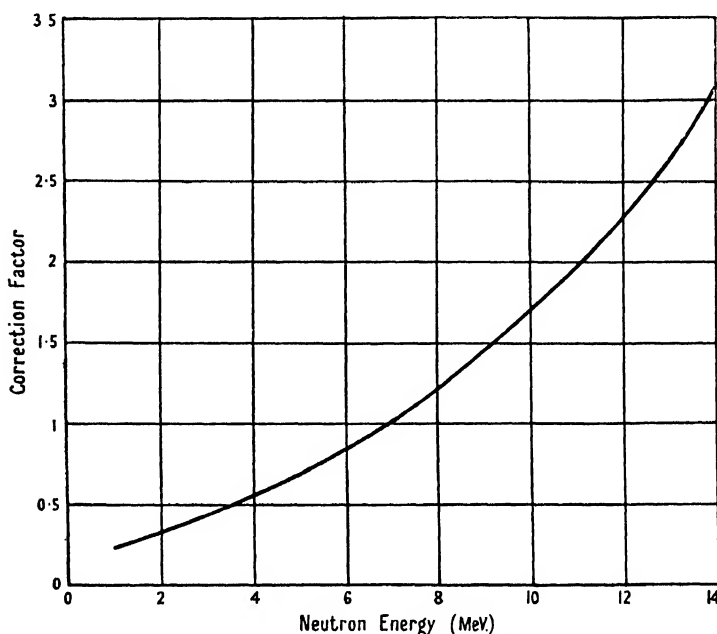
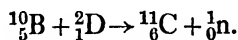


Figure 1. Combined correction for escape and n-p scattering cross section, for a  $250\mu$  emulsion and a "knock-on" angle limit of  $19.5^\circ$ . The correction factor is normalized to unity at 7 Mev.

#### (i) Discussion of Neutron Spectrum from $^{10}\text{B}$ .

It is clear that the groups centred on 6.70 Mev. and 4.85 Mev. (see Figure 2) must be due to the reaction



No other element could give either of these groups if present as contamination of the target, and the almost complete absence of  $^{11}\text{B}$  is shown by the smallness of the 9.4 Mev. group. In particular, comparison of the relative sizes of the 9.4 Mev. and 4.5 Mev. groups in the  $^{11}\text{B}$  spectrum (Figure 3) with those of the 9.4 Mev. and 4.85 Mev. groups in the  $^{10}\text{B}$  spectrum shows that the last-mentioned group could not be due to  $^{11}\text{B}$  contamination even if its mean energy fitted. The unduly low neutron energies (12.2 Mev. and 12.6 Mev.) obtained from the two long tracks in the  $^{10}\text{B}$  spectrum are explained by assuming that the  $^{11}\text{B}$  contamination was not on the  $^{10}\text{B}$  target itself but on the brass holder beside it; this would introduce errors in the calculation of the neutron energy from the proton energy. The peak between 2 Mev. and 3 Mev. in Figure 2 is due to D + D neutrons.

If we assume that the thickness of the target was 30 kev. and the mean energy of the bombarding deuterons therefore 915 kev., we obtain values of  $6.59 \pm 0.10^*$  mev. and  $4.57 \pm 0.10^*$  mev. for the  $Q$  values corresponding to the two groups (we neglect the variation of the excitation function between 900 kev. and 930 kev.). The masses quoted by Bethe (1947) for  $^{10}\text{B}$ ,  $^2\text{D}$ ,  $^{11}\text{C}$  and  $^1_0\text{n}$  give a  $Q$  value of 6.53 Mev., so we must assume that the two groups are produced by the formation of  $^{11}\text{C}$  in its ground state and in an excited state at  $2.02 \pm 0.10^*$  mev. There is as yet no other evidence for such a state, but these results appear conclusive.

### (ii) Discussion of Neutron Spectrum from $^{11}\text{B}$

Figure 3 shows the neutron spectrum from the  $^{11}\text{B}$  target. The groups centred on 13.51 mev., 9.40 mev. and 4.55 mev. must be due to the reaction

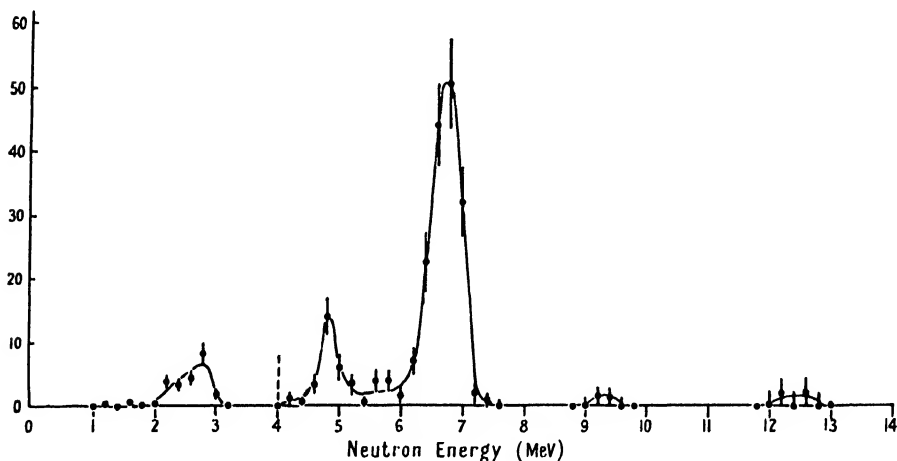
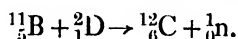


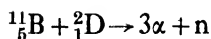
Figure 2. Neutron spectrum from  $^{10}\text{B}$  target, from 285 tracks. Each ordinate is proportional to the number of neutrons in an energy interval of 0.2 mev., and in the region of 7 mev. is equal to the actual number of proton tracks observed in such an interval.

If we assume a target thickness of 120 kev. and use the known excitation function for the reaction (J. V. Jelley, private communication) we obtain an effective mean bombarding energy of 875 kev.; this gives  $Q$  values for the three groups of  $13.92 \pm 0.15$  mev.,  $9.45 \pm 0.15$  mev. and  $4.20 \pm 0.10$  mev., respectively. The masses of  $^{11}_5\text{B}$ ,  $^2_1\text{D}$ ,  $^{12}_6\text{C}$  and  $^1_0\text{n}$  quoted by Bethe (1947) give a  $Q$  value of 13.78 mev., so these three groups may be assumed to be due to the formation of  $^{12}\text{C}$  in its ground state and in levels at  $4.47 \pm 0.10$  mev. and  $9.72 \pm 0.15$  mev. The existence of the lower level has been deduced by many workers, including Holloway and Moore (1940). Independent evidence for the higher level is in the work of Stuhlinger (1939), who observed the onset of slow neutron production in the reaction  $^9\text{Be}(\alpha\text{n})^{12}\text{C}$  at an  $\alpha$ -energy corresponding to a level at 9.5 mev., and of Fulbright and Bush (1948) who studied the inelastic scattering of protons by carbon and inferred the existence of a level at  $9.7 \pm 0.6$  mev.

\* The uncertainties of measurement and the uncertainty of the range-energy relation contribute roughly equally to the error in each  $Q$  value; each alone would give an error of  $\pm 0.07$  mev. The uncertainties of measurement for the two groups are almost independent, but that of the range-energy relation is not. The probable error of the difference of the  $Q$  values is therefore almost entirely due to the uncertainties of measurement, which give 0.10 mev.



The reaction



should have a  $Q$  value of 6.44 mev.; calculation shows that the maximum energy which a  $90^\circ$  neutron from this reaction can have is 6.66 mev., when the deuteron energy is 0.93 mev. There will therefore be a continuous spread of neutrons of all energies up to 6.66 mev., the exact shape of the distribution depending on the detailed mechanism of the reaction.

The spectrum of Figure 3 shows just such a continuous distribution (obscuring the  $\text{D} + \text{D}$  group which would appear between 2 mev. and 3 mev., as in Figure 2). The small peak at 6.4 mev. might be due to this reaction, but is more probably due to a genuine level in  ${}^{12}\text{C}$  at 7.7 mev. Holloway and Moore (1940) give some evidence for such a level, and many workers have found gamma-rays corresponding

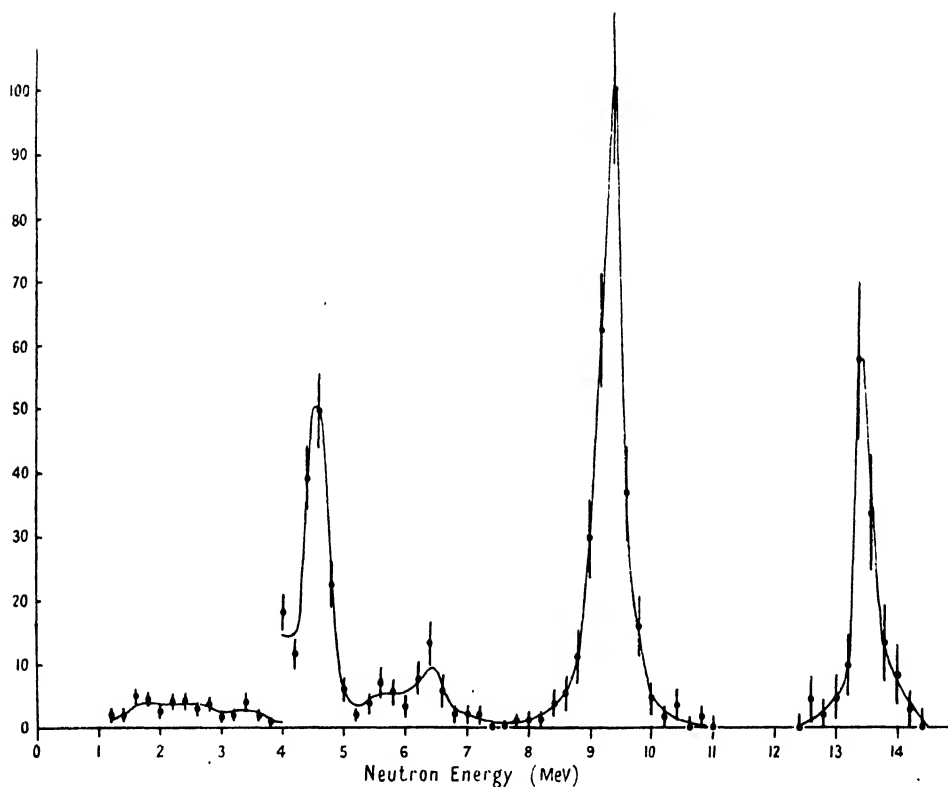


Figure 3. Neutron spectrum from  ${}^{11}\text{B}$  target, from 663 tracks. For ordinate scale see Figure 2.

to transitions to the ground state from a level in this region. This peak cannot be due to  ${}^{10}\text{B}$  contamination since its mean energy is wrong. It may be mentioned that both the 7.7 mev. and the 9.7 mev. levels in  ${}^{12}\text{C}$  are above the threshold for disintegration into three alpha-particles (7.34 mev.).

### (iii) Neutron Spectrum from Unseparated Boron

The spectrum of Figure 4 agrees with that of Powell (1943), and is mainly of interest for the size and mean energy of the group between 6 and 7 mev. This is much larger in proportion to the 9.4 mev. group than in the  ${}^{11}\text{B}$  spectrum; the fact that it is partly due to  ${}^{10}\text{B}$  is shown also by its mean energy, which is 6.5 mev.

compared with 6.4 mev. for the small peak in the  $^{11}\text{B}$  spectrum and 6.7 mev. for the group from  $^{10}\text{B}$ . Otherwise the unseparated-boron spectrum is very similar to that from  $^{11}\text{B}$ .

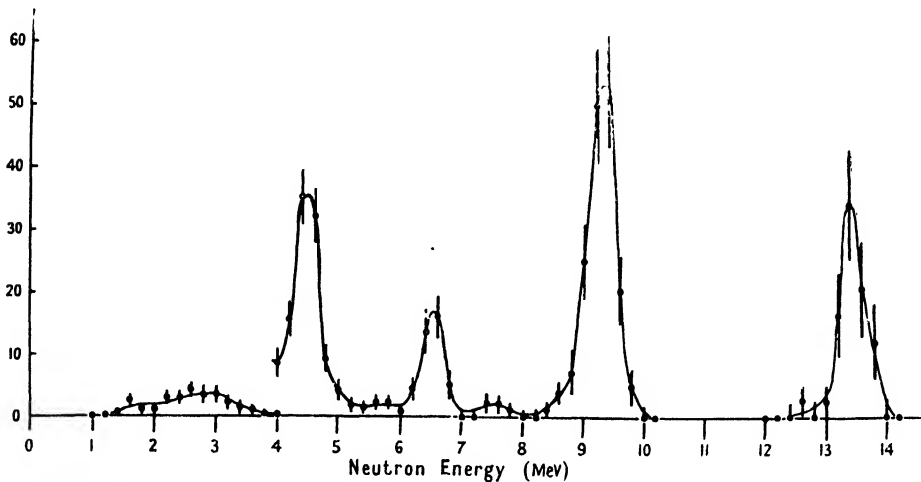


Figure 4. Neutron spectrum from unseparated boron target, from 447 tracks. For ordinate scale see Figure 2.

#### ACKNOWLEDGMENTS

The author's thanks are due to Sir John Cockcroft and Dr. W. D. Allen for providing the specimens of the separated boron isotopes, to Mr. G. H. Stafford for his assistance in estimating the necessary exposure times by the use of a high-pressure hydrogen ionization chamber, to Dr. W. E. Burcham and Professor O. R. Frisch for their helpful advice and criticism, and to the Department of Scientific and Industrial Research for financial support.

#### REFERENCES

- BETHE, H., 1947, *Elementary Nuclear Theory* (New York : John Wiley and Sons), p. 124.  
 DILWORTH, C. C., OCCHIALINI, G. P. S., and PAYNE, R. M., 1948, *Nature, Lond.*, **162**, 102.  
 FULBRIGHT, H. W., and BUSH, R. R., 1948, *Phys. Rev.*, **74**, 1323.  
 GIBSON, W. M., and LIVESSEY, D. L., 1948, *Proc. Phys. Soc.*, **60**, 523.  
 GREEN, L. L., and GIBSON, W. M., 1949, *Proc. Phys. Soc. A*, **62**, 407.  
 HOLLOWAY, M. G., and MOORE, B. L., 1940, *Phys. Rev.*, **58**, 847.  
 LIVESSEY, D. L., and WILKINSON, D. H., 1948, *Proc. Roy. Soc. A*, **195**, 123.  
 PECK, R. A., 1948, *Phys. Rev.*, **73**, 947.  
 POWELL, C. F., 1940, *Nature, Lond.*, **145**, 155 ; 1943, *Proc. Roy. Soc. A*, **181**, 344.  
 RICHARDS, H. T., 1941, *Phys. Rev.*, **59**, 796.  
 SLEATOR, W., 1947, *Phys. Rev.*, **72**, 207.  
 STUHLINGER, E., 1939, *Z. Phys.*, **114**, 185.

## Three-Dimensional Design of Synchrotron Pole-Faces

By C. ROBINSON

*Communication from the Nelson Research Laboratories, English Electric Company, Stafford*

*MS. received 6th April 1949*

**ABSTRACT.** An analytical method for the design of a synchrotron pole-face is outlined, the method taking full account of the cylindrical symmetry. Relaxation methods are employed to determine the exact size and shape of the lips correcting for fringing, and are also used to give a final check on the characteristics of the magnetic field. Practical examples of these methods are then given.

### § 1. INTRODUCTION

TWO recent notes (Davy 1948, Goward and Wilkins 1948) have considered the design of a synchrotron pole-face. This suggests that the methods used by the author may be of interest to other workers in this field. The purpose of their designs has been to produce a field between the poles such that, using cylindrical polar coordinates, the value  $n$  given by

$$n = -(r/H_z)(\partial H_z/\partial r) \quad \dots\dots(1)$$

is almost constant and has a value of about 0.7,  $H_z$  being the  $z$ -component of the field. The contours of the pole-faces have been deduced in two dimensions by neglecting the cylindrical symmetry and by a procedure which amounts to defining a magnetic potential distribution which does not satisfy Laplace's equation. A three-dimensional design in which the potential distribution does satisfy Laplace's equation was given by Coggeshall and Muskat (1944) and independently by Bartlett (1943), but, like that given by Davy, the value of  $n$  defined by (1) is constant only on the plane of symmetry, and is difficult to determine elsewhere. The first object of this paper is therefore to show how to define a magnetic potential distribution which satisfies Laplace's equation and which has an "almost constant" value of  $n$  over the whole area of the pole cross section as distinct from an "exactly constant" value of  $n$  along the plane of symmetry.

### § 2. THE DESIGN OF THE PROFILE

Goward and Wilkins have remarked that a constant value of  $n$  over the whole field is impossible. This is clearly true because the potential distribution which gives

$$H_z = kr^{-n}, \quad \dots\dots(2)$$

where  $k$  and  $n$  are constants, does not satisfy Laplace's equation. The latter, with cylindrical symmetry, has the form

$$\frac{\partial^2 V}{\partial r^2} + \frac{1}{r} \frac{\partial V}{\partial r} + \frac{\partial^2 V}{\partial z^2} = 0. \quad \dots\dots(3)$$

However, all expressions of the form

$$V = \mathcal{C}_0(kr) \sinh(kz) \quad \dots\dots(4)$$

(where  $\mathcal{C}_0(x)$  is a Bessel function of zero order of the first or second kind and  $k$  has any value) are solutions of the equation, have symmetry about  $z=0$ , and have

zero value on  $z=0$ . The problem is, then, to choose a linear combination of terms of the type given in (4) such that the value of  $n$  defined by

$$n = - \left( r / \frac{\partial V}{\partial z} \right) \left( \frac{\partial^2 V}{\partial r \partial z} \right), \quad \dots\dots(5)$$

is "almost constant" over a prescribed cross section.

It is convenient to take as unit of distance the mean value of  $r$  in the area under consideration. Then a potential distribution given by (4) gives at  $r=1$  values of  $n$  defined by

$$n = \{k\mathcal{C}_1(k)\}_s / \mathcal{C}_0(k), \quad \dots\dots(6)$$

and thus for any prescribed  $n$  value at this point it is sufficient for  $k$  to be any root of equation (6). If the potential distribution is given by a linear combination of terms of the type (4), namely,

$$V = \sum_s \{A_s \mathcal{C}_0(k_s r) \sinh(k_s z)\}, \quad \dots\dots(7)$$

then the appropriate value of  $n$  is

$$n = \frac{\sum_s \{A_s k_s^2 r \mathcal{C}_1(k_s r) \cosh(k_s z)\}}{\sum_s \{A_s k_s \mathcal{C}_0(k_s r) \cosh(k_s z)\}}. \quad \dots\dots(8)$$

At the point  $r=1$ ,  $z=0$  this reduces to

$$n = \frac{\sum_s \{A_s k_s^2 \mathcal{C}_1(k_s)\}}{\sum_s \{A_s k_s \mathcal{C}_0(k_s)\}}, \quad \dots\dots(9)$$

and if the constants  $k_s$  are solutions of equation (6) for the prescribed  $n$  (say  $n'$ ) then this reduces to

$$n = \frac{\sum_s \{A_s B_s n'\}}{\sum_s \{A_s B_s\}} = n'. \quad \dots\dots(10)$$

That is to say, if each of the terms of (7) individually has the prescribed  $n$  value at the point  $r=1$ ,  $z=0$ , then the expression (7) also has the prescribed value regardless of the values of  $A_s$ . These  $s$  arbitrary constants can then be chosen so that  $n$  has its prescribed value at  $s$  other points, and in this way a potential distribution is defined which gives a prescribed  $n$  value over an area, and not merely on the line  $z=0$ .

### § 3. THE EXTREMITIES OF THE PROFILE

The remaining problem is the design of a lip correcting for fringing. Relaxation methods can be employed for this purpose, this being a distinct improvement on methods employed hitherto which seem to have been based merely on a qualitative rather than a quantitative basis. The method suggested is as follows, reference being made to Figure 1. Let ABCD be the theoretical pole profile and suppose it must be terminated at a radius  $r=r_1$ , on the line EB. Let HCG be the greatest radius for which the  $n$  values have been specified. A relaxation mesh is then constructed to terminate on HG, GB, BE and HK. The boundary values of the potential are all known except on GB (it being assumed that plausible values are given on the boundary joining E to K, at such a distance that any error in them does not affect the values of  $n$  in the important area). In particular the values of the potential  $V$  and of the potential gradient  $\partial V / \partial r$  along CH are known from

the theoretical potential distribution. The knowledge of the potential gradient  $\partial V/\partial r$  along CH compensates for the unknown boundary BG, and it is an easy matter to put values of the potential along BG which give the correct values of  $\partial V/\partial r$  along CH in the relaxed mesh. When these values are obtained, the equipotential connecting B to C is found by inverse interpolation along each of the mesh lines. The required profile is then EBLMNCD....

#### §4. THE FINAL CALCULATION OF THE $n$ -VALUES

Since approximations must be made in the design of a profile it is desirable to make a final check on the values of  $n$ . Two methods, electrolytic tank measurement and magnetic measurement on the actual synchrotron magnet, have been mentioned as being available. The former method, even when a wedge-shaped tank was used to preserve the cylindrical symmetry, did not prove to be sufficiently accurate. The determination of  $n$  by relaxation methods\* seems to have been overlooked. It has the great advantage of being able to take into account the presence of the adjacent exciting coils and the betatron core and of not requiring

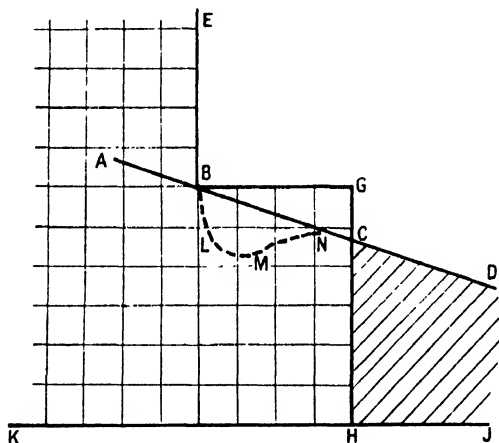


Figure 1. The relaxation mesh for approximating to the extremity of a pole profile.

the manufacture of a magnet or model to test the values of  $n$ . The relaxation mesh is used to determine the values of the magnetic potential, and from this the field and the  $n$  values are readily computed numerically by equation (5). The effect of the betatron core and of the exciting coils is readily found by a variation in the boundary values on the relaxation mesh. In this respect it has been found that the exciting coils do not affect the values of  $n$  appreciably, but that a movement of the betatron core radially outwards may have a considerable effect on the  $n$  values. This effect is easily assessed since the betatron core is a very suitable boundary for the relaxation mesh.

#### §5. COMPARISON OF RELAXATION AND EXPERIMENTAL RESULTS

In the case of one pole profile a check on the  $n$  values obtained by relaxation methods has been made by comparing them with A.C. magnetic measurements made on the actual magnet whose pole profile is shown in Figure 2. In the case of magnetic measurements the  $n$  values were obtained corresponding to various time intervals after field zero. The ones selected for comparison with theoretical values are those before betatron pole saturation.

\* The methods are described by Fox (1947).

Figure 3 compares graphically values obtained by the two methods for  $z=0$  and  $z=1.5$  cm. respectively. There appears to be reasonable agreement between them particularly with respect to maximum and minimum values. The slight displacement radially between corresponding curves may be due to inaccuracies in the experimental technique, whilst the slight difference in slopes at low radii for  $z=0$  may be explained by the effects of pole-packing factors and flux-path reluctance which were not taken into account in the relaxation process.

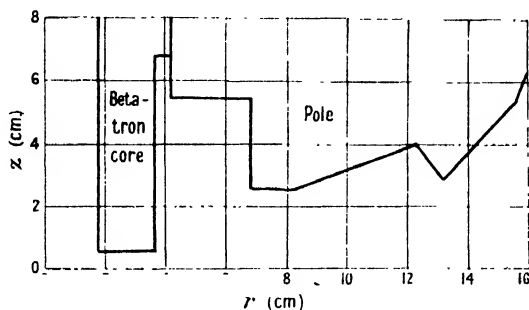


Figure 2. The pole profile used for comparison of relaxation and magnetic measurements.

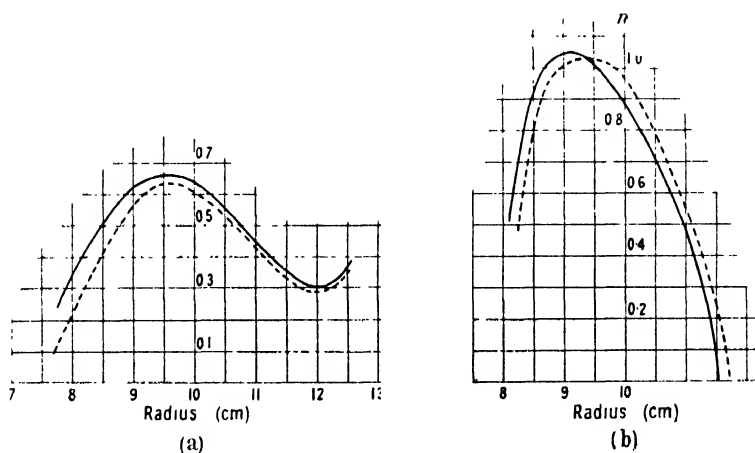


Figure 3. Comparison of relaxation values (continuous lines) and magnetic measurements (broken lines) in the determination of  $n$ .

(a)  $n$  values on the median plane ( $z=0$ ).

(b)  $n$  values on the plane  $z=1.5$  cm.

A check on the boundary values assumed for the relaxation mesh was made by comparing values of the field  $H_z$  obtained by the two methods in the neighbourhood of the poles. It was found that the magnetic measurements at radial distances between 14 cm. and 16 cm. agreed closely with the relaxation values, thus proving that the relaxation boundary conditions were satisfactory.

The relaxation process also enables total flux calculations to be made by a simple summation method and the flux density at any section of the pole to be determined for a given orbit flux density. Values of flux density obtained by this means for a pole profile similar to that in Figure 1(b) of the note by Goward and Wilkins (1948) agreed to within 5% with experimental results. The method has recently been used to modify this profile to that in Figure 2 enabling a 30% increase in maximum orbit flux density to be obtained. This also has been verified by experimental results.

## § 6. PRACTICAL EXAMPLE

As an example of the method of §§ 2-4, a potential distribution which has a value of  $n$  within the range  $0.73 \pm 0.08$  over the area  $0.675 < r < 1.325$ ;  $-0.2 < z < 0.2$  is given by considering only two terms of the series (7), namely,

$$V = -J_0(1.12r) \sinh(1.12z) - 10Y_0(0.26r) \sinh(0.26z), \quad \dots\dots(11)$$

$J_0(x)$  and  $Y_0(x)$  being Bessel functions of the first and second kind respectively, and the radius of the equilibrium orbit again being taken as unit of distance. For an equilibrium orbit of 12 cm. this potential distribution gives a satisfactory  $n$  value over a cross section 8 cm. wide and 5 cm. deep.

Any convenient equipotential of (11) can then be taken as the pole profile. In practice it is found that the equipotentials are almost exactly straight lines, to a very high degree of accuracy in the important area, and it has been found

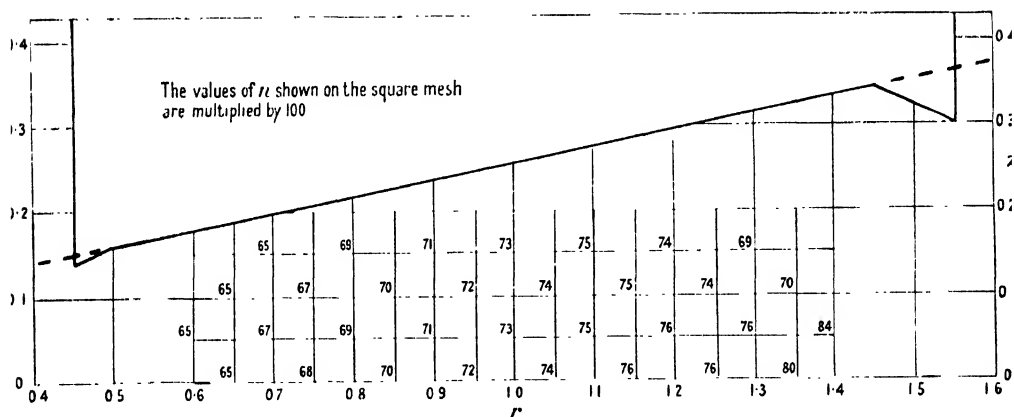


Figure 4. Practical example of the design of a synchrotron pole face showing

- (a) The scale, taking the equilibrium orbit as unit radius.
- (b) The lips correcting for fringing.
- (c) The  $n$  values in the area between the poles.

convenient to approximate to them by straight lines. The linear approximation to that equipotential of equation (11) which passes through the point  $r=0.6154$ ,  $z=0.18$  is

$$z = 0.1867r + 0.0666, \quad \dots\dots(12)$$

and this is a suitable pole profile.

It was required to terminate this profile at  $r=1.55$  and  $r=0.45$  on the outer and inner edges respectively. The prescribed  $n$  values ( $0.73 \pm 0.08$ ) were to hold for values of  $r$  between 0.675 and 1.325. With these conditions the profile was found to be defined by equation (12) modified by the lips shown in Figure 4, these having been designed by the method of § 3.

Relaxation methods were then employed to assess the final values of  $n$  for this profile. The  $n$  values are shown in Figure 4 at the corners of a square mesh. It will be observed that they are exactly constant for variation in  $z$  only and that they vary radially between 0.65 and 0.80—the prescribed limits.

## ACKNOWLEDGMENTS

Work on synchrotrons has been carried out at the Nelson Research Laboratories for the Atomic Energy Research Establishment, and acknowledgment is made to Sir John Cockcroft for permission to publish this paper. The work is also published by permission of the Director of Research, the Nelson Research Laboratories of the English Electric Company.

The magnetic measurements were taken by Mr. D. A. Layne, and the author is indebted to him for the results incorporated in Figure 3 and for the comments thereon which appear in §5.

## REFERENCES

- BARTLETT, J. H., 1943, *Phys. Rev.*, **64**, 185.  
COGGESHALL, N. D., and MUSKAT, M., 1944, *Phys. Rev.*, **66**, 187.  
DAVY, N., 1948, *Proc. Phys. Soc.*, **60**, 598.  
FOX L., 1947, *Proc. Roy. Soc. A*, **190**, 31.  
GOWARD, F. K., and WILKINS, J. J., 1948, *Proc. Phys. Soc.*, **61**, 580.

## REVIEWS OF BOOKS

*Elementary Nuclear Theory*, by H. A. BETHE. Pp. vii + 147. Second Edition. (New York: John Wiley & Sons, Inc.; British Agents: Chapman & Hall, 1948.) 15s.

When the reviewer recently went on a trip visiting Universities in England and Scotland he was struck again by the intense interest in nuclear physics among the graduating scientists. No doubt atomic energy with its many problems has created this favourable situation and has led to popularity of work connected with nuclear physics. It is therefore astonishing that the literature on nuclear physics, in so far as up-to-date books are concerned, is extremely unsatisfactory. Though there are some American textbooks, no book has recently been written which covers nuclear physics experimentally or theoretically with any pretensions to completeness. One reason for this state of affairs is, no doubt, the superior attraction of experimental research for the scientist, in contrast to the labour of writing a book which, even though the work is of modest dimensions, must always be a formidable undertaking. To produce a successful book requires, first of all, a very wide knowledge and a thorough penetration into the field, a requirement which already reduces the number of possible authors, especially as most physicists have become specialists within a small field inside the realm of physics. It is necessary that the author can express himself with lucidity, without which the book will, in general, remain on the shelf and not be read, though it may be bought; and if the author succeeds in injecting a dash of artistic brilliance into his representation, it may even be an eminently readable book. Anybody who knows Professor Bethe also knows that he is eminently qualified on both these points. His vast knowledge of quantum mechanics and the experimental and theoretical side of nuclear physics invariably impresses all physicists in scientific discussions. The astonishing clarity of his lectures secures him an enthusiastic audience. Professor Bethe's book on the *Elementary Nuclear Theory* is, since it contains the subject matter of a series of lectures, necessarily very restricted, but it is admirably clear and it contains a great many of those little pointers which are so often left out but which just make it possible for the reader to understand the problems.

The professional mathematical physicist often presents theory in a form which makes it very difficult for the experimental physicist to see the physical basis behind the formulae. Professor Bethe has very successfully avoided this difficulty, at least in the earlier part of the book.

The subject matter is divided into three main sections. First there is a descriptive part where most of the important facts about the properties of nuclei are condensed into 20 pages. Next there is a section concerned with the quantitative theory of nuclear forces. Since the theory of the deuteron may be said to equal in importance that of the hydrogen atom in



atomic nuclei, it is treated to a considerable extent on 35 pages. The items included under this heading are : the ground state of the deuteron, the scattering of neutrons by free protons and bound protons, and the photo-effect of the deuteron. The rest of this section is concerned with non-central forces, the saturation of nuclear forces, and a very brief account of the meson theory of nuclear forces. Particularly helpful are the discussions about the interaction in the case of tensor forces, from page 73 onwards, a topic which as a rule considerably frightens the experimental physicist.

These two sections alone make the book worth buying.

The third section (Chapter 1) deals with beta-ray disintegrations, containing many useful numerical data about this field, and a discussion of the Gamow-Teller selection rules which are so important. The compound nucleus is treated in the second chapter of the volume, and a very brief survey is made of the relevant features of Bohr's theory. As an appendix the author has supplied a very useful table of nuclear species.

In spite of the excellence of the book, one aspect of the general treatment of the subject matter has puzzled the reviewer though it is not specific to the book under review. It is this : at the beginning of the book it is shown in great detail how the mass-energy relation in nuclear reactions allows one to calculate the energy reaction, and this is demonstrated with a numerical example. From this one will conclude that the book is meant for real beginners in the field. But on page 50 Pauli spin operators are used, and on page 107 the five types of possible interaction in the beta theory, which are covariant under Lorentz transformations, are given, involving the various Dirac operators. The dilemma in which any author finds himself when he writes such a book becomes very clear here. To be consistent, considerably more explanation would have to be given, which, however, is not nuclear physics but quantum mechanics. I do not know if the person who needs to read the explanations given at the beginning of the book is really able to get to the end of it. I would be surprised if the average engineers and physicists of the General Electric Company of America, before whom these lectures were given, could with a good conscience say that they followed these last-mentioned developments completely. These examples were given more as an added illustration of the difficulties to be encountered than as a criticism of this excellent little volume.

E. BRETSCHER.

*Atomic Energy*, by K. K. DARROW. First Edition. Pp. 80. (New York : John Wiley & Sons, Inc. ; London : Chapman & Hall, Ltd., 1948.) \$2.

This book contains the substance of four lectures delivered by Dr. Darrow to an audience of non-physicists in 1947. Dr. Darrow, who is the secretary of the American Physical Society, has a well-deserved reputation for the clarity of his expositions, and the present book is a model of how a work of popularization should be written. The treatment is limited to the essentials, and there are no obscure references intelligible only to the initiated. Where accuracy has had to be sacrificed for the sake of simplicity, as with the distinction between mass and weight, this fact is not disguised.

The first lecture introduces the reader to the atomic structure of matter, the nuclear atom, isotopes, and nuclear masses. In the second lecture the equivalence of mass and energy is considered, and the balance of energy and mass in nuclear reactions is discussed with reference to experiments using the Van de Graaff generator and the Wilson cloud chamber. The third lecture deals with some typical nuclear transformations, leading up to the fission process and the possibility of a chain reaction. In the last lecture the method of obtaining a controlled chain reaction in the atomic pile is described, and the uses of the pile for the production of plutonium and radioactive isotopes are briefly considered.

Within its limits, therefore, the book gives an excellent general account of atomic energy, and it should prove especially valuable to those non-scientists and sixth-form students who wish to obtain a fairly simple but reliable and balanced account of the subject.

H. R. ALLAN.

## CONTENTS FOR SECTION B

	PAGE
Prof. G. I. FINCH. Steam in the Ring Discharge . . . . .	533
Dr. D. K. BUTT. The Electron Optical Properties of the Focal Isolation $\beta$ -Ray Spectrometer . . . . .	551
Mr. J. DYSON. A Unit-Magnification Optical System for the Attainment of Long Working Distances in Microscopy . . . . .	565
Mr. R. WEALE. The Optical Constants of Thin Metallic Films . . . . .	576
Mr. D. H. PEIRSON. The Displacement-Frequency Characteristic of Elastically Coupled Mechanical Systems with Two Degrees of Freedom . . . . .	579
Dr. G. H. METSON. Note on Volt-Dependent Poisoning Effects in Oxide-Cathode Valves . . . . .	589
Reviews of Books . . . . .	592
Corrigenda . . . . .	594
Contents for Section A . . . . .	595
Abstracts for Section A . . . . .	595

## ABSTRACTS FOR SECTION B

### *Steam in the Ring Discharge*, by G. I. FINCH.

**ABSTRACT.** The behaviour of steam and its decomposition products in the ring discharge has been examined.

Dry hydrogen is not dissociated. The production of atomic hydrogen is dependent upon the presence of steam which dissociates into hydroxyl and atomic hydrogen. A secondary source of atomic hydrogen is then afforded by the interaction of hydroxyl with molecular hydrogen.

The escape from the discharge of atomic hydrogen, a long-lived species, favours the dissociation of steam. Mercury vapour, on the other hand, inhibits the formation of atomic hydrogen and thus leads to a high equilibrium steam concentration.

Unlike dry hydrogen, dry oxygen is dissociated into atoms, but these have a short life as such and recombine in the discharge to form molecular oxygen and ozone.

The reaction mechanisms occurring in the discharge are discussed in the light of spectrographic results.

### *The Electron Optical Properties of the Focal Isolation $\beta$ -Ray Spectrometer*, by D. K. BUTT.

**ABSTRACT.** An attempt is made to show theoretically how the performance of a lens spectrometer depends upon the degree of spherical aberration present in the lens. In particular, curves of resolving power and transmission are plotted against radius and area of the central lens annulus, for source and counter window on the axis and of equal diameter.

The resolving properties of a circular source and counter window placed at equal distances off the axis are determined. The arrangement is found to be impracticable.

Lastly, an investigation is made into the resolving properties of a line source placed at right angles to the axis of the spectrometer, the image of which is focused into a slit-shaped window in a counter. The arrangement is shown to be advantageous particularly when long solenoids are employed, as in high energy  $\beta$ -spectroscopy.

*A Unit-Magnification Optical System for the Attainment of Long Working Distances in Microscopy*, by J. DYSON.

**ABSTRACT.** To fill an application for a microscope with a long working distance, several optical systems are reviewed. Of these, a system giving unit magnification to be used in conjunction with a conventional microscope is selected as suitable. This consists of a spherical mirror used with the object near its centre of curvature.

The aberrations of such a system are discussed and means of correcting them described. Modifications necessary to enable vertical illumination to be used are also described, and photographs taken by means of an experimental system are shown.

Other applications of the same system are suggested and designs given for a miniature system capable of being used on an ordinary microscope, for an immersion objective for "nuclear plate" work and for a water immersion system for biological applications.

*The Optical Constants of Thin Metallic Films*, by R. WEALE.

**ABSTRACT.** The optical constants of thin films are shown to depend on the thickness of the films due to the variation of the electrical conductivity with thickness. Good and bad conductors both exhibit maxima in the curves relating absorption coefficient and film thickness: in the two groups these peaks are due to two entirely different causes. The mean free paths of the conducting electrons are calculated from data found in the literature.

*The Displacement-Frequency Characteristic of Elastically Coupled Mechanical Systems with Two Degrees of Freedom*, by D. H. PEIRSON.

**ABSTRACT.** The displacement-frequency characteristic of elastically coupled mechanical systems with two degrees of freedom is calculated. Conditions are obtained for independence of deflection and frequency. The practicability of these conditions is considered and a determination made of the extent of the range for displacement independent of frequency.

The relations between the fundamental constants of the systems are illustrated graphically and the application to galvanometer and accelerometer design is discussed.

*Note on Volt-Dependent Poisoning Effects in Oxide-Cathode Valves*, by G. H. METSON.

**ABSTRACT.** The high vacuum oxide-cathode valve may show cathode poisoning effects when its electrodes are bombarded by electrons of certain discrete energies. Hamaker, Bruining and Aten describe one such effect occurring at about 10 ev. The author confirms this result and describes two other effects occurring at 5.56 ev. and 15.9 ev. The energies of the three effects can be closely associated with the heats of formation of the chlorides, monoxides and sulphates of barium and strontium. It is concluded that the 5.56 ev. effect is due to bombardment dissociation of the monoxides of barium or strontium, the 10 ev. effect to the chlorides and the 15.9 ev. effect either to the sulphates or to a gaseous ionization phenomenon

## CORRIGENDUM

"Temperature Measurements of Flames containing Incandescent Particles", by H. G. WOLFARD and W. G. PARKER (*Proc. Phys. Soc. B*, 1949, **62**, 523). <sup>1</sup>

In the abstract of the above paper in Section A, p. 536, 3 lines from the bottom, for melting point *read* boiling point.

# THE PROCEEDINGS OF THE PHYSICAL SOCIETY

## Section A

VOL. 62, PART 10

1 October 1949

No. 358 A

### On the Ratio of Positive to Negative Particles in the Vertical Cosmic-Ray Beam at Sea Level

BY B. G. OWEN AND J. G. WILSON

The Physical Laboratories, University of Manchester

*Communicated by P. M. S. Blackett ; MS. received 4th April 1949.*

**ABSTRACT.** A method of direct momentum measurement has been used to determine the ratio of positive to negative particles in the cosmic-ray beam at sea level. Measurements on about 12,000 particles give the ratio  $+/- = 1.268 \pm 0.023$ , and it is further shown that to the statistical accuracy of the experiment there is no variation of this ratio with momentum over the momentum range  $10^9$ – $10^{10}$  ev/c.

#### § 1. INTRODUCTION

MEASUREMENTS of the positive excess of energetic cosmic-ray particles, substantially of the meson component, hitherto reported are of two kinds. Blackett (1937), Jones (1939) and Hughes (1940) photographed cloud chamber tracks of single cosmic-ray particles in a magnetic field, and their results give very direct information for the range of momentum which is accepted by the chamber and its associated control and which is measurable in the particular conditions of experiment. However, the technique of accurate measurement of curvature is laborious, and the total number of tracks measured by each of these workers was only of the order of a thousand, a number sufficient to establish the existence of an excess of positive particles, although only within wide limits, but not large enough to yield significant results for separated ranges of momentum.

A different technique, initiated by Bernardini and his co-workers (1941) using a "lens" of magnetized iron has, more recently, been widely used. The results obtained by this method are not susceptible of the same direct interpretation as is possible for the cloud chamber method, for the apparatus becomes unselective at high momenta and has an efficiency of reception varying over the whole spectrum which is a function not only of simple geometry but also of the scattering of the particles traversing the magnetized iron blocks which form the lens. On the other hand the method has the high counting rate and portability which make it particularly suitable for relative measurements, provided that the particle spectrum at the various conditions of observation is sufficiently known.

The new magnetic spectrograph at Manchester University has made possible measurements comparable to those previously obtained in the cloud chamber at

a very much accelerated collection rate. We give here an absolute value of the ratio of positive to negative particles, over a defined angle of collection and momentum spectrum, of considerably greater statistical weight than the early measurements, and we give also some preliminary indication of this ratio as a function of momentum.

## § 2. THE APPARATUS

A detailed description of the spectrograph and its operation will be given elsewhere. The magnetic deflection of particles canalized through the field gap of two large electromagnets (field 12,000 gauss, pole area 30 cm.  $\times$  40 cm., gap 10 cm.) is detected in three rows of Geiger counters, respectively above the upper magnet, between the magnets and below the lower magnet (see Plate). The length of path between the extreme counter rows is 5 m. The individual counters of the three rows are connected to neon lamps, and, on every occasion when a master selection condition is fulfilled, the lamps corresponding to the particular counters discharged flash and are photographed, thus defining the

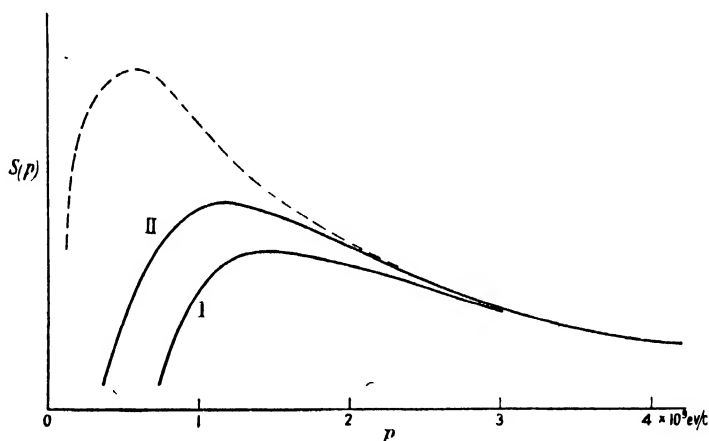
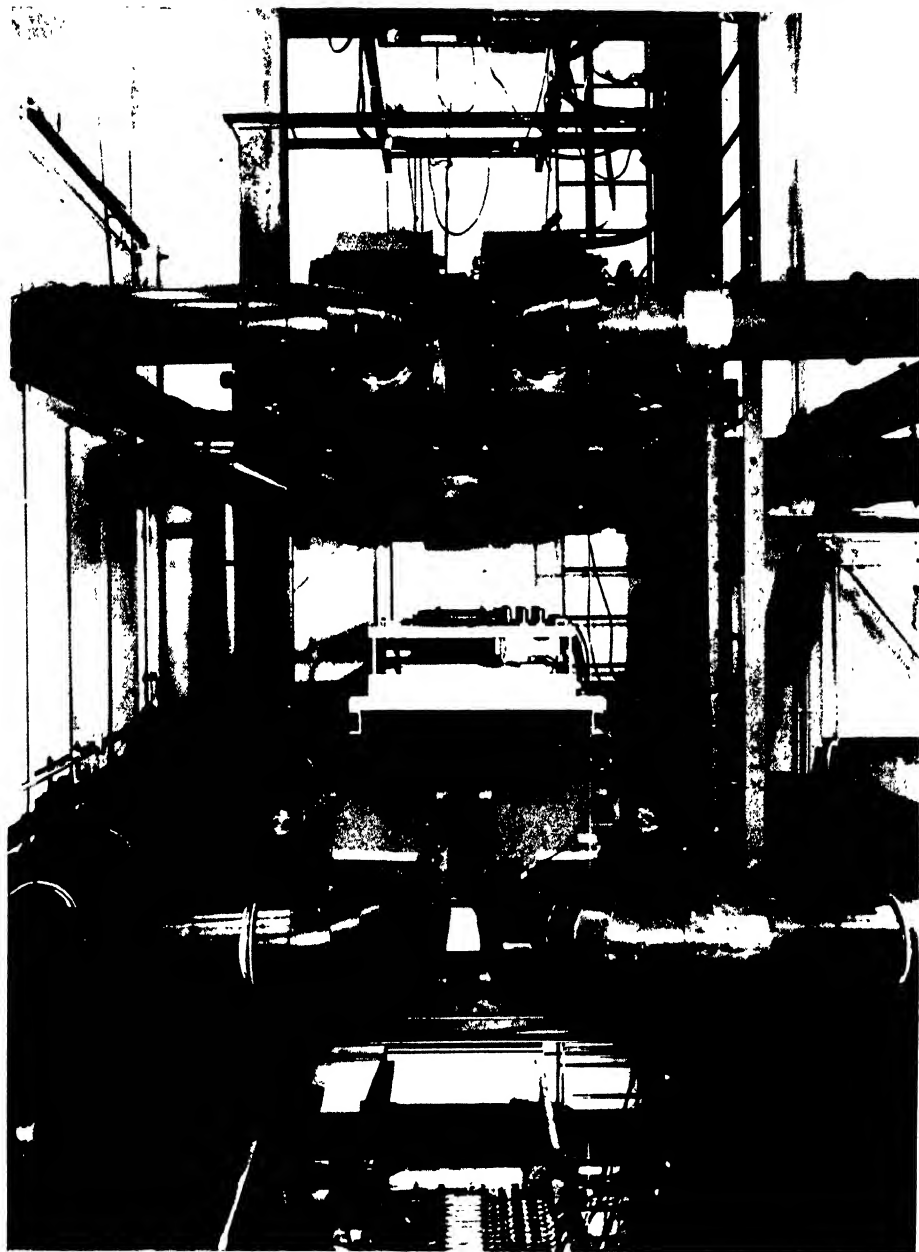


Figure 1. Momentum spectrum included in the determination of the ratio of positive and negative particles.  
I—Measurements with high field. II—Measurements with low field.  
Broken line—Meson sea-level spectrum according to Rossi (1948).

trajectory and deflection of the particle traversing the system. For the work now described the momentum of cosmic-ray particles near the vertical direction is measured with a "maximum detectable momentum" up to about  $3 \times 10^{10}$  ev/c. at a rate varying between 250 and 450 particles per day according to the condition of operation. The precision of measurement quoted is for operation with full magnetic field; in work referred to below with "low field" the corresponding maximum detectable momentum is  $1.5 \times 10^{10}$  ev/c.

The momentum spectrum and angular collection for which our measurements are made are shown in Figures 1 and 2. For comparison with the momentum spectrum of the particles actually used in our determination, the sea-level spectrum of mesons adopted by Rossi (1948) is also given in Figure 1. It is apparent that our measurements, of which the greater part were made with the lower value of magnetic field, give virtually no information about very slow mesons ( $p \lesssim 5 \times 10^8$  ev/c.); all of the other experiments to which we have referred show a similar bias against slow mesons.



Magnetic spectrograph, general view.



In Figure 2 the angular collection of the spectrograph is shown as a function of particle momentum, and it must be noted that the values of the positive-negative ratio given (Table 2) as a function of momentum refer to different collecting directions, a feature which applies also to the other measurements quoted. Our method of measurement in fact defines the direction of every incident trajectory to about  $\pm 1^\circ$ , and hence, were enough data available, a comparison of the ratio for different momenta in similar directions of collection could be made.

### § 3. RESULTS

Measurements were made of groups of approximately 3,000 tracks. This number was chosen in the first instance to correspond to a weekly reversal of the

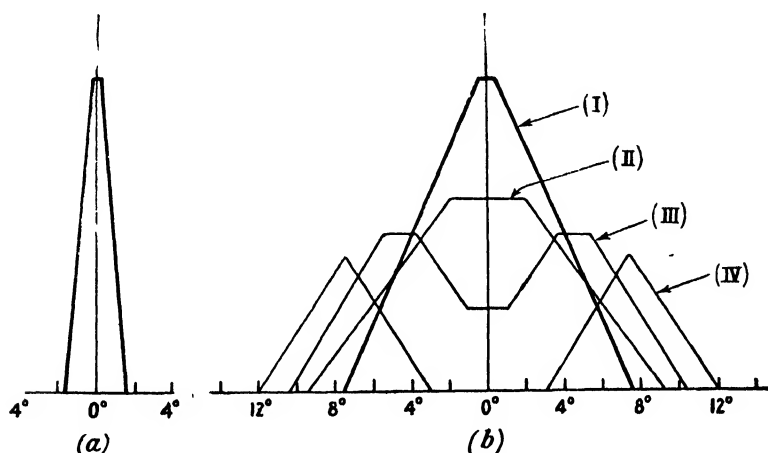


Figure 2. Angular collection of spectrograph (a) in E-W plane, (b) in N-S plane. (b, i) undeviated particles; (b, ii)  $4 \times 10^9$  ev/c. in high field,  $2 \times 10^9$  ev/c. in low field; (b, iii)  $2 \times 10^9$  ev/c. in high field,  $10^9$  ev/c. in low field; (b, iv)  $1.3 \times 10^9$  ev/c. in high field,  $0.7 \times 10^9$  ev/c. in low field.

deflecting field, and the first group in fact consisted of successive runs of about 1,500 tracks between which the field was reversed. For later groups a daily reversal of deflecting field was adopted, but for convenience groups of approximately 3,000 tracks were still collected.

The results for four groups of tracks are given in Table 1 in which are also summarized the results of cloud chamber measurements. The momentum ranges to which the results quoted for cloud chamber measurements apply are given, since particles of low momentum ( $p < 5 \times 10^8$  ev/c.) recorded by Blackett (1937) and by Hughes (1940) have been rejected because of the uncertain number of electrons which are involved in these groups. Hughes measured two groups of tracks for one of which the particles, after traversing the cloud chamber, passed through 10 cm. of lead, but obtained no significant difference in the results; these groups have accordingly been combined. The statistical standard error of the ratio  $+/-$  is given in each instance.

In Table 2 and in Figure 3 our results are shown as a function of particle momentum. Since any variation with momentum of the ratio of positive to negative particles is certainly not large compared with the statistical uncertainty of the various measurements, the mean momentum of each group has not been determined with great precision.



The particles in the group of mean momentum about  $10^{10}$  ev/c. include the particles of highest momentum for which a deflection of trajectory can be recorded. The actual distribution of momentum in this group will be discussed elsewhere.

Table 1. The Ratio of Positive to Negative Particles

Workers	Momentum range	Positive particles	Negative particles	Ratio +/− particles
Blackett (1937)	$p > 5 \times 10^8$ ev/c.	393	336	$1.17 \pm 0.09$
Jones (1939)	$p > 2 \times 10^8$ ev/c.	416	323	$1.29 \pm 0.10$
Hughes (1940)	$p > 5 \times 10^8$ ev/c.	595	487	$1.22 \pm 0.08$
O. & W. (1949)				
I (high field)	See Figure 1	1575	1232	$1.278 \pm 0.049$
II (low field)		1836	1468	$1.251 \pm 0.044$
III (low field)		1569	1250	$1.255 \pm 0.048$
IV (low field)		1763	1385	$1.273 \pm 0.046$
Total I–IV	See Figure 1	6743	5335	$(1.264)$ $1.268 \pm 0.023$

Table 2. Ratio of Positive to Negative Particles of groups I–IV (Table 1) as a Function of Momentum

Approximate mean momentum (ev/c.)	Positive particles	Negative particles	Ratio +/− particles
$10^9$	1781	1430	$1.247 \pm 0.044$
$2 \times 10^9$	1927	1455	$1.324 \pm 0.046$
$4 \times 10^9$	1461	1180	$1.238 \pm 0.048$
$10^{10}$	1576	1276	$(1.235)$ $1.252 \pm 0.046$

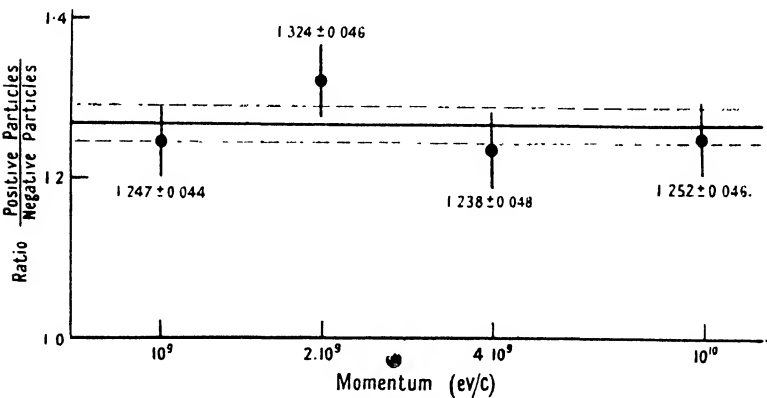


Figure 3. Ratio of positive and negative particles as a function of momentum. The full horizontal line represents the mean value over the whole spectrum, and the broken lines indicate the standard error of this value.

but it is relevant here that approximately 3% of these particles should be of opposite sign to that indicated by the recorded deflection : of the particles of mean momentum  $10^{10}$  ev/c. tabulated as “positive”, 97% are positive and 3% negative, and

similarly for those tabulated as "negative". There is accordingly a correction to be applied which tends to increase the ratio of positive to negative particles in this group. In Table 2 (and also in the total of all measurements in Table 1) the uncorrected ratio is given in brackets, and is followed by the corrected value.

#### § 4. NATURE OF PARTICLES

It is usually assumed that the ratio of positive to negative particles which we have measured is that of  $\mu$ -mesons: it is possible to obtain some confirmation of this assumption for the preliminary results of experiments undertaken in this laboratory by Mr. M. G. Mylroi\* to investigate the penetration of considerable thickness of lead by particles the momenta of which have been measured in the spectrograph.

In part of this work the passage through about 50 cm. lead of 3,500 particles, all of which were of sufficient momentum, if  $\mu$ -mesons, to traverse the absorber, was examined. Of these particles 69 were not detected emerging from the absorber (either because the particles failed to penetrate or because of inefficiency of detection below the lead), 42 being positive and 27 negative.

We conclude that at least 98% of the particles used in our experiment are capable of penetrating about 50 cm. of lead, and these, in the present state of knowledge, must almost certainly be considered to be  $\mu$ -mesons. The rather large positive excess in the small group of particles for which penetration was not observed by Mylroi would lead to a slight reduction of positive-negative ratio of the remaining particles, from  $1.268 \pm 0.023$  to  $1.259 \pm 0.024$ ; it will be noted that, since the effect is a small correction, the statistical weakness of the rejected group has little effect on the uncertainty of the main group.

A result differing from that given in Table 1 by not more than 1 or 2 per cent therefore applies to those particles capable of penetrating about 50 cm. of lead, which, as stated above, must almost certainly be considered to be  $\mu$ -mesons.

#### § 5. DISCUSSION

The agreement between our results and those of other workers using comparable methods shown in Table 1 requires no comment. Other results are, that at sea-level in the momentum range  $10^9 - 10^{10}$  ev/c. there is no variation of the ratio of positive to negative particles to the statistical accuracy of our measurements, and that our experimental value of this ratio applies, to within 1 or 2%, to particles capable of traversing about 50 cm. of lead.

Agreement with results obtained by means of the magnetic focusing method of Bernardini and his co-workers (1941) is less satisfactory; for example, Quercia, Rispoli and Sciuti (1948) find a value 1.16 for the positive-negative ratio at sea-level (a notation differing from ours is used by these and other workers with this technique). The magnetic focusing method is essentially indirect, in that large corrections must be made to the observed quantities, and it therefore seems reasonable to attach more weight to the direct measurements which do not appear to be subject to any uncertainty from which the focusing method is free.

In a recent report, Ballario, Benini and Calamai (1948) describe measurements, using the magnetic focusing method, in which the positive-negative ratio is studied as a function of zenith angle. The ratio is found to decrease with increasing zenith angle and if, in each direction, the ratio is assumed to be independent of

\* We are indebted to Mr. Mylroi for making his data available to us.

momentum, the zenith value of 1.16 is reduced to about 1.06 at  $60^\circ$ . This result is interpreted as demonstrating that the positive-negative ratio at meson formation depends closely upon energy; in particular the ratio is small for particles capable of reaching sea-level at an inclination of  $60^\circ$ , i.e. particles which must have been of energy greater than  $4 \times 10^9$  ev. at formation, and the larger ratio found in the vertical direction is attributed to a large excess of positive particles in the energy range  $2 \times 10^9$ – $4 \times 10^9$  ev. which can penetrate to sea-level vertically, but not at a zenith angle of  $60^\circ$ .

Our measurements give no support to this conclusion. If we make the assumption that there is no significant differential absorption of fast mesons in the atmosphere, the results of Table 2 show no measurable variation of the positive-negative ratio over the energy range at formation,  $3 \times 10^9$  ev. –  $12 \times 10^9$  ev. Since the reduction in sensitivity at high momenta in the magnetic lens apparatus is likely to be considerable at momenta lower than the highest reached in our apparatus, these results include the whole group of particles for which Ballario and his co-workers deduce a very small excess of positive particles. The results of the zenith angle experiment must then be attributed either to differential absorption effects or to an uncertainty in the technique of measurement, as, for example, to the use of an incorrect form of momentum spectrum at large zenith angles.

#### § 6. SIGNIFICANCE OF THE POSITIVE-NEGATIVE RATIO OF MESONS AND ITS MOMENTUM DEPENDENCE

In the absence of differential absorption of fast positive and negative mesons in the atmosphere, the ratio measured at sea-level must be directly connected to the ratio at formation. Further, the multiplicity of meson formation as a function of primary energy may be expected to determine the variation of positive-negative ratio at sea-level, although it is true that if meson formation is a plural process, or if the final states of the nucleons concerned are not equally probable, the relationship may be complicated.

Theoretical treatments which have been given (Heitler and Walsh 1945, Lewis, Oppenheimer and Wouthuysen 1948, Clementel and Puppi 1948) appear all to have discussed experimental values of the positive-negative ratio considerably smaller ( $\sim 1.15$ ) than that which we now propose, and it is clearly of the greatest importance that this discrepancy should be resolved. It is interesting however that Jánossy and Nicolson (1947), using a simplified model—that a primary of energy  $E$  gives rise to  $N$  mesons each of energy  $E/N$  where  $N$  is constant—to investigate the geomagnetic effects, find that  $N$  must be of the order 9. While this result is largely dependent on observations with mesons of lower energy than those measured in our experiment, it is clear that this model would lead to a value close to our measurement and agreeing with it in so far as there is no measurable momentum variation of the ratio.

In a recent discussion of meson production, Lewis, Oppenheimer and Wouthuysen have derived a momentum dependence of the positive-negative ratio approximately of the form  $\{(+/-) - 1\} \sim \epsilon^{-1}$  where  $\epsilon$  is the formation energy of the mesons. Our results at this stage do not completely exclude such a variation, which requires the quantity  $\{(+/-) - 1\}$  to vary by a factor two between the sea-level momenta  $10^9$  ev/c. and  $10^{10}$  ev/c., but they do show it to be unlikely. More extensive data are now being collected which may be expected to establish more clearly the momentum dependence of the positive-negative ratio.

## ACKNOWLEDGMENTS

The construction of the apparatus used in this investigation was made possible by a grant from the Treasury Fund of the Royal Society. The authors wish to thank Professor P. M. S. Blackett for his interest, encouragement and advice throughout the work, and are also grateful to Mr. M. G. Mylroi for his assistance in operating the spectrograph during the collection of data used in the investigation.

## REFERENCES

- BALLARIO, C., BENINI, M., and CALAMAI, G., 1948, *Phys. Rev.*, **74**, 1729.  
BERNARDINI, G., CONVERSI, M., PANCINI, E., and WICK, G. C., 1941, *La Ric. Scient.*, **20**, 1227.  
BLACKETT, P. M. S., 1937, *Proc. Roy. Soc. A*, **159**, 1.  
CLEMENTEL, E., and PUPPI, G., 1948, *Nuovo Cimento*, **5**, 529.  
HEITLER, W., and WALSH, P., 1945, *Rev. Mod. Phys.*, **17**, 252.  
HUGHES, D. J., 1940, *Phys. Rev.*, **57**, 592.  
JÁNOSY, L., and NICOLSON, P., 1947, *Proc. Roy. Soc. A*, **192**, 99.  
JONES, H., 1939, *Rev. Mod. Phys.*, **11**, 235.  
LEWIS, H. W., OPPENHEIMER, J. R., and WOUTHUYSEN, S. A., 1948, *Phys. Rev.*, **73**, 127.  
QUERCIA, I. F., RISPOLI, B., and SCIUTI, S., 1948, *Phys. Rev.*, **74**, 1728.  
ROSSI, B., 1948, *Rev. Mod. Phys.*, **20**, 537.

## The Effect of Holes in a Reacting Material on the Passage of Neutrons

BY D. J. BEHRENS

Theoretical Division, Atomic Energy Research Establishment, Harwell, Berks.

*Communicated by K. Fuchs ; MS. received 31st March 1949*

**ABSTRACT.** In this paper we discuss the increase in the migration length of neutrons in a reactor caused by the presence of holes in the reactor. It is shown how this effect can be evaluated in terms of a simple geometric function of the shape of the holes, and it is found that, in addition to a variation as the inverse overall density of the material in the reactor, the migration length also contains a term which depends upon the size and shape of each hole. When the hydraulic radius of the hole becomes comparable to the mean free path of neutrons in the reactor material, this last term becomes dominant, and it is therefore desirable that all holes should be kept as small as possible. Holes which are totally enclosed, or which contain a uni-directional infinity (cylinders) all give results of the same order of magnitude, but anything in the nature of a two-dimensional plane gash leads to a theoretically infinite increase in the migration length, and hence to a serious escape of spare neutrons.

We have considered the cases both of holes of regular shape and of the interstices between a random arrangement of regular-shaped solid bodies.

### § 1. INTRODUCTION

**I**N order to cool a high power nuclear reactor, it is necessary to introduce into the reactor sufficient space for the passage of the coolant. In many cases the substances used as coolants are of such a low density that neutron scattering and absorption by the coolant does not occur to any appreciable extent, and, for the purposes of calculating the passage of neutrons through the reactor, we may treat the coolant spaces as though they were empty holes. Holes may also be

required to provide space for experiments to be carried out in the reactor. If collisions between neutrons and the coolant can be disregarded, the reproductive constant  $k$  of the reactor \* is unaffected by the presence of holes, and the number  $N$  of collisions made by the average neutron during its lifetime (or during any stage of its life, e.g. slowing down, or thermal diffusion) is also unchanged.

However, owing to the introduction of holes, the scattering atoms of the reactor are less closely spaced than they would be without holes. This effectively raises the mean free path of neutrons in the system, and the average direct distance "as the crow flies" covered in the course of  $N$  collisions increases in the same proportion.

† If the holes are small and closely spaced, so that the mean free path in the solid material is large compared with the hole spacing, then the shape of the holes is of no consequence, and the effective mean free path varies inversely as the overall density of the reactor. Now the critical radius of a reactor of given shape varies as the effective mean free path, i.e. inversely as the density. It follows that the critical volume therefore varies as the inverse cube, and the critical mass as the inverse square, of the overall density of the reactor.

When the holes are large compared with the mean free path in the solid material, this simple treatment is no longer correct. While the arithmetic mean free path is the same, for given overall density, whether many paths are slightly lengthened by small holes or whether a few paths are greatly lengthened by large holes, the root-mean-square free path is substantially greater in the latter case than in the former. And, since the scattering processes are random and near-isotropic, it is with root-mean-square averages that we must be concerned. Consequently the larger the holes at given overall density, the greater will be the increase in the critical dimensions of the reactor.

We can make an estimate of the nature of this size effect. It may be expected that the increase in the square of the mean free path will, apart from the density factor, contain a term proportional to the proportion of neutron paths which pass through the holes and to the square of the amount by which these paths are lengthened.

Let  $\phi$  be the volume ratio of the holes to the material of the reactor, and  $v\phi$  the volume of each hole. Then we may imagine that there is a cell of material of volume  $v$  surrounding each hole, which may be assigned to that hole. Let  $s$  denote the surface area of a hole and let  $\lambda$  be the mean free path in the solid material. We assume that the total volume of the reactor is large compared with the volume  $v$  of a single cell, and that in every direction the dimensions of the reactor are large compared with  $\lambda$ .

Then the proportion of neutron paths which pass through a hole will be proportional to the ratio of a surface layer  $\lambda$  thick over the surface of the hole to the total volume of material in the cell associated with the hole. This ratio is  $\lambda s/v$ .

The amount by which each path is lengthened must be proportional to the dimensions of the hole, i.e. to  $\phi v/s$ . Hence the additional size-effect correction to the mean square free path must vary as  $(\lambda s/v)(\phi v/s)^2$ . Bearing in mind that  $r$ ,

\*  $k$  is the number of neutrons of the second generation which are born in the reactor as the result of processes induced by one neutron of the first generation.  $(k-1)/k$  is the proportion of neutrons which are superfluous to those required to maintain the reaction, and which can therefore be used for experimental purposes—in addition of course to replenishing the losses by leakage from the surface of the reactor.

the hydraulic radius of the hole, varies as  $\phi v/s$ , we may say that the size-effect correction to  $\lambda^2$  must be proportional to  $\phi\lambda r$ . Dividing by  $\lambda^2$ , we get a proportionate increase factor which must vary as  $\phi r/\lambda$ .

This argument is developed in the present report with accuracy and in detail. The numerical coefficient of the term  $\phi r/\lambda$  will be found to vary according to the shape of the hole. For a spherical hole the coefficient is 9/8, and for an infinite circular cylindrical hole it is 4/3.

## §2. PASSAGE OF NEUTRONS IN A SYSTEM WITHOUT HOLES

When, at a later stage, we consider the effect of holes, we shall assume that the ratio of capture probability to scattering probability at the end of each free path is unaffected by the presence of holes\*, and hence that the total number  $N$  of collisions made by each neutron during its lifetime is unchanged. We shall see that the root-mean-square total distance (as the crow flies) travelled by a neutron during the course of a given number  $n$  of collisions is increased owing to the presence of holes in a ratio which for large  $n$  is independent of the actual value of  $n$ . Consequently we may disregard the statistical variation which occurs in  $N$ , the total number of collisions made by a neutron, and calculate what is the mean square distance travelled in the course of  $N$  collisions, without specifying just what the value  $N$  actually is. If the scattering processes are random, then the probability of any particular length of free path must fall off exponentially as the length is increased. If  $\lambda$  is the arithmetic mean free path, then the probability of a free path having a length between  $z$  and  $z + \delta z$  is given by the expression

$$\frac{1}{\lambda} \exp(-z/\lambda) \delta z. \quad \dots\dots (1)$$

Denote by  $L_0^2$  the mean square direct distance, as the crow flies, travelled by a neutron in the course of  $N$  collisions. If  $\lambda$  is unchanged throughout the period considered, we have

$$L_0^2 = \int_0^\infty z^2 \frac{N}{\lambda} \exp(-z/\lambda) dz = 2N\lambda^2 \quad \dots\dots (2)$$

for isotropic scattering. We have made here the tacit assumption that the system is large compared with  $\lambda$ , so that we can integrate without undue error over the full range to infinity of  $z$ .

If the conditions of scattering are not isotropic, we still have  $L_0^2 = Nl^2$ , but  $l^2$  (which may be described as the transport mean square free path) is no longer equal to  $2\lambda^2$ . The result,

$$L_0^2 = Nl^2, \quad \dots\dots (2a)$$

is a general formula, and the particular relation  $l^2 = 2\lambda^2$  holds good for isotropic scattering.

## §3. PASSAGE OF NEUTRONS IN A SYSTEM WITH HOLES

Let us assume now that the system is interspersed with holes, each of which may be taken to be associated with a surrounding cell of material, of volume  $v$ , in which the mean free path is still  $\lambda$ . Let  $\phi$  be the volume ratio hole/material, so that  $v\phi$  is the volume of each hole.

\* This assumption will clearly be justified if the composition of the material of the reactor is of the same nature in all regions in the vicinity of the hole.

Consider now straight passages through the hole in any given direction, as specified by the value of a unit-vector  $\Omega$ . Let  $X$  be the length of such a passage, and let  $\psi(X, \Omega)\delta X$  denote the cross section of passages through the hole in the direction  $\Omega$  which have lengths between  $X$  and  $X+\delta X$ .

Integrating, for any value of  $\Omega$ , we must have

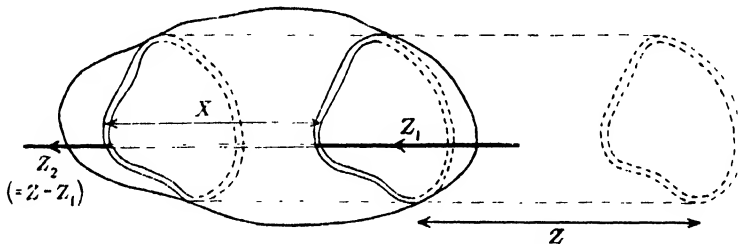
$$\int_0^\infty X\psi(X, \Omega) dX = \phi v. \quad \dots\dots (3)$$

The integral is given as extending to infinity, although of course  $\psi(X, \Omega)=0$  for all  $X$  in excess of the maximum diameter of the hole.

The quantity  $\int_0^\infty \psi(X, \Omega) dX$  is in general a function of the direction  $\Omega$ , as the hole has different projected areas in different directions, except in the special case where it is spherical. Now every passage cuts the surface of the hole twice, once on entering and once on leaving. It is clear that we can write

$$\int_0^\infty \psi(X, \Omega) dX = \iint_s \frac{1}{2} |\Omega \cdot ds|,$$

where the right-hand expression denotes the positive value of the scalar product of  $\Omega$  and  $ds$ , i.e. the element of area multiplied by the cosine of the acute angle between  $\Omega$  and the normal to the surface.



Cross section of annulus is  $\psi(X, \Omega) \delta X$ .

Averaging over all directions, we get

$$\int_\Omega \int_0^\infty \psi(X, \Omega) dX \frac{d\Omega}{4\pi} = \int_\Omega \iint_s \frac{1}{2} |\Omega \cdot ds| \frac{d\Omega}{4\pi} = \frac{1}{4} s, \quad \dots\dots (4)$$

since the mean value of the cosine is  $\frac{1}{2}$ .

Now let  $p(z, \Omega, X)\delta X$  denote the probability that, during the course of a free path in the material of length  $z$  in the direction  $\Omega$ , a neutron will emerge into a hole where the passage length lies between  $X$  and  $X+\delta X$ . Then it is clear that (see diagram)

$$p(z, \Omega, X) = z\psi(X, \Omega)/v. \quad \dots\dots (5)$$

First of all we shall treat the holes as being widely separated, i.e.  $v \gg s\lambda$ , so that no neutron need ever be considered to pass through more than one hole in the course of a single free path. If  $\phi$  is not very small, this implies the case of large holes.

The probability that a free path in the direction  $\Omega$  will be increased in length from  $z$  to  $z+X$ , owing to the presence of a hole, is given by  $p(z, \Omega, X)$ .

Therefore we get, instead of (2) above, the equation

$$L^2 = N \int_{\Omega} \int_0^{\infty} \left[ \int_0^{\infty} (z+X)^2 p(z, \Omega, X) dX + z^2 \left\{ 1 - \int_0^{\infty} p(z, \Omega, X) dX \right\} \right] \\ \times \frac{1}{\lambda} \exp(-z/\lambda) dz \frac{d\Omega}{4\pi} \\ = 2N\lambda^2 + 4\phi N\lambda^2 + N \int_{\Omega} \int_0^{\infty} \frac{\lambda}{v} X^2 \psi(X, \Omega) dX \frac{d\Omega}{4\pi}, \quad \dots\dots(6)$$

which may be combined with (2) to give

$$L^2/L_0^2 = 1 + 2\phi + \frac{1}{2\lambda v} \int_{\Omega} \int_0^{\infty} X^2 \psi(X, \Omega) dX \frac{d\Omega}{4\pi}. \quad \dots\dots(7)$$

This is the general formula for the case of widely separated holes. If, instead of equation (2), we use the more general form (2a), this results in the same proportionate change in  $L^2$  as in  $L_0^2$ , and equation (7) therefore still holds good.

Consider now the opposite extreme, where the holes are very closely spaced, i.e.  $v \ll s\lambda$ . In the limit, the probability of entering a hole is independent of any holes which may already have been entered during the current free path.

The probability of entering no hole at all during a free path in the material of length  $z$  in the direction  $\Omega$  is  $\exp \left[ - \int_0^{\infty} p(z, \Omega, X) dX \right]$ , say  $\exp [-P(z, \Omega)]$ .

The probability of entering  $n$  holes, of lengths respectively  $X_1, X_2 \dots X_n$ , can be shown to be

$$\frac{1}{n!} \prod_{j=1}^n [p(z, \Omega, X_j)] \exp [-P(z, \Omega)].$$

Hence we obtain, instead of the factor between the square brackets in (6) above, the corrected expression

$$\left[ z^2 \exp [-P(z, \Omega)] + \sum_{n=1}^{\infty} \left\{ \prod_{j=1}^n \int_0^{\infty} \right\} \frac{\exp [-P(z, \Omega)]}{n!} \left( z + \sum_{j=1}^n X_j \right)^2 \right. \\ \left. \times \prod_{j=1}^n p(z, \Omega, X_j) \prod_{j=1}^n dX_j \right]. \quad \dots\dots(6a)$$

This expression can, without undue trouble, be separated into three parts, the coefficients respectively of the second, first and zero powers of  $z$ , and reduces to the form

$$z^2(1+\phi)^2 + \int_0^{\infty} X^2 p(z, \Omega, X) dX,$$

so that, instead of (7), we get the expression

$$L^2/L_0^2 = 1 + 2\phi + \phi^2 + \frac{1}{2\lambda v} \int_{\Omega} \int_0^{\infty} X^2 \psi(X, \Omega) dX \frac{d\Omega}{4\pi}. \quad \dots\dots(8)$$

This differs from (7) in the addition of a  $\phi^2$  term.

When  $v$  and  $s\lambda$  are of the same order, the average number of holes entered during the course of a free path of length  $Z$  in the solid is still  $Zs/4v$ . Suppose this number to be  $(n + \epsilon)$ , where  $n$  is an integer and  $\epsilon$  a fraction between the limits



0 and 1. We shall examine the case in which it is assumed that, for a free path of length  $Z$ , there is a probability  $\epsilon$  of entering  $(n+1)$  holes, and  $(1-\epsilon)$  of entering  $n$ .

Then if  $X$  is the lengthening per hole of the passage  $Z$ , we get, instead of  $Z^2$  in equation (2), the quantity

$$\epsilon(Z+X_1+X_2+\dots+X_{n+1})^2+(1-\epsilon)(Z+X_1+X_2+\dots+X_n)^2.$$

Instead of the expression (6a) we therefore obtain

$$\begin{aligned} & \epsilon \left[ \left( Z + \sum_{j=1}^{n+1} X_j \right)^2 \prod_{j=1}^{n+1} \left\{ \frac{p(z, \Omega, X_j)}{P(z, \Omega)} \right\} \prod_{j=1}^{n+1} dx_j \right] + (1-\epsilon) \left[ \left( Z + \sum_{j=1}^n X_j \right)^2 \right. \\ & \quad \left. \times \prod_{j=1}^n \left\{ \frac{p(z, \Omega, X_j)}{P(z, \Omega)} \right\} \prod_{j=1}^n dX_j \right] \\ & = \epsilon [Z^2 + (n+1)2z\bar{X} + (n+1)\bar{X}^2 + n(n+1)\bar{X}^2] \\ & \quad + (1-\epsilon)[Z^2 + n2Z\bar{X} + n\bar{X}^2 + n(n-1)\bar{X}^2] \\ & = Z^2 + 2Z\bar{X}(n+\epsilon) + \bar{X}^2(n+\epsilon) + \bar{X}^2(2n\epsilon + n^2 - n). \end{aligned}$$

Putting now  $\bar{X} = 4\phi v/s$ ,  $\bar{X}^2 = 16Q\phi^2 v^2/s^2$  and  $Z = (n+\epsilon)4v/s$ , we get the expression

$$Z^2 + 2Z\bar{X}\phi + 4Qv\phi^2 z/s + (16\phi^2 v^2/s^2)(2n\epsilon + n^2 - n).$$

The probability of occurrence of  $(Z, \delta Z)$  is  $(1/\lambda) \exp(-z/\lambda) dz$ , so that the corresponding probability of  $(n, \epsilon, \delta\epsilon)$  is  $(4v/s\lambda) \exp[-(n+\epsilon)4v/s\lambda] d\epsilon$ .

We have therefore to evaluate

$$\begin{aligned} & \int_0^\infty (z^2 + 2z^2\phi + 4Qv\phi^2 z/s) \frac{1}{\lambda} \exp(-z/\lambda) dz \\ & \quad + \int_{\epsilon=0}^1 \sum_{n=0}^\infty \exp(-4vn/s\lambda) \frac{4v}{s\lambda} \frac{16\phi v^2}{s^2} (2n\epsilon + n^2 - n) d\epsilon \\ & = 2\lambda^2 + 4\lambda^2\phi + 4Q\phi^2 v\lambda/s + 2\phi^2 \lambda^2 (4v/s\lambda) / [\exp(4v/s\lambda) - 1] \end{aligned}$$

Dividing by  $2\lambda^2$ , we obtain the result that

$$L^2/L_0^2 = 1 + 2\phi + \phi^2(4v/s\lambda)/[\exp(4v/s\lambda) - 1] + \frac{1}{2\lambda v} \int_\Omega \int_0^\infty X^2 \psi(X, \Omega) dX \frac{d\Omega}{4\pi}. \quad \dots\dots(9)$$

It may be verified that, if  $v \gg s\lambda$ , equation (9) reduces to (7), while if  $v \ll s\lambda$  it gives the same result as (8). The last expression is therefore a form which may reasonably be used to cover holes of all sizes.

Now in the case of coolant channels it is customary to define a hydraulic radius, which is given by  $r = 2\phi v/s$  (so that, for an infinite circular cylinder,  $r$  is in fact the radius of the cylinder). It is convenient to use this notation for all holes, so that we may re-write (9) in the form

$$L^2/L_0^2 = 1 + 2\phi + \phi^2(2r/\phi\lambda)/[\exp(2r/\phi\lambda) - 1] + Qr\phi/\lambda, \quad \dots\dots(10)$$

$$\text{where} \quad Q = (1/r^2 s) \int_\Omega \int_0^\infty X^2 \phi(X, \Omega) dX \frac{d\Omega}{4\pi}. \quad \dots\dots(11)$$

(10) is a general expression for holes of any kind, while (11) shows  $Q$  to be a function only of the shape of the hole.  $Q$  is the mean square passage length through the hole divided by the square of the mean, and hence must exceed unity.

Values of  $Q$  for particular shapes of hole are as follows:

Spherical hole	$Q = 1.125$
Regular tetrahedron hole	$Q = 1.583$
Infinite cylinder of circular section	$Q = 1.333$
Infinite cylinder of regular hexagonal section	$Q = 1.397$
Infinite cylinder of square section	$Q = 1.487$
Infinite cylinder of equilateral triangular section	$Q = 1.648$
Cored spherical hole	$Q = 1.125 \times f(\mu)$
Cored circular cylinder	$Q = 1.333 \times F(\mu)$

(where  $\mu$  = inner-radius/outer-radius, and  $f$  and  $F$  are tabulated below).

$\mu$	0.0	0.1	0.2	0.3	0.4	0.5	0.6	0.7	0.8	0.9	1.0
$f(\mu)$	1.000	1.001	1.005	1.016	1.04	1.07	1.11	1.18	1.27	1.43	$\infty$
$F(\mu)$	1.0000	1.0258	1.0536	1.0839	1.1178	1.1567	1.2023	1.2604	1.3422	1.53	$\infty$

The fact that  $f$  and  $F$  tend to infinity as  $\mu \rightarrow 1$  is in accord with the result that  $Q$  is infinite for a two-dimensionally infinite gash extending through the reactor.

The term in  $\phi^2$  falls away rapidly as  $r/\lambda\phi$  increases. When  $r$  reaches the value  $3\frac{1}{2}\lambda\phi$ , this term is already less than  $\phi^2/100$ . The final term in (10) however increases more rapidly than the other decreases, as may be shown by re-writing (10) in the form

$$L^2/L_0^2 = 1 + 2\phi + (r\phi/\lambda)[\coth(r/\phi\lambda) + (Q - 1)]. \quad \dots\dots (12)$$

Since, as we have seen,  $Q$  cannot be less than unity,  $Q - 1$  is essentially non-negative. Again,  $\coth(r/\phi\lambda)$  is at least as great as  $\phi\lambda/r$ , its limiting value as  $r/\phi\lambda \rightarrow 0$ . Thus  $L^2/L_0^2$  is in all cases at least as great as  $(1 + \phi)^2$ .

The following typical values of  $L^2/L_0^2$  apply to a square lattice of cylindrical holes:

Lattice spacing Hole diameter	10	5	3	2
$r/\lambda$ very small	1.016 <i>1.000</i>	1.066 <i>1.000</i>	1.200 <i>1.000</i>	1.548 <i>1.000</i>
$r/\lambda = \frac{1}{2}$	1.019 <i>1.003</i>	1.079 <i>1.012</i>	1.234 <i>1.028</i>	1.609 <i>1.039</i>
$r/\lambda = 1$	1.026 <i>1.010</i>	1.108 <i>1.039</i>	1.319 <i>1.099</i>	1.815 <i>1.172</i>
$r/\lambda = 3$	1.047 <i>1.031</i>	1.194 <i>1.066</i>	1.574 <i>1.312</i>	2.466 <i>1.593</i>

In each case the upper figure is the value of  $L^2/L_0^2$  obtained by the use of (12). The lower figure in italics is the ratio of this value to the simple density correction  $(1 + \phi)^2$ .

#### § 4. ANISOTROPIC EFFECTS

In all cases except those of spherical holes (with or without concentric cores) we have seen that  $\int_0^\infty \psi(X, \Omega) dX$  and  $\int_0^\infty X^2 \psi(X, \Omega) dX$  vary with  $\Omega$ .

This means that  $L^2$ , instead of having a component  $L^2/3$  in all directions, becomes an anisotropic function.

Examining equation (10), and the argument by which we established the equation, it is clear that only the function  $Q$  contributes an anisotropic term to  $L^2$ , and that the contribution in any direction is given by

$$\int_{\Omega} (1/2\lambda v) \int_0^{\infty} X^2 \cos^2 w \psi(X, \Omega) dX \frac{d\Omega}{4\pi},$$

where  $w$  is the angle between the direction under consideration and the direction of  $\Omega$ .

For all cylindrical holes (plain or cored, and of any section) we get an effect twice as great in the axial as in the transverse directions:

$$\left. \begin{aligned} 3L_{\text{axial}}^2/L_0^2 &= 1 + 2\phi + \phi^2(2r/\phi\lambda)/[\exp(2r/\phi\lambda) - 1] + \frac{3}{2}Qr\phi/\lambda, \\ 3L_{\text{transv.}}^2/L_0^2 &= 1 + 2\phi + \phi^2(2r/\phi\lambda)/[\exp(2r/\phi\lambda) - 1] + \frac{3}{4}Qr\phi/\lambda, \end{aligned} \right\}$$

where  $Q$  is still the average value for all directions, namely 1.333 for a circular cylinder, 1.487 for one of square section, etc. It may be verified that  $\Sigma Q$  for the three directions at right angles is unchanged, for  $\frac{3}{2} + 2(\frac{3}{4}) = 3$ .

#### §5. HOLES FORMED AS INTERSTICES BETWEEN A RANDOM ARRANGEMENT OF SOLID BODIES IN POINT OR LINE CONTACT

Hitherto we have dealt only with the case of holes of a regular shape. Sometimes however we are concerned with the holes which arise as interstices between a random arrangement of solid bodies. We shall assume that the solid bodies are in point or line contact, but nowhere in surface contact, so that the total surface area of the bodies will be equal to that of the holes.

Let  $\bar{X}$  and  $\bar{X}'$  denote respectively the mean passage length through a hole and through a solid body respectively. Then, if  $V$  is the total volume of a large part of the reactor, and  $S$  is the surface area of hole (or solid) within  $V$ , we have

$$\bar{X} = \frac{\phi}{1+\phi} \frac{4V}{S}; \quad \bar{X}' = \frac{1}{1+\phi} \frac{4V}{S}.$$

Also, by the definition of  $Q$ ,

$$\bar{X}^2 = \frac{\phi^2}{(1+\phi)^2} Q \frac{16V^2}{S^2}$$

and, defining  $Q'$  by analogy,

$$\bar{X}'^2 = \frac{1}{(1+\phi)^2} Q' \frac{16V^2}{S^2}.$$

Now, if the bodies are randomly arranged, there will be no correlation between the values of  $X$  and of  $(X+X')$  measured in one and the same straight line.

Consequently we have not only  $\bar{X} = (4V/S) - \bar{X}'$ , but also

$$\bar{X}^2 = \frac{16V^2}{S^2} - \frac{8V}{S} \bar{X}' + \bar{X}'^2. \quad \dots\dots(13)$$

This result is equivalent to assuming that the mean square deviations of  $X$  and  $X'$  are equal, i.e.  $\bar{X}'^2 - \bar{X}'^2 = \bar{X}^2 - \bar{X}^2$ . For since  $\bar{X} = (4V/S) - \bar{X}'$  we must have

$$\bar{X}^2 = \frac{16V^2}{S^2} - \frac{8V}{S} \bar{X}' + \bar{X}'^2$$

and if  $\bar{X}^2 - \bar{X}^2 = \bar{X}'^2 - \bar{X}'^2$ .

Then, adding, we obtain equation (13) which, from the equations above, gives

$$\frac{\phi^2}{(1+\phi)^2} Q \frac{16V^2}{S^2} = \frac{16V^2}{S^2} - 2 \frac{1}{1+\phi} \frac{16V^2}{S^2} + \frac{1}{(1+\phi)^2} Q' \frac{16V^2}{S^2}.$$

Multiplying by  $(1+\phi)^2$  and dividing by  $16V^2/S^2$ , we get

$$\phi^2 Q = (1+2\phi+\phi^2) - (2+2\phi) + Q', \quad \text{i.e. } (Q-1) = (Q'-1)/\phi^2. \quad \dots\dots(14)$$

Likewise, if  $r$  denotes the hydraulic radius of the hole and  $r'$  that of the solid, we have

$$r = 2V_{\text{hole}}/S_{\text{hole}}, \quad r' = 2V_{\text{solid}}/S_{\text{solid}}.$$

But the  $S$ 's are equal, so that  $r = r' V_{\text{hole}}/V_{\text{solid}}$ , or

$$r \doteq r' \phi. \quad \dots\dots(15)$$

Substituting in (12) from (14) and (15) we get

$$L^2/L_0^2 = 1 + 2\phi + \frac{r'}{\lambda} \left( \phi^2 \coth \frac{r'}{\lambda} + (Q'-1) \right). \quad \dots\dots(16)$$

Thus we can calculate the streaming effect not only for regular holes but also for those formed between a random arrangement of regular solids. In such cases  $\phi$  is often large, and the coth term must be taken into account. Algebraically, also, equation (12) containing  $Q-1$  is more suitable for substitution by (14) than is (10), which contains  $Q$  itself.

## § 6. CONCLUSIONS

The migration length  $M$  of neutrons in a system is defined so that  $6M^2$  is the mean square distance travelled by a neutron in the whole course of its life. This includes the time spent whilst the neutron is slowing down from its initial energy and the time spent whilst diffusing as a thermal neutron until it is finally absorbed.

The critical size of a reactor depends on  $M^2/(k-1)$ , and, therefore, the migration length is an important design quantity. For a given size of reactor we shall be interested in keeping the migration length as small as possible, since a decrease in  $M^2$  means that a lower value of  $k$  is required to maintain the reaction. Now the value of  $k$  required to maintain the reaction is less than that produced by the lattice by a quantity  $\Delta k$ , usually referred to as "spare  $k$ ", which (while taken up by control rods when not otherwise being utilized) may provide an excess of neutrons for experimental purposes, e.g. irradiation of materials for isotope production.

The theory developed in this paper may be applied to any stage of the neutron's history, provided of course the statistical methods employed are applicable, i.e. within the scope of the age velocity theory and the simple neutron diffusion theory. It is clear that the values of  $L^2/L_0^2$  which we have calculated can be applied directly to the migration length, to give  $M^2/M_0^2$ , where  $M_0$  is the migration length in a system without holes.

To summarize: the effect of holes on  $M^2$  is made up of two parts: firstly, there is an isotropic increase in  $M^2$  proportional to  $(1+\phi)^2$ , i.e. the inverse square of the overall density of the material. In addition to this, there is a further correction term, proportional to the ratio of the hydraulic ratio of the hole to the mean free path in the solid, the volume ratio  $\phi$ , and to a function  $Q$  of the shape of the hole.  $Q$  is in fact the ratio of the mean square chord length through the hole to the square of the mean chord length, and is least for a sphere (for which it is 9/8). For

totally enclosed and cylindrical holes,  $Q$  varies between fairly narrow limits, being seldom in excess of  $5/3$  for reasonable shapes. Any more than unidirectional infinity, however, by offering very long chords over a finite solid angle, results in a theoretically infinite increase of  $Q$ , and, even in the case of a finite reactor surrounded by a reflector, to a substantial increase in  $M^2$ , and hence to a serious loss of spare  $k$ . Such multi-directional holes (e.g. plane gashes) are therefore, if possible, to be avoided from the point of view of conservation of neutrons within the system.

## NOTATION

$k$  = reproductive constant of reactor.

$N$  = number of collisions made by a neutron.

$\lambda$  = mean free path of a neutron through solid material of reactor.

$l^2$  = transport mean square free path (for isotropic scattering,  $l^2 = 2\lambda^2$ ).

$\phi$  = volume ratio: holes/material.

$v\phi$  = volume of each hole.

$s$  = surface area of each hole.

$S$  = surface area of a cell.

$V$  = volume of a cell.

$r$  = hydraulic radius of each hole:  $r = 2v\phi/s$ .

$z$  = length of a (specified) free path through solid material.

$L_0$  = root-mean-square distance travelled by a neutron in  $N$  collisions in the absence of holes.

$L$  = root-mean-square distance travelled by a neutron in  $N$  collisions in the presence of holes.

$X$  = length of a straight passage through a hole.

$\Omega$  = unit vector specifying direction.

$\psi(X, \Omega)\delta X$  = cross section of passages of length between  $X$  and  $X + \delta X$  in the direction  $\Omega$  through a hole.

$p(z, \Omega, X)$  = probability that a neutron, during the course of a free path of length  $z$  in the direction  $\Omega$ , will emerge into a passage of length  $X$ .

$$P(z, \Omega) = \int_0^\infty p(z, \Omega, X) dX.$$

$Q$  = ratio of mean square passage length through hole to square of mean passage length, so that we have

$$Q = \frac{1}{r^2 s} \int_\Omega \int_0^\infty X^2 \psi(X, \Omega) dX \frac{d\Omega}{4\pi}.$$

$\mu$  = ratio of inner to outer radius for a cored hole.

$M$  = migration length of neutrons.

## Betatron Injection into Synchrotrons

By F. K. GOWARD

Atomic Energy Research Establishment, Harwell, Didcot, Berks.

*Communicated by D. Taylor ; MS. received 13th December 1948, and in amended form 23rd May 1949*

**ABSTRACT.** The paper states simply the factors influencing the proportion of electrons which may be trapped and accelerated in a transition from betatron to synchrotron operation; this transition is a vital factor influencing the design of the normal electron-synchrotron. Machines of various energies are studied, and it is shown that the important considerations in the design are quite different in different energy ranges. The theoretical predictions are compared with experimental evidence obtained on 14 and 70 mev. synchrotrons, and the agreement is sufficient to give confidence in the simplified theory.

### §1. INTRODUCTION

SEVERAL adequate papers on the theory of electron-synchrotron operation have been published; it will be convenient to choose only one of them (Bohm and Foldy 1946) as the theoretical basis of the discussion which follows and to assume the results given there without further proof. These theoretical papers have given little detailed attention to the experimental behaviour to be expected from machines of various energies. Such consideration is very necessary, since electron-synchrotrons are now being operated or constructed in Britain (and elsewhere) with energies ranging from 14 to 375 mev., and factors of importance at one energy are quite unimportant at other energies.

To emphasize the difference between the various machines, an idealized picture will be presented of the fraction of electrons captured during the transition from betatron to synchrotron. The process will be over-simplified to separate clearly the more important physical effects, and experimental evidence will be advanced to justify the simplification made. Such a simplified theory is very desirable for general comparison between machines (see for example the paper on synchrotron resonator design by Goward *et al.* 1949) and for initial design purposes. The more exact theories may be applied for more particular considerations.

### §2. THEORY OF INJECTION

#### 2.1. General Factors Influencing Injection Efficiency

The minimum resonator voltage,  $v$ , required to accelerate an electron, if it happens to be at precisely the optimum phase and radius when it is injected from the betatron to the synchrotron, is given by

$$v = 4\pi^2 c^{-1} f E r_0 \cos 2\pi f t, \quad \dots\dots(1)$$

where  $f$  is the frequency of the magnetic field in cycles/sec.,  $E$  is the peak energy of the machine in electron volts, and  $r_0$  is the equilibrium orbit radius in centimetres.  $v$  is maximum at the start of the acceleration, and since  $r_0$  is increased proportionately to  $E$  for the various synchrotrons,  $v_0$ , the maximum value of  $v$  is proportional to  $E^2$ . Taking a peak field of 10,000 gauss,  $r_0$  is equal to  $10^{-6}E/3$ , and, therefore, if  $f$  is 50,

$$v_0 = 2 \cdot 2 \times 10^{-14} E^2. \quad \dots\dots(2)$$

Electrons are normally injected into a synchrotron not only at the correct phase and radius but over quite a range of radii and phases. The resonator voltage must, therefore, be somewhat greater than  $v_0$ , how much greater depending in a rather complex manner on the size of the machine and its operating parameters.

If the electrons are accelerated by betatron action from an initial total energy,  $E_1$ , to a final total energy,  $E_s$ , and the betatron action then ceases suddenly, an electron beam is obtained with a spread of radii given by

$$\rho_0 = \rho_1(E_1\beta_1/E_s\beta_s), \quad \dots\dots(3)$$

where  $\beta$  is the velocity of the electrons relative to the velocity of light. The spread of radii,  $\pm \rho_1$ , about the equilibrium orbit radius  $r_0$ , is, for the moment, assumed to fill the donut entirely at injection, and the energy of the electrons is assumed to be that corresponding to an instantaneous circle at their particular radii, i.e. oscillations about the instantaneous circle are neglected. It is also assumed that the electrons are distributed uniformly in phase and in radius between the limits  $r_0 - \rho_0$  and  $r_0 + \rho_0$ .

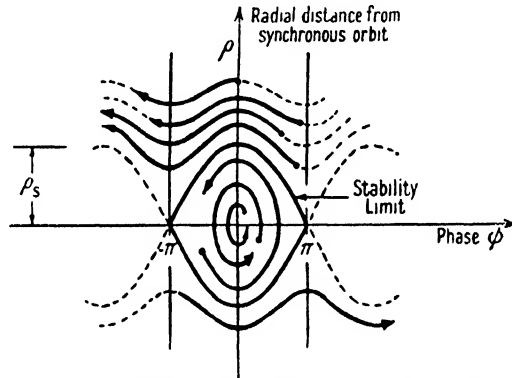


Figure 1. Oscillations in phase and radius ( $V \gg v_0$ ).

Suppose, now, that the betatron action ceases suddenly and that a voltage  $V$  is supplied suddenly to the R.F. resonator, the frequency being such that the synchronous orbit coincides with the betatron equilibrium orbit. The resonator may be considered as producing a wave which travels round the synchrotron with the same angular velocity as the electrons injected from the betatron. Provided the voltage  $V$  is considerably greater than  $v_0$  the electrons will tend to oscillate approximately sinusoidally in phase about the zero phase point. This follows from the relation giving the phase,  $\phi_s$ , at which the electrons are accelerated without oscillations, which is

$$\sin \phi_s = v_0/V. \quad \dots\dots(4)$$

To the phase oscillations correspond equivalent oscillations in radius or energy. These oscillations are represented in Figure 1, where the phase is measured relative to the R.F. wave. It may be seen that, if the spread of radii of the electrons before the radio frequency is turned on is  $\pm \rho_0$ , the final spread of those electrons which are caught is  $\pm \rho_s$ , where  $\rho_s$  is marked on the figure. Only those electrons are trapped which lie within the curve marked "stability limit"; electrons outside this region lose or gain phase continuously as shown. It is assumed that electrons are caught provided

$$\rho < \rho_s \cos \phi/2. \quad \dots\dots(5)$$

$\rho_s$  is given by Bohm and Foldy as

$$\rho_s = \frac{r_0}{(1-n)\beta_s^2} \left[ \frac{2V}{\pi k E_s} \right]^{\frac{1}{2}}, \quad \dots\dots(6)$$

$k$  being given by

$$k = 1 + \frac{n}{(1-n)\beta_s^2}, \quad \dots\dots(7)$$

where  $n$  is the usual index in the magnetic field law. It may be seen that  $\rho_s/\rho_0$  must be substantially greater than unity in order that a large proportion of electrons may be trapped. Examples of inefficient and efficient trapping are shown in Figures 2(a) and 2(b), where it is assumed that the resonator voltage,  $V$ , is varied

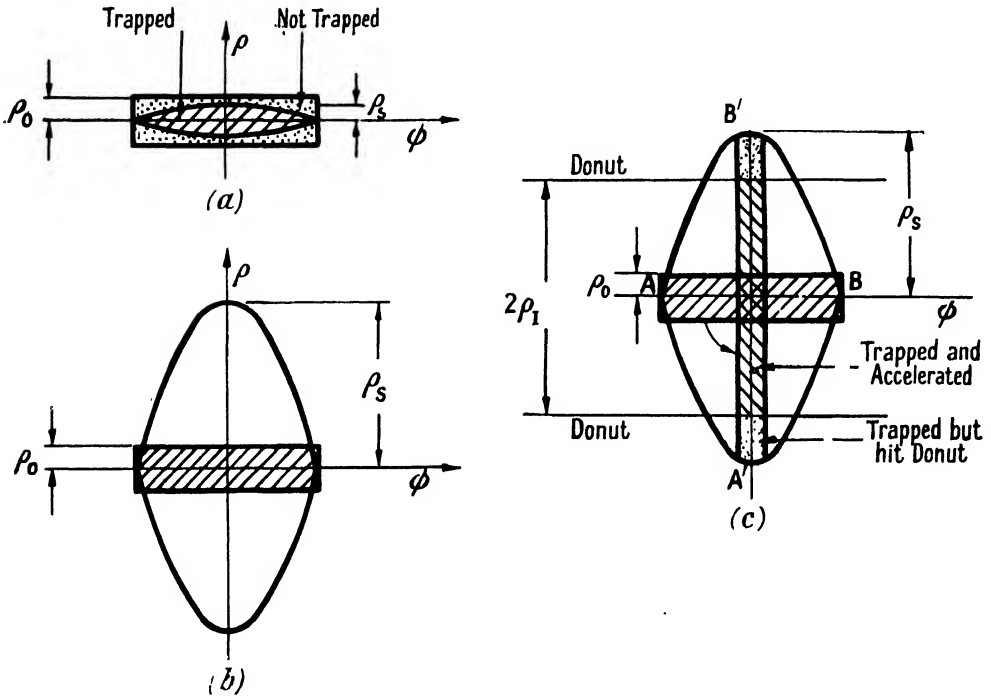


Figure 2. Trapping efficiency ( $V \gg v_0$ ).

- (a) Inefficient trapping (resonator volts small).
- (b) Efficient trapping (resonator volts large).
- (c) Efficient trapping but donut walls hit.

to vary  $\rho_s$ , always keeping it very much greater than  $v_0$ . Figure 2(c) indicates what may happen if  $\rho_s$  is made so large that it exceeds the donut half-width,  $\rho_1$ . Electrons are then lost, even though they are trapped in stable oscillations. In the figure the period of rotation on the phase diagram of all electrons has been assumed constant; in fact the period decreases as the distance from the centre increases, so that  $A'B'$  should be an S-shaped curve. This does not affect the fraction of electrons collected.

Qualitatively, then, the basic curve giving the fraction of electrons accelerated (i.e. injection efficiency) against resonator voltage may be expected to be of the form shown by the full curve in Figure 3, provided always that the voltage across the resonator,  $V$ , is substantially greater than the minimum voltage  $v_0$  required to accelerate the electrons. It will be seen in §§ 2.2 and 2.3 that, not only is this



basic curve of the same form for synchrotrons of various energies, but the absolute values of the resonator voltages at which the effects occur remain approximately constant.

The factor which does differ markedly in synchrotrons of different energies is the voltage  $v_0$  defined by equation (2); this voltage is a few volts in the smaller energy machines and a few kilovolts in the larger energy machines. The efficiency does not rise suddenly to the full curve of Figure 3 at the voltage  $v_0$ , however, since the condition that  $V/v_0$  is much greater than unity does not hold in this region and  $\phi_s$  is therefore not zero (see equation (4)). Electrons are trapped over a limited range of phases only, and the efficiency rises to the curve of Figure 3 relatively gradually, as is shown qualitatively by the dotted curve. Widely differing behaviour may be expected as  $v_0$ , and the position of the dotted curve, varies.

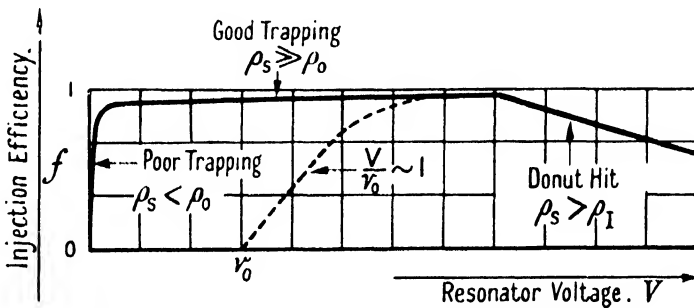


Figure 3. Injection efficiency versus resonator voltage.

The above qualitative considerations will now be developed quantitatively, adopting the same mode of treatment, i.e. considering first the behaviour when  $V \gg v_0$  (§§ 2.2 and 2.3) and later extending it to the region where  $V$  is of the same order as  $v_0$  (§ 2.4).

## 2.2. Trapping Efficiency (for $V \gg v_0$ )

The qualitative picture of the trapping of electrons in stable phase oscillations, when  $V \gg v_0$  (see Figures 2(a) and 2(b)) may readily be expressed quantitatively. Using the condition of equation (5), a simple integration shows that, for  $\rho_0 \leq \rho_s$ , the fraction of electrons trapped,  $f_1$ , is given by

$$f_1 = 1 - (2/\pi) [\sin^{-1}(\rho_0/\rho_s) - (\rho_s/\rho_0) \{1 - \cos \sin^{-1}(\rho_0/\rho_s)\}]. \quad \text{.....(8)}$$

For  $\rho_0 \geq \rho_s$ ,

$$f_1 = 2\rho_s/\rho_0\pi. \quad \text{.....(9)}$$

Using equations (3) and (6), equations (8) and (9) may be expressed in terms of the parameter  $V/V_0$  by the relation

$$(\rho_s/\rho_0) = (V/V_0)^4, \quad \text{.....(10)}$$

where

$$V_0 = \left[ (1-n)^2 \beta_s^2 E_1^2 \left( \frac{\pi k}{2E_s} \right) \right] \left( \frac{\rho_I}{r_0} \right)^2. \quad \text{.....(11)}$$

The resulting curve for the fraction,  $f_1$ , plotted against  $V/V_0$ , is shown in Figure 4. The condition for loss of 36% or less of the electrons is

$$V \geq V_0. \quad \text{.....(12)}$$

Equation (12) gives a simple physical meaning to the parameter  $V_0$  but  $V_0$  is really a parameter derived from the constants of the machine by equation (11).

From equations (11) and (12) follows the interesting fact that the absolute minimum voltage required across the resonator for efficient trapping is practically invariant for different energy machines. This follows because electrons are normally injected into the betatron at the highest energy the standard type of gun permits, which makes  $E_I$  and  $\beta_I$  constant, and also because, for economy in iron and space, the change-over from betatron to synchrotron action is allowed to take place at as low an energy as possible, which gives  $E_s = \text{constant}$ . If the electrons are injected into the betatron at 50 kv., and the change-over to synchrotron operation occurs at  $E_s = 2.5 \text{ mev.}$ , equation (11) gives, for  $n = 0.7$ ,

$$V_0 = 0.97 \times 10^4 (\rho_I / r_0)^2. \quad \dots\dots (13)$$

Since  $\rho_I / r_0$  is practically constant from machine to machine, being about  $1/8$ ,  $V_0$  is of the order of 150 volts. A voltage of at least 150 volts is therefore required on the resonator of a synchrotron to obtain efficient trapping. This condition is a necessary one in all conditions, but may not be a sufficient one if  $v_0$  is not appreciably less than  $V_0$ . This latter condition will be discussed in detail in §2.4.

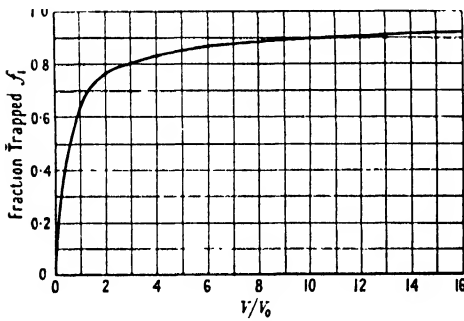


Figure 4. Trapping efficiency,  $f_1$ , for  $V \gg v_0$ .

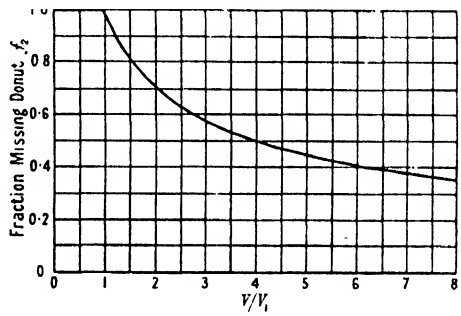


Figure 5. Fraction missing donut,  $f_2$ , for  $V \gg v_0$  and  $V_0$ .

### 2.3. Collision with Donut Walls (for $V \gg v_0$ )

In order that no electrons shall hit the donut wall during the synchrotron injection process, the radial spread after trapping must not exceed the donut half-width. From equation (6), the condition for full collection is

$$V \leq V_1, \quad \dots\dots (14)$$

where

$$V_1 = [\frac{1}{2}(1-n)^2 \beta_s^4 \pi k E_s] (\rho_I / r_0)^2. \quad \dots\dots (15)$$

Equation (14) gives a simple physical meaning to the parameter  $V_1$ , but  $V_1$  is (cf.  $V_0$ ) really a parameter derived from the constants of the machine by equation (15). Substituting the same values as for equation (13) we obtain the result

$$V_1 = 1.11 \times 10^6 (\rho_I / r_0)^2 = 17 \text{ kv.} \quad \dots\dots (16)$$

$V_1$  is not only approximately constant from machine to machine, as  $V_0$  is, but it is also independent of voltage of injection into the betatron.

If  $V$  is greater than  $V_1$ , then, since  $\rho_s$  is proportional to  $V^{\frac{1}{2}}$  by equation (6), the fraction of those electrons trapped which escape collision with the donut is given by

$$f_2 = (V_1/V)^{\frac{1}{2}}. \quad \dots\dots(17)^*$$

This relation is readily deduced from Figure 2(c), where it should be noted that a rotating line on the phase diagram is assumed, rather than a rotating area, as in Figure 2(a), i.e. it is assumed not only that  $V \gg v_0$ , but also that  $V \gg V_0$ . The latter will always be so, since  $V_1 \sim 100 V_0$ . The fraction  $f_2$  is plotted in Figure 5.

It is interesting to observe that the condition for overlap of the rising and falling curves described by  $f_1$  and  $f_2$  is that  $V_1 = V_0$ , i.e. that  $E_s = E_1$ , or that the electrons should be injected directly into the synchrotron, without intermediary betatron acceleration.

#### 2.4. Corrections with $V \sim v_0$

The discussion of §§2.2 and 2.3 is considerably modified if  $V \sim v_0$ . The electrons now oscillate about a phase  $\phi_s$  given by equation (4). The range of phases and radii over which stable oscillations are possible is correspondingly reduced. The oscillations of Figure 1 are now replaced by oscillations such as those shown in Figure 6. This figure shows clearly the mechanism whereby

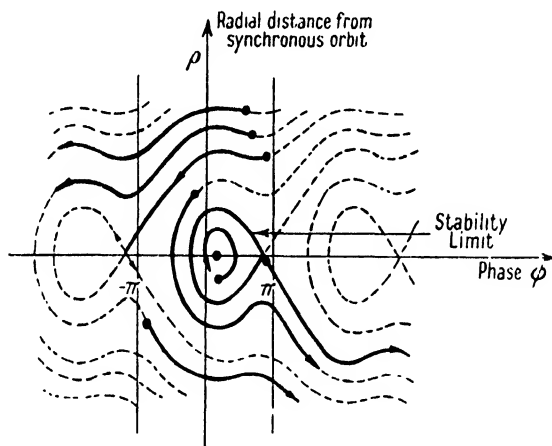


Figure 6. Oscillations in phase and radius for  $V \sim v_0$ .

Note: The figure is to scale and shows the case where  $V = 2v_0$ , i.e.  $\phi_s \sim 30^\circ$ .

electrons, which are at too large an energy and radius to be trapped, pass inwards to hit the donut wall; they pass through the synchronous radius via one of the gaps between the stable regions. The way in which the size of the stable region varies with  $V/v_0$  is given by Bohm and Foldy. A figure similar to theirs, with the addition of a convenient scale of  $V/V_0$ , is shown in Figure 7. The fraction of electrons trapped for any value of  $V/v_0$  and  $V/V_0$  may be found directly by taking area ratios such as EFGH/ABCD on the figure. This fraction would correspond, in the example shown, to  $V/V_0 = 16$  and  $V/v_0 = 2$ .

Rather than consider the problem directly, as above, it is more instructive to consider various limiting conditions. Thus if  $V/V_0$  is less than unity, the fraction

\* Equation (17) assumes a uniform distribution of electrons along A'B' in Figure 2(c). J. J. Wilkins has pointed out that a better approximation would be to assume a uniform distribution along AB, which gives  $f_2 = (2/\pi) \sin^{-1}(V_1/V)^{\frac{1}{2}}$ .

trapped is merely  $f_1$  multiplied by a fraction  $f_3$ ;  $f_3$  is the area of a curve such as EFL, corresponding to a particular  $V/v_0$ , relative to the area of the curve ABM, for which  $V/v_0 = \infty$ . This relationship is valid also for  $V/V_0$  somewhat greater than unity, it being only necessary that the ordinate  $V/V_0$  shall be greater than the maximum height of the particular  $V/v_0$  curve. Thus for  $V$  less than, or of the order of,  $V_0$  ( $V/V_0 \lesssim 1$ ), the fraction of electrons trapped is obtained by multiplying the fraction  $f_1$  by the fraction  $f_3$ , shown in curve (a) of Figure 8.

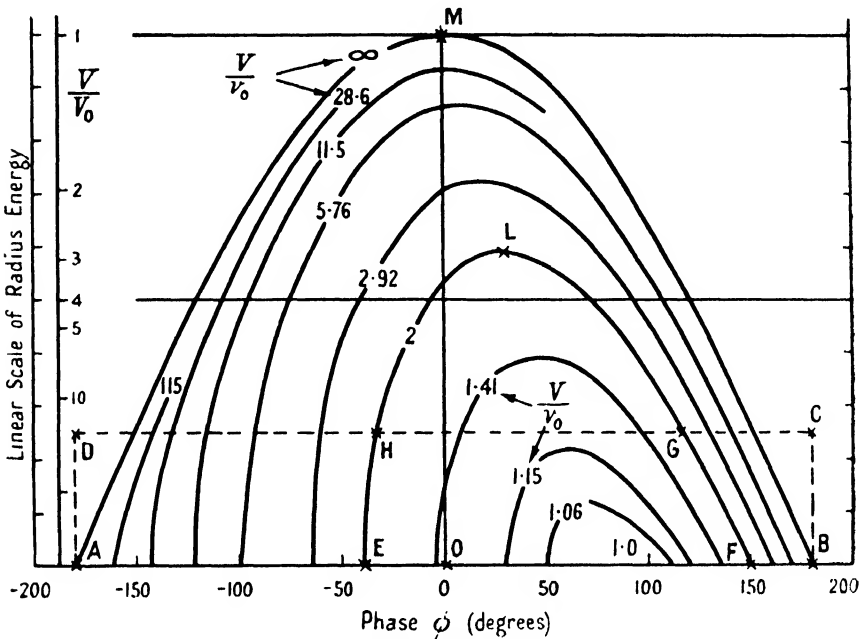


Figure 7. Stability limits for various values of  $V/v_0$ .

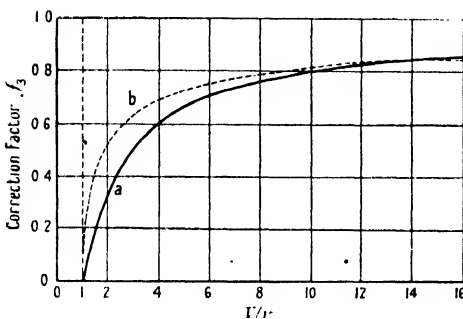


Figure 8. Correction,  $f_3$ , to  $f_1$  when  $V/v_0 \sim 1$ .  
Curve a: Approximation when  $V/V_0 \lesssim 1$   
Curve b: Approximation when  $V/V_0 \gtrsim 1$ .

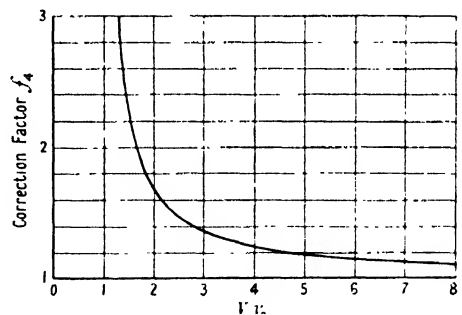


Figure 9. Correction,  $f_4$ , to  $f_2$  when  $V/v_0 \sim 1$ .  
( $V/V_0 \gtrsim 1$ ).

If  $V/V_0$  is very much greater than unity,  $f_3$  approaches the ratio of intercepts of the curves on the  $\phi$  axis in Figure 7, e.g.  $f_3 = EF/AB$ . This ratio is shown in curve (b) of Figure 8.

To obtain the fraction trapped in the transition region between the two curves (a) and (b), the problem must be treated directly by the method already indicated.

It should be noted, however, that the transition curve does not, of necessity, lie between the two limiting curves, although, as will be seen in the examples to be studied, it does so very nearly.

The decrease in trapping efficiency in the region  $V/v_0 \sim 1$  is compensated in certain circumstances by a decreased chance of hitting the donut walls, since there is only a small radial spread for the stable phase oscillations when  $V/v_0 \sim 1$ . To allow for this effect,  $f_2$  in Figure 4 must be multiplied by a factor  $f_4$  (see Figure 9).  $f_4$  is the ratio of the height OM in Figure 7 to the maximum height of a curve such as EFL. If the product of  $f_2$  and  $f_4$  is greater than unity, it must clearly be counted as unity, since hitting the donut walls cannot increase the injection efficiency.

### 2.5. Summary of Calculation of Injection Efficiency

From the foregoing description it may be seen that there are three important parameters determining the injection efficiency at a specified resonator voltage  $V$ . These are

- (a) The particular resonator voltage,  $v_0$ , at which synchronous acceleration is just possible, i.e. the volts required per revolution to accelerate the electrons.  $v_0$  is defined by equations (1) and (2).
- (b) The particular resonator voltage,  $V_0$ , at which the spread of radii, after trapping the electrons, is the same as the radial spread before the R.F. voltage is applied, assuming  $V_0/v_0 \gg 1$ . This latter assumption will not be correct in any but the smallest machines, but  $V_0$  should be defined as if it were so.  $V_0$  is not a hypothetical parameter, however, even in the larger machines since the radio frequency may be turned on when the betatron is still supplying most of the voltage required to accelerate the electrons, in which case  $v_0$  is much smaller than the nominal value.  $V_0$  is defined in terms of the machine dimensions by equation (11).
- (c) The particular resonator voltage,  $V_1$ , at which the spread of radii after trapping it just sufficient to hit the donut walls, assuming as before that  $V_1/v_0 \gg 1$ .  $V_1$  is defined in terms of the machine dimensions by equation (15).

Given these three voltages, each of which is determined from the dimensions of the machine, the injection efficiency may be calculated simply from Figure 4, corrected if necessary by Figure 8, and from Figure 5, corrected if necessary by Figure 9, i.e. the net injection efficiency  $f$ , is given by

$$f = f_1 f_2 f_3 f_4, \text{ if } f_2 f_4 < 1, \\ f = f_1 f_3, \text{ if } f_2 f_4 \geq 1. \quad \dots\dots (18)$$

In circumstances where it is doubtful whether curve (a) or (b) of Figure 8 is appropriate, the efficiency should be obtained directly from Figure 7, by the method outlined in the opening paragraph of §2.4. Calculation by equation (18) is by far the most convenient method, however, and should be used whenever possible.

The procedure described will now be illustrated by examples of machines operating at different energies. The specifications of the machines given will be nominal ones, since they are in early stages of development, where changes of specification are still permissible.

## § 3. EXAMPLES

## 3.1. 30 mev. Synchrotron

The 30 mev. synchrotron built by Fry *et al.* (1948) has  $\rho_1 = 1.5$  cm.,  $r_0 = 10$  cm.,  $E_s = 2.5$  mev., 25 kv. injection voltage, and operates at 50 c/s. The basic parameters are therefore:  $V/v_0 = 5.4$ ;  $v_0 = 20$  v.;  $V_0 = 108$  v.;  $V_1 = 25$  kv. The high value of  $V_1$  means that there is no possibility of hitting the donut wall during injection with any resonator voltage likely to be used. The injection efficiency,  $f$ , is therefore obtained by multiplication of  $f_1$  and  $f_3$ .  $f_1$  is the predominant factor and the  $V \lesssim V_0$  approximation (curve (a)), may be taken for  $f_3$ . The dotted curve of Figure 10 shows  $f$ , obtained in this way, plotted against the resonator voltage, the full curve being the more exact curve deduced directly from Figure 7. It may be seen that a resonator voltage of about 130 volts is required for 50% injection efficiency.

The predominance of the factor  $f_1$  means that the resonator voltage required for efficient synchrotron injection will increase as the voltage at which the electrons are injected into the betatron increases, since this increases  $V_0$ , e.g. about 350 volts are needed for 50% injection efficiency at an injection voltage of 100 kv.

## 3.2. 300 mev. Synchrotron

The 300 mev. synchrotron for Glasgow University will have  $\rho_1 = 7$  cm.,  $r_0 = 125$  cm.,  $E_s = 4.5$  mev. tentatively and 100 kv. injection voltage. The basic parameters are therefore:  $V_0/v_0 = 0.014$ ;  $v_0 = 2.5$  kv.;  $V_0 = 34$  v.;  $V_1 = 6.3$  kv. Since  $V_0/v_0 \ll 1$ ,  $f_1 \approx 1$  for all practical betatron injection voltages. The injection efficiency is therefore independent of betatron injection voltage, in contrast with the 30 mev. machine; the fraction trapped is controlled by  $f_3$ , the  $V/V_0 \gg 1$  approximation being satisfactory for all but the lowest resonator voltages, as is shown in Figure 11.

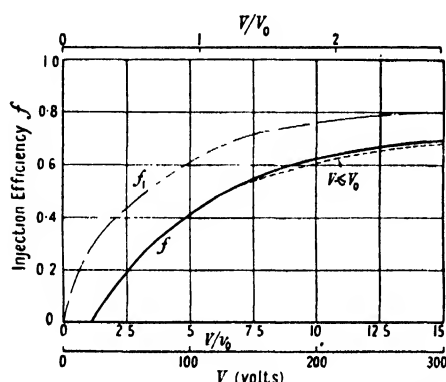


Figure 10. Injection efficiency of 30 MeV. synchrotron.

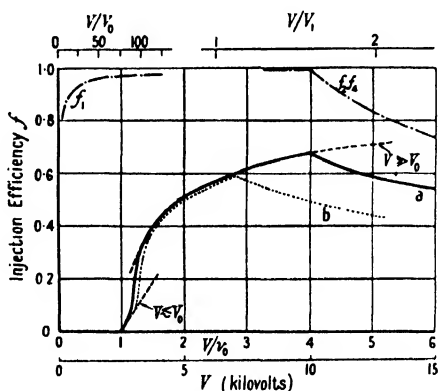


Figure 11. Injection efficiency of 300 MeV. synchrotron.

Curve a:  $E_s = 4.5$  mev. Curve b:  $E_s = 2.5$  mev.

In this synchrotron collision with the donut walls is important and the efficiency of trapping,  $f_1 f_3$ , must now be multiplied by the product  $f_2 f_4$ , giving a diminution in efficiency at resonator voltages in excess of 10 kv. as shown in Figure 11 curve (a).

The effect of reducing  $E_s$  to 2.5 mev. is also shown in Figure 11 by the dotted curve (b). The corresponding values of  $V_0$  and  $V_1$  are  $V_0 = 61$  volts and  $V_1 = 3.5$  kilovolts.

### 3.3. Discussion of Examples and Limitations of Simple Theory

The simple theory outlined has served to show that the operation of the various machines studied in the examples will be influenced by quite different factors. Before studying the experimental information which is available to warrant the approximations made, the importance of some of these approximations will be emphasized.

The main approximation made has been that the betatron action ceases suddenly and in coincidence with the turning on of the radio frequency. In fact the radio frequency is turned on in several R.F. cycles at a time when the betatron acceleration is still considerable, and the betatron acceleration is reduced quite slowly, while the resonator automatically supplies the increasing deficit required to keep the electron in the synchronous orbit.

These gradual transitions may be expected to give approximately the same effects as sudden transitions by the following argument: The resonator is switched on at a time when the volts per turn that it must supply to make up the betatron deficit is very small. The resonator voltage therefore becomes sufficient to accelerate the electrons in a time small compared with the period of the phase cycle, so that to a first approximation the R.F. may be considered as being applied instantaneously. An intermediate condition is then obtained, as shown in Figure 12(b), and most of the electrons are trapped, provided  $V/V_0 \gg 1$ . Now the betatron core begins to saturate, causing a loss of electrons as the stable area on the phase diagram shrinks, due to increase in the effective value of  $v_0$  and therefore decrease in  $V/v_0$ . Finally  $v_0$  obtains its nominal value with the result shown in Figure 12(d), and it may be seen that the fraction of electrons collected is the same as it would be if the intermediate stage of Figure 12(b) had been omitted. The fraction of electrons lost to the donut walls is also unaffected by the presence of the intermediate stage, for although many electrons may be lost to the walls due to the large radial spread of Figure 12(b), they are electrons which would be lost in any case in the transition to Figure 12(c). It is shown in Figures 13(a), (b) and (c), that the injection efficiency is also unaltered by the presence of the intermediate stage if  $V/V_0 \lesssim 1$ , so that it is reasonable to say that the theory of §2 may be applied approximately for all values of  $V/V_0$ .

The above argument would indicate that the effective value of  $E_s$  is that at which the effective value of  $v_0$  is maximum. The effective value of  $v_0$  is here defined as the deficit which must be made up by the synchrotron, and its maximum value will occur in simple cases when the betatron acceleration ceases. For the above value of  $E_s$  to be appropriate, however, the damping in radius must be the same for the trapped electrons as if normal betatron acceleration were still occurring. In fact the synchrotron damping is less, so that the effective value of  $E_s$  will lie nearer to the voltage at which the radio frequency is turned on. It is not intended to study the synchrotron damping in detail in this paper, and it will merely be assumed that the effective value of  $E_s$  lies somewhere between its value when radio frequency is turned on and its value when gamma rays appear during betatron operation. This latter value is usually quoted by experimenters, and the volts per turn supplied by the synchrotron should be approaching a maximum at this point.

A second major approximation made in the theory is that the spread of energies, or radii, on injection into the betatron, is that corresponding to the full width of

the donut. If instead only a fraction  $\Delta$  of the width is filled, equation (11) becomes

$$V_0 = [(1-n)^2 \beta_s^2 E_1^2 \beta_1^2 (\pi k / 2 E_s)] [\rho_1 \Delta / r_0]^2. \quad \dots\dots (19)$$

The fraction  $\Delta$  cannot be estimated because the betatron injection process is not understood, but if synchrotron injection theory is assumed, the possibility of determining  $\Delta$  experimentally arises. This will be discussed in §4.

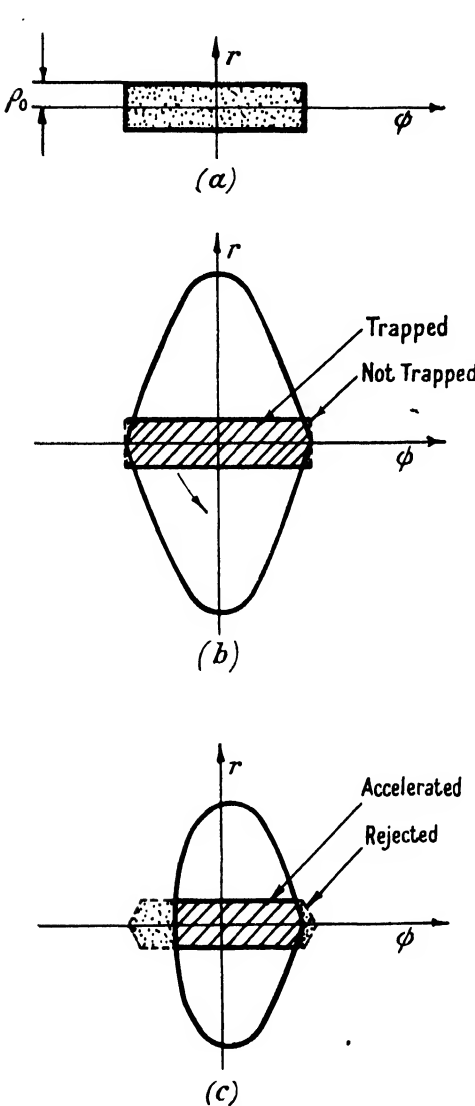


Figure 12. Trapping stages when  $V/V_0$  and  $V/v_0 \geq 1$ .  
 (a) Initial condition: Betatron on, R.F. off.  
 (b) Intermediate condition: Betatron and R.F. on.  
 (c) Final condition: Betatron off, R.F. on.

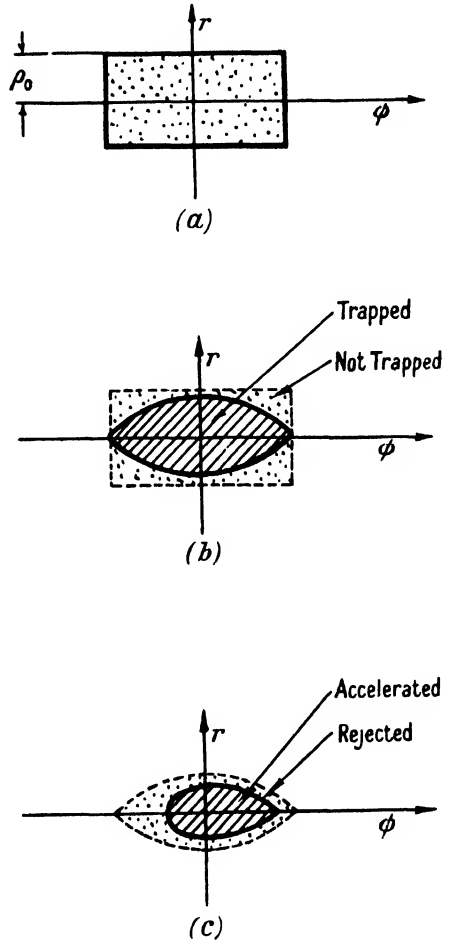


Figure 13. Trapping stages when  $V/V_0 < 1$  and  $V/v_0 \sim 1$ .  
 (a) Initial condition: Betatron on, R.F. off.  
 (b) Intermediate condition: Betatron and R.F. on.  
 (c) Final condition: Betatron off, R.F. on.

The approximations made in the simple theory are seen to be considerable and it is not intended to support the simplifications further on theoretical grounds; clearly synchrotrons could be constructed in which the simplifications are far from justifiable, e.g. de Packh and Birnbaum (1948) have suggested such a



machine. The main justification for the approximations must rest on their agreement with experiment, although it may be observed qualitatively that one would expect a simple theory of this type to give an underestimate of the efficiency.

#### § 4. EXPERIMENTAL RESULTS

##### 4.1. Introduction

Experimental results so far reported are confined to resonator voltages for which the factors  $f_1$  and  $f_3$  are the only ones of importance. It is convenient, therefore, to collect together the curves for these two factors as deduced from the examples. This is done in Figure 14 with the addition of some intermediary

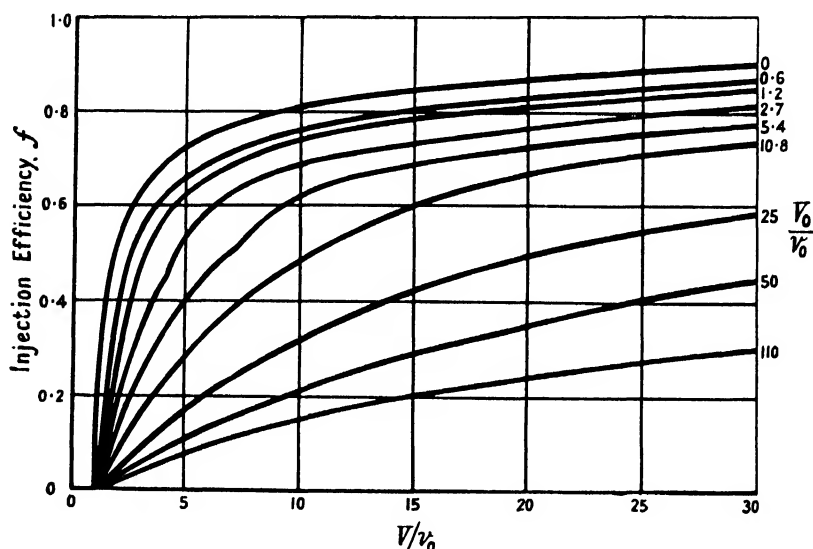


Figure 14. Injection efficiency curves for various values of  $V_0/v_0$ .

curves. The form of these curves changes appreciably as  $V_0/v_0$  varies and it should therefore be possible to determine  $V_0/v_0$  experimentally, even if the scales of  $f$  and  $V/v_0$  are not determined in the experiments, as is unfortunately the case.

##### 4.2. Results on 70 mev. Synchrotron

Some measurements have been reported (Elder *et al.* 1947) on a 70 mev. synchrotron, using an injection voltage of 40 kv.,  $\rho_1 = 3$  cm.,  $r_0 = 29.6$  cm., and  $n = 0.7$ .  $E_s$  is 2.5 mev. when the radio frequency is turned on and the betatron response appears at  $E_s = 4$  mev.  $v_0$  is given as 170 volts, but the effective  $v_0$  supplied by the radio frequency even at its maximum is likely to be less than this by at least 20%, due to betatron acceleration caused by leakage flux cutting the orbit.  $v_0$  will therefore be taken as 136 volts.

The experimental results fit well a theoretical curve for  $V_0/v_0 = 0.56$  as shown in Figure 15 (a), and fit considerably less well a theoretical curve for  $V_0/v_0 = 1.12$ , say, as shown in Figure 15 (b). Taking  $V_0/v_0 = 0.56$ , i.e.  $V_0 = 75$ , and assuming  $E_s = 2.5$  mev.,  $\Delta$  may be determined as 0.95 (see equation (19)). With  $E_s = 4$  mev.,  $\Delta = 1.2$ . The arbitrariness of the value of  $E_s$  and therefore of  $\Delta$  has already been emphasized in § 3.4, but  $\Delta$  may be taken as approximately unity from the above results.

## 4.3. Results on 14 Mev. Synchrotron

Some measurements have been made (Abson and Holmes 1948) on a 14 mev. synchrotron. This synchrotron is a converted 4 mev. betatron, requiring 1.3 volts to accelerate the electrons when the machine operates at 50 c/s., and 3.9 volts when the machine operates at 150 c/s. This low voltage occurs because the betatron gives appreciable accelerating voltage throughout the whole cycle;  $r_0$  is 7.5 cm.,  $\rho_I$  is 1.3 cm.,  $n=0.7$ , and the operating injection voltage 10 kv. The experimental points given by Abson and Holmes are reproduced in Figure 17(a). The betatron output is not negligible compared with the synchrotron output; therefore in

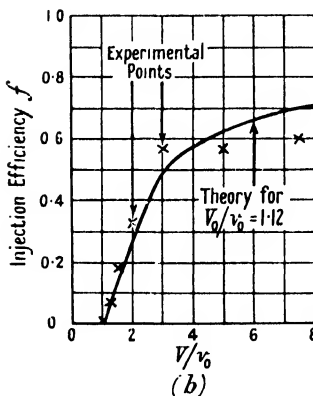
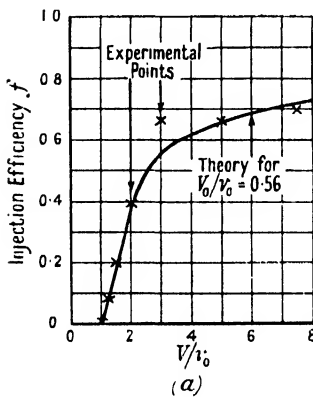


Figure 15. Experiment and theory for 70 mev. synchrotron.

- (a) Good fit for  $V_0/v_0 = 0.56$ .  
(b) Poor fit for  $V_0/v_0 = 1.12$

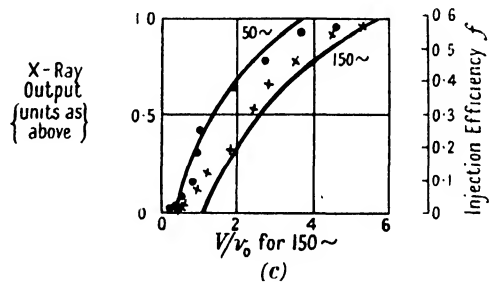
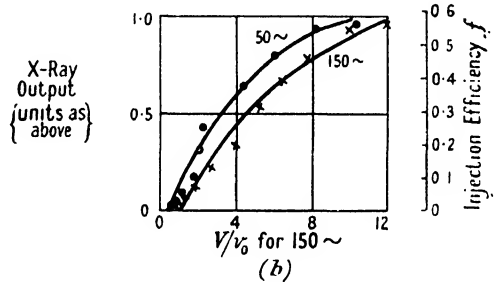
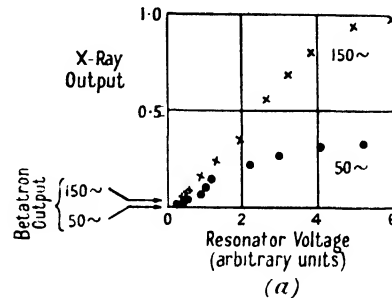


Figure 16. Experiment and theory for 14 mev. synchrotron.

- (a) Experimental results. (Abson & Holmes.)  
(b) Good fit with theory if  $V_0/v_0 = 25$  for 50 c/s. and  $V_0/v_0 = 8.3$  for 150 c/s.  
(c) Poor fit with theory if  $V_0/v_0 = 8.3$  for 50 c/s. and  $V_0/v_0 = 2.8$  for 150 c/s.

Figure 16(b) the betatron output has been subtracted from the experimental points. Further the two curves have been adjusted so that they correspond to the same betatron output and therefore to the same mean electron beam current. The curves are compared with the theory for  $V_0/v_0 = 25$  for 50 c/s., and 8.3 for 150 c/s., and the agreement is quite satisfactory. To illustrate the accuracy of the agreement, in Figure 16(c) it has been assumed that  $V_0/v_0 = 8$  and 2.7 for the respective curves, which gives very poor fit with the experimental points.

Assuming therefore, that  $V_0/v_0$  is 25 for the 50 c/s. case, and that  $v_0 = 1.3$ ,  $V_0$  is determined as 32.5 volts. With  $E_s = 2.5$  mev.,  $\Delta = 0.8$ , while with  $E_s = 4.5$  mev.,  $\Delta = 1.0$ . The value of  $\Delta$  deduced from these measurements is not very reliable since the effective value of  $v_0$  changes very slowly indeed, due to the fact that the machine is a converted betatron.

Abson and Holmes' measurements would make it possible to determine  $\Delta$  more accurately than by arbitrarily assigning a value to  $E_s$ , for they made an experimental determination of the effective value of  $v_0$  for various values of  $E_s$ . It is not intended to study their results in relation to a more comprehensive theory than that already developed here.

### § 5. CONCLUSION

The experimental results indicate that a good estimate of the efficiency of injection into a synchrotron can be made from very simple theoretical considerations. It is sufficient, for most design purposes, to assume (a) that betatron action ceases suddenly at an effective electron voltage lying between that at which the R.F. is applied and that at which the electrons strike the target during betatron

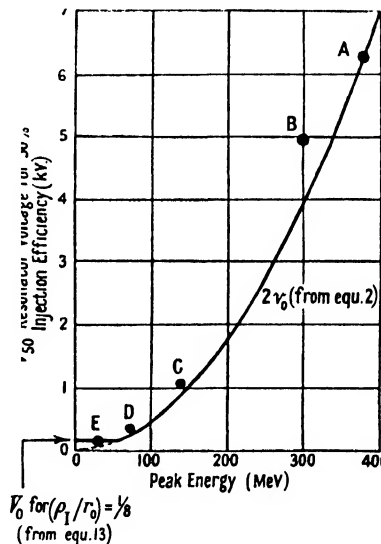


Figure 17. Resonator voltages,  $V_{50}$ , for 50% injection efficiency.

Point A: Glasgow synchrotron at 375 mev.

Point B: Glasgow synchrotron at 300 mev.

Point C: Oxford synchrotron at 140 mev.

Point D: G.E. (America) synchrotron at 70 mev.

Point E: A.E.R.F. synchrotron at 30 mev.

working, and (b) that the donut accepts a spread of energies, during injection into the betatron, corresponding approximately to the donut width, i.e.  $\Delta \simeq 1$ . With these simple assumptions important differences in the behaviour of various synchrotrons, as the resonator voltage is changed, may be explained.

It is convenient to summarize the results by a still greater simplification. For the higher energy machines the resonator voltage for 50% injection efficiency is very nearly equal to  $2v_0$ , as defined by equation (2), since the injection efficiency curve is very nearly curve (b) of Figure 8 for these machines, provided  $V/v_0$  is not near unity. For the lower energy machines the resonator voltage for 50%

injection efficiency is approximately constant and equal to  $V_0$  as defined by equation (13). Thus the required resonator voltages may be expected to follow, roughly, a curve such as that shown in Figure 17. The accuracy of this approximation is shown by the points A to E, which represent the voltages required (according to the foregoing analysis) in some actual synchrotrons.

#### ACKNOWLEDGMENTS

Acknowledgment is made to ideas expressed in a colloquium led by W. Walkinshaw, which directly stimulated the writing of this paper. The paper is published by permission of the Director of the Atomic Research Establishment and of the Controller H.M. Stationery Office, and was written as part of the accelerator programme of the Electronics Group of the Establishment.

#### REFERENCES

- ABSON, W., and HOLMES, L. S., 1948, *A.E.R.E. Report G/R192*.  
 BOHM, D., and FOLDY, L., 1940, *Phys. Rev.*, **70**, 249.  
 ELDER, F. R., GUREWITSCH, A. M., LANGMUIR, R. V., and POLLOCK, H. C., 1947, *J. Appl. Phys.*, **18**, 810.  
 FRY, D. W., GALLOP, J. W., GOWARD, F. K., and DAIN, J., 1948, *Nature, Lond.*, **161**, 504.  
 GOWARD, F. K., WILKINS, J. J., HOLMES, L. S., and WATSON, H. H. H., 1949, *Proc. Instn. Elect. Engrs.*, in the press.  
 KERST, D. W., and SERBER, R., 1941, *Phys. Rev.*, **60**, 53.  
 DE PACKH, D. C., and BIRNBAUM, M., 1948, *J. Appl. Phys.*, **19**, 795.

## A Geiger Counter Spectrometer for the Measurement of Debye-Scherrer Line Shapes

BY W. H. HALL, U. W. ARNDT AND R. A. SMITH  
 Department of Metallurgy, University of Birmingham

*Communicated by C. H. Westcott; MS. received 9th May 1949*

**ABSTRACT.** A spectrometer for the accurate measurement of x-ray powder diffraction line intensities and shapes is described. Monochromatic radiation is used, and the diffracted beam intensity is recorded by a Geiger counter. The intensity of the x-ray source is monitored continuously, and errors due to variations in its output are automatically compensated. The accuracy and resolution obtainable are demonstrated by some typical experimental results.

#### § 1. INTRODUCTION

THE accurate measurement of the shapes and intensities of x-ray diffraction lines from powders has long been an important problem. In this country the most common experimental arrangement involves the use of a specimen in the form of a thin rod placed at the centre of a cylindrical camera (Bradley, Lipson and Petch 1941) and the subsequent densitometry of the photographic record. In another technique, that used by Brentano (1925, 1937) and by Brindley and Spiers (1934), the specimen is in layer form and side reflections from the surface are used. The arrangement has the advantage that a beam

some degrees in aperture may be employed; the use of a focusing monochromator (Smith and Stickley 1943) eliminates the need for the prohibitively long exposures which are required when orthodox cylindrical cameras of comparable resolution are used in conjunction with plane crystal monochromators. The side reflection method has the additional advantage for accurate work that the corrections for absorption in the specimen can be made with greater precision than in the case of a cylindrical specimen.

The spectrometer to be described retains the geometrical arrangement of focusing monochromator and side reflection from a powder layer. The intensity of the diffracted x-ray beam is measured directly and instantaneously by a Geiger counter, thereby eliminating the photographic film and the difficulties of maintaining standard conditions of processing and of densitometry. The Geiger counter method offers considerable advantages in speed, especially where changes in only one or a few lines are to be studied; this factor is important in metallurgical applications since comparatively rapid phase changes can be investigated.

## § 2. THE SPECTROMETER

The geometry of the spectrometer is shown in Figure 1. A curved quartz crystal monochromator *M* rigidly mounted on the x-ray tube provides a monochromatic beam of two or three degrees aperture diverging from *S*<sub>1</sub>, the entrance slit of the spectrometer. The powder block *P*, which is rotated continuously in its own plane, is set so that the angle between its surface and the incident x-ray beam is the Bragg angle for the line under investigation. The diffracted beam is then focused on to an adjustable slit *S*<sub>2</sub> behind which is a Geiger counter *G*. The slit and Geiger counter are mounted on an arm which may be rotated about

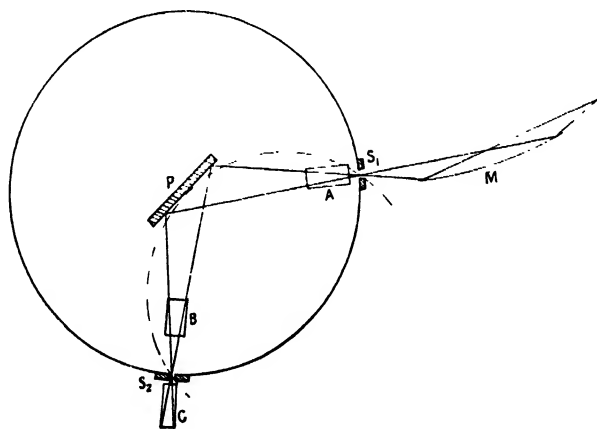


Figure 1. Geometry of spectrometer.

the centre of *P* in such a way that the line joining the centre to *S*<sub>2</sub> makes an angle with the plane of the specimen which is equal to the angle of incidence. Thus the counter arm is rotated about the vertical axis through the centre of the spectrometer at twice the speed of the specimen; for any setting the circle through *S*<sub>1</sub> and *S*<sub>2</sub> tangential to *P* is the focusing circle (Brentano 1937). Soller slits *A* and *B*, limiting the vertical divergence of the beam to 1°, may be added when required (Alexander 1948).

The base of the instrument is that of a commercial ionization spectrometer (Wooster and Martin 1936), supplied by Unicam Instruments Ltd. of Cambridge.



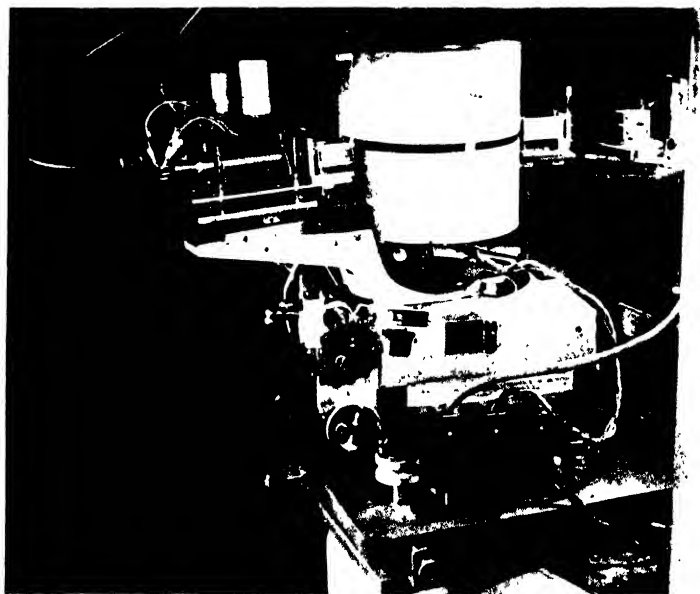


Figure 2. The spectrometer.

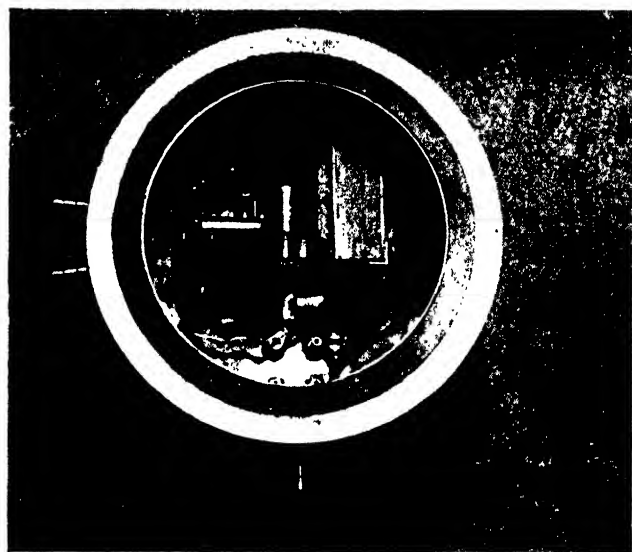


Figure 3. The specimen assembly.

Two concentric tables, one carrying the specimen chamber and the other the Geiger counter arm, can be rotated independently by spring-loaded worm drives or geared together so that the angular rotation of the arm is double that of the specimen table. The angular positions of each can be read on drums calibrated in minutes of arc, an overall accuracy of two minutes being claimed. Considerably greater accuracy is obtainable in measuring small angular differences.

The adjustable entrance slit (Barnes and Brattain 1935) is mounted on a pillar so arranged that scanning of the counter arm up to  $2\theta = 165^\circ$  is possible.

The attainable resolution is limited by the radius of the spectrometer, the slit widths, the lack of perfect focusing, and the vertical divergence of the x-ray beam. A spectrometer radius of 11.46 cm. is convenient since a change in Bragg angle of one degree then corresponds to a traverse of  $S_2$  of exactly 4 mm. The minimum counter slit width found in practice to be compatible with a reasonable counting rate is 0.1 mm.; this subtends an angle of three minutes at P. Perfect focusing at  $S_2$  would be obtained only if the surface of the powder layer coincided with the focusing circle  $S_1PS_2$  (Figure 1). However, for beams of about  $2^\circ$  aperture, the loss of resolution caused by a flat specimen is inappreciable (Brindley 1935). When maximum resolution is required, the vertical divergence of the x-ray beam may be limited by Soller slits, but the available intensity is considerably reduced. It should be noted that when a monochromator is used the small angular separation between the  $\alpha_1$  and  $\alpha_2$  components of the beam entering the spectrometer may either increase or decrease the doublet separation after diffraction by the specimen. All our measurements are carried out on that side of the beam where the dispersions are additive, thus effectively increasing the  $\alpha_1\alpha_2$  resolution.

### § 3. THE SPECIMEN CHAMBER

Experiments have shown that it is difficult to reproduce accurately all the settings of the spectrometer in such a way that after readjustment identical counting rates are obtained for the lines from a given sample. Substances under investigation are therefore compared with a standard reference specimen. The sample holder is a bakelite disc,  $2\frac{1}{4}$  inches in diameter, having an inner circular recess  $\frac{3}{4}$  inch in diameter and an outer annular recess into which sample and reference powders respectively are packed. A small electric motor rotates the disc by a friction drive on its outer rim. The assembly is mounted on an arm which can be tilted about a horizontal axis normal to the plane of the specimen. The throw is limited by two stops so that in one position the x-ray beam strikes the inner sample while in the other it falls on the outer reference specimen; tilting is effected by a mains-operated solenoid. The entire mechanism is mounted in a cylindrical chamber which can be evacuated or filled with hydrogen when necessary, since the absorption of x rays in a 20 cm. air path varies from about 20 per cent for  $\text{CuK}\alpha$  to 55 per cent for  $\text{CrK}\alpha$  radiation. X rays enter and leave the chamber through a  $180^\circ$  slot covered with 'Cellophane', the top being closed by a glass plate and rubber gasket. Three legs allow levelling and height adjustment and locate the specimen chamber accurately on the spectrometer by means of a hole, slot and plane. A screw adjustment to bring the surface of the specimen exactly over the centre of the spectrometer is also provided. The specimen chamber is shown in position on the spectrometer in Figure 2; Figure 3 shows details of the specimen disc assembly inside the chamber.



## § 4. THE GEIGER COUNTER

The counters used in our work are all cylindrical argon-alcohol counters (Friedmann 1945), the x rays entering through an aperture in the front face as close as possible to the axis. The anode wire, which is of 0.1 mm. diameter tungsten, is supported at both ends, care being taken to reduce the dead volume at the front end as much as possible. In view of the high filling pressure used (50 cm. Hg), this latter point is important in order to avoid unnecessary absorption in this dead space. The entrance aperture is covered with 0.01 mm. aluminium foil, and the active length is about 12 cm. The calculated efficiency, i.e. that fraction of the x-ray beam incident on the counter which is absorbed in the active length, ranges from 50 per cent to 65 per cent for wavelengths from  $\text{CuK}\alpha$  to  $\text{CrK}\alpha$ . The starting potential of this counter is about 1600 volts and its dead time is about 200 microseconds.

## § 5. CIRCUITS

The circuits used are all conventional, the arrangement being shown diagrammatically in Figure 4. The output from the measuring counter is first fed into a quenching circuit arranged immediately adjacent to the counter on the counter arm (Figure 2)\*. While the use of an external quenching circuit slightly

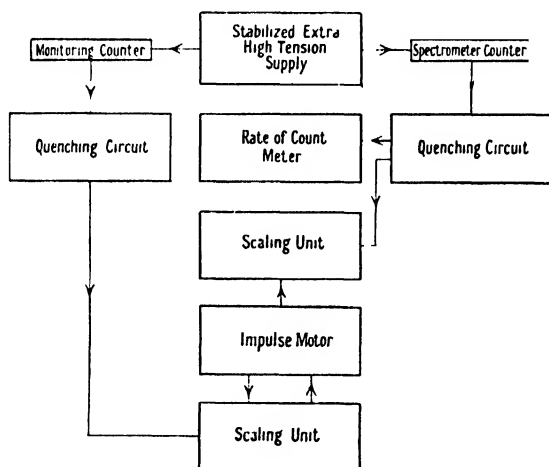


Figure 4. Schematic circuit diagram.

lengthens the resolving time of the system, it improves the plateau and increases the counter life; in addition, the counting characteristics become less dependent on temperature and previous treatment of the counter. We have used circuits of the Neher-Harper type (1936) and of the Getting type (1938) with equal success. A cathode follower output feeds the pulses into cables leading to the measuring circuits.

The pulses are fed either into a scale-of-100 scaling unit (Rotblat, Sayle and Thomas 1948) for accurate measurements, or into a simple integrating circuit (Evans and Alder 1939). The latter has been found very useful during alignment of the apparatus and for rapid surveys of the diffraction pattern of a sample.

\* For Figures 2 and 3 see Plate.

The stabilized E.H.T. supply for the counter follows orthodox design. It contains two independent continuously variable outputs, the one used for the spectrometer counter, the other for a second counter monitoring the x-ray output of the tube.

#### §6. THE MONITOR UNIT

In x-ray diffraction work in which all parts of the pattern are recorded simultaneously on one strip of film, no special precautions are necessary to keep constant the x-ray output of the tube. The use of a spectrometer of the type described, in which the spectrum is scanned by a moving counter, demands either a rigid stabilization of the characteristic x-ray output of the tube or a continuous monitoring of the same, since the scanning of all the lines of a given sample occupies a period of some hours. The latter method was adopted in our work. A plane quartz crystal monochromator is mounted opposite the second window of the x-ray tube; the characteristic radiation from this is allowed to fall on a copper wire. The diffracted rays from the latter are received by a second Geiger counter with its own quenching circuit and scaling unit. In parallel with its Post Office message register the latter drives an impulse motor which breaks a pair of contacts after receiving 104 pulses, i.e. after 10,400 pulses have been registered by the monitoring counter. The contacts operate a relay which switches off both the counting and the monitoring scalars. Consequently, the diffracted intensity is measured, not for a fixed time interval, as in normal practice, but for a fixed quantity of energy emitted by the x-ray tube. The recorded intensity has been found to be virtually independent of x-ray tube current, and voltage fluctuations less than 50 per cent. Any variations outside this range may be due to changes in the focal spot of the x-ray tube which affect the two windows unequally and to differences in the counting losses when the intensity changes greatly.

The counting time can be conveniently adjusted by varying the length of the copper wire bathed by the monochromatic beam by means of an adjusting screw.

#### §7. AUTOMATIC DRIVE

To accelerate the scanning of a line we have fitted a geared motor drive to the spectrometer worm shaft, the motor being energized through a pair of contacts bearing on a disc attached to the shaft. The disc carries at predetermined angular intervals a number of bosses which break the motor circuit when the contacts come opposite them. The motor is started by a push button connected in parallel with the contacts; it is stopped by the opening of the contacts after the spectrometer spindle has turned through the appropriate angular interval. Provision of two field windings on the motor allow it to be operated in either direction.

The process of scanning a line is thus reduced to the operation of two push buttons. Pressing the first starts the count, which stops after 10,400 pulses from the monitoring counter; pressing the second resets the scaler and moves on the spectrometer to the next position.

#### §8. USE OF THE INSTRUMENT

In order to illustrate the setting-up and the operation of the instrument the steps necessary for recording the spectrum of a sample under investigation will now be described.

The monochromator having been adjusted to give a beam of the required aperture, the spectrometer is placed on its table and moved until its entrance slit is at the focus of the monochromator and the beam passes over the exact centre of the spindle. It is convenient to use a centre locator for this purpose, consisting of a vertical rod mounted on a table which can be placed on the spectrometer. The shadow of this rod is observed on a fluorescent screen as the spectrometer is moved into the beam.

The counter is fixed on its table and levelled. The counter arm is swung into position to receive the direct x-ray beam, a sufficient number of absorbing screens being placed in front of the counter entrance slit to prevent the counter from saturating. It is turned about its entrance slit until the indication on the

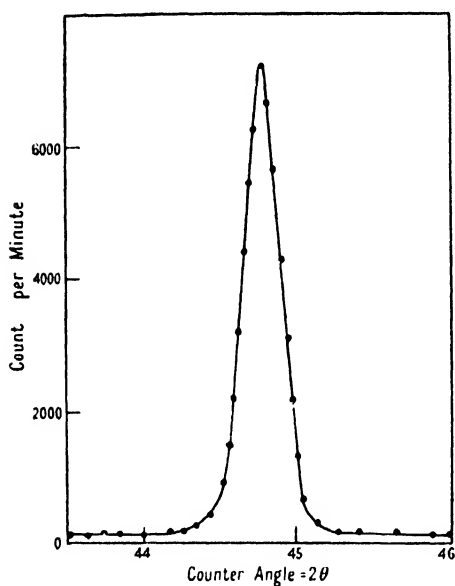


Figure 5. Aluminium line 4.  
CuK $\alpha$  50 kv., 10 ma. G-M slit=0.2 mm.

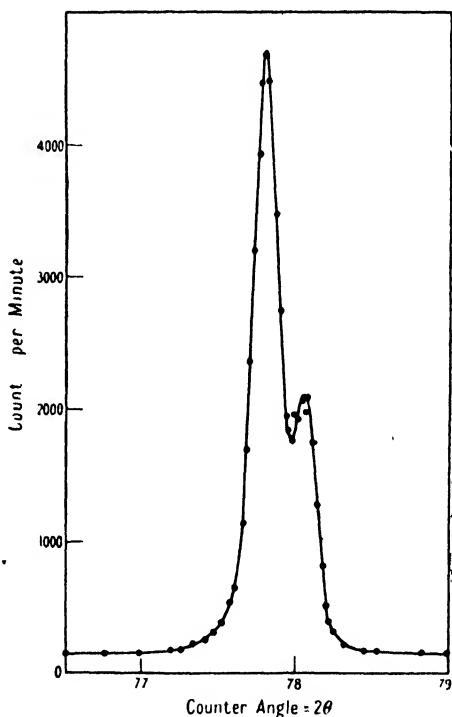


Figure 6. Aluminium line 11.  
CuK $\alpha$  50 kv., 10 ma. G-M slit=0.2 mm.

counting rate meter is a maximum. Both sets of Soller slits are now placed in position if required and, after approximate levelling with the aid of a fluorescent screen, they are adjusted for a maximum meter reading.

The specimen chamber is placed in position and the specimen is brought over the centre spindle, using a microscope for this purpose. The specimen table is turned to the focusing angle (Figure 1) and the two spindles geared together.

The counter entrance slit is set to the required width and the specimen motor switched on.

A preliminary scan of the spectrum is made, using the counting rate meter to determine the positions and the approximate intensities of the lines. The monitor is now set for an appropriate counting time and the spectrum is scanned accurately, using the scaler.

After every line is scanned comparison counts are taken on the reference specimen, both as a check on the stability of the measurements and to enable them to be placed on an absolute intensity scale if required. When the peak counting rate on any line exceeds 20,000 counts per minute one or more absorbing screens are placed in front of the counter since, for intensities greater than this, corrections for counting losses become too great to be accurately determinable.

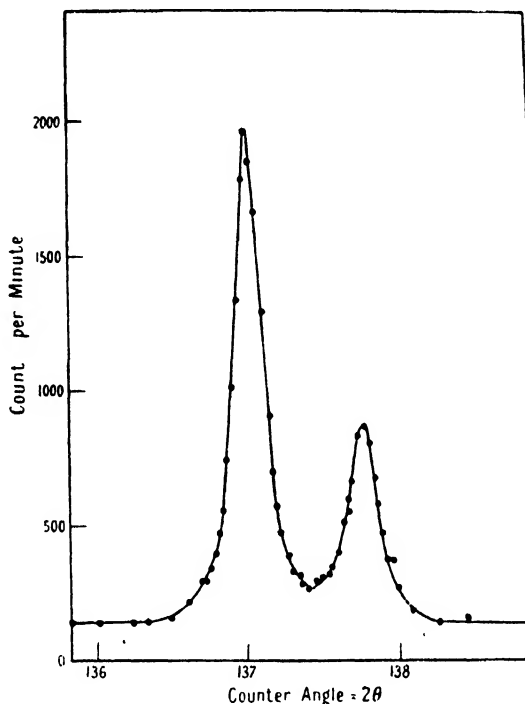


Figure 7. Aluminium line 24.  
CuK $\alpha$  50 kv., 10 ma. G-M slit=0.2 mm.

The time spent in any one position is determined by the required accuracy (Hall 1949). The standard deviation of a single observation is  $[n_1 + n_1^2/n_2]^{\frac{1}{2}}$ , where  $n_1$  is the number of pulses from the specimen and  $n_2$  that from the monitoring counter.

#### § 9. TYPICAL RESULTS

Figures 5, 6 and 7 are typical records of aluminium diffraction lines 4, 11 and 24 using CuK $\alpha$  radiation at 50 kilovolts and 10 milliamperes. The resolution, contrast and small scatter of individual readings, particularly of the background, compare well with microphotometer traces of films. Replacement of the Geiger counter by films showed exposure times of several hours to be necessary under these conditions, whereas the counter records were obtained in times of thirty to sixty minutes each, depending on the angular separation of the K $\alpha$  doublet. Faster scanning can only be carried out at a sacrifice of accuracy, which in these experiments was sufficient to make the standard deviation of the integrated intensity about one per cent.

## ACKNOWLEDGMENTS

It is a pleasure to acknowledge the encouragement given to us by Professor D. Hanson. We have had valuable discussions on the design of the circuits with Mr. C. Wainwright of the National Physical Laboratory, and with Mr. D. Bracher and Mr. A. Ward. The help of Mr. C. Ramm in the construction and filling of counters is gratefully acknowledged, as is the assistance of Mr. G. K. Williamson in the later stages of the work. The work was undertaken under research grants from the Department of Scientific and Industrial Research and from the British Iron and Steel Research Association, and this paper is published by permission of the Director of the National Physical Laboratory and the Director of B.I.S.R.A.

## REFERENCES

- ALEXANDER, L., 1948, *J. Appl. Phys.*, **19**, 1068.  
BARNES, R. B., and BRATTAIN, R. R., 1935, *Rev. Sci. Instrum.*, **6**, 83.  
BRADLEY, A. J., LIPSON, H., and PETCH, N. J., 1941, *J. Sci. Instrum.*, **18**, 216.  
BRENTANO, J. M. C., 1925, *Proc. Phys. Soc.*, **37**, 184; 1937, *Ibid.*, **49**, 61.  
BRINDLEY, G. W., 1935, *Proc. Leeds Phil. and Lit. Soc.*, **3**, 353.  
BRINDLEY, G. W., and SPIERS, F. W., 1934, *Proc. Phys. Soc.*, **46**, 841.  
EVANS, R. D., and ALDER, R. L., 1939, *Rev. Sci. Instrum.*, **10**, 339.  
FRIEDMANN, H., 1945, *Electronics*, **18**, No. 4, 132.  
GETTING, I. A., 1938, *Phys. Rev.*, **53**, 103.  
HALL, W. H., 1949, *J. Sci. Instrum.*, **26**, 61.  
NEIER, H. V., and HARPER, W. W., 1936, *Phys. Rev.*, **49**, 940.  
ROTHBLAT, J., SAYLE, E. A., and THOMAS, D. G. A., 1948, *J. Sci. Instrum.*, **25**, 33.  
SMITH, C. S., and STICKLEY, E. E., 1943, *Phys. Rev.*, **64**, 191.  
WOOSTER, W. A., and MARTIN, A. J. P., 1936, *Proc. Roy. Soc. A*, **155**, 150.

## Surface Forces in Liquids and Solids

By C. GURNEY

Engineering Laboratory, Cambridge University

*MS. received 27th May 1948, and in amended form 1st April 1949*

**ABSTRACT.** The author's recent treatment of the forces in the surfaces of liquids is extended to the surfaces of solids and to interfaces between solids and liquids. Solid surfaces formed by cleavage at temperatures such that no appreciable migration of molecules takes place, will usually be under a state of uniform stress, not necessarily tensile and not numerically equal to the free energy of the surface. If appreciable atomic migration takes place, the surface of a crystalline solid melts, and the solid is covered with a thin liquid film under a tension force greater than that of the corresponding supercooled liquid, and such that the chemical potential of the molecules in the liquid film is equal to that of molecules in the crystal. This tension force is numerically equal to the free energy of the surface. If such a solid is subsequently cooled to a temperature at which atomic migration effectively ceases, it will have frozen in its surface a tension force corresponding to thermal equilibrium at some higher temperature. The Laplace  $Q$  force is discussed in terms of modern theories of atomic bonding and applied to the case of equilibrium at angle of contact between solid and liquid.

### §1. INTRODUCTION—SURFACE FORCES IN LIQUIDS

THE idea that the tension force acting in the surface of liquids is a fiction whose use leads to correct energy relations is very commonly met with in textbooks. The fictitious nature of the force appears to have been first suggested by Laplace, and the idea has persisted because of the failure until recently to account for the force in terms of the position and motion of molecules.

In a recent paper, Brown (1947) has criticized the prevalent textbook treatment and has explained the presence of the tension force in the surface of liquids by a simple argument. In the discussion of Brown's paper, and more fully in a later paper (Gurney 1947), the present author has explained the tension in terms of the position and motion of molecules by giving a molecular interpretation to the thermodynamics of surfaces as developed by Gibbs. Gibbs showed that, at all parts of a system in equilibrium, whether homogeneous or not, the intrinsic or chemical potential  $\mu$  of each species of molecule present must have a constant value;  $\mu$  is defined by

$$dE = TdS + dW + \sum \mu dn,$$

where  $E$  is energy,  $T$  temperature,  $S$  entropy,  $W$  work ( $= \gamma dA$  for surfaces free from pressure) and  $n$  is the quantity of substance. If  $\mu$  has not a constant value, then molecules migrate from parts of the system where  $\mu$  is high, to parts where  $\mu$  is low, until equality of  $\mu$  is achieved. The  $\mu$  of molecules depends on their relative arrangement. At a surface not acted upon by a tension force (stress-free surface), because of their unsymmetrical environment, the  $\mu$  of surface molecules would exceed that of interior molecules, and more molecules would therefore leave the surface region than would enter it, leaving fewer molecules to occupy the given area. The molecules remaining in the surface are therefore at a spacing

exceeding the stress-free spacing and there is consequently a tension force between them. The tension force reduces the  $\mu$  of surface molecules according to the relation

$$(\partial\mu_i/\partial\gamma)T, n = -(\partial A/\partial n_i)T, \gamma, n, \dots \quad (1)$$

where  $\mu_i$  and  $n_i$  are the chemical potential and number of molecules of the species  $i$  at the surface.  $\gamma$  is the tension force per unit width, and  $A$  is area. This expression can be derived from the expression for  $dE$  by changing the independent variables to  $T$ ,  $\gamma$ , and  $n$ , and then equating the crossed differentials of the coefficients of  $d\gamma$  and  $dn$ .

Equilibrium is achieved when, due to continued depopulation of the surface, the tension force reaches such a value that the  $\mu$  of surface molecules equals that of interior molecules. Where more than one species of molecule is present, the variation of the single variable of surface tension force is not sufficient to ensure the equality of the  $\mu$  of each species of molecule at the surface and in the interior. The proportion of different species of molecules at the surface must also vary, and at equilibrium it differs from that in the bulk phase (Gibbs adsorption).

When dealing with interfaces between immiscible liquids a clearer physical picture can be obtained if the force in the plane of the interface is regarded as composed of two parts, the force between molecules of phase A at an interface with phase B being written  $\gamma_{Ab}$  and that between molecules of B at an interface with A being written  $\gamma_{Ba}$ . These forces are conveniently called partial interfacial forces. Their sum is the total force in the interface  $\gamma_{AB}$ . This procedure applied to interfaces between solid and liquid was made use of by Gibbs (1876) and Kelvin (1886). It has recently been advocated by Brown (1947). It is applied here to interfaces between two liquids. Equation (1) then applies to the partial interfacial forces as well as to forces at free surfaces. The partial interfacial force of the phase A is that necessary to cause the  $\mu$  of phase A molecules at the interface to equal that of phase A molecules in the bulk liquid. Because of the positive work of cohesion between all substances, the presence of phase B will cause the  $\mu$  of stress-free phase A molecules at the interface to be less than that of stress-free molecules at a free surface. The partial interfacial force  $\gamma_{Ab}$  will therefore be less than the tension  $\gamma_A$  at a free surface. Similar considerations apply to  $\gamma_{Ba}$ . If there is strong cohesion between A and B molecules, one of the partial interfacial forces may be compressive, but for stability the total interfacial force between liquids must be tensile.

In the case of a liquid covered by a monolayer which is not in equilibrium with a bulk phase, the partial interfacial force between monolayer molecules is not decided by considerations of thermal equilibrium, but may have any value depending on the area in which the monolayer molecules are constrained to occupy. The partial interfacial force of the underlying liquid will be decided by considerations of thermal equilibrium, and will vary in a definite way with the spacing of the monolayer molecules. The usual method of regarding the forces between monolayer molecules as equal to the difference between the total surface when the monolayer is present and the tension in the free surface of the underlying liquid when not covered by monolayer is not strictly correct. This method always leads to compressive forces between monolayer molecules, whereas at suitable larger molecular spacings a tension force would be expected.

The ideas of Laplace which were later extended by Rayleigh and Bakker do not, as these authors suggest, explain the tension force in the surfaces of liquids, because they have not introduced the interchange between surface and interior molecules which is fundamental to the correct explanation. Laplace gave two treatments of the forces in surfaces. The first, which finds a frequent place in textbook treatments, is an extension of ideas first published by Young (1805), and leads to the conclusion that the interior of a body is acted upon by an "intrinsic pressure" of magnitude  $K + H/r$  where  $r$  is the radius of curvature of the surface.

Laplace considered that the term  $H/r$  explained the rise of liquid in a capillary. We have already seen that a static theory such as this does not apply to liquids because interchange of molecules is not taken into account. The equilibrium of liquids under a curved surface is readily explained by the liquid having the real tension which results from the thermodynamic theory. The idea of intrinsic pressure does not lead to any very ready explanation of any of the phenomena discussed in this paper, and we shall not consider it further. For an account of Bakker's extension of the intrinsic pressure theory the reader is referred to the paper by Brown (1947). Bakker's theory does not lead to Gibbs adsorption at the surface of a multicomponent liquid, and if only for this reason it cannot be regarded as correct.

In addition to his intrinsic pressure theory Laplace (1807) gave in his *Nouvelle manière de considérer l'action capillaire* an explanation of the forces between the walls of a capillary tube and the liquid contained in it which does not receive the attention it deserves from modern writers. In §4, when dealing with surface forces in solids, and later, when discussing angles of contact, we shall make use of this theory.

## §2. STRESSES IN THE UNCONTAMINATED SURFACES OF SOLIDS AT TEMPERATURES AT WHICH MIGRATION OF ATOMS TAKES PLACE

At temperatures far below the melting point migration of atoms takes place at a negligible rate and the attainment of thermal equilibrium between surface and interior will be indefinitely delayed. At higher temperatures appreciable atomic migration takes place even in the crystalline state. Evidence for this comes from the conductivity of ionic crystals and the diffusion of solute ions in metals. At such temperatures, possibly after considerable delay, thermal equilibrium between surface and interior will be achieved and the  $\mu$  of surface atoms will then equal that of interior atoms.

Consider first the case of the surface of a liquid. If we imagine a liquid to have a stress-free surface, then the  $\mu$  of surface molecules is higher than that of interior molecules and an excess of molecules enters the interior, increasing the volume of the bulk phase and leaving fewer molecules in the surface to occupy the given area. The spacing of surface molecules thus exceeds the equilibrium spacing and a tension stress in the plane of the surface is set up. This tension has the effect of reducing the  $\mu$  of surface molecules according to equation (1). The tension stress therefore tends to prevent molecules leaving the surface. The manner in which this is effected is illustrated in Figure 1 which represents three stages in the escape of a molecule from the surface into the interior or into the vapour phase.



It is seen that because the liquid molecules cohere to each other and, being mobile, close the hole which would otherwise be formed, the tension during stage 1 of the process of escape tends to pull the escaping molecule back into the surface. Equilibrium is achieved when, due to the continued inward migration of molecules, the tension becomes equal to the value which makes the  $\mu$  of the surface equal to the  $\mu$  of the interior.

Consider now the stress-free surface of a crystalline solid at a temperature such that atoms can migrate. Let us suppose that initially all the lattice points are occupied by atoms. Then just as in the case of a liquid, more atoms leave the surface than enter it, the inward migration of atoms being accommodated by an appropriate increase in the number of interior lattice points. At this stage the remaining surface atoms would still be on lattice points but there would be a number of vacant sites. The entropy of surface atoms would be increased but this does not effect  $\mu$  because  $(\partial\mu/\partial S)_{T,P}=0$ . If this state of affairs persisted, no effective tension would be set up in the surface, and atoms would continue

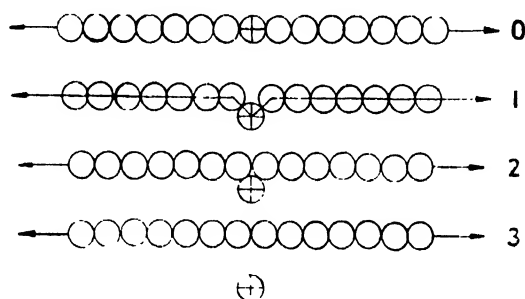


Figure 1.

to leave the surface; thermal equilibrium would be impossible. For thermal equilibrium, it is necessary that the departure of atoms from the surface should set up a force opposing further departure. What is the nature of this force?

At any temperature below the melting point of a crystalline solid thermal equilibrium requires that there should be some interior vacant lattice sites. As the temperature is raised the number of these vacant sites increases and above the melting point the solid phase with its vacant lattice sites is unstable with respect to the liquid phase. The solid therefore melts. We have just seen that an initially perfect surface of a solid would lose atoms to the interior and that there would be an increasing number of vacant lattice sites at the surface. When these reach a given number it is reasonable to expect that the crystalline arrangement of surface atoms will become unstable with respect to the liquid arrangement and the atoms at the surface will melt, forming a liquid film a few atoms thick which completely covers the surface. Thermal equilibrium between surface and interior then becomes possible.

If the liquid film when formed were stress free, atoms would continue to leave the surface until a tension stress was set up in the liquid film such that the  $\mu$  of atoms in the liquid film was equal to the  $\mu$  of interior atoms. As the liquid film is in equilibrium with the solid phase at a temperature below the melting point of the latter, it follows that the tension in the liquid film must be higher than that in the surface of the corresponding supercooled liquid phase. The

necessary value of the tension can be estimated as follows. The equation corresponding to equation (1) for a bulk phase is

$$\partial\mu/\partial p = \partial V/\partial n, \quad \dots\dots (2)$$

where  $p$  and  $V$  are pressure and volume.

At the melting point the  $\mu$ 's of solid and liquid bulk phases are equal and at all temperatures the  $\mu$ 's of solid and liquid must equal those of the corresponding vapour phases so that the difference in the  $\mu$ 's of the solid and liquid bulk phases at temperature  $T$  is given by

$$\Delta\mu = \Delta \int_p^{p_{\text{melting}}} \frac{\partial V}{\partial n} dp, \quad \dots\dots (3)$$

where  $p$  is vapour pressure.

Assuming the vapours to be perfect gases this becomes

$$\Delta\mu = RT \ln p_L/p_S, \quad \dots\dots (4)$$

where the subscripts L and S stand for liquid and solid.

Integrating equation (1) and neglecting variation in  $\partial A/\partial n$ ,

$$\Delta\mu = - \frac{\partial A}{\partial n} \Delta\gamma. \quad \dots\dots (5)$$

Equation (4) gives the difference between the  $\mu$  of solid and liquid bulk phases. Equation (5) shows how the  $\mu$  of a liquid surface phase is altered by tension. If we are to have a liquid surface phase in equilibrium with a solid phase the  $\mu$ 's of the phases must be equal. Using equations (4) and (5) we must therefore have

$$RT \ln p_L/p_S - \frac{\partial A}{\partial n} \Delta\gamma = 0 \quad \dots\dots (6)$$

or

$$\Delta\gamma = \frac{RT \ln p_L/p_S}{\partial A/\partial n}. \quad \dots\dots (7)$$

Chalmers, King and Shuttleworth (1948) have estimated the ratio of  $p_L/p_S$  for silver for the temperature range between the melting point ( $961^\circ\text{C.}$ ) and  $600^\circ\text{C.}$  At  $600^\circ\text{C.}$   $p_L/p_S = 1.42$ .  $\partial A/\partial n$  is the effective area occupied per molecule and for silver is roughly  $10\text{ \AA}^2$ . Using these data the value of  $\Delta\gamma$  is estimated to be about  $40\text{ dynes/cm.}$  The surface tension of the supercooled bulk liquid at  $600^\circ\text{C.}$  would be of the order of  $1,000\text{ dynes/cm.}$  so that it is seen that in this case quite a small increase in tension is sufficient to enable a liquid film to be in equilibrium with a bulk crystalline phase at temperatures well below the melting point. For ice at  $-15^\circ\text{C.}$  the ratio  $p_L/p_S$  is  $1.15$  and  $\partial A/\partial n$  is about  $5\text{ \AA}^2$ . These figures give a value for  $\Delta\gamma$  of approximately  $10\text{ dynes/cm.}$  The surface tension of water at  $-15^\circ\text{C.}$  is about  $80\text{ dynes/cm.}$  so that the tension in the liquid film on the surface of ice at this temperature is about  $90\text{ dynes/cm.}$  This means that ice at  $-15^\circ\text{C.}$  should rise appreciably higher in a capillary tube than liquid water at the same temperature. The effect is extra to the ordinary density effect.

The mobility of surface atoms of solids at temperatures well below the melting point is a well known phenomenon, and is made use of in the sintering of powders. An account of a number of effects associated with the mobility of atoms on surfaces of metals is given by Chalmers *et al.* (1948). Many of the effects may be explained by the presence of liquid films on the surfaces of crystals, and the fact that crystals cannot be superheated above their melting points is readily understood if even

below the melting point the solid already has a film of liquid on it. A bulk liquid phase becomes stable at a temperature such that the tension in the liquid film on the solid is equal to the tension in the bulk liquid phase. The liquid film on ice probably plays an important part in skating.

Frenkel (1945) has considered the subject of surface mobility from a statistical mechanical point of view. He has regarded the surfaces of crystals as having the same atomic arrangement as that of the interior atoms, and has then estimated the number of adsorbed individual atoms which would rest on the top of the surface. He regards these adsorbed atoms as being the source of surface mobility. In his paper he does not apply the statistical mechanical argument to the thermal equilibrium between the surface and the interior of the crystal. If this were done, because surface atoms are in a state of high potential energy, the statistical mechanical argument would presumably predict that they would be less closely packed and would lead to a liquid film on the surface just as the thermodynamic argument does. The isolated movable atoms of Frenkel would then move about on the top of the liquid surface, but they would be too few compared with the number of atoms in the liquid film to play any important part in surface mobility phenomena. They would, however, play an important part in evaporation, the atoms going first to the top of the surface and then later being thrown off.

### §3. UNIFORM STRESSES IN UNCONTAMINATED SURFACES OF SOLIDS AT TEMPERATURES AT WHICH MIGRATION OF ATOMS DOES NOT TAKE PLACE

In solids at temperatures at which no appreciable migration of atoms takes place, a state of thermal equilibrium between surface and interior is not reached, and the process by which the tension force in the surfaces of the liquids is set up does not operate. There will, nevertheless, be uniform stresses acting in the freshly cleaved surfaces of such solids due to the fact that the stress-free spacing of surface atoms differs from that of interior atoms. In the case of liquids, the surface forces are brought to equilibrium at the perimeter by forces between the surface atoms and the walls of the containing vessel. In the case of solids with non-mobile atoms the surface stresses are brought to equilibrium by shear forces between surface and underlying atoms—a state of internal stress is set up near the surface. The detailed explanation of such surface stresses will depend on the predominant type of atomic bonding, covalent, ionic or metallic. To illustrate their nature consider a material having ionic bonding, where each positive ion is surrounded by negative ions and vice versa. Pauling (1940, p. 368) gives a table showing how equilibrium interatomic distances in solids vary with coordination number (number of nearest neighbouring atoms). For positive and negative atoms in a three-dimensional chess-board pattern, the coordination number is six in the interior of the solid but only five at the surface. For this case, Pauling gives the reduction in interionic distance with reduction in coordination to be about four per cent. Lennard-Jones and Dent (1928) have calculated the equilibrium spacing of a two-dimensional array of positive and negative ions, and they find it to be of the order of 5% less than the equilibrium spacing in the bulk phase. The difference, for their calculation, is due to the fact that there is less mutual repulsion between ions of like sign in a two-dimensional than in a three-dimensional array. They have not taken into account the difference in the distribution of electron densities for the plane and for the solid arrays of atoms.

This effect is additional, but the combined result may not be simply additive. The cube surfaces of an ionic bonded material would therefore be in a state of tension relative to the interior, but this would not apply to all surfaces. A surface formed by a 111 plane would contain only ions of like sign, and the mutual repulsion of these would result in a surface having a compression stress in its plane.

Such uniform stresses in surfaces bear no immediate relation to the work of cohesion, so that it is misleading to call these stresses surface tensions. We shall refer to them as induced tangential stresses; they do not play any very direct part in the surface phenomena discussed.

In this section it has been assumed that the surface has been formed at low temperature by mechanical means. If it has been formed by cooling an existing surface from a temperature so high that appreciable atomic migration took place, then it will have a uniform tension frozen into it, corresponding to the equilibrium tension at some higher temperature.

#### §4. THE LAPLACE $\mathcal{Q}$ FORCE AND EQUILIBRIUM AT ANGLES OF CONTACT

If two blocks of material are placed in partial contact as in Figure 2(a), there will be local tangential forces between them, tending to cause relative sliding so that the surfaces on which sliding takes place are eliminated and the two blocks become one.

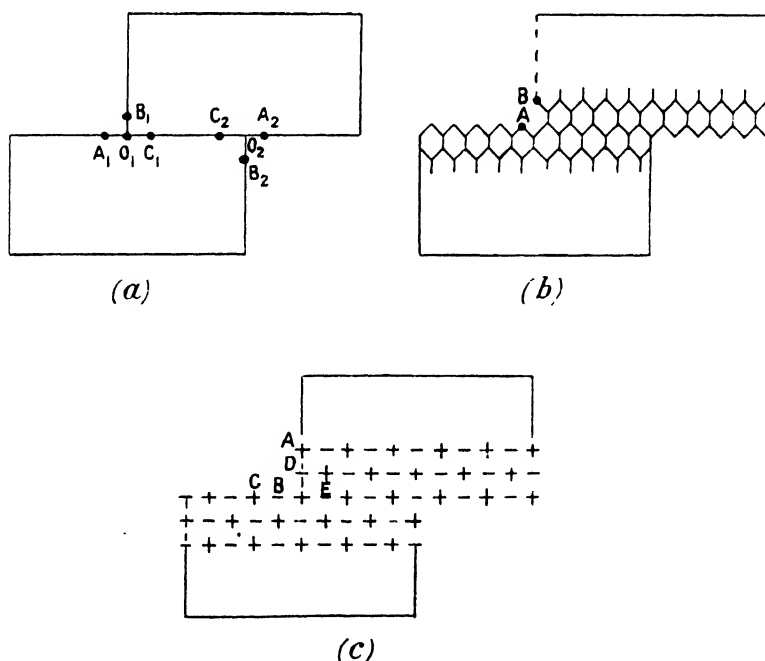


Figure 2.

The tangential forces arise from the tangential components of the cohesive forces between the blocks. On Laplace's model of matter they are explained as follows. The attraction of a particle at C<sub>1</sub> (see Figure 2(a)) for a particle at B<sub>1</sub> is balanced by the intrinsic pressure, so that there is no tendency for the distance B<sub>1</sub>C<sub>1</sub> to shorten. The attraction of a particle at A<sub>1</sub> for a particle at B<sub>1</sub> acts across

space and is unbalanced. There is therefore a resultant tangential force acting in the region of  $O_1$  tending to cause relative sliding of the blocks. There is a similar force at  $O_2$ . We will call these forces the Laplace tangential cohesive forces and denote them as Laplace did by  $Q$ . On more modern ideas of the composition of matter, the explanation of the force  $Q$  must be given in terms of the predominant type of atomic bonding. In Figure 2(b) is a picture of a solid considered as two-dimensional in which for simplicity each atom forms three covalent bonds. In this case the surface atoms will have a free valency and the tangential cohesive force would come from the stretched covalent bond formed between atoms A and B.

In an ionic bonded material shown in Figure 2(c) the tangential cohesive force would arise from attractive forces between ions such as A and B and C and D which act across space not occupied by other ions; and also from polarization (Lennard-Jones and Dent 1928) of the ions B and D which would result in less repulsion between ions B and D than between ions D and E.

Because in an isothermal process, the minimum work to cause a given change is independent of the path, each force  $Q$  is equal to one half of the work of cohesion, since new surfaces may be formed either by normal separation or by sliding. It should be noted that the Laplace  $Q$  force is a local force acting at the junction between the free surface and a bulk phase and does not cause a stress to be set up over the whole of the free surface.

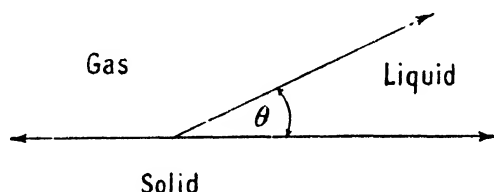


Figure 3.

A Laplace  $Q$  force will also act at the junction of the free surface of a solid and liquid in the case where a solid surface is partly covered with the liquid. Consider the equilibrium at an angle of contact (Figure 3). It is usually written

$$\gamma_{LG} \cos \theta + \gamma_{LS} - \gamma_{SG} = 0, \quad \dots \dots (8)$$

where  $\gamma_{LG}$ ,  $\gamma_{LS}$  and  $\gamma_{SG}$  are tensions in the gas-liquid, liquid-solid and solid-gas interfaces. The nature of the forces involved is usually left unexplained and  $\gamma_{LS}$  and  $\gamma_{SG}$  are referred to as fictitious forces leading to the correct energy relationships.

With our notation we should write

$$\gamma_{Lg} \cos \theta + \gamma_{Ls} - Q = 0, \quad \dots \dots (9)$$

where  $\gamma_{Ls}$  is the partial interfacial force (not necessarily tension) necessary to enforce equality of the  $\mu$ 's of molecules of the liquid at the interface and of molecules in the bulk liquid, and  $Q$  is the Laplace tangential cohesive force.

If the solid is at such a temperature that a liquid layer is formed on its surface equation (8) applies, all the forces being real forces necessary to ensure the various equalities of the  $\mu$ 's. The force  $\gamma_{LS}$  will be made up of the components  $\gamma_{Ls}$  and  $\gamma_{sl}$ , the latter being the force in the liquid surface layer of the solid necessary to ensure equality of the  $\mu$ 's of atoms in surface layer and interior.

# § 5. SURFACE ENERGY AND SURFACE TENSION

Writers on the fundamentals of surface phenomena usually stress the equivalence of surface tension and surface energy and some writers regard the terms as synonymous. The use of these terms is here discussed in the light of the ideas of the preceding section.

The Helmholtz free energy of a surface is the maximum work which can be obtained when the surface is annihilated at constant temperature. This is equal to one half of the work of cohesion. We have seen that there are forces in the planes of the surfaces of solids with non-migratory atoms (induced forces) but that these are not equal to one half of the work of cohesion. To use surface tension as synonymous with surface energy is therefore clearly inadmissible.

In the case of surfaces of liquids and of solids with migratory atoms, if the atoms are exceedingly mobile so that there is no delay in attaining thermal equilibrium after the surface has been formed, then surface tension and surface energy are equivalent provided the latter is understood to be the Helmholtz free energy. If a surface is formed by brittle fracture in a very viscous liquid such as pitch or glass, the surface will be formed before the atomic migrations, which cause the equilibrium tension to be set up in the surface, can take place. If we limit ourselves to events taking place in a short time the considerations already discussed regarding solids with non-migratory atoms apply. If, however, we are interested in a longer period of time, migration of atoms will take place until thermal equilibrium is set up. The final force in the surface will not now be equal to the induced force, but it will be that necessary to ensure the equality of the  $\mu$ 's of surface and interior molecules. The migration of atoms which takes place in order that the system shall reach thermal equilibrium is an irreversible process and the Helmholtz free energy of the system is therefore decreased. It follows that a surface with a tension other than the tension necessary for thermal equilibrium has excess Helmholtz free energy. This can be estimated by calculating what work could be obtained from the surface by operations involving only reversible processes. Let the equilibrium surface tension be  $\gamma_e$  and the tension in the surface whose Helmholtz free energy it is desired to calculate be  $\gamma_0$  and let its area be  $A_0$ . Then we may, by altering the external forces, cause the surface to alter its area elastically and reversibly until the surface tension equals  $\gamma_e$ , the operation being supposed to be sufficiently slow to be isothermal but sufficiently rapid for no appreciable migration of atoms to take place. The work done on the surroundings during the elastic alteration in surface area is equal to

$$\int_{A_e}^{A_0} \gamma dA,$$

where  $A_e$  is the area at which the tension equals  $\gamma_e$ . The surface now has its equilibrium tension and its Helmholtz free energy is  $\gamma_e A_e$ . The initial free energy was therefore

$$\gamma_e A_e + \int_{A_e}^{A_0} \gamma dA.$$

The free energy of a surface having the initial area but the equilibrium value of the tension would be  $\gamma_e A_0$ . The excess free energy of a surface having initial tension  $\gamma_0$  is thus

$$\gamma_e A_e + \int_{A_e}^{A_0} \gamma dA - \gamma_e A_0 = (\gamma_0 - \gamma_e) A_0 + \int_{\gamma_e}^{\gamma_0} A d\gamma.$$

If we assume a linear relationship between area and tension when the number of molecules in the surface is constant the difference can be computed in terms of the effective elastic constant  $E_1$  of the surface. If the initial tension is zero, the fractional excess free energy is  $\gamma_e/2E_1$ . An estimate of  $E_1$  can be obtained from the bulk modulus  $K$  of the liquid by means of the relationship

$$E_1 = \frac{3(1-2\sigma)}{2(1-\sigma)} Kt,$$

where  $\sigma$  is Poisson's ratio and  $t$  the effective thickness of the surface layer. Assuming  $\sigma$  to be  $1/3$  and  $t$  to be equal to the cube root of the volume per molecule, the value of  $\gamma_e/2E_1$  for some common liquids such as water, benzene and mercury is of the order of 5%.

#### REFERENCES

- BROWN, R. C., 1947, *Proc. Phys. Soc.*, **59**, 429.  
 CHALMERS, B., KING, R., and SHUTTLEWORTH, R., 1948, *Proc. Roy. Soc. A*, **193**, 465.  
 FRENKEL, J., 1945, *J. Phys. U.S.S.R.*, **9**, 392.  
 GIBBS, J. W., 1876, *Collected Works* (New York: Longmans, 1928).  
 GURNEY, C., 1947, *Nature, Lond.*, **160**, 166.  
 KELVIN, Lord, 1886, *Popular Lectures and Addresses*, Vol. 1, 1891.  
 LAPLACE, P. S., 1807, *Mécanique céleste*, Bk. IV, Supplement, Paris.  
 LENNARD-JONES, J. E., and DENT, B. M., 1928, *Proc. Roy. Soc. A*, **121**, 256.  
 PAULING, J., 1940, *The Nature of the Chemical Bond*, 2nd Edition (New York: Corner University Press).  
 YOUNG, T., 1805, *Phil. Trans. Roy. Soc.*, **27**, 67.

## The Hydrodynamics of Helium II

By R. B. DINGLE

Royal Society Mond Laboratory, Cambridge

*Communicated by H. N. V. Temperley; MS. received 29th April 1949*

**ABSTRACT.** In this paper expressions are derived for the forces acting on the normal fluid and on the superfluid of helium II, and it is shown that the apparently differing derivations of the velocity of second sound given by Landau and Tisza are, in fact, equivalent, even if thermal expansion is not neglected.

#### § 1. INTRODUCTION

IN discussing the properties of helium II from a phenomenological standpoint it is customary to suppose that the fluid may be considered as some type of mixture of two phases, the normal fluid and the superfluid. The superfluid is assumed to carry little or no entropy, and to be entirely non-viscous. These assumptions are displayed quantitatively as follows. Let  $\rho$  be the density of the fluid as a whole,  $\rho_n$  that of the normal fluid, and  $\rho_s$  that of the superfluid. Then  $\rho = \rho_n + \rho_s$ . Let  $\dot{x}_n$  and  $\dot{x}_s$  be the velocities of the normal and superfluid respectively, so that the current  $j$  is given by  $j = \rho_n \dot{x}_n + \rho_s \dot{x}_s$ . Finally, let  $T$ ,  $p$  and  $t$  be the temperature, the pressure and the time respectively, and  $S$  the entropy of the fluid

considered as a whole. In this notation, Landau (1941) proposed the following equations to describe the hydrodynamics of helium II to the first order\* :

$$\partial p / \partial t + \nabla \cdot \mathbf{j} = 0, \quad \dots\dots (1)$$

$$\partial(\rho S) / \partial t + \rho S \nabla \cdot \dot{\mathbf{x}}_n = 0, \quad \dots\dots (2)$$

$$\partial \mathbf{j} / \partial t + \nabla p = 0, \quad \dots\dots (3)$$

$$\partial \dot{\mathbf{x}}_n / \partial t - S \nabla T + \nabla p / \rho = 0. \quad \dots\dots (4)$$

Equation (1) expresses the conservation of mass, equation (2) the conservation of entropy in a system in which the entropy is transported by the normal fluid only, and equation (3) is the usual kinematical equation giving the acceleration of the bulk fluid in terms of the mechanical force. The fourth equation was derived by Landau from a thermodynamical argument showing that the force acting on unit volume of the superfluid considered alone is given by the gradient of the thermodynamical potential. There appears to be some reluctance to accept equation (4) on the same standing as equations (1), (2) and (3) (see for instance London and Zilsel 1948), apparently on account of the fact that it introduces a new kind of force, a thermal pressure proportional to the temperature at the plane considered.

With the aid of these equations, Landau deduced an approximate expression (neglecting the coefficient of thermal expansion) for the velocity of second sound, and Lifshitz (1944) examined the ratio of the amplitudes of first and second sound produced by various forms of excitation. Approaching the problem from a different standpoint, and assuming the conservation equations (1) and (2), but not the kinematical equations (3) and (4), Tisza (1947) has deduced the same approximate expression for the velocity of second sound.

In this paper we shall deduce Landau's equations (3) and (4), together with further similar equations, by differentiation of a Lagrangian of the complete system similar to that given by Tisza. Hence the Tisza and Landau formulations are equivalent. This equivalence holds even if the coefficient of thermal expansion is not neglected. The work contained in this paper, and in a previous paper by the author (Dingle 1948), shows that it is unnecessary to introduce the concept of "osmotic pressure" as Tisza does, thereby avoiding his assumption † that  $\rho_n \propto S$ . Again, the fact that the equivalence holds even if thermal expansion is not neglected shows that it is unnecessary to repeat (on Tisza's theory) Lifshitz's calculations on the amplitude ratio of first and second sound produced by various processes. The present work shows also that Landau's equation (4), which was deduced assuming perfect reversibility, would still hold, at least approximately, if irreversible processes took place.

As is shown in this paper, (3) and (4) may be derived thermodynamically if we assume the validity of (1) and (2). Since (1) merely expresses the conservation of mass, the only serious assumption of the hydrodynamical theory is contained in (2), which expresses the fact that the entropy is transported only by the normal fluid. This assumption is well-founded experimentally.

\* Quadratic terms are omitted. Thus we neglect the difference between full and partial differentiation with respect to the time (the difference being quadratic in the velocities), and in products such as  $\rho_n \dot{\mathbf{x}}_n$  we ignore the variation of  $\rho_n$ .

† This assumption has been criticized by Dingle (1948) and by Landau (1949), who implies that the whole of Tisza's quantitative theory is incorrect as a result. The present author believes that the proportionality is probably correct for those adiabatic changes in which relaxation effects are negligible.



## § 2. THE POTENTIAL ENERGY OF THE SYSTEM

For the sake of completeness\*, we shall first give the calculation of the potential energy of unit mass of a part of the fluid having excess entropy  $\delta S$  and excess volume  $\delta V$ . Let us suppose that the unit mass forms a sub-system immersed in a surrounding medium at constant temperature  $T_0$  and constant pressure  $p_0$ , the sub-system and the surrounding medium together forming an isolated system.

The work done by the medium on the sub-system is  $p_0\delta V_0$ , and the heat transferred is  $-T_0\delta S_0$ . Let the internal energy change of the sub-system be  $\delta U$ , and the work done on the sub-system by a source of work be  $\delta W$ . Then, by the first law of thermodynamics,  $T_0\delta S_0 = p_0\delta V_0 - \delta U + \delta W$ .

The physical meaning of the ideal processes described may be seen more clearly if we imagine the sub-system to consist of a cylinder fitted with a piston which is always impermeable to normal fluid, but which may be made either permeable or impermeable to superfluid. Neglecting thermal expansion, we alter only the volume per unit mass if the piston is moved whilst impermeable to superfluid, and only the entropy per unit mass if it is moved whilst permeable.  $\delta W$  is the work required to move the piston.

The volume of the whole (medium plus sub-system) will be constant; hence  $\delta V_0 = -\delta V$ . Now the entropy of the whole must either remain constant—perfect reversibility—or increase; thus  $\delta S_0 \geq -\delta S$ . Assuming perfect reversibility for the present, we have  $\delta W + T_0\delta S - p_0\delta V = \delta U$ . Expanding  $\delta U$  in terms of the values appropriate to the surrounding medium, we have

$$\begin{aligned}\delta U &= \left(\frac{\partial U}{\partial V}\right)_{0S} \delta V + \left(\frac{\partial U}{\partial S}\right)_{0V} \delta S + \frac{1}{2} \left(\frac{\partial^2 U}{\partial V^2}\right)_{0S} \delta V^2 \\ &\quad + \left(\frac{\partial^2 U}{\partial V \partial S}\right)_0 \delta V \delta S + \frac{1}{2} \left(\frac{\partial^2 U}{\partial S^2}\right)_{0V} \delta S^2 \dots \\ &= -p_0 \delta V + T_0 \delta S - \frac{1}{2} \left(\frac{\partial p}{\partial V}\right)_{0S} \delta V^2 - \left(\frac{\partial p}{\partial S}\right)_{0V} \delta V \delta S + \frac{1}{2} \left(\frac{\partial T}{\partial S}\right)_{0V} \delta S^2 \dots\end{aligned}$$

$$\text{Hence} \quad \delta W = -\frac{1}{2} \left(\frac{\partial p}{\partial V}\right)_{0S} \delta V^2 - \left(\frac{\partial p}{\partial S}\right)_{0V} \delta V \delta S + \frac{1}{2} \left(\frac{\partial T}{\partial S}\right)_{0V} \delta S^2. \dots\dots (5)$$

$\delta W$  is the work done on the sub-system by the source of work necessary to increase its entropy and its volume above their equilibrium values by amounts  $\delta S$  and  $\delta V$  respectively; i.e. it is the potential energy per unit mass. The derivatives of this energy (taken with a negative sign) will be proportional to the forces called into play. When only the density changes, the force will be entirely mechanical, being proportional to

$$-\left(\frac{\partial \delta W}{\partial \delta V}\right)_{\delta S} = \left(\frac{\partial p}{\partial V}\right)_S \delta V + \left(\frac{\partial p}{\partial S}\right)_V \delta S = \delta p, \quad \dots\dots (6)$$

a remarkably simple result. On the other hand, when only the entropy changes, the force will be entirely thermal, proportional to

$$-\left(\frac{\partial \delta W}{\partial \delta S}\right)_{\delta V} = \left(\frac{\partial p}{\partial S}\right)_V \delta V - \left(\frac{\partial T}{\partial S}\right)_V \delta S = -\delta T, \quad \dots\dots (7)$$

$$\text{since} \quad \left(\frac{\partial p}{\partial S}\right)_V = -\frac{\partial}{\partial S} \left(\frac{\partial U}{\partial V}\right) = -\frac{\partial}{\partial V} \left(\frac{\partial U}{\partial S}\right) = -\left(\frac{\partial T}{\partial V}\right)_S.$$

\* Cf. Landau, L., and Lifshitz, E., *Statistical Physics* (Oxford: University Press).

§ 3. MECHANICAL AND THERMAL FORCES

For the sake of symmetry and generality we shall assume that the superfluid has a small but definite entropy  $S_s$ , that of the normal fluid being  $S_n$ . Then the measured entropy of the bulk fluid,  $S$ , is given by  $\rho S = \rho_n S_n + \rho_s S_s$ . Let  $x_n$  and  $x_s$  be vectors representing the displacements of normal and superfluid respectively. We introduce new coordinates  $x$  and  $y$  such that

$$\rho x = \rho_n x_n + \rho_s x_s, \quad \dots\dots(8)$$

$$\text{and} \quad y = (\rho_n x_n S_n + \rho_s x_s S_s) / (\rho_n S_n + \rho_s S_s) - x. \quad \dots\dots(9)$$

$y$  is defined as the sum of the weighted displacements of the normal and superfluid relative to  $x$ , the displacement of the fluid as a whole. This weighting is taken as proportional to the entropy carried. Thus in these new coordinates the equation of conservation of entropy may be expressed in the simple form

$$\delta S / S + \nabla \cdot y = 0. \quad \dots\dots(10)$$

Also, in these coordinates, the equation of conservation of mass becomes

$$\delta \rho / \rho + \nabla \cdot x = 0,$$

$$\text{i.e.} \quad \delta V / V - \nabla \cdot x = 0. \quad \dots\dots(11)$$

After some reduction, using the fact that  $\rho = \rho_n + \rho_s$ , we obtain for  $y$

$$S \rho^2 y = \rho_n \rho_s S^* (x_n - x_s), \quad \dots\dots(12)$$

where  $S^* = S_n - S_s$ . From these equations we obtain  $x_n$  and  $x_s$  in terms of  $x$  and  $y$  as follows:

$$x_n = x + y \rho S / \rho_n S^*, \quad \dots\dots(13)$$

$$\text{and} \quad x_s = x - y \rho S / \rho_s S^*. \quad \dots\dots(14)$$

Alternatively, relations (10) and (11) may be deduced analytically in the following way. The total entropy per unit volume  $\rho S$  changes with time only by flow through the sides of the volume, the contribution  $\rho_n S_n$  flowing with velocity  $\dot{x}_n$ , and the contribution  $\rho_s S_s$  with velocity  $\dot{x}_s$ . Then, ignoring quadratic effects,

$$\begin{aligned} 0 &= \frac{\partial(\rho S)}{\partial t} + \rho_n S_n \nabla \cdot \dot{x}_n + \rho_s S_s \nabla \cdot \dot{x}_s \\ &= S \left\{ \frac{\partial \rho}{\partial t} + \rho_n \nabla \cdot \dot{x}_n + \rho_s \nabla \cdot \dot{x}_s \right\} + \left\{ \rho \frac{\partial S}{\partial t} - (S - S_n) \rho_n \nabla \cdot \dot{x}_n - (S - S_s) \rho_s \nabla \cdot \dot{x}_s \right\}. \end{aligned}$$

The terms in the first bracket together give zero, since mass is conserved; integrating over time,  $\delta \rho + \rho \nabla \cdot x = 0$ . Using the definition  $\rho S = \rho_n S_n + \rho_s S_s$ , we have

$$-\rho_n (S - S_n) = \rho_s (S - S_s) = \rho_s \rho_n S^* / \rho,$$

where  $S^* = S_n - S_s$ . Thus the terms in the second bracket give

$$\frac{\partial S}{\partial t} + \frac{\rho_s \rho_n}{\rho^2} S^* \nabla \cdot (\dot{x}_n - \dot{x}_s) = 0.$$

Integrating over time, we obtain

$$\delta S + S \nabla \cdot y = 0,$$

where  $y$  is defined by (12).

Since the coordinate  $x$  gives the position of the centre of gravity of the normal and superfluid, the conservation law (11) shows that the density changes on movement of the centre of gravity of the two fluids. Again, since the coordinate  $y$  is proportional to the relative displacement of the normal and the superfluid, the conservation law (10) shows that the entropy changes with the relative displacement of the two fluids.

The potential energy  $\delta W$  of the system may now be expressed simply in terms of  $\nabla \cdot x$  and  $\nabla \cdot y$  by using the conservation laws (10) and (11). The kinetic energy may be expressed in terms of  $\dot{x}^2$  and  $\dot{y}^2$  by means of (13) and (14). Then the velocities of first and second sound may be deduced from the Euler equations

$$\frac{d}{dt} \left( \frac{\partial L}{\partial \dot{x}} \right) - \frac{\partial L}{\partial x} = -\nabla \left( \frac{\partial L}{\partial \nabla \cdot x} \right),$$

and

$$\frac{d}{dt} \left( \frac{\partial L}{\partial \dot{y}} \right) - \frac{\partial L}{\partial y} = -\nabla \left( \frac{\partial L}{\partial \nabla \cdot y} \right),$$

where  $L$  is the Lagrangian of the system, formed by taking the difference between the kinetic and potential energies. The calculation in these coordinates has been previously given (Dingle 1948).

Combining (6) with the equation of mass conservation (11), we have

$$\left( \frac{\partial \delta W}{\partial \nabla \cdot x} \right)_y = -V \left( \frac{\partial \delta W}{\partial \delta V} \right)_s = V \delta p, \quad \dots\dots (15)$$

giving the mechanical force acting on unit mass of the fluid when it is displaced as a whole.

Combining (7) with the equation of entropy conservation (10), we have

$$-\left( \frac{\partial \delta W}{\partial \nabla \cdot y} \right)_x = S \left( \frac{\partial \delta W}{\partial \delta S} \right)_v = S \delta T, \quad \dots\dots (16)$$

giving the thermal force acting on unit mass of the fluid when normal and superfluid are displaced in such a way that the fluid considered as a whole remains at rest.

#### § 4. FORCES ACTING ON THE FLUID

##### (i) *The Force acting on the Superfluid alone*

We wish to calculate the force acting on the superfluid when this alone is displaced, i.e. the value of  $-(\partial \delta W / \partial \nabla \cdot x_s)_{x_n}$ . Now from (8) and (12) we have  $(\partial x / \partial x_s)_{x_n} = \rho_s / \rho$  and  $(\partial y / \partial x_s)_{x_n} = -\rho_n \rho_s S^* / \rho^2 S$ . Then

$$\begin{aligned} \left( \frac{\partial \delta W}{\partial \nabla \cdot x_s} \right)_{x_n} &= \frac{\partial \delta W}{\partial \nabla \cdot x} \cdot \left( \frac{\partial x}{\partial x_s} \right)_{x_n} + \frac{\partial \delta W}{\partial \nabla \cdot y} \cdot \left( \frac{\partial y}{\partial x_s} \right)_{x_n} \\ &= -\frac{\rho_s}{\rho} V \delta p + \frac{\rho_n \rho_s}{\rho^2} S^* \delta T \end{aligned}$$

by (15) and (16). Hence the resultant force acting on unit volume of the fluid is

$$\rho_s \frac{d\dot{x}_s}{dt} = -\rho \nabla \left( -\frac{\partial \delta W}{\partial \nabla \cdot x_s} \right)_{x_n} = \rho_s \left( -\frac{\nabla p}{\rho} + \frac{\rho_n}{\rho} S^* \nabla T \right). \quad \dots\dots (17)$$

The force is therefore partly mechanical and partly thermal.

(ii) *The Force acting on the Normal Fluid alone*

We have, similarly,

$$\begin{aligned}\left(\frac{\partial \delta W}{\partial \nabla \cdot x_n}\right)_{x_s} &= \frac{\partial \delta W}{\partial \nabla \cdot x} \left(\frac{\partial x}{\partial x_n}\right)_{x_s} + \frac{\partial \delta W}{\partial \nabla \cdot y} \left(\frac{\partial y}{\partial x_n}\right)_{x_s} \\ &= -\frac{\rho_n}{\rho} V \delta p - \frac{\rho_n \rho_s}{\rho^2} S^* \delta T.\end{aligned}$$

Hence the resultant force per unit volume of fluid is

$$\rho_n \frac{d\dot{x}_n}{dt} = -\rho \nabla \left( -\frac{\partial \delta W}{\partial \nabla \cdot x_n} \right)_{x_s} = \rho_n \left( -\frac{\nabla p}{\rho} - \frac{\rho_s}{\rho_n} S^* \nabla T \right). \quad \dots\dots(18)$$

The force is again partly mechanical and partly thermal. Equation (18) is important, as it gives directly the force driving the heat current  $\rho S T_0 \dot{x}_n$ .

(iii) *The Force opposing Relative Displacement of Normal and Superfluid*

The force tending to restore equilibrium when the normal and superfluid are displaced relatively to each other will be entirely thermal, since by (12)

$$\frac{\partial \delta W}{\partial \nabla \cdot (x_n - x_s)} = \frac{\rho_n \rho_s S^*}{\rho^2 S} \frac{\partial \delta W}{\partial \nabla y} = -\frac{\rho_n \rho_s S^*}{\rho^2} \delta T, \quad \dots\dots(19)$$

by (16).

(iv) *Action of the Mechanical Force*

Adding equations (17) and (18), and neglecting quadratic terms, we have

$$\partial j / \partial t + \nabla p = 0, \quad \dots\dots(20)$$

since  $\rho = \rho_n + \rho_s$  and  $j = \rho_n \dot{x}_n + \rho_s \dot{x}_s$  by definition. Thus the mechanical force acts on the total current  $j$ . This confirms Landau's equation, (3) of this paper.

(v) *Action of the Thermal Force*

We shall now confirm the proposition that the thermal force acts only in restoring the relative displacement of the normal and superfluid to its equilibrium value zero, a result suggested by (19). We have, from (17),

$$\frac{d}{dt} \dot{x}_s = -\frac{1}{\rho} \nabla p + \frac{\rho_n}{\rho} S^* \nabla T,$$

and from (18)

$$\frac{d}{dt} \dot{x}_n = -\frac{1}{\rho} \nabla p - \frac{\rho_s}{\rho} S^* \nabla T.$$

Eliminating the mechanical force, we obtain

$$\frac{d}{dt} (\dot{x}_n - \dot{x}_s) = -S^* \nabla T. \quad \dots\dots(21)$$

Thus the thermal force acts on the relative velocity of normal and superfluid.

## § 5. CASE WHEN THE SUPERFLUID HAS ZERO ENTROPY

When the entropy of the superfluid is neglected, we usually associate the entropy with the bulk fluid considered as a whole. Then  $S^* = S_n - S_s = \rho S / \rho_n$ . In this case, (17) reduces to

$$\frac{d\dot{x}_s}{dt} = -\frac{1}{\rho} \nabla p + S \nabla T, \quad \dots\dots (22)$$

which is Landau's equation, (4) of this paper, quadratic terms being neglected. Similarly, (18) reduces to

$$\frac{d\dot{x}_n}{dt} = -\frac{1}{\rho} \nabla p - \frac{\rho_s}{\rho_n} S \nabla T, \quad \dots\dots (23)$$

giving the acceleration of the heat current.

## § 6. IRREVERSIBILITIES

The expression (5) for the potential energy of the system was deduced for a reversible process, i.e. for one in which the entropy of the whole system (sub-system plus medium) remains constant. If the entropy increases due to some irreversibility, we must add to the right-hand side of (5) terms of the form  $T_0 \delta S_{\text{irrev}}$ . In addition, irreversible processes will alter the form of the equation of entropy conservation. We shall discuss two types of irreversibility, that due to ordinary thermal conduction and that due to viscous effects.

(i) *Ordinary Thermal Conduction*

In this case the maximum irreversible gain of entropy per unit volume is given by  $\delta Q/T_0 = -K \nabla^2 T \cdot \delta t / T_0$ , where  $K$  is the ordinary heat conductivity, not involving movement of the fluid. Hence we must add a term of the form  $-K \nabla^2 T \delta t$  to the right-hand side of (5),  $\delta t$  being the change in time. The partial differential coefficients with respect to  $\delta V$  and  $\delta S$  do not involve the time, so that the forces, both thermal and mechanical, retain the values already given. However, the equation of entropy conservation must be written as

$$\frac{\partial(\rho S)}{\partial t} + \rho S \nabla \cdot \dot{x}_n - \frac{K}{T_0} \nabla^2 T = 0. \quad \dots\dots (24)$$

The consequences of this change have been discussed in a previous paper (Dingle 1948).

(ii) *Viscous Effects*

The dissipation function per unit volume due to the viscosity  $\mu$  of the normal fluid is given by (cf. Rayleigh 1926)

$$\begin{aligned} \mu \left[ \left( \frac{\partial \dot{x}_{nu}}{\partial u} \right)^2 + \left( \frac{\partial \dot{x}_{nv}}{\partial v} \right)^2 + \left( \frac{\partial \dot{x}_{nw}}{\partial w} \right)^2 - \frac{2}{3} (\nabla \cdot \dot{x}_n)^2 + \frac{1}{2} \left( \frac{\partial \dot{x}_{nv}}{\partial w} + \frac{\partial \dot{x}_{nw}}{\partial v} \right)^2 \right. \\ \left. + \frac{1}{2} \left( \frac{\partial \dot{x}_{nw}}{\partial u} + \frac{\partial \dot{x}_{nv}}{\partial w} \right)^2 + \frac{1}{2} \left( \frac{\partial \dot{x}_{nu}}{\partial v} + \frac{\partial \dot{x}_{nv}}{\partial u} \right)^2 \right], \quad \dots\dots (25) \end{aligned}$$

where  $u$ ,  $v$ , and  $w$  are three Cartesian coordinates.

On differentiation with respect to  $\dot{x}_n$ , this gives rise to a force per unit volume of magnitude

$$\mu[\nabla^2 \dot{x}_n + \frac{1}{3} \nabla \nabla \cdot \dot{x}_n] = \mu[-\nabla_\Lambda(\nabla_\Lambda \dot{x}_n) + \frac{4}{3} \nabla \nabla \cdot \dot{x}_n]. \quad \dots\dots (26)$$

This force acts on the normal fluid only, since the derivative of (25) with respect to  $\dot{x}_s$  vanishes.

The entropy gain to due this irreversible process is quadratic in the velocities, and may be neglected, leaving the equation of entropy conservation unchanged. Thus equation (17) (or (4)) for the force acting on the superfluid is unchanged, but equation (18) for the force acting on the normal fluid becomes

$$\rho_n \frac{d\dot{x}_n}{dt} = -\rho_n \left( \frac{1}{\rho} \nabla p + \frac{\rho_s}{\rho} S^* \nabla T \right) + \mu(\nabla^2 \dot{x}_n + \frac{1}{3} \nabla \nabla \cdot \dot{x}_n), \quad \dots\dots (27)$$

and (20) becomes

$$\frac{\partial j}{\partial t} + \nabla p - \mu(\nabla^2 \dot{x}_n + \frac{1}{3} \nabla \nabla \cdot \dot{x}_n) = 0. \quad \dots\dots (28)$$

#### REFERENCES

- DINGLE, R. B., 1948, *Proc. Phys. Soc.*, **61**, 9.  
 LANDAU, L., 1941, *J. Phys. U.S.S.R.*, **5**, 71; 1949, *Phys. Rev.*, **75**, 884.  
 LIFSHITZ, E., 1944, *J. Phys. U.S.S.R.*, **8**, 110.  
 LONDON, F., and ZILSEL, P. R., 1948, *Phys. Rev.*, **74**, 1148.  
 RAYLEIGH, Lord, 1926, *Theory of Sound*, 2nd edition (London : Macmillan), p. 315.  
 TISZA, L., 1947, *Phys. Rev.*, **72**, 838.

## The Dependence of the Thermal Diffusion Factor on Temperature

BY K. E. GREW

University College of the South-West, Exeter

*Communicated by F. H. Newman; MS. received 18th May 1949*

**ABSTRACT.** The thermal diffusion factor for isotopic mixtures has been calculated from values of the collision integrals given by Hirschfelder, Bird and Spotz which refer to molecules exerting an inverse 13th power repulsion with an inverse 7th power attraction—the (13, 7) model. The theoretical results are compared with experimental ones for the inert gas mixtures previously considered by Grew in relation to the (9, 5) model. The agreement is, as expected, better than for the (9, 5) model. Experimental results for hydrogen-helium mixtures are also given; the behaviour of these mixtures is exceptional in that the thermal diffusion factor appears to be independent of temperature over the range 12 to 600° K.

### § 1. INTRODUCTION

IN the theory of transport phenomena in gases certain integrals involving the collision parameters occur. These integrals can be evaluated only by numerical methods, consequently the number of molecular models for which they are known is small. Recently Hirschfelder, Bird and Spotz (1948) have published results for a special case of the Lennard-Jones type of molecule. This

is one whose force field is represented by an inverse power repulsion with a superposed inverse power attraction : thus the force between two molecules at distance  $r$  apart is

$$F = \kappa r^{-\nu} - \kappa' r^{-\nu'}$$

where  $\kappa, \kappa'$  are the force constants,  $\nu, \nu'$  the force indices, relating to the repulsive and the attractive force respectively. The case treated by Hirschfelder, Bird and Spotz is that in which the potential energy of interaction of two molecules separated by distance  $r$  is

$$E(r) = 4\epsilon[(r_0/r)^{12} - (r_0/r)^6],$$

where  $r_0$  is the separation for zero energy and  $\epsilon$  is the minimum energy (taken as positive). The corresponding force indices are therefore 12 and 6. Hirschfelder, Bird and Spotz have discussed the viscosity and thermal conductivity of a gas composed of molecules of this type (as also have de Boer and v. Kranendonk 1948). In what follows, their results are applied to find the thermal diffusion factor as a function of temperature for this model, after which a comparison of the theoretical results with some experimental ones is made. A similar comparison for another case of the Lennard-Jones molecule, that in which  $\nu=9$ ,  $\nu'=5$ , was made some time ago (Grew 1947); for this case the theoretical results are due to Clark Jones (1941).

## § 2. CALCULATION OF THE THERMAL DIFFUSION FACTOR

The Chapman-Enskog theory of non-uniform gases leads to the result that in a binary mixture in which a temperature gradient exists there is, in the steady state, a concentration gradient such that

$$\nabla n_{10} = -\nabla n_{20} = -\alpha n_{10}n_{20} \cdot \nabla(\ln T),$$

where  $n_{10}, n_{20}$  are the proportionate numbers of the heavier (1) and lighter (2) molecules respectively,  $T$  is the temperature, and  $\alpha$  is the thermal diffusion factor. The thermal diffusion factor in its first approximation may be expressed (following Chapman and Cowling's (1939) notation) as

$$[\alpha]_1 = 5(C-1) \frac{S_1 n_{10} - S_2 n_{20}}{Q_1 n_{10}^2 + Q_2 n_{20}^2 + Q_{12} n_{10} n_{20}},$$

where

$$S_1 = M_1 E_1 - 3M_2(M_2 - M_1) - 4M_1 M_2 A,$$

$$Q_1 = E_1[6M_2^2 + (5-4B)M_1^2 + 8M_1 M_2 A],$$

$$Q_{12} = 3(M_1 - M_2)^2(5-4B) + 4M_1 M_2 A(11-4B) + 2E_1 E_2,$$

and  $S_2, Q_2$  are derived from  $S_1, Q_1$  by interchange of subscripts. Here

$$M_1 = \frac{m_1}{m_1 + m_2}, \quad M_2 = \frac{m_2}{m_1 + m_2},$$

$m_1, m_2$  being the masses of the two kinds of molecules.  $(M_1 - M_2)$  is the proportionate mass difference,  $M$ . The quantities  $A, B, C, E_1, E_2$  involve the collision integrals referred to above. These integrals are denoted in general by

$W^{(l)}(r)$ , with subscript 1, 2 or 12 to distinguish the interactions of like and unlike molecules. Thus

$$A = \frac{W_{12}^{(2)}(2)}{5W_{12}^{(1)}(1)}, \quad B = \frac{5W_{12}^{(1)}(2) - W_{12}^{(1)}(3)}{5W_{12}^{(1)}(1)}, \quad C = \frac{2W_{12}^{(2)}(2)}{5W_{12}^{(1)}(1)},$$

$$E_1 = \frac{2A}{x_{12}(1-M)^{\frac{1}{2}}}, \quad E_2 = \frac{2A}{x_{21}(1+M)^{\frac{1}{2}}},$$

where

$$x_{12} = \left(\frac{r_{012}}{r_{01}}\right)^2 \frac{W_{12}^{(2)}(2)}{W_1^{(2)}(2)}, \quad x_{21} = \left(\frac{r_{012}}{r_{02}}\right)^2 \frac{W_{12}^{(2)}(2)}{W_2^{(2)}(2)}.$$

The integrals  $W$  can be evaluated, as Clark Jones showed in his original work for the (9, 5) model, for assigned values of the ratio  $kT/\epsilon$ . The evaluation of  $[\alpha]_1$  in the general (13, 7) case therefore requires a knowledge of the radii  $r_{01}$ ,  $r_{012}$ ,  $r_{02}$ , and the minimum values  $\epsilon_1$ ,  $\epsilon_{12}$ ,  $\epsilon_2$ , of the energy. But for the isotopic case, in which there is no distinction between the (1, 1), (2, 2) and (1, 2) interactions,  $x_{12} = x_{21} = 1$ , and  $[\alpha]_1$  may readily be found. This has been done for various values of the proportionate mass difference  $M$ , using the values of  $W^{(l)}(r)$  tabulated by Hirschfelder, Bird and Spotz.

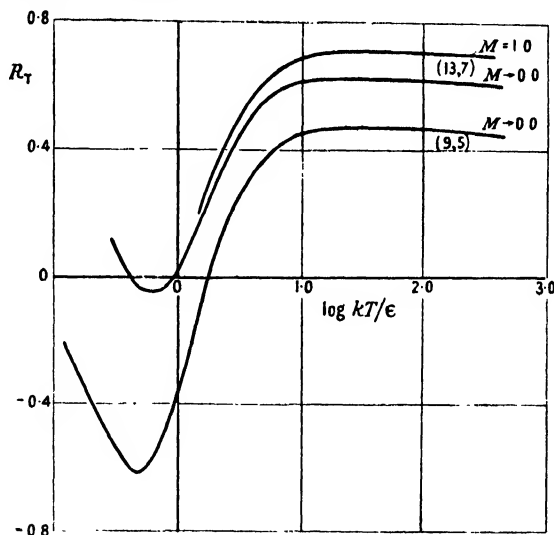


Figure 1. Values of the thermal separation ratio  $R_T$  as a function of  $kT/\epsilon$  for the (13, 7) model, and for the (9, 5) model.

From these values of  $[\alpha]_1$  the thermal separation ratio  $R_T$  has been evaluated. This quantity was first introduced in the discussion of thermal diffusion experiments as a measure of the extent to which the molecular interactions approach the ideally hard ones of rigid spheres. Experimentally  $R_T$  is defined as the ratio of the thermal diffusion factor  $\alpha$ , determined experimentally, to the calculated value (in first approximation) for molecules of the same mass and size as the experimental ones but interacting as rigid elastic spheres. Denoting this latter value by  $[\alpha(\infty)]_1$ ,

$$R_T(\text{exp.}) = \alpha(\text{exp.}) / [\alpha(\infty)]_1.$$

The molecular diameters are found by substitution of the experimental values of the viscosity in the theoretical expression for the viscosity of a gas consisting



of rigid spheres. The corresponding theoretical quantity for a given molecular model is

$$R_T(\text{theor.}) = \alpha(\text{theor.})/[\alpha(\infty)]_1,$$

where  $\alpha(\text{theor.})$  is the calculated exact value of the thermal diffusion factor for that model. In the present case only the first approximation to  $\alpha(\text{theor.})$  is known, and the values of  $R_T(\text{theor.})$  here considered are the ratios of the first approximations  $[\alpha(13, 7)]_1/[\alpha(\infty)]_1$ . This approximate value is likely to be too small, but the error cannot be definitely stated. In the simpler case of molecules which behave as centres of repulsion only, however, an estimate of the error leads to the following values of the ratio of the exact value and the first approximation when  $\nu=13$ :

$M$	0.1	0.5	0.7	1.0
$\alpha/[\alpha]_1$	1.03	1.10	1.13	1.18

The dependence of  $R_T$  on  $kT/\epsilon$  for this (13, 7) case is shown graphically in Figure 1, where the curves refer to the extreme values  $M \rightarrow 0$  and  $M=1.0$ . The corresponding curve for the (9, 5) case, derived from Clark Jones' results, is also given. The marked dependence of  $R_T$  on the temperature (implying of course a similar dependence of the thermal diffusion factor) which results from the introduction of the attractive component of the molecular field, and which was first brought out in Clark Jones' work, appears in the (13, 7) case, but with interesting differences. For the (13, 7) model, the value of  $kT/\epsilon$  at which  $R_T$  changes sign, the range over which  $R_T$  is negative, and the minimum value of  $R_T$  are all smaller than for the (9, 5) model.

### § 3. COMPARISON WITH EXPERIMENT

Although the results deduced above apply to isotopic mixtures, that is those in which the interaction energy is the same for like and unlike molecules, a comparison may be made between these theoretical values of  $R_T$  and experimental values for non-isotopic mixtures such as those of the inert gases. The justification of this, at least as a first step, is that whereas the thermal diffusion factor  $\alpha$  depends strongly on the ratios of the radii  $r_0$  and energies  $\epsilon$ , the value of  $R_T$  is much less sensitive. This is because  $[\alpha(\infty)]_1$  also depends on these ratios, which are taken into account in using the viscosity diameters in its evaluation. A closer comparison in the non-isotopic case requires the theoretical values of  $\alpha$  to be found using appropriate values of the three radii and minimum energies, quantities known in only some cases.

#### *The inert gas mixtures.*

The results of an investigation of thermal diffusion in mixtures of the inert gases have been described elsewhere (Grew 1947). A comparison was there made of the thermal separation ratio  $R_T$  determined experimentally in the range 90 to 600° K. with the theoretical values for the (9, 5) model calculated by Clark Jones (1941). In comparing these same results with the theoretical ones for the (13, 7) model the procedure followed previously has been slightly modified. As  $R_T$  is determined experimentally for a temperature  $T$  it is necessary to determine the corresponding value of  $kT/\epsilon$  before comparison with the theoretical values can be made. The appropriate value of  $\epsilon$  to be used in the reduction has been

taken as  $\epsilon_{12}$ , the minimum energy of unlike molecules. This is a reasonable approximation because in the expression for  $[\alpha]_1$  the factor which is strongly dependent on the temperature is  $(C-1)$ , and this involves the interaction energy of unlike molecules, and that only; the other factor varies but slightly with temperature. There are grounds for taking  $\epsilon_{12}$  as the geometric mean of  $\epsilon_1$  and  $\epsilon_2$ , the values appropriate to the interaction of like molecules; thus  $\epsilon_{12} = (\epsilon_1 \epsilon_2)^{1/2}$ .  $\epsilon_1$  and  $\epsilon_2$  have been calculated from the relation, which for neon and argon at least has experimental justification (Fowler and Guggenheim 1939, p. 345):  $\epsilon = kT_c/1.22$ , where  $T_c$  is the critical temperature.

On this basis it is found that when the values of  $R_T$  for the nine different mixtures examined, after a small modification for the effect of the different mass ratios, are plotted against  $kT/\epsilon_{12}$ , the curves are roughly superposable on a single

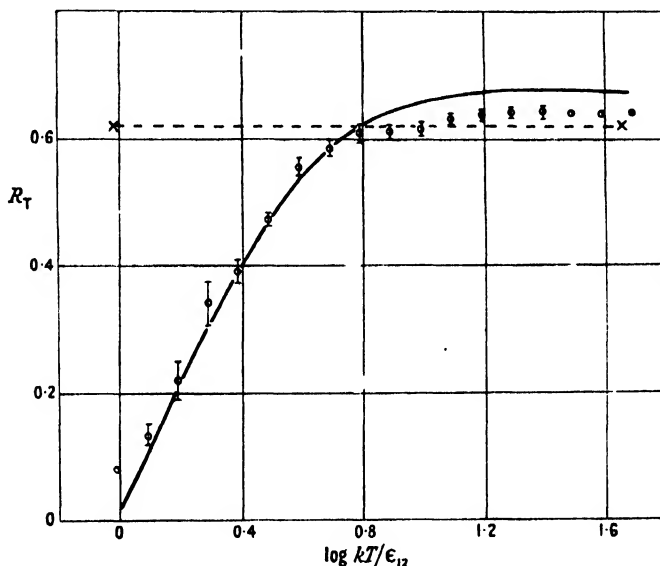


Figure 2. Full curve: values of  $R_T$  for (13, 7) model, with  $M=0.7$ .  
 $\Phi$ : mean experimental values of  $R_T$ , with deviations, for the inert gas mixtures.  
 Broken curve: experimental values of  $R_T$  for the  $H_2$ -He mixtures.

curve. The mean values of  $R_T$  at various values of  $kT/\epsilon_{12}$  are shown in Figure 2. Except at the extreme values of  $kT/\epsilon_{12}$ , the mean is found from values for, usually, four different mixtures. The deviations from the mean, which are indicated, are often considerable, but not so large as to suggest that the mixtures may not be considered as a group. Figure 2 shows also the theoretical values of  $R_T$  for an isotopic mixture in the (13, 7) case when  $M=0.7$ , the value to which the experimental curves were adjusted before their mean was found.

It is clear that the (13, 7) model represents the experimental results much better than does the (9, 5) model, with which the previous comparison was made. There is an appreciable discrepancy at the higher temperatures, where the experimental error is relatively small. It is possible that this would not appear if the comparison were made with theoretical values of  $R_T$  calculated for a non-isotopic mixture. On the other hand the discrepancy may be larger than it appears here, for the theoretical values are first approximations to  $R_T$ , and if the error is comparable with that for molecules interacting as centres of repulsion only, the exact values may be perhaps 10 per cent greater.

*Hydrogen-helium mixtures.*

The behaviour of hydrogen-helium mixtures in thermal diffusion is of interest because it is to be expected that for these light molecules quantum mechanical effects may be apparent at low temperatures. Recently experimental measurements of the thermal diffusion effect in this and other mixtures have been reported by v. Itterbeek, v. Paemel and v. Lierde (1947). In this work the gas mixture was contained in a diffusion vessel consisting of two bulbs, the upper of which was at a fixed temperature  $T$  of  $292^\circ\text{K}$ , the lower at temperatures  $T'$  ranging from  $90$  to  $12^\circ\text{K}$ . The change of composition of the gas in the upper bulb resulting from thermal diffusion was determined from the viscosity change, and from this the separation, that is the difference in composition in the two bulbs, was found. The results for hydrogen-helium mixtures can be supplemented by others, hitherto unpublished, obtained in the course of the experimental work with the inert gas mixtures (Grew 1947). Here the constant temperature  $T$  of one bulb was  $293^\circ\text{K}$ , the variable temperature  $T'$  of the other ranged from  $90$  to  $600^\circ\text{K}$ . The separation, for a mixture containing  $53.6\%$   $\text{H}_2$  is shown as a function of  $\log T'/T$  in Figure 3, the lower four points being found by interpolation from the data of v. Itterbeek *et al.* A similar curve for a hydrogen-nitrogen mixture is shown for comparison.

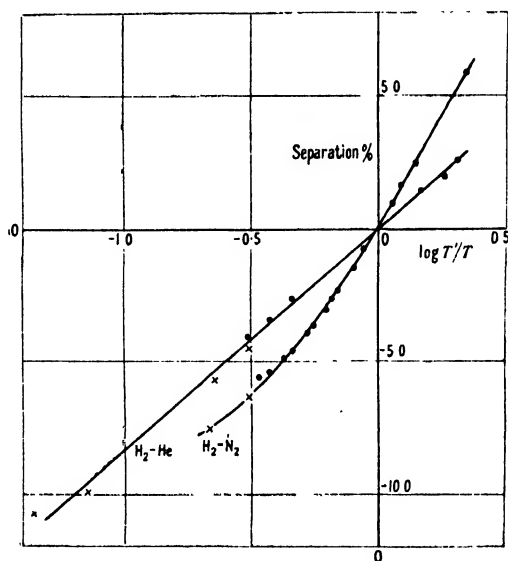


Figure 3. Separation as a function of  $\log T'/T$  for  $\text{H}_2$ -He ( $53.6\%$   $\text{H}_2$ ) and  $\text{H}_2$ - $\text{N}_2$  ( $39.8\%$   $\text{H}_2$ ).  
 $\times$  v. Itterbeek *et al.* ;  $\bullet$  Grew.

The curve for the hydrogen-helium mixture is remarkable in being rectilinear over the whole range of  $T'$  from  $12$  to  $600^\circ\text{K}$ . This implies that the thermal diffusion factor  $\alpha$  and the separation ratio  $R_T$  are independent of temperature in this range. All other mixtures so far examined behave like those of the inert gases in showing a decrease in  $R_T$  as the temperature falls. The value of  $R_T$  for this hydrogen-helium mixture is  $0.59$ ; if it is adjusted to correspond with  $M=0.7$  instead of the actual value  $M=0.33$ , it becomes  $0.62$ , and plotted with respect to  $kT/\epsilon_{12}$ , as for the inert gas mixtures, it gives the curve shown in Figure 2.

Since  $R_T$  is independent of temperature, the interactions can be represented by an inverse power repulsion only. From theoretical values of  $R_T$  calculated for this case, the force index which, for an isotopic mixture, corresponds with  $R_T = 0.59$  when  $M = 0.33$  is found to be 11.3.

The thermal diffusion effect thus illustrates strikingly the abnormal behaviour of hydrogen and helium at low temperatures which is manifested in other ways. The apparent absence of an attractive component of the molecular field at temperatures so near the critical temperature is a point of considerable theoretical interest.

#### REFERENCES

- DE BOER, J., and v. KRANENDONK, J., 1948, *Physica*, **14**, 442.  
 CHAPMAN, S., 1940, *Proc. Roy. Soc. A*, **177**, 38.  
 CHAPMAN, S., and COWLING, T. G., 1939, *Mathematical Theory of Non-uniform Gases* (Cambridge : University Press).  
 FOWLER, R., and GUGGENHEIM, A., 1939, *Statistical Thermodynamics* (Cambridge : University Press).  
 GREW, K. E., 1947, *Proc. Roy. Soc. A*, **189**, 402.  
 HIRSCHFELDER, J. O., BIRD, R., and SPOTZ, E. L., 1948, *J. Chem. Phys.*, **16**, 968.  
 v. ITTERBEEK, A., v. PAEMEL, O., and v. LIERDE, J., 1947, *Physica*, **13**, 231.  
 JONES, R. CLARK, 1940, *Phys. Rev.* **58**, 111; 1941, *Ibid.*, **59**, 1019.

## LETTERS TO THE EDITOR

### A Theory of Emissivity and Reflectivity

The following are some comments on a recent paper of the above title by D. J. Price (1949).

Dr. Price's manner of presenting the optical constants of metals is ingenious. Since the artifice he introduces is mathematical and does not contain any fundamentally new idea, it is not surprising that little agreement with experimental data is obtained. Thus he predicts a change of sign of the temperature coefficient of reflectivity in the region of transparency : but in a previous paragraph he puts the reflectivity  $R$  in that region equal to  $\frac{1}{10}(\lambda/\lambda_0)^4$ , which is clearly independent of the temperature. The intermediate region which is said to extend from  $0.1 \mu$  to  $10 \mu$  is, according to his theory, characterized by a constant reflectivity. In effect, most metals show an increase in  $R$  which extends up to  $3 \mu$  if not more. The Hagen-Rubens approximation can, of course, be derived in a simpler manner. Dr. Price concludes from his failure to predict the observed temperature variation that either the influence of the bound electrons must be emphasized more strongly or a radical change in the theory of dispersion is required. Without some quantitative support such theorizing is unwarranted. Let it be said first of all that the Mott-Zener formulae (1934) describe the behaviour of most metals satisfactorily : the only drawback is that, in the visible, it is necessary to postulate the existence of surface layers of very high resistivity. This will be referred to below. Secondly, an X-point is inherent in the theory of dispersion as based on Maxwell's equations. This is easily seen if only one of the two Hagen-Rubens approximations is carried out. Then the emissivity  $E$  is given by

$$E = \frac{1 + \sqrt{\frac{\lambda}{\rho}}}{1 + 2\sqrt{\frac{\lambda}{\rho}} + 2\frac{\lambda}{\rho}} \quad \dots\dots(1)$$

When this is differentiated with respect to  $\lambda/\rho$ ,  $E$  will be found to have a stationary value at

$$\lambda_X = \frac{1}{2}\rho. \quad \dots\dots(2)$$

This is, of course, too short a wavelength as compared with experimental data. However, when the Mott-Zener theory is made the basis of the calculation (Weil 1948) it is found that

$$\lambda_X = \sqrt{3} \lambda_r, \quad \dots\dots (3)$$

where  $\lambda_r = 2\pi c\tau$ , and  $\tau$  is twice the time of relaxation of the free electrons ( $=m/pe^2f_0$ ).

The writer has compiled a Table which compares calculated values of  $\lambda_X$  (the X-point of Price) with those found in the literature. Corrections have been carried out for the different temperature ranges covered by the various authors. At very high temperatures  $\lambda_X$  is practically constant since the temperature coefficient of resistivity becomes progressively smaller (cf. Ornstein's results). In this connection McCauley's data on tantalum are of interest. He refrained from "smoothing" his experimental curves, and the shift of  $\lambda_X$  in accordance with the above expression (3) is clearly seen. The agreement between the two sets of results is striking although they all occur in a transition region. No agreement could be obtained for copper, silver and gold.

It is seen that there is no need for an increased emphasis of the bound electrons. Nor is there any necessity radically to modify the theory of dispersion. This follows (a) from the agreement obtained above, and (b) from Kent's work (1919) on liquid metals. On the contrary, both (a) and (b) suggest that a large "Restwiderstand", particularly obnoxious at medium temperatures, is responsible for the disagreement found between theory and experiment. It would appear to the writer that the only remedy lies in providing an improved technique for the preparation of mirrors: the development of anodic polishing is highly desirable from this point of view.

Comparison of calculated and observed values of  $\lambda_X$  (in  $\mu$ )

	Ni	Pt	Pd	W	Mo	Ta	Fe	Steel
Calc.	1.6	2.51	2.99	4.32	5.5	1.9	2.43	—
Obs.	<sup>1)</sup> 1.8	<sup>4a)</sup> 0.7	<sup>4b)</sup> 1.0	<sup>5)</sup> 1.27	<sup>7)</sup> 1.4	<sup>4c)</sup> 0.8	<sup>8a)</sup> 1.0	<sup>8b)</sup> 1.0
Calc.	2.77	—	—	3.2	—	1.39	—	—
Obs.	<sup>2)</sup> 2.15	—	—	<sup>6)</sup> 1.65	—	<sup>4d)</sup> 0.6	—	<sup>9)</sup> 0.65
Calc.	2.1	—	—	—	—	—	—	—
Obs.	<sup>3)</sup> 2.5	—	—	—	—	—	—	—

In calculating the values of  $\lambda_X$  it is assumed that there is one free electron per atom.

	Mean temperature (°C.) covered by each author
<sup>1)</sup> HURST, C., 1933, <i>Proc. Roy. Soc. A</i> , <b>142</b> , 46 6	925
<sup>2)</sup> REID, C., 1941, <i>Phys. Rev.</i> , <b>60</b> , 161	470
<sup>3)</sup> CENNAMO, F., 1939, <i>Atti accad. Italia</i> , <b>1</b> , 174	677
<sup>4)</sup> MCCAULEY, G., 1913, <i>Astrophys. J.</i> , <b>37</b> , 164	(a) 1423 (b) 1226 (c) 1717 (d) 2451
<sup>5)</sup> WENIGER, G., and PFUND, A., 1919, <i>Phys. Rev.</i> , <b>14</b> , 427	1451
<sup>6)</sup> ORNSTEIN, L. S., 1937, <i>Physica</i> , <b>3</b> , 561	2027
<sup>7)</sup> PRICE, D. J., 1947, <i>Proc. Phys. Soc.</i> , <b>59</b> , 131	1220
<sup>8)</sup> HAGEN, E., and RUBENS, H., 1910, <i>S.B. preuss. Akad. Wiss.</i> , <b>23</b> , 467	(a) 100 (b) 85
<sup>9)</sup> WEIL, R., 1947, <i>Nature, Lond.</i> , <b>159</b> , 305	100

Vision Research Unit,  
Institute of Ophthalmology,  
London W.C.1.

R. WEALE.

KENT, C. V., 1919, *Phys. Rev.*, **14**, 459.  
MOTT, N. F., and ZENER, H., 1934, *Proc. Camb. Phil. Soc.*, **30**, 249.  
PRICE, D. J., 1949, *Proc. Phys. Soc.*, **62**, 278.  
WEIL, R., 1948, *Proc. Phys. Soc.*, **60**, 8.

## AUTHOR'S REPLY

The dispersion equations and other physical assumptions used in this theory are identical in form with those employed by Mott, Krönig, Zener, and Mr. Weale himself. The removal of certain untractable expressions, and the examination of previous approximations shows that certain consequences of these usual assumptions are in greater conflict with experiment than had been supposed.

Bound electron effects are large in the intermediate region. This is evident in the case of silver, where the clearly differentiated resonance band affects the ordinary reflectivity curve so much that the lower limit of the intermediate region cannot occur before about  $1.0\ \mu$ . This effect, together with the difficulty of accurate measurement, is probably the main reason why a large region of constant reflectivity has not been readily observed.

The excellent agreement obtained by Kent was, as stated, due to the use of a fundamentally different dispersion formula containing an extra term to take account of the bound electron contribution. His work therefore, far from supporting the present theory, is a further indication that some change is necessary.

The postulate of a surface layer having very different properties is widely used and attractive but, at the moment, it is a quite empirical device to reconcile theory and experiment.

The theory predicts that a zero value of the temperature coefficient of reflectivity can only occur near a region of transparency. As a matter of fact, the temperature coefficient is very near zero over the whole of the region of transparency of the model metal considered. There is no contradiction in this since, under such conditions, a true X-point cannot occur. Such phenomena, termed "spurious" X-points, have been noted in a previous paper (Price 1947).

The approximation from Maxwell's equations is not, of course, valid for so short a wavelength as the  $\lambda_X$  deduced from it.

Raffles College,  
Singapore.

D. J. PRICE.

PRICE, D. J., 1947, *Proc. Phys. Soc.*, **59**, 131.

---

## Hyperfine Splitting in Paramagnetic Resonance

Following the illness and sudden death of Dr. R. P. Penrose, after his discovery of the hyperfine structure in the paramagnetic absorption curve of a copper Tutton salt (Penrose 1949), we decided to investigate the behaviour of the hyperfine splitting of  $\text{Cu}^{++}$  in a similar way to that already undertaken for  $\text{Co}^{++}$  (Bleaney and Ingram 1949).

A crystal of  $\text{ZnSO}_4(\text{NH}_4)_2\text{SO}_4 \cdot 6\text{H}_2\text{O}$  in which about one zinc ion in every 1,000 was replaced by a copper ion was investigated, using radiation of 3 cm. wavelength and at a temperature of  $20^\circ\text{K}$ . The procedure was analogous to that used for a systematic survey of the copper Tutton salts (Bleaney, Penrose and Plumpton 1949), except that the sensitivity of the apparatus was increased by modulating the applied d.c. magnetic field, and the amplified output is fed direct to an oscillograph screen, the time-base of this being fed from the modulating coils. In this way the absorption lines can be displayed directly on the screen provided the sweep of magnetic field is considerably larger than the line breadth.

By using the very dilute crystals the line width is so reduced that the hyperfine structure, due to the different orientations of the nucleus in the field of the electrons, can be resolved. The nuclear spin of both the copper isotopes is  $3/2$ , and hence each electronic energy level is split into a further four levels, and for a selection rule  $\Delta M = 0$  four hyperfine lines should be obtained,  $M$  being the resolved component of  $I$  in direction of the field.

A systematic investigation of the variation of the splitting of these lines with orientation to the magnetic axes of the crystal has been undertaken. Like the corresponding cobalt salt (Bleaney and Ingram 1949), the crystal has two ions per unit cell with their tetragonal axes of electric field symmetry in the  $\text{K}_1\text{K}_3$  plane. Measurements in this plane are of the most interest since maximum and minimum values of  $g$  and  $\Delta H$ , the overall hyperfine splitting, are found parallel and perpendicular to a tetragonal axis.

The general results obtained are tabulated below,  $\theta^\circ$  being the angle of the applied magnetic field to the tetragonal axis; and, as in the case of cobalt, it is found that  $g^4(\Delta H)^2$  is a linear function of  $\cos^2\theta$ .

$\theta^\circ$	$\Delta H$	$g^4(\Delta H)^2 \times 10^6$	$\theta^\circ$	$\Delta H$	$g^4(\Delta H)^2 \times 10^6$
0	350	46.0	52	260	17.3
7	345	43.5	63	214	10.5
22	340	39.7	73	146	4.5
32	323	32.8	83	84	1.5
42	301	26.0	90	51	0.53

Two new features of interest arise in the study of this salt, however, namely the existence of an isotope splitting, and a splitting due to nuclear quadrupole moment.

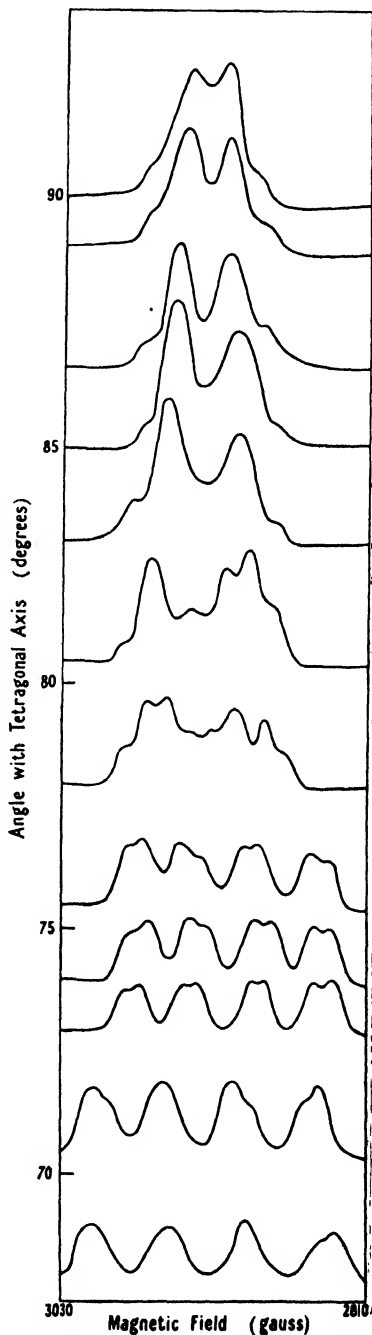


Figure 1.

At directions nearly parallel to a tetragonal axis the extreme lines of the hyperfine pattern are found to have a component of approximately half intensity partially separated on the outer sides. The two different isotopes of copper, of relative abundance 65 to 35, have a slightly different magnetic moment of ratio 1 to 1.071 (Pound 1948). Hence a splitting of  $\frac{1}{2} \times 0.07 \times \Delta H$  would be expected, and for the maximum  $\Delta H$  parallel to a tetragonal axis this is equal to 12 gauss. Experimentally the splitting is equal to  $10 \pm 2$  gauss in this direction, and decreases as  $\Delta H$  decreases; this therefore confirms the effect as due to the two different isotopes.

A very different effect occurs at a direction near the normal to a tetragonal axis, and the behaviour of the lines in this region is shown in Figure 1. As the angle increases from  $60^\circ$  to  $80^\circ$  each of the four lines is seen to split into two equal components of separation of the order of twelve gauss. The intensities of these appear to vary, however, and as the perpendicular direction is approached the whole pattern collapses as shown. By tracing individual lines through the pattern it would seem that a weak component first appears on the inner side of the original line, and that this gradually grows in intensity until it is about twice as strong as the latter.

This splitting is too large to be due to the isotope effect and appears to be caused by a combination of the magnetic interaction and the interaction of the nuclear electric quadrupole moment. Thus, near the tetragonal axis the magnetic effect dominates, but at angles nearly perpendicular to the axis this is weaker and the electric quadrupole moment becomes of the same order of magnitude; under these conditions the selection rule for  $\Delta M$  breaks down, so that more than four lines are obtained.

On this assumption Professor Pryce has made some detailed calculations on the positions and intensities of the lines in the perpendicular direction. The results of this are shown in Figure 2, and are seen to agree quite well with the experimental curve.

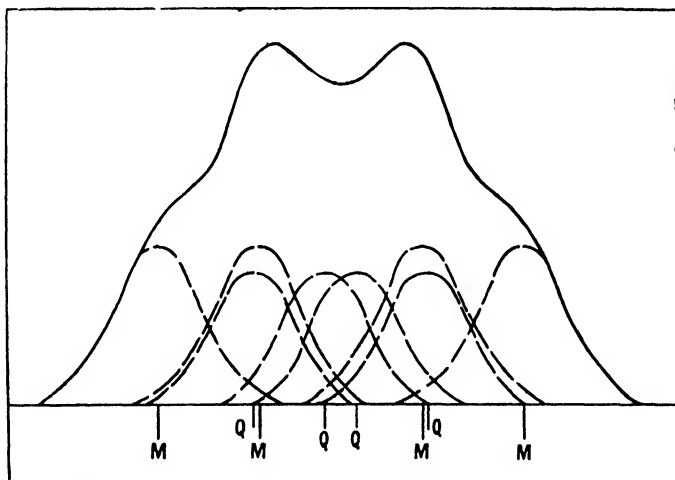


Figure 2. Theoretical prediction of line shape at  $\theta = 90^\circ$ .

M=line due to magnetic interaction. Q=line due to quadrupole interaction.

Measurements have also been made on dilute cobalt and copper fluosilicates. The hyperfine structure of the  $\text{Co}^{++}$  behaves similarly to the Tutton salt,  $g$  varying from 5.4 to 3.4 and  $\Delta H$  from 520 to 193 gauss, parallel and perpendicular to the trigonal axis respectively, but the  $\text{Cu}^{++}$  now appears to have an isotropic  $g$  value.

I should like to thank Professor Pryce and Dr. Bleaney for much guidance whilst the experimental work was being performed.

Clarendon Laboratory,  
Oxford.

4th July 1949.

D. J. E. INGRAM.

BLEANEY, B., and INGRAM, D. J. E., 1949, *Nature, Lond.*, **164**, 116.

BLEANEY, B., PENROSE, R. P., and PLUMPTON, B. I., 1949, *Proc. Roy. Soc. A*, in the press.

PENROSE, R. P., 1949, *Nature, Lond.*, **163**, 992.

POUND, R. V., 1948, *Phys. Rev.*, **73**, 523.



## REVIEWS OF BOOKS

*Compilation of Thermal Properties of Hydrogen in its Various Isotopic and Ortho-para Modifications*, by H. W. WOOLLEY, R. B. SCOTT and F. G. BRICKWEDDE. Pp. 96. (U.S. Department of Commerce, National Bureau of Standards, 1948). 40 cents.

From spectra we learn the term levels and so may calculate the energies of the molecules of gas. The Boltzmann factors show how these will contribute to the physical properties, and so the entropy and free energy of a sufficiently rarefied gas may be calculated as functions of temperature and pressure. The properties of the real gas, at finite densities, are related to these properties for the rarefied (ideal) gas by thermodynamic formulae which involve the constants of the equation of state. Then such derived quantities as specific heat may be deduced in the familiar way.

The authors of this important monograph, which appears as Research Paper RP 1932 in volume 41 of the *Journal of Research of the National Bureau of Standards*, published in November 1948, have carried through this programme for hydrogen in its various forms. Starting with the spectroscopic data and applying statistical mechanics, they compute the thermodynamic functions from  $10^\circ \text{K.}$  to  $2,000^\circ \text{K.}$  for HD and  $\text{D}_2$  and to  $5,000^\circ$  for  $\text{H}_2$ . They then tabulate  $pV/RT$  for the real gas as a function of temperature and density and so deduce the properties for the real gases. Ortho-para modifications and dissociation at high temperature are taken into account.

Other properties which do not follow so directly from basic data are also tabulated; they include viscosity and thermal conductivity, vapour pressure and the equation of state for the condensed phases. As far as data are available, tritium is included in all the fields surveyed.

The compilation will be of value to workers in a great diversity of branches of physics, and will be needed in any reference library. An erratum slip is issued with the reprint, and, since it is easily lost, should be used at once to correct the text. J. H. A.

*Le Noyau atomique*, by A. BERTHELOT. Pp. 32. (Paris: Centre National de la Recherche Scientifique, 1948). Price 25s. 6d. Obtainable from Messrs. H. K. Lewis & Co. Ltd.

This monograph is one of a series issued under the auspices of the French Physical Society. Because it happens that the chief advances in nuclear physics in the last few years have been published in the English language, the book is probably more needed in France than it would be in England.

Of its three chapters, the first surveys the facts about the known stable isotopes. The second deals with radioactivity, and includes an exposition of the Fermi theory, and a short account of Yukawa's field theory. The third chapter, entitled *nuclear fission*, rapidly surveys the facts, and then summarizes the theory of Bohr and Wheeler (the liquid-drop model).

The booklet as a whole fills the same sort of needs as do the articles in *Reports on Progress in Physics*; although it is shorter than most such articles on major subjects, it aims, like them, at helping physicists rather than laymen. It is very well written and, within its limits, is accurate and reliable. J. H. A.

## RECENT PUBLICATIONS RECEIVED

*How to Study Physics*, by SEVILLE CHAPMAN. Pp. iv+28. Revised Edition. (Cambridge, Mass.: Addison-Wesley Press Inc., 1949.) 25 cents.

*Die Brechzahlen einiger Halogenidkristalle*, by H. HARTING. Pp. 25. Sitzungsberichte der Deutschen Akademie der Wissenschaften zu Berlin, Mathematische-Naturwissenschaftliche Klasse, Jahrgang 1948, Nr. IV. (Berlin: Akademie-Verlag, 1948.) 2.50 D.M.

*Max Planck: In Seinen Akademie-Ansprachen* (Erinnerungsschrift der Deutschen Akademie der Wissenschaften zu Berlin). (Berlin: Akademie-Verlag, 1948.)

## CONTENTS FOR SECTION B

	PAGE
Prof. J. D. BERNAL. 'The Physical Basis of Life . . . . .	597
Mr. T. SMITH. The Contributions of 'Thomas Young to Geometrical Optics, and their Application to Present-day Questions . . . . .	619
Mr. R. J. DONATO. The Diffuse Reflectivity of Oxide Layers Formed on Steels under Defined Conditions . . . . .	629
Mr. H. ASHCROFT and Dr. C. HURST. Transit Time Correction Factor for Cylindrical Noise Diodes . . . . .	639
Dr. W. I. PUMPHREY. The Mode of Fracture at the Neck of a Tensile Specimen. .	647
Dr. M. McCAIG. The Magnetostriction of Anisotropic Permanent Magnet Alloys . . . . .	652
Mr. W. HOPWOOD. The Positive Streamer Mechanism of Spark Breakdown .	657
Reviews of Books . . . . .	664
Recent Publications Received . . . . .	666
Contents for Section A . . . . .	667
Abstracts for Section A . . . . .	667

## ABSTRACTS FOR SECTION B

*The Physical Basis of Life*, by J. D. BERNAL.

32nd Guthrie Lecture, delivered 21st November 1947.

*The Contributions of Thomas Young to Geometrical Optics, and their Application to Present-day Questions*, by T. SMITH.

**ABSTRACT.** Thomas Young's constructions for primary and secondary conjugate foci are described, and his algebraic equations are given. The latter are put into the form found most convenient when an instrument of several surfaces is considered. The special forms of these equations referred to the centres of curvature of the reflecting or refracting surfaces are used to show that in spherically symmetrical instruments the number of degrees of freedom—which is equal to the number of surfaces when these are spherical—must exceed the number of aberrations that can be corrected. It is concluded that non-spherical surfaces are likely to be very important, or perhaps essential, for any marked improvement in the correction of optical instruments, and that Young's equations, which relate expressly to spherical surfaces, may prove less useful in the future than they have been in the past.

*The Diffuse Reflectivity of Oxide Layers Formed on Steels under Defined Conditions*, by R. J. DONATO.

**ABSTRACT.** A method to determine the reflectivity of oxide layers formed on steels under defined conditions at various wavelengths in the visible spectrum and at different temperatures up to 660° C. is described. An integrating sphere is used in which the specimen replaces a portion of the sphere wall, and a method is given for the simultaneous comparison of two beams of light using a single photocathode. Except for a correction factor depending upon the geometry of the sphere, the measurements rely solely upon the area of an adjustable aperture. Some results are given for the oxides of various steels.

*Transit Time Correction Factor for Cylindrical Noise Diodes*, by H. ASHCROFT and C. HURST.

**ABSTRACT.** The noise generated by a diode is always less than it would be if the transit of the electrons were instantaneous. The factor by which it is reduced has been evaluated for transit angles up to  $12\frac{1}{2}$  radians and for ratios of anode to cathode radius up to 20. It has been found to fall to zero for one pair of values of these parameters.

*The Mode of Fracture at the Neck of a Tensile Specimen*, by W. I. PUMPHREY.

**ABSTRACT.** Bridgman has shown that in a cylindrical specimen which is deforming plastically under longitudinal tension the tensile stress at the neck of the specimen is greatest on the longitudinal axis and least at the periphery of the specimen. Fracture therefore commences at the centre of the specimen and extends from the centre to the periphery. "Double-cup" fractures encountered during the tensile testing of a number of alloys at elevated temperatures have been accounted for in this way and an examination has been made of the metallurgical factors which govern the occurrence of this type of fracture.

*The Magnetostriction of Anisotropic Permanent Magnet Alloys*, by M. McCAIG.

**ABSTRACT.** Blocks of permanent magnet alloys of the system Fe Ni Al Co Cu have been prepared with columnar crystals. The magnetostriction has been measured in various directions before and after heat treatment in a magnetic field. The results agree well with those predicted theoretically, and so confirm the postulated crystal structure.

*The Positive Streamer Mechanism of Spark Breakdown*, by W. HOPWOOD.

**ABSTRACT.** The essential conditions for streamer onset in spark breakdown are discussed, with particular reference to the production of photo-ionizing radiation in the initial avalanche. It is shown that the process of electron-ion recombination can adequately account for the production of the necessary radiation, and is probably the predominant process. It is also shown that the yield of photons by this mechanism, and consequently the threshold for streamer advance, is critically dependent upon the space-charge field produced by the initial avalanche. While Meek's criterion in its quantitative form gives the order of this critical space-charge field and enables the breakdown voltage for uniform electric fields to be calculated, the newly proposed conditions for photon production give a new physical significance to the criterion.

# THE PROCEEDINGS OF THE PHYSICAL SOCIETY

## Section A

---

VOL. 62, PART 11

1 November 1949

No. 359 A

---

### On the Size-Frequency Distribution of Penetrating Showers

BY W. HEITLER AND L. JÁNOSSY

Dublin Institute for Advanced Studies

*MS. received 30th June 1949*

**ABSTRACT.** We have calculated the relative number of showers containing  $n$  mesons when a fast primary nucleon hits a compound nucleus on the assumption that in a single nucleon-nucleon collision only one meson is produced (pure plural production). The cross section for meson production is assumed to have the form  $\Phi(\epsilon/E)d\epsilon/E$ , where  $E$  is the energy of the primary and  $\epsilon$  the energy lost by it, but the absolute value of  $\Phi$  and its dependence on  $\epsilon/E$  are left open. The fluctuations of the shower size are duly taken into account. For comparison with experiments it is assumed that about half the number of fast shower particles are fast protons as suggested by the positive excess of penetrating shower particles. The theoretical results depend on two constants, the total cross section and some weighted average over the energy distribution  $\Phi(\epsilon/E)$ . Choosing these suitably, the results are in good agreement with the relevant data within the experimental statistical errors, and the agreement extends also to the "large showers" with 20 or so thin tracks. The values of the constants thus determined are physically reasonable. It is concluded that the size-frequency distribution of penetrating showers can be fully understood on the basis of pure plural production, but some—small or large—contribution from multiple processes cannot be excluded.

#### § 1. INTRODUCTION

IN recent papers by Brown, Camerini, Fowler, Heitler, King and Powell (1949) the relative frequency of stars with a given number  $n$  of "thin tracks" is measured. There can be little doubt that these events in the photographic emulsion are identical with the penetrating showers previously found and observed in counter and cloud chamber experiments by Jánossy, Rochester and others. If this is true, then it is also highly probable that we have to deal here with the process of meson-production by fast nucleons (and, indeed, roughly half of the stars are initiated by charged, half by neutral particles) and that at least a considerable fraction of the thin tracks are mesons ( $\pi$ -mesons, presumably, perhaps also  $\tau$ -mesons). Some of the tracks are also likely to be fast protons.

For the interpretation of these events, two widely different hypotheses have been put forward: (i) The occurrence of groups of particles is explained in a natural way as due to a multiple collision of the primary nucleon with *several* of the closely packed nucleons in a compound nucleus, O, C, N or Ag, Br in the photographic plate. We call this process, following J. G. Wilson, plural production. (ii) The groups are assigned to a single elementary process in which the fast

nucleon would produce several mesons in one single collision with a single nuclear nucleon (genuine multiple process). It is assumed here that the emission of several mesons in one act is *more probable* than that of a single meson. The process (ii) would be a type of process for which so far no analogue is known in physics\*, in so far as the emission of the minimum number of particles or quanta (compatible with conservation laws) is always the most probable event. A decision between the two interpretations therefore involves a rather fundamental issue and would be of great importance for the future development of meson theory. In this paper we examine the question whether the data available to date can be understood by the assumption (i) of pure plural production. It will be seen that this is the case quantitatively within the present accuracy of the experimental data, with exception of an irregularity that—possibly—occurs in the experimental distribution curve (cf. §6). But this irregularity is not firmly established.

The agreement also applies to the “large showers” observed so far (up to 22 particles and, perhaps, even to the one case of 31 particles, cf. §6), and there is no necessity to assume a different type of process for these showers.

It will furthermore be seen that the assumptions one has to make about the cross section for meson production etc. to reach this agreement are physically reasonable and they are in harmony with the known facts about the absorption coefficient of fast nucleons†. They are further compatible with the values given in the theory of meson production put forward by Hamilton, Heitler and Peng in its later version‡, within the rather wide limits set by this theory.

Whilst the facts can be explained by the assumption of pure plural production, the issue is not yet decided. It might be possible to explain the facts also by process (ii) (see, e.g., Heisenberg 1949, also Dallaporta and Clementel 1948), making suitable assumptions about the multiplicities and their energy dependence, but a complete theory that would predict them as more probable than the single emission is not available. Nor can it be stated—even if the explanation of mainly plural processes is accepted—that all of the showers in question are plural. It might well be that a fraction of the showers or part of the multiplicity in a given shower is due to genuine multiple processes.

We shall work out the pluralities of the process in a more phenomenological way without assuming any detailed theory of meson production. We shall only make some very general assumptions about the energy dependence of the cross section etc. It will be seen that then two constants occur, the total cross section and some weighted average over the energy distribution of the emitted mesons. We shall try to fix these constants, as far as is possible, by comparison with the facts.

For a first orientation we shall neglect in this paper any secondary production of mesons by fast recoil nucleons within the same nucleus. This effect may not be negligible when the primary is very fast and tends to make an already big shower still bigger, especially in heavy nuclei. This will have to be taken into account in the discussion of the available material (§6).

\* The emission of several extremely soft photons in any electromagnetic process (which is sometimes quoted as an analogue) hardly bears any resemblance to the high energy multiple processes in question. The former is a purely classical phenomenon, translated into the language of quantum theory.

† Cf. Heitler and Jánossy 1949, quoted in the following as HJ.

‡ For references see Heitler 1949, quoted in the following as HHP.

## § 2. THEORY OF PLURAL PRODUCTION

We wish to calculate the probability for  $n$  mesons to be emitted in a collision of a fast nucleon with a given nucleus. Let  $\Phi(\epsilon, E)d\epsilon$  be the cross section for emission of a meson with an energy loss  $\epsilon$  suffered by the nucleon with initial energy  $E$  in a collision with a single nucleon.  $\epsilon$  includes the recoil energy. Instead of  $\epsilon$  we use  $E' = E - \epsilon$ . In a passage through a nucleus in general several acts of meson emission and discontinuous energy losses will occur. We make the following basic assumptions:

(i) 'That 
$$\Phi(E', E) dE' = \Phi\left(\frac{E'}{E}\right) \frac{dE'}{E} \dots\dots (1)$$

shall be a function of  $E'/E$  only. This assumption has a high degree of probability for being at least approximately correct. In the first place the analogous law for Bremsstrahlung has the same form, and in the second place the (very crude) theory of HHP leads to the same result. (1) holds, of course, only for sufficiently high energies  $E$ , say above a certain critical energy  $E_c$ .

(ii) 'The individual acts of emission shall be statistically independent events. This assumption is somewhat doubtful, on account of the large disturbance caused in the nucleus even after the first emission. However, one may argue that the recoil energies produced in each emission act are in most cases small compared with the energy of the primary nucleon. The energy communicated through the recoil to the second nucleon which suffers the second hit from the primary will be even smaller, and since we may treat the nuclear nucleons anyhow as free it will hardly be very wrong to consider them all at rest before they are hit by the primary.

It is convenient to write

$$\Phi\left(\frac{E'}{E}\right) \frac{dE'}{E} = \Phi \cdot \omega\left(\frac{E'}{E}\right) \frac{dE'}{E}, \quad \int_0^E \omega\left(\frac{E'}{E}\right) \frac{dE'}{E} = 1 \dots\dots (2)$$

( $\omega$  differs from the quantity  $w$  used in HJ by the factor  $N d_A \Phi$ ).  $\Phi$  is the total cross section and is, by (1), a constant. Let  $N$  be the density of nuclear matter. The probability for a total loss of energy from  $E$  to  $E' \equiv E_{n-1}$  in  $n-1$  individual acts of emission, each taking place in the intervals of distance between  $x_1$  and  $x_1 + dx_1, \dots, x_{n-1}$  and  $x_{n-1} + dx_{n-1}$ , is

$$\begin{aligned} p_{n-1} dE' &= \int \dots \int \omega\left(\frac{E_1}{E}\right) \frac{dE_1}{E} \omega\left(\frac{E_2}{E_1}\right) \frac{dE_2}{E_1} \times \dots \\ &\times \omega\left(\frac{E_{n-1}}{E_{n-2}}\right) \frac{dE_{n-1}}{E_{n-2}} (\Phi N)^{n-1} \exp(-\Phi N x_n) dx_1 \dots dx_{n-1}, \dots\dots (3) \\ &(E > E_1 > E_2 \dots > E_{n-1}); \quad E_{n-1} \equiv E' > E_c. \dots\dots (3') \end{aligned}$$

The integral is to be extended over all values  $E_1, E_2 \dots E_{n-2}$  ( $E_{n-1}$  is given) satisfying (3'). It is furthermore to be extended over all values of  $x_1, x_2 \dots x_{n-1}$  satisfying

$$0 < x_1 < x_2 < x_3 \dots < x_{n-1} < x_n \text{ say.} \dots\dots (3'')$$

The factor  $\exp(-\Phi N x_n)$  is the probability that within the total distance  $x_n$  no emission act takes place, except in the infinitesimal intervals  $dx_1 \dots dx_{n-1}$  whose total length is, of course, zero compared with  $x_n$ . The reason for denoting the total length by  $x_n$  will become clear below.

We introduce  $y_m = \log(E_{m-1}/E_m), \quad Y = \log(E/E').$

The integration over  $x_1 \dots x_{n-1}$  yields  $x_n^{n-1}/(n-1)!$  because the integration can be performed for each  $x_m$  from 0 to  $x_n$  irrespective of order, and keeping the order (3'') introduces merely the factor  $1/(n-1)!$ . Then (3) becomes

$$p_{n-1} dE' = \int \omega(y_1)\omega(y_2) \dots \omega(y_{n-1}) dy_1 dy_2 \dots dy_{n-2} \left\{ \begin{array}{l} \dots \dots (4) \\ \times \frac{dE'}{E} \exp(-\Phi N x_n) \frac{(\Phi N x_n)^{n-1}}{(n-1)!}, \end{array} \right.$$

$$y_1 + y_2 + y_3 + \dots y_{n-1} = Y, \quad \dots \dots (4')$$

and the normalization for  $\omega$  becomes

$$\int_0^\infty \omega(y_m) dy_m = 1.$$

The length of path in nuclear matter is, of course, limited, and clearly two cases are possible. (i) When  $n$  emission acts take place the primary nucleon may have lost so much energy that it is no longer capable of further meson emission. This is the case if, in the last emission act, the  $n$ th say, the nucleon loses energy from a value  $E' > E_c$  to some value below  $E_c$ . (ii) The primary nucleon may commit  $n$  emission acts and leave the nucleus still retaining an energy  $> E_c$ . We call the probabilities for these two types of events  $p^{(1)}$  and  $p^{(2)}$  respectively.

We consider first the case where one further collision takes place, the  $n$ th, in which  $E$  drops from  $E'$  to a value  $E''$  below the critical energy  $E_c$ . Below  $E_c$ ,  $\omega$  will steadily decrease and will eventually vanish at the meson threshold. We have no exact information as to how rapid this decrease is, but there are reasons, both experimental and theoretical, for believing that it is fairly rapid. We can idealize the situation by assuming that below  $E_c$  the probability for further meson production can be neglected, but that for the jump from  $E'$  to  $E''$  the cross section has still its full value  $\omega\Phi$ . Evidently this idealization is crude, but since it is made only for the last step the total error cannot be very large, except for small showers with only one or two particles which we shall exclude from the comparison with the experiments. The probability for the last step is

$$\Phi N \int_0^{E_c} \omega\left(\frac{E''}{E'}\right) \frac{dE''}{E'} dx_n.$$

Instead of carrying out the integration over the  $y_m$ 's in (4) we first average over the primary spectrum of the incident nucleons. In HJ it was shown that this remains a power spectrum for any depth in the atmosphere if the spectrum falling on the top of the atmosphere was a power spectrum, and this is very probable. We therefore assume a primary spectrum of the form

$$F(E)dE = \gamma E_c^\gamma \frac{dE}{E^{\gamma+1}}, \quad \gamma \sim 1.5. \quad \dots \dots (5)$$

(5) is normalized so that the total number of nucleons above the critical energy  $E_c$  is unity. Primaries with  $E < E_c$  do not contribute according to our assumptions. Actually (5) is only correct if  $E_c$  is larger than the latitude cut-off energy (for Europe  $3 \times 10^9$  ev.). We have reasons to think that  $E_c$  is of about the same order of magnitude (again the theory of HHP suggests this). Even for energies somewhat below the latitude cut-off (5) is still almost correct at some not too small depth below the top of the atmosphere, say at Jungfraujoch or sea level.

We obtain for the probability of emission of  $n$  mesons with the last emission act taking place in the interval  $dx_n$ :

$$p_n^{(1)} dx_n = \gamma E_c^\gamma \int_{E_c}^{\infty} \frac{dE}{E^{\gamma+1}} \int_{E_c}^E p_{n-1} \frac{dE'}{E} \int_0^{E_c} \omega\left(\frac{E''}{E'}\right) \frac{dE''}{E'} \Phi N dx_n. \quad \dots\dots (6)$$

We first carry out the integration over  $E$ , using the variable  $Y = \log(E/E')$ :

$$p_n^{(1)} dx_n = \gamma E_c^\gamma \int_{E_c}^{\infty} \frac{dE'}{E'^{\gamma+2}} \int_0^{\infty} p_{n-1} \exp\{-(\gamma+1)Y\} dY \int_0^{E_c} \omega\left(\frac{E''}{E'}\right) dE'' \Phi N dx_n. \quad \dots\dots (7)$$

The integration over the  $y_m$ 's can now be performed very easily using (4'):

$$\int_0^{\infty} p_{n-1} \exp\{-(\gamma+1)Y\} dY = \frac{(\Phi N x_n)^{n-1}}{(n-1)!} \left\{ \int_0^{\infty} \omega(y_m) \exp\{-(\gamma+1)y_m\} dy_m \right\}^{n-1}.$$

We denote for abbreviation

$$\begin{aligned} \omega_{\gamma+1} &= \int_0^{\infty} \omega(y) \exp\{-(\gamma+1)y\} dy = \int_0^E \omega\left(\frac{E'}{E}\right) \left(\frac{E'}{E}\right)^{\gamma+1} \frac{dE'}{E'} \\ &= \int_0^E \omega\left(\frac{\epsilon}{E}\right) \left(1 - \frac{\epsilon}{E}\right)^{\gamma} \frac{d\epsilon}{E}, \quad \dots\dots (8) \end{aligned}$$

which depends on the elementary distribution  $\omega(\epsilon/E)$  only and is a pure number. The remaining integrations in (7) yield

$$\begin{aligned} \int_{E_c}^{\infty} \frac{dE'}{E'^{\gamma+2}} \int_0^{E_c} \omega\left(\frac{E''}{E'}\right) dE'' &= \int_0^1 \omega(\xi) d\xi \int_{E_c}^{E_c/\xi} \frac{dE'}{E'^{\gamma+1}} \quad (\xi = E''/E') \\ &= \frac{1}{\gamma} \int_0^1 \omega(\xi) d\xi \frac{1 - \xi^\gamma}{E_c^\gamma} = \frac{1}{\gamma} (1 - \omega_{\gamma+1}) \frac{1}{E_c^\gamma}. \quad \dots\dots (9) \end{aligned}$$

Collecting our formulae, we obtain

$$p_n^{(1)} dx_n = \frac{(\Phi N x_n)^{n-1}}{(n-1)!} \exp(-\Phi N x_n) \omega_{\gamma+1}^{n-1} (1 - \omega_{\gamma+1}) \Phi N dx_n. \quad \dots\dots (10)$$

This has now still to be integrated over  $x_n$ , because the last act of emission (and all previous acts) can take place anywhere between 0 and  $x$ , say, if  $x$  is the total length of path. The probability for no emission to take place between  $x_n$  and  $x$  is unity because the energy is there less than  $E_c$ , and therefore  $x_n$  must not be replaced by  $x$  in the exponential  $\exp(-\Phi N x_n)$ . Thus we have to integrate (10) over  $x_n$  from 0 to  $x$ . Denoting the incomplete  $\Gamma$ -function by

$$\int_0^{x(n-1)} e^{-z} dz = \Gamma_n(a), \quad \dots\dots (11)$$

we get finally 
$$p_n^{(1)} = \Gamma_n(\Phi N x) \omega_{\gamma+1}^{n-1} (1 - \omega_{\gamma+1}). \quad \dots\dots (12)$$

This  $p_n^{(1)}$  is the probability for a nucleon to commit within the distance  $x$  in nuclear matter exactly  $n$  acts of meson emission and afterwards to have an energy less than  $E_c$ .

Next we consider the second case where the nucleon has, within the distance  $x$ , committed  $n$  acts of meson emission but has retained an energy greater than  $E_c$ . This probability  $p_n^{(2)}$ , say, is obtained from (4) directly, replacing  $n-1$  by  $n$ ,  $x_n$  by  $x$ , and averaging over the primary spectrum (5). We obtain immediately

$$p_n^{(2)} = \frac{(\Phi N x)^n}{n!} \exp(-\Phi N x) \omega_{\gamma+1}^n. \quad \dots\dots (13)$$



The total probability for emission of  $n$  mesons within the distance  $x$  is the sum

$$p_n = p_n^{(1)} + p_n^{(2)}. \quad \dots\dots (14)$$

$p_n^{(2)}$  can be split up, for a more symmetrical representation,

$$p_n^{(2)} = \omega_{\gamma+1}^n \{ \Gamma_n(\Phi N x) - \Gamma_{n+1}(\Phi N x) \}, \quad \dots\dots (15)$$

and hence

$$p_n = \omega_{\gamma+1}^{n-1} \Gamma_n(\Phi N x) - \omega_{\gamma+1}^n \Gamma_{n+1}(\Phi N x). \quad \dots\dots (16)$$

The last step in the calculation is now to consider the variation in the length of path  $x$ . If the nuclear diameter is  $d_A$ , the probability for a path length  $x$  is  $2x dx/d_A^2$ . This is to be multiplied into (16) and integrated over  $x$  from 0 to  $d_A$ . Changing the order of integration, the integration is elementary and gives (we denote the result by  $P_n$ )

$$\left. \begin{aligned} P_n &= \omega_{\gamma+1}^{n-1} \left\{ \Gamma_n(a_A) - \frac{n(n+1)}{a_A^2} \Gamma_{n+2}(a_A) \right\} \\ &\quad - \omega_{\gamma+1}^n \left\{ \Gamma_{n+1}(a_A) - \frac{(n+1)(n+2)}{a_A^2} \Gamma_{n+3}(a_A) \right\}, \quad \dots\dots (17) \\ a_A &= \Phi N d_A, \quad \omega_{\gamma+1} = \int_0^E \omega\left(\frac{\epsilon}{E}\right) \left(1 - \frac{\epsilon}{E}\right)^\gamma \frac{d\epsilon}{E}. \end{aligned} \right\}$$

(17) is our final result. As can be seen, it depends on (i) the total cross section  $\Phi$ ; (ii) a weighted average over the energy spectrum of the elementary cross section,  $\omega_{\gamma+1}$ , the weight function being  $(1 - \epsilon/E)^\gamma$ ; (iii) the power  $\gamma$  of the primary spectrum ( $\gamma \sim 1.5$ ); (iv) the atomic weight, through  $d_A$ . For sake of completeness we also give the formula for  $P_0$  ( $n=0$ ), because (17) does not immediately permit the transition to  $n=0$ . One gets

$$P_0 = \frac{2}{a_A^2} \Gamma_2(a_A). \quad \dots\dots (17')$$

It can easily be verified that (17) and (17') are normalized to unity:  $\sum_0^\infty P_n = 1$ .

### § 3. SOME GENERALIZATIONS

It is highly probable that amongst the  $n$  mesons emitted some are neutrettos which are not observed directly in either the cloud chamber or the photographic plate. We shall be more interested in the probability,  $P'_\nu$  say, for the emission of  $\nu$  charged mesons than in  $P_n$ . If the probability is known for the particle emitted in an individual emission act to be a neutretto,  $\delta$  say, the probability for  $\nu$  charged mesons to be emitted is derived from  $P_n$  by\*

$$P'_\nu = \sum_{n=\nu}^\infty \binom{n}{\nu} (1-\delta)^\nu \delta^{n-\nu} P_n. \quad \dots\dots (18)$$

\* We do not distinguish here between proton-proton, proton-neutron, neutron-proton etc. collisions. It is by no means evident, or even probable, that the cross sections for these collisions are all equal and that in all of them the probabilities for the emission of a neutretto are the same fraction. In fact Peng and Morette (1948) arrived, for low energies, at the result that the cross sections are quite different, although the charge-symmetrical theory is used. Nothing is known about this point for the energies in which we are interested. Since, however, any such differences must average out in the end, when both neutrons and protons are considered as "primaries", because there is certainly some symmetry in the proton-neutron system, we may assume that the probabilities of neutretto emission are the same fraction of the total, irrespective of the charge of the nucleon.

The evaluation of this sum is straightforward and gives a formula for  $P'$ , that differs from  $P_n$  essentially in a re-definition of the constants. We get

$$P'_\nu = \chi_{\nu+1} \left\{ \omega'^{\nu-1}_{\nu+1} \left[ \Gamma_\nu(a'_A) - \frac{\nu(\nu+1)}{a'^2_A} \Gamma_{\nu+2}(a'_A) \right] - \omega'_{\nu+1} \left[ \Gamma_{\nu+1}(a'_A) - \frac{(\nu+1)(\nu+2)}{a'^2_A} \Gamma_{\nu+3}(a'_A) \right] \right\} \dots\dots (19)$$

with

$$a'_A = \Phi N d_A (1 - \delta \omega_{\nu+1}), \quad \omega'_{\nu+1} = \chi_{\nu+1} \omega_{\nu+1}, \quad \dots\dots (19')$$

$$\chi_{\nu+1} = \frac{1 - \delta}{1 - \delta \omega_{\nu+1}}.$$

Apart from one common factor,  $\chi_{\nu+1}$ , which will be quite close to 1, this means that  $\omega$  is to be replaced by  $\chi\omega$  and  $\Phi$  by  $\Phi(1 - \delta\omega)$ .

For  $P'_0$  one finds

$$P'_0 = 1 - \chi_{\nu+1} + 2\chi_{\nu+1} \frac{\Gamma_2(a'_A)}{a'^2_A}. \quad \dots\dots (19'')$$

$\Phi$  is here the total cross section, including that for emission of neutrettos. In the charge symmetrical theory  $\delta$  has probably the value  $\frac{1}{3}$  and, as will be seen in § 4, the value of  $\omega_{\nu+1}$  is between 0.5 and 1, probably  $\frac{2}{3}$  or so.  $\chi_{\nu+1}$  is then close to 1. Likewise  $a_A$  is only slightly reduced. Since the values of  $\Phi$  and  $\omega_{\nu+1}$  are anyhow not accurately known, we shall work below with formula (17) and evaluate it for a range of values  $\Phi$  and  $\omega_{\nu+1}$ . Since we shall renormalize our results to the total number of showers observed, the constant factor  $\chi$  drops out.

A second generalization concerns the contribution of fast recoil protons. The experiments on the positive excess of shower particles suggest that as many as half the number of shower particles are protons (Rochester 1949). This is not surprising. We expect indeed that one fast recoil nucleon is produced for each meson produced. On the average half of these will however be neutrons. Since neutrettos are also accompanied by recoil nucleons we expect for four charged mesons three fast recoil protons. This figure may be further increased since the strong interaction of the recoil nucleons with the nucleus gives rise not only to a general heating up of the nucleus but also to a few further fast ejected nucleons. Evidently the mechanism of the production of recoil particles is very complicated, much more so than for the mesons, which can be expected to leave the nucleus unhindered (the most that could happen to a meson is a nuclear scattering). Instead of using some model for the ejection of fast protons we adopt a more phenomenological procedure.

Since in the experiments only the total number of fast particles is measured (so far), we would prefer to have the probabilities for a total of  $N$  particles, mesons + protons, rather than those for a given number of mesons. Obviously a certain statistical correlation may exist connecting the number of mesons with the number of protons. (In the first place one recoil nucleon is produced for each nucleon.) If that correlation were quite strict, each meson would be accompanied by one proton, and we should merely need to divide the experimental total number of particles by two to obtain the number of mesons. This is one way of comparing the experiments with the theory (cf. § 6), but it is certainly an exaggeration.

Alternatively we may assume that the fast protons are statistically independent of the mesons. We assume then that each observed particle has a probability  $\xi$ , say, of being a meson and  $1 - \xi$  of being a proton, independently of how many particles there are. The experiments indicate  $\xi \sim \frac{1}{2}$ . We have already the probabilities  $P'_\nu$  for a given number of charged mesons. And we ask, what are then the probabilities  $P''_N$  for a given total of particles to be ejected? This procedure may give too wide a spread of the number of protons relative to that of mesons.  $P''_N$  can be calculated as follows:

Supposing  $P''_N$  were known, on the hypothesis of statistical independence, then the  $P'_\nu$ 's would be determined by

$$P'_\nu = \sum_{N \geq \nu} \binom{N}{\nu} P''_N \xi^\nu (1 - \xi)^{N - \nu}. \quad \dots\dots (20)$$

To give the answer to our question, we have to solve (20) for the  $P''_N$ 's\*.

(20) can be solved for the  $P''_N$ 's. The solution, as can easily be verified, is

$$P''_N = \sum_{\mu \geq N} \binom{\mu}{N} (-1)^{N - \mu} P'_\mu \frac{1}{\xi^\mu (1 - \xi)^{N - \mu}}. \quad \dots\dots (21)$$

It is remarkable that, although for a given  $N$  the number of mesons is certainly less than or equal to  $N$ ,  $P''_N$  is expressed by the  $P'_\mu$ 's with  $\mu \geq N$ . This shows that there can be no arbitrariness in the  $P'_\mu$ 's. (21) has the same form as (18). We get then the explicit expression for  $P''_N$  again by a modification of the constants:

$$P''_N = \chi'_{\gamma+1} \left\{ \omega''_{\gamma+1} \left[ \Gamma_N(a''_A) - \frac{N(N+1)}{a''_A{}^2} \Gamma_{N+2}(a''_A) \right] - \omega''_{\gamma+1} \left[ \Gamma_{N+1}(a''_A) - \frac{(N+1)(N+2)}{a''_A{}^2} \Gamma_{N+3}(a''_A) \right] \right\}, \quad \dots\dots (22)$$

$$a''_A = a'_A \frac{\xi + \omega' - \xi \omega'}{\xi} = a_A \frac{\xi + \omega(1 - \delta - \xi)}{\xi},$$

$$\chi' = \frac{1}{\xi + \omega' - \xi \omega'}, \quad \omega'' = \chi' \omega' = \chi' \chi \omega = \frac{(1 - \delta) \omega}{\xi + \omega(1 - \delta - \xi)}, \quad \dots\dots (22')$$

dropping the index  $\gamma + 1$  in  $\omega$  and  $\chi$ . We get for  $P''_N$  again the same formula, only with different values for the constants. Using this formula below, we shall put  $\xi = \frac{1}{2}$ .

#### § 4. THE NUMERICAL VALUES OF $\Phi$ AND $\omega_{\gamma+1}$

Since  $\omega(\epsilon/E)$  is by definition normalized to 1,  $\omega_{\gamma+1}$  must be less than 1. If we tentatively put  $\omega(\epsilon/E) = (\beta + 1)^{-1} (1 - \epsilon/E)^\beta$  (the true law will probably be well approximated by this with some value of  $\beta$ ), convergence at  $\epsilon = E$  requires  $\beta > -1$ . It is almost certain that  $\beta > 1$  because there is no known law of energy loss in physics that makes high energy losses more probable than small ones. Then  $\omega_{\gamma+1} = (\beta + 1)/(\beta + \gamma + 1)$ . As was mentioned in HJ, the theory of HHP gives

\* It is far from certain that (20) has always solutions with all  $P''_N$ 's positive, when the  $P'_\nu$ 's are given arbitrarily. In fact the assumption of statistical independence of the  $P'_\nu$ 's and the probability  $\frac{1}{2}$  for being a meson or proton may be self-contradictory. In the present case, when the  $P'_\nu$ 's are given by a formula of the type (19) no difficulty arises.

results close to  $\beta=2^*$ . With  $\gamma=1.5$ , we see that  $\omega_{\gamma+1}$  would be 0.4 for  $\beta=0$ , but this is also improbable. For  $\beta=2$ ,  $\omega_{\gamma+1}=\frac{2}{3}$ . It is quite safe to say that  $\omega_{\gamma+1}$  lies between 0.5 and 1 and, more probably, near 0.6 or 0.7. If neutrettos are included, and if we accept, for instance,  $\omega_{\gamma+1}=\frac{2}{3}$ , we get  $\chi_{\gamma+1}=\frac{6}{7}$  (for  $\delta=\frac{1}{3}$ ) and  $\omega'_{\gamma+1}=\frac{4}{7}$ . If we calculate the total number of particles  $N$ , including protons, we get (with  $\xi=\frac{1}{2}$ )  $\chi'_{\gamma+1}=14/11$  and  $\omega''_{\gamma+1}=\chi'_{\gamma+1}\omega'_{\gamma+1}=8/11=0.73$ . If we exclude neutrettos and accept  $\omega'_{\gamma+1}=\omega_{\gamma+1}=\frac{2}{3}$ , we get  $\chi'_{\gamma+1}=6/5$ ,  $\omega''_{\gamma+1}=\frac{4}{5}=0.8$ . If the low energy mesons mentioned in the footnote immediately preceding exist,  $\omega$ ,  $\omega'$ ,  $\omega''$  are still slightly larger. When comparing the results with the experiments we should therefore choose some fairly small value for  $\omega$ , about 0.6 to 0.7, when only mesons are considered, and some higher value, 0.7 or 0.8, when all particles are considered.

The total cross section  $\Phi$  must be expected to be of the order of a few times  $(h/\mu c)^2$ . From the absorption coefficient of fast (meson-producing) nucleons a relation between  $\Phi$  and  $\omega_{\gamma+1}$  was determined in HJ, namely

$$\Phi(1-\omega_{\gamma+1})=1.15(h/\mu c)^2 \quad (\mu=286m). \quad \dots\dots (23)$$

In  $\Phi$  neutrettos are, of course, included. Putting, for instance,  $\omega_{\gamma+1}=\frac{2}{3}$ , we get

$$\Phi=3.5(h/\mu c)^2.$$

This agrees, as was already mentioned in HJ, with the predictions of the HHP theory, within the limits given by that theory.

The quantity  $Nd_A(h/\mu c)^2$  has the value 0.95 for oxygen and about 1.9 for Ag or Br. Thus we should get, if neutrettos are emitted,  $a_A=3.3$ ,  $a'_A=2.6$  for oxygen, and  $a_A=6.6$ ,  $a'_A=5.2$  for Ag or Br. For the calculation of the total number of particles according to (22) we have  $a''_A=4.1$  for oxygen and 8.2 for Ag, Br. These figures increase further if the low energy mesons mentioned in the footnote below exist (as may well be the case, though not in the exaggerated way mentioned). We have then for oxygen  $a_A=6.6$ ,  $a'_A=5.2$  for mesons alone,  $a''_A=8.2$  for the total number of particles, and for Ag, Br twice these values. In all, we can say that for the calculation of mesons alone some values are to be expected as follows:— $a'_A\sim 2.5$ –5 for O or C,  $\sim 5$ –10 for Ag or Br, and for the total number  $a''_A\sim 4$ –9 for O or C,  $\sim 8$ –18 for Ag or Br.

Finally we must also remark that in the derivation of the connection (23) the contribution from recoil nucleons to the effective absorption coefficient has been neglected. It is hardly likely that this will amount to much because  $\Phi$  has already about the largest value it can possibly have, namely a few times  $(h/\mu c)^2$ . In fact we have shown in HJ (in "Note added in proof") that this effect is probably small.

\* Actually this theory predicts also the production of mesons with fairly low energies, of the order  $3 \times 10^8$  ev., which do not follow the law (1). Their number is on the average equal to the number of fast mesons, but their contribution to the energy loss is of a smaller order of magnitude. We have not considered these mesons in this paper. This could easily be done if we neglect the energy loss due to these low energy mesons completely (although this is, of course, a gross exaggeration) and add a term to (1) of the form  $\Phi \delta(\epsilon/E) d\epsilon/E$ . It can then easily be seen that the net effect is a slight increase of the constant  $\omega$  to  $(\omega+1)/2$ , i.e. from  $\frac{2}{3}$  to  $\frac{3}{4}$  (if the numbers of slow and fast mesons are equal) and an increase of  $\Phi$  by a factor 2. The distinction between these two energy groups of mesons is, of course, highly artificial, and the true distribution is certainly a smooth transition between both groups, but the consideration shows that nothing changes, apart from a change of constants, if the law (1) is not strictly obeyed, as long as the main contribution to the energy loss follows from (1).

All this serves only as a guide to the values of the constants to be expected; exact values cannot be predicted, but if the experiments can be explained with some values of  $\omega$  and  $a_A$  similar to the above we can say that this is physically reasonable.

### § 5. NUMERICAL RESULTS

We give the numerical results for  $P_N''$  or  $P_n$  according to formula (17) for a variety of values  $a_A$  and  $\omega_{\gamma+1}$ . The formulae (19) and (22) differ from (17) only by a re-definition of the constants, the constant factors  $\chi_{\gamma+1}$  or  $\chi'_{\gamma+1}$  amount merely to a renormalization of all probabilities for  $n \neq 0$  (the cases  $n=0$  are in any case not observed). The range of values for the constants given,  $a_A=2.5-20$ ,  $\omega=0.6-0.9$ , are wide enough to include the cases considered.  $\omega_{\gamma+1}$  is independent of the atomic weight.

The probabilities are normalized to 100, including the case  $n=0$ , but  $P_0$  is in all cases less than 20%.

$P_n$  decreases more or less rapidly with increasing  $n$ . It is remarkable that for small  $n$ ,  $P_n$  varies very slowly with  $a_A$ , i.e. the atomic weight and the total cross section. It is the number of large showers which depends sensitively on  $\Phi$  and  $A$ .

We see that small showers with one or two mesons are far the most frequent. (Here, however, our approximations are very crude.) In light materials the shower size is limited to a maximum of 3-5 mesons (larger numbers being extremely improbable), in Ag, Br the largest showers to be expected (apart from rare exceptions) are 6-10. The total number of particles (including protons) is larger, as the larger values of constants have to be used.

### § 6. COMPARISON WITH EXPERIMENTS AND DISCUSSION

To compare our results with the data, we consider only showers with at least three thin tracks, for the following reason. The small showers are evidently produced by primaries with energies not much above those in the region where the cross section drops more or less rapidly to a negligible value with decreasing energy. Here the approximation made in § 2 is too crude. The same approximation had been made in HJ in the derivation of the power spectrum at all depths. The power spectrum may therefore not hold in this low energy region either (indeed the decreasing energy loss may make these primaries relatively more frequent). We cannot therefore expect that the present calculation gives the number of small showers very satisfactorily.

Of the thin tracks we take it from the positive excess (Rochester 1949) that roughly half are protons, the rest mesons. We do not expect any of the thin tracks to be electrons, although they accompany as a rule the larger showers in cloud-chamber pictures. These however are very probably the decay products of some short-lived type of meson which the photographic plate would not show to originate from the same grain (unless the lifetime were extremely short).

We compare our results with the experimental data in two ways. We first assume that half the number  $n'$  of the observed thin tracks in each shower are protons. We divide then the experimental numbers  $n'$  by 2 and, when  $n$  is odd, attribute half the number of showers to the preceding, half to the subsequent even number.  $n'/2=n$  is then the number of mesons in the shower. Thus we assume first a very strict correlation between the number of mesons and protons, which is probably much too strict. The ratio  $\frac{1}{2}$  for the number of protons is, of course, none too accurately known, and it is not even known if this ratio is independent of the shower size. The figure  $\frac{1}{2}$  refers to comparatively small showers.

Table 1. Relative Frequency (%) of Showers  $P_n$  with  $n$  Mesons\*

$\omega=0.6$											
$\begin{smallmatrix} n \\ a_A \end{smallmatrix}$	1	2	3	4	5	6	7	8	9	10	
2.5	49	21	5.5	1.5	0.4	0.1	0	0	0	0	
3	48	22	8.3	2.6	0.73	0.18	0	0	0	0	
4	46	24	11	4.3	1.5	0.46	0.13	0	0	0	
5	45	25	13	5.7	2.3	0.85	0.28	0.09	0	0	
7	43	25	14	7.3	3.6	1.6	0.70	0.28	0.10	0	
9	42	25	14	8.0	4.3	2.2	1.1	0.50	0.22	0.09	
11	41	25	14	8.2	4.6	2.5	1.3	0.69	0.34	0.16	

$\omega=0.7$														
$\begin{smallmatrix} n \\ a_A \end{smallmatrix}$	1	2	3	4	5	6	7	8	9	10	11-12	13-14	15-16	
3	43	23	10	4.0	1.3	0.36	0.09	0	0	0	0	0	0	
4	40	25	13	6.3	2.6	0.93	0.30	0.09	0	0	0	0	0	
5	38	25	15	8.1	3.9	1.7	0.66	0.24	0.08	0	0	0	0	
7	34	24	16	10	5.8	3.1	1.6	0.74	0.32	0.13	0	0	0	
9	33	23	16	10	6.7	4.1	2.4	1.3	0.67	0.33	0.2	0	0	
11	32	22	15	11	7.0	4.5	2.8	1.7	1.0	0.55	0.3	0	0	
14	31	22	15	11	7.2	4.7	3.2	2.1	1.3	0.85	0.73	0.25	0.07	

$\omega=0.8$													
$\begin{smallmatrix} n \\ a_A \end{smallmatrix}$	1	2	3	4	5	6	7	8	9	10	11-12	13-14	$\geq 15$
3	37	24	13	5.5	2.1	0.67	0.19	0	0	0	0	0	0
4	33	25	16	8.6	4.1	1.7	0.64	0.22	0.07	0	0	0	0
5	30	24	17	11	6.0	3.0	1.4	0.56	0.21	0.07	0	0	0
7	26	21	17	12	8.4	5.3	3.1	1.7	0.84	0.39	0.3	0	0
9	23	19	16	12	9.2	6.6	4.4	2.8	1.7	1.0	0.9	0.3	0
11	22	18	15	12	9.2	7.0	5.1	3.6	2.4	1.6	1.6	0.6	-
14	22	18	14	11	8.9	7.0	5.4	4.0	3.0	2.2	2.5	1.1	0.58
17	21	18	13	11	8.7	6.9	5.3	4.2	3.2	2.4	3.2	1.6	1.2
20	21	17	13	11	8.5	6.9	5.3	4.2	3.3	2.5	3.4	1.9	1.9

$\omega=0.9$																	
$\begin{smallmatrix} n \\ a_A \end{smallmatrix}$	1	2	3	4	5	6	7	8	9	10	11-12	13-14	15-16	17-18	$\geq 19$		
3	31	24	15	7.3	3.1	1.2	0.4	0.11	0	0	0	0	0	0	0		
4	26	23	17	11	6.0	2.9	1.2	0.46	0.16	0	0	0	0	0	0		
5	22	21	18	13	8.5	4.9	2.5	1.2	0.50	0.20	0	0	0	0	0		
7	17	17	16	14	11	8.1	5.5	3.4	1.9	1.0	0.6	0	0	0	0		
9	14	14	14	13	11	9.4	7.4	5.4	3.8	2.4	2.3	0.4	0	9	0		
11	13	13	12	11	10	9.2	7.9	6.4	5.0	3.7	4.4	1.6	0.4	0	0		
14	12	11	10.5	10	9.2	8.2	7.5	6.5	5.4	5.0	6.9	3.9	1.9	0.75	0.37		
17	11	10.5	9.5	9.2	8.5	7.5	6.9	6.1	5.6	4.8	7.8	5.3	3.3	1.8	1.3		
20	11	10	9.3	8.4	8.0	7.1	6.5	5.7	5.4	4.6	7.8	5.8	4.1	2.7	3.0		

\* or mesons plus protons, cf. text.

However, as our parameters  $\omega$  and  $a_A$  are not determined accurately either, a constant change in this ratio will only change the parameters. For the discussion of large showers, however, the possibility has to be kept in mind that the fraction of protons may be quite different. For the second comparison with experiments we assume a large measure of statistical independence of mesons and protons and use formula (22) to calculate the relative frequencies of the total numbers of particles  $N$ .

The chemical composition of the plate is such that there are 1.04 light atoms C, O, N to one heavy atom Ag or Br. We need not distinguish between C, O, N nor between Ag and Br, as the nuclear diameters of these atoms are not very different. Thus we multiply the theoretical figures of Table 1 for some rather small value of  $a_A$  by 1.04, add the figures for about twice the value of  $a_A$ , and renormalize the total number of showers so as to agree with the actual experimental figures. On account of the renormalization of the theoretical  $P_n$ 's any common factor  $\chi_{\gamma+1}$  as it occurs in (19) or (22) is irrelevant.

Table 2. Experimental and Theoretical Distribution of Shower Sizes (Mesons)

$n$	Experi- mental*	Theoretical		
		$a=3$ and 7 $\omega=0.7$	$a=4$ and 9 $\omega=0.6$	$a=4$ and 9 $\omega=0.7$
2	89	77	83 (41)	70 (37)
3	31.5	42	42 (19)	42 (19)
4	12	23	22 (7.3)	24 (9.6)
5	17	11.5	9.6 (2.5)	13.5 (3.8)
6	9.5	5.6	4.4 (0.8)	7.3 (1.4)
7	0.5	2.7	1.9 (0.2)	3.8 (0.4)
8	0.5	1.2	0.8 (0)	1.9 (0.1)
9	1.5	0.5	0.4 (0)	1.0 (0)
$\geq 10$	1.0	0.3	0.15 (0)	0.75 (0)

\* Results of Powell and collaborators at Bristol.

The figures in brackets show the contribution from light atoms C, O, N.

Since the size-frequency distribution of showers does not seem to vary much with altitude, we may add the results of Powell and his collaborators for Jungfraujoch and balloon heights. Similar data have also been collected in the photographic plate by Rochester and Page. Furthermore, Fretter (1949) has obtained a distribution from cloud-chamber measurements. But, as Fretter himself points out, some particles may be lost for geometrical reasons and also, perhaps, by absorption in the rather thick lead plates, and, indeed, his distribution is more concentrated on smaller showers than the photographic plate results. We therefore base our comparison on the photographic plate results alone. The first comparison with the theory is then given in Table 2 for a few relevant values of the parameters.

The agreement is seen to be very good indeed. The actual values of these parameters could be determined more definitely from the number of large showers if more statistical data were available. The number of small showers ( $n=2-5$ ) is given well by almost any choice of the parameters. It is to be noticed in particular that the large showers, containing a total of 17, 18, 22 particles, are also well accounted for. The theory gives for the total number to be expected with  $n \geq 7$  ( $\omega=0.6$ ,  $a_A=4$  and 9) the value 3.3, whereas a total of 3.5 has been observed.

The number of showers with  $n=1$  would, if calculated in the same way, be smaller than the experimental figure. As mentioned before, we believe that this may be due to the crude approximations made in this energy region as well as to a departure from the power law at lower energies. It may even be that some of these have nothing to do with mesons at all but are merely the effect of the scattering of fairly slow (i.e.  $\sim 10^9$  ev.) protons or neutrons by protons.

We now carry out the same comparison with experiments but calculating the total number of particles and assuming a large amount of statistical independence of meson and proton emission, thus using the constants  $\omega''$ ,  $a''_1$ . These can be compared directly with the experimental figures. We use the latter for  $n \geq 3$ ; this means that we are using more material on small showers than in the former comparison, because there only half of the showers  $n=3$  were attributed to two mesons. According to § 3 we should use now larger values for  $\omega$  and  $a''$ , roughly  $\omega'' = \omega' \{2/(1 + \omega)\}$ ,  $a'' = a'(1 + \omega')$ , but of course, with the assumption of statistical independence, we must expect to have to use somewhat different values.

Table 3. Experimental and Theoretical Distribution of Shower Sizes  
 $N$  = total number of particles

N	Experi- mental*	Theoretical	
		$a''=7$ and 14 $\omega=0.8$	$a''=9$ and 20 $\omega=0.8$
3	61	55 (30)	48 (27)
4	44	41 (21)	38 (21)
5	29	31 (15)	30 (15)
6	14	22 (9.5)	22 (11)
7	6	15 (5.5)	16 (7.6)
8	5	10 (3.0)	11.5 (4.6)
9	8	6.8 (1.5)	8.2 (2.9)
10	9	4.7 (0.7)	5.7 (1.7)
11	8	} 5.0 (0.5)	} 7.1 (1.5)
12	5		
13	1	} 2.0 (0)	} 3.6 (0.6)
14	0		
15-16	0	} 1.0 (0)	} 3.2 (0)
$\geq 17$	3		

\* Results of Powell and collaborators at Bristol.

The figures in brackets show the contribution from light atoms C, O, N.

The agreement is almost equally good, and it is certainly not justifiable to draw any conclusions about a correlation of proton and meson numbers. Since the numerical evaluation of our formula is rather laborious (partly owing to the lack of suitable tables of the incomplete  $\Gamma$ -function) we have not attempted to secure the "best fit" by slightly varying the constants. The accuracy of the present data makes this hardly worth while. The experimental distribution shows a minimum at  $N=7, 8$  (also in Table 2 at  $n=4$ ). The present material is compatible with the assumption that this is a statistical fluctuation and this has to be assumed if we wish to account for the whole distribution. (If this minimum should turn out to be real, a special explanation must be sought, possibly on lines different from those suggested here.) What appears to be certain, however, is that the experimental distribution shows a break in the slope at  $N=7, 8$ .



This is reproduced in the theory—not quite as pronounced as in the experiments—and is due to the rapid falling off of the contribution from light elements so that only the contribution from Ag, Br is left, with its much longer tail.

Also in this comparison there is no reason to conclude that the large showers of 20 particles or so are extraordinary. One shower with 31 thin tracks has been found by Cosyns, Dilworth, Occhialini, Schönberg\* and Vermasen, and the probability for this would, of course, be very small for any reasonable values of  $\omega$  and  $a_A$ . However, even in this case we feel it unwarranted to interpret this shower by a different process, for the following reasons.

Amongst the recoil nucleons which accompany every act of meson production some may be sufficiently fast to produce themselves further mesons and secondary nucleons. These secondary processes have been neglected throughout this paper. The effect would resemble a mild cascade, only probably much less pronounced than in the well-known electron case. The recoil nucleons will also produce further nucleons by nucleon-nucleon scattering if their energy is not high enough to produce mesons. All this tends to make an already large shower still bigger, and the effect is naturally more pronounced in Ag and Br than in C, O, N. If these secondary effects give a substantial contribution, the tail end of our distribution curves would have to be drawn out much longer, and if the effect is important, the values of our constants are smaller than Tables 2 and 3 suggest and, instead, the larger showers owe their large size to some extent to the cascade effect.† Pending an investigation, we feel it unjustified to interpret even the shower with 31 particles as a novel phenomenon.

An indication of the existence of a cascade effect can perhaps be seen in the following fact. As was pointed out to us by Professor Powell, the experiments show that showers with eight or more thin tracks are nearly all produced in Ag, Br (as follows from the number of heavy tracks) and less than one-seventh of these showers are produced in C, O, N (possibly even none). The figures in brackets in Table 3 show that, according to the present calculations, about a quarter or a fifth is still due to light elements. This can be understood if the cascade effect is important; our constants would be smaller and, considering the primary effects only, the distribution would fall off more rapidly than in Tables 2 and 3. Instead, the shower size is increased considerably, and mainly so in Ag, Br by the cascade effects. The fact that large showers are predominantly produced in heavy elements only provides a strong argument for the plural character of the process. If the process were purely multiple, the size of the nucleus should be immaterial.

The conclusions that must be drawn from these results are clear: the statistical data on the size-frequency distribution of penetrating showers can well be accounted for by the assumption of pure plural production (with the possible exception of the minimum). This applies also to the largest showers observed. There is no evidence so far for the existence of any other process such as a genuine multiple process. The values for the total cross section for meson production and other constants which have to be used to represent the experimental data are all reasonable on general physical grounds.

\* We are indebted to Dr. Schönberg for sending us this photograph.

† An interesting cloud-chamber picture has been described (private communication) by Lovati, Mura, Salvini and Tagliaferri: two particles emerging from a penetrating shower create a second penetrating shower in a second lead plate. This means that at least one recoil nucleon has sufficient energy to create a second penetrating shower. It seems that this event is not infrequent. If this can happen in two nuclei in succession, it surely must happen within the same nucleus also.

On the other hand, there is no proof that multiple processes do not occur in appreciable numbers. With a suitably invented dependence of the multiplicity on the primary energy it may be possible to explain the whole of the frequency distribution equally well. It is even more difficult to exclude the possibility that some of the showers, or part of the multiplicity in a given shower, are due to genuine multiple processes. If, for example, the average multiplicity in an individual nucleon-nucleon encounter were 2 or 3, the larger showers would be mixed, partly plural, partly multiple, and the treatment would be much the same as our treatment of the proton contribution. The distribution curve would hardly be much different from the one obtained here (with suitable readjustments of the constants).

The following arguments seem to point in the direction of—at least largely—plural production: the maximum shower size (i.e. excepting comparatively rare fluctuations) agrees roughly with the number of nucleons arranged along the diameter of an Ag or Br nucleus. If the process were purely multiple, the average multiplicity would have to be a similar number, which would be somewhat accidental. Purely multiple processes are difficult to reconcile with the large cross section that follows from the observed absorption coefficient, and so some plurality must surely exist. Finally, as was already mentioned, large showers with eight or more thin tracks occur nearly always in Ag, Br but rarely in C, O, N, and there would be no reason for this correlation were the processes all multiple; this correlation is even stronger than we have reason to expect.

All this tends to show only that the processes are probably to a large extent plural. In order to decide whether multiple processes contribute at all, and if so to what extent, further experiments are needed. The best would be experiments in hydrogen but, failing this, observations on the average shower size in different elements *made separately* would give strong indications. In C, O, N the shower sizes would be roughly half the size of those in Ag, Br if the process is all plural, even less than half if the cascade effects contribute, but the same if the process is all multiple.

#### ACKNOWLEDGMENTS

We are very much indebted to Prof. Powell for communicating to us all the Bristol data before publication and for interesting discussions during his stay in Dublin; to Dr. Rochester for sending us Miss Page's material and for advice regarding the probable ratio of the proton contribution; to Dr. Schönberg for sending us the photograph of a shower with 31 thin tracks; to Dr. Fretter for his manuscript on the cloud-chamber statistics, and finally to Miss M. Houston for computing Table 1 for us.

#### REFERENCES

- BROWN, R. H., CAMERINI, U., FOWLER, P. H., HEITLER, H., KING, D. T., and POWELL, C. F., 1949, *Phil. Mag.*, **40**, 862.  
DALLAPORTA, N., and CLEMENTEL, E., 1948, *Nuovo Cim.*, **4**, 235, 298.  
FRETTER, W. B., 1949, *Phys. Rev.*, in the press.  
HEISENBERG, W., 1949, *Z. Phys.*, **126**, 569.  
HEITLER, W., 1949, *Rev. Mod. Phys.*, **21**, 113 (compare also THOMSON, G. P., 1949, *Phil. Mag.*, **40**, 589).  
HEITLER, W., and JÁNOSSY, L., 1949, *Proc. Phys. Soc. A*, **62**, 374.  
PENG, H. W., and MORETTE, C., 1948, *Proc. R. Irish Acad. A*, **51**, 17, 217.  
ROCHESTER, G. D., 1949, *Rev. Mod. Phys.*, **21**, 20.  
THOMSON, G. P., 1949, *Phil. Mag.*, **40**, 589.

## The Meson Intensity at the Surface of the Earth and the Temperature at the Production Level

BY A. DUPERIER

Turner and Newall Research Fellow of the University of Manchester

*Communicated by P. M. S. Blackett; MS. received 30th March 1949, and in amended form 11th July 1949*

**ABSTRACT.** Meson intensity has been recorded by using a triple-coincidence arrangement with a lead absorber 25 cm. thick between the counters. The comparison of daily mean values with the height of a number of pressure-levels has led us to take into consideration the temperature of the air layer between 200 and 100 mb. The results show that this temperature appears to be a factor closely controlling the meson intensity at the surface of the earth; the intensity increases with increasing temperature at the rate of 0.12% per °C.

Other factors in determining the intensity are the mass of air and the height of the 100 mb. level over the station. The corresponding coefficients of absorption and decay prove to be comparable with those obtained from other measurements for mesons of the same momentum. It has also been found that the coexistence of the three effects permits explanation of the variability exhibited by the barometric coefficient when evaluated from short periods of observations.

These results may therefore be taken as evidence that the bulk of mesons is produced at the height of 100 mb.

If the positive effect of temperature is interpreted as the result of processes of decay and interactions with air nuclei of  $\pi$ -mesons at the production level, then the coefficient 0.12% per °C. leads to a value of  $4.9 \times 10^{-8}$  sec. for the upper limit of the mean life of  $\pi$ -mesons.

### §1. INTRODUCTION

THE results of the comparison of the cosmic-ray intensity, as measured by means of a counter arrangement without using absorbers, with the height of different pressure-levels have been reported in a former paper (Duperier 1944). For this comparison the variation of intensity from day to day was assumed to be given by the regression equation

$$\delta I = \mu \delta B + \mu' \delta H, \quad \dots\dots(1)$$

where  $I$  is the intensity in percentages of the mean,  $B$  the barograph reading at the station and  $\mu$  the true absorption coefficient,  $H$  the height of the pressure-level and  $\mu'$  the probability of meson decay per unit length of path. The partial correlation  $r_{IH \cdot B}$ , or correlation of  $I$  with  $H$  at constant  $B$ , was then obtained by following standard methods of multiple correlation analysis without necessity for reducing the cosmic-ray data beforehand.

Since these results were published, some other observers have made similar studies, but the results obtained are difficult to interpret on account of the procedure followed. Benedetto (1946) has compared the meson intensity at the ground with the height of different pressure-levels, but after reducing the data by applying the so-called barometric coefficient  $\beta$ . This is the coefficient which results from assuming that meson intensity is a function of atmospheric pressure only. It is given by  $\beta = \delta I / \delta B$ . But if  $I$  is in reality represented by equation (1)

then, by substituting, we have  $\beta = \mu + \mu' \delta H / \delta B$ . This expression shows that  $\beta$  by being a function of  $\delta H / \delta B$  will vary with the weather, since the factor  $\delta H / \delta B$  depends on the change in atmospheric temperature accompanying the change in pressure  $\delta B$ . It is therefore clear that the data after being reduced by applying  $\beta$  will appear to be related in one way or another to the height of a certain pressure-level according to the meteorological conditions during the period of observations.

Millican and Loughridge (1948) have compared the intensity of mesons with the temperature of the air mass underlying different pressure-levels, but as they have also reduced the data first by using  $\beta$  the results are again uncertain for the same reason.

It will be seen from the present paper that there is another mechanism, in addition to that expressed by the above expression, which also causes the coefficient  $\beta$  to depend on the weather.

An account is given in this paper of a new study, similar to that made formerly, but using now a lead absorber of 25 cm. thickness between the counter-trays. The comparison of the meson intensity with the height of a number of pressure-levels has led us to take into consideration the temperature of the air layer lying between 200 and 100 mb. The rather unexpected result is found that this temperature appears to be a factor closely controlling the meson intensity at ground-level; the latter intensity is found to increase with the temperature of the layer.

## §2. MEASUREMENTS AND METEOROLOGICAL DATA

The meson intensity has been measured by using a counter arrangement consisting of three trays of counters of three units each. The effective length and the diameter of the tubes were about 60 cm. and 5 cm. respectively. The upper and intermediate trays were directly above each other and separated from the lower tray by a block of lead of 25 cm. thickness. This lead was supported on a steel platform 1 cm. thick. The counting rate was about 7,400 triple coincidences per hour, and was recorded photographically every hour.

The following five periods of observations have been analysed separately :

- (1) 1-4, 7-11 Jan. 1948 (9 days),
- (2) 21 Jan.-9 Feb. 1948 (20 days),
- (3) 12-29 Feb. 1948 (18 days),
- (4) 27 June-3 July, 5-24 July 1948 (27 days),
- (5) 5-10 Nov., 12 Nov.-8 Dec. 1948 (33 days).

During the first three periods the apparatus was installed on the top floor at the Imperial College of Science and during the last two on the top floor at the Birkbeck College, London.

For the analysis, the hourly numbers of coincidences as well as the barograph readings at the station have been averaged in groups of 24 hours centred for convenience at 0030 G.M.T. The barograph was daily compared with a barometer of mercury.

The upper-air data have been extracted from the Daily Weather Report of the Meteorological Office, London, using the radio-sonde observations made every day at 03, 09, 15, 21 hours at Larkhill (about 100 km. to the south-west of London) and at Downham Market (about 75 km. to the north-east). Thus the height of a given pressure-level which corresponds to each 24-hour group is the mean of eight different determinations. This procedure has been considered

necessary in order to minimize the meteorological errors arising from the radio-sonde itself and from rapidly changing weather conditions. The comparison of the means of the four determinations for each day at the two stations has shown however that these means are very closely related. Even in the case of the 100 mb. level the correlation, then appearing at its lowest, has a value not less than 0.70.

When the radio-sonde balloons do not reach the upper levels the missing data have been obtained by interpolation after considering the data from the nearest ascent and the simultaneous ascent at the other station. The error so introduced in the average value for the corresponding 24-hour group is negligible. No level higher than 100 mb. has been considered because the number of balloons reaching these levels is much reduced.

### §3. ANALYSIS OF THE DATA

To begin with, the assumption has again been made that the variation of meson intensity from day to day is a function, and a function only, of the variation in the mass of air over the station and the change in height of the pressure-level at which

Table 1

Period 1; $r_{IB} = -0.96$					Period 2; $r_{IB} = -0.93$				
Pressure-level (mb.)	$r_{IH}$	$r_{BH}$	$r_{IH \cdot B}$	$r_{IB \cdot H}$	Pressure-level (mb.)	$r_{IH}$	$r_{BH}$	$r_{IH \cdot B}$	$r_{IB \cdot H}$
100	-0.75	0.66	-0.52	-0.94	100	-0.81	0.74	-0.49	-0.85
200	-0.95	0.87	-0.84	-0.86	200	-0.97	0.89	-0.82	-0.59
500	-0.97	0.92	-0.77	-0.72	500	-0.98	0.94	-0.84	-0.22
900	-0.98	0.99	-0.65	+0.27	900	-0.94	1.00	-0.52	+0.38

Period 3; $r_{IB} = -0.69$					Period 4; $r_{IB} = -0.69$				
Pressure-level (mb.)	$r_{IH}$	$r_{BH}$	$r_{IH \cdot B}$	$r_{IB \cdot H}$	Pressure-level (mb.)	$r_{IH}$	$r_{BH}$	$r_{IH \cdot B}$	$r_{IB \cdot H}$
100	-0.49	0.04	-0.63	-0.76	100	-0.16	0.01	-0.25	-0.70
200	-0.75	0.26	-0.81	-0.77	200	-0.49	0.17	-0.52	-0.71
500	-0.85	0.39	-0.87	-0.73	500	-0.74	0.60	-0.56	-0.47
900	-0.83	0.89	-0.67	+0.20	900	-0.74	0.99	-0.43	+0.27

Period 5; $r_{IB} = -0.87$				
Pressure-level (mb.)	$r_{IH}$	$r_{BH}$	$r_{IH \cdot B}$	$r_{IB \cdot H}$
100	-0.55	0.24	-0.72	-0.85
200	-0.85	0.64	-0.77	-0.81
500	-0.94	0.84	-0.78	-0.45
900	-0.92	0.94	-0.60	-0.02

mesons originate, that is to say, it is again assumed that equation (1) is valid. Then by comparing the partial correlation coefficients  $r_{IH \cdot B}$  and  $r_{IB \cdot H}$  for different pressure-levels it will be possible to see whether the assumption is justified and if so to obtain the pressure-level at which the bulk of mesons is formed.

Table 1 gives the values which have been obtained for these correlations together with those for  $r_{IB}$ ,  $r_{IH}$  and  $r_{HB}$  (total correlations) for each period.

To facilitate the comparison, the values in the last two columns of the table have been plotted in Figures 1 and 2. It can be seen that in spite of the low values of some coefficients, the change of  $r_{IH \cdot B}$  with the pressure level, as well as the change of  $r_{IH \cdot H}$  is practically the same in all the five cases. The significance of

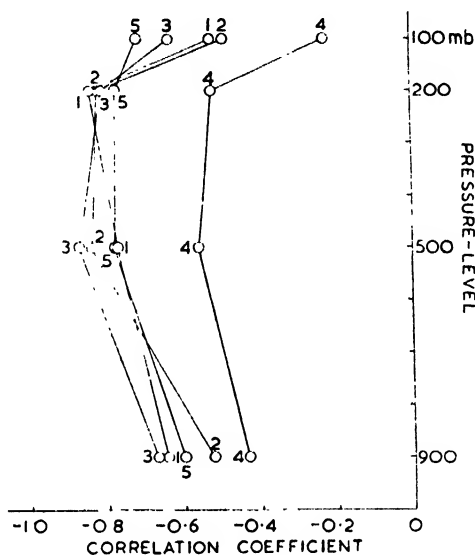


Figure 1. Correlation of meson intensity with height of different pressure-levels at constant ground pressure.

In Figures 1-3 the figures near the points represent the period of observations to which the points correspond.

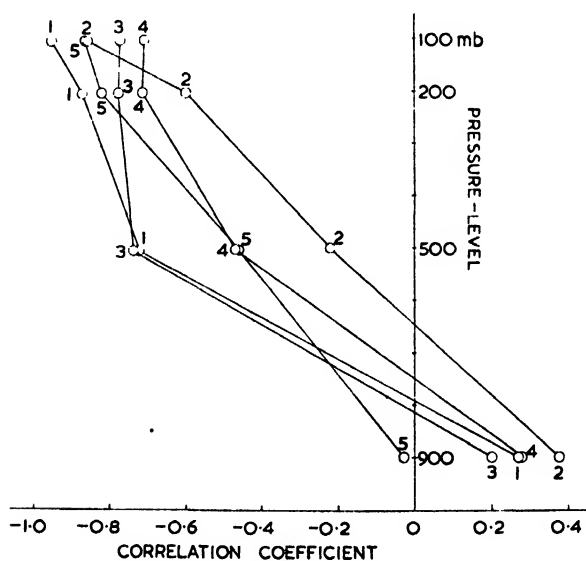


Figure 2. Correlation of meson intensity with ground pressure at constant height of pressure-level for different pressure levels.

both changes could not therefore be questioned, but the fact that  $r_{IB \cdot H}$  increases continually with height while  $r_{IH \cdot B}$  increases only up to about 500 mb., with a very pronounced decrease from 200 to 100 mb., seems to indicate that the variation of meson intensity at ground level is not accounted for entirely by equation (1).

If this had been the case we should have expected the two correlations to have reached their maximum at about the same level, that for which equation (1) would have been valid. Another factor, therefore, must be involved. We will assume that this factor is the density of the air in the proximity of a given pressure-level. For a given pressure-level  $P$  we will consider the mean density of the layer between  $P$  and  $P+100$  mb. Instead of the actual density, it will be convenient to make use of the temperature of the layer, this being inversely proportional to the density. We therefore assume that the variation of meson intensity from day to day at the ground is represented by the regression equation

$$\delta I = \mu \delta B + \mu' \delta H + \alpha \delta T, \quad \dots\dots(2)$$

where the two first terms on the right-hand side have the same meaning as before and  $T$  is the mean temperature of the layer between  $P$ , the chosen pressure-level, and  $P+100$ .

The partial correlations of  $I$  with this particular temperature which have been found by using the third period of observations are given as an example in Table 2. The Table gives also the total correlations between the different variables (with omission of those already given in Table 1) which are necessary to obtain  $r_{IT \cdot BH}$ .

Table 2

Pressure-level (mb.)	$r_{BT}$	$r_{HT}$	$r_{IT}$	$r_{IT \cdot BH}$
100	-0.38	-0.56	+0.80	+0.68
200	-0.28	-0.96	+0.74	+0.01
500	+0.11	+0.92	-0.67	+0.07

As the Table shows, the total correlations  $r_{IT}$  for the two lower pressure-levels are purely accidental, since they both disappear when the other two variables are eliminated. Instead, the correlation for the highest pressure-level remains with its value only slightly reduced after the elimination of  $B$  and  $H$ .

The same result has been obtained for the 100 mb. level with the data for the other four periods. This is shown in Table 3 where the results from period 3 have been inserted to facilitate comparison.

Table 3

Period	$r_{BT}$	$r_{HT}$	$r_{IT}$	$r_{IT \cdot BH}$
1	-0.87	-0.56	0.92	0.75
2	-0.70	-0.30	0.75	0.77
3	-0.38	-0.56	0.80	0.68
4	-0.25	-0.67	0.64	0.74
5	-0.70	-0.58	0.88	0.63

The fact that all the five periods give the same high value for  $r_{IT \cdot BH}$  makes the reality of this correlation unquestionable. Even when taken separately, each value proves to be statistically significant. Following Fisher's method, the probability that correlations of this magnitude should arise from random sampling of uncorrelated observations is about 0.02 in the case of the first period, and less than 0.01 in the case of the others.

In addition, this correlation allows us to explain the rather remarkable change with pressure-level of the correlations  $r_{IH \cdot B}$  illustrated in Figure 1. If  $I$  is closely related to  $T$  we have to expect that the correlations of  $I$  with  $H$  will be similar to those of  $T$  with  $H$ . In Figure 3 has been plotted the correlations  $r_{TH}$  which have

been obtained by using the upper-air data for two of the observation periods and for the same pressure-levels as in Figure 1. It may be noticed that the change with pressure-level in Figure 3 is entirely similar to the change in Figure 1.

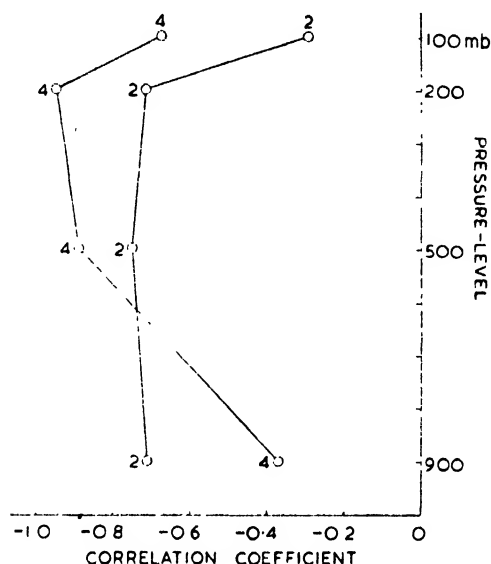


Figure 3. Correlation of the temperature of the 200-100 mb. layer with the height of different pressure-levels.

The conclusion must therefore be that the temperature of the air layer between 200 and 100 mb., or its equivalent, the density, is a controlling factor for the intensity of the penetrating component of cosmic rays at sea-level, this intensity being the greater the higher the temperature of the layer. (According to meteorological observations the mean height of this layer is about 14 km. and its average depth 4.2 km. At mean and high latitudes it lies in the lower stratosphere; in the equatorial belt it is just below the tropopause.)

For the partial correlation of meson intensity with the height of the 100 mb. level and with ground pressure, the following values have been obtained :

Table 4

Period	$r_{IB-HT}$	$r_{IH-BT}$
1	-0.84	-0.74
2	-0.58	-0.79
3	-0.72	-0.33
4	-0.71	+0.28
5	-0.82	-0.49

It can be seen that with the exception of  $r_{IH-BT}$  for the fourth period, all the values are physically of the right sign and sufficiently high to make also these two correlations significant. The exceptional value +0.28 may be partly due to the slight variation of  $H$  during the fourth period, which could accentuate the importance of the meteorological errors. As shown by Table 6, it is just for this period that the standard deviation of  $H$  is at its lowest. In any case, however, if the five periods are taken together, the correlation  $r_{IH-BT}$  proves to be negative and statistically significant, with a level of significance of 0.01.



When the multiple correlation  $r_{I-BHT}$ , or correlation between the two members of equation (2), is considered, the following values are obtained :

Table 5

Period	1	2	3	4	5
$r_{I-BHT}$	0.99	0.98	0.91	0.88	0.96

Equation (2) appears, therefore, to be justified when the pressure-level of 100 mb. is taken.

Figure 4, corresponding to the two first periods of observations, illustrates the daily course of meson intensity and the three meteorological variables.

The coefficients of the equation as well as their probable errors can be determined by using the relevant correlations together with the standard deviations  $\sigma$  of each of the variables. These are given in Table 6, and average values have been obtained as follows :

$$\mu = -(1.05 \pm 0.16)\% \text{ per cm.Hg, or } -(0.77 \pm 0.12) \times 10^{-3} \text{ cm}^2/\text{gm.}$$

$$\mu' = -(3.90 \pm 1.10)\% \text{ per km.}$$

$$\alpha = +(0.123 \pm 0.024)\% \text{ per } ^\circ \text{C.}$$

Table 6

Period	$\sigma_I(\%)$	$\sigma_B(\text{cm.Hg})$	$\sigma_H(\text{m.})$	$\sigma_T(^{\circ} \text{C.})$
1	1.33	0.62	73	4.48
2	1.68	0.86	129	4.44
3	0.67	0.39	63	3.82
4	0.64	0.44	48	3.54
5	1.75	0.66	83	4.50

To check these coefficients in the absence of comparable determinations only indirect methods seem to be possible.

#### *Coefficient of mass absorption.*

For the coefficient  $\mu$  we can use the results of measurements of the absorption curve in water. According to Ehmert (1937), the absorption coefficient in water down to a depth of 45 metres is given by  $\mu = 1.56/h$  where  $h$  is the depth in gm/cm<sup>2</sup>. To use this formula in the present case the range of mesons in air and lead as compared with the range in water must be considered. By using the Bethe-Bloch formula and applying the Fermi correction, Neher and Stever (1940) have found that the range in air is the same as that in water for mesons of rather more than 10<sup>9</sup> ev. energy. From the theoretical results of Rossi and Greisen (1941) it may be seen that the range in lead is about 1.6 times greater than in water for mesons of 10<sup>9</sup> ev. energy. When vertical incidence only is considered, the mass of water equivalent to the mean barograph reading during our observations (757.5 mm.Hg) together with the thickness of the lead block, steel platform, roof and counter-box, then appears to be 1,530 g/cm<sup>2</sup>, which would lead to a coefficient

$$1.56/1,530 \simeq 1.0 \times 10^{-3} \text{ cm}^2/\text{g.}$$

Had, however, the aperture angles of the apparatus been taken into account (18° × 63° to the vertical) this value would have been a little smaller. The two coefficients are, therefore, quite comparable.

### Decay coefficient.

As mentioned before,  $\mu'$  represents the probability of meson decay per unit length of path. The average value  $-3.90\%/km.$  has been obtained after rejecting period 4 because the correlation of  $I$  with  $H$  was positive for this period. The mean range before decay would be  $L = (25.6 \pm 7.2) km.$ , which permits evaluation of the mean life of ordinary mesons.

The cut-off momentum of the apparatus corresponding to about 28 cm. of lead equivalent is estimated to be  $4.5 \times 10^8$  ev/c. From this value and by using Jánosy's expression for the average momentum of the mesons along their path down to sea-level (Jánosy 1948), we obtain  $p = 3.5 \times 10^9$  ev/c. As for the mass,

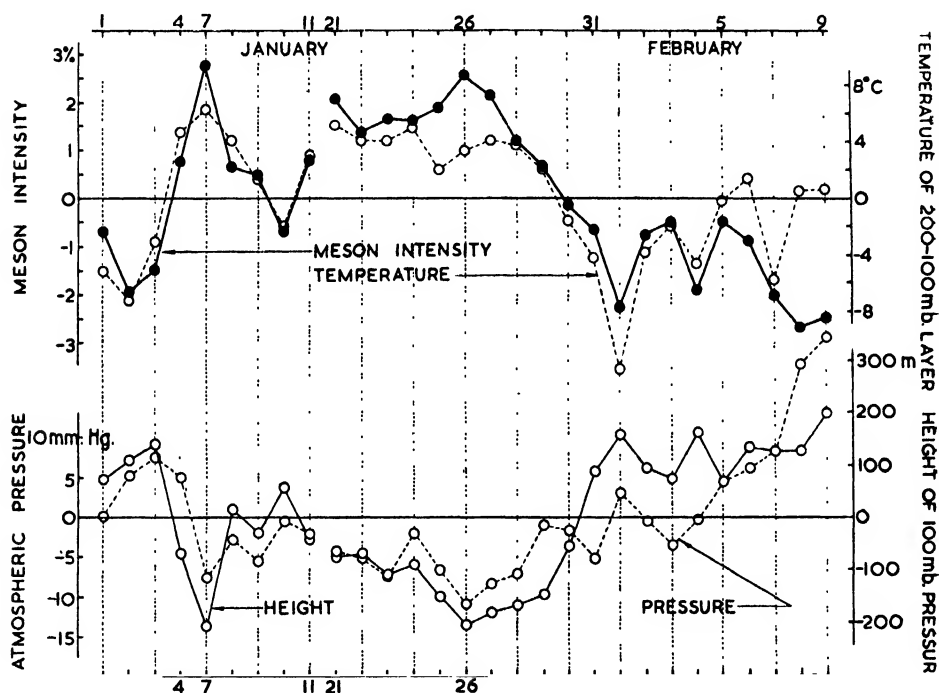


Figure 4. Variation of daily mean values of meson intensity and the three atmospheric variables.

EL

we can take some  $200 m_c$ , the former measurements suggesting an average of  $180 m_c$  while more recent determinations by means both of photographic emulsions and cloud chamber observations give about  $215 m_c$ . Thus from  $L = p\tau_0/m$  we have for the mean life  $(2.49 \pm 0.70) \mu sec.$ , a value which is also comparable with the value  $2.15 \mu sec.$  given by Nereson and Rossi (1943) which is generally accepted.

If the multi-directional character of the radiation recorded by the apparatus had been taken into account, it is clear from equation (2) that  $\mu'$  would have been a little smaller, or  $L$  greater, as  $\delta H$  increases with the secant of the zenith angle. The value for  $\tau_0$ , however, would have been but little affected since the average momentum then to be used would have also been greater.

### Positive temperature effect.

The possible meaning of  $\alpha$  will be discussed in the last section. It may however be noted at this stage that the increase of the cosmic-ray intensity with the temperature of the 200–100 mb. layer (third term of (2)) is not incompatible with the

decrease of intensity with increase of the temperature of the atmosphere as a whole. The latter results from the rising of the meson-producing level caused by the thermal expansion of the atmosphere, and is represented by the second term of equation (2). Thus we must suppose that two separate processes are taking place in the 200–100 mb. layer, one of which leads to an increase and one a decrease of cosmic-ray intensity at sea level with rising temperature of the layer. The latter negative effect is almost certainly due to the decay of  $\mu$ -mesons, and of course also occurs throughout the atmosphere down to the ground. It will be shown that the former positive effect is probably due to the decay of a short-lived intermediate product, probably in fact to  $\pi$ -mesons.

#### § 4. VARIABILITY OF THE BAROMETRIC COEFFICIENT

Further support to the above results is given by the fact that equation (2) also provides an explanation of the variability of the so-called barometric coefficient.

This is the coefficient which results from ascribing the whole variation of cosmic-ray intensity to the variation only of atmospheric pressure. It is given by the regression equation

$$\delta I = \beta \delta B = r_{IB} \cdot \delta B \cdot \sigma_I / \sigma_B. \quad \dots (3)$$

It is well known that  $\beta$ , when determined from observations covering only short periods, say 20 days, shows not infrequently a variability much greater than would be expected from the accuracy of the measurements. In the results obtained by Lindholm (1944) differences up to 100% and more occur among the average values for different periods. In the same way we have great discrepancies among the values given by different observers. To quote only a few: 3.1%/cm.Hg with a shield of 36 cm.Pb (Barnóthy and Forro), 1.1% with 20 cm.Pb (Messerschmidt), 1.6% with 12 cm.Pb (Compton and Turner), all quoted by Rossi (1939); 3.4% with 20.5 cm.Pb and 1.5 with 30 cm.Pb (Smith and Gast, quoted by Millican and Loughridge 1948).

This variability is much reduced when long periods are considered. The results obtained by Hogg (1947) from a period covering more than five years show that the whole range of the variation of monthly mean values is only 33% of the mean for the whole period.

Our results give another example of the variability of  $\beta$ . From the relevant data given in previous tables the following values can be directly obtained as indicated by expression (3):

Table 7

Period	$\beta$ (%/cm.Hg)	$r_{BH}$	$r_{BT}$
1	$-(2.06 \pm 0.22)$	0.66	-0.87
2	$-(1.82 \pm 0.17)$	0.74	-0.70
5	$-(2.33 \pm 0.37)$	0.24	-0.70
Mean	$-(2.22 \pm 0.16)$		
3	$-(1.16 \pm 0.30)$	0.04	-0.38
4	$-(1.00 \pm 0.21)$	0.01	-0.25
Mean	$-(1.07 \pm 0.16)$		

It may be seen that the first three values are about twice as great as the last two. Now if the second term of equation (2) is substituted for  $\delta I$  in (3) we have

$$\beta = \mu + \mu' \delta H / \delta B + \alpha \delta T / \delta B, \quad \dots (4)$$

which shows that  $\beta$ , by depending on the variations  $\delta H$  and  $\delta T$  accompanying the variation of pressure  $\delta B$ , will change with the meteorological conditions during the period. From the correlations given in Table 7 it can be seen that the values of  $\delta H / \delta B$  and  $\delta T / \delta B$  for the first three periods would not only be relatively high but of the right sign to make all the three terms on the right-hand side of (4) negative, thus explaining the high value for  $\beta$ . In fact the values of the second and third terms for these periods are  $-0.36\%$  and  $-0.61\%/\text{cm.Hg}$  respectively.

On the other hand, for the last two periods  $\delta H / \delta B$  is nearly zero, and  $\delta T / \delta B$  is very small, with the result that  $\beta$  is only slightly greater than the coefficient of mass absorption.

It may be noticed that had the term  $\alpha \delta T / \delta B$  been ignored it would not have been possible to account entirely for such a change in the barometric coefficient.

The fact that the values of  $r_{BT}$  are all negative and those of  $r_{BH}$  positive is in accordance with the meteorological result that the stratosphere tends to be warmer over cyclones and colder over anticyclones, whereas most of the troposphere is colder when the pressure is low and warmer with high pressure. On account of this tendency, it is to be expected that over long periods the barometric coefficient will be numerically greater than the coefficient of mass absorption; the observations confirm this.

## § 5. CONCLUSIONS

The above results show that the variation of meson intensity from day to day at the surface of the earth is due to fluctuations in air mass and in the height of the 100 mb. level and in the temperature in its proximity. They may therefore be taken as further evidence that the bulk of mesons is formed at or little above this level.

From a study of the results obtained in different parts of the world of the effects of ground temperature on cosmic-ray intensity, we had already come to the same conclusion regarding the height of meson production (Duperier 1948). It was then suggested that the gradual increase of intensity up to the height of 27 mb. as found by Schein, Jesse and Wollan might be due to primary protons passing through the apparatus. Recently Pomerantz (1949), by investigating the variation of cosmic-ray intensity with altitude in a series of free-balloon flights by using different amounts of absorber between the counters, has been able to evaluate the relative intensity of the electron and proton-plus-meson components. He has found that the maximum of the proton-plus-meson curve occurs at the 80 mb. level while that of the electron component appears to be located a little lower at about 104 mb. These results by Pomerantz seem to suggest that a maximum of the meson component alone must occur somewhere between these two levels, which should be in agreement with our result.

## § 6. INTERPRETATION OF THE POSITIVE EFFECT OF TEMPERATURE

If, as is suggested, the penetrating component is formed by the actions of primary cosmic rays on nuclei of air, the positive effect of temperature in the proximity of the production level appears to indicate that the number of mesons

at the surface of the earth increases as the density of nuclei in that region decreases. This result although apparently anomalous may be explained, at least qualitatively, if we accept the suggestion made by Lattes, Occhialini and Powell (1947) that the greater number of the mesons observed at sea level are the result of decay of  $\pi$ -mesons. Following their view we shall assume that  $\pi$ -mesons originate in the actions of primary rays on nuclei of air and that thereafter they may either be captured by other nuclei with which they collide or disintegrate into  $\mu$ -mesons and presumably a neutral particle. The probability of capture would be the greater the shorter the mean free path of the  $\pi$ -meson for a nuclear collision and the longer its life-time. If  $R$  is the mean free path in gm/cm<sup>2</sup> before a collision takes place and if  $L$  is the range before decay in centimetres, the probability of capture would be given by  $L/(R/\rho)$  where  $\rho$  is the density of air. If  $L/(R/\rho)$  is small, the probability of not being captured, that is the probability of decay of the  $\pi$ -meson, would therefore be  $P = 1 - L\rho/R$ . The temperature coefficient would therefore be

$$\alpha = \frac{\delta P}{\delta T} = - \frac{L}{R} \frac{\delta \rho}{\delta T}, \quad \dots\dots(5)$$

which agrees in sign with the experimental effect.

For a quantitative check we can proceed to estimate the life-time of the  $\pi$ -meson and compare the results with other experiments.

If  $m$  is the mass per unit area and  $h$  the depth of the 200–100 mb. layer,

$$\rho \simeq \frac{m}{h} \quad \text{and} \quad \frac{\delta \rho}{\delta T} \simeq - \frac{m}{h^2} \frac{\delta h}{\delta T}.$$

From meteorological data

$$h \simeq 4.2 \text{ km.}, \quad \delta h / \delta T \simeq 20.5 \text{ m/}^\circ \text{C.}, \quad \text{and} \quad m = 102 \text{ gm.}$$

Consequently

$$\alpha = 1.2 \times 10^{-6} \times L/R. \quad \dots\dots(6)$$

As it appears that it is the temperature of the 200–100 mb. layer only that has an appreciable effect on the meson intensity at sea level, it is to be assumed that the process of decay and capture of the heavy meson occurs mainly on this layer, thus indicating that the mean free path of the heavy meson is of the order of magnitude of the depth of this layer. We might, therefore, take  $R$  to be of the order of 100 gm/cm<sup>2</sup>.

Owing to the very small value of the vertical gradient of temperature in the stratosphere it might be expected, however, that the results obtained in this paper would have been but little altered if a thinner layer starting down at the 100 mb. level had been considered. This has been tested by using the first and the second periods of observations for the 150–100 mb. layer; the results obtained show that the correlation of meson intensity with the temperature of this layer and the coefficient  $\alpha$  are both practically the same as in the case of the 200–100 mb. layer. In fact, they appear to be a little higher, but the difference is not statistically significant. The value 100 gm/cm<sup>2</sup> for the mean free path of the heavy meson might therefore be taken as an upper limit.

For the average energy of the ordinary meson at the production level we may use  $5 \times 10^9$  ev. (derived from Blackett's spectrum at sea level and assuming a total energy loss in air of  $2 \times 10^9$  ev.). Allowing for the energy taken by the

neutral particle originating in the  $\pi$ -disintegration we have  $E_\pi \simeq 10^{10}$  ev. If finally we take for the mass  $286 m_e$  and substitute 0.12% for  $\alpha$  we obtain from (6)  $\tau_\pi \leq 4.9 \times 10^{-8}$  sec.

This is consistent with the results from other experiments. Camerini, Muirhead, Powell, and Ritson (1948) have obtained  $6 \times 10^{-9}$  sec. by comparing the relative number of  $\pi$ - and  $\mu$ -particles in the upward stream of mesons near the ground. Richardson (1948) has given, from other experiments,  $1.1 \times 10^{-8}$  sec. for the mean life of negative  $\pi$ -mesons. Finally, Greisen (1948), by using the results of measurements at great depths underground, has claimed the value  $6 \times 10^{-8}$  sec.

Another consideration can be made which leads to further support for this interpretation. According to (5) the positive effect of temperature, being proportional to  $L$ , should increase with the energy of the particles. Records of the cosmic radiation under 40 metres of water by Rau (1939) show that the intensity had a maximum in June and a minimum in January, the difference between these extreme values being about 4%. As the average energy under 40 metres of water is about five times greater than at the surface, we should expect for the temperature effect at this depth  $5 \times 0.12 = 0.60\%$  c. approximately.

Now, from the Ramanathan diagram for the vertical distribution of temperature of the atmosphere as modified by Gregg (1931) and by Palmen (1934), the change in temperature at 100 mb. from winter to summer in mean latitudes can be estimated at some 5 or 10°C. Using Rau's results this would give for  $\alpha$  some 0.8 or 0.4% per °C., which is quite consistent with the predicted value from the result at the surface.

However, the existence of heavier mesons, as observed by different workers, makes it doubtful if the process of meson formation is as simple as has been visualized. In particular, the recent report by Brown *et al.* (1949) of a meson of  $900 m_e$  which in disintegrating gives rise to  $\pi$ -mesons would seem to suggest that this heavier particle may be partially, at any rate, responsible for the effect of density at the production level.

\* \* \* \* \*

In the experiments referred to in §1, when no absorber was used so that the total radiation was recorded, it was found that the variations of intensity at sea level were well accounted for by the fluctuations of pressure and by the height of the 100 mb. level, that is, the effect of the temperature of the 200–100 mb. layer passed unnoticed. Owing to the smaller value of the average energy of the mesons and to the presence of the electronic component due to the lack of the absorber, it is possible that the greater effects of decay and absorption in this case may have contributed to mask the effect of temperature of the 200–100 mb. layer which, in addition, appears to decrease as the energy of the mesons decreases.

Another possibility is the following. If the electrons of the soft component at sea level are partly the product of meson decay in the lower part of the atmosphere, then it is to be expected that the variations of intensity due to the vertical motion of the 100 mb. level will be partly offset by the electrons resulting from the disintegration of mesons. The fact that these variations appear to be well correlated with the variations in height of the 100 mb. level seems therefore to indicate that something happens or tends to happen in the opposite direction

that compensates for the increase or decrease of the electron component. As mentioned above, the thermal change in the troposphere which accompanies a change of pressure tends to be opposite to that in the stratosphere. When the 100 mb. level rises owing to the warming of the troposphere the number of mesons decreases not only because of the rise in height but also because the 200–100 mb. layer becomes colder. The latter decrease would compensate for the increase in the number of electrons, thus making the intensity appear well correlated with the height of the 100 mb. level.

The former results with the total radiation might therefore be regarded as not inconsistent with the results as given in this paper.

#### ACKNOWLEDGMENTS

The author wishes to express gratitude to Professor J. D. Bernal for providing facilities for this work to be carried out in the Physics Department, Birkbeck College, University of London, and to Professor P. M. S. Blackett for his interest and advice.

#### REFERENCES

- BENEDETTO, F. A., 1946, *Phys. Rev.*, **70**, 817.  
 BROWN, R., CAMERINI, U., FOWLER, P. H., MUIRHEAD, H., POWELL, C. F., and RITSON, D. M., *Nature, Lond.*, **163**, 82.  
 CAMERINI, U., MUIRHEAD, H., POWELL, C. F., and RITSON, D. M., 1948, *Nature, Lond.*, **162**, 433.  
 DUPERIER, A., 1944, *Terr. Magn. Atmos. Elect.*, **49**, 1; 1948, *Proc. Phys. Soc.*, **61**, 34.  
 EHMERT, A., 1937, *Z. Phys.*, **106**, 751.  
 GREGG, W. R., 1931, *Bull. Nat. Res. Coun. of the Nat. Acad. Sci., Wash.*, No. 79, 125.  
 GREISEN, K. I., 1948, *Phys. Rev.*, **73**, 521.  
 HOGG, A. R., 1947, *Proc. Roy. Soc. A*, **192**, 128.  
 JÁNOSSY, J., 1948, *Cosmic Rays* (Oxford: University Press).  
 LATTES, C. M. G., OCCHIALINI, G. P. S., and POWELL, C. F., 1947, *Nature, Lond.*, **160**, 486.  
 LINDHOLM, F., 1944, *Ark. Mat., Astr. Fys.*, **30 A**, No. 13.  
 MILLICAN, F. M., and LOUGHRIDGE, D. H., 1948, *Phys. Rev.*, **74**, 66.  
 NEHER, and STEVER, 1940, *Phys. Rev.*, **58**, 766.  
 NERESON, N., and ROSSI, B., 1943, *Phys. Rev.*, **64**, 199.  
 PALMEN, L., 1934, *Met. Z.*, **51**, 17.  
 POMERANTZ, M. A., 1949, *Phys. Rev.*, **75**, 69.  
 RAU, W., 1939, *Z. Phys.*, **114**, 265.  
 RICHARDSON, J. R., 1948, *Phys. Rev.*, **74**, 1720.  
 ROSSI, B., 1939, *Rev. Mod. Phys.*, **11**, 296.  
 ROSSI, B., and GREISEN, K. I., 1941, *Rev. Mod. Phys.*, **13**, 240.

## On the Decay of $\tau$ -Mesons

BY C. B. VAN WYK\*

Department of Mathematical Physics, University of Birmingham

*Communicated by R. E. Peierls; MS. received 19th April 1949*

**ABSTRACT.** The production of  $\tau$ -mesons (mass about 900 electron masses) by cosmic rays in rather thin layers of air in the upper atmosphere seems to indicate that the nucleon  $\tau$ -meson coupling constant is not very small. The Berkeley experiments show that this is also true for the nucleon- $\pi$ -meson coupling constant. Consequently the decay of a charged  $\tau$ -meson into a photon and a charged  $\pi$ -meson by means of virtual creation and annihilation of nucleons ought to be fairly probable. In this paper this decay process, with the emission of one photon, is studied for the various types of  $\tau$ - and  $\pi$ -mesons. Unless both mesons have zero spin, the matrix elements, and therefore the lifetimes, are found to be of the same order of magnitude, and the  $\tau$ -meson turns out to be too short-lived to be observed photographically.

If both mesons have zero spin the emission of only one photon is forbidden. The detailed discussion of higher order decay processes in this case is reserved for a later paper.

### §1. INTRODUCTION

THE decay of a charged meson into a lighter meson and a photon by means of virtual creation and annihilation of nucleons was discussed by Finkelstein (1947). He carried out a perturbation calculation using as the interaction energy between meson and nucleon fields only that part of the total interaction Hamiltonian which contains the derivatives of the meson wave functions. Assuming both kinds of meson fields to interact reasonably strongly with nucleons—as is the case for the Schwinger mixture of nuclear forces—and taking the mass of the final meson as 177 electron masses, he found a lifetime of about  $10^{-18}$  sec. for a vector meson at rest decaying into a pseudoscalar meson and a photon.

It will be shown that if that part of the total interaction Hamiltonian not containing derivatives of the meson wave functions were used as interaction energy in the calculation referred to above, the position would be improved considerably. With the same parameters the lifetime then becomes  $10^{-12}$  sec. However, it is now certain that the lightest meson ( $\mu$ -meson) of a mass about 200 electron masses is not strongly coupled with nucleons so that a  $\pi$ -meson ( $\sim 300$  electron masses) decaying in the way described by Finkelstein would have a very long lifetime, and may therefore decay in some other way. But in connection with the discovery of a meson having a mass of about 900 electron masses (Powell *et al.* 1949), Oppenheimer† has pointed out that the production of these mesons in fairly thin layers of air leads one to expect it to have a strong coupling with nucleons. In that case Finkelstein's calculations would predict a lifetime too short to be compatible with the observation of tracks of these particles in the photographic plate.

\* Now at the University of Natal.

† Unpublished, remark made at Physics Conference at Birmingham in September 1948.

*Note added in proof.* Through private communication the author learned from Professor Powell and Dr. B. Peters that at present there is no reliable evidence for the existence of short-lived mesons of mass around 900 electron masses. However, this does not affect the validity of this discussion of the possible properties of such particles.



The purpose of the present investigation is to see whether this result is dependent on the character of the mesons which are taking part in the decay process and on the type of the coupling.

If both the initial and final mesons have spin zero, the emission of *one* photon is forbidden by the conservation of angular momentum. In this case the lifetime will be determined by a process of higher order which will be discussed in a subsequent paper.

In all other cases the difference between coupling terms with or without derivatives of the meson field variables, to which reference has been made, is less important here since the dependence expresses itself through a power of  $\mu_0/M$  where  $\mu_0$  is the rest energy of the initial meson and  $M$  that of the nucleon. Since this ratio is about  $\frac{1}{2}$  for  $\tau$ -mesons, this factor is not very important.

Apart from this dependence it will be shown that in all cases the lifetime is very short compared to  $10^{-12}$  sec. so that the difficulty pointed out by Oppenheimer would remain.

Unless both  $\tau$ - and  $\pi$ -mesons have spin zero, one would have to conclude either that the present formalism is not adequate, or that the generation of  $\tau$ -mesons must be due to a process quite different from that usually assumed.

## §2. NUCLEON-MESON INTERACTION TERMS

In the perturbation calculation only interaction terms linear in the coupling constants will be used. For charged scalar mesons this term in the Hamiltonian is (Kemmer 1938)

$$(4\pi)^{\frac{1}{2}} \int \Phi^* \{g\beta + f/\kappa [\partial/\partial x_0 + \alpha \cdot \nabla]\} \{\tau_{PN}U + \tau_{NP}U^*\} \Phi d^3x,$$

where  $g$  and  $f$  are constants with the dimension of charge and  $\kappa = mc/\hbar = \mu/\hbar c$ ;  $m$  = meson mass;  $\Phi$  is the nucleon wave function;  $U$  is the meson wave function;  $\alpha$ ,  $\beta$  are the Dirac matrices;  $\tau_{PN}$  and  $\tau_{NP}$  are operators creating a proton and a neutron respectively.

Imagine the system to be enclosed in a cubic box, side length  $L$ . Introduce the expansions

$$\begin{aligned} \Phi &= L^{-3/2} \sum_l \sum_{r=1,2} \left[ \begin{Bmatrix} v_+^r(l) \\ u_+^r(l) \end{Bmatrix} a^r(l) \exp \{i(lx - l_0 x_0)\} + \begin{Bmatrix} v_-^{r*}(l) \\ u_-^{r*}(l) \end{Bmatrix} b^r(l) \exp \{-i(lx - l_0 x_0)\} \right], \\ U &= (\hbar c L^{-3})^{\frac{1}{2}} \sum_k (2k_0)^{-\frac{1}{2}} U_+(k) \exp \{i(kx - k_0 x_0)\}, \end{aligned}$$

where the upper line refers to the neutron component, and the lower line to the proton component, of the nucleon wave function and where  $v$ ,  $u$ ,  $U(k)$  are the occupation operators for neutrons, protons and mesons respectively (the signs refer to charge in case of protons and mesons and magnetic moment in the case of a neutron).  $a^r(l)$  and  $b^r(l)$  are spinors with the property

$$\begin{aligned} \{(\alpha l) + \beta K\} a(l) &= l_0 a(l), \\ \{(\alpha)l - \beta K\} b(l) &= l_0 b(l), \end{aligned}$$

where  $l_0 = +(l^2 + K^2)^{\frac{1}{2}}$ ,  $K = M/\hbar c$ ,  $M$  = nucleon rest energy. The matrix element then becomes

$$(2\pi/L^3\epsilon)^{\frac{1}{2}} \hbar c u^*(Q) \{g\beta + i\rho(f/\mu)[- \epsilon + (\alpha p)]\} u(P),$$

where  $\rho = 1$  for absorption of a meson,  
 $= -1$  for emission of a meson,

$u(Q)$  can be either  $a(Q)$  or  $b(Q)$ ;  $\epsilon = k_0 \hbar c$ ;  $p = k \hbar c$ ;  $\epsilon^2 = p^2 + \mu^2$ .

For the pseudoscalar case the corresponding expressions are

$$(4\pi)^{\frac{1}{2}} \int \Phi^* \{ig\beta\gamma_5 + (f/\kappa)[\gamma_5 \partial/\partial x_0 + \sigma \nabla]\} \{\tau_{PN} U + \tau_{NP} U^*\} \Phi d^3x \\ (2\pi/L^3 \epsilon)^{\frac{1}{2}} \hbar c U^*(Q) \{ig\beta\gamma_5 + i\rho(f/\mu)[- \epsilon\gamma_5 + (\sigma p)]\} u(P),$$

where  $\gamma_5 = -i\alpha_1 \alpha_2 \alpha_3$   $\sigma = \gamma_5 \alpha$ .

The interaction term for the vector meson field is

$$(4\pi)^{\frac{1}{2}} \int \Phi^* \left\{ \begin{array}{l} [g(-U_0 + \alpha U) + (f/\kappa)(V_0 \cdot \gamma + V\beta\sigma)] \tau_{PN} \\ + [\text{conjugate complex}] \tau_{NP} \end{array} \right\} \Phi d^3x,$$

where  $(U, U_0)$  is the meson vector-field

$$V = \text{curl } U \quad V_0 = -(\partial/\partial x_0)U - \nabla U_0.$$

Introduce

$$U(x) = (\hbar c L^{-3})^{\frac{1}{2}} \sum_k (2k_0)^{-\frac{1}{2}} \left\{ (k_0/\kappa) \mathbf{r} U_{3+}(k) + \sum_{i=1,2} \mathbf{e}_i U_{i+}(k) \right\} \exp \{i(kx - k_0 x_0)\},$$

$$U_0(x) = (\hbar c L^{-3})^{\frac{1}{2}} \sum_k (2k_0)^{-\frac{1}{2}} (k/\kappa) U_{3+}(k) \exp \{i(kx - k_0 x_0)\},$$

where  $\mathbf{r} = \mathbf{k}/k$ ,  $(\mathbf{e}_i, \mathbf{r}) = 0$ ,  $(\mathbf{e}_1, \mathbf{e}_2) = 0$ ,  $(\mathbf{e}_1, \mathbf{e}_1) = (\mathbf{e}_2, \mathbf{e}_2) = 1$   $\gamma = -i\beta\alpha$ .

This leads to the matrix element

$$(2\pi/L^3 \epsilon)^{\frac{1}{2}} \hbar c u^*(Q) \{g[(\epsilon/\mu)(\alpha r) - p/\mu] + \rho f \beta(\alpha r)\} u(P)$$

for longitudinal meson and

$$(2\pi/L^3 \epsilon)^{\frac{1}{2}} \hbar c u^*(Q) \{g(\alpha e) + \rho(f/\mu)\beta[\epsilon(\alpha e) + i\sigma(p_\lambda e)]\} u(P)$$

for transverse meson.

The corresponding expressions for the pseudovector case are

$$(4\pi)^{\frac{1}{2}} \int \Phi^* \left\{ \begin{array}{l} [g(-\gamma_5 U_0 + \sigma U) + (f/\kappa)(V\gamma - V_0 \beta \sigma)] \tau_{PN} \\ + [\text{conjugate complex}] \tau_{NP} \end{array} \right\} \Phi d^3x$$

$$(2\pi/L^3 \epsilon)^{\frac{1}{2}} \hbar c u^*(Q) \{g[(\epsilon/\mu)(\sigma r) - (p/\mu)\gamma_5] - i\rho\beta(\sigma r)\} u(P)$$

$$(2\pi/L^3 \epsilon)^{\frac{1}{2}} \hbar c u^*(Q) \{g(\sigma e) + \rho(f/\mu)\beta[\alpha(p_\lambda e) - i\epsilon(\sigma e)]\} u(P).$$

These matrix elements will be used to describe the transition

$$M^+(0) \rightarrow m^+(-p) + \gamma(p),$$

where the initial meson is at rest with energy  $\mu_0$ , the final meson has energy  $\epsilon_2$ , momentum  $-\mathbf{p}/c$  and the photon has momentum  $\mathbf{p}/c$ . Conservation of energy requires  $\mu_0 = \epsilon_1 + \epsilon_2 = p + \epsilon_2$ . It is convenient to introduce  $\theta_i = \epsilon_i/\mu_0$  ( $i=1,2$ ); thus  $1 = \theta_1 + \theta_2$ .

The matrix elements can be summarized as follows:

*Initial Meson:*

$$S : u^*(Q) \{g_0 \beta - i f_0\} u(P),$$

$$P_s : u^*(Q) \{ig_0 \beta \gamma_5 - i f_0 \gamma_5\} u(P),$$

$$V : u^*(Q) \{g_0(\alpha e_0) + f_0 \beta(\alpha e_0)\} u(P),$$

$$P_v : u^*(Q) \{g_0(\sigma e_0) - i f_0 \beta(\sigma e_0)\} u(P).$$

*Final Meson:*

$$\begin{aligned}
 S & u^*(Q)\{g_2\beta + if_2(\mu_0/\mu_2)[\theta_2 + \theta_1(\alpha r)]\}u(P), \\
 P_s & u^*(Q)\{ig_2\beta\gamma_5 + if_2(\mu_0/\mu_2)\gamma_5[\theta_2 + \theta_1(\alpha r)]\}u(P), \\
 L_v & u^*(Q)\{-g_2(\mu_0/\mu_2)[\theta_2(\alpha r) + \theta_1] + f_2\beta(\alpha r)\}u(P), \\
 T_v & u^*(Q)\{g_2(\alpha e_2) - f_2(\mu_0/\mu_2)\beta[\theta_2(\alpha e_2) - i\theta_1\sigma(r_\lambda e_2)]\}u(P), \\
 L_{pv} & u^*(Q)\{-g_2(\mu_0/\mu_2)\gamma_5[\theta_2(\alpha r) + \theta_1] - if_2\beta(\sigma r)\}u(P), \\
 T_v & u^*(Q)\{g_2(\sigma e_2) + f_2(\mu_0/\mu_2)\beta[\theta_1\alpha(r_\lambda e_2) + i\theta_2(\sigma e_2)]\}u(P).
 \end{aligned}$$

The matrix element for the emission of a photon by a fermion is  $(\alpha e)$  where  $\mathbf{e}$  is the polarization vector of the photon. In all these expressions the factor  $(2\pi/L^3\epsilon)^{1/2}\hbar c$  has been omitted.

### §3. CALCULATION OF THE MATRIX ELEMENT

A typical way in which the transition by means of virtual creation and annihilation of nucleons can take place, is the following:

<i>Process</i>	<i>Matrix Element</i>
$M^+(0) \rightarrow P^+(q) + N^-(-q)$	$a^*(q)Xb(-q)$
$P^+(q) \rightarrow P^+(q_1) + \gamma(p)$	$a^*(q_1)Ya(q)$
$N^-(-q) + P^+(q_1) \rightarrow m^+(-p)$	$b^*(-q)Za(q_1)$

where  $P^\pm$ ,  $N^\pm$  denotes proton or antiproton, neutron or antineutron and where  $X$  is one of the first group, and  $Z$  one of the second group of expressions listed above, and  $Y = (\alpha e)$ . Conservation of momentum requires

$$\mathbf{q} = \mathbf{q}_1 + \mathbf{p}.$$

The matrix element for the three-stage process is  $n_1/4\epsilon_q^2 d_1$  where

$$n_1 = \sum b^*(-q)Za(q_1)a^*(q_1)Ya(q)a^*(q)Xb(-q),$$

$$4\epsilon_q^2 d_1 = (\mu_0 - 2\epsilon_q)(\epsilon_2 - \epsilon_q - \epsilon_{q_1}),$$

$\epsilon_q$  = energy of nucleon with momentum  $\mathbf{q}/c$  and the summation is over the spin states of the nucleons.

The spinors  $a(q)$  and  $b(q)$  have the properties

$$\sum_{r=1,2} a_r^\dagger(q)a_r^*(q) = (1/2\epsilon_q)\{\epsilon_q\delta_{\mu\nu} + (\alpha q)_{\mu\nu} + M\beta_{\mu\nu}\},$$

$$\sum_{r=1,2} b_r^\dagger(-q)b_r^*(-q) = (1/2\epsilon_q)\{\epsilon_q\delta_{\mu\nu} - (\alpha q)_{\mu\nu} - M\beta_{\mu\nu}\}.$$

Introduce  $\mathbf{v} = \mathbf{q}/\epsilon_q, \quad \mathbf{z} = M/\epsilon_q,$

$$E = (\alpha v) + \beta z, \quad v^2 + z^2 = 1.$$

Thus  $n_1 = \frac{1}{8} \text{Sp} Z(1 + E_1)Y(1 + E)X(1 - E).$

Five more ways in which the decay process can take place are obtained by permuting the three processes involving  $X$ ,  $Y$  and  $Z$ . The quantities  $n_i$  are listed below:

$$n_1 = \frac{1}{8} \text{Sp} Z(1 + E_1)Y(1 + E)X(1 - E),$$

$$n_2 = -\frac{1}{8} \text{Sp} Z(1 - E_1)Y(1 + E)X(1 - E),$$

$$n_3 = \frac{1}{8} \text{Sp} Z(1 + E_1)Y(1 - E)X(1 + E),$$

$$n_4 = -\frac{1}{8} \text{Sp} Z(1 - E_1)Y(1 - E)X(1 + E),$$

$$n_5 = -\frac{1}{8} \text{Sp} Z(1 + E_1)Y(1 - E)X(1 - E),$$

$$n_6 = \frac{1}{8} \text{Sp} Z(1 - E_1)Y(1 + E)X(1 + E).$$

The minus signs in processes (2), (4) and (5) result from the commutation properties of the operators  $u$  and  $v$ .

Notice that

$$\begin{aligned}n_2(\mathbf{v}, z, \mathbf{v}_1, z_1) &= -n_1(\mathbf{v}, z, -\mathbf{v}_1, -z_1), \\n_3(\mathbf{v}, z, \mathbf{v}_1, z_1) &= n_1(-\mathbf{v}, -z, \mathbf{v}_1, z_1), \\n_4(\mathbf{v}, z, \mathbf{v}_1, z_1) &= -n_1(-\mathbf{v}, -z, -\mathbf{v}_1, -z_1) \\n_5(\mathbf{v}, z, \mathbf{v}_1, z_1) &= -n_6(-\mathbf{v}, -z, -\mathbf{v}_1, -z_1).\end{aligned}$$

It is therefore only necessary to calculate (say)  $n_1$  and  $n_6$ .

Define

$$x = \frac{\text{mass of initial meson}}{\text{mass of nucleon}}$$

and expand in powers of  $x$

$$\begin{aligned}n_i &= {}^0n_i + x {}^1n_i + \dots, \\d_i &= 1 - x {}^1d_i + \dots.\end{aligned}$$

Then

$$n_i/d_i = {}^0n_i + x \{{}^1n_i + {}^0n_i {}^1d_i\} + x^2 \dots$$

The contribution from these six processes is

$$C_1 \dots C_6 = (\frac{1}{4}\epsilon_q^2) \sum_{i=1}^6 (n_i/d_i).$$

The expansion of the expressions  $d_i$  is carried out as follows:

$$\mathbf{q}_1 = \mathbf{q} - \mathbf{p},$$

or

$$\mathbf{v}_1 = (z_1/z)\mathbf{v} - xz_1\mathbf{l}, \quad \mathbf{l} = \mathbf{p}/\mu_0 = \theta_1\mathbf{r}.$$

Also

$$z_1 = z\{1 - 2xz(lv) + x^2z^2l^2\}^{\frac{1}{2}}$$

hence

$$\epsilon_{q_1} = M/z_1 = \epsilon_q\{1 - xz(lv) + \frac{1}{2}x^2z^2l^2[1 - rv]^2\} \dots$$

Also

$$\begin{aligned}\epsilon_i &= \mu_0\theta_i \\&= xz\theta_i\epsilon_q \quad (i=0, 1, 2; \quad \theta_0=1; \quad \epsilon_0=\mu_0)\end{aligned}$$

hence

$$(\epsilon_q + \epsilon_{q_1} - \epsilon_i)^{-1} = (1/2\epsilon_q)\{1 + \frac{1}{2}xz[\theta_i + (lv)] + \dots$$

Finally

$$\begin{aligned}d_1^{-1} &= 4\epsilon_q^2(2\epsilon_q - \mu_0)^{-1}(\epsilon_q + \epsilon_{q_1} - \epsilon_2)^{-1} \\&= 1 + \frac{1}{2}xz[1 + \theta_2 + (lv)] + \dots\end{aligned} \quad \dots\dots(1)$$

$$\begin{aligned}d_2^{-1} &= 4\epsilon_q^2(2\epsilon_q - \mu_0)^{-1}(\epsilon_q + \epsilon_{q_1} - \epsilon_1)^{-1} \\&= 1 + \frac{1}{2}xz[1 + \theta_1 + (lv)] + \dots\end{aligned} \quad \dots\dots(2)$$

$$\begin{aligned}d_3^{-1} &= 4\epsilon_q^2(2\epsilon_q + \mu_0)^{-1}(\epsilon_q + \epsilon_{q_1} + \epsilon_1)^{-1} \\&= 1 + \frac{1}{2}xz[-1 - \theta_1 + (lv)] + \dots\end{aligned} \quad \dots\dots(3)$$

$$\begin{aligned}d_4^{-1} &= 4\epsilon_q^2(2\epsilon_q + \mu_0)^{-1}(\epsilon_q + \epsilon_{q_1} + \epsilon_2)^{-1} \\&= 1 + \frac{1}{2}xz[-1 - \theta_2 + (lv)] + \dots\end{aligned} \quad \dots\dots(4)$$

$$\begin{aligned}d_5^{-1} &= 4\epsilon_q^2(\epsilon_q + \epsilon_{q_1} + \epsilon_1)^{-1}(\epsilon_q + \epsilon_{q_1} - \epsilon_2)^{-1} \\&= 1 + \frac{1}{2}xz[-\theta_1 + \theta_2 + 2(lv)] + \dots\end{aligned} \quad \dots\dots(5)$$

$$\begin{aligned}d_6^{-1} &= 4\epsilon_q^2(\epsilon_q + \epsilon_{q_1} + \epsilon_2)^{-1}(\epsilon_q + \epsilon_{q_1} - \epsilon_1)^{-1} \\&= 1 + \frac{1}{2}xz[\theta_1 - \theta_2 + 2(lv)] + \dots\end{aligned} \quad \dots\dots(6)$$

*Additional Processes.*

Apart from these processes there are other ways in which a charged meson can decay into a lighter charged meson and a photon.

<i>Process</i>	<i>Matrix Element</i>	
$M^+(0) \rightarrow M^+(-p) + \gamma(p)$		$\left. \begin{array}{l} \\ \\ \end{array} \right\} \dots\dots (7)$
$M^+(-p) \rightarrow P^+(q_1) + N^-( -q)$	$a^*(q_1)X'b(-q)$	
$P^+(q_1) + N^-( -q) \rightarrow m^+(-p)$	$b^*(-q)Za(q_1)$	

Similar to (7) but with last two processes interchanged. .....(8)

$0 \rightarrow P^-( -q_1) + N^+(q) + m^+(-p)$	$a^*(q)Zb(-q_1)$	$\left. \begin{array}{l} \\ \\ \end{array} \right\} \dots\dots (9)$
$M^+(0) \rightarrow M^+(-p) + \gamma(p)$		
$M^+(-p) + P^-( -q_1) + N^+(q) \rightarrow 0$	$b^*(-q_1)X'a(q)$	
$0 \rightarrow P^-( -q) + N^+(q) + m^+(0)$	$a^*(q)Z'b(-q)$	$\left. \begin{array}{l} \\ \\ \end{array} \right\} \dots\dots (10)$
$m^+(0) \rightarrow m^+(-p) + \gamma(p)$		
$M^+(0) + P^-( -q) + N^+(q) \rightarrow 0$	$b^*(-q)Xa(q)$	

$0 \rightarrow P^-( -q) + N^+(q) + m^+(0)$	$a^*(q)Z'b(-q)$	$\left. \begin{array}{l} \\ \\ \end{array} \right\} \dots\dots (11)$
$M^+(0) + P^-( -q) + N^+(q) \rightarrow 0$	$b^*(-q)Xa(q)$	
$m^+(0) \rightarrow m^+(-p) + \gamma(p)$		

Similar to (11) but with first two processes interchanged. .....(12)

The expressions  $X'$ ,  $X$ ,  $Z'$ ,  $Z$  are essentially the same as for processes (1), ..., (6).  $X'$  means  $X$  generalized for a moving meson and  $Z'$  means  $Z$  specialized for a meson at rest.

There are still four more processes by means of which the transition can take place

$0 \rightarrow P^-( -q) + N^+(q) + m^+(-p) + \gamma(p)$	$a^*(q)Z''b(-q)$	$\left. \begin{array}{l} \\ \end{array} \right\} \dots\dots (13)$
$M^+(0) + P^-( -q) + N^+(q) \rightarrow 0$	$b^*(-q)Xa(q)$	

$M^+(0) \rightarrow P^+(q) + N^-( -q)$	$a^*(q)Xb(-q)$	$\left. \begin{array}{l} \\ \end{array} \right\} \dots\dots (14)$
$P^+(q) + N^-( -q) \rightarrow m^+(-p) + \gamma(p)$	$b^*(-q)Z''a(q)$	

$M^+(0) \rightarrow P^+(q_1) + N^-( -q) + \gamma(p)$	$a^*(q_1)X''b(-q)$	$\left. \begin{array}{l} \\ \end{array} \right\} \dots\dots (15)$
$P^+(q_1) + N^-( -q) \rightarrow m^+(-p)$	$b^*(-q)Za(q_1)$	

$0 \rightarrow P^-( -q_1) + N^+(q) + m^+(-p)$	$a^*(q)Zb(-q_1)$	$\left. \begin{array}{l} \\ \end{array} \right\} \dots\dots (16)$
$P^-( -q_1) + N^+(q) + M^+(0) \rightarrow \gamma(p)$	$b^*(-q_1)X''a(q)$	

where  $X$  and  $Z$  are the same as for (1), ..., (6), but  $X''$  and  $Z''$  are derived from the interaction term in the Hamiltonian by replacing

$$\begin{array}{ll} \nabla U & \text{by } \{\nabla - (ie/\hbar c)\mathbf{A}\}U, \\ \nabla U^* & \text{by } \{\nabla + (ie/\hbar c)\mathbf{A}\}U^*, \end{array}$$

where  $\mathbf{A}$  is the electromagnetic vector potential.

This alteration can only affect the  $f$ -terms and the matrix elements are

$$\begin{aligned} Z''_s &= ie(f_2/\mu_2)(\alpha e), \\ Z''_{ps} &= ie(f_2/\mu_2)(\sigma e), \\ Z''_{lv} &= -e(f_2/\mu_2)(\mu_0/\mu_2)\beta\{\theta_1(\alpha e) + i\theta_2\sigma(e_\lambda r)\}, \\ Z''_{lv} &= ie(f_2/\mu_2)\beta\sigma(e_\lambda e_2), \\ Z''_{lpv} &= -e(f_2/\mu_2)(\mu_0/\mu_2)\beta\{\theta_2\alpha(e_\lambda r) - i\theta_1(\sigma e)\}, \\ Z''_{lpv} &= e(f_2/\mu_2)\beta\alpha(e_\lambda e_2). \end{aligned}$$

To get  $X''$ , which refers to the absorption of a meson, the only change is the sign and the replacement of  $f_2$  by  $f_0$  etc.

The matrix elements for the individual processes are as follows:

$$\begin{aligned} n'_7 &= \frac{1}{4} \text{Sp} X'(1-E)Z(1+E_1), \\ n'_8 &= \frac{1}{4} \text{Sp} X'(1+E)Z(1-E_1), \\ n'_9 &= \frac{1}{4} \text{Sp} X'(1+E)Z(1-E_1), \\ n'_{10} &= \frac{1}{4} \text{Sp} X(1+E)Z'(1-E), \\ n'_{11} &= \frac{1}{4} \text{Sp} X(1+E)Z'(1-E), \\ n'_{12} &= \frac{1}{4} \text{Sp} X(1-E)Z'(1+E), \\ n'_{13} &= \frac{1}{4} \text{Sp} X(1+E)Z''(1-E), \\ n'_{14} &= \frac{1}{4} \text{Sp} X(1-E)Z''(1+E), \\ n'_{15} &= \frac{1}{4} \text{Sp} X''(1-E)(Z(1+E_1)), \\ n'_{16} &= \frac{1}{4} \text{Sp} X''(1+E)Z(1-E_1), \end{aligned}$$

where  $n'_7 \dots n'_{12}$  must still be multiplied by the matrix element of the process in which a meson emits a photon to get  $n_7 \dots n_{12}$ . Since this matrix element vanishes for a scalar or pseudoscalar meson finally or initially at rest, some of these matrix elements need not be calculated in these special cases.

The contribution from processes (7), (8) and (9) is

$$C_{789} = (1/2\epsilon_q) \left\{ [1/\mu_0(\theta_3 - \theta_2)] [n_7/d_7 + n_8/d_8] + (1/2\epsilon_q)(n_9/d_9) \right\},$$

$$\text{where } \theta_3 = (\mu_0^2 + p^2)^{1/2}/\mu_0 \quad \theta'_2 = \mu_2/\mu_0$$

$$\begin{aligned} d_7^{-1} &= 2\epsilon_q(\epsilon_q + \epsilon_{q_1} - \epsilon_2)^{-1} \\ &= 1 + \frac{1}{2}xz[\theta_2 + (lv)] + \dots \end{aligned}$$

$$\begin{aligned} d_8^{-1} &= 2\epsilon_q(\epsilon_q + \epsilon_{q_1} + \theta_3\mu_0)^{-1} \\ &= 1 + \frac{1}{2}xz[-\theta_3 + (lv)] + \dots \end{aligned}$$

$$\begin{aligned} d_{10}^{-1} &= 4\epsilon_q^2(\epsilon_q + \epsilon_{q_1} + \epsilon_2)^{-1}(\epsilon_q + \epsilon_{q_1} + \theta_3\mu_0)^{-1} \\ &= 1 + \frac{1}{2}xz[-\theta_2 - \theta_3 + 2(lv)] + \dots \end{aligned}$$

Similarly

$$C_{10,11,12} = (1/2\epsilon_q) \left\{ (1/2\epsilon_q)(n_{10}/d_{10}) - [1/\mu_0(1 - \theta'_2)] [n_{11}/d_{11} + n_{12}/d_{12}] \right\},$$

$$\begin{aligned} \text{where } d_{10}^{-1} &= 4\epsilon_q^2(2\epsilon_q + \mu_2)^{-1}(2\epsilon_q + \mu_0)^{-1} \\ &= 1 + \frac{1}{2}xz(-1 - \theta'_2) + \dots \end{aligned}$$

$$d_{11}^{-1} = 2\epsilon_q(2\epsilon_q + \mu_2)^{-1} = 1 - \frac{1}{2}xz\theta'_2 + \dots$$

$$d_{12}^{-1} = 2\epsilon_q(2\epsilon_q - \mu_0)^{-1} = 1 + \frac{1}{2}xz + \dots$$

Similarly  $C_{13, 14, 15, 16} = -(1/2\epsilon_q) \sum_{i=13}^{16} (n_i/d_i),$

where  $d_{13}^{-1} = 2\epsilon_q(2\epsilon_q + \mu_0)^{-1} = 1 - \frac{1}{2}xz + \dots$

$$d_{14}^{-1} = 2\epsilon_q(2\epsilon_q - \mu_0)^{-1} = 1 + \frac{1}{2}xz + \dots$$

$$d_{15}^{-1} = 2\epsilon_q(\epsilon_q + \epsilon_{q_1} - \epsilon_2)^{-1} = 1 + \frac{1}{2}xz[\theta_2 + (lv)] + \dots$$

$$d_{16}^{-1} = 2\epsilon_q(\epsilon_q + \epsilon_{q_1} + \epsilon_2)^{-1} = 1 + \frac{1}{2}xz[-\theta_2 + (lv)] + \dots$$

The reciprocal of the lifetime of the meson is given by

$$\tau^{-1} = (2\pi/\hbar) |H|^2 \rho$$

where

$$H = (2\pi/L^3)^{3/2} (\hbar c L)^3 \left| [(\epsilon_0 \epsilon_1 \epsilon_2)^{1/2} (2\pi \hbar c)^3] \int d^3 q \{ C_1 \dots C_6 + C_7 \dots C_{12} + C_{13} \dots C_{16} \} \right|$$

and  $\rho$  = density of final states per unit energy.

#### § 4. ADEQUACY OF THE LEADING TERM

The series obtained for  $\Sigma(n_i/d_i)$  by expanding the numerators and denominators in a power series of  $x$  is certainly convergent.

It will be shown that only the leading term is important, even if  $x = \frac{1}{2}$ .

Notice that

$$\mathbf{v}_1(\mathbf{v}, z) = -\mathbf{v}_1(-\mathbf{v}, -z),$$

$$z_1(\mathbf{v}, z) = -z_1(-\mathbf{v}, -z).$$

Anticipate the form

$$n = (z_1/z)A + (1 \pm z_1/z)B + xz_1C,$$

which will be derived in the next section. Suppose the expressions  $X$  and  $Z$  from which  $n$  is derived contain only one type of Dirac matrix like  $\beta(\alpha p)$  and not a linear combination like  $\beta(\alpha p) + \lambda\beta(\sigma k)$ . Then  $A$  and  $B$  contain the same vectors  $\mathbf{v}, \mathbf{e}_i, \dots$  and therefore  $(z_1/z)A$  and  $(1 \pm z_1/z)B$  behave similarly under a change in sign of  $\mathbf{v}$  and  $z$ . From the above this implies also a change in sign of  $\mathbf{v}_1$  and  $z_1$ . Because of the additional factor  $(\alpha r)$  in the spur represented by  $C$ , this expression contains one  $\mathbf{v}$  more (or less) than either  $A$  or  $B$ .

Hence  $n(\mathbf{v}, z) = \pm n(-\mathbf{v}, -z)$ . From the series for  $z_1$  follows that in the expansion

$$n = {}^0n + x^1n + \dots$$

consecutive terms behave differently towards a change in sign of  $\mathbf{v}$ . The same is true for  $d_1^{-1} \pm d_4^{-1}$ . If  $n_1(\mathbf{v}, z) = n_1(-\mathbf{v}, -z)$  then

$$n_1(\mathbf{v}, z) = -n_1(-\mathbf{v}, -z) = -n_1(\mathbf{v}, z),$$

hence  $n_1 d_1^{-1} + n_4 d_4^{-1} = n_1(d_1^{-1} - d_4^{-1})$  which, after integration over the directions of  $\mathbf{v}$ , results in an odd or even series of  $x$ . Closer investigation shows that the second term in the series for  $n_1 d_1^{-1} + n_4 d_4^{-1}$  is smaller than the leading term by about a factor  $\frac{1}{4}x^2 z^2 \theta_1^2 < 4^{-3} z^2$  ( $\theta_1 < \frac{1}{2}, 0 \leq z \leq 1$ ).

The same argument applies to the groups (2, 3), (5, 6), (7, 8, 9), (10, 11, 12), (13, 14, 15, 16). This result holds also for those linear combinations of different types of matrices used in this paper.

*Example.*

Before calculating the matrix element of a particular decay process it is convenient to eliminate  $\mathbf{v}_1$  from the calculation. The equation

$$\mathbf{v}_1 = (z_1/z)\mathbf{v} - xz_1\mathbf{l}$$

is invariant under the various changes in sign of  $\mathbf{v}, z, \mathbf{v}_1$  and  $z_1$ , so that after elimination of  $\mathbf{v}_1$  the calculation of  $n_1$  and  $n_6$  is still sufficient to determine  $n_2, n_3, n_4, n_5$  also.

$$(\alpha v_1) + \beta z_1 = (z_1/z)\{(\alpha v) + \beta z\} - xz_1(\alpha l).$$

Hence  $1 + E_1 = (z_1/z)(1 + E) + 1 - (z_1/z) - xz_1(\alpha l).$

Since  $Y = (\alpha e)$  and  $(1 + E)(\alpha e)(1 + E) = 2(ev)(1 + E)$ , therefore

$$\begin{aligned} n_1 &= \frac{1}{4}(ev)(z_1/z)\text{Sp}Z(1 + E)X(1 - E) \\ &\quad + \frac{1}{8}(1 - z_1/z)\text{Sp}Z(\alpha e)(1 + E)X(1 - E) \\ &\quad - \frac{1}{8}xz_1\text{Sp}Z(\alpha l)(\alpha e)(1 + E)X(1 - E). \end{aligned}$$

Since  $(1 - E)(\alpha e)(1 + E) = 2(\alpha e)(1 + E) - 2(ev)(1 + E)$ ,

therefore 
$$\begin{aligned} n_6 &= -\frac{1}{4}(ev)(z_1/z)\text{Sp}Z(1 + E)X(1 + E) \\ &\quad + \frac{1}{8}(1 + z_1/z)\text{Sp}Z(\alpha e)(1 + E)X(1 + E) \\ &\quad + \frac{1}{8}xz_1\text{Sp}Z(\alpha l)(\alpha e)(1 + E)X(1 + E). \end{aligned}$$

It is evident, from the relationship between  $n_i$  ( $i = 1 \dots 4$ ), that  $\sum_{i=1}^4 n_i = z_1 f(\mathbf{v}, z)$  where  $f(-\mathbf{v}, -z) = f(\mathbf{v}, z)$ . Similarly  $n_5 + n_6 = F(z_1, \mathbf{v}, z)$ , where

$$F(-z_1, -\mathbf{v}, -z) = -F(z, \mathbf{v}, z).$$

Consider now the transition

$$M_v^+(0) \rightarrow m_{ps}^+(-p) + \gamma(p).$$

A vector meson at rest decays into a pseudoscalar meson, momentum  $-p/c$  and a photon with momentum  $p/c$ .

To calculate the term in  $eg_0g_2$  put

$$X = (\alpha e_0), \quad Z = i\beta\gamma_5.$$

$$\text{Sp}Z(1 + E)X(1 - E) = 0,$$

$$\text{Sp}Z(\alpha e)(1 + E)X(1 - E) = 0,$$

$$\begin{aligned} \text{Sp}Z(\alpha l)(\alpha e)(1 + E)X(1 - E) &= -2iz\text{Sp}\gamma_5(\alpha l)(\alpha e)(\alpha e_0) \\ &= 8z(e_\lambda e_0)l. \end{aligned}$$

Thus  $n_1 = -xz_1(e_\lambda e_0)l$  leading to  $-\sum_{i=1}^4 n_i = 0$ .

However  $\sum_{i=1}^4 n_i/d_i = n_1\{d_1^{-1} + d_2^{-1} - d_3^{-1} - d_4^{-1}\} = 3xz_1n_1$ .

Similarly  $n_6 = 0 = n_5$ . Thus neglecting higher powers of  $x$

$$\sum_{i=1}^6 n_i/d_i = -3x^2(e_\lambda e_0)r\theta_1 z^3.$$

The  $ef_0f_2$ -term was calculated by Finkelstein and is of order  $x^0$  (see Table).



It can easily be seen that the additional processes do not contribute.

$$n'_7 = \frac{1}{4} \text{Sp} X' (1 - E) Z (1 + E_1),$$

where  $X' = (\alpha e'_0)$ ,  $Z = i\beta\gamma_5$ , if in the intermediate state the heavy meson is a transverse one. Because of the  $\gamma_5$  in  $Z$

$$n'_7 = \text{const.} (e'_{0\lambda} v) v = 0 = n'_8 = n'_9.$$

Similarly if the heavy meson is longitudinal in the intermediate state.

To get  $n_{10}, n_{11}, n_{12}$ , the expressions  $n'_{10}, n'_{11}, n'_{12}$  must be multiplied by a factor which vanishes if the secondary meson is pseudoscalar.

Processes (13) . . . (16) only contribute to  $f$ -terms. Thus

$$H = (2\pi/L^3 \mu_0 \epsilon_1 \epsilon_2)^{\frac{1}{2}} x^2 (e_{0\lambda} e) r \theta_1 (M/4\pi) e g_0 g_2,$$

$$p = 4\pi \mu_0^2 \theta_1^3 L^3 / (2\pi \hbar c)^3,$$

giving

$$\tau^{-1} = \{(e_{0\lambda} e) r\}^2 \{x^3 \theta_1^4 M / (8\pi^2 \theta_2 \hbar)\} \{e^2 g_0^2 g_2^2 / (\hbar c)^3\}.$$

Summing over the two directions for  $\mathbf{e}$  and averaging over the three directions of  $\mathbf{e}_0$ ,

$$\tau^{-1} = x^3 \theta_1^4 M e^2 g_0^2 g_2^2 / \{12\pi^2 \hbar \theta_2 (hc)^3\} \simeq 10^{12}$$

for the parameters used by Finkelstein.

The picture presented here is however less attractive if it is required to describe the decay of mesons of mass about 900 electron masses.

To get an idea of the order of magnitude in such a case, put  $x = \frac{1}{2}$ ,  $\theta_1 = \frac{1}{4}$ ,  $\theta_2 = \frac{3}{4}$ , giving  $\tau^{-1} = 6 \times 10^{16} g_0^2 g_2^2 / (hc)^2$ . The lifetime  $\tau = 10^{-9}$  sec. would therefore require  $g_0^2 g_2^2 / (hc)^2 \simeq 10^{-8}$ . Since the Berkeley experiments seem to confirm that  $g_2^2 / \hbar c$  is not very small and probably about  $1/10$ , it would follow that  $g_0^2 / \hbar c$  would have to be less than  $10^{-7}$ , which seems incompatible with a reasonable cross section for creation of  $\tau$ -mesons unless some quite new process comes into play.

#### Table.

The matrix elements for all choices of initial and final mesons are tabulated below. The scalar, pseudoscalar, vector and pseudovector mesons are denoted by s, ps, v, pv, respectively. Longitudinal and transverse vector mesons are distinguished by lv and tv respectively, similarly for pseudovector mesons. The symbol  $(i, j)$  denotes the group of four matrix elements containing  $g_i g_j$ ,  $g_i f_j$ ,  $f_i g_j$ ,  $f_i f_j$  (in this order) in the decay process where  $i$  is the initial, and  $j$  the final meson. The second column contains the total matrix element for the first six processes, while the contribution from the rest appears in the third column. The entry  $q^2$  in this column denotes a quadratic divergence. The expressions containing a factor  $z^3$  are finite when integrated over  $q$ , but those containing only  $z$  are logarithmic divergent.

For the sake of consistency all divergences will be ignored. This prescription will in some cases require the calculation of new leading terms.

Process	$4\epsilon_q^2 \int C_1 \dots \frac{d\omega}{4\pi}$	$4\epsilon_q^2 \int C_7 \dots \frac{d\omega}{4\pi}$
(s, tpv)	$-(i/3)x^2(e_\lambda e_2)l\{3+4\theta_1-10\theta_1 z^2\}z^3$ $2x(e_\lambda e_2)l(\mu_0/\mu_2)\{1-(1+\theta_1)z^2\}z$ $2x(e_\lambda e_2)l z^3$ $4i(e_\lambda e_2)l(\mu_0/\mu_2)z$	$2x(e_\lambda e_2)l\theta_2 z^3$
(s, tv)	$4(ee_2)z^3$ $2x(ee_2)(\mu_0/\mu_2)\{\theta_1+(1-4\theta_1+\theta_1^2)z^2\}z$ $(2i/3)x(ee_2)(\theta_2-\theta_1)(z^2+2)z$ $4i(ee_2)(\epsilon_2/\mu_2)z$	$q^2$ $4i(ee_2)(\mu_0/\mu_2)(\theta_2-\theta_1)z$
(ps, tpv)	$-4i(ee_2)z$ $-2x(ee_2)(\mu_0/\mu_2)\{\theta_1+(1-\theta_1+\theta_1^2)z^2\}z$ $(2i/3)x(ee_2)\{2(1-2\theta_1)+(1+7\theta_1)z^2\}z$ $4(ee_2)(\epsilon_2/\mu_2)z^3$	$q^2$ $-4(ee_2)(\mu_0/\mu_2)\theta_1^2 z^3$
(ps, tv)	$3x^2(e_\lambda e_2)l z^3$ $2x(e_\lambda e_2)l(\mu_0/\mu_2)\{1+(1+\theta_2)z^2\}z$ $-4x(e_\lambda e_2)l z^3$ $-4(e_\lambda e_2)l(\mu_0/\mu_2)z^3$	$2x(e_\lambda e_2)l\theta_2 z^3$ $4(e_\lambda e_2)l(\epsilon_2/\mu_2)z^3$
(v, s)	$4(ee_0)z^3$ $-(2i/3)x(ee_0)(\mu_0/\mu_2)\{2+(1+\theta_1^2)z^2+2\theta_1^2 z^4\}z$ $2x(ee_0)\{-\theta_1+(1+2\theta_1)z^2\}z$ $-4i(ee_0)(\epsilon_2/\mu_2)z$	$2(ee_0)a\theta_1^2\theta_3 z^3$ $q^2$ $x(ee_0)a\theta_1^2\theta_2 z^3$ $-4i(ee_0)(\mu_0/\mu_2)z$
(v, ps)	$-3x^2(e_\lambda e_0)l z^3$ $2x(e_\lambda e_0)l(\mu_0/\mu_2)(2+\theta_2)z^3$ $-2x(e_\lambda e_0)l(1+z^2)z$ $4(e_\lambda e_0)l(\mu_0/\mu_2)z^3$	$2x(e_\lambda e_0)l\theta_2 z^3$ $-4(e_\lambda e_0)l(\epsilon_2/\mu_2)z^4$ *
(v, tv)	$(4/3)x(e_0 l)(ee_2)\{2-2z^2-z^4\}z$ $4(e_0 l)(ee_2)(\mu_0/\mu_2)z$ $3x^2(e_0 l)(ee_2)z^3$ $(2/3)x(e_0 l)(ee_2)(\mu_0/\mu_2)\{1+(6-\theta_1)z^2+2\theta_2 z^4\}z$	$q^2$ $2(e_0 l)(ee_2)\{-\mu_0/\mu_2 a(\theta_2-\theta_1)+b\}z$ $2(e_0 l)(ee_2)\{a(\theta_1^2-\theta_2\theta_3)+b-2\}z$ $q^2$
(v, lv)	$(2/3)x(ee_0)\theta_1(\mu_0/\mu_2)\{4+(3-\theta_1)z^2+2\theta_2 z^4\}z$ $3x^2(ee_0)\theta_1 z^3$ $4(ee_0)\theta_1(\mu_0/\mu_2)z$ $(2/3)x(ee_0)\theta_1\{1+7z^2-2z^4\}z$	$q^2$ $2(ee_0)\{a(\theta_1^2-\theta_2\theta_3)+b-2(\mu_0^2/\mu_2^2)\}\theta_1$ $2(ee_0)\{a(\theta_1-\theta_2)(\mu_0/\mu_2)+b\}\theta_1 z$ $q^2$
(v, tpv)	$2ix(e_0 \lambda e)e_2(1+\theta_1)z^3$ $4(e_0 \lambda e)e_2(\epsilon_2/\mu_2)z$ $4i(e_0 \lambda e)e_2 z^3$ $(2/3)x(e_0 l)(e_2 \lambda e)l(\mu_0/\mu_2)\{1-5z^2-2z^4\}z$ $(2/3)x(e_0 \lambda e)^2(\epsilon_2/\mu_2)\{2-\theta_1+(1+4\theta_1)z^2\}z$	$i(e_\lambda e_2)l(e_0 l)a\theta_2 z^3$ $4(e_0 \lambda e)e_2(\mu_0/\mu_2)z$ $2i(e_\lambda e_2)l(e_0 l)a\theta_3 z^3$ $q^2$
(v, lpv)	$2ix(e_\lambda e_0)r(\mu_0/\mu_2)(1+\theta_1^2)z^3$ $4(e_\lambda e_0)r z$ $4i(e_\lambda e_0)r(\epsilon_2/\mu_2)z^3$ $(2/3)x(e_\lambda e_0)r\{2-\theta_1+(1+4\theta_1)z^2\}z$	$4(e_\lambda e_0)r(\mu_0/\mu_2)z$ $-4i(e_\lambda e_0)r\theta_1^2(\mu_0/\mu_2)z^3$ $q^2$

\* This contribution cannot be neglected as Finkelstein suggested. Its inclusion lengthens the lifetime by a factor  $(\epsilon_1/\mu_0)^{-2} \simeq 10$ .

Process	$4\epsilon_q^2 \int C_1 \dots \frac{d\omega}{4\pi}$	$4\epsilon_q^2 \int C_7 \dots \frac{d\omega}{4\pi}$
(pv, s)	$(i/3)x^2(e_\lambda e_0)l\{- (3 + 4\theta_1) + 10\theta_1 z^2\}z^3$ $- 2x(e_\lambda e_0)l\theta_1(\mu_0/\mu_2)z^3$ $2x(e_\lambda e_0)l\{-1 + 2z^2\}z$ $4i(e_\lambda e_0)l(\mu_0/\mu_2)z$	$2x(e_\lambda e_0)l\theta_2 z^3$
(pr, ps)	$4i(ee_0)z$ $-(2i/3)z(ee_0)(\mu_0/\mu_2)\{2 + (1 - 9\theta_1 + \theta_1^2)x^2 + 2\theta_1^2 z^4\}z$ $2x(ee_0)\{\theta_1 - \theta_2 z^2\}z$ $4(ee_0)(\epsilon_2/\mu_2)z^3$	$2i(ee_0)(\theta_1^2/\theta_2)z$ $\frac{q^2}{q^2}$ $- 2x(ee_0)a\theta_1^2\theta_2 z^3$ $2(ee_0)(\epsilon_2/\mu_2)a\theta_1^2 z^3$
(pv, tv)	$2ix(e_\lambda e_0)e_2(2\theta_1 - 1)z^3$ $- 4i(e_\lambda e_0)e_2(\epsilon_2/\mu_2)z^3$ $4(e_\lambda e_0)e_2 z$ $(2/3)x(e_0 l)(e_\lambda e_2)l(\mu_0/\mu_2)\{1 + 4z^2 - 2z^4\}z$ $(2/3)x(e_\lambda e_0)e_2(\epsilon_2/\mu_2)\{2 - \theta_1 + (1 - 5\theta_1)z^2\}z$	$- ix(e_\lambda e_2)l(e_0 l)a\theta_2 z^3$ $2i(e_\lambda e_2)l(e_0 l)(\epsilon_2/\mu_2)z^3$ $\{-2/\theta_1(e_\lambda e_2)l(e_0 l) + 4(e_\lambda e_0)e_2\theta_2\}z$ $\frac{q^2}{q^2}$
(pv, lv)	$2ix(e_\lambda e_0)r(\mu_0/\mu_2)(1 - 3\theta_1 + \theta_1^2)z^3$ $4i(e_\lambda e_0)r z^3$ $- 4(e_\lambda e_0)r(\epsilon_2/\mu_2)z$ $(2/3)x(e_\lambda e_0)r\{-2 + \theta_1 + (-1 + 5\theta_1)z^2\}z$	$- 4(e_\lambda e_0)r(\mu_0/\mu_2)(\theta_2 - \theta_1)z$ $\frac{q^2}{q^2}$
(pv, tpv)	$(2, 3)x(ee_2)(e_0 l)\{4 - 5z^2 - 2z^4\}z$ $- 4i(ee_2)(e_0 l)(\mu_0/\mu_2)z^3$ $-(i/3)x^2(ee_2)(e_0 l)\{3 + 4\theta_1 - 10\theta_1 z^2\}z^3$ $(2/3)x(ee_2)(e_0 l)(\mu_0/\mu_2)\{1 - (3 + \theta_1)z^2 + 2\theta_2 z^4\}z$	$\frac{q^2}{q^2}$ $- 2i(ee_2)(e_0 l)(\mu_0/\mu_2)a\theta_1^2 z^3$ $2i(ee_2)(e_0 l)\{a\theta_1^2 z^2 - (2/3)(1 - 2z^2)\}z$ $\frac{q^2}{q^2}$
(pv, lpv)	$(2/3)x(ee_0)(\epsilon_1/\mu_2)\{3 - \theta_1 - 5z^2 + 2\theta_2 z^4\}z$ $+(i/3)x^2(ee_0)\theta_1\{3 + 4\theta_1 - 10\theta_1 z^2\}z^3$ $4i(ee_0)\theta_1 z^3$ $+(2/3)x(ee_0)\theta_1\{1 - 2z^2 - 2z^4\}z$	$\frac{q^2}{q^2}$ $- 2i(ee_0)a\theta_1^2 z^3$ $2i(ee_0)a\theta_1^2(\mu_0/\mu_2)z^3$ $\frac{q^2}{q^2}$

The notation is as follows:

$\mu_i$  = meson rest energy, where the suffixes 0 and 2 refer to the initial and final mesons respectively.

$\epsilon_2$  = energy of final meson.

$p = e_1$  = energy of photon.

$\mathbf{e}$  = meson polarization vector ( $i=0, 2$ ).

$\mathbf{e}$  = photon polarization vector.

$\mathbf{r}$  = unit propagation vector of photon.

$\theta_1 = p/\mu_0$ ,  $\theta_2 = \epsilon_2/\mu_0$ ,  $\theta'_2 = \mu_2/\mu_0$ ,  $\theta_3 = (\mu_0^2 + p^2)^{1/2}/\mu_0$ .

$\mathbf{l} = \theta_1 \mathbf{r}$ .

$M$  = rest energy of nucleon.

$\epsilon_q = (M^2 + q^2)^{1/2}$ .

$q/c$  = momentum of nucleon in intermediate state.

$x = \mu_0/M$ .

$z = M/\epsilon_q$ .

$a = \{\theta_3(\theta_3 - \theta_2)\}^{-1}$ ,  $b = \{\theta'_2(1 - \theta'_2)\}^{-1}$ ;  $d^3q = q^2 dq d\omega$ .

## § 5. CONCLUSION

From the table it is clear that for  $x = \frac{1}{2}$  all the matrix elements are roughly of the same order of magnitude. Recalling the result of the example it must be concluded that the decay process  $\tau^+ \rightarrow \pi^+ + \gamma$  makes the  $\tau$ -meson too short-lived to agree even approximately with observation.

The situation is however quite different if both the initial and final mesons have zero spin. In this case the emission of a positron-electron pair or of two photons must be considered. If, in particular, one of the two mesons is scalar and the other pseudoscalar, then the production of a pair is forbidden. A calculation, which will be published in a later paper, of the probability of emitting two photons leads in this case to a lifetime of the order of  $\mathcal{G} \times 10^{-12}$  sec. where  $\mathcal{G}$  is the reciprocal of the product of the dimensionless coupling parameters of the two meson fields. This is no longer in direct disagreement with experimental evidence.

Hence the conclusion is that either  $\tau$ -mesons and  $\pi$ -mesons have spin zero, or the nucleon- $\tau$ -meson interaction is different from that represented by the scheme

$$P \rightarrow N + \tau^+,$$

or the usual perturbation theory is not adequate to describe these processes.

#### ACKNOWLEDGMENTS

It is a pleasure to thank Professor R. E. Peierls for suggesting this investigation and for his advice and criticism.

This work was carried out while the author was holding a scholarship from the University of Stellenbosch, S. Africa.

#### REFERENCES

- FINKELSTEIN, R. J., 1947, *Phys. Rev.*, **72**, 415.  
KEMMER, N., 1938, *Proc. Roy. Soc. A*, **166**, 127.  
POWELL, C. F., with others, 1949, *Nature, Lond.*, **163**, 47, 82.

## Excited Electronic Levels in Conjugated Molecules— III: Energy States of Naphthalene\*

By J. JACOBS

Wheatstone Physics Laboratory, King's College, London

*Communicated by C. A. Coulson; MS. received 27th May 1949*

**ABSTRACT.** The electronic states of naphthalene are determined using antisymmetrized molecular orbitals, which are based on wave functions given by the simple molecular orbital theory. This method allows the electronic interaction term to be included explicitly in the Hamiltonian for the system. A clear distinction is made between electronic configurations determined with these wave functions and the actual states of the molecule: states arise from a superposition of configurations of the same symmetry. The ground state becomes considerably stabilized by this configurational interaction, to which even highly excited levels contribute. Calculated energy values for some of the lower transitions agree well with ultra-violet spectral data, as do the newly derived oscillator strengths. A tentative assignment is made regarding the polarization of the electronic transitions in the region of 30,000—55,000  $\text{cm}^{-1}$ .

### § 1. INTRODUCTION

THERE are two main theories known for the theoretical discussion of molecular structure—the valence bond treatment (Heitler, London, Pauling) and the method of molecular orbitals (Hund, Mulliken). Reasonably good results can be obtained with either method for ground state phenomena; but for the interpretation of ultra-violet spectra—involving electronically excited states in relation to the ground state—both treatments are inadequate. Particularly in the polyacenes the two methods lead to different conclusions, neither of which can be correlated satisfactorily with experimental data. Because of this disagreement it seemed worth while to re-examine the method of molecular orbitals and to extend it; this has been done with reference to the naphthalene molecule.

### § 2. METHOD OF MOLECULAR ORBITALS

Our discussion of the molecular orbital (m.o.) theory falls into three stages: (a) the simplest form in which all electronic repulsion is averaged yields the basic m.o. wave functions and levels; (b) inclusion of the electron repulsion term in the potential energy expression leads to individual configurations; (c) configurational interaction gives the states of the molecule. We reserve the term *state* for the final description of the molecule, whereas any allotment of electrons to the available m.o. levels used in (b) is referred to as a *configuration*.

The first stage deals with the method as developed chiefly by Lennard-Jones and Coulson (1939), who applied it to hydrocarbons. The fundamental assumption is that electronic interaction can be averaged over the whole molecule to give a self-consistent field. This means that the effective Hamiltonian contains one-electron functions only and may be written  $\mathcal{H} = \sum_{\nu} H(\nu)$ , where  $H(\nu)$  is the effective Hamiltonian for electron  $\nu$ . Such an approximation enables us to use one-electron wave functions  $\phi_i$  and to associate with each of them a molecular orbital energy  $\epsilon_i$ . The energy of a configuration of the whole molecule is then simply the sum of the energies  $\epsilon_i$  of the occupied m.o. levels. For convenience only  $\pi$ -electrons are usually considered.

\* For parts I and II see C. A. Coulson, *Proc. Phys. Soc.*, 1948, **60**, 257, and H. C. Longuet-Higgins, *Proc. Phys. Soc.*, 1948, **60**, 270.

Coulson (1948) has published detailed calculations for the polyacenes. As these will be required in our later work (stages (b) and (c) above) it will be necessary to begin by summarizing his results. In these molecules the nuclei are arranged symmetrically with respect to the short and long axes. Calling these the  $y$  and  $z$  axes respectively, we can group the nuclei into sets each of which is symmetrical or antisymmetrical to reflection in the planes perpendicular to the plane of the molecule through the  $y$  and  $z$  axes.

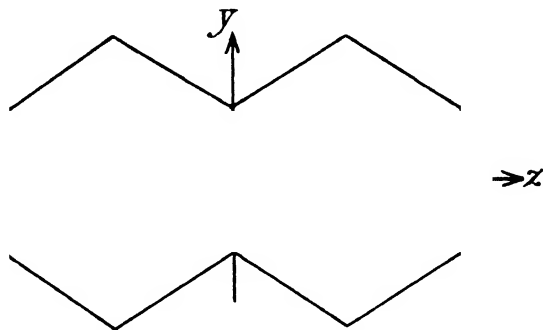


Figure 1.

M.o. wave functions are built up as linear combinations of atomic orbitals at each carbon nucleus  $\phi_i = \sum_r c_r^i \psi_r$ , where  $\phi_i$  = wave function of the  $i$ th m.o.,  $\psi_r$  = atomic  $2p_z$  wave function at carbon atom  $r$ ,  $(c_r^i)^2$  = weight with which  $\psi_r$  enters the  $i$ th m.o. These wave functions themselves must bear the symmetry characteristics of the sets of carbon atoms. Thus four types of wave functions can be written down, which we denote by  $S_z S_y$ ,  $S_z A_y$ ,  $A_z S_y$ ,  $A_z A_y$ , where for example  $S_z$  indicates symmetrical behaviour with respect to reflection in the plane through the  $z$  axis, perpendicular to the plane of the molecule, and  $A_z$  indicates antisymmetrical behaviour with respect to this reflection.

In terms of the effective Hamiltonian  $H(\nu)$  and the normalized m.o. wave functions  $\phi_i$  the energy of a m.o. level is determined by

$$\epsilon_i = \int \phi_i^*(\nu) H(\nu) \phi_i(\nu) d\tau_\nu / \int \phi_i^*(\nu) \phi_i(\nu) d\tau_\nu.$$

Minimizing the energy with respect to the coefficients  $c_r^i$  leads to the secular determinant. Because of the symmetry grouping, the secular determinant factorizes into blocks of these symmetry types called  $P, Q, R, S$  by Coulson. The m.o. energies which are derived as the roots of this determinant are therefore denoted by  $P_1 P_2 P_3, Q_1 Q_2, R_1 R_2 R_3, S_1 S_2$ . Coulson gives a diagram of energy levels which were calculated including the overlap integral of the  $2p_z$  atomic orbitals at adjacent carbon atoms. This diagram shows also relations between the energy groups  $P, Q, R, S$ , and both the symmetry character  $S_z S_y$  etc. and their standard group theory description.

$E_0$  is a Coulomb integral considered constant for all carbon atoms.

In the ground state it is assumed that the five lowest orbitals are each completely filled with  $\pi$ -electrons (each orbital then accommodates two  $\pi$ -electrons according to the Pauli principle); it therefore gives rise to a description  $P_1^2 Q_1^2 R_1^2 P_2^2 S_1^2$ .

Similarly the "first excited configuration"—or, more accurately, the configuration which from this diagram appears to be the first excited one and which arises from the elevation of one electron in m.o.  $S_1$  to the lowest unoccupied one,  $Q_2$ —can be described by  $P_1^2 Q_1^2 R_1^2 P_2^2 S_1 Q_2$ .

To determine the symmetry type to which such a configuration belongs one multiplies the symmetries of the electrons forming it; for the ground state having all m.o.'s doubly filled this gives a totally symmetric configuration. In the "first excited configuration" the symmetry is given by  $S_1 \times Q_2$ , i.e.  $A_z A_y \times S_z A_y$ , i.e.  $A_z$ . A complete table of symmetry types of products of two-electron symmetries is given in Coulson's paper in the more usual notation of group theory first introduced into molecular descriptions by Mulliken (1933).

		<i>Q</i>	<i>R</i>	
<i>P</i>	$A_{1g}$	$B_{1u}$	$B_{2u}$	$B_{3g}$
<i>Q</i>	$B_{1u}$	$A_{1g}$	$B_{3g}$	$B_{2u}$
<i>R</i>	$B_{2u}$	$B_{3g}$	$A_{1g}$	$B_{1u}$
<i>S</i>	$B_{3g}$	$B_{2u}$	$B_{1u}$	$A_{1g}$

An electronic transition from the ground state is spectrally allowed if the product of the electron symmetries in the excited state behaves like a  $y$  or  $z$  vector

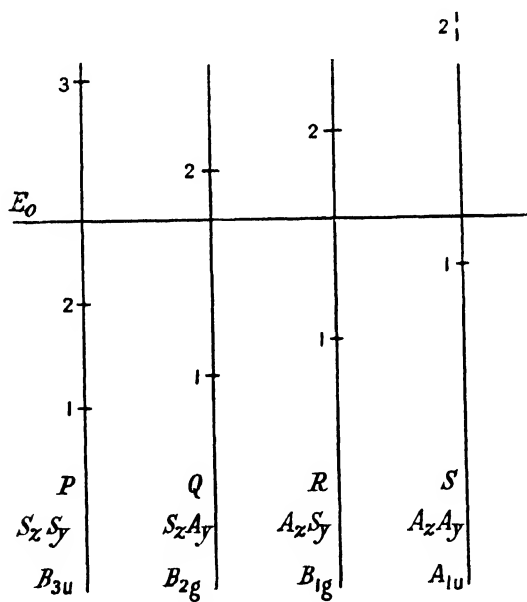


Figure 2.

(symmetry  $A_z$  or  $A_y$  respectively), the direction in which the electric moment vector changes during the excitation, which must be in the plane of the molecule. Above, we deduced  $\tilde{y}$  for the first transition; Coulson's results for higher transitions are given in Table 1 together with values for excitation energies.

Table 1. Naphthalene Energies (Coulson's Results)

Symmetry of excited configuration.	$B_{2u}$	$B_{1u}$	$B_{3g}$	$B_{1u}$	$A_{1g}$	$B_{2u}$	$A_{1g}$
Excitation energy in terms of $\gamma$	1.267	1.532	1.715	1.868	1.884	2.133	2.316
Polarization	$y$	$z$	F	$z$	F	$y$	F

F=forbidden.

In this Table  $\gamma$  is a resonance integral between neighbouring carbon atoms and has a value of 3.4 eV.

In all polyacenes the lowest transition appears to be of  $A_{1g} \rightarrow B_{2u}$  type, i.e. polarized in the  $y$  direction. This result is in direct contrast to valence bond calculations (Craig, in course of publication) which predict  $z$  polarization for the first allowed band in each case.

One limitation of this m.o. method is that no account is taken of electron spin so that the calculated energies of excited configurations are really averages of the corresponding energies for singlet and triplet configurations. The averaging of electron repulsion uniformly over the whole molecule is a further approximation that cannot be justified. Particularly for some excited levels the calculations give electronic charge distributions that are not at all even, so that the potential field for each electron is certainly not equivalent at all atoms of the carbon framework.

### § 3. EXPLICIT INTRODUCTION OF ELECTRON REPULSION

Our first step towards a refinement of this simple method is to include electronic repulsion explicitly in the Hamiltonian of the system with the m.o. wave functions obtained above as basis. This necessitates introducing antisymmetrized determinantal wave functions, as was done by Goeppert-Mayer and Sklar (1938) for benzene.

Let the normalized wave functions for the simple m.o. be  $\phi_i = \sum_r c_r^i \psi_r$ . Then the wave function for the configuration is, in the first approximation,  $\Psi_j = N \Pi_i \phi_i$ , where  $i$  is taken over occupied m.o.'s and  $N$  is a normalizing constant.

Instead of these, the wave functions of the type used by Goeppert-Mayer and Sklar for a configuration  $j$  of the molecule are

$$\Psi_j = N \begin{vmatrix} \phi_1(1)\alpha(1) & & & \\ & \phi_1(2)\beta(2) & & \\ & & \ddots & \\ & & & \phi_i(n)\beta(n) \end{vmatrix},$$

where  $n$  electrons occupy m.o.'s  $1, \dots, i$ .  $\alpha(1)$ ,  $\beta(1)$  define the spin function of electron 1 as  $\alpha$ ,  $\beta$  respectively, and  $N$  is a normalizing constant. This can be written in the form

$$\Psi_j = N \sum_P (-1)^P \Pi_i P \phi_i(\mu) \alpha(\mu) \phi_i(\nu) \beta(\nu),$$

where  $P$  is the permutation operator permuting electrons over all available  $\phi_i\alpha$ ,  $\phi_i\beta$  and  $\mu$ ,  $\nu$  represent electrons.

Including the term  $\sum_{\mu, \nu} e^2/r_{\mu\nu}$  ( $e$  = electronic charge,  $r_{\mu\nu}$  = distance between electrons  $\mu$ ,  $\nu$ ) in the Hamiltonian in their investigation of benzene, these authors obtain fair agreement with experiment. However, all integrals except those for nearest neighbours are neglected and three-or-more centre integrals are omitted altogether (some numerical errors also occur in their integrals (Griffing 1947, Parr and Crawford 1948)). London (1945) has carried out similar calculations for diphenyl and concludes that some of the three-centre integrals may be quite important; they would certainly destroy the good agreement with spectral data for benzene (but see Parr and Crawford). Goeppert-Mayer and Sklar (1938) treat configurations calculated with these antisymmetrized wave functions  $\Psi_j$  as giving the energies of the actual states of the molecule and compare the resulting energy



differences with those observed in the spectrum. The only interactions between configurations which they consider arise from the special degeneracies of benzene that have no parallel in the higher -acenes. However, we find this to be an inadequate description of the energies, and further interactions between some of the calculated configurations can arise in the following way.

#### § 4. CONFIGURATIONAL INTERACTION

Let the wave function  $\Psi_j$  define the electronic configuration  $j$  of the molecule; then the symmetry type of the configuration can be determined from the product of the symmetries of the m.o. wave functions  $\phi$  which form  $\Psi_j$ . Since several such configurations may belong to the same symmetry class (e.g. configurations in which the m.o.'s are each completely filled are all totally symmetric) the possibility of interaction between them must be conceded. Configurations belonging to different symmetry classes or of different multiplicity cannot interact with one another. Parr and Crawford (1948) find in their calculations for ethylene that the configuration in which both  $\pi$ -electrons are excited gives rise to considerable interaction with the lowest configuration, stabilizing it by about 1.3 ev.

This concept of configurational interaction finds confirmation in some recent work carried out in this laboratory on the hydrogen molecule (Coulson and Fischer 1949). For this molecule more accurate values can be obtained as fewer assumptions and approximations have to be made in energy computations. As for the  $\pi$ -electrons in ethylene, there are only two totally symmetric configurations. It is found that even at equilibrium internuclear distance some degree of mixing takes place, which increases for greater nuclear separations. Only after taking configurational interaction into account does the ground state appear as the lowest state of all, with the singly excited state falling below the doubly excited one for all internuclear separations.

The fact that configurational interaction exists indicates that the anti-symmetrized wave functions  $\Psi_j$  are not by themselves suitable for describing the molecule. If we consider a linear combination of  $\Psi_j$ 's including a sufficiently large number of terms we should approximate to the true wave function of a state (Longuet-Higgins 1948). Our procedure is therefore to carry out energy calculations using antisymmetrized wave functions and to obtain the excited configurations and their symmetries. We then allow configurational interaction to take place among the lower levels in the same symmetry class. This third step in the calculations we consider essential as it leads to a sequence of energy levels differing significantly from that obtained in stage two of our method. Only the lower levels in each symmetry class are considered for convenience in computation, although theoretically all levels in one class should be included.

#### § 5. METHOD AND RESULTS FOR NAPHTHALENE

The true Hamiltonian for the system of  $\pi$ -electrons is

$$\mathcal{H} = \sum_{\nu=1}^{10} H(\nu) + \sum_{\nu=1}^{10} T(\nu) + \sum_{\nu < \mu} \frac{e^2}{r_{\nu\mu}},$$

where  $T(\nu)$  is the kinetic energy term for electron  $\nu$  and  $H(\nu)$  is the potential energy of electron  $\nu$  in a field of molecular framework when each C atom is stripped

of its  $\pi$ -electron. This  $H(\nu)$  differs from that introduced in § 1 (first stage of m.o. theory): the earlier  $H(\nu)$  included a term arising from electronic averaging, not found in the present  $H(\nu)$ .

We take  $H(\nu) = \sum_{k=1}^{10} H_k(\nu)$  = a sum of contributions from each carbon atom  $k$  which has lost its  $\pi$ -electron. This may be written

$$H_k(\nu) = H_k^c(\nu) - e^2 \int \frac{|\psi_k^{(\lambda)}|^2}{r_{\nu\lambda}} d\tau_\lambda,$$

where  $H_k^c(\nu)$  is the field acting on electron  $\nu$  due to neutral carbon atom  $k$ . We further assume that the potential field around each carbon atom is the same (so that the form of  $H_k^c$  is independent of  $k$ )—an approximation here, but true in the case of benzene, where Goeppert-Mayer and Sklar introduced this substitution.

The wave function for the ground configuration is

$$\Psi_0 = (10!)^{-1} \sum_P (-1)^P P \phi_1(1) \alpha(1) \phi_1(2) \beta(2) \dots \phi_5(9) \alpha(9) \phi_5(10) \beta(10),$$

where  $P, \phi, \alpha, \beta$  are defined as above, and its energy is

$$\int \Psi_0^* \mathcal{H} \Psi_0 d\tau,$$

with corresponding expressions for other energies and with functions which are all real. It is found that all energy integrals can be given in terms of three series of expressions,  $\epsilon, \gamma, \delta$ , defined by

$\epsilon_i$  = energy of  $i$ th molecular orbital level

$$= \int \phi_i^*(\nu) [T(\nu) + H(\nu)] \phi_i(\nu) d\tau_\nu,$$

$$\gamma_{ll'} = \iint \phi_l^*(\nu) \phi_{l'}^*(\mu) \frac{e^2}{r_{\mu\nu}} \phi_l(\nu) \phi_{l'}(\mu) d\tau_\mu d\tau_\nu,$$

$$\delta_{ll'} = \iint \phi_l^*(\nu) \phi_{l'}^*(\mu) \frac{e^2}{r_{\mu\nu}} \phi_{l'}(\nu) \phi_l(\mu) d\tau_\mu d\tau_\nu.$$

Let us use  ${}^r E_n^{pq}$  to denote an energy level of multiplicity  $r$  for which  $n$  electrons have been raised and the m.o. levels concerned with the excitation are  $p \rightarrow q$ .  $n=0$  will represent the ground configuration,  $n=1$  singly excited configurations which alone are usually considered in m.o. calculations. But doubly excited configurations ( $n=2$ ) are also important as they have the symmetry of the ground state and so may give rise to configurational interaction with it. Using the simple diagram of Coulson's paper (Figure 2) and labelling the m.o. levels in order of magnitude, we expect the following excitations to be significant for low energy differences.

The relation between the notation in Figure 2 and the present enumeration of energy levels is:  $P_1, Q_1, R_1, P_2, S_1, Q_2, R_2$  are equal to 1, 2, 3, 4, 5, 6, 7 respectively;  $p \rightarrow q = 5 \rightarrow 6, 4 \rightarrow 6, 3 \rightarrow 6, 5 \rightarrow 7, 4 \rightarrow 7, \dots$  all of which have been evaluated below.

In terms of the molecular integrals  $\epsilon$ ,  $\gamma$ ,  $\delta$  the energies can be expressed as

$${}^1E_0 = 2(\epsilon_1 + \epsilon_2 + \epsilon_3 + \epsilon_4 + \epsilon_5) + (\gamma_{11} + \gamma_{22} + \gamma_{33} + \gamma_{44} + \gamma_{55}) \\ + 4(\gamma_{12} + \gamma_{13} + \gamma_{14} + \gamma_{15} + \gamma_{23} + \gamma_{24} + \gamma_{25} + \gamma_{34} + \gamma_{35} + \gamma_{45}) \\ - 2(\delta_{12} + \delta_{13} + \delta_{14} + \delta_{15} + \delta_{23} + \delta_{24} + \delta_{25} + \delta_{34} + \delta_{35} + \delta_{45}),$$

$${}^1E_1^{56} = 2(\epsilon_1 + \epsilon_2 + \epsilon_3 + \epsilon_4) + (\epsilon_5 + \epsilon_6) + (\gamma_{11} + \gamma_{22} + \gamma_{33} + \gamma_{44} + \gamma_{56}) \\ + 4(\gamma_{12} + \gamma_{13} + \gamma_{14} + \gamma_{23} + \gamma_{24} + \gamma_{34}) + 2(\gamma_{15} + \gamma_{16} + \gamma_{25} + \gamma_{26} \\ + \gamma_{35} + \gamma_{36} + \gamma_{45} + \gamma_{46}) + \delta_{56} - 2(\delta_{12} + \delta_{13} + \delta_{14} + \delta_{23} + \delta_{24} + \delta_{34}) \\ - (\delta_{15} + \delta_{16} + \delta_{25} + \delta_{26} + \delta_{35} + \delta_{36} + \delta_{45} + \delta_{46}),$$

$${}^1E_2^{56} = 2(\epsilon_1 + \epsilon_2 + \epsilon_3 + \epsilon_4 + \epsilon_6) + (\gamma_{11} + \gamma_{22} + \gamma_{33} + \gamma_{44} + \gamma_{66}) \\ + 4(\gamma_{12} + \gamma_{13} + \gamma_{14} + \gamma_{16} + \gamma_{23} + \gamma_{24} + \gamma_{26} + \gamma_{31} + \gamma_{36} + \gamma_{16}) \\ - 2(\delta_{12} + \delta_{13} + \delta_{14} + \delta_{16} + \delta_{23} + \delta_{24} + \delta_{26} + \delta_{34} + \delta_{36} + \delta_{46}).$$

Similar expressions for other energies are easily written down, and in particular for the singlet triplet separations one obtains, for example,

$${}^1E_1^{56} - {}^3E_1^{56} = 2\delta_{56}.$$

Changing now to integrals over atomic orbitals, we neglect three-or-more centre integrals and introduce the notation of Goeppert-Mayer and Sklar.

$$A = (rr, rr) = \int \psi_r(1)\psi_r(2) \frac{e^2}{r_{12}} \psi_r(1)\psi_r(2) d\tau,$$

$$B = (rr, ss) = \int \psi_r(1)\psi_s(2) \frac{e^2}{r_{12}} \psi_r(1)\psi_s(2) d\tau,$$

$$C = (rs, ss) = \int \psi_r(1)\psi_s(2) \frac{e^2}{r_{12}} \psi_s(1)\psi_s(2) d\tau,$$

$$D = (rs, rs) = \int \psi_r(1)\psi_r(2) \frac{e^2}{r_{12}} \psi_s(1)\psi_s(2) d\tau,$$

$$Q = (H_r^c, ss) = - \int \psi_s(1)H_r^c(1)\psi_s(1) d\tau,$$

$$R = (H_r^c, rs) = - \int \psi_r(1)H_r^c(1)\psi_s(1) d\tau.$$

Let  $W_{2p}$  = energy of a  $\pi$ -electron in a neutral carbon atom so that

$$[T(\nu) + H_j(\nu)]\psi_j(\nu) = W_{2p}\psi_j(\nu),$$

and let the molecular orbital wave functions  $\phi$  be expanded as

$$\phi_l = \sum_r c_r \psi_r, \quad \phi_{l'} = \sum_r d_r \psi_r,$$

in which  $\psi_r$  is the hydrogen-like  $2p_z$  orbital at carbon atom  $r$ , and  $(c_r)^2$ ,  $(d_r)^2$  are the weights with which it enters the m.o.'s  $\phi_l$ ,  $\phi_{l'}$  respectively. With this notation the following expressions are obtained:

$$\gamma_{ll'} = A \sum_r c_r^2 d_r^2 + \sum_r B_{rs} (c_r^2 d_s^2 + c_s^2 d_r^2) + 2 \sum_r C_{rs} (c_r d_s + c_s d_r) (c_r d_r + c_s d_s) + 4 \sum_r D_{rs} c_r c_s d_r d_s, \\ \delta_{ll'} = A \sum_r c_r^2 d_r^2 + 2 \sum_r B_{rs} c_r c_s d_r d_s + 2 \sum_r C_{rs} (c_r d_s + c_s d_r) (c_r d_r + c_s d_s) + \sum_r D_{rs} (c_r d_s + c_s d_r)^2, \\ \epsilon_l = W_{2p} - 2 \sum_r (R_{rs} + C_{rs}) c_r c_s - \sum_r (Q_{rs} + B_{rs}) (c_r^2 + c_s^2).$$

At this stage the following approximations and assumptions are made:

In the atomic  $2p\pi$  functions which are of the form  $r \sin \theta e^{-Zr/2}$  (in the usual notation) the screening constant  $Z$  is taken as 3.18 throughout. The C—C bond-length is taken as 1.39 Å. everywhere, an approximation allowing the naphthalene molecule to consist of two hexagons with the dimensions of benzene. In the evaluation of the integrals  $C$ ,  $D$ ,  $Q$ ,  $R$  only contributions from neighbouring atoms  $r$ ,  $s$  are taken into account, those for non-nearest neighbours being neglected, whereas integrals of type  $B$  (i.e. simple Coulomb terms for the atomic charge clouds on two distant atoms) are taken for all pairs of atoms as  $B$  decreases but slowly with distance between  $r$  and  $s$ . Corrected values for these integrals are used as given by Parr and Crawford (1948), with some extrapolation in type  $B$  integrals. Possible variations of the screening constant  $Z$  and the C—C distance

Table 2

(1)	(2)	(3)	(4)	(5)	(1)	(2)	(3)	(4)	(5)
		0.0	$^1A_{1g}$	Ground state	$^1E_1^{26}$	6.7876			
		0.9840	$^3B_{2u}$	$T$	$^1E_2^{56}$	6.8617			
		1.1015	$^3B_{1u}$	$T$			6.8683	$^1A_{1g}$	$F$
$^3E_1^{56}$	3.1687				$^1E_1^{56}$	6.9349			
		3.2219	$^3B_{2u}$	$T$	$^1E_1^{46}$	7.0614			
$^3E_1^{57}$	3.4648				$^1E_2^{57}$	7.1400			
		3.5210	$^3B_{1u}$	$T$	$^1E_1^{47}$	7.2582			
		3.5624	$^3A_{1g}$	$T$			7.2643	$^1B_{2u}$	$Y$
		3.6214	$^1B_{1u}$	$Z$	$^1E_1^{16}$	7.4488			
		3.6503	$^1B_{2u}$	$Y$	$^1E_1^{17}$	7.5898			
$^3E_1^{26}$	3.6660						7.9080	$^3B_{2u}$	$T$
$^3E_1^{47}$	3.7441						8.5309	$^3B_{1u}$	$T$
$^1E_0$	4.0657						8.6198	$^1A_{1g}$	$F$
$^3E_1^{46}$	4.5572				$^3E_1^{36}$	8.8152	8.8152	$^3B_{3g}$	$T$
$^3E_1^{16}$	4.9513				$^1E_1^{37}$	9.1620			
		4.9873	$^1A_{1g}$	$F$	$^1E_2^{46}$	9.6411			
$^3E_1^{17}$	5.2010						9.9329	$^1A_{1g}$	$F$
$^3E_1^{37}$	5.2936						10.6308	$^1B_{1u}$	$Z$
		5.3972	$^3A_{1g}$	$T$			10.8683	$^1B_{2u}$	$Y$
$^1E_1^{57}$	6.4304				$^1E_1^{36}$	12.3728	12.3728	$^1B_{3g}$	$F$
		6.6883	$^1B_{1u}$	$Z$			13.2497	$^1A_{1g}$	$F$

(1) Description of configuration; (2) Energy (ev.) of configuration: zero at  $-4.0657$ ;  
 (3) Energy (ev.) of state: interaction taken into account; (4) Symmetry; (5) Spectral activity.  $T$ , triplet;  $Z$ ,  $\pi$ -polarized;  $Y$ ,  $y$ -polarized;  $F$ , forbidden.

in excited states are neglected. In the wave functions overlap up to two C—C bond distances is included.

Using the wave functions  $\phi$  obtained by Coulson's method as basis for the antisymmetrized wave functions  $\Psi$ , we determine configurational energies which are recorded in column (2) of Table 2. Finally, resonance among configurations of the same symmetry is allowed for as described below, the results being shown in column (3).

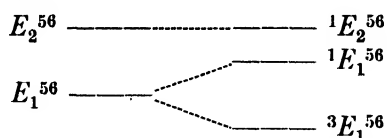
There are six configurations (which are shown in column (1)) of  $^1A_{1g}$  type whose wave functions can be denoted by  $\Psi_1, \Psi_2, \dots$ . To find the energies of the corresponding states of the molecule we take linear combinations of these,

$$\chi = \sum_{r=1}^6 c_r \Psi_r,$$

and minimize the energy calculated from the  $\chi$  with respect to the coefficients  $c_r$ . Such configurational interaction should in principle take place in any symmetry class for all configurations within it. We have here considered it for the six lowest configurations of  $^1A_{1g}$  symmetry and for the three lowest ones in each of the following classes respectively:  $^1B_{1u}$ ,  $^3B_{1u}$ ,  $^1B_{2u}$ ,  $^3B_{2u}$ ,  $^3A_{1g}$  (two levels only). ('Lower' or 'higher' means here as given by calculations of method (a), § 2.) In the  $^1A_{1g}$  configurations this resonance is most pronounced, and it therefore seemed best to include levels up to about 6 ev. above the ground one, assuming that the influence of any higher energies on the ground state would be negligible. In the remaining symmetry types we assume that interactions of the lowest three configurations in each case will suffice as an indication of the effect. But care must be taken to include a sufficient number of configurations in each symmetry group: the differences between taking two or three levels into consideration (in  $^1B_{1u}$  and  $^1B_{2u}$  classes) are considerable both as regards energy separations and calculated oscillator strengths. The values in column (3) must therefore not be taken as final, for inclusion of still higher levels will lower these energies a little further. In so far as these results are valid, therefore, the calculated energy levels must correspond to observed bands at somewhat lower energies.

#### § 6. DISCUSSION

The energy values in column (2) (i.e. of the separate configurations) differ from those found by Coulson both in magnitude and in the order in which they arise because of the corrected Hamiltonian that has included electronic repulsion explicitly. But this improved Hamiltonian leads to the unlikely result that it is energetically sometimes easier to raise two electrons than one, for the  $^1E_2^{56}$  level just precedes the level  $^1E_1^{56}$ . That levels like  $^1E_1^{56}$ ,  $^1E_2^{56}$  should fall fairly close is inherent in our procedure. We start with the simple (Coulson's) molecular orbitals which give levels  $E_1^{56}$ ,  $E_2^{56}$  well separated; we then combine the wave functions  $\phi$  with spin factors  $\alpha$ ,  $\beta$  which separate the singly excited level into a triplet and a singlet level as in the diagram, bringing  $^1E_1^{56}$  near to  $^1E_2^{56}$ , which itself is unaffected by spin.



Only at the third stage—resonance among configurations of the same symmetry—do we reach the final arrangement of states. This resonance is strongest among  $^1A_{1g}$  levels and is particularly effective in lowering the ground level (by about 4.1 ev.). Since spectral term values depend on energy differences with the ground state it is essential to perform calculations like those that lead to column (3) before a comparison with experiment can be attempted.

In Table 3 we give a list of weights ( $c_r^2$ ) to indicate the degree of mixing of configurations in the lowest two states of  $^1A_{1g}$ ,  $^1B_{1u}$ ,  $^1B_{2u}$  symmetry respectively. In this table configurational wave functions are listed in the order in which the corresponding levels occur on an energy scale (column (2), Table 2). The most important conclusion we reach is that this order is not always an indication of the importance of a level in its resonance effect. Judging by the  $^1A_{1g}$  results it is approximately true that the lowest configuration ( $^1E_0$ ) is most important in the

ground state, while the second and third configurations are the chief contributors to the first excited  ${}^1A_{1g}$  state. On the other hand, in  ${}^1B_{1u}$  and  ${}^1B_{2u}$  states the order of configurations is not even approximately in accord with the weights of the wave functions belonging to the final states.

Table 3  
Weights of Configurations in States

${}^1A_{1g}$ configurational wave function	$\Psi_0$	$\Psi_1^{26}$	$\Psi_2^{56}$	$\Psi_2^{57}$	$\Psi_1^{37}$	$\Psi_2^{46}$	
$c_r^2$ in ground state	0.668	0.087	0.017	0.063	0.155	0.009	
$c_r^2$ in 1st excited state	0.001	0.474	0.480	0.009	0.032	0.004	
${}^1B_{1u}$ configurational wave function	$\Psi_1^{57}$ $\Psi_1^{46}$ $\Psi_1^{16}$			${}^1B_{2u}$ configurational wave function $\Psi_1^{56}$ $\Psi_1^{17}$ $\Psi_1^{17}$			
$c_r^2$ in 1st state	0.133	0.499	0.368	$c_r^2$ in 1st state	0.096	0.485	0.419
$c_r^2$ in 2nd state	0.829	0.018	0.153	$c_r^2$ in 2nd state	0.899	0.031	0.070

Returning to Table 2 column (2), we observe that the ground level configuration does not appear as that of lowest energy, for several triplet configurations fall below it: apparently the triplets form a cluster of configurations preceding a group of singlet ones. This may arise in part from too wide a singlet-triplet separation met with in m.o. calculations; the placing of triplets relative to singlets is, however, considered less significant than the order of singlet states alone. It is, indeed, this sequence of states which is perhaps the most unexpected feature of our results. In Coulson's method the sequence of transitions to singlet levels is in the following order

$${}^1E_1^{56}(Y) \quad {}^1E_1^{46}(Z) \quad {}^1E_1^{36}(F) \quad {}^1E_1^{57}(Z) \quad {}^1E_1^{26}(F) \quad {}^1E_1^{47}(Y),$$

whereas now the first of all singlet levels is  $z$ -polarized, very closely followed by a  $y$ -polarized one. The next transition is again long-axis polarized. For comparison we quote the results of valence bond calculations obtained by Craig where the lowest transitions in terms of polarizations are (i) forbidden, (ii)  $z$ -polarized, (iii)  $y$ -polarized. Although this agrees with our determination that a  $z$ -polarized transition occurs energetically below a  $y$ -polarized one, the two predictions do not necessarily support one another. According to our present calculations the first two bands are so close that they could not be detected easily as two distinct bands in the spectrum. Our second  ${}^1B_{1u}$  state (i.e. the third allowed transition, again  $z$ -polarized) should be attributed to the second observed band. This new sequence of singlet levels then gives fairly satisfactory agreement with Kasha's experimental results (in course of publication). He interprets the spectrum of naphthalene as consisting of the 33,100  $\text{cm}^{-1}$  weakly allowed transition preceded by a separate forbidden one at 31,060  $\text{cm}^{-1}$ . These are followed (in order of increasing excitation energy) by the strongly allowed 45,000  $\text{cm}^{-1}$  band; a further weakly allowed band appears at 52,500  $\text{cm}^{-1}$ . Numerically our results for the lowest allowed transition agree fairly closely with the observed values, experiment giving about 4 e.v. while we calculate 3.6 e.v. Energy values for higher excited states are less reliable but should be attributed to bands at energies rather lower than the calculated ones. The uncertainty about the lowest forbidden transition persists, however; several triplet states

fall immediately below our lowest allowed band, whereas the first excited  $^1A_{1g}$  state (to which such a forbidden transition might well have been attributed) occurs 1.4 ev. above the first allowed transition.

A further test of the value of our present extension of the simple molecular orbital treatment is afforded by a comparison of observed and computed oscillator strengths. The intensity of absorption depends on the transition moment  $Q$  associated with that transition, and Mulliken's (Mulliken and Rieke 1941) theoretical formula for determining oscillator strengths is used:

$$f_{\text{theor.}} = 1.085 \times 10^{11} \nu Q^2,$$

where  $\nu$  is the frequency of absorption in  $\text{cm}^{-1}$ ,  $Q$  is in cm. The transition moment  $Q$  is calculated from the integral

$$Q = \int \chi_l^* (\Sigma \mathbf{r}) \chi_k d\tau.$$

Here  $\mathbf{r}$  is the displacement vector of the electron;  $\chi_l, \chi_k$  are the wave functions of the states  $l, k$  between which the excitation takes place.

A comparison with experimental values is given below.

Table 4. Oscillator Strengths

$f_{\text{obs.}}$	0.18	1.7	0.20?	$f_{\text{theor.}} (a)$	0.52 (y)	1.109 (z)	1.306 (z)	
$\nu_{\text{obs.}} \times 10^{-3} \text{ (cm}^{-1}\text{)}$	33	45	52	$\nu_{\text{theor.}} \times 10^{-3} \text{ (cm}^{-1}\text{)}$	29	30	54	59
				$f_{\text{theor.}} (c)$	0.22 (z)	0.36 (y)	1.49 (z)	0.033 (y)

In this Table (a), (c) refer to the first and last of the three stages of m.o. theory described in § 2, so that  $f(a)$  is calculated from the simple m.o. wave functions  $\phi$  using frequencies of the observed spectrum, while  $f(c)$  is determined from wave functions  $\chi$  belonging to the states of the molecule with frequencies corresponding to calculated energy separations.

These new oscillator strengths represent some improvement over those of the simple form of m.o. theory. Although in the m.o. method the calculations for higher states are less reliable than for lower excited states, the new  $f$  values do reproduce the great difference in intensities of the 33,000, 45,000, 52,000  $\text{cm}^{-1}$  bands in the naphthalene spectrum.

A further interpretation emerges from the calculated oscillator strengths  $f(c)$ ; the 33,000  $\text{cm}^{-1}$  band might be attributed to a  $z$ - and a  $y$ -polarized transition nearly overlapping one another. This conclusion differs from results of both the simple m.o. theory and of valence bond theory, but it is not altogether in disagreement with experiment. In 1944 Prikhotko measured the absorption spectrum of naphthalene crystals at low temperatures in polarized light and found both  $z$ - and  $y$ -polarized lines present in the region 29,000–33,000  $\text{cm}^{-1}$ . Nor does a vibrational analysis of this spectral region exclude the possibility of two distinct sequences of lines which might belong to two separate electronic transitions. This dual character in the vibrational lines persists even on substitution by methyl groups.

To summarize: we consider the value of the present investigations to be two-fold. Firstly, they show how unreliable the results of the simple m.o. method are when applied to problems involving excited states; at the same time they

point the way to an improvement which lies in taking electronic interaction into account explicitly together with configurational interaction. However, the calculations become rather long and the new method is probably too laborious to be of use for more complicated molecules. Secondly, in so far as these new calculations have a physical meaning, they suggest a new interpretation of the ultra-violet spectrum of naphthalene. The 'first' allowed observed band may consist of two bands of different polarity almost coinciding with one another. The 'second' strong band (having its peak around  $45,000\text{ cm}^{-1}$ ) is then to be correlated with the next  $\pi$ -polarized transition. The polarity of this band thus agrees with the results of the simple m.o. method, but it is now attributed to the next higher state of that symmetry. For the lowest forbidden transition the symmetry remains uncertain from these calculations.

#### ACKNOWLEDGMENTS

The writer wishes to thank Prof. C. A. Coulson for suggesting this problem and for the great interest he has taken in this work, and Dr. D. P. Craig for many helpful discussions. A grant from the Department of Scientific and Industrial Research, which enabled this work to be carried out, is also acknowledged.

#### REFERENCES

- COULSON, C. A., 1948, *Proc. Phys. Soc.*, **60**, 257.  
 COULSON, C. A., and FISCHER, I., 1949, *Phil. Mag.*, **40**, 386.  
 GOEPPERT-MAYER, M., and SKLAR, A. L., 1938, *J. Chem. Phys.*, **6**, 645.  
 GRIFFING, V., 1947, *J. Chem. Phys.*, **15**, 421.  
 LENNARD-JONES, J. E., and COULSON, C. A., 1939, *T.F.S.*, **35**, 811.  
 LONDON, A., 1945, *J. Chem. Phys.*, **13**, 396.  
 LONGUET-HIGGINS, H. C., 1948, *Proc. Phys. Soc.*, **60**, 270.  
 MULLIKEN, R. S., 1933, *Phys. Rev.*, **43**, 279.  
 MULLIKEN, R. S., and RIEKE, C. A., 1941, *Rep. Prog. Phys.*, **8**, 231 (London: Physical Society.)  
 PARR, R. G., and CRAWFORD, B. L., 1948, *J. Chem. Phys.*, **16**, 526.  
 PRIKHOTKO, A., 1944, *J. Phys. U.S.S.R.*, **8**, 257.



## A New Technique for the Spectroscopic Examination of Flames at Normal Pressures

By H. G. WOLFARD AND W. G. PARKER

Royal Aircraft Establishment, Farnborough

*MS. received 7th June 1949; read on 11th March 1949*

**ABSTRACT.** Up to the present spectroscopic studies of flames supported on a tube have been limited by the geometry of the flame. Thus the important reaction zone presents a three-dimensional problem in which it is impossible to locate the emitters exactly. Moreover this zone is so thin in premixed gas flames that intermediate products cannot be determined from absorption studies. To overcome these difficulties the authors have constructed a burner with a two-dimensional diffusion flame in which the reaction zone at ordinary pressures is 5–10 mm. thick and has an optical depth of 5 cm. or more. With this flame many of the reacting molecules can be located through either their emission or absorption spectra or both. The value of the new technique in the elucidation of combustion processes is demonstrated with reference to  $\text{NH}_3\text{-O}_2$  and  $\text{H}_2\text{-O}_2$  flames, and mention is made of its application to hydrocarbon flames.

### § 1. INTRODUCTION

THE application of spectroscopy to combustion has been widely practised and has provided much of the existing evidence on the subject. It is well known, however, that there are a number of serious limitations in the methods employed, particularly from the structure of the flame. In a Bunsen flame for example, the most interesting reactions occur in the narrow inner cone and not in the large volume of interconal gas above it. The thickness of the inner cone, however, is usually less than 0.1 mm. and it is extremely difficult to study the detail. Moreover, it presents a three-dimensional problem in which it is virtually impossible to decide on the precise location of the emitters. The optical depth of the inner cone is insufficient for absorption studies and this too is a great drawback because absorption spectra can give quantitative as well as qualitative information on the molecules and atoms involved. Spectroscopic evidence is thus limited to overall observations such as the emission of  $\text{C}_2$  and CH bands in the inner cone of hydrocarbon flames or to the emission and absorption of OH radicals in the interconal gases.

Some of these difficulties have been partially overcome by Gaydon and Wolfhard (1948) who used premixed flat flames. Normally a premixed gas flame will strike back when the mass flow is reduced below a critical value and this occurs before the cone has flattened out. Under carefully controlled conditions, with small gas flows which approached the limiting value for self propagation, Wolfhard (1943) found it possible to obtain a flat flame above the burner at any pressure. At 1 atmosphere, however, these flames are very small and require a burner of about 1 mm. diameter. At low pressures (2–20 mm. Hg) the burner diameter may be increased to about 50 mm. and the reaction zone has a thickness of more than 10 mm. depending on the mixture strength. Emission spectra can be observed in different parts of the flame and thus the relative positions of the various emitters may be obtained. At reduced pressures the flat flames are too thin optically for absorption work and it has only been possible to detect OH radicals in absorption using very high resolving power.

Egerton and Powling (1948) have recently developed a large flat premixed gas flame at atmospheric pressure by having a uniform gas flow across the burner, thereby eliminating the usual parabolic velocity distribution which leads to conical flames. The inner cone of the flame is normally very thin but widens for very slow and rich flames. The method is very promising especially for the detection of radicals in the zones before and after the main reaction.

Apart from the last example it may be said that neither premixed gas nor diffusion flames examined hitherto allow full use of absorption spectroscopy. The primary requirements for this are a broad reaction zone with good optical depth for absorption work. These requirements have been met at normal pressure in a diffusion flame of unusual design which is described in this paper.

It should perhaps be pointed out that the chemical reactions in diffusion flames may be different from those in a premixed gas flame. Nevertheless an attempt to understand these reactions is fully justified by the great technical importance of diffusion flames. Apart from calculations on the height and shape of such flames by Burke and Schumann (1928) little fundamental work has been done hitherto.

## §2. DESCRIPTION OF NEW TECHNIQUE

Diffusion flames burning with oxygen have a reaction zone up to 1 cm. in thickness depending on the height of the flame. This zone can be obtained in a more convenient form by using a flat burner in lieu of the usual cylindrical pipe.

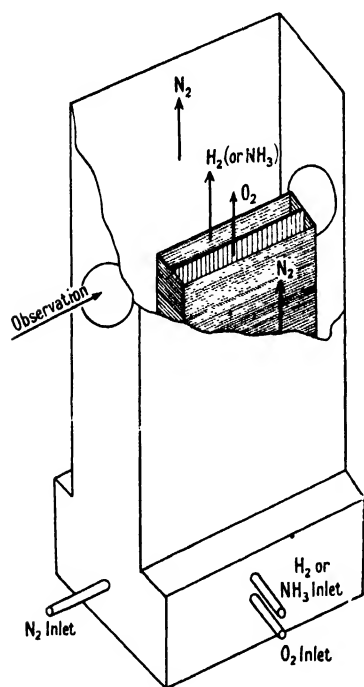


Figure 1. Burner.

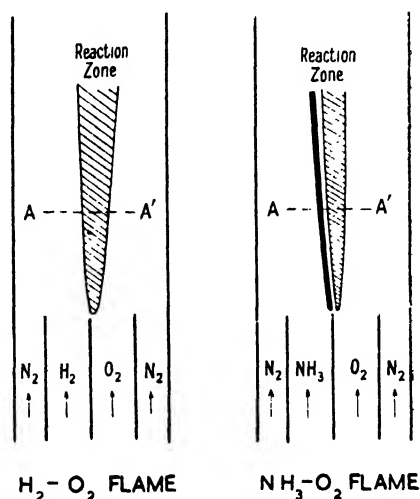


Figure 2. End view of flame.  
Spectroscopic examination made across the reaction zone at A-A'.

Figure 1 shows the design of the burner. The fuel gas and oxygen issue with equal velocities of about 20 cm/sec. from parallel rectangular tubes (5 cm.  $\times$  0.7 cm.) which have one long side in common. The gases rise vertically and diffuse into each other in a laminar flow on account of the low Reynolds number.

On ignition burning takes place at the interface and a flat diffusion flame is obtained which presents a two-dimensional problem, rather similar to the premixed flat flames described in §1. The flame front is kept very steady by stabilizing it with a surrounding stream of nitrogen which flows up the outer jacket. The optical depth of the flame is the length of the interface and is arbitrarily fixed by the burner dimensions; in the investigation described here it was 5 cm. This depth at ordinary pressure is sufficient for absorption studies. Quartz windows are suitably sited in the outer jacket.

This burner has not been used so far for a detailed study of combustion problems, but an assessment of its potential usefulness has been made by finding out what bands can be detected in absorption and emission and the location of these bands in the reaction zone.

Combustion occurs where the fuel and oxygen are in contact at the interface. Figure 2 shows an end view of a  $\text{H}_2\text{-O}_2$  and an  $\text{NH}_3\text{-O}_2$  flame. The reaction zone is thin at first but broadens higher up the flame. The combustion products, viz.  $\text{H}_2\text{O}$  or  $\text{H}_2\text{O}$  and  $\text{N}_2$ , etc., are formed in the reaction zone and diffuse outwards on both sides whereas the oxygen and the hydrogen (or ammonia) diffuse towards the reaction zone and maintain combustion. The reaction zone of the hydrogen flame emits in the visible region a fairly uniform blue continuum similar to that experienced with a premixed  $\text{H}_2\text{-O}_2$  flame, whereas the reaction zone of the  $\text{NH}_3\text{-O}_2$  flame is clearly divided into two parts. On the ammonia side a narrow plane of yellow radiation can be seen, which is due to the ammonia  $\alpha$ -bands; moving across the flame towards the right this is followed by a dark space and then by a fairly thick plane of blue continuum on the oxygen side. The flames are not exactly vertical even when the velocities of both gases are equal, because the diffusion rates of the fuel and oxygen are different. The position of the gas interface in the burner has therefore no relation to any point in the reaction zone above the burner.

A spectroscopic study in emission was made by projecting an image of the end view of the flame (12 mm. above the burner and corresponding to the line AA' in Figure 2), on to the slit of a spectrograph by means of a quartz-fluorite achromatic lens, the aperture being chosen so that the different layers in the flame did not overlap appreciably. For absorption work an image of a carbon arc or a hydrogen discharge lamp was focused on to the flame. This image and the flame were then focused on the slit of the spectrograph. Since the most information about the reactants would be derived in the horizontal direction AA' across the interface and not in a vertical direction parallel to the interface, the images on the spectrograph were made to fall across the slit either by the use of a  $90^\circ$  quartz prism or by putting the spectrograph on its side. Two hairs were placed across the image of the flame on the slit, and cast line shadows over the whole wavelength region of the spectra. These lines served to locate the source of the bands in the flame. A Hilger medium quartz spectrograph was used for most of the investigation.

### §3. THE HYDROGEN-OXYGEN FLAME

The use of a  $\text{H}_2\text{-O}_2$  flame in this assessment is limited because hydrogen cannot be detected in absorption with a quartz spectrograph. The reaction is less complicated than the hydrocarbon reaction, or even the ammonia flame, and it seemed a simple application for the new technique. The results are shown

graphically in Figure 3. The hydrogen diffuses from the left and the oxygen from the right. The abscissa represents the horizontal distance (in millimetres) in the flame 12 mm. above the burner mouth. The ordinate on the right is a rough qualitative measure of the strength of the bands estimated from the negatives. No attempt has yet been made to measure the intensities accurately for calculating the absolute concentration of the molecules. The absorption bands of the OH radical extend over approximately 9 mm. and the emission bands are symmetrically located over the greater part of this distance. The ordinate on the left is a temperature scale. Temperature measurements in the reaction zone were made by the Na line-reversal method. A thin wire coated with sodium chloride was inserted into the flame below the point of measurement. This coloured only the small and relevant part of the flame and eliminated risk of self-reversal. The anode of a carbon arc was used as light source together with a rotating sector to reduce the effective temperature. The results are shown by the top line of

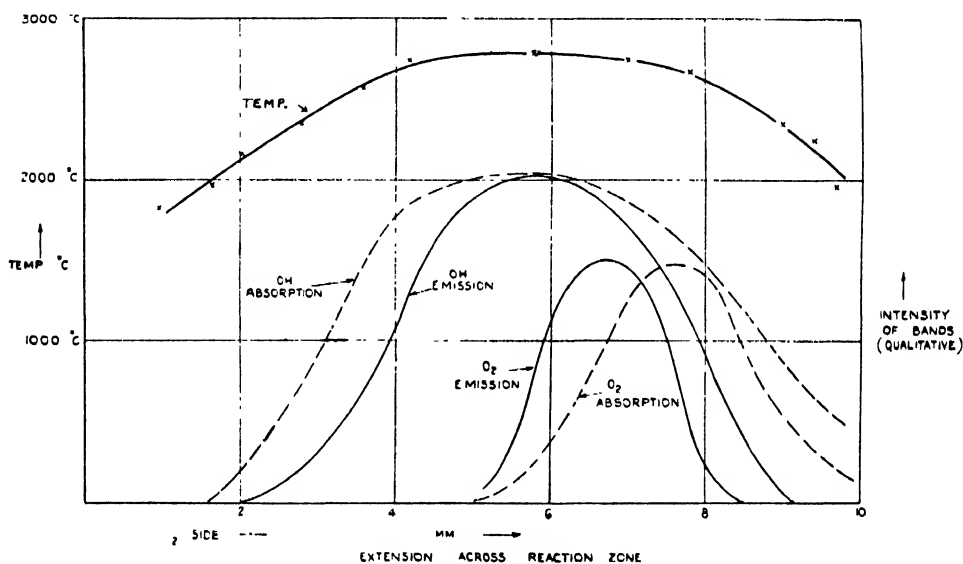


Figure 3.  $\text{H}_2\text{-O}_2$  flat diffusion flame.

Figure 3. The temperature attained a rather flat maximum at  $2,800^\circ\text{C}$ . This agrees very closely with the calculated value for a stoichiometric mixture of  $\text{H}_2$  and  $\text{O}_2$ , allowing for dissociation but not for external heat losses. It appears therefore that diffusion flames are quite as hot as premixed flames.

Comparing the temperature and OH measurements, the latter cease in emission at about  $2,100^\circ\text{C}$ . (though this depends to some extent on the sensitivity of the measurements). The OH absorption extends slightly further on both sides. By using the OH bands for temperature measurements by reversal, instead of the Na lines, the values obtained agreed within the limits of error with the sodium reversal temperature, and proved that in the  $\text{H}_2\text{-O}_2$  diffusion flame the electronic excitation of molecules and atoms is thermal even in the reaction zone. This is believed to be the case in the premixed flame of  $\text{H}_2\text{-O}_2$  also but certainly not in premixed flames of hydrocarbons with oxygen.

Oxygen is normally transparent in the ultra-violet, but hot oxygen absorbs because higher vibrational levels are excited which permit a transition to the upper electronic state above  $2,000\text{ \AA}$ . At  $1,000^\circ\text{C}$  the absorption has already

spread to 2400 Å. and is readily observed. The spectrum contains a vast number of lines which do not form definite heads, and a satisfactory analysis has not been achieved up to the present. The existence of these lines however provides a means of detecting the oxygen in the flame. On the outside of the flame where the temperature is only moderate the absorption by oxygen is a complicated function of the temperature, but in the reaction zone where the temperature is above 2,000° C. the absorption must give at least a qualitative indication as to where the  $O_2$  is used up. These results for the  $H_2-O_2$  flame are also shown in Figure 3. Just beyond the point of maximum temperature the  $O_2$  concentration had fallen to a value where absorption could no longer be detected.

The height of these excited vibrational levels is interesting. The  $O_2$  absorption bands in the flame can be followed up to about 2600 Å. This corresponds to a vibrational energy of about 33 kcal. The reaction  $H + O_2 \rightarrow OH + O$  which can be regarded as an important step in the  $H_2-O_2$  reaction is normally endothermic (16 kcal.), but if this high vibrational energy of the  $O_2$  is available it may be exothermic. At least one metastable  $O_2$  level ( ${}^1\Delta_g$ ) is lower than 33 kcal. and may therefore be partially excited and play an important role in combustion. It seems to be a characteristic of the diffusion flame that the reactants only meet after they have nearly reached the theoretical flame temperature in contrast to the premixed flames where they are continuously in contact and begin to react at the ignition point (800–1,000° C.). The oxygen molecules emit as well as absorb, and the emission is shifted towards higher temperature compared with the absorption. Figure 4 (see Plate) shows an actual spectrum which gives in emission the (0,1) OH band, and the (0,14) and (0,15)  $O_2$  bands. It is noticeable that both  $O_2$  bands and OH bands do not occur at the same position in the flame. The existence of the Schumann-Runge  $O_2$  bands in emission in the flame was rather unexpected since it is very difficult to obtain them in a discharge tube because the potential energy curves of the excited and unexcited states are relatively displaced. In a diffusion flame where the  $O_2$  has high vibrational levels in the ground state it is easier to excite the upper state in accordance with the Frank-Condon principle.

The  $HO_2$  radical could not be detected either in absorption or in emission. The radical is supposed to play an important part in combustion and Minkoff (1947) has calculated that its spectrum should lie around 2900 Å. It has not been reported so far.

In some reaction schemes  $H_2O_2$  has been suggested as an intermediate product and Egerton and Minkoff (1947) found appreciable amounts in an  $H_2-O_2$  flame at low pressure.  $H_2O_2$  has a continuous absorption which is not very strong in the quartz ultra-violet and does not make a very sensitive test. Since no continuum was detected down to 2100 Å., however, it may be said that the  $H_2O_2$  concentration was less than 0.2% of the total pressure.

By a similar reasoning the partial pressure of ozone must be smaller than 0.006% since ozone absorbs quite strongly near 2500 Å., but this continuum was not observed.

#### §4. THE AMMONIA-OXYGEN FLAME

The experimental arrangement for the ammonia flame was in every way similar to that of the  $H_2-O_2$  flame. The ammonia system has an advantage over hydrogen in that the fuel can be observed in absorption. At room temperature  $NH_3$  begins to absorb at 2254 Å. and after a few diffuse bands the absorption becomes a continuum towards the vacuum ultra-violet. The effect of temperature

on this absorption was studied separately in a quartz cell 5 cm. long which was filled with ammonia gas and inserted in a furnace. The length of the optical path was thus similar to that of the flame. As the temperature was raised new band heads appeared and at 1,000°c. these bands had spread up to 2440 Å., the whole absorption becoming more continuous in appearance. Figure 5 (see Plate) shows how the absorption by ammonia in the cell varied with temperatures between 20°c. and 800°c., and Figure 6 shows the ammonia absorption observed in the flat diffusion flame. As the ammonia approaches the reaction zone the bands near 2200 Å. become stronger and later continuous, then they suddenly cease. Figure 7 shows again in graphical form the results for the  $\text{NH}_3\text{-O}_2$  flame of all the absorption and emission spectra observed in a horizontal traverse of the flame 12 mm. above the burner mouth. The height of the curves is again only a qualitative indication of the strength of the bands. The ammonia diffuses

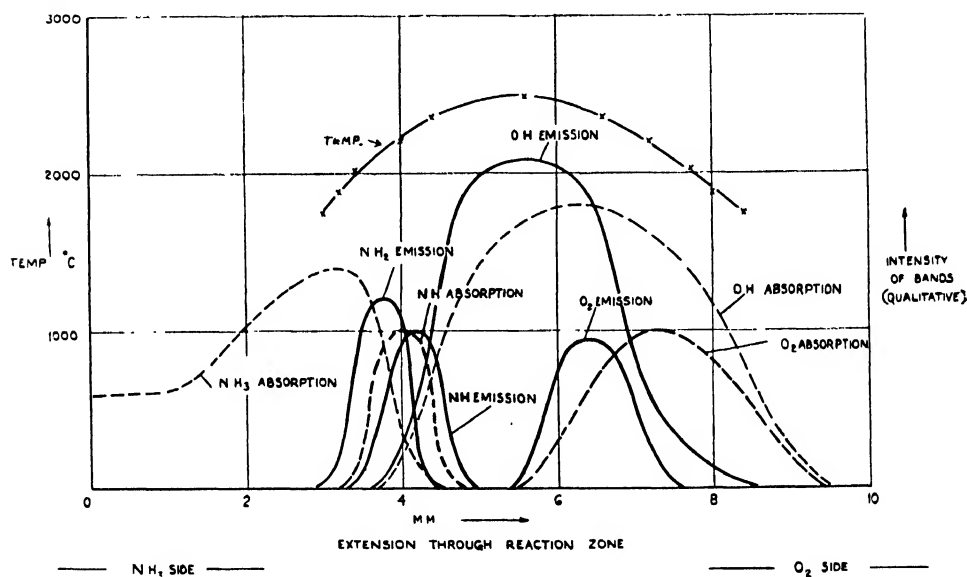


Figure 7.  $\text{NH}_3\text{-O}_2$  flat diffusion flame.

from left to right and the oxygen in the opposite direction. The ammonia is apparently unaffected until about the 1.0 mm. point on the abscissa then the bands increase in strength due to the increasing temperatures and reach a maximum at 3.2 mm. At 4.8 mm. the  $\text{NH}_3$  disappears completely. At the point of maximum decline in the  $\text{NH}_3$  absorption, however, the ammonia  $\alpha$ -bands appear in emission and these bands are usually attributed to  $\text{NH}_2$  radicals. The maximum of these bands is at 3.8 mm. At 4.0 mm. the maximum of the NH bands appears in absorption and the emission bands of this are strongest at 4.2 mm., the shift being due to the higher temperature in this direction. In this way the whole course of the dehydrogenation of the  $\text{NH}_3$  in the flame can be followed.

NH has been detected in absorption by Frank and Reichard (1936) who decomposed pure  $\text{NH}_3$  at 2,000°c.  $\text{NH}_2$  could not be found in absorption possibly because of the small dispersion of the quartz spectrograph in the visible region, and possibly also the multi-line nature of the band renders it difficult to find it in absorption. These bands are discussed again later. The NH band at 3360 Å. is much easier to find because the Q branch forms a strong head and the band looks like a strong line.

O<sub>2</sub> was again detected in absorption and spreads from the right (Figure 7) up to 5.4 mm. Since the ammonia spreading from the left has completely disappeared at 4.8 mm. (see above) it appears that the ammonia and oxygen never come in contact and the whole reaction goes via the intermediate products. The relevant positions of the two bands can be seen in Figure 6.

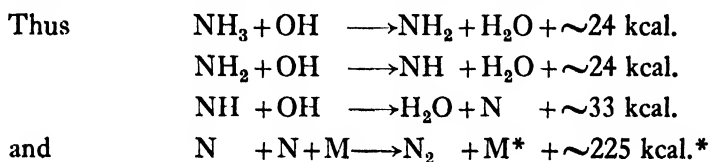
O<sub>2</sub> in emission is again displaced relative to the absorption on account of the temperature gradient in the flame.

OII is the most prominent feature in the spectra, either emission or absorption. It commences near 3.6 mm. and goes far over to the oxygen side (Figure 7).

The temperature of the ammonia flame is plotted in Figure 7 (with reference to the ordinate on the left) from sodium line-reversal measurements. The maximum temperature was found to be very close to the theoretical temperature for a stoichiometric mixture. The fall on either side of the maximum is similar. OH reversal temperature measurements agreed with the Na line results and it was again concluded that the electronic excitation of the OH and Na is purely thermal in the NH<sub>3</sub>-O<sub>2</sub> flame as in the H<sub>2</sub>-O<sub>2</sub> diffusion flame. Even the NH bands may be used to obtain the reversal temperature in the position where they appear and the measurement made with them was 2,200° c. at 4.1 mm. (Figure 7) in agreement with the other values. Figure 8 shows the position of the NH band compared with OH on the plate.

Returning to the problem of the NH<sub>2</sub> bands, the following rather sensitive test was applied. The NH<sub>2</sub> radiation is the only strongly visible radiation and occurs in a narrow vertical plane less than 1 mm. thick; by holding a piece of white paper across the end of the flame and looking at the outside of the paper one should see an equally illuminated field except directly opposite the extension of the luminous plane. Here if absorption is appreciable a vertical shadow will occur on the paper. No such shadow was obtained however. This supports the view that the stationary concentration of NH<sub>2</sub> radicals is very small and that the NH<sub>2</sub> decompose very quickly. The strength of the emission is not exceptional in view of the fact that the temperature at that point is about 2,100° c.

Several additional facts can be gleaned from the analysis. For example, the strongest visible radiation comes from a point some distance from the position of maximum temperature where the reaction rate is highest. Also on the ammonia side the OH in absorption ceases at about 2,100° c., whereas on the O<sub>2</sub> side it is still very strong at that temperature. This may be due to the lower partial pressure of OH in water vapour than in the H<sub>2</sub>O-O<sub>2</sub> mixtures, but it is rather striking that the OH ceases just where the NH<sub>3</sub> dehydrogenation begins. It may be an important dehydrogenation process, though it is unlikely to be the only one, otherwise the temperature distribution in the flame should be somewhat different. This may be shown by assuming that the OH does all the dehydrogenation since it is more exothermic in reaction with NH<sub>3</sub>, NH<sub>2</sub> and NH than the H or O atoms.



\* The symbols M and M\* are the usual convention for denoting collision with a third body to take away energy of recombination  $\text{N} + \text{N}$ .



Figure 4.

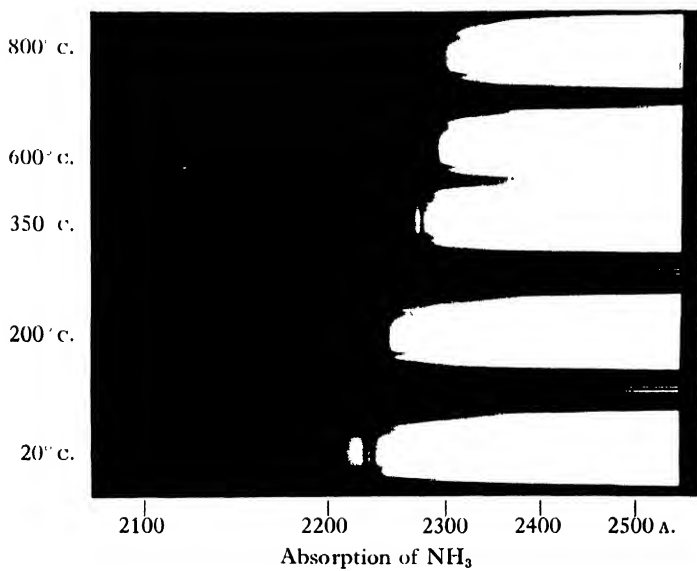


Figure 5.

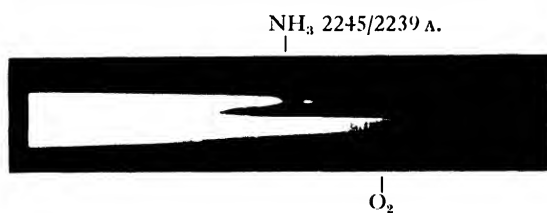


Figure 6.

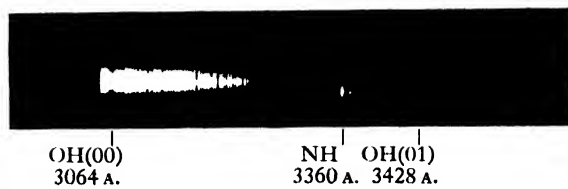


Figure 8.





Hence a very big release of energy would occur at the point of dehydrogenation which does not accord with the temperature plot of the flame. It seems more likely that the product of dehydrogenation is mostly  $\text{H}_2$  and not  $\text{H}_2\text{O}$  and that the  $\text{H}_2$  is subsequently burnt with oxygen and provides the greatest heat release of the reaction at about 5.6 mm. (Figure 7).

A fuller investigation could be made with this technique and more quantitative data obtained from the band strengths would greatly help in completely elucidating the reaction mechanisms.

### § 5. HYDROCARBON FLAMES

Although no extensive work has yet been done with hydrocarbon flames, a few preliminary tests with methane-oxygen flames in this burner are worth recording. On the  $\text{CH}_4$  side of the burner there was a narrow plane of strong luminosity due to radiant soot particles and on the  $\text{O}_2$  side a weak blue continuum which was probably due to recombination of electrons and ions. These two vertical planes, visible to the naked eye, were apparently separated by a thin dark space. Figure 9 gives some of the results graphically represented as before.

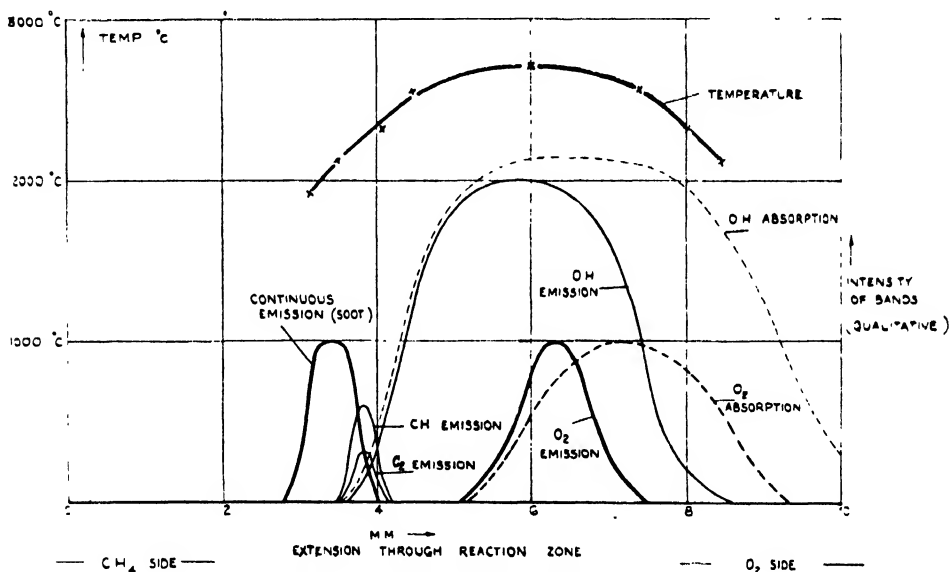


Figure 9.  $\text{CH}_4$ - $\text{O}_2$  flat diffusion flame.

The  $\text{CH}_4$  diffuses from the left and the  $\text{O}_2$  from the right; the distances in the flame are marked in millimetres on the abscissa. The visible continuous radiation (from carbon particles) extends from 2.8 to 4.0 mm. and the OH in absorption and emission just reaches the carbon region. The OH bands are again much stronger on the  $\text{O}_2$  side than at the corresponding temperatures on the  $\text{CH}_4$  side. The maximum temperature (by Na line-reversal method) is close to the theoretical. It is also interesting to note that  $\text{O}_2$  does not reach the luminous zone and the carbon particles cannot therefore burn in oxygen but probably react with OH or  $\text{H}_2\text{O}$ . The region of greatest heat release is at 6.0 mm. and it seems very probable that this is due to combustion of  $\text{H}_2$ - $\text{O}_2$  and perhaps  $\text{CO}$ - $\text{O}_2$ .

The information which this preliminary work gives relevant to carbon formation may be indicated; a discussion of this complex phenomenon will be presented

elsewhere. It is commonly supposed that carbon particles in the flame are formed by condensation of  $C_2$  molecules or even C atoms which are sometimes observed in emission from premixed flames. This theory is quite untenable for the type of flame examined here because the  $C_2$  is not observed prior to the zone of carbon particles, i.e. on the fuel side of the luminous zone (Figure 9). Rather weak  $C_2$  bands occur together with CH bands on the oxygen side of the zone.

#### §6. CONCLUDING REMARKS

It is hoped that sufficient evidence has been presented to show the potential value of the flat flame technique in the application of spectroscopy to diffusion flames. Very full information can be obtained in this way with fuels which absorb light. For the study of hydrocarbon flames other than aromatic flames it may be necessary to use the near vacuum ultra-violet region, but this does not present very great difficulties. Nitrogenous fuels and many other combustible inorganic compounds such as compounds of sulphur can be very fully examined. The behaviour of fuel additives can be investigated and so also can the action of any promoters or inhibitors which give absorption spectra. The problem of carbon formation has already been mentioned and the technique of the flat diffusion flame is at present being used in this connection by the authors.

#### ACKNOWLEDGMENT

The authors are indebted to the Chief Scientist, Ministry of Supply, and to the Controller, H.M. Stationery Office, for permission to publish this communication.

#### REFERENCES

- BURKE, S. P., and SCHUMANN, T. E. W., 1928, *Industr. Engng. Chem.*, **20**, 998.  
EGERTON, A. C., and MINKOFF, G. T., 1947, *Proc. Roy. Soc. A*, **191**, 185.  
EGERTON, A. C., and POWLING, T., 1948, *Colloquium on Combustion* (Paris).  
FRANK, H. H., and REICHARD, H., 1936, *Naturwissenschaften*, **24**, 171.  
GAYDON, A. G., and WOLFHARD, H. G., 1948, *Proc. Roy. Soc. A*, **194**, 169.  
MINKOFF, G. T., 1947, *The Labile Molecule*, Discussion of the Faraday Society, No. 2, p. 151.  
WOLFHARD, H. G., 1943, *Z. techn. Phys.*, **24**, 206.

## Dielectric Changes in Phosphors containing more than One Activator

By G. F. J. GARLICK AND A. F. GIBSON \*

Physics Department, The University, Birmingham

*MS. received 18th May 1949*

**ABSTRACT.** It is well known that some luminescent materials, notably zinc sulphide, show marked changes in dielectric constant and dielectric loss when excited. Recent work by the authors has established that the changes are due to the filling of electron traps, which have large effective diameter and high polarizability.

The present paper describes measurements of the dielectric changes in phosphors containing two or more luminescence activators. Assuming that the dielectric changes are due to electron trapping, it is possible to derive information regarding the nature of electron traps and in particular their apparent association with the luminescence centres. The results support the contention that the introduction of the activating impurity into phosphors produces trapping states for excited electrons and that each trap forms part of a complex which includes the luminescence centre.

### § 1. INTRODUCTION

RECENT studies of the extent to which retrapping occurs in conventional phosphors show that it is a negligible process when the electrons are ejected from the traps by thermal energy only (Garlick and Gibson 1948). This result cannot be reconciled with the conventional model of a luminescent material used by Randall and Wilkins (1945) and other authors. It was suggested, therefore, that each luminescence centre has one electron trap associated with it, the two together forming a closed system from which the excited electron did not normally escape. This view was supported by the experiments described by Garlick (1948) and by Garlick and Gibson (1949). Garlick showed that the introduction of impurities modified the trap distribution in the phosphor specimen. This was illustrated by the production of new peaks, due to the introduction of specific impurities, in the thermoluminescence curve. Garlick also showed that the thermoluminescence curves of phosphors containing two activators could be resolved into 'colour peaks', that is, the colour of the emission at a peak of the thermal curve glow depended upon the particular group of traps being emptied. The colour changes during thermoluminescence might be explained by migration of positive holes and electrons between different types of luminescence centres, as postulated in a recent theory due to Klasens *et al.* (Klasens, Ramsden and Chow Quantie 1948, Klasens and Wise 1948). However, this explanation is unlikely in many cases as the following experiment shows. If a phosphor with more than one type of luminescence centre is excited by radiation of suitable wavelength then it is possible to excite one type of centre only. The resulting thermoluminescence curve obtained after such excitation, using suitable optical filters, may be the same as that after excitation affecting both types of centre, provided that the same optical filters are used to select emission from the same luminescence centres. If this is so, then it is unlikely that any interchange of electrons or

\* Now at T.R.E., Malvern.

positive holes occurs between the different centres. In effect, such a result supports the hypothesis mentioned above (Garlick and Gibson 1948) that retrapping of electrons does not occur in conventional phosphors, such as the zinc sulphides.

Work on the increase in dielectric constant and loss which occurs in zinc sulphide on excitation (Garlick and Gibson 1947) has shown that the increase is due to the filling of electron traps. The present studies, described below, contain further evidence from dielectric measurements to show that electron traps and luminescence centres are closely associated. In particular, the effects of field frequency, temperature, exciting intensity and time of excitation have been studied. It has been shown that the dielectric constant change per filled trap is exponentially dependent on temperature, the exponent varying from phosphor to phosphor. The dependence on field frequency is typical of a dipole system having a relaxation time of about  $10^{-7}$  second. The latter figure also varies among phosphor specimens of different constitution.

It was noticed during the work on dielectric effects that both the relaxation time and the temperature exponent of the polarizability were, to a first approximation, determined by the nature of the activating impurity. The lattice structure (cubic or hexagonal), the constitution of the bulk material (i.e. ZnS or mixed ZnS-CdS) and other parameters were of secondary importance. This suggested that the activating impurity producing the traps largely determined the dielectric properties of the traps.

## § 2. EXPERIMENTAL RESULTS

Garlick (1948) used the phosphor  $\text{CaWO}_4\text{-U}$  as an example of a doubly activated material and gave the thermoluminescence curves of the material, using optical filters to select emission from the different types of luminescence centre.

The same phosphor will be used as an example of the characteristics of the dielectric changes occurring when phosphors containing more than one activator are excited.

### (i) *The Variation of the Dielectric Changes with Applied Field Frequency*

Measurements have been made by the methods described previously (Garlick and Gibson 1947) and over the same frequency range (75 kc/s. to 20 Mc/s.). In a singly activated phosphor the relaxation time  $\tau$  is single valued or nearly so, anomalous dispersion of simple form occurring at about 2 Mc/s. In a doubly activated phosphor, however, it is clear from inspection of the dispersion curve that there are two regions of anomalous dispersion and hence two values of the relaxation time. If the values are sufficiently different it is quite simple to treat the two dispersion regions separately and apply to each region the formula

$$\frac{\Delta\epsilon_0 - \Delta\epsilon}{\Delta\epsilon - \Delta\epsilon_\infty} = \omega^2\tau^2 \quad \dots\dots(1)$$

given as equation (8) by Garlick and Gibson (1947)\*. In Figure 1 the factor on the left-hand side of equation (1) is plotted against the square of the field frequency for the two dispersion regions considered separately. The slopes of the two lines

\*  $\Delta\epsilon$  is the change in the real part of the complex dielectric constant at the given field frequency, while  $\Delta\epsilon_0$  and  $\Delta\epsilon_\infty$  are its values at zero and optical frequencies respectively.

give the two values of the relaxation time. The values obtained are  $\tau_1 = 31 \times 10^{-8}$  second,  $\tau_2 = 5.3 \times 10^{-8}$  second. Measurement of the variation in loss factor change  $\Delta\epsilon''$ , given by (Garlick and Gibson 1947)

$$\Delta\epsilon'' = \frac{(\Delta\epsilon_0 - \Delta\epsilon_\infty)\omega\tau}{0.9 \times 10^{12}(1 + \omega^2\tau)^2}, \quad \dots\dots(2)$$

shows that this factor has two frequency maxima corresponding to the two relaxation times already noted. As  $\Delta\epsilon''$  is a maximum when  $\omega\tau = 1$ , values of  $\tau$  may be obtained. For the specimen of uranium activated calcium tungstate used they are  $\tau_1 = 23 \times 10^{-8}$  second and  $\tau_2 = 4.0 \times 10^{-8}$  second. The agreement with those deduced from the dispersion curve is as good as can be expected.

In view of the results discussed above it seems reasonable to suppose that two different types of electron trap exist in this and similar materials. Each type of trap can be associated with one or other of the two types of luminescent centre in the material. In the above case of  $\text{CaWO}_4\text{-U}$  we may talk loosely of 'WO<sub>4</sub> traps' and 'U traps'. It will be clear from the thermoluminescence curve given by Garlick (1948) that 'U traps' are deeper than 'WO<sub>4</sub> traps'.

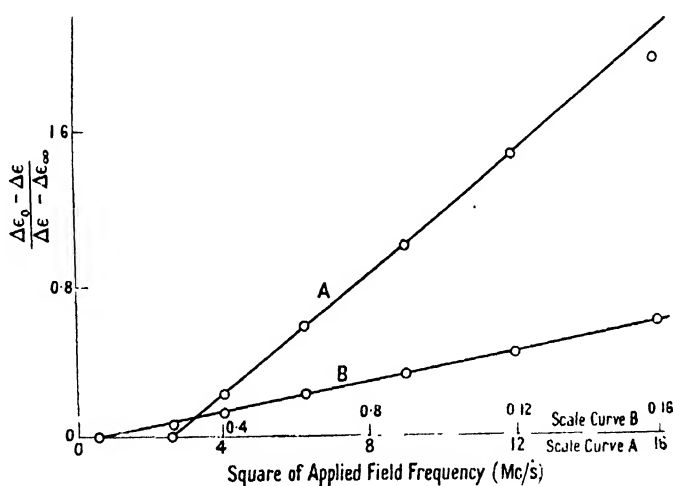


Figure 1. Variation of dielectric constant change with applied field frequency for a  $\text{CaWO}_4\text{-U}$  phosphor. Curves plotted on assumption that phosphor has two types of polarizable centres, as explained in text. A: 'WO<sub>4</sub> traps'; B: 'U traps'.

It is now important to ascribe the two values of  $\tau$  obtained by experiment to the 'WO<sub>4</sub>' and 'U traps' respectively. One method is to determine the reciprocal of  $\tau$  ( $=s$ , Garlick and Gibson 1947) for the two types of trap by luminescence measurements. This can be done by the method due to Randall and Wilkins (1945), but high accuracy cannot be expected. Experiment indicates that the large value of  $\tau$  is associated with the deeper 'U traps'. This result was confirmed by a second method. If the decay of the dielectric constant change after cessation of excitation is measured at frequencies of the order of 5 Mc/s., the decay rate is fast, but becomes slower as the applied field frequency is reduced to a low value ( $\sim 500$  kc/s.). At high frequencies the dipoles of small  $\tau$  are operative, and hence the smaller value of  $\tau$  must be associated with the shallower (in this case WO<sub>4</sub>) traps.

In general, therefore, traps associated with given centres have a relaxation time  $\tau$  peculiar to the impurity involved. Some typical results for zinc sulphide phosphors are summarized in the following table.

Phosphor	$\tau$ (seconds $\times 10^8$ )		
	Zn traps	Cu traps	Mn traps
ZnS-Zn	35	—	—
ZnS-Zn-Cu	34	17	—
ZnS-Zn-Cu-Mn (1)	46	19	2.5
ZnS-Zn-Cu-Mn (2)	36	15	2.4

(ii) *The Variation of the Dielectric Changes during Thermoluminescence*

Measurements of the changes in dielectric constant and loss which occur during the emission of thermoluminescence have been made by methods already described (Garlick and Gibson 1947). The results obtained for doubly activated phosphors may be treated in the way described in the same paper. Ignoring the slow variation in polarizability with trap depth, the magnitude of the dielectric

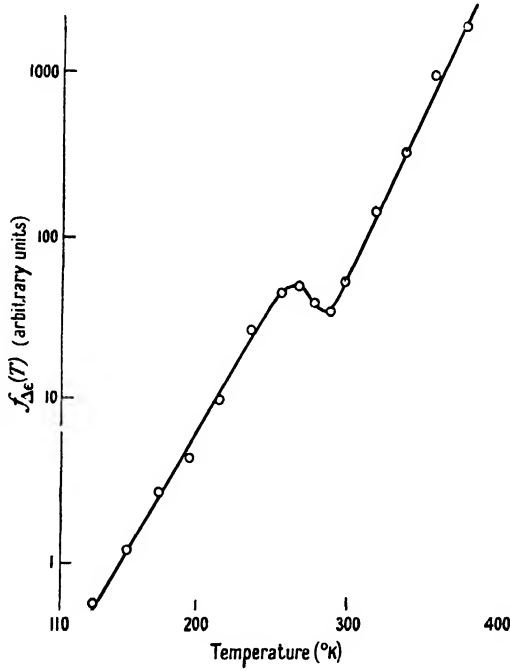


Figure 2. Temperature function  $f_{\Delta\epsilon}(T)$  for the dielectric constant change in a  $\text{CaWO}_4\text{-U}$  phosphor derived from measurements of dielectric changes during thermoluminescence.

constant change at any temperature  $T$  divided by the total number of filled traps remaining at that temperature is taken as a measure of the polarizability of the filled traps. Denoting the polarizability as  $f_{\Delta\epsilon}(T)$ , it was shown by Garlick and Gibson (1947) that

$$f_{\Delta\epsilon}(T) = \text{const.} \exp(\alpha T) \dots\dots (2)$$

where  $\alpha$  is a constant.

The variation of  $f_{\Delta\epsilon}(T)$  with temperature for a doubly activated material ( $\text{CaWO}_4\text{-U}$ ) is shown in Figure 2,  $f_{\Delta\epsilon}(T)$  being plotted logarithmically. The

simple linear relation expected is not obtained, a marked inflection occurring at about 280°K. At about this temperature the emission changes from blue ( $\text{WO}_4$  emission centres) to green (U emission centres). Apparently equation (2) is obeyed while 'WO<sub>4</sub> traps' predominate and while 'U traps' predominate, the inflection occurring intermediately.

This result is explicable if it is assumed that the polarizabilities of 'WO<sub>4</sub>' and 'U traps' are different. As there is a drop in the polarizability-temperature curve at the inflection, it is clear that the polarizability of 'WO<sub>4</sub> traps' ( $P_{\text{WO}_4}$ ) is greater than the polarizability of 'U traps' ( $P_U$ ). The ratio  $P_{\text{WO}_4}/P_U$  can be found by extrapolating both curves to 0°K. and is

$$P_{\text{WO}_4}/P_U = 3.4. \quad \dots\dots(3)$$

It will be clear that such a difference in polarizability will influence the decay of the dielectric constant change at room temperature, making the initial portion relatively faster. This is, in fact, observed.

A difference in apparent polarizabilities of 'WO<sub>4</sub>' and 'U traps' is bound to arise, due to the difference in  $\tau$  value for each kind of trap. As the value of the constant  $\alpha$  obtained from Figure 2 is almost the same for each kind of trap (indicated by the fact that the two linear parts of the curve in Figure 2 are nearly parallel), it is likely that the difference in the values of  $\alpha$  determines the difference in polarizability. The ratio of the apparent polarizabilities may be calculated from equation (1) as  $\omega$ ,  $\Delta\epsilon_0$ ,  $\Delta\epsilon_\infty$ , and  $\tau$  are known. It is found that, at the measurement frequency of 2.7 Mc/s.,

$$P_{\text{WO}_4}/P_U = 3. \quad \dots\dots(4)$$

Agreement with the other experimental value above is better than might be expected.

### § 3. DISCUSSION AND CONCLUSION

Measurements of the increases in dielectric constant and loss of simple phosphors when excited suggest that the increases are due to the filling of electron traps (Garlick and Gibson 1947). If this result is assumed, dielectric measurements may be used to obtain more information on the nature of electron traps.

The study of the dielectric changes occurring in doubly or triply activated materials shows that the theory already developed (Garlick and Gibson 1947) can only be extended to cover such materials if fuller assumptions are made. It is necessary to assume that the introduction of the impurity centres gives rise to the formation of electron traps, and further, that some measurable parameters of the filled traps are determined by the nature of the impurity. This hypothesis has been suggested in previous work (Garlick and Gibson 1948, Garlick 1948), the measurable parameter concerned there being the depth of the electron traps. In the present case the parameter measured was relaxation time  $\tau$  of the filled electron traps.

The relaxation time of such a dipole system is related to the diameter and other fundamental properties of the electron trap. The relation between  $\tau$  and the nature of the activating impurity thus gives further evidence in favour of the view that the impurity ion forms the electron trap, possibly by distortion of the local lattice.



## ACKNOWLEDGMENTS

We wish to thank Professor M. L. E. Oliphant for the provision of facilities for this work and the Ministry of Supply (D.C.D.) for permission for one of us (A.F.G.) to remain in this laboratory for the completion of this work.

## REFERENCES

- GARLICK, G. F. J., 1948, *Solid Luminescent Materials* (New York: John Wiley), paper 5.  
 GARLICK, G. F. J., and GIBSON, A. F., 1947, *Proc. Roy. Soc. A*, **188**, 485; 1948, *Proc. Phys. Soc.*, **60**, 574; 1949, *J. Opt. Soc. Amer.* (in the press).  
 KLASSENS, H. A., RAMSDEN, W., and CHOW QUANTIE, 1948, *J. Opt. Soc. Amer.*, **38**, 60.  
 KLASSENS, H. A., and WISE, M. E., 1948, *J. Opt. Soc. Amer.*, **38**, 226.  
 RANDALL, J. T., and WILKINS, M. H. F., 1945, *Proc. Roy. Soc. A*, **184**, 366.

## Eigenfunctions following from Sommerfeld's Polynomial Method

BY A. RUBINOWICZ

Institute of Theoretical Mechanics, University of Warsaw

MS. received 7th June 1949

**ABSTRACT.** The eigenfunctions following from Sommerfeld's polynomial method were determined in the general case. They are products of a convergence factor  $E$  and a polynomial  $P$  given by a hypergeometric series. The form of  $E$  depends upon whether  $P$  is expressible by the ordinary or the confluent hypergeometric series.

SOMMERFELD'S polynomial method (Sommerfeld 1939) for the solution of the eigenvalue problems of the quantum theory is applicable only to a limited group of such problems. It supposes that the eigenfunctions  $f(x)$  are expressible in the form of a product of two functions  $f(x) = E(x)P(x)$ .

$P(x)$  is a polynomial fulfilling a linear differential equation of the second order of the form

$$x^2(A_2 + B_2x^h) \frac{d^2P}{dx^2} + 2x(A_1 + B_1x^h) \frac{dP}{dx} + (A_0 + B_0x^h)P = 0, \quad \dots\dots (1)$$

where  $A_i$ ,  $B_i$  are constants ( $A_2 \neq 0$ ) and  $h$  is a positive integer.

The factor  $E(x)$  however is responsible for the convergence of the normalization integral and the fulfilment of boundary conditions. In a paper published elsewhere (Rubinowicz 1949) it is proved that  $E(x)$  can appear only in two forms, corresponding to  $B_2 \neq 0$  and  $B_2 = 0$ , provided that  $A_2 \neq 0$ . If the differential equation of the eigenvalue problem has the form

$$\frac{d}{dx} \left( p \frac{df}{dx} \right) - qf + \lambda \rho f = 0,$$

then we have

(I) in the case  $B_2 \neq 0$ ,

$$E = p^{-1} x^{A_1/A_2} (A_2 + B_2 x^h)^{(1/h)(B_1/B_2 - A_1/A_2)}; \quad \dots\dots (2a)$$

(II) in the case  $B_2 = 0$ ,

$$E = p^{-1} x^{A_1/A_2} \exp \{ (1/h)(B_1/A_2)x^h \}. \quad \dots\dots (2b)$$

Since the differential equation of the polynomial (1) is reducible to the hypergeometric differential equation (cf. Riemann-Weber 1901, p. 11) we can now write down the eigenfunctions for all cases accessible to Sommerfeld's polynomial method. For this purpose we must transform equation (1) into the hypergeometric differential equation. Writing

$$y = x^h \quad \dots\dots(3)$$

and

$$P = y^\mu \phi(y), \quad \dots\dots(4)$$

we obtain the differential equation

$$y^2(p_2 + q_2 y) \frac{d^2 \phi}{dy^2} + y(p_1 + q_1 y) \frac{d\phi}{dy} + (p_0 + q_0 y)\phi = 0. \quad \dots\dots(5)$$

Here

$$\left. \begin{aligned} p_2 &= n_2, & p_1 &= n_1 + 2\mu n_2, & p_0 &= n_0 + \mu n_1 + \mu(\mu - 1)n_2, \\ q_2 &= m_2, & q_1 &= m_1 + 2\mu m_2, & q_0 &= m_0 + \mu m_1 + \mu(\mu - 1)m_2, \end{aligned} \right\} \dots\dots(6a)$$

where

$$\left. \begin{aligned} n_2 &= h^2 A_2, & n_1 &= h\{2A_1 + (h-1)A_2\}, & n_0 &= A_0, \\ m_2 &= h^2 B_2, & m_1 &= h\{2B_1 + (h-1)B_2\}, & m_0 &= B_0. \end{aligned} \right\} \dots\dots(6b)$$

Determining  $\mu$  in such a way that  $p_0$  vanishes, that is, from (6a) and (6b), so that

$$\mu h(\mu h - 1)A_2 + 2\mu h A_1 + A_0 = 0,$$

and introducing a new independent variable

$$z = -\frac{q_2}{p_2}y = -\frac{B_2}{A_2}x^h, \quad \dots\dots(7)$$

we get in place of (5) the hypergeometric differential equation

$$z(1-z) \frac{d^2 \phi}{dz^2} + \{\gamma - (\alpha + \beta + 1)z\} \frac{d\phi}{dz} - \alpha\beta\phi = 0. \quad \dots\dots(8a)$$

The constants  $\alpha, \beta, \gamma$  are here given according to (6a) and (6b) by the equations

$$\alpha + \beta + 1 = \frac{q_1}{q_2} = \frac{m_1}{m_2} + 2\mu = \frac{1}{h} \left( 2 \frac{B_1}{B_2} - 1 \right) + 2\mu + 1, \quad \dots\dots(9a)$$

$$\alpha\beta = \frac{q_0}{q_2} = \frac{m_0}{m_2} + \mu \frac{m_1}{m_2} + \mu(\mu - 1) = \frac{1}{h^2 B_2} \{ \mu h(\mu h - 1)B_2 + 2\mu h B_1 + B_0 \}, \quad \dots\dots(9b)$$

$$\gamma = \frac{p_1}{p_2} = \frac{n_1}{n_2} + 2\mu = \frac{1}{h} \left( 2 \frac{A_1}{A_2} - 1 \right) + 2\mu + 1. \quad \dots\dots(9c)$$

From (9a) and (9b) we obtain for  $\xi = \alpha$  or  $\xi = \beta$  the equation

$$(\mu h - \xi h)(\mu h - \xi h - 1)B_2 + 2(\mu h - \xi h)B_1 + B_0 = 0, \quad \dots\dots(10)$$

which is identical with Sommerfeld's condition for the breaking off of the power series.

The function  $\phi$  which is a solution of the hypergeometric differential equation (8a) is given by

$$\phi = F(\alpha, \beta, \gamma, z) = F[\alpha, \beta, \gamma, -(B_2/A_2)x^h], \quad \dots\dots(11)$$

so that from (3), (4) and (11) we obtain for the polynomial  $P$  the expression

$$P(x) = x^{\mu h} F[\alpha, \beta, \gamma, -(B_2/A_2)x^h]. \quad \dots\dots(12a)$$

In order that  $P(x)$  may be a polynomial,  $\alpha$  (or  $\beta$ ) must be a negative integer.

But we must remark that our transformation (7) can be used only in the case where  $B_2 \neq 0$ , and is inapplicable if  $B_2 = 0$ .

In this second case we have to apply the substitution

$$z = -\frac{2}{h} \frac{B_1}{A_2} x^h,$$

which transforms the differential equation (1) into

$$z \frac{d^2 \phi}{dz^2} + (\gamma - z) \frac{d\phi}{dz} - \alpha \phi = 0. \quad \dots\dots(8b)$$

The constant  $\gamma$  is here determined by (9c), whereas  $\alpha$  is given according to (10) by

$$\alpha = \frac{1}{2h} \frac{B_0}{B_1} + \mu.$$

(8b) is the differential equation of the confluent hypergeometric function  $F_1(\alpha, \gamma, z)$ . A solution of Sommerfeld's differential equation (1) is therefore in case (II) given by

$$P(x) = x^{\mu h} F_1\left(\alpha, \gamma, -\frac{2}{h} \frac{B_0}{B_1} x^h\right). \quad \dots\dots(12b)$$

We are now able to write down the complete eigenfunctions  $f(x) = E(x)P(x)$ . We get

(I) in the case  $B_2 \neq 0$  from equations (2a), (9a) and (12a),

$$f(x) = p^{-\frac{1}{2}} \xi^{1/2} h^{\gamma-1/2} (1 + \xi)^{(\alpha + \beta - \gamma + 1)/2} F(\alpha, \beta, \gamma, -\xi) \quad \text{where} \quad \xi = (B_2/A_2)x^h;$$

(II) in the case  $B_2 = 0$  from equations (2b), (9c) and (12b),

$$f(x) = p^{-\frac{1}{2}} \zeta^{1/2} h^{\gamma-1/2} e^{\zeta/2} F_1(\alpha, \gamma, -\zeta) \quad \text{where} \quad \zeta = \frac{2}{h} \frac{B_1}{A_2} x^h.$$

The constants  $\alpha$  or  $\beta$  are here negative integers.

Using these expressions we can determine immediately the eigenfunctions in all cases accessible to Sommerfeld's polynomial method. For this purpose we must know the values of  $A_i$ ,  $B_i$  and  $h$ , which enable us to calculate the constants  $\alpha$ ,  $\beta$ ,  $\gamma$  with the aid of the formulae given in this paper. For all special cases we have dealt with in our former paper (Rubinowicz 1949) the values of  $A_i$ ,  $B_i$  and  $h$  can be found there.

#### REFERENCES

- RIEMANN, B., and WEBER, H., 1901, *Die partiellen Differentialgleichungen der mathematischen Physik*, 4th edition, Vol. II (Braunschweig: Vieweg und Sohn).  
 RUBINOWICZ, A., 1949, *Proc. K. Ned. Akad. Wet. Amst.*, **52**, 351.  
 SOMMERFELD, A., 1939, *Atombau und Spektrallinien*, Vol. II (Braunschweig: Vieweg und Sohn), p. 716.

## LETTERS TO THE EDITOR

### Origin of Low-Energy Electron Lines in the $\beta$ -spectrum of $^{198}\text{Au}$

The low-energy part of the  $\beta$ -spectrum of  $^{198}\text{Au}$  was investigated, using the 254°-radial electrostatic field spectroscopy that has been constructed in this laboratory. Several samples made from pure precipitated gold and also from gold foil were irradiated in the Harwell pile. It was found in all cases that two fairly intense conversion electron lines appear in the spectrum, one at energy 44 kev. and the other at 58 kev. Interpreted as due to internal conversion in gold in K and L shells respectively, they would correspond to  $\gamma$ -ray energies of 0.125 mev. and 0.072 mev. The intensity of these lines was observed over five days and the half-life was found to be of the order of three days.

The conversion-electron peak at 58 kev., which is broad, and due to 0.072 mev. radiation, is in agreement with the observation of Jnanananda (1946), but there is a lack of agreement among observers about  $\gamma$ -rays from  $^{198}\text{Au}$ , other than the well-known one at 0.4 mev. Electron lines due to  $\gamma$ -rays of very nearly the same energies as above have been reported by Valley (1941) and Helmholtz (1942) for  $^{197}\text{Hg}$ , which decays by K-capture to  $^{197}\text{Au}$ , the  $\gamma$ -rays, which are highly converted, being due to transitions from the excited states of  $^{197}\text{Au}$  to the ground state. It is suggested, therefore, that these conversion lines and the corresponding  $\gamma$ -rays are to be associated not with the slow-neutron induced activity,  $^{198}\text{Au}$ , but with the activity induced by fast neutrons during irradiation, giving  $^{197}\text{Pt}$  by (n, p) reaction. Thus,  $^{197}\text{Au}(\text{n}, \text{p})^{197}\text{Pt} \xrightarrow{\beta^-} ^{197}\text{Au}$ . Excited  $^{197}\text{Au}$  produced by the  $\beta$ -decay of  $^{197}\text{Pt}$  would, on transition to the ground level, emit the same  $\gamma$ -rays, highly converted in gold, as are found in the K-capture decay of  $^{197}\text{Hg}$ .

Krishnan and Nahum (1941), who produced  $^{197}\text{Pt}$  by (d, p) reaction on platinum, found that the 2.8 day isotope, as studied by absorption methods, emits strong discrete groups of low-energy electrons of secondary origin, the maximum energy being 0.120 mev. Assuming K, L and M internal conversion in gold to be taking place, this would correspond to a  $\gamma$ -ray energy of 0.124 mev., in good agreement with the energy of the  $\gamma$  ray reported above. They also found evidence for a softer  $\gamma$  ray from  $^{197}\text{Pt}$  and give the energy as 0.075 mev., which again is in close agreement with the other  $\gamma$ -ray energy mentioned above. The half-life for this isotope,  $^{197}\text{Pt}$ , as given by McMillan *et al.* (1937) and Krishnan and Nahum (1941) is of the order of three days, which was also the value found for the decay of these conversion-electron lines.

A long strip of gold foil, made into a small tight roll, was then irradiated at Harwell, so that the inner portion of the coil would be shielded from resonance neutrons, which produce the  $^{198}\text{Au}$  activity. Measurement of the strength of  $^{198}\text{Au}$  activity as indicated by the 0.4 mev.  $\gamma$ -ray from equal areas of the shielded and unshielded portions of the foil showed that the unshielded portion was substantially stronger than the shielded one, as is to be expected. On the other hand, the intensity of the conversion-electron lines, relative to that of the continuous  $\beta$ -ray background of  $^{198}\text{Au}$ , was greater in the spectrum of the shielded foil. This further strengthens the suggestion that the activity responsible for these  $\gamma$ -rays and the conversion lines is induced in gold by fast neutrons and is not the  $^{198}\text{Au}$  activity.

A fuller account of this and other investigations of conversion lines from some other isotopes and also of the electrostatic  $\beta$ -ray spectroscopy used for this purpose will be given at a later date.

The author is very grateful to Professor P. B. Moon for his continued interest and guidance. He also wishes to thank Dr. D. M. Millest, with whom he collaborated in the design and construction of the  $\beta$ -ray spectroscopy, and the Government of India for a State Scholarship.

Physics Department, The University,  
Edgbaston, Birmingham, 15.  
18th September 1949.

B. V. THOSAR.

HELMHOLTZ, A. C., 1942, *Phys. Rev.*, **61**, 204.

JNANANANDA, S., 1946, *Phys. Rev.*, **70**, 812.

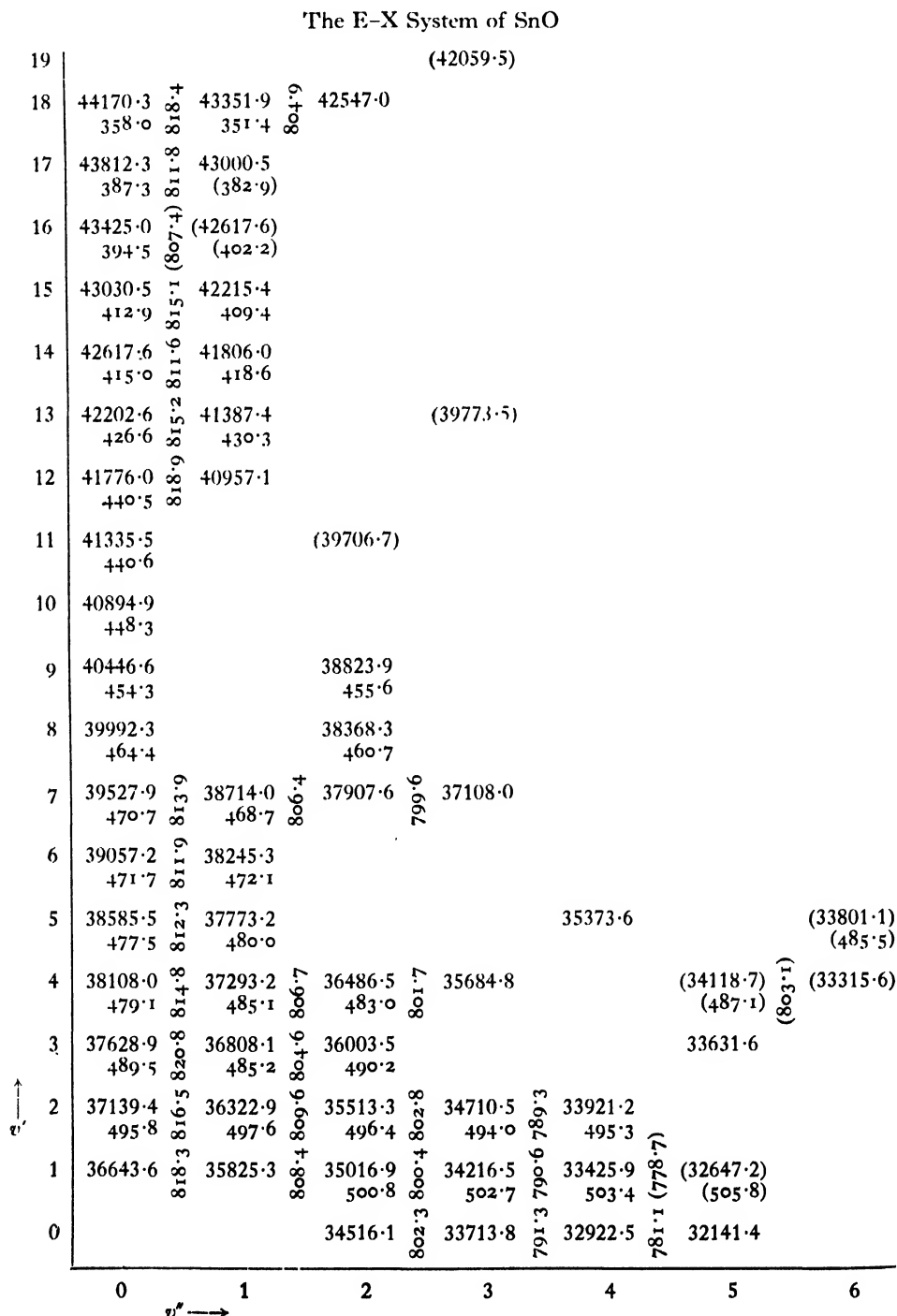
KRISHNAN, R. S., and NAHUM, E. A., 1941, *Proc. Camb. Phil. Soc.*, **37**, 422.

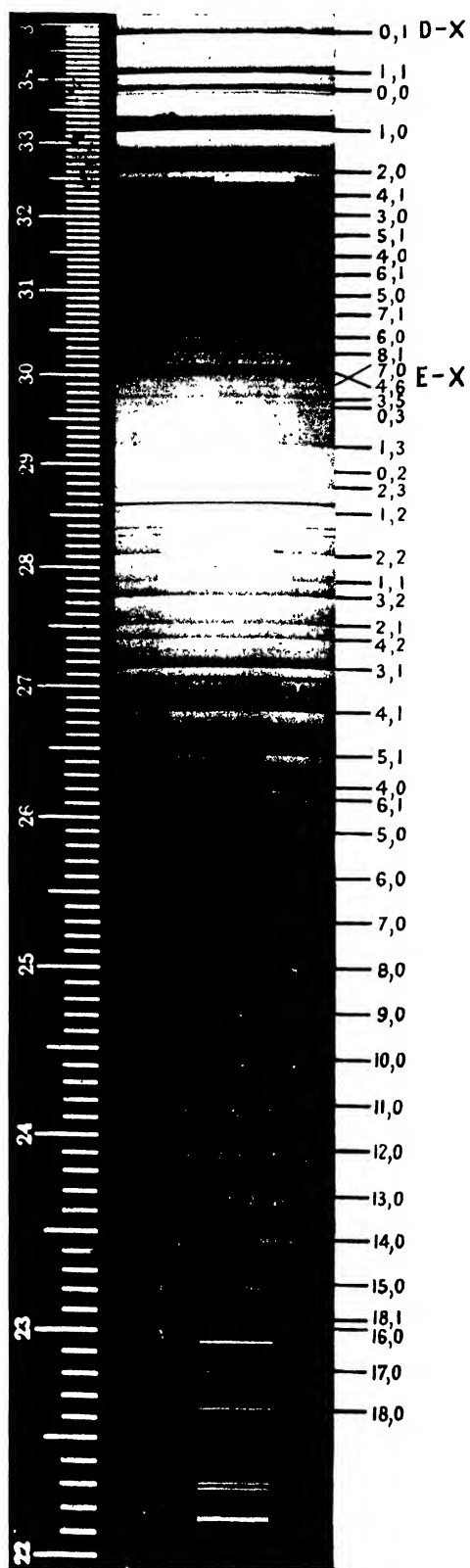
McMILLAN, E., KAMEN, M., and RUBEN, S., 1937, *Phys. Rev.*, **52**, 375.

VALLEY, G. E., 1941, *Phys. Rev.*, **60**, 167.

## The Ultra-Violet Absorption Spectrum of SnO

In the course of other work, we have recently obtained low-dispersion spectrograms of the absorption by SnO in the range 2040–3500 Å. (see Plate). Two band-systems are known in this region: the less refrangible system, D-X, studied especially by Connelly (1933), and the E-X system, first obtained by Loomis and Watson (1934) in emission. The absorption plates add little to our knowledge of the D-X system, but about twenty new





Bands of the D-X and E-X systems of SnO photographed in absorption on Hilger small quartz prism spectrograph: Ilford Q.1 plate.  
Temperature c. 1,400 c., effective path-length c. 25 cm.



bands have been assigned to the E-X system. Apart from the necessity of raising their  $v'$ -values by one unit, the vibrational analysis of Loomis and Watson is unchanged, and the main effect of our measurements, which are summarized in the Table, is to provide more information about the course of the upper-state vibrational levels. (The new values of  $\Delta G'$  are also more consistent than those of Loomis and Watson: the reason seems to be that for the vibrational analysis of a band-system of a molecule which gives an irresolvable complex of isotopic heads it is a positive advantage to use not too high dispersion.)

In attempting to derive an expression for  $G_v'$ , we used the values of  $G_v''$  given by Jevons (1938):  $G_v'' = 822.4(v'' + \frac{1}{2}) - 3.73(v'' + \frac{1}{2})^2$ . No simple expression for  $G_v'$  was however found to fit the levels over the whole range, but up to  $v' = 17$  the equation

$$G' = 508.0(v' + \frac{1}{2}) - 2.9(v' + \frac{1}{2})^2 - 5 \times 10^{-5}(v' + \frac{1}{2})^5$$

is reasonably satisfactory. With this,  $\nu_e = 36,295 \text{ cm}^{-1}$ .

The sharp drop in the vibrational interval beginning at  $v' = 18$  seems to be real and suggests that this point is not far from a dissociation limit. Graphical extrapolation gives  $D_0' \sim 1.2 \text{ eV.}$ , corresponding to a dissociation limit  $5.6_e \text{ eV.}$  above  $\tau'' = 0$ . This value of  $D_0'$  agrees fairly well with that suggested earlier by analogy with SnSe (Vago and Barrow 1946). Linear extrapolation of the ground-state vibrational intervals leads to  $D_0'' = 5.6 \text{ eV.}$ , so it is possible that both states dissociate into the same atomic products.

Band-systems of SnO are also expected at shorter wavelengths than the E-X system. On some of our plates weak red-degraded bands are to be seen with heads at about 2037, 2050, 2054, 2069, 2073, 2084, 2102, 2117 and 2132 Å. These may belong to a new system, but we have so far been unable to get pictures on which the bands are sufficiently well defined for accurate measurement.

To complete the outline of the absorption spectrum of this molecule—so far as it is known at present—it may be mentioned that, contrary to statements in the literature (e.g. Sharma 1944), the stronger bands of the B and C systems (Pearse and Gaydon 1941) are also observed in absorption (Mrs. R. E. Richards, unpublished work): the vibrational analysis of these bands is however still uncertain.

Physical Chemistry Laboratory,  
Oxford.  
21st August 1949.

B. EISLER.  
R. F. BARROW.

CONNELLY, F. C., 1933, *Proc. Phys. Soc.*, **45**, 780.

JEVONS, W., 1938, *Proc. Phys. Soc.*, **50**, 910.

LOOMIS, F. W., and WATSON, T. F., 1934, *Phys. Rev.*, **45**, 805.

PEARSE, R. W. B., and GAYDON, A. G., 1941, *Identification of Molecular Spectra* (London: Chapman and Hall).

SHARMA, D., 1944, *Proc. Nat. Acad. Sci. India*, **14A**, 133.

VAGO, E. E., and BARROW, R. F., 1946, *Proc. Phys. Soc.*, **58**, 707.

## X-Ray Line Broadening in Metals

It is the author's belief that the diverse opinions of different workers on the explanation of x-ray line broadening in metals can be reconciled in terms of the hypothesis of Dehlinger and Kochendorfer (1939 a, b) and Kochendorfer (1944) that both particle size and stress effects are presented simultaneously. The theoretical work of Bragg (1942, 1949) gives mathematical support to the hypothesis.

In the limiting case of pure particle size broadening the line breadth  $\beta_p$  is related to the effective particle size  $\epsilon$ , the x-ray wavelength  $\lambda$  and the Bragg angle  $\theta$  by the equation (Jones 1938)

$$\beta_p = \frac{\lambda}{\epsilon \cos \theta}.$$

For pure stress broadening the breadth  $\beta_s$  is related to the effective strain  $\eta$  (Stokes and Wilson 1944) and the Bragg angle by the equation

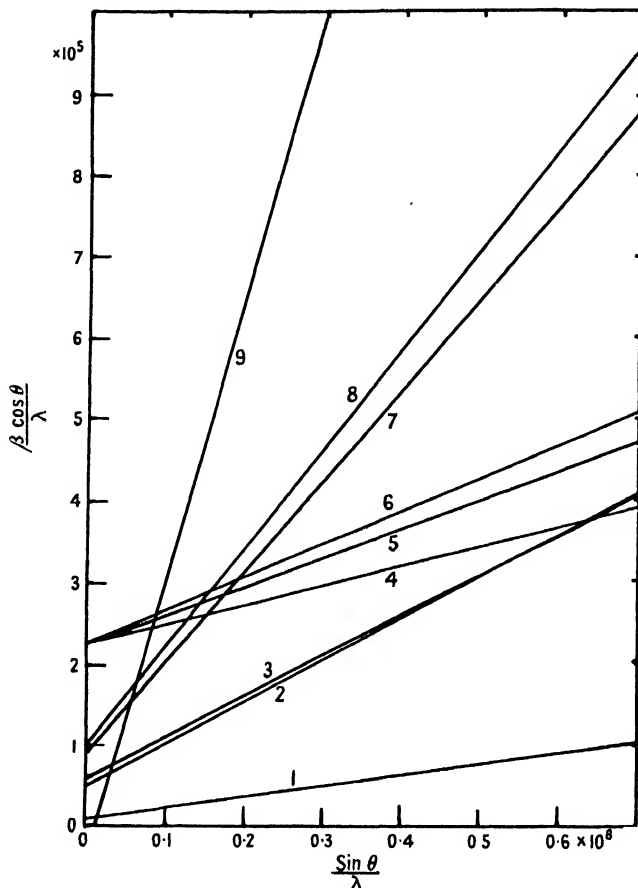
$$\beta_s = \eta \tan \theta.$$



If both types of broadening are present, the resultant line breadth  $\beta$  should be obtained by compounding the component lines as discussed by Jones (1938), Shull (1946) and Stokes (1948), but it has been shown by Wood and Rachinger (1949) that for a commonly occurring line shape the breadths are additive, i.e.  $\beta = \beta_P + \beta_S$ . In this case we may write

$$\frac{\beta \cos \theta}{\lambda} = \frac{1}{\epsilon} + \eta \frac{\sin \theta}{\lambda}.$$

In a distorted lattice the effective particle size  $\epsilon$  must be interpreted as a measure of the volume of regions in the lattice which diffract coherently. In anisotropic metals the strain



Summary of line broadening measurements.

- Key : 1. Aluminium filings, CuK $\alpha$ , Hall and Williamson (unpublished measurements).  
 2. Copper filings, ZnK $\alpha$ , Brindley (1939).  
 3. Copper filings, CuK $\alpha$ , Stokes, Pascoe and Lipson (1943).  
 4. Copper sheet, 20% reduction, CuK $\alpha$ , Dehlinger and Kochendorfer (1939).  
 5. Copper sheet, 60% reduction, CuK $\alpha$ , Dehlinger and Kochendorfer (1939).  
 6. Copper sheet, 99.5% reduction, CuK $\alpha$ , Dehlinger and Kochendorfer (1939).  
 7. Rhodium filings, CuK $\alpha$ , Brindley (1938).  
 8. Rhodium filings, ZnK $\alpha$ , Brindley (1938).  
 9. Martensite rod, FeK $\alpha$ , Wheeler and Jaswon (1947).

distribution is not the same for different crystallographic planes, and a relationship of the type

$$\frac{\beta \cos \theta}{\lambda} = \frac{1}{\epsilon} + \frac{2\sigma}{E_{hkl}} \frac{\sin \theta}{\lambda}$$

is frequently a better representation of the experimental breadths. In this equation  $E_{hkl}$  is the value of Young's modulus for the direction perpendicular to the planes  $\{hkl\}$  and  $\sigma$  is the Laue breadth of the stress distribution function, which is assumed to be independent of direction.

The accurate determination of the value of  $\epsilon$  from these equations is difficult, since the intercept which defines it depends largely on the breadths of lines for which  $\sin \theta/\lambda$  is small. Metals rarely diffract at very low angles, and for such lines the total broadening is small and difficult to measure accurately. A number of published results have been analysed in this way and the best straight lines shown in the diagram determined by the method of least squares. It will be seen that the slopes of the lines (i.e. the stress effects) increase progressively from soft to hard metals. The intercepts are all positive with the exception of that for martensite, and a very small error in the steep slope of the graph would account for this physically unreal result. The mean value of all intercepts corresponds to  $\epsilon = 10^{-5}$  cm. Owing to the uncertainties of the analysis no more than the order of magnitude of this quantity can be regarded as significant. This is about the same as that determined by Wood and Rachinger (1949) by a different method. The physical significance of this value may be understood from the theory of dislocations. There is abundant evidence (Taylor 1934, Brown 1941, Koehler 1941, Cottrell and Churchman 1949) suggesting that the maximum density of dislocations in most cold-worked metals corresponds to an average distance between dislocation lines of about  $10^{-6}$  cm. The coherently diffracting regions of the lattice ought to have an effective particle size rather greater than this, since the dislocation lines are thought to be long compared with their separation. This suggestion agrees well with the experimental values, and it seems that direct calculations of line broadening based on the dislocation model should lead to a much clearer understanding of the problem.

Department of Metallurgy,  
University of Birmingham.  
30th August 1949.

W. H. HALL.

- BRAGG, W. L., 1942, *Nature, Lond.*, **149**, 511; 1949, *Proc. Camb. Phil. Soc.*, **45**, 125.  
BRINDLEY, G. W., 1938, *Proc. Phys. Soc.*, **50**, 501; 1939, *Ibid.*, **51**, 432.  
BROWN, W. F., 1941, *Phys. Rev.*, **60**, 139.  
COTTRELL, A. H., and CHURCHMAN, A. T., 1949, *J. Iron and Steel Inst.*, **162**, 271.  
DEHLINGER, U., and KOCHENDORFER, A., 1939 a, *Z. Metallkde.*, **31**, 231; 1939 b, *Z. Kristallogr. A.*, **101**, 134.  
JONES, F. W., 1938, *Proc. Roy. Soc. A*, **166**, 16.  
KOCHENDORFER, A., 1944, *Z. Kristallogr. A*, **105**, 393.  
KOEHLER, J. S., 1941, *Phys. Rev.*, **60**, 397.  
SHULL, C. G., 1946, *Phys. Rev.*, **70**, 679.  
STOKES, A. R., 1948, *Proc. Phys. Soc.*, **61**, 382.  
STOKES, A. R., PASCOE, K. J., and LIPSON, H., 1943, *Nature, Lond.*, **151**, 137.  
STOKES, A. R., and WILSON, A. J. C., 1944, *Proc. Phys. Soc.*, **56**, 174.  
TAYLOR, G. I., 1934, *Proc. Roy. Soc. A*, **145**, 362.  
WHEELER, J. A., and JASWON, M. A., 1947, *J. Iron and Steel Inst.*, **157**, 161.  
WOOD, W. A., and RACHINGER, W. A., 1949, *J. Inst. Metals*, **75**, 571.

## Magnetic Viscosity in Mn-Zn Ferrite

In a previous paper (Street and Woolley 1949), referred to below as I, a theory of magnetic viscosity, based on activation energy concepts, has been given. The relation between the rate of increase of the intensity of magnetization of a specimen and the time of observation (equation (9) of I), is

$$\frac{dI}{dt} = \frac{\bar{i}p k T}{t} [\exp(-\lambda_0 t) - \exp(-Ct)],$$

where the symbols have the meanings given in I. The general solution of this expression is

$$\Delta I = \bar{i}p k T \left[ Ei(-\lambda_0 t) - Ei(-Ct) + \frac{E_0}{kT} \right], \quad \dots (1)$$

$\Delta I$  being zero at time  $t=0$ .

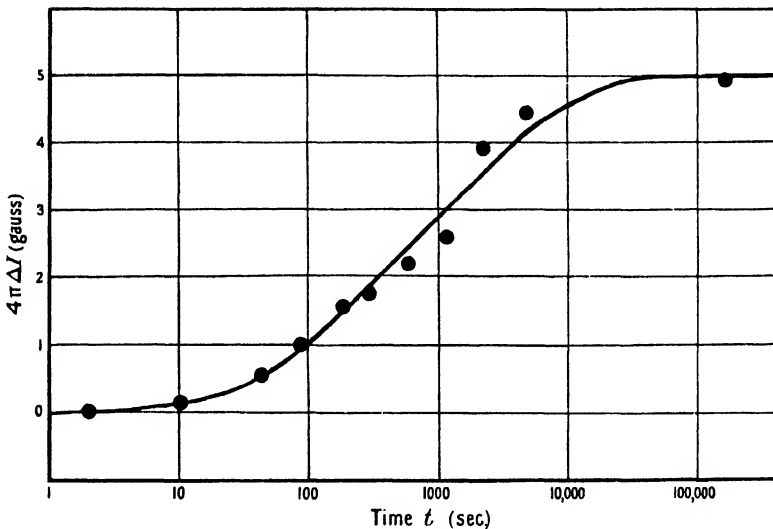
In I it was found that only a limited range of  $t$  need be considered, viz. for values of  $t$  from  $t > t_0$ , where  $Ei(-Ct_0) \ll Ei(-\lambda_0 t_0)$ , to  $t < t_0$ , where  $\lambda_0 t_0 \ll 1$ . Over this range (1) reduces to

$$\Delta I = i p k T \log t + \text{constant}. \quad \dots (2)$$

The results of experiments made on magnetic viscosity in alnico satisfied this simplified equation (2). However, in those cases where observations are extended over time periods greater than the limits detailed above, it is necessary to use the exact form given in equation (1). A convenient test of the expression is provided by considering the experimental results for magnetic viscosity in Mn-Zn ferrite (Snoek 1947). The numerical values of the constants of equation (1) were chosen to fit Snoek's experimental results, and the equation obtained was

$$\Delta B = 0.875[Ei(-5.4 \times 10^{-5}t) - Ei(-1.64 \times 10^{-2}t) + 5.72], \quad \dots (3)$$

where  $\Delta B$  is the difference between the value of the magnetic induction of the specimen at any time  $t$  seconds and that at  $t=0$ . A plot of equation (3) and Snoek's experimental results are shown in the Figure, and it will be seen that satisfactory agreement is obtained.



Magnetic viscosity in Mn-Zn ferrite.

The full line is calculated from equation (3). ● Experimental points obtained by Snoek (1947).

The curve of best fit as drawn by Snoek is almost identical with the theoretical curve of equation (3).

From the numerical equation, the following quantitative results may be obtained :

$$E_0/kT = 5.72 ; \quad C = 1.64 \times 10^{-2} \text{ sec}^{-1} ; \quad 4\pi i p k T = 0.875.$$

Thus, if it is assumed that  $T = 290^\circ \text{K}$ , then the upper value of the activation energy,  $E_0$ , is appropriate to a temperature of  $1,660^\circ \text{K}$ . and  $i p = 1.72 \times 10^{12} \text{ gauss/erg}$ . This value of  $E_0$  is very much smaller than the activation energy suggested by Snoek, viz.  $10,000^\circ \text{K}$ .

Equation (1) is of the same general form as that obtained by Becker and Döring (1939) in their treatment of magnetic viscosity as the analogue of dielectric after-effect. However, the importance of equation (1) lies in the fact that the constants involved are expressed in terms of quantities which are characteristic of the domain processes which lead to magnetic viscosity. Thus, although it is fairly certain that the domain processes are different for soft iron, Mn-Zn ferrite and alnico, it is of interest to compare the available values of the various constants of these three materials, assuming relation (1) to hold in each case :

	Fe*	Mn-Zn ferrite	Alnico
$C \text{ (sec}^{-1}\text{)}$	$2 \times 10^{14}$	$1.6 \times 10^{-2}$	—
$i p \text{ (gauss erg}^{-1}\text{)}$	$2.6 \times 10^{13}$	$1.7 \times 10^{12}$	$3.6 \times 10^{14}$
$E_0/k \text{ (}^\circ \text{K.)}$	10,300	1,660	15,000 (estimate)

\* From analysis of results obtained by Richter (1937) using soft iron at  $55^\circ \text{C}$ .

Snoek considers that the phenomena of magnetic viscosity and time decrease of permeability are two different aspects of identical domain processes. It follows therefore that the activation energy theory of magnetic viscosity given in I should account satisfactorily for time decrease of permeability. From preliminary experimental results using alnico specimens, it appears that the theoretical predictions are confirmed. It is hoped to publish further details of this work at a later date.

The University, Nottingham.  
12th September 1949.

R. STREET.  
J. C. WOOLLEY.

BECKER, R., and DÖRING, W., 1939, *Ferromagnetismus* (Berlin: Springer), p. 247 ff.

RICHTER, G., 1937, *Ann. Phys., Lpz.*, **29**, 605.

SNOEK, J. L., 1947, *New Developments in Ferromagnetic Materials* (Amsterdam: Elsevier), p. 55.

STREET, R., and WOOLLEY, J. C., 1949, *Proc. Phys. Soc. A*, **62**, 562.

## REVIEWS OF BOOKS

*Scientific Foundations of Vacuum Technique*, by SAUL DUSHMAN. Pp. xi + 882.  
First Edition. (New York: John Wiley; London: Chapman and Hall, 1949). 90s.

The introduction of Gaede's mercury diffusion pump marked the commencement of great advances in high-vacuum technique. A new industry—vacuum technology—has grown up, and a small-scale laboratory operation has been transformed within the past forty years into an industrial one, carried out on a scale that would have been almost inconceivable in the minds of the early workers in the field. Speed, and greater speed, is demanded for the exhaustion of all types of electronic equipment, cyclotrons, betatrons, etc., and for vacuum distillation, dehydration and the evaporation of metals and other substances. These higher speeds have been attained by paying more attention to jet design in pumps.

Only a few books have been written on the subject, and the first one to appear was that written by Dr. Dushman in 1922. The recent rapid advances have more than justified the present volume, which workers in this field have required for some time. In spite of its 882 pages, and of the fact that it contains a reference to the researches of practically every investigator in high-vacuum technique, it is no mere encyclopaedia, no catalogue of methods and results, but contains the theory which is so essential if successful operations are to be understood and appreciated. It is not only a complete revision of the earlier work, but it includes a very considerable amount of new material. The diagrams are numerous and good, and a useful feature is the copious references to original papers.

The opening chapters deal with the kinetic theory of gases and their flow through tubes and orifices, features which play important parts in high-vacuum work and which considerably affect pumping speeds. The treatment of mechanical and vapour pumps is interesting and explicit. The rôles of diffusion and condensation are discussed, and the extreme importance of jet design is fully explained. Alexander's modern type of pump is described and reasons are given why all vapour pumps do not function as diffusion ones—a conclusion which agrees with Langmuir's view on their operation. Manometers receive full treatment and the various indispensable leak detectors are included. Then follows a description of other methods whereby gases may be removed from vessels, such as the sorption of gases and vapours by solids, and in particular by activated charcoal, silicates, cellulose and metals. Diffusion through the latter and degassing problems are also fully discussed. The chapter on chemical and electrical clean-up of gases at low pressures gives a comprehensive survey of the clean-up of gases by evaporated metals, technical getters, incandescent filaments, cold and hot cathode discharges, and the production of extremely low pressures in sealed-off devices. The later chapters deal with vapour pressures, rates of evaporation and dissociation pressures—including useful information on vacuum distillation—and the deposition of films.

The book is a complete treatment of the subject, one which should be in the hands of every worker in the fields of physics, engineering and chemistry.

F. H. NEWMAN.

*Thermocinétique*, by PIERRE VERNOTTE. Pp. xxi + 459. Publications Scientifiques et Techniques du Ministère de l'Air. (Paris: Service de Documentation et d'Information Technique de l'Aéronautique, 1949.) No price.

Monsieur Vernotte is a well-known writer on thermal subjects, and those familiar with his work are aware that he does not blindly follow convention without asking the reasons for it. In this book, which deals with the subject that is sometimes described as Heat Transfer, he opens his challenge to tradition by objecting to the traditional names, and selecting eventually that of thermokinetics, so that, between them, thermokinetics and thermodynamics cover the main part of the subject of Heat.

After this, and before we begin on the main subject, we find a stimulating discussion of the question whether the unit of heat is indeed a unit of energy, and whether, therefore, many of us are right in saying that the erg or joule is the proper unit for heat quantities; the author thinks it is not, though it may be used for convenience.

The main part of the book deals with conduction, convection and radiation. In dealing with the first of these, Vernotte sets up the differential equation in the usual way, with a perfectly correct warning that it is only strictly applicable if the thermal constants do not vary with temperature. He claims also that the passage from a difference between two first derivatives to a second derivative is not really valid, though he accepts it in practice. The reviewer confesses to an inability to understand the grounds on which the objection is based.

Having set up the equation, he solves a number of problems; these are well chosen for their illustrative value or for practical use, but they do not illustrate as many methods as might perhaps have been expected in a book of this size. There is no reference to the value of conjugate function methods in two-dimensional problems, nor of the Laplace transform.

Convection is interestingly treated, and the main laws of radiation are brought out.

Altogether, as mentioned earlier, the value of the book is as a stimulus to our own thinking, rather than as a compendium of methods or results, but for its actual purpose it is an extremely successful effort.

J. H. A.

## CORRIGENDUM

"The Physical Basis of Life", by J. D. BERNAL (*Proc. Phys. Soc. A*, 1949, **62**, 537).

Page 540, last clause of footnote \*, viz.: "and secondly, they must originate and develop out of some pre-existing system, or, in plain English, they must work and they must have got there in the first place" *should occur* in the text immediately after the words "dynamic stability" (line 22).

## CONTENTS FOR SECTION B

	PAGE
Prof. E. N. DA C. ANDRADE and Mr. A. J. KENNEDY. An Automatic Recording Apparatus for the Study of Flow and Recovery in Metals . . . . .	669
Dr. H. KOLSKY. An Investigation of the Mechanical Properties of Materials at very High Rates of Loading . . . . .	676
Dr. K. W. HILLIER. A Method of Measuring some Dynamic Elastic Constants and its Application to the Study of High Polymers . . . . .	701
Prof. L. C. MARTIN. The Theory of the Microscope—IV: The Boundary-Wave Theory of Image Formation . . . . .	713
Mr. W. WEINSTEIN. Wave-front Aberrations of Oblique Pencils in a Symmetrical Optical System: Refraction and Transfer Formulae . . . . .	726
Mr. T. S. MOSS. The Temperature Variation of the Long-Wave Limit of Infra-Red Photoconductivity in Lead Sulphide and Similar Substances . . . . .	741
Reviews of Books . . . . .	749
Contents for Section A . . . . .	750
Abstracts for Section A . . . . .	751
Corrigendum . . . . .	752

## ABSTRACTS FOR SECTION B

*An Automatic Recording Apparatus for the Study of Flow and Recovery in Metals,*  
by E. N. DA C. ANDRADE and A. J. KENNEDY.

**ABSTRACT.** An apparatus is described which records continuously on photographic paper the extension-against-time curve of a metal wire creeping under stress. The length and time scales are recorded on the paper at the same time as the extension, so that deformation of the paper during development and drying does not affect the accuracy of the record, which allows an extension of up to 10 cm. to be read to within 0.02 mm. The apparatus also automatically removes and restores, repeatedly if desired, the load at times which can be set before the start of the experiment.

*An Investigation of the Mechanical Properties of Materials at very High Rates of Loading,* by H. KOLSKY.

**ABSTRACT.** A method of determining the stress-strain relation of materials when stresses are applied for times of the order of 20 microseconds is described. The apparatus employed was a modification of the Hopkinson pressure bar, and detonators were used to produce large transient stresses. Thin specimens of rubbers, plastics and metals were investigated and the compressions produced were as high as 20% with the softer materials. It was found that whilst Perspex recovered almost as soon as the stress was removed, rubbers and polythene showed delayed recovery, and copper and lead showed irrecoverable flow. The phenomenon of delayed recovery is discussed in terms of the theory of mechanical relaxation and *memory* effects in the material.

*A Method of Measuring some Dynamic Elastic Constants and its Application to the Study of High Polymers*, by K. W. HILLIER.

**ABSTRACT.** The preliminary work on the measurement of velocity of propagation and attenuation of longitudinal sound oscillations in high polymer filaments already described by Hillier and Kolsky has been continued. It was concluded in that paper that temperature control would be advantageous, and that by varying the temperature and the frequency of oscillations more useful information could be acquired. An apparatus is described whereby the velocity of the propagation and attenuation of longitudinal oscillations throughout the range  $0^{\circ}$  to  $50^{\circ}$  C. and 500 c/s. to 30 kc/s. can be measured. The results obtained with one material, polythene, are discussed in terms of several theories of the elasticity of high polymers, and the constants of the several equations considered are calculated from the data.

*The Theory of the Microscope—IV: The Boundary-Wave Theory of Image Formation*, by L. C. MARTIN.

**ABSTRACT.** The theory of boundary waves (Young, Rubinowicz, and others) is developed for the two-dimensional case and applied to discuss image formation for small apertures, obstacles and phase-retarding laminae. The theoretical predictions are illustrated by diffraction photographs. It is hoped thus to contribute towards a fuller understanding of microscope images for bright-field, dark-field and phase-contrast conditions.

*Wave-front Aberrations of Oblique Pencils in a Symmetrical Optical System: Refraction and Transfer Formulae*, by W. WEINSTEIN.

**ABSTRACT.** The wave-front aberrations which occur in a pencil traversing a symmetrical optical system at a finite field angle are defined in a new way. Refraction and transfer formulae are derived for all the aberration coefficients up to and including those depending on the fourth power of the aperture of the pencil.

*The Temperature Variation of the Long-Wave Limit of Infra-Red Photoconductivity in Lead Sulphide and Similar Substances*, by T. S. MOSS.

**ABSTRACT.** Measurements have been carried out on the spectral distribution of the photoconductive effect in layers of lead sulphide, selenide and telluride, at temperatures ranging from room temperature to that of liquid hydrogen. It is shown that cooling has a marked effect on the long-wave limit of sensitivity, which increases by as much as two microns on cooling with liquid hydrogen.

Brief descriptions of spectral measurements on these materials have already been published by the author. It is shown that depopulation of energy levels due to thermal activation of electrons is not responsible for the shift of spectral sensitivity. The suggestion is made that the shift may be related to the variation of dielectric constant with temperature.

# THE PROCEEDINGS OF THE PHYSICAL SOCIETY

## Section A

---

VOL. 62, PART 12

1 December 1949

No. 360 A

---

### Radiative Reaction and Damping in Scattering

By J. HAMILTON

Manchester University

*Communicated by I. Rosenfeld ; MS. received 14th June 1949*

**ABSTRACT.** The higher order radiative corrections and the damping corrections to the cross section for the scattering of an electron by an electrostatic potential are investigated. It is shown that the perturbation treatment of the radiative corrections at high frequencies joins on to the Bloch-Nordsieck solution for low frequencies. The damping effect arising from the low frequency photons is shown to be negligible, and a modified damping equation is proposed which gives a smooth transition to the damping correction in passing from high to low frequency photons.

#### §1. INTRODUCTION AND SUMMARY

THE emission of low frequency photons during the scattering of an electron by an electrostatic potential has been described by Bloch and Nordsieck (1938), Pauli and Fierz (1938) and others. The method used by these authors suffers from the disadvantage that the upper limit,  $K$ , to the low frequency range considered enters into the final result. The simultaneous emission of high frequency photons can be treated by the ordinary perturbation methods, but the defect remains, for the frequency  $K$  dividing the 'low' from the 'high' frequency photons appears in the cross sections.

It might seem that radiation damping theory could resolve this difficulty. The damping due to the high frequency photons has been discussed by Bethe and Oppenheimer (1946), and it is shown below that the damping due to the low frequency photons is negligible. The resultant total damping effect, though of the right sign, has the wrong dependence on the scattering potential  $V$  to cancel the undesirable effect.

The arbitrary dependence of the cross sections on  $K$  is connected with the fact that, as a result of the Bloch-Nordsieck transformation, the 'free' photon states are modified due to the presence of the electron. At the same time the total Hamiltonian has been separated into an electron and a field part, and the electron part contains a portion of the electron's self energy. Dancoff (1939) studied the corresponding modified 'free' electron and photon states for the high frequency region, but he obtained expressions containing high frequency divergencies. Lewis (1948), Epstein (1948), and Koba and Tomonaga (1948) have shown how Dancoff's results can be made to give finite expressions by subtracting the electron's self energy. The resultant correction to the cross section for scattering without the emission of radiation, which we will call the



radiative reaction effect, is difficult to calculate. It will, however, be shown in the first part of this paper that this reactive effect for the high frequency photons has a complementary dependence on the dividing frequency  $K$  to that of the low frequency photon component, so that  $K$  itself drops out of the cross sections. Further, it is possible to make a rough estimate of the size of the correction to the cross section, and it is seen that the correction is small for a wide range of problems.

The question now arises as to whether there is also a damping correction to the cross section. The mass and charge renormalizing methods have actually enabled the finite, and significant, parts of the matrix elements arising from higher order virtual transitions to be calculated. At the same time they have renormalized the initial and final wave functions. The resultant total matrix elements could be used in a perturbation calculation of the cross sections. However, damping theory goes further in ensuring that the transition probabilities are normalized, so that the rate of decrease of the initial state equals the rate of increase of all the final states. Alternately, in the steady state solution, that particular solution representing the initial state plus outgoing final states is chosen. It thus seems that, even with the new matrix elements resulting from the renormalizing method, damping may give a further correction in calculating the cross sections.

In § 4 the damping effects are investigated using the Bloch-Nordsieck method for low frequency photons, and the ordinary perturbation method (without Dancoff's modified states) for high frequency photons. It appears that the low frequency photons contribute practically no damping, a fact which might have been guessed from the small energy and momentum emitted in the low frequency range. The separation of the Hamiltonian into an electron and a photon component is, in fact, the real cause.

The damping due to the high frequency photons, however, is not satisfactory because the dividing frequency  $K$  again appears in the result. In § 5 a possible method of avoiding this difficulty is discussed. It is, after all, inconsistent to treat the damping due to the high frequency photons without using Dancoff's modified states. The consequent treatment of the damping for transitions between these new 'free' electron and photon states has not been completely investigated. It is probable that the infinities which are neglected in obtaining the damping solution will be replaced by small finite corrections. However, some considerations are made on the effect of the lower frequency photons, and a modified form of damping equation is given in which the dependence of the damping correction on the lower limit of the high frequency photon range is eliminated.

In the Appendix the subtraction method due to Heitler and Peng (1942) is applied to the low frequency photon problem. It is shown that, unless the Bloch-Nordsieck transformation is used, the method is unsatisfactory, as it implies that the low frequency photons produce very strong damping of the electron's motion.

Finally it is worth emphasizing that the satisfactory solutions which have been obtained in the new representations seem to imply some special property of this representation. It may of course be possible, by calculating all the higher order effects, to show that these solutions are, in some way, equivalent to those calculated in any other representation, as would be the case with a system of a finite number of degrees of freedom.

## § 2. THE RADIATIVE REACTION

The Bloch–Nordsieck transformation can be expressed conveniently by Jost's (1947) formalism. The Hamiltonian of the system of electron, scatterer and radiation can be written

$$H = (\boldsymbol{\alpha} \cdot \mathbf{p}) + \beta m + \sum_s (\boldsymbol{\alpha} \cdot \mathbf{a}_s) [q_s \exp \{i(\boldsymbol{\kappa}_s \cdot \mathbf{x})\} + \text{complex conjugate}] + V(\mathbf{x}) + \sum_s n_s \kappa_s, \quad \dots \dots (1)$$

where  $\mathbf{p}$  is the electron's momentum,  $m$  its mass and  $\boldsymbol{\alpha}$ ,  $\beta$  the Dirac matrices.  $V(\mathbf{x})$  is the electrostatic scattering potential, and  $n_s$ ,  $q_s$  are the photon occupation numbers and amplitudes.  $\mathbf{a}_s = \mathbf{e}_s \cdot e \sqrt{(2\pi/L^3 \kappa_s)}$ , where  $\mathbf{e}_s$  is a polarization vector and  $L$  the linear dimension of the enclosing periodic box. Also,  $\hbar = c = 1$ .

The canonical transformations  $F' = S_1^{-1} \cdot F \cdot S_1$ ,  $F'' = S_2^{-1} \cdot F' \cdot S_2$  are applied to the low frequency photons, defined by  $\bar{\kappa} \leq \kappa_s \leq K$ , where  $\bar{\kappa} = 2\pi/L$  is the least frequency allowed by the box. Using  $S_1 = \exp \{i \sum_s n_s (\boldsymbol{\kappa}_s \cdot \mathbf{x})\}$ ,

$$S_2 = \exp \{ \sum_s \eta_s \cdot (\bar{q}'_s - q'_s) \},$$

where  $\bar{q}$  is the Hermetian conjugate of  $q$ , and

$$\eta_s(\mathbf{p}) = \frac{(\mathbf{p}' \cdot \mathbf{e}_s)}{E' - (\mathbf{p}' \cdot \boldsymbol{\kappa}_s)/\kappa_s} (2\pi e^2)^{\frac{1}{2}} (\bar{\kappa}'/\kappa_s)^{\frac{1}{2}} \quad \dots \dots (2)$$

gives

$$\begin{aligned} H''(\mathbf{p}'', \mathbf{x}'', q_t, n_s'', \boldsymbol{\alpha}) &= H(\mathbf{p}, \mathbf{x}, q_t, q_s, \boldsymbol{\alpha}) \\ &= (\boldsymbol{\alpha} \cdot \mathbf{p}'') \left( +\beta m + V(\mathbf{x}'') + \sqrt{2} \sum_s \frac{\partial \eta_s}{\partial \mathbf{p}} P''_s \right) + \sum_t n_t \kappa_t \\ &\quad + \sum_t \{ (\boldsymbol{\alpha} \cdot \mathbf{a}_t) q_t \exp \{i(\boldsymbol{\kappa}_t \cdot \mathbf{x}'')\} + \text{complex conjugate} \} \\ &\quad + \sum_s \{ \mathbf{p}'' \cdot \boldsymbol{\kappa}_s \} [n''_s + \eta''_s] E'' + \text{small terms} \dots \dots \dots (3) \end{aligned}$$

where  $P''_s = (i/\sqrt{2})(q''_s - \bar{q}''_s)$ ,  $\{\mathbf{p} \cdot \boldsymbol{\kappa}\} = E\kappa - (\mathbf{p} \cdot \bar{\boldsymbol{\kappa}})$ , and  $E = (m^2 + p^2)^{\frac{1}{2}}$ .  $t$  refers to high and  $s$  to low frequency photons. The omitted terms are  $-\sum_s (\boldsymbol{\alpha}_1 \cdot \mathbf{a}_s)(q''_s + \bar{q}''_s)$ , where  $\boldsymbol{\alpha}_1 = \boldsymbol{\alpha} - \mathbf{p}''/E''$ , plus terms arising from the recoil of the electron during the emission of the low frequency photons. Solving the wave functions for  $H''$  omitting  $V$ , and transforming back to the  $H'$  system, gives, for example,  $\phi_{(in)} = \phi_i \cdot \Pi_s h_{n_s}(Q'_s - \sqrt{2} \cdot \eta_s(\mathbf{p}_i))$ , where  $\phi_i$  is the wave function of an electron of momentum  $\mathbf{p}_i$ , while  $h_n(Q_s)$  is the free photon wave function, and  $Q'_s = (q'_s + \bar{q}'_s)/\sqrt{2}$ . Then, using the Born approximation, the matrix element for scattering and low frequency emission is  $V_{ki} \Pi_s (m_s \mathbf{p}_k | n_s \mathbf{p}_i)$ , where

$$(m_s \mathbf{p}_k | n_s \mathbf{p}_i) = \exp \{ -z v^2(k, i)/2 \} \sqrt{(m_s! / n_s!)} \sum_{\mu=0}^{\infty} \frac{[w(k, i)]^{m_s - n_s + 2\mu} \cdot (-)^{\mu}}{(n_s - \mu)! \mu! (m_s - n_s - \mu)!}, \quad \dots \dots (4)$$

with  $w(k, i) = \eta_s(\mathbf{p}_k) - \eta_s(\mathbf{p}_i)$  and  $1/\sigma! = 0$ , if  $\sigma < 0$  (cf. Pauli and Fierz 1938).  $V_{ki}$  is the potential matrix element.

The term  $-(\boldsymbol{\alpha}_1 \cdot \mathbf{a}_s)(q''_s + \bar{q}''_s)$  gives further low frequency photon transitions, such as two photon emission, scattering etc. The corresponding transition probabilities are of the order  $\rho_k |V_{ki}|^2 (e^2 K/m)^N$ , where  $N$  is the number of photons emitted or absorbed and  $\rho_k$  the state density. This effect is negligible if  $K \ll m$ , while the omitted recoil terms are small provided  $K \ll |\mathbf{p}|$ , the electron's momentum.

For a finite periodic box the probability of scattering from  $\mathbf{p}$  to  $\mathbf{q}$  without the emission of any photons is, approximately,

$$\rho_q |V_{qp}|^2 \exp \left\{ -\frac{2}{3\pi} \frac{(\mathbf{p}-\mathbf{q})^2}{m^2} \log(K/\bar{\kappa}) \right\}$$

Other transition probabilities, such as that for the emission of any number of low frequency photons  $\kappa_s$ , such that  $\kappa_s \leq K' < K$ , will depend on  $K$  in a similar fashion. Increasing  $K$  to  $K + dk$  gives (for relativistic or slow electrons)

$$d\sigma/\sigma = -(e^2/4\pi^2)K dk \int d\Omega_{\kappa} \{(\mathbf{P}-\mathbf{Q})^2 - (\mathbf{P}-\mathbf{Q} \cdot \hat{\kappa})^2\}, \quad \dots \dots (5)$$

where  $\mathbf{P} = \mathbf{p}/\{\mathbf{p} \cdot \mathbf{K}\}$ , and  $\hat{\kappa}$  is a unit vector which is to be integrated over  $d\Omega_{\kappa}$ .  $d\sigma/\sigma$  is the relative change in the cross section concerned. Treating high frequency photons by the conventional perturbation methods also leads to (5) for the relative change in cross section on varying  $K$ .

The arbitrary factor  $K$  enters the cross sections because the initial and final wave functions for the low frequency photons are, in the  $H'$  system,  $h_n(Q'_s - \sqrt{2} \cdot \eta_s)$ , while those for the high frequency photons are  $h_n(Q'_l)$ . Dancoff (1939) has tried to rectify this asymmetry by using perturbation theory to find the field of high frequency photons which accompanies a freely moving electron, due to the effect of the electron's charge on the vacuum. In fact he tries to find that eigenfunction of

$$H = (\boldsymbol{\alpha} \cdot \mathbf{p}) + \beta m + \sum_l \{(\boldsymbol{\alpha} \cdot \mathbf{a}_l) q_l \exp \{i(\boldsymbol{\kappa}_l \cdot \mathbf{x})\} + \text{complex conjugate}\} + \sum_l m_l \kappa_l,$$

which reduces to a free electron wave function as  $e^2 \rightarrow 0$ . Using such wave functions he calculates the change in the cross section for radiationless scattering. His calculations have been elaborated and corrected by Ito, Koba and Tomonaga (1948), who get

$$\left(\frac{\delta\sigma}{\sigma_0}\right)_{e^2} = -\frac{3e^2}{4\pi} \int \frac{dl}{l} + \frac{3e^2}{2\pi} \frac{m^2(\mathbf{p}-\mathbf{q})^2}{E^2\{E^2 + (\mathbf{p} \cdot \mathbf{q}) + m^2\}} \int^\infty \frac{dk}{k} + \text{finite terms.} \quad (6)$$

The integration over  $l$  refers to electron momenta, and is a vacuum polarization effect, while the  $k$  integration arises from virtual photon processes. It is assumed that the scattering potential is electrostatic. Lewis (1948), Epstein (1948) and Koba and Tomonaga (1948) have shown how the infinite terms can be subtracted. The latter authors write the total Hamiltonian in the form

$$\begin{aligned} H &= \int \bar{\Psi}\{(\boldsymbol{\alpha} \cdot \mathbf{p}) + \beta m\}\Psi d\mathbf{x} + H_{\text{radiation}} + H_{\text{interaction}} \\ &= \int \bar{\Psi}\{(\boldsymbol{\alpha} \cdot \mathbf{p}) + \beta \hat{m}\}\Psi d\mathbf{x} + H_{\text{rad.}} + \hat{H}_{\text{int.}}, \end{aligned}$$

where  $\hat{m} = m + \delta m$  and  $\hat{H}_{\text{int.}} = H_{\text{int.}} - \delta m \int \bar{\Psi}\beta\Psi d\mathbf{x}$ .  $\delta m$  is the electromagnetic self energy of the electron (to order  $e^2$ ) as calculated by Weisskopf (1939) viz.,

$$\delta m = \frac{3}{2\pi} e^2 m \{ \log [(k_\infty + (k_\infty^2 + m^2)^{1/2})/m] - \frac{1}{2} \},$$

where  $k_\infty \rightarrow \infty$ .  $\overset{0}{m}$  is thus the observed electron mass, to order  $e^2$ . The  $\bar{\Psi}, \Psi$  are quantized electron waves,  $H_{\text{rad.}} = \sum_{\nu} n_{\nu} \kappa_{\nu}$ , while

$$H_{\text{int.}} = e \int \bar{\Psi} \alpha \Psi \cdot \sum_{\nu} \{ \mathbf{a}_{\nu} q_{\nu} \exp \{ i(\mathbf{x}_{\nu} \cdot \mathbf{x}) \} + \text{complex conjugate} \} d\mathbf{x} \\ + \frac{e^2}{2} \iint \bar{\Psi}(\mathbf{x}) \Psi(\mathbf{x}) \frac{1}{|\mathbf{x} - \mathbf{x}'|} \bar{\Psi}(\mathbf{x}') \Psi(\mathbf{x}') d\mathbf{x} d\mathbf{x}'.$$

The mass renormalizing term  $-\delta m \cdot \int \bar{\Psi} \beta \Psi d\mathbf{x}$  contributes a correction to the cross section for the scattering from  $\mathbf{p}$  to  $\mathbf{q}$ . For example, this  $\delta m$  term creates an electron pair, denoted by  $\mathbf{q}, (-\mathbf{q})^+$ , and subsequently the potential  $V$  annihilates  $\mathbf{p}$  and  $(-\mathbf{q})^+$ . The resultant correction is

$$\left( \frac{\delta \sigma}{\sigma_0} \right)_m = -\delta m \cdot \frac{\overset{0}{m}(\mathbf{p} - \mathbf{q})^2}{E^2 \{ E^2 + (\mathbf{p} \cdot \mathbf{q}) + m^2 \}}$$

where  $\overset{0}{E} = (\overset{0}{m}^2 + \mathbf{p}^2)^{1/2}$ . Using (6) and the value of  $\delta m$  above, it is clear that the infinite term in  $k$  no longer appears in  $(\delta \sigma / \sigma_0)_{e^2} + (\delta \sigma / \sigma_0)_m$ . Koba and Tomonaga also discuss how the vacuum polarization infinity can be counteracted by re-defining an observed potential  $\overset{0}{V}(\mathbf{x})$ .

It is now of interest to see whether the remaining finite radiative reaction will eliminate the difficulties arising from the arbitrariness of  $K$  in the Bloch-Nordsieck transformation. When the Bloch-Nordsieck transformation is applied to photons such that  $\kappa_s < K$ , Dancoff's procedure will have to be modified.

Following Ito, Koba and Tomonaga (1948) we see that the free electron state  $\Psi_p$  interacts to order  $e$  with the states  $\Psi_p^{(i)}(\mathbf{p} - \mathbf{k}, \tilde{\mathbf{k}})$ ,  $\Phi_p^{(i)}(\mathbf{p}, \mathbf{l}, (-\mathbf{l} + \mathbf{k})^+, -\tilde{\mathbf{k}})$ , where  $\mathbf{l}$  indicates an electron,  $(-\mathbf{l})^+$  a positron and  $\tilde{\mathbf{k}}$  a photon. The wave function  $\Phi_p^{(i)}$  is given by an operator of the type  $\lambda_{1-\mathbf{k}}^-(\alpha \cdot \mathbf{e}) \lambda_1^+ / \{ E(\mathbf{l}) + E(\mathbf{l} - \mathbf{k}) + k \}$ , where  $\lambda_{\mathbf{p}}^{\pm} = \{ E(\mathbf{p}) \pm (\alpha \cdot \mathbf{p}) \pm \beta m \} / 2E(\mathbf{p})$ , and  $E(\mathbf{p}) = (m^2 + \mathbf{p}^2)^{1/2}$ . This will be practically unaltered in the form  $\lambda_{1-\kappa_s}^-(\alpha_1 \cdot \mathbf{e}_s) \lambda_1^+ / \{ E(\mathbf{l}) + E(\mathbf{l} - \mathbf{x}_s) + \kappa_s \}$ , where  $\alpha_1 = \alpha - \mathbf{p} / E$  replaces  $\alpha$  for photons  $\kappa_s$  such that  $\bar{\kappa} \leq \kappa_s < K$ . In fact,  $\lambda_{1-\kappa}^-(\mathbf{l} / E(\mathbf{l})) \lambda_1^+$  gives a contribution  $O(K/E(\mathbf{l}))$ , while  $\lambda_{1-\kappa}^-(\alpha \cdot \mathbf{e}) \lambda_1^+$  gives  $O(1)$ . On the other hand, the state  $\Psi_p^{(i)}(\mathbf{p} - \mathbf{k}, \tilde{\mathbf{k}})$  does not arise for  $\kappa_s < K$ , as there are no transitions of order  $e$  between positive energy states when the Bloch-Nordsieck wave functions are used. The states of order  $e^2$  are reached either through  $\Psi_p^{(i)}$  or  $\Phi_p^{(i)}$ , or directly from  $\Psi_p$  through the Coulomb interaction between electrons. This interaction is unaltered by the Bloch-Nordsieck transformation. Finally, there is the renormalization connection for the wave function  $\Psi_p$ . To order  $e^2$  this arises from  $|\Psi_p^{(i)}|^2$  and  $|\Phi_p^{(i)}|^2$  only.

The amount by which the finite reactive terms will be modified on altering the dividing frequency from  $K$  to  $K + dk$  can now easily be estimated. The important effects arise from  $\int d\mathbf{k} (\bar{\Psi}_q^{(i)}(\mathbf{q} - \mathbf{k}, \tilde{\mathbf{k}}) V \Psi_p^{(i)}(\mathbf{p} - \mathbf{k}, \tilde{\mathbf{k}}))$ , and the renormalization correction  $\Psi_{p(n)}^{(ii)} = -\frac{1}{2} \int d\mathbf{k} |\Psi_p^{(i)}(\mathbf{p} - \mathbf{k}, \tilde{\mathbf{k}})|^2$ , giving  $(\bar{\Psi}_{q(n)}^{(ii)} V \Psi_p)$  and  $(\bar{\Psi}_q V \Psi_{p(n)}^{(ii)})$ . The first gives, in the range  $K, K + dk$ ,

$$I \left( \frac{\delta \sigma}{\sigma_0} \right)_A = \frac{e^2}{2\pi^2} \cdot \int_K^{K+dk} d\mathbf{k} \cdot \sum_{\text{pol.}} \frac{\text{Spur} \{ \lambda_{\mathbf{p}}^+ V \lambda_{\mathbf{q}}^+(\alpha \cdot \mathbf{e}) \lambda_{\mathbf{q}-\mathbf{k}}^+ V \lambda_{\mathbf{p}-\mathbf{k}}^+(\alpha \cdot \mathbf{e}) \}}{\{ E(\mathbf{p}) - E(\mathbf{p} - \mathbf{k}) - k \} \{ E(\mathbf{q}) - E(\mathbf{q} - \mathbf{k}) - k \} \cdot \text{Spur} \{ \lambda_{\mathbf{p}}^+ V \lambda_{\mathbf{q}}^+ V \}}.$$

$\Sigma$  indicates the sum over photon polarizations. Expanding in powers of  $K/m$  or  $K/E$ , both of which are very small, gives

$$d(\delta\sigma/\sigma_0)_A \simeq (e^2/2\pi^2)K dk \int d\Omega_k \{(\mathbf{P} \cdot \mathbf{Q}) - (\mathbf{P} \cdot \hat{\mathbf{x}})(\mathbf{Q} \cdot \hat{\mathbf{x}})\}$$

where  $\mathbf{P}, \mathbf{Q}$  are defined above. Similarly the renormalization terms give

$$d\left(\frac{\delta\sigma}{\sigma_0}\right)_n = -\frac{1}{2}\left(\frac{e^2}{4\pi^2}\right) \int_K^{K+dk} d\mathbf{k} \cdot \sum_{\text{pol.}} \frac{\text{Spur}\{\lambda_{\mathbf{p}}^+(\boldsymbol{\alpha} \cdot \mathbf{e})\lambda_{\mathbf{p}-\mathbf{k}}^+(\boldsymbol{\alpha} \cdot \mathbf{e})\}}{\{E(\mathbf{p}) - E(\mathbf{p}-\mathbf{k}) - k\}^2 \cdot k} + \langle \mathbf{p}, \mathbf{q} \rangle,$$

where  $\langle \mathbf{p}, \mathbf{q} \rangle$  is the same expression with  $\mathbf{p}$  exchanged for  $\mathbf{q}$ . Thus

$$d(\delta\sigma/\sigma_0)_n \simeq -(e^2/4\pi^2)K dk \int d\Omega_k \{\mathbf{P}^2 + \mathbf{Q}^2 - (\mathbf{P} \cdot \hat{\mathbf{x}})^2 - (\mathbf{Q} \cdot \hat{\mathbf{x}})^2\}.$$

Hence

$$d(\delta\sigma/\sigma_0)_A + d(\delta\sigma/\sigma_0)_n = -(e^2/4\pi^2)K dk \int d\Omega_k \{(\mathbf{P} - \mathbf{Q})^2 - (\mathbf{P} - \mathbf{Q} \cdot \hat{\mathbf{x}})^2\} + \text{small terms} \dots\dots\dots (7)$$

The small terms in (7) are of the order of  $K/m$  times the main contribution. For non-relativistic electrons (7) reduces to  $-(2e^2/3\pi)\{(\mathbf{p} - \mathbf{q})^2/m^2\}dk/K$ .

The other terms  $(\delta\sigma/\sigma_0)$  of order  $e^2$  which arise from virtual photon processes are of the same general form as  $(\delta\sigma/\sigma_0)_A$  (cf. Ito, Koba and Tomonaga 1948). The spur in the numerator is of the same order as the spur in the denominator, while the denominator also contains the factor  $k$  and two energy differences. In order to get a result of order  $dk/K$  it is necessary for both energy differences to be of order  $K$ , and this can only arise from transitions between positive energy states, and hence only from  $\Psi_p^{(i)}(\mathbf{p} - \mathbf{k}, \tilde{\mathbf{k}})$ , or  $\Psi_q^{(i)}(\mathbf{q} - \mathbf{k}, \tilde{\mathbf{k}})$ .

Finally, there are the vacuum polarization terms and the self energy to be considered. The vacuum polarization terms are only influenced by the Bloch-Nordsieck transformation when  $|\mathbf{p} - \mathbf{q}| < K$ , and then the effect is negligible for the general reasons stated above. The effect on the self energy can be estimated from the self energy separated off by the Bloch-Nordsieck method. For a non-relativistic electron this is of the order of  $e^2(p/m)^2 K$ . The resultant change in the infinite balancing contribution  $(\delta\sigma/\sigma_0)_m$  is of the order  $\{(\mathbf{p} - \mathbf{q})^2/m^2\}(p/m)^2 K/m$ , which is thus  $K/m$  times the main terms considered. The situation is similar for a relativistic electron.

Comparing (7) and (5) it follows that an increase in  $K$  decreases the cross section as calculated by Bloch and Nordsieck, and increases, by the same amount, the high frequency radiative correction so that  $\partial\sigma/\partial K = 0$ . Thus, to the order  $e^2$  considered,  $K$  no longer enters the final results. The only limitation is that  $K \ll m$ . The small corrections in  $K/m$  can doubtless be eliminated by a more exact treatment. It is also interesting to note that the radiative reaction would give an infra-red divergence in  $(\delta\sigma/\sigma_0)_e$ , if the Bloch-Nordsieck transformation were not applied to the low frequency photons.

It seems to be almost certain that the same treatment will avoid the arbitrariness due to  $K$  in other problems, such as Jost's (1947) treatment of Compton scattering. Finally it should be mentioned that Tati and Tomonaga (1948) have proposed a relativistic generalization of the Bloch-Nordsieck transformation, using the subtraction methods. However, they have not published any precise details of the method to date.

## § 3. THE MAGNITUDE OF THE RADIATIVE CORRECTION

In this section only that part of the reaction which is due to virtual photon processes will be considered. The remainder is the vacuum polarization effect, and will not be discussed here. The exact evaluation of the various terms in  $(\delta\sigma/\sigma_0)$  would be tedious, but it is readily possible to make a rough estimate of the size of the effect, following the formulae of Ito, Koba and Tomonaga. For lower frequencies  $k$  such that  $K < k \ll m$ , the prominent terms are given in the preceding section. For  $k \gg E$ , the electron's energy, those terms which do not converge are of the order of  $e^2\{\log(k_\infty/E) + O(1)\}$  where  $k_\infty$  is the upper limit of the virtual photon integration, which tends to infinity. Subtracting a similar term, giving the effect of the electron self energy, leaves the finite term  $e^2\theta(1)$ . Now it is only necessary to note that the various integrands occurring in  $(\delta\sigma/\sigma_0)$  have the form  $O(e^2/E)$  in the region  $k \sim E$ . It follows that a rough approximation to the finite radiative reaction is  $(\delta\sigma/\sigma_0)_{\text{fin}} \sim O(e^2 \log(E/K))$ , where  $E$  is the relativistic energy of the electron, while  $K$  is the frequency dividing the low from the high frequency photons (this formula overestimates the effect for the lower frequencies when the electron is non-relativistic).

If we can choose  $K$  such that both  $K \ll m$  and  $e^2 \log(E/K) \ll 1$  are satisfied, then the radiative reaction is a small effect (to order  $e^2$ ), and it is sufficient to use perturbation theory for its computation. The limitation on  $E$  is not of practical importance.

It is of interest to see if anything can be deduced about the physical interpretation of the modified cross section analogous to the well-known interpretation of the Bloch-Nordsieck results. For a non-relativistic electron it is clear that if photons of frequency less than  $K$  are neglected, the reactive term for an appreciable energy range behaves like

$$-(2/3\pi)\sigma_0 e^2 \{(\mathbf{p}-\mathbf{q})^2/m^2\} \int_K dk/k.$$

Thus, in this range, the cross section for radiation free scattering is decreased by an amount which is just the total cross section for the emission of one photon. (The emission of more than one photon would have to be compared with terms in  $e^4$  in  $\delta\sigma$ .)

About the higher frequency part ( $k \sim m$ ) of the reaction little can be said without calculating the exact form of  $\delta\sigma$ . However, the ratio of the total probability of the emission of one photon of frequency greater than  $K$  to the scattering probability is, for a relativistic electron, of the order of  $e^2 \log(E/K)$ . This is, according to the rough estimate made above, just the order of  $(\delta\sigma/\sigma_0)_{\text{fin}}$ . Nevertheless the simple interpretation of the correction to the scattering cross section as being the total probability of emission of a photon must break down for two reasons: (i) there are high frequency terms in the radiative reaction which cannot be compared with any real emission; (ii) the emission of a high frequency photon  $k \sim |\mathbf{p}|$  no longer leaves the electron's motion practically unaltered.

## § 4. DAMPING EFFECTS

The damping effects can be readily found on introducing the Bloch-Nordsieck transformation for  $\bar{\kappa} < \kappa_s < K$ , where  $K \ll m$ , and  $\bar{\kappa} = 2\pi/L$  is the least frequency allowed by the finite size of the periodic box. First we will consider the case of a slowly moving electron, with momentum  $\mathbf{p}$  satisfying  $|\mathbf{p}| \ll m$ , so that all the

emitted photons can be treated by the Bloch–Nordsieck method. The simplest form of the damping equation in linear momentum representation is thus

$$U_{mq, np} = H_{mq, np} - i\pi \Pi_s \Sigma_{n'_s} \int H_{m_s q, n'_s p'} \rho_{p'} U_{n'_s p', np}, \quad \dots \dots (8)$$

where  $p, q$  refer to the initial and final electron states, while  $n_s, m_s$  are the numbers of photons of type  $\kappa_s$  in the initial and final states respectively. Also  $H_{mq, np} = \Pi_s(m_s \mathbf{q} | n_s \mathbf{p}) \cdot V_{qp}$ , where  $V_{qp}$  is the matrix element of the scattering potential and  $(m_s \mathbf{q} | n_s \mathbf{p})$  is given by (4).  $\rho_{p'}$  is the state density function. Letting  $e^2 \rightarrow 0$ , equation (8) gives

$$U_{q, p} = V_{qp} - i\pi \int V_{qp'} \rho_{p'} U_{p' p}. \quad \dots \dots (9)$$

It has been shown in another paper (Hamilton 1949 a) that (9) gives an accurate description of the collision (when  $e \rightarrow 0$ ) only when  $V$  is small. Precisely, if  $V_{qp}$  is not strongly dependent on the direction of  $\mathbf{p}$  or  $\mathbf{q}$ , the condition is

$$\rho_p |V_{pq}| \ll 1. \quad \dots \dots (10)$$

This condition will be assumed. (10) is also a necessary condition for the validity of the Born approximation; and it must be expected that the equations (8) in linear momentum representation, which essentially implies the Born approximation, will only be valid under this condition. Equation (8) can be solved by making the substitution  $U_{mq, np} = \Pi_s(m_s \mathbf{q} | n_s \mathbf{p}) \cdot \mathbf{U}_{qp}$ , where the low frequency photons no longer appear in  $\mathbf{U}_{qp}$ . Using the relation (cf. Pauli and Fierz 1938)

$$\Sigma_{n'_s} (m_s \mathbf{q} | n'_s \mathbf{p}') (n'_s \mathbf{p}' | n_s \mathbf{p}) = (m_s \mathbf{q} | n_s \mathbf{p}) \quad \dots \dots (11)$$

the solution is

$$\mathbf{U}_{q, p} = V_{qp} - i\pi \int V_{qp'} \rho_{p'} \mathbf{U}_{p' p}. \quad \dots \dots (12)$$

This solution is obtained by neglecting the recoil and the energy of the low frequency photons. The difficulties arising out of neglecting the energy of the low frequency photons, which were pointed out by Pauli and Fierz (1938), will not be discussed. That part of the interaction between the electron and the radiation field which is neglected in making the Bloch–Nordsieck transformation, and which was discussed in §2, will give a small correction to (12) of the relative order of  $(e^2 K/m)^2$ .

Equation (12) is equivalent to equation (9), so that the low frequency photons give rise to a negligible damping effect. Further, what small effect there is arises from the photons at the higher end of the frequency range  $K$ . From a correspondence principle argument it is not surprising that the large or infinite (case  $\kappa \rightarrow 0$ ) number of low frequency photons produces no appreciable damping effect. The emission of photons of very low frequency is almost a continuous process, so that classical theory can be used with little error. This gives  $E(\kappa) d\kappa = (2e^2/3\pi) \cdot (\mathbf{v} - \mathbf{w})^2 \cdot d\kappa$  for the emitted energy distribution  $E(\kappa) d\kappa$ , where  $\mathbf{v}, \mathbf{w}$  are the initial and final velocities and  $\kappa$  is the frequency of the emitted radiation. This relation holds so long as the frequency  $\kappa$  is less than the reciprocal of the 'collision time'. The reaction due to the emitted radiation must depend on the energy taken from the electron (and scatterer) by the radiation. However, as the integrated energy depends linearly on the range of integration, this reaction is negligible in some small frequency range containing the infinity of photons. As the frequency range increases, the reaction is no longer vanishingly small,

and some damping effect will arise. From the quantum mechanical viewpoint the absence of damping is due to the separation of the electron and low frequency photon variables in the Hamiltonian. This separation is, of course, complete only in the case of infinitesimally small quanta.

The damping of collisions in which high frequency photons may be emitted has been treated by Bethe and Oppenheimer (1946). For convenience they assume that only one photon is emitted, and consequently their results are only valid under the condition  $e^2 \log(T/K) \ll 1$ , where  $T$  is the initial kinetic energy of the electron and  $K$  is the lower limit of frequency of the photons considered. If at the same time  $K \ll m$ , photons of frequency less than  $K$  can be treated by the Bloch-Nordsieck method. The generalization of equation (8) (omitting an unimportant term) is

$$\left. \begin{aligned} U_{mq, np} &= H_{mq, np} - i\pi \Pi_s \sum_{n'_s} \int H_{m_s q, n'_s p'} \rho_{p'} U_{n'_s p', n_s p} \\ &\quad - i\pi \Pi_s \sum_{n'_s} \int H_{m_s q, n'_s p' j'} \rho_{p'} \rho_{j'} U_{n'_s p' j', n_s p} \\ U_{mqj, np} &= H_{mqj, np} - i\pi \Pi_s \sum_{n'_s} \int H_{m_s qj, n'_s p'} \rho_{p'} U_{n'_s p', n_s p} \\ &\quad - i\pi \Pi_s \sum_{n'_s} \int H_{m_s qj, n'_s p' j'} \rho_{p'} \rho_{j'} U_{n'_s p' j', n_s p} \end{aligned} \right\} \dots\dots (13)$$

$n, m$  refer to low frequency quanta and  $j, j'$  to high frequency quanta. The integrations are to be taken over states whose energy equals the initial energy, and  $\rho_{p'}, \rho_{j'}$  are the density functions. The integrations over the high frequency photons go from  $K$  to  $T$ .

Substituting  $H_{mq, np} = \Pi_s(m_s \mathbf{q} | n_s \mathbf{p}) \cdot V_{qp}$ ,  $H_{mqj, np} = \Pi_s(m_s \mathbf{q} | n_s \mathbf{p}) \cdot H_{qj, p}$ , where  $H_{qj, p}$  is the matrix element for the emission of the high frequency photon  $j$ , and, further, substituting  $U_{mq, np} = \Pi_s(m_s \mathbf{q} | n_s \mathbf{p}) \cdot \mathbf{U}_{qp}$ ,  $U_{mqj, np} = \Pi_s(m_s \mathbf{q} | n_s \mathbf{p}) \cdot \mathbf{U}_{qj, p}$ , and using (11), separates off the low frequency photon part and gives the equations

$$\left. \begin{aligned} \mathbf{U}_{q, p} &= V_{qp} - i\pi \int H_{q, p' j'} \rho_{p'} \rho_{j'} \mathbf{U}_{p' j', p} - i\pi \int V_{qp} \rho_{p'} \mathbf{U}_{p' p} \\ \mathbf{U}_{qj, p} &= H_{qj, p} - i\pi \int V_{qp} \rho_{p'} \mathbf{U}_{p' j, p} - i\pi \int H_{qj, p'} \rho_{p'} \mathbf{U}_{p' p} \end{aligned} \right\} \dots\dots (14)$$

Solving (14) by the method of reciprocal kernels, and using the relations  $\rho_p |V_{pq}| \ll 1$ ,  $e^2 \log(T/K) \ll 1$ , gives

$$\begin{aligned} \mathbf{U}_{q, p} &\simeq \{V_{qp} - i\pi \int V_{qp} \rho_{p'} V_{p' p}\} - i\pi \int H_{q, p' j'} \rho_{p'} \rho_{j'} H_{p' j', p} \\ &\quad - \pi^2 \int H_{q, p' j'} \rho_{p'} \rho_{j'} V_{p' p''} \rho_{p''} H_{p'' j', p} - \pi^2 \int V_{qp} \rho_{p''} H_{p'', p' j'} \rho_{p'} \rho_{j'} H_{p' j', p} \\ &\quad - \pi^2 \int H_{q, p' j'} \rho_{p'} \rho_{j'} H_{p' j', p''} \rho_{p''} V_{p'' p} + \text{smaller terms.} \end{aligned} \dots\dots (15)$$

The first term in brackets on the right-hand side of (15) could have been obtained directly from (9), so that the remaining three terms give the radiation damping effect.

The magnitude of the damping correction is obtained by evaluating  $|\mathbf{U}_{q, p}|^2$ . For simplicity it is assumed that  $V_{qp}$  and  $H_{qj, p}$  are real, a statement which is certainly true for the large values of  $H_{qj, p}$  arising from photons  $j$ , whose frequency is near the dividing frequency. It is further assumed that  $V_{qp}$  is almost independent of the directions of  $\mathbf{p}$  and  $\mathbf{q}$ . Then

$$|\mathbf{U}_{q, p}|^2 \simeq |V_{qp}|^2 - O\{e^2 \log(T/K) \cdot \rho_p^2 |V|^4\}. \dots\dots (16)$$



The damping given by (16) has the correct sign but has the wrong dependence on  $\rho|V|$  to cancel the arbitrariness due to the presence of  $K$  in the transition probabilities for the low frequency component. In fact this damping term is smaller than the radiative reaction discussed in §§ 2 and 3 by a factor of order  $\{\rho|V|\}^2$ .

It is troublesome that the factor  $e^2 \log(T/K)$  enters (16). Clearly a similar method would introduce factors of the type  $\{e^2 \log(T/K) \rho^2 |V|^2\}^N$  when states containing  $N$  high frequency photons are considered. Again, it seems that there is a term in the cross section depending on an arbitrary frequency  $K$ . It is not possible, in principle, to omit the damping correction, for as was pointed out in the introduction, damping and radiative reaction are distinct. The latter results from an accurate calculation of the matrix elements, while the former comes from an accurate deduction of the transition probabilities for any given matrix elements.

### § 5. THE MODIFIED DAMPING EQUATIONS\*

The difficulty arising out of the presence of the lower limit,  $K$ , of the 'high' frequency photon spectrum in the damping term cannot be avoided by any consideration of the damping arising from 'low' frequency photons ( $\kappa_s < K$ ), as this effect is negligible. Indeed, the smallness of the damping for  $\kappa_s < K$  suggests that those photons with frequency a little greater than  $K$  should also give rise to a small damping effect. It would also be reasonable to guess that on writing the damping equations in terms of the new wave functions which were introduced in § 2, the undesirable dependence of the results on  $K$  will disappear.

Let  $\Psi_p$  be the wave function of an electron in state  $\mathbf{p}$  (in linear momentum representation) unaccompanied by any photon field,  $\Psi_{p\tilde{\mathbf{k}}}$  that for an electron  $\mathbf{p}$  and a photon  $\tilde{\mathbf{k}}$  with no accompanying photons, etc. Then the corresponding wave functions  $\Psi$  which allow for the influence of the electron on the transverse component of the electromagnetic field are (cf. § 2):

$$\begin{aligned} \Psi_p = & \Psi_p \cdot \{1 - O(e^2)\} + \sum_{\mathbf{k}} \Psi_p^{(1)}(\mathbf{p} - \mathbf{k}, \tilde{\mathbf{k}}) \\ & + \sum_{\mathbf{k}, l} \Phi_p^{(1)}(\mathbf{p}, \mathbf{l}, (-\mathbf{l} + \mathbf{k})^+, -\tilde{\mathbf{k}}) + \text{terms in } e^2 \dots; \end{aligned} \quad \dots \dots (17a)$$

$$\begin{aligned} \Psi_{p\tilde{\mathbf{k}}} = & \Psi_{p\tilde{\mathbf{k}}} \{1 - O(e^2)\} + \sum_{\mathbf{k}'} \Psi_{p\tilde{\mathbf{k}}}^{(1)}(\mathbf{p} - \mathbf{k}', \tilde{\mathbf{k}}, \tilde{\mathbf{k}}') + \Psi_{p\tilde{\mathbf{k}}}^{(1)}(\mathbf{p} + \mathbf{k}) \\ & + \sum_l \Phi_{p\tilde{\mathbf{k}}}^{(1)}[\mathbf{p}, \mathbf{l}, (-\mathbf{l} + \mathbf{k})^+] + \sum_{\mathbf{k}', l} \Phi_{p\tilde{\mathbf{k}}}^{(1)}[\mathbf{p}, \mathbf{l}, (-\mathbf{l} + \mathbf{k}')^+, \tilde{\mathbf{k}}, -\tilde{\mathbf{k}}'] \\ & + \text{terms in } e^2 \dots \end{aligned} \quad \dots \dots (17b)$$

The ordinary matrix element  $H_{q,pj}$  for the absorption of a photon agrees with the matrix element  $(\bar{\Psi}_q V \Psi_{pj})$  in terms of order  $e$ . They differ in the  $e^2$  terms which occur in the latter, partly through higher order virtual transitions, and partly through the renormalization of the initial and final states.

Any attempt to write the damping matrix  $\mathbf{U}$  in terms of the new representation given by  $\Psi_p, \Psi_{p\tilde{\mathbf{k}}}, \dots$  meets with the difficulty that  $\mathbf{U}_{p',p}$  is only defined for  $\mathbf{p}', \mathbf{p}$  which have equal energy. Further, the introduction of the new representation is only possible if the various matrix elements are convergent, or if they can be made to converge by using the mass renormalization method. The damping equations (13) are obtained by neglecting several infinite terms arising from high

\* I am obliged to Professor W. Heitler and Dr. S. T. Ma for letting me see the manuscript of a paper (1949) in which the modified form of the damping equation is considered. However, they do not treat the low frequency problem in any detail.

frequencies, and it is to be hoped that the renormalization method will reduce these infinite terms to small finite corrections.

Using a model in which the frequencies  $\kappa_i$  are limited to the range  $K < \kappa_i < K'$ , where  $K' \ll$  the least of  $|\mathbf{p}|$  or  $m$  ( $\mathbf{p}$  being the initial momentum of the electron), the energy and momentum of the emitted photons can be neglected. Then the damping equation could be assumed to take the form

$$(\bar{\Psi}_q \mathbf{U} \Psi_p) = (\bar{\Psi}_q V \Psi_p) - i\pi \int (\bar{\Psi}_q V \Psi_{p'}) \rho_{p'} (\bar{\Psi}_{p'} \mathbf{U} \Psi_p) \\ - i\pi \int_K^{K'} dE_{j'} \int (\bar{\Psi}_q V \Psi_{p'j'}) \rho_{p'} \rho_{j'} (\Psi_{p'j'} \mathbf{U} \Psi_p) - \dots \quad (18)$$

Writing  $I_{p'} = \Psi_{p'} \bar{\Psi}_{p'} + \sum_{j'} \Psi_{p'j'} \bar{\Psi}_{p'j'} + \sum_{j'j''} \Psi_{p'j'j''} \bar{\Psi}_{p'j'j''} + \dots$

it is clear that it is terms arising from the second, third, ... terms in  $\partial_{p'}$ , which lead to the strong dependence of the damping, as calculated in § 4, upon the lower limit  $K$ .

Owing, however, to the replacement of the wave functions  $\Psi_{p'}$ ,  $\Psi_{p'i}$  by the  $\Psi_p$ ,  $\Psi_{pj}$  etc., it can be seen, on using (17), that

$$I_{p'} = u_{p'}(\mathbf{x}) \cdot \Pi_i \delta(Q_i - Q'_i) \cdot \bar{u}_{p'}(\mathbf{x}') + \text{terms of relative order } (K/m).$$

$U_{p'}(\mathbf{x})$  is the wave function for an electron in state  $\mathbf{p}'$ , while  $\mathbf{x}$ ,  $Q_i$ ;  $\mathbf{x}'$ ,  $Q'_i$  are the variables of integration occurring in the pairs of matrix elements. Using (17), it also follows that the largest part of the terms in  $e$  and  $e^2$  arising in  $I_{p'}$  cancel, leaving only terms of relative order  $(K/m)$ .

Substituting  $I_{p'}$  in equation (18), it follows that the strong dependence of the damping terms on  $K$  (through  $\tilde{i}'$  etc.) is no longer present. This method is clearly a perturbation theory analogue of the Bloch–Nordsieck transformation. However, the modified form of the damping equation requires further investigation.

Finally, it should be noticed that the equation

$$U_{qp} = V_{qp} - i\pi \int V_{qp'} \rho_{p'} U_{p'p}$$

does not give an accurate description of the collision cross section when  $e=0$ . It was pointed out in an earlier paper (Hamilton 1949a) that some extra terms have to be added to this equation to obtain the exact solution. This correction also would have to be incorporated in an accurate damping equation for 'bremsstrahlung'.

#### ACKNOWLEDGMENT

The author wishes to express his thanks to Professor L. Rosenfeld for many helpful discussions.

#### APPENDIX

##### SUBTRACTION PROCEDURES

It is possible to solve the damping equations for the emission of a large number of low frequency photons without having performed the Bloch–Nordsieck transformation. The method fails because it gives a strong damping due to the low frequency photons which greatly influences the electron's motion. Two alternative subtraction methods (of the old kind) can be employed. The details are given briefly.

It is fairly simple to calculate the compound matrix elements for the emission or absorption of any number of low frequency photons. It will be assumed that the incident electron has a non-relativistic velocity, and that the momentum recoil can be neglected. The matrix elements for emission, for example, can be evaluated as follows. Since the photon recoil is to be neglected, there will be a number of emissions during which the electron momentum is approximately  $\mathbf{p}_0$ , then a scattering from  $\mathbf{p}_0$  to  $\mathbf{p}_F$  by the potential  $V$ , and finally further emissions. Only terms linear in  $V$  will be considered.

Using the interaction  $-(\mathbf{p} \cdot \mathbf{e}_s)/mc)(q_s + \bar{q}_s)$  for emission or absorption, the emissions occurring before the scattering give a numerator of the form

$$\{-(e/mc)\sqrt{(2\pi\hbar^2c^2/L^3)}\}^{n_\lambda+n_\mu+\dots}(\epsilon_\lambda^{n_\lambda}\epsilon_\mu^{n_\mu}\dots)^{-1}(\mathbf{p}_0 \cdot \mathbf{e}_\lambda)^{n_\lambda}(\mathbf{p}_0 \cdot \mathbf{e}_\mu)^{n_\mu}\dots\sqrt{(n_\lambda!n_\mu!\dots)}$$

where  $n_\lambda$  photons of energy  $\epsilon_\lambda$ , etc., have been emitted. The factorial term arises from the matrix elements of  $q_s$ . The corresponding energy denominator is easily calculated, using the fact that the order of emission of the individual photons varies. A typical term is

$$(-)^{n_\lambda+n_\mu+\dots}1/\{\epsilon_\lambda(\epsilon_\lambda+\epsilon_\mu)(\epsilon_\lambda+\epsilon_\mu+\epsilon_\nu)\dots(n_\lambda\epsilon_\lambda+n_\mu\epsilon_\mu+\dots)\}.$$

The term  $1/(\epsilon_\lambda+\epsilon_\mu)$  may be preceded by  $1/\epsilon_\lambda$  or  $1/\epsilon_\mu$ , giving, for the two terms,  $(1/\epsilon_\lambda+1/\epsilon_\mu)/(\epsilon_\lambda+\epsilon_\mu)=1/\epsilon_\lambda\epsilon_\mu$ . It is readily seen that allowing for this change in order gives

$$(-)^{n_\lambda+n_\mu+\dots}/\{n_\lambda!\epsilon_\lambda^{n_\lambda}n_\mu!\epsilon_\mu^{n_\mu}\dots\}.$$

Thus the emissions occurring before scattering give the partial matrix element

$$(2\pi e^2/\hbar c)^{(n_\lambda+n_\mu+\dots)/2}(\bar{\epsilon}/\epsilon_\lambda)^{3n_\lambda/2}(\bar{\epsilon}/\epsilon_\mu)^{3n_\mu/2}\dots \\ \times [(\mathbf{p}_0 \cdot \mathbf{e}_\lambda)/mc]^{n_\lambda}[(\mathbf{p}_0 \cdot \mathbf{e}_\mu)/mc]^{n_\mu}\dots 1/\sqrt{(n_\lambda!n_\mu!\dots)}$$

where  $\bar{\epsilon}=\hbar c/L$  is the minimum photon energy. If there had been  $\bar{n}_\lambda, \bar{n}_\mu, \dots$  etc. photons present initially, the factorial term would be replaced by

$$\frac{1}{n_\lambda!}\sqrt{\left(\frac{(n_\lambda+\bar{n}_\lambda)!}{\bar{n}_\lambda!}\right)}\frac{1}{n_\mu!}\sqrt{\left(\frac{(n_\mu+\bar{n}_\mu)!}{\bar{n}_\mu!}\right)}\dots$$

It is now possible to compare the various subtraction methods. Heitler and Peng (1942) suggest using the lowest order elements joining the initial and final states. Thus for  $H_{\bar{n}_\lambda\bar{p}, n_\lambda p}$ , where  $(p, n_\lambda)$ ,  $(\bar{p}, \bar{n}_\lambda)$  are the initial and final states respectively, their method gives

$$(2\pi e^2/\hbar c)^{(\bar{n}_\lambda-n_\lambda)/2}(\bar{\epsilon}/\epsilon_\lambda)^{3(\bar{n}_\lambda-n_\lambda)/2} \\ \times \sum_{n'=n_\lambda}^{\bar{n}_\lambda} \frac{(\bar{\mathbf{p}} \cdot \mathbf{e}_\lambda)^{\bar{n}_\lambda-n'}(\mathbf{p} \cdot \mathbf{e}_\lambda)^{n'-n_\lambda}}{(\bar{n}_\lambda-n')!(n'-n_\lambda)!} (-)^{\bar{n}_\lambda-n'} \sqrt{\left(\frac{\bar{n}_\lambda!}{n_\lambda!}\right)} V_{\bar{p}p},$$

assuming  $\bar{n}_\lambda \geq n_\lambda$ . Thus

$$H_{\bar{n}_\lambda\bar{p}, n_\lambda p} = \frac{(\mathbf{a}_\lambda \cdot \bar{\mathbf{p}} - \bar{\mathbf{p}})^{\bar{n}_\lambda-n_\lambda}}{(\bar{n}_\lambda-n_\lambda)!} \sqrt{\left(\frac{\bar{n}_\lambda!}{n_\lambda!}\right)} V_{\bar{p}p}, \dots (19a)$$

where  $\mathbf{a}_\lambda = \mathbf{e}_\lambda(2\pi e^2/\hbar c)^{1/2}(\bar{\epsilon}/\epsilon_\lambda)^{3/2}$ .

If  $n_\lambda \geq \bar{n}_\lambda$ , the result is

$$H_{\bar{n}_\lambda\bar{p}, n_\lambda p} = \frac{(\mathbf{a}_\lambda \cdot \bar{\mathbf{p}} - \bar{\mathbf{p}})^{n_\lambda-\bar{n}_\lambda}}{(n_\lambda-\bar{n}_\lambda)!} \sqrt{\left(\frac{n_\lambda!}{\bar{n}_\lambda!}\right)} V_{\bar{p}p}, \dots (19b)$$

$V_{\bar{p}p}$  could be replaced by the matrix element for the emission of a high frequency photon without destroying the argument. It will be seen that these matrix elements are just the first term in the expression (4), after omitting the exponential factor. The emission or absorption of other photons merely introduces multiplicative terms got by replacing  $\lambda$  in (19a) and (19b) by  $\mu, \nu, \dots$  etc. For an electron such that  $p, \bar{p} \ll mc$ , it is readily seen that  $(\mathbf{a}_\lambda \cdot \bar{\mathbf{p}} - \mathbf{p}) \ll 1$ .

The most important property of the coefficients  $(mp | np')$  of the Bloch-Nordsieck method is

$$\sum_n (mp | np')(np' | \bar{n}\bar{p}) = (mp | \bar{n}\bar{p}).$$

This relation makes it possible for the emission of low frequency photons to have a very small effect upon the electron's motion, as the low frequency part factorizes out of the damping equations (cf. § 4).

Consider the damping equation for the emission of one high frequency and no low frequency photons using (19). It will contain a term of the type  $\sum_{n'} H_{0\lambda\bar{p}j, n'\lambda p'} U_{n'\lambda p', 0\lambda p}$ . If the emission of low frequency photons is not to influence the scattering of the electron (beyond the small effect due to neglecting the emitted energy and momentum), this term should reduce to the form  $H_{pj, p'} U_{p', p}$ . From the classical result it is clear that  $U_{1\lambda p', 0\lambda p}$  should contain the factor  $(\mathbf{a}_\lambda \cdot \mathbf{p} - \mathbf{p}')$ . Summing over  $n'$  up to 1 gives

$$H_{pj, p'} U_{p', p} + H_{pj, p'} U_{p', p} (\mathbf{a}_\lambda \cdot \bar{\mathbf{p}} - \mathbf{p}') (\mathbf{a}_\lambda \cdot \mathbf{p} - \mathbf{p}').$$

Thus there is a correcting factor  $\{1 + (\mathbf{a}_\lambda \cdot \bar{\mathbf{p}} - \mathbf{p}') (\mathbf{a}_\lambda \cdot \mathbf{p} - \mathbf{p}')\}$ . This factor does not allow  $\mathbf{p}'$  to drop out of the expression, and it is hard to see how higher terms in  $n'$  can rectify that. Also, although for a single low frequency photon the factor is almost unity, when all low frequency photons are considered it becomes

$$\prod_\lambda \{1 + (\mathbf{a}_\lambda \cdot \bar{\mathbf{p}} - \mathbf{p}') (\mathbf{a}_\lambda \cdot \mathbf{p} - \mathbf{p}')\} \simeq \exp \{ \sum_\lambda (\mathbf{a}_\lambda \cdot \bar{\mathbf{p}} - \mathbf{p}') (\mathbf{a}_\lambda \cdot \mathbf{p} - \mathbf{p}') \},$$

which diverges as the lowest energy  $\epsilon \rightarrow 0$ . There is thus a very strong damping, which will greatly influence the angular distribution of the electron wave function. Other forms of  $U_{1\lambda p', 0\lambda p}$ , including higher order terms in  $(\mathbf{a}_\lambda \cdot \mathbf{p} - \mathbf{p}')$ , may be tried, but none of these can cancel the term  $(\mathbf{a}_\lambda \cdot \bar{\mathbf{p}}) (\mathbf{a}_\lambda \cdot \mathbf{p}')$  occurring in  $\{1 + (\mathbf{a}_\lambda \cdot \bar{\mathbf{p}} - \mathbf{p}') (\mathbf{a}_\lambda \cdot \mathbf{p} - \mathbf{p}')\}$  without integrating over  $\mathbf{p}'$ , which again introduces a strong damping of an admissible type into the electron's motion.

An alternative procedure of subtraction (Hamilton 1949b) is to neglect all self energy terms in the original and virtual states. This means neglecting compound matrix elements in which any two states (intermediate or final) have precisely the same quantum numbers or descriptions. Such matrix elements are diagonal terms of the Hamiltonian (if the identical states are initial and final) or contain diagonal terms relating to some intermediate state.

The matrix elements derived in this fashion contain more terms than those of Heitler and Peng. For example, the element  $H_{\bar{n}\lambda\bar{p}, 0\lambda p}$  (to take a simple case) includes terms allowing for the emission of  $n_\mu$  photons  $\epsilon_\mu$ ,  $n_\nu$  photons  $\epsilon_\nu$ , ... etc. before the scattering by  $V$ , and the re-absorption of these photons after the scattering. This gives

$$H_{\bar{n}\lambda\bar{p}, 0\lambda p} = \prod_{\mu \neq \lambda} \exp \{ (\mathbf{p} \cdot \mathbf{a}_\mu) (\bar{\mathbf{p}} \cdot \mathbf{a}_\mu) \} \cdot \left[ \frac{1}{\sqrt{(\bar{n}_\lambda!)}} (\mathbf{p} \cdot \mathbf{a}_\lambda)^{\bar{n}_\lambda} \{ \exp [(\mathbf{a}_\lambda \cdot \mathbf{p}_\lambda) (\mathbf{a}_\lambda \cdot \bar{\mathbf{p}}_\lambda)] - 1 \} \right. \\ \left. + \frac{1}{\sqrt{(\bar{n}_\lambda!)}} (\mathbf{a}_\lambda \cdot \mathbf{p} - \bar{\mathbf{p}})^{\bar{n}_\lambda} \right] \cdot V_{\bar{p}p}.$$

This formula actually bears more relation to  $(\bar{n}_\lambda \bar{p} | 0p)$  of (4) than does the matrix element derived above.

However, there is another type of term to be added. Consider the process  $(0_\lambda, \mathbf{p}) \rightarrow (1_\lambda, \bar{\mathbf{p}})$  during scattering by  $V$ . Then there is a term  $(\mathbf{a}_\lambda \cdot \mathbf{p})$  arising from the emission of photon  $\lambda$  before the scattering. However, one can also have the process  $\nu_e \lambda_e \nu_a$ , where 'e' and 'a' mean emission and absorption respectively. This gives a term of the order  $(\mathbf{a}_\lambda \cdot \mathbf{p})(\mathbf{a}_\nu \cdot \mathbf{p})^2$ , and the only proviso is that  $\nu$  and  $\lambda$  do not represent the same photon. Another allowed process is  $\nu_e \mu_e \nu_a \lambda_e \mu_a$ , giving a term of the order  $(\mathbf{a}_\lambda \cdot \mathbf{p})(\mathbf{a}_\nu \cdot \mathbf{p})^2(\mathbf{a}_\mu \cdot \mathbf{p})^2$ , where  $\nu \neq \lambda$  and  $\mu \neq \nu$  or  $\lambda$ . As a result the original term  $(\mathbf{a}_\lambda \cdot \mathbf{p})$  is modified by a factor of the type

$$\prod_{\nu \neq \lambda} \{1 + \gamma_\nu (\mathbf{a}_\nu \cdot \mathbf{p})^2\} \cdot \prod_{\mu \neq \nu, \lambda} \{1 + \delta_\mu (\mathbf{a}_\mu \cdot \mathbf{p})^2\},$$

where  $\gamma_\nu, \delta_\mu$  are factors of the order of magnitude of unity. Further processes of the type  $\nu_e \mu_e \nu_a \tau_e \mu_a \lambda_e \tau_a, \dots$  etc. can occur, and as a result the product of a large number of factors, each of which are of the order of  $\exp \{\Sigma_\nu (\mathbf{a}_\nu \cdot \mathbf{p})^2\}$ , can enter the matrix element. The method of excluding self energy terms is therefore useless in the present problem. The reason for its failure lies in the strong interaction of the electron with low frequency virtual photons.

#### REFERENCES

- BETHE, H. A., and OPPENHEIMER, J. R., 1946, *Phys. Rev.*, **70**, 451.  
 BLOCH, F., and NORDSIECK, A., 1937, *Phys. Rev.*, **52**, 54.  
 DANCOFF, S., 1939, *Phys. Rev.*, **55**, 959.  
 EPSTEIN, S. T., 1948, *Phys. Rev.*, **73**, 177.  
 HAMILTON, J., 1949 a, *Proc. Phys. Soc. A*, **62**, 2; 1949 b, *Ibid.*, **62**, 12.  
 HEITLER, W., and MA, S. T., 1949, *Phil. Mag.*, **40**, 651.  
 HEITLER, W., and PENG, H. W., 1942, *Proc. Camb. Phil. Soc.*, **38**, 296.  
 ITO, D., Koba, Z., and TOMONAGA, S., 1948, *Prog. Theor. Phys. (Japan)*, **3**, 276, 325.  
 JOST, R., 1947, *Phys. Rev.*, **72**, 815.  
 Koba, Z., and TOMONAGA, S., 1948, *Prog. Theor. Phys. (Japan)*, **3**, 290.  
 LEWIS, H. W., 1948, *Phys. Rev.*, **73**, 173.  
 PAULI, W., and FIERZ, M., 1938, *Nuovo Cim.*, **15**, 167.  
 TATI, T., and TOMONAGA, S., 1948, *Prog. Theor. Phys. (Japan)*, **3**, 391.  
 WEISSKOPF, V. F., 1939, *Phys. Rev.*, **56**, 72.

## Directional Correlation between Successive Internal-Conversion Electrons

By J. W. GARDNER

Department of Mathematical Physics, University of Birmingham

*Communicated by R. E. Peierls ; MS. received 7th June 1949*

**ABSTRACT.** For the internal conversion of successive electric multipole quanta by s-electrons, unaccompanied by spin reversal, the directional correlation between the ejected electrons can be derived by symmetry arguments alone. A general formula is established and special cases likely to be of practical interest are tabulated. Comparison is made with Hamilton's results for  $\gamma$ - $\gamma$  correlation.

### § 1. INTRODUCTION

WHEN an atomic nucleus passes from an excited level A to the ground level C via a second excited level B, by the emission of two successive particles or quanta, one expects from general considerations that the direction of the second emission will be related to that of the first, provided the lifetime of the level B is small compared with the precession period of the nucleus in whatever external field it finds itself. This correlation is expected to depend on the angular momenta of the nuclear levels A, B and C and the angular momenta of the emitted particles or quanta.

One of the earliest calculations of angular correlation in processes of the above type was that by Hamilton (1940), who worked out the correlation between successive  $\gamma$ -quanta emitted by a nucleus in the absence of an external field. Goertzel (1946) extended this work to include the effect of external fields, with particular reference to the magnetic field of the extra-nuclear electrons. More recently there have appeared other calculations, based on various types of interaction, of angular correlation in processes involving  $\beta$ - and  $\gamma$ -decay. References to, and discussion of, these are given by Yang (1948) in a general paper on angular correlation in nuclear processes.

Yang shows that the general form of the angular distribution of the products of nuclear reactions and disintegrations can be derived from symmetry considerations alone, regardless of the particular form of interaction at work. The correlation between successive particles or quanta is specified by the probability  $I(\theta)$  that the direction of propagation of the second makes an angle  $\theta$  with that of the first. Using only the invariance of the properties of the physical process under space rotation and under inversion, Yang is able to expand  $I(\theta)$  as a power series in  $\cos \theta$ , in which the highest power of  $\cos \theta$  is severely limited by the angular momenta of the nuclear levels and the angular momenta of the emitted particles or quanta, so that the expansion frequently reduces to a very few terms. The processes which he considers include  $\beta$ -neutrino,  $\beta$ - $\gamma$  and  $\gamma$ - $\gamma$  correlations; also the general nuclear reaction  $M + P \rightarrow N + Q$ ,  $\theta$  in this case being the angle between the propagation directions of the incident particle P and the emergent particle Q, and M and N being the initial and final nuclei.\*

\* Myers (1938) has given a detailed calculation, based on symmetry arguments, of the angular distribution of resonance disintegration products. This calculation is not as general as Yang's but within the limits of its validity it gives quantitative results, whereas Yang's gives information only about the general form of the distribution.

In general, to evaluate the ratios of the coefficients of the various powers of  $\cos \theta$  appearing in the expansion of  $I(\theta)$  one must make specific assumptions about the interaction. There are, however, certain types of disintegration in which the number of variables is sufficiently small to permit calculation of these ratios merely by an extension of the symmetry arguments. Such a disintegration is one in which the nuclear transitions  $A \rightarrow B \rightarrow C$  are achieved by the ejection from the atom of two successive internal-conversion electrons, subject to certain restrictions stated in the next section. It is the purpose of the present paper to consider such a disintegration by symmetry methods, without specifying the mechanism of internal conversion, and in particular leaving aside the question of whether or not the ejection of an orbital electron is pictured as due to the nucleus emitting and the electron absorbing a  $\gamma$ -quantum. (In the relativistic treatment of internal conversion (cf. Mott and Taylor 1932, 1933) no sharp distinction can be made between the effect of direct interaction and the effect of  $\gamma$ -ray emission and subsequent absorption.)

The function  $I(\theta)$  expressing the angular correlation between the emission directions of successive conversion electrons is expanded in a series of even spherical harmonics whose coefficients are explicit functions of the angular momenta of the nuclear levels and the emitted electrons. These coefficients are tabulated and their general behaviour discussed for most cases likely to be of practical interest. The results are compared with those of Hamilton for  $\gamma$ - $\gamma$  correlation. In conclusion we discuss the extent to which the initial simplifying assumptions limit the applicability of the results.

At least one report of observed angular correlation between successive conversion electrons has appeared (Ward and Walker 1949);  $\beta$ -neutrino and  $\gamma$ - $\gamma$  correlations have been studied experimentally by many workers, references being given in Yang's paper.

## § 2. DERIVATION OF GENERAL CORRELATION FORMULA

We denote the total angular momenta of the nuclear levels A, B and C by the vectors  $\mathbf{J}_A, \mathbf{J}_B, \mathbf{J}_C$  and the orbital angular momenta of the ejected electrons by  $\mathbf{l}_1, \mathbf{l}_2$ ; thus in units of  $\hbar$ ,  $J_A, J_B$  and  $J_C$  may be integer or half-integer,  $l_1$  and  $l_2$  only integer. The projections of these vectors on the (arbitrary)  $z$ -axis we denote by  $M_A, M_B, M_C, m_1, m_2$ . It is assumed that: (a) the total angular momentum of all orbital electrons, other than the ejected ones, remains constant throughout; (b) the ejected electrons have come from an s-state (but not necessarily the K-shell); (c) internal conversion occurs without spin reversal of the ejected electrons.

These assumptions have the effect of restricting the present calculations to internal conversion of electric multipole radiation only (cf. § 5).

Conservation of angular momentum, together with the above assumptions, gives immediately the following vector equations:

$$\mathbf{J}_A = \mathbf{J}_B + \mathbf{l}_1, \quad \dots\dots (1)$$

$$\mathbf{J}_B = \mathbf{J}_C + \mathbf{l}_2, \quad \dots\dots (2)$$

with components in the  $z$ -direction:

$$M_A = M_B + m_1, \quad \dots\dots (3)$$

$$M_B = M_C + m_2, \quad \dots\dots (4)$$

In the final state, the whole system, consisting of the nucleus plus the two ejected electrons,\* is still characterized by the total angular momentum  $\mathbf{J}_A$  with component  $M_A$ ; we therefore introduce  $\psi_A(J_A, M_A)$  for the wave function of the whole system in the final state. Similarly the system consisting of the nucleus plus the second ejected electron is still characterized in the final state by  $\mathbf{J}_B, M_B$ , so for the wave function describing it we introduce  $\psi_B(J_B, M_B)$ , and  $\psi_C(J_C, M_C)$  for the nucleus by itself in the final state. The wave functions of the ejected electrons by themselves we denote by  $\psi_1(l_1, m_1), \psi_2(l_2, m_2)$ . Where no ambiguity occurs we write  $\psi_A(J_A, M_A)$  simply as  $\psi_A$ , with similar abbreviations for the other wave functions.

Because of the vector relation (1),  $\psi_A$  is expressible as a linear combination of the  $2J_B + 1$  possible  $\psi_B$  corresponding to a definite  $J_B$ , and the  $2l_1 + 1$  possible  $\psi_1$  corresponding to a definite  $l_1$  (see for example Condon and Shortley 1935). Thus

$$\psi_A \sim \sum_{M_B, m_1} C_{J_B M_B l_1 m_1}^{J_A M_A} \psi_B \psi_1. \quad \dots\dots (5)$$

Similarly, because of (2),  $\psi_B$  may be written as a linear combination of the  $2J_C + 1$  possible  $\psi_C$  and the  $2l_2 + 1$  possible  $\psi_2$ , which may then be substituted in (5), giving:

$$\psi_A \sim \sum_{M_B, m_1, M_C, m_2} C_{J_B M_B l_1 m_1}^{J_A M_A} C_{J_C M_C l_2 m_2}^{J_B M_B} \psi_C \psi_1 \psi_2. \quad \dots\dots (6)$$

The  $C$ 's in (5) and (6) are the coefficients common to all problems in which two angular momenta are combined to give a resultant; equivalent general formulæ for them have been given by Wigner (1931) and Van der Waerden (1932) using group theoretical methods. Racah (1942) has also given an elementary algebraic derivation of a formula which, apart from a normalizing factor, is the same as Van der Waerden's. In the present calculations it was found most convenient to use the formula of Racah, to whose paper, also, the reader is referred for a concise account of the orthogonality, symmetry and other useful properties of the  $C$ 's.†

The angular parts of  $\psi_1, \psi_2$  are the spherical harmonics  $Y_{l_1, m_1}(\theta_1, \phi_1), Y_{l_2, m_2}(\theta_2, \phi_2)$ . Without loss of generality we may define our  $z$ -axis as the direction of emission of one (say the first) of the conversion electrons, by setting  $\theta_1 = \phi_1 = 0$ . Since  $Y_{l_1, m_1}(0, 0)$  vanishes except for  $m_1 = 0$ , (3) and (4) reduce to

$$M_A = M_B = M_C + m_2. \quad \dots\dots (7)$$

Thus the sum over  $M_B, m_1$  in (6) reduces to one term. Moreover,  $\theta_2, \phi_2$  now define the emission direction of the second electron relative to that of the first, so that the probability  $I(\theta, \phi) d\Omega$  that the second electron is emitted into the solid angle  $d\Omega$  about the direction  $(\theta, \phi)$ —the suffix 2 may now be dropped—expresses directly the angular correlation between the electrons. This probability function is obtained from (6) by

$$I(\theta, \phi) \sim \sum_{M_A} \int \psi_A^* \psi_A d\tau, \quad \dots\dots (8)$$

\* In view of assumption (a) the other orbital electrons can be omitted from the discussion without affecting the validity of the symmetry arguments to be used.

† Our notation differs from Racah's: we define  $C_{j_1 m_1 j_2 m_2}^{j_3 m_3}$  to be the quantity which he writes  $(j_1 j_2 m_1 m_2 / j_3 m_3)$ .



where the integration is over all coordinates except  $\theta, \phi$ , and where the summation over  $M_A$  has to be introduced because  $\psi_A(J_A, M_A)$  refers to a definite  $M_A$ , whereas experimentally it is the average effect over all the  $2J_A + 1$  possible values of  $M_A$  that is observed. The integrand in (8) is a sum, over all possible  $M_C$  and  $m_2$  consistent with (7), of such terms as

$$\{C_{J_B M_A l_1 0}^{J_A M_A} C_{J_C M_C l_2 m_2}^{J_B M_A} \psi_C(J_C, M_C) Y_{l_2, m_2}(\theta, \phi)\}^* \\ \times \{C_{J_B M_A l_1 0}^{J_A M_A} C_{J_C M_C' l_2 m_2'} \psi_C(J_C, M_C') Y_{l_2, m_2'}(\theta, \phi)\}. \quad \dots \dots (9)$$

(The constant factor  $Y_{l_1 0}(0, 0)$  has been omitted; other constant factors will be omitted from time to time without special mention.) Because of the orthogonality of the  $\psi_C$  the only terms which remain after integration are those in which  $M_C' = M_C$ , and hence  $m_2' = m_2$ . Noting the reality of the  $C$ 's, and that  $|Y_{l_2, m_2}(\theta, \phi)|^2$  is independent of  $\phi$ , we see that our angular distribution formula becomes

$$I(\theta) \sim \sum_{M_A, M_C, m_2} \{C_{J_B M_A l_1 0}^{J_A M_A} C_{J_C M_C l_2 m_2}^{J_B M_A} Y_{l_2, m_2}(\theta, 0)\}^2. \quad \dots \dots (10)$$

The fact that this expression is independent of  $\phi$  means that the distribution of the second electron is symmetrical about the direction of the first, while the fact that only squares of spherical harmonics appear means that the distribution is symmetrical about the equatorial plane.

As an example of the use of (10) we may consider the case in which  $J_A = J_C = 0$ , and  $J_B$  has any integral value, say  $L$ . We then have immediately from (1)–(4)  $l_1 = l_2 = L$ ,  $M_A = M_C = m_2 = 0$ , so that the sum in (10) reduces to one term, and  $I(\theta) \sim \{Y_{L, 0}(\theta, 0)\}^2$ . In particular when  $L = 1$ ,  $I(\theta) \sim \cos^2 \theta$ .

However, apart from such extremely simple cases, (10) as it stands is of little value for practical calculation, for if the sum includes more than a very few terms the labour of evaluating it directly becomes prohibitive. It will now be shown that, using an expansion of  $\{Y_{l_2, m_2}(\theta, 0)\}^2$  linear in spherical harmonics, together with Racah's results (1942) for summations of products of  $C$ 's, (10) can be manipulated into a form more convenient both for practical calculation and for making general inferences about the nature of the angular distribution.

### § 3. ANALYSIS AND DISCUSSION OF GENERAL FORMULA

By the customary Fourier method we may obtain the expansion

$$\{Y_{l_2, m_2}(\theta, 0)\}^2 = \sum_k A_k Y_{k, 0}(\theta, 0), \quad \dots \dots (11)$$

where the coefficients are found to be given by

$$A_k = \{(-1)^{m_2}(2l_2 + 1)/2\pi^{1/2}(2k + 1)^{1/2}\} C_{l_2 0 l_2 0}^{k 0} C_{l_2 - m_2 l_2 m_2}^{k 0}. \quad \dots \dots (12)$$

Substitution of (11) and (12) in (10) gives  $I(\theta)$  as a linear expansion in spherical harmonics:

$$I(\theta) \sim \sum_k B_k Y_{k, 0}(\theta, 0) \quad \dots \dots (13)$$

with

$$B_k = (2k + 1)^{-1/2} C_{l_2 0 l_2 0}^{k 0} \sum_{M_A, M_C, m_2} (-1)^{m_2} \{C_{J_B M_A l_1 0}^{J_A M_A} C_{J_C M_C l_2 m_2}^{J_B M_A}\}^2 C_{l_2 - m_2 l_2 m_2}^{k 0}. \quad \dots \dots (14)$$

We see that  $B_k$  involves the summation, over certain common arguments, of the product of five  $C$ 's. Now Racah gives (in effect) the following result for the sum of products of three  $C$ 's:

$$\sum_{\alpha, \beta, \delta} C_{\alpha\beta\delta}^{\gamma} C_{\alpha\beta\delta}^{\epsilon} C_{\alpha\beta\delta}^{\delta} = (2c+1)^{\frac{1}{2}}(2d+1)^{\frac{1}{2}} W(cbfd; ae) C_{c/f\phi}^{\epsilon} \dots \dots (15)$$

The general formula for the function  $W$  and an account of its properties appear in his paper (1942). (Like the  $C$ 's, the  $W$ 's have useful symmetry and orthogonality properties.) It will be shown that a double application of (15) enables the sum in (14) to be evaluated. First let us consider the summation over all possible values of  $M_C, m_2$  subject to  $M_C + m_2 = M_A$ , whilst  $M_A$  is kept constant. We have then to evaluate

$$\sum_{M_C, m_1} (-1)^{m_1} \{C_{J_C M_C l_1 m_1}^{J_B M_A}\}^2 C_{l_2 - m_2 l_1 m_1}^{k0}$$

Using the symmetry properties of the  $C$ 's, it is readily shown that, apart from factors independent of  $M_C$  and  $m_2$ , this sum may be expressed as

$$\sum_{M_C, m_1} \{C_{l_1 m_1 J_C M_C}^{J_B M_A}\}^2 C_{l_1 m_1 k0}^{J_A m_1},$$

which is a form directly evaluable from (15) on making the substitutions

$$\begin{array}{llll} c, e \rightarrow J_B & a, d \rightarrow l_2 & b \rightarrow J_C & f \rightarrow k \\ \gamma, \epsilon \rightarrow M_A & \alpha, \delta \rightarrow m_2 & \beta \rightarrow M_C & \phi \rightarrow 0 \end{array}$$

After carrying out these substitutions and inserting the factors independent of  $M_C$  and  $m_2$ , we have the result:

$$\begin{aligned} \sum_{M_C, m_1} (-1)^{m_1} \{C_{J_C M_C l_1 m_1}^{J_B M_A}\}^2 C_{l_2 - m_2 l_1 m_1}^{k0} \\ = (2k+1)^{\frac{1}{2}} (2J_B+1)^{\frac{1}{2}} (-1)^{k-l_1} W(J_B J_C k l_2; l_2 J_B) C_{J_B M_A k0}^{J_B M_A} \dots \dots (16) \end{aligned}$$

Substituting (16) in (14), we see that the dependence on  $M_A$  is now limited to the factors  $\{C_{J_B M_A l_1 0}^{J_B M_A}\}^2, C_{J_B M_A k0}^{J_B M_A}$ , so that the summation over  $M_A$  reduces effectively to summing this product of three  $C$ 's over all  $M_A$  from  $-J_A$  to  $J_A$ , and this can be done as above using (15) again. (Actually a slightly different formula, obtained from (15) by the symmetry properties of the  $W$ 's, is more suitable in this case.) The result of this summation is

$$\begin{aligned} \sum_{M_A} \{C_{J_B M_A l_1 0}^{J_B M_A}\}^2 C_{J_B M_A k0}^{J_B M_A} \\ = (2J_A+1)(2J_B+1)^{\frac{1}{2}} (2k+1)^{-\frac{1}{2}} (-1)^{-l_1} W(J_B J_A k l_1; l_1 J_B) C_{l_1 0 l_1 0}^{k0} \dots \dots (17) \end{aligned}$$

Thus (16) and (17) in conjunction with (14) enable  $B_k$  to be expressed as a product of 2  $W$ 's, 2  $C$ 's and a few odd factors. Factors independent of  $k$  may, of course, be dropped on substituting  $B_k$  in (13); the factor  $(2k+1)^{-\frac{1}{2}}$  may also be removed if we elect to expand  $I(\theta)$  in terms of  $P_k(\cos \theta)$  rather than  $Y_{k,0}(\theta, 0)$ . [ $P_k(\cos \theta)$  is the Legendre polynomial normalized so that  $P_k(1) = 1$ , and  $Y_{k,0}(\theta, 0)$  is by definition  $\{(2k+1)/4\pi\}^{\frac{1}{2}} P_k(\cos \theta)$ .] The result then assumes the rather neat form

$$I(\theta) \sim \sum_k C_{l_1 0 l_1 0}^{k0} C_{l_2 0 l_2 0}^{k0} W(J_B J_A k l_1; l_1 J_B) W(J_B J_C k l_2; l_2 J_B) P_k(\cos \theta) \dots \dots (18)$$

If in (18) we interchange  $J_A$  with  $J_C$ , and  $l_1$  with  $l_2$ , we see that  $I(\theta)$  is unaffected, in accordance with the physical consideration that it expresses merely the relative angular distribution of the electrons. The properties of either the  $C$ 's or the  $W$ 's limit  $k$  in (18) to the values 0, 2, 4 . . . up to  $2l_1$  or  $2l_2$ , whichever is the lower, showing that  $I(\theta)$  is symmetrical about the equatorial plane. The latter result we had already deduced from the appearance of  $\{Y_{l, m_1}(\theta), 0\}^2$  in formula (10) for  $I(\theta)$ ; the limitation on the highest value of  $k$  is in accordance with the consideration that we could have taken the  $z$ -axis in the direction of the second rather than the first electron and obtained a formula physically equivalent to (10) but expressing  $I(\theta)$  in terms of  $\{Y_{l, m_1}(\theta), 0\}^2$ . Moreover (18) reveals a further limitation on  $k$  which is not apparent from (10), for the  $W$  functions vanish unless  $k \leq 2J_B$ . Thus  $J_B = 0$  or  $\frac{1}{2}$  gives an isotropic distribution, whatever  $l_1$  and  $l_2$ .

The limitations on  $I(\theta)$  discussed in the preceding paragraph apply also to the directional correlation of successive  $\gamma$ -quanta,  $l_1$  and  $l_2$  in this case being interpreted as the multipole orders of the two quanta (Hamilton 1940, Goertzel 1946).

#### § 4. PRACTICAL APPLICATION OF GENERAL FORMULA

##### (i) *Tabulation of the W Functions*

In the practical application of (18) numerical values of the  $C$ 's and  $W$ 's must be obtained either from tables or by direct calculation. Tables of the  $C$ 's for values of the arguments likely to arise in practical cases have been published (see for example Condon and Shortley 1935); however, for  $C$ 's of the type  $C_{ab0}^0$  appearing in (18) the summation formula for the  $C$  with general arguments reduces to a closed form quite suitable for computation.

A series of tables for  $W(abcd; ef)$  may be drawn up, each one characterized by a definite value: 0,  $\frac{1}{2}$ , 1,  $\frac{3}{2}$  . . . of one of the arguments, say  $d$ . In each table the other arguments are kept general, i.e. are allowed to assume any values consistent with the limitations detailed by Racah (1942, p. 444). For a definite numerical value, say  $j$ , of  $d$  these limitations restrict  $f$  to the values  $b+j$ , . . . ,  $|b-j|$  and  $e$  to the values  $c+j$ , . . . ,  $|c-j|$ . The entries in each table are arranged according to these definite values of  $f$  and  $e$ ; there will thus be in general  $(2j+1)^2$  entries in the table for  $d=j$ , although when  $b, c$  have numerical values less than  $j$  some of these entries will be inadmissible.

The selection of  $d$  as the argument to characterize each table by a definite numerical value was quite arbitrary, any other argument being equally suitable; any  $W$  having one or more of its arguments equal to the numerical value assigned to  $d$  in a particular table can be easily obtained from that table by use of the symmetry properties of the  $W$ 's. So far as the author is aware no published tables of  $W$  functions exist\*, but their compilation for the lowest numerical values of  $d$  is not too laborious; as  $d$  increases, however, not only does the number of entries in each table increase as the square of the natural numbers, but the entries themselves become more and more complicated.

##### (ii) *Simplification when $l_1$ and $l_2$ have Lowest Allowed Values*

It is known that for a given nuclear transition accompanied by the ejection of an internal-conversion electron of wave number  $k_0$  the probability that the ejected electron has angular momentum  $l$  varies in general as  $(k_0 r)^2$ ,  $r$  being the

\* Tables for  $d \leq 2$  have been prepared by Professor H. A. Jahn of Southampton for publication in due course, in connection with work on nuclear energy levels.

nuclear radius. Where this is true—exceptions are discussed in the next paragraph—only the lowest value of  $l$  permitted by the magnitude of  $\Delta J$  and by the parity selection rules need be considered: higher values of  $l$  may occur but only with insignificant probability, since in all practical cases  $k_0 r \leq 1$ . (Only for energies greater than 20 Mev. would  $k_0 r$  approach unity.)

For the majority of nuclei, owing to the approximate coincidence of the centres of charge and mass, the transition probabilities for  $l=1$  and  $l=2$  are comparable, and not in the ratio  $(k_0 r)^2 : (k_0 r)^4$ . However, even if  $\Delta J$  permits both  $l=1$  and  $l=2$ , one of these alternatives will be eliminated by the parity rules, and since the transition probabilities for higher  $l$  fall off according to the  $(k_0 r)^{2l}$  rule, the argument for retaining only the lowest allowed  $l$  is not vitiated. More special nuclear symmetries may on occasion make it necessary to retain higher values of  $l$ .

Excepting such special cases, the practical applicability of (18) will not be reduced if we limit  $l_1$  to either of the values  $|J_A - J_B|$  or  $|J_A - J_B| + 1$ , whichever is allowed by the parity relations in a particular case, and similarly limit  $l_2$  to  $|J_B - J_C|$  or  $|J_B - J_C| + 1$ . The general summation formulae for  $W(J_B J_A k l_1; l_1 J_B)$  and  $W(J_B J_C k l_2; l_2 J_B)$  reduce to one or two terms on substituting these values of  $l_1$  and  $l_2$  respectively, and a good deal of cancellation occurs on working out the coefficient of  $P_k(\cos \theta)$  in (18). If we write  $2g$  for  $k$ , so that  $g$  assumes successive integer values, it is found that the angular distribution function can now be written

$$I(\theta) \sim \sum_g b_{2g} \{ [4g+1] [(2g)!]^2 / [g!]^4 \} P_{2g}(\cos \theta). \quad \dots \dots (19)$$

The coefficients  $b_{2g}$  are functions only of  $g$  and the three  $J$ 's; there are sixteen of them corresponding to the various possible combinations of  $l_1 = |J_A - J_B|$  or  $|J_A - J_B| + 1$  with  $l_2 = |J_B - J_C|$  or  $|J_B - J_C| + 1$  for  $J_A \gtrless J_B$  and  $J_B \gtrless J_C$ . In tabulating these coefficients the substitutions  $J_B \rightarrow J$ ,  $J_A - J_B \rightarrow \Delta$ ,  $J_C - J_B \rightarrow \delta$  shorten the formulae somewhat. It will be observed in Table 1 that only ten of the sixteen formulae are given explicitly, the remainder being readily obtained from these ten by symmetry relations.

[continued overleaf]

Table 1. Coefficients  $b_{2g}$  in the Angular Distribution

$$I(\theta) \sim \sum_g b_{2g} \{ [4g+1] [(2g)!]^2 / [g!]^4 \} P_{2g}(\cos \theta)$$

for the Nuclear Transition  $J + \Delta \rightarrow J \rightarrow J + \delta$  with Ejection of Electrons with Angular Momenta  $l_1, l_2$

$\Delta$	$\delta$	$b_{2g}$
$-l_1$	$-l_2$	$\frac{(g-\Delta)! (2J-2g)! (2J+2g+1)! (g-\delta)!}{(2g+1-2\Delta)! (-\Delta-g)! (2g+1-2\delta)! (-\delta-g)!}$
$-l_1$	$-l_2+1$	$\frac{(g-\Delta)! (2J+2g+1)! (2J-2g)! (g+1-\delta)! \{2(1-\delta)(J+1) - 2g(2g+1)(J+\delta)\}}{(-\Delta-g)! (2g+1-2\Delta)! (1-g-\delta)! (2g+3-2\delta)!}$
$-l_1$	$l_2-1$	$\frac{(g-\Delta)! (g+\delta+1)! \{2(\delta+1)J-2g(2g+1)(J+\delta+1)\}}{(2g+1-2\Delta)! (-g-\Delta)! (2g+2\delta+3)! (\delta-g+1)!}$
$-l_1$	$l_2$	$\frac{(g-\Delta)! (g+\delta)!}{(2g+1-2\Delta)! (-g-\Delta)! (\delta-g)! (2\delta+2g+1)!}$
$-l_1+1$	$-l_2$	Interchange $\Delta$ and $\delta$ in $(-l_1, -l_2+1)$
$-l_1+1$	$-l_2+1$	$\frac{(g+1-\Delta)! (2J-2g)! (2J+2g+1)! (g+1-\delta)! \{2(1-\Delta)(J+1) - 2g(2g+1)(J+\Delta)\} \{2(1-\delta)(J+1) - 2g(2g+1)(J+\delta)\}}{(2g+3-2\Delta)! (1-g-\Delta)! (1-g-\delta)! (2g+3-2\delta)!}$
$-l_1+1$	$l_2-1$	$\frac{(g+1-\Delta)! (g+1+\delta)! \{2(1-\Delta)(J+1) - 2g(2g+1)(J+\Delta)\} \times \{2(1+\delta)J - 2g(2g+1)(J+\delta+1)\}}{(2g+3-2\Delta)! (1-g-\Delta)! (\delta+1-g)! (2\delta+2g+3)!}$
$-l_1+1$	$l_2$	$\frac{(g+1-\Delta)! (\delta+g)! \{2(1-\Delta)(J+1) - 2g(2g+1)(J+\Delta)\}}{(2g+3-2\Delta)! (1-g-\Delta)! (\delta-g)! (2g+1+2\delta)!}$
$l_1-1$	$-l_2$	Interchange $\Delta$ and $\delta$ in $(-l_1, l_2-1)$
$l_1-1$	$-l_2+1$	Interchange $\Delta$ and $\delta$ in $(-l_1+1, l_2-1)$
$l_1-1$	$l_2-1$	$\frac{(g+\Delta+1)! (g+\delta+1)! \{2(\Delta+1)J - 2g(2g+1)(J+\Delta+1)\} \times \{2(\delta+1)J - 2g(2g+1)(J+\delta+1)\}}{(2g+2\Delta+3)! (\Delta-g+1)! (2J-2g)! (2J+2g+1)! \times (\delta-g+1)! (2g+2\delta+3)!}$
$l_1-1$	$l_2$	$\frac{(\delta+g)! (\Delta+g+1)! \{2(\Delta+1)J - 2g(2g+1)(J+\Delta+1)\}}{(2\delta+2g+1)! (\delta-g)! (2J-2g)! (2J+2g+1)! \times (\Delta-g+1)! (2\Delta+2g+3)!}$
$l_1$	$-l_2$	Interchange $\Delta$ and $\delta$ in $(-l_1, l_2)$
$l_1$	$-l_2+1$	Interchange $\Delta$ and $\delta$ in $(-l_1+1, l_2)$
$l_1$	$l_2-1$	Interchange $\Delta$ and $\delta$ in $(l_1-1, l_2)$
$l_1$	$l_2$	$\frac{(\Delta+g)! (\delta+g)!}{(2\Delta+2g+1)! (\Delta-g)! (2J-2g)! (2J+2g+1)! (\delta-g)! (2\delta+2g+1)!}$

Table 2. Coefficients  $a_2$  in the Angular Distribution  $1 + a_2 P_2(\cos \theta)$  when  $l_1 = l_2 = 1$ 

$\Delta$	$\delta$	$a_2 \times 5$	$\Delta$	$\delta$	$a_2 \times 5$
-1	-1	$\frac{(2J+3)(J+1)}{J(2J-1)}$	0	1	$-\frac{(2J-1)}{(J+1)}$
-1	0	$-\frac{(2J+3)}{J}$	1	-1	Same as (-1, 1)
-1	1	1	1	0	Same as (0, 1)
0	-1	Same as (-1, 0)	1	1	$\frac{J(2J-1)}{(J+1)(2J+3)}$
0	0	$\frac{(2J-1)(2J+3)}{J(J+1)}$			

Table 3. Coefficients  $a_2$  in the Angular Distribution  $1 + a_2 P_2(\cos \theta)$  when  $l_1 = 2, l_2 = 1$ 

$\Delta$	$\delta$	$a_2 \times 7$	$\Delta$	$\delta$	$a_2 \times 7$
-2	-1	$\frac{2(J+1)(2J+3)}{J(2J-1)}$	1	-1	Same as (-1, 1)
-2	0	$-\frac{2(2J+3)}{J}$	1	0	$\frac{(2J-1)(J+6)}{J(J+1)}$
-2	1	2	1	1	$\frac{-(2J-1)(J+6)}{(J+1)(2J+3)}$
-1	-1	$\frac{-(2J+3)(J-5)}{J(2J-1)}$	2	-1	Same as (-2, 1)
-1	0	$\frac{(2J+3)(J-5)}{J(J+1)}$	2	0	$\frac{-2(2J-1)}{(J+1)}$
-1	1	$\frac{-(J+6)}{J}$	2	1	$\frac{2J(2J-1)}{(J+1)(2J+3)}$

Table 4(a). Coefficients  $a_2$  in the Angular Distribution  
 $1 + a_2 P_2(\cos \theta) + a_4 P_4(\cos \theta)$  when  $l_1 = l_2 = 2$

$\Delta$	$\delta$	$a_2 \times 49$	$\Delta$	$\delta$	$a_2 \times 49$
-2	-2	$\frac{20(2J+3)(J+1)}{J(2J-1)}$	1	-2	Same as (-2, 1)
-2	-1	$\frac{-10(J-5)(2J+3)}{J(2J-1)}$	1	-1	Same as (-1, 1)
-2	1	$\frac{-10(J+6)}{J}$	1	1	$\frac{5(J+6)^2(2J-1)}{J(2J+3)(J+1)}$
-2	2	20	1	2	$\frac{-10(J+6)(2J-1)}{(2J+3)(J+1)}$
-1	-2	Same as (-2, -1)	2	-2	Same as (-2, 2)
-1	-1	$\frac{5(2J+3)(J-5)^2}{J(2J-1)(J+1)}$	2	-1	Same as (-1, 2)
-1	1	$\frac{5(J-5)(J+6)}{J(J+1)}$	2	1	Same as (1, 2)
-1	2	$\frac{-10(J-5)}{(J+1)}$	2	2	$\frac{20J(2J-1)}{(2J+3)(J+1)}$

Table 4(b). Coefficients  $a_4$  in the Angular Distribution  
 $1 + a_2 P_2(\cos \theta) + P_4(\cos \theta)$  when  $l_1 = l_2 = 2$

$\Delta$	$\delta$	$a_4 \times 49$	$\Delta$	$\delta$	$a_4 \times 49$
-2	-2	$\frac{(2J+5)(2J+3)(J+2)(J+1)}{(2J-1)(2J-3)J(J-1)}$	1	-2	Same as (-2, 1)
-2	-1	$\frac{-2(2J+5)(2J+3)(J+2)}{J(2J-1)(J-1)}$	1	-1	Same as (-1, 1)
-2	1	$\frac{-2(2J+5)}{J}$	1	1	$\frac{4(2J+5)(2J-1)(J-1)(2J-3)}{(2J+3)(J+2)(J+1)J}$
-2	2	1	1	2	$\frac{-2(2J-1)(2J-3)(J-1)}{(2J+3)(J+2)(J+1)}$
-1	-2	Same as (-2, -1)	2	-2	Same as (-2, 2)
-1	-1	$\frac{4(2J+5)(J+2)(2J+3)(2J-3)}{J(2J-1)(J-1)(J+1)}$	2	-1	Same as (-1, 2)
-1	1	$\frac{4(2J-3)(2J+5)}{J(J+1)}$	2	1	Same as (1, 2)
-1	2	$\frac{-2(2J-3)}{(J+1)}$	2	2	$\frac{J(2J-1)(2J-3)(J-1)}{(2J+5)(2J+3)(J+2)(J+1)}$

Table 5. Coefficients  $a_2$  in the Angular Distribution  $1 + a_2 P_2(\cos \theta)$  when  $l_1 = 3$ ,  $l_2 = 1$ 

$\Delta$	$\delta$	$a_2$	$\Delta$	$\delta$	$a_2$
-3	-1	$\frac{(2J+3)(J+1)}{3J(2J-1)}$	2	-1	$-\frac{1}{J}$
-3	0	$-\frac{(2J+3)}{3J}$	2	0	$\frac{2J-1}{J(J+1)}$
-3	1	$\frac{1}{3}$	2	1	$\frac{-(2J-1)}{(J+1)(2J+3)}$
-2	-1	$\frac{(2J+3)}{J(2J-1)}$	3	-1	Same as (-3, 1)
-2	0	$-\frac{(2J+3)}{J(J+1)}$	3	0	$\frac{-(2J-1)}{3(J+1)}$
-2	1	$\frac{1}{J+1}$	3	1	$\frac{1}{3} \frac{J(2J-1)}{(J+1)(2J+3)}$

Table 6 (a). Coefficients  $a_2$  in the Angular Distribution  $1 + a_2 P_2(\cos \theta) + a_4 P_4(\cos \theta)$ , when  $l_1 = 3$ ,  $l_2 = 2$ 

$\Delta$	$\delta$	$a_2 \times 7$	$\Delta$	$\delta$	$a_2 \times 7$
-3	-2	$\frac{10(2J+3)(J+1)}{3J(2J-1)}$	2	-2	$-\frac{10}{J}$
-3	-1	$-\frac{5(2J+3)(J-5)}{3J(2J-1)}$	2	-1	$\frac{5(J-5)}{J(J+1)}$
-3	1	$-\frac{5(J+6)}{3J}$	2	1	$\frac{5(J+6)(2J-1)}{2J(J+1)(2J+3)}$
-3	2	$\frac{10}{3}$	2	2	$\frac{-(10(2J-1))}{(2J+3)(J+1)}$
-2	-2	$\frac{10(2J+3)}{J(2J-1)}$	3	-2	Same as (-3, 2)
-2	-1	$-\frac{5(J-5)(2J+5)}{J(J+1)(2J-1)}$	3	-1	$\frac{-(5(J-5))}{3(J+1)}$
-2	1	$-\frac{5(J+6)}{J(J+1)}$	3	1	$\frac{-5(J+6)(2J-1)}{3(2J+3)(J+1)}$
-2	2	$\frac{10}{(J+1)}$	3	2	$\frac{10J(2J-1)}{3(2J+3)(J+1)}$



Table 6 (b). Coefficients  $a_4$  in the Angular Distribution  
 $1 + a_2 P_2(\cos \theta) + a_4 P_4(\cos \theta)$  when  $l_1 = 3, l_2 = 2$

$\Delta$	$\delta$	$a_4 \times 77$	$\Delta$	$\delta$	$a_4 \times 77$
-3	-2	$\frac{3(2J+5)(J+2)(2J+3)(J+1)}{J(2J-1)(J-1)(2J-3)}$	2	-2	$\frac{-(7J+30)}{J}$
-3	-1	$\frac{-6(2J+5)(J+2)(2J+3)}{J(2J-1)(J-1)}$	2	-1	$\frac{2(2J-3)(7J+30)}{J(J+1)}$
-3	1	$\frac{-6(2J+5)}{J}$	2	1	$\frac{(7J+30)(2J-1)(J-1)(2J-3)}{J(J+2)(2J+3)(J+1)}$
-3	2	3	2	2	$\frac{-(7J+30)(2J-1)(J-1)(2J-3)}{(2J+5)(J+2)(2J+3)(J+1)}$
-2	-2	$\frac{-(7J-23)(2J+5)(J+2)(2J+3)}{J(2J-1)(J-1)(2J-3)}$	3	-2	Same as (-3, 2)
-2	-1	$\frac{2(7J-23)(2J+5)(J+2)(2J+3)}{J(J+1)(2J-1)(J-1)}$	3	-1	$\frac{-6(2J-3)}{(J+1)}$
-2	1	$\frac{2(7J-23)(2J+5)}{J(J+1)}$	3	1	$\frac{-6(2J-1)(J-1)(2J-3)}{(J+2)(2J+3)(J+1)}$
-2	2	$\frac{-(7J-23)}{(J+1)}$	3	2	$\frac{3J(2J-1)(J-1)(2J-3)}{(2J+5)(J+2)(2J+3)(J+1)}$

(iii) Coefficients of  $P_2(\cos \theta)$  and  $P_4(\cos \theta)$  for definite numerical  $l_1$  and  $l_2$

Tables 2-6 have been obtained from Table 1 by substituting the numerical values  $l_1 = 1, 2, 3$ ;  $l_2 = 1, 2$ . If in Tables 3, 5, 6(a) and 6(b) we merely interchange the column headings  $\Delta$  and  $\delta$  they become respectively the tables for  $l_1 = 1, l_2 = 2$ ;  $l_1 = 1, l_2 = 3$ ;  $l_1 = 2, l_2 = 3$ , a result which follows from the symmetry of the general formula (18). It will be recalled that  $I(\theta)$  is always isotropic for  $J = 0$  or  $\frac{1}{2}$ ; Tables 1-6 are therefore applicable only for  $J \geq 1$ . It will be clear moreover that certain entries are applicable only for  $J \geq 2$  and others only for  $J \geq 3$ , owing to limitations imposed by the angular momentum relations (1) and (2).

Tables 2-6 refer to angular distributions which contain Legendre polynomials up to the fourth order. If required, more complicated distributions may be calculated in exactly the same way by substituting the appropriate values of  $l_1, l_2$  in Table 1.

In Figure 1 the coefficients  $a_2$ , for the case  $l_1 = l_2 = 1$  (Table 2), are plotted against  $J$ . It is seen that for increasing  $J$  each  $a_2$  tends monotonically to some non-vanishing limit, say  $(a_2)_\infty$ , in the range  $-\frac{2}{5} \leq (a_2)_\infty \leq \frac{4}{5}$ . Similarly curves of  $a_2$  and, where applicable,  $a_4$  against  $J$  may be drawn for Tables 3-6. In all such curves  $a_2$  and  $a_4$  tend to some limiting value numerically less than unity for large  $J$ . For some of the entries in Table 5 and Table 6(a),  $(a_2)_\infty = 0$ , but in Tables 2, 3 and 5(a), i.e. where  $l_1$  and  $l_2$  are both less than 3,  $(a_2)_\infty$  is never numerically less than  $5/49$ , so that in all these cases  $I(\theta)$  exhibits appreciable anisotropy however large  $J$  may be.  $(a_4)_\infty$  does not vanish in any of the cases considered, although its numerical value may be as low as  $1/49$ . Inspection of the tables shows that

although most of the factors in the formulae for  $a_2$  and  $a_4$  do not vanish for allowed values of  $J$ , there are, however, a few which do, namely  $(J-1)$ ,  $(2J-3)$  and  $(J-5)$ , with the result that certain  $a_4$  vanish at  $J=1$  or  $\frac{3}{2}$  and certain  $a_2$  vanish at  $J=5$ . In these cases, which can be quickly spotted in the tables, we have a fortuitous simplification in the angular distribution. A few of the formulae for  $a_4$  have the factors  $(J-1)$  and  $(2J-3)$  in the denominator, but in such cases the values of  $J$  which would give  $a_4 = \pm \infty$  are not allowed by the angular momentum relations.

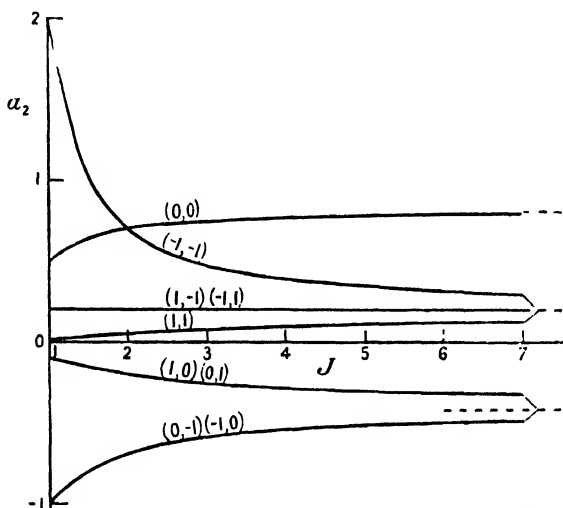


Figure 1. Coefficients  $a_2$  in  $1 + a_2 P_2(\cos \theta)$  as a function of  $J$ :  $l_1 = 1 = l_2$ ; curves labelled  $(\Delta, \delta)$ ; asymptotes shown dotted.

Typical distributions of the form  $I(\theta) \sim 1 + a_2 P_2(\cos \theta) + a_4 P_4(\cos \theta)$  are shown in Figures 2 and 3. The first of these is symmetric about a maximum at  $\theta = \pi/4$ , whilst the second has no turning point in the interval  $0 < \theta < \pi/2$ ; the condition for a turning point in this interval is discussed in (iv) below.

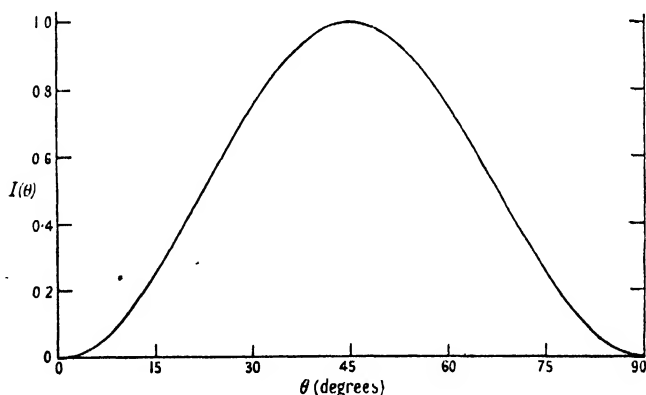


Figure 2.  $l_1 = 2 = l_2$ ,  $J + \Delta = 0$ ,  $J = 2$ ,  $J + \delta = 0$ ,

$$I(\theta) \sim 1 + \frac{5}{7} P_2(\cos \theta) - \frac{12}{7} P_4(\cos \theta) \sim \cos^2 \theta - \cos^4 \theta.$$

It is interesting to compare the present results with the corresponding ones for  $\gamma$ - $\gamma$  correlation (Hamilton 1940). Although Hamilton has tabulated coefficients of  $\cos^2 \theta$  and  $\cos^4 \theta$ , rather than  $P_2(\cos \theta)$  and  $P_4(\cos \theta)$ , it can often be seen by comparing entries in his tables with the corresponding entries in the tables of the

present paper that the  $\gamma\text{-}\gamma$   $I(\theta)$  and the conversion-conversion  $I(\theta)$  for a particular double transition have the same general behaviour. This is borne out in comparing the curves in Figure 1 of the present paper with Hamilton's curves for the coefficient of  $\cos^2\theta$  in a dipole-dipole type transition. However, in every case the conversion-conversion  $I(\theta)$  exhibits stronger anisotropy than the corresponding  $\gamma\text{-}\gamma$   $I(\theta)$ ; none of the entries in Hamilton's tables permits of 100% anisotropy\* in  $I(\theta)$ , whereas this is certainly possible in the conversion-conversion case, as

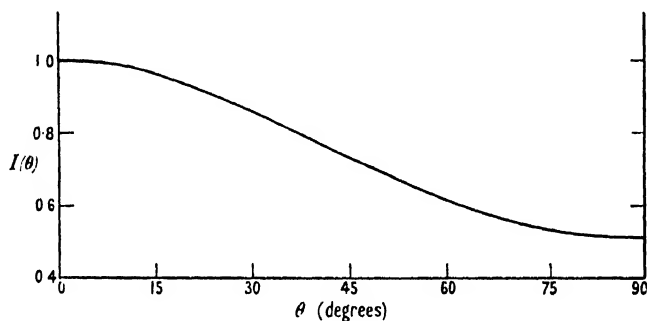


Figure 3.  $l_1=3$ ,  $l_2=2$ ,  $J+\Delta=J-3$ ,  $J\geq 3$ ,  $J+\delta=J+2$ .

$$I(\theta) \sim 1 + \frac{10}{21} P_2(\cos \theta) + \frac{3}{77} P_4(\cos \theta).$$

illustrated by Figure 2 and discussed further in (iv) below. It was reasonable to expect the  $\gamma\text{-}\gamma$  directional correlation to be weaker than the conversion-conversion because in the case of  $\gamma$ -quanta it is the polarization which is directly coupled to the nucleus, and the propagation direction enters only indirectly through the fact that it must be perpendicular to the polarization direction. A preliminary report by Falkoff (1948) on calculations of polarization correlation of successive  $\gamma$ -quanta suggests that this will prove stronger on the whole than their directional correlation.

#### (iv) Conditions for Zero in $I(\theta)$ [100% anisotropy]

It was thought worth while to work out the conditions that the two types of distribution we have been considering, viz.  $I_1(\theta) \sim 1 + a_2 P_2(\cos \theta)$  and  $I_2(\theta) \sim 1 + a_2 P_2(\cos \theta) + a_4 P_4(\cos \theta)$ , shall have zeroes, since a zero in  $I(\theta)$  means 100% anisotropy, and experimentally a large anisotropy should be easier to detect than a small one. We need consider only the interval  $0 \leq \theta \leq \pi/2$ , since we know  $I(\theta)$  is symmetrical about  $\pi/2$ . Since  $I(\theta)$  cannot be negative, zeroes, if they occur, must be at the minima.

$I_1(\theta)$  has either a maximum at  $\theta=0$  and a minimum at  $\theta=\pi/2$ , or vice versa. If the minimum occurs at  $\pi/2$ , the condition  $I_1(\pi/2)=0$  requires  $a_2=2$ ; if it occurs at 0,  $I_1(0)=0$  requires  $a_2=-1$ .

$I_2(\theta)$  also has turning points at  $\theta=0$  and  $\pi/2$ , and will have an additional turning point at some intermediate value of  $\theta$  given by  $\sin^2\theta = 6a_2/35a_4 + 4/7$  when the roots of this equation are real and non-vanishing, i.e. when  $-10/3 < a_2/a_4 < 5/2$ . In the case where there is no intermediate turning point either  $I_2(0)$  or  $I_2(\pi/2)$  will be a minimum.  $I_2(0)=0$  requires  $a_2+a_4=-1$  which, in conjunction with the

\* We define percentage anisotropy as  $100(I_{\text{greatest}} - I_{\text{least}})/I_{\text{greatest}}$ .

condition that  $a_2/a_4$  shall not be within the range  $-10/3$  to  $5/2$ , sets the following individual limits on  $a_2$  and  $a_4$ :

$$a_2/a_4 \leq -10/3: -10/7 \leq a_2 < -1, \quad 0 < a_4 \leq 3/7$$

$$a_2/a_4 \geq 5/2: -1 < a_2 \leq -5/7, \quad -2/7 \leq a_4 < 0.$$

$I_2(\pi/2) = 0$  requires  $4a_2 - 3a_4 = 8$  which, in conjunction with  $a_2/a_4 \leq -10/3$  or  $\geq 5/2$ , sets the following limits:

$$a_2/a_4 \leq -10/3: 80/49 \leq a_2 < 2, \quad -24/49 \leq a_4 < 0$$

$$a_2/a_4 \geq 5/2: 2 < a_2 \leq 20/7, \quad 0 < a_4 \leq 8/7.$$

If a maximum or minimum does occur between  $\theta = 0$  and  $\pi/2$ ,  $I_2(0)$  and  $I_2(\pi/2)$  will be either both minima or both maxima as the case may be; in either event  $I_2(0) \geq I_2(\pi/2)$  according as  $12a_2 \geq -5a_4$ . Let us take first the equality sign and examine the conditions for the vanishing of  $I_2(\theta)$ . If there are minima at 0 and  $\pi/2$ , the vanishing point must occur here and  $I_2(0) = I_2(\pi/2) = 0$  give the conditions  $a_2 = 5/7$ ,  $a_4 = -12/7$ ; if on the other hand there are maxima at  $\theta = 0$  and  $\pi/2$ , with a minimum at some point  $\theta = \alpha$  in between, the condition that  $I_2(\alpha) = 0$  is  $10a_4(7 + a_2 - 3a_4) = 9a_2^2$ , which together with  $12a_2 = -5a_4$  gives  $a_2 = -40/49$ ,  $a_4 = 96/49$ .

Next let us take  $I_2(0) > I_2(\pi/2)$ . In this case vanishing may occur either at  $\theta = \alpha$  or at  $\theta = \pi/2$ , but clearly not at  $\theta = 0$ . Individual limits consistent with the vanishing of  $I_2(\theta)$  may be set to  $a_2$  and  $a_4$  by using in turn the conditions for  $I_2(\alpha) = 0$ ,  $I_2(\pi/2) = 0$  together with  $12a_2 > -5a_4$  and the general condition  $-10/3 < a_2/a_4 < 5/2$  for a turning point at  $\theta = \alpha$ . These limits are as follows:

$$I_2(\alpha) = 0 [0 < \alpha < \pi/2]: -40/49 < a_2 < 7/(6\sqrt{(3/10)} - 1) \simeq 3.06, \quad 8/7 < a_4 < 18/7$$

$$I_2(\pi/2) = 0: 5/7 < a_2 < 80/49 \text{ or } 20/7 < a_2 < +\infty,$$

$$-12/7 < a_4 < -24/49 \text{ or } 8/7 < a_4 < +\infty.$$

Finally we take the case  $I_2(0) < I_2(\pi/2)$ . Zeroes are now possible at either  $\theta = 0$  or  $\theta = \alpha$  but not at  $\theta = \pi/2$ . Using in turn the conditions for  $I_2(\alpha) = 0$ ,  $I_2(0) = 0$  together with  $12a_2 < -5a_4$  and  $-10/3 < a_2/a_4 < 5/2$ , individual limits may be set to  $a_2$  and  $a_4$  as follows:

$$I_2(\alpha) = 0 [0 < \alpha < \pi/2]: -7/(1 + 6\sqrt{(3/10)}) [\simeq -1.63] < a_2 < -40/49, \quad 3/7 < a_4 < 96/49$$

$$I_2(0) = 0: -\infty < a_2 < -10/7 \text{ or } -5/7 < a_2 < 5/7,$$

$$-12/7 < a_4 < -2/7 \text{ or } 3/7 < a_4 < +\infty.$$

## § 5. LIMITATIONS OF PRESENT TREATMENT

In this section we discuss to what extent the validity of the foregoing treatment is limited by the initial assumptions listed at the beginning of § 2.

It may first be remarked that assumptions (a), (b) and (c) have the effect of limiting the whole discussion to internal conversion of electric rather than magnetic multipole radiation, for since we exclude spin reversal, the parity change accompanying the ejection of an electron of angular momentum  $l$  is just  $(-1)^l$ —the parity of  $Y_{l,m}(\theta, \phi)$ , the angular part of the electron wave function—and this is the parity change for an electric  $2^l$ -pole, whereas that for a magnetic  $2^l$ -pole

is  $(-1)^{J+1}$ . In general any nuclear transition is accompanied by the emission of both electric and magnetic multipole radiations, so that it is clearly necessary to consider their relative importance for internal conversion. This has been done in a recent paper by Drell (1949). It is known that a transition in which the angular momentum changes by  $\Delta J$  gives either electric  $2^{\Delta J}$ -pole with magnetic  $2^{\Delta J+1}$ -pole radiation, or magnetic  $2^{\Delta J}$  with electric  $2^{\Delta J+1}$ , according to the parity relations\*. Drell shows that in the former ('parity allowed') case the number,  $N_m$ , of magnetic internal-conversion electrons ejected is quite negligible compared with the number  $N_e$  of electric internal conversion electrons (e.g.  $(N_m/N_e)_{K\text{-shell}} < 10^{-8}$  for electron energies  $< 1$  Mev.), but that in the latter ('parity forbidden') case  $N_m/N_e$  may be appreciable. For soft  $\gamma$ -rays in the neighbourhood of the K-electron threshold magnetic conversion approaches a large finite value, whereas electric conversion vanishes at the threshold; consequently in this energy region  $(N_m/N_e)_{K\text{-shell}}$  may be large—100 or more—the effect increasing with atomic number  $Z$ †. Since the L-shell threshold is one-fourth the K-shell binding energy for the same value of  $Z$ , electric L-shell conversion is predominant in this energy region; however, the magnetic conversion in the K-shell may be large enough to contribute significantly to the total conversion coefficient, so that  $(N_m/N_e)_{\text{total}}$  cannot be neglected. Such cases are therefore outside the treatment of the present paper.‡

The assumption that the internal conversion electrons come from an s-state means that the present treatment can be applied to the L, M etc. shells only if internal conversion in these shells is predominantly by s-electrons. Since, in general, the mean distance of s-electrons from the nucleus is less than that of p-, d-, etc. electrons one would certainly expect internal conversion to be strongest for s-electrons, but that is not to say that conversion by other electrons is necessarily negligible. Hebb and Nelson (1940) have given non-relativistic formulae (valid for  $Z$  less than 40 or 50, and energies very much less than  $mc^2$ ) for the conversion of electric multipole radiation by the two 2s-electrons and the six 2p-electrons of the L-shell. If we denote by  $N_{2s}$  and  $N_{2p}$  the total numbers of internal conversion electrons which have been ejected from 2s and 2p states respectively, during the emission of  $N_q$   $\gamma$ -quanta, then Hebb and Nelson's formulae give in effect the quantities  $N_{2s}/N_q$  and  $N_{2p}/N_q$  in terms of the  $\gamma$ -ray and ejected electron energies, the order  $l$  of the electric multipole radiation, and  $Z$ . To calculate numerical values of  $N_{2p}/N_{2s}$  for definite energies and definite  $l$  and  $Z$  involves one in a somewhat lengthy evaluation of hypergeometric functions. If we admit energies  $\gg mc^2$  the formula certainly gives  $N_{2p}/N_{2s} \rightarrow 0$ , whatever  $l$  and  $Z$ . Such a step is, of course, logically unjustified, since the formula was derived on the assumption of non-relativistic energies; yet the results of an earlier, relativistic, calculation by Hulme (1932) for the case  $l=1$ ,  $Z=84$  suggest that, here at least, the ratios  $N_{1s}:N_{2s}:N_{2p}$  are not very sensitive to energy: thus he finds for  $\gamma$ -energy  $h\nu \rightarrow \infty$ ,  $N_{1s}:N_{2s}:N_{2p} = 6.7:1:0.053$ , and for  $h\nu \simeq 1.4mc^2$   $N_{1s}:N_{2s} \simeq 7.0:1$ . Before one can confidently neglect conversion by p-electrons,  $N_{2p}/N_{2s}$  should be worked out, using e.g. Hebb and Nelson's formulae, for some  $h\nu \ll mc^2$ .

\* Barring special nuclear symmetries, one is justified in retaining only the lowest allowed multipoles of each type (§ 4 (ii)).

† Drell remarks that this point had been missed in earlier literature, giving rise to some inconsistency in values of magnetic internal-conversion coefficients calculated by different authors.

‡ We must also exclude the rare cases with electric multipole radiation absolutely forbidden by the selection rules, e.g. a  $0 \rightarrow 1$  transition without parity change.

Finally we have to consider the limitations introduced by neglecting spin reversal. For magnetic multipole radiation internal conversion by s-electrons must be accompanied by spin reversal but, as we have seen above, magnetic conversion is, with certain exceptions, negligible compared with electric conversion. Spin reversal for electric conversion has been shown by Mott and Taylor (1932) to be a small effect for energies less than  $mc^2$ . They obtain by a relativistic calculation values of the internal conversion coefficients for the K-shell both with and without spin reversal, calling them  $\kappa_B$  and  $\kappa_A$  respectively, and give curves of these quantities against energy for the case of electric quadrupole radiation and  $Z=84$ . The following data are taken from their curves: at  $h\nu=mc^2$ ,  $\kappa_B/\kappa_A \simeq 0.2$ ; at  $h\nu=0.5mc^2$ ,  $\kappa_B/\kappa_A \simeq 0.02$ ; for energies below  $0.5mc^2$ ,  $\kappa_B/\kappa_A$  decreases rapidly.

#### ACKNOWLEDGMENTS

The author is indebted to Professor R. E. Peierls for his suggestion of this problem and general guidance of the work, and to Professor H. A. Jahn for much helpful discussion.

#### REFERENCES

- CONDON, E. U., and SHORTLEY, G. H., 1935, *Theory of Atomic Spectra* (Cambridge: University Press), Chapter III.
- DRELL, S. D., 1949, *Phys. Rev.*, **75**, 132.
- FALKOFF, D. L., 1948, *Phys. Rev.*, **73**, 518.
- GOERTZEL, G., 1946, *Phys. Rev.*, **70**, 897.
- HAMILTON, D. R., 1940, *Phys. Rev.*, **58**, 122.
- HEBB, M. H., and NELSON, E., 1940, *Phys. Rev.*, **58**, 486.
- HULME, H. R., 1932, *Proc. Roy. Soc. A*, **138**, 643.
- MOTT, N. F., and TAYLOR, H. M., 1932, *Proc. Roy. Soc. A*, **138**, 665; 1933, *Ibid.*, **142**, 215.
- MYERS, R. D., 1938, *Phys. Rev.*, **54**, 361.
- RACAH, G., 1942, *Phys. Rev.*, **62**, 438.
- VAN DER WAERDEN, B. L., 1932, *Die Gruppentheoretische Methode in der Quantenmechanik* (Berlin: Springer), Chapter III, § 18.
- WARD, A. H., and WALKER, D., 1949, *Nature, Lond.*, **163**, 168.
- WIGNER, E., 1931, *Gruppentheorie und ihre Anwendung auf die Quantenmechanik der Atom-spektren* (Braunschweig: Vieweg), Chapter XVII.
- YANG, C. N., 1948, *Phys. Rev.*, **74**, 764.

# Applications of the Peierls-McManus Classical Finite Electron Theory

By J. IRVING

Department of Mathematical Physics, The University, Birmingham\*

*Communicated by R. E. Peierls; MS. received 19th April 1949*

**ABSTRACT.** In the case of an electron in a high-frequency field of small amplitude it is found that the scattering cross section for radiation depends only on the mechanical mass  $m$ , instead of the total mass, as in the point electron theory. For the scattering of fast electrons by "protons" the differential cross section for scattering depends on the mass in a more complicated way. Finite values are obtained for the deflection for all values of the impact parameter and for the total energy radiated in the collision.

## § 1. INTRODUCTION

PEIERLS and McManus (McManus 1948) have proposed equations of motion for an electron in an electromagnetic field which can be applied for accelerations and frequencies of any magnitude. Their method depends on the introduction of a Lorentz-invariant form factor  $F(\mathbf{R}^2)$  into the interaction term in the relativistic Lagrangian for the motion. This is equivalent to a space-time distribution of electronic charge and also involves a parameter  $r_0$  of the dimensions of a length. The theory yields the non-linear integro-differential equations of motion:

$$m\dot{U}_i - \frac{2}{3}e^2(\ddot{U}_i + \dot{\mathbf{U}}^2 U_i) = eU^j \int F_{ij}(\mathbf{z}') F(\mathbf{R}^2) d\mathbf{z}'^{(4)} \\ + 2e^2 U^j \int_{-\infty}^{+\infty} [U_j'(z_i - z_i') - U_i'(z_j - z_j')] \frac{dH(\mathbf{R}^2)}{d\mathbf{R}^2} ds', \quad \dots \dots (1)$$

where  $U_j' = U_j(s')$  and  $\mathbf{U}$  is the velocity four-vector in relativistic notation;  $\mathbf{R}^2 = (z^i - z'^i)(z_i - z'_i)$ ,  $i=0, 1, 2, 3$ . The dots denote differentiation with respect to  $s$ , the proper time. This means, for example, that  $U_1 = u_1/\sqrt{1-u^2}$ , where  $u$  is the magnitude of the velocity and  $u_1$  is a component.

$$F(\mathbf{R}^2) = (2\pi)^{-2} \int g(\mathbf{K}^2) \exp(-i\mathbf{K} \cdot \mathbf{R}) d\mathbf{K}^{(4)}$$

is the four-dimensional Fourier transform of  $g(\mathbf{K}^2)$ . The "influence function"  $H(\mathbf{R}^2)$  is the transform of  $-16\pi^3 g^2(|\mathbf{K}^2|)/\mathbf{K}^2$  (McManus 1948). In this paper it is sufficient to know that  $H(\mathbf{R}^2)$  is an even function in  $\mathbf{R}^2$  and

$$\int_{-\infty}^{+\infty} H(\mathbf{R}^2) d\mathbf{R}^2 = 1.$$

Equations (1) reduce to the Lorentz-Dirac equations when the acceleration and its higher derivatives are small.

In this paper two problems are considered: the motion of an electron in a weak electromagnetic field of arbitrary frequency, and the scattering of fast electrons by a small point charge, whose mass is much greater than the mass of the electron. It is found that in both these cases the non-linear integro-differential equations of motion reduce to linear types, when higher powers of the field

\* Now Nuffield Research Fellow in Theoretical Physics in University of Glasgow.

intensities and charges are neglected. Solution of the former problem shows that, for frequencies large compared to the characteristic frequency, only the mechanical mass need be taken into account in the subsequent motion. The scattering cross section for radiation also depends only on the mechanical mass, which indicates an increase in cross section for higher frequencies when compared with the point electron theory. If a similar result held in a quantized theory, this would enable the mechanical mass to be determined experimentally. So far it has not been possible to formulate such a theory.

Solution of the second problem shows that the scattering formula depends on the mechanical and the electromagnetic mass in a more complicated way. In addition it is found that there is a maximum value of the angle of scattering  $\theta$  for a particular value of the impact parameter, that is, a maximum value of the differential cross section for some value of  $\theta$ . Also  $\theta$  has a finite value, namely zero, for zero impact parameter. In contrast with the divergent value for the total energy radiated by the electron in the collision, using a point theory, the theory presented here yields a finite value of the impact parameter.

## § 2. REDUCTION OF EQUATIONS OF MOTION TO APPROXIMATE LINEAR FORM AND METHOD OF SOLUTION

In the particular applications considered in this paper, the external field is of small amplitude and the motion of the electron is rectilinear. The following approximations are then valid:  $s \simeq t$ ,  $z_0 \simeq t$ ,  $z_1 = \zeta$ ,  $z_2 = z_3 = 0$ ,  $\mathbf{R}^2 \simeq (t - t')^2$ , the speed of light being taken as  $c = 1$ . Equation (1) then assumes the form

$$m\ddot{\zeta} - \frac{2}{3}e^2\dot{\zeta} = X(t) + 2e^2 \int_{-\infty}^{+\infty} [(\zeta - \zeta') - \dot{\zeta}'(t - t')]h\{(t - t')^2\}dt', \dots\dots (2)$$

where

$$h\{(t - t')^2\} = dH(\mathbf{R}^2)/d\mathbf{R}^2;$$

$$\zeta = \zeta(t); \quad \zeta' = \zeta(t'); \quad \dot{\zeta} = \frac{d\zeta}{dt}; \quad \dot{\zeta}' = \frac{d\zeta'}{dt'}; \quad \ddot{\zeta} = \frac{d^2\zeta}{dt^2}; \quad \ddot{\zeta}' = \frac{d^2\zeta'}{dt'^2}$$

$X(t)$  is the "averaged external field",

$$eU^j \int F_{ij}(\mathbf{z}')F(\mathbf{R}^2)d\mathbf{z}'^{(4)}.$$

Equation (2) may be solved by means of the Fourier transformation

$$\zeta(t) = \frac{1}{\sqrt{(2\pi)}} \int_{-\infty}^{+\infty} Z(q) \exp(iqt) dq. \dots\dots (3)$$

It is then easily shown, from equation (2), that

$$Z(q) = \frac{\frac{1}{\sqrt{(2\pi)}} \int_{-\infty}^{+\infty} X(t) \exp(-iqt) dt}{-mq^2 + \frac{2}{3}e^2q^3i + \phi(-q)}, \dots\dots (4)$$

with

$$\phi(-q) = -A + \sqrt{(2\pi)}B(q) + \sqrt{(2\pi)}iqC(q), \dots\dots (5)$$

where, with  $u = t - t'$ ,

$$A = 2e^2 \int_{-\infty}^{+\infty} h(u^2) du;$$

$$B(q) = \frac{2e^2}{\sqrt{(2\pi)}} \int_{-\infty}^{+\infty} h(u^2) \exp(-iqu) du;$$

$$C(q) = \frac{2e^2}{\sqrt{(2\pi)}} \int_{-\infty}^{+\infty} uh(u^2) \exp(-iqu) du.$$



The solution of (2) obtained by the above method is valid for any particular form of the "averaging function"  $H(u^2)$ .

When  $q$  is small, equation (5), by expansion of the right-hand side in powers of  $q$ , yields

$$\phi(-q) = -e^2 q^2 \int_0^\infty H(u^2) du = -m_e q^2, \quad \dots\dots (6)$$

where  $m_e$  is the electromagnetic mass.

This result is used in the subsequent calculations. The expression  $X(t)$  is easily evaluated in the first of the following problems. In the second, however, it is most easily found by using the four-dimensional Fourier representation. This arises from the fact that the properties of the "smearing function"  $F(\mathbf{R}^2)$  are simply derived from its transform  $g(\mathbf{K}^2)$  (McManus 1948).

### § 3. MOTION OF AN ELECTRON IN A HIGH-FREQUENCY FIELD

Consider an electron irradiated by a plane wave of small amplitude  $E_0$  and frequency  $\omega/2\pi$ . The electric component may be taken as  $E_0 \exp\{i\omega(x_3 - x_0)\}$  in the  $x_1$ -direction. The averaging process then gives  $E_0 \exp\{i\omega(z_3 - z_0)\}$ , which reduces to  $E_0 \exp(-i\omega t)$ .

Since the amplitude is small, magnetic force and pressure of radiation may be neglected, so that the motion is rectilinear. Since  $X(t) = eE_0 \exp(-i\omega t)$ , then

$$\frac{1}{\sqrt{(2\pi)}} \int_{-\infty}^{+\infty} X(t) \exp(-iqt) dt = \sqrt{(2\pi)} e E_0 \delta(\omega + q).$$

Hence, from (3) and (4),

$$\zeta(t) = \frac{eE_0 \exp(-i\omega t)}{-m\omega^2 - \frac{2}{3}e^2\omega^3 i + \phi(\omega)}. \quad \dots\dots (7)$$

(i)  $\omega$  small; using (6), (7) yields

$$\zeta(t) = \frac{eE_0 \exp(-i\omega t)}{(-M\omega^2 - \frac{2}{3}e^2\omega^3 i)},$$

where  $M = m + m_e$ . This is the usual Lorentz value.

(ii)  $\omega$  large: this case is best illustrated by taking a particular function

$$H(\mathbf{R}^2) = (1/2r_0^2) \exp(-|\mathbf{R}^2|/r_0^2).$$

Since  $\mathbf{R}^2 \simeq (t - t')^2 = u^2$ , we then have  $H(u^2) = (1/2r_0^2) \exp(-u^2/r_0^2)$ . McManus (1948) discusses the general character of  $H(\mathbf{R}^2)$ . This particular choice of  $H(u^2)$  enables the integrals occurring in the expression for  $\phi(\omega)$  to be evaluated exactly by elementary methods, giving

$$\phi(\omega) = -(\sqrt{\pi}e^2/r_0^3) \exp(-\omega^2 r_0^2/4) - (\sqrt{\pi}e^2\omega^2/r_0) \exp(-\omega^2 r_0^2/4) + \sqrt{\pi}e^2/r_0^3. \quad \dots\dots (6')$$

Hence, when  $\omega \gg 1/r_0$ , the characteristic frequency of the electron,  $\phi(\omega) \sim \sqrt{\pi}e^2/r_0^3$ , which is negligible compared with  $2e^2\omega^3/3$ . Thus, from (7),  $\zeta(t)$  involves only the rest-mass  $m$ , instead of the total mass  $M$ , which occurs in the low-frequency case.

The function  $H(u^2) = r_0^2/\{2(r_0^2 + u^2)^2\}$ ,

which gives the electron a greater extension, leads to a similar result, namely  $3\pi e^2/4r_0^3$ . More generally, a discussion of the order of magnitude of the integrals

in  $\phi(\omega)$ , using the fact that  $H(u^2)$  is a function of  $u^2/r_0^2$ , shows that  $\phi(\omega) \sim e^2/r_0^3$  for any even function  $H(u^2)$ , satisfying the normalization condition.

For intermediate frequencies detailed evaluation for a specific  $H(u^2)$  is necessary, as, for example, equation (6').

Consider now the energy radiated by the electron. It is shown in the Appendix that the standard formula for the average rate of radiation of energy, namely  $\frac{1}{2}e^2\ddot{\zeta}\ddot{\zeta}^*$ ,  $\ddot{\zeta}$  being complex in this problem, is applicable. Evaluation then yields  $e^2E_0^2\omega^4DD^*/3$ , where

$$D = 1/\{m\omega^2 + \frac{2}{3}e^2\omega^3i - \phi(\omega)\}.$$

Thus, for  $\omega \gg 1/r_0$ , we have

$$e^2E_0^2/\{3(m^2 + 4e^4\omega^2/9)\}.$$

This means that the scattering cross section for radiation should for high frequencies be greater than the value for a point electron. Quantum effects, however, arise at high frequencies, so that the development of a quantum electrodynamic theory for a finite electron might lead to a different result.

#### § 4. SCATTERING OF ELECTRONS BY PROTONS

(The term "proton" is used here in the sense of a heavy particle with a small charge  $e$ ). The ordinary classical theory of the scattering of fast electrons by protons leads to a divergent result for very small values of the impact parameter when the particle dimensions are neglected. It will be shown that the finite electron theory leads to finite results.

The problem of the scattering of electrons by protons can be converted, by means of a Lorentz transformation, into one in which the electrons are initially at rest and the protons moving. It is convenient to use such a transformation here. Moreover, since the mass of the proton is so much greater than the mass of the electron, the recoil of the proton may be disregarded. For high proton velocities, the proton field will be concentrated in the transverse direction so that the direction of motion of the electron will be approximately at right angles to the direction of motion of the proton. Since the interaction is weak, the speed acquired by the electron will be small.

$$X(t) = eU^j \int F(\mathbf{R}^2) F_{ij}(\mathbf{z}') d\mathbf{z}'^{(4)}$$

is most easily calculated in four-dimensional momentum space.  $F_{ij}(\mathbf{z}')$  is the field at the point  $\mathbf{z}'$  due to the proton at the point  $\mathbf{z}$ , in four-vector notation.  $\mathbf{R} = \mathbf{x} - \mathbf{z}'$ , where  $\mathbf{x}$  is the four-vector for the electron.

$$\text{Now} \quad F_{ij}(\mathbf{z}') = \frac{\partial A_j(\mathbf{z}')}{\partial z'^i} - \frac{\partial A_i(\mathbf{z}')}{\partial z'^j}$$

$$\text{and} \quad A_j(\mathbf{z}') = (2\pi)^{-2} \int \exp(-i\mathbf{K}' \cdot \mathbf{z}') \cdot A_j(\mathbf{K}') d\mathbf{K}'^{(4)}.$$

$$\therefore F_{ij}(\mathbf{z}') = -(2\pi)^{-2} i \int \{k'_i A_j(\mathbf{K}') - k'_j A_i(\mathbf{K}')\} \exp(-i\mathbf{K}' \cdot \mathbf{z}') d\mathbf{K}'^{(4)}$$

$$\text{Hence, since} \quad F(\mathbf{R}^2) = (2\pi)^{-2} \int \exp(-i\mathbf{K} \cdot \mathbf{R}) \cdot g(\mathbf{K}^2) d\mathbf{K}^{(4)},$$

$X(t)$  becomes

$$-eiU^j \int \exp(-i\mathbf{K} \cdot \mathbf{x}) \cdot \{k_i A_j(\mathbf{K}) - k_j A_i(\mathbf{K})\} g(\mathbf{K}^2) d\mathbf{K}^{(4)}.$$

$$\text{Now} \quad \square A_i(\mathbf{z}') \equiv \frac{\partial^2 A_i}{\partial z'_j \partial z'^j} = 4\pi \bar{s}_i(\mathbf{z}'), \quad \dots\dots\dots (8)$$

where  $\bar{s}_i(\mathbf{z}') = \epsilon \int_{-\infty}^{+\infty} U_i^P(\sigma) F(\mathbf{p}^2) d\sigma$ , with  $\mathbf{p} = \mathbf{z}' - \mathbf{z}(\sigma)$ , is the effective charge-current density, and  $\sigma$  is the proper time of the proton,  $\mathbf{U}^P(\sigma)$  being its four-velocity.

$$\therefore \bar{s}_i(\mathbf{K}) = \epsilon \int_{-\infty}^{+\infty} \exp(i\mathbf{K} \cdot \mathbf{z}) \cdot U_i^P(\sigma) g(\mathbf{K}^2) d\sigma.$$

Now from (8)

$$A_i(\mathbf{K}) = \frac{4\pi\bar{s}_i(\mathbf{K})}{\mathbf{k}^2 - k_0^2} + \frac{1}{2}\epsilon i \frac{1}{k} \{\delta(k_0 - |\mathbf{k}|) - \delta(k_0 + |\mathbf{k}|)\}.$$

The second term gives part of the radiation field of the proton. Since the velocity of the proton is constant, this term must vanish. Hence

$$X(t) = 4\pi\epsilon\epsilon i U^j \int \exp(-i\mathbf{K} \cdot \mathbf{x}) \exp(i\mathbf{K} \cdot \mathbf{z}) \cdot \frac{g^2(\mathbf{K}^2)}{\mathbf{K}^2} \{k_i U_j^P - k_j U_i^P\} d\sigma d\mathbf{K}^{(4)}.$$

Choosing the initial position of the electron as origin, we have  $\mathbf{z} = (\tau, -b, v\tau, 0)$ ;  $b$  is the impact parameter;  $\mathbf{U}^P = \left(\frac{d\tau}{d\sigma}, 0, v\frac{d\tau}{d\sigma}, 0\right)$ ;  $\mathbf{x} = (t, \zeta, 0, 0)$ ;  $\mathbf{K} = (k_0, k_1, k_2, k_3)$ ;  $\mathbf{K}^2 = k_0^2 - \mathbf{k}^2$ . The force  $X(t)$  then becomes, since  $U^0 \simeq 1$  and the terms with  $i = 1, 2, 3$  are negligible,

$$4\pi\epsilon\epsilon i \int \exp\{-i(k_0 t - k_1 \zeta)\} \cdot \exp(ik_1 b) \cdot \exp\{i\tau(k_0 - k_2 v)\} \cdot k_1 \frac{g(\mathbf{K}^2)}{\mathbf{K}^2} d\tau d\mathbf{K}^{(4)}.$$

Integration with respect to  $\tau$  and  $k_0$  yields, writing  $\exp(ik_1 \zeta) \simeq 1$ ,

$$8\pi^2\epsilon\epsilon i \int \frac{g^2[-\{k_1^2 + (1-v^2)k_2^2 + k_3^2\}]}{[-\{k_1^2 + (1-v^2)k_2^2 + k_3^2\}]} k_1 \exp(ik_1 b) \cdot \exp(-ik_2 v t) dk_1 dk_2 dk_3.$$

Thus a continuous frequency spectrum enters into this problem.

$$\frac{1}{\sqrt{(2\pi)}} \int_{-\infty}^{+\infty} X(t) \exp(-iqt) dt$$

after integration with respect to  $t$  and  $k'_2$ , where  $k'_2 = k_2 v$ , becomes

$$\frac{8\pi^2\epsilon\epsilon\sqrt{(2\pi)}}{v} i \int \frac{g^2[\ ]}{[\ ]} k_1 \exp(ik_1 b) dk_1 dk_3,$$

where

$$[\ ] \equiv [-\{k_1^2 + k_3^2 + \frac{1-v^2}{v^2} q^2\}].$$

Hence

$$\zeta(t) = c' \int_{-\infty}^{+\infty} \frac{f(q) \exp(iqt)}{-mq^2 + \frac{2}{3}e^2 q^3 i + \phi(-q)} dq, \quad \dots\dots\dots (9)$$

where  $c' = \frac{8\pi^2\epsilon\epsilon i}{v}$  and  $f(q) = \int \frac{g^2[\ ]}{[\ ]} k_1 \exp(ik_1 b) \cdot dk_1 dk_3$ .

Now the velocity acquired by the electron may be written as

$$\begin{aligned} \dot{\zeta} &= \int_{-\infty}^{+\infty} \ddot{\zeta} dt = \int \int_{-\infty}^{+\infty} \frac{c' q^2 f(q) \exp(iqt)}{mq^2 - \phi(-q) - \frac{2}{3}e^2 q^3 i} dq dt \\ &= 2\pi c' \int_{-\infty}^{+\infty} \frac{q^2 f(q) \delta(q)}{mq^2 - \phi(-q) - \frac{2}{3}e^2 q^3 i} dq. \end{aligned}$$

Now  $\phi(-q) \rightarrow -m_e q^2$  for  $q$  small.

$$\therefore \dot{\zeta} = \frac{2\pi c'}{M} \int \frac{g^2 \{-(k_1^2 + k_3^2)\}}{\{-(k_1^2 + k_3^2)\}} k_1 \exp(ik_1 b) dk_1 dk_3, \quad M = m + m_e.$$

$$\therefore \dot{\zeta} = -\frac{2\pi c'}{M} \int_0^\infty g^2(-\kappa^2) d\kappa \int_0^{2\pi} \exp(ib\kappa \cos \theta) \cdot \cos \theta d\theta,$$

where  $(\kappa, \theta)$  are plane polar coordinates. Making use of

$$J_0(b\kappa) = \frac{1}{2\pi} \int_0^{2\pi} \exp(ib\kappa \cos \theta) d\theta,$$

it is found that

$$\dot{\zeta} = -\frac{32\pi^4 e \epsilon}{Mb} \int_0^\infty g^2(-\kappa^2) \frac{\partial}{\partial \kappa} \{J_0(b\kappa)\} d\kappa. \quad \dots\dots (10)$$

Equation (10) could be evaluated for a particular  $g(-\kappa^2)$ . It is of more interest to obtain the magnitude of  $\dot{\zeta}$  for a general function  $g(-\kappa^2)$ . Two extreme cases are those for very large and very small values of the impact parameter, that is,  $b \gg r_0$  and  $b \ll r_0$ , respectively.

(I)  $b \gg r_0$ :

$g$  is an even function in  $\kappa^2$  and is in fact a function of  $\kappa^2 r_0^2$ . It is effectively non-zero if  $\kappa < 1/r_0$ . Now  $J_0(b\kappa)$  has the asymptotic form

$$\sqrt{\left(\frac{2}{\pi}\right)} \frac{\cos(b\kappa - \pi/4)}{\sqrt{(b\kappa)}}.$$

Thus for  $b \gg r_0$  the main contribution will come from  $b\kappa$  small, i.e.  $\kappa \sim 0$ . We may thus replace  $g^2(\kappa^2)$  by  $g^2(0)$ .

$$\therefore \dot{\zeta} = -\frac{32\pi^4 e \epsilon}{bMv} g^2(0) [J_0(b\kappa)]_0^\infty;$$

$$\therefore \dot{\zeta} = \frac{2e\epsilon}{bMv}, \quad \text{since } g(0) = (2\pi)^{-2} \quad (\text{McManus 1948}).$$

Therefore, in the rest system of the proton,

$$\dot{\zeta} = \frac{2e\epsilon}{bMv(1-v^2)^{1/2}}.$$

This is the ordinary classical value.

(II)  $b \ll r_0$ :

Here  $b\kappa \ll 1$ . Hence

$$J_0(b\kappa) \simeq 1 - \frac{1}{4} b^2 \kappa^2 \quad \dots\dots (11)$$

and

$$\begin{aligned} \dot{\zeta} &= \frac{32\pi^4 e \epsilon b}{2Mv} \int_0^\infty \kappa g^2(\kappa^2) d\kappa = \frac{be\epsilon(2\pi)^4}{2Mv} \int_0^\infty g^2(\kappa^2 r_0^2) d\kappa^2 \\ &= \frac{be\epsilon}{2Mv} \frac{1}{r_0^2} \int_0^\infty \mathcal{G}^2(u^2) du^2, \quad \text{where } \mathcal{G}(0) = 1. \\ &= \text{constant} \times \frac{be\epsilon}{2Mv r_0^2}. \end{aligned}$$

Thus, in the rest system of the proton, we have

$$\zeta \propto \frac{be\epsilon}{2Mr_0^2v(1-v^2)^{\frac{1}{2}}},$$

whence  $\zeta \rightarrow 0$  when  $b \rightarrow 0$ .

For intermediate values of  $b$  it is necessary to choose a particular form of  $g(\kappa^2)$  in order to carry out the integration. It is possible, however, to deduce from the above results the general form of the differential scattering cross section. The graph of  $\theta$ , the angle of scattering, in terms of  $b$  has the form indicated in Figure 1.

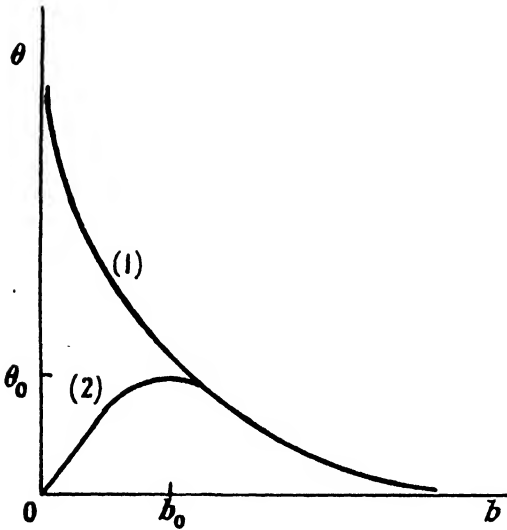


Figure 1. Qualitative graphs of deflection  $\theta$  against impact parameter  $b$ , (1) in point electron theory, (2) in finite electron theory.

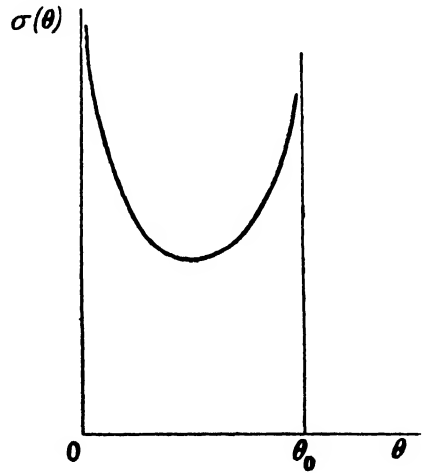


Figure 2. Qualitative graph of differential cross section  $\sigma(\theta)$  against angle of scattering  $\theta$ , in finite electron theory.

Thus  $\theta$  will have a maximum value  $\theta_0$  for some value  $b_0$  of the impact parameter.

Now

$$\sigma(\theta) \propto \frac{b(\theta) db}{\theta \frac{d\theta}{db}}$$

and, near  $\theta_0$ ,

$$\theta \simeq \theta_0 + \frac{1}{2} \frac{d^2\theta}{db^2} (b - b_0)^2.$$

Hence

$$\left| \frac{db}{d\theta} \right| = 1 / \sqrt{\left| \left\{ 2(\theta - \theta_0) \frac{d^2\theta}{db^2} \right\} \right|}.$$

$$\therefore \sigma(\theta) \rightarrow \infty, \text{ as } \theta \rightarrow \theta_0.$$

A qualitative graph of  $\sigma(\theta)$  is shown in Figure 2.

##### § 5. RADIATION EMITTED BY SCATTERED ELECTRON

The theorem proved in the Appendix indicates that the classical radiation formula, namely,  $\frac{2}{3}e^2 \ddot{\zeta} \ddot{\zeta}^*$  or  $\frac{2}{3}e^2 |\ddot{\zeta}|^2$ , since  $\zeta$  in this problem is real, also holds in this case. In this problem it is not very easy to evaluate the radiation spectrum, but the total energy radiated by the electron in the collision may be calculated simply. The radiated energy is

$$\int_{-\infty}^{+\infty} \frac{2}{3}e^2 \ddot{\zeta} \ddot{\zeta}^* dt. \quad \dots\dots (12)$$

From (9),  $\zeta(t)$  may be written in the form  $\int_{-\infty}^{+\infty} \psi(q) \exp(iqt) dq$ , where

$$\psi(q) = \frac{c' f(q)}{-mq^2 + \frac{2}{3}e^2 q^3 i + \phi(-q)}.$$

Equation (12) then becomes

$$\frac{2e^2}{3} \int_{-\infty}^{+\infty} dq dq' \psi(q) \psi^*(q') q^2 q'^2 \int_{-\infty}^{+\infty} \exp\{i(q-q')t\} dt.$$

i.e. 
$$\frac{4\pi e^2}{3} \int_{-\infty}^{+\infty} q^4 |\psi(q)|^2 dq,$$

which is equal to

$$c'^2 \frac{4\pi e^2}{3} \int_{-\infty}^{+\infty} \frac{q^4}{|mq^2 - \phi(-q) - \frac{2}{3}e^2 q^3 i|^2} |f(q)|^2 dq. \quad \dots\dots (13)$$

$|f(q)|$  may be transformed into the integral (cf. equation (10))

$$\frac{2\pi}{b} \left| \int_0^\infty \frac{g^2(\kappa^2 + p^2)}{\kappa^2 + p^2} \kappa^2 \frac{\partial}{\partial \kappa} \{J_0(b\kappa)\} d\kappa \right. \quad (14)$$

where  $p^2 = q^2(1 - v^2)/v^2$ .

Case I:

Now for  $b \gg r_0$  we should expect to obtain the value of the energy radiated by a point electron, that is,  $g^2(\kappa^2 + p^2)$  should be replaced by  $g^2(0) = (2\pi)^{-4}$ . Evaluation of (14) gives in this case

$$2\pi p K_1(bp),$$

since 
$$\int_0^\infty \frac{\kappa^2}{\kappa^2 + p^2} \frac{\partial}{\partial \kappa} \{J_0(b\kappa)\} d\kappa = -2p^2 \int_0^\infty J_0(b\kappa) \frac{\kappa}{(\kappa^2 + p^2)^2} d\kappa = bp K_1(bp),$$

where  $K_1(bp)$  is a modified Bessel function in Watson's (1944) notation. In the following calculation we make use of the Fourier transform of  $PK_1(P)$ , namely

$$\frac{1}{\sqrt{(2\pi)}} \int_{-\infty}^{+\infty} \sqrt{\left(\frac{\pi}{2}\right)} \frac{\exp(iPx)}{(x^2 + 1)^{3/2}} dx,$$

which reduces

$$\int_0^\infty P^2 K_1^2(P) dP \quad \text{to} \quad \frac{\pi}{4} \int_{-\infty}^{+\infty} \frac{dx}{(x^2 + 1)^3} = \frac{3\pi^2}{32}$$

by elementary integration. Equation (13) then becomes

$$\frac{8}{3\pi} \frac{e^4 \epsilon^2}{v^2} \int_0^\infty \frac{q^4 p^2}{[mq^2 - \phi(-q)]^2 + \frac{4}{9}e^4 q^6} \{K_1(bp)\}^2 dq. \quad \dots\dots (15)$$

Consideration of the form of the Bessel function  $K_1$  shows that the main contribution of this integral arises when  $q$  is small. Hence  $\phi(-q) \rightarrow -m_e q^2$ . Equation (15) then gives

$$\frac{8}{3\pi} \frac{e^4 \epsilon^2}{v(1 - v^2)^{1/2} b^3 M^2} \int_0^\infty P^2 K^2(P) dP, \quad M = m + m_e,$$

with  $P = bp = bq(1 - v^2)^{1/2}/v$ .

The energy radiated is thus equal to

$$\frac{\pi}{4} \frac{e^4 \epsilon^2}{M^2 b^3 v(1 - v^2)^{1/2}}.$$

In the rest-system of the proton this becomes

$$\frac{\pi}{4} \frac{e^4 \epsilon^2}{b^3 v M^2} \frac{1}{1-v^2},$$

or, in ordinary units,  $\pi r^3 M c^3 \alpha^2 / 4 b^3 v$ , where  $r = e^2 / M c^2$ ,  $\alpha = (1-v^2)^{-\frac{1}{2}}$ , and  $\epsilon$  is taken equal to  $e$  when  $b$  is large. This is the usual result given by the point electron theory (Jánossy 1948). The value given by this formula diverges as  $b \rightarrow 0$ .

*Case II:*  $b \ll r_0$ .

For  $b \ll r_0$  the function  $g(\kappa^2 + p^2)$  plays a decisive part.

Using the approximation (11) for  $J_0(b\kappa)$ , we may write

$$|f(q)| = \frac{\pi b}{\gamma} \int_0^\infty g^2(P^2 r_0^2) \{1 - p^2/P^2\} dP^2,$$

where  $P^2 = \kappa^2 + p^2$ ,  $p = q(1-v^2)^{\frac{1}{2}}/v$ ; therefore the energy radiated is

$$\frac{e^4 \epsilon^2 b^2}{v^2} (2\pi)^7 \int_0^\infty \frac{q^4 dq}{[\{mq^2 - \phi(-q)\}^2 + \frac{1}{3}e^4 q^6]} \int_0^\infty g^2(P^2 r_0^2) \{1 - p^2/P^2\} dP^2 \dots \dots (16)$$

The function  $g(P^2 r_0^2)$  vanishes unless  $P < 1/r_0$ . Also when  $q$  is large, i.e.  $p$ ,  $P$  large, the term  $(1 - p^2/P^2)$  also becomes very small. The main contribution of the integral (16) will thus arise when  $q$  is small.

Neglecting the  $p^2/P^2$  term will give a value greater than the exact value. We then have

$$\frac{e^4 \epsilon^2 b^2}{3v^2} \cdot \frac{1}{2\pi M^2} \int_0^\infty dq \left| \int_{p^2}^\infty \mathcal{G}^2(P^2 r_0^2) dP^2 \right. \quad (17)$$

where  $\mathcal{G}(0) = 1$ .

To obtain the magnitude of this expression, consider  $\mathcal{G}(P^2 r_0^2) = \exp(-P^2 r_0^2)$ . Evaluation of (17) leads to the result  $e^4 \epsilon^2 b^2 / \{M^2 r_0^5 v (1-v^2)^{\frac{1}{2}} 96 \sqrt{\pi}\}$ . Thus in the rest-system of the proton the energy radiated is  $\{e^4 \epsilon^2 b^2 / M^2 r_0^5 v (1-v^2)\} \times \text{numerical constant}$ . Thus when  $b \rightarrow 0$ , the energy radiated tends to zero. However, in the above calculation the displacement of the electron in the direction of the incident proton has been neglected, and hence, also, the energy radiated in this motion. This radiation is a second-order effect, but in the limiting case of  $b = 0$  would give a finite non-zero contribution. In this case the collision is head-on and the value is easily calculated. Thus, in contrast with the point electron theory, the above theory gives a finite value for the radiated energy for any value of the impact parameter  $b$ .

## § 6. CLOSE COLLISIONS FOR RELATIVISTIC ENERGIES

In the case of close collisions, that is,  $b \sim r_0$ , the momentum acquired by the electron in the direction of the incident proton may be treated qualitatively in the following way. The Coulomb interaction is at most  $e\epsilon/r_0^2$ , and this acts approximately for a time  $r_0/v$ . Hence the momentum acquired by the electron is of the order  $e\epsilon/r_0 v$ . If this is negligible in comparison with  $mv(1-v^2)^{-\frac{1}{2}}$ , where  $m$  is the electron mass, then  $e\epsilon/r_0$  must be less than  $mv^2(1-v^2)^{-\frac{1}{2}}$ . This means that the total energy must be much greater than the self-energy. This is only true for relativistic speeds, that is,  $v$  of the order of  $c$ , with  $c = 1$ . It is of course possible

to evaluate the velocity in the forward direction exactly by the method already used. This will not, however, yield much more than that obtained by the qualitative argument.

McManus has shown that the effective field of a particle of charge  $\epsilon$  is given by

$$\bar{F}_{ij}(\mathbf{x}) = \epsilon \int_{-\infty}^{+\infty} \left[ U_j \frac{\partial}{\partial x^i} - U_i \frac{\partial}{\partial x^j} \right] H\{\mathbf{x} - \mathbf{z}(s)\} ds + \text{radiation term.}$$

Thus for a proton moving with constant speed, only the first term arises. From the form of  $H$  it is then evident that the effective field is reduced for distances of order of magnitude of  $r_0$  or less and is unaffected for distances greater than  $r_0$ . Thus the forward momentum acquired by the electron will be relatively small for high proton speeds.

#### ACKNOWLEDGMENTS

The author wishes to thank Professor Peierls for suggesting the problem and for many valuable discussions, and also Dr. McManus for the use of his thesis.

#### APPENDIX

The expression

$$X(r) = \frac{1}{\sqrt{2\pi}} \int_{-\infty}^{+\infty} \chi(k) \exp(ikr) dk \quad \dots\dots (a)$$

is easily evaluated by the theory of residues (Whittaker and Watson 1935), the contributions coming from the poles of  $\chi(k)$ .

It is shown in the following calculation that the result may be generalized for the case of a four-dimensional integral.

The electromagnetic potentials  $A_i(\mathbf{x})$ ,  $i=0, 1, 2, 3$ , at the point  $\mathbf{x}$ , due to an electron of charge  $e$  at the point  $\mathbf{z}$ , are given by

$$A_i(\mathbf{x}) = (2\pi)^{-2} \int \frac{4\pi \bar{s}_i(\mathbf{k}, k_0)}{\mathbf{k}^2 - k_0^2} \exp(-i\mathbf{K} \cdot \mathbf{x}) d\mathbf{K}^{(4)} + \frac{e}{2} \int U_i(s) \Delta(\mathbf{R}) ds, \quad \dots\dots (b)$$

where 
$$\bar{s}_i(\mathbf{k}, k_0) = e \int_{-\infty}^{+\infty} \exp(i\mathbf{K} \cdot \mathbf{z}) U_i(s) g(\mathbf{K}^2) ds,$$

and

$$\Delta(\mathbf{R}) = \frac{1}{r} [\delta\{(t-t') - r\} - \delta\{(t-t') + r\}], \quad r^2 = (x_1 - z_1)^2 + (x_2 - z_2)^2 + (x_3 - z_3)^2.$$

Consider the first integral of (b), denoting it by  $A^{(1)}(\mathbf{x})$ . In particular, consider the case where

$$\dot{\zeta} = D \exp(-i\omega t'), \quad \mathbf{z} = (t, \zeta, 0, 0).$$

Then

$$A_1^{(1)}(\mathbf{x}) = (e/\pi) \int \frac{g(k_0^2 - \mathbf{k}^2)}{\mathbf{k}^2 - k_0^2} \exp(i\mathbf{k} \cdot \mathbf{r}) \exp(-ik_0 t + ik_0 t') \frac{d\zeta}{dt'} d\mathbf{k}^{(3)} dk_0 dt'.$$

Integration with respect to  $t'$  and  $k_0$  gives

$$A_1^{(1)}(\mathbf{x}) = \exp(-i\omega t) 2i\omega e D \int \frac{g(\omega^2 - \mathbf{k}^2)}{\omega^2 - \mathbf{k}^2} \exp(i\mathbf{k} \cdot \mathbf{r}) \cdot d\mathbf{k}^{(3)}.$$

Using polar coordinates and integrating over the angles yields

$$\frac{4\pi D e}{r} \exp(-i\omega t) \int_{-\infty}^{+\infty} \frac{k}{\omega^2 - k^2} g(\omega^2 - k^2) \exp(ikr) dk. \quad \dots\dots (c)$$



This is an integral of the same type as equation (a). Poles are at points  $k = \pm \omega$ . Thus the contributions come from  $\mathbf{k}^2 = k_0^2$ , i.e.  $g(\mathbf{K}^2) = g(0) = (2\pi)^{-2}$ . It is fairly simple to deduce from this that  $A_1^{(1)}(\mathbf{x})$  may be written in the form

$$\frac{e}{2} \int_{-\infty}^{+\infty} U_1(s) \frac{1}{r} [\delta\{(t-t') + r\} + \delta\{(t-t') - r\}] ds.$$

Hence 
$$A_1(\mathbf{x}) = \int_{-\infty}^{+\infty} U_1(s) \frac{1}{r} \delta\{(t-t') - r\} ds,$$

from (b). It can be shown in the same way that  $A_0(\mathbf{x})$  may be written in a similar form. Then the ordinary form of the retarded potential is valid for a charged particle of finite size, when  $r \gg r_0$ .

The self-field may then be written as

$$F_{ij}^{(s)}(\mathbf{x}) = e \int_{-\infty}^{+\infty} \left( U_j \frac{\partial}{\partial x^i} - U_i \frac{\partial}{\partial x^j} \right) \frac{1}{r} \delta\{(t-t') - r\} ds,$$

thus yielding the standard radiation formula.

In § 4 we had

$$\zeta(t) = \int_{-\infty}^{+\infty} \psi(q) \exp(iqt) dq.$$

This gives a continuous spectrum of poles on the real axis. Thus, in this case too, the contributions come from the poles given by  $\mathbf{k}^2 = k_0^2$ , so that the radiation formula is also valid in this case.

#### REFERENCES

- JÁNOSSY, L., 1948, *Cosmic Rays* (Oxford : University Press).  
 MCMANUS, H., 1948, *Proc. Roy. Soc. A*, **195**, 323.  
 WATSON, G. N., 1944, *Bessel Functions* (Cambridge : University Press).  
 WHITTAKER, E. T., and WATSON, G. N., 1935, *Modern Analysis* (Cambridge : University Press).

# Perturbation Theory in Neutron Multiplication Problems

By K. FUCHS

Theoretical Division, Atomic Energy Research Establishment, Harwell, Didcot, Berks.

*MS. received 24th May 1949*

**ABSTRACT.** The perturbation theory for neutron diffusion problems in the one group theory is developed systematically by expansion in the system of orthogonal solutions of the integral equation in Part I of the paper.

The multiplication of a neutron source inside a fissile system is discussed. The multiplication factor for a near critical system is derived as a function of the position of the source; isotropic sources are considered in Part II and anisotropic sources in Part III.

Part IV is concerned with a few practical applications of the theory.

## INTRODUCTION

**T**HIS report presents the perturbation theory for the calculation of critical sizes of fissile assemblies for small changes in the nuclear properties of the assembly. We confine ourselves to one group theory (all neutrons have the same velocity) and to isotropic nuclear processes. Then a fissile assembly is characterized by two quantities, which in general can be functions of the spatial position: the inverse mean free path  $\alpha(r)$  and the number  $\beta(r)$  of scattered neutrons and fission neutrons emerging from unit path of one neutron.

The problem of a change in  $\beta$  is closely related to the multiplication problem for the neutrons from an isotropic source inside a subcritical fissile assembly. These two problems have been considered by various authors in unpublished papers, in particular by Davison and Fuchs in Birmingham, by Feynman and Serber at Los Alamos, and probably by workers in other fields with which the author did not have personal contact.

The main purpose of the present paper is an extension of the theory to the multiplication problem for anisotropic sources, which permits an application of the perturbation theory to change in the mean free path.

Since the earlier work is not easily accessible and since no systematic account of the general theory exists, the multiplication problem for isotropic sources and an outline of the perturbation theory for exchanges in  $\beta$  is also presented.

## I. GENERAL THEORY

### 1. *The Integral Equation.*

Let  $K(r, r')/v$  be the primary neutron density at the point  $r$ , due to an isotropic point source of unit strength at the point  $r'$ . We shall count all nuclear processes as removal from the primary beam, so that for a homogeneous medium

$$K(r, r') = \exp(-|r - r'|/\alpha)/4\pi|r - r'|^2. \quad \dots\dots(1.1)$$

Here  $\alpha$  is the inverse mean free path of the neutron. In an inhomogeneous system  $K$  is more complicated. However,  $K$  will always be symmetric in  $r$  and  $r'$ , since a neutron is just as likely to penetrate from a point  $r'$  to the point  $r$  as from  $r$  to  $r'$ . Hence

$$K(r, r') = K(r', r). \quad \dots\dots(1.2)$$

The symmetry property is retained if scattering processes without change of energy are not considered as removal from the primary beam, and the general theory developed below applies to this case as well.

Let there be a source per unit volume of strength  $q(r')$  at the point  $r'$ . In a subcritical system this source distribution will give rise to a neutron density  $n(r)$ , which satisfies the equation

$$n(r) = \int \beta(r')K(r, r')n(r')dV' + \int \frac{q(r')}{v}K(r, r')dV'. \quad \dots\dots(1.3)$$

Here  $v$  is the velocity of the neutrons. The second term represents all the primary neutron densities due to the neutron sources. The first term accounts for the secondary contributions of the neutrons removed from the primary beam as well as tertiary contributions and so on. The total number of neutrons removed per unit time from any beam in a unit volume at  $r'$  is  $\alpha(r')n(r')v$ . Let now  $\beta/\alpha$  be the number of neutrons emerging from the volume per neutron removed. We then have a source  $\beta(r')vn(r')$  and multiplication with  $K/v$  yields the contribution of this source to  $n(r)$ .

## 2. Eigensolutions of the Homogeneous Integral Equation

Let us consider the homogeneous integral equation, obtained by omitting the source terms. This equation has solutions  $f_i(r)$  for an infinite number of eigenvalues  $\lambda_i$ . Thus

$$f_i(r) = \lambda_i \int \beta(r')K(r, r')f_i(r')dV'. \quad \dots\dots(2.1)$$

The  $f_i(r)$  form a complete set of functions which are orthogonal to the set  $\beta(r)f_i(r)$ . They may be normalized so that

$$\int \beta(r)f_i(r)f_j(r)dV = \delta_{ij}. \quad \dots\dots(2.2)$$

The kernel  $K$  can be expanded in the form  $K(r, r') = \sum_i f_i(r)f_i(r')/\lambda_i$ . Any arbitrary function  $g(r)$  can be expanded in the form  $g(r) = \sum_i [g]_i f_i(r)$  with coefficients  $[g]_i = \int \beta(r)g(r)f_i(r)dV$ .

## 3. Variation Theory

Let us vary the system under consideration to a slight extent. Such a variation may be expressed as a change  $\Delta\beta$  and  $\Delta K$ . As a result the  $\lambda_i$  and  $f_i$  will change by amounts  $\Delta\lambda_i$  and  $\Delta f_i$ . Variation of the equation (2.1) yields

$$\begin{aligned} \Delta f_i(r) = \lambda_i \int \beta(r')K(r, r')\Delta f_i(r')dV' + \Delta\lambda_i \int \beta(r')K(r, r')f_i(r') \\ + \lambda_i \int [\Delta\beta(r')K(r, r') + \beta(r')\Delta K(r, r')]f_i(r')dV'. \quad \dots\dots(3.1) \end{aligned}$$

Multiplying with  $\beta(r)f_i(r)$  and integrating we find with the help of the integral equation (2.1) and the symmetry property of the kernel  $K$  that the integral of the left-hand side of equation (3.1) cancels the integral of the first term on the right-hand side. The remaining terms yield the equation

$$\frac{\Delta\lambda_i}{\lambda_i} + \int \Delta\beta(r)f_i(r)^2dV + \lambda_i \int f_i(r)\beta(r)\Delta K(r, r')\beta(r')f_i(r')dVdV' = 0. \quad \dots\dots(3.2)$$

This equation is particularly useful if there is no change in the kernel so that the last term vanishes. The resultant equation has been used by Davison and Fuchs (1943) to calculate the effect of a thin reflector on the critical size. It is also used extensively in pile calculations, where it is known as the Statistical Weight Theorem (see for example Goodman (1947)). It is also closely related to the Feynman theorem, which states:

If two critical systems with the same kernel  $K$  differ only in the values of  $\beta(r)$ , then

$$\int [\beta_1(r) - \beta_2(r)] n_1(r) n_2(r) dV = 0, \quad \dots\dots (3.3)$$

where  $n_1$  and  $n_2$  are the neutron densities in the two systems satisfying the integral equations

$$\left. \begin{aligned} n_1(r) &= \int \beta_1(r') K(r, r') n_1(r') dV', \\ n_2(r) &= \int \beta_2(r') K(r, r') n_2(r') dV'. \end{aligned} \right\} \quad \dots\dots (3.4)$$

On multiplying the first equation by  $\beta_2 n_2$  and the second by  $\beta_1 n_1$  and integrating, the equation (3.3) is immediately evident.

#### 4. The Eigenvalue $\lambda$ of a Near Critical System

For a critical system the lowest eigenvalue  $\lambda$  is unity. For a subcritical system  $\lambda$  is greater than unity and it is convenient to use  $\lambda$  as a measure of the criticality of the system.

We may change a critical system into a subcritical system by removing the fissile material from a volume  $\Delta V$  and replacing it, for example, by reflector material. We shall confine ourselves to the special case when the mean free path in the fissile material and reflector are identical. (The more general case requires the methods developed later to deal with anisotropic sources.) The method also applies to a bare fissile system, which can be regarded as being surrounded by an ideal absorber ( $\beta = 0$ ). For equal mean free paths  $\Delta K$  vanishes and

$$\frac{\Delta \lambda}{\lambda} = - \int \Delta \beta(r) f(r)^2 dV. \quad \dots\dots (4.1)$$

Furthermore,  $\beta$  is changed in the volume  $\Delta V$  by the difference of  $\beta$  in core and reflector, but remains the same everywhere else. Hence

$$\frac{\Delta \lambda}{\lambda} = (\beta_c - \beta_r) \Delta V f(r)^2, \quad \dots\dots (4.2)$$

where the bar denotes an average over the volume  $\Delta V$  and the subscripts  $c, r$  refer to the core and reflector.

In the case of a spherical assembly we assume that the system is reduced below critical by slightly reducing the radius  $a$  of the fissile material. Observing that  $\Delta M/M = \Delta V/V_c$  one finds the following relation between the change in  $\lambda$  and the change  $\Delta M$  in the mass of fissile material

$$\frac{\Delta \lambda}{\lambda} = (\beta_c - \beta_r) f(a)^2 V_c \Delta M/M. \quad \dots\dots (4.3)$$

## II. MULTIPLICATION PROBLEMS\*

5. *The Neutron Density from a Source in a Subcritical System*

We now return to the inhomogeneous integral equation (1.3). Expand the neutron density  $n$  in terms of the proper functions  $f_i$

$$n(r) = \sum_i [n]_i f_i(r); \quad [n]_i = \int \beta(r) n(r) f_i(r) dV. \quad \dots\dots (5.1)$$

With the help of the integral equation (1.3), one finds

$$\lambda_i [n]_i = [n]_i + \frac{1}{v} \int q(r) f_i(r) dV.$$

The second term can be considered the expansion coefficient of  $q/\beta$ . Thus

$$(\lambda_i - 1)[n]_i = [q/\beta]_i / v \quad \dots\dots (5.2)$$

and

$$vn(r) = \sum_i \frac{1}{\lambda_i - 1} [q/\beta]_i f_i(r), \quad \dots\dots (5.3)$$

$$[q/\beta]_i = \int q(r) f_i(r) dV. \quad \dots\dots (5.4)$$

For a nearly critical system the first proper value is nearly unity and therefore only the first term in the expansion (5.3) need be considered. Omitting the suffix, we have

$$vn(r) = \frac{1}{\Delta\lambda} [q/\beta] f(r). \quad \dots\dots (5.5)$$

6. *The Multiplication*

Let us calculate now the number of neutrons which escape from the system. In a stationary state this number is identical with the difference between the number created and the number lost in the system, which is given by

$$E = \int vn(r) [\beta(r) - \alpha(r)] dV + \int q(r) dV. \quad \dots\dots (6.1)$$

For  $vn$  we substitute (5.3);  $q$  we write in the form  $\beta q/\beta$  and we expand  $q/\beta$ . Then

$$\begin{aligned} E &= \sum_i [q/\beta]_i \left\{ \frac{1}{\lambda_i - 1} \int f_i(r) \{\beta(r) - \alpha(r)\} dV + \int \beta(r) f_i(r) dV \right\} \\ &= \sum_i \frac{1}{\lambda_i - 1} [q/\beta]_i \int \{\lambda_i \beta(r) - \alpha(r)\} f_i(r) dV. \quad \dots\dots (6.2) \end{aligned}$$

The multiplication  $m$  is defined by  $m = E/Q$ , where  $Q$  is the integrated source of neutrons.

The equation for the multiplication is a special case of the neutron current across a closed boundary. Equation (6.2) evidently holds in general for the current  $E(S)$  across any closed surface  $S$ , provided the integral is extended only over the volume inside the surface  $S$ .

$$E(S) = \sum_i \frac{1}{\lambda_i - 1} [q/\beta]_i \int_{(S)} \{\lambda_i \beta(r) - \alpha(r)\} f_i(r) dV. \quad \dots\dots (6.3)$$

\* Some of the material presented in Part II is a reconstruction of calculations done by Serber at Los Alamos.

### 7. The Multiplication in a Near Critical System

In a near critical system again only the first term in the expansion need be considered. Then we find

$$E = Qm = \frac{1}{\Delta\lambda} \int q(r)f(r) dV \int \{\beta(r) - \alpha(r)\}f(r) dV. \quad \dots\dots(7.1)$$

For a spherical assembly we use (4.3) and find  $m = pM/\Delta M$ , where

$$p = \frac{\int q(r)f(r) dV}{f(a) \int q(r) dV} \frac{\int \{\beta(r) - \alpha(r)\}f(r) dV}{(\beta_c - \beta_r)f(a)V_c}. \quad \dots\dots(7.2)$$

It might be noted that in this form the function  $f$  need not be normalized.

The first factor in (7.2) is the ratio of the average neutron density weighted by the source distribution to the neutron density at the core surface. We may write it symbolically in the form  $\bar{n}_q/n(a)$ . The number of neutrons escaping from the system can also be written in the form of an integral over the surface

$$E = \int \overline{\cos} \nu n(r) dS, \quad \dots\dots(7.3)$$

where  $\overline{\cos}$  is the average direction cosine of the neutrons relative to the normal to the surface. Comparison with the above formula yields

$$\int \overline{\cos} n(r) dS = \int (\beta - \alpha)n(r) dV. \quad \dots\dots(7.4)$$

### 8. The Infinite Perfect Reflector

The second factor in (7.2) is particularly simple if the reflector only scatters but does not absorb neutrons. Then  $\beta - \alpha$  vanishes in the reflector. If we assume further that the mean free path and hence  $\alpha$  in core and reflector are equal, (7.2) reduces to

$$p = \bar{n}_c \bar{n}_c / n(a)^2, \quad \dots\dots(8.1)$$

where  $\bar{n}_c$  denotes the average neutron density in the core.

For simplicity let us apply diffusion theory to the calculation of the neutron density  $n(r)$  in the critical system and let us assume an infinite reflector. The net radial current through the surface of a sphere of radius  $r$  in the reflector is equal to the number of neutrons created in the core minus those absorbed in the core. Hence

$$-D \, dn/dr = \int_{\text{core}} (\beta - \alpha) \nu n(r) dV / 4\pi r^2, \quad \dots\dots(8.2)$$

where the diffusion coefficient  $D = v/3\alpha$ . Thus

$$n = \frac{3}{4\pi r} \alpha (\beta - \alpha) \int_{\text{core}} n dV = a^3 \alpha (\beta - \alpha) \bar{n}_c / r. \quad \dots\dots(8.3)$$

Hence  $d(nr)/dr = 0$ . In the core  $n = \sin(kr)/kr$ , where  $k^2 = 3\alpha(\beta - \alpha)$ . Continuity of  $n$  and  $D \, dn/dr$  implies that the gradient of  $nr$  be continuous. Since it vanishes in the reflector, we require  $ka = \frac{1}{2}\pi$ . Further,  $\bar{n}_c = 3[\sin(ak) - ak \cos(ak)]/(ak)^3$ . Thus

$$n(0) : \bar{n}_c : n(a) = \frac{1}{2}\pi : (12/\pi^2) : 1. \quad \dots\dots(8.4)$$

Hence we have:

$$\left. \begin{array}{l} \text{For a point source at the centre: } p = 6/\pi = 1.91. \\ \text{For a constant source in the core: } p = 144/\pi^4 = 1.49. \\ \text{For a source at the surface of the core: } p = 12/\pi^2 = 1.22. \end{array} \right\} \dots\dots (8.5)$$

For a source distribution in the core proportional to the neutron density one finds  $p = \bar{n}_c^2/n(a)^2$ , which is easily shown to be equal to  $3/2$ .

### III. MULTIPLICATION FOR ANISOTROPIC SOURCE

#### 9. The Angular Velocity Distribution

Let  $N(r, \Omega)$  be the density of neutrons at the point  $r$  with velocities having directions within the element of solid angle  $d\Omega$ .  $N$  satisfies the Boltzmann equation or transport equation.

$$(\Omega \cdot \text{grad})N(r, \Omega) + \alpha(r)N(r, \Omega) = \frac{\beta(r)}{4\pi} n(r), \quad \dots\dots (9.1)$$

$$n(r) = \int N(r, \Omega) d\Omega. \quad \dots\dots (9.2)$$

Assuming  $n(r)$  to be known, we can obtain  $N$  by integration of (9.1),

$$N(r, \Omega) = \frac{1}{4\pi} \int_0^\infty \exp \left[ - \int_0^s \alpha\{r - s'\Omega\} ds' \right] \beta(r - s\Omega) n(r - s\Omega) s^2 ds. \quad \dots\dots (9.3)$$

Here  $\alpha, \beta$  are defined to be zero in free space. This equation can be expressed in the form

$$N(r, \Omega) = \int_0^\infty K(r, r - s\Omega) \beta(r - s\Omega) n(r - s\Omega) s^2 ds. \quad \dots\dots (9.4)$$

Integration over  $\Omega$  leads to the integral equation for  $n$ , since  $s^2 ds d\Omega = dV$ .

#### 10. Anisotropic Source

Let there be a source of distribution such that  $q(r, \Omega) d\Omega dV$  is the rate of emission of neutrons from the volume element  $dV$  with directions within the element of solid angle  $d\Omega$ . We reduce this problem to an isotropic source distribution by considering the neutrons arising from the first collision. These correspond to an isotropic neutron source

$$\left. \begin{array}{l} q_1(r) = 4\pi \beta(r) \int K(r, r') q(r', \Omega) dV', \\ \Omega = (r - r')/|r - r'|. \end{array} \right\} \dots\dots (10.1)$$

In general we should now substitute two source terms into our equations corresponding to  $q$  and  $q_1$ . However, for a near critical system the direct contributions from the source terms are negligible. In this case we can immediately apply the equations derived before. Our problem then reduces to the determination of the coefficient

$$[q/\beta] = \int q_1(r) f(r) dV = 4\pi \int \int f(r) \beta(r) K(r, r') q(r', \Omega) dV dV'. \quad \dots\dots (10.2)$$

We integrate first over  $dV$ . Using a coordinate system centred on the point  $r'$  we have  $dV = s^2 ds d\Omega$  and  $r = r' + s\Omega$ . With (9.4) one finds

$$[q/\beta] = 4\pi \int \int N(r', -\Omega) q(r', \Omega) dV' d\Omega. \quad \dots\dots (10.3)$$

A particularly important case arises if the angular distribution of the source is determined by the angular distribution of the neutron density, i.e.

$$q(r, \Omega) = q(r)N(r, \Omega)/f(r), \quad \dots\dots(10.4)$$

where  $q(r)$  is the total strength of the source, then

$$[q/\beta] = \int q(r)f(r)g(r)dV, \quad \dots\dots(10.5)$$

which differs from the isotropic case by the factor  $g(r)$  defined by

$$g(r) = \frac{4\pi}{f^2(r)} \int N(r, \Omega)N(r, -\Omega)d\Omega. \quad \dots\dots(10.6)$$

The function  $g(r)$  can be worked out for any system for which the neutron density is known.

For a system with spherical symmetry it is evident that at the centre  $g=1$ , and at the boundary of the system  $g=0$ . The latter is true for any system with convex boundaries.

#### IV. APPLICATIONS

##### 11. *Effect of Changes at the Centre of a Spherical System* (Measurement of absorption cross sections)

Let us consider a near critical spherical system with a small hole at the centre. The hole is assumed to be sufficiently small so that the neutron distribution in the hole can be assumed to be isotropic. In that case scattering by a sample introduced into the hole has no effect on the neutron distribution.

If there is some arbitrary distribution of sources in the system, the neutron density is obtained from (5.5),

$$vn_1(r) = \frac{1}{\Delta\lambda} \left[ \frac{q}{\beta} \right] f(r) = S_1 f(r). \quad \dots\dots(11.1)$$

The number of neutrons escaping from the system is given by (6.2),

$$E_1 = \frac{1}{\Delta\lambda} \left[ \frac{q}{\beta} \right] \int (\beta - \alpha) f(r) dV; \quad \dots\dots(11.2)$$

by observing  $E_1$  we can determine  $\Delta\lambda$ .

Let us now introduce a sample of material into the hole and let  $\beta^*$ ,  $\alpha^*$  be characteristic for the material. In that case the neutron density changes and will be

$$vn(r) = Sf(r), \quad \dots\dots(11.3)$$

with a coefficient  $S$  which we shall determine presently.

Since the effect of scattering can be neglected, the only effect of the sample will be to absorb or produce neutrons. This effect can be regarded as a source of neutrons of strength

$$Q = vn(0)(\beta^* - \alpha^*)V = Sf(0)(\beta^* - \alpha^*)V, \quad \dots\dots(11.4)$$

where  $V$  is the volume of the sample. The factor  $S$  is now determined by the primary source distribution and the source  $Q$ , i.e.

$$S = \frac{vn(r)}{f(r)} = S_1 + \frac{1}{\Delta\lambda} \left[ \frac{Q}{\beta} \right] = S_1 + \frac{1}{\Delta\lambda} Sf(0)^2(\beta^* - \alpha^*)V. \quad \dots\dots(11.5)$$



Solving for  $S$  we find

$$S = S_1 / \left[ 1 - \frac{1}{\Delta\lambda} f(0)^2 (\beta^* - \alpha^*) V \right]. \quad \dots\dots (11.6)$$

An experimental measurement of the ratio  $S/S_1$  allows therefore a determination of  $\beta^* - \alpha^*$ . The escape of neutrons is evidently proportional to  $S$ . Hence  $S/S_1 = E/E_1$  can be observed directly.

The result (11.6) could in this particular case have been obtained more directly by application of (3.3). Since scattering does not matter, the empty hole can be replaced by a hole with  $\alpha = \beta = \alpha^*$ . On placing the sample into the hole the kernel is unchanged and  $\beta$  changes by  $\beta^* - \alpha^*$ . Hence  $\Delta\lambda$  changes by  $f(0)^2 (\beta^* - \alpha^*) V$ . Now  $E$  is inversely proportional to  $\Delta\lambda$ : hence  $E_1/E = [\Delta\lambda - f(0)^2 (\beta^* - \alpha^*) V] / \Delta\lambda$ , which is identical with (11.6).

Another use of the equation (11.6) is obtained by observing that for a critical system the neutron density from a source becomes infinite. If we arrange that the system be just critical if the hole is filled with fissile material, it follows that the denominator of (11.6) vanishes for  $\beta^* = \beta$ ,  $\alpha^* = \alpha$  and therefore  $\Delta\lambda = f(0)^2 (\beta - \alpha) V$  is a measure of the effect of the hole on the criticality of the system. Combining this equation with (4.3) we find that a hole increases the critical mass by the amount  $\Delta M$  given by

$$\frac{\Delta M}{M} = \frac{\beta_c - \alpha_c}{\beta_c - \beta_r} \frac{f(0)^2}{f(a)^2} \frac{V}{V_c}. \quad \dots\dots (11.7)$$

This last formula is of course dependent upon the assumption of equal mean free path in core and reflector which was used in order to derive (4.3).

## 12. Effect of a Change of $\alpha$ in a Small Region

In the general case a change of the properties in a small region which changes  $\alpha$  affects the kernel  $K(r, r')$  for any two points which lie on a straight line passing through the affected region. In that case the evaluation by means of formula (3.3) is more complicated and we follow instead the procedure by means of artificial sources.

Let again the suffix 1 refer to the starting system, for which the formulae (11.1) and (11.2) apply. Let us then change the values of  $\beta$  and  $\alpha$  in a small region of volume  $V$  at the point  $r$  by the amounts  $\Delta\beta$  and  $\Delta\alpha$  (not necessarily small). The change in  $\Delta\beta$  corresponds to an isotropic source of strength

$$Q_1 = v n(r_0) \Delta\beta V = S f(r_0) \Delta\beta V. \quad \dots\dots (12.1)$$

An increase in  $\alpha$  on the other hand implies that fewer neutrons pass through the region without collision and it corresponds to an anisotropic source of strength

$$Q_2 = -S N(r_0, \Omega) \Delta\alpha V. \quad \dots\dots (12.2)$$

Corresponding to (11.5) we now find

$$S = S_1 + \frac{SV}{\Delta\lambda} \{ f(r_0)^2 \Delta\beta - f(r_0)^2 g(r_0) \Delta\alpha \}. \quad \dots\dots (12.3)$$

Hence

$$S = S_1 / \left\{ 1 - \frac{V f(r_0)^2}{\Delta\lambda} [\Delta\beta - g(r_0) \Delta\alpha] \right\}. \quad \dots\dots (12.4)$$

Evidently these equations are easily generalized for an extended source and they will, for example, allow us to estimate the error introduced by the neglect of scattering for a finite sample placed at the centre of the assembly. This error may not be negligible even for a small sample, since for most materials  $\beta$  is very close to  $\alpha$  and therefore  $\beta - g\alpha$  may differ appreciably from  $\beta - \alpha$ , even if  $g$  is fairly close to unity.

#### ACKNOWLEDGMENTS

The paper is published by permission of Sir John Cockcroft, Director of the Establishment, and of the Controller, H.M. Stationery Office.

#### REFERENCES

- DAVISON, B., and FUCHS, K., 1943, *British Declassified Report MS.* 97.  
GOODMAN, C., 1947, *The Science and Engineering of Nuclear Power*, p. 176.

### Half-lives of $^{141}\text{Ce}$ and $^{169}\text{Yb}$

By D. WALKER

Physics Department, University of Birmingham

*Communicated by P. B. Moon; MS. received 18th July 1949*

**ABSTRACT.** The half-lives of  $^{141}\text{Ce}$  and  $^{169}\text{Yb}$ , produced through slow neutron capture in cerium and ytterbium, have been redetermined as  $(33.11 \pm 0.23)$  days and  $(31.83 \pm 0.21)$  days respectively. The errors appear to be smaller than in previous determinations.

#### § 1. INTRODUCTION

SLOW neutron capture in cerium produces, in addition to shorter-lived activities, an activity with a half-life of about 30 days. This has been assigned to  $^{141}\text{Ce}$ . Slow neutron capture in ytterbium produces, again in addition to shorter-lived activities, an activity with a half-life of about 33 days. This has been assigned to  $^{169}\text{Yb}$  (Seaborg and Perlman 1948). During the course of some radioactivity experiments, the decay in activity of neutron-activated cerium and ytterbium has been followed over a lengthy period. It seems of value to report the somewhat precise values which have thus been found for the half-lives of  $^{141}\text{Ce}$  and  $^{169}\text{Yb}$ , as the errors appear to be smaller than those in earlier determinations.

#### § 2. HALF-LIFE OF $^{141}\text{Ce}$

A sample of 'Specpure' cerium oxide\* was irradiated in the low power pile at the Atomic Energy Research Establishment, Harwell, intermittently over a period of three weeks. The decay in activity of a source prepared from the irradiated material was followed using a Geiger counter with a  $7 \text{ mg/cm}^2$  window and a standard source-counter geometry. The first point shown on the decay curve (Figure 1) was obtained 11 days after the removal of the sample from the pile. A source of RaE in equilibrium with RaD (22 years half-life) was used to standardize the counter sensitivity, allowance being made for the small but appreciable decay of the RaD. The decay of the cerium source was accurately exponential after 100 days, when the 13-day  $^{143}\text{Pr}$  formed by the decay of 36-hour  $^{143}\text{Ce}$  had decayed

\* Catalogue number J.M.304, Johnson, Matthey and Co. Ltd., London.

away. The exponential portion of the curve in Figure 1 covers about 9 half-lives and the activity decayed steadily, without significant departure from the exponential, until lost in the background. The straight line drawn through the observed points is based on a 'least squares' calculation for the points after and including 165.5 days to ensure that the  $^{143}\text{Pr}$  has a negligible influence. The point at 402.9 days is the last point with any significant weight.

The straight line corresponds to a half-life for  $^{141}\text{Ce}$  of  $(33.11 \pm 0.23)$  days.

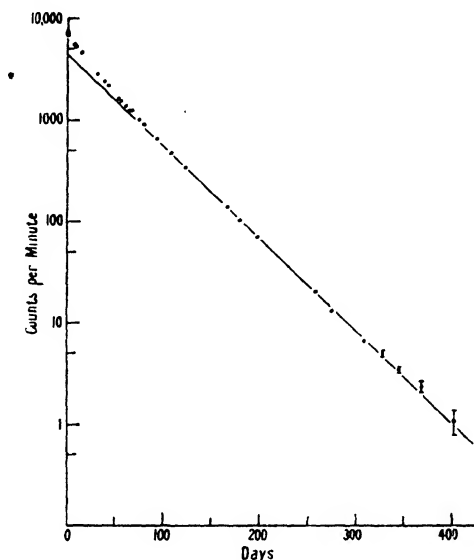


Figure 1. Decay curve of cerium.

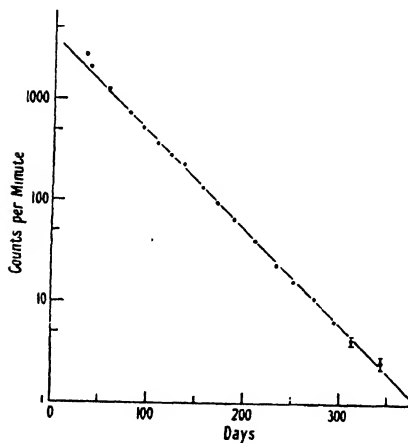


Figure 2. Decay curve of ytterbium.

### § 3. HALF-LIFE OF $^{169}\text{Yb}$

A sample of 'Specpure' ytterbium oxide\* was irradiated in the pile for 4 days. The decay in activity was followed using a procedure similar to that for cerium. Zero time on the decay curve (Figure 2) corresponds to 1 day out of the pile. The decay was accurately exponential after 75 days when the 100-hour  $^{175}\text{Yb}$  had

\* Catalogue number J.M.319, Johnson, Matthey and Co. Ltd., London.

decayed away. The exponential portion of the curve covers about 8 half-lives and the activity decayed steadily, without significant departure from the exponential, until lost in the background. The straight line drawn through the observed points is based on a 'least squares' calculation for the points after and including 92.8 days to ensure that the  $^{175}\text{Yb}$  has a negligible influence. The point at 342.7 days is the last point with any significant weight.

The straight line corresponds to a half-life for  $^{169}\text{Yb}$  of  $(31.83 \pm 0.21)$  days.

## REFERENCE

SEABORG, G. T., and PERLMAN, I., 1948, *Rev. Mod. Phys.*, **20**, 585.

## The Decay and Capture of $\mu$ -Mesons in Photographic Emulsions

By M. G. E. COSYNS, C. C. DILWORTH, G. P. S. OCCHIALINI,  
M. SCHOENBERG \*

Université Libre de Bruxelles, Centre de Physique Nucleaire

AND N. PAGE

Physical Laboratories, The University, Manchester

*Communicated by P. M. S. Blackett ; MS. received 28th July 1949*

**ABSTRACT.** Observations on the decay and capture of  $\mu$ -mesons in Kodak NT4 and Ilford G5 photographic emulsions are described. It is found, in agreement with other workers, that  $63 \pm 4\%$  of all  $\mu$ -mesons stopping in the emulsion decay with the emission of a fast electron, a result which is shown to be in reasonable agreement with theoretical predictions. The emission of *slow* electrons is observed from  $7.2 \pm 1.3\%$  of all slow mesons, and these are ascribed mainly to an Auger effect accompanying the capture of  $\mu$ -mesons.

### § 1. INTRODUCTION

It has already been shown that it is possible to detect the decay electron of the  $\mu$ -meson in the new highly sensitive emulsions (Brown, Camerini, Fowler, Muirhead, Powell and Ritson 1949). In this paper the results of an investigation of the mechanism of stopping and capture or decay of these mesons in the various elements of the emulsion is described. The photographic emulsion is not a very suitable medium for this purpose since it is composed partly of heavy elements, silver and bromine, combined in the form of dielectric crystals, and partly of an amorphous mixture of light elements, carbon, hydrogen, nitrogen and oxygen. Moreover, it has a high stopping power which prevents the recognition of electrons of energy less than 20 kev.

Exposures have been made at the Pic du Midi of batches of plates of the Kodak NT4 and Ilford G5 emulsions, of thicknesses 200, 400 and 600 microns, for 6 days and 12 days. All mesons entering the plate from outside and ending in the emulsion without giving rise to a star or to a secondary meson have been classified as positive or negative  $\mu$ -mesons (formerly designated as  $\rho$ -mesons).

\* University of St. Paulo, Brazil, now on leave at the Université Libre de Bruxelles.

§ 2. OBSERVATIONS AND FRACTION OF  $\mu$ -MESONS WHICH DECAY

In Table 1 are given the observed numbers of mesons in the various exposures, separated into mesons which stop giving rise to no observable electron ( $\mu$ ), those which give a fast electron only ( $\mu + e$ ), those giving a fast electron and one or more slow electrons ( $\mu + e + A$ ), and those giving rise only to slow electrons ( $\mu + A$ ).

Table 1

Exposure (days)	Plates	Thickness (microns)	Area (cm <sup>2</sup> )	Total No.	$\mu$	$\mu + e$	$\mu + e + A$	$\mu + A$
6	Kodak NT4	400	100	65	18	40	1	6
12	Kodak NT4	400	131	205	78	114	0	13
12	Kodak NT4	200	109	61	24	31	1	5
6	Ilford G5	600	50	82	32	45	0	5

A decay electron will be observed only if it is emitted at a sufficiently small angle to the plane of the emulsion. In order to determine the fraction of decay of electrons which have been missed, the lengths of the tracks of all the decay electrons in plates of the same thickness have been measured. Using the usual geometrical argument, the distribution so obtained has been fitted to the calculated distribution. The correction made in this way shows that failure to observe dipping electrons causes a loss of 10% of the observed number in a 400 micron emulsion. The number of tracks available in the other plates is not sufficient to repeat the measurements for 200 and 600 micron plates, but it is assumed that the loss is approximately inversely proportional to the thickness, i.e. 7% for 600 microns and 20% for 200 microns.

In order to find the fraction of mesons giving rise to decay electrons, all mesons giving a fast electron have been put in one group ( $\mu + e$ ) and all without a fast electron in the other group ( $\mu$ ), regardless of the presence or absence of slow electrons. The results after making the geometrical correction are given in Table 2.

Table 2

Plate	Thickness (microns)	Total No. of mesons	$\mu + e$	$\mu$	% of mesons which decay
Kodak NT4	400	270	171	99	$63 \pm 5$
Kodak NT4	200	61	38	23	$62 \pm 10$
Ilford G5	600	82	48	34	$59 \pm 9$

The percentage of decay in the different groups of plates is consistent within the experimental errors, and the results, combined for all the plates, give a total number of 413 mesons, of which 257 decay (i.e.  $62 \pm 4\%$ ) and 156 are captured.

Approximately 2.5% of these particles will be negative  $\pi$ -mesons which are captured by the nucleus and give rise to no visible star. This is deduced from the fact that the number of negative  $\pi$ -mesons giving stars is 10% of the number of  $\rho$ -mesons, and the results of experiments at Berkeley which show that 25% of the negative  $\pi$ -mesons ending in emulsions insensitive to electrons give no ionizing particles. Thus of the 413 mesons which stop in the emulsion, 409 will be  $\mu$ -mesons; of these, 257 decay (i.e.  $63 \pm 4\%$ ) and 152 are captured, a result in good agreement with the Bristol group (Brown *et al.* 1949).

The existence of a positive excess of slow mesons is not definitely established for energies of the order of 10 mev. which are important in the photographic plate.

Preliminary reports from Franzinetti on the magnetic sandwich method indicate that positive and negative  $\mu$ -mesons are present in approximately equal numbers. Thus, in the absence of evidence to the contrary, it will be assumed that the numbers are equal. Then of the 409  $\mu$ -mesons the  $204 \pm 14$  which are positive must all decay, so that of the negatives  $53 \pm 7$  ( $26 \pm 3\%$ ) decay and 74% are captured. If it is assumed that among the various elements of the gelatine the probability of stopping a meson is proportional to  $Z$ , and the probability of capture is proportional to  $Z^4$  (Wheeler 1947), the fraction of negative mesons stopped in gelatine which decay is about 80%. On the same reasoning all the negative mesons stopped in AgBr will be captured. Thus the decay of the negative mesons requires that 30% are stopped in the gelatine. A rough calculation of the relative number stopped, assuming that the stopping power at low energies is still proportional to the number of electrons per unit path, gives a value of 33% for gelatine. This agreement may be considered satisfactory.

### § 3. MESONS WHICH ARE CAPTURED WITH EMISSION OF SLOW ELECTRONS

As indicated in Table 1, the emission of slow electrons has been observed from the ends of  $7.2 \pm 1.3\%$  of the meson tracks, and these are ascribed mainly to an Auger effect accompanying the capture of  $\mu$ -mesons. A detailed analysis shows that this proportion implies an actual occurrence of more than 20% in the cases in which a negative meson stops in the heavy elements of the emulsion.

Although all the slow electrons are ascribed in this paper to  $\mu$ -mesons, it is possible that an appreciable fraction could be due to negative  $\pi$ -mesons which are captured without producing visible stars. Only experiments with artificially produced mesons can give the exact value of this fraction, but certainly not more than one-third of the effect we have observed could be ascribed to this cause. The actual proportion is, in fact, probably much smaller than one-third because this value has been obtained on the assumption that *all* the captured negative  $\pi$ -mesons emit slow electrons. If the emission of slow electrons by these negative  $\pi$ -mesons is the same as for star-producing  $\sigma$ -mesons, the contribution would fall from one-third to one-seventh.

The extent of the loss of slow electrons emitted due to the failure to recognize them as such is very difficult to estimate. These electrons are highly scattered and, therefore, it is not possible to determine their point of origin unless the density of grains in the vicinity of the end of the meson track is high and even. When of very low energy (20–30 kev.) they can easily be obscured by the track of the meson. When of higher energy (50–150 kev.), the beginning of the electron track is frequently well defined, but it is difficult to follow it to the end if the general density of slow electrons in the neighbourhood is high. Electrons of less than 20 kev. will never be recognized, since their range is too short.

It is essential to establish a rigorous criterion for the admission of a slow electron as originating from the end of a meson, since the probability of a chance juxtaposition of the end of the meson track with the beginning of the track of one of the numerous electrons of the background is appreciable. The criterion adopted is that slow electrons should be admitted as Auger electrons only if the beginning of the track can be certainly identified within 1 micron of the end of the meson. The probability of a chance effect has then to be determined. This is done in two ways. First, the number of slow electron tracks on 6,360 microns of

meson track and 6,700 microns of proton tracks are counted. A total of 90 slow electrons is found, giving a frequency of 1.5% for the chance effect. It is realized that some of these slow electrons may be genuine delta rays ejected by the fast particle, and an attempt has been made to repeat the measurement using the image of a fine wire superposed on that of the emulsion. This gives a frequency of slow electrons of the order of 0.2%. A more direct approach has therefore been adopted. Among the protons ejected from the stars, search has been made for those giving an apparent Auger effect, which in this case must certainly have been spurious. In the exposure of 6 days one such effect has been found in 270 protons and in the 12-day exposure one in 220 protons. The probability of a chance effect can therefore be estimated as not more than 0.5% even in a 12-day exposure.

The results given in Table 1 show a frequency of the Auger effect of 7% of the total number of mesons, i.e. 14% of all negative  $\mu$ -mesons (neglecting the contribution from negative  $\pi$ -mesons). This figure is certainly a lower limit since the rigorous criterion excludes possibly as many Auger effects as have been accepted. Of these 7%, less than 1% are associated with a fast electron, which strongly

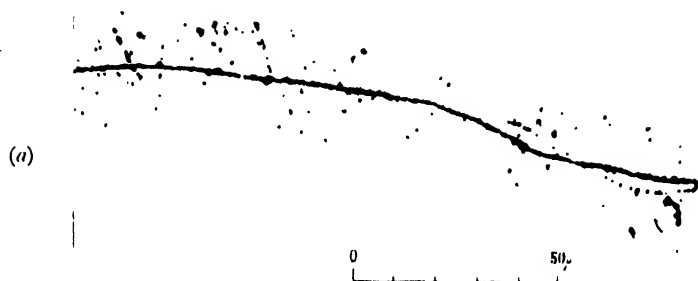
Table 3. Energy of Observable Auger Electrons in the Chief Components of the Emulsion

Element	Energy of Auger Electrons (kev.)							
	Transitions							
	1-2	2-3	3-4	4-5	5-6	6-7	7-8	8-9
Carbon	78	14.5						
Nitrogen	106	19.7						
Oxygen	139	25.8						
Bromine	2650	494	173	80	43.5	26.1	17.0	
Silver	4780	890	311	144	78.4	47.1	30.7	21.4

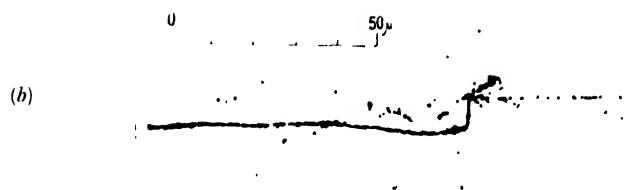
indicates that practically all the Auger electrons are produced in AgBr. From the above estimate of 30% of mesons stopping in gelatine, it follows that of negative mesons stopped in AgBr at least 20% give rise to an observable Auger electron.

The energy of the electrons that should be expected from the Auger effect can be deduced from the position of the orbits of a meson of mass 214 round the nuclei of the various elements of the emulsion. These are given in Table 3. It will be seen that in the gelatine only the last transitions of the meson will give rise to Auger effects observable in the photographic plate (i.e. of energy greater than 20 kev.). According to the theory of Fermi and Teller (1947) it is in the last transitions that the emission of radiation rather than Auger effects become predominant. In the case of AgBr there are several possible transitions before the meson arrives in the region of loss by radiation (for these elements the loss by radiation becomes important for meson orbits whose radii are of the order of  $Zr_K$ ,  $r_K$  being the radius of the meson K orbit corresponding to the atomic number  $Z$ ). The exact values of the relative probabilities of Auger effect and of radiation on this theory have not, to our knowledge, been calculated.

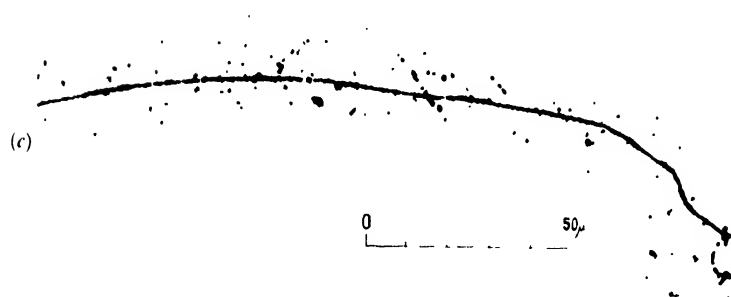
The observed distribution in range of the Auger electrons is given in Figure 1(a). The range-energy relation of slow energy electrons in these emulsions is not yet known with precision and may possibly depend somewhat on the batch, but some idea of the corresponding energies can be obtained from the curve given for Kodak NT2a emulsions. The distribution in energy of the Auger



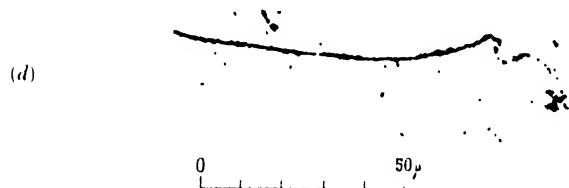
Single slow electron.  
Plate: Kodak NT4, 400  $\mu$ .  
Exposure: 6 days.  
Obs.: Eric Shramm.



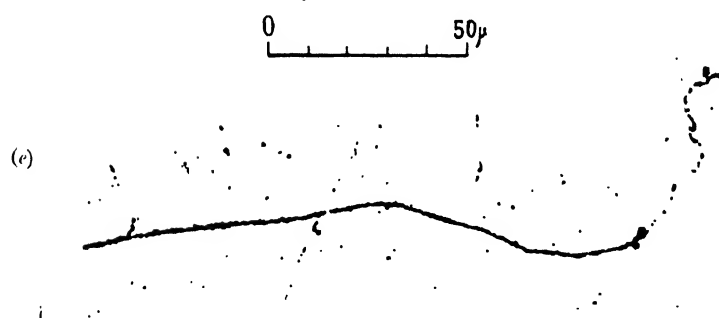
Several slow electrons  
and single fast electron.  
Plate: Kodak NT4, 400  $\mu$ .  
Exposure: 6 days.  
Observer: Mme Hubert.



Two slow electrons.  
Plate: Kodak NT4, 400  $\mu$ .  
Exposure: 6 days.  
Observer: Mme Hubert.



Single slow electron.  
Plate: Ilford G5, 600  $\mu$ .  
Exposure: 6 days.  
Observer: Mme Hubert.



Three slow electrons.  
Plate: Kodak NT4, 400  $\mu$ .  
Exposure: 12 days.  
Observer: Mme Hubert.

Slow electrons observed at the end of meson tracks.





electrons is given in Figure 1 (b) and the spectrum calculated for silver and bromine in Figure 1 (c). Taking into account the difficulties in recognition and measurement of these tracks and the uncertainty of the range-energy curve, there is reasonable agreement. The absence of well-defined lines in the experimental spectrum can be easily explained by the overlapping of the lines of the various elements; moreover, these lines have probably been broadened by the errors of observation and straggling.

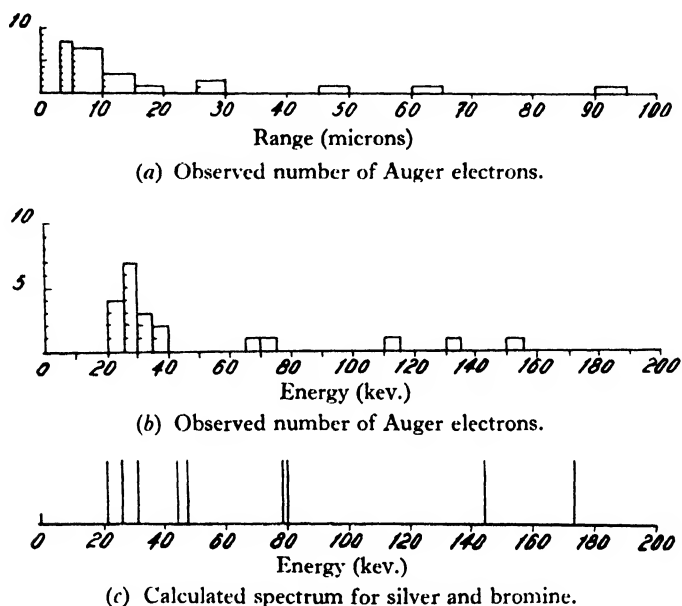


Figure 1.

The conclusions which can be drawn from these measurements seem to be that the existence of the Auger effect—which should more properly be called internal-conversion effect since the transfers of energy correspond to meson orbits well within the electron cloud—has been demonstrated, and its frequency is not large. This indicates that it is largely suppressed by a more probable competing process such as radiation.

#### ACKNOWLEDGMENTS

This work, and other work which is in progress, would not have been possible without the cooperation of many people. We therefore wish to thank Dr. Berriman, of Kodak Ltd. and Mr. Waller of Ilford Ltd. for kindly supplying us with the special thick plates used. We thank Dr. Rösch, Director of the Observatory of the Pic du Midi, and his staff, who arranged the exposures for us. We also take this opportunity to thank Dr. Taylor of Messrs. Cooke, Troughton and Simms, who furnished us with a special long-distance oil immersion objective, with which tracks at the bottom of the 600-micron plates can be viewed through the backing glass.

#### REFERENCES

- BROWN, R., CAMERINI, U., FOWLER, P. H., MUIRHEAD, H., POWELL, C. F., and RITSON, D. M., 1949, *Nature, Lond.*, **163**, 47, 82.  
 FERMI, E., and TELLER, E., 1947 *Phys. Rev.*, **72**, 399.  
 WHEELER, J. A., 1947, *Phys. Rev.*, **71**, 320.

## A Contribution to the Theory of Soft X-ray Emission Bands of Sodium

By P. T. LANDSBERG

Mathematics Department, Imperial College, London

*Communicated by H. Jones ; MS. received 2nd December 1948, and in amended form  
9th May 1949*

**ABSTRACT.** A wave-mechanical treatment of the  $L_{II, III}$  emission spectrum of sodium is given, taking into account (i) the broadening of the energy levels in the conduction band due to electron collisions (§§ 2-4); (ii) the lowering of the potential energy of the electron about to make transition into an inner shell of an ion, due to electrostatic attraction (§§ 5-6). The first problem is treated in the free electron approximation, using a model suggested by Skinner, and the theoretical curve has a 'tail', as found experimentally. The calculation shows that a modification of the wave functions of electrons in a free electron model may be required, and this possibility is discussed. In the second problem, the depression in the electron potential is approximated by using a spherical potential well in the neighbourhood of the ion. The first effect proves to be the more important one, and there is good agreement with experiment.

### § 1. INTRODUCTION

IN the soft x-ray spectroscopy of solids the experimental results are expressed by plotting the intensity  $I$  of the emitted frequency  $\nu$  against either the frequency or the energy  $E$  to which it corresponds (Skinner 1938). The zero of the energy is usually taken at the bottom of the valency electron energy band. If  $P(E)$  is the probability of a transition from a level of energy  $E$  into the ionized inner shell, and  $N(E)$  the density of states of energy  $E$  in the band, then  $I(E)$  is given by  $I(E) \propto \nu^3 P(E) N(E)$ . The factor  $\nu^3$  is unimportant, as it varies only little over the width of a band.

In the theoretical discussion of these curves (Jones, Mott and Skinner 1934, Matyáš 1948), two factors have not so far been considered, although they are bound to affect the theoretically predicted result. First, in calculating the function  $N(E)$ , one must take into account the broadening of the individual energy levels by electron collisions in the conduction band. For the treatment of this problem we shall adopt the model suggested by Skinner (1940). The problem here is to calculate the life-time of an electron vacancy in the valency electron energy levels. This life-time is finite, and the level therefore broadened, because, due to electron collisions, an electron from higher up in the band can drop into the vacant level while another valency electron is transferred to a state above the surface of the Fermi distribution. The details of the present calculations show that the initial and final states of the electrons must be such as to ensure energy and momentum conservation. To find the total broadening one must consider all collisions of this type which will lead to the removal of the initial vacancy. This calculation is made in §§ 2-4, and the  $(I, E)$  curve for sodium so obtained is drawn in Figure 4. The result reproduces the characteristic 'tail' of Skinner's experimental curve.

Secondly, in calculating the transition probability  $P(E)$ , one must take into account the fact that the electron which makes the transition into the inner shell moves in the field of the ionized atom just before the transition is made (cf. also Platt 1946). Thus, in the neighbourhood of the ion the potential of the electron

is lowered, instead of remaining constant as previously assumed. To estimate the effect of this modification, a calculation of  $P(E)$  has been made in §§ 5 and 6, using a potential well of specified radius and depth in the neighbourhood of the ion. Theoretical  $I(E)$  curves predicted with the modified function  $P(E)$  are given in Figure 5. Whereas the first effect causes the  $I(E)$  curve to rise more slowly than  $\sqrt{E}$ , the second effect is seen to cause a rise of the curve at a rate which always exceeds that of  $\sqrt{E}$ . Both results have been combined in Figure 6, and the agreement with Skinner's experimental curve for the sodium  $L_{II,III}$  radiation is satisfactory. The 'bump' near the emission edge remains unaccounted for by these calculations, but it has not been observed by Cady and Tambouliau (1941) who, however, appear to have used a lower resolving power.

In confining attention to a monovalent metal such as sodium in this paper, we do in fact treat the theoretically simplest case, since the function  $N(E)$  becomes complicated as soon as the surface of the Fermi distribution approaches the boundary of the first Brillouin zone. Although the theoretical expressions derived in this paper can be applied to all metals for which the  $N(E)$  curve is similarly simple, only the  $L_{II,III}$  emission of sodium has been treated here.

## § 2. PERTURBATION THEORY FOR THE ELECTRON COLLISIONS

In order to account for the tails obtained in the  $L_{II,III}$  emission spectra Skinner (1938, 1940) and Cady and Tambouliau (1941) have introduced the hypothesis of an Auger effect in the conduction band of a metal which, in this particular case, is equivalent to a collision between a pair of electrons. Cady and Tambouliau supposed that part of the energy difference involved in the transition of a valency electron into a vacant x-ray level is taken up by the transition of a second valency electron into a vacant level above the Fermi surface. This mechanism could very greatly increase the width of an emission band, and seems to be less likely than Skinner's mechanism (cf. § 1). As a detailed discussion of the inter-relation between the electron collisions and the emission of x rays is probably very difficult, we shall restrict ourselves here to calculations based on Skinner's model. In this an electron falls from a full conduction band into a vacant x-ray level emitting radiation, so that there is a single vacant level in the final state of the conduction band. This radiation is not monochromatic since, owing to the Auger effect, which is induced by the Coulomb interactions between the electrons, radiationless transitions occur between this state and a state in which there are *two* vacant levels and one electron above the Fermi surface. The assumed final state of the conduction band after emission of the radiation is, therefore, not a stable state but has a finite and short life-time. Hence this state has no precise energy, and the half-width  $\Delta E$  of the level is related to the life-time  $\Delta t$  of the assumed final state of the conduction band by the relation  $\Delta E \sim \hbar/\Delta t$ . Each energy level in the band can then be replaced by an appropriately broadened level. Finally, by integrating the probability contributions from all broadened levels to a level of fixed energy  $E$ , we obtain a new density of states function which reproduces approximately the tail found by experiment. Throughout the calculation we need consider only the Fermi gas formed by the 3s electrons of sodium.

The perturbation which determines the transition probability is the difference between the complete Hamiltonian, which includes the Coulomb interaction between all electrons, and the Hamiltonian of the Hartree-Fock approximation in which this interaction is replaced by the effect of a self-consistent field. The

perturbation consists therefore of the Coulomb interaction plus a sum of terms each of which depends on the coordinates of only one electron. For the wave functions of the initial and final states of the metal we shall use determinants of normalized plane waves, which implies that we are treating the problem in the one-electron approximation and are assuming the valency electrons of sodium to be free. If the total number of valency electrons is  $2n$ , each determinant is equivalent to a product of two determinants, each having  $n$  rows and columns. One determinant involves the  $n$  functions which refer to one type of spin, whereas the other involves the functions which refer to the other type of spin (cf. Wigner and Seitz 1934). Attention will be confined in the first place to collisions of electrons having opposite spins, and it can then be seen that the matrix element  $U_{if}$  (connecting the initial and the final state) of the perturbation will not involve an exchange term. Suffixes  $i$  and  $f$  denote the initial and final states respectively.

Let  $V$  be the volume of the metal, and let the two electrons partaking in the collision be denoted by suffixes 1 and 2, with wave vectors  $\mathbf{k}_1$  and  $\mathbf{k}_2$  in the initial state and  $\mathbf{k}'_1$  and  $\mathbf{k}'_2$  in the final state. It may then be verified that only the term  $e^2/r_{12}$  of the perturbation, and no other, contributes to  $U_{if}$ , which is given by

$$U_{if} = e^2 V^{-2} \int r_{12}^{-1} \exp \{i[(\mathbf{k}'_1 - \mathbf{k}_1) \cdot \mathbf{r}_1 + (\mathbf{k}'_2 - \mathbf{k}_2) \cdot \mathbf{r}_2]\} d\tau_1 d\tau_2$$

$$= \begin{cases} 4\pi e^2 / V g^2 & \text{if } \mathbf{k}_1 - \mathbf{k}'_1 = \mathbf{k}'_2 - \mathbf{k}_2, \\ 0 & \text{otherwise,} \end{cases} \quad \dots\dots(1)$$

where  $\mathbf{g} = \mathbf{k}_1 - \mathbf{k}'_1 = \mathbf{k}'_2 - \mathbf{k}_2$ . Thus the matrix element vanishes unless the momentum is conserved, and we note particularly that *all* Coulomb interactions between the electrons have been taken into account in (1).

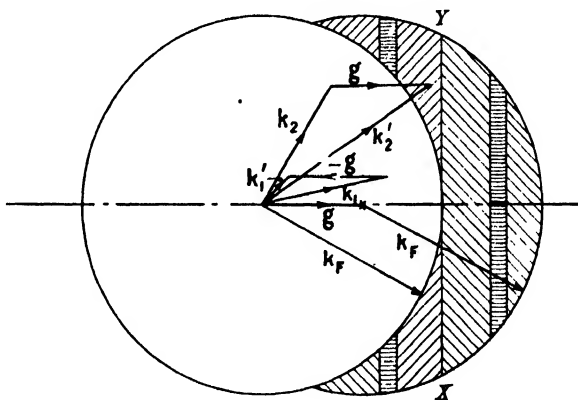


Figure 1. Integration over all wave vectors of electron 2. The figure shows the permissible volume (shaded) for the independently variable vector  $\mathbf{k}'_2$  if  $\mathbf{k}_1$  and  $\mathbf{k}'_1$  (and therefore  $\mathbf{g}$ ) are fixed. The nature of the volume element, which is also shown, changes at the plane  $XY$  so that the integration decomposes into two parts.

If at time  $t=0$  the metal is in a state with total energy  $E_i$ , the probability of a transition to a state of total energy  $E_f$  after a time  $t$  is given by (Heitler 1944, p. 88)

$$P_{if} = (2t^2 U_{if}^2 / \hbar^2) [(1 - \cos x) / x^2], \quad \dots\dots(2)$$

where  $x = t(E_f - E_i) / \hbar$ . It is required to calculate the life-time of the unoccupied level specified by the wave vector  $\mathbf{k}'_1$ . We have therefore to consider transitions from all occupied levels  $\mathbf{k}_1$  with energy greater than the energy of the level  $\mathbf{k}'_1$ ,

and all possible transitions of the second electron from an occupied level  $\mathbf{k}_2$  to a level  $\mathbf{k}'_2$  above the Fermi surface.  $P_{if}$  must therefore be summed over all possible vectors  $\mathbf{k}_1$  and  $\mathbf{k}_2$ . This implies a double volume integration which is carried out in the next section, where it will be shown that the total transition probability into the vacant level at  $\mathbf{k}'_1$  diverges as  $1/g$  for small  $g$ .

### § 3. THE INTEGRATION OF EQUATION (2) OVER ALL PERMISSIBLE COLLISIONS

To sum the probabilities, note that for a fixed change in the momentum of either electron in the collision, i.e. for fixed  $\mathbf{g}$ ,  $x$  can take a range of values, and we shall now determine the number of possible collisions when  $\mathbf{g}$  is fixed and  $x$  lies between  $x$  and  $x + dx$ . The number of states per unit volume of  $k$ -space is  $V/8\pi^3$ , where  $V$  is the volume of the metal. Since we are calculating the life-time of the vacancy specified by  $\mathbf{k}'_1$ , this vector remains constant in the whole calculation. Hence, for given  $\mathbf{g}$ , it follows that  $\mathbf{k}_1$  is also constant, and from the definition of  $x$  we have

$$x = (th/m)(\mathbf{k}'_2 - \mathbf{k}_1) \cdot \mathbf{g}. \quad \dots\dots(3)$$

Thus  $x$  varies by virtue of the variation of  $\mathbf{k}'_2$  only. We have now to find the permissible volume of  $\mathbf{k}'_2$ -space. From (3) it follows that for given  $x$  and  $\mathbf{g}$ ,  $\mathbf{k}'_2$  must lie on a plane at right angles to  $\mathbf{g}$ . The area of this plane is limited by the condition that for the unoccupied state  $\mathbf{k}'_2$ ,  $k'_2 > k_F$ , and that for the occupied state  $\mathbf{k}_2$ ,  $k_2 < k_F$ . If  $\mathbf{k}'_2 \cdot \mathbf{g} \leq k_F g$  we obtain an annulus of area  $\pi(2\mathbf{k}'_2 \cdot \mathbf{g} - g^2)$ , whilst if  $\mathbf{k}'_2 \cdot \mathbf{g} > k_F g$  we obtain a complete disc. The range for which  $\mathbf{k}'_2 \cdot \mathbf{g} > k_F g$  corresponds to collisions in which energy is not conserved, and can therefore be neglected. The limits  $x_1$  and  $x_2$  of the integration over the significant range are determined by the greatest and least value of  $\mathbf{k}'_2 \cdot \mathbf{g}$ , which are, respectively,  $k_F g$  and  $g^2/2$ . Hence

$$x_1 = (th/m)(\frac{1}{2}g^2 - \mathbf{k}_1 \cdot \mathbf{g}); \quad x_2 = (th/m)(k_F g - \mathbf{k}_1 \cdot \mathbf{g}).$$

Since  $k_1 > k'_1$ ,  $x_1$  is always negative;  $x_2$  is always positive if  $\mathbf{k}_1$  lies below the Fermi surface. For the thickness of the volume element we find from (3)

$$g^{-1}d(\mathbf{k}'_2 \cdot \mathbf{g}) = (m/thg) dx.$$

The number of collisions for which  $\mathbf{g}$  is a non-zero constant, and  $x$  lies between  $x$  and  $x + dx$ , is now given by

$$(V/8\pi^3)\pi(2\mathbf{k}'_2 \cdot \mathbf{g} - g^2)(m/thg) dx.$$

The sum over all  $P_{if}$  subject to the above conditions becomes

$$(4\pi me^4/V\hbar^3) t/g^5 \int_{x_1}^{x_2} [(2mx/th) + 2\mathbf{k}_1 \cdot \mathbf{g} - g^2](1 - \cos x)x^{-2} dx. \quad \dots\dots(4)$$

Evaluating (4) in the usual way, we obtain for the probability that in time  $t$  one electron has made a transition from an initial state  $\mathbf{k}_1$  to a final state  $\mathbf{k}'_1$ , all possible transitions of the second electron being taken into account,

$$(4\pi me^4/V\hbar^3)g^{-5}(2\mathbf{k}'_1 \cdot \mathbf{g} + g^2)t. \quad \dots\dots(5)$$

Hence the probability of any electron making a transition into the vacant state  $\mathbf{k}'_1$  in time  $t$ , due to a collision between two electrons, is obtained by summing (5) over all possible values of  $\mathbf{g}$ . The lower limit of the integration over  $g$  should

be  $g=0$  in any theory based on the Bloch model. However, the integral of (5) with respect to  $g$  diverges as  $1/g$  at this limit. A difficulty of a similar nature has recently been found by Heisenberg, and will be discussed in §3.

To see the nature of the divergence, we transfer the origin to the fixed point  $\mathbf{k}'_1$  ( $k'_1 > 0$ ) and take as volume element  $2\pi \sin \theta \, d\theta \, g^2 dg$ , where  $\theta$  is the angle between  $\mathbf{k}'_1$  and  $\mathbf{g}$ . Hence the main contribution to the transition probability, which comes from the region of small  $g$ , is given by

$$(2me^4/\pi\hbar^3)k'_1 t \int \cos \theta \sin \theta \, d\theta \int g^{-2} dg, \quad \dots\dots (6)$$

where the volume element has been multiplied by  $V/8\pi^3$  to give the number of states contained in it.

It is important to notice that only those electrons can make transitions whose initial energy exceeds the energy of the vacant state  $\mathbf{k}'_1$ , since the accompanying transition of the second electron is one which absorbs energy. Thus for a given value of  $g$  the smallest permissible value of  $k_1$  is  $k'_1$ , and in this case the angle between  $\mathbf{k}'_1$  and  $\mathbf{g}$  has its greatest value, which is

$$\theta_1 = \frac{1}{2}\pi + \sin^{-1}(g/2k'_1). \quad \dots\dots (7)$$

The integral over  $\theta$  is therefore  $\frac{1}{2} \int \sin^2 \theta \, d\theta$  which, by (7), is approximately  $\frac{1}{2}$  for small  $g$ . If, in order to obtain a finite life-time for the vacant state, we follow Heisenberg's suggestion and assume that those electrons lying in a spherical shell of  $k$ -space bounded by the energy surfaces  $E_F$  and  $E_F - \epsilon$  ( $\epsilon \ll E_F$ ) do not participate in the collisions, then our previous calculations are not materially affected and the smallest allowable value of  $g$  is given by  $2g/k_F = \epsilon/E_F$ . Thus we obtain from (6) for the probability per unit time of an electron making a transition into the state  $\mathbf{k}'_1$  due to collisions between two electrons

$$P = (4/\pi\hbar)(k'_1/k_F)(E_F/\epsilon)W,$$

where  $W$  is the ionization energy of a normal hydrogen atom. Writing now  $k$  for  $k'_1$ , and denoting by  $\Delta(k)$  the half-width of an energy level on that spherical shell in  $k$ -space for which the wave vector has the magnitude  $k$ , we obtain for  $k > 0$  (Heitler 1944, p. 113)

$$\Delta(k) \sim \hbar P = 17.2 (k/k_F)(E_F/\epsilon) \text{ ev.} \quad \dots\dots (8)$$

For sodium  $E_F \sim 3 \text{ ev.}$ , and if we choose  $\epsilon \sim 1/40 \text{ ev.}$  we see that the theoretical value of the line width can reach several hundred electron volts; even if we choose  $E_F/\epsilon \sim 10$ , expression (8) is in contradiction to the experimental tails found by Skinner, which are only of the order of 1 ev. long.

#### §4. DISCUSSION OF THE PRECEDING CALCULATION OF THE LINE WIDTH

The introduction of  $\epsilon$  was suggested by some considerations of Heisenberg's (1947) in connection with his recent theory of superconductivity. He calculated the second-order perturbation energy which involved matrix elements which correspond to transitions from a state represented by a full Fermi sphere to excited states represented by a sphere with two electrons outside it, the transition being induced by that term of the Hamiltonian which represents the mutual interaction of the electrons. This energy was found to diverge as  $\log p$ , where  $\pm \mathbf{p}$  is the change in momentum of the two electrons. From this comparatively slow

divergence Heisenberg concluded that, whereas for a free electron model the ordinary free electron wave function may still be at least qualitatively correct for electrons inside the Fermi sphere, this is no longer so for the electrons which are in a thin layer at the surface of the sphere. If in the present calculations the electrons in this layer are assumed not to take part in the collisions, one would then expect, on Heisenberg's view, a reasonable result for the line width. That this expectation is not fulfilled is due to the fact that expression (8) for the line width diverges as  $1/\epsilon$ , i.e. much more rapidly than the second-order perturbation energy. Consideration of these electron collisions in a metal suggests, therefore, that a modification of the wave function of electrons in a free electron model is required, which is not confined only to the surface of the Fermi sphere.

As the free electron theory may safely be applied to sodium (von der Lage and Bethe 1947), the discrepancy between theory and experiment found in § 3 is likely to be due to the one-electron approximation. Since we have not been able to find a new  $2n$ -electron wave function which ensures a more reasonable line width when all the terms of the perturbation  $U$  are used, the one-electron functions have been preserved and a screened potential of the form  $r_{12}^{-1} \exp(-\lambda r_{12})$  has been introduced instead. It may be thought that the screening factor takes account of the fact that the Coulomb field due to one electron is screened off by induced charges at distances of the order of the mean distance between electrons in the metal. But this would be inconsistent as all electronic interactions have already been taken into account when calculating  $U_{if}$ , so that they cannot be invoked again at this stage. On the other hand, we have assumed, by adopting the one-electron approximation, that, apart from satisfying the Pauli Principle, the electrons move independently of each other, whereas in fact there are correlations for small distances, and our analysis suggests that there may also be some for larger distances.

For the new matrix element we obtain

$$U_{if} = 4\pi e^2/V(g^2 + \lambda^2) \text{ if } \mathbf{k}_1 + \mathbf{k}_2 = \mathbf{k}'_1 + \mathbf{k}'_2 \text{ and } U_{if} = 0 \text{ otherwise.}$$

This expression remains finite for small  $g$  and should be compared with (1). An argument analogous to, but more complex than, that of § 3 now yields a new and lengthy expression for  $\Delta(k)$ . If  $\lambda \sim 1$  reciprocal Ångström unit,  $\epsilon$  is found to be negligible, and one obtains

$$\begin{aligned} \Delta(k) = 4 \cdot 31 \left\{ \left( \frac{k}{\lambda} - \frac{3\lambda}{4k} \right) \tan^{-1} \left( \frac{2k}{\lambda} \frac{k_F^2 - k^2}{k_F^2 + 3k^2 + \lambda^2} \right) \right. \\ \left. + \frac{k_F^2 - k^2}{2\lambda^2} \left[ \frac{k_F^2 - k^2}{2k\lambda} \tan^{-1} \frac{2k\lambda}{k_F^2 - k^2 + \lambda^2} - 1 \right] \right. \\ \left. + \log \frac{(k_F^2 - k^2)^2 + 2\lambda^2(k_F^2 + k^2) + \lambda^4}{4\lambda^2 k^2 + \lambda^4} \right\}, \quad \dots\dots (9) \end{aligned}$$

$k$  and  $\lambda$  being expressed in the same units. Figures 2 and 3 give  $\Delta(0)$  as a function of  $\lambda$ , and  $\Delta(k)$  as a function of  $k$ . Skinner's results suggest that the maximum line width should be of the order of 1 ev., and hence Figure 2 shows that the value  $\lambda \sim 1 \cdot 2 \text{ Å}^{-1}$  should be suitable.

We now proceed, as explained in § 2, to replace each level by a broadened level. Thus the total probability per unit energy range that a level of energy  $E$  is occupied due to a broadened level at energy  $E_1$ , and of half-width  $\Delta(E_1)$ , is  $[\Delta(E_1)/2\pi]\{(E - E_1)^2 + [\Delta(E_1)/2]^2\}^{-1}$ . The density of states with energies in the



interval  $E_1, E_1 + dE_1$  is, according to the free electron theory,  $2\pi h^{-3}(2m)^{\frac{3}{2}}E_1^{\frac{1}{2}} dE_1$ . Multiplying these two expressions, and integrating over  $E_1$ , one obtains the total number of electron states per unit volume of metal and per unit energy range, at the energy level  $E$  due to all broadened levels. Writing  $\Delta(k_1)$  for  $\Delta(E_1)$ , and putting  $E = \hbar^2 k^2 / 2m$ , we obtain the new density function

$$N(E) = \frac{1}{4\pi^3} \int_0^{k_F} \frac{\Delta(k_1) k_1^2 dk_1}{[\hbar^2(k^2 - k_1^2)/2m]^2 + [\Delta(k_1)/2]^2}. \quad \dots\dots (10)$$

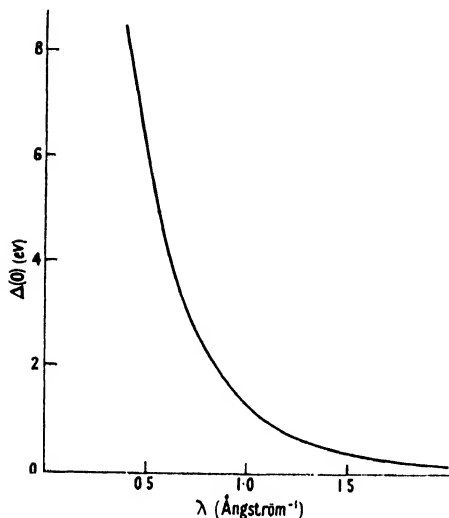


Figure 2. Graph of  $\Delta(0)$  against  $\lambda$  using equation (9) with  $k_F = 0.914 \text{ \AA}^{-1}$  (for sodium).

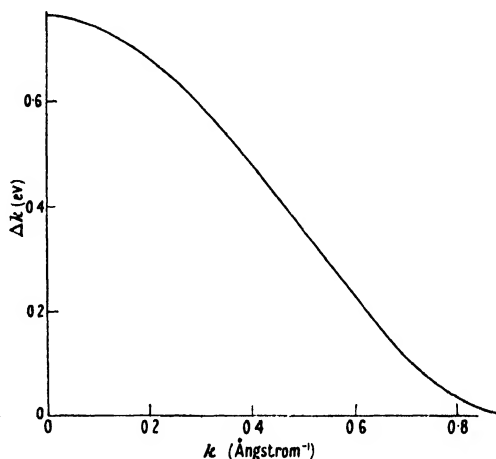


Figure 3. Graph of  $\Delta(k)$  against  $k$  using equation (9) with  $\lambda = 1.21 \text{ \AA}^{-1}$  and  $k_F = 0.914 \text{ \AA}^{-1}$ .

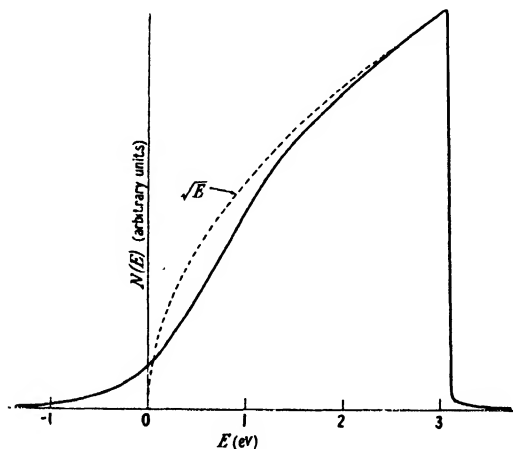


Figure 4. The  $L_{II, III}$  emission curve of sodium according to the theory of §§ 2-4. Graph of the modified  $I(E)$  curve using equation (10) with  $\lambda = 1.21 \text{ \AA}^{-1}$  and  $k_F = 0.914 \text{ \AA}^{-1}$ .

The values of  $N(E)$  for various  $E$  were obtained by graphical integration, and are plotted in Figure 4. As the transition probability into a p-state is approximately independent of  $E$  in the free electron model, the  $I(E)$  and  $N(E)$  curves have the same shape in this approximation. It is seen that the present calculations (with  $\lambda = 1.2 \text{ \AA}^{-1}$ ) lead to a tail of the type found by experiment. Its length is, of course, governed by the value of  $\lambda$  which we have chosen.

### § 5. THE MORE EXACT ONE-ELECTRON WAVE FUNCTIONS BEFORE AND AFTER A RADIATIVE TRANSITION

We now turn to a calculation of the probability that an electron will make a transition from the conduction band into a vacant p-state. As explained in § 1, we wish to take into account that, prior to the transition being made, the potential in the neighbourhood of the ionized atom is not constant, but is depressed by an amount  $D(r)$  which may roughly be represented by  $D(r) = (e/r) \exp(-\mu r)$ , at least for large values of  $r$ . One can obtain qualitative results much more readily by replacing  $D(r)$  by a simpler potential. Accordingly, we shall suppose that the electrons are confined to a sphere of large radius  $R$ , the potential being zero between the radii  $a$  and  $R$  ( $a \ll R$ ), and  $-V$  up to the radius  $a$ . The position of the ionized atom determines the origin of the sphere.

To find the correct one-electron wave function in the two regions of space thus defined, one must solve two Schrödinger equations, whose angular parts lead to spherical harmonics. If  $l$  be the angular momentum quantum number, the radial equations have the general solution

$$R_l(r) = Fr^{-1}J_{l+\frac{1}{2}}(kr) + Gr^{-1}J_{-l-\frac{1}{2}}(kr),$$

with  $k^2 = \alpha^2 = 2m(E+V)/\hbar^2$  for the inner sphere and  $k^2 = \beta^2 = 2mE/\hbar^2$  for the outer region.  $E$  is here the energy of the electron,  $F$  and  $G$  are constants, and the  $J$ 's are Bessel functions. The  $l$ -selection rule ensures that the main contribution to the total wave function comes from the radial terms for which  $l=0$ . Distinguishing the two regions of space by suffixes 1 and 2, and noting that  $\psi_1$  must remain finite at  $r=0$ , one obtains for the radial wave functions

$$\left. \begin{aligned} \psi_1(r) &= Ar^{-1} \sin \alpha r, & 0 \leq r \leq a, \\ \psi_2(r) &= Br^{-1} \sin \beta r + Cr^{-1} \cos \beta r, & a \leq r \leq R, \end{aligned} \right\} \quad (11 a)$$

$A$ ,  $B$  and  $C$  being constants. Since  $\psi_2(R) = 0$ , one finds

$$\psi_2(r) = Dr^{-1} \sin \beta(R-r), \quad D \equiv -B/\cos \beta R. \quad \dots (11 b)$$

The continuity conditions at  $r=a$  for  $\psi$  and its first derivative then yield the equations

$$\frac{A}{D} = \frac{\sin \beta(R-a)}{\sin \alpha a} = - \frac{\beta a \cos \beta(R-a) + \sin \beta(R-a)}{\alpha a \cos \alpha a - \sin \alpha a}, \quad \dots (12 a)$$

and hence  $\tan \beta(R-a) = -(\beta/\alpha) \tan \alpha a. \quad \dots (12 b)$

Since the left-side hand of this equation is a very much more rapidly oscillating function of  $E$  than is the right-hand side, (12) is satisfied only for the discrete set of energies  $E_j$  given approximately by

$$\beta_j R = j\pi, \quad \dots (13)$$

so that  $\psi_{2j}(r) = Br^{-1} \sin \beta_j r, \quad \dots (11 c)$

and the appropriate density of states is

$$N(E) = (R/2\pi)(2m/\hbar^2 E)^{\frac{1}{2}}. \quad \dots (14)$$

In virtue of (12 a) and (12 b)

$$(A/B)^2 = \beta^2 [\alpha^2 \cos^2 \alpha a + \beta^2 \sin^2 \alpha a]^{-1}, \quad \dots (15)$$

and the normalization condition gives approximately

$$|B|^2 = (2\pi R)^{-1}. \quad \dots (16)$$

The normalized wave functions are now obtainable from (11), (15) and (16). With  $V=0$ , they also give the wave functions of the electrons after the radiative transition has been made. It is evident from (13) that under these conditions the set of energy levels remains approximately unchanged, so that one can now specify the initial and final normalized one-electron wave functions,  $\psi_j$  and  $\phi_j$ , thus:

$$\left. \begin{aligned} (2\pi R)^{\frac{1}{2}}\psi_j(r) &= \begin{cases} r^{-1} + (V/E_j) \cos^2 \alpha_j a]^{-\frac{1}{2}} \sin \alpha_j r, & 0 \leq r \leq a, \\ r^{-1} \sin \beta_j r, & a \leq r \leq R, \end{cases} \\ (2\pi R)^{\frac{1}{2}}\phi_j(r) &= r^{-1} \sin \beta_j r, \quad 0 \leq r \leq R. \end{aligned} \right\} \dots\dots (17)$$

If there are  $2n$  electrons,  $j$  goes from 1 to  $n$ , each state being occupied by two electrons with opposite spins, although the spin functions have not been given explicitly in (17). The angular functions have also been omitted. In the final state of the metal one energy level in the valence band is only singly-occupied, the other electron being in a p-state of the L shell, with normalized wave function  $\chi$  (say).

#### § 6. EVALUATION OF THE TRANSITION PROBABILITY

For a system of charged particles the probability of a radiative transition is proportional to  $|M_{if}|^2$ ,  $M_{if}$  being the matrix element of the total dipole moment  $M = e \sum_k x_k$ , the sum being over the  $x$  coordinates of all  $2n$  electrons. The normalized initial and final wave function of the metal,  $\Psi_i$  and  $\Psi_f$  say, are the determinants

$$\Psi_i = [(2n)!]^{-\frac{1}{2}} \sum_P \epsilon(P) P \psi_1(1) \dots \psi_l(t) \dots \psi_{2n}(2n),$$

$$\Psi_f = [(2n)!]^{-\frac{1}{2}} \sum_Q \epsilon(Q) Q \phi_1(1) \dots \chi(t) \dots \phi_{2n}(2n).$$

The normalizing factors are correct since for large  $R$

$$\int \psi_j^* \psi_k d\tau = \int \phi_j^* \phi_k d\tau = \delta_{jk}; \quad \int \phi_j^* \chi d\tau = 0, \quad \int |\chi|^2 d\tau = 1. \quad \dots\dots (18a)$$

Note also that

$$\int \psi_j^* \phi_k d\tau = \delta_{jk}, \quad \int \psi_j^* \chi d\tau = 0. \quad \dots\dots (18b)$$

The numbers in brackets label the electrons, and it is assumed that the  $t$ th electron has been made the transition into the L shell. The summations are over all  $(2n)!$  permutation operators  $P$  and  $Q$ , and  $\epsilon(P)$  is  $+1$  or  $-1$ , depending on whether  $P$  is an even or an odd permutation. In virtue of (18) the matrix element reduces to

$$M_{if} = A \int \psi_i^* x_i \chi d\tau_i / \int \psi_i^* \phi_i d\tau_i,$$

where  $A$  is independent of the energy  $E_t$  of the  $t$ th electron in the initial state of the metal. For large  $R$  the denominator is approximately unity, and since  $\chi$  is a highly localized function, we can replace  $\psi_i$  by its value at  $r=0$  without appreciable error. We then obtain for the transition probability as a function of  $E_t$

$$P \propto E_t(E_t + V)[E_t + V \cos^2 \alpha_t a]^{-1}. \quad \dots\dots (19)$$

Using (14), the intensity is given by

$$I = C \sqrt{E'(E' + V)[E' + V \cos^2 \alpha' a]^{-1}}, \quad \dots\dots (20)$$

where  $C$  is a constant and  $E'$  has been written\* for  $E_i$ .  $I$  goes over into the simple theory,  $I = C\sqrt{E'}$ , if  $V = 0$ , and predicts a steeper rise than the simple theory; this is illustrated by Figure 5, in which some functions (20) are plotted. The

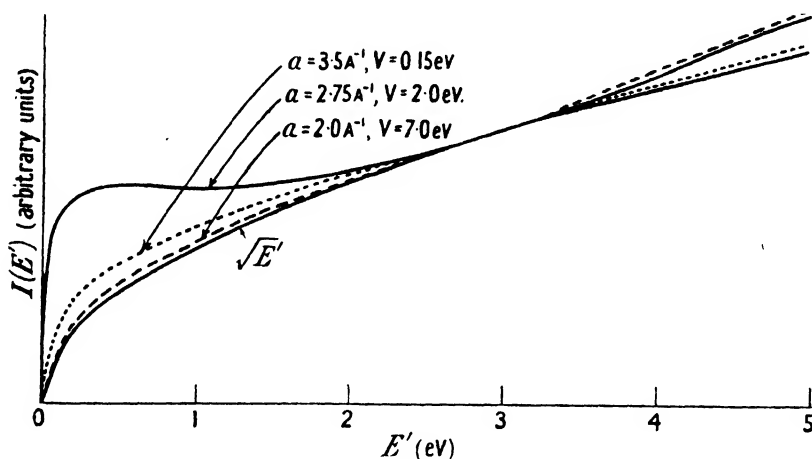


Figure 5. The  $L_{II,III}$  emission curves of sodium according to the theory of §§ 5–6. The modified expression (19) for the transition probability, but not for the density of states, is used here.

values of  $a$  and  $V$  chosen ensure that the curves touch the function  $C\sqrt{E'}$  at about 2.9 eV. The figures show that, although the screening effect must be taken into account, its treatment on the above lines is unlikely to improve agreement with existing experimental evidence. When the results of Figures 4 and 5 are combined, however, it is found that the effect of the screening is almost completely masked by the effect of the electron collisions in the conduction band.

#### § 7. CALCULATION OF THE FINAL INTENSITY CURVE, TAKING INTO ACCOUNT BOTH PHYSICAL EFFECTS

The transition of free electrons into a p-state may be treated by using plane or spherical waves, which will be distinguished by suffixes p and s respectively. If  $P$  be the transition probability and  $N$  the density of states, it is well known that

$$P_p(E) \propto 1, \quad N_p(E) \propto E^{\frac{1}{2}}.$$

On the other hand, reconsideration of §§ 5 and 6 without a potential well ( $\alpha = \beta$ ) shows that

$$P_s(E) \propto E, \quad N_s(E) \propto E^{-1}.$$

The treatment of electron collisions and of the screening effect yielded modified functions  $\bar{N}_p$  and  $\bar{P}_s$  respectively. Since the resulting intensities must, of course, be independent of the method of treatment, we obtain the three equations

$$P_p \bar{N}_p = P_s \bar{N}_s, \quad \bar{P}_p N_p = \bar{P}_s N_s, \quad \bar{P}_p \bar{N}_p = \bar{P}_s \bar{N}_s = \bar{I},$$

$\bar{I}$  being the desired modified intensity curve. Hence

$$\bar{I} = E^{-1} \bar{P}_s \bar{N}_p.$$

\*  $E'$  has been used in Figure 5 in order to distinguish this energy coordinate from that of Figure 4. This difference assists in avoiding confusion when the results of Figures 4 and 5 are combined (cf. § 7).

This shows how the modified curves must be combined. The energy coordinates  $E$  and  $E'$ , of Figures 4 and 5 respectively, must, however, first be fixed relative to each other. Figure 4 shows that the calculated density of states becomes negligibly small for  $E = -1.4$  ev. Hence we chose  $E' = E + 1.4$  ev. In Figure 6 we compare a plot of  $\bar{I}$  with Skinner's experimental results. The agreement is satisfactory, and much better than was previously obtained.

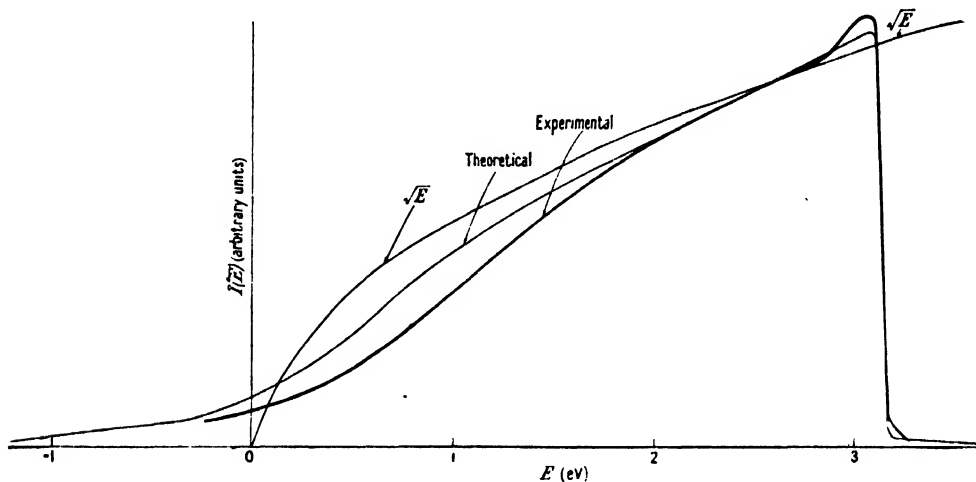


Figure 6. Experimental and theoretical  $L_{II,III}$  emission curves of sodium. The new expressions for the transition probability and the density of states are combined in the theoretical curve, the constants being taken as  $\lambda = 1.21 \text{ \AA}^{-1}$ ,  $k_F = 0.914 \text{ \AA}^{-1}$ ,  $a = 2.75 \text{ \AA}$ ,  $V = 2.0$  ev.

#### ACKNOWLEDGMENTS

The writer is greatly indebted to Professor H. Jones for introducing him to the subject matter of this paper and for many helpful discussions, and to Dr. T. E. Allibone, Manager of the A.E.I. Research Laboratory, Aldermaston, for enabling him to spend a very stimulating time in the Department of Mathematics and Mechanics of the Royal College of Science.

#### REFERENCES

- CADY, W. M., and TAMBOULIAN, D. H., 1941, *Phys. Rev.*, **59**, 381.  
 HEISENBERG, W., 1947, *Z. Naturforsch.*, **2a**, 185.  
 HEITLER, W., 1944, *Quantum Theory of Radiation*, 2nd Edition (Oxford : University Press).  
 JONES, H., MOTT, N. F., and SKINNER, H. W. B., 1934, *Phys. Rev.*, **45**, 379.  
 VON DER LAGE, F. C., and BETHE, H. A., 1947, *Phys. Rev.*, **71**, 612.  
 MATYÁŠ, Z., 1948, *Phil. Mag.*, **39**, 429.  
 PLATT, J. B., 1946, *Phys. Rev.*, **69**, 337.  
 SKINNER, H. W. B., 1938, *Rep. Prog. Phys.*, **5**, 257 (London : Physical Society) ; 1940, *Phil. Trans. Roy. Soc. A*, **239**, 95.  
 WIGNER, E., and SEITZ, F., 1934, *Phys. Rev.*, **46**, 509.

## The Luminescence Characteristics of Tin Activated Zinc Sulphide Phosphors

By G. F. J. GARLICK AND D. E. MASON

Physics Department, University of Birmingham

*MS. received 20th June 1949*

**ABSTRACT.** It has been found that the inclusion of stannous compounds in relatively large concentrations in the preparation of zinc sulphide phosphors results in an intense red luminescence when excitation is by ultra-violet light of long wavelength (3650–4000 Å.). Such characteristics as the luminescence spectra, excitation spectra, phosphorescence and thermoluminescence and the variation of luminescence with temperature have been studied. The hexagonal crystal form of zinc sulphide is essential to the production of efficient phosphors with tin as the activating impurity.

### § 1. INTRODUCTION

It has been found during the study of the effects of such metals as lead, tin and bismuth that tin can function as a luminescence activator in zinc sulphide phosphors. The reason for the absence of an earlier discovery of this activation must be ascribed to the previous use of small amounts of impurity, of the order of 0.1%, in preparation. In recent studies Fonda (1946) has shown that lead can function as a luminescence activator in zinc sulphide if relatively large amounts of lead salts are included when preparing the phosphors (he used 5% lead sulphate or nitrate in his preparations). In our experiments the amount of tin salt included in preparation, e.g. stannous chloride, was in some cases as high as 30% of the weight of zinc sulphide. Semi-quantitative chemical analysis and spectrographic tests indicated that only a very small proportion of tin remained after preparing the phosphor—of the same order as the activator concentrations in copper or silver activated phosphors (0.01%). The same spectrographic tests showed no presence of manganese or other significant impurities which might have given rise to the observed luminescence.

Our studies of tin activated phosphors included the following experimental investigations:

- (i) Methods of preparing the phosphors.
- (ii) Measurement of the spectral distribution of the luminescence for given excitation conditions.
- (iii) Measurement of the excitation spectra of the phosphors—that is, the efficiency of radiation of different wavelengths in exciting luminescence.
- (iv) Measurement of the variation of luminescence efficiency with temperature for the different spectral emission bands of the phosphors.
- (v) Measurement of thermoluminescence characteristics which indicate the effect of tin activation on phosphorescence and electron trapping states in the phosphor.
- (vi) Measurement of the characteristics of luminescence stimulated by infra-red irradiation after excitation of the phosphors by ultra-violet light.

We give the results of these studies and discussion of them in the appropriate sections below.

## § 2. PREPARATION OF TIN ACTIVATED ZINC SULPHIDE

The most suitable compounds of tin for inclusion in the preparation of tin activated zinc sulphide phosphors are stannous chloride and stannous sulphide: both must be of the purity standard of analytical reagents. Since both the chloride and the sulphide have low melting points compared with the temperatures of phosphor preparation, considerable amounts of the materials have to be added in preparation. In some cases, before heating, phosphor specimens contained as much as 30% by weight of stannous chloride. From results mentioned above we conclude that, after firing, the concentration of tin is only of the order of 0.01%. In order to obtain good phosphors it is necessary to use firing temperatures above 1,000°C. This is found to be so even when the tin is added to a zinc sulphide already preformed (i.e. crystallized) by firing at temperatures above 1,000°C. When phosphors are prepared at lower temperatures, with or without flux treatment, products are obtained which are almost non-luminescent in bulk. These contain specks of red-emitting material whose luminescence is characteristic of specimens made at higher temperatures. From this we conclude that the high temperatures are necessary for the diffusion of tin through the crystal lattice. All efficient phosphor specimens possess the hexagonal wurtzite structure, as shown by x-ray diffraction photographs. Phosphor formation is not appreciably influenced by inclusion of fluxes, such as sodium chloride, before firing. All our specimens were heated in silica tubes open to the air (tubes 12 in. long by  $\frac{1}{2}$  in. internal bore,  $\frac{3}{64}$  in. wall thickness).

## § 3. THE LUMINESCENCE SPECTRA OF $\text{ZnS-Sn}$ PHOSPHORS

The luminescence spectra of phosphor specimens were measured by means of a Hilger constant deviation spectrometer, photoelectric cell, electrometer triode system and pen recorder. The phosphor specimen was deposited in a thin layer on a glass slide and mounted in front of the entrance slit of the spectrograph. Excitation was by 3650 Å. radiation from a 125 watt H.P. mercury arc lamp.

A typical emission spectrum is shown by the curves of Figure 1. Curve A is the corrected curve for equal energy while curve B is corrected to give equal quanta conditions. The spectra of all tin activated zinc sulphide phosphors are very much the same, consisting of a broad band in the blue spectral region characteristic of the self-activated phosphor and a broad band in the red region characteristic of the tin impurity. The maxima of these two bands are at 4700 Å. and 6450 Å. respectively. The relative intensity of the two bands is a function of the excitation intensity, the blue band increasing in intensity relative to the red band with increase in intensity of excitation, as in the case of  $\text{ZnS-Mn}$  (0.1%) phosphors (Gisolf and Kröger 1939).

The spectrum of Figure 1 was obtained at room temperature with a fairly high intensity of excitation. Red emission bands have been observed for zinc sulphide phosphors activated by iron (Kröger 1947), but the spectral maximum is then at 6100 Å. and the emission intensity is always very much smaller than that which we observe for tin activation. As shown by Figure 1, the intensity of the red emission band is of the same order as that of the blue emission band and the latter is of the usual magnitude for other zinc sulphide phosphors ( $\text{ZnS-Zn}$ ,  $\text{ZnS-Cu}$  (0.0001%),  $\text{ZnS-Mn}$  (0.1%)).

§ 4. EXCITATION SPECTRA OF ZnS-Sn PHOSPHORS

The excitation spectra of phosphor specimens were obtained by measuring the luminescence intensity produced by radiation of different wavelengths, the

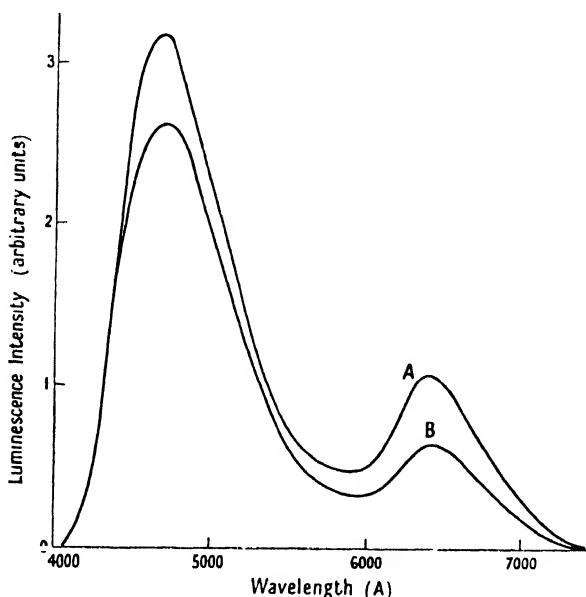


Figure 1. Luminescence emission spectra of a typical ZnS-Sn phosphor ( $\lambda = 3650 \text{ Å}$ ).

A. Spectrum corrected to equal energy scale.

B. Spectrum corrected to equal number of quanta.

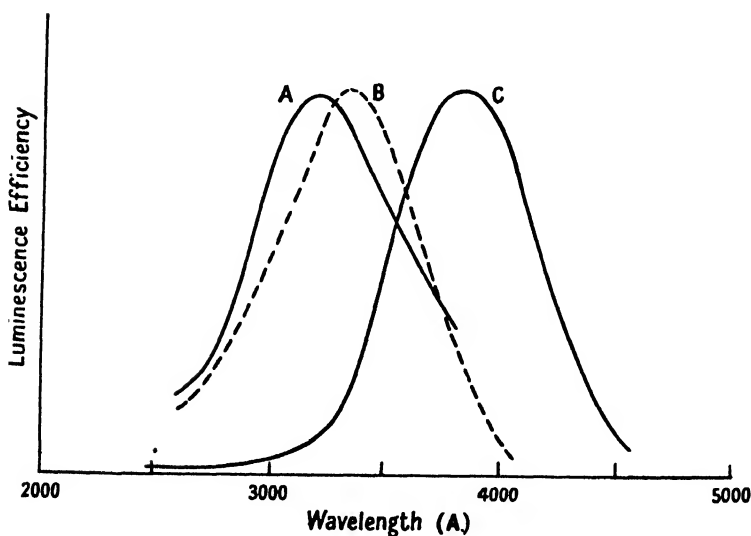


Figure 2. Excitation spectra for a typical ZnS-Sn phosphor at room temperature.

A. ZnS-Sn, blue emission characteristic of Zn activator.

B. ZnS, blue emission characteristic of Zn activator.

C. ZnS-Sn, red emission characteristic of Sn activator.

intensity of the latter being measured by a linear detector (in this case a thermocouple). A quartz prism monochromator provided the necessary monochromatic radiation. Excitation spectra for the blue and red emission of a ZnS-Sn specimen measured at room temperature are given in Figure 2. The spectrum for the blue



emission is similar to that measured for ZnS–Zn phosphors by previous workers (Garlick and Gibson 1948). The excitation spectrum for the red emission due to tin activation lies to longer wavelengths and has a maximum at about 3800 Å. It is a broad band of somewhat similar form to that for the blue emission, but the excitation efficiency becomes negligible at wavelengths shorter than 3000 Å. Excitation by ultra-violet light of short wavelength, by cathode rays or by x rays, produces a predominantly blue emission, the intensity of the red emission being very low. Since the absorption edge of the crystal lattice of zinc sulphide is at 3340 Å., this means that excitation of the red emission (and thus of the tin impurity centres) is negligible when absorption takes place in the phosphor matrix. We hope to make further studies of the excitation spectra of these phosphor specimens at temperatures other than room temperature.

#### § 5. THE VARIATION OF LUMINESCENCE EFFICIENCY WITH TEMPERATURE

The variation of the luminescence efficiency of tin activated zinc sulphide phosphors with temperature was measured separately for the blue and red emission bands, for constant excitation of fixed intensity and 3650 Å. wavelength. Typical results are given in Figure 3. It is found that the blue emission efficiency decreases to zero in the same region (250–350° K.) as for self-activated zinc sulphide

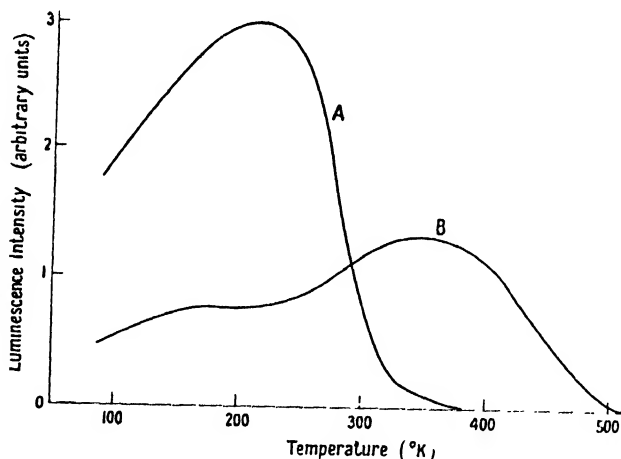


Figure 3. Variation of luminescence with temperature for a typical ZnS–Sn phosphor (constant excitation;  $\lambda = 3650$  Å.).

- A. Blue emission characteristic of Zn activator.
- B. Red emission characteristic of Sn activator.

phosphors (Garlick and Gibson 1948) but that the red emission persists to higher temperatures. As yet we have not studied the variation of luminescence efficiency with excitation intensity in the temperature regions 280–350° K. and 400–500° K. where the efficiency for the respective emission bands decreases rapidly with temperature due to non-radiative processes.

#### § 6. THE THERMOLUMINESCENCE CHARACTERISTICS OF ZnS–Sn PHOSPHORS

To obtain the thermoluminescence characteristics of a ZnS–Sn specimen the phosphor is excited at 90° K. by 3650 Å. radiation and then warmed at a uniform rate (2.5°/sec.) in the dark. The variation of its thermoluminescence emission with temperature is then recorded. Optical filters were used to obtain separately

the thermoluminescence curves for the blue and red emission bands. Typical results for three different specimens are given in Figure 4. The curves for the respective emission bands are very similar for all these specimens. The curves for

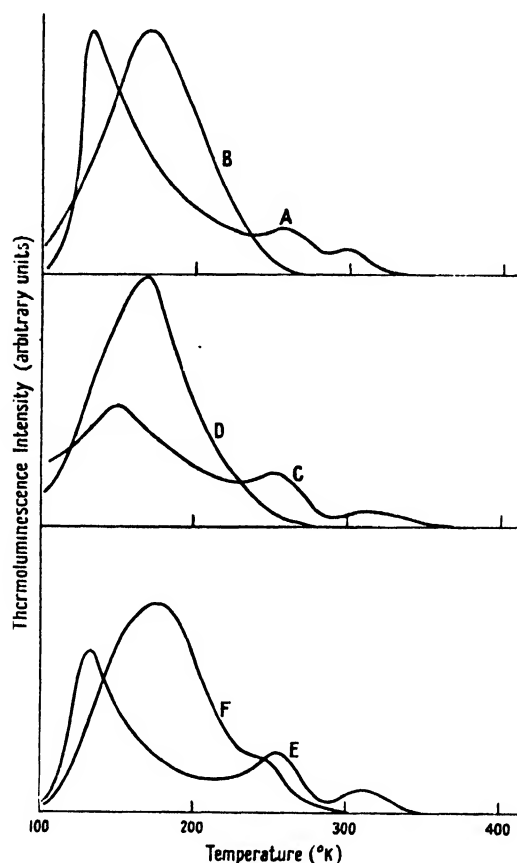


Figure 4. Variation of thermoluminescence intensity with temperature for different specimens of ZnS-Sn phosphor (excitation at 90° K.;  $\lambda = 3650 \text{ \AA}$ ).

A, C & E. Red emission characteristic of Sn activator.  
B, D & F. Blue emission characteristic of Zn activator.

the blue emission are typical of other phosphors also (ZnS-Zn etc.), but those for the red band are characteristic of the tin activator. The peak at 130° K. is slightly variable since it corresponds to phosphorescence of short duration (seconds) at 90° K. The time elapsing between the removal of excitation and beginning of warming, which affects the peak position, was unavoidably different for each specimen in our experiments.

#### § 7. THE INFRA-RED STIMULATION CHARACTERISTICS OF ZnS-Sn PHOSPHORS

Tin activated zinc sulphide phosphors have their blue emission band stimulated by suitable infra-red radiation at low temperatures (90° K.). The characteristics are very similar to those of pure zinc sulphide phosphors at these temperatures (Garlick and Mason 1949). The infra-red stimulation spectrum has a band at  $1.2\mu$  strong compared with that of pure zinc sulphide phosphors. Stimulation does produce red emission in tin activated specimens, but this is too feeble to enable a measurement of the corresponding infra-red stimulation spectrum to be made.

## §8. CONCLUSION

There appears to be no doubt that tin can function as an efficient activator for luminescence in zinc sulphide phosphors provided that the hexagonal crystal form of the phosphor is obtained by preparation at high temperatures. The tin impurity gives rise to phosphors which exhibit specific excitation and emission spectra, and gives rise to a characteristic distribution of electron trapping states as shown by thermoluminescence experiments. Preliminary experiments show that when cadmium sulphide is added to the phosphor in preparation its inclusion does not markedly influence the spectral position of the emission band due to tin impurity. We hope to extend investigations of this new type of phosphor to include measurements of absorption, excitation and emission spectra at various temperatures.

## REFERENCES

- FONDA, G. R., 1946, *J. Opt. Soc. Amer.*, **36**, 382.  
GARLICK, G. F. J., and GIBSON, A. F., 1948, *Nature, Lond.*, **161**, 359.  
GARLICK, G. F. J., and MASON, D. E., 1949, *J. Electrochem. Soc.*, **96**, 90.  
GISOLF, J. H., and KRÖGER, F. A., 1939, *Physica*, **6**, 1101.  
KRÖGER, F. A., 1947, *Some Aspects of Luminescence in Solids* (Amsterdam: Elsevier Publ. Co.).

## CONTENTS FOR SECTION B

	PAGE
Dr. G. LIEBMANN. An Improved Method of Numerical Ray Tracing through Electron Lenses . . . . .	753
Mr. C. G. WYNNE. Field Correctors for Parabolic Mirrors . . . . .	772
Dr. L. C. THOMSON. Shape Irregularities in the Equal Energy Luminosity Curve. . . . .	787
Dr. M. MOKHTAR and Mr. G. ABDEL MESSIH. The Acoustic Characteristics of Conical Pipes . . . . .	793
Prof. A. VAN ITTERBEEK and Dr. L. VERHAEGEN. Measurements of the Velocity of Sound in Liquid Argon and Liquid Methane . . . . .	800
Dr. K. D. FROOME. The Behaviour of the Cathode Spot on an Undisturbed Mercury Surface . . . . .	805
Mr. B. MELTZER. Electron Flow in Curved Paths under Space-Charge Conditions. . . . .	813
Mr. F. A. GOULD. A Knife-Edge Balance for Weighings of the Highest Accuracy. . . . .	817
Dr. J. W. FOX. Onset of Turbulent Flow in certain Arrays of Particles . . . . .	829
Mr. J. K. MACKENZIE and Dr. R. SHUTTLEWORTH. A Phenomenological Theory of Sintering . . . . .	833
Contents for Section A . . . . .	853
Abstracts for Section A . . . . .	853
Obituary Notices :	
WILLIAM BOWEN . . . . .	855
NORMAN ROBERT CAMPBELL . . . . .	855
CECIL LEWIS FORTESCUE . . . . .	858
EDWARD PHILIP HARRISON . . . . .	858
RICHARD ALBERT HULL . . . . .	859
CHRISTOPHER NOEL HUNTER LOCK . . . . .	860
WILLIAM BLAIR MORTON . . . . .	861
ALAN FARADAY CAMPBELL POLLARD . . . . .	862
WILLIAM GEORGE PYE . . . . .	863
MAX PLANCK . . . . .	864
WILLIAM NELSON STOCKER . . . . .	867
Corrigendum . . . . .	869
Index to Section B, Vol. 62 . . . . .	870
Index to Reviews of Books, Section B, Vol. 62 . . . . .	877
Proceedings at the Meetings, 1948-49 . . . . .	viii
Report of Council for the Year 1948 . . . . .	xviii
Report of the Honorary Treasurer for the Year 1948 . . . . .	xxii

## ABSTRACTS FOR SECTION B

*An Improved Method of Numerical Ray Tracing through Electron Lenses*, by  
G. LIEBMANN.

**ABSTRACT.** An improved method is described for the tracing of electron trajectories through electron lenses by integrating the general ray equation with the help of Taylor's series, taking the series up to and including fourth-order terms. The paraxial trajectory is obtained by progressing from point  $P_n$  on the trajectory to point  $P_{n+1}$  with the help of recurrence formulae  $r_{n+1} = Q_1 r_n + Q_2 r'_n$  and  $r'_{n+1} = Q_3 r'_n + Q_4 r_n$ , where the coefficients  $Q_1 \dots Q_4$  are functions of the electrostatic or magnetic field distribution along the axis. The deviation of the first-order trajectory from the paraxial trajectory is built up with the help of similar recurrence formulae. The method is first developed for combined electrostatic and magnetic lenses, using the "equivalent potential"  $U = \Phi - eA^2/2m$ , and then specialized for pure magnetic or pure electrostatic lenses. The case of space charge within lenses is also considered. Comparison of the improved method with other methods shows that it is faster and capable of high accuracy. The factors influencing the accuracy are considered in detail and a short-cut method using extrapolation is given. A fully calculated example is appended.

*Field Correctors for Parabolic Mirrors*, by C. G. WYNNE.

**ABSTRACT.** Optical systems to correct the oblique aberrations of large parabolic mirrors in astronomical telescopes are discussed. The earlier work of F. E. Ross on doublet lens correctors in the converging beam is extended, and the residual first order spherical aberration is shown to depend only on the power of the corrector, its elimination requiring an impracticably large power; these results are independent of the arrangement and the optical constants of the components, and are unaffected by aspherizing the lens surfaces. Correction by two aspheric plates is shown to lead to systems of relatively great length, with consequent heavy vignetting. Finally, systems are discussed consisting of a doublet lens with one aspheric plate or secondary mirror; such a secondary mirror may be used to correct field curvature, giving corrector lenses which are afocal and therefore free from secondary spectrum, and the departure of the secondary mirror from the spherical form may be made zero by a suitable choice of the other variables. Details are given of the calculated performance of four three-component systems.

*Shape Irregularities in the Equal Energy Luminosity Curve*, by L. C. THOMSON.

**ABSTRACT.** The photopic luminosity function of two observers with normal colour vision has been measured. Two shoulders on the curve in the blue region of the spectrum first noticed by Gibson and Tyndall have been confirmed, and the relationship of the curves to the standard C.I.E. luminosity function is discussed.

*The Acoustic Characteristics of Conical Pipes*, by M. MOKHTAR and G. ABDEL MESSIH.

**ABSTRACT.** The paper describes an experimental investigation on slightly tapering conical pipes used as sound transmitters, undertaken in order to determine their acoustic characteristics, their end corrections and the pressure variation along the inside of the pipes.

A hot wire anemometer and a Pitot pressure tube were used for recording particle velocity and pressure variation in the acoustic field. The results obtained for the resonant frequencies show fair agreement with the theoretical formula  $kr = -\tan kl$ , where  $r$  is the radius of the throat of the conical pipe,  $l$  is its slant length and  $k = \omega/c$ ,  $\omega$  being the angular frequency and  $c$  the velocity of sound.

The recording of the acoustic pressure along the axis of the conical pipes shows that the nodes inside are places of minimum but not zero pressure, and that they are not equidistant. The end corrections are deduced from these pressure curves. The correction is always positive, being less than that of a cylindrical pipe of diameter equal to that of the mouth of the cone. It increases with the angle of the cone and with the order of the overtone to which the conical pipe resonates.

*Measurements of the Velocity of Sound in Liquid Argon and Liquid Methane*, by A. VAN ITTERBEEK and L. VERHAEGEN.

**ABSTRACT.** The ultrasonic velocity in liquid argon and methane has been measured between their boiling and melting points and the ratio of specific heats calculated. The compressibilities and degrees of association have also been calculated and compared with the results obtained for other liquified gases (hydrogen, helium).

*The Behaviour of the Cathode Spot on an Undisturbed Mercury Surface*, by K. D. FROOME.

**ABSTRACT.** The cathode spot of transient mercury arcs has been studied by means of a Kerr cell apparatus capable of taking many superimposed photographs. Discussion is limited to times when the spot is moving with sufficient velocity not to disturb the mercury surface. It is found that for a given current the "spot" takes the form of a line, or broken line, of total length proportional to the current. This is also true for a spot in a magnetic field. If the current rises slowly, the length of the line increases proportionally to the current; but if the rate of growth of current is greater than a value lying between  $\pi \times 10^7$  and  $2\pi \times 10^7$  amperes per second, then fresh spots form and spread out radially from the point of formation into lines moving with a maximum velocity of about  $10^6$  cm/sec. It is found that this velocity is never greatly exceeded whatever the experimental conditions. The current density is in excess of  $10^6$  amperes/cm<sup>2</sup>.

*Electron Flow in Curved Paths under Space-Charge Conditions*, by B. MELTZER.

**ABSTRACT.** Further developments in a method of obtaining solutions of space-charge flow, described in a previous paper, are presented. A single example of three-dimensional flow is given, as well as a number of general theorems. A distinction is drawn between "normal" flow, in which all electrons have the same energy (example: a thermionic device with a unipotential cathode) and "abnormal" flow, in which they may have different energies. It is shown that in the case of the former the application of the general method simplifies considerably.

*A Knife-Edge Balance for Weighings of the Highest Accuracy*, by F. A. GOULD.

**ABSTRACT.** A detailed description is given of the balance used at the National Physical Laboratory for the most accurate weighings made in the comparison of fundamental standards of mass. Among the several unique features of this balance are the design of the beam, stirrups and pans, the use of recognized methods of geometrical constraint for precise location of these parts, the accuracy of construction, particularly of the knives, and the fineness of the positional adjustments of the components.

In technique of weighing, this balance also presents novel features. It is installed in a vault and, once it is loaded with the masses to be compared, the operations of controlling and reading the balance are entirely effected from outside the closed vault, mechanical means being employed for interchanging the loads undergoing comparison. Moreover, the technique of weighing is so arranged that a series of weighings of standards of mass from each arm of the balance in turn is completed without disturbing the contacts between the knives and their bearing planes. Largely as the result of using this technique, an accuracy of  $\pm 0.001$  mg., viz. 1 part in  $10^6$ , has been attained in the comparison of kilogram masses of appropriate stability.

*Onset of Turbulent Flow in Certain Arrays of Particles*, by J. W. FOX.

**ABSTRACT.** Reynolds' number has been found for the onset of turbulence in water flowing through a perfectly packed hexagonal array of uniform spheres. Experiments have also been carried out on an imperfectly packed array of the same spheres and on an array of irregular particles (marble chips). A satisfactory differential manometer, which enables differences of head of the order of a hundredth of a millimetre of water to be readily determined, is described.

*A Phenomenological Theory of Sintering*, by J. K. MACKENZIE and R. SHUTTLEWORTH.

**ABSTRACT.** Sintering occurs when powders are heated to temperatures near their melting points. This paper deals with the rapid increase of density during the sintering of single substances. The increase of density cannot be explained by volume diffusion of vacant lattice sites or surface migration of atoms, but must involve macroscopic flow. The driving force for this flow is surface tension, and an equation connecting the rate of shear strain with the shear stress defines the resistance to deformation.

The density of a compact is calculated as a function of the time for two different laws of deformation, (a) that for a solid with a Newtonian viscosity, and (b) that for a Bingham solid which has a yield point and a rate of shear strain proportional to the difference between the applied shear stress and a yield stress. The effect of gas in the pores is calculated in the case of the viscous law.

The theory assumes that the pores are equal spheres and predicts that densification is uniform throughout a compact, independently of its shape and size, and suggests that gas pressures of a few atmospheres applied to the outside of a compact may appreciably increase the rate of sintering.

Relevant experiments and previous theories are examined critically, and it is shown that while the viscous model may explain the sintering of glasses it cannot explain that of metals. However, the experimental data can be explained by a model showing a yield point: on such a model the interaction of one pore with its neighbours is vital, so that pores in powder compacts close and isolated pores do not.

## Obituary Notices

### WILLIAM BOWEN

WILLIAM BOWEN, Managing Director of the Bowen Instrument Co. Leeds, died on 9th February 1949. He was born in September 1886, the eighth child and third son of John and Eliza Bowen. He had three brothers and seven sisters. His father was a coal miner; so was the eldest brother (9½ years older) and the second brother, David Bowen, K.C. (1½ years older).

He was educated at the Pentre Council Schools until the age of twelve. When he reached the school leaving age he wanted to become a coal miner but was persuaded to continue his education by entering the Porth County School; he remained there until, at the age of 17, he won a scholarship to the University College, Cardiff, where he took the courses in engineering. During that time (1904–5) the Welsh Revival movement occurred; with this Bowen was so taken up that he neglected his studies and lost his scholarship. His parents maintained him at College from 1905–6, but he did not succeed in getting his degree in engineering.

For a while after leaving college, in 1906, he taught at an elementary school in Swansea and then at a coaching school in London, after which he obtained a subordinate appointment with the Great Eastern Railway in the Engineers' Department. From there he entered the service of the Cambridge Instrument Company. Towards the end of 1913 he left this company to join his brother David Bowen as consulting engineers in Leeds. There he soon developed his own instrument company specializing in pyrometry, and up to the outbreak of the 1939 war his work was solely concerned with temperature measuring equipment.

In October 1939 he was asked to undertake the manufacture of compensating leads for aero engine temperature equipment. The insulation of these leads was of the plastics type and Bowen brought to bear his knowledge of temperature control equipment to secure a uniform coating of plastic on the cables. He then launched out into the production of plastic-covered wire and a vast amount was supplied in the form of assault cable for military purposes. He also produced a variety of plastic goods.

In the post war years he made strenuous efforts to popularize plastic-covered cables and read a paper on the subject before the Institution of Electrical Engineers. During this period he employed scientific assistance in development work. He contributed funds to the Scientific Instrument Manufacturers Association for the establishment of an award known as 'The Bowen Prize'. The resumption of peace time conditions and business competition imposed a severe strain which his constitution could not stand.

In 1946 Bowen and the writer made a B.I.O.S. trip to Germany and a warm friendship was formed as the result of it. He was a man of charming personality and was highly respected by his employees whose welfare was his first consideration.

In reviewing his life one realizes the profound influence that the higher educational system of Wales has had on the lives of the more ambitious members of the mining community, for without the opportunities given by scholarships and low fees at the University Bowen would probably have followed in the footsteps of his father and become a coal miner. It might be added that four of Bowen's family were students at the University College, Cardiff, during one session.

His brother, David Bowen, worked at the coal face as a miner for seven years then after four years at Cardiff College became the head of the Mining Department at the University of Leeds at the age of 25. David Bowen since the 1914–18 war had been at the Bar and was made K.C. in 1938. To him the writer of this obituary is indebted for details of Bowen's early life.

EZER GRIFFITHS.

### NORMAN ROBERT CAMPBELL

IN the death of Norman Campbell, which occurred on 18th May 1949, at the age of 69, the Physical Society has lost one of its outstanding Fellows. It is true that, because of ill-health, he had not been seen at meetings for ten years and more, but he continued to the very last to make characteristic contributions to the *Proceedings*, and these cannot fail to have reminded Fellows of the times when a paper by Campbell would fill the lecture theatre with an

audience that found his hard-hitting controversial attack on some respectable piece of orthodoxy most stimulating. He had a stammer, which must have been a severe handicap, but he certainly didn't let it stop him; and indeed it sometimes seemed to throw into stronger relief his burning enthusiasm for that particular facet of truth that was engaging his attention at the moment.

And here let it be noted that, though he could show an almost fanatical zeal in certain directions, he was no narrow specialist, but a man who delighted in science in all its aspects. Educated at Eton, and at Trinity College, Cambridge, he worked in the Cavendish Laboratory under the leadership of J. J. Thomson for several years, becoming a Fellow of Trinity College in 1904. He contributed the chapter 1903-9 to *The History of the Cavendish Laboratory*, and in so doing gave a good account of his interests at this period; ionization, radioactivity, penetrating radiation etc. He was appointed to the Cavendish Research Fellowship at Leeds at the time when W. H. Bragg was professor there, and continued on more or less the same lines of research, but he also wrote his *Modern Electrical Theory*, which had a great success, and made his name very familiar to students of that generation. He became an Honorary Fellow of Leeds University in 1913 and seemed well set for an academic career until the first world war brought a complete break by immersing him in applied physics.

Before this occurred, however, he had already shown signs of an interest that certainly forms no part of the Cavendish tradition; an interest in what might loosely be called the logic or philosophy of physics, though Campbell would probably have repudiated both terms. It first appears in a small book on *The Principles of Electricity*, which he wrote for the series of sixpenny books published by Jack, The People's Books. This must have puzzled many a novice. Electricity was presented to him not as that by which marvels have been accomplished, but that which provides wonderful opportunities for clear hard thinking about the first principles of science. Though Campbell subsequently followed many other lines of work, this was probably the one that he had most at heart, and he never abandoned it, although its reception seldom brought him anything but discouragement. In this vein we find his great book *Physics, The Elements* (1930) and the smaller ones *Measurement and Calculation* (1928) and *What is Science?* (1921). All this work leaves the reader with no doubt that to Campbell the primary object of science was the enrichment of the human mind rather than the comfort of the human body. How strange then that he should have been content to spend the greater part of his working life in an industrial research laboratory! The old term 'natural philosopher' seemed to fit him so well that it was hard to see in him also the physicist as the handmaid of industry. But the fact is that he joined the staff of the Research Laboratory of the General Electric Company Ltd. on its foundation in 1919 and worked there until he retired in 1944. Moreover he obviously derived much satisfaction from his position as a member of this large and powerful research organization. This no doubt was partly because he had seen the organization grow up and had played an important part in establishing in it a genuinely scientific tradition, but it was probably partly also because he liked to have a hand in the ordinary workaday world. How else can one explain that after he had retired he voluntarily undertook to prepare a survey of systems of traffic lights, on finding out that one was needed.

As mentioned earlier, it was the War of 1914 that first deflected him towards applied science. He left Leeds for the National Physical Laboratory where he worked on magnetos and spark ignition with C. C. Paterson, work which after the war they published in the *Proceedings*. When Paterson left the N.P.L. in 1919 to organize research laboratories for the G.E.C. Campbell accompanied him and remained with him for the rest of his working life. The two men, so very different on a casual acquaintance, gave ample evidence that they valued the association highly. Paterson's original team indeed gave the impression of being a closely knit band of pioneers. One might be surprised to find Campbell in it, but, once in it was not difficult to understand his reluctance to drop out, and it was only ill-health that eventually forced him to do so.

He worked on the clean-up of gases by the electric discharge, took a leading part in the development of the caesium photoelectric cell, and wrote with Miss Ritchie a book on photoelectric cells. In this work we see Campbell as an experimental worker at the bench. With his tall lean form and intense concentration on the idea of the moment he could, when hard on the trail, be somewhat formidable. A laboratory assistant fresh from school admitted that she found him rather frightening, but for all that the impression that remains



is one of great personal charm. His working bench steadily accumulated a litter of discarded glass tubing, which it was absolutely forbidden to touch. When it reached a depth at which something simply had to be done, he himself would do it. Later on illness took its toll and he had to turn more and more to work on paper as distinct from work on the bench. He was to be found working on many problems in applied science; photometry, colour matching, statistics, 'noise' in valve circuits, and even on the drafting of patent specifications. He confessed that this last, although quite interesting until he had mastered the technique, did become exceedingly boring, and probably nothing but the sense that it at least allowed him to keep his shoulder to the wheel, kept him at it.

All this time he maintained a passionate interest in the fundamentals of physics and produced from time to time the books that have already been mentioned and papers of a similar interest. He himself was convinced that his work on the roots of the subject was far more important than the endless pursuit of novelties, and that sooner or later the need for a far more critical attitude than is customary would be recognized, but he was under no illusion that physicists in general or even his own associates shared this opinion. There were undoubtedly times when he felt like a voice crying in the wilderness, but lest this should give a distorted impression of him it would be well to quote from an unpublished article he wrote in the 1930's. He tells how on a day in 1913 a copy of the *Phil. Mag.* fell out of his bookcase and lay open on the floor.

"Some algebraic formulae caught my eye . . . . It was part of a paper by a Mr. N. Bohr of whom I had never heard . . . . I sat down and began to read. In half an hour I was in a state of excitement and ecstasy, such as I have never experienced before or since in my scientific career. I had just finished a year's work revising a book on *Modern Electrical Theory*. These few pages made everything I had written entirely obsolete. That was a little annoying, no doubt; but the annoyance was nothing to the thrill of a new revelation, such as must have inspired Keats' most famous sonnet. And I had so nearly missed the joy of discovering this work for myself and rushing up to the laboratory to be the first to tell everyone else about it! Twenty years have not damped my enthusiasm . . . ."

His friends will see the authentic Campbell in this fragment, and it is a good example of his writing at its best. One other example may be given; it is from a letter to the present writer, dated November 1944.

"In March this year I carried into effect my long laid plans for retiring from all scientific work and adopting an unintellectual life in the country . . . . Our plans for a peaceful retirement were rudely shattered. After having endured the full length of the London blitz and having so many hairbreadth's escapes that we regarded ourselves as having charmed lives, we were caught by a stray bomb, jettisoned from a plane that was being chased, in an area that had never had a bomb before. Our house and almost all its contents were completely destroyed; I have lost all my papers and nearly all my books; and have had to take refuge here with some kind friends and to resume scientific work in order to give myself occupation."

The quotation speaks for itself. It was followed by the suggestion that we should collaborate on a project that he had much at heart. The outcome can be found in the *Proceedings*, but it is Campbell's extraordinary fortitude in adversity that stands out most in these closing years. He and Mrs. Campbell faced the loss of their son on active service, the loss of their home and severe injury to Mrs. Campbell, but they could still enjoy Chaucer and he could work on the principles of electrical measurement. The death of Mrs. Campbell was a staggering blow, but once more he marshalled his forces, returned to the attack on the principles of magnetism, and looked round for a job (unpaid) in which he could help some scientific organization. It was in this way that he came to make a survey of traffic lights. Having settled down with his daughter near Nottingham, he came up to London for The Physical Society Exhibition of 1949, but the effort was too much for him and he died soon after his return, a man of science to the last.

It would have been pleasant to have had his photograph in the *Proceedings*, but it is characteristic of the man that none could be found.

### PROF. CECIL LEWIS FORTESCUE

PROFESSOR C. L. FORTESCUE's death on 22nd September, only three years after his retirement from the chair of electrical engineering at the Imperial College of Science and Technology, London, came as a shock to his many friends and former colleagues and staff. He was born in 1881 and educated at Oundle School and Christ's College, Cambridge, where he obtained a First Class in the Mechanical Sciences Tripos. He played an active part in school and college life, was a keen oarsman, and reached the 'trial eights' while at Cambridge. This keen interest in student activities, and particularly rowing, never diminished, but probably increased during his later years, and he was rarely away from the river when Imperial College crews were racing.

On leaving Cambridge he spent some years at Messrs. Siemens' dynamo works and as instructor in electrotechnics and applied mechanics at H.M. Torpedo and Gunnery Schools, Portsmouth. During 1911-22 he was professor of electrical engineering at the Royal Naval College, Greenwich, and during this period, in addition to his academic and administrative duties, he carried out experimental work connected with wireless telegraphy during the first world war.

In 1922 he was appointed professor of electrical engineering at the Imperial College of Science and Technology, London. He was the third to occupy this position since 1885, the two previous occupants being Professors W. E. Ayrton and T. Mather. During the whole of the twenty-four years that he was professor and head of the Electrical Engineering Department he was indefatigable in his work for the College, and never seemed to begrudge the long hours spent in the Department. He was always accessible to the students and ready to help them in any way that was possible. He was, until his retirement in 1946, President of the College Radio Society, which involved giving twenty-four Presidential addresses, and he gave considerable time and energy to their preparation so as to present something which was interesting and instructive to the members of the Society. As a lecturer and teacher he was probably more successful with the advanced and postgraduate students than with those in the earlier years, who, in many cases, found his methods of dealing with electrical engineering somewhat difficult to appreciate. He will, generally speaking, be remembered at Imperial College for his very strenuous work in connection with the teaching of the subject of telecommunications at the undergraduate stage and the development of facilities for study and research in this subject for postgraduate students.

This development was so successful that it can be stated that the Electrical Engineering Department of the Imperial College provided a more thorough course of education in the subject of telecommunications than any other college or university in Great Britain, and students from all over the world were attracted to both the undergraduate and postgraduate courses.

As a professor of the University of London he took very seriously the many duties which fell to his lot, and devoted a great deal of care and attention to the work of the many committees and boards of which he was a member. He served on the Senate of the University, was Dean of the Faculty of Engineering and Chairman of the Board of Studies in Electrical Engineering.

In 1942 Prof. Fortescue was elected President of the Institution of Electrical Engineers, which was a fitting recognition not only of his professional standing and academic qualifications, but also of the devoted work he had done for the Institution for very many years.

Prof. Fortescue very rarely took any rest from his work, and since his retirement in 1946 he had been active in the service of the University and also at Southampton Technical College in connection with the development of courses in telecommunications, electronics and electrical measurements. He is survived by his wife, son and daughter.

A. R.

### DR. EDWARD PHILIP HARRISON

E. P. HARRISON, born in London in 1877, died suddenly on 6th May, 1948. He was a Fellow of the Physical Society from 1900 to the time of his death. He was also a Fellow of the Institute of Physics and a Fellow of the Royal Society of Edinburgh.

Whilst a student in University College London he won an 1851 Exhibition Research Scholarship in physics and proceeded to the University of Zurich where he obtained his Ph.D.

In 1904 he went to King's College, Cambridge, and did two years research in physics at the Cavendish Laboratory. Later, he was appointed professor of physics in the Presidency College, Calcutta, where he was also head of the Observatory.

In 1923 he returned to England as Chief Scientist in the Mine Design Department, H.M.S. *Vernon*, Portsmouth, a research post under the (then) Director of Scientific Research, Admiralty. He remained in this post until 1937 when he retired on reaching the age limit. Much of his work for the Admiralty remained unpublished, on grounds of secrecy. His main interests however, centred around the application of magnetostriction to acoustics and magnetic measurements. He was the author of numerous original papers on these subjects. The principle of his 'A-E' magnetometer, employing the change of electrical impedance of a mumetal wire in longitudinal magnetic fields, was used extensively in degaussing ranges during the war to measure the magnetic condition of ships.

On retiring from Admiralty service in 1937 he joined the research staff of Henry Hughes & Sons who at that time were concerned with the Admiralty magnetostriction echo depth sounder. Harrison's fundamental knowledge of magnetostriction helped considerably in the development of this device.

His pleasant personality and his persistence in the face of great difficulties will be remembered by his colleagues in the Admiralty.

Dr. Harrison is survived by his wife and one son. Another son, Robin, was lost in a 'Sunderland' seaplane which failed to return to its base in the early days of the war.

A. B. WOOD.

### RICHARD ALBERT HULL

THE death of Dr. R. A. Hull, who was killed in a climbing accident on Mont Blanc on 22nd August 1949, robs Oxford of a distinguished experimental physicist and an outstanding successful college tutor. His friends will remember him as a man of plain-spoken sincerity and steadfast loyalty.

Richard Albert Hull was born on 27th March 1911 at Church Gresley, Derbyshire, and was educated at Ashby de la Zouch Grammar School. He entered Oxford in 1929 as an Exhibitioner of St. John's College, and read mathematics and physics, taking a first class in physics in the Final Examination in 1932. His first research was an experimental study of the photoelectric properties of transparent thin films of caesium and rubidium. The work was an exacting test of Hull's experimental skill, which was recognized when he was elected a Senior Scholar of Christ Church in 1934. He did not however find it an altogether satisfying field of work, and by the time he submitted his thesis for the degree of D.Phil. he had already turned to low temperature research. Hull took part in the investigation of the range of temperatures below  $1^{\circ}\text{K}$ . accessible by the new method of magnetic cooling. This was a field exactly suited to his temperament and gifts. Interested in experimental technique for its own sake, he enjoyed the exploration of the problems of adiabatic demagnetization, of temperature measurement, and of thermal insulation, which demanded solution before successful experiments could be made in the new field.

The conditions of work were often harassing and difficult. Experiments usually lasted from fifteen to twenty hours, and any accident or delay meant working throughout the night. Specific heat measurements in particular involved long hours of monotonous galvanometer reading. Hull was fortunate in a power of concentration which enabled him to keep command of an experiment in the most trying conditions. He worked himself hard, and the technique of work below  $1^{\circ}\text{K}$ . established in Oxford in 1939 owed much to his patient and ingenious experiments. He had published papers on the vapour pressure of liquid helium, on the attainment of low temperatures by evaporation of helium, and on magnetic effects in iron ammonium alum, one of the most important substances for the magnetic method. In addition, work had been completed on the properties of manganous ammonium sulphate, from which the absolute scale of temperature below  $1^{\circ}\text{K}$ . could be established by using this salt as a magnetic thermometer.

The war interrupted all this. Hull joined the research group formed at Oxford by the Admiralty to work on problems of radio waves of very short wavelengths, and began a study of millimetre waves. His outstanding contribution was the design and construction in 1941 of a velocity modulation oscillator for 9 mm. wavelength, which was used for investigations of propagation and reception of millimetre waves. This was probably the first continuous wave generator in the millimetre wave region.

Hull had been appointed a University Demonstrator and Lecturer in Physics in 1939, and as the war's demands increased he became more and more taken up with the teaching and training of physicists. He took a large part in the working at Oxford of the State Bursary scheme and the Hankey radio training scheme. In 1944 he spent a term as a visiting professor at Harvard, assisting in the U.S. Navy's radio training scheme there. In the same year he was elected a Fellow of Brasenose College. When undergraduates poured back to Oxford at the end of the war, Hull found himself the only science tutor in a large college, at least a quarter of whose undergraduates were reading science subjects. For a time he undertook the general care of all scientific studies in Brasenose, at the same time playing his part in the re-organization of the University physics department, where the number of students was treble the pre-war entry. In 1948 he became a member of the General Board of the Faculties, and soon became an accepted and vigorous representative of the science faculties. These activities made heavy inroads on the time he could give to research, but he returned to the field of work below  $1^{\circ}$  K. in which he had been engaged before the war, and at the time of his death was making experiments on the specific heat of liquid helium in this temperature range.

He was a rock of reliability in any matter entrusted to him. Any problem he took up, whether it was the troubles of a new pupil or the entrance requirements of the University, was considered long and deeply. When his mind was made up, he would speak it, even though it meant saying the difficult and unpopular thing. Something of this same deliberate quality was the secret of his success as a scientist and a teacher: never to accept a partial explanation and, when a satisfying answer was found, to reduce it to its clearest terms. He had many friends from a wide range of University life, from the hockey field, the Bach choir, and the Music Club, as well as those who enjoyed his company and quietly ironical humour in the closer society of common room. His nature however was perhaps too reserved for many to know him intimately. Accustomed to rely upon himself, he would seldom reveal his personal feelings or problems. Yet many brought their problems to him, and found him generous of time and trouble to help them.

He was an enthusiastic and very experienced mountaineer. Climbing was his passion; there can have been few vacations in the last ten years when he did not escape, at least for a short time, to the mountains. At the end of a hard term's work he would slip away to Scotland or Wales, or to the Alps, to return bronzed and refreshed, often with beautiful photographs of the rocks and mountains to delight his friends. He would persuade as many as he could to join him in the sport he loved, and was one of the leaders of this year's Alpine Club party to Switzerland. The climb on which he lost his life was to have been the last of the season—an ascent of Mont Blanc by the Brouillard ridge.

In 1937 Hull married Miss Judith Moore, like himself a research worker in the Clarendon Laboratory. She died in 1943. They leave one daughter.

A. H. C.

### C. N. H. LOCK

CHRISTOPHER NOEL HUNTER LOCK was born on 21st December 1894. He was a Scholar at Charterhouse School and in 1912 was awarded a Major Scholarship at Gonville and Caius College, Cambridge. He became a Wrangler in Part II of the Mathematical Tripos, with distinction in Schedule B, in 1917. He was awarded a Smith's Prize in 1919 for an Essay on External Ballistics and in the following year was elected a Fellow of Gonville and Caius College.

During the 1914–18 war, and for two years afterwards, Lock worked on problems of external ballistics at Whale Island, Portsmouth, and at the National Physical Laboratory, Teddington. The results of an elaborate series of experiments on projectiles undertaken, in collaboration with R. H. Fowler, E. G. Gallop and H. W. Richmond, during the course of this work are given in two classical papers on "The Aerodynamics of a Spinning Shell", published in *Phil. Trans. A*, Vols. 221 and 222. In 1921 he wrote, with R. H. Fowler, a paper on "The Origin of the Disturbances in the Initial Motion of a Shell" (*Proc. Camb. Phil. Soc.*, Vol. 20) and in 1922, also with R. H. Fowler, a paper on "Approximate Solutions of Linear Differential Equations" (*Proc. Lond. Math. Soc.*, Vol. 20).

In 1920 Lock was appointed to the staff of the Aerodynamics Division at the National Physical Laboratory. For about two years he worked on general aerodynamic problems such as the cushioning effect of the ground on aircraft performance and the lateral control

of aircraft, and then began his well-known work on airscrew problems, a subject on which he became an outstanding authority. He carried out both theoretical and experimental researches which contributed much to the development of modern airscrew theory and design. His researches, most of them described in reports published by the Aeronautical Research Committee, cover a wide field and include experiments with a family of airscrews, interference between airscrews and bodies, experimental verification of the independence of the elements of an airscrew blade, a consideration of the accuracy of the vortex theory of an airscrew, an application of Goldstein's theory to airscrew design, the flow around an airscrew in the vortex-ring state, and a graphical method for the calculation of airscrew performance. He also made wind-tunnel experiments on a model autogyro and contributed to the development of autogyro theory.

From 1939 until his death Lock organized and supervised the work undertaken in the High Speed Laboratory of the Aerodynamics Division. He played a prominent part in the design of the high-speed wind tunnels and in the development of the apparatus needed for experimental research, and his wide knowledge of the theory of compressible fluid flow was put to good use in the solution of difficult research problems. He took a very active part in all the work undertaken in the High Speed Laboratory and gave unstinted help to all his colleagues. His individual investigations include development of the pitot-traverse method for the determination of profile drag at high speeds, estimation of tunnel-wall interference at compressibility speeds, calculation of the ideal drag due to a shock wave, and a consideration of the effect of sweepback on the performance of an aerofoil at high Mach numbers.

Lock was a Fellow of the Royal Aeronautical Society and a Fellow of the Physical Society. He was a member of the Power Plant Committee, the Helicopter Committee, the Fluid Motion Sub-Committee and the Engine Aerodynamics Sub-Committee of the Aeronautical Research Council. He gave two lectures to the Royal Aeronautical Society, the first on "Airscrew-Body Interference" in 1929, and the second on "Problems of High-Speed Flight as affected by Compressibility" in 1937.

Lock died on 27th March, 1949, after a short illness. He suffered for many years from asthma and the after-effects of infantile paralysis, but he bore these bodily disabilities with great fortitude.

He married Lilian Mary Gillman in 1924 and his two sons, Robert Christopher and John Michael, are research students at Gonville and Caius College.

A. FAGE.

### WILLIAM BLAIR MORTON

PROFESSOR W. B. MORTON, who died in his native city of Belfast on August 12th at the age of 81, was one of the many physicists of his generation whose formal training had been principally in mathematics. He attended Queen's College, Belfast—then part of the Royal University of Ireland—from 1886 to 1889, reading mathematics under John Purser, and natural philosophy under J. D. Everett, and St. John's College, Cambridge, from 1889 to 1892, when he was eighth wrangler. He was profoundly impressed by Purser's methods of teaching, and strove in later years with conspicuous success to make his own lectures clear and interesting. Morton followed Everett in the chair of natural philosophy at Belfast in 1897 after being his assistant from 1892. He retained the chair until he was retired in 1933 on reaching the age limit. On appointment, one of his first acts was to increase the number of lectures given to undergraduates. Shortly afterwards, with the help of J. Wylie, he extended the laboratory classes. A weekly physical colloquium was started in 1904, after a visit to Germany. The conversion of Queen's College in 1909 into the independent Queen's University of Belfast brought no immediate change beyond the alteration of his title to Professor of Physics, but funds became available in 1911 for the erection of a new physics laboratory. This was designed by Wylie, and completed in 1914. Morton had to meet considerable criticism of its size, which was then considered excessive by some colleagues, and for various periods part of the basement was surrendered to the University's works and engineering departments, and part of the tower to chemistry. Good provision was made in the building for experimental research, although Morton himself took little part in it, preferring to devote such time as he had free from lectures to original theoretical work, and the history of mathematics and physics. Similarly, whilst he was very interested in the undergraduate laboratories, the detailed running of these was

left to Wylie. Although he was author or joint author of a considerable number of papers, he refrained from publishing much which might well have gone into print, preferring to talk about it in colloquium or postgraduate lectures. The present writer and others who were in Belfast in the late 1920's have much reason to be grateful to him for his expositions of quantum theory, which he recognized as being largely a transcription into a new context of the classical work of Rayleigh with which he was intimately acquainted.

Morton was a Fellow of the Royal University of Ireland from 1897 until its dissolution in 1909, a Member and for a time Vice-President of the Royal Irish Academy, and a Founder Fellow of the Institute of Physics. After his retirement, Queen's University conferred the degree of Doctor of Science on him, and he was made a member of Senate, its supreme governing body. He did not, however, seek for honours or public recognition, and was probably most happy in his work when he was in his department with his staff and students. To those who had the privilege of collaborating with him in any capacity his death has been a personal loss.

K. G. E.

### ALAN FARADAY CAMPBELL POLLARD

THE death, on 15th August 1948, of Professor Alan Faraday Campbell Pollard deprived the world of science of one of the few who behold with increasing disquiet the spectacle of a community which spends money lavishly on research and the building up of knowledge, but gives little thought as to the ways in which this knowledge can be made accessible. Some of his favourite examples included the neglect, for 35 years, of the work of Mendel; the patent (1876) of Penaud and Gauchot which described many of the features of the modern aeroplane 27 years before the work of the Wright brothers; and the 81 years between the discovery of 'Herapathite' and the perfection of Polaroid by E. H. Land. Pollard was an enthusiastic advocate of the Universal Decimal Classification and was the first President of the British Society for International Bibliography. For many years he kept up to date a U.D.C. catalogue of the *Proceedings of the Physical Society*. He served on the Council of the Physical Society from 1933-37.

Born in 1878, the son of Lieut.-Colonel B. H. Pollard of the Indian Staff Corps, he studied engineering at University College, London, and was for some time assistant to Professor Karl Pearson, who had a great influence in strengthening his passion for clarity and precision, and who gave him a bent towards the scientific study of instruments. After a period with Nobels Explosives Ltd. and war service (1914-18) with the Royal Scots Fusiliers, the R.A.F., and the Ministry of Munitions, he was appointed Professor of Instrument Design in the Technical Optics Department at the Imperial College and held the last-named post until his retirement from the College in 1943. He continued, however, to work as consultant and scientific adviser to various industrial undertakings until the time of his death.

He was very critical of the usual industrial approach to the design of scientific instruments and based his own ideas on the kinematical theories of Clerk Maxwell, which (used in original ways) led him to ingenious designs of various instruments such as interchangeable nosepieces for microscope objectives and other things. He inspired many students with something of his own enthusiasm, and explained some of his ideas in a small book, *The Kinematical Design of Couplings in Instrument Mechanism*, published by Messrs. Adam Hilger Ltd.

Many will regret that the Chair of Instrument Design has not been filled since his death. The design of instruments as a specific field of study has seemed to some inadmissible, the brewer preferring to design his colorimeter and the surveyor his theodolite. Yet if really adequate instruments are to be made there are fundamental principles of mechanical and optical design the neglect of which makes for failure instead of success. At a time when the scientific instrument industry of this country is making efforts to hold its own against strenuous foreign competition, our instrument industry may yet regret that Pollard's missionary efforts in respect of instrument design have not been followed up.

He was a friendly and helpful colleague; though he deplored the unsystematic and happy-go-lucky methods of some of us, he was always ready to listen and do his best to help. He married Gabrielle, daughter of Mr. Frederick Urwick, in 1915, and had a son and a daughter.

L. C. MARTIN.

## WILLIAM GEORGE PYE

WILLIAM G. PYE, born on 27th October 1869, at Battersea, died at Bexhill on 13th October 1949. He was a son of William Thomas Pye, an expert maker of mechanical models. About 1878, A. G. Dew-Smith began making physiological instruments in Cambridge. In January 1881 Horace Darwin joined him as partner, to form the Cambridge Scientific Instrument Co. In December 1880 they offered W. T. Pye the post of foreman in a workshop they were to start on 1st January 1881. After a trial he was, in 1882, fully established as foreman. In 1895 the Directors of the then newly incorporated company made him Secretary: he had been Manager for some years. The company moved to St. Tibb's Row in 1881. When W. T. Pye came to Cambridge, from Battersea, his son attended the Higher Grade School. Then for a short time he taught at the Chesterton Church School and later did instrument work under his father. When W. T. Pye left, about December 1898, Mr. R. S. Whipple succeeded him as Secretary.

About 1886, W. G. Pye, now a trained youth, went to Elliott Bros., London. In 1892 the post of mechanic at the Cavendish Laboratory became vacant. At the opening of W. G. Pye's works at Chesterton (see below), Sir J. J. Thomson said:—

"It was Mr. Dew-Smith who spoke to him about Mr. W. G. Pye, when they were seeking a new head of the workshop; he had every reason to be grateful for his advice to get Mr. Pye, if he could. He did get him, and they in the Cavendish Laboratory owed a great deal to him. He immensely improved the workshops and made a great many exceedingly effective instruments, and not the least he did was to train his successor, Mr. F. J. Lincoln. Mr. Pye, in addition to his great skill as a workman, possessed the qualities of great energy and business capacity, and so he encouraged him to start as an instrument maker."

I began to teach at the 'Cav. Lab.' in 1888. As a boy I did a lot of mechanical work. I naturally appreciated Pye's 'new broom' and cordially echo the words of 'J. J.' There was leeway to make up. Maxwell made no provision for a workshop; he discovered his mistake and made a small beginning. When Pye came, in September 1891, the equipment was still meagre.

By 1892 the number of students had grown and class apparatus was needed. Pye made many things for the Medical Students—all very simple. Great additions for my own Class and for the Advanced Class were made by him or, under his direction, by Lincoln, who started as a 'lab. boy' in 1891. With his first-rate mechanical knowledge, instinct for good design, handiness and skill of hand, Pye was very helpful. Research was developing and he made much of what the researchers could not 'pinch' from the Practical Classes or make of 'sealing wax and string'.

Many research students, on leaving the Laboratory, wanted apparatus like that used there. To meet this demand, W. G. Pye, about 1895, set up a small workshop in St. Andrew's Street, with his brother, Frederick W. Pye, as foreman. On leaving the 'Cav. Lab.', in 1902, he equipped a workshop in a granary of a disused water-mill. He prospered and, in 1913, built works at Chesterton. In 1921 these works, which had grown, were attacked by the 'Radio Beetle' and a rapid expansion followed. In 1927 the works and the radio business were bought by a company, under the name of Pye Radio Ltd., now Pye Ltd.

Pye and his younger son, H. J. Pye, then built the "Granta" works in Newmarket Road. Here the manufacture of electrical and mechanical apparatus for Practical Classes was continued by W. G. Pye & Co. Ltd. Mr. W. G. Pye soon became a 'sleeping partner'; the business was then run by H. J. Pye. In 1930 W. G. Pye left Cambridge and later went to Bexhill. There he took a leading part in the "Senlac Metal Casements Co." till early in 1949. In 1946 W. G. Pye & Co. Ltd. was amalgamated with Pye Ltd.\*

Many things devised for my Class were put on the market, often in improved forms, by Pye, and had a wide distribution and appeared in textbooks. The Conductivity of Copper apparatus stimulated a girl to write: "Conductivity for Heat, discovered by Dr. Searle". When we were settling a design, a flashing suggestion from Pye sometimes altered the whole plan. I knew the destructive ways of students and demonstrators and Pye loathed things which 'came ungummed'. Sturdy and reliable apparatus was the result.

It is on record that I was pleased when, in 1911, I saw six sets of apparatus for the Mechanical Equivalent of Heat at Harvard University.

\* Up to this point some of the dates given above may be only approximate.

From 1892 I had the friendship of W. G. Pye, and later of his son. We used to seek each other's help. They showed me much kindness in my work in Physics.

Sir J. E. Townsend, F.R.S., who began research in 1895, testifies :—

"I am sure that the Research Students who worked in the Cavendish when Pye was head instrument maker feel that they are much indebted to him. I certainly appreciated very much the assistance he was to me. The cheerful way he undertook to make apparatus of various designs contributed substantially to the success of the research work."

C. T. R. Wilson, F.R.S., writes :—

"I just remember him as being always most kind and helpful in his difficult task of supplying one's requirements from the Laboratory workshop."

In 1910 Pye went for his health to Torquay. With my wife and me he paid two or three visits to Oliver Heaviside.

I could not be at the opening of the Chesterton works in 1913. I wrote to Pye :—

"You have the happy power of making a feeling of sunshine around you. This will go far to secure in the future, as it has done in the past, the loyal and enthusiastic co-operation of all those who help you in any way."

In July 1892 he married Miss Annie E. Atkins, who survives him. The surviving children are: (1) Donald Walter, of New College, Oxford, now Senior Master at Llandovery College, (2) Marjorie Irene, and (3) Harold John, of St. John's College, Cambridge, who attended my Practical Class.

G. F. C. SEARLE.

### MAX PLANCK \*

UNDOUBTEDLY Planck, who died at Göttingen on 4th October 1947, was one of the greatest of all those who ever turned their minds to scientific inquiry. His achievements place him among the three or four most outstanding men of science of this or any other time and, quite apart from his greatness as a contributor to our knowledge and comprehension of physical phenomena, he was a man of perfect integrity and great nobility of character, the like of whom rarely appears on our horizon.

Max Karl Ernst Ludwig Planck was born on the 23rd April 1858 at Kiel, where his father was a professor in the faculty of law. He was taken in his early years to Munich and was a pupil at the Maximilian Gymnasium for four years. In his recently published *Wissenschaftliche Selbstbiographie* † he remembers with affectionate appreciation a mathematical teacher there: one Hermann Müller, who was evidently a strong contributory influence in inclining him to take up the study of physics.

With the *abitur* of the Gymnasium Planck entered the University of Munich at the age of seventeen, where he studied under von Jolly, Ludwig Seidel and Gustav Bauer. After the manner of the German student, who was wont to migrate from one university to another, Planck spent a year at Berlin attending the lectures of Hermann von Helmholtz and Gustav Kirchhoff. He was promoted Doctor of Philosophy (*summa cum laude*) at Munich in 1879, his dissertation being entitled *Ueber den zweiten Hauptsatz der mechanischen Wärmetheorie*. Thereafter he became *Dozent*, the subject of his *Habilitationsschrift* being *Gleichgewichtszustände isotroper Körper in verschiedenen Temperaturen*. In 1885 he was called to the university of his native town, Kiel, as Professor *Extraordinarius*, having in the meantime completed the now well-known essay on the Principle of Conservation of Energy, which he submitted for the prize offered by the Göttingen Philosophical Faculty. Planck was adjudged second and one has a suspicion that the Faculty of that day were perhaps hardly capable of appreciating his essay at its full value.

In the spring of 1889 he was called to Berlin (as *extraordinarius*) to succeed Kirchhoff, on the recommendation, or initiative, of Helmholtz. He became Professor *Ordinarius* in 1892 and filled the office of Rector during the Semester of 1913–1914. His inaugural address was entitled *Neue Bahnen der physikalischen Erkenntnis*. In 1926 he retired and was succeeded by Erwin Schroedinger. He was awarded the Nobel Prize in 1918, taking as the subject of his address to the Royal Swedish Academy (on the 2nd June 1920) The

\* This was received soon after the December 1948 issue of the *Proceedings* had gone to press.

† I am indebted to Professor Flint for providing me with a copy of this.



Origin and Development of the Quantum Theory. The Royal Society elected him a Foreign Member in 1926 and awarded him its Copley Medal in 1929. In 1930 he became President of the Kaiser Wilhelm Society. He also served for many years as one of the secretaries of the Prussian Academy, to which he was elected soon after the death of Hertz in 1894.

Planck's most important work was his investigation of the nature of black body (cavity) radiation, which led to the solution of the problem of the distribution of energy in the so-called normal spectrum and, as is well known, to the discovery of the quantum of action,  $h$ , and the quantum theory. Before his attention was directed to the radiation problem, he spent many years in the study of thermodynamics and in securing its foundations. No doubt this long thermodynamical training enabled him to appreciate better than anybody else, the nature of the formidable problem which he eventually solved.

His early work on thermodynamics evoked little response. Apparently it was not even read by Helmholtz, Kirchhoff or Clausius. This is perhaps not so surprising, when we reflect that thermodynamics must have impressed them as a finished product in which only trivial modifications could be contemplated. Indeed it still retains substantially the form which Clausius gave to it. It is perhaps easier to forgive this great triumvirate than later specialists in thermal science for their neglect of Planck. His attitude to thermodynamical principles was different from that of all his predecessors. He was not hypnotized by the literal sense of the terms 'reversible' and 'irreversible'. He did not begin with reversibility at all, but by defining an irreversible process, which for him was a process which could not *in any way whatsoever* be completely undone (*rückgängig gemacht*). Any other processes were defined to be reversible. He seems to have been led to this attitude by studying the axiom of Clausius that heat cannot of itself pass from a colder to a warmer body. Notwithstanding Planck's criticisms this axiom is still used, quite uncritically, in quite recent textbooks.

Beyond doubt Planck succeeded in giving the second law a sound foundation, and his work, as set forth in his great book *Thermodynamik*, is rigorous; but there are alternatives to his approach, or at least one. One finds some indication of this in an unknown work by Carl Neumann (1875); but Neumann and Planck seem to have been unable to understand one another. They seem to me to be both equally sound.

In approaching the problem of the distribution of energy in the normal spectrum Planck made use of the fact, pointed out by Kirchhoff, that the character of the radiation within a vacuous enclosure, in temperature equilibrium, is independent of the nature of the emitting and absorbing material constituting the enclosing wall. He realized that this fact entitled him—in investigating the character of the radiation under temperature equilibrium—to assume *any sort* of emitting or absorbing systems he liked and so he assumed what seemed to him the simplest thing, namely the Hertzian oscillator. He had for his guidance the two formulae obtained by W. Wien (1896); in particular the exponential one which Lummer and Pringsheim had shown to fit the observations in the region of very short wavelengths. Probably at that time Rayleigh had not yet developed his formula; but its experimental equivalent had emerged from the work of Rubens and Kurlbaum in the region of very long waves—the residual radiation from rocksalt, fluorspar etc. Planck's preoccupation with thermodynamical studies, as he himself has indicated, made it natural that he should study the relation between the entropy of an oscillator and its energy. Wien's formula gives for  $U$ , the mean energy of an oscillator in temperature equilibrium,

$$U = ae^{-b/T},$$

$a$  and  $b$  being constants. Now remembering that  $dU/dS = T$ , it easily follows that

$$1 \left/ \frac{d^2S}{dU^2} \right. = -bU,$$

$S$  and  $T$  meaning entropy and temperature respectively. On the other hand the results of Rubens and Kurlbaum suggested  $U = cT$ , where  $c$  is a constant. This in effect is Rayleigh's formula. Consequently

$$\left/ \frac{d^2S}{dU^2} \right. = -\frac{U^2}{c}.$$

Naturally Planck tried the experiment of combining these two in the following simple way :

$$\frac{d^2S}{dU^2} = -bU - \frac{U^2}{c},$$

the solution of which yields

$$U = bc/(e^{-b/T} - 1),$$

which is virtually Planck's final formula; but the problem of deducing it from fundamental principles still remained. In order to make progress in this direction Planck turned to Boltzmann's H theorem and its implication of a functional relationship between the entropy of an assemblage and the probability of its state. He was thus led to equate the entropy of an assemblage to the product of a universal constant and the logarithm of what he called the thermodynamical probability. This universal constant, which he represented by  $k$ , is usually called Boltzmann's constant; but was in fact first introduced by Planck. Indeed as Planck has said, his theory is distinguished from that of Boltzmann precisely by the assumption or premiss that a definite finite number,  $k$ , actually exists, with the property that its product with the logarithm of the thermodynamical probability is equal to the entropy.

The rest is very simply told. In any case, whether a departure from classical principles were contemplated or not—and probably Planck did not have this in mind at first—it was necessary to divide the extension in phase of the oscillators—each assumed to have one degree of freedom—into elements with the dimensions *energy × time*. The classical procedure necessarily involves that these elements approach the limit zero. Planck realized however that this gave the oscillators the average energy  $U = cT$ , which could only fit the observations in the region of very long waves. Thus he was forced to endow each element of the phase space with a precise numerical value, *different from zero*. He represented this element by the symbol,  $h$ , and called it the *elementary quantum of action*. It was a consequence of this that the energy of each oscillator took the form

$$\text{Integer} \times h\nu,$$

or, in his later and slightly modified theory—in which he assumed that *energy emission only* was discontinuous—

$$(\text{Integer} - \frac{1}{2}) \times h\nu.$$

Just as the constant  $k$  was suggested to Planck by Boltzmann's theory, so the much earlier work of Sir William Hamilton might have suggested the constant  $h$ . It appears later, in wave mechanics, not only as the quotient of energy by frequency, but also as the quotient of momentum by wave number. Indeed the study of Hamilton's analogy between geometrical optics and classical mechanics might well have suggested a more general mechanics analogous to optics or wave propagation in the widest sense.

Planck communicated his theory to the German Physical Society and it was published in their *Proceedings* and in the *Annalen der Physik* at the very close of the century. Anyone who can remember the state of physical science in 1900 and the outlook of physicists at that time will appreciate that Planck's theory of radiation was at first regarded as very eccentric if not quite mad; but when one re-reads it one realizes that it is an almost inevitable consequence of the actual facts of black-body radiation already known. A very strong impression was made by Planck's computation of Loschmidt's (or Avogadro's) number and consequently of the elementary ionic charge, which he found to be  $4.6 \times 910^{-10}$  E.S.U. Rutherford and Geiger found  $4.65 \times 10^{-10}$  E.S.U. a year or two later by counting alpha particles and estimating their total charge. Planck's result is remarkably close to  $4.803 \times 10^{-10}$  E.S.U., which I think is the present estimate. He computed  $h$  to be  $6.55 \times 10^{-27}$  ergs  $\times$  sec., a value which has not been appreciably modified since, and  $k$  he found to be  $1.34 \times 10^{-16}$  ergs per  $^\circ\text{K.}$ , now estimated to be  $1.372 \times 10^{-16}$  ergs per  $^\circ\text{K.}$  Many important consequences soon followed from Planck's theory of *Quanten-emission* even before a coherent quantum mechanical theory was built up: Einstein's photoelectric theory; the dependence of specific heats on temperature, especially Debye's brilliant treatment of the atomic heats of solid elements; Bohr's theory of the hydrogen atom and of the extra-nuclear structure of atoms and the theory of spectra; the contributions of Sommerfeld, Epstein, Kramers and others and then the triumph of quantum mechanics (L. de Broglie, E. Schroedinger, W. Heisenberg, M. Born and P. Dirac).

Planck was twice married and is survived by his second wife (Margaret, née von Hoesslin) and a son. Until the outbreak of the first world war he might indeed have been described as a happy and fortunate man, particularly fortunate in his teachers, in his academic career and in making one of the greatest of all scientific discoveries. But then calamities came. His eldest son, Karl, fell before Verdun in 1916 and he lost his twin daughters. In the last war his house in the Grunewald quarter of Berlin was destroyed in an air raid and his fine library lost. He happened to be in Cassel when that town was destroyed and was buried for hours in an air-raid shelter. After the attempt on Hitler's life, on 20th July 1944, his son Erwin was arrested, condemned and executed on 23rd Jan. 1945, solely on the ground, apparently, that some of those involved belonged to his circle of acquaintances.

Planck was found in May 1945 by the Americans at Rogätz on the Elbe and conveyed by them to Göttingen where he remained till his death and where his remains now lie.

Many Fellows of the Physical Society will remember his Guthrie lecture in 1932 and his profoundly interesting and illuminating discussion of causality. He had been elected an Honorary Fellow of the Physical Society in 1924. In 1936 he attended, as a guest, the centenary celebrations of the University of London, and it was on this occasion, I believe, that the University conferred on him the degree of Doctor of Science *honoris causa*. He obviously much enjoyed his visits to St. Paul's Cathedral and to the Guildhall and the dinner in his honour at the Waldorf Hotel.

His last visit to England was in 1946, little more than a year before his death, to attend the Royal Society's Newton celebrations. He was no longer the erect and vigorous man that many of us remember; but he retained his mental clarity and alertness.

Planck was an enthusiastic musician and a fine pianist. He was also a great mountaineer and continued to make strenuous ascents of 3000 metres or more after reaching 70 years of age. I have it on the authority of Professor Sommerfeld that Planck made personal representations to Hitler on behalf of persecuted Jewish scientists. He was of course 'schroff zurückgewiesen'.

I remember him as a modest, kindly man, who, in the words of one of the greatest of his countrymen,

**weit entfernt von allem Schein,  
Nur in der Wesen Tiefe trachtet.**

WM. WILSON.

## WILLIAM NELSON STOCKER

THE name of W. N. Stocker, who died on 2nd August 1949 at Oxford, in his 99th year, will probably sound unfamiliar to most readers of the *Proceedings of the Physical Society*. Even in, Oxford where he taught physics on and off for over forty years, his name is better known to those interested in original 'Oxford characters' than to the physicists. And yet Stocker, who was born in the year Kelvin formulated the Second Law of Thermodynamics, who took Finals in the year Maxwell published his *Treatise*, and who, in his own words, 'lost the habit of work' in the year Einstein announced the Special Theory of Relativity, was for the last ten years or so the *doyen* of British physicists.

William Nelson Stocker was born on 29th January 1851 at Horsforth, near Leeds, the son of the Rev. William Henry Browell Stocker. After education at Stony Stratford School he matriculated at Oxford in 1869 with the intention of reading classics and taking Holy Orders. His interest in science soon caused him to change his plans, and in 1870 he started studying mathematics and physics, gaining a First in Mathematical Moderations in 1872 and two Firsts in the Final Honour Schools of Mathematics (1873) and Natural Science (1874). It was presumably for lack of sufficient money that he had started as a non-collegiate student and remained one until 1873, when he gained an Exhibition at Christ Church, and his first five years in Oxford must have been a period of hard work, modest living and recreations chosen with an eye on a tight budget. Little is known about these years, but from the detailed entries of his account book covering the years 1869-1878 one pictures young Stocker as an undergraduate who, within his modest means, enjoyed the amenities that Oxford could offer. Boating and skating alternated with long walks in Oxford and its neighbourhood, books and music were bought for study and for leisure; then there were public concerts (the Hallé Society's concerts seem to have been regular features in those



*Dr. Max Planck.*



WILLIAM NELSON STOCKER

days) and the private enjoyment of playing the piano and the organ. We also learn from this account book that the cost of his fifteen terms at Oxford, including University expenses, board and lodging, books, etc. was just under £400, a very modest sum even for those days.

He took his degree in 1874, and in the same year accepted a demonstratorship at the then new Clarendon Laboratory under Professor R. B. Clifton in preference to becoming a science master in Cheltenham. In 1877 he was elected to a Fellowship at Brasenose for life, and his death marks the disappearance of the last of these Oxford life-Fellows. In the same year he became a Fellow of the Physical Society and, having held this Fellowship for 72 years, established a record which will be very hard indeed to break. His generous contribution to the Physical Society's Holweck Fund, one of his many donations to deserving causes, will be gratefully remembered. He was one of the first members of the Oxford University Mathematical and Physical Society, founded in 1888, and although there is no record of his ever reading a paper to that Society he took a lively interest in its functions, and he was genuinely disappointed when, in November 1948, failing health prevented him from attending the dinner commemorating the Society's 300th Meeting. Stocker was a conscientious if not inspiring teacher. He was more interested in experiment than in theory, and many generations of undergraduates who passed through his hands in the Clarendon Laboratory learned from him how to carry out physical experiments carefully, honestly and accurately.

In 1883, at the age of 32, Stocker was appointed Professor of Physics at the Royal Indian Civil Engineering College at Cooper's Hill, near Egham, Surrey. He held this post for the next 18 years till 1901 and delivered regular courses of lectures on heat, electricity and magnetism, light, etc. He used to visit Oxford for occasional week-ends during these years, keeping up his old connections with Brasenose, so that when in 1901, at the age of 50, he retired from Cooper's Hill and returned to Brasenose it was like coming home. He continued to do some teaching for the College and demonstrating in the Clarendon Laboratory, but these activities were on a diminishing scale, and came to an end soon after the 1914-18 war. One important event during this period was his "around the world trip", as he called it. He went to Australia via the Indian Ocean in the summer of 1914 to attend the British Association Meeting there and returned via Canada, arriving back in England in October.

Little can be said about the last 30 years of Stocker's life, especially about his scientific pursuits. He was never much interested in new developments in physics and with 'Einstein and all that' he did not even attempt to cope. He did, however, like to hear gossip about what was going on in the laboratories and about the doings of some of the old guard whom he still knew. A few years before his death he was shown round the new Clarendon Laboratory by the late Dr. R. A. Hull, his third successor as Physics Tutor at Brasenose. He seemed to have been impressed by what he saw in the new laboratory, but perhaps even more by the sight of the old Clarendon being partly pulled down and rebuilt. It must have given Stocker some satisfaction to see that he survived not only all his human contemporaries but even the Laboratory which he knew when it was first built.

If it is difficult to give an account of Stocker's life—partly because it was so uneventful—it is even more difficult to describe his personality without the fear of doing him an injustice. What we know about him is bound to be superficial; he had very few intimate friends—most of whom have been dead for a long time—and even to them he was never communicative. This does not mean he did not like company; in fact among his greatest pleasures were the long, friendly evenings in Brasenose Senior Common Room, and he had little patience with some of the younger generation who would 'use the place as a restaurant' and go off after dinner to meetings or lectures or—*horribile dictu*—to the laboratory to continue experiments.

To those who met Stocker in the last one or two decades the mere fact of talking to a man really belonging to quite a different age was a thrilling experience. Stocker himself was rather proud of his old age and of his reminiscences going back well over 90 years. He could remember Tsar Nicholas I being burnt in effigy at Horsforth during the Crimean War; one of his 'earlier' recollections was of Queen Victoria and the Prince Consort driving in state to the opening of the new Guildhall of Leeds, and he would delight in mentioning that his uncle, Dr. C. W. Stocker, Fellow of St. John's, had examined Gladstone in 1831. It is no wonder that after hearing such reminiscences one almost believed Stocker's classic

remark about lectures on electricity : " In my days you took a piece of sealing wax, rubbed it against your sleeve, picked up a piece of paper with it, and there was your course of electricity ".

By no means a brilliant conversationalist, Stocker had the gift of a dry, biting humour which enabled him to drive home a point with a minimum outlay of words and, very often, the maximum embarrassment to the unfortunate victim. Among the many stories told about him the following quite authentic one may be given as an example. It so happened that on VJ Day in 1945 a party of only four was dining in Common Room; Stocker, two people he very much disliked, and a fourth person who, the last to arrive, greeted Stocker with the remark, " A small but select gathering for this memorable day ! " After a brief pause came Stocker's grunting reply, " Yes . . . humph . . . small." In spite of this mordant wit he had an air of measured old-world courtesy, and many a young guest in the Common Room must have felt surprised and flattered at being addressed as " Sir " by an old gentleman more than 70 years his senior.

Stocker's great hobby—it was an integral part of his life—was walking. His regular daily walks at Oxford and Cooper's Hill were followed in the vacations by long walking tours during which he explored the countryside and observed the flora and geology of all parts of Britain. He always carried a pedometer and a barometer on him, and kept an exact record of the distances covered and the heights ascended. His endurance was fabulous. Even when he was over 70 he could average twenty miles a day over several weeks, and one can quite believe that in his life-time he all but covered the distance to the moon and did over a hundred ascents of Everest. These and similar data are contained in some seventy-five volumes of diaries which also present a faithful record of the weather from 1873–1949 with thermometric and barometric readings.

One might wonder why it was that Stocker, undoubtedly an able man with a capacity and a constitution for hard work and with a deep interest in nature, never made a name for himself in the world of physics. One should remember, however, that in 1874, when Stocker became a demonstrator, and for nearly 50 years afterwards, the Clarendon Laboratory was a place of teaching from which research was virtually banned. Whatever may have been Professor Clifton's merits as a teacher or as a collector of the choicest scientific instruments of his day, he certainly was not a man who could have inspired young Stocker to engage in research and to take up physics as his hobby. It is perhaps not idle to speculate whether, given a more inspiring scientific environment during his earlier years, Stocker might not have become the Grand Old Man of Oxford Physics. As it is, one thinks of him as an original and therefore typical old bachelor don of the Victorian era whose sayings, doings and habits, enriched and embellished by the passage of time, will probably be handed down as a legend to posterity.

N. KURTI.

## INDEX

	PAGE
Absorption of meson-producing nucleons . . . . .	374
Absorption spectrum of cosmic rays. . . . .	356
Air showers, extensive, momentum spectrum of the particles in . . . . .	364
Anisotropy, diamagnetic, and structure, of p-benzoquinodimethane . . . . .	505
Andrade, E. N. da C. : Lantern model to illustrate dislocations in crystal structure (Letter) . . . . .	394
Andrew, E. R. : Critical field measurements on superconducting tin foils . . . . .	88
Andrew, E. R. : Size-variation of resistivity for mercury and tin . . . . .	77
Application of the Peierls-McManus classical finite electron theory . . . . .	780
Arndt, U. W., <i>see</i> Hall, W. H.	
Band spectra, CN tail bands emitted by the carbon arc in air . . . . .	121
Band spectra, intensity distribution for bands of the $\gamma$ -system of $MgH^+$ . . . . .	237
Band spectra, Schumann-Runge $O_2$ bands emitted at atmospheric pressure . . . . .	114
Band spectra, ultra-violet bands of $Na_2$ . . . . .	124
Bands, emission, of sodium, theory of soft x-ray, . . . . .	806
de Barr, A. E. : A stereographic projector . . . . .	559
Barrow, R. F., <i>see</i> Eisler, B.	
Basis of electron theory of metals, with special reference to transition of metals . . . . .	416
Bauer, E. : A theory of ultrasonic absorption in unassociated liquids . . . . .	141
Beghian, L. E., and Halban, H. H. : Electron collection in high pressure methane ionization chambers (Letter) . . . . .	395
Behrens, D. J. : The effect of holes in a reacting material on the passage of neutrons . . . . .	607
Bending vibrations of linear chain . . . . .	200
Bernal, J. D. : The physical basis of life . . . . .	537
Bernal, J. D. : The physical basis of life. Corrigendum . . . . .	746
Beta-particles, fast, scattering through large angles by nitrogen nuclei (Discussion) . . . . .	264
Beta-spectrum of $^{198}Au$ , origin of low-energy electron lines in (Letter) . . . . .	739
Betatron injection into synchrotrons. . . . .	617
Bilby, B. A., <i>see</i> Cottrell, A. H.	
Bishop, G. R., <i>see</i> Wilson, R.	
Bombardment of $^{10}B$ and $^{11}B$ by deuterons, neutrons emitted . . . . .	586
Booth, F. : On the radiation from transient light sources . . . . .	95
Bowen, E. J., Mikiewicz, E., and Smith, F. W. : Resonance transfer of electronic energy in organic crystals . . . . .	26
Bowers, R., and Mendelssohn, K. : Viscosity and superfluidity in liquid helium (Letter) . . . . .	394
Bright, R. J., Jackson, D. A., and Kuhn, H. : The resolving power and intensity relationships of the Fabry Perot interferometer with silvered reflecting surfaces . . . . .	225
Bunyan, D. E., Lundby, A., and Walker, D. : Experiments with the delayed coincidence method, including a search for short-lived nuclear isomers . . . . .	253
Bunyan, D. E., Lundby, A., and Walker, D. : Experiments with the delayed coincidence method, including a search for short-lived nuclear isomers. Corrigendum . . . . .	398
Campbell, N. R., and Hartshorn, L. : The experimental basis of electromagnetism—Part III : The magnetic field . . . . .	422
Champion, F. C., and Roy, R. R. : The scattering of fast $\beta$ -particles through large angles by nitrogen nuclei (Discussion) . . . . .	264
CN tail bands emitted by the carbon arc in air . . . . .	121
Collision problems and the theory of radiation damping . . . . .	2
Computation of wave functions in momentum space—I : The helium atom . . . . .	509
Computation of wave functions in momentum space—II : The hydrogen molecule ion . . . . .	519



	PAGE
Conductivity, electrical, of germanium . . . . .	284
Continuous $\gamma$ -emission in neutron-proton collisions . . . . .	19
Cooke, A. H. : The establishment of the absolute scale of temperature below $1^\circ \text{K}$ . . . . .	269
Cooke, A. H. : The establishment of the absolute scale of temperature below $1^\circ \text{K}$ . Corrigendum. . . . .	534
Corrigenda . . . . . 298, 398, 534, 600,	746
Cosmic rays at sea level, ratio of positive to negative particles . . . . .	601
Cosmic rays, absorption spectrum . . . . .	356
Cosmic rays, evidence for stellar origin . . . . .	491
Cosyns, M. G. E., Dilworth, C. C., Occhialini, G. P. S., Schoenberg, M., and Page, N. : The decay and capture of $\mu$ -mesons in photographic emulsions . . . . .	801
Cottrell, A. H., and Bilby, B. A. : Dislocation theory of yielding and strain ageing of iron . . . . .	49
Coulson, C. A., <i>see</i> McWeeny, R.	
Counter, Geiger-Müller, experiments with adjustable . . . . .	32
Counters, argon-alcohol, effect of external quenching on life . . . . .	369
Critical field measurements on superconducting tin foils . . . . .	88
Crystal dislocations, equations of motion . . . . .	131
Crystals, inert gas and ionic, surface energies . . . . .	167
Cut-off methods for the electron self-energy . . . . .	386
Daly, E. F., and Sutherland, G. B. B. M. : The performance of infra-red spectro- meters as limited by detector characteristics . . . . .	205
Damping in scattering and radiative reaction . . . . .	749
Damping theory and the propagation of radiation . . . . .	12
Decay and capture of $\mu$ -mesons in photographic emulsions . . . . .	801
Decay constant of radio sodium, $^{24}\text{Na}$ (Letter) . . . . .	457
Decay of $^{170}\text{Tm}$ and $^{186}\text{Re}$ . . . . .	573
Decay of $\tau$ -mesons . . . . .	697
Delayed coincidence method and search for short-lived nuclear isomers . . . . .	253
Dependence of the thermal diffusion factor on temperature . . . . .	655
Devons, S. : A note on the $^{10}\text{B}(n, \alpha)^7\text{Li}$ reaction . . . . .	580
Dielectric changes in phosphors containing more than one activator . . . . .	731
Dilworth, C. C., <i>see</i> Cosyns, M. G. E.	
Dingle, R. B. : The hydrodynamics of helium II . . . . .	648
Dingle, R. B. : Second sound and the behaviour of helium II . . . . .	154
Direct method of measuring nuclear spin-lattice relaxation times . . . . .	301
Directional correlation between successive internal-conversion electrons . . . . .	763
Disintegration of carbon by fast neutrons . . . . .	296
Disintegration of lithium by deuterons, neutrons emitted in . . . . .	407
Disintegration, the $^{10}\text{B}(n, \alpha)^7\text{Li}$ reaction . . . . .	580
Dislocation theory of yielding and strain ageing of iron . . . . .	49
Dislocations in crystal structure, lantern model to illustrate (Letter) . . . . .	394
Dislocations, sessile (Letter) . . . . .	202
Dislocations, uniformly moving . . . . .	307
Drain, L. E. : A direct method of measuring nuclear spin-lattice relaxation times . . . . .	301
Duperier, A. : The meson intensity at the surface of the earth and the temperature at the production level . . . . .	684
Effect of external quenching on the life of argon-alcohol counters . . . . .	369
Effect of holes in a reacting material on the passage of neutrons . . . . .	607
Eigenfunctions following from Sommerfeld's polynomial method . . . . .	736
Eisenschitz, R. : The steady non-uniform state for a liquid . . . . .	41
Eisler, B., and Barrow, R. F. : The ultra-violet absorption spectrum of $\text{SnO}$ (Letter) Electrical conductivity of germanium . . . . .	740
Electrical properties of nickel oxide, temperature variation . . . . .	284
Electron collection in high pressure methane ionization chambers (Letter) . . . . .	446
Electron self-energy, some cut-off methods . . . . .	395
	386

Electron theory of metals, transition of metals . . . . .	416
Electron theory, Peierls-McManus classical finite, applications . . . . .	780
Electron trap mechanism of luminescence in sulphide and silicate phosphors (Letter) . . . . .	317
Electronic energy, resonance transfer of, in organic crystals . . . . .	26
Electronic levels, excited, in conjugated molecules—III: Energy states of naphthalene . . . . .	710
Electrons ejected by polarized radiation (Letter) . . . . .	529
Electrons, successive internal-conversion, directional correlation between . . . . .	763
Elleman, A. J., and Wilman, H. : The structure and epitaxy of lead chloride deposits formed from lead sulphide and sodium chloride . . . . .	344
Elliot, H. : The effect of external quenching on the life of argon-alcohol counters . . . . .	369
Emission spectrum of sodium hydride . . . . .	191
Emissivity and reflectivity, theory (Letter) . . . . .	661
Epitaxy of lead chloride deposits, formed from PbS and NaCl . . . . .	344
Equations of motion of crystal dislocations . . . . .	131
Eshelby, J. D. : Uniformly moving dislocations . . . . .	307
Establishment of the absolute scale of temperature below 1° K. . . . .	269
Evans, M. G., de Heer, J., and Gergely, J. : Structure and diamagnetic anisotropy of p-benzoquinodimethane in connection with those of p-benzoquinone . . . . .	505
Evidence for the stellar origin of cosmic rays . . . . .	491
Ewles, J., and Farnell, G. C. : The luminescence of wetted solids . . . . .	216
Excited electronic levels in conjugated molecules—III : Energy states of naphthalene . . . . .	710
Experimental basis of electromagnetism—Part III : The magnetic field . . . . .	422
Experimental basis of electromagnetism—Part IV : Magnetic materials . . . . .	429
Experiments with an adjustable Geiger-Müller counter . . . . .	32
Experiments with delayed coincidence method, including search for short-lived nuclear isomers . . . . .	253
Farnell, G. C., <i>see</i> Ewles, J.	
Feast, M. W. : 'The CN tail bands emitted by the carbon arc in air . . . . .	121
Feast, M. W. : On the Schumann-Runge O <sub>2</sub> bands emitted at atmospheric pressure . . . . .	114
Fenton, A. G., and Fuller, E. W. : Further experiments with an adjustable Geiger- Müller counter . . . . .	32
Finch, G. I. : Steam in the ring discharge . . . . .	465
Flames at normal pressures, spectroscopic examination, a new technique . . . . .	722
Frank, F. C. : On the equations of motion of crystal dislocations . . . . .	131
Frank, F. C. : Sessile dislocations (Letter) . . . . .	202
Frank, F. C., <i>see also</i> van der Merwe, J. H.	
Fuchs, K. : Perturbation theory in neutron multiplication problems . . . . .	791
Fuller, E. W., <i>see</i> Fenton, A. G.	
Gamma-emission, continuous, in neutron-proton collisions . . . . .	19
Gardner, J. W. : Directional correlation between successive internal-conversion electrons . . . . .	763
Garlick, G. F. J., and Gibson, A. F. : Dielectric changes in phosphors containing more than one activator . . . . .	731
Garlick, G. F. J., and Mason, D. E. : The luminescence characteristics of tin acti- vated zinc sulphide phosphors . . . . .	817
Garlick, G. F. J., <i>see also</i> Johnson, J. S.	
Geiger counter spectrometer for the measurement of Debye-Scherrer line shapes . . . . .	631
George, E. P., and Jason, A. C. : Nuclear disintegrations in photographic plates exposed to cosmic rays under lead absorbers . . . . .	243
George, E. P., and Jason, A. C. : Nuclear disintegrations in photographic plates exposed to cosmic rays under lead absorbers. Corrigendum . . . . .	268
Gergely, J., <i>see</i> Evans, M. G.	
Gibson, A. F., <i>see</i> Garlick, G. F. J.	
Gibson, W. M. : The neutrons emitted in the bombardment of <sup>10</sup> B and <sup>11</sup> B by deuterons . . . . .	586
Gibson, W. M., <i>see also</i> Green, L. L.	
Goward, F. K. : Betatron injection into synchrotrons . . . . .	617

	PAGE
Goward, F. K., Titterton, E. W., and Wilkins, J. J. : The photo-disintegration of oxygen into four alpha-particles (Letter) . . . . .	460
Grant, P. J., and Richmond, R. : The decay of $^{170}\text{Tm}$ and $^{186}\text{Re}$ . . . . .	573
Green, L. L., and Gibson, W. M. : The disintegration of carbon by fast neutrons . . . . .	296
Green, L. L., and Gibson, W. M. : The neutrons emitted in the disintegration of lithium by deuterons . . . . .	407
Grew, K. E. : The dependence of the thermal diffusion factor on temperature . . . . .	655
Gurney, C. : Surface forces in liquids and solids . . . . .	639
Halban, H. H., <i>see</i> Beghian, L. E.	
Half-life of $^6\text{He}$ , measurement. . . . .	293
Half-lives of $^{141}\text{Ce}$ and $^{169}\text{Yb}$ . . . . .	799
Hall, W. H. : X-ray line broadening in metals (Letter) . . . . .	741
Hall, W. H., Arndt, U. W., and Smith, R. A. : A Geiger counter spectrometer for the measurement of Debye-Scherrer line shapes . . . . .	631
Hamilton, J. : Collision problems and the theory of radiation damping . . . . .	2
Hamilton, J. : Damping theory and the propagation of radiation . . . . .	12
Hamilton, J. : Radiative reaction and damping in scattering . . . . .	749
Hartshorn, L. : The experimental basis of electro-magnetism—Part IV : Magnetic materials . . . . .	429
Hartshorn, L., <i>see also</i> Campbell, N. R.	
de Heer, J., <i>see</i> Evans, M. G.	
Heitler, W., and Jánosy, L. : On the absorption of meson producing nucleons . . . . .	374
Heitler, W., and Jánosy, L. : On the size-frequency distribution of penetrating showers . . . . .	669
Helium, liquid, viscosity and superfluidity (Letter) . . . . .	392
Helium II, behaviour and second sound . . . . .	154
Helium II, hydrodynamics of . . . . .	648
Holmes, J. E. R. : Measurement of the half-life of $^6\text{He}$ . . . . .	293
Huang, K., and Wyllie, G. : On the surface free energy of certain metals . . . . .	180
Huby, R. : Investigations on the binding energy of heavy nuclei . . . . .	62
Hudson, R. P., Hunt, B., and Kurti, N. : The use of liquid helium in magnetic cooling experiments (Letter) . . . . .	392
Hunt, B., <i>see</i> Hudson, R. P.	
Hydrodynamics of helium II . . . . .	648
Hyperfine splitting in paramagnetic resonance . . . . .	664
Increased sensitivity of infra-red photoconductive receivers (Letter) . . . . .	456
Infra-red photoconductivity in layers of tellurium and arsenic (Letter) . . . . .	264
Ingram, D. J. E. : Hyperfine splitting in paramagnetic resonance . . . . .	664
Intensity distribution for bands of the $\gamma$ -system of $\text{MgH}^1$ . . . . .	237
Interferometer, Fabry Perot, the resolving power and intensity relationships . . . . .	225
Investigations on the binding energy of heavy nuclei . . . . .	62
Ionization chambers, high pressure methane, electron collection in (Letter) . . . . .	395
Irving, J. : Applications of the Peierls-McManus classical finite electron theory . . . . .	780
Jackson, D. A., <i>see</i> Bright, R. J.	
Jacobs, J. : Excited electronic levels in conjugated molecules—III : Energy states of naphthalene . . . . .	710
Jánosy, L., <i>see</i> Heitler, W.	
Jason, A. C., <i>see</i> George, E. P.	
Johnson, J. S., and Williams, F. E. : The electron trap mechanism of luminescence in sulphide and silicate phosphors (with reply by G. F. J. Garlick) . . . . .	317
Jones, T. K., Scott, R. A., and Sillars, R. W. : The structure and electrical properties of surfaces of semiconductors—Part I : Silicon carbide . . . . .	333
Kellermann, E. W., and Westerman, K. : On the absorption spectrum of cosmic rays . . . . .	356
Kellner, L. : Bending vibrations of a linear chain . . . . .	200

Krook, M. : Continuous $\gamma$ -emission in neutron-proton collisions. . . . .	19
Kuhn, H., <i>see</i> Bright, R. J.	
Kurti, N., <i>see</i> Hudson, R. P.	
 Landsberg, P. T. : A contribution to the theory of soft x-ray emission bands of sodium . . . . .	806
Lantern model to illustrate dislocations in crystal structure (Letter) . . . . .	394
Light sources, transient radiation from . . . . .	95
Liquid, steady non-uniform state . . . . .	41
Long, D. A., <i>see</i> Miller, C. H.	
Luminescence characteristics of tin activated zinc sulphide phosphors . . . . .	817
Luminescence, electron trap mechanism, in sulphide and silicate phosphors (Letter) . . . . .	317
Luminescence of wetted solids . . . . .	216
Lundby, A., <i>see</i> Bunyan, D. E.	
 McWeeny, R. : 'The computation of wave functions in momentum space—II : 'The hydrogen molecule . . . . .	519
McWeeny, R., and Coulson, C. A. : The computation of wave functions in momentum space—I : The helium atom . . . . .	509
Magnetic cooling experiments, use of liquid helium (Letter) . . . . .	392
Magnetic field—experimental basis of electromagnetism—Part III . . . . .	422
Magnetic materials—experimental basis of electromagnetism—Part IV . . . . .	429
Magnetic viscosity . . . . .	562
Magnetic viscosity in Mn-Zn ferrite . . . . .	743
Mason, D. E., <i>see</i> Garlick, G. F. J.	
Measurement of the half-life of $^6\text{He}$ . . . . .	293
Mendelssohn, K., <i>see</i> Bowers, R.	
van der Merwe, J. H., and Frank, F. C. : Misfitting monolayers (Letter) . . . . .	315
Meson intensity at the surface of the earth and the temperature at the production level . . . . .	684
Mesons, $\mu$ -, decay and capture, in photographic emulsions . . . . .	801
Mesons, slowing down of (Letter) . . . . .	136
Mesons, $\tau$ -, on the decay of . . . . .	697
Metallic films, thin, resistivity (Letter) . . . . .	135
Metals, electron theory of, transition of metals . . . . .	416
Metals, surface free energy . . . . .	180
Metals, $\alpha$ -ray line broadening in . . . . .	741
Mikiewicz, E., <i>see</i> Bowen, E. J.	
Miller, C. H., Long, D. A., Woodward, L. A., and Thompson, H. W. : A recording spectrometer for Raman spectroscopy . . . . .	401
Misfitting monolayers (Letter) . . . . .	315
Mitra, S. M., and Rosser, W. G. V. : Momentum spectrum of the particles in extensive air showers . . . . .	364
Momentum spectrum of the particles in extensive air showers . . . . .	364
Monolayers, misfitting (Letter) . . . . .	315
Moss, T. S. : Infra-red photoconductivity in layers of tellurium and arsenic (Letter) . . . . .	264
Mott, N. F. : The basis of the electron theory of metals, with special reference to the transition of metals . . . . .	416
Mott, N. F. : Note on the slowing down of mesons (Letter) . . . . .	136
 Neutrons emitted in the bombardment of $^{10}\text{B}$ and $^{11}\text{B}$ by deuterons . . . . .	586
Neutrons emitted in the disintegration of lithium by deuterons . . . . .	407
Neutrons, fast, disintegration of carbon . . . . .	296
Neutrons, passage, effect of holes in a reacting material . . . . .	607
New technique for the spectroscopic examination of flames at normal pressures . . . . .	722
Note on the $^{10}\text{B}(n, \alpha)^7\text{Li}$ reaction . . . . .	580
Nuclear disintegrations in photographic plates exposed to cosmic rays under lead absorbers . . . . .	243

	PAGE
Nuclear spin-lattice relaxation time, direct method of measuring . . . . .	301
Nuclei, heavy, investigation on binding energy . . . . .	62
Nucleons, meson-producing, absorption of . . . . .	374
Obituary Notices . . . . .	826
Occhialini, G. P. S., <i>see</i> Cosyns, M. G. E.	
Organic crystals, resonance transfer of electronic energy in . . . . .	26
Origin of low-energy electron lines in the $\beta$ -spectrum of $^{198}\text{Au}$ (Letter) . . . .	739
Owen, B. G., and Wilson, J. G. : On the ratio of positive to negative particles in the vertical cosmic-ray beam at sea level . . . . .	601
Page, N., <i>see</i> Cosyns, M. G. E.	
Pair-production in different elements by $\gamma$ -rays . . . . .	499
Pankhurst, R. C. : The emission spectrum of sodium hydride . . . . .	191
Paramagnetic resonance, hyperfine splitting (Letter) . . . . .	664
Parker, W. G., <i>see</i> Wolfhard, H. G.	
Performance of infra-red spectrometers as limited by detector characteristics . .	205
Penetrating showers, size-frequency, distribution . . . . .	669
Perturbation theory in neutron multiplication problems . . . . .	791
Phosphors, containing more than one activator, dielectric changes . . . . .	731
Phosphors, zinc sulphide, tin activated, luminescence characteristics . . . . .	817
Photoconductive receivers, infra-red increased sensitivity of (Letter) . . . . .	456
Photoconductivity, infra-red, in layers of tellurium and arsenic (Letter) . . . .	264
Photoconductivity of semiconducting layers, theory (Letter) . . . . .	530
Photo-disintegration of oxygen into four $\alpha$ -particles (Letter) . . . . .	460
Photographic plate, nuclear disintegration in . . . . .	243
Physical basis of life . . . . .	537
Pillow, M. E. : Intensity distribution for bands of the $\gamma$ -system of $\text{MgII}^1$ . . . . .	237
Price, D. J. : A theory of reflectivity and emissivity . . . . .	278
Price, D. J., <i>see also</i> Weale, R.	
Propagation of radiation and damping theory . . . . .	12
Putley, E. H. : The electrical conductivity of germanium . . . . .	284
Radio-frequency emission from the sun, intense, significance of the observation . .	483
Ratio of positive to negative particles in the vertical cosmic-ray beam at sea level . .	601
Radio-sodium, $^{24}\text{Na}$ , decay constant (Letter) . . . . .	457
Radiation damping, theory of, and collision problems . . . . .	2
Radiation from transient light sources . . . . .	95
Radiation, polarized, electrons ejected by (Letter) . . . . .	529
Radiation, propagation of, and damping theory . . . . .	12
Radiative reaction and damping in scattering . . . . .	749
Recording spectrometer for Raman spectroscopy . . . . .	401
Reflectivity and emissivity, theory . . . . .	278
Reflectivity and emissivity, theory (Letter) . . . . .	661
Resistivity for mercury and tin, size-variation . . . . .	77
Resistivity of thin metallic films (Letter) . . . . .	135
Resolving power and intensity relationships of the Fabry Perot interferometer with silvered reflecting surfaces . . . . .	225
Resonance transfer of electronic energy in organic crystals . . . . .	26'
Robinson, C. : Three-dimensional design of synchrotron pole-faces . . . . .	592
Rosser, W. G. V., <i>see</i> Mitra, S.M.	
Roy, R. R. : Pair-production in different elements by $\gamma$ -rays . . . . .	499
Roy, R. R., <i>see also</i> Champion, F. C.	
Rubinowicz, A. : Eigenfunctions following from Sommerfeld's polynomial method .	736
Ryle, M. : Evidence for the stellar origin of cosmic rays . . . . .	491
Ryle, M. : The significance of the observation of intense radio-frequency emission from the sun . . . . .	483
Rzewuski, J. : Some cut-off methods for the electron self-energy . . . . .	386

Scattering of fast $\beta$ -particles through large angles by nitrogen nuclei (Discussion) . . . . .	264
Schoenberg, M., <i>see</i> Cosyns, M. G. E.	
Schumann-Runge O <sub>2</sub> bands emitted at atmospheric pressure . . . . .	114
Schwarz, E. : Theory of photoconductivity of layers of semi-conducting substances (Letter) . . . . .	530
Scott, R. A., <i>see</i> Jones, T. K.	
Second sound and the behaviour of helium II . . . . .	154
Semiconductors, surfaces, structure and electrical properties-- Part I : Silicon carbide	333
Sessile dislocations (Letter) . . . . .	202
Shuttleworth, R. : The surface energies of inert-gas and ionic crystals . . . . .	167
Significance of the observation of intense radio-frequency emission from the sun . . . . .	483
Silicon carbide : surface structure and electrical properties . . . . .	333
Sillars, R. W., <i>see</i> Jones, T. K.	
Sinha, S. P. : Ultra-violet bands of Na <sub>2</sub> . . . . .	124
Size-frequency distribution of penetrating showers . . . . .	669
Size-variation of resistivity for mercury and tin . . . . .	77
Slowing down of mesons (Letter) . . . . .	136
Smith, F. W., <i>see</i> Bowen, E. J.	
Smith, R. A., <i>see</i> Hall, W. H.	
Sodium hydride, emission spectrum. . . . .	191
Sommerfeld's polynomial method, eigenfunctions following from . . . . .	736
Spectrometer, Geiger counter, for the measurement of Debye-Scherrer line shapes	631
Spectrometers, infra-red, performance . . . . .	205
Spectrometer, recording, for Raman spectroscopy . . . . .	401
Spectroscopic examination of flames at normal pressures, a new technique . . . . .	722
Spring, K. II. : Electrons ejected by polarized radiation (Letter) . . . . .	529
Steady non-uniform state for a liquid . . . . .	41
Steam in the ring discharge . . . . .	465
Stereographic projector . . . . .	559
Strain ageing of iron and dislocation theory of yielding . . . . .	49
Street, R., and Woolley, J. C. : A study of magnetic viscosity . . . . .	562
Street, R., and Woolley, J. C. : Magnetic viscosity in Mn-Zn ferrite (Letter) . . . . .	743
Structure and diamagnetic anisotropy of p-benzoquinodimethane in connection with those of p-benzoquinone . . . . .	505
Structure and electrical properties of surfaces of semiconductors—Part I : Silicon carbide . . . . .	333
Structure and epitaxy of lead chloride deposits formed from lead sulphide and sodium chloride . . . . .	344
Study of magnetic viscosity . . . . .	562
Superconducting tin foils, critical field measurements . . . . .	88
Surface energies of inert-gas and ionic crystals . . . . .	167
Surface forces in liquids and solids . . . . .	639
Surface free energy of certain metals . . . . .	180
Sutherland, G. B. B. M., <i>see</i> Daly, E. F.	
Synchrotron pole-faces, three-dimensional design . . . . .	592
Synchrotrons, betatron injection into . . . . .	617
Temperature, absolute scale, establishment below 1° K. . . . .	269
Temperature variation of the electrical properties of nickel oxide . . . . .	446
Theory of emissivity and reflectivity (Letter) . . . . .	661
Theory of photoconductivity of layers of semi-conducting substances (Letter) . . . . .	530
Theory of reflectivity and emissivity . . . . .	278
Theory of ultrasonic absorption in unassociated liquids . . . . .	141
Thermal diffusion factor, dependence on temperature . . . . .	655
Thompson, H. W., <i>see</i> Miller, C. H.	
Thosar, B. V. : Origin of low-energy electron lines in the $\beta$ -spectrum of <sup>198</sup> Au (Letter) . . . . .	739
Three-dimensional design of synchrotron pole-faces . . . . .	592
Titterton, E. W., <i>see</i> Goward, F. K.	

	PAGE
Ultrasonic absorption in unassociated liquids, theory . . . . .	141
Ultra-violet bands of $\text{Na}_2$ . . . . .	124
Ultra-violet absorption spectrum of $\text{SnO}$ (Letter) . . . . .	740
Uniformly moving dislocations . . . . .	307
Use of liquid helium in magnetic cooling experiments (Letter) . . . . .	392
 Vibrations, bending, linear chain . . . . .	 200
Viscosity and superfluidity in liquid helium (Letter) . . . . .	394
 Walker, D. : Half-lives of $^{141}\text{Ce}$ and $^{169}\text{Yb}$ . . . . .	 799
Walker, D., <i>see also</i> Bunyan, D. E.	
Watts, B. N. : Increased sensitivity of infra-red photoconductive receivers (Letter)	456
Wave functions, computation in momentum space, helium atom . . . . .	509
Wave functions, computation in momentum space, hydrogen molecule ion . . . . .	519
Weale, R. : The resistivity of thin metallic films (Letter) . . . . .	135
Weale, R., and Price, D. J. : A theory of emissivity and reflectivity (Letter) . . . . .	661
Westerman, K., <i>see</i> Kellermann, E. W.	
Wilkins, J. J., <i>see</i> Goward, F. K.	
Williams, F. E., <i>see</i> Johnson, J. S.	
Wilman, H., <i>see</i> Elleman, A. J.	
Wilson, J. G., <i>see</i> Owen, B. G.	
Wilson, R., and Bishop, G. R. : The decay constant of radio sodium, $^{24}\text{Na}$ (Letter)	457
Wolfhard, H. G., and Parker, W. G. : A new technique for the spectroscopic examination of flames at normal pressure . . . . .	722
Wolfhard, H. G., and Parker, W. G. : Temperature measurements of flames containing incandescent particles (abstract). Corrigendum . . . . .	600
Woodward, L. A., <i>see</i> Miller, C. H.	
Woolley, J. C., <i>see</i> Street, R.	
Wright, R. W., and Andrews, J. P. : Temperature variation of the electrical properties of nickel oxide . . . . .	446
van Wyk, C. B. : On the decay of $\tau$ -mesons . . . . .	697
Wyllie, G., <i>see</i> Huang, K.	
 X-ray emission bands of sodium, soft, theory . . . . .	 806
X-ray line broadening in metals (Letter) . . . . .	741

## INDEX TO REVIEWS OF BOOKS

	PAGE
Attwood, C. : <i>Practical Five-figure Mathematical Tables</i> . . . . .	71
Berthelot, A. : <i>Le Noyau atomique</i> . . . . .	666
Bethe, H. A. : <i>Elementary Nuclear Theory</i> . . . . .	597
Booth, A. D. : <i>Fourier Technique in X-ray Organic Structure Analysis</i> . . . . .	328
Centre de Documentation : <i>Bulletin Analytique</i> . . . . .	323
Comrie, L. J. : <i>Chambers' Six-figure Mathematical Tables</i> . . . . .	461
Cottrell, A. H. : <i>Theoretical Structure Metallurgy</i> . . . . .	397
Dale, J. B. : <i>Five-figure Tables of Mathematical Functions</i> . . . . .	462
Dallavalle, J. M. : <i>Micromeritics</i> . . . . .	330
Darrow, K. K. : <i>Atomic Energy</i> . . . . .	598
Dushman, S. : <i>Scientific Foundations of Vacuum Technique</i> . . . . .	745
Fonda, G. R., and Seitz, F. : <i>Preparation and Characteristics of Solid Luminescent Materials</i> . . . . .	138
Glasstone, S. : <i>Theoretical Chemistry</i> . . . . .	321
Green, S. L. : <i>The Theory and Use of the Complex Variable</i> . . . . .	462
Hartman, R. J. : <i>Colloid Chemistry</i> . . . . .	325
James, R. W. : <i>The Optical Principles of the Diffraction of X Rays</i> . . . . .	326
Jánossy, L. : <i>Cosmic Rays</i> . . . . .	319
Kaye, G. W. C., and Laby, T. H. : <i>Tables of Physical and Chemical Constants</i> . . . . .	322
Korff, S. A. : <i>Electrons and Nuclear Counters</i> . . . . .	73
Kröger, F. A. : <i>Some Aspects of the Luminescence of Solids</i> . . . . .	72
Mathieu, J. P. : <i>Les Théories moléculaires du Pouvoir rotatoire naturel</i> . . . . .	322
Miller, A. R. : <i>The Theory of Solutions of High Polymers</i> . . . . .	532
Milne, E. A. : <i>Kinematic Relativity</i> . . . . .	327
Milne-Thomson, L. M. : <i>Theoretical Aerodynamics</i> . . . . .	74
Mott, N. F., and Sneddon, I. N. : <i>Wave Mechanics and its Applications</i> . . . . .	329
Robertson, J. K. : <i>Radiology Physics</i> . . . . .	533
Slater, J. C., and Frank, N. H. : <i>Electromagnetism</i> . . . . .	321
Spreadbury, F. G. : <i>Electronics</i> . . . . .	321
Tolansky, S. : <i>Multiple-beam Interferometry of Surfaces and Films</i> . . . . .	266
Vernotte, P. : <i>Thermocinétique</i> . . . . .	746
Weld, L. D. : <i>A Text-book of Heat</i> . . . . .	532
Wilson, A. J. C. : <i>X-ray Optics</i> . . . . .	533
Wilson, J. G. : <i>About Cosmic Rays</i> . . . . .	322
Woolley, H. W., Scott, R. B., and Brickwedde, F. G. : <i>Compilation of Thermal Properties of Hydrogen in its Various Isotopic and Orthopara Modifications</i> . . . . .	666
Worthing, A. G., and Halliday, D. : <i>Heat</i> . . . . .	324





L.A.R.1. 75

INDIAN AGRICULTURAL RESEARCH  
INSTITUTE LIBRARY, NEW DELHI.

[illegible]